F 1103

Vegyiml

04

ACADÉMIE DE LA RÉPUBLIQUE SOCIALISTE DE ROUMANIE

REVUE ROUMAINE DE CHIMIE

Hommage à l'académicien
ELENA CEAUȘESCU

TOME 29

N° 1

Janvier 1984

EDITURA ACADEMIEI REPUBLICII SOCIALISTE ROMÂNIA

Rev. Roumaine Chim.

RRCHAX, 29, *1*, p. 1–140 (1984), Bucarest

ACADÉMIE DE LA RÉPUBLIQUE SOCIALISTE DE ROUMANIE

COMITÉ DE RÉDACTION

Rédacteur en chef:

I. G. MURGULESCU, membre de l'Académie de la République Socialiste de Roumanie

Rédacteurs en chef adjoints:

A. T. BALABAN et V. EM. SAHINI, membres correspondants de l'Académie de la République Socialiste de Roumanie

Collège de rédaction:

EM. BRATU, ELENA CEAUŞESCU, ECATERINA CIORĂNESCU-NENITZESCU, CR. SIMIONESCU, membres de l'Académie de la République Socialiste de Roumanie; P. SPACU, membre correspondant de l'Académie de la République Socialiste de Roumanie; MARGARETA AVRAM, M. BANCIU, I. HAIDUC, D. I. MARCHIDAN, I. MOLDOVAN, G. NIAC et D. SĂNDULESCU

La Revue Roumaine de Chimie paraît 10 fois par an. Toute commande de l'étranger pour les travaux parus aux Editions de l'Académie de la République Socialiste de Roumanie sera adressée à ILEXIM – Departamentul Export-Import Carte (Livres)/Departamentul Export-Import Presă (Revues), P.O.B. 136–137, télex 11226, str. 13 Decembrie, 79517, Bucarest, Roumanie

Les manuscrits, les livres et les revues proposés en échange, ainsi que toute correspondance seront envoyés à la rédaction

REVUE ROUMAINE DE CHIMIE

125, Calea Victoriei, 79717 Bucarest, Roumanie, téléphone 50 76 80

EDITURA ACADEMIEI REPUBLICII SOCIALISTE ROMÂNIA
125, Calea Victoriei, 79717, Roumanie, téléphone 50 76 80

ORSZÁGOS MŰSZAKI INFORMÁCIÓS KÖZPONT ÉS KÖNYVTÁR
1883

HOMMAGE À L'ACADÉMICIEN
ELENA CEAUȘESCU

IN HONOUR OF
ELENA CEAUȘESCU, D. CHEM. ENG.
MEMBER OF THE ACADEMY OF THE SOCIALIST REPUBLIC OF ROMANIA

On January 7, this year, we celebrate 45 years of revolutionary action of Academician Elena Ceaușescu. A Doctor in Chemical Engineering, Member of the Executive Political Committee of the Romanian Communist Party, First Vice-Prime Minister of the Government of the Socialist Republic of Romania, President of the National Council for Science and Technology, Dr. Elena Ceaușescu conducts a vast scientific, political and social activity devoted to the implementation of the overall policy of Romania's Communist Party and State, to progress and assertion of the Romanian science. The organization and management of the scientific research in this country, most evidently in the field of chemistry, chemical technology and engineering, rely largely upon the innovative scientific spirit and direct guidance of Dr. Elena Ceaușescu.

As a direct outcome, the whole research and development enterprise in chemistry has been given an appropriate coordination and has been integrated, along with the higher education in the field, into the industrial enterprise.

The research work undertaken by Dr. Elena Ceaușescu focussed mainly on the chemistry and technology of macromolecular compounds; she contributed to elucidating a number of major problems in the area — a most dynamic one in chemistry today, while also providing valuable contributions in all stages of applied research and engineering, thus fostering the implementation of fundamental research results in industry. The topics of her studies include procedures of monomer and solvent purification; procedures for obtaining polymers via stereospecific polymerization and emulsion polymerization; procedures for obtaining polycondensates; studies on structural characteristics of polymers and relationship between structure and properties; as well as methods for the characterization of polymers. A series of studies deal with the use of complex catalysts for polymer synthesis in solution with special emphasis on transitional metal-based catalysts. Other works treat on the obtention of polymers modified by isomerization, degradation and substitution reactions.

The stereospecific polymerization of isoprene holds an important place in the research work developed by Dr. Elena Ceaușescu, owing to the paramount relevance of this problem in today's chemistry of synthetic rubber. Part of the results were gathered in her doctoral thesis. The studies borne upon the synthesis of *cis*-1,4-polyisoprenic rubber that displays properties and structure similar to those of the natural rubber, a substitute of the latter in the tyre and technical item industry. The theoretical aspects connected with the reaction mechanism and kinetics and with the properties of the polyisoprene were also dealt with. Research was focussed on the optimization of the basic parameters, the obtention of catalytic systems and development of the main steps of the technological flow-chart. The results led to the elaboration of the industrial process of manufacturing *cis*-1,4-polyisoprenic rubber in Romania.

The scientific activity of Dr. Elena Ceaușescu is also reflected by the numerous papers published in scientific journals and in the four monographs issued at Editura Academiei, Bucharest: "Research Work on Synthesis and Characterization of Macromolecular Compounds" (1974), "Stereospecific Polymerization of Isoprene" (1979), "Recent Research in the Field of Macromolecular Compounds" (1981) and "Research in Chemistry and Technology of Polymers" (1984).

Dr. Elena Ceaușescu acted as Chairwoman of the National Congresses of Chemistry (1978, 1981) and IUPAC, Macro '83 Symposium. Her opening address at the IUPAC 1983 offers important guidelines to the chemical research, the strengthening of co-operation, the expansion of modern domains of science, and of a technological development aimed at providing for further progress. Dr. Elena Ceaușescu contributed to the two National Congresses and the IUPAC International Symposium on Macromolecular Chemistry a series of valuable papers — an outcome of her comprehensive scientific and applied activity in the field of elastomer chemistry.

Dr. Elena Ceaușescu's scientific merits led to her election as full member of the Academy of the Socialist Republic of Romania and to her worldwide recognition as a remarkable scientist. She was elacted member of numerous international chemical societies of high renown and was nominated honorary professor at important foreign higher education institutions. She is honorary member of the International Society of Industrial Chemistry, France; active member of the Academy of Sciences, New York; honorary member of the College of Chemists and Chemical Engineers in Costa Rica; honorary member of the University Council and of the Management Council of the Central University in Ecuador; honorary member of the Ecuador Institute of Natural Sciences; honorary member of the School of Information Science of the Central University of Ecuador; honorary professor of the National Engineering University, Peru; honorary member of the American Institute of Chemists (A.I.C.); Doctor Honoris Causa of the University of Buenos Aires; Doctor Honoris Causa of the South University — Bahia Blanca, Argentina; Doctor Honoris Causa of the Feminine University of Manilla, the Philippines; honorary member of the Chemical Society of Mexico; Doctor Honoris Causa of the University of Yucatan, Mexico; Extraordinary Professor of the Autonomous National University of Mexico; Doctor Honoris Causa of Sciences, University of Teheran; honorary member of the Society of Polymer Science of Japan; corresponding member of the Academy of Athens; distinguished with the Silver Medal of the Science University of Kuweit; honorary member of the Academy of Arts and Sciences of Ghana; associated member of the Institute of Egypt; honorary member of the Academy of Sciences of Illinois, USA; Fellow of the Royal Institute of Chemistry, U.K.; Professor Honoris Causa of the Central London Polytechnic; full member of the European Academy of Sciences, Arts and Humanities and member of the Honorary Committee of the Academy; Doctor Honoris Causa of the Technical University of the Middle East, Ankara; Doctor Honoris Causa of the University of Malta.

The high appreciation enjoyed by Dr. Elena Ceaușescu's many-sided activity is reflected also in the important titles and distinctions of merit she was awarded: the highest title of honour "Hero of the Socialist Republic of Romania", "Hero of Socialist Work", "Star of the Socialist Republic of Romania" and other Romanian and foreign orders and medals. She was also awarded the Gold Medal of the Institute for the Problems of a New International Economic Order, the Gold

Medal "Marie Curie" and the Jubilee Gold Medal of the Institute of International Relations in Rome, the Gold Badge of the European Academy of Sciences, Arts and Humanities.

The Presidium of the Academy of the Socialist Republic of Romania, the Executive Bureau of the National Council for Science and Technology, the Section of Chemical Sciences of the Academy of the Socialist Republic of Romania and the Editorial Board of the "Revue Roumaine de Chimie", joining whole heartedly the feelings of great esteem and appreciation in which the Romanian people holds Academician Elena Ceauşescu for her exceptional contribution to the development of scientific research in Romania, of Romanian chemistry and engineering, express their best wishes of good health, happiness, long and fruitful activity, for raising science, education and culture in the Socialist Republic of Romania onto ever higher levels.

THE PRESIDIUM
OF THE ACADEMY OF THE SOCIALIST
REPUBLIC OF ROMANIA

THE EXECUTIVE BUREAU
OF THE NATIONAL COUNCIL FOR
SCIENCE AND TECHNOLOGY

THE SECTION OF CHEMICAL SCIENCES
OF THE ACADEMY OF THE SOCIALIST REPUBLIC
OF ROMANIA

THE EDITORIAL BOARD
OF THE "REVUE ROUMAINE DE CHIMIE"

REVUE ROUMAINE DE CHIMIE

Tome 29, N° 1 Janvier, 1984

IN HONOUR OF ELENA CEAUȘESCU, D. CHEM. ENG. MEMBER OF THE ACADEMY OF THE SOCIALIST REPUBLIC OF ROMANIA

ELENA CEAUȘESCU, R. BORDEIANU, P. GHIOCA, R. STANCU, I. CERCHEZ and E. BUZDUGAN. Dilute block copolymer systems. III. Hardness of oil-extended butadiene-styrene block copolymers 3–11

C. ANDREI, ELENA MOLDOVAN, GEORGETA ANDREI, GALINA NICOLESCU and VIORICA DOBRESCU, Alternating copolymers of maleic anhydride with ethylene and vinyl acetate – ion exchangers . . . . 13–18 R

OLGA BUTUFEI and ION GAVĂT, Polyaminochlorquinones. I. Polycondensation of chloranil with piperazine 19–24

CORNELIA CERCASOV, FELICIA CORNEA, MARIANA CIUREANU, MIHAELA HILLEBRAND, V. EM. SAHINI and ELENA VOLANSCHI, ESR and ^{1}H-NMR spectra of some nitrosubstituted thiobenzamides . . 25–29 Bc

EMIL CHIFU, CĂLIN GHEORGHIU and IOAN STAN, Surface mobility of surfactant solutions. XI. Numerical analysis for the Marangoni and the gravity flow in a thin liquid layer of triangular section 31–42

IULIA CONTINEANU and D. I. MARCHIDAN, The enthalpies of combustion and formation of D-alanine, L-alanine, DL-alanine and β-alanine . . . . 43–48 R

AURELIA GHENCIULESCU, MIRCEA D. GHEORGHIU, LUCIAN ENESCU, ILIE G. DINULESCU and MARGARET AVRAM, Regio- and stereoselective bromine addition to 2-chloro-*endo*-benzocyclobutenonorbornene 49–53

MONIMUL HUQUE and D. SĂNDULESCU, Studies on aqueous electrolytes and nonelectrolytes. I. Effects of electrolytes on viscosity and structure of aqueous solutions of polyvinyl alcohol . . . . 55–65 R

C. LUCA, G. SEMENESCU and A. ANDREI, Considerations on the equilibrium state of metal/oxide electrolyte system . . . . 67–75 R

Rev. Roumaine Chim. 29, *1*, p. 1 – 140 (1984) Bucarest

CR. I. SIMIONESCU and MARIANA BEZDADEA, Matrix polymerization in the presence of urea . . . . 77–82 Bc

Z. SIMON, G. I. MIHALAŞ and E. CASPI, Structure-binding affinity correlations for iodo- and selenoestrogen analogs and mapping of the estrogen receptor by the MTD-method 83–97

P. SPACU, LUMINIŢA PATRON and ADRIANA CONŢESCU, Coordination compounds of Co(II) (d^7) with tryptophan 99–104

SOLOMON STERNBERG and MIHAELA DRĂGĂNOIU, Thermodynamic activity of $ZnSO_4$ in ternary systems. I. $ZnSO_4 + Me^{I}_{2}SO_4 + H_2O$ and $ZnSO_4 + Me^{II}SO_4 + H_2O$ systems 105–112

I. TEOREANU, N. ANGELESCU and D. ŢUCLEA, $CA-CA_2$ Aluminous cement hydration kinetics and the nature of its hydration products (in French) . . 113–120 R

CORNELIA UNCUŢA, IOANA BALLY, C. DRĂGHICI, F. CHIRALEU and A. T. BALABAN, Heterocyclic organoboron compounds. XVII. Axial chirality of boron chelates evidenced by ^1H-NMR spectroscopy in the presence of chiral additives. 121–129

RODICA VÎLCU and ELENA DIMITRIU, A correlation between surface tension and the adiabatic compressibility . . . . 131–140 C

Revue Roumaine de Chimie, 29, *1*, 3–11 (1984)

DILUTE BLOCK COPOLYMER SYSTEMS. III[1]

HARDNESS OF OIL-EXTENDED BUTADIENE-STYRENE BLOCK COPOLYMERS

ELENA CEAUŞESCU, R. BORDEIANU, P. GHIOCA, R. STANCU, I. CERCHEZ
and E. BUZDUGAN
Chemical Research Institute ICECHIM, Spl. Independenţei 202, 77208
Bucharest, Romania

Received May 23, 1983

The effect of oil extension on hardness of butadiene-styrene block copolymers was investigated. Both linear and star block copolymers with varying initial styrene contents were diluted with mineral oils in the range 0–140 phr. It was found that hardness is controlled by the amount and chemical composition of oil added, the initial composition of the thermoplastic elastomer, and the nature of the casting solvent. A quantitative relationship between hardness and the factors controlling it was derived. A probably morphological transition similar to that found earlier for the tensile modulus of oil-extended block copolymers was identified.

Hardness is defined as the resistance opposed by an elastic material to a deformation produced by pressing down an indentor of specified shape with a specified force. It is customary to regard hardness as being a measure of the elastic modulus (E),[2] although the deformations involved in the process of measuring it are rather complicated. Nonlinear relationships exist between shear modulus (G) and the commonly used hardness scales.[3,4] However, as hardness measurements were performed on non-standard test pieces, we have refrained in our work from interpreting the hardness data in terms of G or E. Nevertheless, the study of hardness can give a fairly accurate, albeit qualitative picture of the mechanical behaviour of the material at low strains. The aim of this work was to investigate the effect of oil-extension upon hardness of linear and star butadiene-styrene block copolymers.

EXPERIMENTAL

Linear S–B–S triblock copolymers (L) were synthesized by sequential monomer addition in a three-step anionic polymerization process in toluene, using *n*-butyllithium as catalyst. Styrene initiation was accelerated by catalyst modification with diphenyl ether (DPE) at a molar ratio DPE/n–BuLi = 2. Star block copolymers, $(S-B-)_4$ were obtained by coupling active styrene-butadiene diblocks (S–B–Li) with a tetrafunctional linking agent ($SiCl_4$). The polymers were stabilized with 0.8 percent of 2,6-*bis-tert*-butyl-*p*-cresol, and then recovered by steam-hot water stripping. Polymer properties are given in Table 1.

Weighed amounts of polymer were redissolved in toluene and known amounts of extender oil were added. The properties of the extender oils used are given in Table 2. Two of the oils (Oils I and II) were paraffinic-naphthenic and the third was a highly aromatic oil.

Table 1

Properties of Block Copolymers

Polymer	Structure	Styrene content, wt.—%	Molecular weight ($\overline{M}_n$), g·mole^{-1}		
			Total	$\overline{M}_B$	$\overline{M}_S$
L—1	linear	34.5	123,200	80,000	21,200
L—3	linear	27.8	78,500	57,100	10,700
L—4	linear	40.3	98,000	58,600	19,700
S—1	star	42.7	120,000	68,800	12,800
S—2	star	30.7	141,400	98,200	10,800

From the homogeneous solutions 0.8 mm thick polymer films were spin-cast as described in an earlier paper.[5] Hardness was measured on multilayer piles of film with a total thickness of approx. 6 — 8 mm according to ISO R—868 on a dead load Zwick hardness tester Mod. 7206 at 25° in the Shore A scale. A good blocking of rubber layers was obtained even for pure gum (nonextended) samples, due to the smooth surface of the spin-cast films. Care was taken to prevent inclusion of air bubbles. For all practical purposes a multilayer test piece behaved like a solid block of material.

Table 2

Properties of Extender Oils

Property	Unit	Oil I	Oil II	Oil III
Color	—	colorless	pale yellow	black
Density at 25°	kg·m^{-3}	866.5	897.1	1009.6
Refractive index at 25°	—	1.4740	1.4929	1.5785
Average molecular weight	g·mole^{-1}	418	450	
Kinematic viscosity at 37.8°	m^2·h^{-1}	0.134	0.432	
Saybolt viscosity at 100°	deg. Saybolt			118
Structural composition *				
Aromatic C	wt.—%	3.5	7	45
Naphthenic C	wt.—%	29.9	38	21
Paraffinic C	wt.—%	66.6	55	34

* Calcd. from n_D, d, and M.

RESULTS AND DISCUSSION

1. Hardness of Triblock Copolymers

1.1. *Effect of Oil Level*

Taking as a measure of matrix dilution the volume fraction of rubber in the oil-extended matrix,[1] φ_R, calculated in the reasonable assumption (at least for paraffinic-naphthenic oils) that oil is compatible with the polydiene phase only,[1] it can be seen from Figure 1 (in which data on toluene-cast films of S – B – S triblocks extended with paraffinic-naphthenic oils are plotted against φ_R), that, after an initially slower decrease of hardness with oil content, a transition interval follows after which hardness decreases faster with further oil extension. The onset of the transition is dependent on the composition of base polymer.

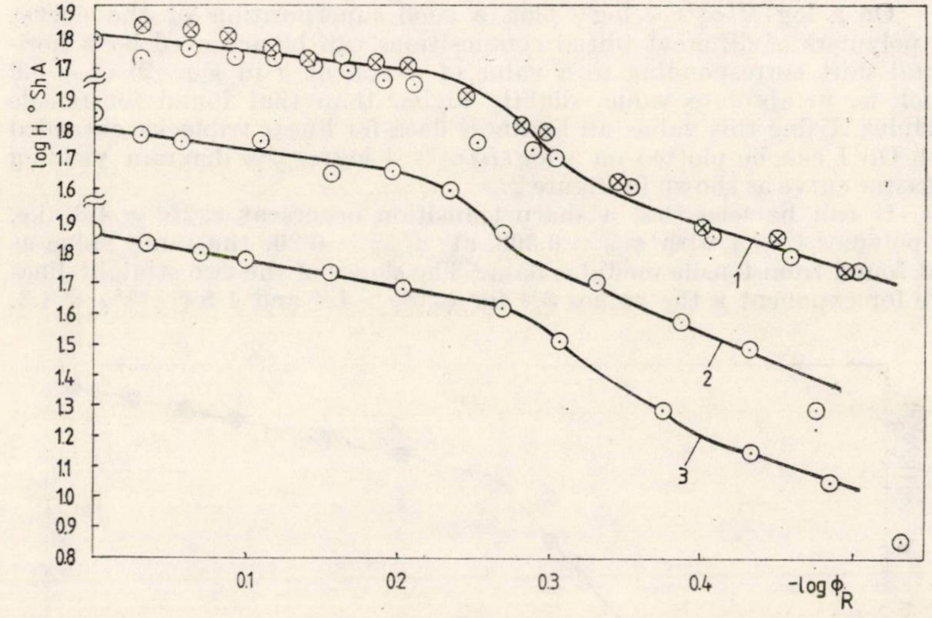

Fig. 1. — Hardness of linear block copolymers vs. volume fraction of rubber in the oil-diluted matrix.

⊙ Oil I; ⊗ Oil II

1, L – 1 ; *2*, L – 3 ; *3*, L – 4.

In an attempt to find a quantitative relationship between hardness, amount of extender oil added and composition of base polymer, a data treatment similar to that applied for tensile modulus [1] was employed. Our previous investigations have shown that the large strain tensile modulus (f) of oil-extended S – B – S block copolymers is given by the following equation :

$$f = (C_1' + C_2'/\lambda)(\lambda - 1/\lambda^2)\,\varphi_R^{1/3}(\varphi_{S,0}^{-1/2}\gamma)^n \qquad (1)$$

where λ = extension ratio, $\varphi_{S,0}$ = volume fraction of polystyrene domains in base polymer, C_1' and C_2' = constants. The Guth-Smallwood function, γ, is defined as [6]

$$\gamma \equiv E/E_0 = 1 + 2.5\,\varphi_S + 14.1\,\varphi_S^2$$

where E is the elastic modulus of the material, E_0 is the elastic modulus of the matrix, and φ_S is the volume fraction of polystyrene domains in the oil-extended material. The exponent n in Eq. 1 is 4/3 for $\varphi_{S,0}^{-1/2} > 3.7$, and 4 for $\varphi_{S,0}^{-1/2} < 3.4$.

By analogy, and under the same assumptions, the validity of a similar model for hardness (H) was tested :

$$H = H_0 \varphi_R^{1/3} (\varphi_{S,0}^{a} \gamma)^n \qquad (2)$$

where, H_0, a, and n are constants.

On a $\log(H/\varphi_R^{1/3}) - \log\gamma$ plot, a good superposition of the curves for polymers of different initial compositions can be achieved by a horizontal shift corresponding to a value of exponent a in Eq. (2) of -0.6 which is, in absolute value, slightly higher than that found for tensile modulus. Using this value, all hardness data for linear triblocks extended with Oil I can be plotted on a $\log(H/\varphi_R^{1/3}) - \log(\varphi_{S,0}^{-0.6}\gamma)$ diagram yielding a master curve as shown in Figure 2.

It can be seen that a sharp transition occurs at $\varphi_{S,0}^{-0.6}\gamma = 4.3$, i.e, for polymer L — 1 with $\varphi_{S,0} = 0.308$, at $\varphi_{S,crit} = 0.20$, the same value as that found from tensile modulus data.[1] The slopes of the two straight lines give for exponent n the values 3/4 for $\varphi_{S,0}^{-0.6}\gamma > 4.3$ and 4 for $\varphi_{S,0}^{-0.6}\gamma < 4.3$.

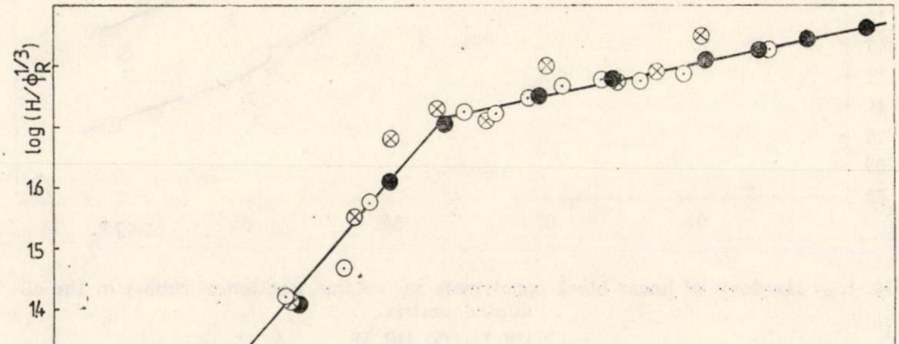

Fig. 2. — Master curve of hardness dependence on decomposition of base polymer and Guth-Smallwood function.

⊙ L—1 ; ⊗ L—3 ; ● L—4.

From the intercepts the values 17.3 °ShA and 0.15 °ShA respectively were found for H_0. While the slope of the master curve is, at high dilutions, equal with that of the tensile modulus curve (see Figure 6 in Ref.[1]) which may be fortuitous in view of the fact that no simple relationship exists between *f* and *H*, at low dilutions the slope is smaller. These findings fortify the conclusions drawn earlier from analyzing tensile modulus data. Indeed, the most probable explanation of the behavior of toluene-cast films of oil-extended block copolymers consists in a morphological transition induced by the decreasing volume fraction of the glassy phase, from a more or less continuous polystyrene phase (resulted from fusing together the glassy domains over distances significantly larger than their characteristic length) to – probably spherical – isolated polystyrene domains in a continuous oil-diluted polybutadiene matrix. It seems that this transition is assisted by oil separation from the matrix at concentrations higher than the equilibrium value.[1]

In contrast to large strain testing, which is accompanied by a massive disruption of the polystyrene continuum, at the low strains involved in determining hardness the original morphology of spin-cast polymer films is left largely unperturbed. This can easily explain the smaller value of exponent n in the hardness equation (2) compared with the tensile modulus equation (1) at $\varphi_{S,0}^{-0.6}\gamma > 4.3$. At higher oil concentrations where domains are isolated the behavior of the dilute block copolymer system is governed by the properties of the extended matrix and the volume fraction of polystyrene only, hence a similar response to tensile and hardness testing is to be expected.

1.2. *Effect of Oil Composition*

If data on toluene-cast films of polymer L—1 extended with variable proportions of oils of different composition (Oils II and III, containing higher amounts of aromatic hydrocarbons) are similarly treated (Figure 3), a behavior different from that encountered with Oil I is revealed. The most prominent feature of the plot is the increase in hardness begin-

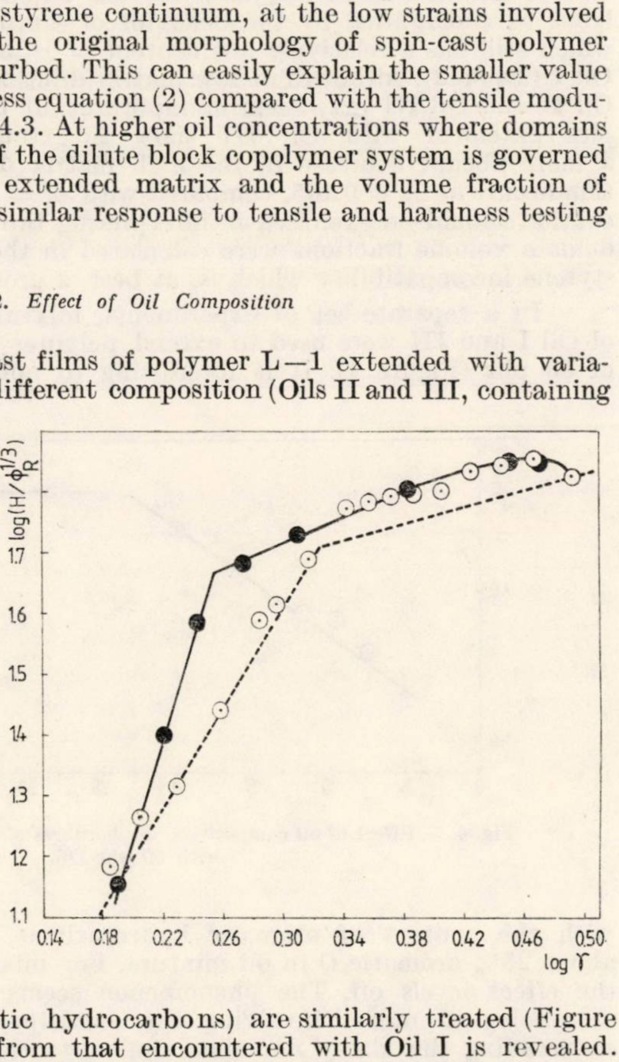

Fig. 3.—Hardness dependence on Guth-Smallwood function for polymer L—1 extended with oils of different compositions.

⊙ Oil II; ● Oil III;
– – – Master curve for Oil I.

ning from the lowest oil concentrations (Figure 3, see also curve 1, Figure 1).

Previous investigations[1] confirmed that the compatibility of polystyrene with oils increases with the content of aromatic hydrocarbons. As in the case of tensile testing, the effect of aromatics in oil is primarily a swelling of the glassy domains, hence an increase of polystyrene volume fraction. Since the elastic modulus of two-phase materials consisting of an elastic matrix and a dispersed rigid phase is dependent on the volume fraction of the latter (e.g. through the Guth-Smallwood function), it is self-evident that the absorption of some of the oil fractions in the domains can bring about an increase in hardness. This effect is felt in the case of hardness even for relatively low amounts of aromatic hydrocarbons, as exemplified by the behavior of samples extended with Oil II which still has a relatively low content of aromatics, albeit twice that of Oil I (Table 2). Although at low matrix dilutions the differences between Oil II and Oil III may seem unimportant, at higher concentrations samples extended with Oil III show an extended plateau, followed by a more abrupt decrease in the high matrix dilution range. The transition occurs at $\varphi_S = 0.165$, compared with $\varphi_S = 0.205$ for Oil I. However, caution should be exercised in interpreting the data in terms of φ_S since domain volume fractions were calculated in the assumption of oil-polystyrene incompatibility which is, at best, a gross approximation.

In a separate set of experiments, mixtures in various proportions of Oil I and III were used to extend polymer L—1 at a constant level of 50 phr (Figure 4). It is interesting to note that hardness increases with the content of aromatic hydrocarbons, up to a concentration of about 25% aromatic C in oil mixture. For mixtures richer in aromatics, the effect levels off. The phenomenon seems to be consistent with a morphological model involving the participation of interphase layers surrounding the glassy domains, similar to that proposed by Leblanc.[7] In the domain-interphase layer system (DILS) the interphase layer is

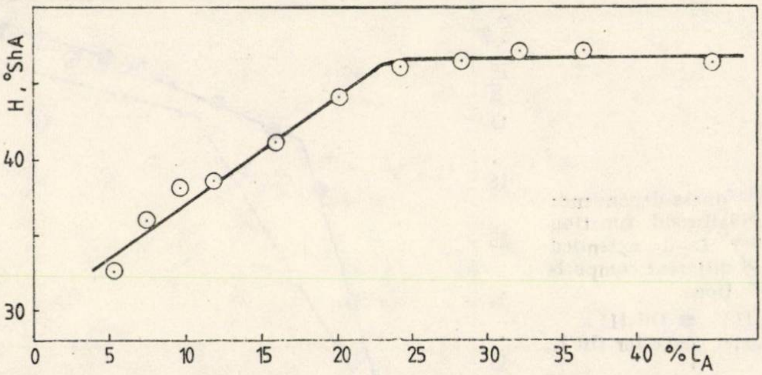

Fig. 4. — Effect of oil composition on hardness of polymer L—1 extended with 50 phr Oil.

probably the main locus of swelling; the leveling of hardness with an increasing content of aromatics may be attributed to a "saturation" of the DILS, or at least of its glassy core.

1.3. *Effect of Casting Solvent*

Solvent has a profound effect on the morphology of cast polymer films and hence on their mechanical behaviour. In solvents selective for the diene center block, the plastomeric blocks collapse early in the process of film deposition conducing thus to the formation of isolated polystyrene domains. Films of polymer L—1 cast from cyclohexane (a θ solvent for polystyrene at 34.5°) show a lower hardness than that of toluene-cast films extended with the same amount of Oil I (Figure 5). Down to $\gamma \approx 2.1$ the slope of hardness decrease with γ is virtually equal to that of toluene-cast films. At higher oil concentrations hardness decreases abruptly, along the same slope as found for films cast from toluene. This is an indication that even for cyclohexane-cast films a morphological transition occurs. The fact that this transition could not be identified by large strain tensile testing[1] can probably be explained by a much more loose aggregation of the domains in the low dilution range, which was easily broken at the high extension ratios ($\lambda = 4$ or $\lambda = 6$) involved in determining tensile modulus.

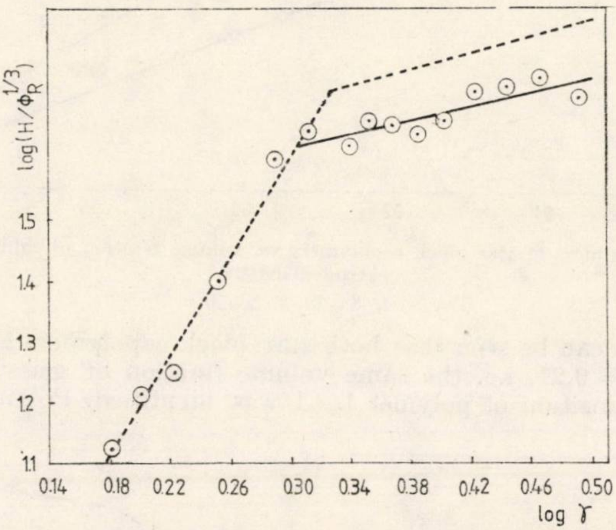

Fig. 5. — Hardness dependence on Guth-Smallwood function for films of polymer L—1 cast from cyclohexane.

2. **Hardness of Star Block Copolymers**

The effect of matrix dilution on the hardness of star block copolymers seems to be more complicated than in the case of linear triblocks, as illustrated in the diagram given in Figure 6. Although the polymer with a lower styrene content (S–2) shows in the $\log H - \log \varphi_R$ plot only one transition (like the linear block copolymers), the star block copolymer richer in styrene (S–1) yields a curve of a more complicated shape. The differences become even more obvious in the $\log H/\varphi_R^{1/3} - \log \gamma$ plot

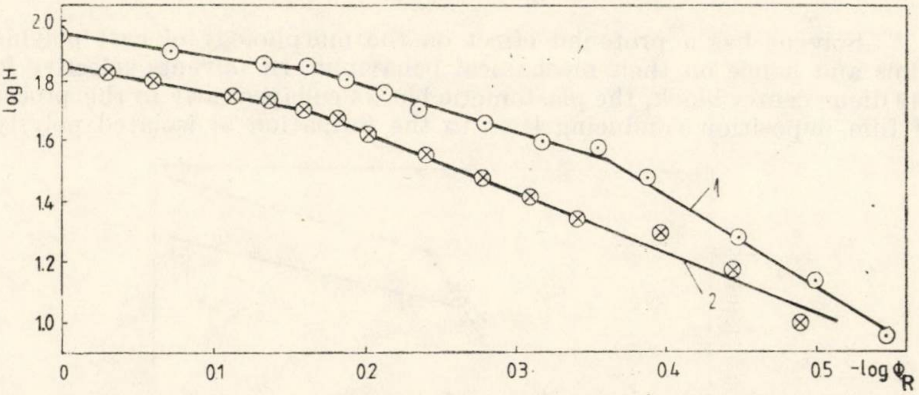

Fig. 6. – Hardness of star block copolymers vs. volume fraction of rubber in the oil-extended matrix.
1, S–1 ; *2*, S–2.

(Figure 7). It can be seen that both star block copolymers exhibit a transition at $\varphi_S = 0.21$, i.e. the same volume fraction of glassy domains at which the transition of polymer L–1 was identified. Polymer S–1 also

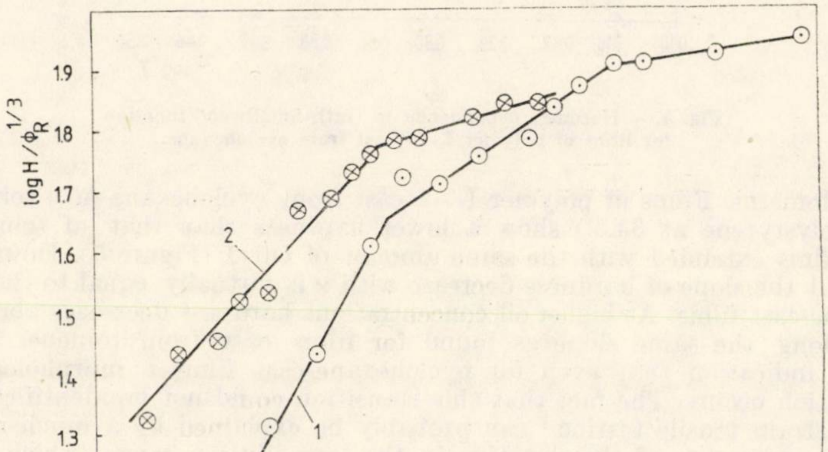

Fig. 7. – Hardness dependence on Guth-Smallwood function for star block copolymers extended with Oil I.
1, S–1 ; *2*, S–2.

shows a transition at a higher concentration of polystyrene domains ($\varphi_S = 0.3$) which could not be detected so far in the case of linear triblock copolymers.

REFERENCES

[1] E. Ceauşescu, R. Bordeianu, P. Ghioca, I. Cerchez, E. Buzdugan, and R. Stancu, *Rev. Roumaine Chim.*, **28**, 229 (1983).

[2] R. P. Brown, "Physical Testing of Rubbers", Applied Science Publishers, London, 1979, p. 114.

[3] A. V. Tobolsky, and H. F. Mark, "Polymer Science and Materials", Wiley, New York, 1971, ch. 13.

[4] A. N. Gent, in "Science and Technology of Rubber", F. R. Eirich, ed., Academic Press, New York, 1978, ch. 1.

[5] E. Ceauşescu, R. Bordeianu, P. Ghioca, and M. Bălănescu, *Mat. Plast.*, **17**, 201 (1980).

[6] H. M. Smallwood, *J. Appl. Phys.*, **15**, 758 (1944).

[7] J. L. Leblanc, *J. Appl. Polymer Sci.*, **21**, 2419 (1977).

Revue Roumaine de Chimie, 29, 1, 13–18 (1984)

ALTERNATING COPOLYMERS OF MALEIC ANHYDRIDE WITH ETHYLENE AND VINYL ACETATE — ION EXCHANGERS*

C. ANDREI[a], ELENA MOLDOVAN[a], GEORGETA ANDREI[a], GALINA NICOLESCU[a]
and VIORICA DOBRESCU[b]
[a] ICECHIM, Brazi Research Dept. 2000 Ploiești, Romania
[b] ICECHIM Bucharest, Splaiul Independenței 202, Bucharest, Romania

Received February 18, 1983

Some aspects regarding the high yield synthesis of the copolymers of maleic anhydride with ethylene and vinyl acetate, their crosslinking with monoethylene glycol, diethylene glycol and polyethylene glycol 200 (Mn = 200) are presented. The crosslinked copolymers were tested as ion exchangers; their total ion exchange capacity and the volume change from H^+ form to Na^+ form were determined.

INTRODUCTION

The tendency of some pairs of monomers to form alternating copolymers is one of the most important features of the radical copolymerization chemistry. The most frequently studied example is the copolymerization of maleic anhydride with various polar and non-polar monomers.

The investigations on copolymerization of maleic anhydride with ethylene [1] and vinyl acetate [2–4] have evidenced that alternating copolymers are obtained. The alternance was ascribed to the formation of a complex with charge transfer between the two monomers, which participate in the copolymerization reaction as a single unit.

Besides the theoretical importance of copolymerization, the copolymers of maleic anhydride with ethylene (EMA) and vinyl acetate (VAMA) are suitable for important practical utilization.

These copolymers may be hydrolized, amonolized, esterified, crosslinked, employed as adhesives, agents for coating textile fabrics, plastifiers, lubricants and additives for paper.

Previous works have reported studies of characterization of these copolymers (structure, molecular weight, thermal properties) [5–7] as well as aspects regarding their esterification. [8–9]

---

* The paper was presented at the 23rd microsymposium "Selective Polymeric Sorbents" Prague, July 19–22, 1982.

This contribution studies the synthesis of VAMA copolymers in the presence of free radicals, modification by crosslinking of EMA and VAMA copolymers and some results on utilization of crosslinked copolymers as ion exchangers in purification of water.

EXPERIMENTAL

The EMA copolymer was synthesized by radical copolymerization, in benzene in the presence of benzoyl peroxide at 120–150 atm and 80°C.

The product was purified by extraction with benzene and dried at 50°C in vacuum.

The VAMA copolymer was also obtained by radical copolymerization in toluene in the presence of AIBN or diethyl peroxydicarbonate. It was conditioned as EMA.

Crosslinking of EMA and VAMA copolymers was performed with monoethylene glycol (MEG), diethylene glycol (DEG) or polyethylene glycol 200 (PEG 200) in methyl ethyl ketone medium at 80°C.

The testing of crosslinked copolymers as ion exchangers was effected by determining their total ion exchange capacity in 0.1 n NaOH solution. The stability of cationites in electrolyte solution was determined from the variation of cationite volume as sodium salt or acid form.

RESULTS AND DISCUSSION

1. On the synthesis of VAMA copolymers

The synthesis of VAMA copolymers was performed both at low and high yields in order to elucidate theoretical aspects and establish the possibilities of industrial production.

Figure 1 shows the variation of the yield into copolymer with reaction time at copolymerization of maleic anhydride with vinyl acetate at various temperatures.

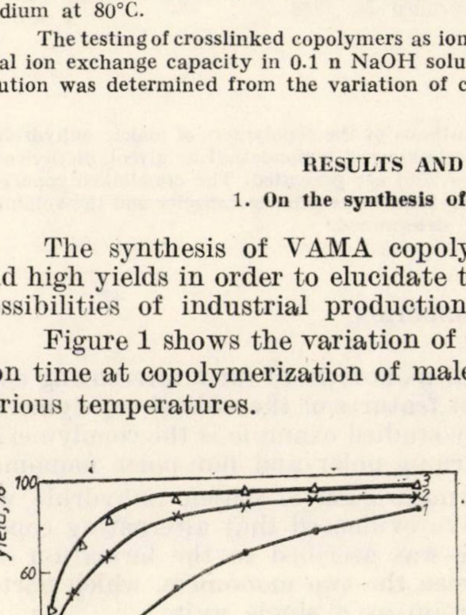

Fig. 1. — The variation of yield *versus* reaction time at copolymerization of maleic anhydride with vinyl acetate at various temperatures ; 1. 50°C ; 2. 60°C ; 3. 70°C ; initiator : diethyl peroxydicarbonate ; monomer ratio : AM/AcV = 1/1 ; toluene/monomer = 8/1.

Examination of figure 1 shows that the yield is strongly dependent on temperature ; at 70°C, the reaction is very fast and strongly exothermal.

To remove the heat of reaction (so that the reaction can be controlled) and to obtain polymers of adequate molecular weight one has to select a certain solvent/ monomer ratio which also ensures a high yield.

Figure 2 shows the variation of yield into copolymer with the solvent/ monomer ratio.

One can notice that the yield decreases with the increase of this ratio.

It was found out that in order to eliminate the heat of reaction and reach an adequate yield the optimum solvent/monomer ratio is (6–10)/1.

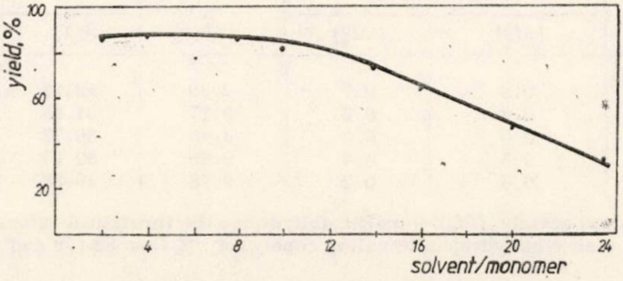

Fig. 2. – The variation of yield with the solvent/monomer ratio at copolymerization of maleic anhydride with vinyl acetate; molar ratio: AM/AcV = 1/1; reaction temperature, 60°C; reaction time, 60 minutes; initiator: diethyl peroxydicarbonate; solvent: toluene.

Figure 3 presents the variation of yield *versus* the mole fraction of maleic anhydride in the composition of feed. The maximum of yield is reached at a mole fraction of 0.4. This agrees with Caze and Loucheux's data.[2]

The latter diagram supports the idea that the reaction of copolymerization of maleic anhydride with vinyl acetate occurs through a donor-acceptor complex of vinyl acetate and maleic anhydride.

The alternating structure of the copolymer was evidenced by its elemental analysis.

Table 1 lists the results of the analysis of copolymers obtained at various mole ratios; most values are close to the theoretical ones for alternating structure.

The decrease of yield with solvent/monomer ratio (Fig. 2) is accounted for in terms of the decrease of donor-acceptor complex concentration.

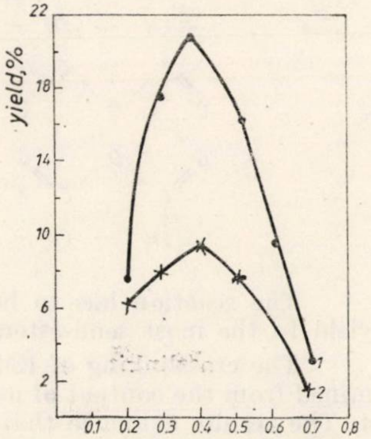

Fig. 3. – The variation of yield with the mole ratio of monomers in the feed composition at copolymerization of maleic anhydride with vinyl acetate; 1. temperature, 60°C; time, 35 minutes; 2. temperature, 70°C; time, 25 minutes; initiator: diethyl peroxydicarbonate; toluene/monomer = 8/1.

2. Crosslinking of EMA and VAMA copolymers

The alternating EMA and VAMA copolymers easily solve in water and polar organic solvents. They may become insoluble if crosslinked with dialcohols, diamines and amino-alcohols and this enlarges their field of application.

Table 1

The elemental analysis of VAMA copolymers

Sample	Feed composition (mole fraction)		Yield %	Elemental analysis	
	$[M_1^0]$	$[M_2^0]$		%C	%H
VAMA 1	0.3	0.7	2.59	52.22	4.41
VAMA 2	0.4	0.6	5.17	51.58	3.95
VAMA 3	0.5	0.5	4.45	50.73	3.33
VAMA 4	0.6	0.4	9.89	52.17	4.38
VAMA 5	0.8	0.2	9.78	49.88	2.71

(M_1) – vinyl acetate, (M_2) – maleic anhydride ; the theoretical values of C and H for vinyl acetate – maleic anhydride alternating copolymer : % C = 52.179 and %H = 4.38

Investigations on crosslinking of some copolymers of maleic anhydride were also performed by Decroix *et al.* [10] and by Frank, [11] but their aim was not utilization as ion exchangers.

This contribution also deals with the obtaining of EMA and VAMA copolymers crosslinked in the presence of MEG, DEG and PEG 200.

The crosslinking process of EMA and VAMA copolymers occurs according to the following reaction :

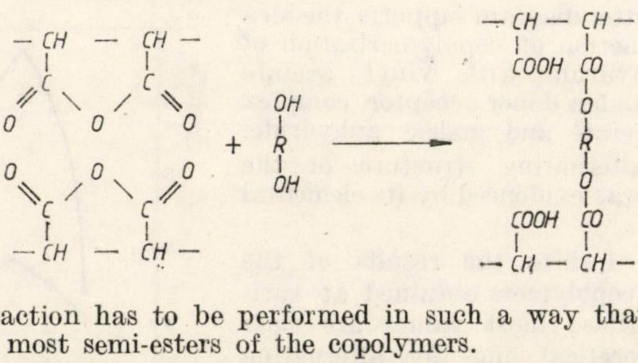

The reaction has to be performed in such a way that it showed yield to the most semi-esters of the copolymers.

The crosslinking of EMA and VAMA copolymers with MEG determined from the content of polymer insoluble in acetone is shown in figure 4. The results evidence that the crosslinking rate of VAMA copolymers is higher than that of EMA.

A comparison between the relative values of the degree of crosslinking for EMA and VAMA copolymers crosslinked with various diols is given in table 2.

In all the diols tested the crosslinking of VAMA occurs easier than crosslinking of EMA.

The table also shows that the higher the etoxilation of diol, the lower the degree of crosslinking.

Figure 5 illustrates the dependence of the degree of crosslinking on VAMA/MEG molar ratio.

The degree of crosslinking decreases with the increase of VAMA/MEG ratio and reaches a plateau at a VAMA/MEG ratio of about 7.

Table 2

The degree of crosslinking of EMA and VAMA with various diols, %

Diol	EMA	VAMA
MEG	38.70	90.50
DEG	19.55	72.30
PEG 200	10.16	58.20

Reaction temperature, 80°C ; reaction time, 180 minutes ; copolymer/diol ratio = 1/1.

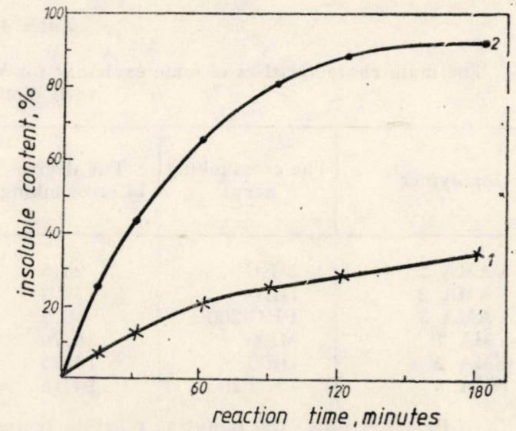

Fig. 4.— The time dependence of crosslinking degree for EMA (curve 1) and VAMA (curve 2) copolymers with MEG ; copolymer/MEG, 1/1 ; temperature, 80°C.

For practical reasons i.e. in view of testing the crosslinked copolymers as ion exchangers, the crosslinking of EMA and VAMA copolymers was effected at copolymer/diol molar ratios of 1/1.

3. The behaviour of EMA and VAMA copolymers as ion exchangers

After crosslinking and drying the EMA and VAMA copolymers were ground and sorted by sieving so that only copolymer fraction whose dimension exceeded 0.2—0.6 mm was retained for ion exchange studies.

The main properties that define the activity of polymers as ion exchangers are : the total ion exchange capacity and the variation of volume from H^+ to Na^+ ionic form.

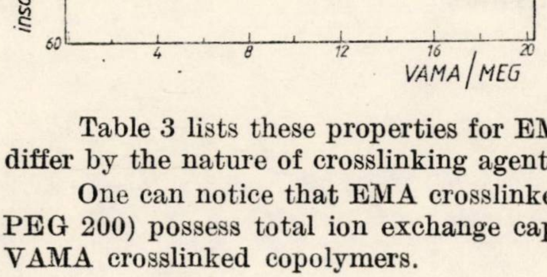

Fig. 5. — The dependence of insoluble content at crosslinking of VAMA copolymer with MEG for various VAMA/MEG ratios ; time of reaction, 180 minutes ; reaction temperature, 80°C.

Table 3 lists these properties for EMA and VAMA copolymers that differ by the nature of crosslinking agent and the degree of crosslinking.

One can notice that EMA crosslinked copolymers (MEG, DEG and PEG 200) possess total ion exchange capacities comparable to those of VAMA crosslinked copolymers.

The volume changes from H^+ to Na^+ forms in electrolyte solutions are lower in EMA than in VAMA copolymers.

Table 3

The main characteristics of ionic exchange for VAMA and EMA copolymers crosslinked with diols

Copolymer	The crosslinking agent	The degree of crosslinking	The total capacity of ionic exchange in 0.1 n NaOH solution (mVal/g)	The volume change from H^+ to Na^+ %
VAMA 1	MEG	90.5	9.80	280
VAMA 2	DEG	72.3	7.00	122
VAMA 3	PEG 200	58.2	5.30	78
EMA 1	MEG	38.70	10.50	160
EMA 2	DEG	19.55	7.50	120
EMA 3	PEG 200	10.16	6.10	70

Reaction time, 180 minutes ; reaction temperature, 80°C ; copolymer/diol = 1/1.

This behaviour evidences a better chemical stability of EMA crosslinked copolymer.

The nature of crosslinking agent influences the chemical stability of the product.

One can notice that the increase of the degree of etoxilation of diol raises the chemical stability of EMA and VAMA crosslinked copolymers ; however the total ion exchange capacity remains satisfactory.

REFERENCES

[1] S. Machi, T. Sakai, M. Gotoda and T. Kagiya, *J. Polym. Sci. A – 1*, **4,** 821 (1966).

[2] C. Caze and C. Loucheux, *J. Macromol. Sci., Chem.*, **A 9,** 29 (1975).

[3] R. Arnaud and C. Caze, *J. Macromol. Sci., Chem.*, **A 14,** 1269 (1980).

[4] C. Caze and C. Loucheux, *J. Macromol. Sci., Chem.*, **A 15,** 95 (1981).

[5] C. Andrei, E. Moldovan, *Rev. Chim. (Bucureşti)*, **27,** 154 (1976).

[6] C. Andrei, V. Tomescu, E. Moldovan, *Mat. Plastice*, **13,** 36 (1976).

[7] E. Moldovan, C. Andrei, M. Cocirla, *Rev. Chim. (Bucureşti)*, **32,** 960 (1981).

[8] E. Moldovan, C. Andrei, *Rev. Chim. (Bucureşti)*, **30,** 416 (1979).

[9] C. Andrei, E. Moldovan, G. Musca, "27e Symposium International sur les Macromolécules", Strassbourg, 6–9 Juillet 1981.

[10] J. C. Decroix, J. M. Bouvier, R. Roussel, A. Nicco and C. M. Bruneau, *J. Polymer Sci., Symposium* **52,** 299 (1975).

[11] H. P. Frank, *Makromol. Chem.*, **114,** 113 (1968).

Revue Roumaine de Chimie, 29, *1*, 19–24 (1984)

POLYAMINOCHLOROQUINONES. I

POLYCONDENSATION OF CHLORANIL WITH PIPERAZINE

OLGA BUTUFEI and ION GAVĂT
ICECHIM – Research Center for Plastic Materials, Splaiul
Independenţei no. 202 Bucharest – 77208 Romania

Received June 22, 1982

New polyaminochloroquinones were obtained by low temperature solution polycondensation of chloranil with piperazine in the presence of acceptors for hydrochloric acid resulted by polycondensation, sodium acetate or an excess of diamine. The obtained polymer was purified and studied by IR spectroscopy and elemental analysis. The formation of the low molecular chloranil-piperazine interaction products of the chloranil and piperazine mixtures in dilute alcoholic solution and of the polymerization mixtures diluted with ethylic alcohol was made evident by IR, UV and visible spectroscopy.

Chloranil interacts with amines with the formation of charge-transfer complexes, low molecular substitution compounds and polymers.[1] The character of amines and the reaction conditions enable the formation of one compound or another.

The formation of polyaminochloroquinones based on chloranil and amines like benzidine, p-phenylendiamine, hexametylendiamine[2] was made evident.

This work reports on the obtention of new polyaminochloroquinones by polycondensation of chloranil with piperazine.

For rendering evident the polycondensation mechanism of chloranil with piperazine the low molecular chloranil-piperazine interaction products were studied. The study was performed by IR, UV and visible spectroscopy. The intermediate products like radical-ion of chloranil, charge-transfer complex chloranil-piperazine, the monosubstituted product of chloranil with piperazine and the dihydrochloride of dipiperazine-chloranil were also evidenced.

1. EXPERIMENTAL

1.1. Preparation and purification of the polymer

Over 0.3 g chloranil solution, dissolved into 75 ml ethylic alcohol, under reflux conditions, 0.105 g piperazine solution in 25 ml ethylic alcohol and 0.331 g sodium acetate were added. This mixture was kept under reflux conditions and stirred for 30 min. The formed polymer was filtered hot. After drying at 105°C the polymer was kept, under reflux conditions, as 200 ml water suspension and then filtered and dried. The polymer was kept again under reflux conditions, in 200 ml ethylic alcohol and then filtered. Finally the polymer was washed in 100 ml ethylic ether. There resulted 0.181 g polymer.

1.2. Ultraviolet and visible spectroscopy of the alcoholic solutions of chloranil and piperazine

For this study a UV—VIS spectrophotometer with 0.5—1 cm quartz cells was employed. The concentrations of the reagents varied between 10^{-3} and 10^{-5} moles/L in p.a. ethylic alochol.

The determinations were made by separate preparation of the reagent of solutions in ethylic alcohol, by their mixture in molar ratio of 2 : 1, 1 : 1, 1 : 2 and 1 : 100 chloranil-piperazine, by registering the spectra for each mixture, immediately at mixing and from time to time. The spectrograms were performed at room temperature.

1.3. Infrared spectroscopy

The spectrograms were performed on a UR—10 Carl-Zeiss-Jena spectrophotometer, on potassium bromide tables.

1.4. Elemental analysis

Carbon, hydrogen, chlorine and nitrogen were determined by an elemental analysis apparatus.

2. RESULTS AND DISCUSSIONS

2.1. Chloranil polycondensation with piperazine

The chloranil polycondensation with piperazine takes place in ethylic alcohol solution under reflux conditions, in the presence of sodium acetate like acceptor for the hydrochloric acid resulted from the polycondensation reaction. Preparing the polymer by the method presented in section 1.1. but at different condensation times, the results presented in table 1 were obtained.

It is clear from table 1 that the necessary time for obtaining a high yield for the polymer is maximum 2 hours. After purification, as shown in section 1.1., the polymer appears as a dark-brown powder insoluble in common organic solvents, little soluble in dimenthylformamide and soluble in concentrated sulphuric acid.

Table 1

Dependence of polymer quantity on condensation time

Condensation time, minutes	Polymer amount
30	0.186
60	0.198
120	0.232
180	0.233

Elemental analysis of the polymer.

	%C	%H	%Cl	%N
Calculated	46.36	3.08	27.38	10.81
Found	46.39	3.23	26.40	10.92

The analysis corresponds to a raw formula $C_{10}Cl_2H_8O_2N_2$. In the IR spectrum of the polymer appear the IR absorption bands of the chloranil and piperazine.

The band characteristic of the presence of two adjoining chlorine atoms in the chloranil molecule (1115 cm^{-1}) diminishes its intensity due to the chlorine substitution in chloranil by the piperazine in the 2nd and 5th positions.

2.2. The study of the low molecular interaction products of chloranil and piperazine

The low molecular interaction products between chloranil and piperazine were studied by ultraviolet and visible spectroscopies.

The interaction of chloranil with piperazine was studied in very dilute solutions by ultraviolet and visible spectroscopies in order to make evident the formation and the disappearance of some intermediary reaction products, as in such dilute solution both the reagents that come into reaction and the products that arise are practically soluble.

Chloranil in ethylic alcohol solution has the following absorption maxima : 260 mμ, 287 mμ and 362 mμ.

Piperazine does not absorb in visible or in ultraviolet. The mixtures of chloranil solutions with piperazine and ethylic alcohol at 2 : 1, 1 : 1, 1 : 2 and 1 : 100 chloranil-piperazine molar ratios were photometered immediately at mixing and from time to time.

In all cases, when mixing the alcoholic solutions of chloranil and piperazine at room temperature in spectrograms, there appear absorption maxima characteristic of chloranil [3] radical-ion at 333 mμ, 425 mμ and 456 mμ.

The chloranil radical-ion is not stable, when it appears it turns into reaction products. The process of the radical-ion changing into reaction products cannot be followed due to the appearance of other characteristic maxima of other reaction products. It is only in the first moments after mixing that isosbestic points are rendered evident, a fact that proves the change of the radical-ion into other reaction products.

Thus in the case of employing the 2 : 1 chloranil-piperazine molar ratio it was observed that in the first moments after mixing the alcoholic solutions of the reagents, the intensity of the characteristic band for the chloranil radical-ion at 333 mμ diminishes whereas the absorption band of maximum 302 mμ enlarges and shifts towards lower wavelengths as the molar ratio of the reagents varies from 2 : 1 to 1 : 1, to 1 : 2 and 1 : 100. This change is probably due to the pH-variation of solution or the changes of the piperazine concentration. At the 1 : 100 chloranil-piperazine molar ratio, the band shifts towards 318 mμ wavelength. The isosbestic point that shows the chloranil radical-ion change into the absorption product at 302 mμ is better visible at the 2 : 1 chloranil : piperazine molar ratio when the change develops at a lower rate. The isosbestic point appears at 312 mμ wavelength.

At the 1 : 1 and 1 : 2 chloranil : piperazine molar ratios an isosbestic point at 403 mμ was noticed that indicates the change of the chloranil radical-ion, that also absorbs at 426 mμ into products of characteristic absorption of the 370 mμ. At the 1 : 1 chloranil : piperazine molar ratio an isosbestic point stands out, also in the first moments of mixing the alcoholic solution of the reagents at the 476 mμ wavelength, that indicates the change of the chloranil radical-ion into the absorption product at 540 mμ.

Therefore, in the first moments of mixing the chloranil and piperazine alcoholic solutions, at different molar ratios, the characteristic bands of 333 mμ, 426 mμ and 456 mμ chloranil radical-ion disappear, appearing bands at 302 mμ, 370 mμ, 540 mμ, as well as bands from 240 mμ and 430 mμ.

Nogami[4] shows that the interaction rate of chloranil with amines is extremely high, whereupon the intermediary reaction products are difficult to be rendered evident. Dipiperazine chloranil dihydrochloride was synthesized as a unit product[5] and it was established by studying the DPCDHC* solutions in ethylic alcohol in ultraviolet and in visible, that it has absorption maxima at 240 mμ and 430 mμ.

If piperazine has a reduction action on chloranil, the tetrachlorhydroquinone can be formed.

Tetrachlorhydroquinone,[2] in alcoholic solution, in ultraviolet has two absorption maxima at 206 mμ, and at 301 mμ, respectively.

Tetrachlorhydroquinone forms with piperazine the adduct studied and characterized in a previous paper.[5] The adduct of tetrachlorhydroquinone with piperazine taken in a 1 : 1 molar ratio, has in ultraviolet an absorption band at 321 mμ. In absolute ethylic alchohol solution, the adduct obeys the Lambert-Beer line variation law of the absorption intensity *versus* concentration from 312 mμ. In a 1 : 1 ethylic alcohol : water ratio solution, the adduct is not stable in time and changes. One can notice that a new band appears at about 370 mμ and the chloranil radical-ion bands at 333 mμ, 426 mμ, 412 mμ become stable in products with absorption at 310 mμ and 375 mμ.

Back to the spectra of the products resulted from the mixing of the chloranil and piperazine solutions, at different molar ratios, respectively to the changes that take place in time one can say that the chloranil radical-ion turns into secondary oxidoreduction products responsible for the absorptions at 302—318 mμ, 370 mμ similar to those of piperazine-tetrachlorhydroquinone adduct prepared in ethylic alcohol solution or in a mixture of alcohol and water. Likewise, the 240 mμ and 430 mμ bands can be assigned to the disubstituted product of the chloranil with piperazine in form of hydrochloride. The 540 mμ band that appears more clearly in the spectrum of the product obtained at the molar ratio of reagents 2 : 1 chloranil : piperazine can be assigned to the charge-transfer complex that generally has its absorption within this range. [7–9] The monosubstituted product of the chloranil with piperazine has been made evident this way, although the absorption of this product can be partly covered by the absorption of the other products and it could not be synthesized as a unit product by the methods studied. Therefore, at the 2 : 1 chloranil : piperazine molar ratio, in the first moments after mixing, it is easy to watch the formation of the chloranil radical-ion and of the change-transfer complex. At the 1 : 1 molar ratio, there are extremely evident the chloranil radical-ion, the change-transfer complex and the secondary products identified at the adduct of the tetrachlorhydroquinone with piperazine that have absorptions at 312 mμ and 375 mμ. At the 1 : 2 molar ratio the bands of the disubstituted product at 240 mμ and 430 mμ are already clearly visible. At the 1 : 100 molar ratio this is extremely well visible.

2.3. The study in ultraviolet and visible of the polycondensation of chloranil with piperazine

The above accomplished study for the interaction of chloranil and piperazine in dilute solution is useful for the identification of the reaction products under polymerization conditions where everything takes place at higher (about 10^{-2}) mole/L concentrations of the compounds and at the reflux temperature of the alcoholic solution of the reagents. Syntheses were made after the method described in section 1.1. and the alcohol synthesis solutions were spectrophotomeasured, from time to time and at the end of the polycondensation, after the filtering of the unsoluble products. The alcohol solutions were diluted as required by the measurements.

The periodical spectrophotometry of the synthesis alcohol solutions indicated, in the first moments of the polycondensation, the formation of the product that absorbs about 300 mμ and 540 mμ, then disubstituted product of chloranil and piperazine appears that absorbs at a maximum of about 430 mμ. During polycondensation, the spectrophotometry did not allow the pursuit of the changes of the products from one into another due to the superposition of the absorptions with those of the reaction by-products that result.

Carrying out syntheses after the method shown in 1.1. with 1 : 1 : 2, 1 : 2 : 2 and 1 : 3 : 2 molar ratios for chloranil-piperazine and sodium acetate and performing the spectrophotometry of the alcohol solutions isolated after the synthesis, there was noticed that at a 1 : 1 : 1 molar ratio for chloranil-piperazine and sodium acetate, the product that absorbs about 300 mμ appears in the synthesis alcohol. This could be assigned to the absorption of the monosubstituted product of chloranil with piperazine since by adding another mole of piperazine into the alcohol a visible change takes place in spectrum at the product that absorbs at 430 mμ and corresponds to the disubstituted product of chloranil with piperazine in the form of hydrochloride.

One can notice that in the UV spectra at the 1 : 2 : 2 and 1 : 3 : 2 molar ratios of the reagents, the concentration of the disubtituted product increases with the intensity of the absorption bands from 430 mμ.

Therefore it can be concluded that the polycondensation of chloranil with piperazine takes place by forming monosubstituted, disubstituted products and then polymer. The highest yield of the polymer is obtained as expected, at a 1 : 1 molar ratio of the chloranil and piperazine reagents and as the piperazine amount increases the amount of disubstituted product increases whereas the polymer amount diminishes.

REFERENCES

[1] O. Butufei, *Rev. Chim. (Bucureşti)*, **31**, 140 (1980).
[2] A. A. Berlin, *Vysokomol. Soedineya*, **1961**, 402.
[3] S. Carter, J. N. Murrel and E. J. Rosh, *J. Chem. Soc.*, **1967**, 477.
[4] T. Nogami, K. Ioshihara and S. Nagakura, *Bull. Chem. Soc. Japan*, **45**, 122 (1972).
[5] O. Butufei and I. Gavăt, *Rev. Roumaine Chim.*, under print.
[6] I. Gavăt, O. Butufei and M. Munteanu, *Rev. Roumaine Chim.*, **22**, 1261 (1977).
[7] S. B. Satih and A. S. Murthy, *J. Phys. Chem.*, **79**, 326 (1975).
[8] H. Hosoya and S. Nagakura, *J. Phys. Chem.*, **73**, 2670 (1969).
[9] Z. Joshida and T. Kabayashi, *Tetrahedron*, **26**, 267 (1970).

Revue Roumaine de Chimie, **29**, *1*, 25–29 (1984)

ESR AND ^{1}H-NMR SPECTRA OF SOME NITROSUBSTITUTED THIOBENZAMIDES

CORNELIA CERCASOV, FELICIA CORNEA, MARIANA CIUREANU, MIHAELA HILLEBRAND, V. EM. SAHINI and ELENA VOLANSCHI

National Institute of Chemistry,
Polytechnic Institute of Bucharest,
Bd. Republicii 13, Bucharest, Romania

Received February 2, 1983

The ESR spectra of the anion radicals obtained from *p*-nitro-thiobenzoyl pyrrolidine (**1**) and -homopiperidine (**2**) are reported and discussed. The hf splittings show that the rotation around the C(S)-N bond is frozen in a position favourable to the conjugation of the thioamide nitrogen with the nitroaromatic moiety. The evidence of the hfs of two protons for **1** and of none for **2** is discussed in terms of ring inversions. ^{1}H-NMR data on the neutral compounds are also presented and discussed.

A number of ESR and ^{1}H-NMR studies have been performed in order to get a better understanding of the structural problems of the thiobenzamide series.[1–5] The influence of the electronic structure on the rotational barrier around the C(S)—N and C(S)—phenyl bonds, the spin density distribution in the anion radicals were previously investigated for some substituted thiobenzoylpiperidines and morpholines.[6–8]

The purpose of the present work is to complete this information by new ^{1}H-NMR and ESR data, outlining the influence of the saturated tertiary thioamide on the electronic structure of these compounds. Therefore, the following nitrothiobenzamides containing five- and seven-membered saturated rings were synthetised and investigated:

1 4-nitrothiobenzoylpyrrolidine (X = pyrrolidine)
2 4-nitrothiobenzoylhomopiperidine (X = homopiperidine)

The ^{1}H-NMR spectra, as well as the ESR patterns of the anion radicals will be compared to the previously reported results[8] on 4-nitrothiobenzoylpiperidine (**3**) and -morpholine (**4**).

EXPERIMENTAL PART

The ^{1}H-NMR spectra were recorded on a VARIAN EM–360 spectrometer in both deuterated chloroform ($CDCl_3$) and *o*-dichlorobenzene (ODCB). TMS was used as an internal standard.

The anion radicals were prepared by electrochemical reduction in dimethylsulphoxide, using tetra-*n*-butylammonium perchlorate as supporting electrolyte.

The ESR spectra were registered on a JES−3B spectrometer, operating at the X-band frequency.

Potassium peroxylamine disulphonate was used as standard ($a_N = 1.300$ mT).

The hyperfine splittings (hfs) were checked by simulation using a program written in FORTRAN.

RESULTS AND DISCUSSION

1. ESR spectra

The hyperfine couplings of the anion radicals under investigation are collected in Table 1. The experimental patterns, together with the spectra simulated using these hfs are presented in figure 1.

Inspection of Table 1 allows the following observations:

a) The anion radicals of **1** and **2** exhibit the general pattern of the nitroaromatic anion radicals.[9,10] The nitro nitrogen atom has the largest splitting ($a_N^{NO_2} = 0.808-0.882$ mT), showing that the unpaired electron is mainly localized on the nitro group. A comparison with the hfs obtained for the anion radicals of the related compounds **3** and **4** reveals a slight increase of this constant in the order: $\mathbf{1} < \mathbf{3} \approx \mathbf{4} < \mathbf{2}$.

The hf couplings of the aromatic protons ($a_o^H = 0.323-0.328$ mT and $a_m^H = 0.082-0.100$ mT) are influenced only to a small extent by the nature of the thioamide.

b) The hfs of the thioamide nitrogen has nearly the same value for all the anion radicals in Table 1. This fact suggests, as already pointed out for the anion radicals of **3** and **4**[8] that, although the π-electron system is not planar,[11] the position of the nitrogen lone pair is favourable to the delocalization of the odd electron via the thiocarbonyl group, to the thioamide nitrogen.

c) More important differences are revealed when the thioamide proton splittings are examined: for the anion radical of **1** the coupling due to two protons of the saturated ring was evidenced, with values close to that of the thioamide nitrogen atom, whereas for the anion radical of **2** no hfs due to the heteroring protons were detected, although the thioamide nitrogen has essentially the same value as for **1**.

We believe that these results can be interpreted in terms of a preferred half-chair conformation of the pyrrolidine ring[12,13] with the nitrogen lone pair in a pseudoaxial position. In this case only the two pseudoaxial β-protons are expected to have appreciable splittings, comparable to that of the thioamide nitrogen.

A similar behaviour of the five-membered heteroring was encountered for the anion radical of 1,3-dinitro-4-pyrrolidine benzene,[14] in which the amine is directly bonded to the nitroaromatic moiety. In that case too, only two proton splittings, equivalent to the amine nitrogen ($a_{2H} = a_N^{am} = 0.091$ mT) are apparent from the pyrrolidine ring.

For the anion radical formed by **2** the absence of the hfs due to the thioamide ring protons cannot be explained by the lack of conjugation

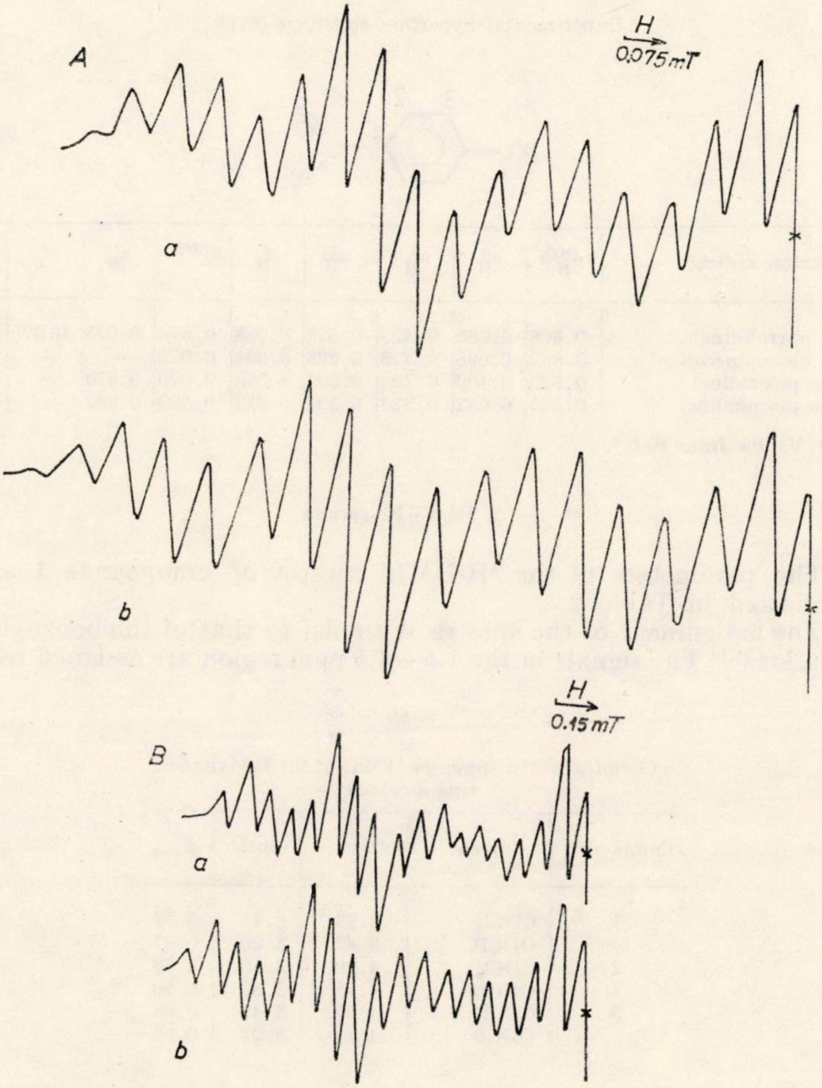

Fig. 1. — Low-field half of the ERS spectra of the anion radicals obtained from **1** (A) and **2** (B). a) experimental (electrochemical reduction, DMSO) b) simulated.

between the aromatic ring and the thioamide group : the existence of a nitrogen coupling which is about the same as that of the anion radical of **1** rules out this supposition. Therefore it may be inferred that the mobility of the seven-membered ring, which is considerably larger than that of the five-membered heterocycle, averages the hfs of the axial and equatorial protons to a value which is smaller than the experimental line-width.

Table 1

Experimental hyperfine splittings (mT)

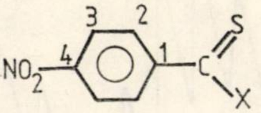

Anion radical	$a_N^{NO_2}$	a_H^2	a_H^3	a_H^5	a_H^6	a_N^{thioam}	a'_H	a'_H	Line width
1 (X = pyrrolidine)	0.808	0.088	0.323	0.323	0.088	0.070	0.075	0.075	0.045
2 (X = homopiperidine)	0.882	0.096	0.328	0.328	0.096	0.075	—	—	0.045
3* (X = piperidine)	0.825	0.100	0.324	0.324	0.085	0.070	0.070	—	0.049
4* (X = morpholine)	0.825	0.082	0.324	0.324	0.082	0.082	0.082	—	0.038

* Values from Ref. [8]

2. ¹H-NMR spectra

The parameters of the ¹H-NMR spectra of compounds **1** and **2** are collected in Table 2.

The assignment of the spectra is similar to that of thiobenzoylpiperidines. [1-4,15,16] The signals in the 1.5—4.5 ppm region are assigned respectively to the saturated ring protons : the low-field signal (3.93—4.29 ppm) to the NCH$_2$ protons *syn* with respect to the C=S bond and the signal at 3.41—3.50 ppm to the NCH$_2$ protons in *anti*. This assignment is supported by the shift of the signals in an aromatic solvent (ODCB) : both signals are shifted towards higher fields in ODCB, but the effect is considerably larger for the protons in *anti*.

Table 2

Chemical shifts (ppm vs. TMS) of the thioamide ring protons

Compound	Solvent	syn	anti	Δ_{s-a}
1	CDCl$_3$	3.93	3.41	0.52
	ODCB	3.87	3.20	0.67
2	CDCl$_3$	4.20	3.50	0.70
	ODCB	4.15	3.35	0.80
3	CDCl$_3$	4.29	3.41	0.88
	ODCB	4.19	3.23	0.96

The signal at high field (1.5—2.3 ppm) is due to the remaining protons of the heteroring.

Both *syn* and *anti* signals in the spectrum of **1** display a triplet pattern, owing to the coupling with the protons on the neighbouring carbon atoms ($J = 6$ Hz) ; the equivalence of the geminal protons shows that the ring inversion is rapid on the ^{1}H-NMR time scale. In the spectrum of **2** the signals of the *syn* and *anti* protons have different patterns : the former is a triplet, whereas the latter is a broad singlet. It is difficult to assess whether this difference is due to the existence of two rotameric conformations with unequal populations, or to intrinsic molecular asymmetry.

A comparison of the chemical shifts ($CDCl_3$) of the NCH_2 protons in **1**, **2** and **3** shows the following trends for the *anti* ($\delta_1 \approx \delta_3 < \delta_2$) and the *syn* protons ($\delta_1 < \delta_2 < \delta_3$).

These trends point out that, owing to the molecular geometry of the five-membered heteroring, the averaged position of the *syn* protons in **1** allows a more important shielding by the anisotropic thiocarbonyl group. Owing to the same reason, the *anti* protons in **1** are shielded to a larger extent than in **2** by the ring current of the aromatic ring.

It may be concluded, from the non-equivalence of the *syn* and *anti* NCH_2 protons that, on the ^{1}H-NMR time scale, the rotation about the C(S)—N bond is frozen in both compounds **1** and **2**; the ring inversion is rapid on the same time scale and leads to equivalent geminal protons. The ESR data show that the rotation around the C(S)-N bond is frozen in a position favourable to the conjugation with the nitroaromatic moiety for both anion radicals, as reflected by the hfs of the thioamide nitrogen. As for anion radical of 1 the ring inversion is frozen too, on the ESR time scale, since otherwise four equivalent β-proton splittings from the pyrrolidine ring would have been expected. For the anion radical of **2** the ring inversion is probably rapid on this time scale, but the hfs are averaged to a value which is below the experimental resolution.

REFERENCES

[1] A. O. Fulea and P. J. Krueger, *Canad. J. Chem.*, **53**, 3315 (1975).

[2] A. O. Fulea, *Rev. Roumaine Chem.*, **24**, 1265 (1979).

[3] U. Berg, *Canad. J. Chem.*, **55**, 2297 (1977).

[4] U. Berg, *Acta Chem. Scand.*, **B 30**, 695 (1976).

[5] J. Voss and W. Walter, *Liebigs Ann. Chem.*, **743**, 177 (1970).

[6] M. Ciureanu, V. E. Sahini, F. Cornea and C. Cercasov, *Org. Magn. Reson.*, **15**, 148 (1981).

[7] C. Piccinni-Leopardi, C. Fabre, D. Zimmerman, J. Reisse, F. Cornea and C. Fulea, *Canad. J. Chem.*, **55**, 2649 (1977).

[8] C. Cercasov, F. Cornea, M. Ciureanu, M. Hillebrand, V. E. Sahini and E. Volanschi, *Org. Magn. Reson.*, (1982).

[9] P. H. Rieger and G. K. Fraenkel, *J. Chem. Phys.*, **39**, 609 (1963).

[10] A. H. Maki and D. H. Geske, *J. Amer. Chem. Soc.*, **83**, 1852 (1961).

[11] a) R. P. Shibaeva and R. O. Atovmyan, *Zhur. strukt. Khim.*, **9**, 73 (1978) ; b) J. Sandstrom, *Acta Chem. Scand.*, **16**, 1616 (1962).

[12] E. L. Eliel, N. L. Allinger, S. J. Angyal and G. A. Morrison, "Conformational Analysis", Interscience Publishers, Wiley, New York, 1966, p. 202.

[13] B. C. Gilbert, R.O.C. Norman and M. Trenwith, *J.C.S. Perkin II*, 1033 (1974).

[14] M. Hillebrand, Em. Ionescu and E. Volanschi, *Rev. Roumaine Chim.*, to be published.

[15] M. Ciureanu, C. Cercasov, F. Cornea and M. Contineanu, *Rev. Chim. (București)*, **32**, 861 (1981).

[16] C. Piccinni-Leopardi, O. Fabre, D. Zimmermann, J. Reisse, F. Cornea and C. Fulea, *Org. Magn. Reson.*, **8**, 536 (1976).

ring inversion is rapid on the [illegible] NMR timescale. In the spectrum of 2 the signals of the [illegible] protons have different patterns: the former is a triplet, whereas the latter is a broad singlet. It is difficult to assess whether this difference is due to the existence of two exchanging conformations with different populations or to different molecular asymmetry.

A comparison of the chemical shifts (CDCl$_3$) of the NCH$_2$ protons in 1 and 2 shows the following trends for the [illegible] and the [illegible] protons [illegible].

These trends indicate that, owing to the molecular geometry of the [illegible] heteroring, the averaged position of the [illegible] protons in 1 allows a more important shielding by the [illegible] group. For the same reason, the [illegible] protons in 1 are shielded to a larger extent than in 2 by the ring current of the aromatic ring.

It may be concluded, from the nonequivalence of the [illegible] and [illegible] NCH$_2$ protons that, on the ^{1}H-NMR timescale, the rotation about the [illegible]–N bond is frozen in both compounds 1 and 2, the ring inversion is rapid on the same time scale and leads to [illegible] protons. The ESR data show that the rotation around the [illegible]–N bond is frozen in a position favourable to the conjugation with the [illegible] for both anion radicals, as reflected by the hfs of the [illegible] nitrogen. As for anion radical of 1, the ring inversion is frozen too on the ESR time scale, since otherwise four equivalent proton splittings from the pyrrolidine ring would have been expected. For the anion radical of 2 the ring inversion is probably rapid on this time scale, but the hfs are averaged to a value which is below the experimental resolution.

REFERENCES

[illegible]

Revue Roumaine de Chimie, 29, *1*, 31–42 (1984)

SURFACE MOBILITY OF SURFACTANT SOLUTIONS. XI[1]

NUMERICAL ANALYSIS FOR THE MARANGONI AND THE GRAVITY FLOW IN A THIN LIQUID LAYER OF TRIANGULAR SECTION

EMIL CHIFU*,1), 2) CĂLIN GHEORGHIU** and IOAN STAN*
* University of Cluj-Napoca, Romania
** Polytechnic Institute of Cluj-Napoca, Romania

Received May 17, 1983

The numerical calculation method of the "simplex" finite element is applied to the Marangoni flow undergone by the surfactant solutions, as well as to the simultaneous gravitational flow inversely oriented and occurring in competition with the former. The order of magnitude, for the experimental rates of flow corresponding to the two types of thin liquid layer movement in "surface canals" of angular section, is in agreement with that obtained by applying the above-mentioned method of calculation.

INTRODUCTION

In previously published papers[1,3–5] a theoretical treatment has been presented, for a Marangoni-type flow, according to the model of a semi-infinite thin liquid layer situated on an inclined solid plane and acted by a surface tension gradient.

The Ox axis is directed towards the maximum slope of the plane, Oz is perpendicular to the plane, and Oy links the points situated at the same level h (Fig. 1 and Fig. 2a).

The surface tension gradient at the liquid/gas interface is created by means of two reservoirs containing a surfactant solution with $\sigma = \sigma_1$ at the distance $x = H$ (reservoir 1) and the pure solvent or a more diluted solution with $\sigma = \sigma_0$ at the distance $x = 0$ (reservoir 2). Like this, the surface tension varies at the liquid/gas interface along the Ox axis ($\sigma_1 < \sigma_0$).

In the thin liquid layer a competitive flow occurs due to the simultaneous action of the surface tension and gravity forces, inversely oriented to one another (Fig. 1). Indeed, the liquid/gas interface moves towards negative values of the Ox axis, due to the surface tension difference

---

[1] To whom correspondence should be sent : Department of Physical Chemistry, str. Arany J., No. 11, 3400 Cluj-Napoca, Romania.

[2] This paper was communicated at the first Symposium on Colloid and Surface Chemistry, Bucharest, 13 – 14 May 1983

$\sigma_0 - \sigma_1$; it also drags, by viscosity forces, subjacent strata of liquid (Marangoni flow). But, simultaneously, the liquid in the thin layer is stressed towards the positive direction of the *Ox* axis, due to the inclination of the plane, or to the gravity forces, respectively.

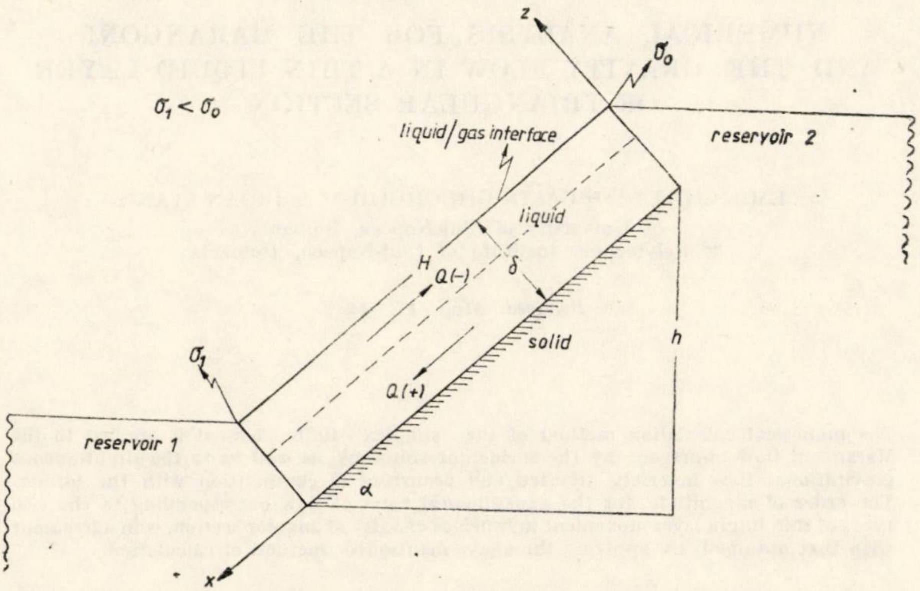

Fig. 1. — Longitudinal section of the thin liquid layer in which the Marangoni flow is in competition with the gravity flow.

The total rate of flow Q(cm^3/s) in the semi-infinite thin liquid layer of section $1 \times \delta$ is given by the equation[1]:

$$Q = -\frac{\sigma_0 - \sigma_1}{2\mu H}\delta^2 + \frac{1}{2\mu H}\Gamma g h \delta^2 + \frac{1}{3\mu H}\rho g h \delta^3 \qquad (1)$$

where δ is the thickness of the layer, H its length, ρ the liquid density, Γ the surface density of the liquid, μ the viscosity; g the acceleration of gravity and h the level difference between reservoir 1 and reservoir 2 (Fig. 1).

The theory mentions that, at h values found in the interval

$$\frac{\sigma_0 - \sigma_1}{g(\rho\delta + \Gamma)} < h < \frac{\sigma_0 - \sigma_1}{g\left(\rho\frac{\delta}{2} + \Gamma\right)}, \qquad (2)$$

or if the surface density Γ ($\Gamma \approx 10^{-7}$ g/cm^2) is neglected, in the interval

$$\frac{\sigma_0 - \sigma_1}{\rho g \delta} < h < 2\frac{\sigma_0 - \sigma_1}{\rho g \delta}, \qquad (2a)$$

an "antiparallel" flow must occur : a layer of liquid moves upwards on the inclined plane, due mainly to the surface tension forces, at a flow rate Q_- ; simultaneously, another layer, found under the former, moves downwards, due especially to the gravity forces and its flow rate is Q_+.

In the h values range given by the inequality (2) it is obvious that the total rate of flow given by Eq. (1) is $Q = |Q_-| + Q_+$.

At h values such as :

$$h \leqslant \frac{\sigma_0 - \sigma_1}{g\rho\delta}$$

the liquid/gas interface drags the whole liquid in the layer towards the negative direction of the Ox axis (Fig. 1), and we have only the rate of flow Q_-. In conformity with Eq.(1),

$$Q = Q_- < 0.$$

For h values

$$h > 2\,\frac{\sigma_0 - \sigma_1}{g\rho\delta}$$

the whole liquid in the layer flows towards the positive direction of the Ox axis, and the rate of flow is now only Q_+, and :

$$Q = Q_+ > 0.$$

Experimentally, the existence of the two types of flow has been revealed[6] in the case of a thin liquid layer bordered by two solid walls. The thin liquid layer arises, by adhesion, in the canal formed by longitudinally sealing two glass rods (Fig. 2b), i.e. in an angular "surface canal". The transversal section of the liquid layer is then a triangle having slightly curved sides, and this section is obviously different from that of the semi-infinite thin liquid layer (Fig. 2a).

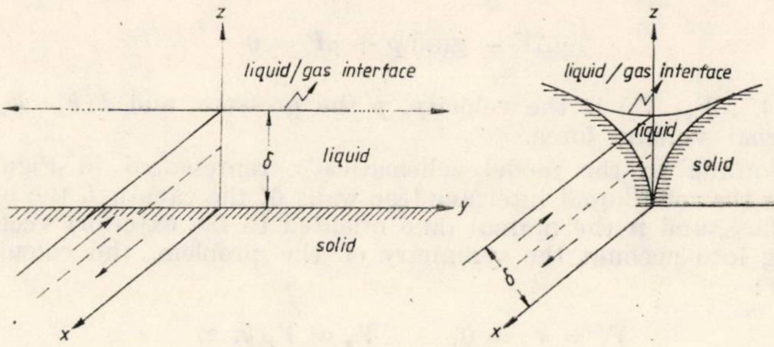

Fig. 2 a. — Transversal section of the semi-infinite thin liquid layer ; along the Oy axis the layer is indefinitely expanded ; b. — Transversal section of the experimental thin liquid layer.

The aim of the present work is to quantitatively examine the two types of flow occurring in experimentally obtained pellicles of triangular section.

A method of numerical calculation has been used in this view, namely, the method of the finite element.

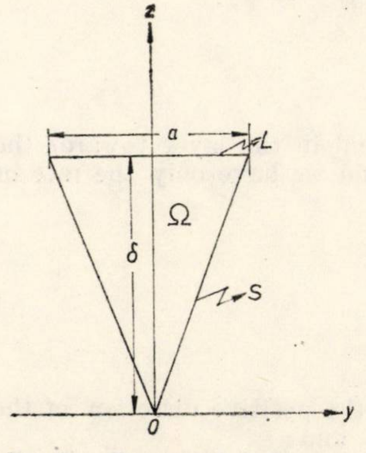

Fig. 3. — Transversal section assummed for the thin liquid layer in the numerical calculation.

In the following, the section of the thin liquid layer in Fig. 2a will be assimilated to a proper triangle (Fig. 3).

The results given in the present paper are compared with the experimental previously reported.[6] The study of the Marangoni-type processes is timely in various fields such as the space science and technology of liquids, the biophysics, and others.[2]

THE MARANGONI FLOW THROUGH A LIQUID LAYER OF TRIANGULAR SECTION SITUATED ON AN INCLINED PLANE

We assume that the liquid in the thin liquid layer is viscous and incompressible and that the flow is both laminar and stationary. In such a case the problem is reduced to the working out of a Navier-Stokes equation:

$$\mu \Delta \boldsymbol{V} - \operatorname{grad} p + \rho \boldsymbol{F} = 0 \tag{3}$$

where $\boldsymbol{V}(V_x, V_y, V_z)$ is the velocity, p the pressure, and $\boldsymbol{F}(F_x, F_y, F_z)$ the external volume force.

According to the model schematically represented in Figure 3, S denotes the solid/liquid interface (the walls of the canal), L the liquid/gas interface, and $\boldsymbol{n}$ the normal (and oriented to the exterior) vector to L. Taking into account the symmetry of the problem, the calculation results in:

$$V_y = V_z = 0, \qquad V_x = V_x(y, z) \tag{4}$$

because the flow occurs along the Ox axis. Supposing also that the pressure p is constant, equation (3) becomes:

$$-\mu\left(\frac{\partial^2 V_x}{\partial y^2} + \frac{\partial^2 V_x}{\partial z^2}\right) = \rho F_x. \tag{5}$$

The boundary conditions for Eq.(5) are:

$$V_x = 0 \qquad \text{on } S \tag{6}$$

i.e. the condition for the viscous fluid to adhere to the solid walls; and

$$\frac{\partial V_x}{\partial n} = \text{constant} \quad \text{on} \quad L. \tag{7a}$$

In what the value of the constant in Eq.(7a) is concerned, it would be necessary to take into account the Navier-Stokes equations applied to the liquid interface.[1,2,7] If we neglect, in a first approximation, the surface shear and dilatational viscosity $(\varepsilon + \varkappa)$ and the surface density Γ the condition (7a) becomes:

$$\frac{\partial V_x}{\partial n} = \frac{1}{\mu}\frac{\partial \sigma}{\partial x} \quad \text{on} \quad L. \tag{7b}$$

So, the surface tension gradient $\partial \sigma / \partial x$ gives rise to a tangential tension which is balanced by the tangent force due to the viscosity of the liquid.

Admitting that the surface tension gradient is a constant (see Fig. 1)

$$\frac{\partial \sigma}{\partial x} = \frac{\sigma_1 - \sigma_0}{H}. \tag{8}$$

and introducing (8) into (7b), the boundary condition (7b) has the final form:

$$\frac{\partial V_x}{\partial n} = \frac{\sigma_1 - \sigma_0}{\mu H}. \tag{7c}$$

In the following, Eq.(5) will be numerically integrated with the boundary conditions (6) and (7). For that, it is necessary to introduce the function:

$$\varphi(y, z) = 4\pi \frac{H}{h} \frac{\mu}{g} V_x(y, z). \tag{9}$$

Because (see Fig. 1):

$$F_x = g \frac{h}{H} = g \sin \alpha, \tag{10}$$

and taking into account relationships (9) and (10), equation (5) becomes:

$$-\Delta \varphi = 4\pi \rho. \tag{11}$$

Eq.(11) has the well-known form of Poisson's equation in the electrostatics.[8]

The physical meaning of Eq.(11) in the present case lies in the fact that this equation is valid inside the liquid pellicle (Fig. 3) – the range termed Ω – while at the solid/liquid interface we have, from the condition (6):

$$\varphi = 0 \quad \text{on} \quad S \,. \tag{12}$$

Analogously, at the liquid/gas interface the condition (7) is fulfilled, so that, if we take Eq. (9) into account, we have:

$$\frac{\partial \varphi}{\partial n} + (\sigma_0 - \sigma_1)\frac{4\pi}{gh} = 0 \quad \text{on} \quad L \,. \tag{13}$$

THE SOLUTION OF THE FLOW EQUATION BY THE FINITE ELEMENT METHOD

This problem represents the mathematical model of the laminar as well as of the stationary flow of an incompressible viscous fluid, under the action of a surface tension gradient, through an inclined canal having a certain section, in the case studied, a triangular section (Fig. 3).

A numerical calculation, by the finite element method and using simplex elements,[9,10] has been employed to obtain the solution of this problem.

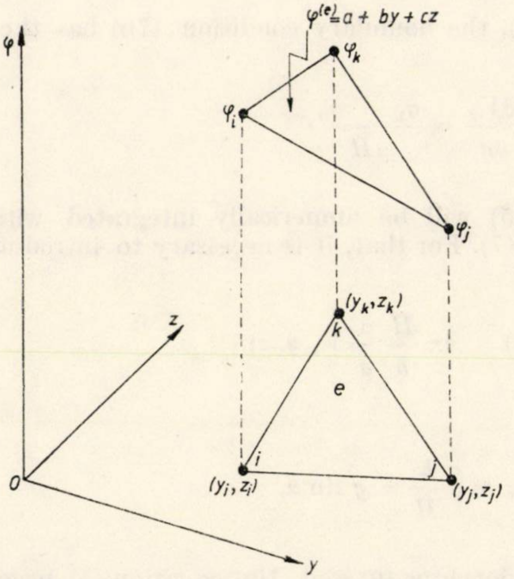

Fig. 4. – The finite element.

In this way, the equivalent functional to be minimized, corresponding to (11), is:

$$J(\varphi) = \int\limits_{\Omega} \frac{1}{2}\left[\left(\frac{\partial \varphi}{\partial y}\right)^2 + \left(\frac{\partial \varphi}{\partial z}\right)^2 - 8\pi\rho\varphi\right] \mathrm{d}\Omega + \int\limits_{L} (\sigma_0 - \sigma)\frac{4\pi}{gh}\varphi \,\mathrm{d}L. \tag{14}$$

By following the usual proceeding with the finite element method[9], we consider a triangulation of the domain (Fig. 4), containing E finite elements, so that:

$$J(\varphi) = \sum_{e=1}^{E} J^{(e)}.$$

On a typical finite element "e" (Fig. 4), a linear variation is considered for φ:

$$\varphi^{(e)}(y, z) = a^{(e)} + b^{(e)}y + c^{(e)}z,$$

otherwise:

$$\varphi^{(e)}(y, z) = N_i^{(e)}\varphi_i + N_j^{(e)}\varphi_j + N_k^{(e)}\varphi_u,$$

where:

$$N_i^{(e)} = (2A^{(e)})^{-1}[a_i^{(e)} + b_i^{(e)}y + c_i^{(e)}z], \quad a_i^{(e)} = Y_jZ_k - Y_kZ_j,$$

$$b_i^{(e)} = Z_j - Z_k, \quad c_i^{(e)} = Y_k - Y_j$$

$$N_j^{(e)} = (2A^{(e)})^{-1}[a_j^{(e)} + b_j^{(e)}y + c_j^{(e)}z], \quad a_j^{(e)} = Y_kZ_i - Y_iZ_k,$$

$$b_j^{(e)} = Z_k - Z_i, \quad c_j^{(e)} = Y_i - Y_k$$

$$N_k^{(e)} = (2A^{(e)})^{-1}[a_k^{(e)} + b_k^{(e)}y + c_k^{(e)}z], \quad a_k^{(e)} = Y_iZ_j - Y_jZ_i,$$

$$b_k^{(e)} = Z_i - Z_j, \quad c_k^{(e)} = Y_j - Y_i$$

$$2A^{(e)} = Y_jZ_k - Y_kZ_j + Z_jY_i - Z_kY_i + Y_kZ_i - Y_jZ_i.$$

The method of minimizing $J(\rho)$ against φ leads to:

$$\frac{\partial J}{\partial\{\varphi\}} = \frac{\partial}{\partial\{\varphi\}}\left(\sum_{e=1}^{E} J^{(e)}\right) = \sum_{e=1}^{E}\frac{\partial J^{(e)}}{\partial\{\varphi\}} = 0 \tag{15}$$

or, moreover:

$$\frac{\partial J^{(e)}}{\partial\{\varphi\}} = [k^{(e)}]\{\varphi^{(e)}\} + \{f^{(e)}\}$$

where :

$$[k^{(e)}] = \int_{\Omega_e} [B^{(e)}]^{\mathrm{T}} I [B^{(e)}]\,\mathrm{d}\Omega, \quad \{\varphi^{(e)}\}^{\mathrm{T}} = \{\varphi_i \varphi_j \varphi_k\}$$

$$\{f^{(e)}\} = \int_{\Omega_e} 4\pi\rho [N^{(e)}]^{\mathrm{T}}\,\mathrm{d}\Omega + \int_{L^{(e)}} (\sigma_0 - \sigma)\frac{4\pi}{gh}[N^{(e)}]^{\mathrm{T}}\,\mathrm{d}L$$

$$[B^{(e)}] = \begin{bmatrix} \dfrac{\partial N_i^{(e)}}{\partial y} & \dfrac{\partial N_j^{(e)}}{\partial y} & \dfrac{\partial N_k^{(e)}}{\partial y} \\ \dfrac{\partial N_i^{(e)}}{\partial z} & \dfrac{\partial N_j^{(e)}}{\partial z} & \dfrac{\partial N_k^{(e)}}{\partial z} \end{bmatrix}, \quad [N^{(e)}] = [N_i^{(e)} \; N_j^{(e)} \; N_k^{(e)}]$$

and I is the unit matrix of the second order.

Turning back to Eq. (15), we have :

$$\frac{\partial J}{\partial\{\varphi\}} = \sum_{e=1}^{E} ([k^{(e)}]\{\varphi^{(e)}\} + \{f^{(e)}\}) = 0$$

or, more briefly :

$$[K]\cdot\{\varphi\} = \{F\} \tag{16}$$

where :

$$[K] = \sum_{e=1}^{E} [k^{(e)}], \quad \{F\} = -\sum_{e=1}^{E} \{f^{(e)}\}.$$

Eq. (16) represents a linear algebraic system in which $[K]$ is a symmetrical banded matrix and $\{\varphi\}$ is the column vector of the unknown nodal values of the function φ in the nodes of the triangulation applied to the domain Ω (Fig. 5).

From the nodal values of φ, by using Eq.(9), the nodal values of the velocity V_x are derived and finally the rates of flow Q (respectively, Q_+ and Q_-).

The above-described algorithm has been transcribed into a FORTRAN IV programme and run on a Felix C 256 computer.

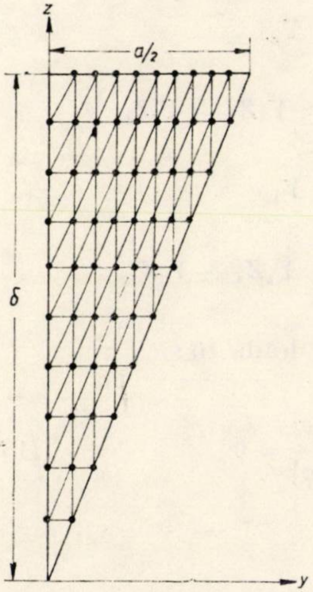

Fig. 5. — Triangulation of the Ω-domain.

DISCUSSION

The numerical calculation aimed at solving the problem (11) — (13) for the systems : aqueous butyl alcohol (reservoir 1) — solvent (reservoir 2) (see Fig. 1). The characteristic parameters of the studied systems are given in Table 1.

Table 1

Parameters of experimentally studied systems *

System N°	Reservoir 1				Reservoir 2 — solvent		
	Surfactant : Aqueous butyl alcohol (% w)	Interfacial tension difference $\sigma_0 - \sigma_1$ (mN/m)	Viscosity μ (P)	Density ρ (g/cm^3)	Interfacial tension difference $\sigma_0 - \sigma_1$ (mN/m)	Viscosity μ (P)	Density ρ (g/cm^3)
1	0.32	8.6	9.69×10^{-3}	0.9974	7.5	9.41×10^{-3}	0.9977
2	0.68	16.4	9.77×10^{-3}	0.9969	14.8	9.41×10^{-3}	0.9977
3	1.04	20.4	9.98×10^{-3}	0.9962	19.1	9.41×10^{-3}	0.9977
4	3.20	33.0	10.8×10^{-3}	0.9927	32.5	9.41×10^{-3}	0.9977

* Dimensions of the thin liquid layer : $\delta = 4.80 \times 10^{-2}$ cm, $a = 3.87 \times 10^{-2}$ cm (Fig. 3); $\alpha = 40°$ (Fig. 1).

Like this, for each set of values $(\sigma_0 - \sigma_1)$, μ and ρ we have obtained, besides the nodal values of the function φ at several level differences h, the velocity fields V_x and the values of the corresponding rates of flow Q_+ and Q_-, as well.

In Figure 6 the velocity field V_x, corresponding to a set of values for the parameters in Eqs. (11) — (13), is illustrated as an example. The existence of two fluxes of inverse orientation is observed (see the arrows) inside the thin liquid layer of triangular section, in general accordance with our experimental data reported before. [6]

In the concrete calculation performed in order to evaluate the values of the rates of flow Q_- (calc.) when the flow occurs from the reservoir 1 towards reservoir 2, the parameters corresponding to the liquid in the reservoir 1 have been introduced. Similarly, for the calculation of the values Q_+ (calc.) the parameters of the solvent in reservoir 2 have been used. This is reasonable, even if this approach represents a certain simplification of the reality. Indeed, the existence of the surface tension gradient on the thin liquid layer which undergoes the flow implies the variation of the surfactant concentration as well as of the density and viscosity of the liquid along this layer. Nevertheless, the differences in μ and ρ for the liquid in the two reservoirs are minor.

As to the surface tension difference $(\sigma_0 - \sigma_1)$, it should be the same for a given system, no matter what the direction of the flow is. Yet, from the experimental point of view, small differences have occurred and they can be seen in Table 1. They result from the corrections applied to the surface tension for the liquids in the two reservoirs, at the end of the time interval (of the order of minutes) in which the flow is observed.

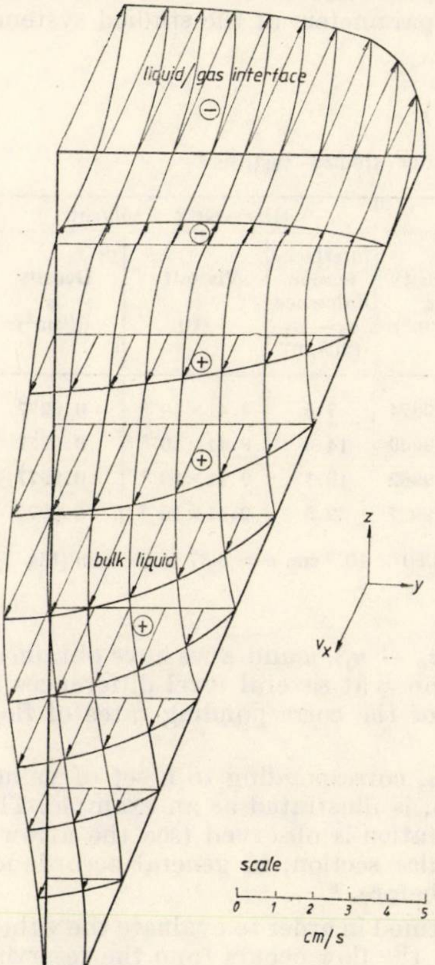

Fig. 6. – The velocity field corresponding to the system 3 in Table 1; $\sigma_0 - \sigma_1 = 20.4$, $\mu = 9.98 \cdot 10^{-3}$, $\rho = 0.9962$, $h = 1.8$ cm.

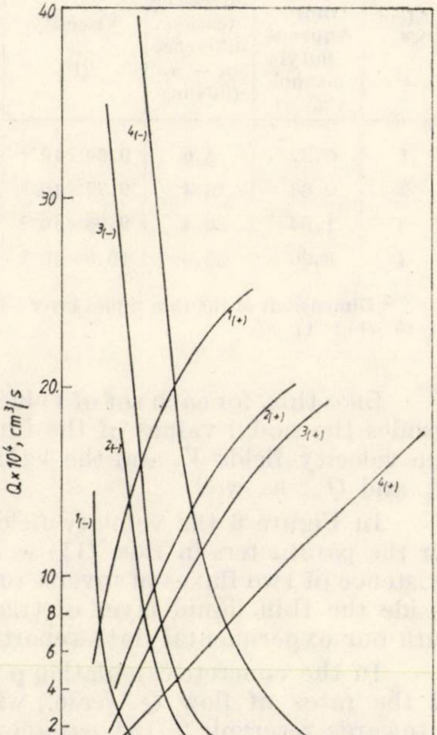

Fig. 7. – $Q_-(h)$ curves $(1_{(-)} \div 4_{(-)})$ and $Q_+(h)$ curves $(1_{(+)} \div 4_{(+)})$ numerically calculated for the systems $1 \div 4$ in Table 1.

Figure 7 shows the curves resulted in this work by numerical calculation for the systems 1 – 4 in Table 1. The fluxes $Q_-(h)$ curves $1_{(-)} \div 4_{(-)}$ and $Q_+(h)$ curves $1_{(+)} \div 4_{(+)}$ have the same aspect as those experimentally obtained.[6]

The range of h values in which the "antiparallel" flow arises has also been calculated and it is given by the inequalities :

$$1.5\,\frac{\sigma_0 - \sigma_1}{\rho g \delta} < h < 7.5\,\frac{\sigma_0 - \sigma_1}{\rho g \delta} \tag{17}$$

This is much different from the domain calculated for the semi-infinite liquid layer (see Eq.(2a)), but comparable with that obtained in the experimental measurements,[6]

$$2\,\frac{\sigma_0 - \sigma_1}{\rho g \delta} < h < 6\,\frac{\sigma_0 - \sigma_1}{\rho g \delta} \tag{18}$$

For a more detailed analysis, in Tables 2—3 the numerically calculated values (see the curves $2_{(-)} \div 3_{(-)}$, $2_{(+)} \div 3_{(+)}$ in Figure 7) have been listed besides those experimentally determined, for the systems 2 and 3 in Table 1.

Table 2

Calculated and experimental rates of flow (cm³/s) for the system 2 in Table 1

h (cm)	Q_- (calc.) ($cm^3\ s^{-1}$)	Q_- (exp.) ($cm^3\ s^{-1}$)	Q_+ (calc.) ($cm^3\ s^{-1}$)	Q_+ (exp.) ($cm^3\ s^{-1}$)
0.7	1.68×10^{-3}	—	0.50×10^{-3}	0.2×10^{-3}
0.9	0.94×10^{-3}	0.23×10^{-3}	0.72×10^{-3}	0.7×10^{-3}
1.1	0.5×10^{-3}	0.16×10^{-3}	0.90×10^{-3}	1.2×10^{-3}
1.3	0.28×10^{-3}	0.12×10^{-3}	1.10×10^{-3}	1.6×10^{-3}
1.5	1.30×10^{-4}	0.58×10^{-4}	1.30×10^{-3}	2.0×10^{-3}
1.7	0.46×10^{-4}	0.50×10^{-4}	1.42×10^{-3}	2.4×10^{-3}
1.9	1.44×10^{-5}	2.0×10^{-5}	1.58×10^{-3}	2.7×10^{-3}
2.1	0.56×10^{-5}	—	1.7×10^{-3}	3.2×10^{-3}
2.3	0.22×10^{-5}	—	1.82×10^{-3}	3.5×10^{-3}

The theoretical model presented above implies some simplifications, such as : neglect of the convective terms in the Navier-Stokes equations, as well as of the surface viscosity ; accepting that the surface tension gradient is a constant ; assimilation of the curvilinear walls of the canal to planes ; use of a finite element-simplex method.

Nevertheless, the order of magnitude for the experimental rates of flow is correctly reproduced by the numerical calculation employed (see Tables 2 — 3). This result is of the first importance especially when compared with the model of the semi-infinite pellicle [1,3-5] which led to flux values circa 40 times greater than the experimental ones.[6]

Table 3

Calculated and experimental rates of flow (cm^3/s) for the system 3 in Table 1

h (cm)	Q_- (calc.) ($cm^3\ s^{-1}$)	Q_- (exp.) ($cm^3\ s^{-1}$)	Q_+ (calc.) ($cm^3\ s^{-1}$)	Q_+ (exp.) ($cm^3\ s^{-1}$)
0.6	0.34×10^{-2}	—	0.28×10^{-3}	—
0.9	1.56×10^{-3}	0.23×10^{-3}	0.50×10^{-3}	0.25×10^{-3}
1.2	0.76×10^{-3}	0.18×10^{-3}	0.74×10^{-3}	0.8×10^{-3}
1.5	0.36×10^{-3}	0.125×10^{-3}	0.98×10^{-3}	1.5×10^{-3}
1.8	1.6×10^{-4}	0.75×10^{-4}	1.18×10^{-3}	2.0×10^{-3}
2.1	0.49×10^{-4}	0.4×10^{-4}	1.36×10^{-3}	2.5×10^{-3}
2.4	1.24×10^{-5}	1.0×10^{-5}	1.56×10^{-3}	2.1×10^{-3}
2.7	0.38×10^{-5}	—	1.70×10^{-3}	3.5×10^{-3}
3.0	1.32×10^{-5}	—	1.82×10^{-3}	3.9×10^{-3}

The concrete values of the experimental fluxes Q_- are, however, smaller than those calculated — for low level differences h — ; then the experimental Q_- values gradually amount with h, approaching the calculated ones. As to the experimental fluxes Q_+, they are also smaller at low h values, then go up with h and even pass beyond the calculated fluxes.

In conclusion, the Marangoni and gravity-type flow processes through the thin liquid layer of triangular section bordered by two solid walls are satisfactorily described in the theoretical model presented in this work.

REFERENCES

[1] Part X : E. Chifu and I. Stan, *Rev. Roumaine Chim.*, **27,** 703 (1982).

[2] E. Chifu, I. Stan, Z. Finta and E. Gavrilă, *J. Colloid Interface Sci.*, (1983) ; E. Chifu and I. Stan, *Rev. Roumaine Chim.*, **25,** 1149 (1980).

[3] R. Deutsch and E. Chifu, *Studia Univ. Babeş-Bolyai, Chem.*, **9** (1), 101 (1964).

[4] E. Chifu, *Studia Univ. Babeş-Bolyai, Chem.*, **10** (2), 85 (1965).

[5] E. Chifu and R. Deutsch, *Rev. Roumaine Chim.*, **11,** 873 (1966).

[6] E. Chifu and I. Albu, *Studia Univ. Babeş-Bolyai, Chem.*, **13** (1), 99 (1968).

[7] L. E. Scriven, *Chem. Eng. Sci.*, **12,** 98 (1960) ;
R. Aris, "Vector, Tensor and the Basic Equations of the Fluid Mechanics",Prentice Hall, New Jersey, 1962, Chap. X.

[8] R. Deutsch, H. Szöcs and E. Chifu, *Studia Univ. Babeş-Bolyai, Chem.*, **10** (2), 99 (1965).

[9] L. Segerlind, "Applied Finite Element Analysis", Wiley, New York, 1976.

[10] J. J. Connor and C. A. Brebbia, "Finite Element Techniques for Fluid Flow", Newnes-Buttersworth, London, 1976.

Revue Roumaine de Chimie, **29**, *1*, 43 – 48 (1984)

THE ENTHALPIES OF COMBUSTION AND FORMATION OF D-ALANINE, L-ALANINE, DL-ALANINE AND β-ALANINE

IULIA CONTINEANU and D. I. MARCHIDAN
Center of Physical Chemistry, Splaiul Independenţei 202, Bucharest 77208, Romania

Received May 28, 1983

The enthalpy of combustion of D-alanine, L-alanine, DL-alanine and β-alanine has been determined in an oxygen static-bomb calorimeter. The enthalpy of formation has been derived using data from the available literature. The results obtained are as follows:

$$C_3H_7O_2N(c) + 3^3/_4\ O_2(g) = 3\ CO_2(g) + 3^1/_2\ H_2O\ (l) + {}^1/_2\ N_2(g)$$

D-Alanine

$\Delta cH^0(298.15\ K) = -1576 \pm 3.46$ kJ/mol (-376 ± 0.83 kcal/mol)

$\Delta fH^0(298.15\ K) = -605 \pm 3.46$ kJ/mol (-144.5 ± 0.83 kcal/mol)

L-Alanine

$\Delta cH^0(298.15\ K) = -1621 \pm 1.73$ kJ/mol(-387 ± 0.41 kcal/mol)

$\Delta fH^0(298.15\ K) = -560 \pm 1.73$ kJ/mol (-134 ± 0.41 kcal/mol)

DL-Alanine

$\Delta cH^0(298.15\ K) = -1602 \pm 2.85$ kJ/mol (-382 ± 0.68 kcal/mol)

$\Delta fH^0(298.15\ K) = -578.93 \pm 2.85$ kJ/mol (-138.30 ± 0.68 kcal/mol)

β-Alanine

$\Delta cH^0(298.15\ K) = -1871 \pm 1.52$ kJ/mol(-447 ± 0.36 kcal/mol)

$\Delta fH^0(298.15\ K) = -310 \pm 1.52$ kJ/mol (-74 ± 0.36 kcal/mol)

The amino acids, organic compounds that include in their molecule the carboxyl and amino groups, are considered to be the first substances of importance for the living organism that have appeared on Earth. It is from them that the living matter has formed and developed. Indeed, in biological systems both structural and functional proteins consist almost exclusively of L-amino acids. Under these circumstances it has been very important to acquire detailed information on the structure and the properties of these organic compounds ; the amino acids have been studied by the most diverse experimental techniques among which the combustion calorimetry.

Alanine exists as two isomers : α-alanine (2-aminopropionic acid with the formula $CH_3.CH(NH_2).COOH$) and β-alanine (3-aminopropionic acid with the formula $NH_2 \cdot CH_2 \cdot CH_2 \cdot COOH$) ; α-alanine exhibits optical isomery : it exists as D-alanine, L-alanine and the racemic mixture of the two enantiomers, DL-alanine.

In order to determine the heat of formation of D-alanine, L-alanine, DL-alanine and β-alanine, heats of combustion were measured. Use has been made of a calorimetric bomb and the procedure of processing data described elsewhere.[1] In this work the calorimeter constant was 8465 J/K and the pressure of oxygen employed in the bomb 30 bars. Throughout this paper 1 cal = 4.186 J and the following values of heat of formation of carbon dioxide and water [2] were used :

$$\begin{aligned}\Delta fH^0(298.15\mathrm{K})CO_2\ (g) &= -393.51 \pm 0.13\ \mathrm{kJ/mol}\\ &\ -94.051 \pm 0.031\ \mathrm{kcal/mol}\\ \Delta fH^0(298.15\ \mathrm{K})H_2O\ (l) &= -285.83 \pm 0.042\ \mathrm{kJ/mol}\\ &\ -68.315 \pm 0.01\ \mathrm{kcal/mol}\end{aligned}$$

These values were obtained by critical evaluation of data in the literature [3] and are recommended as key values to be employed in scientific works. We have adopted the following values : $\Delta\ fH^0(HNO_3) = 219.5$ cal/g and $\Delta fH^0(Fe_2O_3) = 1600$ cal/g. To calibrate the calorimeter we employed BDH-benzoic acid, thermochemical standard. Benzoic acid has been certified at the Thermochemical Laboratory of the University of Manchester (U.K.) to have a caloric value (for combustion carried out under standard bomb conditions) of 26432 ± 4 J/g (corrected to mass in vacuo). As secondary standard we employed research grade crystalline salicylic acid (2-hydroxybenzoic acid) — Serva, Heidelberg (B.R.D.). Oxygen was purified by flowing it through copper oxide heated at 550°C, to burn combustible impurities, through Ascarite (sodium hydroxide-asbestos compound) to retain the carbon dioxide and through drying agents (P_2O_5 and $Mg(ClO_4)_2$). Ignition of the sample was achieved with an iron wire. The amount of nitric acid in the solution of the bomb (originating partly in the nitrogen from oxygen and partly in the nitrogen from the sample) was determined analytically by titration with a sodium hydroxide solution (0.1 N) in the presence of methyl orange. The volume of the calorimeter bomb was 0.3 L.

The combustion calorimetry of organic compounds containing nitrogen introduces few if any additional problems to those already described which apply to compounds containing carbon, hydrogen and oxygen. The generalised combustion reaction is :

$$C_aH_bO_cN_d\ (\mathrm{l\ or\ c}) + (a + b/4 - c/2)\ O_2(g) = aCO_2(g) + b/2H_2O(l) + + d/2N_2(g)$$

About ninety per cent of the nitrogen appears in the combustion products as elementary nitrogen, the remainder giving rise to aqueous nitric acid.

All chemicals used in experiments were Fluka chromatographic reagent grade. The molecular mass was taken as 89.10. The results obtained for the heat of combustion of solid compounds are listed in Tables 1 – 4. For the reaction :

$$C_3H_7O_2N(c) + 3^3/_4\,O_2(g) = 3\,CO_2\,(g) + 3^1/_2\,H_2O\,(l) + 1/2\,N_2\,(g)$$

Table 1

Heat of combustion of D-alanine

g substance	K ΔT	Joules (ΔT × calorim. const.)	ΔfH (Fe_2O_3)	ΔfH (HNO_3)	J/g ($-\Delta U_B$)	kJ/mol ($-\Delta U_B$)
0.7101	1.493	12 638	56	33	17 672.5	1 574
0.7777	1.63	13 798	56	42	17 616	1 569
0.8390	1.758	14 881.47	57	33	17 630	1 571
0.8608	1.805	15 279	56	47	17 630.5	1 571
1.2164	2.575	21 797	57	61	17 822.57	1 588

average value = –1 575 kJ/mol

Standard deviation $\sigma = \sqrt{\Sigma D^2/n(n-1)} = \pm 3.46$ kJ/mol

$$\%\ \text{Washburn correction} = \frac{-0.3 \times 30 \times 3}{-1\,575}\left[1 - \frac{1.1\,(7-4)}{12} + \frac{2}{30}\right] = -0.0136\,\%$$

$$\text{hence } \Delta c\,U^\circ(298.15\ \text{K}) = \frac{-1576 \times 99.986}{100} = -\ 1575\ \text{kJ/mol}$$

For the reaction $C_3H_7O_2N(c) + 3^3/_4\ O_2(g) = 3\ CO_2\ (g) + 3^1/_2\ H_2O\ (l) + {}^1/_2\ N_2(g)$ volume change is 1/4 so that

$\Delta c H^\circ(298.15\ \text{K}) = -1575 - 0.25\ RT = -1575 - 0.62 = -1576 \pm 3.46(0.219\,\%)$ kJ/mol

$-376.5 \pm 0.83(0.219\,\%)$ kcal/mol

Table 2

Heat of combustion of L-alanine

g substance	K ΔT	Joules (ΔT × calorim. const.)	ΔfH (Fe_2O_3)	ΔfH (HNO_3)	J/g ($-\Delta U_B$)	kJ/mol ($-\Delta U_B$)
0.7766	1.675	14 179	57	36	18 138	1 616
1.0066	2.17	18 369	58	40	18 151	1 617
1.0414	2.25	19 046	58	56	18 179	1 619
1.0764	2.33	19 723	56	42	18 332	1 624
1.2334	2.67	22 602	58	63	18 227	1 624

average value = –1 620 kJ/mol

Standard deviation $\sigma = \sqrt{\Sigma\Delta^2/n(n-1)} = \pm 1.73$ kJ/mol

$$\%\ \text{Washburn correction} = \frac{-0.3 \times 30 \times 3}{-1620}\left[1 - \frac{1.1(7-4)}{12} + \frac{2}{30}\right] = -0.0132\ \%$$

$$\text{hence } \Delta c U^0(298.15\ \text{K}) = \frac{-1\,620 \times 99.987}{100} = -1\,620\ \text{kJ/mol}$$

Volume change for the reaction is of 1/4, so that

$\Delta c H^0(298.15\text{K}) = -1620 - 0.25\ RT = -1\,620 - 0.62 = -1621 \pm 1.73(0.107\%)$ kJ/mol

$-387 \pm 0.41(0.107\%)$kcal/mol

Table 3

Heat of combustion of DL-alanine

g substance	K ΔT	Joules (ΔT × calorim. const.)	ΔfH (Fe_2O_3)	ΔfH (HNO_3)	J/g ($-\Delta U_B$)	kJ/mol ($-\Delta U_B$)
0.9969	2.127	18 005	55.6	48.3	17 957	1 600
1.0227	2.195	18 581	55.6	48.1	18 067	1 609
1.0779	2.306	19 520	57.6	60.6	18 000	1 604
1.2765	2.735	23 152	57.6	64.7	18 041	1 607
1.3599	2.921	24 726	57	73.3	18 086	1 611

average value = −1 602 kJ/mol

Standard deviation $\sigma = \sqrt{\Sigma\Delta^2/n(n-1)} = \pm 2.85$ kJ/mol

$$\%\ \text{Washburn correction} = \frac{-0.3 \times 30 \times 3}{-1\,602}\left[1 - \frac{1.1(7-4)}{12} + \frac{2}{30}\right] = -0.014\%$$

$$\text{hence } \Delta cU^0(298.15\ \text{K}) = \frac{-1602 \times 99\,986}{100} = -1\,601\ \text{kJ/mol}$$

Volume change for the reaction is of 1/4, so that

$$\Delta cH^0(298.15\ \text{K}) = -1601 - 0.25\,RT = -1601 - 0.62 = -1602 \pm 2.85(0.178\%)\ \text{kJ/mol}$$
$$-382 \pm 0.68(0.178\%)\text{kcal/mol}$$

Table 4

Heat of combustion of β-alanine

g substance	K ΔT	Joules (ΔT × calorim. const.)	ΔfH (Fe_2O_3)	ΔfH (HNO_3)	J/g ($-\Delta U_B$)	kJ/mol ($-\Delta U_B$)
0.9098	2.268	19 199	56	42	20 994	1 871
0.9396	2.343	19 833.5	54	49	20 998.8	1 871
1.0938	2.725	23 067	58	54	20 987	1 870
1.1201	2.798	23 685	56	52	21 049	1 875
1.3412	3.33	28 188	56	65	20 927	1 865
1.4968	3.718	31 473	58	68	20 943	1 866

average value = −1870 kJ/mol

Standard deviation $\sigma = \sqrt{\Sigma\Delta^2/n(n-1)} = \pm 1.52$ kJ/mol

$$\%\ \text{Washburn correction} = \frac{-0.3 \times 30 \times 3}{-1870}\left[1 - \frac{1.1(7-4)}{12} + \frac{2}{30}\right] = -0.0114\%$$

$$\text{hence } \Delta cU^0(298.15\text{K}) = \frac{-1870 \times 99.99}{100} = -1869.8\ \text{kJ/mol}$$

Volume change for the reaction is of 1/4, so that

$$\Delta cH^0(298.15\text{K}) = -1870 - 0.25\,RT = -1870 - 0.62 = -1871 \pm 1.52(0.08\%)\ \text{kJ/mol}$$
$$= -447 \pm 0.36(0.08\%)\text{kcal/mol}$$

volume change is 1/4. To bring values obtained to standard state, calculations were the more intricate, the more complex the structure of the substance. In the case of compounds with carbon, hydrogen and oxygen of $C_aH_bO_c$ general formula the corrections of the procedure of reduction to standard state are summed by Washburn's equation :[4]

$$\% \text{ correction} = \frac{-0.3 \times P_i \times a}{-\Delta U_B}\left[1 - \frac{1.1(b-2c)}{4a} + \frac{2}{P_i}\right]$$

where P_i stands for initial oxygen pressure (in bars) and $-\Delta U_B$ for the heat of combustion ; the correction is calculated in percents of experimental value. The above equation applies fairly well in the case of nitrogen compounds as well. The calculation of standard heat of combustion was effected after application of Washburn's corrections, by summation of the products RT (equal to $-$ 2.479 kJ/mol) times the number of volumes that entered and emerged from reaction. Application of the Hess rule allows the calculation of the heats of formation. The following relation was obtained :

$$\Delta fH^0(298.15\ \text{K})C_3H_7O_2N\ (c) = -\Delta cH^0(298.15\ \text{K})C_3H_7O_2N\ (c) + 3\,\Delta fH^0(298.15\ \text{K})CO_2\ (g) + 3^1/_2\,\Delta fH^0(298.15\ \text{K})H_2O\ (l)$$

the enthalpies of formation of elements were assumed to be zero. The results obtained for the heat of formation are listed in table 5.

Table 5

The enthalpies of combustion and formation of D-alanine, L-alanine, DL-alanine and β-alanine

Substance	$-\Delta cH^0$(298.15 K)		$-\Delta fH^0$(298.15 K)	
	kJ/mol	kcal/mol	kJ/mol	kcal/mol
D-alanine	1576±3.46	376±0.83	605±3.46	144.5±0.83
L-alanine	1621±1.73	387±0.41	560±1.73	134±0.41
DL-alanine	1602±2.85	382±0.68	579±2.85	138.3±0.68
β-alanine	1871±1.52	447±0.36	310±1.52	74 ±0.36

As one expects, the heats of combustion and formation of the racemic mixture range between the values for the two enantiomers of which it consists. The heat of combustion of alanine was determined[5] in 1936 by Huffman, Ellis and Fox who published values assigned to the D-isomer ; in Domalski's compilation[6] issued in 1972, the values were assigned to the L-isomer, as other properties were considered as well, e.g. the configuration and the specific rotation. The values obtained in this contribution confirm Domalski's assignment. For DL-alanine the ΔcH° (298.15 K) and ΔfH° (298.15 K) values obtained by Huffman, Fox and Ellis are also published.[5]

REFERENCES

[1] I. Contineanu and D. I. Marchidan, *Rev. Chim.* (*Bucureşti*), **30**, 1096 (1979).

[2] CODATA Bulletin no 28 (April 1978) : "CODATA Recommended Key Values for Thermodynamics 1977".

[3] CODATA Task Group on Key Values for Thermodynamics. *J. Chem. Thermodynamics*, **4**, 331 (1972) ; *Teplofiz. Vys. Temperatur*, **9**, 657(1971) ; CODATA Bulletin no 5 (1971).

[4] E. W. Washburn, *J. Res. Nat. Bur. Standards*, **10**, 525 (1933).

[5] H. M. Huffman, E. L. Ellis and S. W. Fox, *J. Amer. Chem. Soc.*, **58**, 1728 (1936).

[6] E. G. Domalski, *J. Phys. Chem. Ref. Data*, **1**, 221 (1972).

Revue Roumaine de Chimie, **29**, *1*, 49–53 (1984)

REGIO- AND STEREOSELECTIVE BROMINE ADDITION TO 2-CHLORO-*endo*-BENZOCYCLOBUTENONORBORNENE[1]

AURELIA GHENCIULESCU, MIRCEA D. GHEORGHIU, LUCIAN ENESCU,
ILIE G. DINULESCU and MARGARET AVRAM *

Laboratory of Organic Chemistry, Polytechnic Institute-TCH, Spl. Independenţei 313,
72206 Bucharest 16, Romania

Received October 10, 1983

The synthesis of 2-chloro-*endo*-benzocyclobutenonorbornene **(11)** from 1-chloro-benzocyclobutadiene and cyclopentadiene is described. Evidences for regio- and stereoselective course of solvolytic bromine addition to **11** are presented.

It was shown in earlier papers that the solvolytic bromine addition to benzocyclobutenonorbornenes occurs with skeletal rearrangement.[2a,b,c] Thus, in the reaction of *endo*-isomer **(1)** with NBS in acetic acid, the bromo-acetoxy derivative **4** was obtained.

Due to the symmetry of the bromonium ion **2**, the same intermediate non classical ion **3** can result by the σ-attack of the bond C_1-C_2 or C_5-C_6 leading consequently to the same reaction product.

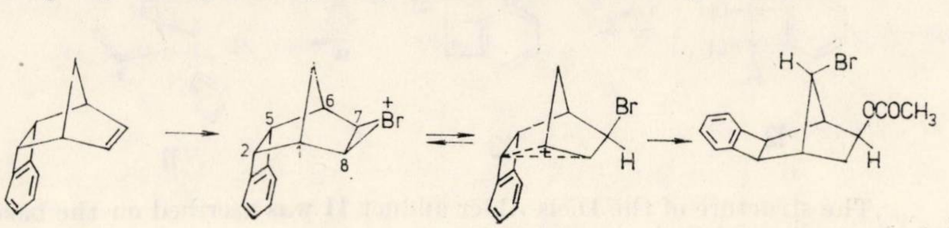

1 2 3 4

Taking into account that in 2-substituted benzocyclobutenonorbornenes **(5)** the 1,2 and 5,6 σ-bonds are not equivalent, two different intermediate non classical ions **7** and **8** may be formed by the opening of the bromonium ion **6**, during the solvolytic bromine addition, leading to two isomeric addition products **9** and **10**.

---

* Deceased October 28, 1983

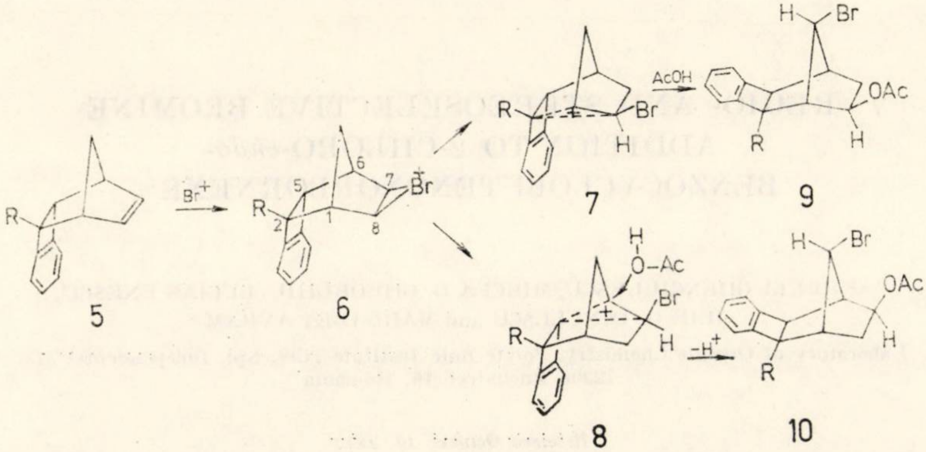

As an extension of our studies concerning the skeletal rearrangement of benzocyclobutenonorbornenes in reactions involving ionic intermediates, [2] the behaviour of benzocyclobutenonorbornenes having in 2 position substituents with various electronic demands was considered of interest.

In this paper we present the synthesis and behaviour in the solvolytic bromine addition of 2-chloro-*endo*-benzocyclobutenonorbornene **(11)**.

The synthesis of **11** was achieved from trichlorobenzocyclobutene **(12)**. [3] The treatment of **12** with lithium amalgam in ethereal solution, in the presence of cyclopentadiene **(14)**, afforded as intermediate the 1-chloro-benzocyclobutadiene **(13)** which by Diels-Alder reaction with **14** gave the adduct **11**. (Together with **11** small amounts of dimeric compounds were formed).

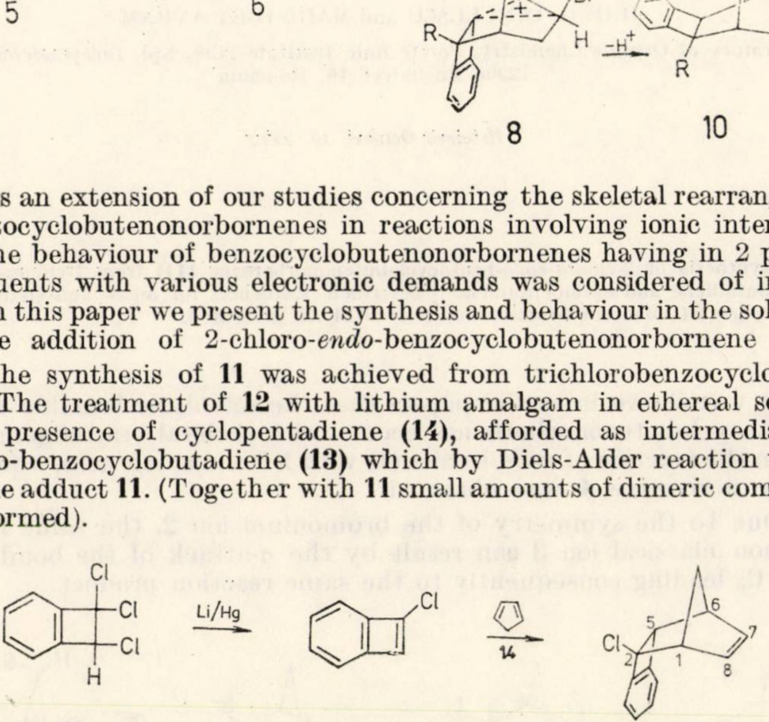

The structure of the Diels-Alder adduct **11** was ascribed on the basis of the analytical and spectral data.

The NMR spectrum (CCl_4, δ, ppm) presents beside a multiplet at 6.57—7.40 ppm (4 aromatic H) a broad singlet at 5.67 ppm (2H) ascribed to H-7 and H-8 coupled with H-1 and H-6 respectively (3.03 ppm, bs), a doublet at 3.77 ppm (1H) for H-5 coupled with H-6 ($J = 4.0$ Hz) and two doublets at 2.35 ppm (H-9-*anti*) and 2.03 ppm (H-9-*syn*) ($J_{gem} = 9.0$ Hz).

The mass spectrum of **11** presents for $m/e = 167$ the parent ion ; the molecular ion $m/e = 202$ is of 3.6 % intensity. The fragmentations of the molecular ion are M—Cl and M—CH_3 and are followed by elimination of

CH_3 and Cl, respectively, leading to fragments $m/e = 152$, probably biphenylene. This kind of fragmentation is characteristic for compounds with benzocyclobutenonorbornene skeleton [4] and represents the support for benzocyclobutene fragment. The third route of fragmentation of the molecular ion is a retro Diels-Alder reaction leading finally to chlorophenylacetylene ($m/e = 136$).

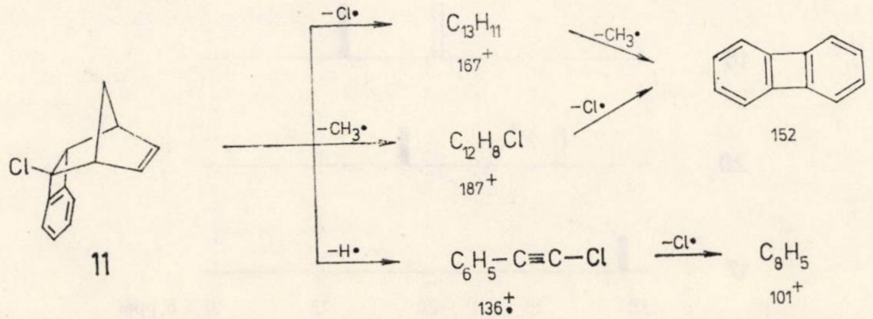
Cl
11
−Cl•
$C_{13}H_{11}$
167+
−CH3•
−Cl•
152
−CH3•
$C_{12}H_8Cl$
187+
−H•
$C_6H_5-C\equiv C-Cl$
136+•
−Cl•
C_8H_5
101+

Reaction of 2-chloro-*endo*-benzocyclobutenonorbornene **(11)** with NBS in acetic acid afforded as single reaction product the bromo-acetoxy derivative **15**.

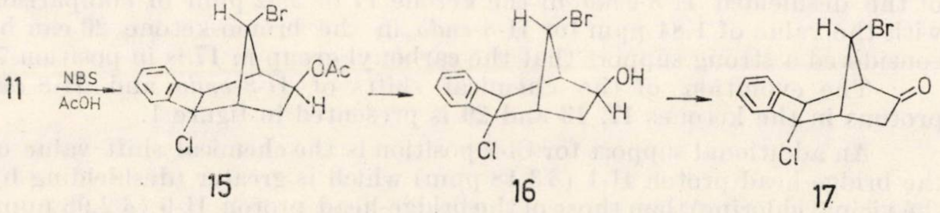
11
NBS
AcOH
H
Br
OAc
H
Cl
15
H
Br
OH
H
Cl
16
H
Br
O
Cl
17

Hydrolysis of **15** afforded the bromo-hydroxy derivative **16** and oxidation of the latter, the bromo-ketone **17**.

The ^{1}H-NMR spectral data of **15**, **16** and chiefly of **17** and specially those obtained in the presence of $Eu(fod)_3d_{27}$ support the ascribed structures.

The small coupling between the benzylic proton H-5 and the bridgehead proton H-6 supports the *exo* configuration of the benzocyclobutene ring. The *syn* orientation of bromine at C-9 is supported by the deshielding of H-8-*exo* proton in **17** with 0.70 ppm in comparison with the parent ketone **18**.

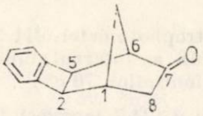

18

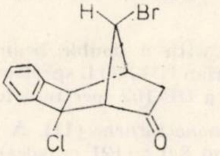

19

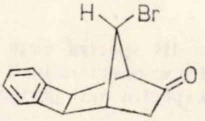

20

The relative position of the carbonyl group in respect to Cl-2 in the ketone **17** was ascribed on the basis of the chemical shift value of vicinal H-8-*endo* proton. In the structure **17** it is expected a greater deshielding of this proton due to the proximity of the Cl-2-*endo*. In an isomeric structure **19** the distance between the chlorine and H-8-*endo* proton is greater than in **17** so that smaller deshielding is to be expected. The signal of the deshielded H-8-*endo* in the ketone **17** of 2.82 ppm in comparison with the value of 1.84 ppm for H-8-*endo* in the bromo-ketone **20** can be considered a strong support that the carbonyl group in **17** is in position 7.

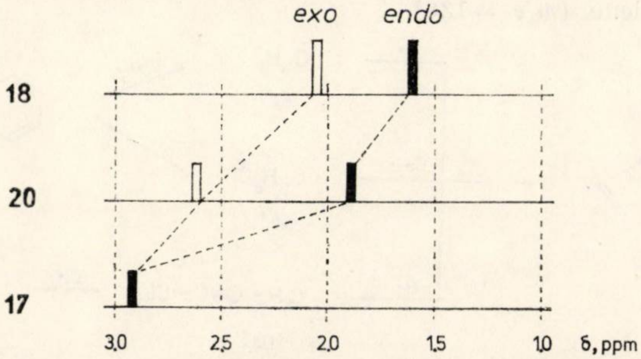

Fig. 1. — Chemical shifts of the α-ketonic protons (H-8-*exo* and *endo* protons).

The evolution of the chemical shifts of H-8-*endo* and H-8-*exo* protons in the ketones **17, 18** and **20** is presented in figure 1.

An additional support for Cl-2 position is the chemical shift value of the bridge-head proton H-1 (δ 3.18 ppm) which is greater (deshielding by the vicinal chlorine) than those of the bridge-head proton H-6 (δ 2.98 ppm) near to the carbonyl group. In the ketone **20** the both bridge head protons H-1 and H-6 present approx. the same chemical shifts (2.95 and 2.98 ppm, respectively).

The obtention of the bromo-acetoxy derivative **15** as the single addition product to **11** evidences that the —*I* effect of chlorine has an essential role on the participation of the σ-bond to the opening of the intermediate bromonium ion **6** (R = Cl). This occurs regioselectively leading to the intermediate non classical ion **8** (R = Cl). Reaction of the latter with the solvent nucleophile molecule takes place stereoselectively, as usual.[2]

EXPERIMENTAL

IR spectra were recorded with a double beam UR 20 spectrophotometer. ^{1}H-NMR spectra were determined with a Varian EM-360 L spectrometer, using TMS as internal standard. Mass spectra were performed with a DP-102 spectrometer in EJ, with ionisation 70 eV.

2-Chloro-endo-benzocyclobutenonorbornene **(11)**. A solution of 5.0 g (24.7 mmoles) 1,1,2-trichloro-benzocyclobutene **(12)** and 8.0 g (121 mmoles) cyclopentadiene **(14)** in 100 ml anhydrous diethyl ether was treated with 180 g (130 mmoles Li) 0.5% lithium amalgam and the mixture was shaken for 5 hrs in a stopped bottle, at room temperature. The ethereal layer was separated, washed with water, dried and the solvent evaporated yielding 2.9 g residue (yellow oil). By distillation pure **11** (1.9 g, 38%), b.p. 115°/2 mm, were obtained. – $C_{13}H_{11}Cl$ Molecular weight calcd. : 202.6 ; found (by mass spectrometry) : 202. – ^{1}H-NMR (CCl_4,δ, ppm) : 2.03 (d, 1H, H-9-*syn*, $J_{9\text{-}syn.9\text{-}anti} = 9.0$ Hz), 2.35 (d, 1H, H-9-*anti*, $J = 9.0$ Hz), 3.03 (bs, 2H, H-1, H-6), 3.77 (d, 1H, H-5, $J_{5.6} = 4.0$ Hz), 5.67 (bs, 2H, H-7, H-8), 6.57–7.40 (m, 4 aromatic H).

exo-7-Acetoxy-syn-9-bromo-2-chloro-exo-benzocyclobutenonorbornene **(15)**. A solution of 0.81 g (4.0 mmoles) **11** in 40 ml anhydrous acetic acid was treated with 0.72 g (4.0 mmoles) of N-bromo-succinimide, and the mixture was left at room temperature. After 24 hrs, 100 ml water were added, the product was extracted with dichloromethane and the organic layer washed with water and 5% sodium hydrogen carbonate solution in order to remove the acetic acid. After drying and evaporation of the solvent, the oily residue (1.2 g) was purified by chromatography with petroleum ether on alumina column, yielding 1.1 g (85%) **15**, colourless oil. – $C_{15}H_{14}BrClO_2$ Molecular weight calcd. : 341.6 ; found (by mass spectrometry) : 342. – IR (CCl_4, cm^{-1}) : ν_{CO}1745. – ^{1}H-NMR (CCl_4, δ, ppm) : 2.05 (s, 3H, CH_3COO), 2.10–2.90 (m, 2H, H-8-*endo*, H-8-*exo*), 2.71 (bs, 2H, H-1, H-6), 3.40 (s, 2H, H-5, H-9-*anti*), 4.77 (m, 1H, H-7-*endo*), 6.95–7.62 (m, 4 aromatic H).

exo-7-Hydroxy-syn-9-bromo-2-chloro-exo-benzocyclobutenonorbornene **(16)**. Into a solution of 1.0 g (18.0 mmoles) potassium hydroxide in 15 ml methanol, 0.68 g (2 mmoles) **15** were added and the mixture was boiled for 5 hrs. After evaporation of methanol, water was added, the product extracted with dichloromethane, the organic layer washed until neutral and the solvent was removed yielding 0.54 g (90%) **16**, viscous oil. – IR (CCl_4, cm^{-1}) : ν_{OH}3582. – ^{1}H-NMR (CCl_4, δ, ppm) : 1.72 (m, 2H, H-8-*endo*, H-8-*exo*), 2.72 (m, 2H, H-1, H-6), 3.22 (s, 1H, H-5), 3.47 (bs, 1H, H-9-*anti*), 3.93 (m, 1H, H-7-*endo*), 6.98–7.58 (m, 4 aromatic H).

syn-9-Bromo-2-chloro-exo-benzocyclobutenonorbornen-7-one **(17)**. A solution of 0.6 g (2.0 mmoles) **16** in 6 ml pyridine was added to a suspension of chromic anhydride – pyridine complex obtained from 0.60 g chromic anhydride and 6 ml pyridine, and the mixture was left for 24 hrs at room temperature with occasional shaking. Water was added and the product extracted with diethyl ether. After washing with water, with 2% hydrochloric acid, with water, and drying, the solvent was removed, yielding 0.55 g (93%) **17**, m.p. 67° (from methanol). – IR (CCl_4, cm^{-1}) : ν_{CO} 1770. – ^{1}H-NMR ($CDCl_3$, δ, ppm) : 2.82 (m, 2H, H-8-*endo*, H-8-*exo*), 2.98 (s, 1H, H-6), 3.81 (m, 1H, H-1), 3.28 (bs, 1H, H-9-*anti*), 3.67 (s, 1H, H-5), 7.05–7.70 (m, 4 aromatic H).

REFERENCES

[1] Part LV in the series "Investigations in the Cyclobutane Series". For part LIV see : L. Enescu, M. D. Gheorghiu, A. Ghenciulescu, I. G. Dinulescu and M. Avram, *Rev. Roumaine Chim.*, **28**, 1001 (1983).

[2] a. M. Avram, I. Pogany, F. Badea, I. G. Dinulescu and C. D. Nenitzescu, *Tetrahedron Letters*, **1969**, 3851 ; b. M. Avram, I. Pogany, I. G. Dinulescu, F. Chiraleu and C. D. Nenitzescu, *Rev. Roumaine Chim.*, **15**, 1207 (1970) ; c. I. G. Dinulescu, H. L. Prasad, L. Enescu, A. Ghenciulescu and M. Avram, *Rev. Roumaine Chim.*, **24**, 833 (1979) ; d. L. Enescu, H. L. Prasad, I. G. Dinulescu, A. Ghenciulescu, F. Chiraleu and M. Avram, *Rev. Roumaine Chim.*, **24**, 999 (1979) ; e. A. Ghenciulescu, I. G. Dinulescu, H. L. Prasad, L. Enescu and M. Avram, *Rev. Roumaine Chim.*, **24**, 1159 (1979).

[3] P. Filip, N. Ştefan, F. Chiraleu, I. G. Dinulescu and M. Avram, *Rev. Roumaine Chim.*, in press.

[4] M. D. Gheorghiu, A. Ghenciulescu, L. Enescu and M. Avram, unpublished results.

was separated, washed with water, dried and the solvent evaporated leaving 2.9 g [illegible] yellow oil. By distillation pure 11 [illegible] were obtained. [illegible] Molecular weight calcd. [illegible] found (by mass spectrometry) [illegible] [illegible] aromatic H).

[illegible] (12). A solution of 0.81 g [illegible] 11 in 40 ml anhydrous acetic acid was treated with 0.73 g [illegible] of [illegible] and the mixture was left at room temperature. After 24 hrs, the [illegible] was added, the product was extracted with [illegible] and the organic layer washed with water and [illegible] sodium carbonate solution in order to remove the acetic acid. After drying and evaporation of the solvent, the [illegible] was purified by chromatography with [illegible] [illegible] aromatic H).

[illegible] (16). [illegible] 1.0 g [illegible] potassium hydroxide in 15 ml methanol [illegible] were added and the mixture was [illegible] for [illegible] hrs. After evaporation of methanol, water was added, the product extracted with [illegible], the organic layer washed until neutral and the solvent was removed yielding [illegible] 16. [illegible] aromatic H).

[illegible] (17). A solution of 0.6 g [illegible] 16 in 6 ml pyridine was added to a suspension of chromic anhydride – pyridine complex obtained from [illegible] g chromic anhydride and [illegible] ml pyridine, and the mixture was left for 24 hrs at room temperature with occasional shaking. Water was added and the product extracted with diethyl ether. After washing with water, with [illegible] hydrochloric acid, with water, and drying, the solvent was removed, yielding 0.25 g [illegible] 17 [illegible] aromatic H).

REFERENCES

[1] Part LV in the series [illegible] L. [illegible], M. D. [illegible], A. [illegible], L. [illegible] and M. Avram, Rev. Roumaine Chim. [illegible]

[2] M. Avram, [illegible] Tetrahedron Letters, [illegible]

[3] [illegible] and M. Avram, Rev. Roumaine Chim., in press.

[4] M. D. [illegible], A. [illegible], L. [illegible] and M. Avram, unpublished results.

Revue Roumaine de Chimie, **29**, *1*, 55–65 (1984)

STUDIES ON AQUEOUS ELECTROLYTES AND NONELECTROLYTES. I

EFFECTS OF ELECTROLYTES ON VISCOSITY AND STRUCTURE OF AQUEOUS SOLUTIONS OF POLYVINYL ALCOHOL

MONIMUL HUQUE and D. SĂNDULESCU
Department of Chemistry, Institute of Petroleum and Gas,
Blvd. București, No. 39, 2000 Ploiești, Romania

Received December, 1982

As a sequel to a previous study, the '*B*' coefficient of Jones-Dole equation, $[\eta]$, ΔH, ΔG, $T\Delta S$ and apparent specific volume (φ) have been determined for aqueous solutions of polyvinyl alcohol (PVA) in the presence of NaCl and KCl at 20°, 30° and 40°C from experimentally determined viscosity coefficient and density. Thermodynamic quantities of flow phenomena indicate a strong interaction between Na^+ and solvents.

The viscosity of aqueous solutions of electrolytes has been studied extensively [1] since Arrhenius began his investigation on electrolytes in 1880's [2]. In literature some general and complete works are known in this domain: the classical theory of Falkenhagen and Dole interprets the viscosity of electrolytes by means of interionic forces and the empirical equation of Jones-Dole, $\eta_{rel.} = 1 + A\sqrt{C} + BC$, where A is the theoretical coefficient of Falkenhagen which has a small positive value (0.01 ... ... $0.0051^{\frac{1}{2}}\,\text{mol}^{-\frac{1}{2}}$) and B is an empirical coefficient which corresponds to ion-solvent interaction and has a positive or a negative value depending upon the nature of electrolytes and temperature. The positive value of B corresponds to ions which intensify the structure of solution through hydration, e.g. Li^+, Na^+ and the negative value corresponds to ions which destroy the structure i.e. have an effect which disorders in molecular arrangement of water or solution e.g. K^+, Cl^-. This equation is verified in various solvents including water [3-6] as well as in aqueous solution of polyvinyl alcohol (PVA). From these studies it is reflected that the study of coefficient B is important for qualitative and, within certain limits, quantitative determination of the effects of ions on the structure of solvents, and for establishing the possibility of comparing the B values of one electrolyte in different solvents respectively.

In the previous study[1], the B coefficient was determined for aqueous solutions of PVA in the presence of electrolytes: LiCl, NaCl, KCl, NH_4Cl, $MgCl_2$ and $CaCl_2$ at 20°C. Considering a very small value of coefficient 'A' $\left(\frac{A}{B} \ll 1\right)$, the validity of Jones-Dole equation $\left(\frac{\eta - \eta_0}{\eta_0} = BC\right)$ was verified at 20°C for different concentrations of PVA (0.125 ... 2%) solution. The effect of PVA on the 'B' coefficient was interpreted as the intensification in volume, respectively by the number of cluster in pseudotetrahedral structure of water formed by the effect of hydrophobic linkage of polymer chains. It was also interpreted as the effect of polar group, $-OH$, which links directly to the hydrogen bonding network of water.

Undoubtedly, one of the most difficult problems in this field corresponds to the establishment of ion-solvent interactions, interpretation of thermodynamic processes and transport phenomena of ions in solutions on the basis of their effective state. For this reason the present study was proposed as a sequel to the previous work to complete it with the effect of temperature and molecular weight of polymers. The study was limited to the solutions of NaCl, KCl and PVA ($\bar{M} = 1.72 \times 10^4$, 1.8×10^4 and 3.0×10^4) and to temperatures 20°, 30° and 40°C. This study was extended by the determination of Ultrasonic velocity and velocity of flow through different granular beds. [7]

EXPERIMENTAL

Redistilled water was used to prepare stock solution of different fractions of PVA. The concentration of stock solution was determined by evaporating 5 ml solution under vacuum pressure at 80°C to a constant weight. The stock solution was used to prepare solutions of desired concentration of PVA under study. The electrolytes used were AR grade NaCl and KCl. The required amount of salts was weighed by using an analytical balance to yield the exact molality. To avoid hygroscopic effect the salts of sodium and potassium chloride were dried for 24 hrs at 110—115°C and then kept in a desiccator over $CaCl_2$ prior to use. Molecular weight of different fractions of PVA were determined by viscometric method using the formula[8] :

$$[\eta] = 5.83 \times 10^{-4} \cdot \bar{M}_\eta^{0,63} \text{ at } 25°\text{C}.$$

A viscometer (Höppler, type BH 2, VEB MLW, PRUFGERATEWERK MEDINGEN with an ultra-thermostate (U 10) was used for viscosity measurement at 20°, 30° and 40°C (± 0.05°C). The densities were determined by hydrostatic method using a hydrometer with an analytical balance and an ultra-thermostate [7]. Both the apparatus for viscosity and density measurements were calibrated with redistilled water on the basis of the following data at different temperatures : [2,9]

t°C	$g \cdot cm^{-3}$	10^2 (P)
25	0.9971	0.8903
30	0.9957	0.7975
35	0.9941	0.7194
40	0.9922	0.6531

RESULTS

Experimentally determined viscosity data for different solutions of VA ($\bar{M}_\eta = 1.72 \times 10^4$) having concentrations 0.25%, 0.50% and 1% by wt./vol. in the presence of electrolytes (NaCl and KCl) are presented in the diagram $\frac{\eta - \eta_0}{\eta_0}$ vs C (Fig. 1), where C is the concentration of electrolytes (mole l^{-1}), η and η_0 are the viscosity coefficients of solutions and solvent respectively. Figure 1 shows that the application of Jones-Dole equation agrees well with the results obtained in the previous study[1] and also with the value of coefficient 'B' for Na^+ and K^+ in pure water at 20° C[4,10,11].

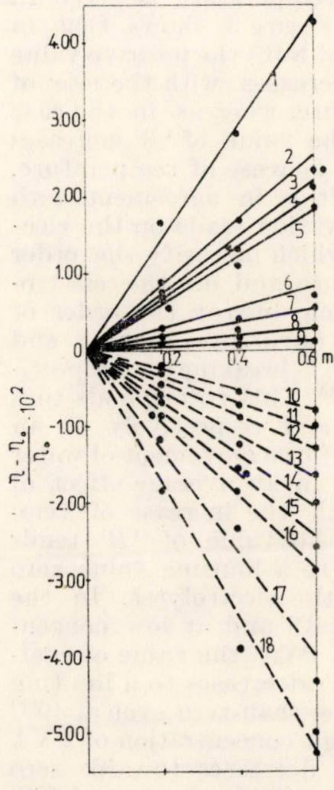

Fig. 1. — Variation of $\frac{\eta - \eta_0}{\eta_0}$ with concentration of electrolytes at different temperatures and concentrations of PVA ($\overline{M} = 1.72 \cdot 10^4$): 1—9 for NaCl; 10—18 for KCl; 1, 4, 6, 14, 17, 18, for 20°C; 2, 5, 7, 12, 15, 16 for 30°C; 3, 8, 9, 10, 11, 13 for 40°C; 1, 2, 3, 10, 12, 14 for 0.25 % PVA; 4, 5, 8, 11, 15, 17 for 0.5 % PVA; 6, 7, 9, 13, 16, 18 for 1.0124 % PVA.

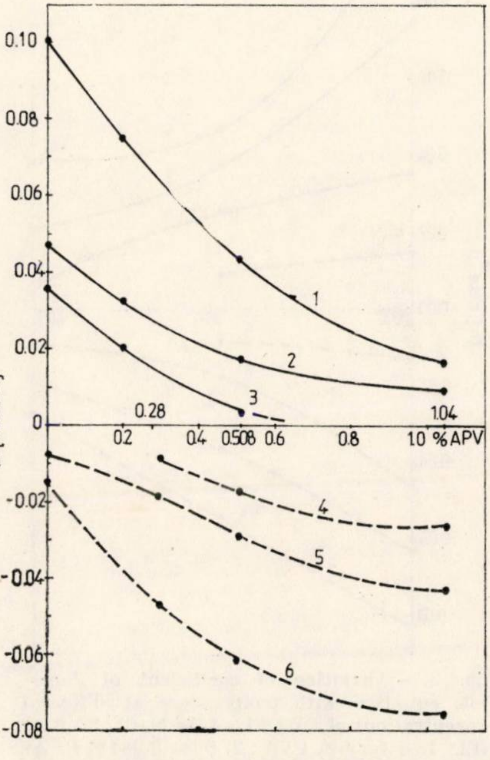

Fig. 2. — Variation of B coefficient of Jones-Dole equation with concentration of PVA at different temperatures: 1—3 for NaCl; 4—6 for KCl; 1,6 for 20°C; 2,5 for 30°C; 3, 4 for 40°C.

The variation of coefficient 'B' ($B > 0$ for NaCl and $B < 0$ for KCl) with the concentration of PVA at 20°, 30° and 40°C is given in figure 2. From figure 2, it is evident that the value of coefficient 'B' decreases with the increase of the concentration of PVA and has a tendency to reach a limiting value at relatively high concentration of PVA (above 0.6 %PVA), which indicates the attainment of a structure predominated by the presence of cluster formed by the interaction of H_2O-PVA.

The variation of coefficient 'B' with temperature is given in figure 3. Figure 3 shows that in the case of NaCl the positive value of 'B' decreases with the rise of temperature, whereas in the case of KCl the value of 'B' increases with the increase of temperature. This result is in agreement with the observation made on the electrolytes which intensify the order of structure and on the electrolytes which destroy the order of structure (structure making and structure breaking) respectively.[12,13,14] This corresponds to a decrease and respectively to an increase of free movement of water molecules in an average effect of time. With the increase of temperature the value of 'B' tends probably to a limiting value zero for both the electrolytes. In the case of NaCl and at low concentration of PVA, the value of coefficient 'B' decreases to a limiting value other than zero even at 40°C but at high concentration of PVA the value decreases towards zero at around 40°C. In the case of KCl and at low concentration of PVA the value of coefficient 'B' increases towards zero with the increase of temperature but at high concentration of PVA the 'B' coefficient attains a limiting value (negative) other than zero even at a temperature higher than 40°C.

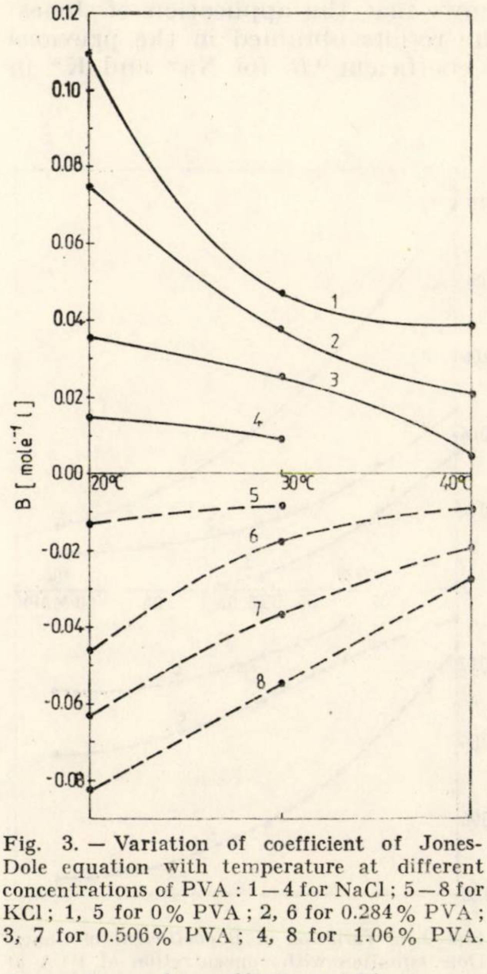

Fig. 3. — Variation of coefficient of Jones-Dole equation with temperature at different concentrations of PVA : 1—4 for NaCl ; 5—8 for KCl ; 1, 5 for 0% PVA ; 2, 6 for 0.284% PVA ; 3, 7 for 0.506% PVA ; 4, 8 for 1.06% PVA.

DISCUSSIONS

The study of viscosity permits to obtain an interesting information about the structure and on the interaction between the particles in liquid solution. Though, within certain limits, this information leads only to a qualitative conclusion, because a complete mathematical theory on the relation between viscosity and the nature of liquid is very difficult to establish with the exception of polymer solution, [15] the values of thermodynamic quantities of flow phenomena provide a series of interesting semiquantitative discussions. [6,10,16,17]

If there is no chemical interaction in solution, measurements of viscosity and corresponding data of flow process are related to the change in size and interactions between hydrodynamic groups which characterize the flow process. The increase of enthalpy of activation corresponds to the increase in energy of interactions between the hydrodynamic units; at the same time there is a possibility of increasing the dimensions of these units which in general shows the increase of rigidity of the structure of liquid.

With the application of Eyring theory [18] the enthalpy of activation and other thermodynamic quantities were calculated from the diagram $\ln \eta$ VS $\frac{1}{T}$ and by the relations:

$$\Delta H_\eta^\ddagger \approx E_\eta^\ddagger = R \frac{\mathrm{d} \ln \eta}{\mathrm{d} \frac{1}{T}}$$

Free enthalpy $\Delta G^\ddagger$ is expressed as

$$\Delta G_\eta^\ddagger = RT \ln \frac{V\eta}{hN_A} = \Delta H_\eta^\ddagger - T\Delta S_\eta^\ddagger \text{ or } \Delta S_\eta^\ddagger = \frac{\Delta H_\eta^\ddagger - \Delta G_\eta^\ddagger}{T}$$

Therefore $\Delta S_\eta^\ddagger = \frac{H_\eta^\ddagger}{T} + R \ln \frac{hN_A}{V}$.

Experimental results for $\Delta H^\ddagger$, $\Delta G^\ddagger$ and $T\Delta S^\ddagger$ are presented in Figs 4, 5 and 6 respectively. It is observed from figure 4 that the enthalpy of activation of flow increases with the increase of concentrations of both PVA and NaCl but in the case of a solution of PVA with KCl the enthalpy of activation of flow decreases with the increase of concentration of KCl. For a solution of PVA only the increase of enthalpy of activation of flow is about 1500 cal in the concentration range 0–1% PVA. In the case of 0.25% PVA solution with NaCl the increase of enthalpy of activation is about 100 cal for a concentration range 0–0.6 mol. L^{-1} of NaCl, but for a solution of 1% PVA with the same range of concentration of NaCl the increase of enthalpy of activation is about 50 cal. In the case of PVA solution with KCl the enthalpy of activation decreases by 150–250 cal within the same range of concentration of KCl as indicated above for electrolytes.

It is evident from figure 5 that the free enthalpy of flow process increases with the increase of concentration of PVA. The value of free enthalpy also changes (increases or decreases) with the change of concentration of electrolytes. For a solution of PVA the effect on the change of free enthalpy decreases with the increase of temperature and also with the increase of concentration of PVA.

In a similar way, figure 6 indicates the similar effect of electrolytes and of concentration of PVA on the entropy of activation of flow. In the case of NaCl the entropy of activation of flow increases remarkably with the increase of concentration of electrolytes but this effect is annihilated with a large increase of PVA concentration. In the case of KCL the opposite effect is observed i.e. $\Delta S^{\ne}$ decreases with the increase of concentration of KCl and PVA. Similar curves are also obtained for polymer (PVA) of different molecular weights.

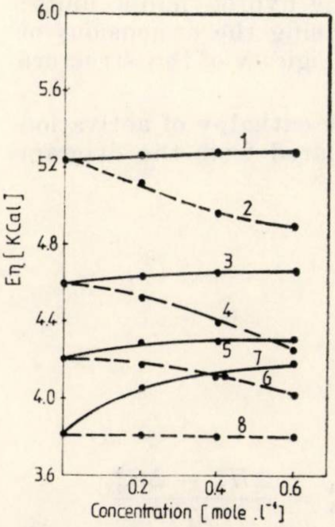

Fig. 4. — Variation of energy of activation ($E^{\ne}_{\eta}$) with concentration of electrolytes at different concentrations of PVA: 1, 3, 5, 7 for NaCl; 2, 4, 6, 8 for KCl; 1, 2 for 1.0142% PVA; 3, 4 for 0.507% PVA; 5, 6 for 0.25% PVA; 7, 8 for 0% PVA.

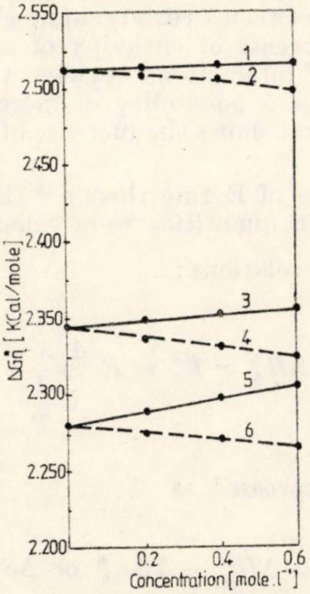

Fig. 5. — Variation of $\Delta G^{\ne}_{\eta}$ with concentration of electrolytes at different concentrations of PVA: 1, 3, 5 for NaCl; 2, 4, 6 for KCl; 1, 2 for 1.014% PVA; 3, 4 for 0.507% PVA; 5, 6 for 0.25% PVA.

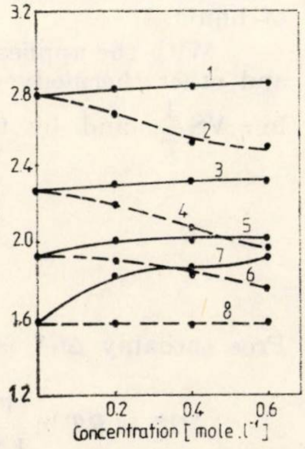

Fig. 6. — Variation of $T\Delta S^{\ne}_{\eta}$ with concentration of electrolytes at different concentrations of PVA: 1, 3, 5, 7 for NaCl; 2, 4, 6, 8 for KCl; 1, 2 for 1.014% PVA; 3, 4 for 0.507% PVA; 5, 6 for 0.25% PVA; 7, 8 for 0% PVA.

The experimental result shows an increase of $\Delta H^{\ne}_{\eta}$, $\Delta G^{\ne}_{\eta}$ and $T\Delta S^{\ne}_{\eta}$ with the molecular weight of polymers but at the same time it shows the annihilation of the effect of electrolytes on polymers of higher molecular weight.

It is to be noted that the form of the curves of activation enthalpy, free enthalpy and change of entropy correspond to the usual form for solutions of electrolytes, especially in the case of KCl [19] but in the case of NaCl entropy of activation increases with the increase in concentration of electrolytes which indicates the relatively significant energetic effect in comparison with the geometric effect of the structure of liquid. This is in agreement with the hypothesis implied to hydrated or nonhydrated

Na^+ in hydrodynamic block of polymer stated in the previous study,[1] which confirms the wedge effect of Na^+ between these hydrodynamic blocks through the values of thermodynamic quantities $\Delta H^{\ddagger}_{\eta}$ and $\Delta G^{\ddagger}_{\eta}$.

One more aspect of interaction of particles in liquid solution corresponds to the modification of intrinsic viscosity defined by

$$[\eta] = \lim_{C\to 0} \frac{\eta - \eta_0}{\eta_0 C} = \lim_{C\to 0} \frac{\eta_{sp.}}{C}$$

where C is the concentration of polymer, η and η_0 are the viscosities of solutions of electrolytes with and without polymer respectively. Huggins defined the reduced viscosity as

$$\eta_{red.} = \frac{\eta_{sp.}}{C} = [\eta] + K[\eta]^2 C + \dots$$

where K is a constant which measures the hydrodynamic interaction in solution. Figure 7 representing the variation of $\frac{\eta_{sp.}}{C}$ with the concentration of electrolytes, leads to an analogous conclusion as indicated in the previous study.[1] In general, the value of $[\eta]$ decreases with the increase of concentration of electrolytes. At a higher temperature the decrease of $[\eta]$ is more influenced by KCl than by NaCl. The intrinsic viscosity also decreases with the increase of temperature and with the decrease of molecular weight of PVA.

The decrease of intrinsic viscosity due to the presence of electrolytes can be explained by the decrease of hydrodynamic radius 'r' of macromolecules according to the well known equation :

$$[\eta] = \text{Ø}(\bar{r}^2)^{3/2}/M,$$

where Ø is the Flory constant for solvent and M is the molecular weight of macromolecules. This relation shows the possibilities of crowdness of chains in macromolecules. This crowdness is more in the case of Na^+ for which the intensive hydration decreases the intensity of electric ionic field. In the case of K^+, the hydration is less at temperatures higher than 20°–30°C.

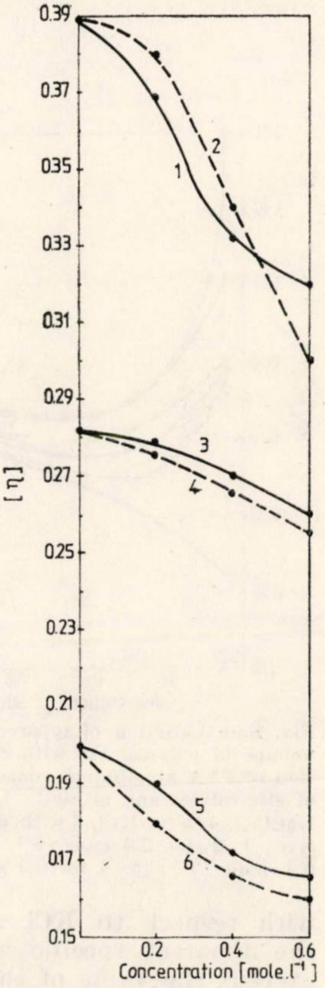

Fig. 7. — Variation of $[\eta]$ with concentration of electrolytes at different temperatures : 1, 3, 5 for NaCl ; 2, 4, 6 for KCl ; 1, 2 for 20°C ; 3, 4 for 30°C ; 5, 6 for 40°C.

Other aspects of interaction between the particle in aqueous solutions of electrolytes and PVA can be explained by the change of apparent specific volume of polymer in solution with the change of concentration of electrolytes and temperature. By definition, the apparent specific volume is expressed as

$$\varphi = \frac{1}{\rho_0}\left[1 + \frac{\rho_0 - \rho}{C}\right],$$

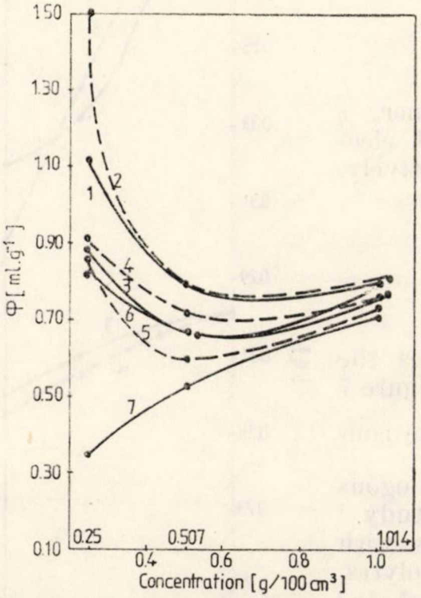

Fig. 8. — Variation of apparent specific volume of polymer (φ) with concentration of PVA at different concentrations of electrolytes and at 20°C : 1, 6, 7 for NaCl ; 2, 4, 5 for KCl, 3 without electrolyte ; 1, 2 for 0.6 mole · l^{-1} ; 4, 6 for 0.4 mole · l^{-1} ; 5, 7 for 0.2 mole · l^{-1}.

where ρ and ρ_0 are the densities of the solutions of electrolytes with polymer and without polymer respectively and C is the concentration of PVA. The results calculated from the experimentally determined densities of solutions are shown in figure 8. An examination of the results presented in figure 8 indicates that in the case of KCl the value of φ increases with the increase in concentration of KCl. In the case of NaCl the value of φ also increases with the concentration of NaCl but less remarkable than KCl. The form of the curves is a little different in the case of NaCl than in the case of KCl. With a concentration $m < 0.4$ mol./L of NaCl, the apparent specific volume of PVA is smaller than that of PVA solution with zero concentration of electrolytes, but with a higher concentration of NaCl this value exceeds the value of PVA solution.

With the increase of temperature the effect of electrolytes decreases remarkably the φvs C curves approach to each other keeping a reverse order with respect to KCl and NaCl. At temperatures around 30°—40°C the apparent specific volume of polymer in solution of polymer only exceeds the value of that in solution containing electrolytes. It is also observed from figure 8 that with the increase of concentration of PVA, the value of φ tends towards a common limiting value through the formation of H_2O-PVA linkage for both the electrolytes.

The increase of the molecular weight of polymer has the effect of increasing φ, appearance of a minimum value of φ at 30°—40°C and also a common limiting value of φ in the presence of electrolytes at higher concentration of PVA. The apparent specific volume of polymer in aqueous solution increases with the increase of temperature and molecular weight of polymer. A general tendency is observed to reach a limiting value with the increase of concentration of PVA which corresponds to the formation of a limiting structure of the solution by increasing the number of H_2O-PVA cluster or by the formation of hydrogen bonds or hydrophobic linkages. Surely, the presence of a nonelectrolyte having a disordering effect shows opposite results, e.g. dioxane.[20]

A complete theory of coefficient 'B' is not known, but in keeping with the classical theory of Einstein for big molecules the 'B' coefficient undoubtedly results from the interaction of solvent and dissolved solutes which modifies the structure of the medium and also from the share of their own volume. An activated complex theory applied to the viscosity of electrolytes in water and extended to the solute of electrolytes and nonelectrolytes by Feakins, Freemantle and Lawrence[6] has shown that the value of coefficient 'B' can be represented mathematically by

$$B = \lim_{C\to 0} \frac{\eta_{rel} - 1 - A\sqrt{C}}{C}, \quad \text{where } \eta_{rel.} = \frac{\eta}{\eta_0}$$

hence by analogy it corresponds to the usual intrinsic viscosity of solutions as shown before.

Thus by using relations:

$$\ln \eta_{rel.} = \ln \frac{V_0}{V} \exp\left(\frac{\Delta G_1^{\ddagger} - \Delta G_0^{\ddagger}}{RT}\right)$$

with $\Delta G^{\ddagger} = x_0 \Delta\mu_0^{\ddagger} + x_1 \Delta\mu_1^{\ddagger}$ and for dilute solution

$$\Delta G^{\ddagger} = x_1 \Delta\mu_1^{0\ddagger} + (1 - x_1)\Delta\mu_0^{0\ddagger}$$

or $\Delta G - \Delta G_0 = x_1\ (\Delta\mu_1^{0\ddagger} - \Delta\mu_0^{0\ddagger})$, the difference between the free enthalpy of activation for the transfer of one mole of solution having the concentration C and for one mole of solvent can be represented by

$$x_1 (\Delta\mu_1^{0\ddagger} - \Delta\mu_0^{0\ddagger} = RT \ln \frac{(1 + BC)}{V_0}\ V, \quad \text{where } x \text{ is the}$$

mole fraction, $\Delta\mu^{0\ddagger}$ is the chemical potential contributed by two components: solvent and dissolved solute, V is the molar volume of the solution and V_0 is that of solvent at the working temperature. This equation also represents the effect of displacing x mole of solvent by x_1 mole of solute showing the contribution of both the substances on the free enthalpy of activation, which actually shows the relation existing between coefficient B of transport phenomena and the state of dissolved substances. Experimentally determined values of $\Delta\mu_1^{0\ddagger} - \Delta\mu_0^{0\ddagger}$ for solutions under study are given in table 1.

An examination of the data presented in table 1 indicates that the value of $\Delta\mu_1^{0\ddagger} - \Delta\mu_0^{0\ddagger}$ (positive for a solution with NaCl and negative for a solution with KCl) decreases with the increase of concentration of electrolytes, in the case of a solution of electrolytes on pure water. For a solution PVA with KCl a decreasing tendency is observed with the increase of the concentration of both PVA and KCl, but for a solution of

Table 1

$\Delta\mu_1^{0\ddagger} - \Delta\mu_0^{0\ddagger}$ for different solutions under study at 20°, 30° and 40°C

Conc. of PVA (g./100 cm³)	Conc. of electrolytes (mol./L)	$\Delta\mu_1^{0\ddagger} - \Delta\mu_0^{0\ddagger}$ (cal. mol^{-1}		
		20°C	30°C	40°C
0	0.2 NaCl	3600	1700	1500
	0.4 NaCl	3400	1540	1360
	0.6 NaCl	3420	1500	1350
	0.2 KCl	−240	20	50
	0.4 KCl	−240	50	480
	0.6 KCl	−280	−4	440
0.25	0.2 NaCl	2350	830	580
	0.4 NaCl	2400	940	640
	0.6 NaCl	2420	1020	710
	0.2 KCl	−1100	−470	30
	0.4 KCl	−1160	−350	40
	0.6 KCl	−1180	−270	90
0.507	0.2 NaCl	1360	580	150
	0.4 NaCl	1300	530	100
	0.6 NaCl	1410	610	160
	0.2 KCl	−1560	−630	−230
	0.4 KCl	−1650	−650	−240
	0.6 KCl	−1700	−650	−220
1.014	0.2 NaCl	480	290	30
	0.4 NaCl	410	300	20
	0.6 NaCl	520	330	10
	0.2 KCl	−2110	−1110	−500
	0.4 KCl	−2150	−1055	−470
	0.6 KCl	−2260	−1120	−490

PVA with NaCl the value $\Delta\mu_1^{0\ddagger} - \Delta\mu_0^{0\ddagger}$ (positive) decreases with the increase of concentration of PVA and increases relatively little with increase of concentration of NaCl containing the same amount of PVA. Increasing temperature has the effect of decreasing the value of $\Delta\mu_1^{0\ddagger} - \Delta\mu_0^{0\ddagger}$ for a solution with NaCl but for a solution with KCl it increases towards zero with the increase of temperature. The variation of B with temperature is a measure of difference between enthalpy of activation of the process indicated. It is observed that the negative or positive value of B corresponds to the conditions $\Delta\mu_1^{0\ddagger} < \mu_0^{0\ddagger}$ for KCl and $\Delta\mu_1^{0\ddagger} > \Delta\mu_0^{0\ddagger}$ for NaCl and it measures the tendency of ions to attract and orientation of polar molecules. It is seen that in the solution structured by PVA these effects decrease more and more (the difference decreases) in the case of NaCl. The increase of temperature also decreases the differences to near about zero by annihilation of the specific efects of ions.

CONCLUSIONS

Experimental data presented in this study are a sequel and completion of a previous work.[1] The validity of Jones-Dole equation for solutions of NaCl, KCl and PVA was verified. Effects of temperature corresponding to the annihilation of the formation of structure of solvent are represented by the tendency of decreasing the coefficient of interaction *B*. Thermodynamic quantities of activation of flow phenomena show a strong interaction between Na^+ and solvent (water or polyvinyl alcohol); the value of these thermodynamic quantities increases with the increase of concentration of NaCl, concentration of PVA and with the molecular weight of dissolved polymer.

Efects on structure formation also result from the study of the variation of apparent specific volume and from the values of intrinsic viscosity.

The value of coefficient *B* provided the possibility for calculation of the difference of free enthalpy of activation at the transfer of dissolved solute – solvent, the magnitude of which confirms the effect of orientation in solvent, in solution of NaCl in water and also in solution of PVA in comparison with the solution of KCl.

REFERENCES

[1] C. Hölszky, C. Suciu and D. Săndulescu, *Rev. Roumaine Chim.*, **19**, 887 (1974).

[2] R. Stokes and R. Mills, "Viscosity of Electrolytes and Related Properties", Pergamon Press, New York, 1971.

[3] I. Padova, "Modern Aspects of Electrochemistry", vol. 7, Ed. B. Conway, I.O.M. Bokris, Butterworths, London, 1972.

[4] M. Palma and J. Morel, *Canad. J. Chem.*, **55**, 1521 (1977).

[5] D. Feakins and K. Lawrence, *J. Chem. Soc.*, **1966**, 212 A; **1966**, 212.

[6] D. Feakins, D. Freemantle and K. Lawrence, *J. Chem. Soc., Faraday Trans.*, **70**, 795 (1974).

[7] M. Hugue, Ph. D. Thesis, Inst. of Petroleum and Gas, Ploiești, 1982.

[8] A. Beresnewicz, *J. Polymer. Sci.*, **35**, 321 (1959).

[9] R. Robinson and R. Stokes, "Electrolytes Solutions", 2nd edition Butterworths, London, 1959.

[10] D. Goldsack and R. Francetto, *Canad. J. Chem.*, **55**, 1062 (1977).

[11] M. Kaminsky, *Discuss. Faraday Soc.*, **24**, 171 (1957).

[12] R. Gurney, "Ionic Process in Solution", Mc. Graw Hill, New York, 1953.

[13] H. Frank and M. Evans, *J. Chem. Phys.*, **13**, 507 (1948).

[14] H. Frank and W. Wen, *Discuss. Faraday Soc.*, **24**, 133 (1957).

[15] H. Morawetz, "Macromolecules in Solutions", Wiley, New York, 1975.

[16] F. Ratkovics, T. Salamon and L. Domonkos, *Acta Chim. Acad. Sci. Hung*, **4**, 313 (1981).

[17] E. Nightingale, Jr., In "Chemical Physics of Ionic Solutions", Edited by B. Conway, R. Barradas, Wiley, New York, 1966.

[18] S. Glasstone, K. Laider and H. Eyring, "Theory of Rate Processes", Mc. Graw Hill, New York, 1941.

[19] W. Good, *Electrochimica Acta*, **9**, 203 (1964).

[20] B. Oliver and A. Campbell, *Canad. J. Chem.*, **47**, 4207 (1969).

CONCLUSIONS

Experimental data presented in this study are a sequel and completion of a previous work.[8] The validity of Jones-Dole equation for solutions of NaCl, KCl and PVA was verified. Effects of temperature corresponding to the annihilation of the formation of structure of solvent are represented by the tendency of decreasing the coefficient of interaction B. Thermodynamic quantities of activation of flow phenomena show a strong interaction between Na+ and solvent (water or polyvinyl alcohol); the value of these thermodynamic quantities increases with the increase in concentration of NaCl, concentration of PVA and with the molecular weight of dissolved polymer.

Effects on structure formation also result from the study of the variation of apparent specific volume and from the values of intrinsic viscosity.

The value of coefficient B provided the possibility for calculation of the difference of free enthalpy of activation at the transfer of dissolved solute → solvent, the magnitude of which confirms the effect of orientation in solvent, in solution of NaCl in water and also in solution of PVA in comparison with the solution of KCl.

REFERENCES

[1] [illegible] G. Stein and [illegible], [illegible] Chem. 13, [illegible] (1974).
[2] [illegible] and R. Mills, "Viscosity of Electrolytes and Related Properties", Pergamon Press, New York, [illegible].
[3] [illegible], "[illegible] Aspects of [illegible]", vol. 7, Ed. [illegible], Butterworths, London, [illegible].
[4] [illegible] and [illegible], J. [illegible], 53, [illegible].
[5] D. Feakins and K. G. Lawrence, J. Chem. Soc. 1966, 212 A.
[6] D. Feakins, D. Freemantle and K. G. Lawrence, J. Chem. Soc. Faraday Trans. I, 70, 795 (1974).
[7] [illegible], Ph. D. Thesis, [illegible], 1968.
[8] [illegible], [illegible] 33, [illegible].
[9] R. A. Robinson and R. H. Stokes, "Electrolyte Solutions", 2nd edition, Butterworths, London, [illegible].
[10] [illegible] and [illegible], [illegible] Chim. 25, 1067 ([illegible]).
[11] M. Kaminsky, Discuss. Faraday Soc. 24, 171 (1957).
[12] [illegible], "Water [illegible]", Plenum Press, New York, 1972.
[13] H. S. Frank and M. G. Evans, J. Chem. Phys. 13, 507 (1945).
[14] H. S. Frank and W. Y. Wen, Discuss. Faraday Soc. 24, 133 (1957).
[15] R. A. Horne, "Water and aqueous solutions", Wiley, New York, 1972.
[16] [illegible], [illegible].
[17] [illegible], in "[illegible]", Edited by [illegible], Wiley, New York, [illegible].
[18] S. Glasstone, K. J. Laidler and H. Eyring, "Theory of Rate Processes", Mc Graw Hill, New York, 1941.
[19] W. [illegible], [illegible].
[20] [illegible] and A. [illegible], J. [illegible] Chem. [illegible].

Revue Roumaine de Chimie, **29**, *1*, 67–75(1984)

CONSIDERATIONS ON THE EQUILIBRIUM STATE OF METAL/OXIDE ELECTROLYTE SYSTEM

C. LUCA,[a] G. SEMENESCU[b] and A. ANDREI[b]
[a]Central Institute of Chemistry, Department of Physical Chemistry, Splaiul Independenţei 202, Bucharest, Romania
[b]Institute for Nuclear Power Reactors, Piteşti, Romania

Received December 1, 1983

The thermodynamic equilibrium at solid/electrolyte interface was studied in the complex metal/oxide/electrolyte system. A "transition layer model" is advanced which accounts for the Nernstian behaviour of some systems, including the insoluble oxide/electrolyte interface.

GLOSSARY OF SYMBOLS:

D^- — donor ionic species;
$\mathscr{A}$ — acceptor active site;
A^+ — acceptor ionic species;
$\mathscr{D}$ — donor active site;
t — subscript which identifies a species belonging to a "transition layer";
K_{a1}, K_{a2} — anodic rate constants for reactions 1 and 2, respectively;
K_{c1}, K_{c2} — cathodic rate constants for reactions 1 and 2, respectively;
$\Gamma(D_t^*)$ — surface concentrations of D^* species in adsorbed state;
Γ_{sd} — surface concentration of active sites $\mathscr{D}$ for donor species;
$\Gamma(A_t^*)$ — surface concentration of A^* species in adsorbed state;
Γ_{sa} — surface concentration of active sites $\mathscr{A}$ for acceptor species;
Γ_{SD} — saturated surface concentration for D species in adsorbed state;
Γ_{SA} — saturated surface concentration for A species in adsorbed state;

$$\alpha = \frac{1}{2}\frac{F}{RT}$$

$\varphi = \varphi_t - \varphi_e$ — inner potential difference between transition layer and electrolyte;
a_{D^-} — donor species activity in electrolyte;
a_{A^+} — acceptor species activity in electrolyte;

i_a — net current density associated with charge transfer reaction of A^+ species ;
i_d — net current density associated with charge transfer reaction of D^- species ;
m — subscript which identifies a species belonging to oxide/ metal interfacial region ;

INTRODUCTION

To understand corrosion of metals in aqueous media, one has to know what phenomena occur at the interface with the electrolyte. Most papers deal with solid/ electrolyte interface [1] of metal/ oxide/ electrolyte type. [2]

Although the studies on solid electrolyte interface supply a great deal of thermodynamic and electrochemical data on the interface they give no information regarding its structure. [2]

The classical approach of solid/ electrolyte interface requires the thermodynamic characterization of the interface and its response to removal from equilibrium state as measured by current, charge and potential measurements. The difficulty with these electrochemical methods is that despite good sensitivity they lack sufficient molecular specificity. [3] These methods do not reveal the site where a particular species can be adsorbed, the nature of the interactions with the substrate and not even the charge of the adsorbed species.

The electrosorption of species on electrode surface is frequently followed by chemical changes of these species whose nature cannot be revealed by electrochemical methods alone. [3]

The knowledge about absorption is still empirical [4] both for liquid and solid electrodes.

Parsons [4] showed that theoretical studies on the equations of state for adsorbed monolayer and the effect of the change of the electrical state are required in order to understand the differences between adsorption on surface of different structures.

The electrochemist is most interested in information on gas-solid interface including the energetics of adsorption, the type of adsorption sites, the configuration, electronic and vibrational properties of adsorbed species, the modification of adsorbate following adsorption. [5]

Most electrochemists specialized in electrocatalysis are interested in literature on solid/ gas interface and their interest will certainly increase. [5]

The techniques that surface science has developed recently allow the experimental and theoretical study of adsorption and catalysis. [6]

Elaboration of an electronic science of chemosorption is a very active frontier of surface physics. It involves various electronic spectroscopic measurements and the electronic theories of surface ; the latter tend towards unification of the extended wave and many body viewpoints of solid-state physics with the local molecular orbital approach of quantum chemistry. [6]

In expectation of the development of new techniques that would allow one to acquire direct information on the structure of surface, the theory can do no better than issue adquate theoretical approaches which do not conflict with the experimental data. [2]

Rechnitz [7] has shown that the advancement of science is limited not only by the inflow of new ideas but by the development of new experimental techniques as well.

The mechanisms have to be regarded as hypotheses subjected to continuous adjusting and refining; they are not sought for the sake of personal enjoyment but because they guide and organize ideas, evidence the fruitful areas of practical research that empirical research lacks and mostly rationalize and systematize observations into a coherent point of view. [7]

CONSIDERATIONS ON MECHANISTIC ASPECTS OF SOLID/ELECTROLYTE INTERFACE

The semiconductor character of nonstoichiometric oxides is well known. The detailed nature of the compact inner Helmholtz layer between the electrode and electrolyte is poorly understood both for semiconductors and metals. [8]

Some difficulties arise in connection with the explanation of Nernstian behaviour in some interfaces with the generally accepted ion — exchange mechanism. [7] In ref. 2 the interfacial system AgI/ electrolyte is examined first, then the oxide/ electrolyte interfacial system compared with it, for both slightly soluble and essentially insoluble oxide. Rechnitz [7] showed that for AgI/ electrolyte system, the ion exchange equilibrium is doubtful.

The present contribution introduces a "transition layer" model which accounts for the distinct behaviour of various interfacial systems (including insoluble oxide/electrolyte).

THE "TRANSITION LAYER" MODEL

Owing to the specific chemical short range interactions at solid/ electrolyte interface, reversible specific adsorption can occur in some ionic species from the bulk of electrolyte.

Depending on the donor or acceptor character of active surface sites, on the strength of specific interactions, homogeneous or heterogeneous character of solid phase at interface, anion — cation or mixed — selective Nernstian or non-Nernstian behaviour is possible.

The model considers a "transition layer" including Helmholtz inner plane and adjacent solid phase layer. Reversibly adsorbed species in transition layer participate in electron exchange.

For simplicity, we consider monoelectronic exchange and concentrated solution, so that the Gouy-Chapman diffuse double layer is negligible.

In open circuit, the algebraic sum of currents associated with charge exchange reactions at interface is zero. When thermodynamic equilibrium is not attained many exchange reactions are simultaneously possible at interface, among which at least one is anodic and one cathodic so that the open circuit condition is satisfied.

For simplicity we consider only an electronation and a deelectronation reaction at interface :

$$\begin{array}{c} \mathrm{D}^- \rightleftharpoons \mathrm{D}_t^* + \mathrm{e}^- \\ \mathscr{A} + \mathrm{D}_t^* \rightleftharpoons (\mathscr{A}\mathrm{D}_t)^* \\ \hline \mathrm{D}^- + \mathscr{A} \overset{K_{a1}}{\underset{K_{c1}}{\rightleftharpoons}} (\mathscr{A}\mathrm{D}_t)^* + \mathrm{e}^- \end{array} \tag{1}$$

$$\begin{array}{c} \mathrm{A}^+ + \mathrm{e} \rightleftharpoons \mathrm{A}_t^* \\ \mathrm{A}_t^* + \mathscr{D} \rightleftharpoons (\mathscr{D}\mathrm{A}_t)^* \\ \hline \mathrm{A}^+ + \mathscr{D} + \mathrm{e}^- \overset{K_{c2}}{\underset{K_{a2}}{\rightleftharpoons}} (\mathscr{D}\mathrm{A}_t)^* \end{array} \tag{2}$$

In this case :

$$\frac{\mathrm{d}\Gamma(\mathrm{D}_t^*)}{\mathrm{d}t} = K_{a_1} \exp\left(-\beta_1 \frac{\Gamma_{sd}}{\Gamma_{SD} - \Gamma(\mathrm{D}_t^*)}\right) a_{\mathrm{D}^-} e^{\alpha\varphi} [\Gamma_{sd} - \Gamma(\mathrm{D}_t^*)] - K_{c1} e^{-\alpha\varphi} \Gamma(\mathrm{D}_t^*) \tag{3}$$

$$\frac{\mathrm{d}\Gamma(\mathrm{A}_t^*)}{\mathrm{d}t} = K_{c2} \exp\left(-\beta_2 \frac{\Gamma_{sa}}{\Gamma_{SA} - \Gamma(\mathrm{A}_t^*)}\right) a_{\mathrm{A}^+} e^{-\alpha\varphi} [\Gamma_{sa} - \Gamma(\mathrm{A}_t^*)] - K_{a_2} e^{-\alpha\varphi} \Gamma(\mathrm{A}_t^*) \tag{4}$$

Eqs (3) and (4) which describe adsorption kinetics are of bimolecular type.

Factors $\exp\left(-\beta_1 \frac{\Gamma_{sd}}{\Gamma_{SD} - \Gamma(\mathrm{D}_t^*)}\right)$ and $\exp\left(-\beta_2 \frac{\Gamma_{sa}}{\Gamma_{SA} - \Gamma(\mathrm{A}_t^*)}\right)$ are introduced to take account of the interactions between the species adsorbed.

Regarding the sign of the current, we adopt the following convention : when there is a net flow of electrons from the solution to the solid, the current is taken as positive. Thus :

$$i_d = F\,\mathrm{d}\Gamma(\mathrm{D}_t^*)/\mathrm{d}t \tag{5}$$

$$i_a = -F\,\mathrm{d}\Gamma(\mathrm{A}_t^*)/\mathrm{d}t \tag{6}$$

Owing to the double layer charging, the inner potential difference between the electrode and the electrolyte changes :

$$\mathrm{d}\varphi/\mathrm{d}t = (i_d + i_a)/c \tag{7}$$

At fixed a_{A^+} and a_{D^-} values, φ reaches a steady state value $\overline{\varphi}$, when $\mathrm{d}\varphi/\mathrm{d}t = 0$.

Then, according to (7), the open circuit condition is satisfied:

$$i_d + i_a = 0 \tag{8}$$

According to eqs. (3)–(8) it results

$$\varphi = \frac{1}{2\alpha} \ln \frac{K_{c1}\overline{\Gamma}(D_t^*) + K_{c2}[\Gamma_{sa} - \overline{\Gamma}(A_t^*)] \exp[-\beta_2 \Gamma_{sa}/(\Gamma_{SA} - \overline{\Gamma}(A_t^*) a_{A^+}}{K_{a2}\overline{\Gamma}(A_t^*) + K_{a1}[\Gamma_{sd} - \overline{\Gamma}(D_t^*)] \exp[-\beta_1 \Gamma_{sd}/(\Gamma_{SD} - \overline{\Gamma}(D_t^*) a_{D^-}} \tag{9}$$

where $\overline{\Gamma}(D_t^*)$ and $\overline{\Gamma}(A_t^*)$ are steady state values.

The steady state is characterized by the "mixed steady state" value $\overline{\varphi}$.

We consider the interfaces with $\Gamma_{sa} = 0$. In this case $\Gamma(A_t^*) = 0$ and at the interface only reaction (1) occurs. According to (3) and (8) it results that $d\Gamma(D_t^*)/dt = 0$; hence we may conclude that the adsorption isotherm can be written as:

$$\frac{\Gamma(D_t^*)}{\Gamma_{sd} - \Gamma(D_t^*)} \exp(\beta_1 \Gamma_{sd}/[\Gamma_{SD} - \Gamma(D_t^*)]) = \mathscr{B} a_{D^-} \tag{10}$$

where $\mathscr{B} = \exp(-\Delta G_1/RT)$ and ΔG_1 is the standard free energy of adsorption.

In the activity range of donor species there is a value $a_{D^-} = a^{\circ}_{D^-}$ beginning with which $\overline{\Gamma}(D_t^*)$ reaches a near saturation value (Fig. 1):

$$\overline{\Gamma}(D_t^*) = \gamma \Gamma_{SD} \text{ where } \Gamma_{SD} \leqslant \Gamma_{sd} \text{ and } \gamma < 1.$$

For $a_{D^-} > a^{\circ}_{D^-}$ the dependence of $\overline{\Gamma}(D_t^*)$ on a_{D^-} can be considered negligible.

According to eq. (9) it results:

$$\overline{\varphi} = \frac{1}{2\alpha} \ln \frac{K_{c1}\gamma\Gamma_{SD}}{K_{a1}[\Gamma_{sd} - \gamma\Gamma_{SD}] \exp\left(\dfrac{-\beta_1\Gamma_{sd}}{\Gamma_{SD}(1-\gamma)}\right) a_{D^-}} = C - \frac{RT}{F} \ln a_{D^-} \tag{11}$$

$$C = \frac{RT}{F}\left\{\ln\frac{K_{c1}}{K_{a1}} + \ln\left[\frac{\gamma\Gamma_{SD}}{\Gamma_{SD} - \gamma\Gamma_{SD}} \exp\left(\frac{\beta_1\Gamma_{sd}}{\Gamma_{SD}(1-\gamma)}\right)\right]\right\} =$$

$$= \Delta G_1/F + \frac{RT}{F} \ln f(\gamma\Gamma_{SD}) \tag{12}$$

For activities $a_{D^-} > a^{\circ}_{D^-}$ the interface exhibits an anion selective Nernstian behaviour. When a_{D^-} increases from $a^{\circ}_{D^-}$ to the maximum attainable value ($10^{-7} - 1$ M) the β_1 exponent is so that γ approximately does not change.

Similarly, for $\Gamma_{sa} = 0$ which implies $\Gamma(D_t^*) = 0$ throughout the activity range $a_{A^+} > a^{\circ}_{A^+}$, $\Gamma(A_t^*)$ is not a function of activity and a cation — selective Nernstian behaviour results.

Considering reaction (1), the anion — selective Nernstian behaviour can be deduced by equating the electrochemical potentials of the species involved:

$$\mu_{(\mathscr{A})} + \bar{\mu}_{(D^-)} + \mu_{(AD_t^*)} = \bar{\mu}_{(e)} \tag{13}$$

Taking into account that:

$$\mu_{(\mathscr{A})} = \mu^{\circ}_{(\mathscr{A})} \tag{14}$$

$$\bar{\mu}_{(e)} = -F\varphi_t \tag{15}$$

$$\mu_{(AD_t)^*} = \mu^0_{(AD_t)^*} + RT \ln f\,[\Gamma(D_t^*)] \tag{16}$$

where $f\,[\Gamma(D_t^*)]$ is a function of surface concentration which represents just the adsorbate activity:

$$\mu_{(D^-)} = \mu^0_{(D^-)} + RT \ln a_{D^-} - F\varphi e \tag{17}$$

It results:

$$\varphi = \varphi_t - \varphi_e = C - \frac{RT}{F} \ln a_{D^-} \tag{18}$$

where:

$$C = \frac{\mu^0_{(AD_t)^*} - \mu^0_{(\mathscr{A})} - \mu^0_{(D^-)} + RT \ln f[\Gamma(D_t^*)]}{F} = \Delta G_1/F + RT/F \ln f[\Gamma(D_t^*)] \tag{19}$$

It is necessary that $\bar{\Gamma}(D_t^*)$ be not a function of a_{D^-} which is possible if $\bar{\Gamma}(D_t^*)$ reaches the saturation value:

$$\bar{\Gamma}(D_t^*) = \gamma\Gamma_{SD}$$

Similarly, when at interface only reaction (2) occurs, $\bar{\Gamma}(A_t^*)$ is not a function of a_{A^+} which is possible when $\Gamma(A_t^*)$ reaches saturation; one has to do with the cation — selective Nernstian behaviour.

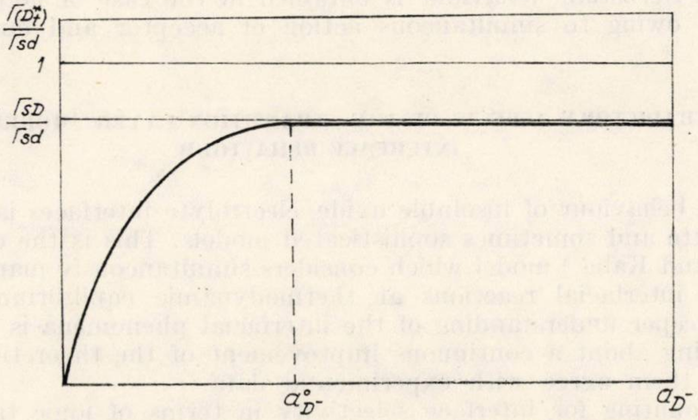

Fig. 1. — Adsorption isotherm $\overline{\Gamma}(D_t^*)/\Gamma_{\text{sd}} = f(a_{\text{D}^-})$.

TRANSITION LAYER MODEL FOR INSOLUBLE OXIDE/ ELECTROLYTE INTERFACE

In the case of insoluble oxide (MO)/ electrolyte interface, the pH — selective Nernstian behaviour can be explained by means of the "transition layer" model admitting the following electron exchange mechanism :

1. In basic medium :

$$(\text{OH}^-) \rightleftharpoons (\text{OH})_t^* + e^-$$

$$(\text{OH})_t^* + \text{MO} \rightleftharpoons (\text{HO} \ldots \text{MO})_t^*$$

$$(\text{HO} \ldots \text{MO})_t^* + (\text{HO} \ldots \text{MO})_t^* \rightleftharpoons (\text{MO} \ldots \text{O} \ldots \text{OM})_t^* + \text{H}_2\text{O}$$

$$(\text{MO} \ldots \text{O} \ldots \text{OM})_t^* \rightleftharpoons 2\text{MO} + \text{O}_t^*$$

$$\text{O}_t^* \rightleftharpoons (\text{O}_t^*)_\text{m}$$

$$\text{M} + (\text{O}_t^*)_\text{m} \rightleftharpoons \text{MO}$$

Equating the electrochemical potentials of the species involved in the reversible reaction mentioned above, one obtains the pH — selective Nernstian behaviour as in the case of anion-selective interface.

2. In acid medium :

$$\text{H}^+ + e^- \rightleftharpoons \text{H}_t^*$$

$$\text{MO} + \text{H}_t^* \rightleftharpoons (\text{MO} \ldots \text{H})_t^*$$

$$(\text{MO} \ldots \text{H})_t^* + (\text{MO} \ldots \text{H})_t^* \rightleftharpoons (\text{M} \ldots \text{O} \ldots \text{M})_t^* + \text{H}_2\text{O}$$

$$(\text{M} \ldots \text{O} \ldots \text{M})_t^* \rightleftharpoons \text{M}_t^* + \text{MO}$$

$$\text{M}_t^* \rightleftharpoons (\text{M}_t)_\text{m}$$

According to these reactions, as in the cation — selective interface case, H⁺ — selective Nernstian behaviour results.

Non-Nernstian behaviour is obtained in the case of heterogeneous interfaces owing to simultaneous action of acceptor and donor active sites.

CONTRADICTORY ASPECTS OF THE "TRANSITION LAYER" MODEL OF INTERFACE BEHAVIOUR

The behaviour of insoluble oxide/electrolyte interfaces is explained by intricate and sometimes sophisticated models. This is the case of the Dignam and Kalia [2] model which considers simultaneously many electron exchange interfacial reactions at thermodynamic equilibrium.

A deeper understanding of the interfacial phenomena is needed; it would bring about a continuous improvement of the theoretical models to make them agree with experimental data.

Accounting for interface selectivity in terms of ionic transport is sometimes difficult. Thus, according to Rechnitz [7] it is difficult to explain the Nernstian behaviour and the selectivity of platinum wire on which a "liquid membrane" is deposited with some intermediate binder. The question arises: what process in the covering liquid may cause variations of potential in the electron-conducting wire?

The ion exchange mechanism leaves also unexplained the behaviour of glass electrode. Whenever the internal solution and the reference element of the glass electrode are replaced with liquid mercury, or platinum is deposited in vacuum on the inner surface of glass, the system continues to be pH-selective.

There must be an explanation of the coupling between the cation transport through a glass membrane and the electron conduction in the metal.

Radioactive tracer experiments (making use of tritium [7]) have shown that the H^+ ion is not carried through a membrane even at high temperature and voltage.

Rechnitz [7] has also revealed many other experimental data that contradict the theory of ionic exchange equilibrium.

The "transition layer" model allows one to explain the selective behaviour of interfaces taking into account the determining part played by the adsorption phenomena that originate in the chemical affinity of the ionic species in the electrolyte against the surface active sites of the interfaces.

The mechanism advanced here suggests that for insoluble oxide/electrolyte interface, the glass electrodes whose apparent detection limit lies at 10^{-14} M H^+ works reversibly in turn for H^+ (in acid medium) and OH^- (in basic medium).

CONCLUSIONS

The "transition layer" model is presented; it explains to a large extent the distinct behaviour of anion-, cation- and mixed-selective interfaces.

The model employs electron transfer electrochemical reactions, in which the selective adsorption is determining.

The Nernstian behaviour of interfaces is not conditioned by the simultaneous presence of ionic species involved in the solid and the electrolyte (as in the mechanism based on ionic exchange equilibrium).

The "transition layer" model allows the unitary treatment of solid/ electrolyte interface.

A treatment of oxide/ electrolyte interfaces at thermodynamic non-equilibrium by means of "transition layer" model yields a qualitative study of the growth and dissolution of oxide films which applies to evaluation of metal corrosion. This aspect will make the object of a future study.

REFERENCES

[1] J. O' M. Bockris, "Modern Electrochemistry", Plenum Press, New York, 1970.
[2] M. J. Dignam, R. K. Kalia, *Surf. Sci.*, **100**, 154 (1980).
[3] E. Yeager, *Surf. Sci.*, **101**, 1 (1980)
[4] R. Parsone, *Surf. Sci.*, **101**, 316 (1980).
[5] C. D. Duke, *Surf. Sci.*, **101**, 624 (1980).
[6] T. E. Fischer, "CRC Critical Reviews in Solid State Sciences", **401** (1976).
[7] G. A. Rechnitz, "Mechanistic aspects of ion — selective membrane electrodes", paper presented at the International Symposium on Selective Ion — Sensitive Electrodes, held at Cardiff, U.K. 9—12, April, 1973.
[8] R. H. Wilson, "CRC Critical Reviews in Solid State and Materials Sciences", **10**, 1 (1980).
[9] C. Luca, G. Semenescu, *Rev. Chim. București*, **11**, 946 (1975).
[10] G. Semenescu, *Rev. Chim. București*, **32**, 170 (1982).

Revue Roumaine de Chimie, **29**, *1*, 77–82 (1984)

MATRIX POLYMERIZATION IN THE PRESENCE OF UREA

CR. I. SIMIONESCU and MARIANA BEZDADEA
Polytechnic Institute, Iassy, Splai Bahlui 71,
Romania, 6600

Received January 21, 1983
Revised October 10, 1983

The polymerization conditions of vinyl acetate have been studied in the presence of urea by using UV and γ radiations as well as ultrasound. We also investigated the synthesis of polyacrolein by UV radiation.

INTRODUCTION

In 1965 Clasen reported the polymerization of some monomers included in the thiourea channels. In this way he obtained macromolecular compounds with regular structure by radicalic polymerization using γ irradiation of butadiene, acrylonitrile, vinyl chloride, vinylidene chloride, cyclohexadiene and so on (75 monomers in all).[1]

The subsequent studies have shown that 2,3-dimethylbutadiene, butadiene, 2,3-dichlorobutadiene as well as 1,3-cyclohexadiene led in these conditions to 1,4-crystalline polymers.[2]

The present paper reports on the investigation of matrix polymerization of *vinyl acetate* (*VAc*) and *acrolein* in the presence of urea.

EXPERIMENTAL

The monomers were distilled under vacuum and used directly. The urea, purified by repeated recrystallizations from water and ethanol, was activated by addition of freshly distilled methanol (the weight ratio urea to methanol being 1 g/0.05 ml). The mixture urea-methanol was cooled within the temperature range −30 to − 70°C. Then *VAc* was added, cooled at the same temperatures.

Initiation of *VAc* polymerization reaction was carried out by UV and γ radiations as well as ultrasound waves.

The photopolymerizations were accomplished in an inert medium at −70°C (time 30 hrs) while both the ultrasound waves (3.3 hrs) and γ irradiation were carried out at room temperature. After the urea was removed by dissolution in water, the obtained polymer was purified by filtration and reprecipitations in the system toluene/petroleum ether, followed by drying under vacuum at 30°C. The polyvinylacetate (*PVAc*) obtained by UV irradiation was a white powder with $\overline{M}v$ of 2158 and melting points between 155 and 200°C, while *PVAc* obtained by ultrasound waves was present as transparent and thin films with $\overline{M}v$ of 1674 and melting points between 155 and 200°C. The γ irradiation led to trace of polymer. The experimental conditions and some characteristics of *PVAc* obtained by matrix polymerization of *VAc* in the presence of urea are shown in table 1.

Table 1

The experimental data and some characteristics of PVAc obtained by matrix polymerization of VAc[a]

	Experimental conditions							
	Monomer (VAc) (ml)	Solvent (CH_3OH) (ml)	Temperature of the complex formation (°C)	Time of the complex formation (h)	Temp. of irradiation (°C)	Time of irradiation (h)	Mode of irradiation (g)	Amount of polymer
M	3	0.1	−70	24	+25	30	UV*	0.21
1	2	0	−70	24	−60 − −70	7	UV	0
2	2[b]	0.1	−30 − −70	24	−60 − −70	7	UV	0.012
3	2	0.1	−30 − −70	24	−60 − −70	7	UV	0.01
4	3[b,c]	0.1	−70	24	−60 − −70	30	UV	0.55
5	3	0.05	−60	24	−30	5	UV	0
6	2	0.1	−60	120	−60	5	UV	0
7	3	0.1	−70	24	−30	30	UV	0.4
8	2	0.1	−70	96	+25	336	irradiation **	traces
9	3	0.1	−70	168	+25	1200	irradiation **	traces
10	1	0.05	−50	48	+25	3.3	ultrasounding***	0.05
11	3[d]	0.1	−70	24	+25	3.3	ultrasounding***	0.1

* UV lamp ; 125 W

** source Co^{60} ; 60 mr/h

*** Czechoslovakian Apparatus — ULA 250

[a] In all but the first case, 2 g of urea matrix were used

[b] M.p = 155 — 200°C

[c] $\overline{M_v} = 2158$

[d] M.p = 120—180°C and $\overline{M_v} = 1674$

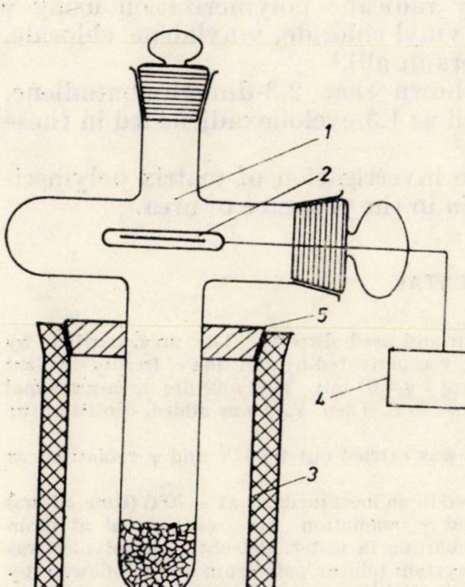

Fig. 1. — Installation of polymerization by UV irradiation :

1 — ampoule of polymerization ; 2 — UV lamp by 125 W ; 3 — Dewar with the refrigerator mixture ; 4 — feeder ; 5 — thermal insulation.

The complex acrolein — urea (3 g urea, 0.05 ml methanol and 2 ml acrolein) was prepared under the same conditions and photopolymerizations were carried out in an inert medium at $-70°$, for 5 hrs. The isolated polymer is presented as white fine particles, being insoluble in the usual solvents.

The scheme of the installation used for UV irradiation is shown in figure 1.

The ^{1}H-NMR spectra of *PVAc* were recorded with Jeol JNMC — 60 — HL equipment, by using TMS as internal standard. The estimation of tacticity was accomplished by extended bands technique.

The ^{1}H-NMR spectra of *PVAc* were recorded in ethane tetrachloride at temperatures between 100 and 130°C.

The IR spectra were recorded with a Perkin — ELMER 577 spectrophotometer within the range of 400 — 4 000 cm^{-1}.

The *PVAc* viscosity was measured in acetone at 25 ± 0.05°C with an Ubbelohde viscosimeter.

The melting points were determined with a Boetius microscope.

RESULTS AND DISCUSSION

1. The VAc polymerization

The *PVAc* obtained both by UV irradiations and ultrasound waves has been characterized by IR spectroscopy. The IR spectra show a shifting of the band characteristic of the carbonyl group from 1760 cm^{-1} for monomer towards 1740 cm^{-1} for polymer.[3]

The *PVAc* was not obtained by UV irradiation at -70°C in the absence of urea, a fact also reported by other authors. [4]

The experimental data listed in table 1 show that the methylic alcohol used on complex formation tends to direct the process towards obtaining macromolecular compounds.

In the case of UV irradiation of VAc included in the urea channels the yield is practically independent of the polymerization temperature (-70°C— -30°C).

The nuclear magnetic resonance spectroscopy (NMR) has shown that the *PVAc* obtained by UV irradiation is isotactic, while the *PVAc* obtained by ultrasound waves (sample 11, Table 1) is a statistic polymer.

The ^{1}H-NMR spectra of the sample obtained in the absence of urea (M) by photochemical initiation at 25°C, similar with those for the polymer obtained by ultrasound and for sample 4, are shown in figure 2.

The signal of the methylic protons of the etalon sample (M) $\tau = 2.02$ ppm (low level), $\tau = 2$ ppm (centre) and $\tau = 1.98$ ppm (high level) allows the establishment of a ratio polymer isotactic/heterotactic/syndiotactic of 33%/41%/26%.

The ^{1}H-NMR measurements made on the samples obtained in the presence of urea indicate the existence of a signal peak corresponding to the methylic protons which, by comparison, certify the isotacticity of the poylmer synthesized on matrix [5].

2. Acrolein polymerization

The literature indicates the existence of various structures in the acrolein polymerization, as a function of the reaction conditions. [6-8]

The investigation of IR spectra of the samples obtained by matrix polymerization of acrolein evidences the presence of a strong absoption

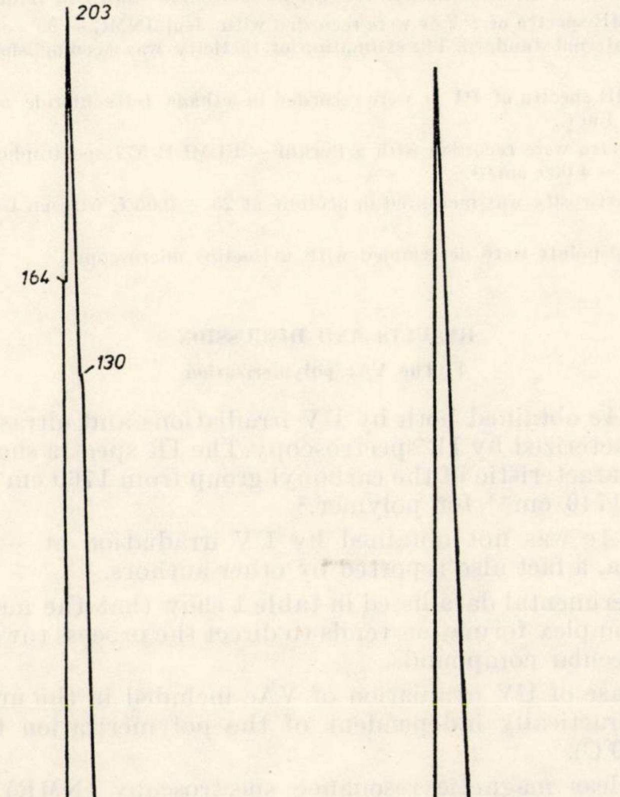

Fig. 2. — ^{1}H-NMR spectra of PVAc solutions in deuterated chloroform, samples M (a) and 4 (b) in table 1 respectively.

within the range 1100 cm^{-1}—900 cm^{-1}, a fact in favour of the cyclic structure —1,2, characteristic of the bands of the type —C—O—C—.

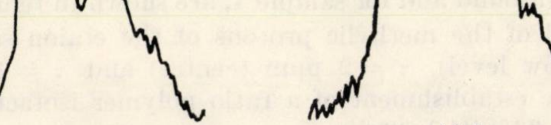

The absence of some broad absorption bands in the IR spectrum of the studied sample at 3100 cm^{-1}, 1650 cm^{-1} and 950 cm^{-1} suggests the absence of the structures as follows:

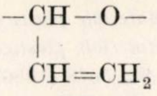

$$\begin{array}{l} -CH-O- \\ \ \ | \\ CH=CH_2 \end{array}$$

III

and confirms the existence of the cyclic forms presented previously. The absorptions from 1700 cm^{-1}, 1650 cm^{-1} and 1450 cm^{-1} indicate the presence of the groups: $-C=O$, $-C=C-$ and $-CH_2-$ respectively and the shoulder from 3040 cm^{-1} the group $-CH$, probably from the $-C\begin{smallmatrix} \diagup O \\ \diagdown H \end{smallmatrix}$ as well as $R-\underset{\underset{O}{\|}}{C}-R$ groups from the chain.

The vibrations from 2900 cm^{-1} and 2840 cm^{-1} are assigned to ν asym $-CH_2$ and ν sym $-CH_2$ respectively.

It is mentioned that around the normal vinylic polymerization (1,2 addition) the samples obtained by UV irradiation of acrolein in the presence of urea can have cyclic forms:

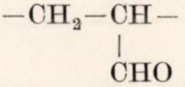

$$\begin{array}{l} -CH_2-CH- \\ \qquad\quad | \\ \qquad\ CHO \end{array}$$

IV

The polymer is practically insoluble in the normal solvents and has not a definite melting point.

CONCLUSIONS

The present paper focuses on the investigation of the possibilities of matrix polymerization of *VAc* and *acrolein* in the presence of urea and UV irradiation (*VAc acrolein*) as well as ultrasound waves (VAc).

The results have shown that *PVAc* obtained is isotactic, with low molecular weight and the yield is dependent on the amount of solvent (CH_3OH) in the reaction medium, on the ratio matrix/monomer, as well as on initiation of reaction and the nature of the complex formed.

In the case of acrolein the polymer obtained also contains cyclic structures, is practically insoluble in normal solvents, and has not a definite melting point.

REFERENCES

[1] H. Clasen, *Z. Electrochem.*, **60**, 982 (1956).

[2] M. Bezdadea and Cr. Simionescu, *Materiale plastice*, **10**, 63 (1973).

[3] M. Bezdadea and Cr. Simionescu, *Materiale plastice*, **19**, 57 (1982).

[4] M. D. White, *J. Amer. Chem. Soc.*, **82**, 5678 (1960).

[5] F. A. Bovey, E. W. Anderson, D. C. Douglas and J. A. Manson, *J. Chem. Phys.*, **39**, 1199 (1963).

[6] R. C. Schulz, *Makromol. Chem.*, **17**, 62 (1955).

[7] A. Henglein, W. Schnabel and R. C. Schulz, *Makromol. Chem.*, **31**, 181 (1959); R. C. Schulz, *ibid*, **17**, 62 (1955–1956); R. C. Schulz and W. Kern, *ibid* 18–19, 4 (1956).

[8] H. Schulz and H. Wagner, *Angew. Chem.*, **62**, 105, 112 (1956).

Revue Roumaine de Chimie, **29,** *1,* 83–97 (1984)

STRUCTURE-BINDING AFFINITY CORRELATIONS FOR IODO- AND SELENOESTROGEN ANALOGS AND MAPPING OF THE ESTROGEN RECEPTOR BY THE MTD-METHOD

Z. SIMON, G. I. MIHALAŞ and E. CASPI *)

Institute of Medicine, Department of Biophysics, Piaţa 23 August 2,
Timişoara 1900, Romania

*) The Worcester Foundation for Experimental Biology, Shrewsburg, Massachusetts
01545, USA

Received October 10, 1983

A structure-binding affinity correlation of iodoestrogen and selenoestrogen analogs was carried out by the MTD method. A correlation coefficient $r = 0.80$ was obtained for the whole series of 30 compounds, including the inactive ones. Structure-affinity correlations were also performed for another series of estrogen and stilbestrol derivatives. The attributions of the vertices of the hypermolecule to the receptor cavity, wall and exterior regions were verified by comparing the 17 common attributions for the iodo- and selenoestrogens with those of the structure-affinity correlation for the separate series of estrogen and stilbestrol derivatives : there are 13 identical and 4 different attributions, 2 of which may be explained by differences in the polar or apolar nature of atoms occupying the vertices. The estrogen receptor site should be mostly hydrophobic, with two groups bonding estrogenic 0-atoms at, or nearby positions 3 and 17 and with some large later openings.

INTRODUCTION

The previous communications [1-3] described an original approach to the possible noninvasive differentiation of hormone dependent mammary tumours from hormone independent tumours with the use of radioactive ^{125}I and ^{127}I-labelled iodoestrogen analogs. In the course of these studies, several ^{127}I-iodoestradiol analogs and selenoestrogens were prepared [4] and tested for competitive binding affinity with estradiol for the uterine receptor. In the present paper we describe the application of the MTD procedure for the structure-binding affinity correlation with iodoestrogen and selenoestrogen analogs. We shall map hereby the estrogen receptor using also the results of the MTD-method for the structure-binding affinity correlation with other estrogen analogs.[5-7]

The minimal steric (topologic) difference method – the MTD method [8] maps the receptor site by correlating minimal steric differences with biological activities. The minimal steric difference is a measure for the misfit of a molecule with respect to the receptor cavity. For the series of compounds for which a structure-activity relation is sought, a "hypermolecule" is constructed first, which is a network of the locations in the receptor of the atoms, of these molecules. The M vertices "j" of this network are attributed to the receptor cavity (annotation $\varepsilon_j = -1$), to the receptor walls ($\varepsilon_j = +1$) or to regions outside the receptor ($\varepsilon_j = 0$), by an optimisation procedure. These vertex attributions, $\varepsilon_1, \varepsilon_2, \ldots, \varepsilon_M$, constitute the receptor map, S.

METHOD

The experimental activities, A_i, considered here for correlations are relative affinities for the estrogen receptor:

$$A_i = \log\ [K_D(\text{estradiol})/K_D(i)] \tag{1}$$

with K_D (estradiol) and K_D (i) the dissociation constants for the estradiol-receptor complex and the molecule "i" – receptor complex respectively. If estrogenic activities for in vivo administration are considered:

$$A_i = \log\ [C\ (\text{estradiol})/C(i)] \tag{2}$$

with C (estradiol) and $C(i)$ the minimal molar concentrations which produce a certain physiologic effect.

The data for iodo-, and selenoestrogens (Table 1) are considered separately for structure-activity correlations. Binding affinity data of Dandliker *et al.*,[5] Katzenellenbogen[6] and of Famchenko *et al.*[7] will be considered, for a second correlation, as a single series (Table 2); for common compounds, these authors find similar relative binding affinities. Estrogenic activities in rats, as quoted by Malcolm-Dyson and May[9] and estrogenic activities in mice, as quoted by Nazarov and Bergelson[10] will be considered only qualitatively because there are large differences between bonding affinities and biological activities for the compounds for which both types of measurements were performed (Table 3).

For inactive compounds only an upper limit for the biological activity is known, not the real value of A_i. We shall include, nevertheless, also inactive compounds in correlations, with the upper limit for A_i, in order to discover wall vertices.

A single hypermolecule is constructed for both series of compounds by the approximative atom per atom superposition procedure of the MTD-method. A rational numbering of the vertices j is adopted here: the annotation j corresponds to the usual numbering of C-atoms in the steranic nucleus of estradiol. Annotations α, β and γ refer to the stereochemical orientation of substituents (γ – refers to substituents at sp^2-C-atoms), bars below or above the number indicate downward or upward displacements with respect to the normal atomic positions in estradiol (Figs 1 and 2).

Molecular models (Framework Molecular Models, Prentice Hall, 1965), consideration of van der Waals radii and some approximative atomic coordinate calculations[11] were used to construct the hypermolecule. Details are given in Appendix 1.

As examples, estradiol occupies the vertices $j = 1-18$, 3γ and 17β of the hypermolecule, diethylstilbestrol-vertices $j = 1-5$, $7-11$, $13-19$, 3γ, 7α, 11β and 19γ. The two phenyl rings of diethylstilbestrol are superimposed upon rings A and D of estradiol, the two ethyl groups are in vertices, 7,7α and 11,11β such as to avoid van der Waals repulsions with the benzenic rings. The superposition of molecules with condensed cycles, such as equiline, equilenine, estradiol is not quite unambiguous. Atoms are considered displaced upwards or downwards (as compared to positions in estradiol) following comparison of molecular models and atomic coordinates (Appendix 1). Atoms within cca 0.5 Å from a common centre are "condensed" into a unique vertex j.

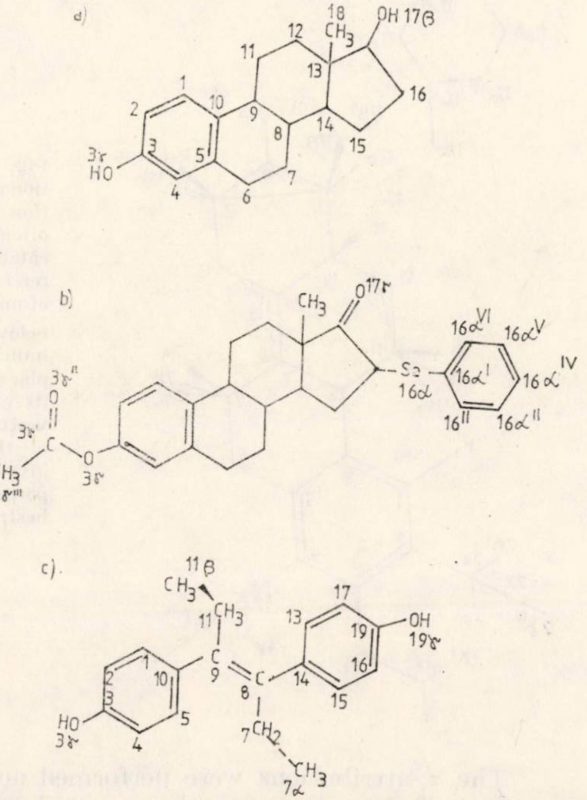

Fig. 1.—Molecules and numeration of atomic positions: (a) estradiole-3,17β-dioxy-estra 1,3,5 (10) triene; (b) 16 α-Selenophenyl estrone-3-acetate, 16 α-Selenophenyl-estra 1,3,5 (10) triene-301, 17-one 3-acetate; (c) diethylstilbestrol-trans 1,2 diethyl 1,1,2, di(4-hydroxyphenylene)-ethylene.

The way we superimpose diethylstilbestrol upon estradiol differs from that of Hospital *et al.*[12] who consider the asymmetric "DES-2" conformation for diethylstilbestrol (obtained in the crystals grown in polar solvents) and an exact superposition of one phenoxy moiety with the A-ring of estradiol. Instead, we consider the centrosymmetric "Des-1" conformation (obtained in the crystal grown in nonpolar solvents) and allow the 0.5 Å tolerance also in superimposing the phenoxy moiety upon the A-ring. There is no reason to suppose a really significant energy difference between the two diethylstilbestrol conformations and the "DES-1" conformation allows for a better superposition of the two molecules.

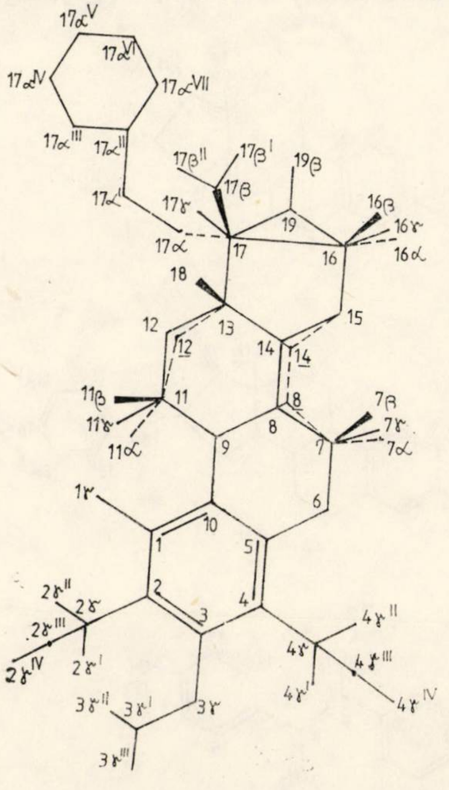
17αV
17αVI
17αIV
17αVII
17αIII
17αII
17βII
17βI
19β
17αI
17β
17γ
16β
16γ
19
17α
17
16
16α
18
12
13
15
12
14
14
11β
11
8
7β
11γ
8
7γ
11α
9
7
7α
1γ
6
10
1
5
2γII
2γ
2
4
3
4γII
2γIII
4γ
4γIII
2γIV
2γI
3γII
3γI
3γ
4γI
4γIV
3γIII

Fig. 2. — The hypermolecule and rational numbering of vertices j. Annotation α and β refer to stereochemical orientations of substituents at the indicated carbon atom. The γ-annotation refers to subtituents on an sp^2-carbon atom (e.g. 2-iodo, 17-keto, etc.). Bars below or above the number (e.g. $\underline{8},\overline{8}$) indicate a downward and upward displacement of the indicated atom from its normal position in estradiol. Not all vertices, describing the stereochemistry of the molecules considered here, are given. Vertex $j = 19$ results by the superposition of a benzene-ring of stilbestrol derivatives upon the D-ring of the estrogen nucleus.

The ε_j-attributions were performed according to a trial and error procedure. [13] Details upon the ε_j-attributions and their reliability are given in Appendix 2.

The model of Malcolm Dyson [9] for the estrogen receptor requires, for active molecules, the presence of two oxygen atoms at cca 8.3 Å distance. We will include, therefore, two indicator variables in the correlational equation (3) used in this paper :

$$A_i = a_0 + a_1\,\delta_{1i} + a_2\,\delta_{2i} - \beta MTD_i \tag{3}$$

with $\delta_{1i} = 1$ and $\delta_{2i} = 1$ if, in molecule i, an oxygen atom is bound to C_3 ($j = 3\ \gamma$) and respectively to C_{17} or nearby (i.e. for $j = 17\ \alpha, \beta, \gamma$, $16\ \alpha, \beta, \gamma$ and $19\ \gamma$).

The ε_j-attributions corresponding to the structure-activity correlations for the compounds of Tables 1 and 2 are listed in Table 4.

The calculations were performed on the M-18 computer of the High School of Medicine, of Timișoara.

Structure-Binding Affinity Correlations for Iodo- and Selenoestrogens

The iodoestrogens and selenoestrogens considered for the first structure-binding affinity correlation are listed in Table 1.

Table 1

Iodoestrogen and selenoestrogen molecules used in the construction of the hypermolecule and of the correlational equation (6)

No. (i)	Name	A_i	δ_1	δ_2	MTD		
					S_1	S_1''	S_1'
1	16 α-Iodoestradiol	+0.02	1	1	0	0	—
2	Estradiol	+0.00	1	1	1	1	2
3	16 β-Iodoestradiol	−0.25	1	1	1	1	—
4	6-Iodoestra-1,3,5(10),6 -tetraene-3,17 β-diol	−0.31	1	1	2	1	—
5	17 α-[Methyl]-Selenomethyl -estradiol	−0.51	1	1	2	—	3
6	16 α-Iodoestrone	−0.54	1	1	1	1	—
7	16 α-Selenomethyl-estradiol	−0.55	1	1	1	—	2
8	16 α-Selenophenyl-estrone	−0.64	1	1	2	—	3
9	16 α-Iodomethyl-estrone	−1.05	1	1	2	2	—
10	3-Acetoxy, 16 α-selenomethyl-estrone	−1.15	1	1	3	—	4
11	7α-Selenomethyl-6 β-hydroxy-estradiol	−1.22	1	1	2	—	4
12	3-Acetoxy, 16 α-iodo-estrone	−1.30	1	1	2	2	—
13	17 α-Selenomethyl-estra-1,3,5(10) -trien 3,16 β-diol-16 acetate	−1.30	1	1	3	—	4
14	17 α-[Phenyl]selenomethyl- -estradiol	−1.30	1	1	3	—	4
15	7 α-[Phenyl] selenomethyl-estra- -1,3,5(10) trien-3,6 β,17 β-triol, triacetate	−1.40	1	1	3	—	4
16	7 α-[Phenyl] selenomethyl-estra- -1,3,5(10) trien-3,6 β,17 β-triol, 3,17 diacetat	−1.40	1	1	3	—	4
17	17 α-Selenomethyl-estra-1,3,5, (10)-trien-3,16 β-diol	−1.52	1	1	3	—	4
18	4-Iodo-3-hydroxy-estra-1,3,5(10) 9(11)-tetraene-17 one	−1.70	1	1	3	2	—
19	7α-Iodo-3,17 β-diacetoxy-estra- -1,3,5(10)-triene-6 one	−1.70	1	1	3	2	—
20	7 α-Iodo, 6 β-hydroxy-estradiol	−1.70	1	1	2	2	—
21	7α-Iodo-3,6 β,17 β trihydroxy-estra-1,3,5(10)-triene-3,17-diacetate	−2.00	1	1	3	3	—
22	17 α-Iodoestra-1,3,5(10)-triene- -3,16 β-diol	−2.00	1	1	3	3	—
23	17α-Iodoestra-1,3,5(10)-triene-3- -01	−2.00	1	0	3	3	—
24	17α-Iodoestra-1,3,5(10), 6-tetraene-3-01	<−3	1	0	3	—	—
25	2,4,17-Triodoestra-1,3,5,(10), 16-tetraene-3-01	<−3	1	0	4	—	—
26	17-Iodoestra-1,3,5(10),16-tetra-ene-3-01	<−3	1	0	2	—	—

Table 1 (continued)

No. (i)	Name	A_i	δ_1	δ_1	MTD		
					S_1	S_1''	S_1'
27	2,6-Diiodo-1,3,5(10), 6-tetraene--3,17 β-diol	<-3	1	1	3	—	—
28	2-Iodoestradiol	<-3	1	1	2	-	—
29	2,4,17 α-Triodoestra-1,3,5(10)—-trienne-3,16 β-diol	<-3	1	1	5	—	—
30	4,17 α-Diiodoestra-1,3,5(10)--triene-3,16 β-diol	<-3	1	1	4	—	—

Activities $A_i = -\log$ of relative binding affinities to uterine cytosol; the affinity of estradiol is taken as 1.0. MTD-minimal steric differences calculated from the optimised map S_1 and respectively S_1' or S_1''; $\delta_1 = 1$ marks the presence of an O-atom at $j = 3$, $\delta_1 = 0$ its absence; $\delta_2 = 1$ marks the presence of an O-atom in the vicinity of C_{17}. Estradiol is estra-1,3,5(10) triene — 3.17 β-diol, estrone is estra-1,3,5(10)-triene-3-01-17-one.

In a separate correlation for the ten selenoestrogens of Table 2 (i: 2, 5, 7, 8, 10, 11, 13—17; estradiol also included), following receptor map S_1' and correlational equation (4) were obtained:

$$S_1' \begin{cases} j(\varepsilon = -1): 7\alpha'',\ 16\alpha,\ 17\,\beta \\ j(\varepsilon = \ \ 0): 3\gamma'', \gamma''', 6\beta' - \beta''', 7\alpha', \alpha''' - \alpha^{\mathrm{VI}}, 16\alpha'' - \alpha^{\mathrm{VI}} \\ \qquad\qquad 16\beta' - \beta''', 17\alpha', \alpha''' - \alpha^{\mathrm{VII}}, 17\beta' - \beta''', 17\gamma \\ j(\varepsilon = +1): 3\gamma', 6\beta, 7\alpha, 16\,\alpha', 17\,\alpha, \alpha'' \end{cases}$$

$$\hat{A} = 0{,}924 - 0{,}557\ \mathrm{MTD},\ r = 0.929,\ s = 0.181,\ \mathrm{EV} = 0.848,\ F = 25.3 \qquad (4)$$

A separate correlation for the active iodoestrogens of Table 2 ($i = 1-4$, 6, 9, 12, 18—23; estradiol also included) yields the following results:

$$S_1'' \begin{cases} j(\varepsilon = -1): 16\alpha,\ 17\beta \\ j(\varepsilon = \ \ 0): 3\gamma'', \gamma''', 4\gamma, 6\,\gamma, 7\alpha, 16\,\beta,\ 17\alpha', 17\beta' - \beta'''. \\ \quad 17\gamma,\ \varepsilon_{12} = \varepsilon_{\underline{12}}\ \varepsilon_{14} = \varepsilon_{\underline{14}} \\ j(\varepsilon = +1): 3\gamma', \bar{6}\beta,\ 17\,\alpha \end{cases}$$

$$\hat{A} = 0.567 - 0.170\ \delta_2 - 0.856\ \mathrm{MTD},\ r = 0.943,\ s = 0.273,\ \mathrm{EV} = 0.87 \qquad (5)$$

$$F = 24.2,\ r\,(\delta_2) = 0.327,\ r = (\mathrm{MTD}) = -0.942,\ r(\delta_2, \mathrm{MTD}) = -0.399$$

The linear correlation coefficient is r, the partial correlation coefficients — $r(\delta_2)$ and $r(\mathrm{MTD})$, the intercorrelation coefficient, $r(\delta_2, \mathrm{MTD})$.

For all 30 compounds of Table 1, the receptor map S_1, listed in Table 4 and the correlational equation (6) were obtained:

$$\hat{A} = -0.866 + 1.004\ \delta_2 - 0.628\ \mathrm{MTD},\ r = 0.804,\ s = 0.592,\ \mathrm{EV} = 0.620 \qquad (6)$$

$$F = 15.8,\ r(\delta_2) = 0.483,\ r\,(\mathrm{MTD}) = -0.728,\ r(\delta_2, \mathrm{MTD}) = -0.204$$

The modest r-value is probably due to the seven inactive compounds, whose real binding affinities may differ sensibly from the upper limit, $A = -3$, considered for the correlation. All 2-iodo-derivatives are inactive; vertex $j = 2$ falls into a very rigid wall region. Other predicted detrimental positions for substituents at the estrogen nucleus are: 4 γ, 6β, 6 γ, 17 α, while the beneficial positions are 16 α and 17 β, at least for small hydrophobic and hydrophylic substituents respectively. Substituents at 7 α and 16 β are predicted to have only minor effects. Acetylation of the $3-OH$ group is also detrimental ($\varepsilon_{3\gamma'} = +1$).

If a supplementary indicator variable for the presence of a 2-I-substituent is added to eq. (6), $r = 0.853$ is obtained, while if the MTD's are calculated with a more elaborate formula which accounts for the large size of third period and fourth or higher period atoms, [8] $r = 0.846$ results.

Structure-Binding Affinity Correlations for Various Estrogen and Stilbene Derivatives

Relative affinities of various estrogen and stilbene derivatives for the estrogen receptor were published by Dandliker *et al.* [5] and by Katzenellenbogen. [6] We omitted some highly distorted stilbene derivatives with large substituents at the ethylenic C-atoms but some of the compounds studied by Famchenko *et al.*[7] were included in the series listed in Table 2.

For the compounds of Table 2, the receptor map S_2 (see Table 4), and the correlational equation (7) were obtained.

$$\hat{A} = 0.309 + 2.409\,\delta_1 + 1.203\,\delta_2 - 1.122\,\mathrm{MTD},\ r = 0.849,\ s = 0.518 \qquad (7)$$

$$\mathrm{EV} = 0.698,\ \ F = 22.6,\ \ r(\delta_1) = 0.468,\ \ r(\delta_2) = 0.220,\ \ r(\mathrm{MTD}) = -0.632$$

$$r(\delta_1, \delta_2) = -0.037,\ \ r(\delta_1, \mathrm{MTD}) = 0.009,\ \ r(\delta_2, \mathrm{MTD}) = -0.069$$

For vertex $j = 11\ \beta$, occupied by the hydrophobic CH_3 group in diethylstilbestrol and hexestrol, $\varepsilon_{11\beta} = -1$ is attributed by S_2. A polar substituent at 11β is markedly detrimental, $A = -1.7$ for 11 β-hydroxy-estradiol, demonstrating the hydrophobic character of the receptor cavity bordering the $j = 11\ \beta$ vertex.

Structure-affinity studies with the MTD-method for the compounds of Dandliker *et al.* and Katzenellenbogen were performed by Niculescu-Duvăz and Crăescu, [14] and for in vivo data by Popoviciu *et al.*,[11] but on a somewhat different basis than the general correlational equation (3).

IN VIVO ACTIVITIES

The large differences between relative binding affinities and in vivo activities, as already discussed in the second paragraph (see also Table 3), do not allow to use in vivo biological activity data [9,10] for QSAR's to be compared with eqs (6) and (7). Some of the data quoted by Nazarov and Bergelson[10] concerning activities of estrane-nucleus-isomers will be considered to have an at least qualitative idea of the effects of changes in ring-stereochemistry.

Table 2

Estradiol and stilbestrol derivatives used to obtain the correlation equation (7). Relative affinities to the estrogen receptor

No. (i)	Name	A	δ_1	δ_2	MTD(S_2)
1	17α-Ethynyl-estradiol	0.28	1	1	3
2	Hexestrol	0.26	1	1	3
3	Diethylstilbestrol	0.08	1	1	3
4	3-Fluoro-hexestrol	0.01	1	1	3
5	Estradiol	0.00	1	1	3
6	17-Epiestriol	−0.05	1	1	4
7	3-Azido-hexestrol	−0.15	1	1	3
8	17 α-Butylestradiol	−0.15	1	1	3
9	16-Epiestriol	−0.36	1	1	3
10	3-Iodo-hexestrol	−0.40	1	1	3
11	Estrone	−0.41	1	1	4
12	16 α-Hydroxyestrone	−0.60	1	1	4
13	Equilin	−0.62	1	1	4
14	Methyl-ethylstilbestrol	−0.62	1	1	3
15	17-Epiestradiol	−0.70	1	1	4
16	Coumestrol	−0.68	1	1	4
17	6-Keto-estradiol	−0.68	1	1	4
18	4-Methoxy-hexestrol	−0.72	1	1	4
19	Estriol	−0.80	1	1	3
20	3-Nitrohexestrol	−0.84	1	1	4
21	16-Ketoestradiol	−0.85	1	1	4
22	Dimethylstilbestrol	−0.87	1	1	4
23	Estra-1,3,5(10),9-tetraene-3,17 β-diol-12-one	−0.91	1	1	4
24	Estra-1,3,5(10),6-tetraene-3,17 β,diol	−1.00	1	1	4
25	3-Methoxy-17α-ethynyl-estradiol	−1.00	1	1	4
26	Estradiol-3-benzoate	−1.03	1	1	4
27	3,3-Difluorohexestrol	−1.05	1	1	4
28	Equilenine	−1.10	1	1	4
29	4-Nitroestradiol	−1.21	1	1	4
30	2-Azido-estradiol	−1.52	1	1	4
31	3-Methoxy-estradiol	−1.52	1	1	4
32	Estradiol-17 β-valerianate	−1.73	1	1	4
33	4-Azido-estradiol	−2.05	1	1	4
34	16-Azoestrone	−2.30	1	1	4
35	2-Bromoestradiol	−2.21	1	1	4
36	4-Bromoestradiol	−2.30	1	1	4
37	17-Deoxyestradiol	−2.39	1	0	4
38	3-Deoxyestradiol	−2.47	0	1	3
39	3-Deoxy-estrone	−3.60	0	1	4
40	2-Nitro-estradiol	<-4	1	1	6

Activities, A and MTD — see Table 1. Estriol is estra-1,3,5(10)-triene-3,16 α, 17 β triol; 17-epi etc. means that the corresponding substituent is in the isomeric position at the same C-atom (e.g. 17-epi-estradiol has the 17-OH group in 17 α instead of 17 β). Hexestrol is 1,2-diethyl-1,2-di(4-hydroxyphenylene) ethane. Diethylstilbestrol is *trans*-1,2-diethyl-1,2-di(4-hydroxyphenylene) ethylene. Coumestrol occupies vertices j : 1−7, *8*, *13*, 14 -17, 19,3 γ, 7γ, 19 γ. Equilin is estra-1,3,5 (10), 7-tetraene-3-01-17-one; equilenine is estra-1,3,5(10),6,8-pentene-3-01-17 one.

Hydrogenation of the A-ring inactivates the estrogen derivatives (in octahydroestrone, 6-hydroxy-1, 2, 3, 4-tetrahydro-17—equilenone) or strongly reduces activity (3β, 17β-dihydroxy-estra-6, 8 (9), 5(10)-triene,

Table 3

Relative binding affinities to the estrogenic receptor and relative biological activities

Substance	RBA	In vivo act,	
	(1)	(2)	(3)
17-α-Ethynyl estradiol	0.28	0.0	0.0
Hexestrol	0.26	−0.2	—
Estradiol	0.0	0.0	0.0
Diethylstilbestrol	0.08	−0.1	—
16-Epiestradiol	−0.36	—	−2.0
Estrone	−0.41	−1.1	−0.8
Equilin	−0.62	−1.2	−0.8
6-Ketoestradiol	−0.68	−0.8	—
17-Epiestradiol	−0.70	−1.5	−1.8
Estriol	−0.80	−2.1	−2.0
Estradiol-3-benzoate	−1.03	—	−1.0
Equilenin	−1.10	−2.4	−2.5

Column (1)—relative binding affinities, according to eq.(1) and Table 2. Columns (2) and (3) — relative in vivo activities calculated according to eq.(2) and data listed by Malcolm-Dyson and May[9] (for rats) and by Nazarov and Bergelson[10] (for mice) respectively. For the reference, estradiol, one has the value zero in all three columns.

$A \simeq -2.5$). A general change of shape in the estrone nucleus inactivates the compounds — norequilenine (*cis* C/D-isomer), 17-*iso*-equilenine, lumiestrone are inactive. Strong modifications of the D-ring stereochemistry also produce strong decrease of activity (in D-homoestrone, $A \simeq -2.3$, in D-homoestradiol, $A \simeq -2.4$ and in the C_{13}-antipode of equilenine, $A \simeq -3$). In contrast, increase of the alkyl group in position 19 ($j = 18', 18''$ etc. in the hypermolecule of Fig. 2) does not produce a sensible change of estrogenic activity: equilenine, 19-homo-,19-homo-bis- and 19-homo-tris-equilenine are all 100 to 500 times less active than estradiol.

The tentative conclusions concerning the detrimental effects of the corresponding upwards and downwards shifts of atoms are indicated in column S_3 of Table 4.

RESULTS. THE MAP OF THE ESTROGEN RECEPTOR SITE

The results of our structure-activity studies concerning the series of compounds of Tables 1 and 2 are synthetised in columns S_1 and S_2 of Table 4; the last column, S^*, gives the most probable ε_j-attributions and the polar/apolar character of the receptor regions bordering the respective vertices.

Based upon the correlational equations (6) and (7), one MTD unit corresponds to cca one logarithmic affinity unit, the presence of the O-atom at position 3 to cca two logarithmic units, the presence of the O-atom in the vicinity of 17β to cca one logarithmic unit. One substituent in the position of a cavity vertex should thus increase about 10 times the affinity, one sub-

Table 4

Results of the estrogen receptor site mapping by the MTD-method

j	$\varepsilon_j : S_1$	S_2	S_3	S
2,3	—	—	−1 : A	−1 *c*, A
$\underline{2}, \underline{3}$(or $\overline{2},\overline{3}$)	—	—	0 :A	0 ; *w*, A
6	—	0, *A*		−1 ; *c*, *A*
8.$\underline{8}$	—	$\varepsilon_8 = \varepsilon_{\underline{8}}$; *A*		
11, $\overline{11}$	—	$\varepsilon_{11} = \varepsilon_{\overline{11}}$ *A*		
12	$\varepsilon_{12} = \varepsilon_{\underline{12}}$	−1 ; *A*	$\varepsilon_{12} = \varepsilon_{\underline{12}} = \varepsilon_{\overline{12}}$, *A*	
$\underline{12}$		0 ; *A*		
$\overline{12}$	—	−1 ; *A*		
14	$\varepsilon_{14} = \varepsilon_{\underline{14}}$; *A*		−1 : A	
$\underline{14}$			0 : A	
15, 16, 17	—	—	−1. A	
$\underline{15}$, $\underline{16}$, $\overline{16}$, $\underline{17}$, $\overline{17}$	—	—	0 : A	0 ; *w*
18	—	$\varepsilon_{18} = \varepsilon_{\underline{19}}$; *A*	—	0 ; *e*
19	—		—	
$\overline{19}$	—	—	+1 : A	+1 : *w*
1 γ	—	—	0 : A	0 ; *w*, *A*
2 γ	+1 ; *A*	+1 ; *A*,*P*	—	+1 ; *w*
2 γ', γ''	—	+1, *P*	—	
2 γ''', γ^{IV}	—	0, *P*	—	
3 γ	—	0 ; *P*	—	0 (*c*, *P*)*
3 γ'	+1 ; *P*	+1 ; *P*, *A*	—	+1
3 γ'',...,γ^{VII}	0 ; *P*	0 ; *P*, *A*	—	0 ; *e*
4 γ	+1 ; *A*	+1 ; *P*, *A*	—	+1 ; *w*
4 γ',...,γ^{IV}	—	0 ; *P*	—	0 ; *e*
6β	+1, *P*	—	—	+1 ; *w*
6 β',...,β'''	0, *P*	—	—	0
6 γ	+1, *P*, *A*	—	—	+1 ; *w*
7α	0 ; *A*	0(or−1) ; *A*	—	0 ; *e*, *A*
7α',..., α^{VII}	0 ; *A*	—	—	0 ; *e*
7β	—	+1(or 0) ; *A*	—	+1 *w*
11α	—	+1(or 0) ; *A*	—	+1 ; *c*, *w*, *A*
11β	—	−1(or 0) ; *A*	—	−1 ; *c*, *A*
$\overline{12}\gamma$	—	+1, *P*	—	+1 ; *w*
16α	−1, *A*	0 ; *P*	0 ; *P*	−1 ; *c*, *A*
16α'	+1, *A*	—	—	+1 ; *w*
16α'',..., α^{VI}	0 ; *A*	—	—	0 ; *e*
16β	0 ; *P*, *A*	—	—	0(*c*/*e*, *P*)**
16β',...,β'''	0 ; *P*, *A*	—	—	0 ; *e*
16γ	—	+1, *P*	—	0(*c*/*w*, *P*)**
17α	+1 ; *A*	0 ; *A*, *P*	—	
17α'''	+1 ; *A*	0 ; *A*	—	+1, *w*
17α', α'', α^{IV},..., α^{VII}	0 ; *A*	0 ; *A*	—	0, *e*
17β	−1 ; *P*	−1 ; *P*	—	−1(*c*, *P*)**
17β'	0 ; *P*	+1 ; *P*	—	0(*c*/*w*)
17β'',...,β^{VI}	0 ; *P*	0 ; *A*	—	0 ; *e*
17γ	0 ; *P*, *A*	0 ; *P*	—	0(*c*/*w*, *P*)**

Table 4 (continued)

j	$\varepsilon_j : S_1$	S_2	S_3	S
18′, 18″, 18‴	—	—	0 ; A	0 ; e
19γ	—	−1 ; P	—	1 ; (w, P)**
19γ′	—	+1 ; P	—	+1 ; w

Column j marks the vertices or group of vertices, for which ε_j-values are assigned in the two receptor maps. S_1 is the receptor map obtained for the compounds listed in Table 1, S_2 — the map obtained for the compounds of Table 2, S_3 — qualitative assignments based upon in vivo data.[10] Column S^* synthetises the results of the previous columns and indicates the most probable ε_j-assignments. P and/or A indicate the polar-hydrophilic or apolar-hydrophobic character of the atoms (groups) which occupy the corresponding j vertex in the compounds of Tables 1 and 2. In the S^*-column, c, w and e indicate that the corresponding j-vertex is a cavity, wall or outer (exterior) vertex, A or P indicate the hydrophobic or hydrophilic character of the corresponding receptor region ; c/w indicates a vertex probably situated at the boundary between a cavity and a wall region. Asterisks (*) and double asterisks (**) indicate vertices which are occupied by the O-atoms in positions 3 and 17.

stituent in the position of a wall vertex should decrease about 10 times this affinity.

Concerning the two oxygen atoms required by the Malcolm Dyson model for the estrogen receptor, the phenolic OH group at C_3 acts as a proton donor in a hydrogen bond with the receptor : the attribution $\varepsilon_{3\gamma'} = +1$ should correspond not to a steric effect but to the methylation or acylation of the OH-group. The O-atom at $j = 3\gamma$ must be bound also by another bond to the receptor in order to explain the high regressional coefficient of δ_1. The O atom at 17 β, or nearby, is probably bound to a cationic receptor site : doisynolic acid, with a carboxylate group (at $j = 16, 17, 17\gamma$), is about 20 times more active than estradiol.[9] The most favourable position for this second O-atom is 17 β ($\varepsilon_{17\beta} = -1$), although the interaction with the receptor is possible also for other, nearby, positions.

The vertex assignments of Table 4 indicate most atoms of the estrogen-nucleus in a hydrophobic cavity ($\varepsilon_j = -1$, A). This cavity should mould rather tightly around rings A and D of the nucleus : changes of atomic positions from $j = 2, 3, 15, 16, 17$ by upwards or downwards shifts produce detrimental effects. The cavity should be rather specious around the B and C rings ($\varepsilon_8 = \varepsilon_{\bar{8}}$, $\varepsilon_{11} = \varepsilon_{\overline{11}}$, etc) and opened upwards : $\varepsilon'_{18} = \varepsilon''_{18} = \varepsilon'''_{18} = 0$ for substitution of the methyl in $j = 18$ by larger alkyl groups.

Beneficial vertices for hydrophobic substituents are $j = 11$ β and 16 α ; the vertex corresponding to 11 β was assigned as beneficial also in the paper of Popoviciu et al.[11] The most detrimental vertex is 2γ : all 2-substituted derivatives are inactive or with low activity. Other detrimental vertices are $j = 4\gamma$, 6 β, $\overline{12}\gamma$, 16 α′, 17γ′, 19 γ′. The detrimental vertices indicate the extent of receptor walls. According to the vertices with $\varepsilon_j = 0$ attributions — especially to those for larger substituents (as 3 γ″, . . ., . . . γ^{VII}, etc.), the receptor cavity should be opened to the exterior in the vicinity of positions 3, 7, 16, 17 and 18 — above the C-ring.

A general view of this model for the receptor site, with an estrogen molecule in it, is presented in Fig. 3.

This model is in good agreement with the estrogen receptor model of Duax *et al.*[15] in which the steroid A ring is primarily responsible for the hormone binding, the D-ring controls expression of activity, while modifications of the median region of the hormone molecule do not alter much activity (if the relative orientation of the A and D rings is not changed). This receptor should consist of two fragments, bond together by the hormone molecule.

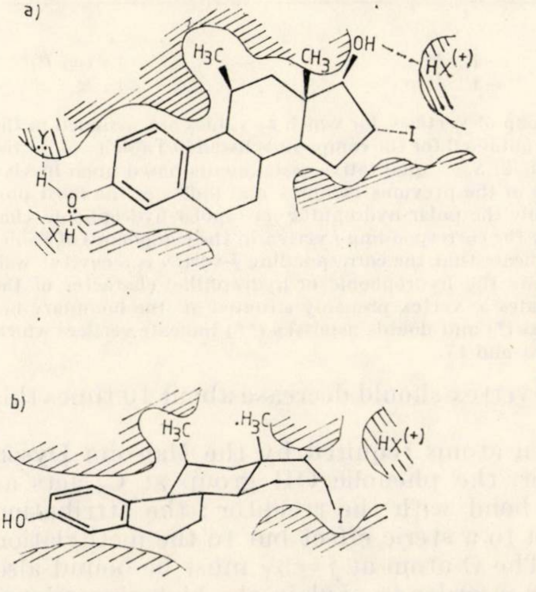

Fig. 3. — Probable shape of the estrogen receptor site. View from above (a); lateral viwe (b). Dashed zones-limits of walls of the receptor cavity; ▨-hydrophobic receptor zones; ▩-hydrophylic receptor zones. XH and Y -hydrogen donor, respectively acceptor group of the receptor site for hydrogen bonding. An 11 β-methyl, 16 α-iodo estradiol molecule is depicted in the interior of the receptor cavity.

A reliability test for our vertex attribution is the degree of concordance for the common attributions of the receptor maps S_1 and S_2, obtained for almost entirely different series of compounds. Of the 17 common attributions, 13 are identical, 4 disagree (for $j = 12$, 16 α, 17 α, 17 β′). Of the 4 disagreements, 2 can be explained by the different polar, or apolar, character of atoms occupying the vertices in the molecules of Table 1 and Table 2 : $j = 16$ α is occupied by apolar atoms (I, Se) in Table 1 and by polar groups (OH) in Table 2 ; 17 α only by apolar atoms (CH_2, I, Se) in Table 1, both by polar and apolar (C, CH_2, OH) in Table 2.

The most active molecules predicted by our structure-affinity correlations are estradiol derivatives with small hydrophobic substituents at 16 α and 11 β. The 11 βn-propyl and isopropyl derivatives of 17α-ethynyl estradiol were synthesized by Bélanger, Philibert and Teutsch[16] and found to have an estrogen receptor affinity about 3 times larger than 17α-ethynyl estradiol and 7 times larger than estradiol.

DISCUSSIONS

The description of the receptor-effector molecule interaction for the estrogen and stilbene derivatives, considered in this paper, requires the characterisation of about 50 vertices, describing the molecular stereochemistry. This description implies at least the attribution to cavity, wall or outer regions and the indication of the apolar character for the corresponding receptor region. Affinity data for 70 compounds are available to extract, by QSAR-methods, the required information. It seems therefore likely that QSAR-methods could give realistic and reliable descriptions of receptor sites only if combined with supplementary information about the receptor. This explains, at least in part, the rather modest correlational results obtained here with the MTD-method.

The MTD method has the advantage of simplicity and allows to extract much of the information concerning the receptor, contained in the available series of molecules with known biological activities. The MTD method could be a useful first approximation to more elaborate receptor mapping methods, like the distance geometry approach of Crippen,[17] which requires a preliminary receptor model before the approach, per se, can be applied.

ACKNOWLEDGEMENT. The described MTD studies were made possible by a grant received by Eliahu Caspi from the John E. Fogarty International Center for Advanced Studies, in the framework of the exchange program of the U.S. Public Health Service and the Romanian Ministry of Health Services.

The authors are indebted to dr. Tamara Bânzaru from our Biophysics Department for assistance in computations and to dr. S. Holban and dr. D. Ciubotariu from the Polytechnical Institute "Traian Vuia", Timişoara, for adaptations of programs for the M—18 computer.

REFERENCES

[1] T. Arunchalam, C. Longcope and E. Caspi, *J. Biol. Chem.*, **254**, 5900 (1979).
[2] C. Longcope, T. Arunachalam, I. Rafkind and E. Caspi, in "Hormones and Cancer", W. W. Leavitt, editor, Plenum Publ. Co, New York 1982, p. 191.
[3] C. Longcope, T. Arunachalam, I. Rafkind and E. Caspi, *J. Steroid. Biochem.*, **14**, 26 (1981).
[4] T. Arunachalam, C. Longcope and E. Caspi, *Canad. J. Biochem.*, **60**, 152 (1981).
[5] W. B. Dandliker, R. J. Brawn, M. L. Hsu, P. J. Brawn, J. Levin, C. Y. Meyers and W. M. Kolb, *Cancer Res.*, **38**, 4212 (1978).
[6] J. A. Katzenellenbogen, *Cancer Treatm. Rep.*, **62**, 1243 (1978).
[7] N. D. Famchenko, L. S. Minina and R. N. Shchedrina, *Voprosy Mediz. Himii (Moscow)*, **2**, 198 (1978).
[8] A. T. Balaban, A. Chiriac, I. Moţoc and Z. Simon, "Steric Fit in Quantitative Structure-Activity Relations", Lecture, Notes in Chemistry, vol. 15 (1980), Springer Verlag, Berlin, 1980, chap. 5.
[9] C. Malcolm-Dyson and P. May, "May's Chemistry of Synthetic Drugs", Logmans, London, 1955, chap. 22.
[10] I. N. Nazarov and L. S. Bergelson, "Chemistry of Steroid Hornomes", Edition of the Soviet Acad. of Sci., Moscow 1955, chap. VI.
[11] V. Popoviciu, S. Holban, I. I. Bădilescu and Z. Simon, *Studia Biophys. (Berlin)*, **69**, 75 (1978).
[12] M. Hospital, B. Busetta, C. Courseille and G. Precigoux, *J. Steroid. Chem.*, **6**, 221 (1975).
[13] Z. Simon, N. Dragomir, M. G. Plauchithiu, S. Holban, H. Glatt and F. Kerek, *Eur. J. Medic. Chem.*, **15**, 520 (1980).
[14] I. Niculescu-Duvăz and T. Crăescu, *Oncologia (Bucharest)*, **19**, 211 (1980).
[15] W. L. Duax, J. F. Griffin, D. C. Rohrer and Ch. M. Weeks, in "Hormone Antagonists", M. K. Agarwal, editor, Walter de Gruyter, Berlin, 1982, p. 3.
[16] A. Belanger, D. Philibert and G. Teutsch, *Steroids*, **37**, 36 (1981).
[17] G. M. Crippen, *J. Medic. Chem.*, **22**, 988 (1979); **23**, 599 (1980); **24**, 198 (1980).

APPENDIX 1

CONSTRUCTION OF THE HYPERMOLECULE

The hypermolecule is constructed by a maximal atom-per-atom superposition of the molecules, considered.[8] Hydrogen atoms are neglected. The general orientation of the molecules is determined by the superposition of two essential O-atoms, corresponding to the vertices $j = 3\gamma$ (the phenolic OH-group) and as near as possible to $j = 17\gamma$ (ketonic O-atom of estrone) and to the superposition of at least one benzenoid ring upon the A-ring of estradiol. Molecular models were constructed by use of framework molecular models, to have a general idea of their shapes.

Coordinates of the atomic centres within the steranic nucleus or the stilbene moiety are calculated using a standard bond length, 1.5 Å, and tetrahedral or trigonal bond angles.[11] For nearby atomic centres, unique vertices are considered and all atomic centres within less than cca 0.5 Å of a vertex, j, are superimposed upon j. Following z-coordinates, in Å, with respect to the plane of the benzenoid A-ring of estradiol result (cf. Figs. 1, 2) :

Estradiol : $z_1 = z_2 = \ldots = z_7 = z_9 = z_{10} = 0.0$; $z_8 = z_{11} = z_{12} = z_{14} = z_{15} = 0.75$; $z_{13} = 1.5$; $z_{16} = 1.9$; $z_{17} = 1.7$; $z_{18} = 3.0$

6,7-Dehydro-estrone : $z_1 = z_2 = \ldots z_6 = z_9 = z_{10} = 0.0$; $z_7 = 0.4$; $z_8 = z_{11} = z_{15} = 0.75$; $z_{12} = z_{14} = -0.4$; $z_{13} = z_{16} = z_{17} = 1.1$; $z_{18} = 2.8$

Equilin (7,8-dehydro-estrone) : $z_1 = z_2 = \ldots = z_{10} = 0.0$; $z_{11} = z_{12} = z_{13} = z_{16} = z_{17} = 1.5$; $z_{14} = 0.2$; $z_{15} = 0.4$; $z_{18} = 3.0$

Equilenin (7, 8, 9, 10-dehydro-estrone) : $z_1 = z_2 = \ldots = z_{12} = 0.0$; $z_{13} = 0.75$; $z_{14} = 0.2$; $z_{15} = z_{17} = 0.9$; $z_{16} = 1.1$; $z_{18} = 2.3$

Hexestrol : $z_1 = z_2 = \ldots = z_5 = z_9 = z_{10} = 0.0$; $z_8 = 0.75$; $z_{13} = 0.7$; $z_{14} = 0.9$; $z_{15} = 1.1$; $z_{16} = 1.3$; $z_{17} = 0.9$; $z_{19} = 1.5$; C-atoms in ethyl groups : 0.75 and 1.7 ; 0.0 and −1.0

Stilbestrol : $z_1 = z_2 = \ldots = z_5 = z_9 = z_{10} = 0.0$; $z_8 = 0.6$; $z_{13} = 0.7$; $z_{14} = 0.9$; $z_{15} = 1.1$; $z_{16} = 1.3$; $z_{17} = 0.9$; $z_{19} = 1.5$: C-atoms in ethyl groups : − 0.2 and 0.8 ; 0.8 and −0.2

Following z° coordinates were considered for the vertices $j = 1-19$ of the hypermolecule (in Å) :

$z_1^0 = z_2^0 = \ldots = z_6^0 = z_9^0 = z_{10}^0 = 0.0$; $z_7^0 = 0.4$; $z_8^0 = 0.8$; $z_{11}^0 = 0.2$; $z_{12}^0 = 0.5$; $z_{13}^0 = z_{15}^0 = 1.1$; $z_{14}^0 = 0.8$; $z_{16}^0 = z_{17}^0 = 1.2$; $z_{19}^0 = 1.4$

As example, the first CH_2 group of the ethyl groups, with $z = 0.75$ Å in hexestrol, and the one with $z = -0.2$ Å in stilbestrol are both superimposed upon vertex $j = 7$ ($z_7^0 = 0.4$ Å) of the hypermolecule.

APPENDIX 2

THE OPTIMISATION PROCEDURE

The optimisation procedure is based upon computations of the increase $\Delta Y(\varepsilon_j')$ of the mean standard deviation between the experimental and calculated activities, when ε_j is substituted by ε_j' in the receptor map S^x. If all $\Delta Y(\varepsilon_j')$-values are positive or zero, S^x is considered optimal.[8,13]

In certain circumstances only less specific assignments can be done. For example, for the series of molecules of Table 2, vertices 3 γ', γ'', γ''' are either all empty or all occupied (in 3-acetylated derivatives) : any one of those vertices can be assigned as detrimental ($\varepsilon_j = +1$), the other two as neutral ($\varepsilon_j = 0$). For the same series (see the receptor map S_1 of Table 4), $\varepsilon_{12} = \underline{\varepsilon_{12}}$ and $\varepsilon_{14} = \underline{\varepsilon_{14}}$ but any value (−1.0 or +1) can be attributed to these pairs of vertices.

For the selenoestrogens of Table 1 ($N = 11$, $i = 2, 5, 7, 8, 10, 11, 13-17$) with the calculated $\hat{A}_i$s (eq. 4) $Y = 0.33$ results, and for an at least 95% reliability of the ε_j-attributions, according to Fischer statistics, $\Delta Y(\varepsilon_j') \geqslant 0.59$ is required. For the active iodoestrogens of Table 2 ($N = 13$, $i = 1-4, 6, 9, 12, 18-23$), $Y = 0.94$ and $\Delta Y(\varepsilon_j') \geqslant 1.65$ is required for a 95% reliability. The ΔY-values are given in Table 5.

Table 5

Reliability of vertex attribution and $\Delta Y(\varepsilon'_j)$-values

j	Selenoestrogens			Iodoestrogens		
	ε'_j: −1	0	+1	ε'_j: −1	0	+1
3 γ'	2.83	0.74	**0**	8.10	1.85	**0**
3 γ'', γ'''	0.56	0	0.66	2.56	0	1.85
4 γ		—		0.78	0	0.63
6 β	2.45	0.56	0	4.05	0.74	0
6 β', β'', β'''	0.18	0	0.38		—	
6 γ		—		1.92	0	0.65
7 α	2.99	0.81	**0**		—	
7 α'	0.82	0	0.56		—	
7 α''	**0**	0.72	2.47		—	
7 α''', . . . , α^{VI}	0.72	0	0.28		—	
16 α	**0**	0.80	2.78	**0**	1.73	7.85
16 α'	2.39	0.53	0		—	
16 α'', . . . , α^{VI}	0.39	0	0.16		—	
16 β	0.28	0	0.72	0.81	0	1.74
16 β', β'', β'''	0.26	0	0.30		—	
17 α	3.20	0.82	**0**	5.61	0.97	0
17 α'	0.82	**0**	0.72	0.33	0	1.08
17 α''	0.77	0	0.23		—	
17 α'''	1.14	0.28	0		—	
17 α^{IV}, . . . , α^{VII}	0.29	0	0.27		—	
17 β	**0**	0.84	3.24	**0**	2.76	10.10
17 β', β'', β'''	0.30	0	0.70	1.83	0	0.75
17 γ	0.79	0	0.21	2.55	0	1.06

The values under the headings −1, 0, +1, Selenoestrogens and respectively Iodoestrogens are $\Delta Y(\varepsilon'_j)$ values, for substituting the ε_j of the maps S'_1 and respectively S''_1 by ε'_j. The 0 values correspond to $\varepsilon'_j = \varepsilon_j$, i.e. to the attributions in S'_1 and S''_1. The **0** values corresponding to attributions of at least 95% reliability are underlined.

Revue Roumaine de Chimie, **29**, *1*, 99 – 104 (1984)

COORDINATION COMPOUNDS OF Co(II) (d^7) WITH TRYPTOPHAN

P. SPACU, LUMINIȚA PATRON and ADRIANA CONȚESCU
Center of Physical Chemistry, Bucharest, Romania

Received December 15, 1982

In order to establish the bond nature in coordination compounds of amino acids with 3d metal ions as well as the reactivity of these complexes towards small molecules (O_2), some Co(II)-coordination compounds with tryptophan (trp) were studied. The syntheses of these compounds were carried out in different experimental conditions. The compounds were characterized by elemental analysis, electronic spectra, magnetic susceptibility and electrical molecular conductivity.

Our systematic study regarding the formation of metal–aminoacid compounds has been extended to Co(II)(d^7) – DL – tryptophan. In a previous paper we reported the synthesis and properties of Co(II) – aminoacids complexes of [CoL_2] and (CoL_2)O_2(OH) type (L stands for phenylalanine, lysine.HCl and tyrosine)[1].

The synthetic reversible oxygen carriers have been studied in order to find some simple hypothetical models for the natural oxygen-carriers. Natural oxygen complexes play a significant role in absorption, transport and storage of molecular oxygen in biological systems. These oxygen carriers, including hemoglobin, myoglobin, hemerithrin and hemocyanin are generally oxygen-complexes, in which oxygen is coordinated to a metal ion firmly bound to a multidentate ligand. The metal-oxygen combining ratio is 1 : 1 for heme-proteins (mononuclear compounds) and 2 : 1 for non-heme proteins (dinuclear compounds).[2]

The oxygenated forms of most synthetic dioxygen carriers seem to be polynuclear complexes in which two metal ions are coordinated to an oxygen molecule, but mononuclear dioxygen complexes have also been synthesized.[3,4]

Synthetic dioxygen carriers are, normally, compounds which combine reversibly with oxygen and thus do not effect oxygen reduction. Dioxygen may be removed from the complex by heating or by pressure variation.

All metal ions whose complexes combine with dioxygen exist in more than one oxidation state. Apparently, the oxidation potential of the metal ion is suitably modified by chelating agents so that combination with molecular oxygen is effected without appreciable irreversible oxidation of the metal ion. The oxidation potential of Co(II) has an intermediate value in the series [5]:

$$Fe^{II} < Co^{II} < Ni^{II} < Cu^{II}$$

for the reaction:

$$M(II) + O_2 \longrightarrow M(III)$$

The vast majority of metal complexes which take up dioxygen to form 2 : 1 adducts contain Co(II) as metal ion. The frequent use of Co(II) requires further details. On the one hand, it has been shown that replacement of Fe(II) in natural pigments with Co(II) does not alter essentially the most relevant properties related to oxygen fixation of the biological systems. On the other hand, the synthesis of oxygen carriers with Fe(II) has been marred by considerable difficulties.[6] In this way, a lot of Co(II) complex compounds with amino acids (alanine, phenylalanine, lysine, tyrosine, glycine) may reversibly absorb, in solution, molecular oxygen.[7,8] However, only data regarding Co(II)-histidine system are available. The kinetic evidence for this mechanism has generally agreed that dinuclear dioxygen-bridged complexes are formed in a two-step process:

$$\text{I}\ \ Co(his)_2 + O_2 \rightleftarrows Co(his)_2O_2$$

$$\text{II}\ \ Co(his)_2O_2 + Co(his)_2 \rightleftarrows [Co(his)_2]_2O_2$$

It is worth remarking that the isolation of $[Co(his)_2]_2O_2$ complex compound was possible.[5,9–13]

RESULTS AND DISCUSSION

In this paper we extend our previous investigation to study the coordination ability of another substituted alanine derivative, indolylalanine(trp).

The presence of the $-COOH$, $-NH_2$ and N-indolyl groups in trp allows it to act (theoretically) as a tridentate ligand. The potentiometric data suggested the conclusion that the potential donor sites are oxygen atoms of $-$ COOH and nitrogen atoms of NH_2 groups.[14] Battaglia and Pellacani [15] were particularly interested in the donor properties of N-protected aminoacids and have recently suggested that $-$ COOH group behaves as both mono and bidentate species. A few studies on the coordination ability of trp towards metal ions are available [16–18]; the addition of molecular oxygen has not been investigated. Generally, addition of molecular oxygen to Co(II) $-$ ion of the aminoacid compounds requires strongly basic solutions[6–8]; this is particularly true about the Co(II)-trp system. Usually, the synthesis of the non-oxygenated compounds has been carried out also in strongly basic solution.

Our attempts to obtain the oxygen adduct have been most successful in ethanol solution. Surprinsingly, we isolated the non-oxygenated precursor at pH = 6 $-$ 7; it is a pink compound formally corresponding to $[Co(trp)_2(EtOH)_2]$. The brown solution, which suggested the presence of oxygenated species, has been observed repeatedly, at pH = 8. Reversible oxygenation can be repeated several times, also, by heating. It was possible to isolate the brown solid compound by bubbling air through the solution. As already reported,[12] we proposed the formula :

$$[Co(trp)_2(EtOH)]_2O_2 \cdot EtOH$$

The electronic reflectance spectra for both compounds revealed the characteristic bands of Co(II)(d^7) ions with octahedral structure.[19] The spectrum of the pink compound consists of two peaks, one in the higher wave-number range, 950 – 1000 nm, assigned to the $T^4_{1g}(F) \rightarrow \rightarrow T^4_{2g}(F)$ transition and the other at 530 nm assigned to $T^4_{1g}(F) \rightarrow T^4_{1g}(P)$ (Fig. 1). The electronic spectrum of dioxygen adduct is similar with that of $[Co(his)_2]_2 \cdot O_2$, in respect of both the position and the number of the bands in the visible range. The spectra show the characteristic bands at 330 nm and 390 nm. This analogy of electronic spectra suggests that the stereochemistry of two dioxygen adducts does not differ significantly ; we also proposed a dimeric monobridged octahedral structure of our compound.[11, 12]

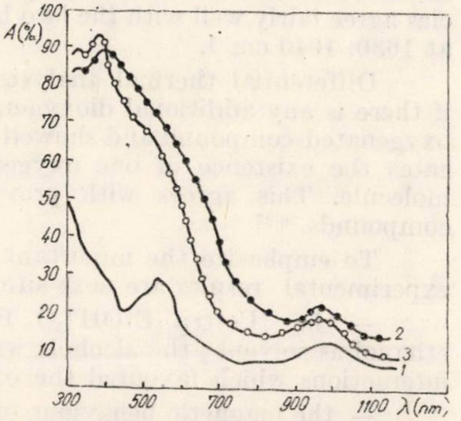

Fig. 1. – Electronic spectra of complexes : *1.* $[Co(trp)_2(EtOH)_2]$ —— ; *2.* $[Co(trp)_3(EtOH)]_2O_2 \cdot EtOH$ –●–●–● *3.* $[Co(trp)_2(EtOH)]_2O_2$ on the film –o–o–o

This assumption has been confirmed by the magnetic behaviour. The magnetic moment of the brown compound is lower (μ = 1.05 MB) than that of the pink compound (μ = 5.06 MB). The difference is most likely due to the change from the high-spin Co(II)(d^7) monomeric species to the low-spin dimeric one.[4, 20, 21] However, the low value found for the dioxygen adduct magnetic moment is due to the contribution of precursor impurities ; this values is similar to those in the literature.[22]

The molecular conductivities in DMF and DMSO at 25° range between 20 and 40 $ohm^{-1}cm^2mole^{-1}$, which correspond to the non-electrolyte type compounds.[23]

In order to supply additional support for the various modes of the trp coordination, the IR spectra of free ligand, parent compound and dioxygen adduct were recorded. A comparison of the vibrational spectra of the free ligand with those of its complexes shows the characteristic bands of the coordinated aminoacid :

–3400 – 3200, 1600 – 1570, 640 – 650 cm^{-1} – for NH_2 group ;
–1640 – 1600, 1400 – 1380, 870 – 730, 550 – 540, 490 – 460 cm^{-1} for carboxyl group.[24]

Taking into account that the trp acts as a bidentate ligand (the chromophore group in the complex compounds is N_2O_2) the ranges 500 – 600 cm^{-1} and 1400 – 1600 cm^{-1} are characteristic to the metal-nitrogen bond from $-NH_2$ group and metal-oxygen bond from carboxyl group, respectively [25]. The IR spectra of both reported complex compounds exhibit a medium intensity absorption band in the $500 - 600\ cm^{-1}$ region ($565\ cm^{-1}$) assigned to $Co-N\ (NH_2)$ bond. The spectra of both compounds also show two strong bands between $1400 - 1600\ cm^{-1}$, which have been assigned to the symmetric and asymmetric ν_{COO^-} —stretch. The higher value of separation $\nu_{asym}(COO^-) - \nu_{sym}(COO^-)$, in the aminoacids coordinated series, provides evidence for the strength of the bond $-COOM$. The IR spectrum of the parent compounds shows ν_{asym} at $1600\ cm^{-1}$ and ν_{sym} at $1415\ cm^{-1}$; the $\Delta\nu$ separation takes a value of $185\ cm^{-1}$, in a good agreement with that found for other tryptophan complexes.[15] The $\nu_{sym}(COO^-)$ of the dioxygen adduct is shifted to $1390\ cm^{-1}$, but $\nu_{asym}(COO^-)$ is observed with additional site splitting. The splitting of the $\nu_{asym}(COO^-)$ mode is tentatively ascribed to dioxygen bridge formation. These frequencies agree fairly well with the two bands reported by Sano and Watters[11,12] at 1630, $1640\ cm^{-1}$.

Differential thermal analysis was therefore preformed to establish if there is any additional dioxygen. The DTA curve was recorded on the oxygenated compound and showed a weight loss (6.81 %) at 53°. This indicates the existence of one oxygen molecule and one solvent (ethanol) molecule. This agrees with previous investigation on oxygen adduct compounds.[26,27]

To emphasize the important features of the dioxygen adduct, the experimental results are next summarized :

— the $[Co(trp)_2EtOH]_2O_2.EtOH$ compound was prepared with ethanol as solvent ; the alcohols were chosen owing to the hydrogen bond interactions which favoured the oxygen uptake [28] ;

— the magnetic behaviour of both compounds confirms the change from the high spin Co(II) (d^7) monomeric species to the low spin dimeric, peroxo-bridged species ;

— the weight loss at 53°(DTA curve) corresponds only to a dinuclear compound ;

— the dinuclear, mono-peroxo bridged species is characterized by the appearance of two bands at 330 and 390 nm (in the electronic spectra) ; the dinuclear dibridge compound is associated to one band at 355 nm .[29]

These data on dioxygen adduct have allowed us to advance the following structural configuration (Fig. 2).

According to previous research, Co-aminoacid complex compounds in solution take up molecular oxygen reversibly. In solid state, this uptake of dioxygen is irreversible.

In order to supply the evidence for the existence of dioxygen in $[Co(trp)_2 \cdot EtOH]_2O_2 \cdot EtOH$, we have sought a new pathway which applies particularly to simulating the natural "oxygen carriers". It consists of the formation of

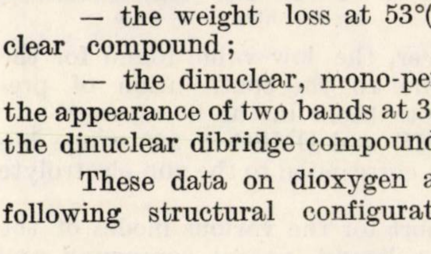

Fig. 2. — Configuration of $[Co(trp)_2(EtOH)]_2O_2$
S is EtOH.

active centers (complex compounds) on silicagel or polymer film. Attempts have been made to attach the aminoacid complex compounds either to modified aerosil[30] or to polyvinyl alcohol (PVA).[31] In our experiments we tried to attach Co-trp compound to polyvinyl alcohol film.

Brown-red films were obtained whose spectra were similar to those observed for the dioxygen adduct (Fig. 1). Each spectrum exhibits the two characteristic bands at 330 and 390 nm.

The behaviour of the films in oxygen adsorption — desorption has been checked by a volumetric method. The amount of adsorbed oxygen (605 μmole/g film) was evaluated from pressure variations.

EXPERIMENTAL

Preparation of the complexes

$[Co(trp)_2(EtOH)_2]$: 2,5 mmole $CoCl_2 \cdot 6H_2O$ and 5 mmoles DL-tryptophan were solved in 20 ml ethanol and HCl conc. ($d = 1.19$) was then added; a solution of 1 : 1 ammonia in ethanol was then added in drops up to a $pH = 6 - 7$. A pink precipitate formed which was filtered, washed with ethanol and dried in air.

Found : C, 56.07 ; N, 9.67 ; Co, 10.34. $C_{26}H_{34}O_6N_4Co$ requires :

C, 56.01 : N, 10.05 ; Co, 10.59

$[Co(trp)_2(EtOH)]_2O_2.EtOH$: This complex was prepared in the same way but up to $pH = 9 - 10$. We succeeded in isolating the brown crystalline compound by flowing air through the brown solution.

Found : C, 54.96 ; N, 9.70 ; Co, 10.33. $C_{50}H_{62}O_{13}N_8CO_2$ requires : C, 54.54 ; N, 10.18 ; Co, 10.72.

Physical measurements

Electronic spectra were recorded on a VSU —1 Zeiss Jena spectrophotometer within a 260 — 1100 nm range using MgO as the standard.

IR spectra on KBr pellets (400 — 4000 cm^{-1}) were recorded with UR-10 Zeiss-Jena spectrophotometer.

Magnetic susceptibilities of solid samples were measured by the Faraday method using Mohr salts as standard.

Molecular electrical conductivities were determined in DMF and DMSO solution at 25° by means of an OK — 102/1 Radelkis Conductometer with a 0.1 μ S—0.25 S measuring range.

REFERENCES

[1] P. Spacu, C. Mărculescu and L. Patron, *Rev. Roumaine Chim.*, **24**, 191 (1979).

[2] L. Roman and O. Bârzu, "Implicații biomedicale ale combinațiilor complexe", Ed. Dacia, Cluj-Napoca, 1979.

[3] J. S. Valentine, *Chem. Rev.*, **73**, 235 (1973).

[4] R. W. Erskine and B. O. Field, "Structure and Bonding", Springer-Verlag, Berlin, 1976.

[5] J. Simplicio and R. G. Wilkins, *J. Amer. Chem. Soc.*, **89**, 2092 (1967).

[6] G. Henrici-Olivé and S. Olivé, "Coordination and Catalysis", Verlag-Chemie, Weinheim, 1977.

[7] J. H. Hearon, *J. Natl. Cancer Instit.*, **9**, 1 (1948).

[8] J. H. Hearon, *J. Natl. Cancer Instit.*, **9**, 333 (1948).

[9] L. Y. Zompa, *J. Chem. Soc. Chem. Commun.*, **1969**, 783.

[10] H. K. Powell, *J. Amer. Chem. Soc.*, **94**, 2664 (1972).

[11] K. Watters and R. G. Wilkins, *Inorg. Chem.*, **13**, 752 (1974).

[12] Y. Sano and H. Tanabe, *J. Inorg. Nuclear Chem.*, **25**, 11 (1963).

[13] M. Woods, *Inorg. Chem.*, **11**, 1713 (1972).
[14] S. T. Chow and C. A. McAuliffe, "Progress in Inorganic Chemistry", vol. **19**, Ed. Wiley-Interscience Publishers, London, 1975, p. 51.
[15] L. P. Battaglia and G. C. Pellacani, *J. Amer. Chem. Soc.*, **102**, 2663 (1980).
[16] O. A. Weber, *J. Inorg. Nuclear Chem.*, **36**, 1341 (1974).
[17] A. Quick, *J. Chem. Soc. Chem. Commun.*, **1973**, 207.
[18] A. Quick, *J. Chem. Soc. Dalton Trans.*, **1975**, 2569.
[19] B. N. Figgis, "Introduction to Ligand Field", Interscience Publishers, New York, 1966.
[20] C. C. McDonald and W. D. Phillips, *J. Amer. Chem. Soc.*, **85**, 3736, (1963).
[21] C. J. Willis, *J. Chem. Soc. Chem. Commun.*, **1974**, 117.
[22] C. Floriani and F. Calderazzo, *J. Chem. Soc.*, (*A*), **1969**, 946.
[23] D. J. Phillyss and S. Y. Tyree, *J. Amer. Chem. Soc.*, **83**, 1806 (1961).
[24] W. L. Kwik and K. P. Ang, *J. Inorg. Nuclear Chem.*, **42**, 302 (1980).
[25] N. H. Cernova, V. V. Strukov, G. B. Avetikian and V. N. Cernojkin, *Zhur. neorg. Khim.*, **25**, 1569 (1980).
[26] B. Jezowska-Trzebiatowska, A. Vogt, H. Kozlovski and A. Jezierski, *Bull. Acad. Polon, Sci. Chim.*, **20**, 187 (1972).
[27] Yu. I. Bratushko and N. G. Melnikova, *Zhur. neorg. Khim.*, **26**, 3007 (1981).
[28] R. S. Drago, P. Cannady and K. A. Leslie, *J. Amer. Chem. Soc.*, **102**, 6014 (1980).
[29] W. R. Harris, G. McLendon and A. E. Martell, *J. Amer. Chem. Soc.*, **92**, 8378 (1976).
[30] K. B. Yatsimirskii and Yu. I. Bratushko, *Doklady Acad. Nauk S.S.S.R.*, **252**, 376 (1980).
[31] A. V. Savitschi, V. N. Kuzovkina and V. K. Beliakov, *Doklady Acad. Nauk S.S.S.R.*, **257**, 1417 (1981).

Revue Roumaine de Chimie, **29**, *1*, 105 – 112 (1984)

THERMODYNAMIC ACTIVITY OF $ZnSO_4$ IN TERNARY SYSTEMS. I

$ZnSO_4 + Me^I_2SO_4 + H_2O$ and $ZnSO_4 + Me^{II}SO_4 + H_2O$ SYSTEMS

SOLOMON STERNBERG and MIHAELA DRĂGĂNOIU
Dept. of Physical Chemistry and Electrochemical Technology,
Polytechnical Institute, Bucharest, str. Polizu 1, Romania

Received January 21, 1983

The mean thermodynamic activity coefficient of $ZnSO_4$ has been determined in ternary systems of the types : $ZnSO_4 + Me^I_2SO_4 + H_2O$ and $ZnSO_4 + Me^{II}SO_4 + H_2O$ using measurements of electromotive forces. The deviations from the ideal behaviour are discussed as a function of the molality of $ZnSO_4$ and the ionic strength of the solutions.

In the present work we set the task of bringing some new contributions to the thermodynamic study of the solutions of polyelectrolytes. In this respect we have studied the variation of the activity coefficient of a 2 : 2 electrolyte ($ZnSO_4$) in the presence of other electrolytes with common anion, symmetrical as well as asymmetrical, as follows :

– electrolytes 1 : 2 – Na_2SO_4, K_2SO_4
– electrolytes 2 : 2 – $MgSO_4$, $MnSO_4$

The determinations have been made in aqueous solutions, at 25° C, using measurements of electromotive forces.

EXPERIMENTAL PART

The cells used for the determinations have been of the types :

$$Pt - Hg_2SO_4 - Hg/ZnSO_4(m_1),\ Me^I_2SO_4(m_2)/Zn_xHg - Pt$$

or, for the mixtures with 2 : 2 electrolytes :

$$Pt - Hg_2SO_4 - Hg/ZnSO_4(m_1),\ Me^{II}SO_4(m_2)/Zn_xHg - Pt.$$

The electrodes we used have been as follows :

– the zinc electrode – a two-phase (25 wt% Hg) – amalgam – was obtained by dissolving zinc powder – 99.9% from Merck – in mercury ;[1]

– the mercury-mercurous sulphate electrode has been chosen in spite of its disadvantages – its tendency to hydrolyze and its rather high solubility – because of the compensating advantage of promoting extremely efficient depolarization and this, coupled with the virtues of mercury, makes this electrode almost as good as the hydrogen electrode in being capable of outstanding reproducibility.[2]

The electrical contacts to the electrodes were obtained with platinum wire.

The emf of the cell was measured with an accuracy of ± 0.1 mV.

The thermodynamic activities have been calculated by the relation : [3]

$$E = E^0 - \frac{\nu RT}{nF} \ln a_{\pm} \qquad \text{(I)}$$

where :

$$\nu = 2$$

$$n = 2$$

It follows :

$$\ln a_{\pm} = \frac{F}{RT}(E^0 - E) = \frac{F}{RT}\Delta E \qquad \text{(II)}$$

The mean activity coefficient in an aqueous solution of two electrolytes is :

$$\gamma_{\pm} = \gamma_{+} \cdot \gamma_{-} = \frac{a_{\pm}}{[m_1(m_1 + m_2)]^{1/2}} \qquad \text{(III)}$$

Different groups of determinations have been made for six given ionic strengths and varying proportions of the two electrolytes in each of the four systems of binary electrolytes.

RESULTS AND DISCUSSION

The results are presented in tables 1 and 2 and the graphic representations in figures 1 respectively 2.

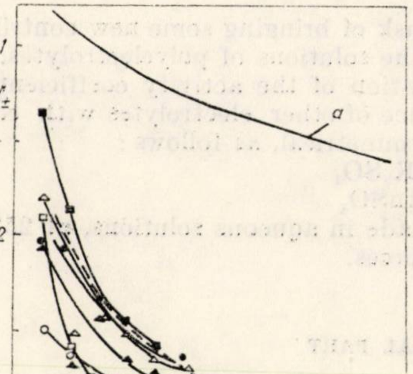

Fig. 1. — The dependence $\ln\gamma_{\pm} = f(m_1)$ in the ternary system $ZnSO_4 + Na_2SO_4 + H_2O$; a — the dependence $\ln\gamma_{\pm Na_2SO_4} = f(m_{Na_2SO_4})$ in the binary system $Na_2SO_4 + H_2O$; b — the dependence $\ln\gamma_{\pm ZnSO_4} f(m_{ZnSO_4})$ in the binary system $ZnSO_4 + H_2O$; —□—□— $I = 3$; —○—○— $I = 2.7$ —▲—▲— $I = 2.4$; —●—●— $I = 2.1$; —△—△— $I = 1.8$; —■—■— $I = 1.5$.

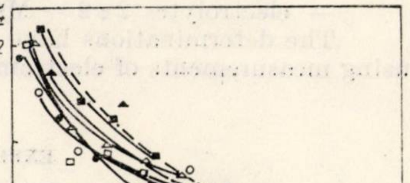

Fig. 2. — The dependence $\ln\gamma_{\pm} = f(m_1)$ in the ternary system $ZnSO_4 + MnSO_4 + H_2O$; b — the dependence $\ln\gamma_{\pm ZnSO_4} = f(m_{ZnSO_4})$ in the binary system $ZnSO_4 + H_2O$; —□—□— $I = 3$; —○—○— $I = 2.7$; —▲—▲— $I = 2.4$; —●—●— $I = 2.1$; —△—△— $I = 1.8$; —■—■— $I = 1.5$.

Table 1

The determination of $\gamma_\pm$ values in aqueous solutions of zinc sulphate + 2 : 2 electrolyte with common ion

Ionic strength	Concentrations mol/1000 g H_2O	$ZnSO_4 + Na_2SO_4$		$ZnSO_4 + K_2SO_4$	
		$-\Delta E \cdot 10^2$	$\gamma_\pm \cdot 10^2$	$-\Delta E \cdot 10^2$	$\gamma_\pm \cdot 10^3$
$I = 3$	$m_1 = 0.75$ $m_2 = 0$	8.55	5.05	8.55	5.05
	$m_1 = 0.675$ $m_2 = 0.1$	8.71	4.59	8.35	5.29
	$m_1 = 0.6$ $m_2 = 0.2$	8.40	5.41	8.60	5.01
	$m_1 = 0.525$ $m_2 = 0.3$	8.39	4.66	8.35	5.82
	$m_1 = 0.45$ $m_2 = 0.4$	9.52	4.78		
	$m_1 = 0.375$ $m_2 = 0.5$	9.06	5.06		
	$m_1 = 0.3$ $m_2 = 0.6$	9.25	5.18		
	$m_1 = 0.225$ $m_2 = 0.7$	9.04	6.41		
	$m_1 = 0.15$ $m_2 = 0.8$	9.16	7.40		
	$m_1 = 0.075$ $m_2 = 0.9$	8.22	14.90		
$I = 2.7$	$m_1 = 0.675$ $m_2 = 0$	8.35	5.35	8.35	5.35
	$m_1 = 0.6$ $m_2 = 0.1$	9.22	5.12	8.23	6.19
	$m_1 = 0.525$ $m_2 = 0.2$	8.77	5.27	8.07	6.17
	$m_1 = 0.45$ $m_2 = 0.3$	8.86	5.40	8.13	7.16
	$m_1 = 0.375$ $m_2 = 0.4$	8.79	5.97		
	$m_1 = 0.3$ $m_2 = 0.5$	8.60	5.48		
	$m_1 = 0.225$ $m_2 = 0.6$	9.24	6.28		
	$m_1 = 0.15$ $m_2 = 0.7$	9.39	7.15		
	$m_1 = 0.075$ $m_2 = 0.8$	9.93	8.04		
$I = 2.4$	$m_1 = 0.6$ $m_2 = 0$	8.64	5.69	8.64	5.69
	$m_1 = 0.525$ $m_2 = 0.1$	8.64	5.97	8.55	6.18
	$m_1 = 0.45$ $m_2 = 0.2$	8.72	6.13	7.93	8.51
	$m_1 = 0.375$ $m_2 = 0.3$	8.71	6.61	8.81	6.36

Table 1 (continued)

Ionic strength	Concentrations mol/1000 g H_2O	$ZnSO_4 + Na_2SO_4$		$ZnSO_4 + K_2SO_4$	
		$-\Delta E \cdot 10^2$	$\gamma_\pm \cdot 10^2$	$-\Delta E \cdot 10^2$	$\gamma_\pm \cdot 10^2$
$I = 2.4$	$m_1 = 0.3$ $m_2 = 0.4$	8.87	6.79	7.49	11.69
	$m_1 = 0.225$ $m_2 = 0.5$	8.57	8.70		
	$m_1 = 0.15$ $m_2 = 0.6$	9.72	6.69	9.02	8.79
	$m_1 = 0.075$ $m_2 = 0.7$	8.94	12.62	10.41	7.11
$I = 2.1$	$m_1 = 0.525$ $m_2 = 0$	8.79	6.15	8.79	6.15
	$m_1 = 0.45$ $m_2 = 0.1$	8.57	7.07	8.77	6.53
	$m_1 = 0.375$ $m_2 = 0.2$	8.82	6.86	7.91	9.80
	$m_1 = 0.3$ $m_2 = 0.3$	8.43	8.75	8.94	7.46
	$m_1 = 0.225$ $m_2 = 0.4$	9.24	15.22	8.64	9.12
	$m_1 = 0.15$ $m_2 = 0.5$	8.29	12.56	8.44	11.85
	$m_1 = 0.075$ $m_2 = 0.6$	9.09	12.75	8.55	28.41
$I = 1.8$	$m_1 = 0.45$ $m_2 = 0$	8.96	6.75	8.96	6.75
	$m_1 = 0.375$ $m_2 = 0.1$	9.03	6.96	9.36	6.11
	$m_1 = 0.3$ $m_2 = 0.2$	8.83	8.20		
	$m_1 = 0.225$ $m_2 = 0.3$	9.03	8.55	9.29	7.71
	$m_1 = 0.15$ $m_2 = 0.4$	9.87	7.87	7.98	7.05
	$m_1 = 0.075$ $m_2 = 0.5$	10.85	16.48	9.26	12.10
$I = 1.5$	$m_1 = 0.375$ $m_2 = 0$	9.57	7.45	9.57	7.45
	$m_1 = 0.3$ $m_2 = 0.1$	8.99	8.61	9.17	8.03
	$m_1 = 0.225$ $m_2 = 0.2$	9.09	9.28	9.09	9.28
	$m_1 = 0.15$ $m_2 = 0.3$	8.20	15.64	8.36	14.66
	$m_1 = 0.075$ $m_2 = 0.4$	7.47	25.64	9.33	18.38

Table 2

The determination of $\gamma_\pm$ values in aqueous solutions of zinc sulphate + 2 : 2 electrolyte with common anion

Ionic strength	Concentrations mol/1000 g H_2O	$ZnSO_4 + MgSO_4$		$ZnSO_4 + MnSO_4$	
		$-\Delta E \cdot 10^2$	$\gamma_\pm \cdot 10^2$	$-\Delta E \cdot 10^2$	$\gamma_\pm \cdot 10^2$
$I = 3$	$m_1 = 0.75$ $m_2 = 0$	8.55	5.05	8.55	5.05
	$m_1 = 0.65$ $m_2 = 0.1$	8.12	6.00	8.35	5.86
	$m_1 = 0.55$ $m_2 = 0.2$	8.33	6.01	8.34	5.97
	$m_1 = 0.45$ $m_2 = 0.3$	8.58	6.00	8.45	6.34
	$m_1 = 0.35$ $m_2 = 0.4$	8.56	6.86	8.54	6.94
	$m_1 = 0.25$ $m_2 = 0.5$	8.81	7.36	8.70	7.71
	$m_1 = 0.15$ $m_2 = 0.6$	9.07	8.59	9.52	7.23
	$m_1 = 0.05$ $m_2 = 0.7$	9.16	14.41	9.29	13.71
$I = 2.7$	$m_1 = 0.675$ $m_2 = 0$	8.35	5.35	8.35	5.35
	$m_1 = 0.575$ $m_2 = 0.1$	8.24	6.39	8.32	6.22
	$m_1 = 0.475$ $m_2 = 0.2$	8.53	6.30	8.28	6.95
	$m_1 = 0.375$ $m_2 = 0.3$	8.51	7.15	8.82	6.33
	$m_1 = 0.275$ $m_2 = 0.4$	8.45	8.47	9.41	5.87
	$m_1 = 0.175$ $m_2 = 0.5$	8.50	10.50	9.39	7.42
	$m_1 = 0.075$ $m_2 = 0.6$	9.07	12.85	9.59	10.49
$I = 2.4$	$m_1 = 0.6$ $m_2 = 0$	8.64	5.69	8.64	5.69
	$m_1 = 0.5$ $m_2 = 0.1$	8.78	5.91	8.78	5.91
	$m_1 = 0.4$ $m_2 = 0.2$	6.90	6.90	8.84	6.46

Table 2 (continued)

Ionic strength	Concentrations mol/1000 g H_2O	$ZnSO_4 + MgSO_4$		$ZnSO_4 + MnSO_4$	
		$-\Delta E \cdot 10^2$	$\gamma_\pm \cdot 10^2$	$-\Delta E \cdot 10^2$	$\gamma_\pm \cdot 10^2$
$I = 2.4$	$m_1 = 0.3$ $m_2 = 0.3$	8.95	7.11	8.09	9.99
	$m_1 = 0.2$ $m_2 = 0.4$	9.73	6.42	9.70	6.52
	$m_1 = 0.1$ $m_2 = 0.5$	6.64	9.65	9.47	11.64
$I = 2.1$	$m_1 = 0.525$ $m_2 = 0.0$	8.79	6.15	8.79	6.15
	$m_1 = 0.425$ $m_2 = 0.1$	7.80	10.05	9.21	5.79
	$m_1 = 0.325$ $m_2 = 0.2$	9.36	6.25	9.47	5.99
	$m_1 = 0.225$ $m_2 = 0.3$	10.05	5.74	9.72	7.33
	$m_1 = 0.125$ $m_2 = 0.4$	6.82	8.10	9.60	9.18
	$m_1 = 0.025$ $m_2 = 0.5$	11.19	15.99	10.87	12.48
$I = 1.8$	$m_1 = 0.45$ $m_2 = 0$	8.96	6.75	8.96	6.75
	$m_1 = 0.35$ $m_2 = 0.15$	9.95	7.85	8.11	7.40
	$m_1 = 0.25$ $m_2 = 0.2$	10.02	6.40	9.30	7.88
	$m_1 = 0.15$ $m_2 = 0.3$	9.98	7.80	9.72	8.63
	$m_1 = 0.05$ $m_2 = 0.4$	10.14	12.69	9.97	13.78
$I = 1.5$	$m_1 = 0.375$ $m_2 = 0$	9.57	7.45	9.57	7.45
	$m_1 = 0.275$ $m_2 = 0.1$	8.66	10.55	9.55	9.18
	$m_1 = 0.175$ $m_2 = 0.2$	10.02	18.58	9.38	9.99
	$m_1 = 0.075$ $m_2 = 0.3$	7.14	36.61	9.47	14.75

The exclusive dependence on the ionic strength, according to the Debye-Hückel theory, should have given a constant value $\gamma_{\pm}$ for any ratio between the concentrations of the two electrolytes, which is not the case for the dependence formerly quoted. Harned described in his works [2] a linear dependence $\ln\gamma - I$ for the ternary mixtures of hydrochloric acid + alkali halides + H_2O.

In the systems studied by us variations of the mean activity coefficient of $ZnSO_4$ appear at a constant total ionic strength, depending on the ratio of the two electrolytes. These deviations have a greater value than those mentioned in literature for 1 : 1 electrolytes [4] or for H_2SO_4 in solutions of alkali sulphates.[5]

As far as figures 1 and 2 are concerned it is obvious that the dependences $\ln \gamma_{\pm} = f(m_1)$ at I = constant for the ternary mixture follow that of the $ZnSO_4 + H_2O$ system, although the latter does not refer to constant ionic strength. At small ionic strengths, in the limit of the experimental errors, the behaviour of the ternary mixture is practically identical with that of the binary mixture. At greater values of the ionic strengths. although the type of dependences maintained is that for the binary mixture, the appearing negative deviations from ideality are much greater.

This behaviour can be explained by the formation of ionic associates in which zinc cation is involved.

Harned's law was based on experiments with mono-monovalent electrolytes where the ionic associations are less probable, the tendency to associate growing strongly with the valence of the associating ions.

The difference between the behaviour of bivalent sulphate solutions, where the formation of ionic pairs is more important, and those of 1 : 2 sulphates, where the association is weaker, can be noticed in figure 1, the curve $\ln\gamma = f(m)$ representing the binary system $Na_2SO_4 + H_2O$, which presents smaller deviations from the ideal behaviour.

The increase of the ionic strength favours the formation of ionic associates thus explaining the arrival at a practically constant value for $\ln\gamma_{\pm}$ at smaller concentrations of $ZnSO_4$ as compared with the binary system.

For the other systems studied by us dependences very similar to those in figure 1 have been obtained.

The mean activity coefficient of $ZnSO_4$ in the ternary solution $\gamma_{\pm}$, at a molality m_1, can be expressed by an equation of the type :

$$\ln \gamma_{\pm}(t, m_1) = \ln \gamma_{\pm}(b, m_1) + \Delta \ln \gamma_{\pm} \qquad \text{(IV)}$$

where $\gamma_{\pm}$ (b, m_1) refers to a binary solution of $ZnSO_4$ at the same molality m_1 and $\Delta\ln \gamma_{\pm}$—the correction factor—is function of m_2, of the ionic strength I as well as of the load and the nature of the second cation. For the compositions $m_1 \cong m_2$ — where the correction is the most significant — the factor $\Delta \ln \gamma_{\pm}$ does not exceed 10% of the $\ln \gamma_{\pm}$ (t, m_1) value (figure 3).

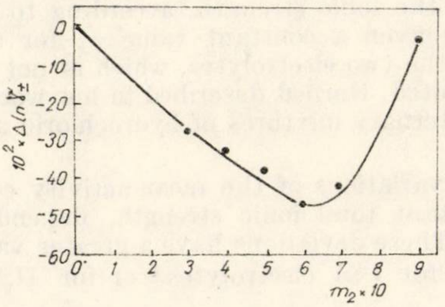

Fig. 3. – The variation of the correction factor $\Delta \ln \gamma_{\pm}$ with the increase of the concentration m_2 for the ternary system $ZnSO_4 + Na_2SO_4 + H_2O$ at $I=3$.

REFERENCES

[1] A. Lewandowski, *Electrochim. Acta*, **23**, 1303 (1978).

[2] D. J. D. Ives and G. J. Janz, "Reference Electrodes", Academic Press, New York, 1961, p. 403.

[3] S. Sternberg and F. Daneş, "Termodinamică chimică aplicată", Ed. Academiei, Bucureşti, 1978, p. 342.

[4] H. Harned and B. Owen, "The Physical Chemistry of Electrolytic Solutions", third ed., Reinhold Publishing, New York, 1958, p. 592.

[5] G. A. Motornaya and E. Ya. Ben'yash, *Zhur fiz. Khim.*, **47**, 459 (1973).

Revue Roumaine de Chimie, **29**, *1*, 113–120 (1984)

LA CINÉTIQUE DE L'HYDRATATION DU CIMENT ALUMINEUX CA—CA_2 ET LA COMPOSITION DE SES PRODUITS D'HYDRATATION

I. TEOREANU*, N. ANGELESCU** et D. ŢUCLEA**
*L'Institut Polytechnique — Bucarest, Polizu 1
**L'Institut de Recherches Métallurgiques — Bucarest, Mehadiei 39, Roumanie

Reçu le 14 juillet, 1982

Dans ce travail on examine, du point de vue quantitatif et qualitatif, les processus d'hydratation du $CaO \cdot Al_2O_3$ (CA), $CaO \cdot 2Al_2O_3$ $(CA)_2$ et d'un ciment alumineux de type CA+CA_2, par la méthode de diffraction des rayons X.

In the present paper, hydration processes of $CaO \cdot Al_2O_3$ (CA), $CaO \cdot 2Al_2O_3$(CA_2) and of a CA + CA_2 type aluminous cement are quantitatively and qualitatively examined by the X-ray diffraction method.

1. INTRODUCTION

La cinétique de l'hydratation des ciments alumineux et de leurs composés minéraux, avec des implications sur la connaissance de ses facteurs d'influence et du mécanisme du processus, a été assez peu étudiée.

L'examen par diffraction des processus d'hydratation des ciments alumineux, des ciments hydrauliques en général, utilisé comme méthode d'investigation, fournit des renseignements qualitatifs — concernant la composition des produits, et quantitatifs — concernant le degré d'hydratation, la cinétique du processus et la composition de phase du système.

Les renseignements quantitatifs se basent sur le fait que l'intensité intégrale d'une ligne de diffraction est proportionnelle au volume de la substance cristalline, le coefficient de proportionnalité dépendant des propriétés du faisceau incident, de la méthode expérimentale utilisée et des propriétés de la structure étudiée.

La méthode expérimentale et les propriétés du faisceau incident étant établies, il faut tenir compte, nécessairement, dans la description mathématique de la méthode, des propriétés d'absorption du constituant structural examiné. Supposant qu'il y a un échantillon de composition homogène, formé par plusieurs constituants différents du point de vue de la structure et ayant été soumis à un broyage très fin, on peut considérer négligeables les effets de la microabsorption et de l'extinction.

De même, l'échantillon doit avoir une épaisseur suffisante pour donner le maximum d'intensité à la diffraction.

Dans ces conditions, par l'évaluation de l'intensité d'une ligne appartenant à un certain composant de l'échantillon examiné par diffraction on déduit la proportion de celui-ci.

2. CONDITIONS EXPÉRIMENTALES

On a examiné la cinétique de l'hydratation d'un ciment alumineux de type $CA-CA_2$ (Alicem 2), ainsi que la cinétique de l'hydratation de l'aluminate de calcium et du dialuminate de calcium synthétisés individuellement (étalons). Dans ce but, par l'analyse de diffraction, X, on a suivi, par la mesure des impulsions, l'évolution de l'intensité des principales lignes du CA et CA_2 dans le spectre de diffraction du liant en cours d'hydratation, en considérant que l'intensité de la ligne de diffraction (I) dans le composé anhydre correspond à la proportion initiale de ces composants.

La loi de la variation de l'intensité, lors du processus d'hydratation, fournira des renseignements sur la cinétique de l'hydratation des composants analysés (tant les constituants du ciment que ceux des liants monominéraux étalon).

En même temps, ont été effectuées des analyses qualitatives à l'aide des spectres de diffraction, afin d'obtenir des renseignements sur la composition des produits d'hydratation résultés des processus d'hydratation-hydrolyse du ciment Alicem 2 et des échantillons-étalon, en utilisant des durées différentes.

2.1. L'appareillage utilisé

Dans le cadre des recherches on a utilisé un générateur de rayons X Seifert, muni d'un tube de cuivre alimenté à 40 KV et 20 mA et un goniomètre HZG3, ayant la fente d'entrée de 2mm et la fente du compteur de 0,28 mm, muni d'un dispositif pour la rotation de l'échantillon.

Pour chaque durée d'hydratation, l'échantillon a été broyé à moins de 40 μm et légèrement compacté dans un support d'aluminium. On a tracé un diffractogramme ordinaire suivi par la mesure (comptage) à l'aide d'un compteur, correspondant aux lignes caractéristiques de l'aluminate de calcium et du dialuminate de calcium.

Avant de commencer les recherches proprement dites, on a mis l'appareil dans les mêmes conditions de travail, la vérification étant réalisée par le comptage de la ligne de l'aluminium en commençant de 19°18′, qui doit avoir une intensité de 100 000 impulsions/min.

Pour les mesures, on a utilisé les lignes à partir de $d = 2{,}96$ Å dans le cas de l'aluminate de calcium et de $d = 3{,}52$ Å pour le dialuminate de calcium. Le comptage a été effectué pendant une minute, la fente étant largement ouverte ; afin de comprendre la ligne de diffraction dans toute sa largeur et du nombre d'impulsions correspondant aux pics analysés, on a soustrait le fond continu, déterminé en le mesurant dans les mêmes conditions dans la zone du fond voisin aux pics envisagés. Pour chaque durée d'hydratation on a effectué des comptages sur trois échantillons du même composant, le résultat étant la moyenne des trois mesures.

2.2. Liants soumis à l'hydratation

Le ciment alumineux Alicem 2 a été obtenu par voie industrielle, par frittage à $\theta = 1\,460°C$.

Les composants minéraux-étalon ont été synthétisés par réaction en phase solide, à partir de mélanges homogènes de substances pures du point de vue chimique : Al_2O_3 et $CaCO_3$.

Les mélanges réagissants correspondants aux composants minéraux-étalon (CA et CA_2), dosés dans les proportions indiquées dans le tableau 1, ont été homogénéisés dans un broyeur en agate pendant 4 h. Les compositions homogénéisées, liées à vinarol, ont été agglomérées sous forme de cylindres ayant le rayon de 2,5 cm et la hauteur de 5 cm, et ensuite calcinées en deux phases, à 1520°C avec une durée de maintien à la température maximale de synthèse de 5 h, dans un four électrique à résistance de superkanthal. Les échantillons ainsi calcinés ont été broyés ensuite au-dessous de 40 μm dans le broyeur en agate.

Le ciment alumineux Alicem 2, ainsi que les aluminates de calcium-étalon, en état broyé, mélangés avec de l'eau (rapport eau/solide = 0,3), ont été hydratés durant 6 h, 12 h, 24 h, 3 jours et 7 jours, à la température et pression normales.

Les échantillons anhydres et ceux hydratés dans les conditions ci-dessus ont été analysés par diffraction de la manière indiquée.

Tableau 1

La composition des mélanges de réaction des minéraux-étalon (CA et CA_2)

Composant oxydique	CA	CA_2
Alumine, %	50,5	67,11
Carbonates de calcium %	49,5	32,89

3. RÉSULTATS EXPÉRIMENTAUX

Les diffractogrammes des échantillons examinés ont été présentés dans les figures 1 — 3.

De l'analyse quantitative par diffraction des rayons X des échantillons anhydres — la méthode de l'étalon externe — on a obtenu les résultats présentés dans le tableau 2 (pour les échantillons des substances minérales-étalon — en comparaison avec la composition minérale potentielle calculée à partir de leur composition oxydique).

En suivant l'évolution de l'intensité des principales lignes du CA et du CA_2 des échantillons en cours d'hydratation — tant de ciment Alicem 2 que de liants monominéraux-étalon (tel qu'on a déjà montré : 2,96 Å — pour l'aluminate de calcium et 3,52 Å — pour le dialuminate de calcium), on peut constater, du point de vue cinétique, l'existence, dans les limites de temps utilisées à la recherche, de deux intervalles différents : un intervalle initial—caractérisé par une vitesse plus basse de développement du processus (qu'on peut considérer comme une ***étape d'induction***) et un autre — caractérisé par une vitesse évidemment accrue de développement du processus (qu'on peut considérer comme une ***étape d'accélération***).

Les données expérimentales, présentées dans les tableaux 3 — 4 et dans la figure 4, ont mis en valeur la vitesse d'hydratation plus élevée du CA par rapport à CA_2, surtout dans le ciment Alicem 2. Le degré de frittage plus élevé des liants monominéraux-étalon, pour des intervalles équivalents, conduit à l'obtention d'un degré d'hydratation de ceuxci beaucoup plus réduit que dans le ciment de type $CA-CA_2$ examiné, surtout dans le cas de l'aluminate de calcium — composant plus actif par rapport à l'eau et dont l'activité est, par conséquent, beaucoup plus affectée par l'accroissement du degré de frittage. La différence plus grande entre le degré d'hydratation, pour des durées plus élevées d'hydratation, entre CA_2 du ciment Alicem 2 et CA_2-étalon, pourrait s'expliquer aussi par l'activation de l'hydratation de ce dernier dans le ciment $CA-CA_2$, à la suite de l'hydratation antérieure, beaucoup plus puissante, de l'aluminate de calcium.

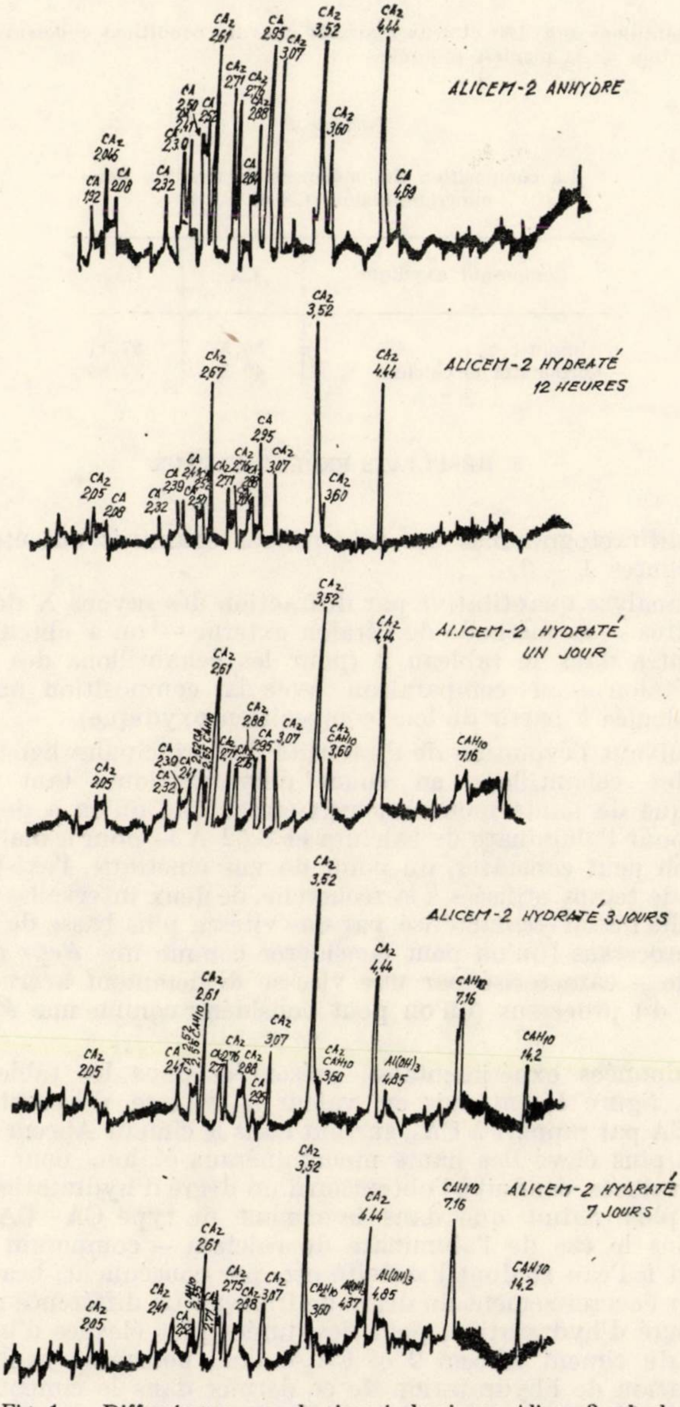

Fig. 1. — Diffractogrammes du ciment alumineux Alicem 2 anhydre et hydraté, en utilisant des durées différentes.

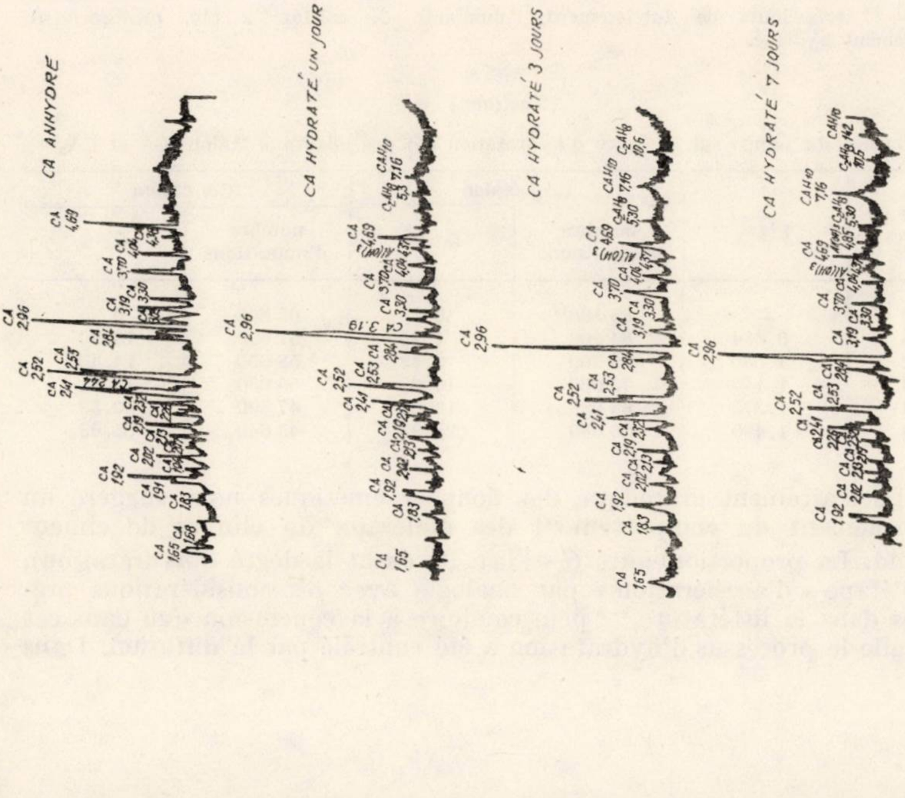

Fig. 2. — Diffractogrammes du CA étalon anhydre et hydraté, en utilisant des durées différentes.

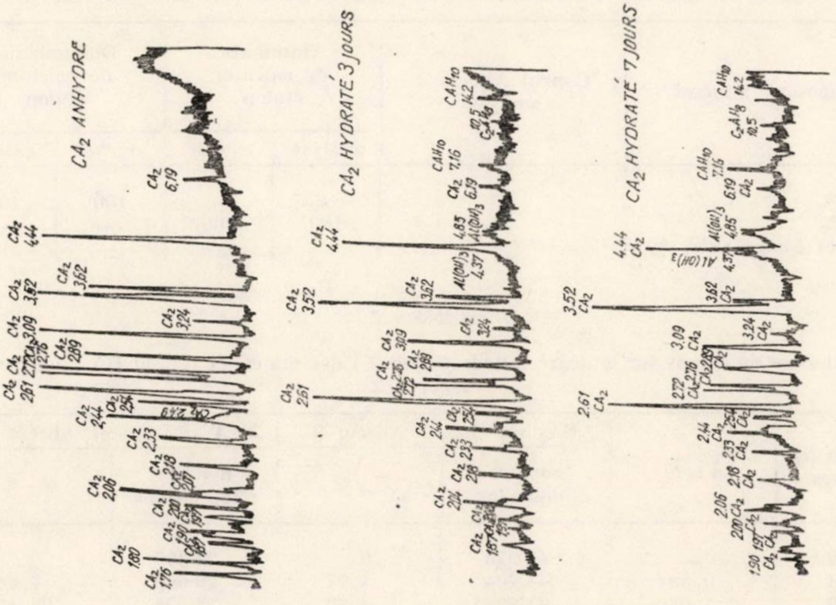

Fig. 3. — Diffractogrammes du CA$_2$ étalon anhydre et hydraté, en utilisant des durées différentes.

Tableau 2

La composition minérale des liants monominéraux et du ciment Alicem 2 ($CA+CA_2$)

Composant minéral	Ciment Alicem 2 analysé	Aluminate de calcium étalon		Dialuminate de calcium étalon	
		analysé	calculé	analysé	calculé
CA_2, %	60	—	—	100	100
CA, %	32	100	100	—	—
d'autres composants, %	8	—	—	—	—

Tableau 3

L'influence du temps sur le degré d'hydratation (*G*) des minéraux CA_2 et CA du ciment Alicem 2

Temps (*t*) heures	$\sqrt{\lg t}$	CA_2 du ciment Alicem 2		CA du ciment Alicem 2	
		nombre d'impulsions	*G*, %	nombre d'impulsions	*G*, %
0	—	43 270	0	22 406	0
6	0,884	41 204	4,77	20 666	7,36
12	1,040	41 198	4,80	16 031	28,45
24	1,175	37 294	13,81	8 598	61,18
72	1,370	25 968	39,98	—	*)
168	1,490	12 833	70,34	—	—

---

*) à trois jours de durcissement, l'aluminate de calcium a été, pratiquement, complètement hydraté.

Tableau 4

L'influence du temps sur le degré d'hydratation (*G*) des minéraux-étalon (CA et CA_2)

Temps (*t*) heures	$\sqrt{\lg t}$	CA_2 étalon		CA étalon	
		nombre d'impulsions	*G*, %	nombre d'impulsions	*G*, %
0	—	85 166	0	68 866	0
6	0,884	84 100	1,25	61 800	10,20
12	1,040	82 200	3,48	58 650	14,83
24	1,175	76 600	10,05	56 050	18,61
72	1,370	68 966	19,02	47 800	30,59
168	1,490	63 080	25,93	43 640	36,63

Le traitement graphique des données cinétiques nous suggère un rapprochement du comportement des minéraux du clinker de ciment portland. La proportionnalité $G \sim \sqrt{\lg t}$ (G étant le degré d'hydratation), dans l'étape « d'accélération » par analogie avec les considérations présentées dans la littérature,[1-3] peut conduire à la conclusion que dans cet intervalle le processus d'hydratation a été contrôlé par la diffusion. Dans ces conditions, on peut supposer que dans l'étape « d'induction », le processus d'hydratation se produisant à la surface, celui-ci a été probablement contrôlé, pour la plupart de la durée de développement, par l'apparition des germes cristallins appartenant aux nouvelles phases hydratées. La période « d'induction » est évidemment plus basse pour le CA (6 heures environ, par rapport à 24 heures pour le CA_2) dans le ciment Alicem 2 ; sa durée pour les deux substances minérales-étalon fortement frittées s'approche effectivement, en se prolongeant, pour l'aluminate de calcium par rapport à son comportement dans le ciment Alicem 2.

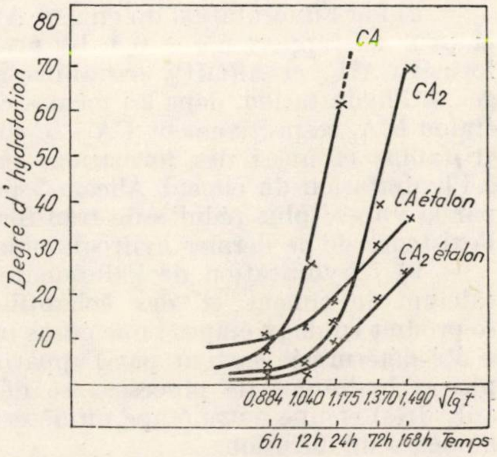

Fig. 4. — L'influence du temps sur le degré d'hydratation du CA et CA_2 du ciment alumineux Alicem 2 et des composants minéraux-étalon.

L'examen de la composition des composants hydratés, à base des diffractogrammes présentés dans les figures 1 — 3, relève, de ce point de vue aussi, certaines différences entre les échantillons de ciment Alicem 2 et ceux de liants monominéraux-étalon.

Dans les conditions du développement des processus d'hydratation (conditions normales de température et pression) on constate la formation, dans le cas des pâtes de ciment Alicem 2, de l'hydroaluminate CAH_{10} (les lignes 14,2 Å, 7,16 Å, 3,60 Å, 2,55 Å), ainsi que de l'hydroxyde d'aluminium (les lignes 4,85 Å, 4,37 Å). A l'hydratation des liants monominéraux-étalon, on constate la formation des hydroaluminates de calcium CAH_{10} (lignes 14,2 Å, 7,16 Å) et C_2AH_8 (lignes 10,6 Å, 5,30 Å), ainsi que de l'hydroxyde d'aluminium (4,85 Å, 4,37 Å). Ces observations sont, en général, en accord avec les informations de la littérature [4,5] concernant l'hydratation des aluminates de calcium, dans les conditions de travail mentionnées.

L'absence des lignes caractéristiques pour l'hydroaluminate C_2AH_8 dans les échantillons hydratés du ciment Alicem 2, pourrait, éventuellement, s'expliquer par la vitesse plus réduite de transformation du CAH_{10} en C_2AH_8 ainsi que par l'existence de ce dernier en état de gel (le fond de radiations plus élevé dans les diffractogrammes des échantillons hydratés de ciment, par rapport à celui des diffractogrammes des échantillons de liants monominéraux, pourrait être un argument à ce propos).

4. CONCLUSIONS

Les résultats des recherches effectuées conduisent à quelques conclusions plus importantes concernant la composition des produits d'hydratation et la cinétique de l'hydratation du ciment alumineux $CA-CA_2$, ainsi que celle des liants monominéraux-étalon (CA respectivement CA_2), à savoir :

a) Par l'hydratation du ciment Alicem 2 dans des conditions normales et pour un rapport a/c = 0,3, les premiers 7 jours du processus, se sont formés CAH_{10} et $Al(OH)_3$ cristallins, ainsi que des formations en état de gel. A l'hydratation, dans les mêmes conditions, des liants monominéraux-étalon (CA, respectivement CA_2) se sont formés CAH_{10}, C_2AH_8, $Al(OH)_3$ – cristallins et aussi des formations en état de gel. L'absence du C_2AH_8 à l'hydratation du ciment Alicem 2 pourrait s'expliquer, éventuellement, par la vitesse plus réduite de transformation du CAH_{10} en C_2AH_8 et par l'existence de ce dernier hydroaluminate prépondérant en état de gel.

b) L'hydratation de l'aluminate de calcium et du dialuminate de calcium du ciment et des échantillons de liant monominéral-étalon, se produit en deux étapes : une étape initiale – où la vitesse d'hydratation a été déterminée surtout par l'apparition des germes cristallins dans les phases hydratées (le processus se développant à la surface des grains anhydres) et une autre étape où déterminantes de la vitesse sont les phénomènes de diffusion.

c) La cinétique de l'hydratation du CA et du CA_2 est plus accélérée pour les constituants minéraux du ciment Alicem 2 par rapport aux mêmes constituants minéraux synthétisés comme liants monominéraux (étalon).

Les différences apparaissant à l'hydratation du CA et du CA_2 du ciment, par rapport à l'hydratation des échantillons, sont dues, surtout, au degré de frittage plus élevé de ces derniers.

BIBLIOGRAPHIE

[1] I. Teoreanu et M. Muntean, *Silicat. Ind.*, **39**, 49 (1974).
[2] I. Teoreanu et C. Hriţcu, *Mat. Constr.* **6**, 157 (1976).
[3] I. Teoreanu et C. Hriţcu, *Memoriile Secţiilor Ştiinţifice – Acad. R. S. România. Seria IV*, **3**, 251 (1980).
[4] I. Teoreanu, V. Moldovan, M. Georgescu, M. Muntean et A. Puri, « Bazele fizico-chimice ale întăririi lianţilor anorganici ». Bucureşti, Ed. Didactică şi Pedagogică, 1972.
[5] A. Fleurence et L. Lecrivain, *Bull. Soc. Franç. Ceram.*, **1971**, 29.

Revue Roumaine de Chimie, **29**, *1*, 121 – 129 (1984)

HETEROCYCLIC ORGANOBORON COMPOUNDS. XVII.[1]

AXIAL CHIRALITY OF BORON CHELATES EVIDENCED BY ^{1}H–NMR SPECTROSCOPY IN THE PRESENCE OF CHIRAL ADDITIVES

CORNELIA UNCUŢA,[a] IOANA BALLY,[b] C. DRĂGHICI,[a] F. CHIRALEU[a] and A.T. BALABAN*[c]

[a] Centre for Organic Chemistry, Bucharest
[b] Institute of Physics, and Nuclear Engineering, Bucharest
[c] Correspondence author : The Polytechnic Institute, Department of Organic Chemistry — TCH, Splaiul Independenţei 313, 76206 Bucharest — 16, Romania

Received May 28, 1983

Chiral chelatic organoboron compounds of general formulas 1 – 4 were synthetized from 1,3,2-benzodioxaboroles or diarylborinic esters and tropolones or 1,3-diketones. Intermolecular enantiomeric splittings were observed for signals in the ^{1}H–NMR spectra recorded in the presence of a chiral shift reagent. The site of complexation is discussed. An intramolecular splitting was also observed with the same shift reagent for the prochiral boron chelate 2a derived from acetylacetone.

1. INTRODUCTION

In a series of communications, several organoboron chelate compounds of general formulas **1** – **4** were synthetized and characterized by absorption IR and UV spectroscopy [2] as well as by ^{1}H–NMR spectroscopy.[2b,3] Dipole moment measurements[4] confirmed the proposed structures of these chelates : the experimental values were in fairly good agreement with the theoretical values calculated for a chelated structure with a delocalized charge distribution on both oxygen atoms of the chelatic ring.

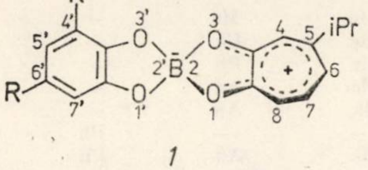

1

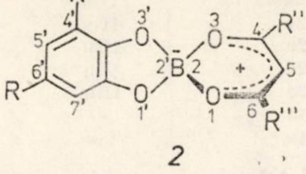

2

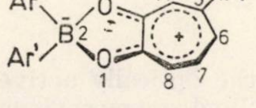

3

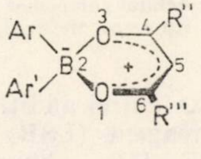

4

The tetracoordinated boron atom of these compounds is a good candidate in generating molecular chirality with suitable substituents. Indeed, as early as 1968, a previous part of this series [5] reported the preparation of a compound **3** (Ar = Ph, Ar′ = An, where An stands for a *p*-anisyl residue) and suggested that such a compound could be resolved in enantiomers. NMR techniques in the presence of chiral additives have become an effective tool for the direct and unambiguous evidence of chirality without having to resolve the enantiomers and to perform polarimetric measurements;[6] other quotations [7] refer particularly to axial chirality. We decided therefore to investigate the chirality of the organoboron chelatic compounds with general formulas **1** — **4** by this particular technique.

2. RESULTS

Table 1 presents the compounds which were investigated; in the experimental part, the general method of synthesis and the characterization of the compounds are given. The chosen substitution pattern (R and/or R′ ≠ H, Ar ≠ Ar′ and R″ ≠ R‴) ensures the lack of reflexion symmetry and hence the axial chirality of these compounds. The choice of the substituents was primarily determined by the necessity to have in the ^1H-NMR spectra intense and non-overlapping singlets, whose splitting can be easily observed.

Table 1

Chiral organoboron chelates

Group[b]	R	R′	R″	R‴	Ar	Ar′
Position	6′	4′	4	6	—	—
Comp.						
1a[a]	H	H	—	—	—	—
1b	tBu	H	—	—	—	—
1c	tBu	tBu	—	—	—	—
2a[a]	tBu	tBu	Me	Me	—	—
2b	tBu	H	Me	Ph	—	—
2c	tBu	tBu	Me	Ph	—	—
2d	tBu	tBu	Me	An	—	—
2e	tBu	tBu	Ph	An	—	—
3a	—	—	—	—	Ph	An
4a	—	—	Me	An	Ph	An

[a] Achiral compound for comparison
[b] An = $p-MeOC_6H_4$

As chiral additive, we have chosen the optically active lanthanide shift reagent (LSR) tris(heptafluoropropylhydroxymethylene)-d-camphorato—Eu(III), abbreviated $Eu(hfcam)_3$, of commercial source. The ^1H-NMR spectra were recorded in methylene chloride solution at 60 MHz and room temperature, with TMS as internal standard. On progressive addition of the chiral shift reagent, the expected intermolecular enantiomeric splitting of the signals appeared. This means that the two enantiomeric boron chelates constituting the racemic mixture become diastereomers when complexed with the chiral LSR. Figure 1 presents a representative example, namely that of the compound **2c**. The relative amount

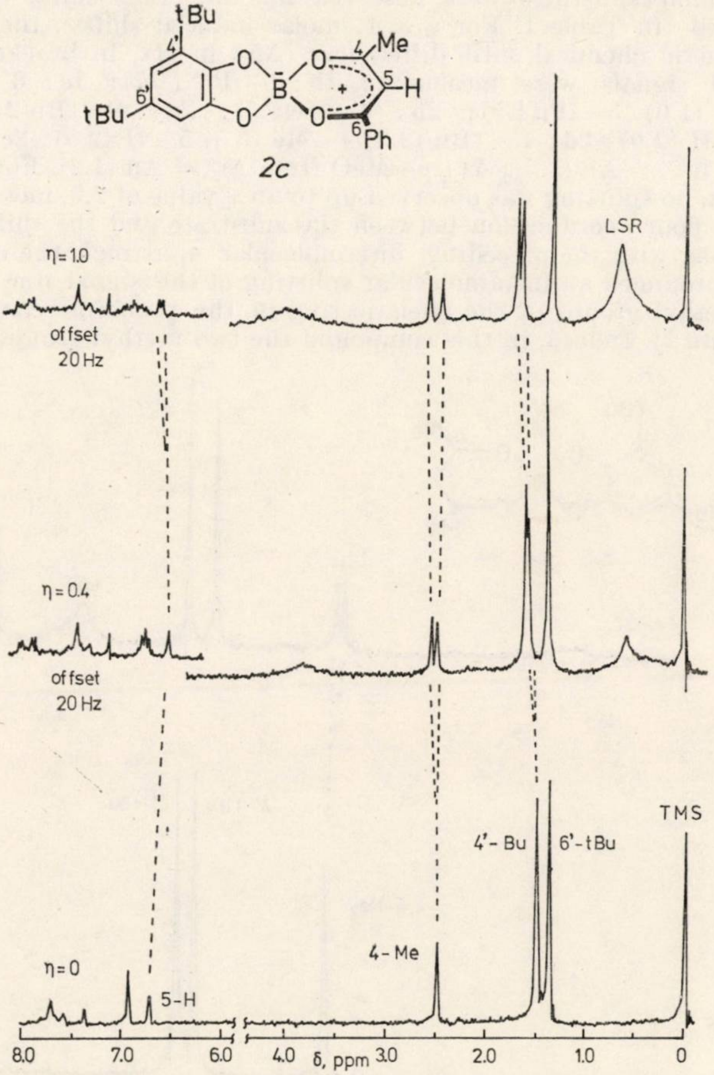

Fig. 1. — Intermolecular splitting of the signals in the ^1H-NMR spectra of the chiral compound **2c** recorded in methylene chloride in the presence of increasing relative amounts (η) of the chiral shift reagent $Eu(hfcam)_3$. The peak denoted by LSR is the signal due to the lanthanide shift reagent.

of LSR is expressed by the molar ratio : η = moles Eu(hfcam)$_3$/moles boron chelate.

Similar splittings were observed for the other chiral compounds mentioned in Table 1. For $\eta = 1$ (molar induced shifts), the following enantiomeric chemical shift differences ($\Delta\Delta\delta$ in Hz, in brackets) of the indicated signals were measured : **1b** : 5–iPr (1.7) ; **1c** : 6′–tBu(0.5) 4′–tBu (1.0) 5–iPr(1.7) ; **2b** : 4–Me(5.5) ; **2c** : 4′–tBu(2.9) 4–Me (7.3) 5–H (2.0) ; **2d** : 4′–tBu (3.2) 4–Me (6.5) 5–H (2.5) ; **2e** : p–MeO from 6–R‴ = An (1.5) ; **4a** : p–MeO from Ar′ = An (1.2). For the compound **3a**, no splitting was observed up to an η value of 2.2, most probably due to a poor coordination between the substrate and the shift reagent.

Along with the preceding intermolecular splittings, the chiral shift reagent produced an intramolecular splitting of the signal due to the 4- and 6-methyl groups of the chelatic ring in the prochiral compound **2a** (see Figure 2). Indeed, in this compound the two methyl groups are enantiotopic by internal comparison and isochronous in the normal spectrum (Fig. 2A), but become diastereotopic by internal comparison due to the interaction with the chiral shift reagent and consequently anisochronous in the spectrum recorded in its presence (Fig. 2B). Unlike the splitting observ-

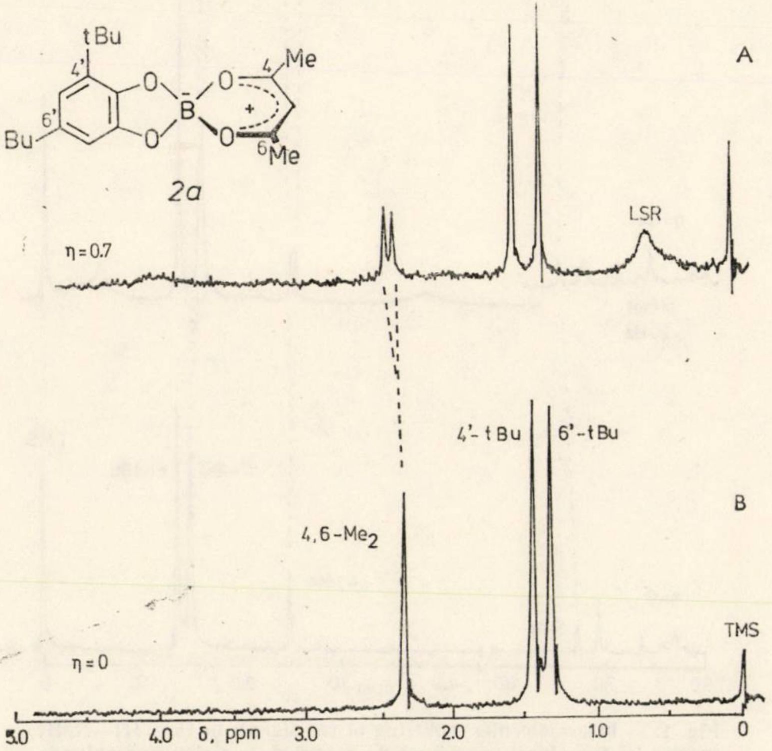

Fig. 2. — Intramolecular splitting of the signal of the 4,6-methyl groups in the ^{1}H–NMR spectra of the prochiral compound **2a** recorded in the presence of the chiral shift reagent Eu(hfcam)$_3$ Solvent : CDCl$_3$; Temp. : 30 – 32°C.

ed for the chiral compounds (e.g. Fig. 1) evidencing the existence of a pair of enantiomers, in this case the splitting is due to chemical shift non-equivalence within the same molecule. A raise in temperature from 30 to 70°C leads to an apparent increase of the splitting. This process is reversible, as returning to room temperature restores the initial spectrum. It might be a proof that the chelatic B—O bond is stable on the NMR time-scale, because otherwise coalescence would be observed.

Another stereochemical aspect deserves attention. In the chiral compounds of general formulas **1** and **3**, the two methyls of the 5-isopropyl group are diastereotopic and might be anisochronous, but they appear accidentally isochronous in all the compounds investigated. Figure 3 presents the chemical shifts of the protons of the 5-isopropyl group in the chiral compounds **1b** and **1c** compared to those of the achiral reference compound **1a**. In spite of their different spatial relationships, the methyl groups are isochronous in the achiral as well as in the chiral compounds.

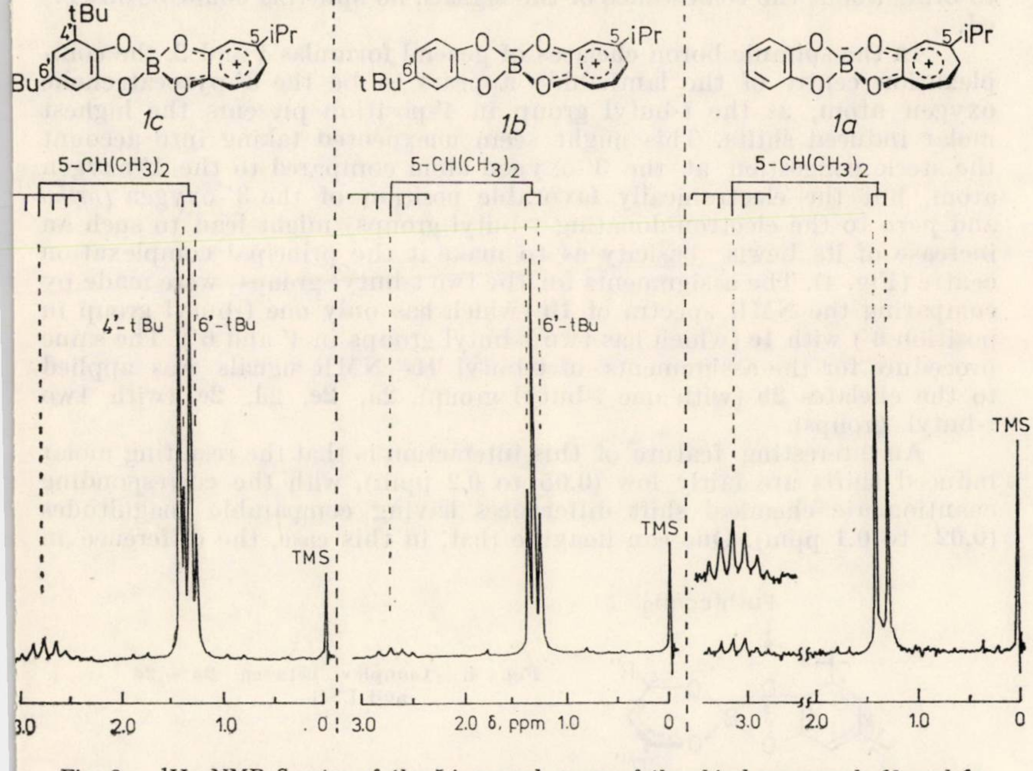

Fig. 3. — ^{1}H—NMR Spectra of the 5-isopropyl group of the chiral compounds **1b** and **1c** in comparison with the achiral compound **1a** (solvent : CDCl$_3$).

All attempts to remove the chemical shift degeneracy of the diastereotopic methyl groups in these chiral compounds by changing the solvent or by recording the NMR spectra, in the presence of an achiral lanthanide shift reagent, failed. Probably these groups are too far away from the molecular axis of chirality to be sensitive to the difference in their environments.

3. DISCUSSION

The intermolecular enantiomeric splitting observed in the ^1H-NMR spectra of the chelatic organoboron compounds with the general formulas **1**–**4** recorded in the presence of the chiral shift reagent Eu(hfcam)$_3$ represents a definite proof for the chirality of these compounds. It confirms, by stereochemical evidence, the structure attributed to these compounds by the previous investigations.[2–5] On the other hand, one can conclude that the chelatic boron-oxygen bond is stable on the NMR timescale, at least under normal temperature conditions. An easy breaking and reforming of this chelatic bond would be equivalent to an enantiomerization process; would this be fast enough on the NMR time scale to bring about the coalescence of the signals, no splitting could be observed.

In the spiranic boron chelates of general formulas **1** and **2**, the complexation centre of the lanthanide appears to be the 3′-pyrocatecholic oxygen atom, as the t-butyl group in 4′-position presents the highest molar induced shifts. This might seem unexpected taking into account the steric congestion at the 3′-oxygen atom compared to the 1′-oxygen atom, but the electronically favorable position of the 3′-oxygen *(ortho* and *para* to the electron-donating t-butyl groups) might lead to such an increase of its Lewis basicity as to make it the principal complexation centre (Fig. 4). The assignments for the two t-butyl groups were made by comparing the NMR spectra of **1b** (which has only one t-butyl group in position 6′) with **1c** (which has two t-butyl groups in 4′ and 6′). The same procedure for the assignments of t-butyl ^1H-NMR signals was applied to the chelates **2b** (with one t-butyl group), **2a**, **2c**, **2d**, **2e** (with two t-butyl groups).

An interesting feature of this interaction is that the resulting molar induced shifts are fairly low (0.05 to 0.2 ppm), with the corresponding enantiomeric chemical shift differences having comparable magnitudes (0.02 to 0.1 ppm). One can imagine that, in this case, the difference in the geometry of the two diastereomeric complexes, rather than the difference in the equilibrium constants of complexation, is the main factor in obtaining the enantiomeric splitting of the signals.

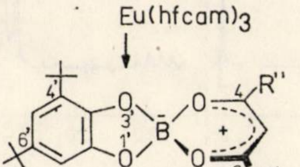

Fig. 4. — Complex between **2a** — **2d** and LSR.

For the compounds **3a** and **4a**, the complexation centre of the lanthanide seems to be the oxygen atom in the anisyl group attached to boron, as these methoxy group protons present molar induced shifts of 0.4 and 0.6 ppm respectively, whereas the other signals in the spectrum are practically unshifted. This complexation centre is too far away from the chiral axis to produce large enantiomeric splittings, which is indeed the case: for the compound **4a** the enantiomeric chemical shift difference was only 0.02 ppm while **3a** gave no splittings as mentioned earlier. In the compound **4a** there is another potential centre of complexation, namely the methoxy group in the 6-anisyl group. From the limiting structures for **4a** one can see, however, that the basicity of the 6-anisyl methoxy group is reduced owing to the conjugation of its p electrons with the π electrons in the chelating ring; thus this group no longer competes for the complexation of the lanthanide (Fig. 5).

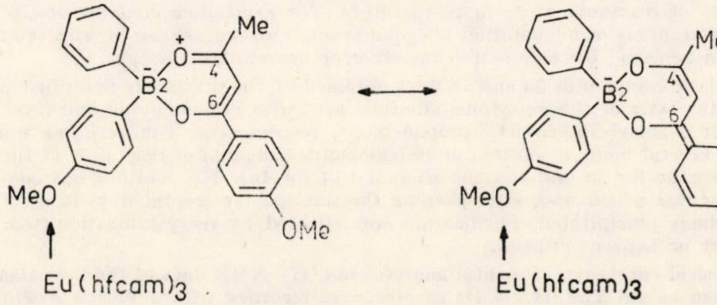

Fig. 5. — Complex between **4a** and LSR.

A similar situation holds for **2e**, in which a 6-anisyl group and the benzodioxaborole oxygens are potential complexation centres: though the methoxy protons evidence an intermolecular enantiomeric splitting in the presence of Eu(hfcam)$_3$, their MIS value is much lower than for the 4′-t-butyl protons. Therefore complexation occurs at the benzodioxaborole oxygen as in the other compounds **2** (Fig. 6).

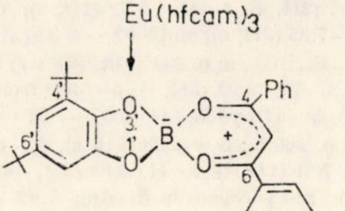

Fig. 6. — Complex between **2e** and LSR.

Thus for all compounds presented in this paper, complexation never occurs at the β-diketone or tropolone bidentate ligands, probably because of the partial positive charge of these moieties.

EXPERIMENTAL PART

The chelatic compounds of general formulas **1** and **2** were obtained according to the previously described procedure[2] starting from 2-*n*-butoxy-1,3,2-benzodioxaborole (or the correspondingly 6′-t-butyl and 4′,6′-di-t-butyl substituted derivatives) and β-isopropyltropolone or 1,3-diketones, respectively. The reaction was effected in benzenic solution with stoichiometric amounts of reactants at room temperature. The crystalline chelates precipitate from this solution on standing or on addition of cyclohexane. Purification can be effected by recrystallization from benzene, benzene/petroleum ether or benzene/cyclohexane.

The chelatic compounds **3a** and **4a** were obtained by the previously described procedure[5] starting from the ester of the anisylphenylborinic acid with ethanolamine and from β-isopropyltropolone or 1-anisyl-3-phenyl-1,3-propanedione, respectively. The reaction was effected by heating for several hours a solution of stoichiometric amounts of reactants at the reflux of the solvent (benzene for **3a** and benzene-ethanol 1 : 1 for **4a**). The solution was concentrated, petroleum ether was added and, after keeping the solution for several days in a refrigerator, crystalline chelates precipitated. Purification was effected by recrystallization from benzene/petroleum ether or benzene/ethanol.

The physical constants, elemental analysis and ^{1}H—NMR data of the investigated compounds are given below. The ^{1}H—NMR spectra were recorded with a Varian A-60A spectrometer in $CDCl_3$; chemical shifts are given in δ-scale from TMS as internal standard.

1a : $C_{16}H_{15}BO_4$; m.p. 155 — 157°C (lit.[8] 157°C) ; $\delta = 1.34$ (6H, d, $J = 7$ Hz), 3.13 (1H, septet, $J = 7$ Hz), 5—iPr ; 6.82 (4H, unresolved multiplet), aromatic protons in the pyrocatechol moiety ; 7.55 — 8.17 (4H, m), tropolonic protons.

1b : $C_{20}H_{23}BO_4$; m.p. 222 — 223°C ; $\delta = 1.32$ (9H, s), 6′ — tBu ; 1.36 (6H, d, $J = 7$ Hz), 3.17 (1H, septet, $J = 7$Hz), 5—iPr ; 6.73 (2H, unresolved multiplet), 4′—H and 7′—H ; 6.89 (1H, unresolved multiplet), 5′—H ; 7.43 — 8.10 (4H, m), tropolonic protons.

1c : m.p. 257°C ; $\delta = 1.34$ (9H, s), 6′—tBu ; 1.44 (9H, s), 4′—tBu ; 1.33 (6H, d, $J = 7$ Hz), 3.12 (1H, septet, $J = 7$ Hz), 5—iPr ; 6.82 (2H, unresolved multiplet), 5′—H and 7′—H ; 7.48—8.17 (4H, m), tropolonic protons ; Found : C, 72.81 ; H, 8.03 ; B, 2.76 ; $C_{24}H_{31}BO_4$ requires : C, 73.10 ; H, 7.92 ; B, 2.74 %.

2a : m.p. 205 — 207°C (lit.[9] 193°C) ; $\delta = 1.31$ (9H, s), 6′—tBu ; 1.43 (9H, s), 4′—tBu ; 2.33 (6H, s), 4,6—Me$_2$; 6.10 (1H, s), 5—H ; 6.88 (2H, unresolved multiplet), 5′—H and 7′—H ; Found : C, 68.70 ; H, 8.50 ; B, 3.59 ; Calc. for $C_{19}H_{27}BO_4$: C, 69.11 ; H, 8.24 ; B, 3.27%.

2b : $C_{20}H_{21}BO_4$; m.p. 204 — 205°C ; $\delta = 1.34$ (9H, s), 6′—tBu ; 2.45 (3H, s), 4—Me ; 6.74 (1H, s), 5—H ; 6.91 (2H, unresolved multiplet) 4′—H and 7′—H ; 7.07 (1H, m), 5′—H ; 7.42 — 7.85 (3H, m) and 8.17 (2H, m), aromatic protons in 6—Ph.

2c : $C_{24}H_{29}BO_4$; m.p. 198 — 199°C (lit.[9] 201°C) ; $\delta = 1.35$ (9H, s), 6′ — tBu ; 1.48 (9H, s), 4′—tBu ; 2.45 (3H, s), 4—Me ; 6.72 (1H, s), 5—H ; 6.92 (2H,unresolved multiplet), 4′—H and 7′—H ; 7.50—7.85 (3H, m) and 8.03 — 8.28 (2H, m), aromatic protons in 6—Ph.

2d : $C_{25}H_{31}BO_5$; m.p. 244°C(lit.[9]248°C) ; $\delta = 1.35$ (9H, s), 6′—tBu ; 1.48 (9H, s), 4′—tBu ; 2.40 (3H, s), 4—Me ; 3.98 (3H, s), *p*—MeO from 6—An ; 6.65 (1H, s), 5—H ; 6.98 (2H, unresolved multiplet), 5′—H and 7′—H ; 6.87—7.32 (4H, m), aromatic protons in 6—An.

2e : m.p. 260°C ; $\delta = 1.38$ (9H, s), 6′—tBu ; 1.52 (9H, s), 4′—tBu ; 4.00 (3H, s) *p*—MeO from 6—An ; 7.31 (1H, s), 5—H ; 6.98 (2H, unresolved multiplet), 5′—H and 7′—H ; 7.13 (2H, d, $J = 7$ Hz), *m*-hydrogens in 6—An ; 7.60 — 7.85 (3H, m), *m*- and *p*-hydrogens in 4—Ph ; 8.13 — 8.43 (4H, m), *o*-hydrogens in 4—Ph and 6—An ; Found : C, 73.96 ; H, 7.10 ; B, 2.49 ; $C_{30}H_{33}BO_5$ requires : C, 74.39 ; H, 6.87 ; B, 2.23%.

3a : m.p. 110 — 115°C ; $\delta = 1.27$ (6H, d, $J = 6.5$ Hz), 2.93 (1H, septet, $J = 6.5$ Hz), 5—iPr ; 3.71 (3H, s), *p*-MeO from Ar′ = An ; 6.70 (2H, d, $J = 8$ Hz), *m*-hydrogens in Ar′ = An ; 6.97 — 7.82 (11H, m), aromatic protons in Ar = Ph, Ar′ = An and tropolonic protons ; Found : C, 76.79 ; H, 6.78 ; B, 2.86 ; $C_{23}H_{23}BO_3$ requires : C, 77.11 ; H, 6.47 ; B, 3.02%.

4a : m.p. 141 — 142°C (lit.[5] 142°C) ; $\delta = 2.37$ (3H, s), 4—Me ; 3.89 (3H, s), *p*-MeO from Ar′ = An ; 4.00 (3H, s), *p*-MeO from 6—R‴ = An ; 6.38 (1H, s), 5—H ; 7.03 (2H, d, $J = 8.5$ Hz), *m*-hydrogens in Ar′ = An ; 7.15 (2H, d, $J = 9$ Hz), *m*-hydrogens in 6—R‴ = An ; 7.35 — 7.88 (7H, m) and 8.25 (2H, d, $J = 9.0$ Hz), other aromatic protons in 6—R‴ = An, Ar = = Ph and Ar′ = An ; Found : C, 74.23 ; H, 6.24 ; Calc. for $C_{24}H_{23}BO_4$: C, 74.63 ; H, 6.00%.

REFERENCES

[1] Preceding part, I. Bally and A. T. Balaban, *Tetrahedron*, **29**, 3183 (1973).

[2] a) A. T. Balaban, G. Mihai, R. Antonescu and P. T. Frangopol, *Tetrahedron*, **16**, 68 (1961); b) A. T. Balaban, C. N. Renţea, M. Mocanu-Paraschiv and E. Romaş, *Rev. Roumaine Chim.*, **10**, 849 (1965); c) I. Bally, A. Arsene, M. Băcescu-Roman and A. T. Balaban, *Tetrahedron Letters*, **1965**, 3929; d) A. Arsene, A. T. Balaban, I. Bally, A. Barabás, M. Paraschiv and C. N. Renţea, *Spectrochimica Acta*, **23A**, 1373 (1967).

[3] A. Trestianu, H. Niculescu-Majewska, I. Bally, A. Barabás and A. T. Balaban, *Tetrahedron*, **24**, 2499 (1968).

[4] a) A. T. Balaban, I. Bally, R. J. Bishop, C. N. Renţea and L. E. Sutton, *J. Chem. Soc.*, **1964**, 2382; b) A. T. Balaban, I. Bally, V. I. Minkin and A. I. Usachev, *Tetrahedron*, **33**, 3265 (1977).

[5] I. Bally, E. Ciornei and A. T. Balaban, *Rev. Roumaine Chim.*, **13**, 1507 (1968).

[6] a) G. M. Whitesides and D. W. Lewis, *J. Amer. Chem. Soc.*, **92**, 6979 (1970); b) G. M. Whitesides and D. W. Lewis, *ibid.*, **93**, 5914 (1971); c) H. L. Goering, J. N. Eikenberry and G. S. Koermer, *ibid.*, **93**, 5913 (1971); d) H. L. Goering J. N. Eikenberry, G. S. Koermer and C. J. Lattimer, *ibid.*, **96**, 1493 (1974).

[7] a) B. A. Behnam, D. M. Hall and B. Modarai, *Tetrahedron Letters*, **1979**, 2619; b) E. Diaz, E. Rojas-Dávila, A. Guzman and P. Joseph-Nathan, *Org. Magn. Reson.*, **14**, 439 (1980); c) R. W. Lang and H. J. Hansen, *Helv. Chim. Acta*, **62**, 1025 (1979).

[8] A. T. Balaban, *Rev. Roumaine Chim.*, **10**, 879 (1965).

[9] I. Bally A. Arsene, M. Roman, M. Paraschiv, E. Romaş and A. T. Balaban, *Rev. Roumaine Chim.*, **13**, 1225 (1968).

Revue Roumaine de Chimie, **29**, *1*, 131–140 (1984)

A CORRELATION BETWEEN SURFACE TENSION AND THE ADIABATIC COMPRESSIBILITY

RODICA VÎLCU[a] and ELENA DIMITRIU[b]

[a] National Institute of Chemistry, Department of Physical Chemistry and Electrochemical Technology, Bd. Republicii, 13 – Bucharest, Romania

[b] Institute of Physics and Technology of Materials, Măgurele, Bucharest, Romania

Received July 21, 1982

A linear empirical relation is proposed between the surface tension γ and the adiabatic compressibility β_s as calculated from the velocity of propagation of ultrasounds. The relation has the form : $\gamma^{3/2} = a + b\,\beta_s^{-1}$, where a and b are constants specific to each homologous series of substances. The percent errors occurring in estimating surface tension by the proposed relation are around 1%. The linear relationship between $\gamma^{3/2}$ and β_s^{-1} has a general character for homologous series.

INTRODUCTION

The surface tension of a pure liquid has been correlated with many experimental quantities, [1-16] such as the critical temperature, the parachor and the isothermal compressibility.

A quantitative relationship between surface tension and adiabatic compressibility has not been established so far. In this work we propose such a correlation. The adiabatic compressibility values are calculated using the well-known[17] relation

$$\beta_s = \frac{1}{\rho v^2} \tag{1}$$

where ρ is the liquid density and v, the ultrasound propagation velocity. Literature data were used for velocity[18-21] and for surface tension[22,23] values.

The Correlation between γ and β_s

The values of $\gamma^{3/2}$ and β_s^{-1} were calculated and the correlation between these values was investigated by estimating for each class of substances the correlation coefficient r,[24] which for this case has the form

$$r = \frac{\sum\limits_{k=1}^{n} \left[(\beta_{s,k}^{-1} - \overline{\beta_s^{-1}})(\gamma_k^{3/2} - \overline{\gamma^{3/2}})\right]}{\left[\sum\limits_{k=1}^{n} (\beta_{s,k}^{-1} - \overline{\beta_s^{-1}})^2 \sum\limits_{k=1}^{n} (\gamma_k^{3/2} - \overline{\gamma^{3/2}})^2\right]^{1/2}} \tag{2}$$

Table 1

Values of $\underline{a}$ and $\underline{b}$ in relation (4) for homologous series of substances, and percent error of the surface tension values determined from relation (4)

Class of substance	Substance	Temp. (K)	$\gamma^{3/2}$ $\left(\frac{dyn}{cm}\right)^{3/2}$	$\beta_s^{-1}\times 10^{-10}$ $\left(\frac{dyn}{cm^2}\right)$	r Eq. (4)	$\underline{a}$ $\left(\frac{dyn}{cm}\right)^{3/2}$	$\underline{b}\times 10^8$ $\left(\frac{dyn}{cm}\right)^{1/2}$	$\gamma^{3/2}_{calc.}$	E% Eq. (4)
1	2	3	4	5	6	7	8	9	10
HYDROCARBONS									
	n-pentane	288.15	67.81	0.702	0.998	−10.83	1.112	67.26	−0.54
		293.15	64.48	0.821	0.998	− 8.62	1.091	63.83	−0.68
		303.15	58.09	0.592	0.998	− 5.64	1.064	57.39	−0.86
	n-hexane	288.15	80.47	0.858	0.998	−10.83	1.112	84.63	+1.94
		293.15	79.05	0.821	0.998	− 8.62	1.091	80.96	+1.57
		303.15	72.58	0.747	0.988	− 5.64	1.064	73.89	−0.45
	n-heptane	288.15	95.20	0.951	0.998	−10.83	1.112	94.97	−0.19
		293.15	91.59	0.91	0.998	− 8.62	1.091	90.68	−0.68
		303.15	84.59	0.836	0.998	− 5.64	1.064	83.37	−0.98
	n-octane	288.15	104.59	1.046	0.998	−10.83	1.112	105.53	
		293.15	101.43	1.000	0.998	− 8.62	1.091	100.50	−0.64
		303.15	91.39	0.921	0.998	− 5.64	1.064	92.42	−1.69
	n-nonane	288.15	113.33	1.126	0.998	−10.83	1.112	114.43	
		293.15	109.65	1.09	0.998	− 8.62	1.091	110.32	+0.39
		303.15	102.55	1.025	0.998	− 5.64	1.064	103.49	+0.59
	n-decane	288.15	120.89	1.189	0.998	−10.83	1.112	121.44	
		293.15	116.98	1.15	0.998	− 8.62	1.091	116.87	−0.08
		303.15	109.65	1.070	0.998	− 5.64	1.064	108.83	−0.87
ISO-HYDROCARBONS									
	2-methylpentane	293.15	72.01	0.733	0.984	6.76	0.896	72.60	+0.40
	2-methylhexane	293.15	83.93	0.851				83.01	−0.73
	3-methylhexane	293.15	86.50	0.886				86.22	−0.25
	2,4-dimethylpentane	293.15	77.13	0.790				77.61	+0.38
	iso-ocrane	293.15	81.84	0.852				83.17	+1.06
AROMATIC AND CYCLIC HYDROCARBONS									
	benzene	293.15	154.39	1.54	0.998	−10.34	1.066	153.87	−0.24

	toluene	293.15	152.38	1.527	0.998	−10.34	1.066	152.49	+0.03
	o-xylene	293.15	164.56	1.637	0.998	−10.34	1.066	164.22	−0.16
		303.15	155.60	1.531	0.995	1.91	1.021	154.4	−0.48
	m-xylene	293.15	155.36	1.558	0.998	−10.34	1.066	155.79	+0.17
		303.15	144.52	1.447	0.995	− 1.91	1.021	145.81	+0.61
	p-xylene	293.15	150.62	1.532	0.998	−10.34	1.066	153.02	+1.02
		303.15	142.01	1.411	0.995	− 1.91	1.021	142.15	+0.03
	ethylbenzene	293.15	156.49	1.553	0.998	−10.34	1.066	155.20	−0.55
		303.15	147.60	1.439	0.995	− 1.91	1.021	145.01	−1.25
	butylbenzene	293.15	158.03	1.573	0.998	−10.34	1.066	157.34	−0.27
		303.15	149.67	1.47	0.995	− 1.91	1.021	148.17	−0.78
	cyclohexane	293.15	124.92	1.268	0.998	−10.34	1.066	124.87	−0.04
	methylcyclohexane	293.15	116.54	1.188	0.998	−10.34	1.066	116.34	−0.12
CARBOXYLIC ACIDS									
	acetic acid	293.15	143.48	1.387	0.974	39.279	0.716	138.58	−2.33
	propionic acid	293.15	137.96	1.371	0.974	39.279	0.716	137.52	−0.22
	butyric acid	288.15	142.79	1.442	0.984	23.14	0.822	141.79	−0.44
		293.15	138.74	1.387	0.974	39.279	0.716	138.67	−0.22
	valeric acid	288.15	146.81	1.505	0.984	23.14	0.822	146.97	+0.03
		293.15	142.79	1.457	0.974	39.279	0.716	143.68	+0.40
	caproic acid	288.15	150.54	1.573	0.984	23.14	0.822	152.57	+0.91
		293.15	148.55	1.522	0.974	39.279	0.716	148.34	−0.07
	caprylic acid	288.15	161.85	1.671	0.984	23.14	0.822	160.64	−0.47
		293.15	154.70	1.608	0.974	39.279	0.716	154.50	−1.36
ETHERS									
	ethyl ether	293.15	70.46	0.722	0.998	− 6.88	1.068	70.225	−0.05
		303.15	63.70	0.642	1.00	− 3.209	1.042	63.70	0.00
	1-4-dioxane	293.15	195.65	1.929	0.998	− 6.88	1.068	199.14	+0.08
		303.15	182.72	1.784	1.00	− 3.209	1.042	182.718	0.00
	anisole	293.15	211.69	2.016	0.998	− 6.88	1.068	208.43	−0.19
KETONES									
	acetone	293.15	112.61	1.122	0.996	−15.41	1.127	111.127	−0.9
		297.95	108.15	1.071	0.994	−15.24	1.155	108.42	+0.13
	2-butanone	297.95	117.35	1.143	0.994	−15.29	1.155	116.74	−0.37
	3-pentanone	297.95	122.98	1.200	0.994	−15.29	1.155	123.32	+0.16
	cyclohexanone	293.15	203.52	1.992	0.996	−15.41	1.127	209.25	+1.8
	acetophenone	293.15	247.78	2.296	0.996	−15.41	1.127	243.54	−1.16
ESTERS									
	ethylacetate	293.15	115.74	1.248	0.999	−33.106	1.197	116.37	+0.33
	prophylacetate		119.63	1.273				119.36	−0.16

Table 1 (continued)

1	2	3	4	5	6	7	8	9	10
	butylacetate		126.50	1.324				125.47	−0.55
	amylacetate		131.04	1.376				131.70	+0.31
AMINES									
	diethylamine	293.15	89.30	0.935	0.999	2.33	0.943	90.58	+0.95
	triethylamine		93.90	0.953				92.28	−1.16
	o-toluidine		253.93	2.613				248.96	−1.27
	m-toluidine		234.43	2.515				239.71	+1.47
CHLORINATED HYDROCARBONS									
	dichloromethane	293.15	149.11	1.584	0.986	54.34	0.594	148.48	−0.28
		303.15	136.72	1.455	0.977	60.52	0.521	136.45	−0.15
	chloroform	293.15	141.54	1.489	0.986	54.34	0.594	142.84	+0.58
		303.15	131.81	1.377	0.977	60.52	0.521	132.38	+0.27
	carbon tetrachloride	293.15	138.35	1.402	0.986	54.34	0.594	137.67	−0.33
		303.15	129.14	1.309	0.977	60.52	0.521	128.83	−0.15
	1,2-dichloromethane	293.15	189.97	1.851	0.996	47.49	0.766	189.40	−0.13
	tetrachloroethane	293.15	216.36	2.189	0.996	47.49	0.766	215.31	−0.30
	pentachloroethane	293.15	204.58	2.07	0.996	47.49	0.766	206.19	+0.51
	trichloroethylene	303.15	143.81	1.465	0.995	−40.88	1.282	147.01	+1.49
	tetrachloroethylene	303.15	174.86	1.687				175.48	+0.22
	3-chloropropene	303.15	101.09	1.1034				100.63	−0.91
	chlorobenzene	393.15	181.95	1.718				179.46	−0.93
BROMINATED HYDROCARBONS									
	bromoethane	293.15	118.67	1.183	0.998	−22.15	1.187	118.37	−0.20
	1,2-dibromoethane	293.15	242.71	2.217				241.19	−0.43
	bromobenzene	293.15	219.79	2.046				220.87	+0.55

RI									
	iodomethane	293.15	165.46	1.585	0.998	19.66	0.923	165.97	+0.19
		303.15	152.94	1.458	0.998	12.23	0.971	153.91	+0.38
	iodoethane	293.15	154.79	1.48	0.998	19.66	0.923	156.28	+0.55
		303.15	144.56	1.382	0.998	12.23	0.271	146.53	+1.45
	iodopropane	293.15	160.79	1.507	0.998	19.66	1.923	158.77	−0.85
		303.15	151.40	1.409	0.998	12.23	0.971	149.15	−1.22
RCN + RNO_2									
	acetonitrile	293.15	156.97	1.323	0.996	16.74	1.019	151.68	−2.26
	propionitrile		142.25	1.271				146.38	+1.90
	nitromethane		224.88	2.063				227.16	+0.16
	nitrobenzene		285.42	2.623				284.28	−0.27
ALCOHOLS									
	methanol	293.15	107.08	0.998	0.989	62.192	0.454	107.54	+0.44
	ethanol		105.44	1.07				110.81	+1.18
	n-propanol		115.37	1.202				116.81	+0.80
	n-butanol		121.78	1.292				120.90	+0.48
	n-pentanol		129.52	1.366				124.27	−2.73
	n-hexanol		121.12	1.433				127.31	+3.34
	n-octanol		133.02	1.525				131.49	−0.80
	n-butanol	303.15	115.74	1.207	0.998	−27.79	1.189	115.83	+0.04
	sec-butanol	303.15	107.58	1.143				108.22	+0.35
	isobutanol	303.15	103.96	1.099				102.74	−0.81
	tert-butanol	303.15	83.47	0.937				83.70	+0.15
	glycerine	293.15	498.85	4.409		−27.79	1.189	496.44	−0.31
ETHYLENE GLYCOLS									
	ethyleneglycol	293.15	316.98	3.09	0.987	201.83	0.372	317.04	+0.01
	diethyleneglycol		303.98	2.745				304.18	+0.02
	triethyleneglycol		307.60	2.832				307.35	−0.06

where

$$\overline{\beta_s^{-1}} = \frac{1}{n} \sum_{k=1}^{n} \beta_{s,k}^{-1}$$

and

$$\overline{\gamma^{3/2}} = \frac{1}{n} \sum_{k=1}^{n} \gamma_k^{3/2}$$

are the mean values of β_s^{-1} and $\gamma^{3/2}$.

Since the values of the correlation coefficient are very close to +1(see Table 1), we can state that a linear relationship occurs between $\gamma^{3/2}$ and β_s^{-1} for all classes of substances considered ; hence

$$\gamma^{3/2} = a + b\,\beta_s^{-1} \tag{3}$$

The values of constants a and b were calculated by the least-square method for each homologous series of organic liquids. Table 1 shows that a and b depend on temperature : with the exception of iodine derivatives and of ketones, a increases as the temperature increases, whereas b decreases as the temperature increases. Lack of sufficient literature data on surface tension and adiabatic compressibility at various temperatures has prevented us from establishing a linear dependence of a and b on temperature.

After checking up the linear relation (3) with available values of β_s^{-1}, calculated values of surface tension resulted which were very close to the experimentally measured ones. The percent error E of the surface tension calculated by the relation (3), γ_{calc}, as compared to that measured experimentally, γ_{expt},

$$E = \frac{\gamma_{\text{calc}} - \gamma_{\text{expt}}}{\gamma_{\text{expt}}} \times 100 \tag{4}$$

was generally less than 1% for nonpolar liquids as well as for strongly associated liquids (see Table 1).

For hydrocarbons, ethers, ketones, esters, and amines, b has an approximate value of 1×10^{-8} (dyn. cm)$^{1/2}$ at 293.15 K. Since b is the slope of the straight line, we can state that a single linear relation exists between $\gamma^{3/2}$ and β_s^{-1} for all these compounds. The correlation coefficient r is 0.999 for all hydrocarbons, which confirms the linear dependence of $\gamma^{3/2}$ on β_s^{-1}. The relation which describes the behaviour of surface tension as a function of adiabatic compressibility is similar to relation (3), i.e.

$$\gamma^{3/2} = -2.768 + 1.018 \times 10^{-8} \beta_s^{-1} \tag{5}$$

The coefficients in relation (5) are the mean values of a and b given in Table 1 for linear, cyclic or branched-chain aliphatic hydrocarbons and for aromatic hydrocarbons.

Estimation by relation (5) of surface tension of organic liquids as a function of adiabatic compressibility led to the values listed in Table 2.

Table 2

Percent error in determining surface tension values by relation (5)

Class of substance	Substance	Temp. (°K.)	$\gamma_{\text{exptl.}}$ $\left(\frac{\text{dyn}}{\text{cm}}\right)$ Eq. (6)	$\gamma_{\text{calcd.}}$ $\left(\frac{\text{dyn}}{\text{cm}}\right)$ Eq. (6)	$E(\%)$ Eq. (5)	$E(\%)$ Ref.[2]	$E(\%)$ Brook-Bird relation (Ref.[2])
1	2	3	4	5	6	7	8
HYDROCARBONS		293.15					
	n-pentane		16.08	16.13	+0.31	− 5.6	−0.7
	n-hexane		18.43 (ref.[23])	18.69	+1.41	−10.0	−0.4
	n-heptane		20.32	20.06	−1.27	−12.6	−4.3
	n-octane		21.75	21.40	−1.60	−15.9	−0.3
	n-nonane		22.91	22.70	−0.87		
	n-decane		23.92	23.55	−1.54		
	2-methylpentane		17.31	17.28	−0.17	−10.0	−0.7
	3-methylpentane		18.10	17.88	−1.21		
	2-methylhexane		19.17	19.15	−0.10		
	3-methylhexane		19.56	19.70	+0.71		
	2,4-dimethylpentane		18.12	18.20	+0.44		
	iso-octane		18.85	19.17	+1.69		
	benzene		28.78	28.73	−0.17	−6.8	−3.4
	toluene		28.53	28.59	+0.21	−6.7	−2.0
	o-xylene		30.03	30.07	+0.13	−8.2	−1.7
	m-xylene		28.90 (ref.[23])	28.96	+0.20		
	p-xylene		28.31	28.63	+1.13		
	ethylbenzene		29.04	28.90	−0.48	−10.3	+2.9
	butylbenzene		29.23	29.15	−0.20		
	cylohexane		24.99	25.17	+0.72		
	methylcyclohexane		23.85	24.08	+0.96		
	1,2,3,4-tetrahydronaphthalene		35.70	35.79	+0.25		
CARBOXYLIC ACIDS							
	formic acid	293.15	37.58	34.46	−8.30		
	acetic acid		27.42	26.76	−2.40	+47.7	+53.6
	propionic acid		26.70	26.55	−0.56	+31.1	+65.6
	butyric acid		26.8 (ref.[23])	26.79	−0.03	+17.7	+90.0
	valeric acid		27.32	27.67	+1.28		
	caproic acid		28.31 (ref.[23])	28.50	+0.67		
	caprylic acid		29.20	29.59	+1.33		
ETHERS							
	ethyl ether	293.15	17.01 (ref [23])	17.01	0.00		
	1,4-dioxane		33.7	34.41	+2.10		
	anisole		35.22	35.48	+0.73		
KETONES							
	acetone	293.15	23.32	23.16	−0.68	+3.3	+7.0
		297.95	22.7	22.44	−1.14		
	2-butanone	297.95	23.97	23.85	−0.50		
	3-pentanone	297.95	24.73	24.62	−0.44		

Table 2 (continued)

1	2	3	4	5	6	7	8
	cyclohexanone	293.15	34.6	34.20	−1.09		
	acetophenone	293.15	39.8 (ref.^{23})	37.65	−5.40		
ESTERS		293.15					
	ethyl acetate		23.75	24.90	+4.82	−10.5	+2.1
	propyl acetate		24.28	25.54	+3.80		
	butyl acetate		25.20	25.95	+2.97		
	isobutyl acetate		23.7 (ref.^{23})	24.47	+3.24		
	amyl acetate		25.80	26.62	+3.17		
AMINES		293.15					
	diethylamine		19.98	20.44	+2.30		
	triethylamine		20.66	20.71	+0.24	−8.0	−2.4
	o-toluidine		40.10	41.08	+2.44		
	m-toluidine		38.02	40.03	+5.28		
	aniline		42.79	43.13	+0.79		
	aniline		42.58 (ref.^{23})	43.13	+1.31	−5.6	+8.5
CHLORINATED HYDROCARBONS		293.15					
	dichloro-methane		28.12	29.29	+4.16		
	chloroform		27.24 (Ref. ^{23})	28.08	+3.08		
	carbon tetrachloride		26.75	26.98	+0.85	−5.6	−3.5
	dichloroethane		32.23	32.55	+0.99		
	tetrachloroethane		36.04	36.45	+1.13		
	pentachloroethane		34.72	35.10	+1.09		
	1-chloropropane		21.78	22.13	+1.60		
	1-chlorobutane		23.86	23.55	−1.29		
	trichloroethylene		29.5	29.80	+1.01		
	tetrachloroethylene		32.28	31.82	−1.42		
	chlorobenzene		33.28	32.34	−2.82	−3.6	−3.1
	m-dichlorobenzene		36.16	36.10	−0.16		
BROMINATED HYDROCARBONS		293.15					
	bromoethane		24.15	24.01	−0.57	−3.7	+12.7
	1,2-dibromoethane		38.91	36.17	−5.49		
			36.34	34.83	−4.15	−7.8	−3.8
	bromobenzene	293.15					
RI		293.15					
	iodomethane		30.14	29.30	−2.78		
	iodoethane		28.83	27.97	−2.98		
	iodopropane		29.57	28.31	−4.26		
ROH							
	methanol	293.15	22.55	21.37	−5.23	+58.6	+91.6
	ethanol	293.15	22.27 (ref.^{23})	22.30	+0.13	+18.6	+67.9
	n-propanol	293.15	23.8 (ref. ^{23})	24.27	+1.97		
	iso-propanol	293.15	21.7 (^{3}ef.^{23})	22.49	+3.64		
	n-butanol	293.15	24.57	25.63	+4.31	+7.5	+36.2
		303.15	23.75	24.34	+2.48		
	iso-butanol	293.15	22.98	23.94	+4.17		
		303.15	22.11	22.83	+3.15		
	sec-butanol	303.15	22.62	23.45	+3.66		

Table 2 (continued)

1	2	3	4	5	6	7	8
	tert-butanol	303.15	20.7	20.47	+1.11		
	amyl alcohol	293.15	35.60	26.48	+3.43		
	iso-amyl-alcohol	293.15	24.33	25.54	+4.97		
	m-cresol	293.15	37.4 (Ref.[23])	38.00	+1.60		
	benzyl alcohol	293.15	39.71 (Ref.[23])	39.63	−0.20		
	2-propenol	303.15	24.92	24.88	−0.16	+7.5	+35.3
	ethylene glycol	293.15	46.90	44.88	−4.30		
	diethylene glycol	293.15	35.21	42.46	−6.08		
	triethylene glycol	293.15	45.57	43.34	−4.89		
RNO_2	nitromethane	293.15	36.82 (Ref.[23])	35.06	−4.67		
	nitrobenzene	293.15	43.38 (Ref. [23])	41.18	−5.07		

The percent error was of about 1% for all classes of substances for which the value of *b*, as calculated from relation (3), was no less than 0.716 and no greater than 1.15 $(\text{dyn.cm})^{1}/_{2}$. The value of 8.30% obtained for the percent error in the case of formic acid may be accounted for by the fact that propagation of ultrasound waves in this liquid is accompanied by their absorption, due to the structural relaxation from **HCOOH**. The percent error was greater than 2% in the case of nitroderivatives and nitriles, and of any class of substances for which $b < 0.716$ or $b > 1.15$ $(\text{dyn.cm})^{1/2}$.

Though for associated substances γ can be calculated, using relation (5), with an error of about 3%, the error is far less than that reported in literature [2] (from 17.7 to 47% for acids and from 7.5 to 58.6% for alcohols) on the basis of correlations between γ and other quantities, different from β_s. Since in all these compounds a velocity dispersion occurs we believe that the errors in estimating γ for these classes of substances by the method proposed herein could be much less if values of ultrasound propagation velocities, measured at identical ultrasound frequencies, would be available.

CONCLUSIONS

For all considered classes of substances, $\gamma^{3/2}$ depends linearly on β_s^{-1}. The percent error in estimating surface tension values by relation (3) is generally less than 1% and much less than the percent errors resulted by using other correlations proposed in literature. Since relation (3) was checked up for 83 organic liquids belonging to 9 different classes of organic liquids, we might conclude that the linear dependence of $\gamma^{3/2}$ on β_s^{-1} is quite general.

REFERENCES

[1] R. C. Reid and T. K. Sherwood, "The Properties of Gases and Liquids. Their Estimation and Correlation", McGraw-Hill, New York, 1966.

[2] J. Lielmezs and A. P. Watkinson, *Chem. Ind.*, **1970**, 1019.

[3] R. V. G. Rao and V. V. Subba Rao, *Z. phys. Chem. (Leipzig)*, **221**, 357 (1962).

[4] D. B. Macleod, *Trans. Faraday Soc.*, **19**, 38 (1923).

[5] S. W. Mayer, *J. Chem. Phys.*, **38**, 1803 (1963).

[6] V. R. Shastry and W. V. Bhagwat, *J. Indian Chem. Soc.*, **46**, 287 (1969).

[7] D. G. LeGrand and C. L. Gaines, Jr., *J. Colloid Interface Sci.*, **42**, 181 (1973).

[8] W. Porteus, *J. Chem. Eng. Data*, **20**, 339 (1975).

[9] R. Ulbrich, *Z. Naturforsch.* A, **22**, 407 (1967).

[10] W. B. Strickfaden and L. DeSobrino, *Canad. J. Phys.*, **48**, 3061 (1970).

[11] G. W. Woodburg, Jr., *J. Chem. Phys.*, **60**, 3674 (1974).

[12] R. V. Rao, *Indian J. Pure Appl. Phys.*, **13**, 459 (1975).

[13] A. J. M. Yang, P. D. Fleming and J. H. Gibbs, *J. Chem. Phys.*, **64**, 3732 (1976).

[14] F. F. Abraham, *J. Chem. Phys.*, **63**, 157 (1975).

[15] C. G. Gray and K. E. Gubbins, *Mol. Phys.*, **30**, 179 (1975).

[16] A. J. Richard and K. S. Rogers, *Canad. J. Chem.*, **49**, 3956 (1971).

[17] W. van Dael, in B. Le Neindre and B. Vodar (ed.) "Experimental Thermodynamics", vol. II, Butterworths, London, 1975, Chapter 11.

[18] Landolt-Börnstein, "Numerical Data and Functional Relationships in Science and Technology", Vol. 5, "Molecular Acoustics", Springer-Verlag, Berlin, 1967.

[19] R. Vîlcu, E. Dimitriu and I. Dima, *Rev. Roumaine Chim.*, **24**, 1247 (1979).

[20] E. Dimitriu, V. Dima, *Rev. Roumaine Phys.* (in press).

[21] R. Vîlcu, E. Dimitriu, V. Dima, *Bul. Inst. Politeh. București* (in press).

[22] A. Wassberger, E. S. Proskauer, J. A. Riddlick and E. E. Toops, Jr., "Technique of Organic Chemistry", Vol. III: "Organic Solvents, Physical Properties and Methods of Purification", Interscience, New York, 1965.

[23] E. W. Washburn (editor), "International Critical Tables of Numerical Data, Physics, Chemistry and Technology", vol. IV, McGraw-Hill, New York, 1928.

[24] I. Todoran, "Tratarea matematică a datelor experimentale. Funcții empirice", Ed. Academiei, București, 1976.

ORSZÁGOS MŰSZAKI INFORMÁCIÓS KÖZPONT ÉS KÖNYVTÁR 1983

CONST. GH. MACAROVICI, **Analiza chimică cantitativă anorganică** (L'analyse chimique quantitative inorganique), 1979, 457 p.

I. G. MURGULESCU, E. SEGAL, **Introducere in chimia fizică. Vol. II.1. Teoria molecular-cinetică a materiei** (Introduction à la chimie physique. Vol. II.1.La théorie moléculaire-cinétique de la matière), 1979, 1036 p.

S. STERNBERG, FL. DANEȘ. **Termodinamica chimică aplicată** (La thermodynamique chimique appliquée), 1978, 400 p.

I. G. MURGULESCU, V. EM. SAHINI, **Introducere în chimia fizică. Vol. I.2. Structura și proprietățile moleculelor** (Introduction à la chimie physique. Vol. I.2. La structure et les propriétés des molécules), 1978, 604 p.

I. ZUGRĂVESCU, MAGDA PETROVANU, **N-ylid chemistry**, coédition avec McGraw-Hill International Book Company, U.S.A., 1977, 604 p.

I. G. MURGULESCU, **Introducere in chimia fizică. Vol. I.1. Atomi, molecule, legătură chimică** (Introduction à la chimie physique. Vol. I.1. Atomes, molécules, liaison chimique), 1976, 560 p.

CR. SIMIONESCU, VIORICA RUSAN, V. POPA, **Chimia algelor marine** (La chimie des algues marines), 1974, 212 p., 1 pl.

TRAVAUX PARUS AUX ÉDITIONS DE L'ACADÉMIE DE LA RÉPUBLIQUE SOCIALISTE DE ROUMANIE

ELENA CEAUŞESCU, **Cercetări în chimia şi tehnologia polimerilor** (Recherches de chimie et de technologie des polymères), 1984, 508 p.

ELENA CEAUŞESCU, **Noi cercetări în domeniul compuşilor macromoleculari** (Nouvelles recherches dans le domaine des composés macromoléculaires), 1981, 536 p.

ELENA CEAUŞESCU, **Polimerizarea stereospecifică a izoprenului** (La polymérisation stéréospécifique de l'isoprène), 1979, 307 p.

ELENA CEAUŞESCU, **Research work on synthesis and characterization of macromolecular compounds. Contributions**, 1974, 251 p.

E. SEGAL, D. FĂTU, **Introducere în cinetica neizotermă** (Introduction à la cinétique non isotherme), 1983, 209 p.

N. IONESCU, MONICA CĂLDĂRARU, **Oxidarea catalitică a olefinelor inferioare** (L'oxydation catalytique des oléfines inférieures), 1983, 178 p.

C. CAŞCAVAL, **Studiul polimerilor prin piroliză şi cromatografie de gaze** (L'étude des polymères par pyrolyse et chromatographie à gaz), 1983, 220 p.

C. I. SIMIONESCU, F. DENEŞ, **Originea vieţii** (L'origine de la vie), 1983, 110 p.

C. BODEA (sous la direction de), **Tratat de biochimie vegetală** (Traité de biochimie végétale) IIe p., T. IV, 1982, 408 p.

I. G. MURGULESCU, RODICA VÎLCU, **Introducere în chimia fizică. Vol.III. Termodinamica chimică** (Introduction à la chimie physique. Vol. III. Thermodynamique chimique), 1982, 626 p.

I. G. MURGULESCU, J. PĂUN, **Introducere în chimia fizică. Vol. I.3. Nucleul atomic, reacţii nucleare, particule elementare** (Introduction à la chimie physique. Vol. I.3. Noyau atomique, réactions nucléaires, particules élémentaires), 1982, 606 p.

ELENA JERCAN, **Analiza cromatografică** (Analyse chromatographique), 1982, 286 p.

I. G. MURGULESCU, TATIANA ONCESCU, E. SEGAL, **Introducere în chimia fizică. Vol. II.2. Cinetică chimică şi cataliză** (Introduction à la chimie physique. Vol. II.2. Cinétique chimique et catalyse), 1981, 1024 p.

V. DRĂGUŢAN, A. T. BALABAN, M. DIMONIE, **Metateza olefinelor şi polimerizarea prin deschidere de inel a cicloolefinelor** (La métathèse des oléfines et la polymérisation par ouverture annulaire des cyclooléfines), 1981, 254 p.

LYDIA-MARIA VAICUM, **Epurarea apelor uzate cu nămol activ. Bazele biochimice** (L'épuration des eaux résiduelles à boue active. Les bases biochimiques), 1981, 218 p.

I. GĂLĂŢEANU, **Procese şi metode radiochimice în energetica nucleară** (Processus et méthodes radiochimiques dans l'énergétique nucléaire), 1981, 234 p.

O. IORDACHE, **Procese polistocastice aplicate în fenomenele de transfer** (Processus polystochastiques appliqués aux phénomènes de transfert), 1981, 187 p.

CR. SIMIONESCU, VALERIA GORDUZA, **Polimeri biocompatibili şi biologic activi** (Polymères biocompatibles et biologiquement actifs), 1980, 497 p.

M. FLORESCU, **Metode ştiinţifice în dezvoltarea industriei chimice moderne** (Méthodes scientifiques dans le développement de l'industrie chimique moderne), 1979, 256 p.

A. T. BALABAN, I. GĂLĂŢEANU, G. GEORGESCU, LIGIA SIMIONESCU, **Compuşi marcaţi şi radiofarmaceutici cu aplicaţii în medicina nucleară** (Composés marqués et radiopharmaceutiques à application en médecine nucléaire), 1979, 495 p.

(continued on the reverse side)

1984 APR 12

ISSN 0035–4090

I. P. INFORMAŢIA c. 1633

43 426

Lei 40

$ 75 (pour un abonnement annuel)

1103 04

ACADÉMIE DE LA RÉPUBLIQUE SOCIALISTE DE ROUMANIE

REVUE ROUMAINE DE CHIMIE

TOME 29

N° 2

Février 1984

EDITURA ACADEMIEI REPUBLICII SOCIALISTE ROMÂNIA

Rev. Roumaine Chim.

RRCHAX, 29, 2, p. 141–230 (1984), Bucarest

ACADÉMIE DE LA RÉPUBLIQUE SOCIALISTE DE ROUMANIE

COMITÉ DE RÉDACTION

Rédacteur en chef :

I. G. MURGULESCU, membre de l'Académie de la République Socialiste de Roumanie

Rédacteurs en chef adjoints :

A. T. BALABAN et V. EM. SAHINI, membres correspondants de l'Académie de la République Socialiste de Roumanie

Collège de rédaction :

EM. BRATU, ELENA CEAUŞESCU, ECATERINA CIORĂNESCU-NENITZESCU, CR. SIMIONESCU, membres de l'Académie de la République Socialiste de Roumanie ; P. SPACU, membre correspondant de l'Académie de la République Socialiste de Roumanie ; MARGARETA AVRAM, M. BANCIU, I. HAIDUC, D. I. MARCHIDAN, I. MOLDOVAN, G. NIAC et D. SĂNDULESCU

La Revue Roumaine de Chimie paraît 10 fois par an. Toute commande de l'étranger pour les travaux parus aux Editions de l'Académie de la République Socialiste de Roumanie sera adressée à ILEXIM — Departamentul Export-Import Carte (Livres)/Departamentul Export-Import Presă (Revues), P.O.B. 136 — 137, télex 11226, 3, str. 13 Decembrie 79517 Bucarest, Roumanie

Les manuscrits, les livres et les revues proposés en échange, ainsi que toute correspondance seront envoyés à la rédaction

REVUE ROUMAINE DE CHIMIE

125, Calea Victoriei, 79717 Bucarest, Roumanie, téléphone 50 76 80

EDITURA ACADEMIEI REPUBLICII SOCIALISTE ROMÂNIA
125, Calea Victoriei, 79717 Bucarest, Roumanie, téléphone 50 76 80

ORSZÁGOS MŰSZAKI INFORMÁCIÓS KÖZPONT ÉS KÖNYVTÁR 1983

REVUE ROUMAINE DE CHIMIE

Tome 29, N° 2 Février, 1984

I. G. MURGULESCU and EUGENIA SĂLĂGEAN, Equations of state for ionic liquids 143–149

A. CIOCHINĂ, M. CARP and RODICA VÎLCU, Thermal conductivimeter for nonmetallic solids 151–163

A. MASCAŞ and S. STERNBERG, Thermal conductivity of $Co(NO_3)_2 \cdot 6\,H_2O - nH_2O$ system 165–174

A. BĂLDEA and G. NIAC, Kinetics of lignite and lignite char gasification with carbon dioxide and steam 175–183

R. BACALOGLU, I. HAVLIK and C. CSUNDERLIK, Synthesis and characterization of substituted 2-(aryl-azoarylamino)-4,6-dichlor- and 2-chlor-4,6-bis (aryl-azoarylamino)-1,3,5-triazines (in German) 185–191

DUMITRU MĂNOIU, MARIA MĂNOIU, I. G. DINULESCU and MARGARET AVRAM, Friedel-Crafts acylation of alkynes. I. The reaction of 1-alkynes with acetyl chloride$\cdot AlCl_3$-complex in the presence of halogenated nonnucleophilic solvents 193–199

DUMITRU MĂNOIU, MARIA MĂNOIU, I. G. DINULESCU and MARGARET AVRAM, Friedel-Crafts acylation of alkynes. II. The reaction of 1-alkynes with acetyl chloride$\cdot AlCl_3$-complex in aromatic and saturated hydrocarbons as solvents 201–206

JÁNOS FAZAKAS, Effect of atomisation temperature on the sensitivity of lead in atomic absorption spectrometry under electrothermal atomisation and tube wall or platform vaporization (in French) 207–210

L. ROMAN, MARIA ŞERBAN and VICTORIA GUG, Mercaptothiadiazole derivatives-sensitive reagents for the potentiometric determination of Hg (II) (in German) 211–217

C. I. CHIRIAC, A new convenient method for the synthesis of aromatic hydrazides directly from acids using ethylene chlorophosphite as reagent 219–222

M. K. SHARMA and B. K. SHARMA, On the aging of turpentine (montan wax) in water emulsions as functions of viscosity and particle size distribution 223–229

Rev. Roumaine Chim. **29**, *2*, 141–230 (1984), Bucarest

Revue Roumaine de Chimie, **29**, 2, 143–149 (1984)

EQUATIONS OF STATE FOR IONIC LIQUIDS

I. G. MURGULESCU and EUGENIA SĂLĂGEAN
Chair of Physical Chemistry, The Polytechnic Institute of Bucharest, Romania

Received February 15, 1983

The paper deals with the estimation of thermodynamic properties (expansion and compressibility coefficients, entropies and heat capacities) of molten alkaline halides, from Thiele's and Buehler-Hirschfelder-Curtiss' equations, with solid state radii as structural parameter.

A simple and attractive approach to ionic liquids is based on the model of identical rigid spheres fluid, which is assumed to have a perfect solid type lattice.

In order to use the rigid spheres model for ionic liquids, whose ions differ both in size and charge, Stilinger [1] has suggested to replace the true ions by equivalent identical mean particles, as the charge seems to have no significant influence on the thermodynamic properties.

According to Stilinger assumption, several liquid state equations have been tried for ionic liquids, with rather promising results. Particularly useful proved to be the equation of Thiele [2,3] and that of Buehler, Hirschfelder and Curtiss[4,5] but the latter was not so systematically studied as the former one.

This paper aims to prove and compare the adequacies of the two above-mentioned equations to the prediction of thermodynamic properties-expansion and compressibility coefficients, entropies and heat capacities of ionic liquids. The molten alkaline halides have been selected as typical ionic liquids.

THE EQUATIONS OF STATE

For a ν ions molten salt, Thiele's equation may be written as:

$$pV = \nu RT \frac{1 + x + x^2}{(1 - x)^3} \tag{1}$$

where:

$$x = \frac{1}{6}\pi \cdot \sigma^3 \cdot \nu \cdot \frac{N}{V} \tag{2}$$

and σ is the mean ionic diameter.

In the B.H.C. equation, the hypothetical liquid with identical particles is assigned a particular solid like structure, determined by a structure factor γ, so that the equation is:

$$pV = \nu RT \frac{1}{1 - \dfrac{\nu^{1/3}N^{1/3}\sigma}{\gamma^{1/3}V^{1/3}}} \tag{3}$$

As distance measurements in molten alkaline halides revealed a shortage of the nearest neighbours distances, the most compact packing structure has been assumed, i.e., the face centered cubic lattice with γ equal to $2^{1/2}$.

THE THERMAL EXPANSION COEFFICIENTS

From Thiele's equation we have the thermal expansion coefficient:

$$\alpha = \frac{1}{V}\left(\frac{\partial V}{\partial T}\right)_p = \frac{1}{T}\,\frac{1 - x^3}{(1 + 2x)^2} \tag{4}$$

The thermal expansion coefficient of B.H.C. equation follows directly from (3), with $\gamma = 2^{1/2}$:

$$\alpha = \frac{1}{V}\left(\frac{\partial V}{\partial T}\right)_P = \frac{1}{T}\,\frac{1 - \dfrac{\nu^{1/3}N^{1/3}\sigma}{2^{1/6}V^{1/3}}}{1 - \dfrac{2}{3}\,\dfrac{\nu^{1/3}N^{1/3}\sigma}{2^{1/6}V^{1/3}}} \tag{5}$$

The experimental expansion coefficients were obtained from the temperature dependence of liquid densities using the data of Janz [6]

$$\rho = \mathrm{a} - \mathrm{b}\mathrm{T} \tag{6}$$

$$\alpha = \frac{\mathrm{b}}{\rho} \tag{7}$$

In table 1 the experimental and calculated values of the expansion coefficients are given.

From table 1 it turns out that:

- Both equations fail for Li halides
- Equation (5) produces better thermal coefficients values, except for Li, and to some insignificant extent, Na halides.
- The above mentioned discrepancies are easily explained by the simplicity of the model, as well as by the way the mean particle was set up; as expected, the greater the difference between anion and cation radii, the greater the deviation from the experimental value is.

Table 1

Expansion coefficients of molten alkaline halides at their melting points

Salt	T_m, K	V cm^3 mol^{-1}	σ, Å	$\alpha \cdot 10^4 \cdot K^{-1}$				
				exp.	eq (4)	Δ%	eq(5)	Δ%
LiF	1121	14.2	2.010	2.71	2.87	5.9	3.99	47.2
LiCl	883	28.2	2.570	2.87	3.46	20.5	4.85	69
LiBr	823	34.6	2.732	2.59	3.79	46.3	5.15	99
LiI	742	43.1	3.002	2.96	3.94	33	4.54	87
NaF	1268	21.0	2.306	2.89	2.48	−14.2	3.47	20.1
NaCl	1073	37.6	2.814	3.49	2.89	−17	4.05	16
NaBr	1020	44.0	2.980	3.50	2.99	−14.3	4.20	20
NaI	933	54.7	3.232	3.48	3.19	− 8.4	4.48	29
KF	1131	30.4	2.664	3.41	2.61	−23.5	3.66	7.33
KCl	1043	48.9	3.138	3.84	2.78	−28	3.91	1.8
KBr	1007	56.0	3.284	3.91	2.88	−26	4.06	3.8
KI	954	67.8	3.526	3.89	2.96	−24	4.17	7.2
RbCl	995	53.8	3.268	3.95	2.83	−28	3.87	− 2
RbBr	965	60.9	3.408	3.95	2.91	−26	4.05	2.5
RbI	920	73.4	3.656	3.96	2.97	−25	4.18	6
CsF	976	41.6	3.004	3.52	2.87	−18.5	4.03	14.5
CsCl	918	60.3	3.566	3.84	2.56	−33	3.54	− 7.8
CsBr	909	67.9	3.712	3.89	2.58	−34	3.55	− 8.7
CsI	899	81.8	3.946	3.74	2.62	−30	3.62	− 3.2

THE ISOTHERMAL COMPRESSIBILITY COEFFICIENT

The Isothermal Compressibility of Thiele's equation is given by:

$$\beta_T = -\frac{1}{V}\left(\frac{\partial V}{\partial P}\right)_T = -\frac{V}{2RT}\,\frac{(1-x)^4}{(1+2x)^2} \tag{8}$$

and that of B.H.C., by:

$$\beta_T = \frac{V}{2RT}\,\frac{\left(1-\dfrac{2^{5/6}N^{1/3}\sigma}{V^{1/3}}\right)^2}{\left(1-\dfrac{2}{3}\,\dfrac{2^{5/6}N^{1/3}\sigma}{V^{1/3}}\right)} \tag{9}$$

The reference experimental values are those of Bockris, Pilla and Barton,[7] obtained from ultrasound velocity measurements.

The comparison between experimental and calculated values is shown in table 2.

The comparison reveals that all estimated values have the right order of magnitude, but the deviations from experiment are more marked than for the thermal expansion coefficient.

A rather strange agreement between calculated and experimental values of compressibility coefficients for Li halides, where the thermal expansion coefficients give the worst results, can be noticed.

Table 2

Isothermal compressibility coefficients of molten alkaline halides at their melting points

Salt	T_m, K	V cm^3 mol^{-1}	σ, Å	$\beta_T \cdot 10^{11}$ cm^2 dyne^{-1}				
				exp	eq (8)	Δ%	eq (9)	Δ%
LiCl	883	28.2	2.57	2.14	1.84	−14	1.64	−23.3
LiBr	823	34.5	2.732	2.27	2.55	12.3	2.19	− 3.5
NaCl	1073	37.6	2.814	2.87	2.13	−25.7	1.87	−35
NaBr	1020	44.0	2.980	2.83	2.50	−11.7	2.22	−21.6
NaI	973	55.4	3.232	4.00	3.19	−20.2	2.93	−26.7
KCl	1043	48.9	3.138	3.95	2.29	−42	2.15	−45.6
KBr	1073	57.4	3.284	4.38	2.85	−35	2.71	−38
KI	973	68.3	3.526	4.99	3.24	−35	3.13	−37
CsCl	973	61.6	3.566	4.29	1.77	−58.7	2.04	−52
CsBr	973	69.7	3.712	5.58	2.44	−56	1.49	−73.3

THE ENTROPY

For a rigid spheres fluid, according to Yosim and Owens, [8] the entropy of the liquid is given by:

$$S_{(l)} = S_{(g)} - \int_{V_l}^{V_g} \frac{P}{T}\,\mathrm{d}V \tag{10}$$

where we use the notations:

$S_{(g)}$ — the molar entropy of a rigid spheres gas;

$V_{(g)}$ — the molar volume of the gas, at the melting temperature, under atmospheric pressure;

$V_{(l)}$ — the molar volume of the liquid at the melting temperature.

With the two equations of state, the corresponding expressions for the molar liquid entropies are:

$$S_{(l)} = S_{(g)} - 2R\left[\ln \frac{V_{(g)}}{V_{(l)}(1-x)} + \frac{3}{2}\,\frac{x(2-x)}{(1-x)^2}\right] \tag{11}$$

$$S_{(l)} = S_{(g)} - 6R\ln\frac{V_g^{1/3} - 2^{5/6}N^{1/3}\sigma}{V_l^{1/3} - 2^{5/6}N^{1/3}\sigma} \tag{12}$$

As the rigid spheres gas may be assimilated to two moles of monoatomic ideal gas, Sackur-Tetrode equation may be used for the molar entropy of the gas, i.e. at one atmosphere pressure:

$$S_{(g)} = 2(1.5\mathrm{R}\ln\overline{\mathrm{M}} + 2.5\mathrm{R}\ln\mathrm{T} - 2.311) \tag{13}$$

In this equation, $\overline{\mathrm{M}}$ is the mean weight of anion and cation of the salt.

Yosim and Owens have made such calculations for molten alkaline halides, using equation (11), derived from Thiele's equation of state.

Table 3 allows a comparison between experimental, Yosim's and our calculated values.

Table 3

Entropies of molten alkaline halides at their melting points

Salt	T_m, K	V cm^{3}mol^{-1}	V_g cm^{3}mol^{-1}	σ Å	S, cal. mol$^{-1}K^{-1}$				
					exp	eq (11)	Δ%	eq (12)	Δ%
LiF	1121	14.2	92600	2.010	30.6	34.2	11.8	31.14	1.7
LiCl	883	28.2	72740	2.570	33.5	37.8	18.8	32.35	−3.4
LiBr	823	34.6	67540	2.732	34.4	41.6	21	36.73	6.7
LiI	742	43.1	60890	3.002	34.6	45.2	30.6	39.34	13.7
NaF	1268	21.0	104070	2.306	37.4	37.9	1.3	33.24	−11
NaCl	1073	37.6	88060	2.814	40.8	41.8	2.4	36.80	−9.8
NaBr	1020	44.0	83710	2.980	42.4	43.5	2.5	40.34	−4.8
NaI	933	54.7	76570	3.232	43.2	47.1	9.0	42.61	−1.3
KF	1131	30.4	92820	2.664	39.2	38.0	−3.0	35.88	−8.4
KCl	1043	48.9	85600	3.138	42.2	41.8	−0.9	41.19	−2.4
KBr	1007	56.0	82635	3.284	45.6	43.7	−4.2	46.2	1.3
KI	954	67.8	78340	3.526	46.8	45.9	−1.9	43.00	−8.1
RbCl	990	53.8	81250	3.268	44.3	42.6	−3.8	40.77	−7.9
RbBr	965	60.9	79200	3.408	47.6	45.3	−4.8	42.90	−9.8
RbI	920	73.4	75500	3.656	49.0	45.9	−6.3	44.67	−8.8
CsF	976	41.6	80100	3.004	40.3	47.4	17.6	41.04	1.8
CsCl	918	60.3	75340	3.566	45.0	41.6	7.6	40.05	−11
CsBr	909	67.9	74600	3.712	47.8	46.7	−2.3	41.35	−13.5
CsI	899	81.8	73780	3.946	50.7	46.8	−7.7	42.86	−15.4

The experimental entropy values are those used by Yosim.

As for the previous thermodynamic properties, the two equations seem to complete each other; while equation (11) approximates better the heavier salts, equation (12) is more fitted to lighter salts.

THE HEAT CAPACITY

The heat capacity equation is derived from the entropy expression, through the relationship :

$$C_p = T\left(\frac{\partial S}{\partial T}\right)_P \tag{14}$$

and is :

$$C_{p(l)} = C_{p(g)} - T\frac{\partial}{\partial T}\left(\int_{V_l}^{V_g}\frac{P}{T}\,\mathrm{d}V\right) \tag{15}$$

After performing the calculations, the following relation is obtained :

$$C_{p(l)} = C_{p(g)} + \alpha_l V_l P - \alpha_g V_g P \tag{16}$$

As $C_{V(g)}$ for two moles of monoatomic ideal gas is $3R$ and $\alpha_{(g)}$ is T^{-1}, the two equations of state give for the liquid heat capacities :

$$C_{p(l)} = 3R + 2RT\alpha_{(l)} \frac{1 + x + x^2}{(1 - x)^3} \tag{17}$$

$$C_{p(l)} = 3R + 2RT\alpha_{(l)} \frac{1}{1 - \dfrac{2^{1/6}N^{1/3}\sigma}{V_l^{1/3}}} \tag{18}$$

Yosim's and our calculated values together with the Janz's experimental ones, are tabulated in table 4.

Table 4

Heat capacities of molten alkaline halides at their melting points

Salt	T_m, K	V cm^{3}mol^{-1}	σ, Å	$\alpha \cdot 10^4$ K^{-1}	C_p cal. mol$^{-1}K^{-1}$				
					exp	eq. (17)	Δ%	eq. (18)	Δ%
LiF	1121	14.2	2.010	3.99	15.5	13.255	−14.4	14.28	− 7.9
LiCl	883	28.2	2.570	4.85	15.3	13.71	−10.4	14.41	− 5.7
LiBr	823	34.6	2.732	5.15	15.6	13.507	−13.5	14.20	− 8.9
LiI	742	43.1	3.002	5.54	15.1	14.14	− 6.3	14.58	− 3.4
NaF	1268	21.0	2.306	3.47	16.4	13.42	−18.2	14.23	−13.2
NaCl	1073	37.6	2.814	4.05	17.0	13.56	−20.2	14.58	−15.4
NaBr	1020	44.0	2.980	4.20	16.7	13.68	−17	14.42	−13.6
NaI	933	54.7	3.232	4.48	16.5	13.96	−15.4	14.52	−12
KF	1131	30.4	2.664	3.66	16.0	14.04	−12.2	14.53	− 9.2
KCl	1043	48.9	3.138	3.91	16.7	14.21	−15	14.66	−12.6
KBr	1007	56.0	2.284	4.06	16.7	14.23	−14.8	14.62	−12.4
KI	954	67.8	3.526	4.17	17.3	14.47	−16.4	14.67	−15.2
RbCl	995	53.8	3.268	3.87	18.4	14.51	−21	14.50	−21.2
RbBr	965	60.9	3.408	4.05	17.6	14.53	−17.4	14.71	−16.4
RbI	920	73.4	3.656	4.18	17.4	14.84	−17.7	14.80	−14.9
CsF	978	41.6	3.004	4.03	17.7	14.58	−17.6	14.70	−16.9
CsCl	918	60.3	3.566	3.54	18.5	16.887	− 8.7	15.24	−17.6
CsBr	909	67.9	3.712	3.55	18.5	16.92	− 8.5	15.16	−18
CsI	899	81.8	3.946	3.62	18.0	16.87	− 6.2	15.25	−15.2

In heat capacity prediction, the two equations of state have about the same degree of inaccuracy as for the entropy prediction.

CONCLUSIONS

Both equations of state use as structural data only the mean ionic diameter, and, unfortunately, all the properties estimated above, are largely sensitive to this value. Due to the lack of structural information on the liquid, solid state ionic radii were used, although some authors [9] have recommended a smaller radius, at least for compressibility calculations.

There are many other equations of state for liquids, but they do not produce better results and are far too complicated; Till now, no equation predicts equally well all the thermodynamic properties.

Our results emphasize that both equations of state are good, as a first approximation, to the prediction of thermodynamic properties of molten alkaline halides.

Also, our result proves that the larger use of Thiele's equation is just a matter of preference, the B.H.C. equation being at least as good as that of Thiele.

REFERENCES

[1] F. H. Stilinger jr, *J. Chem. Phys.*, **35**, 1581 (1961).
[2] H. Reiss, H. L. Frisch and J. L. Lebowitz; *J. Chem. Phys.*, **31**, 369 (1959).
[3] E. Thiele, *J. Chem. Phys.*, **39**, 474 (1963).
[4] J. O. Hirschfelder, C. F. Curtiss and R. Byron Bird, "Molecular Theory of Gases and Liquids", New York, 1954, p. 286.
[5] I. G. Murgulescu and E. Sălăgean, *Rev. Roumaine Chim.*, **17**, 603 (1972).
[6] G. Janz, "Molten Salts Handbook", New York, 1967.
[7] J. O'M Bockris, A. Pilla and J. Barton, *Rev. Chim. Acad. R.P.R.*, **7**, 59 (1962).
[8] S. J. Yosim and B. B. Owens, *J. Chem. Phys.*, **41**, 2032 (1964).
[9] C. A. Coulson, "Valence", Oxford University Press, Oxford, 1959.

Revue Roumaine de Chimie, **29**, *2*, 151–163 (1984)

THERMAL CONDUCTIVIMETER FOR NONMETALLIC SOLIDS

A. CIOCHINĂ*, M. CARP* and RODICA VÎLCU**

* Centre of Physical Chemistry – ICECHIM, Spl. Independenței no. 202, Bucharest 77208, Romania

** The Polytechnic Institute, Department of Physical Chemistry and Electrochemical Technology, Blvd. Republicii 13, Bucharest, Romania

Received February 22, 1983

This contribution presents a method and an apparatus for absolute measurement of thermal conductivity of homogenous and dry nonmetallic solids, within the 0.02–5 W/(m°C) range. The apparatus employs the steady-state hot wire method and the test specimen is a parallelipiped of square section. Data on different materials within the –30 – 150°C range show that the accuracy and the precission of measurements are 5% and 3% respectively. Some computation relations for samples with other sections are also presented.

1. INTRODUCTION

The most series instruments available (dr. BOCK, KARL WEISS – G.D.R., CEAST – Italy, LINSEIS – F.R.G., DYNATECH – U.S.A.) for thermal conductivity measurements on homogenous nonmetallic solids operate according to the principle of steady-state plate (or disk) [1,2]. These instruments have some inconveniences such as: – samples are big and with imposed shapes and dimensions; – sample surfaces have to be plane, condition difficult to satisfy for large areas; – complicated electronic apparatus are employed which process the signals from a great number of temperature transducers; – if the conditions for sample preparation (dimensions, state of surfaces) are met the accuracy of the measurements is in the best of cases of 5%; – instruments are quite expensive.

In the present paper the method and apparatus are presented for absolute measurement of thermal conductivity on homogeneous and dry nonmetallic solids, within the 0.02 – 5 W/(m°C) range. [3] The apparatus is based on the steady-state hot wire method. The sample is a parallelepiped of square section made up by superposing two identical plates, P_1 and P_2, of length L, width l and thickness $\frac{l}{2}$. In-between the two semi-samples a heating metallic wire and a thermocouple are introduced, the latter disposed parallelly against the heater. The assembly is thermostated at temperature t_0 in the cell C (Fig. 1).

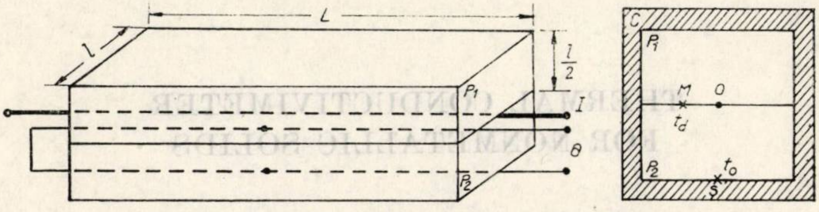

Fig. 1. — Principle of the measurement method.

2. MATHEMATICAL MODEL

Let us consider a linear source of heat dissipating a constant power q on its unit length. The heat source is disposed axially within a parallelepiped sample of infinite length and a square section with an edge l, having a thermal conductivity λ. The external faces of the sample are maintained at the temperature t_0. The temperature t_d reached by the sample in the steady-state regime is then calculated in the point M situated at a distance d against the heating source in 0 (Fig. 2).

Inside the sample, the temperature field $t(x, y)$ satisfied Laplace's equation:

$$\frac{\partial^2 t}{\partial x^2} + \frac{\partial^2 t}{\partial y^2} = 0 \tag{1}$$

Along the frontier of the square, $(x, y) = \pm \frac{l}{2}$, and thence:

$$t\Big|_{\substack{x=\pm l/2 \\ y=\pm l/2}} - t_0 = 0 \tag{2}$$

Considering a system of polar coordinates, r and φ, with the center in 0 $(r = (x^2 + y^2)^{1/2}$, $\mathrm{tg}\,\varphi = y/x)$ we must also have:

$$\lim r \frac{\partial t}{\partial r}\Big|_{r=0} = -\frac{q}{2\pi\lambda} \tag{3}$$

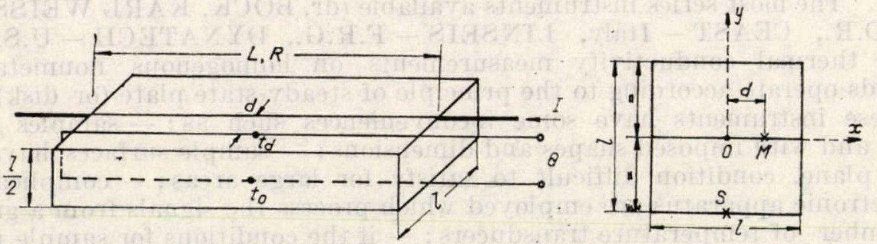

Fig. 2. — Quantities employed in calculations.

Equation (1) with limit conditions (2) and (3) determines the temperature field distribution. The conformal plot which transforms the complex plane of the circle unity (complex variable ξ) into the complex plane of the square of edge l (complex variable z) is:

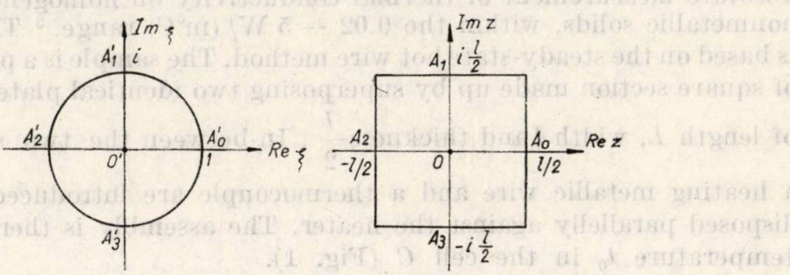

$$z(\xi) = \frac{lC}{2}\int_0^{\xi}\frac{du}{(1+u^4)^{1/2}} \tag{4}$$

$$C = \left(\int_0^1 \frac{du}{(1+u^4)^{1/2}}\right)^{-1} = 1.0787\ldots \tag{5}$$

From relation (4) it results that the inverse of the function $z(\xi)$ in the vicinity of the origin is given by the development:

$$\xi(z) = \frac{2z}{lC}\left[1 + \frac{1}{10}\left(\frac{2z}{lC}\right)^4 + \frac{1}{120}\left(\frac{2z}{lC}\right)^8 + \ldots\right] \tag{6}$$

This is the expression of the conformal transformation of the given square into the circle of radius unity. For the case with homogeneous Dirichlet conditions along the square frontier and with the source in $z = 0$, the Green function is:

$$G(z, 0) = \frac{1}{2\pi}\ln\frac{1}{|\xi(z)|} \tag{7}$$

The temperature distribution which satisfies equations (1)—(3) is:

$$t_z - t_0 = \frac{q}{2\pi\lambda}\ln\frac{1}{|\xi(z)|} \tag{8}$$

where $\xi(z)$ is given by relation (6). For the point M:

$$t_d - t_0 = \frac{q}{2\pi\lambda}\ln\frac{1}{|\xi(d)|} \tag{9}$$

$$\lambda = \frac{q}{2\pi(t_d - t_0)}\ln\frac{1}{|\xi(d)|} \tag{10}$$

Here:

$$\xi(d) = \frac{2d}{lC}\left[1 + \frac{1}{10}\left(\frac{2d}{lC}\right)^4 + \frac{1}{120}\left(\frac{2}{lC}\right)^8 + \ldots\right] \tag{11}$$

If $[2d/(Cl)]^4 \leqslant 0.01$ or $(d/l) \leqslant 0.17$, it results that $\xi(d) = 2d/(Cl)$. Therefore:

$$\lambda = \frac{q}{2\pi\theta}\ln[Cl/(2d)] = \frac{q}{2\pi\theta}K \tag{12}$$

where $\theta = t_d - t_0$ and $C = 1.0787\ldots$

The computation relations of K for a finite cylinder embedded in samples of various shapes [4,5] are given in tables 1 and 2.

Table 1

Computation relations of K for samples of various shapes

Geometry	Arrangement	K	Error
cylinder in square-section sample	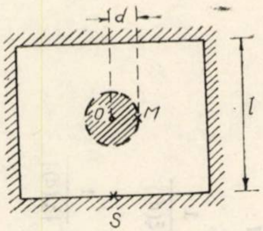	$\ln\,[1.0787l/(2d)]$	$\leqslant 0.1\%$ for $d/l \leqslant 0.171$ $\leqslant 1\ \%$ for $d/l \leqslant 0.303$
cylinder in rectangular-section sample	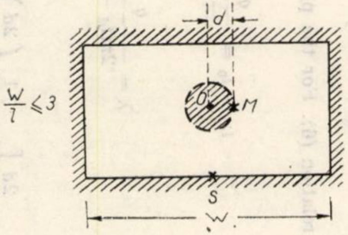	Table 2.	$\leqslant 0.1\%$ for $W/l \leqslant 3$
cylinder in semiinfinite plane sample	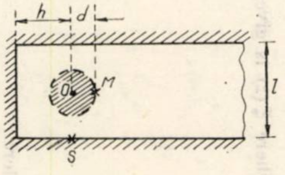	$\ln\left[\frac{2l}{\pi d}\,\mathrm{tgh}\left(\frac{\pi h}{l}\right)\right]$	good accuracy for $2d/l < 0.5, \quad h/l < 0.5$

cylinder in semiinfinite sample	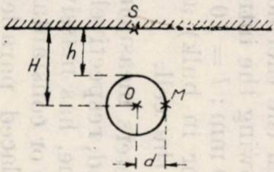	$\ln\left[\frac{H}{d}+\sqrt{\left(\frac{H}{d}\right)^{2}-1}\right]$; $H = h + d$	good accuracy
		$\ln\left[\left(1+\frac{h}{d}\right)+2\sqrt{\frac{h}{2d}\left(1+\frac{h}{2d}\right)}\right]$	good accuracy
		$\ln(2h/d)$ or $\ln(2H/d)$	good accuracy for $H, h > 4d$
cylinder in large plane sample	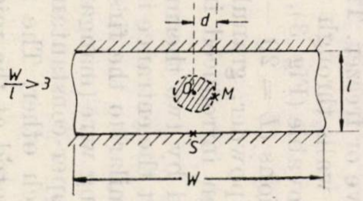	$\ln\left[\frac{\sqrt{X}+\sqrt{Y}}{\sqrt{X-Y}}\right]-\frac{R^4}{30}+0.014R^8$ $X = 1 + 2\sinh^2 R$; $Y = 1 - 2\sin^2 R$ $R = \pi d/(2l)$	accurate for $0.10 \leqslant \frac{2d}{l} \leqslant 0.99$
		$X \ln(\operatorname{ctg} R) + XY(\operatorname{ctgh} R)$ $X = 1/(1 + Y)$; $R = \pi d/(2l)$ $Y = \left(\frac{\operatorname{tg}^4 R - 1}{\operatorname{tgh}^4 R - 1}\right)\frac{\operatorname{tgh}^2 R}{\operatorname{tg}^2 R}$	accurate
		$\ln\left(\frac{2l}{\pi d}\right)-\frac{0.01346\,(2d/l)^4}{1-0.355125\,(2d/l)^4}$	$\leqslant 1\%$ for $2d/l \leqslant 0.6$
		$\ln\left[\frac{1+\sqrt{1-(\operatorname{tg}^2 R-\operatorname{tgh}^2 R)}}{\operatorname{tg} R+\operatorname{tgh} R}\right]$ $R = \pi d/(2l)$	$\leqslant 1\%$ for $2d/l \leqslant 0.54$
		$\ln[2l/(\pi d)]$	$\leqslant 1\%$ for $2\ d/l \leqslant 0.55$

Table 2

Computed values of K for cylinder in rectangular – section sample

W/l $2d/l$	1.0	1.25	1.50	1.75	2.00	2.50	3.00
0.05	3.072	3.160	3.202	3.220	3.229	3.236	3.237
0.10	2.378	2.467	2.508	2.528	2.537	2.543	2.544
0.20	1.685	1.774	1.815	1.834	1.843	1.849	1.850
0.30	1.280	1.368	1.409	1.429	1.438	1.444	1.445
0.40	0.992	1.079	1.120	1.140	1.149	1.155	1.156
0.50	0.769	0.834	0.896	0.915	0.924	0.930	0.931
0.60	0.586	0.668	0.709	0.729	0.737	0.743	0.745
0.70	0.432	0.506	0.547	0.566	0.575	0.581	0.582
0.80	0.297	0.360	0.400	0.418	0.426	0.431	0.432
0.90	0.174	0.219	0.253	0.267	0.274	0.279	0.280
0.99	0.045	0.059	0.072	0.077	0.080	0.082	0.082

3. THERMAL CONDUCTIVIMETER

The thermal conductivimeter consists of measurement cell, transducer and measuring apparatus. [3] *The cell* has been made in two versions : one thermostated with circulating fluid from the thermostat or cryostat and the other thermostated in a drying stove or freezer. The first cell is made up of four metallic plates with double walls through which the thermostating fluid flows. The cell walls are movable (Fig. 3), allowing the introduction of samples of different dimensions ($L = 20 - 400$ mm ; $l = 10 -$ 150 mm). The non-coherent samples (powder, granules or in bulk) are placed in a metallic case which is then introduced into the cell.

The cell thermostating is followed by two thermometers measuring the temperatures t_i and t_e of the fluid, at the entrance in and, respectively, exit from the cell. The second cell, similar to the first one, has massive walls. *The transducer* consists of a heating wire (manganine or constantan) and a thermocouple (for example copper-constantan) placed parallely at a distance $d = 2 - 5$ mm from each other. The measuring bead of the thermocouple is approximately located at the middle of the heating wire. The wire diameters are smaller or equal to 0.1. mm. The wires are mechanically secured at the ends or sandwiched in-between plastic foils (Fig. 4).

The transducer made as a flexible band was used between – 50 – 250°C. Zone I of the transducer is introduced in-between the two semi-samples. Zone II is placed between the cell wall and sample (Fig. 5).

The measuring apparatus consists of a d.c. constant current source (to supply the heating wire) and a d.c. microvoltmeter (to measure the t.e.m.f. of the thermocouple). The values of the heating current and

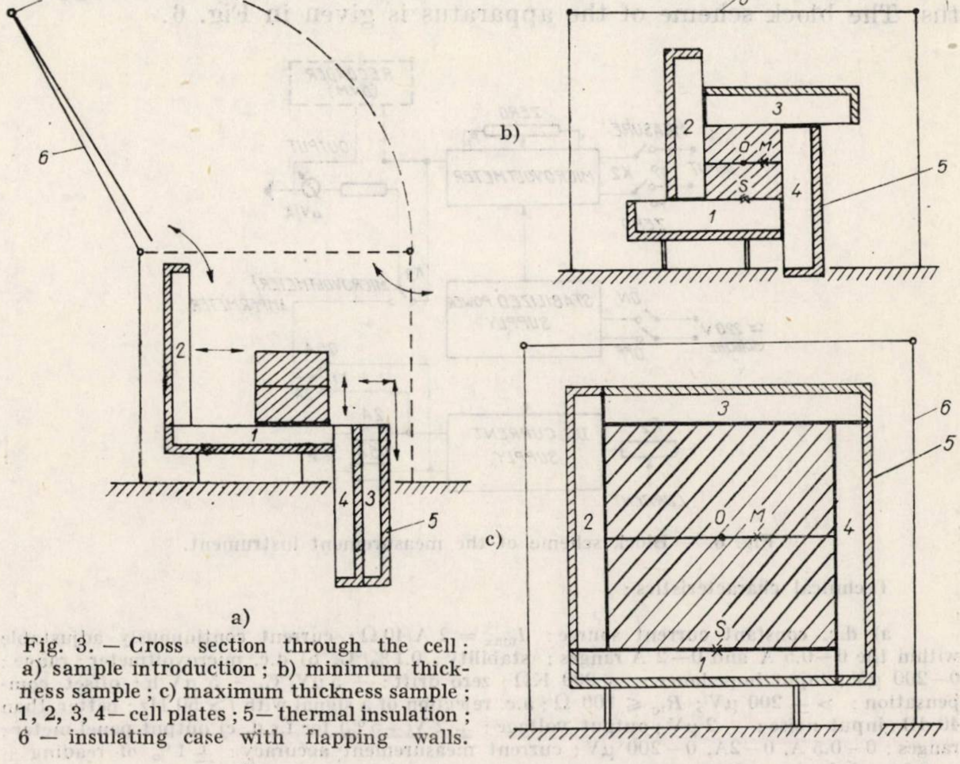

Fig. 3. — Cross section through the cell: a) sample introduction; b) minimum thickness sample; c) maximum thickness sample; 1, 2, 3, 4 — cell plates; 5 — thermal insulation; 6 — insulating case with flapping walls.

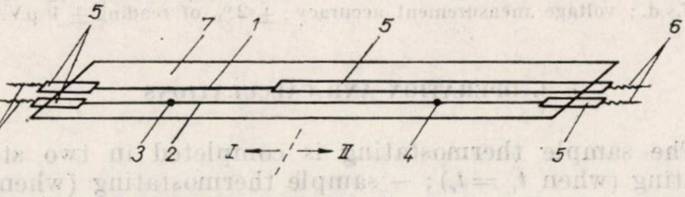

Fig. 4. — Scheme of the transducer: 1 — heating wire; 2 — copper — constantan thermocouple; 3 — measurement junction; 4 — reference junction; 5 — copper foil; 6 — copper leads; 7 — plastic foil.

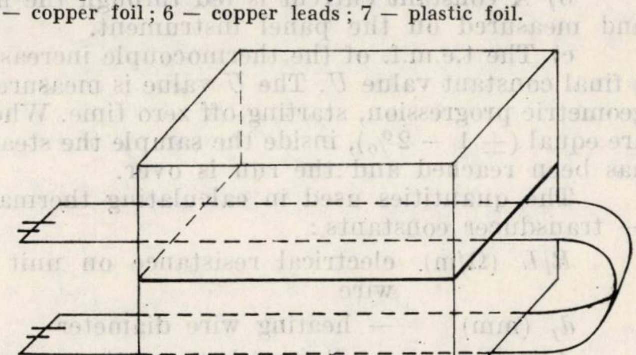

Fig. 5. — Sample-transducer assembly.

t.e.m.f. are alternatively readout on the panel instrument of the apparatus. The block scheme of the apparatus is given in Fig. 6.

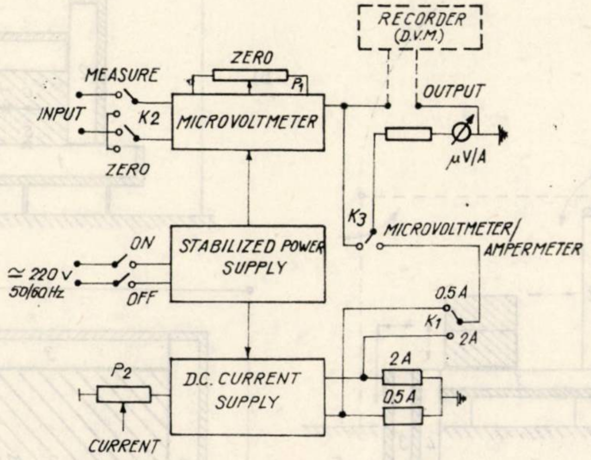
RECORDER
(D.V.M.)
ZERO
MEASURE
P_1
OUTPUT
INPUT
K2
MICROVOLTMETER
ZERO
μV/A
K3
MICROVOLTMETER/
AMPERMETER
ON
STABILIZED POWER
SUPPLY
≃ 220 V
50/60 Hz
OFF
0.5 A
K1
2A
2A
P2
D.C. CURRENT
SUPPLY
0.5A
CURRENT

Fig. 6. — Block scheme of the measurement instrument.

Technical characteristics:

a) d.c. constant current source: $I_{\max} = 2\ \mathrm{A}/40\ \Omega$; current continuously adjustable within the 0—0.5 A and 0—2 A ranges; stability: 0.1 %/°C. b) d.c. microvoltmeter: range: 0—200 μV; input impedance: $> 200\ \mathrm{K\Omega}$; zero drift: $\pm 5\ \mu\mathrm{V}/°\mathrm{C}$, $\pm 5\ \mu\mathrm{V/h}$; offset compensation: $> \pm 200\ \mu\mathrm{V}$; $R_{tc} \leqslant 100\ \Omega$; a.c. rejection of a signal with $f \geqslant 50$ Hz: better than 40 dB; input noise: $\pm 2\ \mu\mathrm{V}$; output voltage: $\pm 2\ \mathrm{V} (\pm 5\%)$ for f.s.d. c) output panel meter: ranges: 0—0.5 A, 0—2A, 0—200 μV; current measurement accuracy: $\pm 1\%$ of reading $\pm$ $\pm 0.5\%$ of f.s.d.; voltage measurement accuracy: $\pm 2\%$ of reading $\pm 1\ \mu\mathrm{V}$.

4. OPERATION AND CALCULATIONS

a) The sample thermostating is completed in two steps: — cell thermostating (when $t_i = t_e$); — sample thermostating (when t.e.m.f. is zero).

b) A constant current is fed through the heating wire (zero time) and measured on the panel instrument.

c) The t.e.m.f. of the thermocouple increases in time from zero to a final constant value U. The U value is measured at times selected in a geometric progression, starting off zero time. When two successive values are equal ($\pm 1 - 2\%$), inside the sample the steady-state thermal regime has been reached and the run is over.

The quantities used in calculating thermal conductivity are:

— transducer constants:

R/L (Ω/m) electrical resistance on unit length of the heating wire

d_f (mm) — heating wire diameter

d (mm) — distance between the measuring bead of the thermocouple and heating wire

$U(t_0)$ (μV (°C)) — thermocouple equation
— geometric constant of the sample :
l (mm) — sample thickness
— experimental parameters :
t_0 (°C) — reference function temperature of the thermocouple ($t_0 = t_i = t_e$)
I (A) — current through the heating wire
U (μV) — steady-state t.e.m.f. value of the thermocouple.

The thermal conductivity, λ, expressed in W/(m, °C) is obtained by relation :

$$\lambda = 0.367 \frac{R}{L} \frac{I^2}{\theta} \log \left(0.54 \frac{l}{d} \right) \tag{13}$$

where : $\theta = U / \varepsilon (t_0)$; $\varepsilon (t_0) = \mathrm{d} U / dt_0$
The thermal conductivity is measured at the temperature $t = t_0 + (\Delta t/2)$, where Δt is calculated by :

$$t = \theta \frac{\log \left(1.08 \dfrac{l}{d_f} \right)}{\log \left(0.54 \dfrac{l}{d} \right)} \tag{14}$$

5. EXPERIMENTAL DATA

Both method and apparatus have been tested by experiments on a rich assortment of materials and under different experimental conditions (the following parameters have been observed : — nature and homogeneity of the samples ; — sample dimensions (L and L/d) ; — degree of the sample surface processing ; — quality of the thermal contact between sample, transducer and cell ; — value of the heating current ; — distance between transducer wires ; — deviation from the wire parallelism ; — eccentricity of the heating wire ; — constructive non-identity of the transducers ; — position of the measuring junction along the longitudinal axis of the sample ; — the way the transducers were secured between the semi-samples (without plastic foil ; included totally or partially in different parts into the foil ; fixed with adhesive tape onto one of the semi-samples ; included in the material ; disposed in the grooves machined in the material) ; — type and dimensions of the plastic foil ; — quality of the thermostating ; — degree of reaching the initial thermal equilibirum). When large plane samples were possible to obtain, our results, λ, were compared with λ_S and λ_T values obtained by the plate method in single — plate system versions (dr. Bock) and, respectively, twinplate system (Poensgen). Both apparatus were calibrated with cork and Flintglass standard discs with which dr. Bock apparatus was endowed. Our apparatus was tested with a SUPEREX (Portugal) cork standard. Some of our results obtained during the last four years are presented in Table 3.

6. DISCUSSIONS

For SUPEREX cork standard which has λ (0°C) $= 0.0373$ W/(m°C), the value λ (0°C) $= 0.0375 - 0.0377$ W/(m°C) was obtained, that is with an error of $0.53 - 1.06\%$. For materials with $\lambda = (0) \times 10^{-1}$ W/(m°C), determinations at different temperatures were carried out and the temperature coefficient, β, of thermal

Table 3

Experimental data (τ = total duration of the measurement, steps 4.a. to 4.c.; the λ data are extreme values obtained by measurements with the same transducer on different test specimens and with different transducers on the same test specimen)

Sample (density)	Our apparatus					Plate apparatus ($t = 25°$; $\tau = 8$ h)
	L (mm)	l (mm)	t (°C)	τ (h)	λ (W/(m°C))	λ_s, λ_T (W/(m°C))
Superex Cork (150 kg/m³)	100	40	0	4	0.0375−0.0377	
	250	70	25	2.5	0.0405−0.0406	
	250	60	25	2.5	0.0406−0.0420	0.0420−0.0430
Paraffine (920 kg/m³)	300	60	20	2	0.260 −0.267	
Rigid polyurethane foam (28.5−31.5 kg/m³)	190	40	30	2.5	0.0290−0.0304	
Poly(methyl methacrylate) (plexiglas) (1175 kg/m³)	150	40	25	3,5	0.190 −0.195	
Expanded polystyrene (24 kg/m³)	250	50	25	2	0.0350−0.0357	0.0357−0.0364
			50	4	0.0382−0.0387	
Cell concrete (400 kg/m³)	200	70	25	5	0.100 −0.102	
			40	5.5	0.114 −0.116	
(450 kg/m³)	200	80	25	5	0.103 −0.107	0.115 −0.118
(525 kg/m³)	200	80	25	5	0.117 −0.120	0.120 −0.124
			100	8	0.147 −0.148	
(540 kg/m³)	200	80	25	5	0.130 −0.134	
			40	5.5	0.135 −0.136	
(662 kg/m³)	200	60	30	5	0.164 −0.169	
(675 kg/m³)	200	80	25	5	0.168 −0.172	0.170 −0.175
Glass — wool (70 kg/m³)	250	60	20	2.5	0.0317−0.0319	0.0325−0.0330
Mineral — wool (90 kg/m³)	250	80	−30	8	0.0342−0.0344	
			25	3.5	0.0387−0.0388	0.0389−0.0393
			80	6	0.0448−0.0450	
			150	8	0.0536−0.0538	
Stabilite (300 kg/m³)	250	80	25	3	0.082 −0.099	
Expanded perlite (120 kg/m³)	250	70	25	4	0.0426−0.0429	0.0435−0.0440
Felt (100 kg/m³)	250	70	25	3	0.0695−0.0720	0.0710−0.0730
Polyurethanic wastes (70 kg/m³)	250	70	25	3	0.047 −0.048	0.0490−0.050

Table 3 (continued)

Sample (density)	Our apparatus					Plate apparatus ($t = 25^0$; $\tau = 8$ h)
	L (mm)	l (mm)	t (°C)	τ (h)	λ (W/(m°C))	λ_s, λ_T (W/(m°C))
Thermal insulators with :						
— wood-refuse (200kg /m³)	250	40	25	3	0.0917–0.0950	0.0970–0.100
— ash from thermal power station						
(400 kg/m³)	250	80	25	3	0.0900–0.0920	
(500 kg/m³)	250	80	25	3	0.100 –0.103	
— perlite (200 kg/m³)	250	60	25	3	0.0630–0.0650	
Concrets :						
C–200 (2090 kg/m³) agent : ash from thermal power station aggregate : gravel 0–3 mm 22% ; 3–7 mm 28% 7–16 mm 25% ; 16–31 mm 25%	300	80	20	5	0.81 –0.84	
C – 250 (2290 Kg/m³) agent : cement aggregate : gravel 0–3 mm 30% 3–7 mm 30% 7–16 mm 40%	300	80	20	5	1.23 –1.28	

conductivity was calculated. The values $\beta = 0.00245 - 0.0026$ (°C)$^{-1}$ were found, as comparad with the mean value $\beta = 0.0025$ (°C)$^{-1}$) proposed in literature for building materials. Our results agree within the experimental errors, with the λ_s and λ_T values. In order to do correct measurements, an as good as possible thermal contact is recommended between sample, transducer and cell as well as $L \geqslant 2\,l$. The duration of the measurement is function of the thermal diffusivity and thickness of the sample. In our case, the samples can be much smaller than those used in plate apparatus. For non-homogeneous materials (for example concrete mixed with gravel) there will be a scatter of the results owing to sample non-homogeneity and therefore bigger samples are recommended. The determinations are carried out on more samples from the same material which will be characterized by the mean value and standard deviation of the results ; the latter indicates the degree of the thermal transfer variance due to the sample non-homogeneity. Moreover, determinations can be made on the same sample by moving the thermocouple measuring junction as to scan the sample surface. Studies carried out on such materials have shown that the results are correct and conclusive if thermal conductivity values of the components are of the same order of magnitude. For $\lambda = 0.02 - 5 \frac{\mathrm{W}}{\mathrm{m^\circ C}}$ the error due to the plastic foil of the transducer is within the measurement accuracy. The foil improves the thermal contact between transducer and sample, especially for hard samples. The transducer obtained in this way has the advantage of a simple and rapid handling and it protects the wires from mechanical deterioration. Unfortunately, a mathematical model has not been worked out as yet to take the perturbation due to the plastic foil into account.

We consider that the above presented results are conclusive enough to highlight some of the advantages of both method and apparatus described, against the plate method and respective series instruments : — determinations are absolute and the calculation is simple ; — apparatus is quite easily feasible and easy to operate ; it has good viability and low electricity consumption ; — parallelepiped samples of different sections are easy to obtain for every type of materials ; — dimensions of the samples are not imposed ; — measurement cell has adjustable inner space ; — determinations can be carried out at different temperatures ; — the thermal field is created and measured inside the sample ; — heat losses are avoided by the measuring procedure ; — time evolution and moments when inside the sample the initial thermal equilibrium and, the final steady-state thermal regime respectively, are reached, are both accurately and directly measurable — measurement duration is directly available ; — surfaces of thermal contact of the sample are small and can be easily machined ; — measurement accuracy (± 5%) and precision (±3%) are at least equal to those of the best series apparatus abroad.

In a subsequent paper we will show that our apparatus allows also the determination of the sample thermal conductivity and thermal diffusivity by the transient hot wire method. Thermal properties of the sample are thus measured with the same apparatus by method different in principle, a fact utterly important. In the first place, it offers the possibility of choosing one of the methods depending on the sample nature (homogeneity, humidity) and/or its dimensions. In the second place, the concordance between the values is the most objective and severe test for the measurements accuracy and for the correctness in running the experiments with respect to the conditions imposed by the theory of the methods.

ANNEXE

A. 1. Error calculation

From the law of error propagation, the most probable random error of λ is :

$$\delta\lambda/\lambda = \left[\left(\frac{\delta R}{R}\right)^2 + \left(\frac{\delta L}{L}\right)^2 + 4\left(\frac{\delta I}{I}\right)^2 + \left(\frac{\delta \varepsilon}{\varepsilon}\right)^2 + \left(\frac{\delta U}{U}\right)^2 + \left(\frac{\delta A}{A}\right)^2\right]^{1/2}$$

where $A = \ln(0.54\ l/d)$ and :

$$\left(\frac{\delta A}{A}\right)^2 = \frac{1}{[\ln(0.54l/d)]^2}\left[\left(\frac{\delta l}{l}\right)^2 + \left(\frac{\delta d}{d}\right)^2\right]$$

For the most unfavourable case, with $l = 10$ mm, $\delta l = 0.1$ mm, $d = 2$ mm, $\delta d = 0.05$ mm, one obtains : $(\delta A/A)^2 = 7.35 \times 10^{-4}$. With the following maximum relative errors : $\delta R/R = 1 \times 10^{-3}$; $\delta L/L = 1 \times 10^{-3}$; $\delta I/I \leqslant 1.5 \times 10^{-2}$; $\delta U/U \leqslant 2 \times 10^{-2}$; $\delta\varepsilon/\varepsilon \leqslant 2 \times 10^{-2}$, it results :

$$\delta\lambda/\lambda \leqslant 4.94 \times 10^{-2}$$

The influence of the eccentricity has been examined for cylindrical symmetry [6-9]. The eccentricity, e, is defined as the distance from the sample axis to the axis of the heating wire. If eccentricity exists the λ values are lower than the real ones. Using percent eccentricity $E = 100\ (2\ e/l)$, the computed relative errors, $\Delta\lambda/\lambda\ (\%)$, are listed in Table A.1.

Table A.1.

Relative error $(\Delta\lambda/\lambda)\%$ values due to the eccentricity

$E(\%)$ \ $\frac{l}{2d}$	3	4	5	6	7	8	9	10	20	30	40	50
2	0.04	0.03	0.03	0.02	0.02	0.02	0.02	0.02	0.01	0.01	0.01	0.01
3	0.09	0.07	0.06	0.05	0.05	0.04	0.04	0.04	0.03	0.03	0.02	0.02
4	0.16	0.12	0.10	0.09	0.08	0.08	0.07	0.07	0.05	0.05	0.04	0.04
5	0.26	0.19	0.16	0.14	0.13	0.12	0.12	0.11	0.08	0.07	0.07	0.06
6	0.37	0.28	0.23	0.21	0.19	0.18	0.17	0.16	0.12	0.11	0.10	0.09
7	0.50	0.38	0.32	0.28	0.26	0.24	0.23	0.21	0.16	0.14	0.13	0.12
8	0.65	0.49	0.41	0.37	0.33	0.31	0.29	0.28	0.21	0.19	0.17	0.16
9	0.82	0.62	0.52	0.46	0.42	0.39	0.37	0.35	0.27	0.24	0.22	0.21
10	1.02	0.76	0.64	0.57	0.52	0.49	0.46	0.44	0.33	0.29	0.27	0.25
20	4.0	3.0	2.5	2.3	2.1	1.9	1.8	1.7	1.3	1.2	1.1	1.0
30	8.7	6.6	5.6	4.9	4.5	4.2	4.0	3.8	2.9	2.5	2.3	2.2
40	14.8	11.3	9.5	8.5	7.8	7.2	6.8	6.5	5.0	4.4	4.0	3.8
50	22.0	16.8	14.3	12.7	11.6	10.9	10.3	9.8	7.5	6.6	6.1	5.7

REFERENCES

[1] "Thermal Conductivity", ed. R. P. Tye, Academic Press, London, 1969 ; vol. I, chap. 4 ; vol. II, chap. 4.

[2] Y. S. Touloukian, P. E. Liley and S. C. Saxena, "Thermophysical Properties of Matter", vol. 2, TPRC Data Series, Plenum Press, New York, 1970, p. 15 .

[3] Gh. Vasu, A. Ciochină and D. Serbănescu, Romanian Patent No. 75282 (1980).

[4] M. A. R. Gunston, "Microwave Transmission — Line, Impedance Data", Van Nostrand Reinhold Comp. Ltd., New York, 1972, chap. 4.

[5] S. S. Kutateladze and V. M. Borishanskii, "A Concise Encyclopedia of Heat Transfer", Pergamon Press, Oxford, 1966, p. 36.

[6] R. Vîlcu and A. Ciochină, *Rev. Roumaine Chim.*, **17**, 1679 (1972).

[7] R. Vîlcu and A. Ciochină, *Studii și Cercetări de Chimie, Acad. R.S.R.*, **21**, 571 (1973).

[8] R. Vîlcu and A. Ciochină, *Studii și Cercetări de Chimie, Acad. R.S.R.*, **21**, 643 (1973).

[9] R. Vîlcu and A. Ciochină, *Rev. Roumaine Chim.*, **26**, 161 (1981).

Revue Roumaine de Chimie, **29**, *2*, 165–174 (1984)

THERMAL CONDUCTIVITY OF $Co(NO_3)_2 \cdot 6H_2O - nH_2O$ SYSTEM

A. MASCAŞ [*,★] and S. STERNBERG [**]

[*] Laboratory of Physical Chemistry, Institute of Higher Education, Str. Armatei Roşii No. 5, Oradea, 1976, Romania

[**] Dept. of Physical Chemistry, The Polytechnic Institute, str. Polizu No. 1, Bucharest, 78126, Romania

Received February 27, 1983

The thermal conductivity of $Co(NO_3)_2 \cdot 6H_2O - nH_2O$ system was studied within the concentration range corresponding to $n = 0$ and $n = 491$ at temperatures between 303 K and 353 K. For $n > 5$ a linear dependence of thermal conductivity on molar concentration of nitrate was obtained ; at higher concentration there are considerable deviations from linearity. At low concentrations the dependence of thermal conductivity λ of the system on temperature is described by an Arrhenius-type equation. At higher concentrations the dependence of thermal conductivity on concentration is described by the equation : $\Delta\lambda = A_1 \exp -\left[\frac{B_i n}{c}\right]$ where A and B are empirical constants while the dependence on temperature is described by an equation with three constants (Vogel-Tamann-Fulcher).

INTRODUCTION

Fused crystal hydrates have been focusing increasing attention because of their theoretical importance as well as their practical applications among which the energy storage. [1-11]

Of the transport properties electrical conductivity, viscosity and diffusion were studied. The data on thermal conductivity are scarce.

In previous papers [1,11] the thermal conductivity of $Ca(NO_3)_2 + 4H_2O - nH_2O$ was studied. This contribution deals with thermal conductivity of hexahydrated cobalt nitrate and of hexahydrated cobalt nitrate-water system, for concentrations ranging from $n = 0$ to $n = 491$ at temperatures between 303 K and 353 K.

EXPERIMENTAL

Preparation of chemicals. Reagent grade $Co(NO_3)_2 \cdot 6H_2O$ and twice distilled water degased by boiling were employed. The cobalt content was determined by complexometry with ethylene diamine tetra-acetic acid (EDTA). [12]

[★] Aurel Mascaş deceased on October 5, 1982

Equipment. Various types of devices and methods of determination of thermal conductivity in liquids [13,14] are presented in the literature. All have advantages and drawbacks. No equipment has enjoyed general utilization.

In this study use has been made of an apparatus designed by ourselves, [1] based on the principle of the catharometer employed as detector in gas chromatography.

A relative method and at least two convenient standard liquids (whose thermal conductivity was known) were employed. The procedure was described elsewhere. [1] The standard liquid was in most instances ethylene glycol—water mixtures. With the apparatus utilized at a sensitivity of $2.10^{-4}\mathrm{W.m^{-1}\,K^{-1}}$ the precision was of ± 1.0%.

RESULTS AND DISCUSSION

Table 1 lists the values of thermal conductivity of fused cobalt nitrate hexahydrated without or with water.

Table 1

The values of thermal conductivity of $Co(NO_3)_2 \cdot 6\,H_2O - n\,H_2O$ system

System	$\lambda(\mathrm{W.m^{-1}.k^{-1}})$					
	303 K	313 K	323 K	333 K	343 K	353 K
$Co(NO_3)_2 \cdot 6H_2O - 0{,}0H_2O$	0.2954*	0.3268*	0.3594*	0.3826	0.4041	0.4233
$Co(NO_3)_2 \cdot 6H_2O - 0{,}5H_2O$	0.3152*	0.3442*	0.3745	0.3966	0.4164	0.4350
$Co(NO_3)_2 \cdot 6H_2O - 1{,}0H_2O$	0.3400*	0.3665*	0.3935	0.4133	0.4340	0.4512
$Co(NO_3)_2 \cdot 6H_2O - 1{,}6H_2O$	0.3652*	0.3884	0.4152	0.4338	0.4512	0.4675
$Co(NO_3)_2 \cdot 6H_2O - 2{,}0H_2O$	0.4124	0.4210	0.4330	0.4495	0.4670	0.5058
$Co(NO_3)_2 \cdot 6H_2O - 3{,}7H_2O$	0.4547	0.4722	0.4931	0.5082	0.5216	0.5350
$Co(NO_3)_2 \cdot 6H_2O - 3{,}9H_2O$	0.4594	0.4768	0.4978	0.5129	0.5257	0.5385
$Co(NO_3)_2 \cdot 6H_2O - 5{,}3H_2O$	0.5197	0.5247	0.5350	0.5470	0.5570	0.5695
$Co(NO_3)_2 \cdot 6H_2O - 5{,}9H_2O$	0.5285	0.5338	0.5418	0.5514	0.5605	0.5746
$Co(NO_3)_2 \cdot 6H_2O - 10{,}0H_2O$	0.5408	0.5513	0.5664	0.5768	0.5856	0.5939
$Co(NO_3)_2 \cdot 6H_2O - 24{,}5H_2O$	0.5745	0.5850	0.6001	0.6100	0.6187	0.6270
$Co(NO_3)_2 \cdot 6H_2O - 40{,}2H_2O$	0.5885	0.5989	0.6141	0.6234	0.6324	0.6407
$Co(NO_3)_2 \cdot 6H_2O - 68{,}4H_2O$	0.5989	0.6094	0.6245	0.6338	0.6429	0.6512
$Co(NO_3)_2 \cdot 6H_2O - 85{,}4H_2O$	0.6024	0.6129	0.6280	0.6373	0.6463	0.6546
$Co(NO_3)_2 \cdot 6H_2O - 153H_2O$	0.6082	0.6187	0.6344	0.6437	0.6524	0.6607
$Co(NO_3)_2 \cdot 6H_2O - 491H_2O$	0.6148	0.6251	0.6402	0.6495	0.6583	0.6665

* Values obtained by extrapolation.

Figure 1 shows the $\lambda = f(x_1)$ dependence where x_1 is the mole fraction of hexahydrated cobalt nitrate in $Co(NO_3)_2 \cdot 6\,H_2O + H_2O$. Relatively high negative deviations from ideality were found. Similar findings were mentioned by other authors for other transport phenomena (electrical conductivity, viscosity) in the similar systems.

It is worth mentioning (Fig. 2) that when volume fractions φ_i are used instead of mole fractions: [15,17,18]

$$\varphi_i = \frac{n_i V_i}{\sum_i n_i V_i} \qquad (1)$$

positive deviations are obtained which are comparatively lower than those in figure 1.

The experimental data published in works[1,11] yield for the $Ca(NO_3) \cdot 4\,H_2O + H_2O$ a behaviour which is similar to that shown in figures 1 and 2.

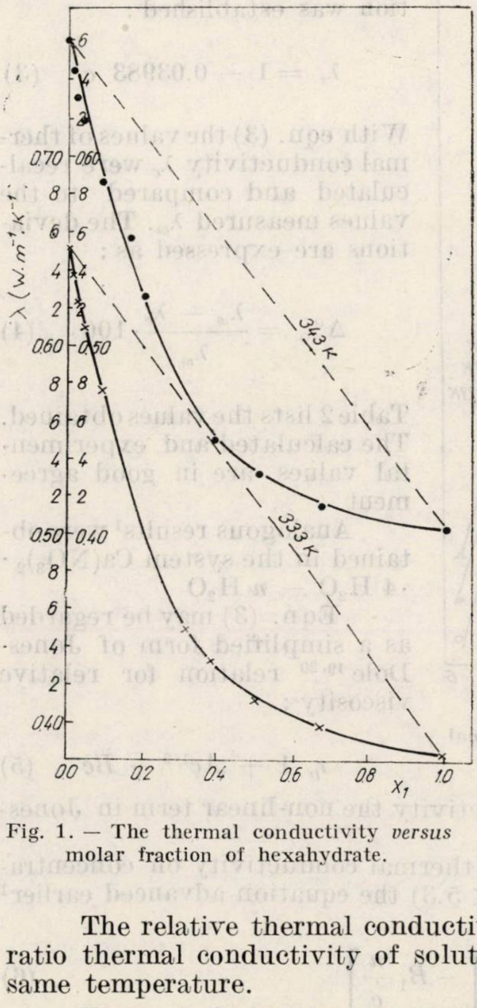

Fig. 1. — The thermal conductivity *versus* molar fraction of hexahydrate.

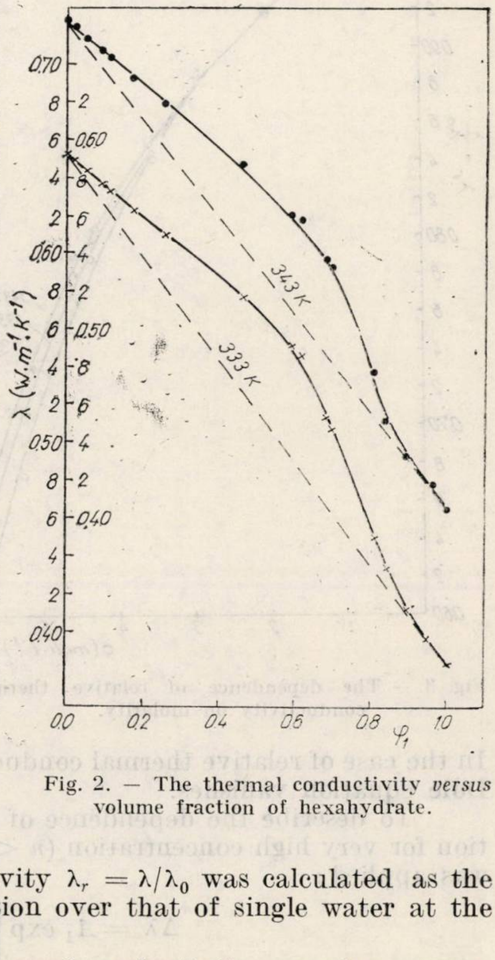

Fig. 2. — The thermal conductivity *versus* volume fraction of hexahydrate.

The relative thermal conductivity $\lambda_r = \lambda / \lambda_0$ was calculated as the ratio thermal conductivity of solution over that of single water at the same temperature.

Figure 3 shows the plot of thermal conductivity *vs* molar concentration. The dependence $\lambda_r = f(c)$ is different in two concentration ranges. In the first the dependence is linear, independent of temperature, described by the equation :

$$\lambda_r = 1 - \beta_c \tag{2}$$

If constant β for a certain electrolyte is known, eqn. (2) allows calculation of thermal conductivity for any concentration and temperature within the linearity range of $\lambda_r = f(c)$.

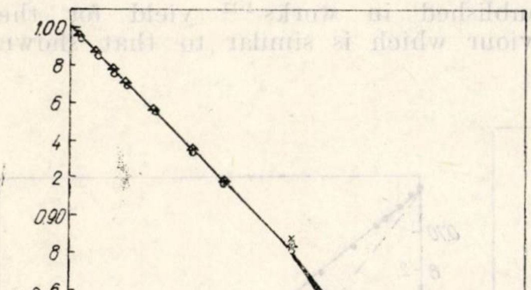

Fig. 3. — The dependence of relative thermal conductivity on molarity.

Starting up from experimental data the value of β was calculated for the system in question and the following equation was established:

$$\lambda_r = 1 - 0.03983\ c \qquad (3)$$

With eqn. (3) the values of thermal conductivity λ_c were recalculated and compared to the values measured λ_m. The deviations are expressed as:

$$\Delta\% = \frac{\lambda_m - \lambda_c}{\lambda_m} \cdot 100 \qquad (4)$$

Table 2 lists the values obtained. The calculated and experimental values are in good agreement.

Analogous results[1] were obtained in the system $Ca(NO_3)_2 \cdot 4\,H_2O - n\,H_2O$

Eqn. (3) may be regarded as a simplified form of Jones-Dole [19, 20] relation for relative viscosity:

$$\eta_r\ 1 + Ac^{1/2} + Bc \qquad (5)$$

In the case of relative thermal conductivity the non-linear term in Jones-Dole equation vanishes.

To describe the dependence of thermal conductivity on concentration for very high concentration ($n < 5.3$) the equation advanced earlier[1] was applied:

$$\Delta\lambda = A_1 \exp\left[-B_1 \frac{n}{c}\right] \qquad (6)$$

where $\Delta\lambda$ is the difference between thermal conductivity of pure water λ_0 and that of electrolyte solution λ, c is the molar concentration, n is the number of moles of water in excess versus that contained in the crystal hydrate, A_1 and B_1 are empirical constants.

Constants A_1 and B_1 were calculated by least squares from the experimental thermal conductivities. Eqn. (6) was employed to recalculate thermal conductivities, λ_c, which were then compared with values λ_m; the deviations were calculated by eqn. (5). The results are listed in Table 3. The calculated and experimental values are in good agreement. A similar behaviour was obtained [1] for $Ca(NO_3)_2 \cdot 4\,H_2O$.

Table 2

Verification of the applicability of $\lambda_r = 1 - \beta_c$ equation in $Co(NO_3)_2 \cdot 6\ H_2O - H_2O$ system for $n \geqslant 10$

System	323 K			333 K			343 K		
	λ_m	λ_c	%Δ	λ_m	λ_c	%Δ	λ_m	λ_c	%Δ
$Co(NO_3)_2 \cdot 6H_2O - 491\ H_2O$	0.6402	0.6403	+0.02	0.6495	0.6497	+0.03	0.6583	0.6583	0.00
$Co(NO_3)_2 \cdot 6H_2O - 153\ H_2O$	0.6344	0.6347	+0.05	0.6437	0.6437	0.00	0.6524	0.6523	−0.02
$Co(NO_3)_2 \cdot 6H_2O - 85{,}4\ H_2O$	0.6280	0.6281	+0.02	0.6373	0.6372	−0.02	0.6463	0.6458	−0.08
$Co(NO_3)_2 \cdot 6H_2O - 68{,}4\ H_2O$	0.6245	0.6247	+0.03	0.6338	0.6338	0.00	0.6429	0.6425	−0.06
$Co(NO_3)_2 \cdot 6H_2O - 40{,}2\ H_2O$	0.6141	0.6141	0.00	0.6234	0.6231	−0.05	0.6324	0.6317	−0.11
$Co(NO_3)_2 \cdot 6H_2O - 24{,}5\ H_2O$	0.6001	0.6003	+0.05	0.6100	0.6092	−0.13	0.6187	0.6176	−0.18
$Co(NO_3)_2 \cdot 6H_2O - 10{,}0\ H_2O$	0.5664	0.5667	+0.05	0.5768	0.5754	+0.24	0.5856	0.5836	−0.34

Table 3

The verification of the applicability of $\Delta\lambda = A_1 \exp\left(-B_1 \frac{n}{c}\right)$ equation in $Co(NO_3)_2 \cdot 6\ H_2O - n\ H_2O$ for $n \leqslant 10.0$

n	323 K				333 K				343 K			
	λ_m	λ_c	Δ	%Δ	λ_m	λ_c	Δ	%Δ	λ_m	λ_c	Δ	%Δ
0.0	0.3594	0.3594	0.0000	0.00	0.3826	0.3826	0.0000	0.00	0.4041	0.4041	0.0000	0.00
0.5	0.3745	0.3766	+0.0021	+0.56	0.3866	0.3866	+0.0022	+0.55	0.4164	0.4189	+0.0025	+0.60
1.0	0.3935	0.3947	+0.0012	+0.30	0.4133	0.4153	+0.0020	+0.48	0.4340	0.4345	+0.0005	+0.12
1.6	0.4152	0.4169	+0.017	+0.41	0.4338	0.4357	0.0019	+0.44	0.4512	0.4534	+0.0022	+0.49
2.0	0.4330	0.4314	−0.0016	−0.37	0.4495	0.4495	0.0000	0.00	0.4670	0.4665	−0.0005	−0.11
3.7	0.4931	0.4918	−0.0013	−0.26	0.5082	0.5060	−0.0022	−0.43	0.5216	0.5195	−0.0021	−0.40
3.9	0.4978	0.4968	−0.010	−0.20	0.5129	0.5118	−0.0019	−0.37	0.5257	0.5243	−0.0014	−0.27
4.2	0.5062	0.5078	+0.0016	+0.28	0.5194	0.5207	+0.0013	+0.25	0.5318	0.5332	+0.0014	+0.26
5.3	0.5350	0.5382	+0.0032	+0.59	0.5470	0.5504	+0.0034	+0.62	0.5570	0.5605	+0.0035	+0.63
5.9	0.5418	0.5530	+0.0112	+2.07	0.5514	0.5642	+0.0128	+2.32	0.5605	0.5748	+0.0143	+2.55
7.5	0.5514	0.5868	+0.0354	+6.42	0.5616	0.5971	+0.0355	+6.32	0.5705	0.6060	+0.0355	+6.22
10.0	0.5664	0.6219	+0.0555	+9.80	0.5768	0.6308	+0.0540	+9.36	0.5856	0.6393	+0.0537	+9.17

For the temperature dependence of thermal conductivity, the Arrhenius type equation:

$$\lambda(T) = A_2 \exp\left[-B_2/RT\right] \tag{7}$$

and the Vogel-Tamann-Fulcher equation:

$$\lambda(T) = A_3 \cdot T^{-\frac{1}{2}} \exp\left[-B_3/(T - T_0)\right] \tag{8}$$

were employed.

The graph in figure 4 shows a plot of $\ln \lambda = f(1/T)$. Within the first concentration range the Arrhenius type equation describes satisfac-

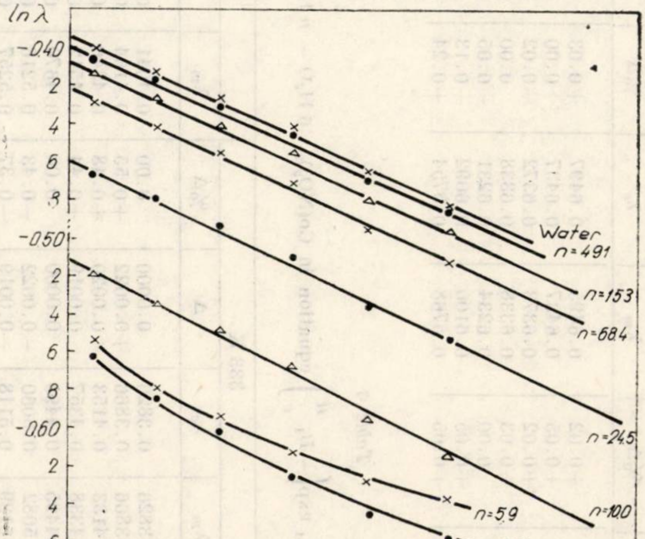

Fig. 4. — The Arrhenius dependence of thermal conductivity on temperature.

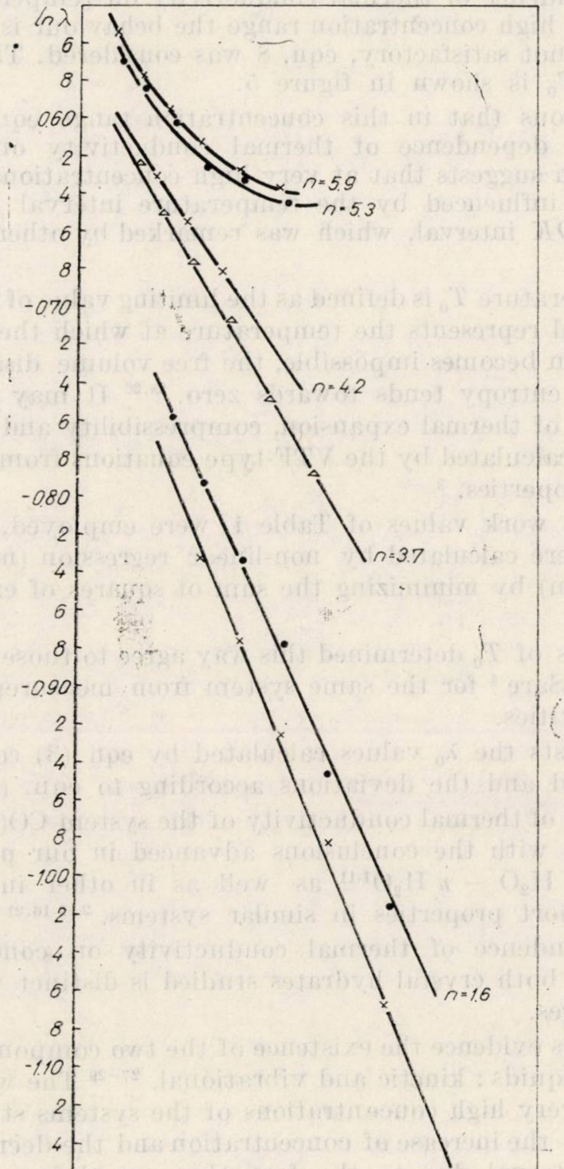

Fig. 5. — The non-Arrhenius dependence of thermal conductivity on temperature.

torily the dependence of thermal conductivity on temperature. Because within the very high concentration range the behaviour is non-Arrhenius and eqn. (7) is not satisfactory, eqn. 8 was considered. The plot of ln λ *versus* $1/T - T_0$ is shown in figure 5.

It is obvious that in this concentration range eqn. (8) describes adequately the dependence of thermal conductivity on temperature. This observation suggests that at very high concentrations the transport phenomenon is influenced by the temperature interval $T - T_0$ rather than the $T - OK$ interval, which was remarked by other researchers as well.[2]

The temperature T_0 is defined as the limiting value of glass transition temperature and represents the temperature at which the ionic and molecular migration becomes impossible, the free volume disapears and the configurational entropy tends towards zero. [25,26] It may de determined by experiments of thermal expansion, compressibility and heat capacity. It may also be calculated by the VTF-type equations from measurements of transport properties. [3]

As in this work values of Table 1 were employed, the A, B and T_0 constants were calculated by non-linear regression (non-linear parameter estimation) by minimizing the sum of squares of errors according to eqn. (5).

The values of T_0 determined this way agree to those communicated by Angell and Sare [4] for the same system from measurements of other transport quantities.

Table 4 lists the λ_0 values calculated by eqn. (3) compared to λ_m values measured and the deviations according to eqn. (4).

The study of thermal conductivity of the system $CO(NO_3)_2 \cdot 6\, H_2O - nH_2O$ agrees with the conclusions advanced in our previous studies on $Ca(NO_3)_2 \cdot 4\, H_2O - n\, H_2O$[1.11] as well as in other investigations on different transport properties in similar systems. [2-9.16,21-24]

The dependence of thermal conductivity on concentration and temperature of both crystal hydrates studied is distinct within two concentration ranges.

The results evidence the existence of the two components of thermal conduction in liquids : kinetic and vibrational. [27-29] The weight of kinetic component at very high concentrations of the systems studied decreases sensitively with the increase of concentration and the decrease of $T - T_0$ temperature interval due to the fact that, on the one hand, the free volume decreases considerably and, on the other, the motion of rearrangement is not attended by single particles (ions, molecules) but by larger groups of particles whose motion is sluggish.

At T_0 the transport process related to viscosity ceases, the electrical conductivity is ensured by electronic conduction if allowed by the nature of substances and the thermal conductivity is reduced to the vibrationa component of the transport process.

Table 4

Comparison of calculated (λ_c) and experimental (λ_m) thermal conductivities for the system $Co(NO_3)_2 \cdot 6 H_2O - n H_2O$

T (K)	$\lambda(W.m^{-1}.K^{-1})$ experimental	calculated	Deviation $(W.m^{-1}.K^{-1})$	$\Delta\%$
	$n = 0.0$	$T_0 = 206.5K$	$A = 18.63$	$B = 124.70$
303	0.2954	0.2938	−0.0016	−0.54
313	0.3268	0.3263	−0.0005	−0.15
323	0.3594	0.3552	−0.0042	−1.17
333	0.3826	0.3807	−0.0019	−0.50
343	0.4041	0.4032	−0.0009	−0.22
353	0.4233	0.4231	−0.0002	−0.05
	$n = 0.5$	$T_0 = 202.3$	$A = 17.98$	$B = 118.56$
303	0.3152	0.3182	+0.0030	+0.95
313	0.3442	0.3483	+0.0041	+1.19
323	0.3745	0.3746	+0.0001	+0.03
333	0.3966	0.3974	+0.0008	+0.20
343	0.4164	0.4180	+0.0016	+0.38
356	0.4350	0.4358	+0.0008	+0.18
	$n = 1.0$	$T_0 = 197.1$	$A = 18.19$	$B = 119.54$
303	0.3400	0.3380	−0.0020	−0.59
313	0.3665	0.3665	−0.0000	−0.00
323	0.3935	0.3916	−0.0019	−0.48
333	0.4133	0.4136	+0.0003	+0.07
343	0.4340	0.4328	−0.0012	−0.28
353	0.4512	0.4497	−0.0015	−0.33
	$n = 1.6$	$T_0 = 193$	$A = 17.83$	$B = 114.28$
303	0.3652	0.3624	−0.0028	−0.77
313	0.3884	0.3888	+0.0004	+0.10
323	0.4152	0.4118	−0.0034	−0.82
333	0.4338	0.4319	−0.0019	−0.44
343	0.4512	0.4493	−0.0019	−0.42
353	0.4675	0.4645	−0.0030	−0.64

REFERENCES

[1] S. Sternberg and A. Mascaş, *Rev. Roumaine Chim.* in press.

[2] C. A. Angell, *J. Phys. Chem.*, **68**, 1917 (1964); **69**, 2137 (1965); 2793, 3988 (1966).

[3] C. T. Moyniham, *J. Phys. Chem.*, **70**, 3399 (1966).

[4] C. A. Angell and E. J. Sare, *J. Chem. Phys.*, **52**, 1058 (1970).

[5] C. A. Angell and R. D. Bressel, *J. Phys. Chem.*, **71**, 2759 (1967).

[6] C. T. Moyniham and C. A. Angell, *J. Phys. Chem.*, **74**, 736 (1970).

[7] J. Novak, I. Slama and Z. Kodejs, *Coll. Czech. Chem. Comm.*, **41**, 2838 (1976).

[8] J. Malà, J. Novak, Z. Kodejsand, I. Slama, *Coll. Czech. Chem. Comm*, **43**, 183 (1978).

[9] J. Novak, I. Slama and Z. Kodejs, *Chem. Zvesti*, **31**, 29 (1977).

[10] S. Zuca and N. Ene, *E.E.A. — Electrotehnica*, **27**, 15 (1979).

[11] S. Sternberg and A. Mascaş, *Rev. Roumaine Chim.*, in press.

[12] C. Liteanu and E. Horpîrteanu, "Quantitative Analytical Chemistry", Ed. Didactică şi Pedagogică, Bucharest, 1973.

[13] N. V. Tsederberg, "Thermal Conductivity of Gases and Liquids", Edward Arnold Ltd, London, 1965.
[14] L. Faraday and L. Bencze, *Magyar Kém. Lapjá*, **31**, 347 (1976).
[15] I. G. Murgulescu and S. Zuca, *Electrochim. Acta*, **11**, 1383 (1966).
[16] J. Mc. Donald and H. T. Davis, *J. Phys. Chem.*, **74**, 725 (1970).
[17] I. G. Murgulescu and S. Zuca, *Electrochim. Acta*, **14**, 519 (1969).
[18] B. F. Markov and L. A. Sunina, *Doklady Akad. Nauk. S.S.S.R.*, **110**, 411 (1956).
[19] G. Jones and S. K. Talley, *J. Amer. Chem. Soc.*, **55**, 624, 124 (1933).
[20] G. Jones and M. Dolle, *J. Chem. Soc.*, **51**, 2950 (1929).
[21] L. H. White and H. T. Davis, *J. Chem. Phys.*, **47**, 5433 (1967).
[22] C. A. Angell and R. D. Bresse, *J. Phys. Chem.*, **76**, 3244 (1972).
[23] C. A. Angell, E. J. Sare and R. D. Bressel, *J. Phys. Chem.*, **71**, 2759 (1967).
[24] C. A. Angell, *J. Electrochem. Soc.*, **112**, 1224 (1965).
[25] M. H. Cohen and D. Turnbull, *J. Chem. Phys.*, **31**, 1164 (1959).
[26] G. Adamand, H. J. Gibbs, *J. Chem. Phys.*, **43**, 139 (1965).
[27] J. K. Horrokand, E. Mc. Laughlin, *Trans. Faraday Soc.*, **58**, 1357 (1962).
[28] S. H. Lin, H. Eyring and H. T. Davis, *J. Phys. Chem.*, **68**, 3017 (1964).
[29] J. K. Horroks and E. Mc. Laughlin, *Trans. Faraday Soc.*, **56**, 206 (1960) ; **59**, 1709 (1963).

Revue Roumaine de Chimie, **29**, 2, 175 – 183 (1984)

KINETICS OF LIGNITE AND LIGNITE CHAR GASIFICATION WITH CARBON DIOXIDE AND STEAM

A. BÂLDEA* and G. NIAC**

* Institute for Isotopic and Molecular Technology, Cluj-Napoca, Str. Donath 65 – 103, P.O. Box 700

** Polytechnic Institute, Cluj-Napoca, Str. Podgoriei 103 – 155, Romania

Received March 8 1982

The kinetics of the reaction between carbon dioxide and steam with Rovinari lignite and two chars obtained from it in a differential reactor on line with a gas chromatograph are presented. For the reaction with carbon dioxide activation energies of 90.7 kJ/mol with lignite, 101.0 and 156.8 kJ/mol with chars obtained at 600° (C-600) and 800° (C-800) respectively and 92.2 kJ/mol with active charcoal were found. With C-600 the reaction order with respect to steam was 0.6. Two temperature zones were found in the Arrhenius plots of the steam-char reaction. The first was ascribed to chemical control and the second to diffusion control respectively. Increase of the steam partial pressure shifts the diffusion control to higher temperatures. With C-800 114.0 kJ/mol was obtained for steam gasification. The kinetics of gasification reactions is discussed in terms of surface area, pore distribution and chemical composition of the carbonaceous matter.

In order to control the coal gasification process in each of the usual procedures (underground gasification "in situ" or in a gasification plant), knowledge of the coal-carbon dioxide and the coal steam reaction kinetics is required. Although the practice of coal gasification began a long time ago, its engineering study started only recently. This is due to the complex physical and chemical properties of solid fuels and to the great number of reactions involved in the gasification process which cannot be accurately specified for reactor design.[1–5] As the gasification proceeds the solid fuel dries and pyrolyses so the resulted residue has a greater carbon content and reacts further with the products of thermal decomposition and reactant gases (steam, oxygen).

In the present paper the gasification kinetics of lignite and its chars with carbon dioxide and steam at atmospheric pressure is described.

EXPERIMENTAL

The experimental device, the materials and the used procedure were described previously[6,7]. For steam gasification a vapor saturator was attached to a differential reactor. The saturator allowed different steam partial pressures to be realised in a helium stream. The excess steam was condensed at the reactor exit. The reaction rate was calculated using the instant unreacted coal amount,calculated by subtracting the amount of gasified coal from the initial weight by a graphic integration procedure described previously[6]. For steam gasification an overall reaction rate was calculated using a material balance involving the carbon bearing species : methane, carbon monoxide and dioxide.

As with the nitric oxide reduction[6], the reaction rate decrease until 2 – 5% of the char was gasified and remains further approximately stationary. Since the states of the C-600 and C-800 chars are those expected in a practical gasification system, the gasification kinetics experiments were performed on lignite, lignite chars and active charcoal.

RESULTS AND DISCUSSIONS

Figure 1 presents a gasification] run for C-600 char. Similar behavior has been obtained with lignite and C-800 char. The temperature, the coal amount, the carbon monoxide concentration and the rate of its appearance are also included. The lignite is very reactive with carbon dioxide, the start of the reaction can be observed just above 400° along with its thermal decomposition. The highest reaction rates are observed with the C-600 char. The reaction rate of the C-800 char increases faster with temperature than the rate of the C-600 char. While at 700° the rate of the C-800 char is but one half of the rate of the C-600 char at the same temperature, at 815° the two rates become equal. The lignite reaction rate increases slower than the rate of C-600 char.

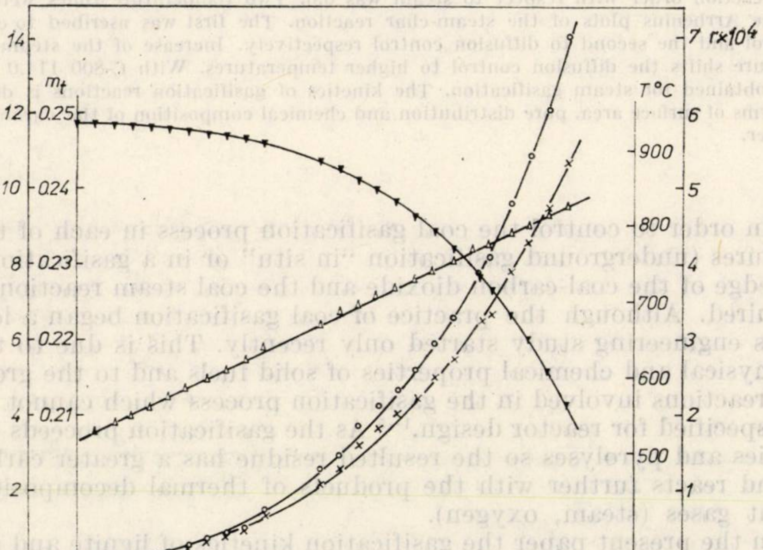

Fig. 1. – Carbon monoxide concentration, reaction rate, char amount and temperature *versus* time for C-600 char-carbon dioxide reaction (× carbon monoxide concentration ; ○ reaction rate ; ▼ char amount ; Δ temperature).

The kinetics of thermal decomposition of lignite leads to an activation energy of 146.5 kJ/mol for hydrogen evolution. The slower increase of the lignite reaction rate as compared to the char at a given temperature even above 600° can be explained by the observed higher hydrogen content of the lignite, which inhibits the reaction with carbon dioxide.

In the temperature range of 400 – 600° the most reactive groups are consumed. As lignite pyrolyses, its reactivity decreases continuously along with the change in chemical composition[8]. There is a "thermodynamic range" of changing reactivity where the determined reaction rates are erratic. C-600 and C-800 chars behave in the same way. This modification of reactivity may be correlated with the "organic oxygen" content.[2,3] Assuming that hydrogen acts as a retarding agent by occupying the active sites, the kinetic behaviour of the lignite and its chars can be explained.

An alternative explanation could rely on the difference of the BET surface areas. Taking into account the surface area of 10.0, and 4.7 m^2/g for C-600 and C-800 respectively the twice higher reaction rate for C-600 at 700° could be explained. The surface area of mineral matter cannot be neglected because of the high ash content of the two chars. BET surface area of 7.1 m^2/g was measured for ash, but the mineral matter of the coals differs from its ash, as expected. Both explanations are consistent with the experimental facts.

Elemental analyses of coal samples give 11.5% for O + S (by difference) with C-600 and 7.7% with C-800. The higher organic oxygen content enhances the reactivity. The higher reaction rates for C-600 below 800° and the faster increase of C-800 reaction rates can be explained by competing effects between oxygen promotion and hydrogen inhibiting effects. The heating of C-600 over its obtaining temperature decreases its organic oxygen content rather than its hydrogen content. The same explanation could be done in the case of lignite.

The reaction rate for active charcoal is an order of magnitude lower than that of the chars, although the surface area is with two orders of magnitude higher. This can be explained by the larger diameter of the carbon dioxide molecule compared with that of nitric oxide, for which the rates have the same order of magnitude. It can be assumed that the reactant molecules flow through the charcoal pores by activation.

With water vapor the reaction rate was calculated using the sum $\Sigma c_i = CO_2 + CO + CH_4$ in the rate expression described previously.[6,7] The product concentrations and the instant coal amount, m_t, are shown in Figs 2 and 3 for two chars. Similar experiments were performed for C-600 at 12.33 kPa and 31.15 kPa steam pressures. The reaction order was found to be 0.6 using the reaction rates for 3 partial pressures (Fig. 4).

The activation energies shown in Table 1 were obtained by linear plots as shown in Fig. 5.

Assuming that the carbon dioxide-char reaction obeys a first order dependence with respect to the consumption of the solid, the function

$$g(x) = -\ln(1 - x)$$

is defined, where x stands for char conversion. Using a Coates-Redfern expansion[9], log $[g(x)/T^2]$ can be plotted against $1/T$, as presented in Fig. 6. Activation energies were found as follows: 97.9 kJ/mol for lignite, 104.6 and 168.2 for C-600 and C-800 respectively and 92.0 kJ/mol for active charcoal, in good agreement with the values given in Table 1. The reaction between carbon dioxide and chars is chemically controlled. The

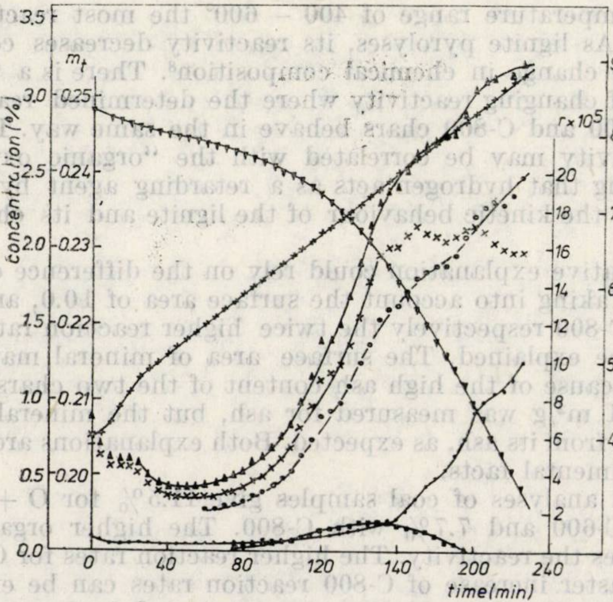

Fig. 2. — Product concentrations, reaction rate, char amount and temperature *versus* time for C-600 char-steam (19.90 kPa) reaction (● carbon monoxide; ■ methane; × carbon dioxide; ▲ the sum $CO_2 + CO + CH_4$; ○ reaction rate; ▼ char amount, m_t; + temperature).

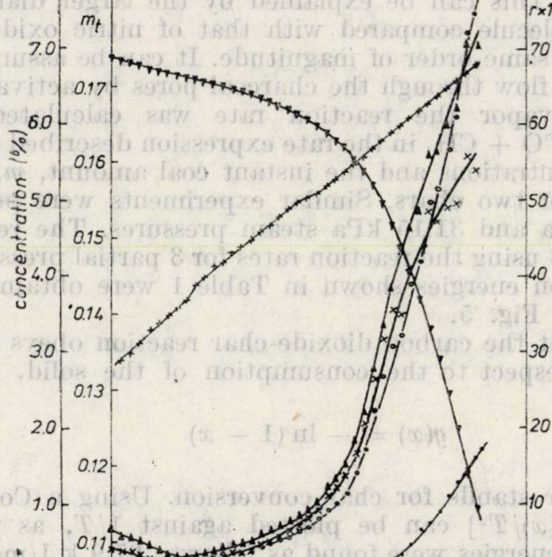

Fig. 3. — Product concentrations, reaction rate, char amount and temperature *versus* time for C-800 char-steam (19.90 kPa) reaction (The same notation as in Fig. 2).

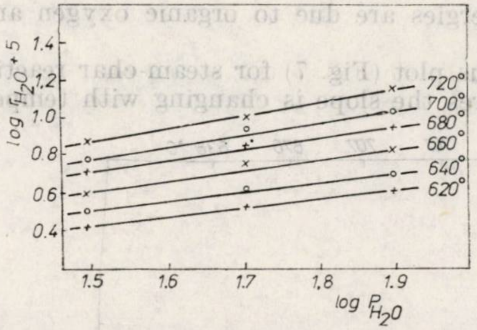

Fig. 4. — The plot of the reaction rate logarithm against steam partial pressure logarithm for C-600 char.

Table 1

Activation energies for chars gasification with carbon dioxide and steam

Reaction	E kJ/mol
Active charcoal-carbon dioxide	95.2±2.1
Lignite-carbon dioxide	90.7±2.1
C-600 char-carbon dioxide	101.0±1.8
C-800 char-carbon dioxide	156.8±2.8
C-600 char-steam (12.33 kPa)	79.1 ±3.9
C-600 char-steam (19.90 kPa)	81.4±3.6
C-600 char-steam (31.15 kPa)	106.7±4.8
C-800 char-steam (19.90 kPa)	114.2±5.7

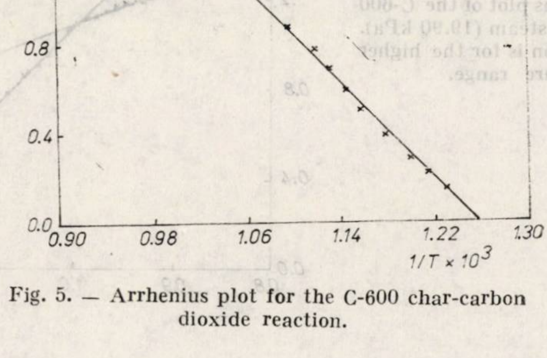

Fig. 5. — Arrhenius plot for the C-600 char-carbon dioxide reaction.

low activation energies are due to organic oxygen and mineral matter content catalysis.

The Arrhenius plot (Fig. 7) for steam-char reactions shows that at low partial pressures the slope is changing with temperature, suggesting

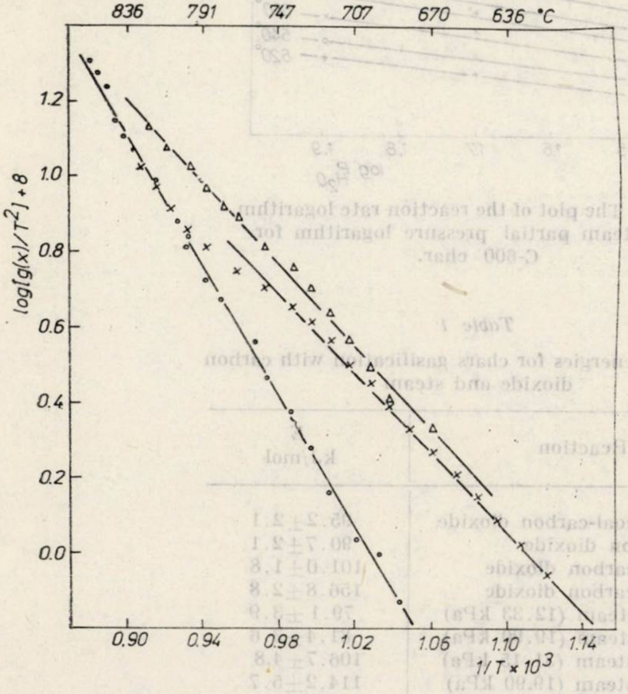

Fig. 6. — Arrhenius plot of the function $g(x)/T^2$ for the reactions of lignite (×), C-600 (△) and C-800 (○) chars with carbon dioxide.

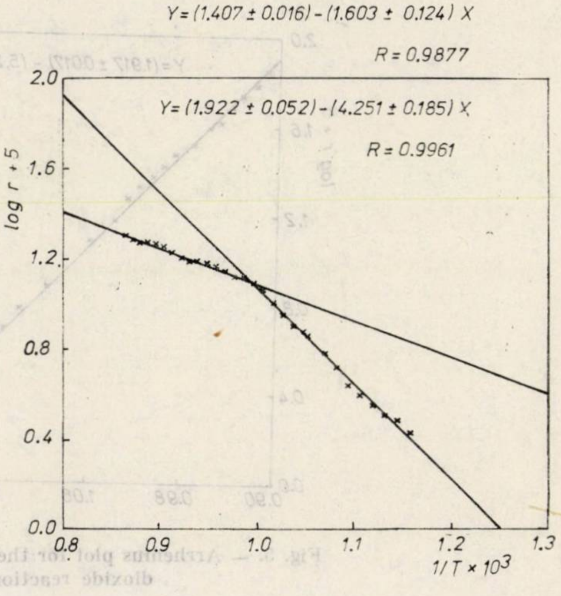

Fig. 7. — Arrhenius plot of the C-600 char reaction with steam (19.90 kPa). The upper equation is for the higher temperature range.

a transition from chemical to diffusion control. At higher vapor pressure this transition zone is moved to higher temperatures. Obviously, with increasing pressures, the number of molecules reaching the surface increases, the diffusion providing enough reactant molecules such that the reaction rate remains uninfluenced. Another possible explanation consists in the fact that at higher reaction rates, char consumption leads to pore opening and the surface increases causing the shift of the transition range. Surface decrease due to thermal treatment cannot be excluded at 750°, as observed for carbon dioxide and steam reactions. This surface modification is consistent with BET surface areas measured for both chars. It can be assumed that the benzene rings are linked together while surface area and pore volume decrease, as shown in Fig. 8 obtained using mercury porosimetry. The surface decrease cannot explain the activation energy decrease. Within a range of 100° and a linear decrease of the surface to one half, the computed activation energy change is less than 21 kJ/mol. Therefore this fact alone cannot explain the behavior of the char-steam

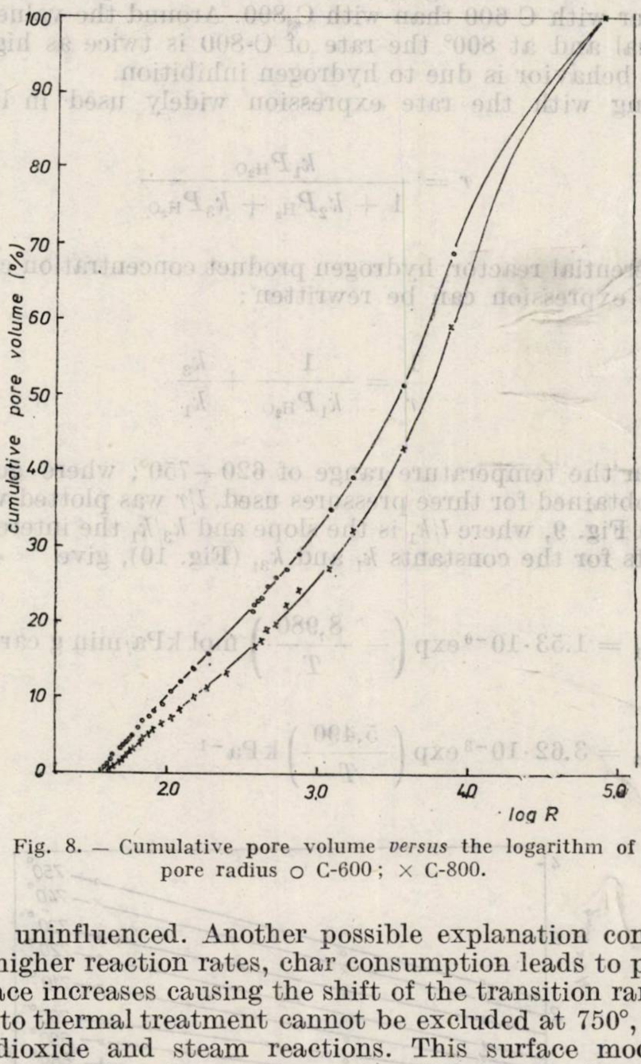

Fig. 8. — Cumulative pore volume *versus* the logarithm of pore radius ○ C-600 ; × C-800.

reaction. We must admit that the main factor determining the rate is diffusion either alone or in association with one or more of the above discussed factors.

A similar discussion as for the carbon dioxide reaction can also be made for the steam-char gasification. At low temperature the reaction rate is higher with C-600 than with C-800. Around the value of 750° they become equal and at 800° the rate of C-800 is twice as high as that of C-600. This behavior is due to hydrogen inhibition.

Starting with the rate expression widely used in literature [10-13]:

$$r = \frac{k_1 P_{H_2O}}{1 + k_2 P_{H_2} + k_3 P_{H_2O}}$$

for our differential reactor, hydrogen product concentration can be neglected and the expression can be rewritten:

$$\frac{1}{r} = \frac{1}{k_1 P_{H_2O}} + \frac{k_3}{k_1}$$

Within the temperature range of 620–750°, where good Arrhenius plots were obtained for three pressures used, l/r was plotted versus l/P_{H_2O} as shown in Fig. 9, where l/k_1 is the slope and k_3/k_1 the intereept. The Arrhenius plots for the constants k_1 and k_3, (Fig. 10), give

$$k_1 = 1.53 \cdot 10^{-6} \exp\left(-\frac{8{,}980}{T}\right) \text{ mol kPa/min g carbon}$$

$$k_3 = 3.62 \cdot 10^{-3} \exp\left(\frac{5{,}490}{T}\right) \text{kPa}^{-1}$$

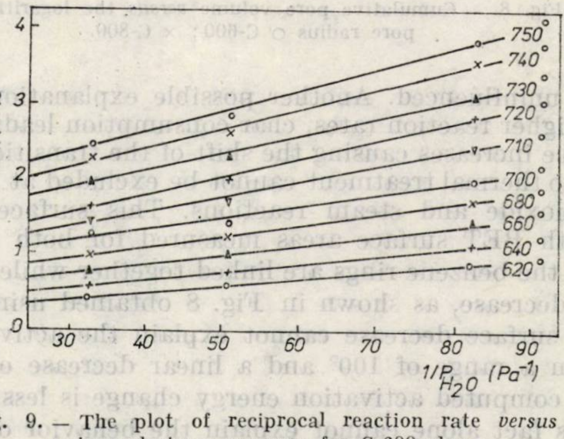

Fig. 9. — The plot of reciprocal reaction rate *versus* reciprocal steam pressure for C-600 char.

The adsorption constant of steam has a negative dependence on temperature, and the amount of adsorbed water decreases with temperature as expected. The results are quite consistent with the literature results [12,13] but the activation energies are somewhat lower.

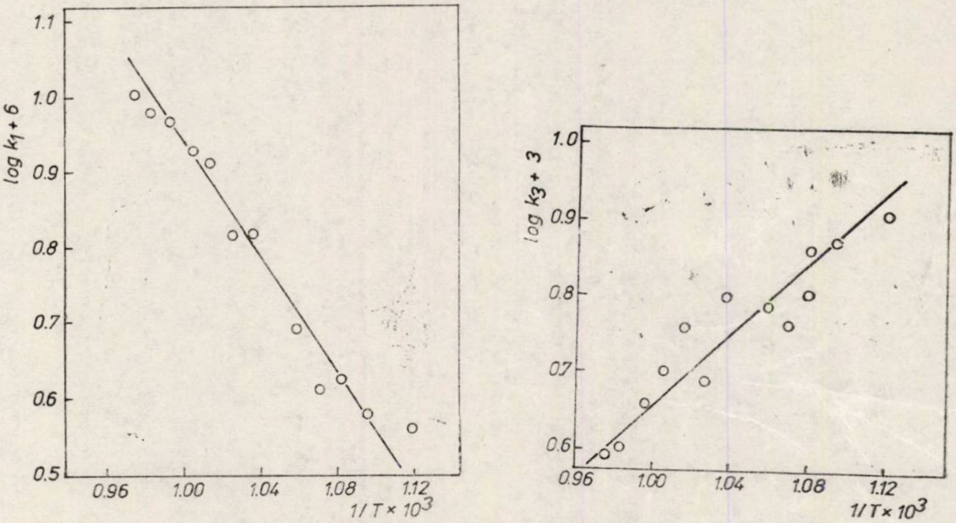

Fig. 10. — Arrhenius plots for k_1 and k_3 rate constants.

REFERENCES

[1] C. Heuchamps, *Bull. Soc. chim. France.*, **1967**, 4205.

[2] J. T. Sears, H. S. Muralidhara and C. Y. Wen, *Ind. Eng. Chem. Process Des. Dev.*, **19**, 358 (1980).

[3] A. K. Agrawal and J. T. Sears, *Ind Eng. Chem. Process Des. Dev.*, **19**, 364 (1980).

[4] J. Bjerle, H. Ekleund and O. Svenson, *Ind. Eng. Chem. Process Des. Dev.*, **19**, 345 (1980).

[5] R. T. Yang and M. Steinberg, *J. Phys. Chem.*, **80**, 965 (1976).

[6] A. Bâldea and G. Niac, *Rev. Chim.* (*București*), **33**, 835 (1982) ; **34**, 224 (1983).

[7] A. Bâldea, Thesis, Craiova, 1981.

[8] G. Niac, *Metalurgia*, **31**, 551 (1979).

[9] A. W. Coates and J. P. Redfern, *Nature*, **201**, 68 (1964).

[10] P. L. Walker Jr., F. Rusinko Jr. and L. G. Austin, *Adv. in Catalysis*, **11**, 133 (1959).

[11] J. O. Blackwood, *Ind. Chemist.*, **55**, 171 (1960).

[12] A. P. Malinauskas, *Chem. Eng. Progr. Symp. Series, 104*, **66**, 81 (1970).

[13] S. H. Wong, J. E. Young and J. E. Johnson, 14-th IECEC, 5 — 10 Aug. 1979 (preprint).

Revue Roumaine de Chimie, **29**, *2*, 185 — 191 (1984)

SYNTHESE UND CHARAKTERISIERUNG DER SUBSTITUIERTEN 2-(ARYLAZOARYLAMINO)-4,6-DICHLOR- UND 2-CHLOR-4,6-BIS (ARYLAZOARYLAMINO)-1,3,5-TRIAZINE

R. BACALOGLU[a], I. HAVLIK[b] und C. CSUNDERLIK[a]
[a] Polytechnisches Institut „Traian Vuia", Timişoara, Str. Bocşa Nr. 6, Rumänien
[b] Chemie-Forschungszentrum, Timişoara, Blvd. M. Viteazul, Nr. 24, Rumänien

Eingegangen am Dezember 15, 1982

Es wurden Herstellungsverfahren für die substituierten 2-(Arylazoarylamino)-4,6-dichlor- und 2-Chlor-4,6-bis(arylazoarylamino)-1,3,5-triazine ausgearbeitet und die synthetisierten Produkte wurden IR—, UV—VIS— und 1H NMR-spektroskopich charakterisiert.

Syntheses of 2-arylazoarylamino-4,6-dichloro- and 2-chloro-4,6-arylazoarylamino-1,3,5-triazines are described. The structures of these compounds are proved by infrared, ultraviolet-visible and nuclear magnetic resonance spectroscopy.

Die durch die Reaktion des Cyanurchlorids mit verschiedenen Aminoarylazofarbstoffen hergestellten reaktiven s-Triazinfarbstoffe haben eine besondere Bedeutung für die Technologie gewonnen.

In vorliegender Arbeit wird die Synthese einiger einfachen Modellverbindungen dieser Reihe beschrieben, die für kinetische und Mechanismusstudien eingesetzt wurden und durch IR—, ^{1}H—NMR— und UV—VIS—Spektroskopie charakterisiert wurden.

ERGEBNISSE UND DISKUSSION

Die substituierten 2-(Arylazoarylamino)-4,6-dichlor-1,3,5-triazine (I) wurden durch Monokondensation des Cyanurchlorids mit hochreinen 4′-substituierten 4-Aminoazobenzolen in Aceton-Wasser hergestellt. Die substituierten 2-Chlor-4,6-bis(arylazoarylamino)-1,3,5-triazine (II) wurden durch Dikondensation des Cyanurchlorids mit Aminoazofarbstoffen in Dioxan-Wasser erhalten.

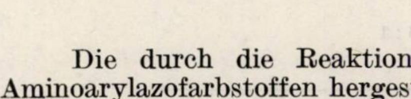

I

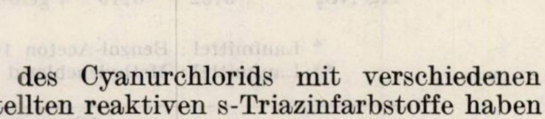

II

Die Produkte wurden durch fraktioniertes Umkristallisieren, Extraktionen und Umfällen gereinigt, wobei die Reinheit der Stoffe durch Elementaranalyse und Dünnschichtchromatographie auf Kieselgel G-Platten und mit Benzol-Aceton und Methylenchlorid als Laufmittel (Tabelle 1) überprüft wurde.

Tabelle 1

Charakterisierung der synthetisierten substituierten 2-(Arylazoarylamino)-4,6-dichlor-(I) und 2-Chlor-4,6-bis(arylazoarylamino)-1,3,5-triazine (II)

Produkt Nr.	X	Dünnschichtchromatographie R_f(A)*	R_f(B)**	Fleckfarbe	Schmelzpunkte °C
Ia	$(H_3C)_2N$	0,56	0,22	gelb-braun	>360
Ib	HO	0,21	nicht-eluiert	gelb-grünlich	>360
Ic	H_3C	0,52	0,35	gelb	200–201,5
Id	H	0,55	0,35	gelb	216–217
Ie	Cl	0,67	0,38	gelb	203–204,5
If	H_3C-CO	0,48	0,16	gelb	267–268
Ig	NO_2	0,57	0,32	gelb-orange	270–271
IIa	$(H_3C)_2N$	0,34	0,23	gelb-braun	>360
IIc	H_3C	0,39	0,18	gelb-grünlich	231–232
IId	H	0,40	0,19	gelb-grünlich	220–221,5
IIe	Cl	0,46	0,16	gelb	309–310
IIg	NO_2	0,32	0,19	gelb-braun	>360

* Laufmittel : Benzol-Aceton 16 : 1

** Laufmittel : Methylenchlorid

Nr.	Elementaranalyse berechnet %C	%H	%N	%Cl	gefunden %C	%H	%N	%Cl
Ia	52,3	3,9	25,25	—	52,95	3,62	24,8	—
Ib	—	—	21,7	19,65	—	—	22,0	19,25
Ic	74,0	6,2	19,9	—	74,2	6,1	19,3	—
Id	52,19	2,92	24,34	—	51,13	2,83	24,17	—
Ie	47,46	2,39	22,14	—	46,59	2,26	22,51	—
If	52,75	3,12	21,7	—	52,70	2,94	21,73	—
Ig	—	—	22,64	18,2	—	—	22,32	17,9
IIa	—	—	26,02	6,50	—	—	25,85	6,12
IIc	—	—	23,5	6,64	—	—	23,62	6,87
IId	—	—	24,9	7,02	—	—	25,2	7,11
IIe	—	—	21,9	18,52	—	—	21,6	18,21
IIg	—	—	27,2	6,29	—	—	27,45	6,33

Aus Tabelle 1 geht hervor, daß die Produkte genügend rein waren um einer spektralen Analyse unterworfen werden zu können.

In Tabelle 2 sind die Wellenlängen und die molaren Extinktionskoeffizienten der Absorptionsspektren in Methanol und 1,2-Dichlorethan für die Mono- und Dikondensationsfarbstoffe angegeben, die in diesen Lösungsmitteln löslich waren.

Tabelle 2

Sichtbare und ultraviolette Absorptionsspektren der Farbstoffe I und II.
(Die Wellenlängen des Absorptionsmaximums in nm und der Logarithmen in Zehnerbasis des molaren Extinktionskoeffizienten — in Klammern).

	X	Monokondensationsprodukte (I)		Dikondensationsprodukte (II)
		CH_3OH	$C_2H_4Cl_2$	$C_2H_4Cl_2$
a	$(H_3C)_2N$	318(3,95) 428(4,38)	322(4,23) 430(4,39)	
c	H_3C	358(4,41)	360(4,44)	363(4,67)
d	H	352(4,34)	352(4,40)	360(4,61)
e	Cl	362(4,40)	362(4,44)	386(4,60)*
f	H_3C-CO	—	368(4,48)	—
g	NO_2	—	380(4,37)	—

* Dimethylformamid

Mit Ausnahme der 4′-substituierten Dimethylaminoderivate (Ia und IIa), hat in allen Fällen die Kondensation mit Cyanurchlorid einen wesentlichen hypsochromen Effekt von cca 20 — 50 nm auf den $\pi \rightarrow \pi^*$— Übergang des Azosystems. So wird im Vergleich zu der Absorption der nichtkondensierten Produkte[1] eine Verschiebung von 22 nm (Ic), 30 nm (Id), 36 nm (If) und 46 nm (Ig) in Dichlorethan für die monokondensierten Produkte festgestellt. Diese Verschiebung läßt sich durch die Konjugation des Triazinsystems mit den unbeteiligten Elektronen des Aminstickstoffs — die folglich nur noch in einem geringen Ausmaß an der globalen Konjugation mit dem Azosystem teilnehmen können — vollkommen erklären. Die Verschiebung ist um so größer, je größer der mezomere elektronenanziehende Effekt des Substituenten aus der 4′-Stellung ist.

Im gleichen Sinn kann bemerkt werden, daß im Falle der in 4′-mit Dimethylaminogruppen substituierten Derivate (Ia und IIa) durch die Kondensation ein leichter bathochromer Effekt verzeichnet wird, was auf den Anstieg des elektronenspendenden Effekts der Dimethylaminogruppe infolge einer Positivierung des Aminstickstoffs am entgegengesetzten Ende des konjugierten Systems zurückzuführen ist.

Die wichtigsten Banden des IR-Spektrums, die die vorgeschlagene Struktur bestätigen, sind in Tabelle 3 angegeben.

Der Triazinring erscheint — wie zu erwarten war — durch vier charakteristische Banden, und zwar die Valenzschwingungen des Triazinrings um 1530—1570 und 1490 cm^{-1}, sowie die in der Ebene Deformationsschwingungen bei 850 — 870 cm^{-1} und beziehungs weise die außerhalb der Ebene dei 790 cm^{-1}. [3-7]

Die durch Arylaminogruppen disubstituierten Produkte unterscheiden sich von jenen monosubstituierten nur durch eine um 20 cm^{-1} verschobene Valenzbande des Rings, und zwar bei 1530 — 1570 cm^{-1}. Die Triazinverbindungen mit zwei Chloratomen besitzen eine Bande bei 840 cm^{-1}, die der C—Cl—Valenzschwingung [7] zugeschrieben wird.

Tabelle 3

Die charakteristischen Banden aus dem IR-Spektrum der substituierten 2-(Arylazoarylamino)-4,6-dichlor-(I) und 2-Chlor 4,6-bis(arylazoarylamino)-1,3,5-triazine (II). (cm^{-1})

Produkt	X	Triazinstruktur							
		ν_{Ring}	ν_{Ring}	δ_{Ring}	γ_{Ring}	ν_{CCl}	$\nu_{N=N}$	ν_{CN}	ν_{NH}
Ia	$(CH_3)_2N$	1 540	1 490	870	790	840	1 400	1 220 1 370	3 280
Ib	HO— [d)]	1 530	1 490	870	790	840	1 420	1 220 1 380	3 280
Ic	CH_3—	1 540	1 490	870	790	840	1 410	1 220 1 380	3 280
Id	H—	1 540	1 490	880	790	840	1 420	1 220 1 380	3 320
Ie	Cl—	1 540	1 500	880	790	840	1 410	1 220 1 380	3 280
If	H_3C—CO[c)]	1 530	1 490	870	790	840	1 420	1 220 1 390	3 280
Ig	NO_2— [e)]	1 540	1 480	870	790	840	1 420	1 220 1 390	3 280 3 360
IIa	$(CH_3)_2N$	1 560	1 480	860	790	—	1 400	1 220 1 380	3 200
IIc	H_3C—	1 570	1 490	870	795	—	1 410	1 220 1 380	3 200
IId	H—	1 560	1 480	850	790	—	1 420	1 220 1 380	3 200
IIe	Cl—	1 560	1 490	860	790	—	1 420	1 220 1 380	3 200
IIg	NO_2— [e)]	1 560	1 490	860	790	—	1 410	1 220 1 390	3 300

c) $\nu_{CO} = 1680$; d) $\nu_{OH} = 3110, 3180$

e) $\nu^{s}_{NO_2} = 1320$; $\nu^{a}_{NO_2} = 1550$

	Aromatischer Ring (cm^{-1})				
	ν_{arom}	ν_{arom}	γ_{CH}		
Ia	1 600	1 520	—	—	820 [b]
Ib	1 580 1 605	1 510	—	—	810 [b]
Ic	1 590	1 510	—	—	820 [b]
Id	1 600	1 520	680 [a]	770 [a]	830 [b]
Ie	1 590 1 605	1 510	—	—	830 [b]
If	1 590 1 605	1 510	—	—	830 [b]
Ig	1 595 1 610	1 510	—	—	820 [b]
IIa	1 590	1 530	—	—	810 [b]
IIc	1 600	1 510	—	—	830 [b]
IId	1 595 1 610	1 510	680 [a]	770 [a]	820 [b]
IIe	1 600 1 610	1 510	—	—	830 [b]
IIf	1 600	1 510	—	—	830 [b]

a) monosubstituiert

b) 1,4-disubstituiert

Im IR-Spektrum kann man die N=N– und CN–Valenzbanden beobachten die von den in para zur Azogruppe liegenden Struktur-elementen wenig beeinflußt sind. Die Banden des aromatischen Rings bestätigen die Substitutionsweise — di-1,4 oder mono-dieser Systeme.[8]

In Tabelle 4 sind die chemischen Verschiebungen und die Kopplungskonstanten für die aromatischen Protonen und jene der Substituenten X der Verbindungen (I) und (II) angegeben.

Tabelle 4

Chemische Verschiebungen und Kopplungskonstanten der substituierten 2-(Arylazoarylamino)-4,6-dichloro-(I) und 2-Chlor-4,6-bis(arylazoarylamio)-1,3,5-triazine (II)

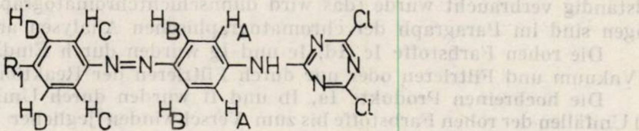

(I)

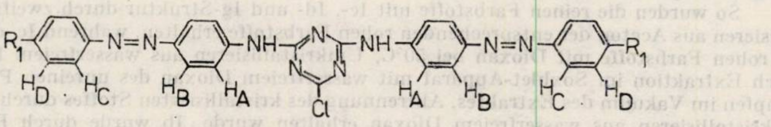

(II)

Struktur	X	δ(ppm)						J(Hz)	
		δ_A	δ_B	δ_C	δ_D	δ_X	δ_{NH}	J_{AB}	J_{CD}
I_a	$(H_3C)_2N$	7,87	7,87	7,89	6,80	3,13	11,25	0	8,75
I_c	H_3C	7,90	7,90	7,82	7,36	2,47	11,39	0	8,5
I_d	H	7,93	7,93	7,90	7,51	7,58	11,18	0	—
I_e	Cl	7,91	7,91	7,89	7,54	—	11,21	0	8,75
I_f	H_3C-CO	7,97	7,97	7,96	8,14	2,68	11,35	0	8,50
I_g	NO_2	7,99	7,99	8,05	8,40	—	11,25	0	9,00
II_c	H_3C	7,97	7,97	7,83	7,37	2,48	10,50	0	8,50
II_d	H	8,00	8,00	7,90	7,53	7,60	10,42	0	—
II_e	Cl	7,99	7,99	7,93	7,56	—	10,60	0	8,75

Zum Unterschied von den 4′-substituierten 4-Aminoazobenzolen[1] weisen die A- und B-Protonen des an den Triazinring gebundenen aromatischen Rings der Verbindungen I und II praktisch identische chemische Verschiebungen auf, was eine Umwandlung des Quartetts vom AB-Typ in ein spitzes Singulett zur Folge hat. Dieses Singulett wird von der Natur der Substituenten aus 4′ wenig beeinflußt ($\delta = 7,87 - 7,99$ ppm). Die C- und D-Protonen aus der 2-Stellung weisen den entsprechenden Protonen aus 4′-substituierten 4-Amino-azobenzolen[1] naheliegende chemische Verschiebungen auf. Die Protonen der NH-Gruppe hingegen sind durch den elektronenanziehenden Effekt des Triazinrings Tieffeld-verschoben (11,2–11,4 ppm).

So kann auch auf diese Weise unterstrichen werden, daß es zu einer beträchtlichen Konjugation der unbeteiligten Elektronen des Aminstickstoffs mit dem Triazinring kommt, wodurch die Rolle des Elektronenspenders dieses Atoms dem Azostickstoff gegenüber fast gänzlich aufgehoben wird.

VERSUCHSTEIL

Substanzen

Die substituierten 2-(Arylazoarylamino)-4,6-dichlor-1,3,5-triazine (I) wurden durch die Kondensation des Cyanurchlorids mit 4′-substituierten 4-Aminoazobenzolen (Molverhältnis 1 : 1), in Aceton bei 0—5°C und einer Reaktionszeit von 1 — 3 Stunden, je nach der Reaktivität des Aminoazofarbstoffes hergestellt.

Die auf 0°C abgekühlte acetonische Cyanurchloridlösung (10—15%) wird in cca 30 Minuten unter kräftigem Rühren zu der auf 0— 5°C abgekühlten acetonischen Azofarbstofflösung (3 — 8%) hinzugetropft, wonach noch cca 30 Minuten weitergerührt wird. Anschließend wird die durch die Kondensation freigesetzte Salzsäure mit einer 10%-igen Na_2CO_3-Lösung neutralisiert, wobei der Reaktionsverlauf pH-metrisch verfolgt wird. Im Verlaufe der Neutralisation wird das pH streng bei 6 — 6,5 gehalten. Die Kondensation wird als abgeschlossen angesehen, wenn das pH der Reaktionsmasse sich allmählich verändert und der Aminofarbstoff vollständig verbraucht wurde (das wird dünnschichtchromatographisch bestimmt ; die Bedingungen sind im Paragraph der chromatographischen Analysen angegeben).

Die rohen Farbstoffe Ic, Id, Ie und Ig wurden durch Eindampfen der Reaktionsmasse im Vakuum und Filtrieren oder nur durch Filtrieren der Reaktionsmasse erhalten.

Die hochreinen Produkte Ia, Ib und If wurden durch Umkristallisieren, Extraktionen und Umfällen der rohen Farbstoffe bis zum Verschwinden jeglicher Parasitflecken im Dünnschichtchromatogramm erhalten.

So wurden die reinen Farbstoffe mit Ic-, Id- und Ig-Struktur durch zweifaches Umkristallisieren aus Aceton der entsprechenden rohen Farbstoffe erhalten, während Ic durch Waschen des rohen Farbstoffe mit Dioxan bei 50°C, Umkristallisieren aus wasserfreiem Dioxan und Ia durch Extraktion im Soxhlet-Apparat mit wasserfreiem Dioxan des unreinen Produktes, Eindampfen im Vakuum des Extraktes, Abtrennung des kristallisierten Stoffes durch Abkühlen und Umkristallisieren aus wasserfreiem Dioxan erhalten wurde. Ib wurde durch Extraktion mit wasserfreiem Dioxan im Soxhlet-Apparat und Kristallisieren durch Abkühlen, Fällen mit Wasser bei 2 — 5°C des Produktes, Filtrieren, Waschen des Rückstandes mit Aceton, Auflösung in Dimethylformamid bei 35 — 40°C, Umfällen mit Wasser bei 5°C und rasches Waschen mit Aceton erhalten.

Die reinen Stoffe wurden in allen Fällen im Vakuum getrocknet.

Die substituierten 2-Chlor-4,6-bis(arylazoarylamino)-1,3,5-triazine (II) wurden durch Kondensation des Cyanurchlorids mit 4′-substituierten 4-Aminoazobenzolen (Molverhältnis 1 : 2) in Dioxan-Wasser synthetisiert. Die 2 — 8%-ige Aminoazofarbstofflösung in wasserfreiem Dioxan wurde unter Rühren der Cyanurchloridlösung (cca 5%) im selben Lösungsmittel zugefügt und cca 30 Minuten bei 12—15°C gehalten. Dann wurde unter kräftigen Rührem eine 10%-ige Natriumcarbonatlösung bis zu pH = 6 zugesetzt, wonach die Temperatur in 30 Minuten auf 60—65° C gesteigert wurde und für IIa 2 Stunden lang, für IIc und IId 3,5 Stunden lang beibehalten wurde.

Infolge der geringeren Reaktionsfreude der Aminoazoderivate, war für die Farbstoffe der Struktur IIe und IIg eine Reaktionszeit von 4 bzw. 5,5 Stunden für die Dikondensation notwendig, sowie eine Temperatur von 70 — 75°C. Während der Kondensation wurde von Zeit zu Zeit eine wäßrige 10%-ige Natriumcarbonatlösung zugefügt zwecks Konstanthaltung des pH bei 6,2 — 6,5 (pH-metrisch gemessen). Die Dikondensation gilt als abgeschlossen, wenn das pH 15 minutenlang konstant bleibt.

Die Verbindungen sind in der Reaktionsmasse schwer löslich, so daß die Abtrennung in allen Fällen durch Filtrieren bei 50 — 60°C durchgeführt wurde.

Die rohen Verbindungen IIa und IIg wurden durch Waschen mit Dioxan-Wasser (80/20 V/V) auf dem Filter, Aufschlämmen in wasserfreiem Dioxan, Filtrieren bei 80°C und Waschen mit wasserfreiem Dioxan (auf dem Filter) gereinigt.

Die reinen Verbindungen IIc und IIe wurden durch Soxhlet-Extraktion der rohen Farbstoffe mit Aceton, Auflösung des Rückstandes in Dimethylformamid bei 5°C, Fällen mit kaltem Wasser, Filtrieren und rasches Waschen mit wasserfreiem Aceton erhalten.

Die reine Verbindung IIe wurde durch einfaches Waschen des rohen Produktes mit wasserfreiem Dioxan erhalten.

Alle Verbindungen wurden im Vakuum getrocknet.

Die *dünnschichtchromatographische Analyse* wurde auf mit Kieselgel G Merck bedeckten Platten, von einer Schichtdicke von 0,25 mm und 15 — 18 cm Höhe durchgeführt.

Die in der Literatur[2] für die Analyse der Azotriazinfarbstoffe angegebenen Laufmittel sind für die in vorliegender Arbeit beschriebenen Farbstoffe nicht geeignet, da sie eine zu große Polarität aufweisen. Deshalb setzten wir es uns zur Aufgabe eine mobile Phase zu finden, die zu einem unterschiedlichen R_f für eine größtmögliche Anzahl von Farbstoffen unserer Reihe führt, und zwar in den Bedingungen einer klaren Abtrennung der Aminoazofarbstoffe von den Mono-und Dikondensationsprodukten mit Cyanurchlorid. Die vorgeschriebenen Bedingungen wurden vom Gemisch Benzol-Aceton 16 : 1 (A) und unter Umständen auch vom Methylenchlorid (B) erfüllt.

Die *sichtbaren und ultravioletten Spektren* wurden mit einem UNICAM SP 800 Spektrographen in Methanol und 1,2-Dichlorethanlösungen aufgenommen.

Die *infrarot Spektren* wurden mit einem Specord IR 75 Spektrographen an KBr- Preßlingen gemessen.

Die *protonischen kernmagnetischen Resonanzspektren* wurden in einer 2-5%-igen Lösung eines Gemisches von Deuterochloroform-Hexadeuterodimethylsulfoxid ($CDCl_3$—DMSO—d_6), in Volumverhältnissen von 3 : 1 bzw. 1 : 3, mit einem ,,Tesla'' BS 487C NMR-Spektrometer (80 Hz) aufgenommen, wobei als interner Standard Tetramethylsilan (TMS) verwendet wurde.

Die *Elementaranalyse* für C, H und N wurde mit einem Perkin Elmer ,,Elemental — Analyzer'' 240 B durchgeführt, während N und Cl nach Kjeldahl bzw. Schöniger bestimmt wurden.

Die *Schmelzpunkte* wurden mit einem Boetius-Apparat bestimmt.

Die *pH-Messungen* wurden mit einem MV 85 pH-Meter Präcitronic DDR, mit Glaselektrode und als Bezugselektrode eine Kalomelektrode durchgeführt.

LITERATURVERZEICHNIS

[1] I. Havlik, C. Csunderlik, A. Toth und R. Bacaloglu, *Rev. Roumaine Chim.*, im Druck.

[2] V. Pelloni-Tamaş und F. Iolian, ,,Cromatografia în strat subţire,'' Editura tehnică, Bucureşti, 1971, S. 259.

[3] E. Allenstein, P. Kiemle, E. Schlipf und W. Podszum, *Spectrochim. Acta*, **34A**, 423 (1978).

[4] E. Allenstein, W. Podszum und I. Weideim, *Z. anorg. Chem.*, **40B**, 53 (1974).

[5] C. Msoumoto, *Nippon Kagaku Zasshi*, **87**, 797 (1966).

[6] A. R. Katritzky, ,,Physical Methods in Heterocyclic Chemistry'', vol. II, Academic Press, New York, 1963.

[7] W. A. Heckle, H. A. Ory und J. M. Talbert, *Spectrochim. Acta*, **17**, 600 (1961).

[8] N. B. Colthup, L. H. Daly und S. E. Wiberay, ,,Introduction to Infrared and Raman Spectroscopy'', Academic Press, New York, 1975.

Revue Roumaine de Chimie, **29**, *2*, 193 – 199 (1984)

FRIEDEL-CRAFTS ACYLATION OF ALKYNES. I

THE REACTION OF 1-ALKYNES WITH ACETYL CHLORIDE·$AlCl_3$-COMPLEX IN THE PRESENCE OF HALOGENATED NON-NUCLEOPHILIC SOLVENTS

DUMITRU MĂNOIU[a], MARIA MĂNOIU[a], ILIE G. DINULESCU[b]
and MARGARET AVRAM[b,*]

[a] Institute of Research Technological Engineering and Design for Rafineries, Ploiești, Romania
[b] Laboratory of Organic Chemistry, Polytechnic Institute-TCH, Spl. Independenței 313, 72206 Bucharest 16, Romania

Received April 19, 1983

The acylation of 1-alkynes with $AlCl_3$-complexed acetyl chloride, in the presence of non-nucleophilic solvents, gives rise to normal addition products, β-chloro-α,β-unsaturated ketones, variable amounts of isomeric β-chloro-β,γ-unsaturated ketones as well as of chlorodienic compounds. The mechanisms of formation of these compounds are discussed.

INTRODUCTION

The chemistry of acetylenes was the object of several studies, treatises and monographs.[1-10] Although the chemistry of the Friedel-Crafts acylation of acetylenes leading to β-chloro-α,β-unsaturated ketones [9] as well as the chemistry of vinyl cations [11-17] were investigated intensively, little is known about the behaviour of vinyl cations generated in the Friedel-Crafts acylation of acetylenes. Due to the practical importance of β-chloro-α,β-unsaturated ketones, the majority of studies are limited to synthetical aspects of this reaction.[9,10]

Our interest in the chemistry of acetylenes [18] prompted us to investigate the behaviour of mono- and disubstituted acetylenes toward a variety of acyl chlorides, in the presence of Lewis acids, in order to obtain more information concerning the course of this reaction.

In this paper we report on the reaction of 1-alkynes with the formula $R-C\equiv CH$ (**1**, $R=C_6H_5$; **2**, $R=CH_3$; **3**, $R=C_2H_5$; **4**, $R=C_3H_7$; **5**, $R=C_4H_9$) with the soluble acetyl chloride·$AlCl_3$ complex (Perrier's reagent) in non-nucleophilic halogenated solvents.

RESULTS

The reaction of acetyl chloride with 1-alkynes (**1**–**5**) was performed in comparable experimental conditions, using a standard procedure (see experimental part).

The general results of these reactions are presented in table 1.

Table 1

Reaction of $R-C\equiv CH$ with $CH_3COCl \cdot AlCl_3$ in carbon tetrachloride

Reaction products (%g) \ R		C_6H_5 (1)	CH_3 (2)	C_2H_5 (3)	C_3H_7 (4)	C_4H_9 (5)
β-Chloro- -α,β-unsaturated ketones	*E*	84.0	96.20	64.77	31.75	56.18
	Z	16.0	3.80	12.87	3.55	1.98
Other products		—	—	22.69	64.70	41.84

As expected, the experimental data concerning the products formed in the acylation of 1-alkynes with the soluble acetyl chloride · $AlCl_3$ complex present a more complex pattern as reported earlier in the literature.[9,10]

In all cases we identified, besides the well-known normal addition products, namely the *E*-β-chloro-α,β-unsaturated ketones (*trans*-β-chlorovinyl ketones), variable amounts of the corresponding *Z* isomer. Methyl- and phenylacetylene gave only these two components. In the reaction of phenylacetylene the amount of the *Z* isomer becomes significant.

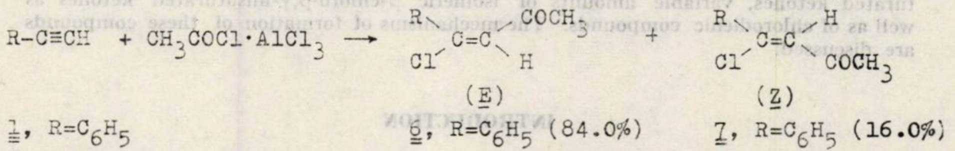

1, $R=C_6H_5$ 6, $R=C_6H_5$ (84.0%) 7, $R=C_6H_5$ (16.0%)

2, $R=CH_3$ 8, $R=CH_3$ (96.2%) 9, $R=CH_3$ (3.8%)

In the reaction of acetylenes bearing higher alkyl groups (**3 — 5**) and having CH_2 or CH groups next the triple bond three types of reactions products were identified (Scheme 1). Along with the normal addition products, namely β-chloro-α,β-unsaturated ketones (*E* and *Z* isomers) (type A, **10 — 15**), they gave significant amounts of isomeric ketones (type B, **16 — 20**) with β-chloro-β,γ-unsaturated ketonic structure, as well as small amounts of higher condensation products with acylated chlorodienic structure (type C, **21 — 23**).

The conjugated β-chloro-α,β-unsaturated ketones present in the ^1H-NMR spectrum the signal of the vinylic proton at δ 6.2 ppm, in accordance with literature data,[20] while the signals of the vinylic proton in the unconjugated β-chloro-β, γ-unsaturated ketones, appear more shielded at δ 5.0—5.5 ppm.

Some *E* and *Z* isomers difficult to separate were identified on the basis of spectral data of their mixture as shown in the experimental part.

The dienic compounds were isolated and their structures were ascribed on the basis of analytical data.

Using (instead of carbon tetrachloride) other non-nucleophilic halogenated solvents such as dichloroethane, dichloromethane or mixtures of these solvents, the yield of the acylation presented only small variation

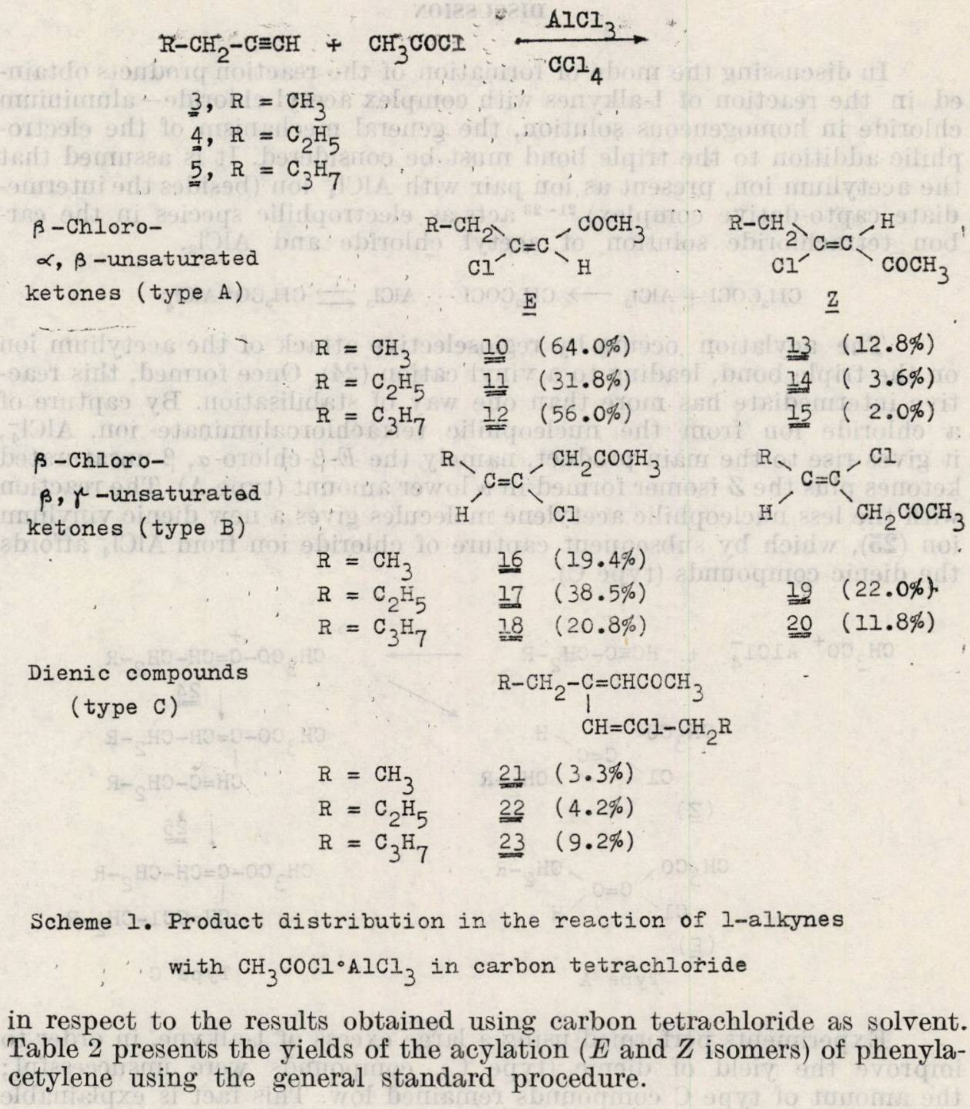
R-CH₂-C≡CH + CH₃COCl
AlCl₃
CCl₄
3, R = CH₃
4, R = C₂H₅
5, R = C₃H₇
β-Chloro-α,β-unsaturated ketones (type A)
E
Z
R = CH₃ 10 (64.0%) 13 (12.8%)
R = C₂H₅ 11 (31.8%) 14 (3.6%)
R = C₃H₇ 12 (56.0%) 15 (2.0%)
β-Chloro-β,γ-unsaturated ketones (type B)
R = CH₃ 16 (19.4%)
R = C₂H₅ 17 (38.5%) 19 (22.0%)
R = C₃H₇ 18 (20.8%) 20 (11.8%)
Dienic compounds (type C)
R-CH₂-C=CHCOCH₃
CH=CCl-CH₂R
R = CH₃ 21 (3.3%)
R = C₂H₅ 22 (4.2%)
R = C₃H₇ 23 (9.2%)

Scheme 1. Product distribution in the reaction of 1-alkynes with $CH_3COCl \cdot AlCl_3$ in carbon tetrachloride

in respect to the results obtained using carbon tetrachloride as solvent. Table 2 presents the yields of the acylation (*E* and *Z* isomers) of phenylacetylene using the general standard procedure.

Table 2

Yield of acetylation of phenylacetylene in various halogenated solvents and in carbon disulphide

Solvent	Yield %	Solvent	Yield %
CCl_4	81	CCl_4-CHCl_3 (1 : 1)	62
CH_2Cl_2	68	$CCl_4-C_2H_4Cl_2$ (1 : 1)	68
$CHCl_3$	60	$CH_2Cl_2-C_2H_4Cl_2$ (1 : 1)	67
$C_2H_4Cl_2$	74	CS_2	73

DISCUSSION

In discussing the mode of formation of the reaction products obtained in the reaction of 1-alkynes with complex acetyl chloride—aluminium chloride in homogeneous solution, the general mechanism of the electrophilic addition to the triple bond must be considered. It is assumed that the acetylium ion, present as ion pair with $AlCl_4^-$ ion (besides the intermediate capto-dative complex),[21–23] acts as electrophilic species in the carbon tetrachloride solution of acetyl chloride and $AlCl_3$.

$$CH_3COCl + AlCl_3 \longrightarrow CH_3COCl \cdots AlCl_3 \rightleftarrows CH_3CO^+ AlCl_4^-$$

The acylation occurs by regioselective attack of the acetylium ion on the triple bond, leading to a vinyl cation (**24**). Once formed, this reactive intermediate has more than one way of stabilisation. By capture of a chloride ion from the nucleophilic tetrachloroaluminate ion, $AlCl_4^-$, it gives rise to the main product, namely the *E*-β-chloro-α, β-unsaturated ketones plus the *Z* isomer formed in a lower amount (type A). The reaction with the less nucleophilic acetylene molecules gives a new dienic vinylium ion (**25**), which by subsequent capture of chloride ion from $AlCl_4^-$ affords the dienic compounds (type C).

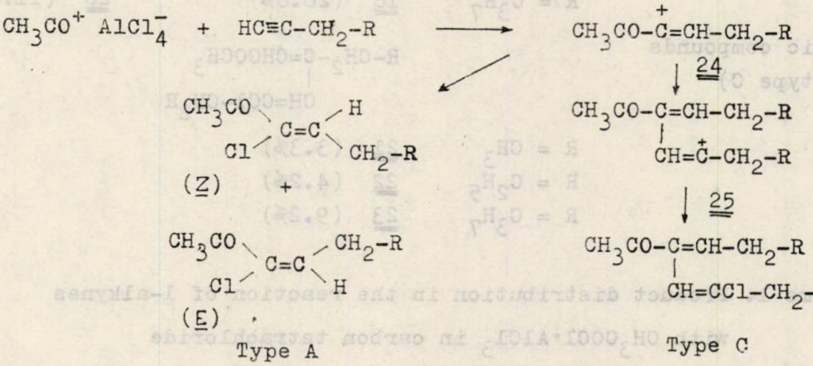

Experiments performed using a large excess of 1-alkyne, in order to improve the yield of dienic (type C), compounds were unsuccessful; the amount of type C compounds remained low. This fact is explainable by the lower nucleophilicity of acetylene molecules in respect to the tetrachloroaluminate ion, $AlCl_4^-$. It can be concluded that the product distribution is under kinetical control.

For the formation of β-chloro-β,γ-unsaturated ketones (type B) observed in the reaction of higher alkynes, one must take into account the intermediacy of allenic compounds. Thus the initially formed acylvinyl cation **24**, by losing a proton, gives as intermediate the acylated allenic compound **26**, which by reprotonation leads to the vinyl cation **27**. The latter by capture of a chloride ion from $AlCl_4^-$, affords finally the double bond isomeric β-chloro-β,γ-unsaturated ketones (type B), which in turn exist as two stereoisomeric *E* and *Z* forms.

The formation of allenes from acetylenes in acid catalysis was reported earlier in heterogeneous reaction conditions.[23] Although 1,2-dienes and acetyl chloride give, in the presence of $AlCl_3$, the same β-chloro-β,

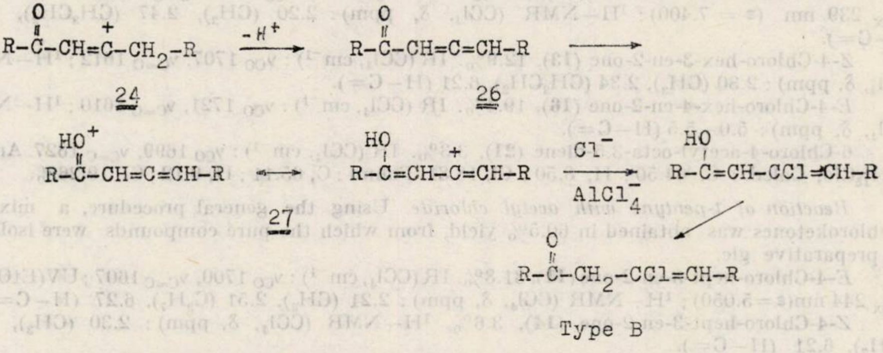

γ-unsaturated ketones as those formed starting with acetylenes, the occurrence of compounds of type B via this reaction can be ruled out. Several attempts to illustrate the isomerisation of 1-alkynes to 1,2-dienes under Friedel-Crafts acylation conditions were unsuccessful.

EXPERIMENTAL

IR spectra were recorded with a double beam UR-20 spectrophotometer. ^1H-NMR spectra were determined with a Tesla 60 and Varian A—60A spectrometer. Glc analyses were carried out on a Varian chromatograph, equipped with a flame ionisation detector, using a 4m × 3mm of 10% QF-1 on kisselgur 60 — 80 mesh column; column temperature 120°, detector temp. 240°; carrier gas hydrogen, 45 ml/min. Preparative glc was carried out on a Beckmann Meghachrom chromatograph equipped with catharometer, using a 6m × 3 mm of 10% QF-1 on kisselgur.

Reagents: all the reagents used were obtained from commercial source in high purities. Acetyl chloride and $AlCl_3$ were purified just before use.

Standard procedure. All experiments were performed in comparable experimental conditions using a standard procedure. The acylating reagent was prepared according to Perrier's method,[19] by stirring equimolar quantities of acetyl chloride and anhydrous aluminium chloride in carbon tetrachloride or other halogenated solvents (2500 ml/mol) until all $AlCl_3$ disappeared and a homogeneous solution was formed. This solution, cooled at 0°, was added dropwise during 10 min to a vigorously stirred solution of an equimolar amount of alkyne in the halogenated solvent, kept at −40° to −60°. After additional stirring for 15 min at this temperature, the reaction mixture was poured into ice and hydrochloric acid, extracted with diethyl ether and the organic layer was washed with water, neutralised with sodium hydrogen carbonate, dried and the solvent removed in vacuo. The crude reaction product was analysed by means of gas chromatography.

Reaction of phenylacethylene with acetyl chloride. The acetylation products were isolated in 81% yield. The following compounds were separated by thin layer chromatography:

E-4-Chloro-4-phenyl-but-3-en-2-one (**6**), 84%; IR (CCl_4, cm^{-1}): ν_{CO} 1710, $\nu_{C=C}$ 1630; UV(EtOH): λ_{max} 235 nm(ε = 10.300); ^1H-NMR (CCl_4, δ, ppm): 2.20 (CH_3), 6.42 (H—C=).

Z-4-Chloro-4-phenyl-but-3-en-2-one (**7**), 16%. IR (CCl_4, cm^{-1}): ν_{CO} 1710, $\nu_{C=C}$ 1630; ^1H-NMR (CCl_4, δ, ppm): 2.33 (CH_3), 6.74 (H—C=).

Reaction of propyne with acetyl chloride. From the acylation product, formed in 60% yield, the following compounds were isolated:

E-4-Chloro-pent-3-en-2-one (**8**), 96.2%. IR (CCl_4, cm^{-1}): ν_{CO}1707, $\nu_{C=C}$1612; UV(EtOH): λ_{max} 239 nm (ε = 7.300); ^1H-NMR (CCl_4, δ, ppm): 2.20 (CH_3), 2.54 (CH_3C=), 6.47 (H—C=).

Z-4-Chloro-pent-3-en-2-one (**9**), 3.8%. IR (CCl_4, cm^{-1}) : ν_{CO} 1707, $\nu_{C=C}$ 1612 ; ^1H-NMR (CCl_4, δ, ppm) : 2.31 (CH_3), 2.25 ($CH_3-C=$), 6.30 ($H-C=$).

Reaction of 1-butyne with acetyl chloride. From the acylation product, obtained in 58.3% yield, the following ketones were isolated :

E-4-Chloro-hex-3-en-2-one (**10**), 64.4%. IR (CCl_4, cm^{-1}): ν_{CO} 1707, $\nu_{C=C}$ 1612 ; UV (EtOH) : λ_{max} 239 nm (ε = 7.400) ; ^1H-NMR (CCl_4, δ, ppm) : 2.20 (CH_3), 2.47 (CH_3CH_2), 6.27 ($H-C=$).

Z-4-Chloro-hex-3-en-2-one (**13**), 12.9%. IR (CCl_4, cm^{-1}) : ν_{CO} 1707, $\nu_{C=C}$ 1612 ; ^1H-NMR (CCl_4, δ, ppm) : 2.30 (CH_3), 2.34 (CH_3CH_2), 6.21 ($H-C=$).

E-4-Chloro-hex-4-en-2-one (**16**), 19.4%. IR (CCl_4, cm^{-1}) : ν_{CO} 1721, $\nu_{C=C}$ 1610 ; ^1H-NMR (CCl_4, δ, ppm) : 5.0 – 5.5 ($H-C=$).

6-Chloro-4-acetyl-octa-3,5-diene (**21**), 3.3%. IR (CCl_4, cm^{-1}) : ν_{CO} 1699, $\nu_{C=C}$ 1627. Anal. : $C_{10}H_{15}Clo$, Calcd. : C, 64.50 ; H, 8.50 ; Cl, 18.81. Found : C, 65.11 ; H, 9.12 ; Cl, 19.26%.

Reaction of 1-pentyne with acetyl chloride. Using the general procedure, a mixture of chloroketones was obtained in 60.5% yield, from which the pure compounds were isolated by preparative glc.

E-4-Chloro-hept-3-en-2-one (**11**), 31.8%. IR (CCl_4, cm^{-1}) : ν_{CO} 1700, $\nu_{C=C}$ 1607 ; UV(EtOH) : λ_{max} 244 nm(ε=5.050) ; ^1H-NMR (CCl_4, δ, ppm) : 2.21 (CH_3), 2.51 (C_3H_7), 6.27 ($H-C=$).

Z-4-Chloro-hept-3-en-2-one (**14**), 3.6%. ^1H-NMR (CCl_4, δ, ppm) : 2.30 (CH_3), 2.34 (C_3H_7), 6.21 ($H-C=$).

4-Chloro-hept-4-en-2-one, mixture of *E* (**17**, 38.5%) and *Z* (**19**, 22.0%), isomers. assuming 60.5%. IR(CCl_4, cm^{-1}) : ν_{CO} 1727, $\nu_{C=C}$ 1612 ; ^1H-NMR (CCl_4, δ, ppm) : 5.1 – 5.6 ($H-C=$).

6-Chloro-4-n-propyl-nona-3,5-dien-2-one (**22**), 4.2%. IR(CCl_4, cm^{-1}) : ν_{CO}1696, $\nu_{C=C}$ 1628. Anal. : $C_{12}H_{18}ClO$, Calcd. ; C, 67.50 ; H, 8.45 ; Cl, 16.43. Found : C, 67.13 ; H, 9.05 ; Cl, 16.02%.

Reaction of 1-hexyne with acetyl chloride. In the fraction with b.p. 90 — 110°/1 mm of the reaction product, the following compounds were identified :

E-4-Chloro-oct-3-en-2-one (**12**), 56.0%. IR (CCl_4, cm^{-1}) : ν_{CO}1695, $\nu_{C=C}$1605 ; UV(EtOH) : λ_{max} 239 nm (ε = 12.600) ; ^1H-NMR (CCl_4, δ, ppm) : 2.20 (CH_3), 2.37 (C_4H_9), 6.25 ($H-C=$).

Z-4-Chloro-oct-3-en-2-one (**15**), 2.0%. ^1H-NMR (CCl_4, δ, ppm) : 2.31 (CH_3), 2.35 (C_4H_9), 6.30 ($H-C=$).

4-Chloro-oct-4-en-2-one, mixture of *E* (**18**, 20.8%) and *Z* (**20**, 11.8%) isomers. IR (CCl_4, cm^{-1}) : ν_{CO} 1724, $\nu_{C=C}$ 1610 ; ^1H-NMR (CCl_4, δ, ppm) : 5.0 – 5.5 ($H-C=$).

6-Chloro-4-n-butyl-deca-3,5-dien-2-one (**23**, 8.8%). IR (CCl_4, cm^{-1}) : ν_{CO}1701, $\nu_{C=C}$ 1625. Anal. : $C_{14}H_{23}ClO$, Calcd. : C, 69.42 ; H, 9.51 ; Cl, 14.46. Found : C, 70.51 ; H, 10.42 ; Cl, 15.04 %

REFERENCES

[1] V. A. Nieuwland and R. Vogt, "The Chemistry of Acetylene", Reinhold Book Corp., New. York, 1945.

[2] H. G. Viehe, "Chemistry of Acetylenes". M. Dekker, New York, 1969.

[3] S. A. Miller, "Acetylene. Its Properties, Manufacture and Uses", E. Benn Ltd., London, 1965.

[4] T. F. Rutlege, "Acetylenic Compounds. Preparation and Substitution Reactions", Reinhold Book Comp., New York, 1968.

[5] V. Jäger, Alkine, Di- und Polyine, Allene, Kumulene, in Houben-Weyl, "Metoden der organischen Chemie", vol 5/2 A, Georg Thieme Verlag, Stuttgart, 1977.

[6] J. Iwai, Base-Catalyzed Rearrangements of Acetylene Derivates, in B. S. Thyagarajan, "Mechanism of Molecular Rearrangements", vol. 2, Interscience Publ., New York, 1969, p. 73.

[7] C. A. Thomas, "Anhydrous Aluminium Chloride in Organic Chemistry", vol. 2, Reinhold Publ. Corp., New York, 1950, p. 760.

[8] C. D. Nenitzescu and A. T. Balaban, Aliphatic Acylation, in G. A. Olah, "Friedel-Crafts and Related Reactions", vol 3/2, Interscience Publ., London, 1964, p. 1081.

[9] A. E. Pohland and W. R. Benson, *Chem. Rev.*, **66**, 161 (1966).

[10] R. Gipp, Direkte Einführung von R–CO–Gruppen durch Acylierung von Alkinen und Vinylhalogeniden, in Houben-Weyl, "Metoden der Organischen Chemie", vol. 7/2 A, Georg Thieme Verlag, Stuttgart, 1978, p. 480.

[11] H. G. Richey and J. M. Richey, Disubstituted Carbonium Ions, in G. A. Olah, "Carbonium Ions". vol. 2, Interscience Publ., London, 1970, p. 900.

[12] M. Hanack, *Acc. of Chem. Res.*, **3**, 209 (1970).

[13] G. Modena and U. Tonelato, *Adv. Phys. Org. Chem.*, **9**, 185 (1971).

[14] P. Y. Stang, *Adv. Phys. Org. Chem.*, **30**, 205 (1973).

[15] A. Schegolev, W. A. Smit, G. V. Raitburg and W. F. Kucherov, *Tetrahedron Letters*, **1974**, 3373.

[16] G. J. Martin and G. Daviand, *Bull. Soc. Chim. France*, **1970**, 3098.

[17] H. Martens and G. Hoornaret, *Tetrahedron Letters*, **1970**, 1821.

[18] M. Avram and coworkers, series of Reaction of Acetylenes with Transition Metals : Part X : I. G. Dinulescu, S. Staicu, E. Avram, F. Chiraleu and M. Avram, *J. Organometal. Chem.*, **136**, 15 (1977).

[19] G. Perrier, *Ber. dtsch. chem. Ges.*, **33**, 815 (1900).

[20] D. Cook, *Canad. J. Chem.*, **37**, 48 (1959).

[21] B. P. Susz and J. J. Wuhrmann, *Helv. Chim. Acta*, **40**, 722 (1957).

[22] B. P. Susz and J. J. Wuhrmann, *Helv. Chim. Acta*, **40**, 971 (1957).

[23] D. Mănoiu, Ph. D. Thesis, Polytechnical Institute, București, 1979.

Revue Roumaine de Chimie, 29, 2, 201–206 (1984)

FRIEDEL-CRAFTS ACYLATION OF ALKYNES. II[1]

THE REACTION OF 1-ALKYNES WITH ACETYL CHLORIDE·$AlCl_3$-COMPLEX IN AROMATIC AND SATURATED HYDROCARBONS AS SOLVENTS

DUMITRU MĂNOIU [a], MARIA MĂNOIU [a], ILIE G. DINULESCU [b] and MARGARET AVRAM [b,*]

[a] Institute of Research Technological Engineering and Design for Rafineries, Ploieşti, Romania
[b] Laboratory of Organic Chemistry, Polytechnic Institute-TCH, Spl. Independenţei 313, 72206 Bucharest 16, Romania

Received April 19, 1983

The reaction of 1-alkynes with the complex acetyl chloride·$AlCl_3$ was investigated in carbon tetrachloride solution, in the presence of aromatic solvents such as benzene or hydride donor solvents such as cyclohexane and methylcyclopentane or methylcyclohexane. Competition between both nucleophilic species, chloride ion and the aromatic hydrocarbon, takes place. No hydride transfer from the saturated hydrocarbon to the acetylvinyl cation could be evidenced. The reaction mechanisms are discussed.

INTRODUCTION

It was shown in the previous paper[1] that the acetylvinyl cations (I) generated in the reaction of 1-alkynes with the complex acetyl chloride·$AlCl_3$ give rise, in non-nucleophilic halogenated solvents, to three types of reaction products: the normal addition products, namely *E* and *Z* β-chloro-α, β-unsaturated ketones (II), the structurally isomeric β-chloro-β, γ-unsaturated ketones (IV) resulted from an acylallenic intermediate (III) (also existing as two *E*/*Z* stereoisomers) and the chlorodienic compounds (V) (whose *E*/*Z* stereoisomers were not separable) resulted from the reaction of intermediate acetylvinyl cation I with the alkyne.

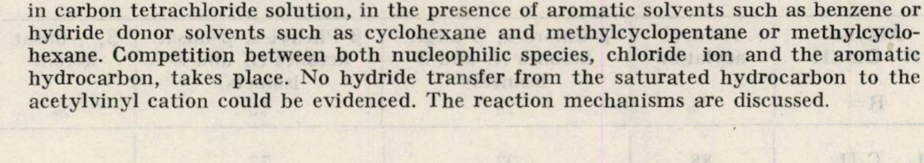

In order to obtain a more complete picture on the behaviour of the acetylvinyl cations (I), generated in the presence of $AlCl_3$, we investigated the reaction using as solvents aromatic hydrocarbons with nucleophilic character as well as saturated hydrocarbons with hydride donor properties, well known as reactive partners in the acylation of alkenes.[2]

In this paper we present the results obtained in the reaction of the complex acetyl chloride·$AlCl_3$ in homogeneous carbon tetrachloride solution, in the presence of variable amounts of benzene or cyclohexane and methylcyclopentane. The following 1-alkynes $R-C\equiv CH$ were used: **1**, $R=C_6H_5$; **2**, $R=CH_3$; **3**, $R=C_2H_5$; **4**, $R=C_3H_7$; **5**, $R=C_4H_9$.

REACTION OF 1-ALKYNES WITH THE ACETYL CHLORIDE·$AlCl_3$ COMPLEX IN THE PRESENCE OF BENZENE

The reactions were performed using the same standard procedure as in the reactions carried out in non-nucleophilic halogenated solvents.[1] The general results obtained in the reaction of 1-alkynes (**1** – **5**) with acetyl chloride·$AlCl_3$ in CCl_4-benzene, based on gas chromatographic analysis of the crude reaction mixture, are presented in table 1.

Table 1

Reaction of $R-C\equiv CH$ with $CH_3COCl\cdot AlCl_3$ in CCl_4-benzene solution

Alkyne $R-C\equiv CH$ R=	Yield of acylation %	β-Chloro-α, β-unsat. ketones (*E* and *Z* isomers) %	β-Phenyl-α, β-unsat. ketones (*E* and *Z* isomers) %	β, γ-unsat. ketone %
1, C_6H_5	88	23	77	–
2, CH_3	48	58	42	–
3, C_2H_5	62	51*	47	2.0
4, C_3H_7	64	42*	44	3.2
5, C_4H_9	71	37*	52	11.0

* Because not all compounds were identified, the total is different from 100%

Phenylacetylene gave two major components, which were isolated and identified as *E*-β-chloro- and β-phenyl-α,β-unsaturated ketones (**6** and **7** respectively).

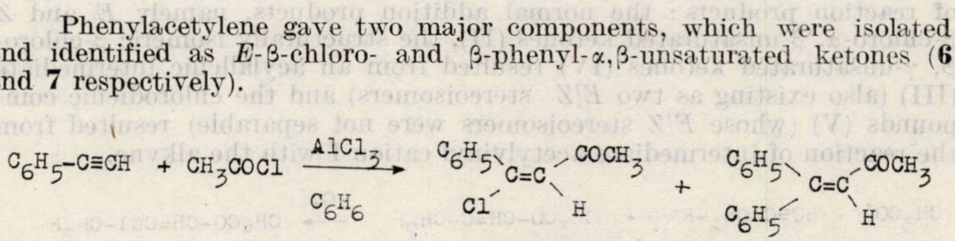

The alkynes **2** – **5** gave a more complex mixture. From the reaction product two groups of major components were isolated by preparative gas chromatography coupled with thin layer chromatography. They were identified as β-chloro-α,β-unsaturated ketones (**8**–**15**) and β-phenyl-α,β-unsaturated ketones (**16** – **23**). Small amounts of β-chloro-β,

γ-unsaturated ketones could be identified by comparison with authentic samples from precedent work.[1]

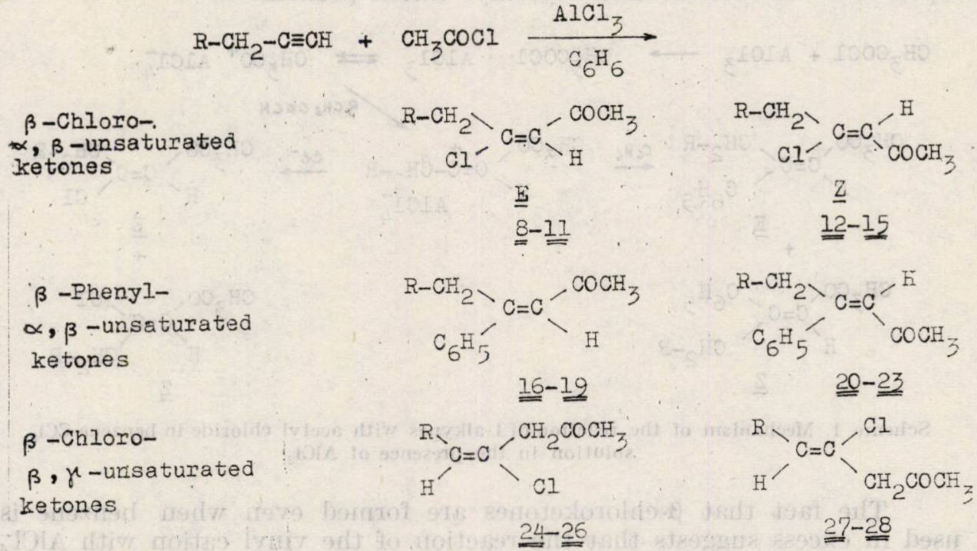
R-CH2-C≡CH + CH3COCl
AlCl3
C6H6
β-Chloro-α,β-unsaturated ketones
R-CH2 Cl C=C COCH3 H
E
8-11
R-CH2 Cl C=C H COCH3
Z
12-15
β-Phenyl-α,β-unsaturated ketones
R-CH2 C6H5 C=C COCH3 H
16-19
R-CH2 C6H5 C=C H COCH3
20-23
β-Chloro-β,γ-unsaturated ketones
R H C=C CH2COCH3 Cl
24-26
R H C=C Cl CH2COCH3
27-28

The ratios of the individual compounds are presented in table 2.

Table 2

Product distribution in the reaction of 1-alkynes in benzene-CCl_4 solution (% moles)

Compound \ Alkyne R−C≡CH		R				
		C_6H_5 (1)	CH_3 (2)	C_2H_5 (3)	C_3H_7 (4)	C_4H_9 (5)
β-Chloro-α,β--unsat. ketone	*E*	**6**, 23.0	**8**, 55.0	**9**, 48.4	**10**, 36.84	**11**, 32.9
	Z	—	**12**, 3.0	**13**, 2.6	**14**, 5.6	**15**, 4.1
β-Phenyl-α,β--unsat. ketone	*E*	**7**, 77.0	**16**, 39.5	**17**, 46.3	**18**, 40.5	**19**, 48.36
	Z	—	**20**, 2.5	**21**, 0.7	**22**, 3.25	**23**, 3.64
β-Chloro-β,γ-unsat. ketone	*E*	—	—	**24**, 2.0	**25**, 1.84	**26**, 3.9
	Z	—	—	—	**27**, 1.34	**28**, 7.1

Using a larger excess of benzene, two- or three-fold in respect to the chloride ion, in order to improve the yield of the phenylated ketones, the same results were obtained as in the reference experiments; in all cases the ratio between β-chloro- and β-phenylketones were found approximately the same.

It is notable that the amount of isomerised β-chloro-β,γ-unsaturated ketones, if present, is insignificant. No dienic compounds could be decelated.

These results are explainable by the competition which takes place between the benzene molecule and the tetrachloroaluminate ion for the capture of the intermediate acylvinyl cation (Scheme 1)

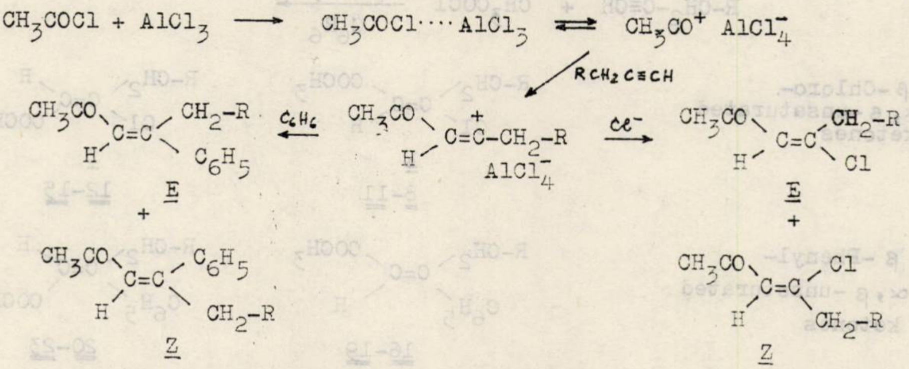

Scheme 1. Mechanism of the reaction of 1-alkynes with acetyl chloride in benzene-CCl_4 solution in the presence of $AlCl_3$

The fact that β-chloroketones are formed even when benzene is used in excess suggests that the reaction of the vinyl cation with $AlCl_4^-$ occurs even in the ion pair stage. The reaction with benzene takes place when the vinyl cation is separated from the $AlCl_4^-$ ion by the solvent.

Concerning the reactivities of the acetylium ion and of the acetylvinyl cation towards the alkyne or the aromatic hydrocarbon, the reaction products evidence that the alkyne is a better partner towards CH_3CO^+ than benzene; the contrary is valid for the acylvinyl cation.

REACTION OF 1-ALKYNES WITH ACETYL CHLORIDE·$AlCl_3$ IN THE PRESENCE OF SATURATED HYDROCARBONS

In order to investigate the ability of the acetylvinyl cations, generated in the reaction of alkynes with acetyl chloride · $AlCl_3$, to abstract hydride ion from saturated hydrocarbons used as solvents, experiments were performed in the presence of cyclohexane, methylcyclohexane and methylcyclopentane at temperatures between —60° and 25°. As alkynes we used phenylacetylene and 1-butyne.

The reaction of phenylacetylene gave only the normal addition products, namely the mixture of *E* and *Z* isomers of β-chloro-α,β-unsaturated ketone **6**. Although the temperature was varied from —60° to + 25° no detectable amounts of benzylidene-acetone could be detected.

In the reaction of 1-butyne, the same complex mixture as previously reported [1] was identified gas chromatographically.

It is notable that at + 80° in cyclohexane solution, besides the acylation of the alkyne, it was observed that the isomerisation at equilibrium of cyclohexane to methylcyclopentane [3] takes place, together with the acylation of methylcyclopentane, as established earlier for both processes by Nenitzescu and coworkers.[2;3]

Although in this reaction hydride ion transfer takes place between the carbocations involved in the isomerisation of the cyclohexane used as solvent, we are not able to detect the intermolecular hydride ion transfer to the acetylvinyl cation.

This result shows that the "hot" acylvinyl cation is short-lived and reacts fast with the $AlCl_4^-$ ion possessing nucleophilic character even in the ion pair step.

EXPERIMENTAL

IR spectra were recorded with a double beam UR-20 spectrophotometer. ^1H-NMR spectra were determined with a Tesla 60 and Varian A-60A spectrometer. Glc analyses were carried out on a Varian chromatograph, equipped with a flame ionisation detector, using a 4m × 3 mm of 10% QF-1 on kisselgur 60 — 80 mesh column; column temperature 120°, detector temp. 240°; carrier gas hydrogen, 45 ml/min. Preparative glc were carried out on a Beckmann Megachrom chromatograph, equipped with catharometer, using a 6m × 3 mm of 10% QF-1 on kisselgur column.

Reagents. The alkynes used in this work were commercialy available in high purities. Acetyl chloride and aluminium chloride were purified just before use.

REACTION OF 1-ALKYNES WITH ACETYL CHLORIDE·$AlCl_3$ IN THE PRESENCE OF BENZENE

Standard procedure. The reactions were carried out using the same standard procedure as in the reactions performed in non-nucleophilic halogenated solvents.[1] The homogeneous solution of the acylating complex (prepared from equimolar ratios of acetyl chloride and freshly sublimed $AlCl_3$, in carbon tetrachloride) was dropped in course of 10 to 15 min into a stirred mixture of the alkyne, benzene and CCl_4, cooled at $-60°$. After stirring for additional 10 min at this temperature, the mixture was poured on ice (and hydrochloric acid), extracted with diethyl ether, washed until neutral, dried and the solvent evaporated *in vacuo*. The crude reaction product was analysed gas chromatographically.

The components were identified by comparison with authentical samples isolated by means of preparative gas chromatography coupled with thin layer chromatography. The structures were ascribed on the basis of IR, ^1H-NMR and current analytical data.

Reaction of phenylacetylene with acetyl chloride·$AlCl_3$. Into a solution of 3.42 g (33.5 mmoles) phenylacetylene in 5 ml benzene and 5 ml carbon tetrachloride, a solution of 33.5 mmoles of complex acetyl chloride·$AlCl_3$ in 10 ml carbon tetrachloride was dropped at $-60°$. After working up as described in the standard procedure, in the crude reaction product (isolated in 88% yield) the following ketones were evidenced by means of glc:

E-4-Chloro-4-phenyl-but-3-en-2-one (**6**), 23%, identical with those previously described.[1]

4,4-Diphenyl-but-3-en-2-one (**7**), 77%, isolated by preparative glc; b.p. 168°/5 mm. ^1H-NMR (CCl_4, δ, ppm): 2.21 (CH_3-CO-), 6.62 ($H-C=$), 7.27 (C_6H_5-). Analysis: $C_{16}H_{14}O$ Calcd.: C, 86.48; H, 6.30. Found: C, 85.91; H, 6.42%.

Reaction of propyne with acetyl chloride·$AlCl_3$. Working as above, from 2.7g (6.73 mmoles) propyne in 2 ml carbon tetrachloride and 2 ml benzene and 6.8 mmoles acylating complex $CH_3COCl \cdot AlCl_3$ in 2.5 ml carbon tetrachloride, a crude reaction product was obtained in 48% yield. In this product, by means of glc, were evidenced the β-chloro-α, β-unsaturated ketones **8** (55.0%) and **12** (3.0%), identical with those previously described, [1] and the phenylated ketones **16** (39.5%) and **20** (2.5%). These new compounds were separated by preparative glc:

E-4-Phenyl-pent-3-en-2-one (**8**), b.p 104°/5mm. IR (CCl_4, cm^{-1}): ν_{CO} 1706, $\nu_{C=C}$ 1618; ^1H-NMR (CCl_4, δ, ppm): 2.20 (CH_3-CO-), 2.41 ($CH_3-C=$), 5.98 ($H-C=$), 7.28 (C_6H_5-).

Z-4-Phenyl-pent-3-en-2-one (**20**), b.p. 118°/5 mm; ^1H-NMR (CCl_4, δ, ppm): 2.31 (CH_3-CO-), 2.10 ($CH_3-C=$), 5.98 ($H-C=$), 7.14 (C_6H_5-).

Reaction of 1-butyne with acetyl chloride·$AlCl_3$. The reaction was carried out after standard procedure, using 8.7 mmoles acylating complex in 5 ml carbon tetrachloride and 4.65 g (8.6 mmoles) 1-butyne in 10 ml benzene. After working up, in the crude product (isolated in 62% yield), the previously described[1] ketones **9** (48.4%), **13** (2.6%) and **24** (2.0%) together with the new ketones **17** (46.3%) and **21** (0.7%) were evidenced by glc. The new compounds were isolated by preparative glc.

E-4-Phenyl-hex-3-en-2-one (**17**), b.p. 106 – 108°/5 mm. IR (CCl_4, cm^{-1}) : ν_{CO}1710, $\nu_{C=C}$ 1627 ; ^1H-NMR (CCl_4, δ, ppm) : 2.24 (CH_3-CO-), 2.36 ($C_2H_5-C=$), 6.43 ($H-C=$), 7.27 (C_6H_5-) ; Anal. $C_{12}H_{13}O$ Calcd : C, 82.75 ; H, 8.04. Found : C, 82.31 ; H, 8.07%.

Z-4-Phenyl-hex-3-en-2-one (**21**), b.p. 112 – 114°/5 mm ; ^1H-NMR (CCl_4, δ, ppm) : 2.31 (CH_3-CO-), 1.90 ($C_2H_5-C=$), 5.97 ($H-C=$), 7.14 (C_6H_5-).

Reaction of 1-pentyne with acetyl chloride·$AlCl_3$. Working as above, in the crude reaction product, isolated in 64.0% yield, the previously described[1] chloroketones **10** (36.8%), **14** (5.6%), **25** (1.84%) and **27** (1.34%), together with the new phenylated ketones **18** (40.5%) and **22** (3.25%) were evidenced by glc. The new compounds were isolated by preparative glc.

E-4-Phenyl-hept-3-en-2-one (**18**). IR (CCl_4, cm^{-1}) : ν_{CO} 1718, $\nu_{C=C}$1605 ; ^1H-NMR (CCl_4, δ, ppm) : 2.20 (CH_3-CO-), 2.36 ($C_3H_7-C=$), 6.40 ($H-C=$), 7.31 (C_6H_5-). Anal. $C_{13}H_{16}O$ Calcd. : C, 82.97 ; H, 8.51. Found : C, 82.53 ; H, 8.16 %.

Z-4-Phenyl-hept-3-en-2-one (**22**). ^1H-NMR (CCl_4, δ, ppm) : 2.31 (CH_3-CO-), 1.93 ($C_3H_7-C=$), 5.95 ($H-C=$), 7.12 (C_6H_5-).

Reaction of 1-hexyne with acetyl chloride·$AlCl_3$. In the crude reaction product, isolated in 71.0% yield, the previously described[1] chloroketones **11** (32.9%), **15** (4.1%), **26** (3.9%) and **28** (7.1%) together with the new phenylated ketones **19** (48.36%) and **23** (3.64%) were evidenced. The new compounds were separated by preparative glc.

E-4-Phenyl-oct-3-en-2-one (**19**). IR (CCl_4, cm^{-1}) : ν_{CO} 1695, $\nu_{C=C}$ 1607 ; ^1H-NMR (CCl_4, δ, ppm) : 2.42 ($C_4H_9-C=$), 2.95 (CH_3-CO-), 6.25 ($H-C=$), 7.45 (C_6H_5-) ; Anal. : $C_{14}H_{18}O$ Calcd. : C, 83.17 ; H, 8.69. Found : C, 83.87 ; H, 8.69%.

Z-4-Phenyl-oct-3-en-2-one (**23**). ^1H-NMR (CCl_4, δ, ppm) : 2.07 ($C_4H_9-C=$), 2.82 (CH_3-CO-), 5.98 ($H-C=$), 7.14 (C_6H_5-).

REACTION OF 1-ALKYNES WITH $CH_3COCl·AlCl_3$ IN SATURATED HYDROCARBONS

The reactions were carried out using the same standard procedure as for the reactions performed in the presence of benzene, with the difference that the order of the introduction of the reagents was changed, namely the solution of the alkyne in the saturated hydrocarbon (cyclohexane, methylcyclohexane or methylcyclopentane) was dropped into the carbon tetrachloride solution of the acylating reagent.

In these experimental conditions at temperatures varying from −60° to +25° in the reaction of phenylacetylene, the glc analysis of the reaction product indicates the presence of the β-chloro-α, β-unsaturated ketones **6** and **7** and in the reaction of 1-butyne the presence of chloroketones **9**, **13** and **24**, in the same ratios as those obtained in the reactions performed in non-nucleophilic halogenated solvents, previously reported.[1]

In the reaction between phenylacetylene and the acylating complex $CH_3COCl·AlCl_3$ in cyclohexane after boiling for 3 hours, in the fraction with b.p. 70–80° cyclohexane and methylcyclopentane were identified by glc analysis in the ratio 3 : 1. In the reaction mixture, after removal of the solvents, the chloroketones **6** and **7** were identified together with 1-acetyl-1-methylcyclopentane.[2]

REFERENCES

[1] Part I : D. Mănoiu, M. Mănoiu, I. G. Dinulescu and Margaret Avram, *Rev. Roumaine Chim.*, **29**, 193 (1984).

[2] C. D. Nenitzescu and I. Chicoș, *Ber. dtsch. Chem. Ges.*, **66**, 969 (1933) ; C. D. Nenitzescu and I. Cantuniari, *Liebigs Ann. Chem.*, **510**, 269 (1934) ; C. D. Nenitzescu and E. Ciorănescu, *Ber. dtsch. chem. Ges.*, **69**, 1820 (1936).

[3] C. D. Nenitzescu and I. Cantuniari, *Ber. dtsch. chem. Ges.*, **66**, 1907 (1933).

Revue Roumaine de Chimie, **29**, *2*, 207–210 (1984)

EFFET DE LA TEMPÉRATURE D'ATOMISATION SUR LA SENSIBILITÉ DU PLOMB EN SPECTROMÉTRIE D'ABSORPTION ATOMIQUE AVEC ATOMISATION ÉLECTROTHERMIQUE ET AVEC VAPORISATION À PARTIR DE LA PAROI DU TUBE OU D'UNE PLATE-FORME

JÁNOS FAZAKAS
Centre de spectrochimie analytique
Bd. Mărăşti 61
R-71331 Bucarest, ROUMANIE

Reçu le 2 février 1983

La sensibilité optimale du plomb est atteinte à des températures d'atomisation différentes qui dépendent de la nature du tube et de la plate-forme. A certaines températures, la combinaison tube + plate-forme en graphite ordinaire donne de meilleurs résultats que la combinaison tube + plate-forme en graphite pyrolytique. Dans tous les cas, la vaporisation à partir d'une plate-forme détermine un accroissement de la sensibilité.

The optimal sensitivity of lead is attained at different temperatures depending on the nature of the furnace and the platform. At certain temperatures the normal tube + normal platform combination gives a better sensitivity than the pyrofurnace + pyroplatform combination. In all cases platform vaporization leads to an enhancement of sensitivity as compared to wall vaporization.

1. INTRODUCTION

La transformation de la spectrométrie d'absorption atomique en méthode absolue d'analyse est un ancien rêve des spectroscopistes. Parmi les facteurs qui ont empêché une telle transformation on peut citer principalement l'existence d'interactions, très fréquentes et souvent peu prévisibles. De nombreuses méthodes ont été proposées pour leur prévention et élimination.[1–3] Une démarche très intéressante a été abordée par L'vov.[3,4] L'échantillon étant vaporisé à partir d'une plate-forme placée dans le tube, les interactions en phase de vapeur sont réduites ou entièrement éliminées. Des travaux ultérieurs[5–8] ont pu confirmer partiellement la validité de la démarche de L'vov.

Slavin et Manning[6] ont étudié en détail les interactions lors de la détermination du plomb atomisé à partir d'une plate-forme. L'influence de certains paramètres analytiques comme la température d'atomisation n'a toutefois pas fait l'objet de leur étude. Un article plus récent des mêmes auteurs[8] recommande la modification de l'analyte avec $NH_4H_2PO_4$ et une température optimale d'atomisation de 1900°C.

Le but de notre travail a été d'étudier la sensibilité du plomb en fonction de la température d'atomisation mais aussi en fonction de la nature du tube et de la plate-forme.

2. MATÉRIEL ET MÉTHODE

Le travail a été réalisé avec un atomiseur HGA – 500 (Perkin-Elmer). Les tubes étaient en graphite spectrographique ordinaire ou recouverts d'une couche de graphite pyrolytique formée « in situ ». Les plates-formes utilisées étaient soit en graphite ordinaire soit en graphite pyrolytique massif[6]. Les échantillons (en HNO_3 0,05%) ont été introduits dans l'atomiseur à l'aide d'un injecteur automatique AS – 1 (20 μl). Après séchage (200°C/60 S) et décomposition thermique (400°C/30 S) des échantillons, l'atomisation était réalisée à la plus grande vitesse d'élévation de la température (Ramp 0, 2000°C/S) et en argon avec gas stop. Le programme électrothermique était complété par un cycle de nettoyage (Clean, 2600°C/5 S). Il est à noter que les températures sont celles du tube de graphite, celles de la plate-forme étant moins élevées dans tous les cas.

Les signaux d'absorption ont pu être suivis à l'aide d'un spectromètre PE – 5000 (résolution en temps d'environ 20 mS). La raie de résonance de 283,3 nm a été utilisée avec une bande passante de 0,7 nm.

3. RÉSULTATS ET DISCUSSION

Étant donné que lors de la vaporisation d'une plate-forme les pertes de l'analyte par convection sont réduites[3] par comparaison à la vaporisation à partir de la paroi du tube, on peut s'attendre à une augmentation de la hauteur et de la surface des signaux d'absorption. Ceci a été confirmé par nos expériences. Nous allons toutefois insister principalement sur l'effet de la nature du tube et de la plate-forme et de la température d'atomisation qui permettent d'atteindre la sensibilité la plus haute.

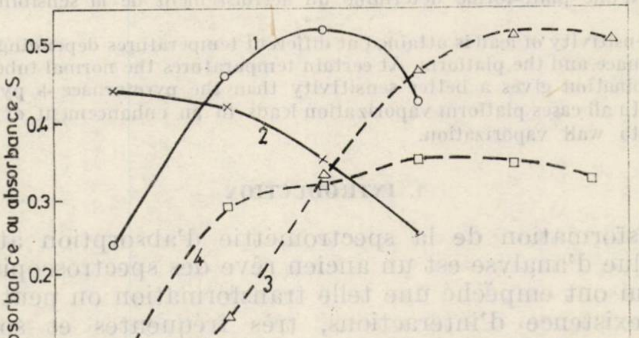

Fig. 1. — Effet de la température d'atomisation sur la sensibilité du Pb en spectrométrie d'absorption atomique avec atomisation électrothermique avec vaporisation d'une plate-forme : 1. ○ – ○ – ○ Hauteur du pic, tube + plate-forme pyro ; 2. × – × – × Surface du pic, tube + plate-forme pyro ; 3. Δ – Δ – Δ Hauteur du pic, tube + plate-forme en graphite ordinaire ; 4. □ – □ – □ Surface du pic, tube + plate-forme en graphite ordinaire.

La figure 1 permet d'observer que la combinaison « tube + plate-forme pyro » entraîne la réduction de la surface du pic pour les températures d'atomisation excédant 1000°C. En utilisant la combinaison « tube + plate-forme en graphite ordinaire », on observe toutefois son augmentation jusqu'à 1600°C. Il est à noter qu'à partir d'environ 1450°C, la surface du pic obtenue avec la combinaison « ordinaire » est plus élevée qu'avec la combinaison « pyro ».

La hauteur du signal est également plus grande en vaporisant de la plate-forme [3] par comparaison à celle obtenue par atomisation conventionnelle (de la paroi). Un travail antérieur [9] a permis de montrer que lors de la vaporisation à partir d'une plate-forme d'un élément moins volatile que le plomb (palladium), la hauteur du pic est plus petite que celle obtenue lors de l'atomisation à partir de la paroi du tube. L'explication du phénomène résiderait dans la vitesse d'élévation de la température qui était plus réduite dans le cas de la plate-forme.

Il semble tout de même que dans le cas d'un élément volatile tel que le plomb, la réduction de la vitesse de chauffage de la plate-forme est plus que compensée par la diminution des pertes de l'analyte par convection.

On peut observer (Figure 1) que la sensibilité (exprimée en hauteur du pic) est similaire pour les deux combinaisons plate-forme— tube. Il faut cependant souligner que la meilleure sensibilité est atteinte à 1400°C pour la combinaison « pyro » et à 1800°C pour la combinaison en graphite ordinaire. Il est à noter qu'à nouveau, comme dans le cas de la surface du pic, au-delà d'une certaine température (içi 1600°C) la combinaison en graphite ordinaire détermine une meilleure sensibilité que la combinaison « pyro ».

4. CONCLUSION

Notre travail a montré que l'optimalisation du programme électrothermique en vue d'améliorer la sensibilité du plomb nécessite également une prise en considération de la nature de la surface de vaporisation (plate-forme, paroi), mais aussi de celle du réservoir atomique. Ainsi, si la matrice présente dans l'échantillon nécessite une atomisation à température élevée, il semblerait que du point de vue « sensibilité » l'utilisation de la combinaison tube + plate-forme en graphite ordinaire serait plus avantageuse.

L'auteur veut remercier le Dr. Michel Hoenig pour la révision linguistique du manuscrit et pour avoir fait des observations critiques qui ont amélioré le manuscrit.

BIBLIOGRAPHIE

[1] C. W. Fuller, « Electrothermal Atomisation in AAS », The Chemical Society, London, 1977.
[2] J. Matousek, *Progr. Anal. At. Spectr.*, **4**, 247 (1981).
[3] B. V. L'vov, *Spectrochim. Acta*, **33B**, 153 (1978).
[4] B. V. L'vov, L. A. Pelieva et A. J. Sharnopolski, *Zhur. prikl. Spektrosk.*, **27**, 395 (1977).
[5] D. C. Grégoire et C. L. Chakrabarti, *Analyt. Chem.*, **49**, 2018 (1977).
[6] W. Slavin et D. C. Manning, *Analyt. Chem.*, **51**, 261 1979).
[7] E. J. Hinderberger, M. L. Kaiser et S. R. Koirtyohan, *At. Spectr.*, **2**, 1 (1981).
[8] W. Slavin, D. C. Manning et G. R. Carnick, *At. Spectr.*, **2**, 137 (1981).
[9] J. Fazakas, *Analyt. Letters*, **15**, 245 (1982).

Revue Roumaine de Chimie, **29**, *2*, 211–217 (1984)

MERCAPTOTHIADIAZOLDERIVATE EMPFINDLICHE REAGENZIEN FÜR POTENTIOMETRISCHE BESTIMMUNGEN DES Hg(II)

L. ROMAN, MARIA ŞERBAN und VICTORIA GUG
Lehrstuhl für analytische Chemie der Fakultät für Pharmazie, Institut für Medizin und Pharmazie, Cluj-Napoca, Rumänien

Eingegangen am November 23, 1981

Für die potentiometrische Titration von Hg(II) im Konzentrationsbereich $10^{-3}-10^{-7}$ M werden fünf neue Reagenzien vorgeschlagen: 2-Mercapto-5-amino-1,3,4-thiadiazol und seine Acetyl-, Allyl-, Phenyl- und Naphtyl-substituierten Amino-derivate. Die Titrationen wurden mit einer Quecksilberindikatorelektrode und einer gesättigten Kalomelelektrode durchgeführt. Die Titrationskurven zeigen, dass sich zwei Komplexe Hg : L, im Verhältnis 1 : 1 und 1 : 2, bilden, Tatsache, die auch mit den Ergebnissen der Elementaranalyse und den Elektronenspektren übereinstimmen. Die experimentellen Resultate sind sehr gut, die relativen Fehler sind auch bei sehr niederen Konzentrationen (10^{-7}M) kleiner als 1%.

Five new organic reagents are suggested for the potentiometric titration of Hg(II) in the concentration range $10^{-3} - 10^{-7}$ M : 2-mercapto-5-amino-1,3,4-thiadiazole and the 5-amino-substituted derivatives with acetyl, alyl, phenyl and naphthyl groupings. The titrations were made with a mercury indicator electrode and a saturated calomel electrode. The titration curves indicate the formation of two Hg : L complexes in the ratios 1 : 1 and 1 : 2 ; this corresponded to the results of the elementary analysis and to the electronic spectra of the complexes. The experimental results are very good, the relative errors being below ±1% even at very low concentrations (10^{-7} M).

Organische Reagenzien mit Schwefel und Stickstoff als Spenderatome finden in der qualitativen und quantitativen analytischen Chemie häufig Verwendung. Sie bilden stabile koordinative Verbindungen, die meistens farbig und in Wasser schwerlöslich, dafür aber extrahierbar mit organischen Lösungsmitteln, mit Komplexgeneratoren (kräftig polarisierenden und polarisierbaren) wie Ionen der transitionellen Metalle und im allgemeinen Schwermetallionen sind. Die von uns verwendeten Reagenzien dieser Art sind: Bis-thio-harnstoff, seine mono- und disubstituierten Derivate, Mercapto-thiadiazolverbindungen,[1–6] sowie auch Derivate von 1-Benzoyl-4-R-thiosemicarbazid.[7–9]

Die vorliegende Arbeit untersucht die Reaktionen von Hg(II) – Ionen mit den Mercaptothiadiazolverbindungen wie 2-Mercapto-5-amino-1,3,4-thiadiazol (I, MATD), 2-Mercapto-5-acetylamino-1,3,4-thiadiazol (II, MAATD), 2-Mercapto-5-allylamino-1,3,4-thiadiazol (III, MAlATD), 2-Mercapto-5-phenylamino-1,3,4-thiadiazol (IV, MPhATD) und 2-Mercapto-

5-naphtylamino-1,3,4-thiadiazol (V, MNATD). In Lösung existieren diese Reagenzien in einem tautomeren Thion-thiol-gleichgewichtszustand (Abb.1):

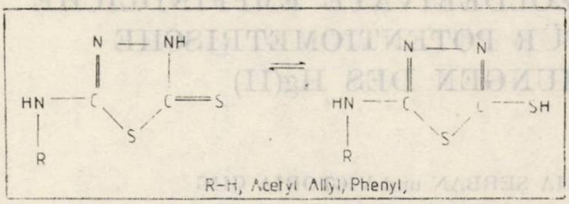

Abb. 1.—Tautomere Strukturen der verwendeten Reagenzien.

In saurem Medium ist die Thionform, in alkalischem Medium die Thiolform vorherrschend.[10]

Die Hg(II)-Ionen bilden mit den angeführten Reagenzien amorphe, schwach gelbliche oder gelbe, in Waser und wässr. Äthanol schwer lösliche Niederschläge, die bei der quantitativen Dosierung von Quecksilber, in der chemischen Analyse, in der analytischen Toxikologie, bei der Analyse und Kontrolle von Medikamenten usw. Anwendung finden können. Die Bestimmung von Quecksilber mit den angeführten Reagenzien (I—V) kann in dem weiten Konzentrationsbereich von $10^{-3} - 10^{-7}$ M durchgeführt werden.

EXPERIMENTELLER TEIL

Die Bestimmungen wurden mit einem MV 84 pH-Meter, unter Verwendung einer Quecksilberindikatorelektrode und einer gesättigten Kallomelelektrode (S.C.E.) vorgenommen. Um die Verseuchung der zu analysierenden Lösung mit Chlorionen zu vermeiden, wurde zwischen der Kallomelelektrode und der zu analysierenden Lösung eine Agar-agar Brücke in gesättigter Kaliumnitratlösung angebracht. Die Quecksilberindikatorelektrode auf Platin wurde nach der Methode von Ramaley und Mitarbeiter[11] durch reduzierende, elektrochemische Behandlung des Platindrahtes, gefolgt von seinem Eintauchen in p.a. reines Quecksilber, erhalten.

Bei der potentiometrischen Titration von Hg(II) mit I und seinen 5-N-substituierten Derivaten müssen die zu analysierenden Lösungen ein Optimal-pH=5 haben und die ionische Stärke während der Titration muss durch Zugabe einer grossen Menge von Kaliumnitrat konstant gehalten werden. Die Titration des Quecksilbers erfolgt mit Reagenzienlösungen, die eine wenigstens zenhmal höhere Konzentration als die der zu bestimmenden Quecksilberlösungen besitzen. Die bis zum Äquivalenzpunkt der Titration verbrauchten Volumen an Reagenslösung werden durch die Rechenmethode von Hostetter und Roberts[12] bestimmt. Die Titrationen mit I und II werden in Wasser, die mit III, IV und V in wässr. (1 : 1) Äthanol durchgeführt (in letzteren Fällen muss die Abscheidung des Überschusses an schwerer löslichen Reagens vermieden werden). Im Falle der Titration mit IV und V darf die Konzentration der Hg(II) Lösung nicht höher als $5 \cdot 10^{-4}$ M sein, damit die Bildung von zu grossen Niederschlagsmengen vermieden wird.

Verwendete Lösungen

1. $5 \cdot 10^{-2}$ M $Hg(NO_3)_2$-Lösung in Wasser ($T = 0{,}0105448$ g Hg(II), bestimmt mit $EDTANa_2$, im Gegenwart von Xylenolorange).
2. $2 \cdot 10^{-1}$ M Acetatpufferlösung, pH = 5, mit Zugabe von wässr. 10^{-1} M KNO_3-Lösung.
3. $2 \cdot 10^{-1}$ M Acetatpufferlösung in Äthanol-Wasser 1 : 1.
4. $10^{-3} - 10^{-4}$ M $Hg(NO_3)_2$-Lösungen, hergestellt durch Verdünnung von Lösung 1 mit Wasser oder mit den Pufferlösungen 2 und 3.

5. $2\cdot10^{-2}$ M wässr. Acetatpufferlösung, pH = 5, mit Zugabe von wässr. 10^{-2} M KNO_3-Lösung.

6. 10^{-7} M $Hg(NO_3)_2$-Lösung, durch Verdünnung von Lösung 1 mit Lösung 5 im Messkolben, frisch vor der Dosierung hergestellt.

7. 10^{-2} M Lösungen von I und II, hergestellt durch genaues Wägen von I und II im Messkolben und Lösen in 70% wässr. Äthanol.

8. 10^{-2} M Lösungen von III, IV und V, hergestellt durch genaues Wägen der Substanzen im Messkolben und Lösen in absolutem Äthanol.

9. 19^{-6} M Lösung von I, frisch vor der Titration durch Verdünnung von 10^{-2} M Lösung mit 70% wässr. Äthanol hergestellt.

RESULTATE UND DISKUSSIONEN

Die bei der potentiometrischen Titration von 10^{-3} M $Hg(NO_3)_2$-Lösung mit I erhalten Kurven werden vergleichend bei zwei pH-Werten, uzw. pH = 2 (Kurve 1) und pH = 5 in Acetatpuffer (Kurve 2), in Abb. 2 gezeigt.

Beim Fortschreiten der Titrationsreaktion fällt die Hg(II)—Ionenkonzentration und implizite auch das Potential der Quecksilberelektrode. Der Äquivalenzpunkt der Titration wird durch plötzlichen Sprung des Potentials angezeigt. Die Titrationskurven weisen entsprechend der Bildung von zwei Komplexen des Verbindungsverhältnisses Hg : Ligand 1 : 1 bzw. 1 : 2 zwei Potentialsprünge auf. Der erste Potentialsprung, dem die Bildung des Komplexes 1 : 1 entspricht, impliziert die im saurem Medium, dank der Verschiebung des tautomeren Gleichgewichtes, vorherrschende Thionform des Reagens, während der zweite Sprung die bei pH = 5 in höherer Konzentration als in stark saurem Medium vorkommende Thiolform impliziert und die Bildung des Komplexes 1 : 2 anzeigt. Dieser zweite Potentialsprung ist deutlicher und besitzt einen höheren Wert als der erste, Tatsache, die höhere Stabilität des Komplexes 1Hg : 2 MATD anzeigt.

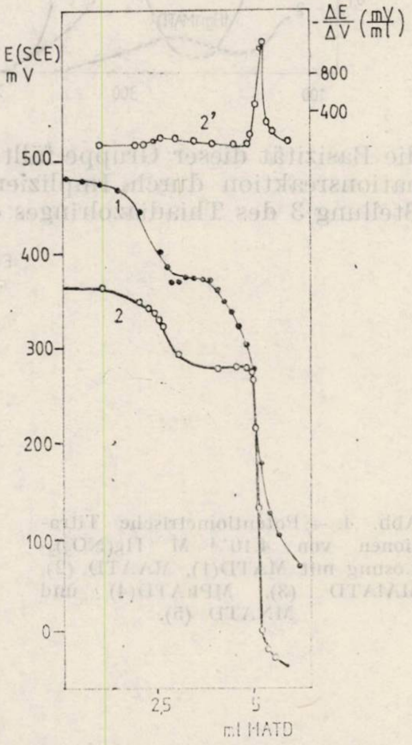

Abb. 2. — Potentiometrische Titration von 10^{-3} M $Hg(NO_3)_2$-Lösung mit MATD bei pH = 2 (Kurve 1) und pH = 5 (Kurve 2).
Kurve 2' — die Ableitung 1-ter Ordnung der Kurve 2.

Es wurden die UV-Absorptionspektren der Reagenzien und ihrer Komplexe mit Quecksilber (II) aufgenommen. Im Spektrum der Liganden erscheint ein intensives Absorptionband bei 315 — 320 nm, im Falle von MATD z.B. bei 316 nm (Abb. 3). Dieses Band erleidet durch Koordination eine hypsochrome Verscheibung von 37 nm im Falle des Komplexes

1 : 2 und von 41 nm im Falle des Komplexes 1 : 1 (Abb. 3). Anderseits fällt die Intensität des Bandes durch Koordination — sehr wenig im Falle des Komplexes 1 : 2 und sehr kräftig im Falle der Verbindung 1 : 1 — d.h. gleichzeitig mit dem Anwachsen der Quecksilberkonzentration im Molekül.

Ausgehend von der Tatsache, dass durch Einführen von Substituenten wie Phenyl- oder Naphtylradikalen usw. in die C-5-Aminogruppe die Basizität dieser Gruppe fällt, kann erwartet werden, dass die Koordinationsreaktion durch Implizieren des basischeren Stickstoffatoms aus Stellung 3 des Thiadiazolringes erfolgt.

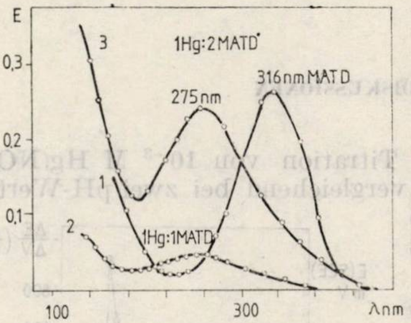

Abb. 3. — Elektronenspektren des MATD-Reagenzes und seiner Komplexen 1Hg : 1 MATD und 1Hg : 2 MATD.

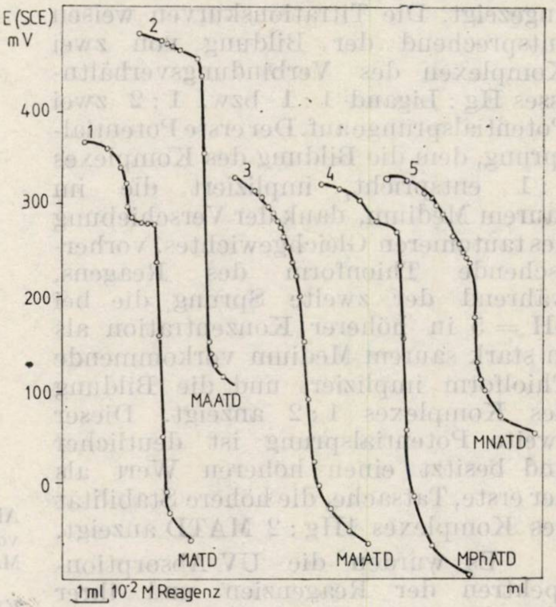

Abb. 4. — Potentiometrische Titrationen von 4.10^{-4} M Hg(NO$_3$)$_2$-Lösung mit MATD(1), MAATD (2), MAlATD (3), MPhATD(4) und MNATD (5).

Abbildung 4 zeigt vergleichend die bei der potentiometrischen Titration von $4 \cdot 10^{-4}$ M Hg $(NO_3)_2$—Lösungen mit I, II, III, IV und V erhaltenen Titrationskurven. Die mit II, III, IV und V im Verhältnis 1 : 1

gebildeten Komplexe besitzen sehr reduzierte Stabilität — auf den entsprechenden Titrationskurven erscheinen niedere Potentialsprünge.

Der zweite, der Bildung des Komplexes 1 : 2 entsprechende Potentialsprung dagegen ist höher und kann in bei pH=5 gepuffertem Medium analytisch verwertet werden. Die Resultate der statistischen Bearbeitung der bei der Titration von 10^{-3} M—2.10^{-4} M Hg $(NO_3)_2$-Lösungen mit I und II und von $4\cdot 10^{-4}$ M — 10^{-4} M $Hg(NO_3)_2$-Lösungen mit IV erhaltenen Daten werden in Tabelle 1, 2 und 3 angeführt.

Tabelle 1

Potentiometrische Titration von 10^{-3} — $2\cdot 10^{-4}$ M $Hg(NO_3)_2$-Lösungen mit 10^{-2} M MATD(I)-Lösung

Ord. zahl	Hg(II) bearbeitet, g	Hg(II) gef. g	Hg(II) gef. % (X_i)	$\overline{X} - X_i$	Statistische Berechnung
1	0,005272	0,005287	100,284	+0,414	$\overline{X} = 99,870\%$
2	0,005272	0,005258	99,734	−0,136	$P = 95\%$; $t = 2,78$
3	0,002109	0,002093	99,241	−0,629	$s_{\overline{X}} = 0,026$
4	0,003163	0,003145	99,430	−0,440	
5	0,001054	0,001061	100,664	+0,794	$A = 99,870 \pm 0,072$ %

Tabelle 2

Potentiometrische Titration von 10^{-3} — $2\cdot 10^{-4}$ M $Hg(NO_3)_2$-Lösungen mit 10^{-2} M MAATD (II)-Lösung

Ord. zahl	Hg(II) bearbeitet, g	Hg(II) gef. g	Hg(II) gef. % (X_i)	$\overline{X} - X_i$	Statistische Berechnung
1	0,005272	0,005272	100,000	+0,005	$\overline{X} = 100,005\%$
2	0,005272	0,005281	100,170	+0,165	$P = 95\%$; $t = 2,78$
3	0,003163	0,003166	100,095	+0,090	$s_{\overline{X}} = 0,062$
4	0,002109	0,002108	99,952	−0,053	
5	0,001054	0,001052	99,810	−0,195	$A = 100,005 \pm 0,172$ %

Tabelle 3

Potentiometrische Titration von $4\cdot 10^{-4}$ — 10^{-4} M $Hg(NO_3)_2$-Lösungen mit 10^{-3} M MPhATD(IV)-Lösung

Ord. zahl	Hg(II) bearbeitet, g	Hg(II) gef. g	Hg(II) gef. % (X_i)	$\overline{X} - X_i$	Statistische Berechnung
1	0,002109	0,002090	99,099	−0,777	$\overline{X} = 99,876\%$
2	0,002109	0,002097	99,431	−0,445	$P = 95\%$; $t = 2,78$
3	0,001054	0,001063	100,854	+0,978	$s_{\overline{X}} = 0,384$
4	0,000527	0,000523	99,240	−0,636	
5	0,000527	0,000531	100,759	+0,883	$A = 99,876 \pm 1,068$ %

Es wurde eine potentiometrische Titration von Quecksilber (II) mit MATD (I) auch bei sehr niederen (10^{-7} M) (Abb. 5) Hg(II)-Konzentrationen durchgeführt. Wie aus Tabelle 4 hervorgeht, ist die Präzision der Titration von sehr verdünnten Quecksilber (II)-Lösungen mit 10^{-6} M I-Lösungen gut. Die Kurven der potentiometrischen Titration zeigen auch bei diesen grossen Verdünnungen Potentialsprünge die der Bildung der zwei erwähnten Komplexe entsprechen.

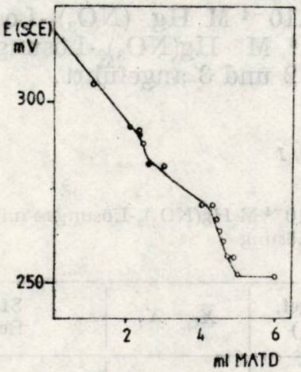

Abb. 5. — Potentiometrische Titration von 10^{-7} M $Hg(NO_3)_2$—Lösung mit MATD.

Tabelle 4

Potentiometrische Titation von 10^{-7} — $8 \cdot 10^{-8}$ M $Hg(NO_3)_2$ - Lösungen mit 10^{-6} M MATD(I) -Lösung

Ord. zahl	Hg(II) bearbeitet, µg	Hg(II) gef. µg	Hg(II) gef. % (X_i)	$\overline{X} - X_i$	Statistische Berechnung
1	0,527	0,523	99,241	−0,664	$\overline{X} = 99{,}905\%$
2	0,527	0,522	99,051	−0,854	$P = 95\%$; $t = 2{,}78$
3	0,527	0,531	100,759	+0,854	$s_{\overline{X}} = 0{,}333$
4	0,633	0,636	100,474	+0,569	
5	0,422	0,422	100,000	+0,095	$A = 99{,}905 \pm 0{,}925\%$

SCHLUSSFOLGERUNGEN

In der vorliegenden Arbeit werden zur Dosierung von Hg(II) — Ionen im Konzentrationsbereich 10^{-3} — 10^{-7} M die Präzipitationsreaktionen dieser Ionen mit 2-Mercapto-5-amino-1,3,4-thiadiazol (I) und seinen Acetyl-(II), Allyl-(III), Phenyl-(IV) und Naphtyl-(V)-substituierten Aminoderivaten, mit potentiometrischer Anzeige des Äquivalenzpunktes, empfohlen. Zu diesem Zweck wurden die optimalen pH-, Konzentrations- und Ionenkraft-Bedingungen bestimmt. Die Titrationen wurden mit einer Quecksilberindikatorelektrode und einer gesättigten Kalomelelektrode durchgefüht.

Die Titrationskurven weisen zwei Potentialsprünge, die der Bildung von zwei Komplexen im Verbindungsverhältnis 1 : 1 bzw. 1 : 2 (Hg : L) entsprechen, auf. Diese Tatsache stimmt auch mit den Resultaten der Elementaranalyse und den Elektronenspektren der Komplexe, Spektren die in der Arbeit vergleichend mit den Elektronenspektren der Liganden beschrieben werden, überein.

Die experimentellen Ergebnisse sind in einem weiten Konzentrationsbereich gut und reproduzierbar, so dass die potentiometrische Titration von Hg(II) mit I, II, III, IV und V sowohl in der chemischen Analyse als auch in der analytischen Toxikologie und bei Hygienesanitären Analysen zur Bestimmung von sehr geringen Quecksilbermengen verwendet werden kann.

LITERATUR

[1] E. Popper, N. Ariton und R. Crăciuneanu, *Studii și Cercetări Chim. Fil. Cluj*, **7**, 85 (1956).
[2] E. Popper, L. Popa, L. Proinov, R. Crăciuneanu und L. Roman, *Z. analyt. Chem.*, **184**, 184 (1961).
[3] E. Popper, L. Roman, R. Crăciuneanu und E. Florean, *Bull. Soc. chim. France*, **1963**, 991.
[4] L. Roman, R. Crăciuneanu und E. Popper, *Mikrochim. Acta*, **3**, 660 (1968).
[5] L. Roman und M. Serban, Conferința Națională de Chimie analitică, Mamaia, Constanța, 1969, p. 60.
[6] L. Roman, E. Florean, M. Echim-Grosu und E. Dordea, *Rev. Roumaine Chim.*, **23**, 929 (1978).
[7] R. Crăciuneanu und E. Florean, *Rev. Roumaine Chim.*, **14**, 753 (1979).
[8] R. Crăciuneanu, E. Florean und P. Marcu, *Rev. Roumaine Chim.*, **16**, 951 (1971).
[9] R. Crăciuneanu und L. Chiorean, *Pharmazie*, **27**, 108 (1972).
[10] E. Popper, L. Roman und P. Marcu, *Talanta*, **11**, 515 (1964).
[11] L. Ramaley, R. L. Brubaker und C. G. Enke, *Analyt. Chem.*, **35**, 1088 (1963).
[12] J. C. Hostetter und H. S. Roberts, *J. Amer. Chem. Soc.*, **41**, 1337 (1919).

Revue Roumaine de Chimie, **29**, *2*, 219–222 (1984)

A NEW CONVENIENT METHOD FOR THE SYNTHESIS OF AROMATIC HYDRAZIDES DIRECTLY FROM ACIDS USING ETHYLENE CHLOROPHOSPHITE AS REAGENT

C. I. CHIRIAC
"P. Poni" Institute of Macromolecular Chemistry, Aleea Ghica Vodă no. 41 A, Iaşi, Romania

Received November 3, 1982

Various aromatic hydrazides were prepared by a condensation reaction of aromatic carboxylic acids with hydrazines using as reagent ethylene chlorophosphite in pyridine at 100 – 110°.

In a previous paper,[1] we showed that ethylene acylphosphites prepared "in situ" from aromatic acids and ethylene chlorophosphite in pyridine can react with amines (nucleophilic reagents), affording the corresponding amides.

In this paper we have investigated the reactivity of the ethylene acylphosphites *versus* other nucleophilic reagents such as hydrazines, in order to obtain the corresponding hydrazides.

The classical methods for the synthesis of N-monosubstituted hydrazides use the reactions of hydrazines with acyl chlorides or esters.[2,3]

As reagents for the synthesis of hydrazides starting directly from carboxylic acids, there could be mentioned: acylimidazoles,[4] phosphonitrilic chloride [5] and 2,4,6-trichloro-s-triazine.[6]

RESULTS AND DISCUSSION

For the synthesis of aromatic hydrazides from ethylene acylphosphites and hydrazines, we used the described procedure,[1] starting from ethylene acylphosphites prepared "in situ". In this way, the synthesis becomes very simple.

The reaction between ethylene acylphosphites and hydrazines has not been investigated. Our studies have shown that ethylene acylphosphites manifest high reactivity towards hydrazines. In this way we prepared a number of ethylene acylphosphites (reactive compounds) in pyridine as solvent and acceptor for hydrochloric acid. These reactive compounds prepared "in situ" reacted with phenylhydrazine or hydrazine, affording hydrazides or diacylhydrazines, in high yields.

The reaction was checked up with pure ethylene benzoyl-phosphite, prepared from ethylene chlorophosphite and sodium benzoate in benzene as solvent.[1] The pure benzoylphosphite reacts with hydrazines in solution of pyridine in the same conditions as the compound prepared "in situ". The purity and the yields of hydrazides obtained from ethylene benzoylphosphite prepared "in situ" were similar to those obtained from pure ethylene benzoyl-phosphite. Therefore, it is not necessary to isolate these reactive compounds (sensible to moisture). In this reaction, we tried many tertiary amines, but pyridine was found to be the most suitable base, which served also as reaction medium. The ethylene acylphosphites (1 mole) prepared "in situ" can react with phenylhydrazine (1 mole) affording acylphenylhydrazines (1 mole), or with hydrazine (0.5 moles) affording diacylhydrazines (1 mole).

As a result of these investigations, we propose the following mechanism of reaction :

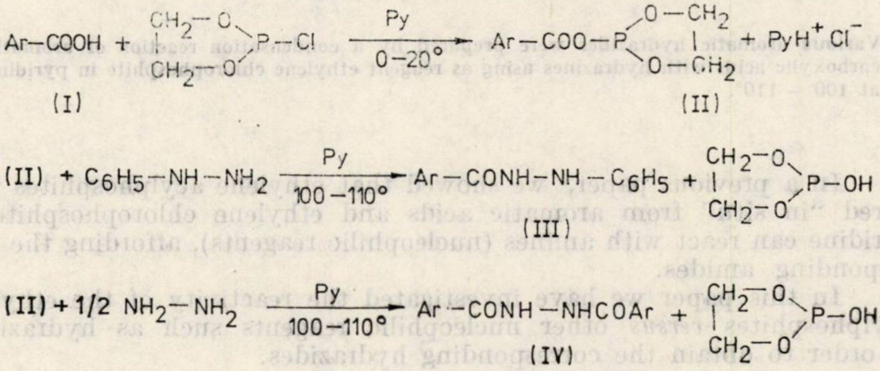

In this reaction, ethylene hydroxyphosphite and PyH^+Cl^- result as by-products which do not affect the reaction, similar to other cases.[1,7–9] We suppose, as in other cases [1,10,11] that this reaction involves a four centre transition state (V) :

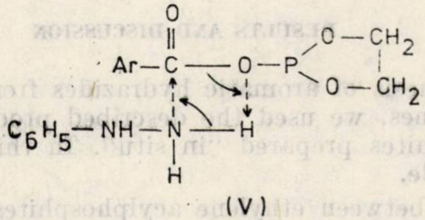

(V)

In a typical experiment, to a stirred solution of 1 mole (I) in dried pyridine cooled to 0°, 1 mole ethylene chlorophosphite was added slowly (the reaction is exothermal), and then 1 mole phenylhydrazine or 0.5 moles hydrazine were also added. After 4 hours at 100 — 110°, the desired products resulted in high yields. At room temperature the yield is low. In the case of phenylhydrazine, an excess of 5 — 10% is necessary in order to improve the yield. The yields of this method ranged from 68 to 89% (table 1).

By this new direct synthesis, we obtained hydrazides which are difficult to be obtained by heating aromatic acids with hydrazines.

Table 1

Hydrazides from "in situ" prepared ethylene acylphosphites

Acid	Hydrazine	Hydrazides[a]		
		Yield[b] %	M.p.[c] °C	Reported m.p.[d] °C
Benzoic	Phenylhydrazine	70	167–168	167–168
Benzoic	Hydrazine	87	237–239	238–239
p-Toluic	Phenylhydrazine	71	165–167	166–167
p-Toluic	Hydrazine	89	251–253	253–254
Anisic	Phenylhydrazine	77	179–180	178–180
Anisic	Hydrazine	82	223–225	224–225
m-Bromobenzoic	Phenylhydrazine	68	150–152	151–153
m-Bromobenzoic	Hydrazine	72	264–266	264–266

[a] The products were identified by comparing m.p. and IR spectra with autehntic samples.

[b] Yield calculated on the acid employed, before recrystallisation.

[c] After recrystallisation.

[d] From "Beilstein Handbuch der organiscen Chemie".

EXPERIMENTAL

1. β-benzoylphenylhydrazine

To 2.44 g (0.02 mole) of benzoic acid in 15 ml dried pyridine in a 50 ml three-necked flask, 1.8 ml (0.02 mole) of ethylene chlorophosphite[12] was added slowly under stirring and cooling, when the reactive product resulted "in situ" and pyridine hydrochloride precipitated partially, the solution being very concentrated. The rate of addition is regulated such that the temperature of the reaction mixture be kept in the interval 0 — 10°. The mixture was stirred for 1 — 2 hours at room temperature. Then 2.37 g (0.02 mole + 10% excess) phenylhydrazine was added under stirring. The obtained solution was heated 4 hours at 100—110° and poured into a large volume of water and ice (100 — 150 ml) under vigorous stirring. The precipitated product was collected by filtration, washed with 20 — 30 ml 10% Na_2CO_3 solution, 20 — 30 ml 10% HCl solution, three times with 20 — 30 ml water and dried at 80 — 100° under vacuum. After recrystallisation from ethanol, 3 g β-benzoylphenylhydrazine with m.p. 167 — 168° were obtained (mixed m.p. with pure β-benzoylphenylhydrazine underpressed). Yield 70% (calculated on benzoic acid employed).
Anal. Calculated for $C_{13}H_{12}N_2O$; C, 73.58 ; H, 5.66 ; N, 13.20%. Found : C, 73.41 ; H, 5.47 ; N, 13.11%.

2. Dibenzoylhydrazine

By a similar procedure, using 1.04 (0.01 mole) $NH_2-NH_2.2HCl$ for [2.44 g (0.02 mole) of benzoic acid, 2.1 g (87%) dibenzoylhydrazine with m.p. 237 — 239° (ethanol) was obtained (mixed m.p. with pure dibenzylhydrazine undepressed).

Anal. Calculated for $C_{11}H_{12}N_2O_2$; C, 70.00 ; H, 5.00 ; N.11.66%. Found : C, 69.13 ; H, 4.84 ; N, 11.37%.

In similar conditions, the other hydrazides (presented in table 1) were prepared from the corresponding aromatic carboxylic acids and phenylhydrazine or hydrazine.

REFERENCES

[1] C. I. Chiriac, *Rev. Roumaine Chim.*, **28,** 863 (1983).
[2] E. Fischer, *Liebigs Ann. Chem.*, **190,** 125 (1878).
[3] Th. Curtius and G. Struve, *J. prakt. Chem.*, **50,** 295 (1894).
[4] H. A. Staab, *Chem. Ber.*, **95,** 1280 (1962)
[5] L. Cagliati and M. Peloni, *J. Org. Chem.*, **33,** 2979 (1968).
[6] G. Baccolini and G. Rosini, *Chimica Industria (Milano)*, **51,** 287 (1969) ; *Chem. Abstr.*, **72,** 3441 (1970).
[7] C. I. Chiriac and J. K. Stille, *Macromolecules*, **10,** 716 (1977).
[8] B. Iselin and W. Rittel, *Helv. Chim., Acta*, **40,** 373 (1957).
[9] N. Yamazaki, *Tetrahedron Letters*, **49,** 5047 (1972).
[10] C. I. Chiriac, *Rev. Roumaine Chim.*, **26,** 1001 (1981).
[11] H. O. Becker and K. F. Tunk, *J. prakt. Chem.*, **14,** 55 (1961).
[12] H. J. Lucas and W. F. Mitchell, *J. Amer. Chem. Soc.*, **72,** 5491 (1950).

Revue Roumaine de Chimie, **29**, *2*, 223 — 229 (1984)

ON THE AGING OF TURPENTINE (MONTAN WAX)-IN-WATER EMULSIONS AS FUNCTIONS OF VISCOSITY AND PARTICLE SIZE DISTRIBUTION

M. K. SHARMA[a] and B. K. SHARMA[b]

[a] Instruments Research and Development Establishment, Dehra, Dun, India
[b] Oil and Natural Gas Commission, Calcutta, India

Received March 22, 1980

The influence of aging on the viscosity and particle size distribution of turpentine (montan wax)-in-water wax emulsions, stabilized with polyoxyethylene sorbitan monostearate, has been studied at 30°C. There is a variation in the shape, height and width of the particle size distribution curves of the wax emulsions on aging. The inhomogeneity of the emulsions increases with aging time. On aging, the progressive increase in the mean particle size (D_m) exerts a measurable effect on the fall in viscosity of wax emulsions. D_m exerts the same influence on the viscosity of aged emulsions as on the viscosity of freshly prepared emulsions of the same composition. The rate of increase in D_m and the viscosity — particle size relationship for fresh wax emulsions are determined and from these data viscosity changes over longer aging periods can be predicted.

When emulsions are aged, substantial changes are observed in the degree of dispersion of the dispersed phase before it separates out in the bulk. The accumulated data in the literature suggest the following sequence of events : particle flocculation leading to the formation of aggregates, thinning of the film of continuous phase separating adjacent particles within the aggregates, surmounting of the energy barrier and finally particle coalescence. Thus, during the course of aging changes do occur in the particle size distribution and flow properties of emulsions.

In continuation of earlier work on wax emulsions [1], the present investigation deals with the influence of aging on the viscosity and particle size distribution of wax emulsions prepared with water and binary mixture of turpentine and montan wax as two phases and polyoxyethylene sorbitan monostearate (nonionic surfactant) as emulsifying agent.

EXPERIMENTAL

Montan wax (South Arcot, Tamil Nadu ; m.p. 84° ± 2°C), turpentine (sp. gr. 0.814 at 30°C), double distilled water (pH 6.8 and conductivity 0.85×10^{-6} ohm^{-1} cm^{-1} at 30°C) and polyoxyethylene sorbitan monostearate (Tween 60 ; Koch-Light) were employed for the formation of wax emulsions. 2.0% concentration of Tween 60 (w/v % of emulsion) and the volume fraction of 2.0% solution of montan wax in turpentine ranging from 0.1 to 0.65 were employed for the preparation of turpentine (montan wax)-in-water wax emulsions. The time (5 min) and temperature (30°C) of emulsification were kept the same for the preparation of each wax emulsion.

The particle size distribution and the viscosity of wax emulsions were determined at different intervals of time during the course of aging of emulsions. Aging of wax emulsions was carried out at room temperature (30°C) over several weeks in stoppered bottles.

Particle size analyses of wax emulsions were carried out by the photomicrographic method,[2] taking photomicrographs of the microscopic slides of emulsions of ORWO, NP 27, 400 ASA cut films with the help of Carl Zeiss Jena microscope equipped with an attachment camera using a 25 × projection system and a 40 × objective. The mean volume globule diameter (D_m) was calculated as described earlier.[3]

A Weissenberg rheogoniometer model R.16 (Sangamo Weston, Bognor, Regis, England) was used for viscosity determinations of wax emulsions at 30°C, as described in the previous work.[4] A high rate of shear (1467.6 $\sec^{-1}$) was employed. Cone diameter and cone angle were 7.5 cm and 1°32′, respectively. The relative viscosity, $\eta_{\mathrm{rel}}(\eta_{\mathrm{rel}} = \eta_{\infty}/\eta_0$, where η_{∞} is the viscosity at high rate of shear such that it is independent of rate of shear and η_0 is the continuous phase viscosity) of the wax emulsions was determined during aging.

RESULTS AND DISCUSSION

In order to find the influence of aging on the particle size distribution of wax emulsions, the size distribution data have been summarised in terms of an inhomogeneity factor. The inhomogeneity, I, is defined as "the mean square deviation of the number distribution curve with respect to the diameter" [5]

$$I = \frac{\int_0^{\infty} (D - D_n)^2 n_1 \, \mathrm{d}l}{\int_0^{\infty} n_1 \, \mathrm{d}l} \tag{1}$$

where D is the globule diameter, D_n in the number average diameter $(\Sigma nD/\Sigma n)$ and n_1 is the rate of changes in the number of particles with their diameter.

On expansion, Eq. (1) reduces to

$$I = a_n/\lambda - D_n^2 \tag{2}$$

where a_n is the number average area $(\Sigma na/\Sigma n)$. The value of I was calculated for all fresh and aged emulsions.

Figure 1 shows the influence of aging period in days on the inhomogeneity of wax emulsions prepared with different dispersed phase volume concentrations (Φ) and 2.0% Tween 60 concentration. There is an increase in the inhomogeneity with an increase in the value of Φ of the emulsions. From the curves, it is clear that the inhomogeneity of the emulsions increases with the aging time.

The effect of aging on the particle size distribution data of a typical turpentine (montan wax)-in-water wax emulsion prepared with 0.5 dispersed phase volume concentration and 2.0% Tween 60 is shown in Fig.2.

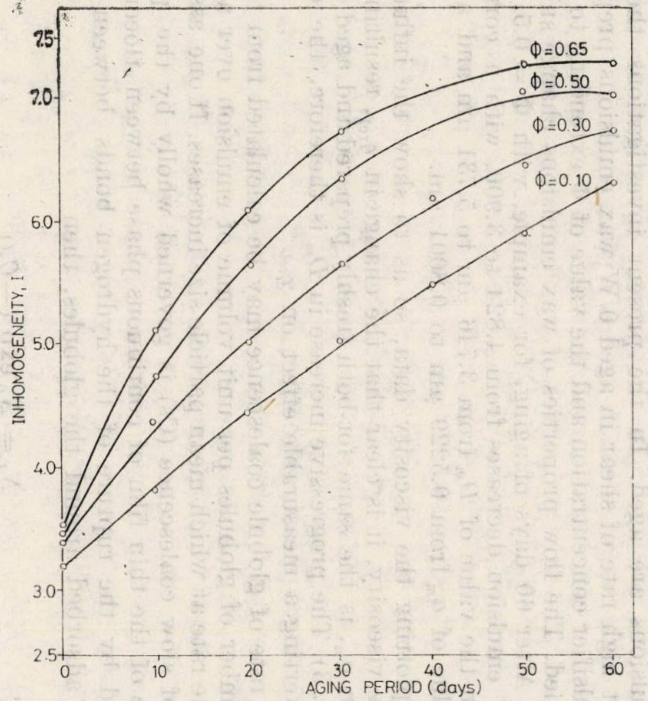

Fig. 1. — The rate of change in the inhomogeneity of wax emulsions at different dispersed phase volume concentrations.

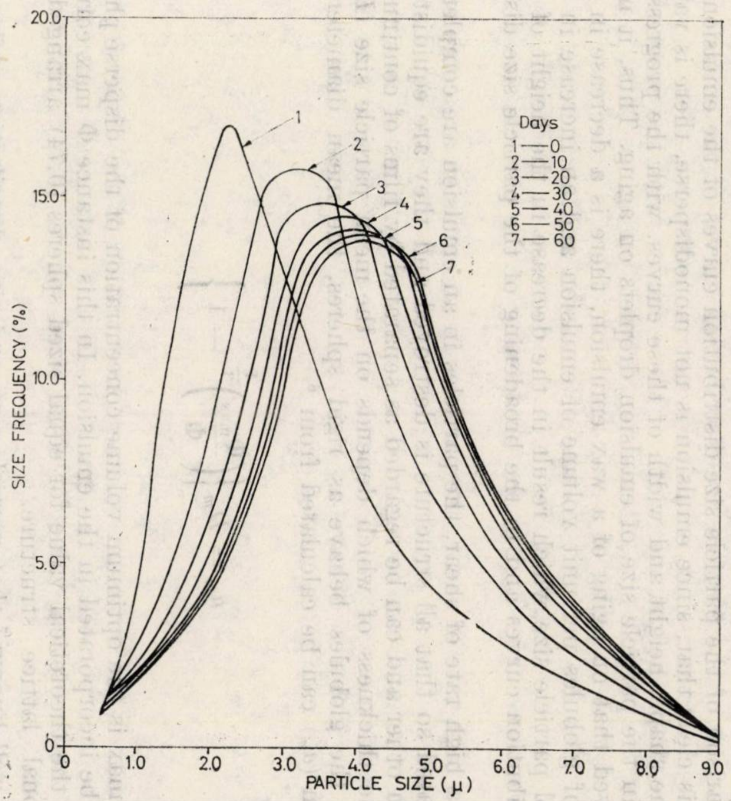

Fig. 2. — The influence of aging on the particle size distribution data of turpentine (montan wax)-in-water emulsion stabilized with a nonionic surfactant.

By comparison of the particle size distribution curves of the emulsion on aging, it is clear that, since emulsion is not monodisperse, there is variation in the shape, height and width of these curves, with the progressive increase in the particle size of emulsion droplets on aging. Thus, it may be observed that on aging of a wax emulsion, there is a decrease in the number of globules per unit volume of emulsion and an increase in the individual particle size which result in the decrease in the height of the size distribution curves and in the broadening of the particle size distribution.

At a high rate of shear, the particles in an emulsion are completely deflocculated so that all structure is destroyed and they are equidistant from each other and can be regarded as separated by films of continuous phase, the thickness of which depends on the mean particle size (D_m). Provided the globules behave as rigid spheres, the mean diameter of separation (a_m) can be calculated from [6]

$$a_m = D_m \left\{ \left(\frac{\Phi_{\max}}{\Phi} \right)^{\frac{1}{3}} - 1 \right\} \tag{3}$$

where Φ max is the optimum volume concentration of the disperse phase that can be incorporated in the emulsion. In this instance Φ max corresponds to the theoretical value for equal sized spheres (0.74) arranged in a hexagonal lattice structure.

It is well known [7] that particle size and size distribution influence viscosity of emulsions, so the latter would be expected to change also when emulsions are aged. In the present investigations the viscosity changes at high rate of shear in aged 0/W wax emulsions prepared with 2.0% emulsifier concentration and the value of Φ extending to 0.65, have been studied. The flow properties of wax emulsions change substantially on aging. After 60 days of aging, for example, with $\Phi = 0.5$, the value of η_{rel} of emulsion decreases from 4.824 to 3.900, with a corresponding increase in the value of D_m from 3.746 μm to 5.731 μm and an increase in the value of a_m from 0.5229 μm to 0.8001 μm.

By plotting the viscosity data, so as to show the influence of a_m on relative viscosity, it is clear that the change in η_{rel}, resulting from an increase in a_m, is the same for both freshly prepared and aged wax emulsions (Fig. 3). The progressive increase in D_m is therefore, the only aging process exerting a measurable effect on η_{rel}.

The rate of globule coalescence may be calculated from the change in the number of globules per unit volume of emulsion over a few days or from the rate at which mean particle size increases. If one assumes that the rate of slow coalescence (Cs) is governed wholly by the probability of rupture of the thin film of continuous phase between flocculated globules [8] and by the rupture of the hydrogen bonds between emulsifier molecules adsorbed around the globules, then

$$N_t = N_0 \exp\left(-C_s t\right) \tag{4}$$

where N_0 is the original number of globules per unit volume and N_t is the number after aging time t.

It follows that

$$\ln Dt = \ln \; D_0 + C_s t/3 \tag{5}$$

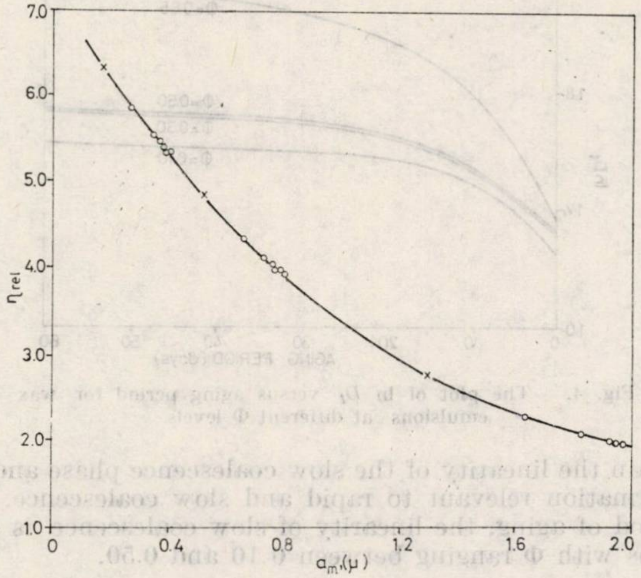

Fig. 3. — The influence of a_m on η_{rel} for freshly prepared (o), and aged (×), oil-in-water wax emulsions

where D_t and D_0 are the values of D_m at zero time and after aging time t, respectively, because

$$N = \frac{6\Phi \times 10^{12}}{\pi \, D_m^3} \, . \tag{6}$$

The mathematical development of Eq. (4) or (5) is based on the assumption that C_s is independent of number of globules (N) per cc of emulsion. This condition applies only for slow coalescence. The wax emulsions do not show a uniform rate of coalescence throughout the whole of the aging period. An initial phase of rapid coalescence, which occasionally lasts for several days, is followed by a second phase of slow coalescence which extends over the remainder of the aging period. Rapid coalescence, in its present connotation, does not imply that all globules coalesce immediately after flocculation. It merely indicates a somewhat faster rate than for slow coalescence. The O/W wax emulsions do not cream to a significant extent during the first few days of aging so that rapid coalescence cannot be attributed to this phenomenon.

Eq.(5) applies only for slow coalescence. During rapid coalescence the globules coalesce more rapidly than is suggested by this equation since many more factors are involved. Therefore, this ln $D_t - t$ plot should be continued until such time as the linearity of the slow coalescence phase is well established, if changes in η_{rel} are to be predicted accurately. Fig. 4 shows the plot of ln D_t against t for wax emulsions within Φ range 0.10 – 0.65. The plot has been continued for several days in order to obtain the linearity of the slow coalescence phase and the curves provide information relevant to rapid and slow coalescence. During the 60 days period of aging, the linearity of slow coalescence is observed for the emulsions with Φ ranging between 0.10 and 0.50.

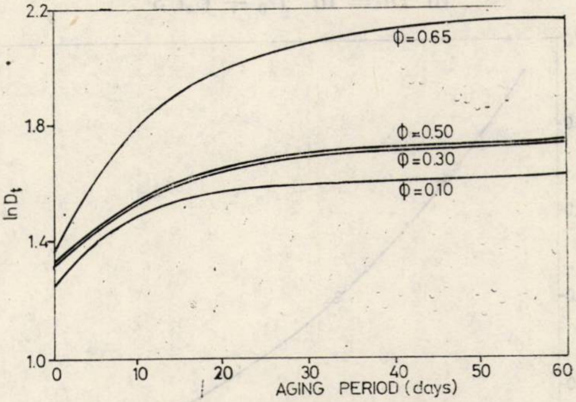

Fig. 4. – The plot of ln D_t versus aging period for wax emulsions at different Φ levels.

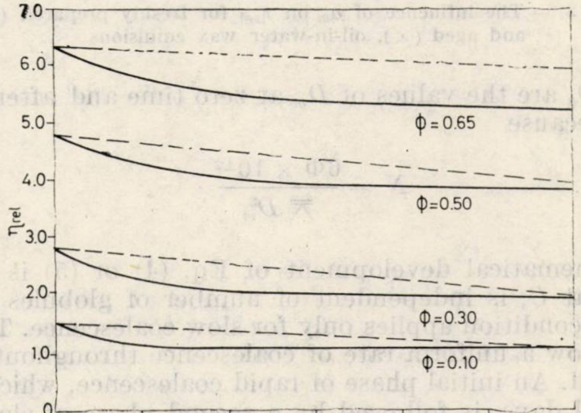

Fig. 5. – The comparison of the theoretical (dotted lines) and experimental changes in relative viscosity on aging of wax emulsions.

During slow coalescence, the value of C_s is determined from the linear portions of the curves and its value for the wax emulsions is found to be 21.605×10^{-8} sec^{-1}. The values of D_t for various aging periods have been calculated from Eq. (5). The value of η_{rel} corresponding to any value of D_t or a_m is derived from Fig. 3. The values of η_{rel} obtained in this way have been plotted with the values determined experimentally over a 60-day period of aging, in Fig. 5.

The theoretical (dotted lines) and experimental data do not agree satisfactorily because the wax emulsions do not coalesce at uniform rate throughout the whole of the aging period studied. The theoretical value of η_{rel} is based on slow coalescence whereas both rapid and slow coalescence do take place during aging of 0/W wax emulsions.

REFERENCES

[1] M. K. Sharma, K. D. Jain, A. K. Jain and B. K. Sharma, *Indian J. Technol.* (in press).

[2] C. P. Shillaber, "Photomicrography in Theory and Practice", Wiley, New York, 1949, p. 41.

[3] M. K. Sharma, *Progr. Colloid and Polymer Sci.*, **63,** 90 (1978).

[4] M. K. Sharma, *Progr. Colloid and Polymer Sci.*, **63,** 87 (1978).

[5] H. G. H. Jellinek, *J. Soc. Chem. Ind.*, **69,** 225 (1950).

[6] P. Sherman, "Emulsion Science", Academic Press, London, 1969, p. 304.

[7] P. Sharman, "Proc. 3rd Intern. Congr. Surface Activity", Cologne, vol. 2, 1960, p. 586.

[8] M. Van den Tempel, "Proc. 2nd Intern. Congr. Surface Activity", London, vol. 1, 1957, p.439.

NOTE POUR LES AUTEURS

La Revue Roumaine de Chimie publie des articles en anglais, français, russe, allemand ou espagnol. Les auteurs sont priés d'envoyer des articles et des comptes rendus inédits.

Les manuscrits seront dactylographiés à deux intervalles. La bibliographie, les tableaux et la légende des figures seront placés après le texte.

Si l'article fait partie d'une série numérotée, la partie précédente sera donnée comme première référence.

Chaque article sera précédé d'un résumé comprenant quinze lignes au maximum.

Les références bibliographiques dans le texte seront faites par des exposants sans parenthèses et paraîtront à la fin de l'ouvrage.

Les publications périodiques mentionées dans la bibliographie seront présentées suivant les prescriptions internationales : le nom de l'auteur précédé de l'initiale du prénom, le titre du périodique abrégé conformément à « Chemical Abstracts » et souligné par une ligne, le numéro du tome indiqué par des chiffres arabes et souligné par deux lignes, suivi de la première page de l'article : à la fin, l'année de la parution sera placée entre parenthèses. Le numéro de la revue ne sera pas indiqué si les pages du volume seront numérotées consécutivement.

Les textes des livres ou traités incluеront : le nom des auteurs, précédés de l'initiale du prénom, le titre du livre entre guillements et sans être souligné, le numéro du tome précédé par l'abréviation « vol. » (ou « Bd. »), le numéro de l'édition, les éditions (the publisher), la localité de la parution du livre, l'année de la parution et la page de référence précédée(s) par l'abréviation « p » (ou « S »).

Les brevets seront indiqués comme suit : l'auteur ou la firme, le pays et le numéro du brevet, la date de la revue (*Chem. Abstr.*).Par ex. : M. Jones (to Union Carbide Co.). Brit. Pat. 610 238, 2 Sept. 1959 : cf. *Chem. Abstr.*, **54**, 12808 (1960).

Si la référence n'a pas été lue en original, on indiquera aussi la revue de références consultée.

Les diagrammes seront tracés à l'encre de Chine sur papier calque. Les tableaux et les figures (en nombre strictement nécessaire), ainsi que les courbes dans les figures seront numérotés par des chiffres arabes. Leur explication sera donnée dans la légende des figures. Prière de ne pas inscrire les mêmes données dans les tableaux et les figures. Chaque tableau aura un titre. On indiquera dans le texte la place approximative des tableaux et des figures. Les formules chimiques seront incluses dans le texte : en outre, elles seront transcrites sur papier calque à l'encre de Chine.

Les auteurs sont priés d'indiquer les caractères italiques (en soulignant les lettres au crayon), ainsi que tout autre caractère spécial : les préfixes *ortho, meta, para, cis, trans,* etc. seront soulignés pour indiquer leurs caractères italiques, et ne seront jamais écrits avec des majuscules.

Aucune correction à la main ne sera admise sur le manuscrit. Les corrections seront frappées à la machine. Les lettres grecques ou autres symboles spéciaux seront insérés à la main à l'encre clairement.

Le manuscrit sera signé par l'auteur.

Le titre-courant aura 50 lettres au maximum.

L'entière responsabilité du contenu des articles appartient aux auteurs.

Sur demande on peut obtenir une note plus complete.

PRINTED IN ROMANIA

ORSZÁGOS MŰSZAKI INFORMÁCIÓS KÖZPONT ÉS KÖNYVTÁR
1968

TRAVAUX PARUS AUX ÉDITIONS DE L'ACADÉMIE DE LA RÉPUBLIQUE SOCIALISTE DE ROUMANIE

ELENA CEAUŞESCU, **Cercetări în chimia şi tehnologia polimerilor**, 1983, 519 p.
N. ASANDEI, AURELIA GRIGORIU, **Chimia şi structura fibrelor**, 1983, 395 p.
N. IONESCU, M. CĂLDĂRARU, **Oxidarea catalitică a olefinelor inferioare**, 1983, 178 p.
C. CAŞCAVAL, **Studiul polimerilor prin piroliză şi cromatografie de gaze**, 1983, 220 p.
C. I. SIMIONESCU, F. DANEŞ, **Originea vieţii**, 1983, 110 p.
C. BODEA (sub redacţia), **Tratat de biochimie vegetală**, partea II, volumul IV, 1982, 408 p.
I. G. MURGULESCU, RODICA VÎLCU, **Introducere în chimia fizică. Vol. III. Termodinamica chimică**, 1982, 624 p.
I. G. MURGULESCU, J. PĂUN, **Introducere în chimia fizică. Vol. I, 3. Nucleul atomic, reacţii nucleare, particule elementare**, 1982, 606 p.
ELENA JERCAN, **Analiza cromatografică**, 1982, 606 p.
ELENA CEAUŞESCU, **Noi cercetări în domeniul compuşilor macromoleculari**, 1981, 536 p.
I. G. MURGULESCU, TATIANA ONCESCU, E. SEGAL, **Introducere în chimia fizică. Vol. II.2. Cinematică chimică şi cataliză**, 1981, 1024 p.
V. DRĂGUŢAN, A. T. BALABAN, M. DIMONIE, **Metateza olefinelor şi polimerizarea prin deschidere de inel a cicloolefinelor**, 1981, 254 p.
LYDIA-MARIA VAICUM, **Epurarea apelor uzate cu nămol activ. Bazele biochimice**, 1981, 218 p.
I. GĂLĂŢEANU, **Procese şi metode radiochimice în energetica nucleară**, 1981, 234 p.
O. IORDACHE, **Procese polistocastice aplicate la fenomenele de transfer**, 1981, 186 p.
CR. SIMIONESCU, VALERIA GORDUZA, **Polimeri biocompatibili şi biologic activi**, 1980, 479 p.
ELENA CEAUŞESCU, **Polimerizarea stereospecifică a izoprenului**, 1979, 307 p.
CONST. GH. MACAROVICI, **Analiza chimică cantitativă anorganică**, 1979, 457 p.
M. FLORESCU, **Metode ştiinţifice în dezvoltarea industriei chimice moderne**, 1979, 256 p.
A. T. BALABAN, I. GĂLĂŢEANU, G. GEORGESCU, LIGIA SIMIONESCU, **Compuşi marcaţi şi radiofarmaceutici cu aplicaţii în medicina nucleară**, 1979, 495 p.
I. G. MURGULESCU, E. SEGAL, **Introducere în chimia fizică. Vol. II. 1. Teoria molecular cinetică a materiei**, 1979, 1036 p.
S. STERNBERG, FL. DANEŞ, **Termodinamica chimică aplicată**, 1978, 400 p.
I. G. MURGULESCU, V. EM. SAHINI, **Introducere în chimia fizică. Vol. I. 2. Structura şi proprietăţile moleculelor**, 1978, 604 p.
I. ZUGRĂVESCU, MAGDA PETROVANU, **N-ylid chemistry**, coédition avec McGraw Hill International Book Company, U.S.A., 1977, 396 p.
I. G. MURGULESCU, **Introducere în chimia fizică. Vol. I. 1. Atomi, molecule, legătură chimică**, 1976, 560 p.
ELENA CEAUŞESCU, **Research work on synthesis and characterization of macromolecular compounds. Contributions**, 1974, 251 p.
CR. SIMIONESCU, VIORICA RUSAN, V. POPA, **Chimia algelor marine**, 1974, 212 p., 1 pl.

1984 MAR 2 1

ISSN 0035–4090

I. P. INFORMAŢIA c. 1712

43426

Lei 40.—
$ 75 (pour un abonnement annuel)

1103
66
R
Vegyészet

ACADÉMIE DE LA RÉPUBLIQUE SOCIALISTE DE ROUMANIE

REVUE ROUMAINE DE CHIMIE

REFERÁLVA

TOME 29
N° 3
Mars 1984

EDITURA ACADEMIEI REPUBLICII SOCIALISTE ROMÂNIA

Rev. Roumaine Chim.

RRCHAX, 29, 3, p. 231–306 (1984) Bucarest

ACADÉMIE DE LA RÉPUBLIQUE SOCIALISTE DE ROUMANIE

COMITÉ DE RÉDACTION

Rédacteur en chef:

I. G. MURGULESCU, membre de l'Académie de la République Socialiste de Roumanie

Rédacteurs en chef adjoints:

A. T. BALABAN et V. EM. SAHINI, membres correspondants de l'Académie de la République Socialiste de Roumanie

Collège de rédaction:

EM. BRATU, ELENA CEAUŞESCU, ECATERINA CIORĂNESCU-NENITZESCU, CR. SIMIONESCU, membres de l'Académie de la République Socialiste de Roumanie ; P. SPACU, membre correspondant de l'Académie de la République Socialiste de Roumanie; MARGARETA AVRAM, M. BANCIU, I. HAIDUC, D. I. MARCHIDAN, I. MOLDOVAN, G. NIAC et D. SĂNDULESCU

La Revue Roumaine de Chimie paraît 10 fois par an. Toute commande de l'étranger pour les travaux parus aux Editions de l'Académie de la République Socialiste de Roumanie sera adressée à ILEXIM—Departamentul Export—Import Carte (Livres)/Departamentul Export—Import Presă (Revues), P.O.B. 136—137, télex 11226, 3, str. 13 Decembrie, 79517 Bucarest, Roumanie

Les manuscrits, les livres et les revues proposés en échange, ainsi que toute correspondance seront envoyés à la rédaction :

REVUE ROUMAINE DE CHIMIE

125, Calea Victoriei, 79717 Bucarest, Roumanie, téléphone 50 76 80

EDITURA ACADEMIEI REPUBLICII SOCIALISTE ROMÂNIA

125, Calea Victoriei, 79717 Bucarest, Roumanie, téléphone 50 76 80

REVUE ROUMAINE DE CHIMIE

ORSZÁGOS MŰSZAKI INFORMÁCIÓS KÖZPONT ÉS KÖNYVTÁR

Tome 29, N° 3 **Mars, 1984**

ȘTEFANIA ZUCA and RODICA BORCAN, Viscosity of certain charge-unsymmetrical molten chloride mixtures : $CaCl_2-(Na, K, Rb, Cs)Cl$ . . . . . 233–239 R

MARIA ZAHARESCU, MARINA BĂLĂȘOIU, MARIA CRIȘAN, D. CRIȘAN, T. TĂVALĂ and N. BRÎNZAN, The influence of the properties of ferric oxides on barium hexaferrite formation 241–246

MARIA ZAHARESCU, MARINA BĂLĂȘOIU, MARIA CRIȘAN, D. CRIȘAN, T. TĂVALĂ and VERONICA MOSER, The influence of the properties of ferric oxides on the formation of Mn–Zn ferrite . . . . 247–252 R

DOMNINA POPESCU, D. OANCEA, V. GOȘA, N. I. IONESCU and B. ALBU, The explosive combustion of propylene. III. The explosive combustion of propylene in a constant volume bomb . . . . 253–259 BC

GH. MIHĂILĂ, N. BÎLBĂ, D. DRANGA and C. LUCA, Vapour – liquid equilibrium at atmospheric pressure of the toluene – acetic anhydride and acetic anhydride – *o*-xylene systems 261–265

D. NEGOIU, S. NEAGOE and MARIA NEGOIU, Contributions to the chemistry of thiocomplexes. I. Complex combinations of Pd(II) with 4-(arylsulfonyl)-thiobenzamides 267–273

D. NEGOIU, S. NEAGOE and IOANA ȘARAMET, Contributions to the chemistry of thiocomplexes. II. Complex combinations of Pt(II), Cu(I), Au(III) and Hg(II) with 4-(arylsulfonyl)-thiobenzamides 275–282

MOHAMED M. SHOUKRY, Potentiometric studies on transition metal chelates of acetoacetanilide . . . . 283–288 BC

NICULINA PĂUNESCU, A spectrophotometric study of uranyl complexes formed in the $UO_2^{2+}-Cl^-$-acetone system 289–293

H. W. LANGFELD and S. IONIȚĂ, On the quaternization of *p*-aminophenylazo-azols. I. Mechanism of 2-(4′-aminophenylazo)-azol alkylation (in German) 295–306

Rev. Roumaine de Chim. **29**, *3*, 231–306 (1984) Bucarest

Revue Roumaine de Chimie, **29**, 3, 233–239 (1984)

VISCOSITY OF CERTAIN CHARGE-UNSYMMETRICAL MOLTEN CHLORIDE MIXTURES : $CaCl_2$—(Na, K, Rb, Cs)Cl

ŞTEFANIA ZUCA and RODICA BORCAN
Institute of Physical-Chemistry — ICECHIM, Spl. Independenţei 202,
Bucharest, Romania

Received September 28, 1983

The density and the viscosity of molten $CaCl_2$—(Na, K, Rb, Cs)Cl systems have been investigated over a temperature range of about 150 K in the whole concentration range. The viscosity isotherms show positive deviations from linearity increasing systematically as the tendency to form chemical compounds and/or the difference in the cationic radii in the mixture increased. A linear dependence of the observed $\Delta\eta$ vs. distance parameter, $(d_1 - d_2)^2$, was established.

Our study on the viscosty of binary molten salt systems was extended with a systematic investigation in $CaCl_2$—(Na, K, Rb, Cs)Cl series. Thus, it was intended to provide additional information regarding the nature of ionic interactions in these mixtures and to supply a new set of viscosity data which are scarce for these systems.

RESULTS AND DISCUSSION

The oscillating sphere method and Archimedean method have been employed for viscosity and density measurements, respectively. Details on the experimental set up were given elsewhere.[1] All salts were p.a. reagent grade, purified by the special technique which ensured the removal of any trace of water and hydrolysis products.[2] In order to keep the samples anhydrous, their handling (weighing, transferring into crucible for measurement) took place in a dry box. They were also remelted in vacuum by slowly increasing the temperature of the furnace. The neutrality of all salt samples was tested before and after each run. Only the results obtained with consistently neutral melts were retained.

Both density and viscosity were determned as a function of temperature over the whole concentration range from single $CaCl_2$ to single AlkCl. The temperature range covered through the run was of about 150 K above the melting point. For each system studied the density as a function of temperature was fitted by the linear equation $d = a - bT$. The constants *a* and *b* as determined by the least squares method are listed in Table 1, together with the standard deviations of density and the experimental temperature range over which the data were obtained. A comparison with the available literature data [3] indicated a satisfactory agreement. The data in Table 1 were used for subsequent calculation of molar volume, V_m, and of viscosity, η.

Table 1

Density of $CaCl_2$–(Na, K, Rb, Cs)Cl systems, g·cm^{-3}.

$d = a - bT$

System	x_{CaCl_2}	a	$b \cdot 10^3$	Standard deviations	Temperature range, K
$CaCl_2-NaCl$	0.10	2.1682	0.5296	0.0007	1074–1201
	0.25	2.2024	0.4791	0.0006	1100–1280
	0.40	2.2559	0.4529	0.0005	1080–1240
	0.50	2.3141	0.4569	0.0003	1080–1280
	0.75	2.4051	0.4327	0.0003	1082–1270
$CaCl_2-KCl$	0.15	2.1786	0.5559	0.0011	1060–1120
	0.25	2.2011	0.5307	0.0008	1075–1140
	0.35	2.2532	0.5403	0.0006	1060–1155
	0.50	2.2946	0.4990	0.0002	1070–1160
	0.75	2.2967	0.3868	0.0005	1080–1185
$CaCl_2-RbCl$	0.10	2.9863	0.7966	0.0008	1080–1245
	0.25	2.8746	0.7120	0.0005	1085–1265
	0.40	2.8065	0.7349	0.0004	1090–1230
	0.50	2.7042	0.5875	0 0007	1125–1270
	0 25	2.5636	0.4760	0.0004	1080–1275
$CaCl_2-CsCl$	0.25	3.3320	0.8471	0.0009	1145–1295
	0.60	2.7827	0.5466	0.0006	1190–1305
	0.75	2.7269	0.5166	0.0010	1140–1285

The viscosity of $CaCl_2$ – (Na, K, Rb, Cs,)Cl mixtures as a function of temperature and compostion is given in Tables 2–5.

Table 2

Viscosity of $CaCl_2-NaCl$ system, mN.s.m^{-2}

10 mole % $CaCl_2$		25 mole % $CaCl_2$		40 mole % $CaCl_2$		50 mole % $CaCl_2$		75 mole % $CaCl_2$	
T	η	T	η	T	η	T	η	T	η
1130.2	1.210	1123	1.485	1146	1.744	1104	2.130	1073	2.853
1150	1.123	1130.5	1.430	1168	1.604	1116	2.040	1093	2.745
1164.4	1.110	1143.6	1.385	1183	1.570	1133.5	1.932	1124.9	2.519
1184.2	1.040	1163.3	1.345	1200.5	1.484	1149	1.859	1131	2.377
1200.5	1.032	1182	1.285	1231.4	1.407	1167.3	1.744	1153.5	2.280
1217	0.980	1202.4	1.205			1201.4	1.633	1170.4	2.150
1236	0.962	1225	1.142			1218	1.574	1192.5	2.082
		1242.5	1.112			1233	1.522	1214.5	1.974

Table 3

Viscosity of Ca_2Cl_2—KCl system, $mN.s.m^{-2}$

15 mole % $CaCl_2$		25 mole % $CaCl_2$		35 mole % $CaCl_2$		50 mole % $CaCl_2$		75 mole % $CaCl_2$	
T	η	T	η	T	η	T	η	T	η
1098	1.463	1107	1.620	1091.7	1.945	1092.4	2.305	1070.3	3.075
1101	1.440	1147	1.432	1103.9	1.894	1105	2.203	1102	2.772
1115.8	1.354	1164	1.373	1128	1.756	1115	2.145	1125.7	2.562
1131	1.300	1186	1.290	1150.7	1.623	1128.3	2.048	1148	2.400
1144.5	1.236	1217.2	1.142	1177.5	1.501	1148	1.945	1172.4	2.261
1171	1.160	1232	1.120	1202	1.418	1168.7	1.834	1220.3	2.014
1199	1.082	1248.5	1.090	1228.4	1.340	1185.2	1.758	1242.5	1.914
1228.6	1.015					1206	1.648		
						1225	1.578		
						1243.5	1.500		

Table 4

Viscosity of $CaCl_2$—RbCl system, $mN.s.m^{-2}$

10 mole % $CaCl_2$		25 mole % $CaCl_2$		40 mole % $CaCl_2$		50 mole % $CaCl_2$		75 mole % $CaCl_2$	
T	η	T	η	T	η	T	η	T	η
1088	1.449	1102.2	1.805	1125.7	2.040	1170.4	1.947	1101.3	2.952
1095.8	1.410	1131	1.644	1136	2.004	1201.4	1.820	1124	2.621
1111.3	1.350	1173.4	1.465	1150.7	1.887	1219	1.730	1148.5	2.323
1124.8	1.266	1194.3	1.365	1194.3	1.647	1228	1.704	1170	2.227
1145.5	1.185	1204.7	1.318	1206.6	1.588	1236.4	1.659	1187	2.135
1194.8	1.015	1219	1.263	1223.4	1.515	1246.5	1.642	1208	1.958
1218.5	0.958	1235.5	1.201	1238.7	1.480	1251.3	1.613	1228.6	1.958
1240.8	0.891							1245.2	1.855

Table 5

Viscosity of $CaCl_2$—CsCl system, $mN.s.m^{-2}$

25 mole % $CaCl_2$		60 mole % $CaCl_2$		75 mole % $CaCl_2$	
T	η	T	η	T	η
1138.3	1.732	1214.5	2.123	1156	2.748
1160.7	1.595	1227.7	2.060	1179.2	2.530
1181	1.532	1248.6	1.958	1205.7	2.347
1207.1	1.427	1262.5	1.880	1233	2.210
1233.6	1.319	1278.5	1.790	1250.8	2.060
1253.8	1.256	1297	1.704	1275	2.030
1281.4	1.169				

The present results on pure components $CaCl_2$, KCl, RbCl, CsCl, are in very good agreement (within ± 1%) with our earlier data.[2,4] Their agreement with literature was already discussed.[2,4] In addition we mention the more recent data for $CaCl_2$ issued by Otha,[5] which agree within ± 5% with the present data. For NaCl, a fairly good agreement (1—3%) with Tørklep and Øye's data,[6] recommended as reference standard,[7] is obtained.

Due to the above discussed differences for the viscosity of pure components, similar differences are expected for the mixtures investigated. Thus, a comparison with literature data [5,8,9] indicated indeed differences of ± 5%, although the dependence of the viscosity on the composition is very similar.

In all studied systems the temperature dependence of the viscosity was of Arrhenius type over the whole temperature range covered for each composition. The parameters E_η and A_η of the Arrhenius equation, as determined by the least squares method are listed in Table 6 along with the corresponding standard deviations and the validity temperature range.

Table 6

A_η and E_η for molten $CaCl_2-$(Na, K, Rb, Cs)Cl systems

System	x_{CaCl_2}	$A_\eta \cdot 10^2$	E_η kJ/mol	Standard deviations for E_η	Temperature range K
$CaCl_2-NaCl$	0	8.23	22.81	0.12	1033–1260
	0.10	7.51	25.92	1.15	1130–1236
	0.25	7.62	27.64	1.13	1123–1242
	0.40	8.41	28.82	0.97	1140–1230
	0.50	8.40	29.65	0.92	1104–1233
	0.75	9.09	29.38	0.44	1073–1215
	1	10.99	30.24	0.65	1068–1180
$CaCl_2-KCl$	0	7.67	22.92	0.31	1073–1200
	0.15	4.65	31.39	1.10	1098–1230
	0.25	4.61	32.69	1.19	1100–1253
	0.35	5.67	32.08	0.84	1090–1230
	0.50	6.53	32.46	0.22	1090–1240
	0.75	9.95	30.48	0.58	1070–1240
$CaCl_2-RbCl$	0	6.84	24.65	0.12	1010–1110
	0.10	3.97	32.63	0.49	1080–1245
	0.25	4.29	34.30	0.69	1105–1240
	0.40	5.04	34.70	1.02	1125–1240
	0.50	5.55	34.79	0.90	1170–1250
	0.75	7.66	32.89	1.05	1100–1245
$CaCl_2-CsCl$	0	8.65	22.45	0.35	963–1080
	0.25	3.60	36.03	0.88	1135–1290
	0.60	5.69	36.63	0.92	1215–1300
	0.75	9.03	32.24	1.09	1150–1275

The composition dependence, as illustrated by the viscosity isotherms in Fig. 1, is directly influenced by the alkaly chloride present in the mixture. Thus, for $CaCl_2-NaCl$ system, the viscosity varies practically linearly with melt composition, while for the remaining systems of the series, the viscosity isotherms show positive deviations from linearity increasing systematically in the sequence K < Rb < Cs. Moreover, at $x_{CaCl_2} = 0.75$, the viscosity isotherm for $CaCl_2-CsCl$ system exhibits a maximum. As seen in Fig. 1, similar trends are evidenced by the E_η vs. composition curves. The large positive deviations from linearity observed for $CaCl_2-$(K, Kb, Cs)Cl systems entail significant changes in the cation-anion bonding energy on mixing, which render the viscous flow more difficult especially as the radius of alkali cation increases. For these three systems the molar volume isotherms (Fig. 2) show considerable positive deviations from linearity which point out to a systematical weakening of ionic packing on mixing.

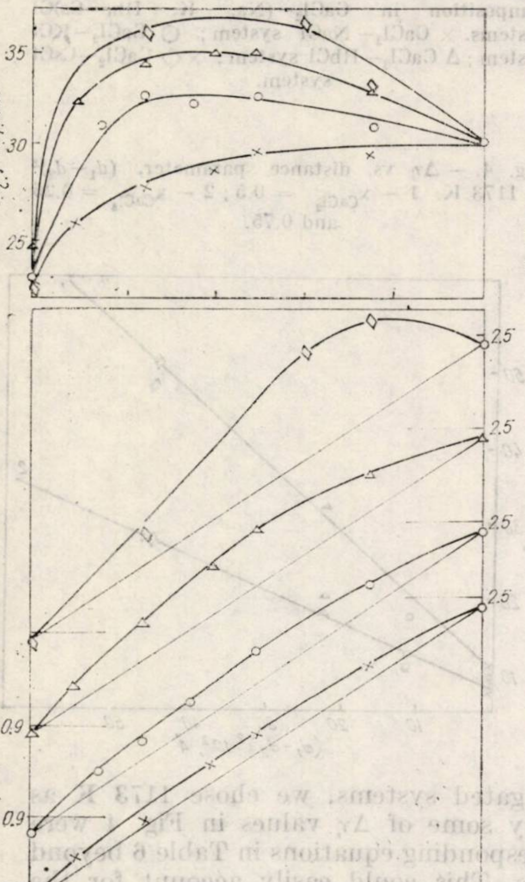

←Fig. 1. — Viscosity and activation energy vs. composition in $CaCl_2$ — (Na, K, Rb, Cs)Cl systems at 1173 K. × $CaCl_2$—NaCl system ; ○$CaCl_2$—KCl system ; Δ $CaCl_2$—RbCl system ; ×◇ $CaCl_2$—CsCl system.

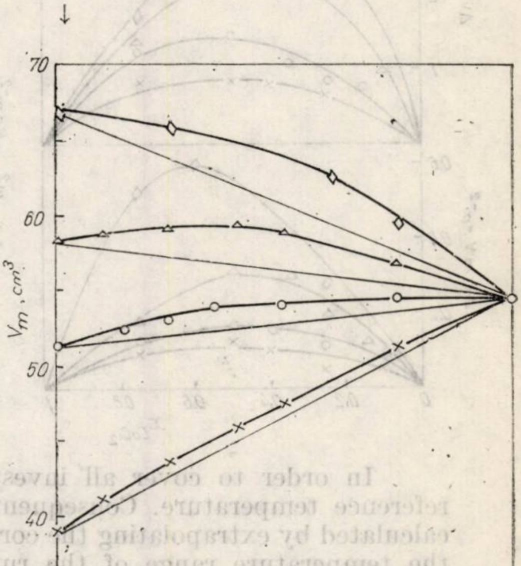

Fig. 2. — Molar volume isotherms at 1173 K. × CaCl—NaCl system ; ○ $CaCl_2$ — KCl system ; Δ $CaCl_2$—RbCl system ; ×◇ $CaCl_2$—CsCl system.

Regarding $CaCl_2$—NaCl system, the experimental data illustrated in Figs 1 and 2 suggest no important changes on mixing.

The above mentioned facts are better emphasized in Fig. 3 where the excess quantities, $\Delta\eta$, ΔV, ΔE_η, are plotted against mole fraction of the mixture.

It is obvious from the figure that the departure from linearity is larger as the tendency to form chemical compounds is more pronounced (as indicated by the phase diagram information [10-13]) and/or the difference in the cationic radii increases. A quatitative relationship $\Delta\eta$ — distance parameter is thus suggested. As seen in Fig. 4, by plotting $\Delta\eta$ vs. $(d_1 - d_2)^2$ parameter at constant concentration, a linear dependence is obtained. For interionic separation d_1 and d_2 in $CaCl_2$ and AlkCl respectively, we have used the values for the crystals.[14,15]

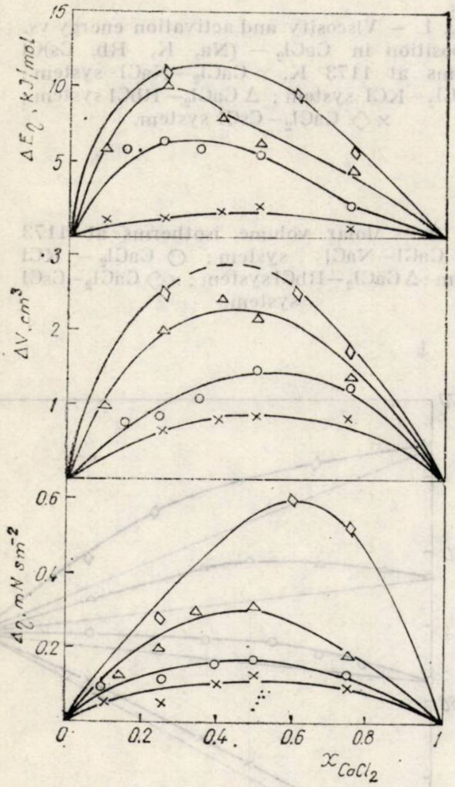

←Fig. 3. — Excess quantities, $\Delta\eta$, ΔV, ΔE_η, vs. composition in $CaCl_2$—(Na, K, Rb, Cs)Cl systems. × $CaCl_2$—NaCl system ; ○ $CaCl_2$—KCl system ; Δ $CaCl_2$—RbCl system ; ×◇ $CaCl_2$—CsCl system.

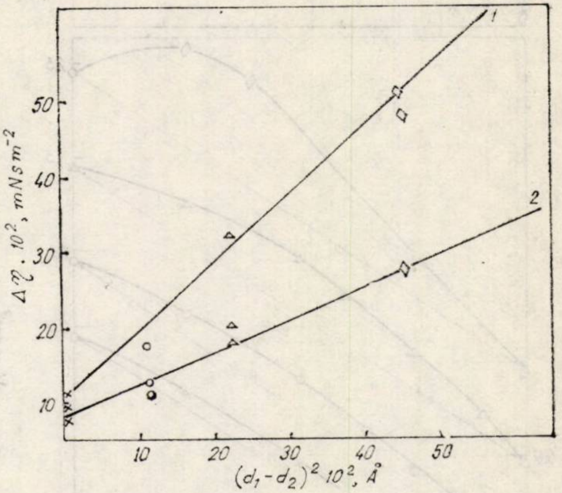

Fig. 4. — $\Delta\eta$ vs. distance parameter, $(d_1-d_2)^2$ at 1173 K. 1 — $x_{CaCl_2} = 0.5$; 2 — $x_{CaCl_2} = 0.25$ and 0.75.

In order to cover all investigated systems, we chose 1173 K as reference temperature. Consequently some of $\Delta\eta$ values in Fig. 4 were calculated by extrapolating the corresponding equations in Table 6 beyond the temperature range of the runs. This could easily account for the relatively high differences (2—3%) obtained between the experimental values of the viscosity and the calculated ones (by subtracting from the value of the viscosity calculated additively the $\Delta\eta$ yielded by the linear fit in Fig. 4). The agreement is perfect ($\leqslant$ 1%) below 1123 K, but the discussion is restricted therefore to $CaCl_2$—(Na, K, Rd)Cl systems whose melting points lie within the range mentioned. Nevertheless, the data in Fig. 4 prove obviously that the distance parameter is sufficient to account quantitatively for the changes in the ionic interactions on mixing. In this respect, we mention the special trends shown by $CaCl_2$—CsCl system, whose tendency to form complex ions is most pronounced in the series [13,16] (see also Fig. 1). For $CaCl_2$—rich mixtures ($x_{CaCl_2} > 0.5$) where, according to Pelton's complex ion model [17], the complexation of Ca^{2+} ion is total, the above discussed linearity is no longer verified. The different behaviour of NaCl, KCl, RbCl containing systems, might be explained in terms of the kinetic stability of the complex ion in the melt ($CaCl_4^{2-}$ and/or $CaCl_3^-$ as advanced by Hagiwara et al.[18] and Roewer and Emons [19] respectively). Its relaxation time may be so much shorter that it is not manifested in the viscosity and in this case the $\Delta\eta$ — distance parameter relationship is not affected.

REFERENCES

[1] S. Zuca and R. Borcan, *Electrochem. Acta*, **15**, 1817 (1970).

[2] S. Zuca and R. Costin, *Rev. Roumaine Chim.*, **12**, 1813 (1970).

[3] G. J. Janz, R. P. Tomkins, C. B. Allen, R. J. Downey, G. L. Gardener and S. K. Singer, *J. Phys. Chem. Ref. Data*, **4**, 871 (1975).

[4] S. Zuca and R. Borcan, *Rev. Roumaine Chim.*, **19**, 553 (1974).

[5] T. Otha, Ph. D. Thesis, Trondheim, 1974.

[6] K. Tørklep and H. A. Øye, *J. Phys. E : Sci. Instrum.*, **12**, 875 (1979).

[7] G. J. Janz, *J. Phys. Chem. Ref. Data*, **9**, 791 (1980).

[8] D. Dumas, B. Fjeld, K. Grjotheim and H. A. Øye, *Acta Chem. Scand.*, **27**, 319 (1973).

[9] W. Brockner, K. Grjotheim, T. Otha and H. A. Øye, *Ber. Bunsen Gesellschaft*, **79**, 344 (1975).

[10] A. Seltveit and A. Flood, *Acta Chem. Scand.*, **12**, 1036 (1958).

[11] T. Sato and T. Amano, *Kinzoku-no-Kenkyu, 11*, 549 (1934).

[12] I. V. Shakhano and V. E. Plyuschev, *Zhur. neorg. Khim.*, **5**, 1172 (1960).

[13] E. P. Dergurov and A. G. Bergman, *Doklady Akad. Nauk S.S.S.R.*, **75**, 815 (1950).

[14] R. W. Wyckoff, "Crytsal Structure", Interscience, New York, 1948.

[15] L. Pauling, "The Nature of Chemical Bond", Cornwell University Press, New York, 1963.

[16] T. Østvold, *J. Phys. Chem.*, **76**, 1629 (1972).

[17] A. D. Pelton, *Canad. J. Chem.*, **49**, 3919 (1971).

[18] H. Hagiwara, R. Oyomoda and S. Fukushima, *J. Electrochem. Soc. Japan*, **36**, 35 (1968).

[19] G. Roewer and H. H. Emons, *Z. anorg. Chem.*, **370**, 128 (1969).

Revue Roumaine de Chimie, 29, 3, 241—246 (1984)

THE INFLUENCE OF THE PROPERTIES OF FERRIC OXIDES ON BARIUM HEXAFERRITE FORMATION

MARIA ZAHARESCU*, MARINA BĂLĂȘOIU*, MARIA CRIȘAN*,
D. CRIȘAN*, T. TĂVALĂ** and N. BRÎNZAN**

* ICECHIM, Center of Physical Chemistry, Splaiul Independenței 202
Bucarest, Romania

** Center of Chemistry, Blvd Mihai Viteazu 24, Timișoara, Romania

Received September 1, 1982

A comparative study on the reactivity of eight iron oxides in the formation of barium hexaferrite has been made. The reactivity was estimated working under nonisothermal conditions (by DTA/TG) and isothermal conditions (by X-ray diffraction of samples annealed at temperatures between 600 and 1200°C).

1. INTRODUCTION

The ceramic materials made from barium hexaferrite can be used as permanent magnets, being therefore of much practical interest. The $BaO.6Fe_2O_3$ was described first by Adelsköld,[1] together with other analogues as $SrO.6Fe_2O_3$ and $PbO.6Fe_2O_3$.

Barium hexaferrite formation from $BaCO_3$ and Fe_2O_3 was studied by many authors.[2-6] The reaction mechanism has two steps : in the first (up to about 900°C), $BaCO_3$ completes its decomposition, and the formation of an intermediate phase, $\gamma BaO.Fe_2O_3$, is noticed.[7] In the second step, the monoferrite reacts with excess Fe_2O_3, resulting in barium hexaferrite. Further, densification and crystallization processes occur, which are necessary for good magnetic properties of the ceramic body. This process is finished around 1200°C.

The differences in the physical-chemical properties of the ferric oxide lead to differences in the ranges of formation and stability of the monoferrite, which exert an important influence on the range of formation and the microstructure of the final product — barium hexaferrite —.[8]

In practice, for better magnetic properties, nonstoichiometric compositions of the formula $BaO.nFe_2O_3$ (where $5.5 \leqslant n \leqslant 5.9$) are used. The values of the B_r (remanent induction) and H_c (coercive force) are much greater at $n = 5.5-5.7$.[5] The magnetic should be dense (close to the theoretical value), and the grain size should be around 2 μ ; at approximately equal densities, the BH_{max} of the masses with inhomogeneous grain size distributions above 2 μ are approximately 30 % lower.[9] For convenient grain size, additives whose role is to inhibit the crystal growth are used, the most usual being SiO_2.[10-12] The study of the $BaO-SiO_2-Fe_2O_3$ system[11,13] has determined low temperature eutectics, which alow liquid phase sintering, thus accelerating all stages of the formation process of barium hexaferrite.

This work is a comparative study on the reactivity of eight iron oxides in the formation of barium hexaferrite from nonstoichiometric mixtures of the mole ratio $BaCO_3 : \alpha-Fe_2O_3 = 1 : 5.7$. The reactivity was estimated under nonisothermal conditions (by DTA/TG) and isothermal conditions (by X-ray diffraction of samples annealed at temperatures between 600 and 1200°C).

2. EXPERIMENTAL PART

The physical-chemical properties of the studied oxides are listed in Table 1.

Table 1

Physical-chemical properties of investigated iron oxides

Sampl	Crystal structure	Surface area m^2/g	Particle size and shape
1	$\alpha-Fe_2O_3$	12	Needles Ø = 0.2–0.3 μ; L = 0.4–1 μ
2	$\alpha-Fe_2O_3$	6	Spheres Ø = 0.2–0.5 μ
3	$\gamma-Fe_2O_3$	11	Spheres Ø = 0.2–0.5 μ
4	$\alpha-FeOOH$	14	Needles Ø = 0.3–0.5 μ L = 0.5–1 μ
5	Fe_3O_4		
6	$\alpha-Fe_2O_3$	4.5	Needles Ø = 0.3 μ L = 0.8–1.4 μ
7	$\alpha-Fe_2O_3$	7.6	Spheres Ø = 0.6–1.5 μ Needles Ø = 0.2 μ
B* (Bayer) 1640 HM	$\alpha-Fe_2O_3$	5.7	Spheres Ø = 0.3–0.6 μ (predominant 0.4 μ)

* — contained approximately 1 % SiO_2.

The selection of these oxides was made in such a manner as to allow the study of the effect of some parameters, such as : chemical composition (e.g. Fe_2O_3, Fe_3O_4, $FeOOH$), crystal structure ($\alpha-Fe_2O_3$, $\gamma-Fe_2O_3$), particle shape (needles, spheres, complicated shapes), particle size (0.5 to 1.5 μ) and surface area (4 to 12 m^2/g).

The other starting material was in all cases $BaCO_3$ p.a supplied by UCB Belgium.

All mixtures were prepared according to the non-stoichiometric mole ratio $BaO : Fe_2O_3 = 1 : 5.7$. The mixtures were labelled MB, the index corresponding to the ferric oxides listed in Table 1. The wet homogenization was done in a laboratory planetary ball mill (Pulverisette Fritsch).

The reactivity of the ferric oxides under non-isothermal conditions was done by DTA and TGA of all unreacted mixtures. The variation of the temperature range of the $BaCO_3$ decomposition, and the thermal effects due to starting materials and the intermediate compound — barium monoferrite — were determined. An OD-103 Derivatograph supplied by MOM was used; the heating rate up to 1300°C was 7.5°C/min.

The treatment under isothermal conditions was done for 1 hr. on pressed tablets on a furnace heated by silicon carbide resistance, between 600—1200°C, in 100°C steps. The variation in the ferrite amount as a function of the annealing temperature and the type of ferric oxide used was determined measuring the variation in the relative intensities of the main diffraction peaks of the starting materials, and the intermediate and final product. In order to diminish the errors due to degree of crystallization and preferential orientation of the crystallites in the annealed samples,[14] the reacted mixtures were ground and screened on 20 μm sieve. The X-ray diffraction measurements were done with a HZG-3 diffractometer equipped with a proportional counter, with $Co_{k\alpha}$ radiation filtered by Fe.

3. RESULTS AND DISCUSSIONS

3.1. Results under non-isothermal conditions

The DTA curve of the MB_B mixture and the decarbonation intervals of $BaCO_3$ in all mixtures are shown in Figure 1. The changes in temperatures marking the beginning and the end of $BaCO_3$ decarbonation are taken as the measure of the iron oxide reactivity. The temperature of decarbonation beginning (610—650°C) is lower than that of pure $BaCO_3$, which is above 1100°C. In all mixtures the process is completed up to 940°C. The weight losses are comparable (around 4%) and agree with the theoretical values. The DTA curves exhibit some thermal effects due to the starting materials: endothermal effect at 675°C due to the Néel point of Fe_2O_3 (all mixtures) exothermal polymorphic transformation $\gamma-Fe_2O_3 \longrightarrow \alpha-Fe_2O_3$ at about 600°C (MB_3, MB_5); Fe_3O_4 oxidation to $\gamma-Fe_2O_3$ at about 300°C (MB_5); $\alpha-FeOOH$ decomposition to $\alpha-Fe_2O_3$ at about 300°C (MB_4) and the endothermal polymorphic transformation at 810°C of non-decomposed $BaCO_3$ (all mixtures). In all cases, the endothermal effect of barium monoferrite formation at 870°C,[5-7] is noted.

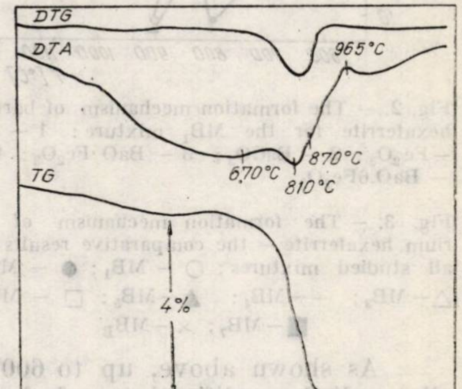

Fig. 1. — The DTA and TG/DTG curves of the MB_B mixture and the $BaCO_3$ decomposition temperature ranges for all mixtures: 1 — MB_1; 2 — MB_2; 3 — MB_3; 4 — MB_4; 5 — MB_5; 6 — MB_6; 7 — MB_7; 8 — MB_B.

The differences in the temperatures marking the beginning and the end of $BaCO_3$ decarbonation are relatively small, arond 50°C; the lowest temperature is recorded for iron oxide Bayer 1640 (MB_B). For less reactive oxides, the decarbonation range is narrower: the end of the process is noted at temperatures close to those of the reactive oxides. The lowest temperatures of the end of decarbonation are noted for the MB_B and MB_4 mixtures, which exhibit also an exothermal effect at 960°C assignated to barium hexaferrite formation.

3.2. Results under isothermal conditions

The results are shown in figures 2 and 3. In figure 2 the formation mechanism of barium hexaferrite for the MB_1 mixture is shown, and figure 3 gives the comparative results for all studied mixtures.

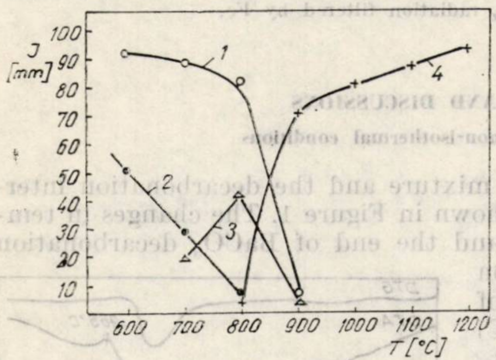

Fig. 2. — The formation mechanism of barium hexaferrite for the MB_1 mixture: 1 — α—Fe_2O_3; 2 — $BaCO_3$; 3 — $BaO \cdot Fe_2O_3$; 4 — $BaO.6Fe_2O_3$.

Fig. 3. — The formation mechanism of barium hexaferrite — the comparative results for all studied mixtures: ○ — MB_1; ● — MB_2; △ — MB_3; + — MB_4; ▲ — MB_5; □ — MB_6; ■ — MB_7; × — MB_B. →

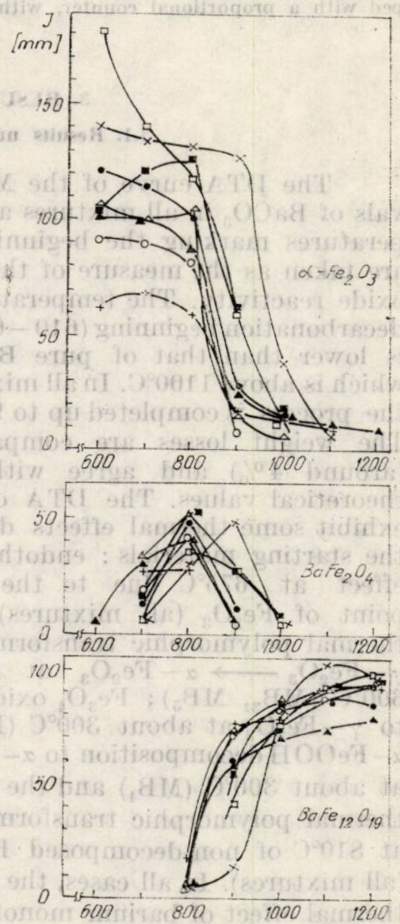

As shown above, up to 600°C, all studied modifications of ferric oxide are completely transformed into $\alpha-Fe_2O_3$.

In the case of the starting oxides with $\alpha-Fe_2O_3$ structure, the intensities determined at 600°C are very close to those in the initial, unfired mixtures. In some cases, up to 800°C, even an apparent increase in the amount of ferric oxide is recorded, as, e.g., in MB_B, MB_4, MB_7. This is due to the much smaller reaction rate in solid phase than the rate of Fe_2O_3 sintering, because both DTA and X-ray analysis confirm the $BaCO_3$ decomposition from 600°C and the formation of barium monoferrite from 700°C. Above 800°C a marked decrease of the Fe_2O_3 amount is noted, because it begins to react. This does not hold for the Bayer oxide for-which the inflexion of the curve occurs at 900°C. Fe_2O_3 peaks vanish at different temperatures : for MB_1 above 900°C (here $BaCO_3$ disappeared rapidly, too), and for all other mixtures (except MB_5, where unreacted Fe_2O_3 is identified even at 1200°C), above 1000—1100°C.

The characteristic features of the studied ferric oxides affect mainly the stability range of barium monoferrite, and the temperature where the maximum amuont of the new phase is seen. At 600°C, the presence of the monoferrite is recorded (in a small amount) in the MB_5 mixture only; at 700°C all mixtures contain variable amounts of monoferrite. The monoferrite is noted roughly between 700 and 900°C (MB_1—MB_3, MB_5) and between 700 and 1000°C (MB_6, MB_7, MB_B). The greatest amount of monoferrite is seen at 800°C (except MB_B —at 900°C), in the MB_2, MB_3, MB_7 and MB_B mixtures. At the same time, the goethite (MB_4) causes the mixture to behave in a different manner ; thus, the monoferrite exists between 700 and 800°C, in equal, small amounts.

Barium hexaferrite is seen from 800°C in most mixtures, but no connection can be made with the maxima in the amount of monoferrite formed in the previous stage. At 900°C, the amounts of formed hexaferrite differ very much from one sample to the other. A steep increase of the amount formed is noted between 800 and 900°C for the mixtures whose formation had begun at 800°C, and between 900 and 1000°C for the others. This phenomenon is connected with a rapid decrease, over the same temperature range, of the amounts of ferric oxide and barium monoferrite. The mixture MB_B presents equal amounts at 800 and 900°C, then the amount of hexaferrite increases sharply.

Upon an increase of temperature up to 1000 and 1100°C, the amounts of hexaferrite become equal in all samples (around 90% of the maximum value), except MB_B, which exhibits the maximum value, and MB_5, which, even at 1200°C, has only 75% of the maximum value. At 1200°C, the amounts of hexaferrite are almost the same in the most mixtures (MB_B, MB_1, MB_3, MB_4, MB_6, MB_7), excepting, of course, MB_5.

The different reactivity of the ferric oxides in the barium hexaferrite formation is visible over a wide temperature range, mainly at low temperatures, between 600 and 900°C, where it exerts its influence on $BaCO_3$ decarbonation, barium monoferrite formation and the initiation of the formation process of barium hexaferrite. The initiation at 600—700°C of the monoferrite formation, and at 800°C of hexaferrite formation, takes place in mixtures prepared with high surface area oxides, hence with greater areas of reaction ; this feature might be present from the start (MB_1, MB_3) or might be obtained later, by a decomposition (MB_4, MB_5). The Bayer oxide, though it has the lowest surface area, initiates the formation of mono- and hexaferrite at low temperatures, but the formed amounts are small. The loss of reactivity is compensated by the content of SiO_2 which, as shown above, accelerates the reaction in solid phase, but does not allow increases in the grain size.

At temperatures above 1000—1100°C the densification of the material is enhanced by SiO_2 and MB_B mixture exhibits the maximum amount of hexaferrite formed. The reactivity of the other oxides above 900°C is lowered, probably because of a partial sintering, and at 1200°C the amounts of hexaferrite are close to the MB_B value, but smaller.

No correlation between the reactivity of ferric oxides and the grains shape was noted.

4. CONCLUSIONS

The differences in the reactivity of eight ferric oxides in the barium ferrite formation were studied and correlated with their physical-chemical properties.

The differences in reactivity between ferric oxides are noted mainly at relatively low temperatures (600–900°C) in the barium monoferrite formation and the initiation of the barium hexaferrite formation.

At high temperatures, the differences in reactivity are smaller, and the final hexaferrite amounts are relatively closer.

No correlation could be made between the reactivity of ferric oxides and the grains shape.

The important role played in the barium hexaferrite formation by SiO_2 initial additions in the ferric oxide composition was confirmed.

REFERENCES

[1] V. Adelsköld, *Arkiv. Kemi Mineral. Geol.*, **12A**, 1 (1938).
[2] J. Suchet, *Bull. Soc. franc. Céram.*, **33**, *33*, (1956).
[3] C. G. Bye and C. R. Howard, *J. Appl. Chem. Biotechnol.*, **21**, 319 (1971); **22**, 1053 (1972).
[4] H. Wullkopf, *Int. J. Magnetism*, **3**, 179 (1972).
[5] H. Wullkopf, *Int. J. Magnetism*, **5**, 147 (1973).
[6] F. Haberey, M. Velicescu and A. Kockel, *Int. J. Magnetism*, **5**, 161 (1973).
[7] F. Haberey, A. Kockel and J. Kuncl, *Ber. dtsch. Keram. Ges.*, **51**, 131 (1974).
[8] H. Wullkopf, *Physica*, **80B**, 129 (1975).
[9] H. Wullkopf and W. Grienke, *Powder Metall. Intern.*, **7**, 68 (1975).
[10] H. Stäblein, *Ber. dtsch. Keram. Ges.*, **55**, 305 (1978).
[11] F. Kools, *Ber. dtsch. Keram. Ges.*, **55**, 301 (1978).
[12] H. E. Schütz and H. W. Hennicke, *Ber. dtsch. Keram. Ges.*, **55**, 308, (1978).
[13] F. Haberey, *Ber. dtsch. Keram. Ges.*, **55**, 297, (1978).
[14] H. P. Klug and L. E. Alexander, "X-Ray Diffraction Procedures for Polycrystalline and Amorphous Materials", Wiley, New York, 1966.

Revue Roumaine de Chimie, **29**, *3*, 247–252 (1984)

THE INFLUENCE OF THE PROPERTIES OF FERRIC OXIDES ON THE FORMATION OF Mn – Zn FERRITE

MARIA ZAHARESCU*, MARINA BĂLĂȘOIU*, MARIA CRIȘAN*,
D. CRIȘAN*, T. TĂVALĂ** and VERONICA MOSER**
* ICECHIM, Center of Physical Chemistry, Splaiul Independenței 202,
Bucharest, Romania
** Center of Chemistry, Blvd Mihai Viteazu 24, Timișoara, Romania

Received December 15, 1982

A comparative study on the reactivity of six iron oxides in the formation of Mn – Zn ferrite has been done. The reactivity was estimated working under nonisothermal conditions (by DTA/TG) and isothermal conditions (by X-ray diffraction of samples annealed at temperatures between 600 and 1200°C).

1. INTRODUCTION

The Mn – Zn ferrites are soft magnetic ceramics, with spinel structure; their initial magnetic permeability is high, and the magnetic losses are low. These materials are solid solutions between the Zn ferrite and the Mn ferrite, corresponding to the general formula:[1,2]

$$Mn_{1-x}Zn_xFe_2O_4 \quad \text{where} \quad 0 \leqslant x \leqslant 1$$

The magnetic properties and the structural features are strongly influenced by their composition. On the other hand, the microstructure of the final product exhibits a great influence on its characteristics. When the grain size is great, and the pores are situated in the grain boundary areas, the initial permeability is high; on the contrary, a fine microstructure determines small magnetic losses. The impurities introduced by the starting materials, mainly the ferric oxide, usually lead to an exaggerated grain growth during sintering, which is undesirable in the manufacturing process.[3]

The manufacturing process of Mn – Zn ferrites is a complicated multi-stage sequence of solid phase reactions,[4] and requires a very attentive monitoring of all stages in order to obtain the desired properties.

The formation and the quality of the final ceramic product are also influenced by the reactivity of the ferric oxide, which constitutes the greatest portion of the initial mixture. The reactivity of the ferric oxide is determined by its physical-chemical properties, i.e. chemical composition (purity), crystal structure, particle size and shape, surface area, tapped bulk density.

This work is a comparative study on the reactivity of six iron oxides in the formation of Mn–Zn ferrite.

2. EXPERIMENTAL

The properties of the studied ferric oxides are listed in Table 1.

Table 1

The main physical-chemical properties of the studied ferric oxides

Sample	Crystal structure	Surface area m²/g	Grain shape and size
1	$\alpha-Fe_2O_3$	12	Needles 0.2–0.3 diameter and 0.4–1 μ long.
2	$\alpha-Fe_2O_3$	6	Spheres 0.2–0.5 μ diameter.
3	$\gamma-Fe_2O_3$	11	Spheres 0.2–0.5 μ diameter.
4	$\alpha-FeOOH$		Needles 0.3–0.5 μ diameter and 0.5–1 μ long.
5	Fe_3O_4		
B Bayer 1352 WF	$\alpha-Fe_2O_3$	4.4	Needles 0.2–0.3 μ diameter and 0.5–1.5 μ long.

There were investigated the variations in the chemical composition (Fe_2O_3, Fe_3O_4, FeOOH), crystal structure ($\alpha-Fe_2O_3$, $\gamma-Fe_2O_3$), particle shape (needles, spheres, complicated shapes), particle size (0.5–1.5 μ) and BET surface area (4–12 m²/g).

The other starting materials are $MnCO_3$ (Reactivul) and ZnO (Merck).

The composition of the initial mixture was Fe_2O_3 = 52.5 mole %, $MnCO_3$ = 25.4 mole %, ZnO = 22.10 mole %. The mixtures were labelled MM, and the indexes correspond to those of the ferric oxides in Table 1.

In order to clarify the formation mechanism of the Mn–Zn ferrite, there were prepared the binary ferrites $ZnO.Fe_2O_3$ and $MnO.Fe_2O_3$, using Fe_2O_3 supplied by Bayer. The wet homogenization was done in a planetary laboratory ball mill Pulverisette Fritsch.

The reactivity study was done working under non-isothermal and isothermal conditions. The experimental procedure was the same as presented in a previous work.[5] At the same time, there was determined the temperature variation of the lattice parameter a_0 of the Mn–Zn spinel.

3. RESULTS AND DISCUSSIONS

3.1. Results under non-isothermal conditions

The DTA and TG curves of $MnCO_3$ and mixtures corresponding to Mn and Zn binary ferrites are shown in figures 1–3.

The graph on $MnCO_3$ has a decarbonation effect at 495°C, followed by the formation of Mn_3O_4. At about 600°C, Mn_3O_4 passes into Mn_2O_3, which is reduced at 950°C back to Mn_3O_4. The decarbonation range of $MnCO_3$ is situated between 300 and 550°C (Fig. 1).

The X-ray diffraction pattern of the sample after thermal analysis up to 1100°C shows that the only phase present is Mn_3O_4.

The DTA curve of the sample corresponding to the formation of the Mn ferrite drows effects due to $MnCO_3$ only, proving that the formation of the ferrite does not occur up to 1100°C (Fig. 2). Unlike the Mn ferrite, the mixture corresponding to the Zn ferrite shows a marked exothermal effect at 785°C, which is due to its formation at a relatively low temperature (Fig. 3).

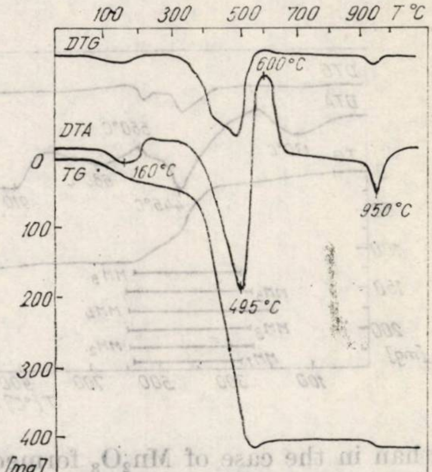

Fig. 1. — DTA and TG curves of $MnCO_3$.

Figure 4 shows the DTA curve of a ternary mixture MM_2 and the decarbonation ranges of all studied ternary mixtures. The decarbonation range of $MnCO_3$ in these mixtures is approximately the same, except MM_4 which contains the ferric oxide as FeOOH. In the latter mixture, the decompositions of $MnCO_3$ and FeOOH occur simultaneously; this lowers the initiation temperature of the decarbonation by 200°C. MM_4 is the only mixture having an exothermal effect at 730°C; the comparison with the DTA curve of the Zn binary ferrite shows that this effect could be assigned to the formation of the solid solution with the initial structure of Zn ferrite.

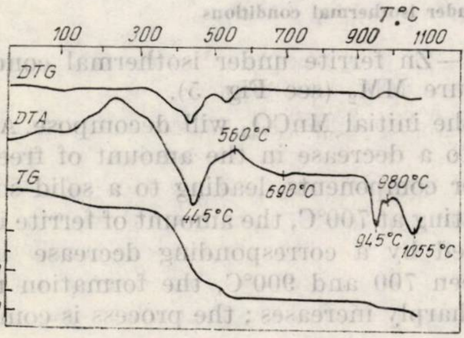

Fig. 2. — DTA and TG curves of the Mn binary ferrite.

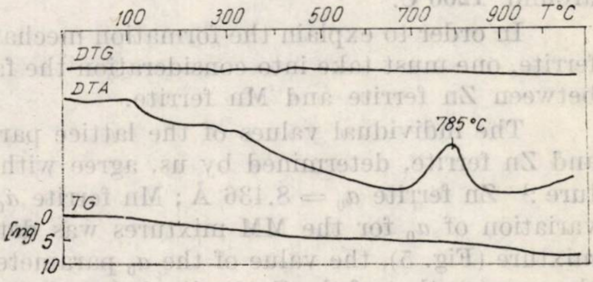

Fig. 3. — DTA and TG curves of the Zn binary ferrite.

All mixtures exhibit an exothermal effect at 675°C, due to the Néel point of Fe_2O_3, and another effect, due to the reduction of Mn_2O_3 to Mn_3O_4 at temperatures varying between 860 and 930°C; these are lower than in the case of Mn_2O_3 formed from pure $MnCO_3$, showing that under dynamic conditions the manganese oxide did not react completely up to 1000°C.

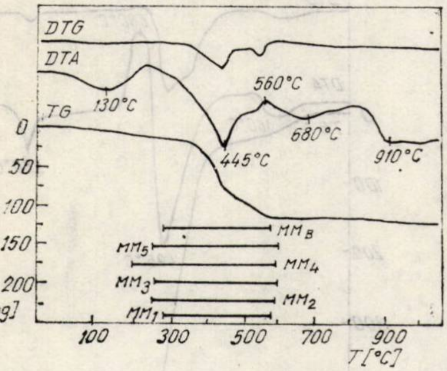

Fig. 4. — DTA and TG curves of ternary mixture MM_2 and the decarbonation ranges for all ternary mixtures studied.

Among the mixtures studied under non-isothermal conditions, MM_4 appears to be the most reactive.

3.2. Results under isothermal conditions

The formation of the Mn—Zn ferrite under isothermal conditions will be described for the mixture MM_2 (see Fig. 5).

By heating up to 600°C, the initial $MnCO_3$ will decompose. Annealing at this temperature leads to a decrease in the amount of free ZnO, because it reacts with the other components, leading to a solid solution with Zn ferrite structure. By heating at 700°C, the amount of ferrite increases; this process is accompanied by a corresponding decrease in the amounts of pure oxides. Between 700 and 900°C, the formation rate is much slower, and above 900°C sharply increases; the process is completed around 1200°C.

In order to explain the formation mechanism of the ternary Mn—Zn ferrite, one must take into consideration the fact that it is a solid solution between Zn ferrite and Mn ferrite.

The individual values of the lattice parameter a_0 of the Mn ferrite and Zn ferrite, determined by us, agree with the values found in literature:[1] Zn ferrite $a_0 = 8.436$ Å; Mn ferrite $a_0 = 8.50$ Å. The temperature variation of a_0 for the MM mixtures was determined, too. For the MM_2 mixture (Fig. 5), the value of the a_0 parameter at 600°C is approximately the same as that of the Zn ferrite, being almost identical with the a_0 parameter of the latter at 700°C. This agrees with the DTA results which suggest that the formation of the Zn ferrite is the first stage of the process.

The differences in the a_0 values for the Zn ferrite and the MM_2 mixture at 600°C are due to the incomplete formation of the Zn ferrite in the latter. Between 700 and 900°C a sharp increase of the a_0 parameter occurs, which is explained by the inclusion of Mn in the lattice of the initial Zn ferrite. This is supported by the shape of the amount of Fe_2O_3 and ZnO curves, which, instead of decreasing, mark a slight increase in the 700—900°C range. The explanation is that their crystallization rate is greater than the rate of the reaction between the two oxides. The inclusion of Mn in the Zn ferrite lattice over this temperature range has also been reported by Chol et al.[1] who used Mössbauer spectroscopy data. Disordering of the initial Zn ferrite lattice occurs consequently, which is recorded as a flat of the formation curve.

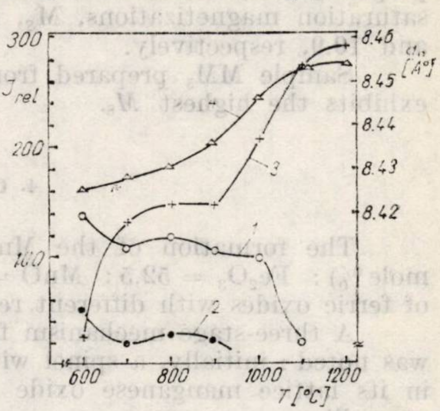

Fig. 5. — The formation mechanism of the Mn—Zn ferrite under isothermal conditions in the case of the ternary mixture MM_2 : 1 — $\alpha-Fe_2O_3$; 2 — ZnO ; 3 — $ZnFe_2O_4$; 4 — a_0.

Above 900°C, the inclusion of Mn is practically finished and the formation curve begins to go up again as the reaction between oxides and the Mn—Zn spinel formation comes closer to their completion. On the other hand, the a_0 versus temperature curve reaches above 900°C a value close to that for the Mn ferrite.

The other mixtures behave in a similar way, except MM_1 (Fig. 6). This mixture contains $\alpha-Fe_2O_3$ with the highest surface area among all used oxides (12 m²/g), which determines its higher reactivity at low temperatures. The solid solution with Zn ferrite structure formed at 600 and 700°C is consequently stable, and probably cannot subsequently include Mn. The formation curve of Mn—Zn ferrite in this mixture has no flat portion between 700 and 900°C, and the lattice parameter a_0 has, up to 1200°C, values close to those for Zn ferrite. Though the amount of ferrite formed at 1200°C is greater for the MM_1 mixture, it cannot be taken into consideration because it is not a Mn—Zn spinel.

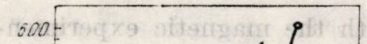

Fig. 6. — The formation mechanism of the Mn—Zn ferrite under isothermal conditions for all ternary mixtures studied : 1 — MM_1 ; 2 — MM_2 ; 3 — MM_3 ; 4 — MM_4 ; 5 — MM_5 ; 6 — MM_B.

Among the other mixtures, at 1200°C the highest amounts of Mn—Zn ferrite and, consequently, the highest reactivities of the ferric oxides under study are noted for the MM_B, MM_3 and MM_5 mixtures.

The reactivity of ferric oxides used is in correlation with the magnetic properties of resulting ferrites : the magnetic properties of the samples prepared from oxides close in reactivity are accordingly close. Thus, the saturation magnetizations, M_S, for the samples MM_B and MM_5 are 10 and 10.9, respectively.

Sample MM_5 prepared from spinel-type Fe_3O_4 with Fe^{2+} content exhibits the highest M_S.

4. CONCLUSIONS

The formation of the Mn—Zn ferrite with the composition (in mole %) : $Fe_2O_3 = 52.5$; $MnO = 25.4$; $ZnO = 22.1$, using six types of ferric oxides with different reactivities, has been studied.

A three-stage mechanism for the formation of the Mn—Zn ferrite was noted : initially, a spinel with the Zn ferrite structure forms ; then, in its lattice manganese oxide is included ; then the Mn—Zn spinel crystallizes.

Under non-isothermal conditions, by DTA, no significant differences in the reactivities of the ferric oxides used were noted ; an exception is mixture MM_4, which contains FeOOH.

Under isothermal conditions, the optimum value of the specific surface for $\alpha-Fe_2O_3$ is about 5 m²/g ; greater values lead to unsatisfactory reactivity at the higher temperatures at which the Mn—Zn ferrite formation process is completed.

The structural results are correlated with the magnetic experimental data.

The use of oxides with spinel structure which exhibit phase transformations enhances the formation of Mn—Zn ferrite.

REFERENCES

[1] G. Chol and F. Damay, *Bull. Soc. franc. Céram.*, **75**, 61 (1967).
[2] A. R. Corradi, L. Benzoni, N. Burriesci, C. A. Nannetti, M. Petrera and S. Pizzini, *J. Phys.*, **38**, Supplement C_1 291 (1977).
[3] M. F. Yan and D. W. Johnson Jr., *J. Amer. Ceram. Soc.*, **61**, 342 (1978).
[4] A. Withop, *IEEE Trans. Magn.*, **MAG—14**, 439 (1978).
[5] M. Zaharescu, M. Bălășoiu, M. Crișan, D. Crișan, T. Tăvală and N. Brînzan, *Rev. Roumaine Chim.*, **29**, 241 (1984).

Revue Roumaine de Chimie, **29**, *3*, 253–259 (1984)

III. THE EXPLOSIVE COMBUSTION OF PROPYLENE. III[1]

THE EXPLOSIVE COMBUSTION OF PROPYLENE IN A CONSTANT-VOLUME BOMB

DOMNINA POPESCU*, D. OANCEA**, V. GOŞA*, N. I. IONESCU* and B. ALBU*
* Center of Physical Chemistry, Spl. Independenţei 202, Bucharest, 77208, Romania
** The Polytechnic Institute, Department of Physical Chemistry and
Electrochemical Technology, Bd. Republicii 13, Bucharest, Romania

Received December 15, 1982

The normal burning velocities of propylene-oxygen mixtures at constant equivalence ratio, in the presence of nitrogen or carbon dioxide, have been measured in the pressure range $(0.4-1.2)\cdot 10^5$ Pa. The measurements have been carried out in a constant-volume cylindrical bomb, at room temperature. The normal burning velocities were correlated with the mixture pressure using a power law and the overall reaction orders were estimated from the baric exponent of the burning velocities.

The flame velocities of several propylene-air mixtures, at subatmospheric initial pressures, have been reported in a previous paper.[1] More complete information concerning the combustion process in these mixtures can be obtained by using the constant-volume bomb technique, allowing the measurements in a wide range of initial conditions (pressure and temperature).

In this paper, we present the results concerning the normal burning velocities for some near-stoichiometric propylene-oxygen mixtures, in the presence of various amounts of inert additives (nitrogen or carbon dioxide).

EXPERIMENTAL

The explosions were performed in a cylinder-shaped stainless steel bomb, with the volume of 1000 cm^3 and the inner diameter of 10 cm. Stainless steel electrodes having plane and parallel surfaces formed the spark gap at the center of the bomb; the spark was produced by the discharge of a standard induction coil.

The continuous change of the pressure in the explosion bomb was measured by means of a piezoelectric pressure transducer Kistler, type 601 A, mounted at the cell bottom. The output signal of the transducer was amplified by a Kistler Charge Amplifier, type 5001 SN, and monitored with a cathodic oscilloscope Hewlett Packard type 1707 B.

The gaseous mixtures were prepared by the partial pressures method using the glass installation previously described,[2] for total pressures lower or equal to the atmospheric pressure. A similar installation, having several 10 l metallic cylinders for the storage of gaseous mixtures, was used for the preparation of mixtures at a total pressure of $(4 \div 5)\cdot 10^5$ Pa. The mixing of gases was supposed to be complete after 3 days (checked by gas chromatographic analyses).

Reagents: Propylene had 99.4 % purity, oxygen and nitrogen 98.6 and 99.0 % respectively. Carbon dioxide was technical grade. Oxygen, nitrogen and air were dried before use according to the method previously described.[2]

Operating mode: From the oscillograms, photographically recorded, the pressure in the explosion bomb was measured in any moment after ignition. Any detectable pressure rise in the bomb was considered as an explosion. A typical oscillogram is shown in figure 1, where ΔP_f is the maximum pressure rise observed in the explosion.

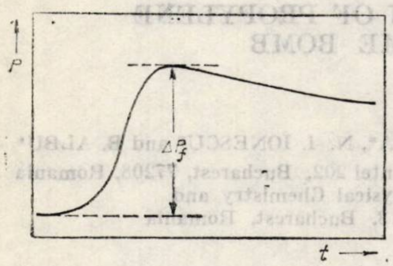

Fig. 1. — The pressure rise in a closed bomb during an explosion.

From the instantaneous values of the pressure in the bomb, the normal burning velocities corresponding to each of these presssures were calculated, according to the equations developed by Lewis and von Elbe [3,4] for the case of explosions in closed spherical vessels:

$$v_n = \left(\frac{r_0}{r_f}\right)^2 \left(\frac{P_0}{P}\right)^{1/\gamma} \frac{dr_0}{dt} \tag{1}$$

where P_0 is the initial pressure of the gaseous mixture

P is the pressure in the bomb, at the time t

r_0 is the radius of the sphere which contained the fraction x of gas, before its combustion

r_f is the radius of the sphere occupied by the fraction x of burned gas (the radius of the sphere of burned gas, at any instant)

$\gamma = \frac{C_P}{C_V}$; C_P and C_V are the mean heat capacities of the mixture at constant pressure and volume,

and

$$r_0 = R_0 x = R_0 \frac{P - P_0}{P_f^* - P_0} \tag{2}$$

$$r_f = R_0 \left[1 - \left(\frac{P_0}{P}\right)^{1/\gamma} \cdot \frac{P_f^* - P}{P_f^* - P_0}\right]^{1/3} \tag{3}$$

Here, P_0 and P have the same meaning as above, P_f^* is the maximum pressure obtained in the explosion, corrected according to the model of adiabatic combustion [5] and R_0 is the radius of a sphere equivalent to the explosion bomb (having the same volume).

Equations (1)—(3) were used only for the analysis of the early stage of explosions, when the radius of the sphere of burned gas, r_f, is less than the inner radius of the cylindrical cell. One can suppose that under these conditions, the spherical propagation of the combustion wave is not disturbed. Usually, this situation corresponds to a fraction of burned gas, x, less or equal to 0.3. In view of this, the pressure recording during the explosion of a mixture with a well-known composition, at constant initial pressure, was made twice. The first record gives the peak pressure P_f, from which the values P_f^* are determined.[5] The second record was made at a greater sensitivity of the charge amplifier, as to measure accurately the pressure P in the early phase of the explosion, using 15—30 points on the oscillogram.

The evaluation of r_0, r_f, dr_0/dt and v_n from the experimental data was made on a computer CORAL type 4011, using a program written in FORTRAN.

Experimental conditions: The explosive mixtures enlisted in table 1 were kept at constant initial temperature (20°C) and various initial pressures, within the range $(0.4 \div 1.2)10^5$ Pa

For each mixture, the value of the equivalence ratio φ, calculated by the formula:

$$\varphi = \frac{[C_3H_6]/[O_2]}{([C_3H_6]/[O_2])_{\text{stoichiometric}}} \tag{4}$$

is also given, where the square brackets indicate the partial pressure.

Table 1

The composition of the studied systems

Mixture no.	$[C_3H_6]$	$[O_2]$	$[N_2]$	$[CO_2]$	φ
	(vol. %)				
I	10.5	44.5	45.0	—	1.060
II	8.3	36.7	55.0	—	1.013
III	6.0	25.1	68.9	—	1.076
IV	4.5	20.1	75.4	—	1.014
V	10.2	45.9	—	43.9	0.999
VI	8.0	36.1	—	55.9	0.998
VII	6.0	27.0	—	67.0	0.993

RESULTS AND DISCUSSIONS

The combustion of gaseous mixtures in closed vessels is a nonstationary process, characterized by the continuous change of the explosion parameters, as long as the explosion proceeds : the radius of the combustion wave, the flame front velocity, the normal burning velocity, the temperature of burned and unburned gases, respectively. The possibility of evaluating the momentary values of all these parameters only from the pressure-time records of the explosion is given by equations (1)—(3), provided that their use is limited to small values of the fraction x of burned gas. This limitation was done after the analysis of the experimental records $\Delta P = f(t)$ obtained for several mixtures. It was observed that in all cases, the pressure rise ΔP during the early stage of an explosion changed according to the equation :

$$\Delta P = a\, t^b \tag{5}$$

where b takes positive values between 2.8 and 3.5 for the studied mixtures. This type of equation, already found in the case of combustions in spherical vessels,[6] holds until the fraction of burned gas is less or equal to 0.4, which is a rather large value. Afterwards, ΔP has a slower increase, due to a greater extent of heat losses to the walls. At the same time, the values of r_0 change according to the following relationship :

$$r_0 = ct + d \tag{6}$$

which was also found for all the studied systems. The slopes $\mathrm{d}r_0/\mathrm{d}t$ have been used for calculating the normal burning velocities v_n, according to equation (1). A typical set of values of ΔP, r_0, r_f and v_n is given in table 2.

The data show that the normal burning velocities decrease during the explosion, as the pressure in the bomb increases. The typical aspect of the dependence $v_n = f(P)$ is shown in figure 2, for two systems having the same initial conditions, but different inert diluents. It can be seen that the values of the normal burning velocity of system I ($C_3H_6-O_2-N_2$) are twice the values of the normal burning velocity of system V ($C_3H_6-O_2-CO_2$).

Table 2

The characteristic parameters of the explosion in the mixture : 6.0 % C_3H_6–27.0 % O_2–67.0 % CO_2, in a closed cylindrical bomb of volume $V = 1000$ cm^3 ; $P_0 = 9.19 \cdot 10^4$ Pa, $P_f^* = 5.48 \cdot 10^5$ Pa ; $T_0 = 295$ K

$t \cdot 10^3$ (s)	$P \cdot 10^{-4}$ (Pa)	r_0 (cm)	r_f (cm)	v_n (cm/s)
0	9.19	0	0	21.56
4	9.31	0.917	1.546	21.55
8	9.43	1.155	1.940	21.49
12	9.68	1.454	2.424	21.38
16	9.93	1.665	2.775	21.27
20	10.43	1.973	3.220	21.07
24	10.93	2.206	3.552	20.88
28	11.68	2.486	3.925	20.61
32	12.42	2.713	4.208	20.36
36	13.42	2.967	4.500	20.06
40	14.67	3.233	4.777	19.72
44	15.67	3.418	4.955	19.47
48	17.45	3.701	5.201	19.09
52	19.20	3.046	5.393	18.75
56	20.95	4.164	5.546	18.44
60	23.20	4.414	5.706	18.10

For each experiment, the dependence of the normal burning velocity on the pressure reached during the explosion has the form :

$$v_n = mP^{-n} \qquad (7)$$

The values of m and n for three of the studied systems, are given in table 3. This table also gives the values of the normal burning velocities at normal pressure (v_n^0), calculated by extrapolation of equation (7) to initial pressure, in experiments starting from $P_0 = 1.013 \cdot 10^5$ Pa. For instance, for system IV (stoichiometric mixture of propylene and air), it was found

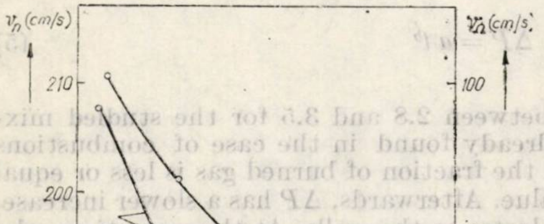

Fig. 2. — The influence of pressure on normal burning velocities during the explosion in a closed bomb. (1) — system I ; (2) — system V.

that $v_n^0 = 42.7$ cm/s, which is in very good agreement with the values obtained by the tube method [7] or by the burner method.[8]

The values of the normal burning velocities at normal atmospheric pressure, for all systems, have been enlisted in table 4 and can be compared, taking into account that systems I—VII have approximately the same equivalence ratio ($\varphi \simeq 1$) and increasing amounts of inert additives :

Table 3

The coefficients of the dependency $v_n = mP^{-n}$, for some propylene-oxygen-inert mixtures

System	$[C_3H_6]$ (vol. %)	φ	$P_0 \cdot 10^{-4}$ (Pa)	m	n
Propylene-oxygen-nitrogen	4.5	1.014	4.74	264.3	0.1036
			5.36	273.2	0.1646
			6.76	270.0	0.1648
			8.12	278.2	0.1623
			9.45	278.0	0.1625
			10.70	277.5	0.1636
	6.0	1.076	3.45	433.0	0.1530
			4.77	469.5	0.1559
			6.11	488.8	0.1524
			7.34	489.0	0.1542
			8.73	488.9	0.1552
Propylene-oxygen-carbon dioxide	6.0	0.993	4.08	182.2	0.1891
			5.33	188.2	0.1904
			6.67	183.8	0.1838
			7.85	186.8	0.1880
			9.20	186.9	0.1889

— the increase of nitrogen concentration from 45 % to 75 % results in a decrease of normal burning velocities at normal atmospheric pressure, v_n^0, for the systems I—IV. The same remark holds for systems V—VII, at the increase of carbon dioxide concentration from 44 % to 67 %.

Table 4

The influence of the nature on inert gas on the normal burning velocities of propylene-oxygen mixtures, at normal atmospheric pressure

$C_3H_6-O_2-N_2$					$C_3H_6-O_2-CO_2$				
$[C_3H_6]$ (vol %)	$[O_2]$ (vol %)	$[N_2]$ (vol %)	φ	v_n^0 (cm/s)	$[C_3H_6]$ (vol %)	$[O_2]$ (vol %)	$[CO_2]$ (vol %)	φ	v_n^0 (cm/s)
10.5	44.5	45.0	1.060	225	10.2	45.9	43.9	0.999	85
8.3	36.7	55.0	1.013	116	8.0	36.1	55.9	0.998	55
6.0	25.1	68.9	1.076	83	6.0	27.0	67.0	0.993	21

— the substitution of nitrogen from systems I—III by carbon dioxide (systems V—VII) leads to a systematic decrease of normal burning velocities, which is a strong proof for the good stabilisation effect of carbon dioxide. Moreover, system VIII, analogous to system IV and containing carbon dioxide instead of nitrogen, is outside the flammability limits of the $C_3H_6-O_2-CO_2$ mixture.

By extrapolation of equation (7), the normal burning velocities corresponding to each initial pressure have been calculated. These values $v_n[P_0]$ are given in table 5, for some of the studied mixtures.

Table 5

The normal burning velocities of some propylene mixtures, at different initial pressures

$C_3H_6-O_2-N_2$				$C_3H_6-O_2-CO_2$	
System I		System II		System VII	
$P_0\cdot10^{-4}$ (Pa)	$v_n[P_0]$ (cm/s)	$P_0\cdot10^{-4}$ (Pa)	$v_n[P_0]$ (cm/s)	$P_0\cdot10^{-4}$ (Pa)	$v_n[P_0]$ (cm/s)
2.29	201.8	3.95	110.8	4.07	24.47
3.60	202.3	5.27	117.6	5.32	23.71
4.76	208.1	6.64	123.8	6.65	22.58
6.08	216.7	7.97	125.6	7.84	22.36
7.58	236.0	8.07	126.1	9.18	21.57

From these data, the pressure influence on normal burning velocities was found to be expressed by the relationship:

$$v_n[P_0] = \alpha P_0^{\beta} \tag{8}$$

This type of dependence was also found for other hydrocarbon-oxygen-inert systems, by soap bubble[9] or constant-volume bomb measurements.[10-12] As Strauss and Edse remarked,[9] the baric exponent β is negative in the mixtures having normal burning velocities at atmospheric pressure less than 50 cm/s and the mixtures with v_n^0 higher than 50 cm/s have positive values of the baric exponent respectively. Indeed, the β values calculated from the data given in table 5 are:

$$\beta = 0.157 \text{ (system I)}$$

$$\beta = 0.188 \text{ (system II)}$$

$$\beta = -0.157 \text{ (system VII)}$$

Taking into account the relationship between β, the baric exponent of normal burning velocities and s, the overall reaction order of the combustion process:

$$\beta = \frac{s-2}{2} \tag{9}$$

suggested by Potter and Berlad[10] for the case when dissociation reactions as well as the dependence of flame temperature on pressure could be neglected, the reaction orders for the studied systems have been calculated and are given in table 6.

Table 6

The overall reaction order, *s*, for the explosion of several propylene-oxygen-diluent mixtures with constant equivalence ratio

Explosive system	Mixtures no.	$[C_3H_6]$ (vol %)	β	*s*
$C_3H_6-O_2-N_2$	I	10.5	0.157	2.31
	II	8.3	0.188	2.38
$C_3H_6-O_2-CO_2$	VII	6.0	−0.157	1.69

The substitution of nitrogen by carbon dioxide seems to change not only the physical properties of the propylene-oxygen-inert system, but also the course of the chemical reactions. The lack of complete data concerning the pressure dependence of normal burning velocities for the propylene-oxygen-diluent systems does not allow any further correlations.

In conclusion, our results indicate that the model of the burning process in a closed cylindrical bomb was correct and in good agreement with the experiment. If only the early stage of an explosion (i.e. until the flame radius is less than the inner radius of the cylindrical cell) is used, one can obtain the same information on the burning process as in the case of a spherical bomb.

REFERENCES

[1] R. H. Schuster, N. I. Ionescu, D. Oancea, D. Popescu and V. Goșa, *Rev. Roumaine Chim.*, **26**, 819 (1981).

[2] D. Popescu, V. Goșa, R. H. Schuster, N. I. Ionescu and D. Oancea, *Rev. Roumaine Chim.*, **26**, 927 (1981).

[3] J. Manton, G. von Elbe and B. Lewis, in "Proceedings of the IVth Symposium (International) on Combustion", The Williams and Wilkins Company, Baltimore, 1953, p. 358.

[4] B. Lewis and G. von Elbe, "Combustions, Flames and Explosions of Gases" Academic Press Inc., New York, 1961, p. 374.

[5] D. Oancea, V. Goșa, N. I. Ionescu and D. Popescu, (to be published).

[6] H. Perlee, F. Fuller and C. Saul, "U. S. Bureau of Mines Report of Investigations" no. 7839, 1974.

[7] M. Gerstein, L. Levine and E. Wong, *J. Amer. Chem. Soc.*, **73**, 418 (1951).

[8] T. Scholte and V. Vaags, *Combust. Flame*, **3**, 495 (1959).

[9] W. Strauss and R. Edse, in "Proceedings of the VIIth Symposium (International) on Combustion", Butterworths, London, 1959, p. 377.

[10] A. Potter and A. Berlad, in "Proceedings of the VIth Symposium (International) on Combustion", Reinhold Publ. House, New York, 1957, p. 27.

[11] V. Babkin and L. Kozacenko, *Fizika Gorenyia i Vzryva*, **3**, 77 (1966).

[12] M. Metghalchi and J. Keck, *Combust. Flame*, **38**, 143 (1980).

Revue Roumaine de Chimie, **29**, *3*, 261–265 (1984)

VAPOUR – LIQUID EQUILIBRIUM AT ATMOSPHERIC PRESSURE OF THE TOLUENE – ACETIC ANHYDRIDE AND ACETIC ANHYDRIDE – *o*-XYLENE SYSTEMS

GH. MIHĂILĂ, N. BÎLBĂ, D. DRANGA and C. LUCA
Department of General and Technological Chemistry,
Polytechnic Institute, Splai Bahlui 71, Iaşi, Romania

Received September 27, 1982

Vapour–liquid equilibrium of the toluene – acetic anhydride and acetic anhydride – *o*-xylene systems was measured at atmospheric pressure using a Bushmakin recirculation glass still. The acetic anhydride–*o*-xylene system presents an azeotropic point (62.3% acetic anhydride and 37.7% *o*-xylene) with minimum boiling temperature (133.5°C). The experimental data were tested for thermodynamic consistency by means of Herington's procedure.

INTRODUCTION

Vapour – liquid equilibrium in the binary and ternary systems with acetic anhydride has been little studied. Thus, up to now, there have been studied its systems with pyridine,[1,2] methylenediacetate and cyclohexane.[2] The binary systems to be studied in this paper are connected to the antimony acetate manufacture by means of the reaction between antimony trioxide and acetic anhydride in aromatic hydrocarbons medium in which, after separation of the reaction product, a mixture of acetic anhydride excess and solvents remains. In order to obtain the data necessary for a separation plant design, the vapour – liquid equilibrium in the binary systems toluene–acetic anhydride and acetic anhydride–*o*-xylene was measured at atmospheric pressure.

EXPERIMENTAL

Reagents. Toluene, *o*-xylene, and acetic anhydride were supplied at chromatography grade and used without further purification. The three-parameters equation, $\lg p = A + B/t + C$, was used to calculate the vapour pressure of components in pure state at equilibrium temperature. The necessary physical constants were found in the literature and are reported in table 1.

Apparatus. Experimental vapour – liquid equilibrium data were determined by using a conventional Bushmakin recirculation glass still described in the literature.[4] Pressure was regulated by an electric manostat.[5] Variation of pressure in the system was estimated to be, at the most, 1 mm of mecury. Boiling temperature of the mixtures was determined with a precision as high as ± 0.1°C. A total load of about 100 ml was used for each experiment. After 90 minutes of gentle boiling, the steady state was established, and liquid and vapour samples were taken simultaneously and directly analysed.

Table 1

Physical constants of pure components [3]

Physical constant	Component		
	Toluene	*o*-Xylene	Acetic anhydride
Boiling point, °C	110.6	144.4	139.6
Refractive index, n_D^{20}	1.49693	1.50545	1.39020
Parameters for equation $p = f(t)$: A	6.95334	6.99891	7.12165
B	1343.94	1474.68	1427.77
C	219.38	213.69	198.04

Analytical method. The equilibrium samples were analysed refractometrically, using an Abbé refractometer. For this reason a calibration curve, refractive index vs. composition, was constructed on the basis of refractive index measurement for several mixtures with known composition of the two systems. Dependence of refractive index on composition for the two investigated systems is listed in table 2.

Table 2

Dependence of the refractive index, n_D^{20}, on composition for the two investigated systems

Content of light volatile component, % mol	System	
	Toluene-acetic anhydride	Acetic anhydride-*o*-xylene
0.0	1.3902	1.5051
10.0	1.4014	1.4946
20.0	1.4122	1.4842
30.0	1.4230	1.4738
40.0	1.4337	1.4630
50.0	1.4443	1.4519
60.0	1.4550	1.4411
70.0	1.4658	1.4295
80.0	1.4764	1.4173
90.0	1.4870	1.4033
100.0	1.4962	1.3902

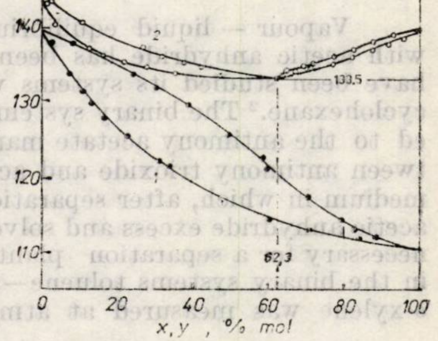

Fig. 1. — The $t - X, Y$ diagram at 760 mm Hg: 1 — Toluene—acetic anhydride; 2 — Acetic anhydride—*o*-xylene.

Results. The experimental data as regards the composition of the phases and their boiling temperature at steady state are summarized in table 3. The content of light volatile component, expressed in molar percents, in the liquid phase, was noted by X_1 and, in the gaseous phase, by Y_1. Together with these data, in table 3, are also given the activity coefficients γ_1 and γ_2, as well as $\lg\gamma_1/\gamma_2$, data needed for the thermodynamic consistency test. Using the data set out in table 3, the $t - X, Y$ diagram was constructed in figure 1 and $Y - X$ diagram, in figure 2.

As it comes out from both figure 1 and figure 2 the acetic anhydride—*o*-xylene system presents an azeotropic point with minium boiling temperature (133.5°C) at $X_1 = 62.3\%$.

Fig. 2. — The Y — X diagram at 760 mm Hg : 1 — Toluene-acetic anhydride ; 2 — Acetic anhydride—o-xylene.

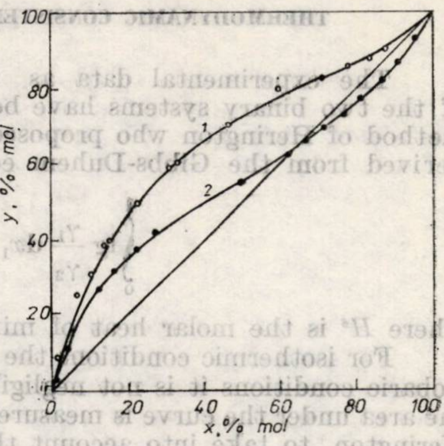

Table 3

Experimental data of the vapour — liquid equilibrium

t, °C	X_1, % mol	Y_1, % mol	γ_1	γ_2	$\lg(\gamma_1/\gamma_2)$
1. *Toluene—acetic anhydride*					
139.6	0.00	0.00	1.8100	1.0000	0.2576
138.0	2.40	8.80	1.7877	0.9662	0.2672
133.6	7.80	24.00	1.6710	0.9788	0.2322
131.6	10.80	30.50	1.6123	0.9869	0.2131
129.5	14.40	38.80	1.5803	0.9537	0.2195
127.5	16.00	39.70	1.5722	1.0294	0.1839
125.5	22.70	49.70	1.4622	0.9890	0.1698
122.4	31.50	58.50	1.3443	1.0232	0.1185
121.6	33.90	60.00	1.3087	1.0452	0.0976
117.5	46.80	70.20	1.2386	1.0915	0.0348
114.4	60.00	79.80	1.1962	1.0811	0.0439
113.2	71.50	82.80	1.0768	1.3294	−0.0915
113.0	79.00	85.60	1.0132	1.5327	−0.1797
112.3	84.30	88.00	1.0057	1.7340	−0.2365
112.0	88.00	90.50	0.9837	1.8232	−0.2679
110.7	100.00	100.00	1.0000	2.2500	−0.3522
2. *Acetic anhydride—o-xylene*					
144.2	0.00	0.00	2.5900	1.0000	0.4132
143.2	1.00	2.86	2.5572	1.0314	0.3943
140.5	4.00	10.20	2.4782	1.0804	0.3605
137.2	12.50	26.20	2.1972	1.0645	0.3147
136.2	16.30	31.22	2.0795	1.0657	0.2903
135.2	22.10	37.30	1.9003	1.0694	0.2496
134.7	27.50	41.95	1.7699	1.0905	0.2103
133.7	35.50	47.00	1.5722	1.1354	0.1413
133.6	50.00	54.00	1.2865	1.2736	0.0043
133.5	62.30	62.30	1.1968	1.3894	−0.0648
134.2	67.00	65.80	1.1395	1.4115	−0.0929
134.7	71.40	69.50	1.1208	1.4370	−0.1079
135.0	77.00	72.10	1.0621	1.6174	−0.1826
135.8	81.50	77.00	1.0482	1.6290	−0.1914
137.2	87.20	82.06	0.9864	1.7694	−0.2537
137.9	91.20	87.00	0.9931	1.8226	−0.2636
138.8	96.00	93.00	0.9817	2.0978	−0.3297
139.6	100.00	100.00	1.0000	2.3000	−0.3617

THERMODYNAMIC CONSISTENCY OF EXPERIMENTAL DATA

The experimental data as regards vapour—liquid equilibrium of the two binary systems have been tested thermodynamically by the method of Herington who proposed an equation for isobaric conditions derived from the Gibbs-Duhem equation:

$$\int_0^1 \lg \frac{\gamma_1}{\gamma_2}\, dx_1 = \int_{T_1}^{T_2} \frac{2H^e}{RT^2}\, dT$$

where H^e is the molar heat of mixing.

For isothermic conditions the right-hand term is negligible, but for isobaric conditions it is not negligible. From the graph $\lg(\gamma_1/\gamma_2) = f(x_1)$, the area under the curve is measured and compared with values given by Herington to take into account this second term of the integral. The entire method is reported by Hála et al.[6]

The activity coefficients from experimental data (X_i, Y_i, P and t) were calculated for each component using equation

$$\gamma_i = \frac{PY_i}{p_i X_i}$$

where P is the total pressure and p_i is the pressure of ith component in pure state.

For both systems the plot, $\lg(\gamma_1/\gamma_2) = f(x_1)$, is represented in figure 3. Values of positive areas (A_i), negative areas (B_i), integral (I) and Herington's terms are listed in table 4.

As can be seen in table 4, the experimental data as regards vapour — liquid equilibrium of the two systems investigated are thermodynamically consistent, according to Herington consistency test, because either $I = 0$, or $D - J < 10$.

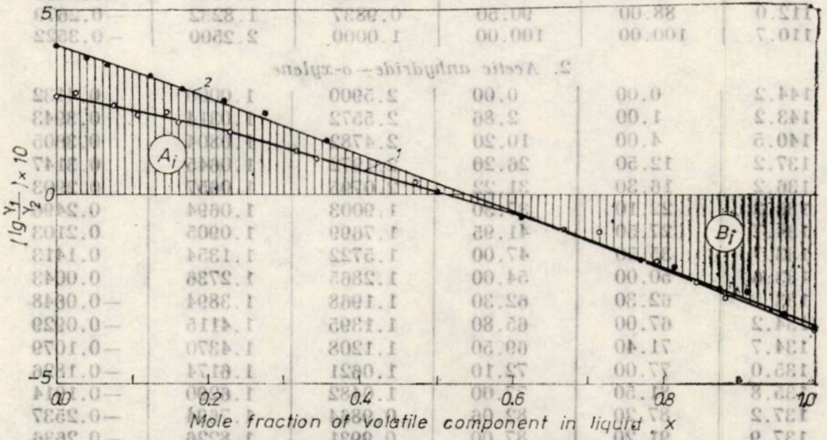

Fig. 3. — Herington consistency test: 1 — Toluene—acetic anhydride; 2 — Acetic anhydride—*o*-xylene.

Table 4

Data as regards Herington consistency test

System	*A*, a.u.	*B*, a.u.	*I*, a.u.	*D*	*J*	*D−J*
Toluene—acetic anhydride	0.0761	−0.0764	−0.0003	—	—	—
Acetic anhydride—*o*-xylene	0.0810	−0.0782	0.0028	1.75	2.25	−0.5

CONCLUSIONS

From the experimental results presented above, the following conclusions may be drawn:

1. The $t - X$, Y and $Y - X$ diagrams of the toluene — acetic anhydride and acetic anhydride — *o*-xylene systems were constructed.

2. The acetic anhydride — *o*-xylene system presents an azeotropic point with minimum boiling temperature (133.5°C) which contains 62.3% mol acetic anhydride and 37.7% mol *o*-xylene.

3. The vapour — liquid experimental data of both investigated systems satisfy the Herington's criterion of thermodynamic consistency.

REFERENCES

[1] P. A. Helson and A. E. Markham, *J. Amer. Chem. Soc.*, **72**, 2417 (1950).

[2] H. E. Jones, *J. Chem. Eng. Data*, **7**, 13 (1962).

[3] * * * "Spravochnik khimika", vol. I, Goskhimizdat, Leningrad, 1962, p. 706 and 1031.

[4] V. B. Kogan, V. M. Fridman and V. V. Kafarov, "Ravnovesie mezhdu zhidkosti i parom". Nauka, Moscow, 1966, p. 17.

[5] Gh. Mihăilă and Gh. Bendescu, *Anal. St. Univ. "Al. I. Cuza" Iaşi*, **11**, 99 (1965).

[6] E. Hála, J. Pick, V. Fried and O. Vilim, "Vapour — Liquid Equilibrium", Pergamon Press, Oxford, 1967, p. 331.

Revue Roumaine de Chimie, **29**, *3*, 267—273 (1984)

CONTRIBUTIONS TO THE CHEMISTRY OF THIOCOMPLEXES. I

COMPLEX COMBINATIONS OF Pd(II) WITH 4-(ARYLSULFONYL)-THIOBENZAMIDES

D. NEGOIU*, S. NEAGOE** and MARIA NEGOIU*

* Polytechnical Institute of Bucharest, Faculty of Chemical Technology, 1 Str. Polizu, 78126-Bucharest, Romania

** Institute of Petroleum and Gases, Ploiești, Romania

Received May 4, 1983

Three complex combinations of palladium (II) with 4-(arylsulfonyl)-thiobenzamides of the type [$PdLCl_2$] were synthesized. Elemental chemical analysis suggested a formulation for these combinations. Conductivity measurements were carried out and infrared, visible and ultraviolet spectra were recorded and interpreted.

The chemical literature provides information on the complex combinations of some transition metals with donor ligands such as sulfur,[1] sulfur and oxygen,[2-6] sulfur and nitrogen, [7-11] and sulfur, nitrogen and oxygen.[12] Data concerning the complex combinations with 4-(arylsulfonyl)-thiobenzamides are, however, scarce.

It is known [13,14] that sulfur, as a donor atom, has empty *d* orbitals which can be used to form $d_\pi - d_\pi$ bonds with transition metals, even when these are in lower, uncommon oxidation states.

The donors with sulfur form much stronger bonds with group B metals than the donors with oxygen.[15] The oxidation state of the metal affects the character of group B elements, which is more significant in the case of the lower oxidation states.

Transition metals, which contain pairs of nonbonding *d* electrons, can form $d_\pi - d_\pi$ bonds by donating these electrons to the ligand. Thus, the low-spin metal ions, such as Pd(II), Pt(II) and Au(III), having the electronic configuration d^8, or Cu(I), Ag(I), Au(I) and Hg(II), having the electronic configuration d^{10}, form complex combinations in which strong σ bonds as well as $d_\pi - d_\pi$ bonds occur with sulfur-containing donor ligands.

Ligands which involve sulfur and nitrogen donor atoms behave similarly to those containing only sulfur donor atoms. However, the nitrogen atoms have a tendency to decrease the solutibility of the complex combinations in non-aqueous solvents, so that the complexes with sulfur- and nitrogen-containing ligands are in general less soluble or even insoluble in nonpolar solvents. Based on published experimental data,[14] we concluded that ligands containing sulfur and nitrogen cause a slight decrease of the interelectronic repulsion energy as compared to ligands containing only sulfur.

Since the thioamides are ligands which include in their molecules sulfur and nitrogen donor atoms, they are in fact weak Lewis bases and, according to Pearson's principle,[16] they are preferred by the weak Lewis acids, which belong to the B-type class of acceptors.[15]

This paper presents the results of our research on the complex combinations of Pd(II) with ligands of the 4-(arylsulfonyl)-thiobenzamide series,[17] known from the chemical literature:

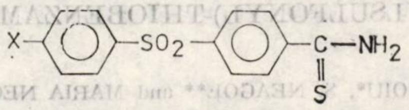

where X = H; 4-(phenylsulfonyl)-thiobenzamide ($C_{13}O_2NS_2H_{11}$);
X = Cl; 4-(4'-chlorophenylsulfonyl)-thiobenzamide ($C_{13}O_2NS_2H_{10}Cl$);
X = Br; 4-(4'-bromophenylsulfonyl)-thiobenzamide ($C_{13}O_2NS_2H_{10}Br$).

RESULTS AND DISCUSSION

The complex combinations of Pd(II) with 4-(arylsulfonyl)-thiobenzamides appear as microcrystals, coloured in various shades of brown depending on the nature of the ligand. They are sparsely soluble in inorganic and organic solvents (with the exception of dimethylsulfoxide (DMSO), in which the solubility is large) and have high melting points compared to the corresponding thioamides (Table 1). The complex combinations were prepared by mixing under refrigeration an ethanolic solution of thioamide with an aqueous solution of palladium dichloride.

Table 1

Elemental chemical analysis of the complex combinations of Pd(II) with 4-(arylsulfonyl)-thiobenzamides

Compound	Element analyzed (%) theor./exptl.					Melting point (°C)	Colour
	Pd	C	H	S	N		
$C_{13}O_2NS_2H_{11}$	—	56.29 56.40	3.99 4.02	—	5.05 5.25	180	yellowish-white
$C_{13}O_2NS_2H_{10}Cl$	—	50.07 50,27	4.20 4.32	—	4.48 4.89	178	yellow-orange
$C_{13}O_2NS_2H_{10}Br$	—	43.82 44.10	2.85 3.05	—	3.03 4.10	245	yellow-orange
$[Pd(C_{13}O_2NS_2H_{11})Cl_2]$	19.94 19.88	29.23 28.74	1.87 1.82	11.99 12.50	—	299	light brown
$[Pd(C_{13}O_2NS_2H_{11}Cl)Cl_2]$	21.75 21.68	31.88 31.70	2.04 1.60	13.08 12.82	—	254	brown
$[Pd(C_{13}O_2NS_2H_{10}Br)Cl_2]$	23.40 23.18	34.33 35.20	2.42 2.90	13.55 14.08	—	175	dark brown

The results of the elemental chemical analysis of the obtained compounds are given in Table 1. The results support the following formulation for these complex combinations:

$$[PdLCl_2]$$

where $L = C_{13}O_2NS_2H_{11}$, $C_{13}O_2NS_2H_{10}Cl$ or $C_{13}O_2NS_2H_{10}Br$.

Complex combinations of the type $[PdL_2]Cl_2$ between Pd(II) and thioamides are also known.[9-11] Only one molecule of thioamide is included in the molecule of the complex combinations obtained by us, which may be caused by the large volume of the ligand, producing steric hindrance.

Conductometric measurements also supported the formulas presented in Table 1 for our complex combinations. The values of the molar conductivities of the complexes of Pd(II) with 4-(arylsulfonyl)-thiobenzamides are given in Table 2. Molar conductivity determinations were carried out after dissolving the complexes in DMSO. The values obtained allowed us to conclude that these complex combinations have non-electrolytic properties, in agreement with the limits mentioned in the literature for the molar conductivities in DMSO.[18]

Table 2

Molar conductivities of the complex combinations of Pd(II) with 4-(arylsulfonyl)-thiobenzamides

Compound	Concentration ($\times 10^{-4}$ *M*)	Molar conductivity (Ω^{-1} cm^2 mole^{-1})
$[Pd(C_{13}O_2NS_2H_{11})Cl_2]$	1.77	7.37
$[Pd(C_{13}O_2NS_2H_{10}Cl)Cl_2]$	1.43	4.05
$[Pd(C_{13}O_2NS_2H_{10}Br)Cl_2]$	1.16	9.23

SPECTRA OF THE COMPLEX COMBINATIONS

The IR spectra of thioamides and of their corresponding complex combinations obtained by us are systematized in Table 3 and discussed below by spectral regions.

The bands which are characteristic of associated $-NH_2$ groups, $\nu_{assoc.\ NH_2}$, both in the ligands and in the complex combinations appear in the 3500—3000 cm^{-1} range; we note that in the spectra of the complexes the peaks are slightly shifted towards lower frequencies and have smaller intensities. This fact confirms the assumption that the $-NH_2$ group participates in the formation of the investigated complex combinations.

Bands assignable to coupled vibrations ($\delta_{NH_2} + \nu_{CN}$) appear in the range 1650—1600 cm^{-1}. The strong absorption bands characteristic of the coupled vibrations $\delta_{NH_2} + \nu_{CN}$ in thioamides occur at lower frequencies in the spectra of the complex combinations (Table 3) and with varying

Table 3

Characteristic IR frequencies of thioamides and of the complex combinations of Pd(II) with thioamides (cm^{-1}).*

Compound	Vibrations of $-\underset{\underset{S}{\parallel}}{C}=NH_2$ group				Vibrations of benzenic rings			Vibrations of SO_2 group		Vibrations of C—X bond
	3500—3000 ν_{NH_2}	1650—1600 $\delta_{NH_2}+\nu_{CN}$	1600—1400 $\nu_{CN}+\delta_{NH}$	1400—1200 $\nu_{C=S}$	3100—3000 ν_{C-H}	1600—1400 $\nu_{C\cdots C}$	900—700 γ_{C-H}	1350—1300 $\nu_{asym.SO_2}$	1200—1100 $\nu_{sym.SO_2}$	ν_{C-X}
$C_{13}O_2NS_2H_{11}$	3375s 3355sh 3290m 3190s	1640s	1420s	1290s	3080sh 3060sh	1600 1580sh 1480w	850s 775 710	1310m	1170s	—
$C_{13}O_2NS_2H_{10}Cl$	3400s 3300w 3290m 3160s	1625s	1420s	1290s	3095w 3060w	1595s 1580m 1490w	850s	1315m	1170s	770s
$C_{13}O_2NS_2H_{10}Br$	3370s 3330w 3290m 3170s	1650s	1420s	1290s	3085w 3065sh	1600w 1580s 1480m	850s	1310m	1170s	580s
$[Pd(C_{13}O_2NS_2H_{11})Cl_2]$	3350w 3280w	1630m	1400m	1315	3095w	1590sh	850m 770sh 720sh	1310w	1165m	—
$[Pd(C_{13}O_2NS_2H_{10}Cl)Cl_2]$	3410w 3355w	1600sh	1405m	1285w	3105w	1590m	845m	1330w	1165m	770s
$[Pd(C_{13}O_2NS_2H_{10}Br)Cl_2]$	3410w	1580w	1490m	1280w	3060w	1580w 1475sh	850m	1330w	1160m	580s

* Abbreviations : s — strong, m — medium, w —weak, sh — shoulder.

intensities. This also supports the assumption that the $-NH_2$ group participates in the bond formation.

Bands assignable to the coupled vibrations $\nu_{CN} + \delta_{NH}$ appear in the 1600—1400 cm^{-1} range. The relatively strong absorption band occurring in this region of the spectra, due to the coupled vibrations $\nu_{CN} + \delta_{NH}$ in thioamides, appears at somewhat lower frequencies (1400—1390 cm^{-1}) and with diminished intensity in the spectra of our complex combinations.

The increased intensity of this band in the spectra of thioamides can be attributed to its overlap with the absorption band produced by the valence vibration $\nu_{C\overset{...}{=}C}$ in aromatic rings. Its modifications can be accounted for by p-π-type electronic displacements in the thioamide group caused by complexation.

The band due to the vibration of the thiocarbonyl group, $\nu_{C=S}$, appears in the 1400—1200 cm^{-1} range. The band, located at 1290 cm^{-1} in the spectra of thioamides, was assigned to $\nu_{C=S}$. The increased intensity of this band is accounted for by its overlap with the absorption band $\nu_{asym.\,SO_2}$, located also at 1290 cm^{-1}. In the spectra of the complex combinations, this band, due to the vibration of the C = S bond, is shifted towards higher frequencies. Only intensity changes occur in the case of the $Pd(II)-C_{13}O_2NS_2H_{10}Cl$ and $Pd(II)-C_{13}O_2NS_2H_{10}Br$ complexes. All these observations allowed us to accept the idea of the sulfur atom participation as a donor atom in the chemical bond formation.

The presence of the aromatic rings is evidenced in the spectra of thioamides by bands at 3095—3060 cm^{-1}, due to the valence vibrations ν_{CH}, and at 850 cm^{-1}, due to the bending vibrations γ_{CH}, which are characteristic of the p-substituted aromatic ring. At frequencies between 1600—1480 cm^{-1}, absorption bands due to valence vibrations $\nu_{C\overset{...}{=}C}$ in the two aromatic rings appear in the spectra.

A slight shift towards lower frequencies of the bands corresponding to the valence vibrations ν_{CH} and $\nu_{C\overset{...}{=}C}$ in the aromatic rings was noticed in the spectra of the complex combinations. These shifts can be accounted for by the influence of the $p-\pi$ conjugation, which takes place as a consequence of complexation.

The frequency of the bending vibration γ_{CH} in the p-substituted aromatic ring, located at 850 cm^{-1}, remains unchanged in the spectra of the complex combinations, but its intensity is smaller.

The absorption bands of thioamides due to the asymmetric valence vibration of the SO_2 group, $\nu_{asym.\,SO_2}$, located at 1310—1315 cm^{-1}, and those due to the symmetric valence vibration, $\nu_{sym.\,SO_2}$, located at 1170 cm^{-1}, are only slightly affected by complexation. The valence vibration ν_{C-X} (X = Cl, Br), located at 770 and 580 cm^{-1}, respectively, is practically not influenced by complexation, probably due to the large separation of this bond from the thioamidic group which takes part in bond formation.

Investigation of the IR spectra of the complex combinations of Pd(II) with thioamides strengthens the conclusion that the chemical bond in complexes is formed by participation of both the sulfur atom and the nitrogen atom of the thioamidic group.

To investigate in depth in the complex combinations of Pd(II) with 4-(arylsulfonyl)-thiobenzamides, the UV/Vis electronic reflection spectra were also recorded (Fig. 1). Absorption bands in the visible range were assigned on the basis of the data provided by Gray and Ballhausen,[19] who applied the molecular orbital theory to square-planar complexes of the elements with d^8 electronic configuration.

The band located at 380 nm (26,300 cm^{-1}) in the spectra of complexes was assigned to the spin-allowed and parity-forbidden $d-d$ transition $^1A_{1g} \rightarrow {}^1E_{1g}\,(e_g(\pi^*) \rightarrow b_{1g}(\sigma^*))$. The shoulder noticed at 435 nm (23,300 cm^{-1}) was assigned to the spin-allowed, parity-forbidden $d-d$ transition $^1A_{1g} \rightarrow {}^1B_{1g}(a_{1g}(\sigma^*) \rightarrow b_{1g}(\sigma^*))$. The band located at 577 nm (17,500 cm^{-1}) was assigned to the spin-allowed, parity-forbidden $d-d$ transition $^1A_{1g} \rightarrow {}^1A_{2g}(b_{2g}(\pi^*) \rightarrow b_{1g}(\sigma^*))$. These correlations allowed us to draw the conclusion that the prepared complex combinations have a square-planar conformation, belonging to the D_{4h} point group.

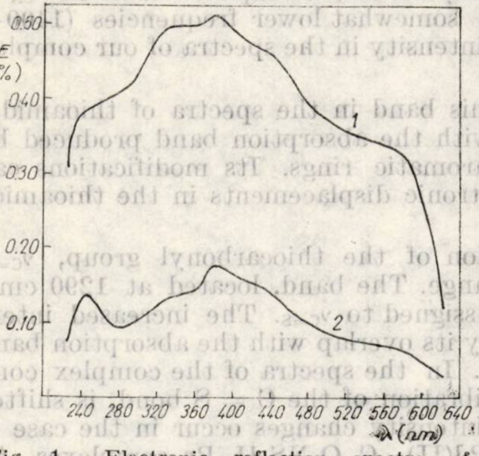

Fig. 1. — Electronic reflection spectra of $Pd(C_{13}O_2NS_2H_{10}Br)Cl_2$ (1) and of $Pd(C_{13}O_2NS_2H_{10}Cl)Cl_2$ (2).

Alongside these bands, bands assignable to the ligands appear in the range 200 to 350 nm; these were assigned to electronic $\pi-\pi^*$ transitions occurring in the complex chromophore, which includes the two aromatic rings, the central SO_2 group and the substituents in positions 4 and 4′, i.e. thioamide and the halogens, respectively. These bands can also be found, bathochromically shifted, in the spectra of the complex combinations obtained by us, which proves the formation of the corresponding complexes.

EXPERIMENTAL

Reagents: $PdCl_2$, 0.02 M solution in HCl. The thioamides were dissolved in hot 96 % ethanol.

Preparation of the complex combinations: The ethanolic solution of thioamides was added, under continuous stirring, to 10 cm^3 of 0.02 M solution of $PdCl_2$. A fine precipitate was formed, which was left to deposit during one hour. The precipitate wad filtered through a G_4-grade sintered-glass filter, washed with ethanol and dried under vaccum. The complex combinations prepared in this way are brown-coloured microcrystalline powders, stable in time and having low solubilities in various inorganic and organic solvents.

Instrumentation: The IR spectra of thioamides and of the complex combinations were recorded with a UR-20-type Carl Zeiss Jena spectrophotometer, using anhydrous KBr pellets. The UV/Vis reflection spectra were recorded with a VSU-1-type Carl Zeiss Jena spectrophotometer, using MgO pellets.

CONCLUSIONS

Based in this study, the conclusion was drawn that the prepared complex combinations of Pd(II) with thioamides in the series of 4-(arylsulfonyl)-thiobenzamides have the conformation

$$[\mathrm{Pd\,L\,Cl_2}]$$

Analysis of IR spectra proved that the chemical bond in the investigated complex combinations is formed through the sulfur atom and through the nitrogen atom of the $-NH_2$ group. Correlation of the results of chemical analysis with physico-chemical studies makes plausible the following formula for these complex combinations:

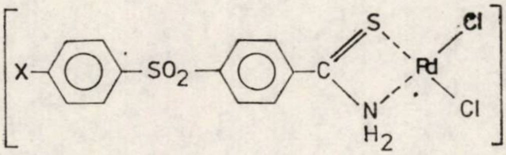

The thioamides take part as "thioaceto" ligands, since the complex combinations are non-electrolytes; this proves that two of the four coordinating points of the central metal atom are occupied by the bidentate ligand, while the other two are occupied by chlorine atoms.

The electronic reflection spectra of the complex combinations lead to the conclusion that these have a square-planar conformation of D_{4h} symmetry.

REFERENCES

[1] L. F. Lindoy, *Coord. Chem. Rev.*, **4**, 41 (1969).
[2] J. A. McCleverty, *Progr. Inorg. Chem.*, **10**, 49 (1968).
[3] D. Coucouvanis, *Progr. Inorg. Chem.*, **11**, 233 (1969).
[4] R. Eisenberg, *Progr. Inorg. Chem.*, **12**, 295 (1970).
[5] M. Cox and J. Darken, *Coord. Chem. Rev.*, **7**, 29 (1971).
[6] S. E. Livingstone, *Coord. Chem. Rev.*, **7**, 59 (1971).
[7] B. P. Kennedy and A.B.P. Lever, *Canad. J. Chem.*, **50**, 3488 (1972).
[8] V. V. Sibirskaia and YuN. Kukushkin, *Koord. Khim.*, **4** (7), 963 (1978).
[9] D. Negoiu and V. Mureșan, *Anal. Univ. București, Ser. Chim.*, **20** (1) 121 (1971).
[10] D. Negoiu, V. Mureşan and G. Fulea, *Rev. Roumaine Chim.*, **18**, 1749 (1973).
[11] D. Negoiu, V. Mureşan and S. Florea, *Rev. Roumaine Chim.*, **18**, 1875 (1973).
[12] M. Negoiu and I. Saramet, *Bul. Inst. Politeh. "Gh. Gheorghiu-Dej" (Bucureşti), Ser. Chim.-Metalurgie*, 43 (1) 73 (1981).
[13] S. E. Livingstone, *Quart. Rev.*, **19**, 386 (1965).
[14] M. Akbar Ali and S. E. Livingstone, *Coord. Chem. Rev.*, 13, 101 (1974).
[15] D. Ahrland, J. Chatt and N. R. Davies, *Quart. Rev.*, **12**, 265 (1958).
[16] R. G. Pearson, *J. Amer. Chem. Soc.*, **35**, 3533 (1963).
[17] Ioana Saramet, Florea Cocu, *Rev. Chim (Bucureşti)*, **32**, 855 (1981).
[18] W. J. Geary, *Coord. Chem. Rev.*, **7**, 81 (1971).
[19] H. B. Gray and C. J. Ballhausen, *J. Amer. Chem. Soc.*, **85**, 260 (1963).

Revue Roumaine de Chimie, **29**, 3, 275–282 (1984)

CONTRIBUTIONS TO THE CHEMISTRY OF THIOCOMPLEXES. II[1]

COMPLEX COMBINATIONS OF Pt(II), Cu(I), Au(III) and Hg(II) WITH 4-(ARYLSULFONYL)–THIOBENZAMIDES

D. NEGOIU*, S. NEAGOE** and IOANA ŞARAMET***

* Polytechnical Institute of Bucharest, Faculty of Chemical Technology,
1, Str. Polizu, 78126—Bucharest, Romania
** Institute of Petroleum and Gases, 3, Şos. Bucureşti—Ploieşti,
2000—Ploieşti, Romania
*** Institute of Medicine and Pharmacy, Faculty of Pharmacy,
6, Str. Traian Vuia, 70139—Bucharest, Romania

Received May 23, 1983

Eight complex combinations of the type (PtL_2), ($PtLCl_2$), $[AuLCl_2]Cl$, $[CuLCl]_2$, and $[HgLCl_2]$, where L is 4-(arylsulfonyl)-thiobenzamide or one of its halogenated derivatives, were synthesized. Elemental analysis allowed formulation of the corresponding combinations. Conductivity measurements were carried out and the infrared and ultraviolet spectra were recorded and interpreted.

The ability of thioamides to form complex combinations with transition metals has attracted the attention of many workers. Mollin and Kásparek [8] synthesized complex combinations of Ag^+, Hg^{2+}, Cu^{2+}, Au^{3+}, Pd^{2+} and other ions with thiobenzamide. Other authors synthesized complex combinations of Pt(II) with thioamides and showed that these can have the formulas $[PtL_2X_2]$, $[PtL_4]X_2$ [2,3] or $[PtLCl_2]$.[4] Gold in oxidation states III and I forms with thioamides complex combinations [5,6] with square-planar conformation.[7]

In this work we intend to further the study of the complex combinations formed by 4-(arylsulfonyl)-thiobenzamides [1] with those ions of the transition metals which have the electronic configurations d^8 (e.g. Pt(II), Au(III)) and d^{10} (e.g. Cu(I), Hg(II)). These metals are typical *b*-group elements [9] (i.e. weak Lewis acids) and therefore they have an affinity for weak Lewis bases.[10]

The ligands in the series of 4-(arylsulfonyl)-thiobenzamides are bidentate and comprise in their molecule sulfur and nitrogen donor atoms; they have the structural formula

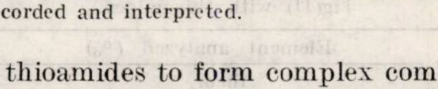

where X = H (4-(phenylsulfonyl)-thiobenzamide) ($C_{13}O_2NS_2H_{11}$);
X = Cl (4-(4′-chlorophenylsulfonyl)-thiobenzamide) ($C_{13}O_2NS_2H_{10}Cl$);
X = Br (4-(4′-bromophenylsulfonyl-thiobenzamide) ($C_{13}O_2NS_2H_{10}Br$).

RESULTS AND DISCUSSION

The complex combinations which will be studied in what follows were obtained by similar means : the ethanolic solution of the thioamide was added under stirring to an aqueous solution of $PtCl_2$ Cu_2Cl_2, $HgCl_2$, or $AuCl_3$. The obtained complexes are solid substances, coloured differently from yellow to dark brown, stable in time with the exception of those containing Hg(II) ions. They are partly soluble in inorganic and organic solvents, with the exception of dimethylsulfoxide and dimethylformamide, in which the solubility is higher. Their melting points are lower than those of the corresponding thioamides.

The results of the elemental chemical analysis are given in Table 1.

These results suggest the following formulations :

$[Pt^{II}L_2]$, where $L = C_{13}O_2NS_2H_{10}Br$;

$[Pt^{II}LCl_2]$, where $L = C_{13}O_2NS_2H_{10}Cl$ or $C_{13}O_2NS_2H_{11}$;

$[Au^{III}LCl_2]Cl$, where $L = C_{13}O_2NS_2H_{10}Cl$ or $C_{13}O_2NS_2H_{10}Br$;

$[Cu^{I}LCl]_2$, where $L = C_{13}O_2NS_2H_{11}$ or $C_{13}O_2NS_2H_{10}Br$;

$[Hg^{II}LCl_2]$, where $L = C_{13}O_2NS_2H_{10}Br$.

Table 1

Elemental chemical analysis of the complex combinations of Pt(II), Au(III), Cu(I) and Hg(II) with thioamides

Compound	Element analyzed (%) theor./exptl.				M.p.	Colour
	M*	C	H	S		
$[Pt(C_{13}O_2NS_2H_{11})Cl_2]$	$\frac{35.88}{35.81}$	$\frac{28.72}{29.86}$	$\frac{2.02}{1.20}$	$\frac{11.78}{12.40}$	154	yellow-orange
$[Pt(C_{13}O_2NS_2H_{10}Cl)Cl_2]$	$\frac{33.75}{33.68}$	$\frac{26.99}{28.10}$	$\frac{1.73}{1.80}$	$\frac{11.07}{11.77}$	132	yellow
$[Pt(C_{13}O_2NS_2H_9Br)_2]$	$\frac{21.54}{21.4}$	$\frac{34.50}{35.60}$	$\frac{1.99}{2.40}$	$\frac{14.14}{13.33}$	165	yellow-orange
$[Au(C_{13}O_2NS_2H_{10}Cl)Cl_2]Cl$	$\frac{32.02}{—}$	$\frac{25.36}{26.50}$	$\frac{1.62}{1.30}$	$\frac{10.40}{10.82}$	164	dark brown
$[Au(C_{13}O_2NS_2H_{10}Br)Cl_2]Cl$	$\frac{29.86}{—}$	$\frac{23.65}{24.30}$	$\frac{1.51}{2.80}$	$\frac{9.70}{10.10}$	148	black
$[(CuCl)_2(C_{13}O_2NS_2H_{11})_2]$	$\frac{16.88}{16.80}$	$\frac{41.45}{40.47}$	$\frac{2.92}{2.80}$	$\frac{17.00}{16.82}$	116	light brown
$[(CuCl)_2(C_{13}O_2NS_2H_{10})_2]$	$\frac{13.96}{14.08}$	$\frac{34.26}{35.30}$	$\frac{2.19}{2.30}$	$\frac{14.06}{14.62}$	120	orange
$[Hg(C_{13}O_2NS_2H_{10}Br)Cl_2]$	$\frac{31.96}{32.20}$	$\frac{24.85}{26.10}$	$\frac{1.59}{1.70}$	$\frac{10.19}{9.58}$	—	dark yellow

* M =metal

These formulations are supported by electrical molar conductivity measurements (Table 2).

In order to understand the nature of the chemical bond formed by complexation, we used the IR and UV/Vis spectra. The results of the comparative study carried out on the ligands and on their corresponding complex combinations are given in Table 3 and discussed by spectral regions.

Table 2

Molar conductivities of the complex combinations of Pt(II), Au(III), Cu(I) and Hg(II) with 4-(arylsulfonyl)-thiobenzamides

Compound	Concentration ($\times 10^{-4}$ *M*)	Molar conductivity (Ω^{-1} cm^2 mole^{-1})
$[Pt(C_{13}O_2NS_2H_{11})Cl_2]$	1.19	5.47
$[Pt(C_{13}O_2NS_2H_{10}Cl)Cl_2]$	1.90	1.86
$[Pt(C_{13}O_2SN_2H_9Br)_2]$	1.43	7.50
$[Au(C_{13}O_2NS_2H_{10}Cl)Cl_2]Cl$	1.13	32.00
$[Au(C_{13}O_2NS_2H_{10}Br)Cl_2]Cl$	1.23	30.00
$[(CuCl)_2(C_{13}O_2NS_2H_{11})_2]$	0.99	6.57
$[(CuCl)_2(C_{13}O_2NS_2H_{10}Br)_2]$	2.30	1.16
	—	—

In the spectra of the complex combinations, the maxima corresponding to the $-NH_2$ groups are located either at the same wavelength with those found in the spectra of the ligands, or shifted; in both these situations the band intensities decrease. We specify that in the spectra of the complexes, the thioamide ν_{NH_2} bands, located at $3400-3160$ cm^{-1}, appear at somewhat lower wavenumbers and have lower intensities; this suggests that the $-NH_2$ group participates in bond formation.

In the range $3500-3000$ cm^{-1} (assigned to $\nu_{assoc.NH_2}$), the maxima characteristic of the $-NH_2$ group in the spectra of thioamides are slightly shifted towards lower wavenumbers in the spectra of the complex combinations with Pt(II) and towards higher wavenumbers in the spectra of the complex combinations of thioamides with Au(III), Cu(I) and Hg(II). The spectra of the complexes are, moreover, damped. The fact that the shape characteristic of the uncomplexed thioamides is not preserved, confirms the assumption that the $-NH_2$ group takes part in bond formation.

The strong absorption bands characteristic of the coupled vibrations $\delta_{NH_2} + \nu_{CN}$ in thioamides appear in the range $1650-1600$ cm^{-1} and are shifted towards lower wavenumbers in the complex combinations $[Pt^{II}(C_{13}O_2NS_2H_{11})Cl_2]$ and $[Pt^{II}(C_{13}O_2NS_2H_9Br)_2]$ and towards higher wavenumbers in the complex combinations $[Pt^{II}(C_{13}O_2NS_2H_{10}Cl)Cl_2]$ (see Table 3). In the spectra of the complex combinations the intensity of these bands is diminished and is different in value from one compund to another.

We also mention that in the spectra of the complex combinations of Au(III), Cu(I) and Hg(II) with 4-(phenylsulfonyl)-thiobenzamide and 4-(4′-bromophenylsulfonyl)-thiobenzamide, the bands characteristic of thio-

Table 3

Characteristic IR frequencies of thioamides and of the complex combination of Pt(II), Au(III), Cu(I) and Hg (II) with thioamides (in cm^{-1})*

Compound	Vibrations of $-\underset{\overset{\|}{S}}{C}-NH_2$ group				Vibrations of benzenic rings			Vibrations of SO_2 group		Vibrations of C–X bond
	3500–3000 ν_{NH_2}	1650–1600 $\delta_{NH_2}+\nu_{CN}$	1600–1400 $\nu_{CN}+\delta_{NH}$	1400–1200 $\nu_{C=S}$	3100–3000 ν_{C-H}	1600–1400 C=C	900–700 γ_{C-H}	1350–1300 $\nu_{asym.SO_2}$	1200–1100 $\nu_{sym.SO_2}$	ν_{C-X}
$C_{13}O_2NS_2H_{11}$	3375s 3355sh 3290m 3190s	1640s	1420s	1290s	3080sh 3060m	1600 1580sh 1480w	850s 775 710	1310m	1170s	—
$C_{13}O_2NS_2H_{10}Cl$	3400s 3330w 3290m 3160s	1625s	1420s	1290s	3095w 3060w	1595s 1580m 1490w	850s	1315m	1170s	770s
$C_{13}O_2NS_2H_{10}Br$	3370s 3330w 3290m 3170s	1650s	1420s	1290s	3085w 3065sh	1600w 1580s 1480m	850s	1310m	1170s	580s
$[Pt(C_{13}O_2NS_2H_{11})Cl_2]$	3320sh 3280w 3195w	1630m	1400m	1315sh	3100w 3070sh	1580sh 1470sh	850m 770sh 720w	1310m	1160m	—
$[Pt(C_{13}O_2NS_2H_{10}Cl)Cl_2]$	3390w 3180w 3120sh	1635w	1390m	1285w	3100sh	1590m 1480w	845m	1330m	1165m	770s
$[Pt(C_{13}O_2NS_2H_9Br)_2]$	3320sh 3150sh	1630w	1440w	1280w	3050sh	1580w 1475sh	850m	1330w	1165m	580s
$[Au(C_{13}O_2NS_2H_{10}Cl)Cl_2]Cl$	3500w 3425w 3335sh	1670m	1400w	1285sh	3100w 3075sh	1580w 1480w	830m	1330w	1160m	770m
$[Au(C_{13}O_2NS_2H_{10}Br)Cl_2]Cl$	3420w 3380w 3320sh	1635w	1395m	1285w	3095w 3080sh	1600sh 1575w 1480m	845m	1330w	1165m	580m
$[(CuCl)_2(C_{13}O_2NS_2H_{11})_2]$	3345w 3280w 3100w	1630m	1400w	1290sh	3070sh	1590sh 1465sh	850m 770w 720w	1315w	1160m	—
$[(CuCl)_2(C_{13}O_2NS_2H_{10}Br)_2]$	3420w 3380sh 3100sh	1630m	1390m	1290s	3080sh	1580w 1600sh	850m	1320m	1170s	580s
$[Hg(C_{13}O_2NS_2H_{10}Br)Cl_2]$	3425w 3350sh	1615m	1390m	1290sh	2950w	1580w	850w	1320w	1160m	580s

* Abbreviations : s — strong ; m — medium ; w — weak ; sh — shoulder.

amides appear at wavenumbers somewhat lower, whereas in the spectrum of the complex combination of Au(III) with 4-(4′-chlorophenylsulfonyl)-thiobenzamide, they are located around 1670 cm^{-1} and are weak. These facts strengthen the idea of the $-NH_2$ group participation to bond formation.

The absorption band due to the coupled vibrations $\nu_{CN} + \delta_{NH}$ in thioamides appears, quite strongly, in the 1600 — 1400 cm^{-1} region. In the complex combinations, this band is located at lower wavenumbers, except in the spectrum of the compound of Pt(II) with 4-(4′—bromophenylsulfonyl) — thiobenzamide (where a weaker band appears at 1440 cm^{-1}). In this region, the bands in the spectra of thioamides have a slightly larger intensity, due to their overlap with the absorption band assigned to the valence vibration $\nu_{C=C}$ of the aromatic rings.

The modification occurring in the spectra may be accounted for on the basis of the $p-\pi$ — type electronic displacements taking place in the thioamidic group as a consequence of complexation.

In the range 1400—1200 cm^{-1}, the band located at 1290 cm^{-1} in the spectra of thioamides is assignable to the valence vibration of the thyocarbonyl group, $\nu_{C=S}$. Because it is overlapped by the absorption band $\nu_{asym.SO_2}$, also located at 1290 cm^{-1}, this is a strong band. In the spectra of the complex combinations, this band appears weaker or is shifted towards lower wavenumbers (Table 3), due to the fact that the sulfur atom takes part, as a donor atom, in the formation of the chemical bond in complexes.

In the spectra of thioamides, the benzenic rings are evidenced by bands in the range 3095—3060 cm^{-1}, assignable to the valence vibrations ν_{CH}, as well as by a band located at 850 cm^{-1} assignable to the deformation vibration γ_{CH}, both characteristic of the *p*-substituted aromatic ring.

The frequency of the deformation vibration γ_{CH} at 850 cm^{-1} and that of the vibrations $\nu_{asym.SO_2}$, $\nu_{sym.SO_2}$ and ν_{C-X} are scarcely affected by complexation (Table 3).

Analysis of the IR spectra of the complex combinations obtained by us confirms the participation in the chemical bond of the sulfur atoms as well as of the nitrogen atoms of the thioamidic group.

The UV/Vis electronic reflection spectra were also recorded, both for the ligands and for the complex combinations (Fig. 1). Assignment of the bands was made on the basis of the data published by Gray and Ballhausen [11] for the complexes of $[PtCl_4]^{2-}$, $[AuCl_4]^-$

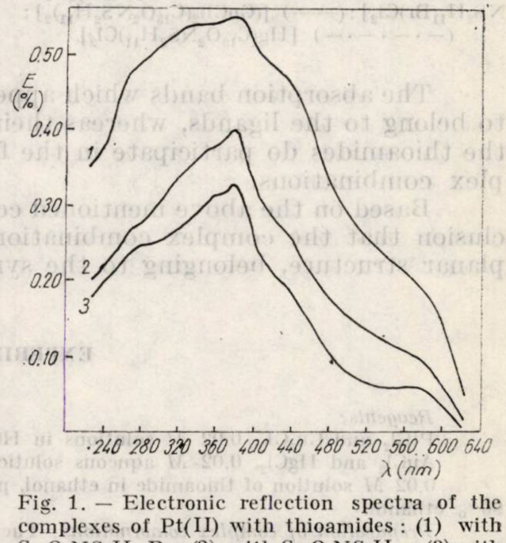

Fig. 1. — Electronic reflection spectra of the complexes of Pt(II) with thioamides : (1) with $C_{13}O_2NS_2H_{10}Br$; (2) with $C_{13}O_2NS_2H_{11}$; (3) with $C_{13}O_2NS_2H_{10}Cl$.

and $[AuBr_4]^-$. Thus, the following assignments were made for the complexes of Pt(II) with thioamides :

— The band located at 380 nm (26,200 cm^{-1}) in the spectra of the complex combinations is assigned to the spin-allowed and parity-forbidden $d-d$ transition $a_{1g}(\sigma^*) \rightarrow b_{1g}(\sigma^*)$ $(^1A_{1g} \rightarrow {}^1B_{1g})$.

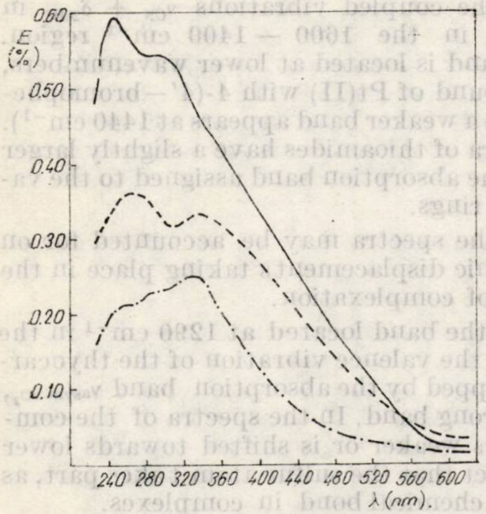

Fig. 2. — UV/Vis electronic reflection spectra of the complex combinations of Cu(I) and Hg(II) with thioamides : (———) $[Hg(C_{13}O_2NS_2H_{11}Br)Cl_2]$; (-------) $[(CuCl)_2(C_{13}O_2NS_2H_{11})_2]$; (— · — · —) $[Hg(C_{13}O_2NS_2H_{11})Cl_2]$.

— The shoulder located at 436 nm (23,100 cm^{-1}) is assigned to the spin-allowed, parity-forbidden transition $b_{2g}(\pi^*) \rightarrow b_{1g}(\sigma^*)$ $(^1A_{1g} \rightarrow {}^1A_{2g})$.

— The shoulder located at 577 nm (17,500 cm^{-1}) is assigned to the weak, spin-forbidden transition $^1A_{1g} \rightarrow {}^3A_{2g}$.

For the complex combinations of Au(III) with thioamides, the weak band located at 390 nm (25,800 cm^{-1}) is assigned to the transition $a_{1g}(\sigma^*) \rightarrow a_{2u}(\pi^*)$ $(^1A_{1g} \rightarrow {}^1A_{2u})$.

For the complex combinations of Hg(II) and Cu(I), the shape of the absorption curves in the visible region agrees with the fact that the central metal ion has the electronic configuration d^{10}, for which the crystal field theory predicts the absence of any absorption bands (Fig. 2).

The absorption bands which appear in the UV region are considered to belong to the ligands, whereas their slight shifts may be a proof that the thioamides do participate in the formation of the investigated complex combinations.

Based on the above mentioned considerations, we can draw the conclusion that the complex combinations prepared by us have a square-planar structure, belonging to the symmetry point group D_{4h}.

EXPERIMENTAL

Reagents:

$PtCl_2$ and Cu_2Cl_2, 0.02 *M* solutions in HCl ;

$AuCl_3$ and $HgCl_2$, 0.02 *M* aqueous solutions ;

0.02 *M* solution of thioamide in ethanol, prepared by dissolving the thioamide in hot 96 % ethanol.

Preparation of complex combinations: The ethanolic solution of thioamide was added, under weak stirring, to 10 cm^3 of a 0.02 *M* solution of $PtCl_2$, $HgCl_2$, Cu_2Cl_2 or $AuCl_3$. Fine precipitates formed, which were allowed to deposit during 30 minutes to one hour ; they were filtered through a G_4-grade sintered crucible, under reduced pressure, then washed with ethanol and ethyl ether and dried in vacuum.

Instrumentation: The IR spectra of thioamides and the complex combinations were recorded with a Carl Zeiss Jena UR-20 spectrophotometer, with samples prepared as pellets in anhydrous KBr. The UV/Vis electronic reflection spectra were recorded with a Carl Zeiss Jena VSU-1 spectrophotometer, using MgO pellets. Electrical conductivity measurements were carried out with a Radelkis OK-102/1 conductimeter.

CONCLUSIONS

The results obtained by elemental chemical analysis, molar conductivity measurements, and spectrometric analysis in infrared and ultraviolet/visible allowed us to ascertain the following formulas for the complex combinations of Pt(II), Au(III), Cu(I) and Hg(II) with 4-(arylsulfonyl-thiobenzamides :

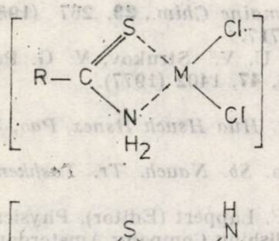

M = Pt(II) ; R = I, II
M = Hg(II) ; R = III

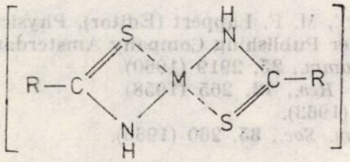

M = Pt(II); R = III

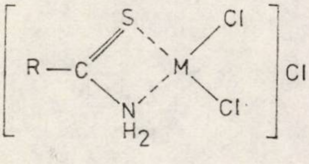

M = Au(III) ; R = II, III

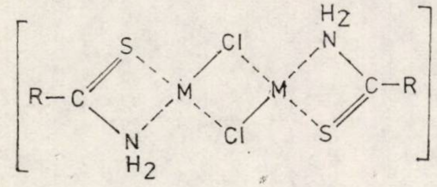

M = Cu(I) ; R = I, III

where

I

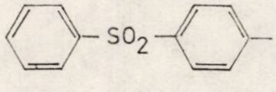

II

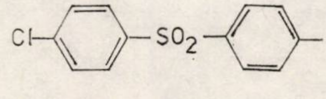

III

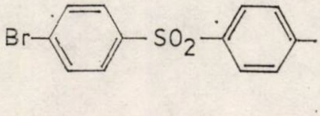

In general terms, thioamides take part in the formation of the chemical bonds in complexes as "thioketo" functions. In the complex combination of Pt(II) with 4-(4′-bromophenylsulfonyl)-thiobenzamide, the ligand is bonded as a "thiol" function, a fact which agrees with the results of the elemental chemical analysis.

The UV/Vis reflection spectra allowed the conclusion that the investigated complex combinations have a square-planar structure with D_{4h} symmetry.

REFERENCES

[1] Part I., D. Negoiu, S. Neagoe and M. Negoiu, *Rev. Roumaine Chim.*, **29**, 267 (1984).

[2] T. Tarantelli and C. Furlani, *J. Chem. Soc., A*, **1968**, 1717.

[3] Yu. N. Kukushkin, V. U. Sibirskaia, V. N. Samuseva, U. V. Strukov, V. G. Pogoreva and T. K. Mihalcenko, *Zhur. obshchei Khim.*, **47**, 1402 (1977).

[4] C. Schafer and C. Curran, *Inorg. Chem.*, **5**, 265 (1966).

[5] Zhang Jian Min, Yang Bing Yu and Liu Chuan Sheng, *Hua Hsuch Hsnex Pao*, **38**, 521 (1980).

[6] A. M. Gevorgyan, V. S. Kostylev and N. V. San'kova, *Sb. Nauch. Tr. Tashkent. Un.*, **622**, 60 (1980).

[7] A.B.F. Lever, "Inorganic Electronic Spectroscopy", M. F. Lappert (Editor). Physical Inorganic Chemistry, Monograph. 1. Elsevier Publishing Company Amsterdam 1968.

[8] F. Kasparek and J. Mollin, *Coll. Czech. Chem. Comm.*, **25**, 2919 (1960).

[9] D. Ahrland, J. Chatt and N. R. Davies, *Quart. Rev.*, **12**, 265 (1958).

[10] R. G. Pearson, *J. Amer. Chem. Soc.*, **35**, 3533 (1963).

[11] H. B. Gray and C. J. Ballhausen, *J. Amer. Chem. Soc.*, **85**, 260 (1963).

Revue Roumaine de Chimie, **29**, *3*, 283–288 (1984)

POTENTIOMETRIC STUDIES ON TRANSITION METAL CHELATES OF ACETOACETANILIDE

MOHAMED M. SHOUKRY*

Department of Chemistry, Faculty of Science, Cairo, University Giza, A. R. Egypt

Received April 20, 1981
Revised September 12, 1983

The metal chelates of some 3d transition metal ions formed with acetoacetanilide have been studied potentiometrically employing the methods of Bjerrum and Irving and Rossotti in 70% ethanol-water medium of $\mu = 0.1$ M (NaCl) at 25°C. It is observed that the chelation of Cu(II), Zn(II) and Mn(II) occurs in two steps forming ML and ML_2 chelates, whereas in the case of Ni(II) three chelates ML, ML_2 and ML_3 are formed stepwise. In the case of Co(II), the oxidation to Co(III) seems possible. The observed stability sequence of the divalent metal ions is $Zn < Cu > Ni > Mn$.

INTRODUCTION

There has been interest in the metal chelates of aroylacetanilides from the standpoint of synthesis and characterization. In the previous publications [1,2] from this laboratory, physicoanalytical studies on cyanoanilide were reported. Very little attention has been paid to the investigation of stability of the metal complexes of acetoacetanilide. This paper describes systematic potentiometric studies of complex formation by Cu(II), Zn(II), Ni(II), Co(II) and Mn(II) with acetoacetanilide in 70% ethanol-water medium and ionic strength $\mu=0.1$ M (NaCl). The proton and metal-ligand formation constants have been determined. Log K_1 and log β_2 were correlated with atomic number of metals.

EXPERIMENTAL

All chemicals used were of A. R. Grade. Acetoacetanilide was obtained from Eastman Organic Chemicals.

a) *Solution:* Double distilled water and carbonate free sodium hydroxide solution were prepared. [3] Hydrochloric acid (0.1M), sodium chloride (1M) and metal chloride solutions (0.004M) in double distilled water. Ligand solution (0.004M) was made in ethanol. Estimation of metal ions was made by EDTA method. [4]

b) *Apparatus:* A Pye Unicum pH meter equipped with a combined glass electrode was used for the present study. The pH-meter readings (B) recorded in ethanol-water solutions were converted to hydrogen ion concentration $[H^+]$ by means of the widely used equation [5]

---

* Present address: University of Alberta, Department of Chemistry, Edmonton, Alberta, Canada, T6G 2G2.

$$„- \log[H^+] = B + \log U_H"$$

where $\log U_H$ is the correction factor for the solvent composition and ionic strength for which B is read. For this purpose, readings were made on a series of solutions containing known amounts of HCl and NaCl such that μ was 0.1. The value of $\log U_H$ in 70% ethanol-water solutions and ionic strength 0.1 at 25±0.1°C was found to be −0.30.

C) *Titration* : The method of Bjerrum and Irving and Rossotti [6-8] was followed to determine the proton and metal-ligand formation constants. The following sets of titrations were performed :

- i) 4 ml of 0.1M HCl + 4 ml of 1M NaCl + 4 ml H_2O + 28 ml ethanol.
- ii) 4 ml of 0.1M HCl + 4 ml of 1M NaCl + 20 ml of 0.004M ligand + 4 ml H_2O + 8 ml ethanol.
- iii) 4 ml of 0.1M HCl + 4 ml of 1M NaCl + 20 ml of 0.004M ligand + 4 ml of 0.004M metal ion + 8 ml ethanol.

The total volume in each case was 40 ml and ionic strength was 0.1M NaCl. The ratio of the ligand to the metal salt was maintained at 5 : 1 in all the titrations in order to satisfy the maximum coordination possibility of the metal ions.

Calculations : From the titration curves using the solution (i) and (ii) the $\bar{n}_H$ (average number of protons associated/ligand molecule) values were calculated using the Irving-Rossotti relation. Proton-ligand formation curve was drawn by plotting $\bar{n}_H$ against $-\log [H^+]$ values. From this curve proton-ligand formation constant, $\log K_1^H$ was evaluated by using (i) Half $\bar{n}$-method and (ii) Average value method [9] using the relation

$$\log K_1^H = - \log[H^+] + \log \frac{\bar{n}_H}{1 - \bar{n}_H}$$

From the titration curves using the solutions (ii) and (iii), $\bar{n}$ (metal-ligand formation number) and pL (free ligand concentration) were calculated using the following relations :

$$\bar{n} = \frac{(V''' - V'')(N^0 + E^0)}{(V^0 + V')T^0_{CM}\,\bar{n}_H}$$

$$pL = \log \frac{B_n^H\,[H^+]^n\,(V^0 + V''')}{(T^0_{CL} - \bar{n}\,T^0_{CM})V^0}$$

where V′, V″ and V‴ denote the volume of alkali required to reach the same pH in the titrations of mixtures i, ii and iii respectively, V^0 the initial volume of the titrated solution, N^0 the normality of alkali, E^0 the initial concentration of the free acid, T^0_{CM} the total metal ion concentration, T^0_{CL} the total ligand concentration and β_n^H the overall proton-ligand formation constant value.

Metal-ligand formation curves were obtained by plotting different $\bar{n}$-values against pL values (Fig. 2). From these formation curves log K values (metal-ligand formation constants) were obtained by using the usual computational methods.[10] The values are given in table 1.

RESULTS AND DISCUSSION

Proton-ligand formation constant

In order to calculate the formation constants of the metal chelates, it is essential to have a prior knowledge of the proton-ligand formation constant. The protonation constant of the ligand is calculated from the potentiometric titration curves of the hydrochloric acid in the presence and absence of the ligand. The formation curve for the proton-ligand

Table 1

Formation constants for some 3d metal ion chelates formed with acetoacetanilide. (Temp. =25°C, $\mu = 0.1$ M NaCl)

Metal ion		Formation constant (computational method)		
		log K_1	log K_2	log K_3
H		10.70 (a)	—	—
		10.70 (b)	—	—
	Mean	10.70	—	—
Cu(II)		7.40 (a)	6.10 (a)	—
		7.43 (c)	6.13 (c)	—
		7.41 (d)	6.18 (d)	—
		7.41 (e)	6.15 (e)	—
	Mean	7.41	6.14	—
Zn(II)		6.40 (a)	5.50 (a)	—
		6.24 (c)	5.56 (c)	—
		6.29 (d)	5.60 (d)	—
		6.23 (e)	5.63 (e)	—
	Mean	6.29	5.57	—
Mn(II)		4.90 (a)	4.10 (a)	—
		4.77 (c)	4.23 (c)	—
		4.74 (d)	4.18 (d)	—
		4.72 (e)	4.21 (e)	—
	Mean	4.78	4.18	—
Ni(II)		5.17 (a)	4.13 (a)	3.00 (a)
		4.93 (c)	4.27 (c)	3.05 (b)
		4.98 (d)	4.20 (d)	3.03 (c)
		4.88 (e)	4.23 (e)	—
	Mean	4.98	4.21	3.03
Co(III)		5.60 (a)	4.70 (a)	3.50 (a)
		5.49 (c)	4.83 (c)	3.43 (b)
		5.44 (d)	4.72 (d)	3.47 (e)
		5.46 (e)	4.79 (e)	—
	Mean	5.50	4.76	3.47

---

a is half $\bar{n}$ method ; b is average value method ; c is successive approximation method ; d is correction term method and e is least-square method.

system, depicted in Fig. 1, is extended between 0 and 1 in the $\bar{n}_H$ scale and it indicated that the ligand has one dissociable proton. The value of log K_1^H is obtained directly from its formation curve. Likewise log K_1^H is calculated by the average value method. The results are given in table 1.

Metal-ligand system

For metal complex or chelate formation taking place in steps in a homogenous solution, the step formation constants are given by the following equation

$$K_n = \frac{C_{MLn}}{C_{MLn-1} \cdot C_L} \qquad (n = 1, 2, 3, \ldots, N)$$

where K_n is called the n-th metal-ligand formation constant.

In the present case the metal titration curves show significant separation from the ligand titration curve. This indicates the release of protons due to complex formation. Fig. 2 contains the formation curves of the metal chelates of acetoacetanilide. It is observed that for Cu(II), Zn(II) and Mn(II) chelates the $\bar{n}$ values attain a maximum value of approximately 2. It is thus clear with Cu(II), Zn(II) and Mn(II) that two chelates ML and ML_2 are formed in solutions, whereas in the case of Ni(II), $\bar{n}$ value approaches 2.5. This indicates that in the case of Ni(II) three chelates ML, ML_2 and ML_3 are formed stepwise. In the case of cobalt complex, $\bar{n}$ value approaches 2.5. The oxidation of Co(II) to give a complex of the type CoL_3 by the release of three protons seems possible in view of the reversal of stability order in the case of Co(III) complex. The formation constants were computed[10] by half $\bar{n}$, successive approximation, correc-

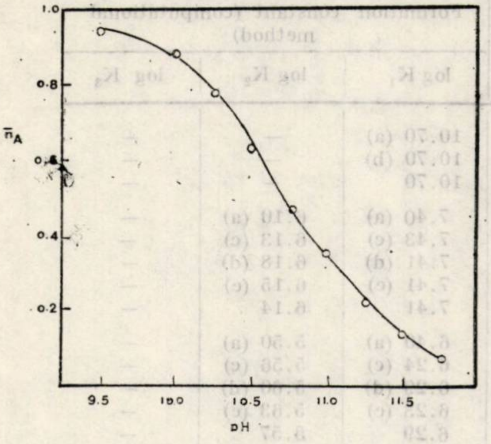

Fig. 1. — Formation curve for proton ligand complex of acetoacetanilide.

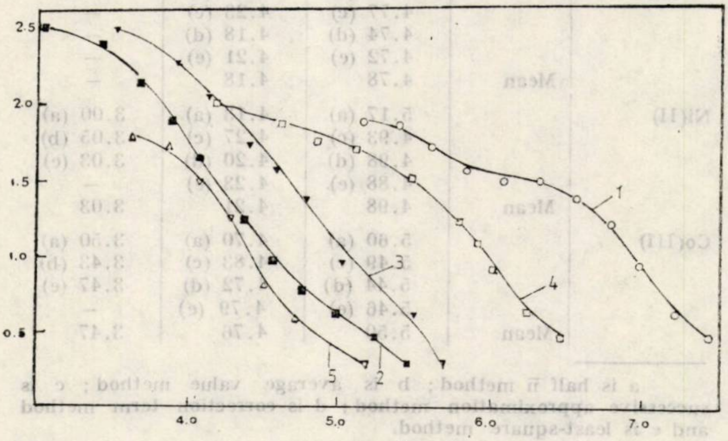

Fig. 2. — Formation curves for metal chelates of acetoacetanilide. 1. Cu ; 2. Ni ; 3. Co ; 4. Zn ; 5. Mn.

tion term and average value method. The stepwise formation constants for bis- and tris-chelates were also calculated by a linear least-square fit of the following equation

$$\frac{\bar{n}}{(L)(1-\bar{n})} = \beta_2 \cdot \frac{(2-\bar{n})(L)}{(1-\bar{n})} + K_1$$

$$\frac{\bar{n}}{(L)(1-\bar{n})} = \beta_2 \cdot \frac{(2-\bar{n})(L)}{(1-\bar{n})} + \beta_3 \cdot \frac{(3-\bar{n})(L)^2}{(1-\bar{n})} + K_1$$

The ratio of successive formation constants

As the tendency of metal ion to take up ligand is proportional to the number of the vacant sites, the ratio between consecutive constants, to a certain extent, is statistically determined.[6] For anionic ligand columic attraction is more for M^{2+} as compared to ML^+. As such $\log K_1 - \log K_2$ and $\log K_2 - \log K_3$ values are usually positive.[11] Table 1 shows that for all metal ions studied here $\log K_1 - \log K_2$ and $\log K_2 - \log K_3$ values lie within 0.60 – 1.27 and 1.18 – 1.29 log K units respectively.

The electronic configuration of the metal ion and stability order

The complex forming ability of transitional metal ions is frequently characterized by stability order. This is displayed graphically in figure 3.

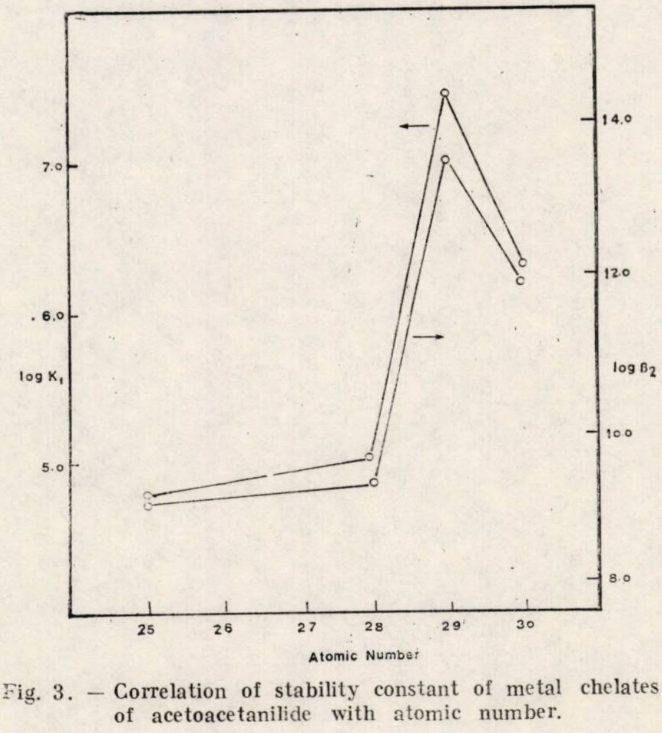

Fig. 3. — Correlation of stability constant of metal chelates of acetoacetanilide with atomic number.

It can be seen that log K_1, log β_2 (log K_1K_2) order Zn $<$ Cu $>$ Ni $>$ Mn are in accordance with Irving and Williams order[12] for 3d divalent metals.

It is clear from table 1 that the formation constants of the Cu(II) complex is considerably larger as compared to other metals of 3d series. This exceptional behaviour in the case of Cu ($3d^9$) may be explained on the basis of Jahn-Teller distortion.[13] Such distortion will result in a more reduction in metal-donor bond distance.

REFERENCES

[1] M. M. Shoukry, M. H. Elnagdi and A. E. Mahgoub, *Ann. Chim. (Ital.)*, **69**, 211 (1979).

[2] M. M. Shoukry, A. E. Mahgoub and M. H. Elnagdi, *Ann. Chim. (Ital.)*, **70**, 319 (1980).

[3] A. I. Vogel, "Quantitative Inorganic Analysis", Longmans, London, 1961.

[4] F. J. Welcher, "The Analytical Uses of Ethylenediaminetetraacetic Acid", Van Nostrand, Princeton, 1965.

[5] L. G. Van Uitert and C. G. Hass, *J. Amer. Chem. Soc.*, **75**, 451 (1953).

[6] J. Bjerrum, "Metal Ammine Formation in Aqueous Solution" Haase, Copenhagen, 1941.

[7] M. Calvin and K. W. Wilson, *J. Amer. Chem. Soc.*, **62**, 2003 (1945).

[8] H. Irving and H. Rossotti, *J. Chem. Soc.*, **1954** 2904.

[9] M. M. Shoukry, A. E. Mahgoub and M. H. Elnagdi, *J. Inorg. Nuclear Chem.*, **42**, 1171 (1980).

[10] M. T. Beck, "Chemistry of Complex Equilibria", Akademiai Kiado, Budapest 1970.

[11] "Stability Constants of Metal Ion Complexes", Part I, The Chemical Society, London, 1957.

[12] H. Irving and R. P. J. Williams, *Nature*, **162**, 746 (1948).

[13] L. E. Orgal, "An Introduction to Transition Metal Chemistry Ligand Field Theory", Methuen, London, 1966.

Revue Roumaine de Chimie, **29**, *3*, 289–293 (1984)

A SPECTROPHOTOMETRIC STUDY OF URANYL COMPLEXES FORMED IN THE $UO_2^{2+}-Cl^{-}-$ACETONE SYSTEM

NICULINA PĂUNESCU
Central Institute of Physics, P.O.Box MG–6, R–76900
Bucharest–Măgurele, Romania

Received July 21, 1982

The complex species formed in the $UO_2^{2+}-Cl^{-}-$acetone system were investigated by spectrophotometric methods. The $[UO_2Cl_n]^{(2-n)+} (n = 1, 2, 3, 4)$ species were observed, and their overall stability constants β_n were calculated giving the following values: $(120.6\ \ 6.6)$; $(5.12 \pm 0.75).10^3$; $(3.20 \pm 0.36) \cdot 10^5$; $(8.94 \pm 1.24) \cdot 10^5$. The presence of water in the system diminishes the amount of formed complexes.

INTRODUCTION

The uranyl ion forms complex species with many anions, in various liquid media.

The complexes formed with Cl^- were studied by different methods, in aqueous medium,[1–3] or in water–alcohol mixed solvents.[4–5] The formation of some species of the type $[UO_2Cl]^+$, UO_2Cl_2 and $[UO_2Cl_3]^-$ was observed. From the IR spectroscopic measurements, the existence of $[UO_2Cl_4]^{2-}$ complex ion was also deduced.[6]

In the present work, the complexes formed in the $UO_2^{2+}-Cl^{-}$acetone system were studied by spectrophtometric methods, and all four species $[UO_2Cl_n]^{2-n}$ cited previously, were found in this system. Their stability constants were determined.

EXPERIMENTAL

Reagents and equipment, $UO_2(ClO_4)_2.3H_2O$ and $UO_2(ClO_4)_2.6H_2O$ were prepared from $UO_2(NO_3)_2.6H_2O$ by repeated evaporation with perchloric acid, until complete absence of NO_3^- ion. The lithium chloride was used either as $LiCl.H_2O$, or in anhydrous form (dehydrated at 98°C and kept in vacuum).

$LiClO_4$ was prepared from $LiOH.H_2O$ (p.a., Chemapol, Praha), in two forms: $LiClO_4.3H_2O$ and $LiClO_4$ anhydrous, obtained by alcohol crystallisation and kept in vacuum.

The acetone was purified by stirring with 1 M NaOH and $AgNO_3$ solution, dehydration with K_2CO_3 and distillation.

The quaternary ammonium salts (p.a., made by BDH Laboratories) were purified by recrystallisation.

Two spectrophotometers, C. Zeiss Jena type Specord UV–VIS with automatic recording and Pye Unicam SP 500 were employed.

PROCEDURE, RESULTS AND DISCUSSION

The complexation ability of UO_2^{2+} with different anions in aqueous solution, increases in the following order: $ClO_4^- < NO_3^- < Cl^- < SO_4^{2-}$. This order is also maintained in acetone solutions except for SO_4^{2-} anion, because of the insolubility of UO_2SO_4 in acetone.

A proof of this are the absorption spectra of the systems containing UO_2^{2+} ions and different anions; their absorption bands became more intensive and better vibrationally resolved by replacing the ClO_4^- ion with NO_3^- and Cl^-.

In the $UO_2^{2+}-NO_3^-$-acetone system three successive complexes were noticed; their overall stability constants were determined at different ionic strengths.[7]

In this study quaternary ammonium salts or lithium salts, which do not absorb in the range of the studied wave-lengths, have been used as ligands [A].

The $UO_2Cl_2.3H_2O-(C_4H_9)_4NCl-$ $-HCl-$acetone system was studied with the aid of continuous variations method.[8]

Equimolar solutions of 0.1 M concentration were used. The results obtained are shown in Fig. 1.

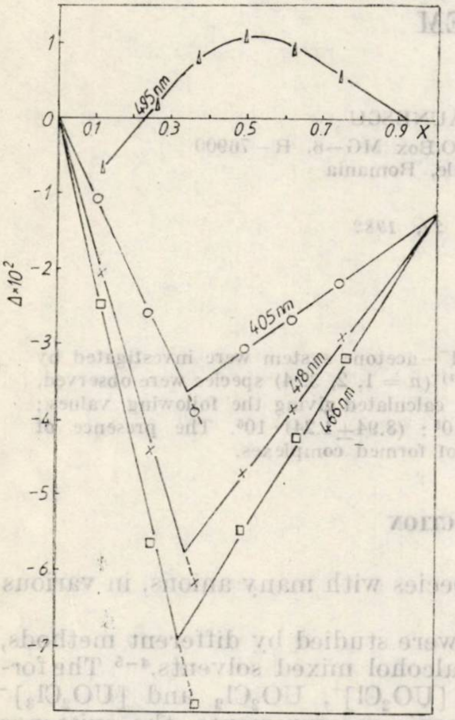

Fig. 1. — The continuous variation curves for $UO_2Cl_2.3H_2O-(C_4H_9)_4NCl-$ acetone system. (Δ is the absorbance difference between a mixed system and one containing only the metal ion).

The continuous variation curves obtined at the wavelength, corresponding to maximum absorption, show the formation of two complexes, in which the ratios $UO_2^{2+}:Cl^-$ are 1 : 3 and 1 : 4. Using the molar ratio method,[9] in the system $UO_2(ClO_4)_2\cdot 6H_2O-LiCl.H_2O$-acetone (ionic strength : $\mu = 0.1$ M maintained with $LiClO_4$) even lower ratio complexes were detected. The measurements were carried out at 446, 466, 480 and 495 nm.

Our data show that in acetone solutions the $[UO_2Cl]^+$, UO_2Cl_2, $[UO_2Cl_3]^-$ and $[UO_2Cl_4]^{2-}$ species are present.

In order to calculate the overall stability constants $\beta_i (i = 1, \ldots, 4)$ the Yatsimirski-Asawa [10-11] method was used.

For this purpose, sets of 30 samples containing 0.005 M $UO_2(ClO_4)_2$ and increasing amounts of $LiCl.H_2O$ were prepared.

The constant ionic strength ($\mu = 0.1$ M) was maintained with $LiClO_4$. The molar absorptivities (e) at the wave-length corresponding to the maximum absorption: 446, 466 and 495 nm were determined.

With the obtained values, the following functions:

$$\Delta\bar{e}([A]),\ f_1 = \Delta\bar{e}[A]^{-1},\ f_i = (f_{i-1} - a_{i-1})[A]^{-1} \quad (i = 2, 3, 4)$$

and

$$\varphi_1 = (\Delta\bar{e} - b_1)[A],\ \varphi_i = (\varphi_{i-1} - b_i)[A] \quad (i = 2, 3)$$

were calculated, with the aid of a Hewlett-Packard 9810 computer.

The set of values a_n and $b_n (n = 1, \ldots, 4)$ were introduced in the equation system of four unknowns:

$$b_1\beta_1 + b_2\beta_2 + b_3\beta_3 + b_4\beta_4 - a_1 = 0$$

$$-a_1\beta_1 + b_1\beta_2 + b_2\beta_3 + b_3\beta_4 - a_2 = 0$$

$$-a_2\beta_1 - a_1\beta_2 + b_1\beta_3 + b_2\beta_4 - a_3 = 0$$

$$-a_3\beta_1 - a_2\beta_2 - a_1\beta_3 + b_1\beta_4 - a_4 = 0$$

The equation system was solved with an adequate computer program, and the values of the overall stability constants β_i, were obtained.

Table 1

The values of a_n and b_n coefficient

λ (nm)	a_1	a_2	a_3	a_4	b_1	b_2	b_3	b_4
446	710.20	$1.56.10^5$	$1.60.10^7$	$6.50.10^8$	16.20	$6.84.10^{-2}$	$5.3.10^{-2}$	$1.5.10^{-3}$
466	669.71	$1.70.10^5$	$1.20.10^7$	$8.28.10^8$	15.63	$10.0.10^{-2}$	$4.5.10^{-2}$	$2.8.10^{-3}$
495	662.40	$1.37.10^5$	$0.98.10^7$	$9.38.10^8$	17.62	$10.5.10^{-2}$	$1.9.10^{-2}$	$6.9.10^{-3}$

The values of the a_n and b_n coefficients are presented in Table 1, and the overall stability constants β_n are listed in Table 2.

Table 2

The overall stability constants

λ (nm)	β_1 ($l.mol^{-1}$)	β_2 ($l^2.mol^{-2}$)	β_3 ($l^3.mol^{-3}$)	β_4 ($l^4.mol^{-4}$)
446	107.67	5894	$2.793.10^5$	$8.501.10^5$
466	129.08	5842	$3.934.10^5$	$7.099.10^5$
495	124.9	3620	$2.878.10^5$	$11.32.10^5$
Average	(120.6 ± 6.6)	$(5.12 \pm 0.75)10^3$	$(3.20 \pm 0.36)10^5$	$(8.94 \pm 1.24)10^5$

A small value for β_1 constant and a low stability of $[UO_2Cl]^+$ ion is observed.

The large standard deviation that affects the β_4 constants value can be explained by the accumulation of some errors during successive extrapolations used in order to determine the a_n and b_n coefficient values.

The stability in time of these complexes was followed by measuring the changes in the absorption spectra. For this purpose solutions containing $UO_2(ClO_4)_2.6\ H_2O$ and LiCl at different concentrations were prepared. The constant ionic strength was maintained with $LiClO_4$.

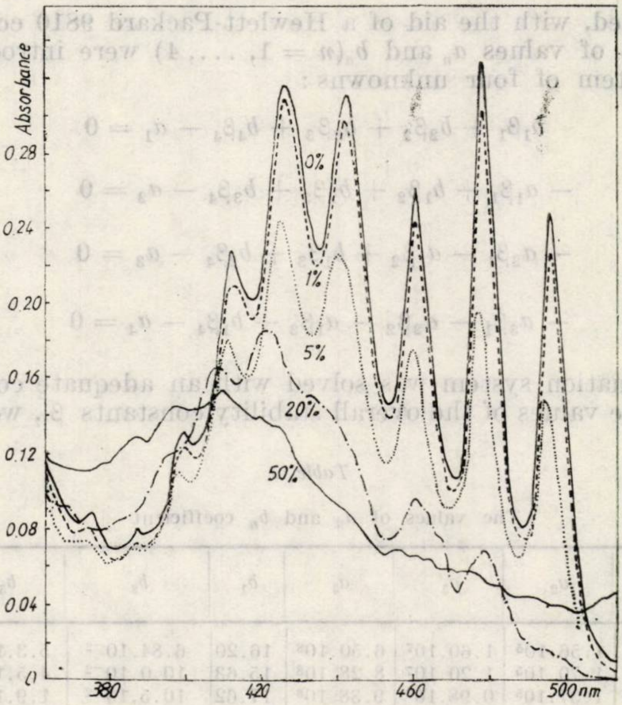

Fig. 2. — The influence of water upon the system $UO_2Cl_2-(C_4N_9)_4NCl$—acetone. The percent water content is inscribed on the curves.

For the solutions containing the complexes in 1 : 1, 1 : 2 and 1 : 3 ratio, the modification of absorption spectrum was small during 24 hours.

The influence of water was also studied by following the modifications of the absorption spectra (Fig. 2).

The presence of water in the system diminished the corresponding amount of formed complexes, which was evident by the dissapearance of vibrational structure in aqueous solutions. This could be explained by a modification of the dielectric constant of the solvent and also by the competition between water, solvent molecules and anion, for a position in the coordination sphere of UO_2^{2+} cation.

The data obtained in this work demonstrate a remarkable complexation ability of the UO_2^{2+} cation with the Cl^- anion in acetonic medium.

The stability constants in acetonic medium (Table 2) are much greater than β_1 and β_2 constants obtained in aqueous medium (ionic strength $\mu = 2.0$) which are less than unity.[3]

REFERENCES

[1] S. Ahrland, *Acta Chem. Scand.*, **5**, 1271 (1951).
[2] F. Bunuș, *J. Inorg. Nuclear Chem.*, **36**, 917 (1974).
[3] L. Bednarezyk and I. Fidelis, *J. Radioanal. Chem.*, **45**, 325 (1978).
[4] J. D. Hefley and E. Amis, *J. Phys. Chem.*, **64**, 870 (1960).
[5] Y. Marcus and J. T. Wei, *J. Inorg. Nuclear Chem.*, **40**, 549 (1978).
[6] Ken Ohwada, *J. Inorg. Nuclear Chem.*, **40**, 1369 (1978).
[7] N. Păunescu, in press.
[8] I. Ostromisslenski, *Ber. deutsch. Cehm. Ges.*, **44**, 268 (1911). P. Job, *Ann. Chim. (France)*, **9**, 113 (1928).
[9] J. H. Yoe and L. Jones, *Ind. Eng. Chem. Analyt. Ed.*, **16**, 111 (1944).
[10] K. B. Yatsimirski, *Zhur. neorg. Khim*, **1**, 2306, 2310 (1956).
[11] H. G. Asawa and L. Dhoot, *Z. phys. Chem. (Leipzig)*, **250**, 177, 180 (1972).

Revue Roumaine de Chimie, **29**, 3, 295–306 (1984)

ÜBER DIE QUATERNISIERUNG DER *p*-AMINOPHENYLAZO—AZOLE. I.

ALKYLIERUNGSMECHANISMUS DER 2-(4′-DIALKYL-AMINOPHENYLAZO)-AZOLE

H. W. LANGFELD und S. IONIŢĂ
Farbstoffunternehmen „Colorom“ — Codlea

Eingegangen am Oktober 6, 1982

Auf Grund von spektrophotometrischen Bestimmungen wurde eine kinetische Untersuchung der Alkylierung mit Dimethylsulfat in Essigsäure des als Modellsubstanz dienenden Azoderivat 6-Methoxy-2-amino-benzthyazol → N-Phenylmorpholin unternommen. Es wurde eine Kinetik zweiter Ordnung festgestellt, was die Annahme eines bimolekularen SN_2-Mechanismus unterstützt.

On the basis of spectrophotometrical determinations a kinetic research of the alkylation with dimethylsulfat in acid acetic was made in which the azoderivative 6-methoxy-2-aminobenzothyazole → N-phenylmorpholine was used as model substance. A kinetic of the second order was found, a fact that encourages the acceptance of a bimolecular SN_2 mechanism.

EINLEITUNG

In einer anderen Arbeit, [1] die der Untersuchung der kationischen 2-(4′-Aminophenylazo)-azol-Farbstoffe der allgemeinen Formel :

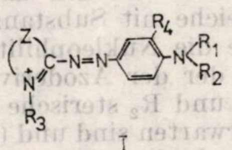

I

in welcher R_1 und R_2 aliphatische Reste (Alkyl, Hydroxyalkyl, Cyanalkyl, Halogenalkyl, Benzyl), die in einem den aliphatischen Charakter bewahrenden Ring (z.B. Morpholin oder Piperazin) eingeschlossen sein können.

R_3 ein Alkyl-, Hydroxyalkyl-, Cyanalkyl-, Carboxyalkyl-Rest, R_4, R_5-Wasserstoff- oder Halogenatome oder Alkyl-, Alkoxy-, Acylamino-Reste.

Z — das Heteroatom aus einer, gegebenenfalls zu einem Benzolring *ortho*-kondensierten Azolstruktur, die in geeigneten Stellungen Alkyl-, Alkoxy-, Acylamino-, Acyl-(Azetyl-, Benzoyl-), Nitro- oder Alkylsulfonyl-Substituenten tragen kann, darstellen, gewidmet war, haben wir auch spezifische Aspekte betreffend die Alkylierungsreaktion der nichtquaternierten Azoderivate behandelt. Diese hat eine besondere praktische Bedeutung, da sie in der Regel die Syntheseendstufe der genannten Farbstoffe darstellt. [2] Als Alkylierungsmittel können dabei Dialkylsulfate, [2-4] Alkylhalogenide, [5-8] Alkylester der Arylsulfosäuren, [9-11] Trialkyloxonium-Borofluoride, [12, 13] sowie einige ungesättigte Verbindungen, wie z.B. Alkylamid, [14] oder Epoxyde (z.B. Propylenoxyd [15]) eingesetzt werden.

Von anderen Autoren unternommene Versuche zur Bestimmung des Einflusses den verschiedene Reaktionsparameter auf den Verlauf der Alkylierung haben, führten zur Feststellung einer Abhängigkeit der Reaktionsgeschwindigkeit ausschliesslich von der Konzentration des Alkylierungsmittels (Dimethylsulfat) und auf dieser Grundlage zur Annahme eines SN1-Mechanismus; [3,4] in einigen Fällen, wurde sogar der Vorschlag das Alkylierungsagens als Lösungsmittel anzuwenden [16] gemacht. Die entsprechenden Schlüsse beziehen sich auf Farbstoffe des Typus I mit Benzthyazolstruktur und basieren auf ein reiches experimentelles Material, das leider nicht stichhaltige kinetische Argumente liefert. Zum Teil resultieren sie durch Extrapolieren der Messergebnisse von parallel bei Alkylierungen von Pyrazolonderivaten der Formel II durchgeführten Bestimmungen

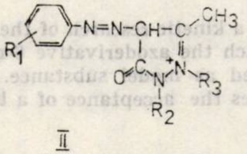

II

$R_1 = H$, Alkyl, Alkoxy, Halogen, NO_2

$R_2 = H, C_6H_5$

$R_3 = CH_3, C_2H_5$

Sie wurden erklärt durch die angeblich geringe Nukleophilität des heterozyklischen Stickstoffatoms, hergeleitet aus der niedrigen Basizität, die ihrerseits aber nicht unmittelbar bestimmt werden konnte. [3]

Dabei muss hervorgehoben werden dass die Substanzen II kein passendes Modell für Vergleiche mit Substanzen des Typus I darstellen, da : (a) die Carbonylgruppe die Nukleophilität beträchtlich beeinflusst, so dass diese nur begrenzt der der Azoderivate I gleichgestellt werden kann, (b) die Gruppen CH_3 und R_2 sterische Effekte hervorrufen die bei den Substanzen I nicht zu erwarten sind und (c) der kationische Farbstoff II keine Polymethinstruktur besitzt und dementsprechend ist seine Bildung energetisch weniger bevorzugt gegenüber den Substanzen I, deren Chromophor den Heptamethinen zugeordnet werden kann. [1,17]

Die erwähnten Festellungen wiedersprechen auch allgemeinen Kenntnissen bezügkich des möglichen Mechanismus der Alkylierung mit Primäralkyl-Halogeniden und -Arylester. [18] Desgleichen befinden sie sich in Gegensatz zu den Kenntnissen über den Reaktionsmechanismus der Alkylierung von Aminen (Menschutkin-Reaktion), [19] der gegenüber die Quaternierung der 2-(4′-Dialkylaminophenylazo)-azole einen Sonderfall darstellen muss.

In der vorliegenden Arbeit wird ein Beitrag zur Klärung des Alkylierungsmechanismus der Substanzen III (R_1, R_2, R_4, R_5 und Z haben dieselbe Bedeutung wie in der Formel I) auf Grund des kinetischen Kriteriums, das häufig zu diesem Zweck angewendet wird,[18,19] erbracht.

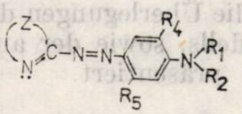

III

ERGEBNISSE

Die Bestimmungsmethode und die angewendeten Messbedingungen. Allgemeines über den möglichen Reaktionsmechanismus

Die untersuchte Reaktion entspricht einer nukleophilen Substitution, wobei das Azoderivat III die Rolle des Nukleophils einnimmt und das Alkylierungsagens die des Reaktionssubstrats. Bezeichnet man die Substanz III mit Y :, den Alkylrest im Molekül des Alkylierungsmittels mit R und die verdrängte Gruppe aus demselben mit X, kann die Reaktion folgendermassen geschrieben werden :

$$\mathrm{Y:} + \mathrm{R{-}X} \longrightarrow \overset{+}{\mathrm{Y}}\mathrm{{-}R} + \mathrm{:X^-}$$

Bekanntlich können sich derartige Reaktionen nach zwei Verschiedenen Mechanismen entwickeln :[20,21] einem bimolekularen (SN2) bzw. einem unimolekularen (SN1).

Dem bimolekularen Mechanismus entspricht eine Kinetik II. Ordnung :

$$-\frac{\mathrm{d\,RX}}{\mathrm{d}t} = k_2\cdot[\mathrm{RX}]\cdot[\mathrm{Y:}] \qquad (2)$$

während der unimolekulare einer Kinetik der I. Ordnung verläuft :

$$\frac{d\,\mathrm{RX}}{\mathrm{d}t} = k_1\cdot[\mathrm{RX}] \qquad (3)$$

wobei k_2, k_1 die Geschwindigkeitskonstanten der II. Ordnung, $\mathrm{l\cdot Mol^{-1}\cdot s^{-1}}$, bzw. der I. Ordnung, $\mathrm{s^{-1}}$, und [RX], [Y :] die Konzentrationen des Substrats, bzw. der nukleophilen Agens, Mol/l, darstellen).

Zwischen dem bi- und unimolekularen Mechanismus kann nicht in allen Fällen klar unterschieden werden,[21,22] da sie eigentlich Grenzsituationen darstellen. Die dazwischenliegenden Abstufungen sind in erster Reihe durch die Struktur des Restes R und durch die Stärke der Bindung R—X debingt. Eine Erkennung des Reaktionsmechanismus auf

Grund von kinetischen Untersuchungen kann nicht allein auf die Prüfung der Geschwindigkeitsgleichung basieren, sondern auch auf die gleichzeitige Bestimmung sämtlicher Faktoren die die Reaktionsgeschwindigkeit beeinflussen, sowohl die strukturellen (internen), wie auch die des Reaktionsmediums (Agens, Lösungsmittel, Salzeffekte etc.).[18]

In der Folge werden die Überlegungen die zu Grunde der Wahl des untersuchten Reaktionsmodells, sowie der angewandten Untersuchungsmethode gestanden haben präsentiert.

Die Substanz III (das nukleophile Reagens)

Infolge der äusserst niederen Stabilität der heterozyklischen Diazoniumsalze,[2] ist die Anzahl der zur Darstellung von Azoderivaten der Formell III einsetzbaren heterozyklischen Amine gering. In der Technik haben sich durchgesetzt: das 2-Aminothyazol[23] und seine Derivate (5-Methylsulfonyl-,[24] 5-Nitro-[25]) für violette und rötlich-blaue kationische Farbstoffe, das 2-Aminobenzthyazol[26] und seine Derivate (6-Nitro-,[27] 6-Benzoyl-,[28] 6-Methyl-,[29] 6-Methoxy-[30]) für sämtliche blaue Nuancen, das 3- und 5-Amino-1,2,4-triazol[31] und seine Derivate[32] für rote Nuancen das 3- und 6-Aminoindazol und seine Derivate[33] für rötlich-orange, sowie verschiedene Benzimidazolderivate[34] für Nuancen die von gelb bis rot reichen.

Die Alkylierung der Triazolderivate stellt die interessanteren Fragen, da sie notwendigerweise zwei aufeinanderfolgende Stufen durchlaufen muss: zunächst den Ersatz des Protons durch ein Alkylrest, dann erst die Quaternierung. In ihrem Fall wurde eine Untersuchung des Vorgangs einerseits zur Erläuterung des Einflusses der Azol-Tautomerie auf die Verteilung der Isomere führen und andererseits die Art in der sich verschiedene Chromophortypen herausbilden: der polyenische (bei den eigentlichen Azoderivaten) und der polymethinische (bei den quaternierten Produkten),[1] klären. Da aber viele Isomere entstehen, sind die Triazolderivate nicht geeignete Modelle für kinetische Untersuchungen; diesem Zweck entsprechen besser die Benzthyazolabkömmlinge.

In der vorliegenden Arbeit wurde als Modellsubstanz das Azoderivat 6-Methoxy-2-aminobenzthyazol → N-Phenylmorpholin IV eingesetzt

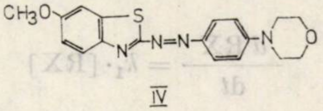

IV

da es einerseits in der Technik als Zwischenprodukt Anwendung findet[2] und andererseits ein praktische einheitliches Reaktionsprodukt liefert. Die Alkylierung am heterozyklischen Stickstoffatom verläuft mit ähnlich hoher Selektivität auch bei anderen Benzthyazolderivaten, zum Unterschied, beispielsweise, von den entsprechenden Triazolderivaten, die in chromatographisch erkennbaren Mengen Alkylierungsprodukte am Amin-Stickstoff bilden.[1]

Diese Beobachtung ist nur scheinbar in Widerspruch zum ausgewogeneren Hemicyanincharakter der Benzthyazolfarbstoffe der Formel I, der sich in ihrer blauen Farbe äussert. Da dieser dem geringen Basizitätsunterschied zwischen den zwei Stickstoffatomen (dem heterozyklischen und dem der Aminogruppe) zuzuschreiben ist [35-38], könnte er eine weitgehendere Bevorzugung der Alkylierung am Aminstickstoff als Folge haben. Das ist aber nicht der Fall, denn die durch Alkylierung am heterozyklischen Stickstoffatom resultierte Struktur V:

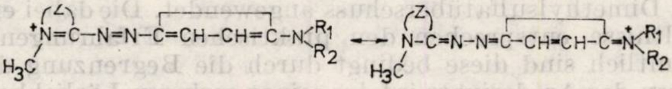

Va Vb

besitzt ausgesprochene Heptamethineigenschaften und ist dementsprechend gegenüber dem Alkylierungsprodukt am Aminstickstoff, dem die Struktur VI mit Polyencharakter entspricht:

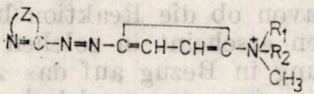

VI

energetisch stabilisierter (in Vergleich zu anderen Hemicyaninen der Formel I).

Wiederum kann die Identifizierung eines sekundären blauen Farbstoffs im Chromatogram des Reaktionsproduktes anderer Benzthyazolderivate (z.B. 6-Methoxy-2-aminobenzthyazol → N,N-Diäthylanilin) nicht, so wie andererorts[3] angenommen wurde, als Beweis der teilweisen Alkyllierung am Aminstickstoff gedeutet werden; denn das Produkt einer solchen Reaktion kann nicht blau, sondern nur rot sein, da es das intramolekular-ionoide polyenische System der nichtquaternierten Azoderivate bewahrt. Der entsprechende Fleck im Chromatogram ist wahrscheinlich auf ein Rest nichtumgewandelten Azoderivats zurückzuführen, der in Berührung mit dem angewandten sauren Fliessmittel durch Protonierung quaterniert wurde.

Das Alkylierungsmittel (das Reaktionssubstrat)

In der vorliegenden Arbeit wurde Dimethylsulfat eingesetzt, weil dieses das meistverwendete Agens der Technik darstellt.[2] Die in der Literatur erwähnen Untersuchungen sind aber hauptsächlich mit Alkylhalogeniden und -arylsulfonaten durchgeführt worden,[18] während der Einsatz von Dialkylsulfaten zu diesem Zweck nur spärlich Erwähnung findet.[3]

Bei Anwendung der Dialkylsulfate stellt sich die Frage ob und in welchem Ausmasse sie nur eine oder beide Alkylreste austauschen; die zugänglichen Literaturangaben [3,4] berücksichtigen die Beteiligung nur im Rahmen der Gleichung (4):

$$Y\,; + (CH_3)_2SO_4 \longrightarrow \overset{+}{Y}-CH_3 + CH_3SO_4^- \qquad (4)$$

Um die günstigsten Bedingungen zur Einschränkung des Alkylierungsprozesses auf die durch Gleichung (4) beschriebene Reaktionsstufe zu schaffen, wurde bei allen Bestimmungen der vorliegenden Untersuchung ein Dimethylsulfatüberschuss angewendet. Die dabei eingesetzten Molarverhältnisse entsprechen den praktischen Erfahrungen der Technik.[2] Bekanntlich sind diese bedingt durch die Begrenzung der einsatzbaren Mengen des Azoderivats infolge seiner geringen Löslichkeit im Reaktionsmittel.[4] Im Falle des Alkylierungsagens stellt sich die Frage nicht, da es selbst als Reaktionsmedium dienen kann.[3,4,16]

Im selben Zusammenhang muss betont werden dass in Konzentrationsbereichen oberhalb der Sättigungsgrenze des Azoderivats im Reaktionsmedium, eine weitere Steigerung der Reaktionsgeschwindigkeit nur durch Erhöhung der Konzentration des Alkylierungsmittels erreicht werden kann, unabhängig davon ob die Reaktion bi- oder monomolekular verläuft. In beiden Fällen erscheint in solchen Bereichen die Kinetik, formal, von erster Ordnung in Bezug auf das Alkyleirungsmittel. Deswegen muss die Annahme eines monomolekularen Mechanismus [3,4] auf Grund einer Argumentation die diesen Aspekten nicht Rechnung trägt, als unschlüssig betrachtet werden. Nur eine genaue Prüfung der kinetischen Gleichung, so wie wir uns weiter unten vorgenommen haben, kann die gewünschte Klarheit bringen.

Andererseits ist bekannt dass der Mechanismus der nukleophilen Substitution (Gleichung (1)) in erster Reihe von der Beschaffenheit des Restes R aus dem Substrat und nur in zweiter Reihe von der Nukleophilität des Reagens Y : und der Art der verdrängten Gruppe X abhängt.[19] Da aber die Reaktionen der Primäralkyl-Abkömmlinge in der Regel nach bimolekularem Mechanismus verlaufen [18,39] (und weil im Falle der Anwendung von Dimethylsulfat $R = CH_3$), haben wir auch unserer Untersuchung diese Voraussetzung zu Grunde gelegt.

Das Lösungsmittel

In der Literatur werden eine Anzahl protischer, aprotischer und aprotischdipolarer Lösungsmittel erwähnt.[18,19,40] Bekanntlich beteiligt sich das Lösungsmittel am Verlauf der Reaktion indem es durch das Ionisationsvermögen und durch die nukleophile Aktivität den Mechanismus beinflusst,[18] so dass seiner Wahl eine grosse Bedeutung zukommt. Für den Fragenkreis unserer Arbeit ist von Interesse dass protische und aprotisch-dipolare Lösungsmittel, die Kationen stark solvatisieren, sowohl den SN1-Mechanismus (in dem Carbokationen gebildet werden), wie auch den SN2-Mechanismus bei dem im Übergangszustand neue Ladungen entstehen (wie im Falle der Menschutkin-Reaktion) begünstigen.[18,14–45] Die Feststellung einer Steigerung der Reaktionsgeschwindigkeit proportional zur dielektrischen Konstante des Lösungsmittels,[4] kann deswegen in unserem Fall nicht als Argument zugunsten des monomolekularen Mechanismus betrachtet werden.

Als Reaktionsmedium für Alkylierungen von Benzthyazol-Azoderivaten wurden folgende Lösungsmittel vorgeschlagen: Chlorbenzol,[46–48,50–52] *m*-Dichlorobenzol,[48] Benzol,[46,48] Toluol,[46,48] Xylol,[46,48,49] Chloroform,[46,48,50] Tetrachloräthan,[46,48] Azetonitril,[49] Äthanol,[48] Essigsäure,[53] sogar Wasser.[54] Einen wesentlichen Faktor bei der Wahl des Lösungsmittels stellt die Löslichkeit des zu alkylierenden Azoderivats dar, da der Reaktionsumsatz unmittelbar von der Homogenität der Masse abhängt.[4]

In der vorliegenden Arbeit haben wir die Essigsäure von vornherein bevorzugt, da sie die Homogenität der Reaktionsmasse gewährt indem sie ein gutes Lösungsmittel sowohl für den kationischen Farbstoff, wie auch für das nichtalkylierte Azoderivat darstellt. Bei Anwendung von Chlorbenzol, das sehr gut Letzteres, aber gar nicht das Reaktionsprodukt löst, leidet die Reproduktibilität der Messergebnisse wesentlich infolge von Agglomerierungen, Verklebungen u.s.w. Aus diesem Grunde konnten die im Rahmen von anderen Untersuchungen gewonnenen Daten[3] von uns nicht geprüft werden. Es fällt dabei auf, dass Autoren deren Schlüsse auf Bestimmungen in Chlorbenzol basieren, zuletzt Essigsäure als optimales Lösungsmittel vorschlagen.

Die Essigsäure ist letztens auch ein geeigneteres Lösungsmittel für die Untersuchungen von nukleophilen Substitutionen, da es eine geringe nukleophile Aktivität und gleichzeitig ein niedriges Ionisationsvermögen besitzt.[18]

Das Prinzip der Bestimmungsmethode

Die Ergebnisse anderer Arbeiten [3] stützen sich ausschliesslich auf gravimetrische Bestimmungen, die eine komplizierte und langwierige Arbeitsweise voraussetzen. Die nötigen Trennungen durch Ausfällung und anschliessender Filtrierung, Auswaschungen u.s.w. beeinträchtigen alle den Genauigkeitsgrad und führen Fehler ein, die die annehmbaren Grenzen überschreiten können.

In der vorliegenden Arbeit haben wir auf spektrophotometrische Messungen zurückgegriffen, da diese eine höhere Genauigkeit voraussetzen.[55]

Die spektralen Bereiche in deen das Azoderivat IV und sein Alkylierungsprodukt absorbieren: $\lambda_{\max} = 495$ nm, bzw. $\lambda_{\max} = 627$ nm, sind genügend differenziert um das Verschwinden der Ersten aus der Reaktionsmasse (Reaktionsumsatz), bzw. die Bildung des Zweiten (Ausbeute) spektrometrisch verfolgen zu können.

Die den Messungen unterzogenen Proben wurden, aus der gut durchrührten, homogenen und thermostatierten Reaktionsmasse, nach genauen Zeiten gewonnen.

Die kinetische Untersuchung der Alkylierung

Setzt man in der Gleichung (2) die Symbole *a* und *b* für die ursprünglichen Konzentrationen (bei $t = 0$) des Alkylierungsmittels RX(Dimethylsulfat) und des nukleophilen Reagens Y : (Substanz IV), bzw. das Symbol x für die Variation der Konzentration in der Zeit t ein, so erhält man durch Integrieren die Beziehung (5) :

$$\frac{1}{b-a} \ln \frac{a(b-x)}{b(a-x)} = k_2 t \tag{5}$$

Die Kinetik zweiter Ordnung wird bewiesen durch die Konstanz des k_2-Wertes.[19] Graphisch lässt sich die Gleichung (5) durch die Liniarität der Funktion $\log \frac{b-x}{a-x} = f(t)$ bestätigen.

Die vorliegende Untersuchung besteht aus drei Massreihen, denen drei verschiedene Paare von Anfangskonzentrationen a und b (in allen Fällen aber $b < a$) entsprechen. Die Bestimmungstemperature its mit Hilfe eines Thermostates auf 41°C gehalten worden, was einen befriedigenden Verlauf der Alkylierung sicherte; unterhalb dieser Temperatur ist die Reaktionsgeschwindigkeit zu gering.

Tabelle 1

Ergebnisse der kinetischen Untersuchung der Alkylierung des Azoderivats IV mit Dimethylsulfat in Essigsäure, bei 41°C

t min.	$(b-x)$ Mol/l	$x = b-(b-x)$ Mol/l	$(a-x)$ Mol/l	k_2 berechnet nach Gleichung (9) l/Mol.min.
Fall A : $a = 0{,}459$ Mol/l $b = 0{,}0925$ Mol/l				
1	0,09000	0,00250	0,45650	0,05945
5	0,08120	0,01130	0,44770	0,05748
30	0,04370	0,04880	0,41020	0,05800
49	0,02700	0,06550	0,39350	0,05997
67	0,01810	0,07440	0,38460	0,05926
105	0,00787	0,08463	0,37437	0,05874
132	0,00425	0,08825	0,37075	0,05926
			Durchschnitt :	0,05888
Fall B : $a = 0{,}1946$ Mol/l $b = 0{,}0392$ Mol/l				
1,15	0,03866	0,00054	0,19406	0,05970
13	0,02770	0,01150	0,18310	0,05989
24	0,02100	0,01820	0,17640	0,05989
42	0,01370	0,02550	0,16910	0,05923
50	0,01140	0,02780	0,16680	0,05912
62	0,00860	0,03060	0,16400	0,05926
85	0,00500	0,03420	0,16040	0,05995
			Durchschnitt :	0,05976
Fall C : $a = 0{,}046$ Mol/l $b = 0{,}0095$ Mol/l				
23	0,00875	0,00075	0,04525	0,05811
34	0,00860	0,00100	0,04500	0,05971
84	0,00775	0,00175	0,04425	0,05946
114	0,00700	0,00250	0,04350	0,05956
165	0,00613	0,00337	0,04263	0,05922
			Durchschnitt :	0,05921

Die Messergebnisse sind in der Tabelle 1 enthalten. Dabei entspricht die Differenz $(b-x)$ der Konzentration des nichtumgesetzten Azoderivat IV; ihre Bestimmung auf spektrophotometrischem Wege wird im experimentellen Teil beschrieben.

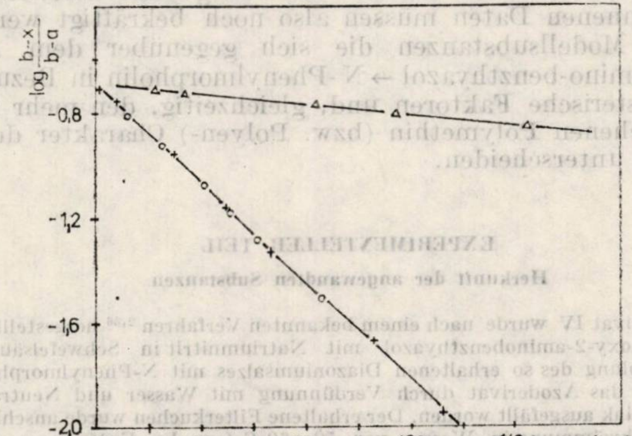

Bild 1. — Graphische Prüfung der kinetischen Gleichung II. Ordnung bei der Alkylierung des Azoderivats IV : (a, b und x wurden der Tabelle 1 entnommen) Fall A : + ; Fall B : o ; Fall C : Δ.

In Bild 1 wird die graphische Prüfung der kinetischen Gleichung auf Grund von der Tabelle 1 entnommenen Daten, dargestellt. Die Neigung der erhaltenen Geraden, multipliziert durch 2,303 $(b-a)$ ergibt dabei den k_2-Wert.

Sowohl die Werte der Geschwindigkeitskonstante aus der Tabelle 1, als auch die graphische Darstellung im Bild 1 bestätigen also die Annahme der Kinetik zweiter Ordnung, bzw. die Bimolekularität der Alkylierungsreaktion des Azoderivats IV.

Schlussfolgerungen

Die in der vorliegenden Arbeit durchgeführten Bestimmungen beweisen dass die mit Hilfe von Dimethylsulfat in Essigsäure durchgeführte Alkylierungsreaktion des Azoderivats 6-Methoxy-2-aminobenzthyazol → N-Phenylmorpholin nach einer Kinetik zweiter Ordnung verläuft, was auf einen bimolekularen Reaktionsmechanismus schliessen lässt.

Diese Feststellung widerlegt entgegengesetzte Schlüsse bezüglich der Alkylierung anderer, ähnlicher Benzthyazol-Azoderivate, die aber nicht auf eine strenge Prüfund der Reaktionsgeschwindigkeitsgleichung basieren.

Sie bestätigt wiederum allgemeinere Kenntnisse bezüglich des Mechanismus von nukleophilen Substitutionen bei denen als Reaktionssubstrat Primäralkyl-Abkommlinge wirken.

Ein vollkommenes Bild des Alkylierungsmechanismus der *p*-Aminophenylazo-azole benötigt aber die Bestimmung sämtlicher Faktoren die die Reaktionsgeschwindigkeit beeinflussen, zunächst die strukturellen, dann die in Zusammenhang mit dem Reaktionsmedium (Lösungsmittel, Salzeffekte etc.) stehenden. Die bei der vorliegenden kinetischen Untersuchung gewonnenen Daten müssen also noch bekräftigt werden durch ähnliche, auf Modellsubstanzen die sich gegenüber dem Azoderivat 6-Methoxy-2-amino-benzthyazol → N-Phenylmorpholin in Bezug auf Nukleophilität, sterische Faktoren und, gleichzeitig, den mehr oder weniger ausgesprochenen Polymethin (bzw. Polyen-) Charakter des alkylierten Produkts, unterscheiden.

EXPERIMENTELLER TEIL

Herkunft der angewandten Substanzen

Das Azoderivat IV wurde nach einem bekannten Verfahren [2,56] hergestellt, durch diazotieren von 6-Methoxy-2-aminobenzthyazol mit Natriumnitrit in Schwefelsäure/Essigsäure/Wasser und Kupplung des so erhaltenen Diazoniumsalzes mit N-Phenylmorpholin. Aus der sauren Lösung ist das Azoderivat durch Verdünnung mit Wasser und Neutralisierung mit wässrigem Ammoniak ausgefällt worden. Der erhaltene Filterkuchen wurde anschliessend durch wiederholte Aufschwämmung in Wasser von 50—60°C (zwecks Entfernung der mineralen Salze) und Spülen mit Essigsäure (zur Entfernüng der vorhandenen Reaktantenüberschüsse, die in Essigsäure leichter löslich sind) gereinigt. Die Reinheit des Produktes wurde papierchromatographisch (wobei die untersuchte Probe in viel Wasser mit etwas Essigsäure gelöst wurde und als Fliessmittel die Mischung 10 Teile Dioxan/10 Teile Ameisensäure 80%/30 Teile Wasser diente) und titanometrisch, auf Grund einer bekannten Methode,[2] sichergestellt. Das der kinetischen Untersuchung unterstellte Produkt hatte im trockenen Zustand eine titanometrisch bestimmte Konzentration von 98,5%.

Das Dimethylsulfat war technisches Produkt von „Sojushimexport“ — Moskau/UdSSR : Konzentration min 99%; Säuregehalt max. 0,5% $d^{20} = 1{,}325 - 1{,}330$; $n_{20} = 1{,}3874 \pm 0{,}0005$; Gehalt an Monomethylsulfat max. 0,5%.

Als Lösungsmittel diente Essigsäure „zur Analyse“ von „Reactivul“ Bukarest, N.I. 4176—76.

Durchführung der kinetischen Bestimmungen

Zu der sich in einem geschlossenen, von Aussen durch ein thermostatiertes Wasserbad erhitzten Glasbehälter, genau gemessenen Menge Essigsäure, wurden auf einmal und unter sehr guter Rührung genau gemessene Mengen Azoderivat IV und Dimethylsulfat gegeben. Die dabei angewandten Konzentrationen entsprechen den Fällen A, B und C aus der Tabelle 1. Um eine genügende Homogenität der Masse zu sichern ist die Rührung während der ganzen Bestimmungsdauer nicht unterbrochen worden.

Den spektrometrischen Messungen wurden, nach bestimmten Zeitspannen, mit Hilfe von geeichten Pipetten aus der Reaktionsmasse gewonnene Proben unterstellt. Die Volumina der Proben schwankten zwischen 0,01—0,1 ml (je nach Fall A, B oder C) und wurden alle, vor der Messung, mit Essigsäure von 40°C auf 2 ml gebracht.

Die spektrometrische Bestimmung der Konzentration $(b-x)$

Obwohl das Azoderivat IV und sein Alkylierungsprodukt gut unterscheidbare Absorptionsmaxima zeigen, sind die Spektralbereiche in denen die Absorption nur einem von beiden zuzuschreiben ist sehr schmal und am äusseren Rand situiert : unter 350 nm, bzw. über 670 nm. In den entsprechenden Zonen nimmt aber die Extinktion kleine, vom Standpunkt der Messgenauigkeit nichtannehmbare Werte an.

Da $(b-x)$ der augenblicklichen Konzentration des Azoderivats IV entspricht, wurden alle Messungen bei der Wellenlänge die dem λmax-Wert des nichtalkylierten Produkts entspricht durchgeführt. Die gemessene Extratkion E ist dabei gleich der Summe der Extinktionen E_1 des nichtalkylierten Azoderivats und E_2 seines Alkylierungsprodukts:

$$E = E_1 + E_2$$

Es war deswegen nötig eine Beziehung $(b - x) = f(E)$ festzulegen. Zu diesem Zweck wurden auf Grund von Sonderbestimmungen, vorerst die Eichkurben $E_1 = f(C_1)$, bzw. $E_2 = f(C_2)$ graphisch dargestellt; die Konzentrationen C_1 und C_2 des Azoderivats IV und seines Aklylierungsprodukts sind hierfür titanometrisch bestimmt worden. Weil x annähernd gleich der Konzentration des zu einem gewissen Zeitpunkt gebildeten Alkylierungsprodukts ist, konnte durch Kombinieren der erwähnten Eichkurven die Abhängigkeit $(b - x) = f(E)$ ihrerseits graphisch dargestellt werden; die Werte $(b - x)$ der Tabelle 1 sind dieser graphischen Darstellung entnommen.

Die Näherung betreffend x wird rechtfertigt durch die Tatsache dass die Differenz zwischen Ausbeute (% gebildetes Alkylierungsprodukt bezogen auf die ganze, im Prozess eingesetzte Menge Azoderivat) und Umsatz (% in der Reaktion umgewandeltes Azoderivat), die auf Grund der Absorptionen in den obenerwähnten Randspektralbereichen bestimmt werden konnte, in keinem geprüften Fall die 1,5%-Grenze überschritten hat.

Die Messungen sind mit Hilfe eines Spektrophotometers UNICAM SP 800 der Firma Pye Unicam Ltd — Grossbritannien, bei 41°C (Einstellung eines Thermostats) durchgeführt worden. Die angewandte Küvettenbreite war in allen Fällen 0,501 cm.

Die in der Tabelle 1 aufgenommenen Werte stellen Durchschnittsergebnisse von je drei Messungen für jeden der Fälle A, B und C dar.

LITERATUR

[1] H. W. Langfeld, E. Barbacaru und S. Ioniţă, „Beitrag zur Untersuchung der kationischen 2-(4'-Aminophenylazo)-azol-Farbstoffe", Mitteilung beim Simposion über Forschungen und angewandte Aspekte im Bereich der Zwischenprodukte, der Textylhilfsmittel und der organischen Synthesefarbstoffe, Zentrum für Chemie/Polytechnisches Institut, Timişoara, Oktober 1982; *Buletin informativ Laborator Aplicare Industrială Coloranţi Bucureşti*, **3/1982**, 7; *Rev. Chim. (Bucureşti)*, im Druck 1983.

[2] L. Floru, H. W. Langfeld und C. Tăbărăşanu-Mihăilă, „Coloranţi azoici", Ed. tehnică, Bucureşti, 1981, S. 186, 387, 391, 490.

[3] A. Spiliadis, Doktorarbeit, Institutul Politehnic Timişoara, 1968.

[4] A. Spiliadis, „Tehnologii noi în industria coloranţilor", Centrul de documentare MICh, Bucureşti 1968, S. 74, 219, 244.

[5] H. C. Brown und A. Cohn, *J. Amer. Chem. Soc.*, **77**, 1715 (1955); H. C. Brown und N. Nagakova, *J. Amer. Chem. Soc.* **27**, 175 (1950).

[6] W. Few, A. R. Gilby, R. H. Ottewill und H. C. Perrera, *J. Chem. Soc.*, **1958**, 1489.

[7] J. S. Ioffe und N. A. Selesnova, *Zhur obshchei Khim.*, **31**, 50 (1961)

[8] USA-Patent 2945037 (1956).

[9] S. Berg, *J. Chem. Soc.*, **1961**, 4041.

[10] Y. S. Rozum, *Zhur obshchei Khim.*, **30**, 1661 (1960).

[11] Französisches Patent 1145751 (1956); Belgisches Patent 544767 (1956); Britisches Patent 791932 (1956); USA-Patent 2883373 (1956).

[12] H. Balli und F. Kersting, *Liebigs Ann. Chem.*, **647**, 1 (1961).

[13] H. Meerschwein, E. Baltenberg, H. Gold, E. Pfeil und G. Willfarg, *J. prakt. Chem.*, **154**, 83 (1939).

[14] USA-Patent 3156751 (1961).

[15] Japanisches Patent 15791 (1971); Deutsches Bundespatent 1906709 (1969).

[16] Rumänisches Patent 43248 (1964).

[17] U. Mayer, *Textilveredlung*, **7**, 492 (1972).

[18] F. Badea, „Mecanisme de reacţie în chimia organică", Ed. Ştiinţifică Bucureşti 1973, S. 140, 211.

[19] C. D. Neniţescu, „Chimie organică", Ed. didactică şi pedagogică, Bucureşti 1980, I. Band, S. 158, 185, 425, 554.

[20] C. D. Hughes, C. K. Ingold und C. S. Patel, *J. Chem. Soc.*, **1933**, 526.

[21] C. K. Ingold, ,,Structure and Mechanism in Organic Chemistry", Cornell University Press, Ithaca/New York 1953, S. 309; II. Aufl. 1969, S. 313, 422.

[22] J. Hine, ,,Physical Organic Chemistry", Mc. Graw. Hill Book Comp., New York 1962, S. 138.

[23] Britisches Patent 974523 (1964); Schweizerisches Patent 570503 (1963) USA-Patent 2893816 (1959), 2889315 (1959).

[24] USA-Patent 3033847 (1962).

[25] Japanischse Patent 2181 (1966), 6910 (1969). Schweizerisches Patent 500924 (1971). Britisches Patent 831118 (1963).

[26] L. Dawidenkow und S.B. Porai-Koschitz, Zhur obshchei Khim **36**, 868 (1953); L. Mokow, *Zhur obshchei Khim*, **29**, 804 (1956).

[27] Schweizerisches Patent 464849 (1968).

[28] Britisches Patent 1162665 (1969). Französisches Patent 1496352 (1967).

[29] S. G. Friedmann, *Zhur. obshchei Khim*, **20**, 1191 (1950).

[30] Deutsches Bundespatent 1906709 (1969), 1937885 (1970), 1619328 (1970), 2155694 (1972), 2159587 (1972).

[31] Belgisches Patent 634376 (1963). Deutsches Bundespatent 2010013 (1971). DDR-Patent 1541464, (1968). Britisches Patent 974623 (1964).

[32] Deutsches Bundespatent 1117233 (1961). Britisches Patent 891515 (1962).

[33] Französisches Patent 1337224 (1963), 1322331 (1963). Deutsches Bundespatent 1927416 (1970).

[34] Französisches Patent 1322331 (1963), 1380628 (1964), 2016982 (1970); Deutsches Bundespatent 1816985 (1970), 2031561 (1969).

[35] H. Kuhn, *Chimia*, **4**, 203 (1950); *Z. Elektrochem.* **53**, 165 (1949); Experientia, *9*, 41 (1956).

[36] L.G.S. Brooker, *J. Amer. Chem. Soc.*, **62**, 116 (1941).

[37] L.G.S. Brooker und R. H. Sprague, *J. Amer. Chem. Soc.*, **63**, 3203 (1941).

[38] I. Voltz, *Chimia*, **15**, 168 (1961).

[39] A. Streitwieser Jr., C. L. Wilkins und E. Kiehlmann, *J. Amer. Chem. Soc.*, **90**, 1598 (1968).

[40] C. F. Duffin, ,,Advances in Heterocyclic Chemistry", A. R. Katritzky, New York 1964, S. 2–57.

[41] K. J. Leidler, ,,Chemical Kinetiks", Mc. Graw Hill, New York 1950, S. 116.

[42] J. O. Leffler, *J. Org. Chem.*, **20**, 1202 (1955).

[43] J. Miller und A. J. Parker, *J. Amer. Chem. Soc.*, **83**, 117 (1961).

[44] A. J. Parker, *J. Chem. Soc.*, **1961**, 1328.

[45] S. G. Smith und S. Winstein, *Tetrahedron*, **3**, 317 (1958).

[46] Deutsches Bundespatent 1050940 (1959).

[47] Deutsches Bundespatent 1056757 (1959).

[48] Französisches Patent 1145235 (1957).

[49] A. J. Kiprianow und F. A. Michajlenko, *Zhur obshchei Khim.*, **33**, 1415 (1963).

[50] Britisches Patent 891515 (1961), 896673 (1962).

[51] USA-Patent 3132133 (1962).

[52] Sowjetisches Patent 154286 (1962).

[53] A. Spiliadis, Rumänisches Patent 53072 (1968).

[54] Deutsches Bundespatent 1943799 (1970).

[55] I. Pogany und M. Banciu, ,,Metode fizice in chimia organică", Editura Ştiinţifică, Bucureşti 1972.

[56] H. W. Langfeld, D. Gageonea und K. Gross, Rumänisches Patent 77298 (1981).

NOTE POUR LES AUTEURS

La Revue Roumaine de Chimie publie des articles en anglais, français, russe, allemand ou espagnol. Les auteurs sont pries d'envoyer des articles et des comptes rendus inédits.

Les manuscrits seront dactylographiés à deux intervalles. La bibliographie, les tableaux et la légende des figures seront placés après le texte.

Si l'article fait partie d'une série numérotée, la partie précédente sera donnée comme première référence.

Chaque article sera précédé d'un résumé comprenant quinze lignes au maximum.

Les références bibliographiques dans le texte seront faites par des exposants sans parenthèses et paraîtront à la fin de l'ouvrage.

Les publications périodiques mentionnées dans la bibliographie seront présentées suivant les prescriptions internationales : le nom de l'auteur précédé de l'initiale du prénom, le titre du périodique abrégé conformément à « Chemical Abstracts » et souligné par une ligne, le numéro du tome indiqué par des chiffres arabes et souligné par deux lignes, suivi de la première page de l'article : à la fin, l'année de la parution sera placée entre parenthèses. Le numéro de la revue ne sera pas indiqué si les pages du volume sont numérotées consécutivement.

Les textes des livres ou traités incluеront : le nom des auteurs, l'initiale du prénom, le titre du livre entre guillemets et sans être souligné, le numéro du tome précédé par l'abréviation « vol. » (ou « Bd. »), le numéro de l'édition, les éditions (the publisher), la localité de la parution du livre, l'année de la parution et la page de la référence précédée(s) par l'abréviation « p » (ou « S »).

Les brevets seront indiqués comme suit : l'auteur ou la firme, le pays et le numéro du brevet, la date et la revue *(Chem. Abstr.)* Par ex. : M. Jones (to Union Carbide Co.) Brit. Pat. 601 238, 2 Sept. 1959, cf. *Chem. Abstr.*, **54**, 12808 (1960).

Les diagrammes seront tracés à l'encre de Chine sur papier calque. Les tableaux et les figures (en nombre strictement nécessaire), ainsi que les courbes dans les figures seront numérotées par des chiffres arabes. Leur explication sera donnée dans la légende des figures. Prière de ne pas inscrire les mêmes données dans les tableaux et les figures. Chaque, tableau aura un titre. On indiquera dans le texte la place approximative des tableaux et des figures. Les formules chimiques seront incluses dans le texte : en outre, elles seront transcrites sur papier calque, à l'encre de Chine.

Les auteurs sont priés d'indiquer les caractères italiques (en soulignant les lettres au crayon). ainsi que tout autre caractère spécial : les préfixes *ortho*, *meta*, *para*, *cis*, *trans*, etc. seront soulignés pour indiquer leurs caractères italiques, et ne seront jamais écrits avec des majuscules.

Aucune correction à la main ne sera admise sur le manuscrit. Les corrections seront frappées à la machine. Les lettres grecques ou autres symboles spéciaux seront insérés à la main à l'encre clairement.

Le manuscrit sera signé par l'auteur.

Titre-courant aura 50 lettres au maximum.

L'entière responsabilité du contenu des articles appartient aux auteurs.

Sur demande on peut obtenir une note plus complète.

PRINTED IN ROMANIA

TRAVAUX PARUS AUX ÉDITIONS DE L'ACADÉMIE DE LA RÉPUBLIQUE SOCIALISTE DE ROUMANIE

1984 MAJ 17

ELENA CEAUŞESCU, **Cercetări în chimia şi tehnologia polimerilor** (Recherches de chimie et de technologie des polymères), 1983, 395 p.

E. SEGAL, D. FĂTU, **Introducere în cinetica neizotermă** (Introduction à la cinétique non isotherme), 1983, 299 p.

N. IONESCU, M. CĂLDĂRARU, **Oxidarea catalitică a olefinelor inferioare** (L'Oxydation catalytique des oléfines inférieures), 1983.

C. CAŞCAVAL, **Studiul polimerilor prin piroliză şi cromatografie de gaze** (L'étude des polymères par pyrolyse et chromatographie à gaz), 1983, 220 p.

C. I. SIMIONESCU, F. DENES, **Originea vieţii** (L'origine de la vie), 1983, 110 p.

C. BODEA (sous la direction de), **Tratat de biochimie vegetală** (Traité de biochimie végétale), IIe p., T. IV, 1982, 408 p.

I. G. MURGULESCU, RODICA VÎLCU, **Introducere în chimia fizică. Vol. III. Termodinamica chimică** (Introduction à la chimie physique, Vol. III, Thermodynamique chimique), 1982, 624 p.

I. G. MURGULESCU, J. PĂUN, **Introducere în chimia fizică. Vol. I.3. Nucleul atomic, reacţii nucleare, particule elementare** (Introduction à la chimie physique. Vol. I. 3. Noyau atomique, réactions nucléaires, particules élémentaires), 1982, 606 p.

ELENA JERCAN, **Analiza cromatografică** (Analyse chromatographique), 1982, 286 p.

ELENA CEAUŞESCU, **Noi cercetări în domeniul compuşilor macromoleculari** (Nouvelles recherches dans le domaine des composés macromoléculaires), 1981, 536 p.

I. G. MURGULESCU, TATIANA ONCESCU, E. SEGAL, **Introducere în chimia fizică. Vol. II. 2 Cinetică chimică şi cataliză** (Introduction à la chimie physique. Vol. II.2. Cinétique chimique et catalyse), 1981, 1024 p.

V. DRĂGUŢAN, A. T. BALABAN, M. DIMONIE, **Metateza olefinelor şi polimerizarea prin deschidere de inel a cicloolefinelor** (La métathèse des oléfines et la polymérisation par ouverture annulaire des cyclooléfines), 1981, 254 p.

LYDIA-MARIA VAICUM, **Epurarea apelor uzate cu nămol activ. Bazele biochimice** (L'épuration des eaux résiduelles à boue active. Les bases biochimiques), 1981, 218 p.

I. GĂLĂŢEANU, **Procese şi metode radiochimice în energetica nucleară** (Processus et méthodes radiochimiques dans l'énergétique nucléaire), 1981, 234 p.

OCTAVIAN IORDACHE, **Procese polistocastice aplicate la fenomenele de transfer** (Processus polystochastiques appliqués aux phénomènes de transfert), 1981, 186 p.

CR. SIMIONESCU, VALERIA GORDUZA, **Polimeri biocompatibili şi biologic activi** (Polymères biocompatibles et biologiquement actifs), 1980, 479 p.

ELENA CEAUŞESCU, **Polimerizarea stereospecifică a izoprenului** (La polymérisation stéréospécifique de l'isoprène), 1979, 307 p.

CONST. GH. MACAROVICI, **Analiza chimică cantitativă anorganică** (L'analyse chimique quantitative inorganique), 1979, 457p.

M. FLORESCU, **Metode ştiinţifice în dezvoltarea industriei chimice moderne** (Méthodes scientifiques dans le développement de l'industrie chimique moderne), 1979, 256 p.

A. T. BALABAN, I. GĂLĂŢEANU, G. GEORGESCU, LIGIA SIMIONESCU, **Compuşi marcaţi şi radiofarmaceutici cu aplicaţii în medicina nucleară** (Composés marqués et radiopharmaceutiques à application en médecine nucléaire), 1979, 495 p.

I. G. MURGULESCU, E. SEGAL, **Introducere în chimia fizică, vol. II.1. Teoria molecular cinetică a materiei** (Introduction à la chimie physique. Vol. II.1. La théorie moléculaire-cinétique de la matière), 1979, 1036 p.

S. STERNBERG, FL. DANEŞ, **Termodinamica chimică aplicată** (La thermodynamique chimique appliquée), 1978, 400 p.

I. G. MURGULESCU, V. EM. SAHINI, **Introducere în chimia fizică, Vol. I.2. Structura şi proprietăţile moleculelor** (Introduction à la chimie physique. Vol. I.2. La structure et les propriétés des molécules), 1978, 604 p.

I. ZUGRĂVESCU, MAGDA PETROVANU, **N-ylid chemistry**, coédition avec McGraw-Hill International Book Company, U.S.A., 1977, 936 p.

I. G. MURGULESCU, **Introducere în chimia fizică. Vol. I.1. Atomi, molecule, legătură chimică** (Introduction à la chimie physique, Vol. I.1. Atomes, molécules, liaison chimique), 1976, 560p.

ELENA CEAUŞESCU, **Research work on synthesis and characterization of macromolecular compounds. Contributions**, 1974, 251 p.

CR. SIMIONESCU, VIORICA RUSAN, V. POPA, **Chimia algelor marine** (La chimie des algues marines), 1974, 212 p., 1 pl.

ISSN 0035–4090

43 426

Lei 40

I. P. INFORMAŢIA c. 1755

$ 70 (pour un abonnement annuel)

= 1103

REFERÁLVA Vegyészet

ACADÉMIE DE LA RÉPUBLIQUE SOCIALISTE DE ROUMANIE

REVUE ROUMAINE DE CHIMIE

TOME 29
N° 4
Avril 1984

EDITURA ACADEMIEI REPUBLICII SOCIALISTE ROMÂNIA

Rev. Roumaine Chim.

RRCHX, 29, 4, p. 307–392 (1984), Bucarest

ACADÉMIE DE LA RÉPUBLIQUE SOCIALISTE DE ROUMANIE

COMITÉ DE RÉDACTION

Rédacteur en chef :

I. G. MURGULESCU, membre de l'Académie de la République Socialiste de Roumanie

Rédacteurs en chef adjoints :

A. T. BALABAN et V. EM. SAHINI, membres correspondants de l'Académie de la République Socialiste de Roumanie

Collège de rédaction :

EM. BRATU, ELENA CEAUŞESCU, ECATERINA CIORĂNESCU-NENITZESCU, CR.SIMIONESCU, membres de l'Académie de la République Socialiste de Roumanie : P. SPACU, membre correspondant de l'Académie de la République Socialiste de Roumanie : MARGARETA AVRAM, M. BANCIU, I. HAIDUC, D. I. MARCHIDAN, I. MOLDOVAN, G. NIAC et D. SĂNDULESCU

La Revue Roumaine de Chimie paraît 10 fois par an. Toute commande de l'étranger pour les travaux parus aux Editions de l'Académie de la République Socialiste de Roumanie sera adressée à ILEXIM — Departamentul Export-Import Carte (Livres)/Departamentul Export-Import Presă (Revues). P.O.B. 136—137, télex. 11226, 3, str. 13 Decembrie, 79517 Bucarest, Roumanie

Les manuscrits, les livres et les revues proposés en échange, ainsi que toute correspondance seront envoyés à la rédaction :

REVUE ROUMAINE DE CHIMIE

125, Calea Victoriei, 79717 Bucarest, Roumanie, téléphone 50 76 80

EDITURA ACADEMIEI REPUBLICII SOCIALISTE ROMÂNIA

125, Calea Victoriei, 79717 Bucarest, Roumanie, téléphone 50 76 80

REVUE ROUMAINE DE CHIMIE

ORSZÁGOS MŰSZAKI INFORMÁCIÓS KÖZPONT ÉS KÖNYVTÁR

Tome 29, N° 4 **Avril, 1984**

ŞTEFANIA ZUCA, I. GALASIU and I. BĂLU, On anode effect in aluminium electrolysis . . . . . 309–314 R
AL. CECAL and N. MIHAI, Radiochemical study on the corrosion kinetics of the carbon-steel OL-32 . . . . . 315–322 R
P. BAHADUR, K. SINGH and A. GUPTA, Influence of added salt on the adsorption characteristics of alkaline earth metal soaps at benzene-water interface . . . . . 323–328 Bc
C. I. CHIRIAC, Synthesis of aromatic thioureas under mild conditions using a new condensation reaction . . . . . 329–331 C
M. IOVU and M. IQBAL, Condensation of bis(chloromethyl)ether with secondary amines. A new reaction . . . . . 333–343 Bc
H. A. DESSOKI and A. ESSAWY, Synthesis of 2-cyano-2-arylazo-methyl-3,1-benzoxazin-4(*H*)-ones and studies of their spectral behaviour . . . 345–351
I. I. SCHIKETANZ, F. BADEA, ANA HANEŞ and ILEANA NECŞOIU, Étard reaction. XII. Oxidation of dibenzo [*b, f*] bicyclo [3, 2, 1] octa-2,6-diene and of dibenzo [*b, e*] bicyclo [2.2.2] octa-2,5-diene with chromyl chloride 353–365
DOLORES VAZQUES BARBADO, Determination of Fe (III) by complexometric potentiometry. Determination of the binary mixtures of Ca(II)-Pb(II), Ca(II)-Fe(III) and Pb(II)-Fe(III). 367–374
DOLORES VAZQUES BARBADO, Applications of the amalgamated gold electrode to the complexometric determination of Ca(II) and Pb(II). . . . . 375–382 R
SANJAY KUMAR, RAVI KANT and OM PRAKASH, Sensitised colour reaction for spectrophotometric determination of uranium . . . . 383–388 R
BOOK REVIEWS 389–391

Rev. Roumaine Chim. **29, *4*,** 307–392 **(1984), Bucarest**

Revue Roumaine de Chimie, **29**, *4*, 309—314 (1984)

ON ANODE EFFECT IN ALUMINIUM ELECTROLYSIS

ŞTEFANIA ZUCA*, I. GALASIU* and I. BĂLU**
*Institute of Physical Chemistry — ICECHIM, Splaiul Independenţei 202, 77208
Bucharest — Romania
* * Aluminium Plant Slatina, Romania

Received April 18, 1983

The onset of anode effect in cryolite — alumina melt was studied with carbon anodes of different porosities : vitreous carbon, a non-porous material, spectral graphite which contains micropores, industrial baked carbon and graphitized carbon of porosity of 8—26 % and 3—13.5 % respectively. The porosity referred to (P_l) is due to pores larger than 7.5 μm. It was established that : the critical current density, (ccd), decreases as P_l increases ; there is an "upper" limit $P_l \leqslant 8\%$ and a "lower" limit $P_1 \geqslant 18\%$ whose exceeding entails no change of ccd with P_l ; for comparable P_l, the ccd's do not depend on the nature of carbon anode ; for vitreous carbon the probability of occurrence of the anode effect is the same as for very porous carbon. It was proved that these findings support the mechanism of anode effect based on the partial or total blockage of anode surface by a gas film formation.

The anodic overvoltage and the anode effect of the two phenomena accounting for the relatively low current and low energy efficiency respectively of Hall — Heroult process, have been extensively investigated in various laboratories. Nevertheless, as pointed out in Grjotheim *et al.* excellent up-to-date reviews on the problem, [1,2] the mechanism of these processes is still disputed and awaits further elucidation. Anyway, it is beyond any doubt and commonly accepted, that both of them are basically controlled by the reactions on the anode surface. This result of immediate practical importance focuses the attention on the properties of carbon anode and promotes possibilities of improving aluminium electrolysis by the adequate modification of carbon anode material, as well.

Starting up from this viewpoint, we carried out an investigation on the influence exerted by the porosity of anode material upon the above mentioned processes.

The porosity — anodic overvoltage correlation has already been discussed. [3] Now, we present the data regarding the influence of anode porosity upon the onset of anode effect.

We recall here that the porosity referred to is due to pores larger than 7.5 μm which is denoted by P_l and called "large porosity"; it differs from the "total porosity", currently considered one of the quality criteria for the baked carbon anodes, which sums up the total volume of pores, macropores included.

EXPERIMENTAL TECHNIQUE

The critical current density, ccd, was measured by the usual technique of gradually rising the potential which causes the current to increase up to a maximum value and then to fall off sudenly. The peak current observed on the obtained current/ voltage curves, as generally accepted, was designed as ccd. The power supply delivered a continuously increasing voltage for currents up to 20 A. The sweep rates were those normally used (0.1—0.5 V/s depending on the Al_2O_3 concentration in the melt). The potential was measured between the carbon anode and the liquid aluminium cathode. The anodes were made of carefully polished cylinders of 14 mm dia. positioned in the melt by a micrometer screw. The geometric surface aria exposed to the melt was always the same, namely 2.3 cm^2. Details on the electrolysis cell were given elsewhere.[4]

The scatter in ccd due to the wear of anode during electrolysis was minimized by changing the anode after each run. The anode materials employed were: vitreous carbon (a nonporous material); compact spectral graphite (containing micropores only); graphitized carbon ($d = 1.55 - 1.68$ g/cm^3 and $P_l = 3 - 13.5\%$); baked carbon sampled from various industrial anode batches with and without Al_2O_3 addition in their bulk ($d = 1.48 - 1.57$ g/cm^3 and $P_l = 8 - 26\%$).

In order to improve the reproductibility of obtained ccd values, prior to the run, the anode was conditioned by pre-electrolysis for 30 min at 0.2 A/cm^2. Each ccd value considered was the average of 8—10 measurements with a dispersion of less than 5%. All experiments were carried out 950° ± 1° in argon atmosphere. The composition of the electrolyte employed was the following: 95 wt.% NaF/AlF_3 of molar ratio 2.7, 5 wt% CaF_2 and different Al_2O_3 additions. Substances of purity not less than 99% were employed. The porosity P_l was measured by mercur penetration method.[3]

RESULTS AND DISCUSSIONS

In order to delimit the influence exerted by the concentration of Al_2O_3 and the parameter P_l on the initiation of anode effect, AE, we have studied the dependence of ccd on Al_2O_3 content at constant P_l, as well as the dependence of ccd on P_l at constant content of Al_2O_3.

The experimental data regarding the influence exerted by Al_2O_3 content on ccd are shown in figure 1; all ccd values plotted were obtained on baked carbon anodes of $P_l = 14.1\%$.

Figure 1 shows that the present data indicate a dependence similar to that already reported.[5,6] In fact, all investigators have reported a systematic increase of ccd with increasing Al_2O_3 content in the melt, but due to the fact that the measured ccd's depend to a great extent upon the experimental arrangement, the geometry of the anode, the procedure to induce the AE etc., there is a considerable difference between the numerical values of ccd obtained in various laboratories.

New in figure 1 is the fact that curve I was obtained in the usual way, by varying the Al_2O_3 content in the molten electrolyte while curve II was obtained in an electrolyte of constant alumina content (1.5%) but on baked carbon anodes with various contents of Al_2O_3 in their bulk (sampled from specially elaborated industrial batches containing Al_2O_3 additive in the anode paste). Nevertheless, the two curves show similar trends; it is obvious that the interfacial phenomena at the anode — electrolyte boundary are the same no matter of the Al_2O_3 addition origin. According to the literature data, there is a strong inverse proportionality between the contact angle of anode wetting and ccd [7,8] and a systematic increase of wetting of carbon materials by cryolite — alumina melts with the increasing concentration of Al_2O_3. [8-11] The experimental data in figure 1 curve II, prove that Al_2O_3 addition in anode paste improves as well, the anode wettability and implicitly its surface activity which renders the onset of AE more difficult as compared to the usual carbon anode.

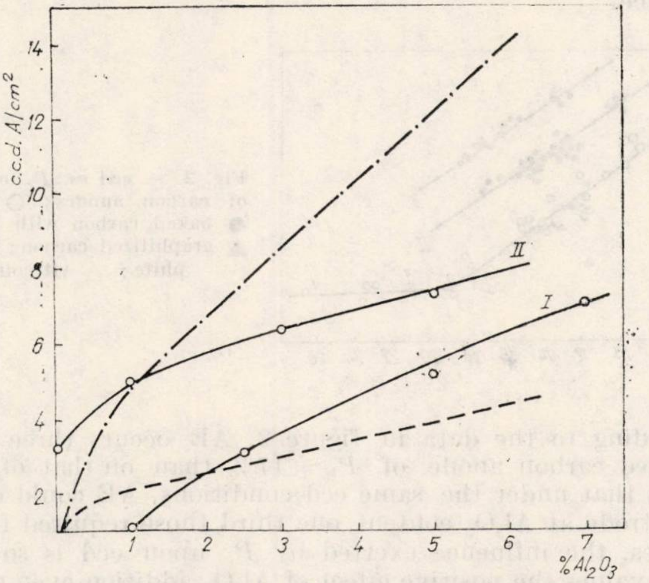

Fig. 1. — ccd *vs.* Al_2O_3 content on carbon anode of $P_l = 14.1\,\%$; —— this work, I Al_2O_3 added in electrolyte ; II Al_2O_3 added in anode bulk ; — · — · —Thonstad [5] ; — — — — — Schischkin [6].

The influence exerted by P_l on ccd is illustrated by the experimental data in fig. 2. Taking into account that the data were obtained on different types of carbon anodes characterized by various P_l's but in an electrolyte of constant Al_2O_3 content (1.5 wt.%), it is obvious that the parameter P_l itself assumes a determining share in the onset of AE: there is a regular decrease of ccd with increasing P_1.

On the other hand, figure 2 evidences the perfect parallelism of the lines yielded by baked anodes with or without Al_2O_3 addition. The equations of these lines calculated by the least square method for the range of $P_l = 9 - 19\%$:

$$\text{I. ccd} = 8.32 - 0.372\ P_l$$

$$\text{II. ccd} = 9.66 - 0.350\ P_l$$

$$\text{III. ccd} = 11.27 - 0.376\ P_l$$

show indeed slopes which are identical within experimental error. This proves that the increase of ccd on anodes containing Al_2O_3 is due exclusively to the presence of alumina into anodic bulk and to the extent of this presence.

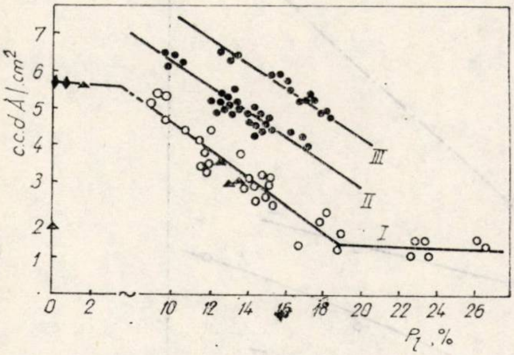

Fig. 2. — ccd *vs.* P_l for various types of carbon anodes: ○ baked carbon; ● baked carbon with Al_2O_3 addition; ▲ graphitized carbon; ◆ spectral graphite; △ vitreous carbon.

According to the data in figure 2, AE occurs three times easier on the baked carbon anode of $P_l = 17\%$ than on that of $P_l = 10\%$. This means that under the same ccd conditions, AE could occur on the former electrode at Al_2O_3 content, one third those required for the latter one. Besides, the influence exerted by P_l upon ccd is so strong that at high P_l values the positive effect of Al_2O_3 addition even at important concentrations is no longer sensed. Both facts are important for the operating of industrial cells. If they are equipped with baked anodes of very different P_l values, then the onset of AE may occur at concentrations of Al_2O_3 in the electrolyte higher than the usually admited limit ($\simeq 1.5$ wt. %).

Special interest deserve some other experimental results shown in figure 2. So it is obvious that:

— for comparable P_l, the ccd's do not depend on the nature of anode materials;

— there is an "upper limit" ($P_l \leqslant 8\%$) and a "lower limit" ($P_l \geqslant 18\%$) whose exceeding entails no change of ccd with P_l;

— for vitreous carbon, a non-porous material, the probability of occurrence of AE is the same as for very porous carbon of $P_l \geqslant 18\%$.

In our opinion all these facts supply major information designed to contribute to the explanation of AE mechanism. Several hypotheses have been advanced so far to describe this mechanism but only few of them may be considered acceptable. One hypothesis [12] considers that the ultimate cause of the phenomenon is the blockage of anode surface by discharged fluorine which occurs when the concentration of the oxygen-containing ions at the anode surface approaches zero. According to other hypotheses the blockage of anode surface is due to an isolating gaseous film generated either by electrostatic attraction of negatively charged gas bubbles [13] or as a result of hydrodynamic effects. [14–16] Recently Calandra *et al.* [17], assuming that the anode surface is blocked by the adsorbed gaseous species, developed a model based on Temkin — Frumkin adsorption isotherm, which was in a good agreement with the experimental data.[18]

Presently established P_l — ccd dependence in figure 2 suggests that the accumulation and the desorption of anodic gas "into" and "out of" the large size pores are indeed important for the onset of the AE. The gas accumulation and the implicit tendency to form very large bubbles adhering to the anode surface are enhanced with increasing P_l. As a result, an additional ohmic drop, systematically increasing in this same sequence, was measured on these anodes.[3] Such large bubbles remaining between the anode surface and the electrolyte somehow block the anode surface thus obstructing the mass transfer of the oxygen-containing ions to the anode ,which explains the permanent decrease of ccd with increasing P_l. Meanwhile, the free sites at the anode surface, the protrusions, could carry high enough current to promote the fluorine discharge. Nevertheless this is not absolutely necessary for the onset of the AE.

Most probably, when P_l reaches a very high value, it is possible to get en entire coverage of the anode surface by a large gas bubble so that any further increase of P_l does no longer affect the ccd value. This may explain the "lower" plateau illustrated on curve I (Fig. 2). As for the "upper" plateau on this curve, it suggests that the coalescence of gas bubbles and their rapid escape is facilitated as $P_l \to 0$ so that within this range the onset of the AE is rendered with much more difficulty.

It is of interest to mention that the point of view of a partial or total coverage of the anode surface by adsorption or gas film formation was also supported by the chronopotentiometric measurements on graphite anodes, performed by Lantelme *et al.*[19–21] and by Wasilewski *et al.*[22]

The vitreous carbon, as seen in figure 2, gives very low ccd values although it is a non-porous material. Similarly, low values compared to those obtained on carbon and graphite anodes were also reported by Mazza *et al.*[15] Certainly this special behaviour has to be connected with the surface gas layer formation rendered evident[3,23] even during the normal electrolysis with vitreous carbon.

It is certain that all facts above mentioned supply experimental evidence to support the hypotheses advanced by several authors[24–27] that the dependence of ccd on the anode material results from a different porosity. It is noteworthy that only the porosity contributed by "large pores" is decisive for the onset of AE. As already established,[3] P_l is also decisive in determining the contribution of various types of overvoltage to the total anodic overvoltage. Therefore it seems very useful to consider it as a distinctive quality criteria for the baked carbon anodes, more so as none of the discussed relationships holds true for the "total porosity".

REFERENCES

[1] K. Grjotheim, C. Krohn, M. Malinovsky, K. Matiasovsky and J. Thonstad, "Aluminium Electrolysis", Aluminium Verlag, Düsseldorf, 1982, p. 227—283.

[2] K. Grjotheim and B. J. Welch, "Aluminium Smelter Technology", Aluminium Verlag, Düsseldorf, 1980, p. 59—65.

[3] S. Zuca, C. Herdlicka and M. Terzi, *Electrochim. Acta*, **25**, 221 (1980).
[4] S. Zuca, I. Galasiu, D. Găgescu and M. Onişor, *Rev. Chim., (Bucureşti)*, **25**, 553 (1974).
[5] J. Thonstad, *Electrochim. Acta*, **12**, 1219 (1967).
[6] V. Schischkin, *Z. Electrochem*, **33**, 83 (1927).
[7] A. I. Belyaev, M. B. Rapaport and L. A. Firsanova, "Elektrometallurgia aluminia", Metallurghizdat, Moscow, 1953.
[8] E. A. Zemchuzhina, "Proceedings Research Institute for Non-Ferrous Metals", Akad. Kiadó, Budapest, 1971, p. 232.
[9] L. Piszczek, *Chem. Stosowana*, **12**, 479 (1968).
[10] A. Vajna, *Bull. Soc. franc. Elec.*, **1952**, 85.
[11] K. Matiasovsky, M. Paucirova and M. M. Malinovsky, *Chem. Zvesti*, **17**, 181 (1963).
[12] J. Thonstad, *Electrochim. Acta*, **19**, 761 (1974).
[13] H. Wartenberg, *Z. Electrochem.*, **32**, 330 (1926).
[14] R. Piontelli, B. Mazza and P. Pedeferri, *Electrochim. Met.*, **1**, 217 (1966).
[15] B. Mazza, P. Pedeferri and A. Tognoni, *Chim. Ind.*, **53**, 123 (1971).
[16] Qiu Zhu Xian, Wei Ching Bin and Chang Ming Ji, *Leight Metals*, **1982**, 279.
[17] A. J. Calandra, C. M. Ferro and C. E. Castello, *Electrochim. Acta*, **25**, 201 (1980).
[18] A. J. Calandra, C. E. Castello and C. M. Ferro, *ibid.*, **25**, 425 (1979).
[19] F. Lantelme, D. Daminiacos and J. Chevalet, *Electrochim. Acta*, **23**, 717 (1978).
[20] F. Lantelme, D. Daminiacos, J. Chevalet and M. Chemla, *Electrochim. Acta*, **24**, 425 (1979).
[21] F. Lantelme, D. Daminiacos and M. Chemla, *J. Electrochem. Soc.*, **127**, 498 (1980).
[22] L. Wasilewski and L. Piszczek, *Chem. Stosowana.*, *2 A*, **1964**, 223.
[23] J. Thonstad, *J. Electrochem. Soc.*, **15**, 1569 (1970); **15**, 158 (1970).
[24] A. Vajna and R. Bacchiega, *Alluminio*, **35**, 173 (1966).
[25] B. J. Welch and R. J. Snow, *J. Electrochem. Soc.*, **113**, 1338 (1966).
[26] B. J. Welch and R. J. Snow, *Australian Inst. Min. Met. Proceedings*, **221**, 43 (1967).
[27] N. Watanabe, F. Kato and K. Amura, *Denki Kagaku*, **37**, 274 (1969).

Revue Roumaine de Chimie, **29**, *4*, 315–322 (1984)

ÉTUDE RADIOCHIMIQUE SUR LA CINÉTIQUE DE LA CORROSION DE L'ACIER AU CARBONE OL-32

ALEXANDRU CECAL et NICOLAE MIHAI *
Faculté de technologie chimique, Institut Polytechnique de Jassy, Splai
Bahlui 71, 6600-Jassy

Reçu le 21 janvier 1983

Cet article comprend une étude sur la cinétique de la corrosion de l'acier au carbone OL-32 en milieu de HCl, en l'absence et en présence de certaines substances organiques à rôle d'inhibiteurs. On présente une méthode radiochimique qui se fonde sur la dilution isotopique. Le processus de corrosion est décrit à l'aide d'un paramètre cinétique appelé « le degré de résistance de l'échantillon métallique envers l'action du milieu corrosif ».

The present paper studies the corrosion kinetics of the carbon-steel OL-32, in HCl medium, without and with some organic substances as corrosion inhibitors. A radiochemical method based on the isotopic dilution is presented. The corrosion process is described by a kinetic parameter named "degree of resistance of the carbon-steel sample against the action of the corrosive medium".

INTRODUCTION

L'étude du processus complexe de la corrosion des métaux à l'aide des radioisotopes a préoccupé un grand nombre de chercheurs.

Ainsi, Bardeen et collab. [1] ont suivi la corrosion de certains échantillons métalliques après avoir déposé au préalable sur leurs surfaces, sous forme de couches minces, les radioisotopes de ces métaux ; Turos et Wilhelmi [2] ont étudié la corrosion des métaux par la rétrodiffusion de certaines particules lourdes comme : $^{2}_{1}H$, $^{3}_{2}He$ et $^{4}_{2}He$.

Pour étudier la cinétique du processus de corrosion de certains types d'acier en différents milieux corrosifs, Close et Hines [3] ont préalablement activé ces échantillons avec les neutrons, pour obtenir les radioisotopes $^{59}_{26}Fe$ et $^{51}_{24}Cr$. Puisque les isotopes respectifs ont été retrouvés dans le milieu corrosif donné à la suite de la corrosion de ces échantillons (à certains intervalles de temps), les auteurs ont tiré des conclusions sur le déroulement de ce processus et sur la résistance des aciers étudiés envers des agents corrosifs étudiés.

---

* Adresse actuelle : Lycée de Cogealac – Constanţa.

Schwabe et collab. [4,5] ont étudié le processus de corrosion de certains métaux en suivant l'adsorption de certains anions marqués sur les surfaces métalliques antérieurement exposées à l'attaque du milieu corrosif respectif.

Kolotyrkin [6] a fait appel aux méthodes électrochimiques et aux radioisotopes pour rechercher les réactions de corrosion à vitesse réduite et Akerman [7] a utilisé des atomes marqués dans l'étude de la corrosion des métaux et de la passivation de ces réactions à l'aide de certains inhibiteurs.

On connaît aussi des monographies [8,9] et d'autres études [10-15] où l'on décrit des procédés d'étude de la corrosion de différents échantillons métalliques dans certains milieux corrosifs.

Ce travail est la suite d'une étude cinétique antérieure [16-21] sur le processus de corrosion de certains aciers en différents milieux corrosifs, en utilisant une technique de travail basée sur la dilution isotopique. [22] En effet, dans cette étude on a essayé de mettre en évidence l'action corrosive différente de la solution d'acide chlorhydrique en présence et en l'absence de certaines substances organiques à rôle d'inhibiteurs dans une plus grande ou plus petite mesure, par l'intermédiaire de la dilution isotopique produite par les ions de fer inactifs qui passent du métal dans la solution, sur les ions radioactifs $^{55+59}Fe^{3+}$, présents dès le début dans ce milieu corrosif.

A cette fin on a introduit un paramètre cinétique, « le degré de résistance de l'échantillon métallique envers l'action du milieu corrosif », à l'aide duquel on a pu décrire le processus de corrosion dans différentes conditions expérimentales.

SECTION EXPÉRIMENTALE

On a d'abord coupé des échantillons de dimensions égales d'un tuyau d'acier au carbone OL-32, au diamètre de 1,7 cm. Ces échantillons ont été ensuite polis, lavés à l'eau, dégraissés avec de l'éthanol et de l'acétone et séchés dans un dessiccateur avec P_2O_5, dans le vide.

La composition de l'acier au carbone OL-32 est la suivante : Fe ; 0,17 %C ; 0,21 – 0,60 % Mn ; 0,017 % Si et 0,055 % S.

On a pris ensuite 4 béchers où l'on a introduit 20 ml de solution $5 \cdot 10^{-3}$ M HCl comme agent corrosif et 20 ml de solution $1 \cdot 10^{-3}$ $M^{55+59}FeCl$ avec une activité spécifique de $1,12 \cdot 10^5$ Bq/ml.

Dans le premier bécher on a ajouté 60 ml d'eau et dans les autres béchers, 60 ml de solution $5 \cdot 10^{-2}$ M de substance organique à rôle d'inhibiteur : pyrocatéchine dans le deuxième, pyrogalol dans le troisième et trion dans le dernier. Ensuite l'on a introduit dans chaque bécher un échantillon d'acier au carbone OL-32, préparé au préalable, pour être soumis au processus de corrosion.

A certains intervalles de temps on a extrait séparément des prélèvements d'un millilitre, qui ont été introduits dans des creusets de porcelaine. Après l'évaporation des solutions respectives, sous une lampe infrarouge, on a déterminé l'activité du résidu de chacun des creusets R_2 (coups/ min. ml) à l'aide d'un tube Geiger-Müller β (3 mg/cm²) connecté à un compteur « Orion-Decimal Scaler ».

A la suite des déterminations effectuées à certains intervalles de temps au cours du processus de corrosion respectif, on a constaté une diminution de l'activité spécifique R_2.

Pour démontrer que cette diminution d'activité n'est pas due seulement au processus de désintégration radioactive du radioisotope $^{55+59}Fe^{3+}$, on a préparé une solution étalon de la manière suivante :

Dans un bécher l'on a introduit 20 ml de solution $1 \cdot 10^{-3}$M $^{55+59}FeCl_3$ et 80 ml d'eau (pour que le volume de la solution soit égal à celui des solutions qui contenaient les échantillons métalliques) d'où l'on a extrait, au commencement des déterminations, un volume d'un ml. Cette dernière solution a été introduite dans un creuset de porcelaine et après son évaporation l'on a réalisé l'étalon respectif, ayant l'activité spécifique R_1 (coups/ min. ml).

Chaque fois qu'on déterminait l'activité d'un échantillon avec le milieu corrosif, on mesurait aussi l'activité de l'étalon et l'on trouvait toujours une différence

$$R = R_1 - R_2 \tag{1}$$

Dans cette expression, R représente l'activité spécifique de la solution due seulement à la dilution isotopique effectuée sur les ions $^{55+59}Fe^{3+}$ par les ions Fe^{n+}, qui résultent après la corrosion de l'échantillon d'acier au carbone OL-32 introduit dans le milieu corrosif respectif.

Cette différence d'activité a été attribuée au processus net de corrosion de l'échantillon d'acier au carbone OL-32.

Dans les systèmes ci-dessus, le processus de corrosion a été étudié à quatre températures différentes. On a suivi aussi l'influence de la concentration du trion, à rôle d'inhibiteur, sur la vitesse de la réaction de corrosion, dans le même milieu agressif.

Les réactifs chimiques ont été obtenus de la firme « Fluka » tandis que le fer radioactif, $^{55+59}FeCl_3$, a été fourni par IFIN Bucarest.

RÉSULTATS ET DISCUSSION

On sait que le processus de corrosion du fer peut être représenté par deux réactions qui ont lieu en même temps [23-25] :

— la dissolution anodique de l'échantillon métallique respectif :

$$Fe \rightarrow Fe^{2+} + 2e^-$$

$$Fe^{2+} \rightarrow Fe^{3+} + e^-$$

— la réduction des ions H^+ (à rôle de dépolarisant dans un milieu acide) :

$$3\,H^+ + 3e^- \rightarrow 3/2H_2$$

Le procédé d'étude de la cinétique de la corrosion des échantillons d'acier au carbone OL-32 proposé dans cet article peut être considéré comme une variante de la méthode d'analyse fondée sur la dilution isotopique.

Tandis qu'en général la dilution isotopique est réalisée par l'introduction extérieure de l'agent isotopique (radioactif ou non) ayant un rôle de diluant, dans la variante que nous proposons la dilution isotopique des ions $^{55+59}Fe^{3+}$, qui se trouvent dans le système depuis le commencement, est effectuée de l'intérieur par les ions Fe^{2+} et Fe^{3+} non radioactifs, qui résultent de la corrosion de l'échantillon métallique immergé dans la solution corrosive.

Par conséquent, au fur et à mesure que le processus de corrosion avance, dans la solution nous trouverons des ions de fer qui ne sont pas radioactifs et ainsi, la concentration par ml (exprimée en fractions molaires) des ions radioactifs $^{55+59}Fe^{3+}$ diminuera selon l'expression :

$$X_{^{55+59}Fe^{3+}} = \frac{[^{55+59}Fe^{3+}]}{[^{55+59}Fe^{3+}] + [Fe^{n+}]}, \qquad (2)$$

où $$[Fe^{n+}] = [Fe^{2+}] + [Fe^{3+}]. \qquad (3)$$

Par conséquent, l'activité spécifique de la solution extraite du milieu corrosif (qui contient aussi des ions $^{55+59}Fe^{3+}$) et où l'on a initialement immergé l'échantillon d'acier au carbone OL-32 diminuera parce que la fraction molaire $X_{^{55+59}Fe^{3+}}$ diminuera et que la concentration des ions de fer qui ne sont pas radioactifs, ayant un rôle d'agent isotopique diluant, augmentera :

$$R \text{ (coups/ min. ml)} = f\,(X_{^{55+59}Fe^{3+}}) = f\,(1/\,[Fe^{n+}]). \qquad (4)$$

(L'activité spécifique de la solution extraite est inversement proportionnelle à la concentration des ions inactifs de fer engendrés par la dissolution anodique de l'échantillon donné).

De plus, à mesure que le processus de corrosion avance, la quantité de fer qui passe de l'échantillon d'acier au carbone OL-32 dans la solution corrosive augmentera et par conséquent, la quantité de résidu qui en résulte après l'évaporation de ce millilitre de solution extraite à des intervalles différents de temps, augmentera. Ce résidu peut agir dans une certaine mesure comme « écran » contre les radiations β émises par le $^{55+59}Fe^{3+}$, en contribuant, proportionnellement de cette manière aussi, à la diminution de l'activité de ces échantillons extraits du milieu corrosif.

Pour caractériser du point de vue cinétique le processus de corrosion, nous proposons un paramètre appelé « le degré de résistance de l'échantillon métallique envers l'action de l'agent corrosif » :

$$q = \frac{R_0 - R}{R_0}\,100 \text{ (en \%)}, \qquad (5)$$

paramètre qui rend compte justement de la croissance en temps de la concentration des ions inactifs de Fe^{n+} dans la solution respective à cause de la corrosion. R_0 représente ici l'activité spécifique de la solution initiale (coups/ min. ml), identique en réalité à l'activité spécifique de l'étalon au temps $t = 0$, tandis que R est l'activité spécifique nette (coups/ min. ml) à un certain moment, correspondant seulement au processus de corrosion. La valeur de R est donnée par la relation (1).

En tenant compte du fait que le paramètre q dépend de la constante de vitesse de n'importe quelle réaction, la relation d'Arrhenius peut être écrite :

$$q = A.\ \exp\,(-\Delta E/RT). \qquad (6)$$

Par la représentation graphique : $\ln q = f\,(1/T)$ on obtient une droite et de sa pente on peut calculer la valeur de l'énergie d'activation apparente pour le système réactant donné.

Les données expérimentales ont été représentées dans les figures 1—4.

A l'aide de ces figures on constate qu'à mesure que la température du système réactant augmente, le degré de résistance de l'échantillon métallique envers l'action du milieu corrosif (*q*) baisse, ce qui indique

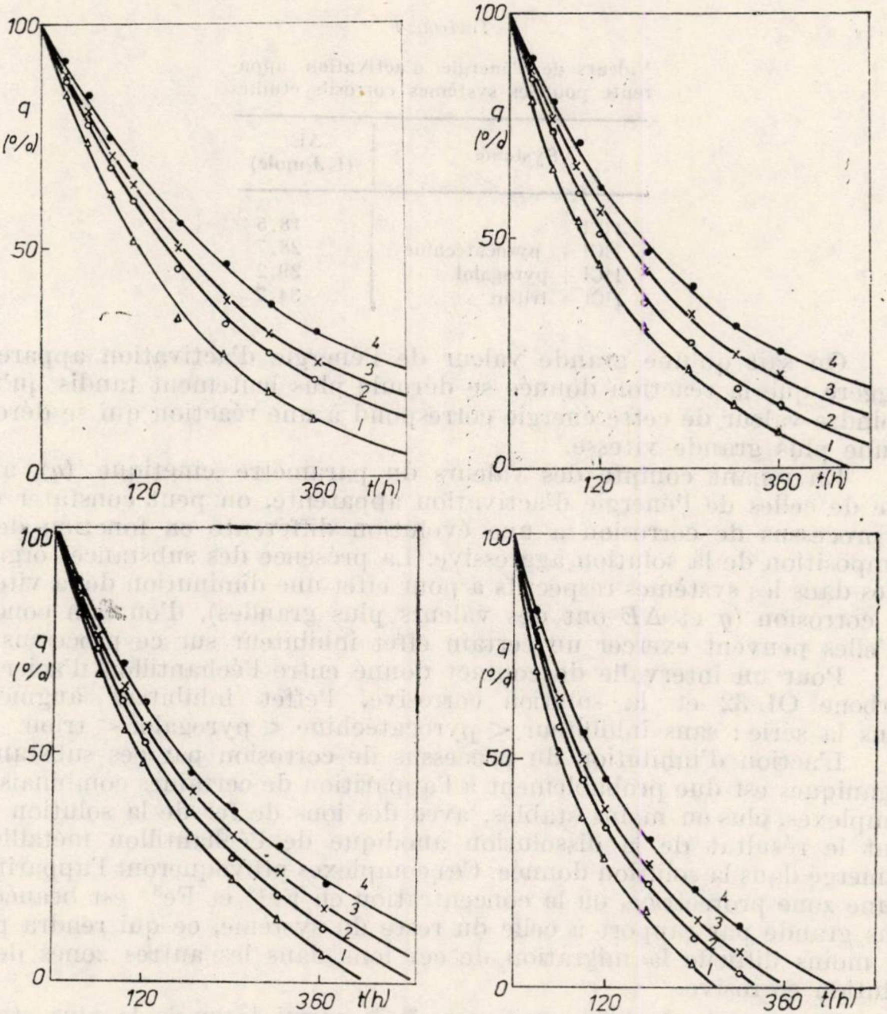

Fig. 1—4. Influence du temps de contact sur le degré de résistance de l'échantillon d'acier au carbone OL-32 envers l'action du milieu corrosif, à quatre températures différentes : 293,7 K (fig. 1) ; 301,4 K (fig. 2) ; 309,2 K (fig. 3) et 319,7 K (fig. 4). Les milieux corrosifs sont : HCl (1) ; HCl + pyrocatéchine (2) ; HCl + pyrogalol (3) et HCl + trion (4).

que la vitesse de corrosion est beaucoup plus grande aux températures plus élevées que dans le cas des températures plus basses, fait déjà connu.

Si l'on représente graphiquement ln $q = f(l/T)$, par une certaine valeur donnée de l'intervalle de contact entre l'échantillon métallique et le milieu corrosif, pour tous les systèmes étudiés, il en résulte des droites des pentes desquelles on peut ensuite déduire les valeurs de l'énergie d'activation apparente. Les données obtenues sont synthétisées dans le tableau 1.

Tableau 1

Valeurs de l'énergie d'activation apparente pour les systèmes corrosifs étudiés

Système	ΔE/ (KJ/mole)
HCl	18,5
HCl + pyrocatéchine	28,7
HCl + pyrogalol	29,2
HCl + triton	34,7

On sait qu'une grande valeur de l'énergie d'activation apparente suggère que la réaction donnée se déroule plus lentement tandis qu'une moindre valeur de cette énergie correspond à une réaction qui se déroule à une plus grande vitesse.

En tenant compte des valeurs du paramètre cinétique (q), ainsi que de celles de l'énergie d'activation apparente, on peut constater que le processus de corrosion a une évolution différente en fonction de la composition de la solution aggressive. La présence des substances organiques dans les systèmes respectifs a pour effet une diminution de la vitesse de corrosion (q et ΔE ont des valeurs plus grandes), d'où l'on conclut qu'elles peuvent exercer un certain effet inhibiteur sur ce processus.

Pour un intervalle de contact donné entre l'échantillon d'acier au carbone OL-32 et la solution corrosive, l'effet inhibiteur augmente dans la série : sans inhibiteur < pyrocatéchine < pyrogalol < trion.

L'action d'inhibition du processus de corrosion par ces substances organiques est due probablement à l'apparition de certaines combinaisons complexes, plus ou moins stables, avec des ions de fer de la solution qui sont le résultat de la dissolution anodique de l'échantillon métallique immergé dans la solution donnée. Ces complexes provoqueront l'apparition d'une zone protectrice, où la concentration en Fe^{2+} et Fe^{3+} est beaucoup plus grande par rapport à celle du reste du système, ce qui rendra plus ou moins difficile la migration de ces ions dans les autres zones de la solution corrosive.

On connaît de tels complexes, [26-28] parmi lesquels le plus stable est celui avec trion, et l'apparition de telles zones protectrices pour d'autres systèmes corrosifs a été postulée aussi par d'autres auteurs. [29-31]

Il est toutefois probable qu'une molécule organique plus volumineuse et ayant plusieurs groupements fonctionnels capables de fixer des ions Fe^{2+} et Fe^{3+} exerce un effet inhibiteur plus accentué sur le déroulement du processus de corrosion de l'échantillon métallique respectif, que la molécule de trion.

Dans la figure 5 on a représenté graphiquement la variation dans le temps du degré de résistance de l'échantillon métallique envers l'action du milieu corrosif lorsque cellui-ci contenait du trion en concentrations différentes.

Dans cette figure on constate qu'au fur et à mesure que la concentration de cette substance organique dans la solution respective augmente, la valeur du degré de résistance de l'échantillon d'acier au carbone OL-32 envers l'action de l'agent corrosif augmente aussi, ce qui peut confirmer la supposition concernant l'existence, au voisinage de cet anneau métallique immergé, d'une couche de protection réalisée à l'aide des complexes de trion avec les ions Fe^{2+} et Fe^{3+}.

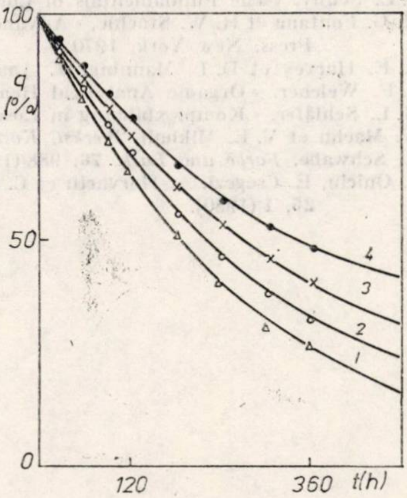

Fig. 5. Influence de la concentration du trion sur le degré de résistance de l'échantillon métallique soumis à la corrosion par l'acide chlorhydrique ($5 \cdot 10^{-3}$ M), à différents intervalles de temps. Les concentrations des solutions de trion sont : 1.10^{-2} M(1) ; 5.10^{-2} M(2) ; 1.10^{-1} M(3) et 5.10^{-1} M(4).

BIBLIOGRAPHIE

[1] J. Bardeen, W. H. Brattain et W. Shockley, *J. Chem. Phys.*, **14**, 714 (1946).

[2] A. Turos et Z. Wilhelmi, *Nukleonika*, **14**, 319 (1969).

[3] J. H. Close et B. D. Hines, *Isotop. Radiat. Technol.*, **7**, 104 (1970).

[4] K. Schwabe, K. Wagner et C. Weissmantel, *Z. phys. Chem. (Leipzig)*, **206**, 308 (1957).

[5] K. Schwabe, *Chem. Technol.*, **10**, 469 (1958).

[6] Ya. M. Kolotyrkin, *Electrochim. Acta*, **18**, 593 (1973).

[7] K. Akerman, *Chem. Anlagen Verfahren*, **5**, 68 (1972).

[8] J. G. N. Thomas, *Werkst. Korr.*, **19**, 957 (1968).

[9] F. Wormwell et J. G. N. Thomas, *Soc. Chem. Ind. London, Monogr.*, **28**, 365 (1968).

[10] R. Chan, *Nucleonics*, **9**, 13 (1951).

[11] K. H. Lieser, O. Kalvenes et S. Compostelle, *Corros. Sci.*, **4**, 51 (1964).

[12] R. Dreyer, I. Dreyer et J. Redlich, *Z. phys. Chem. (Leipzig)*, **228**, 404 (1965).

[13] I. Dreyer et R. Dreyer, *Z. phys. Chem. (Leipzig)*, **236**, 177 (1967).

[14] J. Redlich et R. Dreyer, *Z. phys. Chem. (Leipzig)*, **239**, 406 (1968).

[15] L. Grzelewski, H. Paluchowa, N. Krawczykowa, H. Piotrowska et M. Dukielski, *Przem. Chem.*, **52**, 165 (1973).

[16] Al. Cecal, N. Calu et P. Harabor, *Bull. Soc. chim. France*, **1975**, 1076.

[17] Al. Cecal et St. Roșu, *Radiochim. Acta*, **23**, 22 (1976).

[18] Al. Cecal et D. Ciobanu, *Radiochim. Acta*, **28**, 171 (1981).

[19] Al. Cecal, *Isotopenpraxis*, **17**, 328 (1981).
[20] Al. Cecal et V. Stan, *Z. phys. Chem. (Leipzig)*, **263**, 117 (1982).
[21] Al. Cecal et D. Ciobanu, *Radiochem. Radioanal. Letters*, **51**, 9 (1982).
[22] H.A.C. McKay, « Principles of Radiochemistry », Butterworths, London, 1971.
[23] U. R. Evans, « An Introduction to Metallic Corrosion », Arnold Publ., London, 1963.
[24] J. C. Scully, « The Fundamentals of Corrosion », Pergamon Press, New York, 1966.
[25] M. G. Fontana et R. W. Staehle, « Advances in Corrosion Science and Technology », Plenum Press, New York, 1970.
[26] A. E. Harvey et D. L. Manning, *J. Amer. Chem. Soc.*, **72**, 4488 (1950).
[27] J. F. Welcher, « Organic Analytical Reagents », Van Nostrand Comp., New York, 1955.
[28] H. L. Schläfer, « Komplexbildung in Lösung », Springer Verlag, Berlin, 1961.
[29] W. Machu et V. E. Mikhail, *Werkst. Korr.*, **13**, 276 (1962).
[30] K. Schwabe, *Farbe und Lack*, **76**, 988 (1970).
[31] L. Oniciu, E. Csegezi, A. Horvarth et C. Csegezi, *Studia Univ. Babeş-Bolyai, Cluj-Napoca*, **25**, 1 (1980).

Revue Roumaine de Chimie, **29**, *4*, 323–328 (1984)

INFLUENCE OF ADDED SALT ON THE ADSORPTION CHARACTERISTICS OF ALKALINE EARTH METAL SOAPS AT BENZENE-WATER INTERFACE

P. BAHADUR, K. SINGH and A. GUPTA
Chemistry Department, D.A.V. College, Muzaffarnagar-251001, India

Received February 27, 1981
Revised August 25, 1983

Adsorption characteristics of alkaline earth metal soaps in electrolytic solutions at benzene-water interface have been studied and the influence of KNO_3 and $Mg(NO_3)_2$ on the interfacial tension γ and consequently on CMC has been observed. Surface activity, the area per molecule of the soaps and the number of molecules adsorbed/cm^2 have been calculated using the appropriate form of Gibbs adsorption equation.

INTRODUCTION

Lower soaps (C_5 to C_8) of alkaline earth metals (Second Main Group) are water soluble where they form micellar aggregates. The micelle formation of calcium, [1] strontium [2] and magnesium [3] soaps in aqueous solution has been studied using physical methods such as conductivity, viscosity etc. Calcium soaps (valerate, caproate and caprylate) promote oil-in-water emulsions and their role in emulsion stability has been examined quantitatively. [4] Some preliminary studies on adsorption characteristics of these soaps at xylene-water interface have also been made. [5] We have studied [6] the influence of additives on micellar behaviour of alkaline earth metal soaps conductometrically and have reported that inorganic salts with varying anions have got the same effect on the micellization of these soaps in water. The present paper deals with the studies on adsorption of soaps at benzene-water interface in the presence of salt.

EXPERIMENTAL

Alkaline earth metal soaps were prepared by metathesis of the corresponding sodium soaps. [6] Double distilled water and AnalaR grade chemicals were always used.

Interfacial tensions at benzene-water interfaces were measured using the drop-volume technique with an Agla micrometer syringe which can deliver liquids accurate up to 0.0002 ml. The drops of aqueous soap solutions (in the presence of salt) were developed in benzene at a very slow speed for about 3 minutes in all the systems. The equilibrium was established within this time and no significant change in interfacial tension was observed on further ageing.

Measurements were made at a constant temperature of 40°C and the volume of single drop was averaged from five to six measurements. The correlation factor was also included in the interfacial tension calculation. The results were reproducible up to 1 %.

RESULTS AND DISCUSSION

The interfacial tension γ of metal soaps at benzene-water interface in the presence of inorganic salts is recorded in Tables 1 and 2. The CMC values obtained by γ vs. C plots (a representative set of curves is shown in Figs 1 and 2) are in close agreement with our previous findings by conductivity method.[6] Figures 1 and 2 show that the metal soaps reduce interfacial tension with a greater amount below CMC, and that above CMC the decrease in interfacial tension is very slow (or almost similar values of γ were seen at concentrations above CMC). Such a trend can be well understood from adsorption of molecules/ micelles at the interface. However, none of these soaps could lower γ values for more than

Table 1

Values of interfacial tension, surface pressure, area, number of molecules adsorbed and the surface excess for soaps in 0.002 N KNO_3 (aq.) against benzene

$\gamma_0 = 35.01$ dyne cm^{-1} Temp. 40°C

Soaps	Conc. of soap (mole litre^{-1})	Interfacial tension (dynes cm^{-1})	Surface pressure (dynes cm^{-1})	Number of molecules adsorbed/cm^2 $\times 10^{-12}$	Area/ molecule (A°)^2	Γg cm^{-2} $\times 10^{11}$
Ca valerate	0.001	34.18	0.83	5.03	1988	0.83
	0.003	33.80	1.21	15.08	663	2.50
	0.005	33.46	1.55	20.10	498	3.34
	0.006	33.50	1.71	23.12	433	3.84
	0.008	33.03	1.98	30.15	332	5.00
	0.010	32.75	2.26	30.15	332	5.00
	0.015	32.55	2.46	—	—	—
Sr caprylate	0.001	33.98	1.03	33.47	298	5.56
	0.002	32.65	2.36	47.74	209	7.92
	0.003	31.65	3.36	62.81	159	10.42
	0.005	30.00	5.01	85.43	117	14.18
	0.007	28.78	6.23	89.65	111	14.89
	0.008	28.57	6.44	—	—	—
	0.010	28.34	6.65	—	—	—
Ca caprylate	0.0005	33.73	1.28	22.61	442	3.75
	0.0008	33.30	1.71	36.88	271	6.12
	0.0010	33.04	1.97	56.98	176	9.46
	0.0015	32.16	2.85	—	—	—
	0.0020	31.85	3.16	—	—	—
	0.0030	31.75	3.26	—	—	—
Mg caprylate	0.001	31.98	3.03	34.27	298	5.68
	0.002	30.65	4.35	59.30	169	9.83
	0.003	29.69	5.32	62.81	159	10.42
	0.004	28.70	6.30	85.43	117	14.18
	0.005	28.25	6.75	—	—	
	0.006	28.15	6.85	—	—	—

Table 2

Values of interfacial tension, surface pressure, area, number of molecules adsorbed and the surface excess for soaps in 0.002 N $Mg(NO_2)_2$ (aq.) against benzene

$\gamma_0 = 35.01$ dynes cm^{-1} Temp. = 40°C

Soaps	Conc. of soap (mole $litre^{-1}$)	Interfacial tension (dynes cm^{-1})	Surface pressure (dynes cm^{-1})	Number of molecules adsorbed/cm^2 $\times 10^{-12}$	Area/ molecule $(A°)^2$	$\Gamma g \cdot cm^{-2} \times 10^{11}$
Ca valerate	0.001	34.01	1.00	10.05	995	1.67
	0.003	33.36	1.65	26.53	376	4.40
	0.005	32.83	2.18	33.47	298	5.56
	0.006	32.50	2.51	37.69	265	6.26
	0.008	32.42	2.59	—	—	—
	0.010	32.36	2.65	—	—	—
Sr caprylate	0.001	33.76	1.25	27.65	362	4.59
	0.002	32.54	2.47	55.28	180	9.18
	0.003	31.25	3.76	78.19	128	12.98
	0.004	30.22	4.79	100.50	99	16.68
	0.005	28.76	6.25	140.70	71	23.35
	0.008	28.24	6.77	—	—	—
	0.010	28.05	6.96	—	—	—
Ca caprylate	0.005	33.92	1.09	23.42	426	3.89
	0.0006	33.68	1.33	33.47	298	5.56
	0.0008	33.31	1.70	50.25	199	8.34
	0.0010	32.74	2.27	75.38	132	12.51
	0.0015	32.18	2.83	—	—	—
	0.0020	32.06	2.95	—	—	—
Mg caprylate	0.0005	32.21	1.80	32.56	307	5.40
	0.0006	32.94	2.07	35.88	278	5.96
	0.0008	32.46	2.55	39.09	256	6.49
	0.0010	32.00	3.01	50.25	199	8.34
	0.0015	30.90	4.11	62.81	159	10.42
	0.0020	30.15	4.86	75.37	133	12.51
	0.0030	29.52	5.49	—	—	—

6.86 dyne cm^{-1} even up to the concentration of 0.015 M. Such a little decrease shows their poor adsorption at the interface and consequently less surface activity. Furthermore the relative lowering in values was

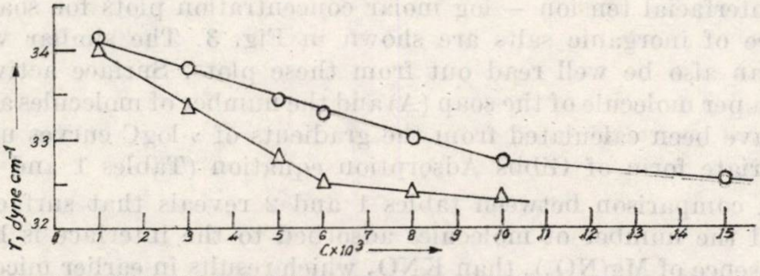

Fig. 1. — Plots of interfacial tension *vs.* concentration of calcium valerate in the presence of inorganic salts. ○ → 0.002 N KNO_3 ; △ → 0.002 N $Mg(NO_3)_2$.

dependent upon the number of carbon atoms in the hydrocarbon chain of the soap. The order of soap efficacy in lowering the interfacial tension is Mg caprylate > Ca caprylate > Sr caprylate > Ca valerate. This can be attributed to the dissociation of soap, *i. e.* the easier the dissociation of soap into ions, the greater the adsorption. It may also be concluded (Fig. 1) that metal soaps reduce the interfacial tension to greater amount in the presence of $Mg(NO_3)_2$ than KNO_3. This may be due to the greater tendency of Mg ions in approaching the monomers and thereby reducing the magnitude of electrical forces between the polar head groups. This enhances adsorption of soap molecules which ultimately brings in micellization.

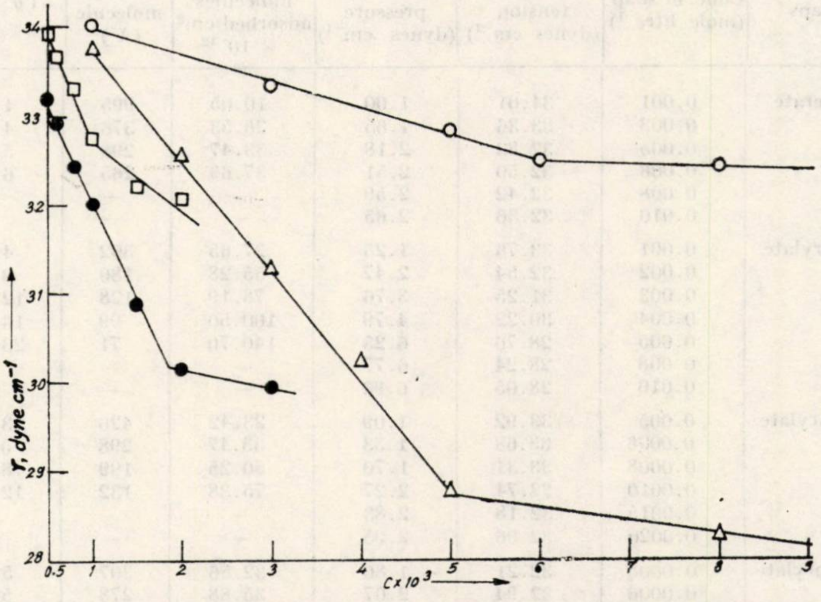

Fig. 2. — Plots of interfacial tension *vs.* concentration of soap in the presence of 0.002 N $Mg(NO_3)_2$ at 40°C. ○ → Ca valerate ; △ → Sr caprylate ; □ → Ca caprylate ● → Mg caprylate.

Interfacial tension — log molar concentration plots for soap in the presence of inorganic salts are shown in Fig. 3. The similar values of CMC can also be well read out from these plots. Surface activity (Γ), the area per molecule of the soap (A) and the number of molecules adsorbed/ /cm² have been calculated from the gradients of ν-logC curves using the appropriate form of Gibbs Adsorption equation (Tables 1 and 2).

A comparison between tables 1 and 2 reveals that surface excess (Γ) and the number of molecules adsorbed to the interface is higher in the presence of $Mg(NO_3)_2$ than KNO_3 which results in earlier micellization of soaps in the presence of $Mg(NO_3)_2$. It is obvious that with the increase in concentration of the soaps, the number of molecules adsorbed to the surface and the values of surface excess are always increased which shows positive adsorption of these soaps. Increase in these values is much sharper initially and at higher concentrations it reaches a limiting value. Furthermore a comparison of these values for soaps confirms the finding that metal caprylates are more strongly adsorbed than valerate ones.

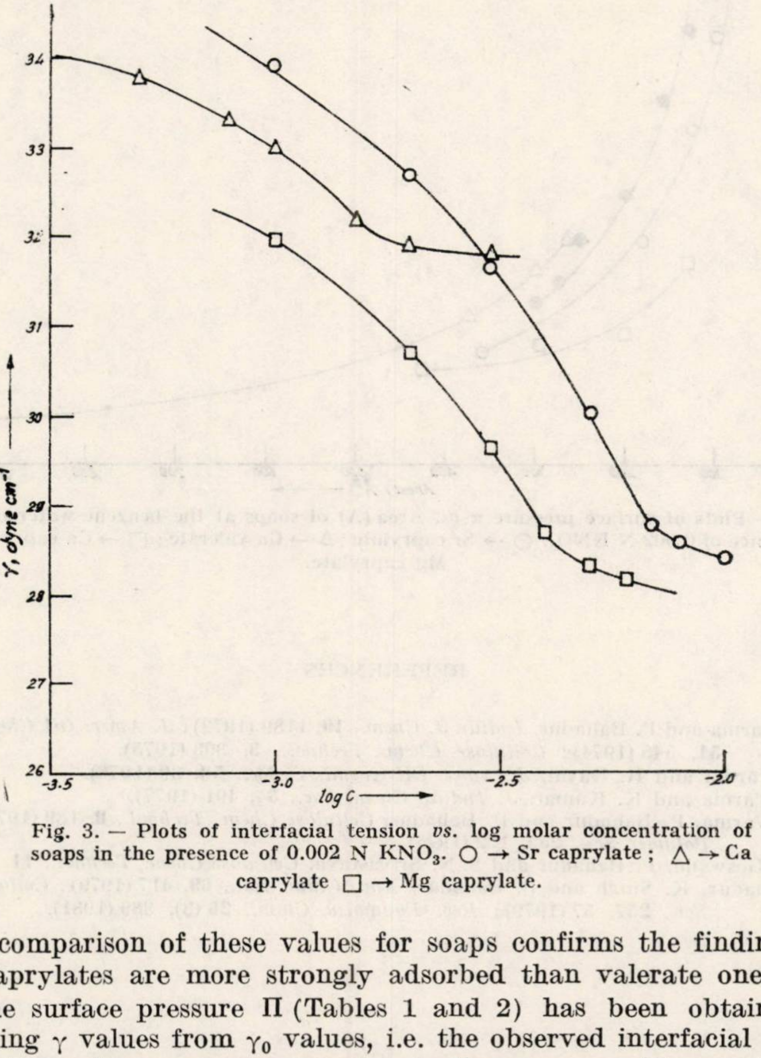

Fig. 3. — Plots of interfacial tension *vs.* log molar concentration of soaps in the presence of 0.002 N KNO_3. ○ → Sr caprylate ; △ → Ca caprylate □ → Mg caprylate.

The surface pressure Π (Tables 1 and 2) has been obtained by subtracting γ values from γ_0 values, i.e. the observed interfacial tension values of pure benzene-water interface in the presence of inorganic salts, which was 35.01 dynes cm^{-1} at 40°C. It is clear from Π – A curves (Fig. 4) that initially, *i.e.* at low soap concentrations, only slight increase in surface pressure is capable of reducing the area to greater extent but at higher concentrations a large increase in force produces very little decrease in area. The same trend has also been observed earlier with a large decrease in area at low pressure and then with the attainment of limiting value of area even the pressure increases sharply.

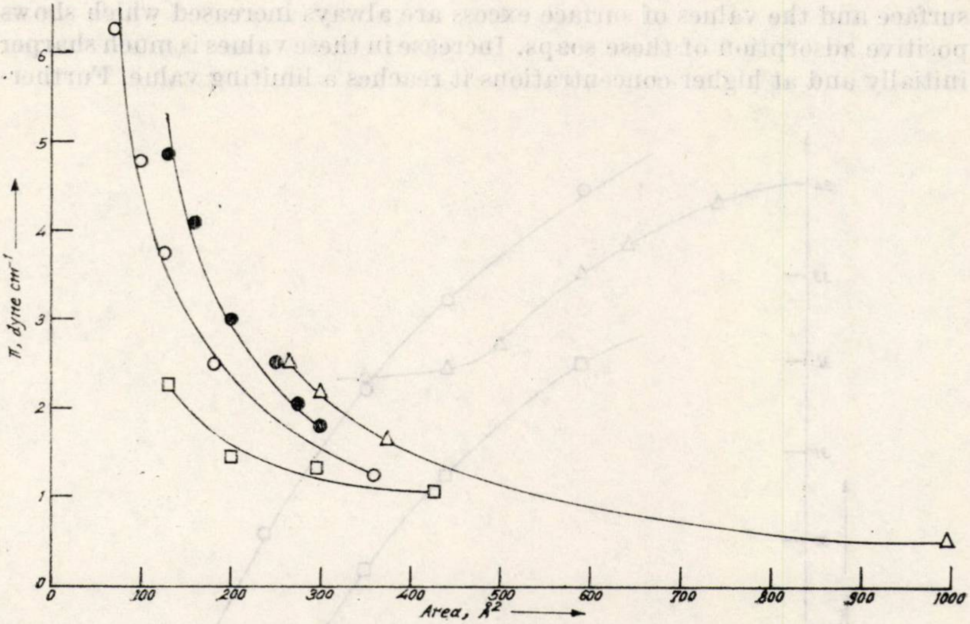

Fig. 4. — Plots of surface pressure π *vs.* Area (A) of soaps at the benzene-water interface in the presence of 0.002 N KNO_3. ○ → Sr caprylate ; Δ → Ca valerate ; □ → Ca caprylate ; ○ → Mg caprylate.

REFERENCES

[1] R. P. Varma and P. Bahadur, *Indian J. Chem.*, **10**, 1189 (1972) ; *J. Amer. Oil Chemists' Soc.*, **51**, 545 (1974) ; *Cellulose Chem. Technol.*, **9**, 393 (1975).

[2] R. P. Varma and R. Dayal, *J. Amer. Oil Chemists' Soc.*, **53**, 39 (1976).

[3] R. P. Varma and K. Kumar, *J. Indian Chem. Soc.*, **54**, 491 (1977).

[4] R. P. Varma, P. Bahadur and P. Bahadur, *Cellulose Chem. Technol.*, **8**, 189 (1974) ; *Colloid Polymer Sci.*, **253**, 132 (1975).

[5] A. K. Goswami, P. Bahadur and S. N. Srivastava, *Cellulose Chem. Technol.*, **11**, 377 (1977).

[6] P. Bahadur, K. Singh and P. Bahadur, *Ann. Chim. Ital.*, **69**, 417 (1979) ; *Colloid Polymer Sci.*, **257**, 57 (1979) ; *Rev. Roumaine Chim.*, **26** (3), 389 (1981).

Revue Roumaine de Chimie, **29**, *4*, 329—331 (1984)

SYNTHESIS OF AROMATIC THIOUREAS UNDER MILD CONDITIONS USING A NEW CONDENSATION REACTION

C. I. CHIRIAC

"P. Poni" Institute of Macromolecular Chemistry, Aleea, Gr. Ghica Vodă 41 A, Iași, Romania

Received February 2, 1983

Aromatic thioureas are prepared in good yields by the reaction between aromatic amines and carbon disulfide in the presence of ethylene chlorophosphite in pyridine as reagent at room temperature.

Phosphorus acid hexaalkyltriamide prepared from phosphorus trichloride and secondary amines afforded the corresponding carbamoyloxy compounds by inserting carbon dioxide. [1] Other phosphorus-nitrogen compounds prepared from phenyldichlorophosphite and amines can react with carbon dioxide and carbon disulfide, affording ureas or thioureas. [2]

RESULTS AND DISCUSSION

A previous communication from this laboratory showed that ethylene chlorophosphite in pyridine is a useful reagent in synthesis of amides. [3]

In this work we have investigated the applicability of this reaction in synthesis of aromatic thioureas. We found that ethylene chlorophosphite is a very good reagent in this field. We obtained aromatic thioureas in high yields, just at room temperature. Thus from a solution of aniline and carbon disulfide in pyridine in the presence of ethylene chlorophos phite at room temperature, diphenyl thiourea resulted in high yield.

By addition of ethylene chlorophosphite to a solution of an aromatic amine (I) in pyridine, a reactive compound results, similar to many other cases. [1–4] In this case, we supposed that this reactive intermediate is an amide of ethylene phosphorous acid (II), which can further react with

CS_2, affording (III) and (IV):

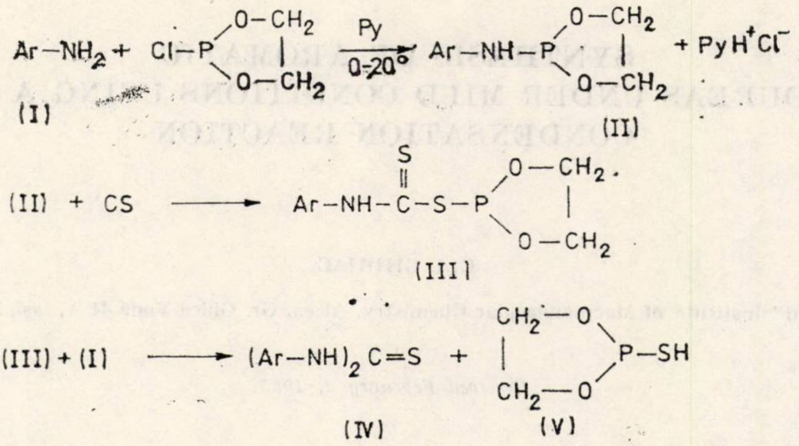
Ar—NH2 + Cl—P(O—CH2)2 —Py, 0-20°→ Ar—NH—P(O—CH2)2 + PyH+Cl−
(I)
(II)
(II) + CS → Ar—NH—C(=S)—S—P(O—CH2)2
(III)
(III) + (I) → (Ar—NH)2 C=S + (CH2—O)2P—SH
(IV)
(V)

Thus, from reaction between aniline (1 mole), ethylene chlorophosphite (1 mole) and pyridine (1 mole) in dried benzene as solvent at room temperature, after 2—3 hours, pyridine hydrochloride (about 1 mole with m.p. 80—82°) results as by-product, insoluble in this solvent. The pyridine hydrochloride was filtered and the filtrate was evaporated, resulting the reactive intermediate II ($Ar-C_6H_5$) as a syrup capable to react with CS_2. The separation of pyridine hydrochloride is an indirect argument for the structure (II). Tertiary amine plays an important role in the reaction. We tried many tertiary amines, but the pyridine was found to be the most suitable base as acceptor for hydrochloric acid and as solvent for the final products. The by-product (V) and PyH^+Cl^- do not affect the reaction, similar to other cases. [3,4] We supposed, also similar to other cases, [3,5,6] that this reaction involves a four-centred transition state (VI):

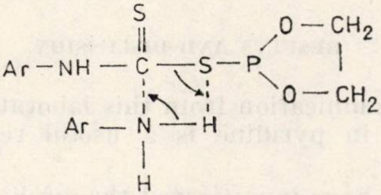

(VI)

The mechanism of the reaction, on which the method is based, will be extensively discussed in a separate communication.

In a typical procedure, to a solution of a 2 moles (I) and 1 mole CS_2 in dried pyridine cooled to 0°, 1 mole ethylene chlorophosphite was added very slowly, under stirring. After 24 hours at room temperature, the final product (IV) was separated by precipitation with water and ice.

Table 1 shows the aromatic thioureas obtained in this way. The yields ranged from 67 to 91%.

Table 1

Aromatic thioureas obtained from aromatic amines and CS_2 in the presence of ethylene chlorophosphite/Py, as reagent

$(Ar-NH)_2C=S$ a) Ar :	Yield b) %	M.p. c) °C	Reported m.p. d) °C
C_6H_5	91	153—155	154—155
p-CH_3-C_6H_4	89	177—179	178—179
-naphthyl	85	206—208	207
-naphthyl	88	192—193	192—193
p-Cl-C_6H_4	68	172—174	173—174
m-Cl-C_6H_4	73	130—132	131—133
p-Br-C_6H_4	67	187—189	188—189
p-CH_3O-C_6H_4	90	184—186	184—185

a) The products were identified by comparison of m.p. and IR spectra with those of authentic sample.
b) Yields determined by isolation of the crude products.
c) After recrystallisation.
d) From "Beilstein Handbuch der organischen Chemie".

By this new synthesis, we obtained in high yields, aromatic thioureas at room temperature.

EXPERIMENTAL

Diphenyl thiourea

To 10 ml dried pyridine in a 50 ml three-necked flask, 3.64 ml (0.04 moles) aniline and 1.2 ml (0.02 moles) carbon disulfide were added. Then under stirring and cooling, 1.8 ml (0.02 moles) ethylene chlorophosphite were added. After stirring 24 hours at room temperature, the obtained solution was poured into a large volume of water with ice (50—70 ml), when the diphenyl thiourea precipitated. The product was collected by filtration and washed with 40—50 ml 7% HCl solution and three times with 20—30 ml water. After drying under vacuum at 100—120° and recrystallisation from ethanol, 4.15 g diphenyl thiourea with m.p. 153—155° were obtained (mixed m.p. with pure diphenyl thiourea undepressed). Yield 91% (calculated on aniline employed). Anal. Calculated for : $C_{13}H_{12}N_2S$; C, 68.41 ; H, 5.21 ; N ; 12.28%. Found : C, 68.33 ; H, 5.48 ; N, 12.39%.

In similar conditions, the other aromatic thioureas (presented in table 1) were prepared.

REFERENCES

[1] G. Ortel and H. Holtschmidt, *Chem. Ber.* **97**, 891 (1964).
[2] N. Yamazaki, T. Tomioka and F. Higashi, *Bull. Chem. Soc. Japan*, **49**, 3106 (1976).
[3] C. I. Chiriac, *Rev. Roumaine Chim.*, (in press).
[4] N. Yamazaki, T. Iguchi and F. Higashi, *Tetrahedron Letters*, **1974**, 1191 ; *Tetrahedron*, **31**, 3031 (1975).
[5] C. I. Chiriac, *Rev. Roumaine Chim.*, **26**, 1001 (1981).
[6] H. O. Becker and K. F. Funk, *J. prakt. Chem.*, **14**, 55 (1961).

Table I

Aromatic thioureas obtained from aromatic amines and CS_2 in the presence of ethylene chlorophosphite. Py, as reagent

$(Ar-NH)_2C=S$ a) Ar	Yield b) %	M.p. °C c)	Reported m.p. °C d)
C_6H_5	91	153	154–155
$p\text{-}CH_3\text{-}C_6H_4$	89	177–179	178–179
α-naphthyl	85	206–208	207
β-naphthyl	88	182–183	192–193
$p\text{-}ClC_6H_4$	86	172–174	172–174
$m\text{-}ClC_6H_4$	78	130–132	131–132
$p\text{-}BrC_6H_4$	87	187–189	188–189
$p\text{-}CH_3O\text{-}C_6H_4$	90	184–186	184–185

a) The products were identified by comparison of m.p. and IR spectra with those of authentic sample.
b) Yields determined by isolation of the crude products.
c) After recrystallisation.
d) From Beilstein Handbuch der organischen Chemie.

By this new synthesis, we obtained in high yields, aromatic thioureas at room temperature.

EXPERIMENTAL

Diphenyl thiourea

To 10 ml dried pyridine in a 50 ml three-necked flask, 3.64 ml (0.04 moles) aniline and 1.2 ml (0.02 moles) carbon disulfide were added. Then under stirring and cooling, 1.8 ml (0.02 moles) ethylene chlorophosphite were added. After stirring 24 hours at room temperature, the obtained solution was poured into a large volume of water with ice (50–70 ml), when the diphenyl thiourea precipitated. The product was collected by filtration and washed with 40–50 ml 7% HCl solution and three times with 20–30 ml water. After drying under vacuum at 100–120° and recrystallisation from ethanol, 4.15 g diphenyl thiourea with m.p. 153–154° were obtained (mixed m.p. with pure diphenyl thiourea undepressed). Yield 91% (calculated on aniline employed). Anal. Calculated for $C_{13}H_{12}N_2S$, C, 68.41; H, 5.21; N, 12.28%. Found: C, 68.32; H, 5.48; N, 12.30%.

In similar conditions, the other aromatic thioureas (presented in table I) were prepared.

REFERENCES

1 G. Oertel and H. Holtschmidt, Chem. Ber. 97, 891 (1964).
2 N. Yamazaki, T. Tomioka and F. Higashi, Bull. Chem. Soc. Japan, 49, 3106 (1976).
3 C. I. Chiriac, Rev. Roumaine Chim., (in press).
4 N. Yamazaki, T. Iguchi and F. Higashi, Tetrahedron Letters 1975, 1191; Tetrahedron 31, 3031 (1975).
5 C. I. Chiriac, Rev. Roumaine Chim., 26, 1291 (1980).
6 G. O. Becker and K. F. Funk, J. prakt. Chem. 14, 35 (1961).

Revue Roumaine de Chimie, **29**, *4*, 333–343 (1984)

CONDENSATION OF BIS (CHLOROMETHYL)ETHER WITH SECONDARY AMINES. A NEW REACTION

M. IOVU[a] and M. IQBAL[b]

[a] Faculty of Pharmacy, Bucharest, str. Traian Vuia no. 6, Romania
[b] Case Western Reserve University, Cleveland, Ohio, 44106, SUA

Received January 11, 1983

In the attempted synthesis of diaminoethers through the condensation of bis(chloromethyl) ether with secondary amines, methylenebisamines resulted by a reaction not yet mentioned in the literature. The methylenebisamines thus synthesized are identical with those prepared by the condensation of formaldehyde with the corresponding secondary amines. The physical constants and the infra-red or ^{1}H-NMR spectra are also identical. The proposed reaction mechanism implies the participation of secondary amine and bis (chloromethyl) ether in a molar ratio of 6 : 1 in order to form methylenebisamines and the hydrochloride of the initial secondary amine in the highest yields. This assumption was experimentally confirmed.

INTRODUCTION

Bis(chloromethyl)ether being halogen compounds with enhanced reactivity take easily part in nucleophilic substitution reactions. For example through attack on phenoxide ions, trisethers are formed. [1–5] Using dihydroxylic phenols or bisphenols, macromolecular polyethers can be obtained.

It was thought that bis (chloromethyl) ether would react with amines in a similar fashion e.g. with *sec*-amines, diaminoethers could occur. Keeping in mind the above analogy the bis(chlormethyl) ether was treated with different *sec*-amines, a reaction which has not been mentioned in literature.

Diaminomethyleneethers are unknown compounds. All the efforts made for the separation of diaminomethyleneethers did not succeed.

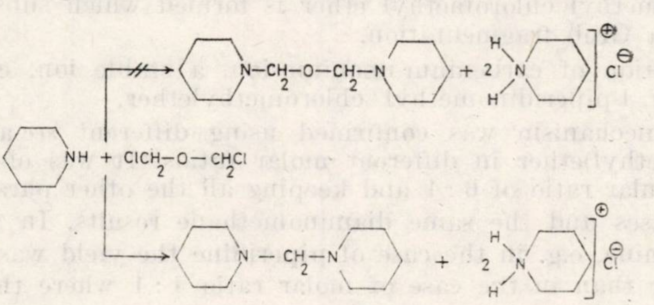

From the reaction tertiary amines, namely methylenebisamines, less basic than the secondary amines, are formed. Therefore the secondary amines were taken in excess to make sure the complete participation of bis(chloromethyl)ether in the reaction.

Hydrochlorides of *sec*-amines were precipitated and separated using non polar solvents such as benzene and petroleum ether.

Formation of methylenebisamines was confirmed using IR and ^{1}H-NMR spectroscopy.

In IR-spectra we could not identify the corresponding νC$-$O antisymmetric bands, but in ^{1}H$-$NMR spectra a signal appears at $\delta = 5.4$ ppm in the case of methylenebispiperidine corresponding to two protons of methylene group and not to the 4 protons expected in the case of bis (piperidinemethylene)ether.

To verify the unexpected reaction products, the methylenebisamines were synthesized by a different method, namely through condensation of *sec*-amines with formaldehide.

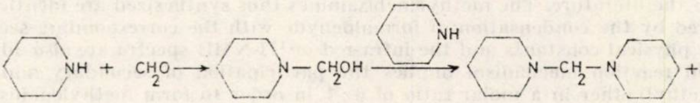

This reaction has been known for a long time,[6-9] different authors showing the reaction of formaldehyde (35$-$40%) with *sec*-amines in the molar ratio of 1 : 2 when hydroxymethyleneamine was formed as intermediate.

1,1′-Methylenebispiperidine which separates from the aqueous layer, in our reaction was separated by decantation, dried and distilled under vacuum. IR spectrum of 1,1′-methylenebispiperidine is identical with that of our product obtained from the condensation of bischloromethyl-ether with piperidine.

Other authors have reported the synthesis of methylenebisamines using paraformaldehyde and trioxymethylene instead of formaldehyde in aqueous solution.[10-12]

In the condensation of bis(chloromethyl)ether with piperidine using the molar ratio of 1 : 4, 1,1′-methylenebispiperidine and piperidine hydrochloride were formed as unique products. It was supposed that firstly l-piperidinomethyl chloromethyl ether is formed which subsequently is broken by a Grob fragmentation.

Formation of carbenium-imonium-ion, a stable ion, explains the breakage of l-piperidinomethyl chloromethylether.

This mechanism was confirmed using different *sec*-amines with bis(chloromethyl)ether in different molar ratios. It was observed that using molecular ratio of 6 : 1 and keeping all the other parameters the yield increases and the same diaminomethane results. In the case of every *sec*-amine, e.g. in the case of piperidine the yield was 77%, thus much better than in the case of molar ratio 4 : 1 where the observed yield was 42.5%.

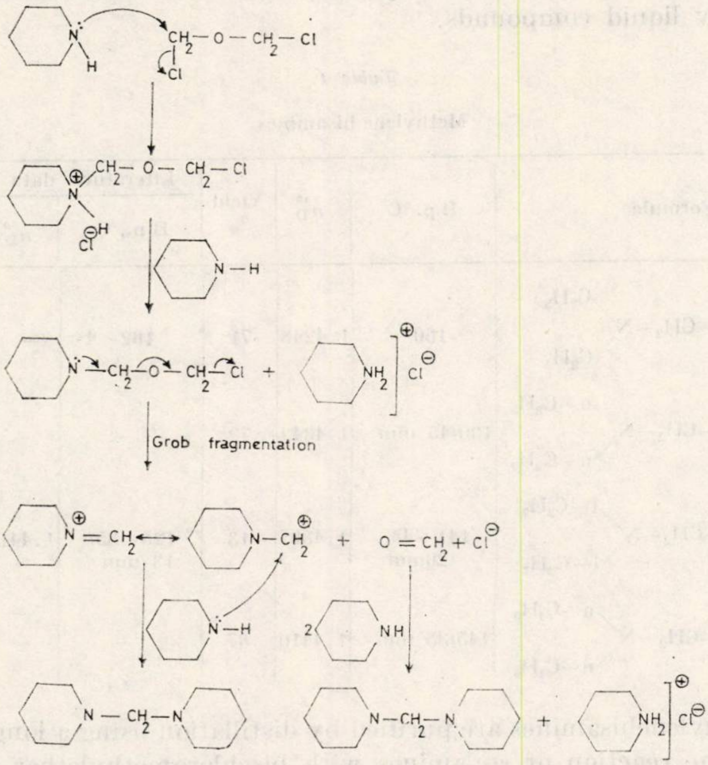

In the case of 2 : 1 molar ratio of *sec*-amines and bischloromethyl-ether, hydrochlorides of methylenebispiperidine were formed (in 78% yield) and were converted to methylenebispiperidine by treating with bases.

It was very interesting to find out that working at a molar ratio of 6 : 1, directly methylenediamines were formed while in the case of molar ratio 2 : 1, firstly the dihydrochlorides were formed which were converted into methylenediamine by treating them with sodium hydroxide solutions.

RESULTS AND DISCUSSION

In agreement with the reaction mechanism presented above when the *sec*-amine is taken in excess, every molecule of bischloromethyl-ether uses 6 molecules of *sec*-amine for the completion reaction affording methylenebisamines and hydrochloride of the starting *sec*-amine which is more basic than the methylenebisamines.

$$6\ {>}NH+ClCH_2-O-CH_2Cl-2\ {>}N-CH_2-N{<}\ +2\ \left[{>}N{<}^{H}_{H}\right]^{+}Cl^{-}+H_2O$$

Hydrochlorides being solid substances can be precipitated with petroleum ether and can be separated easily from the methylenebisamines which are usually liquid compounds.

Table 1

Methylene bisamines

Formula	B.p. °C	n_D^{23}	Yield %	Literature data		Reference
				B.p., °C	n_D^{20}	
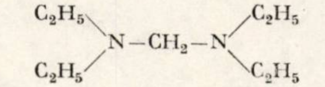	160	1.4248	71	162–4	—	9,12,17
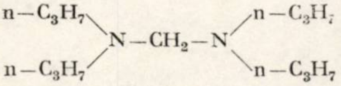	130/45 mm	1.4342	72	—	—	15
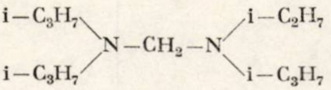	141–45/ 26mm	1.4397	13	128--35/ 13 mm	1.4415	13,14
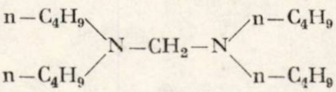	145/33 mm	1.4410	87	—	—	16

Methylenebisamines are purified by distillation using a long column.

In the reaction of *sec*-amines with bischloromethylether in molar ratio 6 : 1, the acyclic amines : diethylamine, di-*n*-propylamine, di-*iso*-propylamine, di-*n*-buthylamine and cyclic amines : pyrrolidine, piperidine, 2-, 3-, and 4-methylpiperidine, 2,6-dimethylpiperidine, 2-ethylpiperidine, 4-benzylpiperidine, hexamethylenimine, morpholine, 2,6-dimethylmorpholine, *N*-methylpiperazine, *N*-phenylpiperazine and *N*-benzylpiperazine were used. Some of the methylenebisamines are already known in the literature (Table 1).

Even the compounds previously described, were characterised by us for the first time especially by spectroscopic methods.

SPECTRAL CHARACTERISTICS

Although methylenebisamines have been synthesized and used by many authors, [17,18,21] their spectral characteristics were not dealt with.

In a paper [22] referring to *gem*-di(*N*-amines), the authors have mentioned "De façon tout à fait général", for morpholine nucleus a band ν as C–O at 1100 cm^{-1} and other ν s C–O at 930 cm^{-1} in IR.

Table 2

Methylenebisamines

Formula	B p °C	n_D^{23}	Yield %	C% calc. found	H% calc. found	N% calc. found	Literature B p °C	data n_D^{20}	Reference
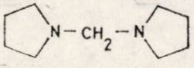	112/42 mm	1.4756	63	70.08 69.78	11.76 11.59	18.15 17.95	94–5/30mm		17,23
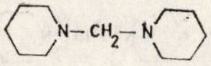	115/25 mm	1.4814	77	71.84 71.63	12.92 12.69	15.12 15.42	120–5/22mm	1.4835	7,17
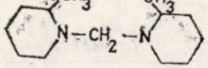	145/26 mm	1.4794	82	74.23 73.95	12.45 12.31	13.31 13.40	—	—	—
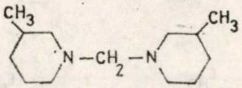	137/25 mm	1.4723	74	74.23 73.94	12.45 12.25	13.31 13.80	—	—	—
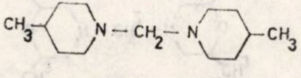	142/24 mm	1.4702	86	74.23 73.81	12.45 12.09	13.31 13.63			18
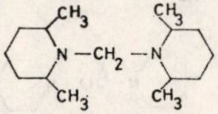	165/24 mm	1.4727	22	75.56 75.38	12.68 12.19	11.74 11.30	—	—	15
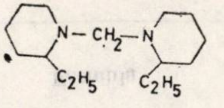	168/24 mm	1.4830	51	75.56 75.21	12.68 12.43	11.74 11.31	—	—	—
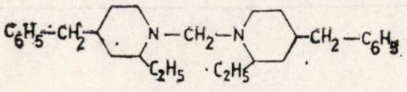	95	—	80	82.82 82.91	9.45 9.21	7.72 7.76	—	—	—
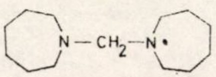	175/46 mm	1.4901	86	74.24 73.95	12.45 12.19	13.31 13.56	128–34/4 mm	1.4930	10

Table 3

Methylenebisamines

Formula	B p °C	n_D^{23}	Yield %	C% calc. found	H% calc. found	N% calc. found	Literature B p °C	data n_D^{20}	Reference
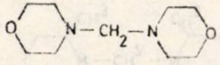	145/35 mm	1.4783	82	58.04 58.46	9.47 9.59	15.04 15.26	113–4/9 mm	1.4803	11
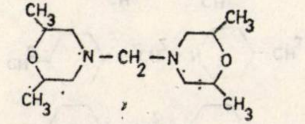	165/70 mm	1.4600	25	64.42 64.29	10.72 10.91	11.55 11.23	—	—	—
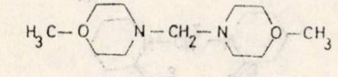	162/36 mm	1.4838	73	62.22 62.01	11.39 11.48	26.37 26.59	—	—	—
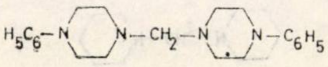	119	—	85	72.57 72.81	9.61 9.30	17.80 17.61	—	—	—
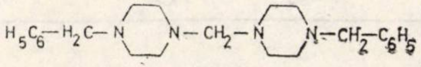	127	—	80	75.78 75.46	8.84 8.62	15.36 15.21	123–4	—	22

Infra-red spectra

IR spectra of methylenebisamines are characterized by the presence of an absorption band in the region of ν C—H at lower wavenumber values than hydrocarbons. A band of a similar type is also mentioned for methyl groups bonded with aminic nitrogen. [22 23]

At methylenebis(dialkylamines) absorption bands due to stretching vibrations of methyl and methylene groups have been presented.

The bands arising from asymmetric vibrations of C—H linkage of CH_3 and CH_2 are present at 2950 cm^{-1} and 2927 cm^{-1}.

The band due to ν s CH_3 is mixed with the band from ν sCH_2 e.g. in the case of methylenebis(di-*n*-buthylamine), or it is observed separately with a very low intensity at 2883 cm^{-1} as in the case of methylene(di-*n*-propylamine). The band due to ν sCH_2 is more intense and is present at 2863 cm^{-1}.

Stretching vibrations of CH_2 groups in the neighbourhood of nitrogen atom present a band with medium intensity at 2790 cm^{-1} and another weak band at 2730 cm^{-1}.

Due to deformation vibrations of methyl group and due to scissoring vibrations of methylene groups a single bond (which in some of the cases is splitted) at 1465 cm^{-1} is observed, while due to δsCH_3 deformation vibrations a medium band at 1368 cm^{-1} is observed.

Methylenebisamines with a single heteroatom presents an intense band due to ν $asCH_2$ from methylene groups. This band increases in intensity from methylenebispyrrolidine to methylenebispiperidine and methylenebis (hexamethylenimine) with the increase of CH_2 groups in the ring and at the same time its value decreases from 2954 cm^{-1} for pyrrolidine to 2927 cm^{-1} for hexamethylenimine.

The ν sCH_2 band is less intense and is also shifted from 2800 to 2850 and to 2847 cm^{-1}.

The bisamines show two bands in this region, one due to stretching vibrations of CH_2 in the neighbourhood of nitrogen atom of the ring and of CH_2 which links two nitrogen atoms.

In the fingerprint region, bands due to stretching vibration of C—N are present at 1134 and at 1090 cm^{-1}. Due to methyl or ethyl, the substitution at the ring spectra becomes more complicated.

Methylenebis (4-benzylpiperidine) due to benzenic nucleus shows characteristic stretching vibrations of C—H at 3085, 3065, 3030 cm^{-1} and in fingerprint region vibrations at 1600 and 1492 cm^{-1} due to C=C stretching.

Heterocyclic methylenebisamines with two heteroatoms (Table 3). In IR spectra of these amines characteristic bands are present *e.g.* in the case of methylenebismorpholine in the region of C—H stretching vibration many bands at 2952, 2912, 2890 and at 2846 cm^{-1} are found.

Electronic spectra

Methylenebisamines do not absorb in UV because they have only σ bonds while the unsharing electrons can have $n \rightarrow \sigma^*$ transitions which take place at higher energy and therefore have lower values. Methylenebisamines with benzene nucleus absorb in UV e.g. methylenebis (4-benzylpiperidine), and methylenebis(N-phenylpiperazine).

In the case of methylenebis (4-benzylpiperidine) many absorption maxima are observed: 224, 249, 252, 260, 262, 265, 268 nm.

The band at 224 is of E type, shifted bathochromically due to substitution at benzene nucleus.

The spectra show similarity with that of benzene in the region of benzenoid bands.

^{1}H-Nuclear magnetic resonance spectra

It is mentioned [22] that protons from α carbon atoms to nitrogen show signals at $\delta = 2.60 - 2.40$ ppm.

Methylenebis (dialkyl)amines (Table 1) show very well resolved spectra. Methylenebis (di-N-propyl)amine spectrum registered in $CDCl_3$, shows a singlet for protons between the nitrogen atoms which are deshielded and have higher value of δ (Table 4). The other signals correspond to propyl protons.

Table 4

^{1}H-NMR Analysis of Methylenebisamines

Formula	δ_{ppm}	Number of protons	Spin-spin splitting	Type of protons
$(CH_3CH_2CH_2)_2N-\underset{a}{CH_2}-N(\underset{b}{CH_2}\underset{c}{CH_2}\underset{d}{CH_3})_2$	2.93	2	singlet	a
	2.40	8	triplet	b
	1.43	8	multiplet	c
	0.87	12	triplet	d
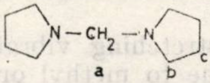	3.20	2	singlet	a
	2.55	8	multiplet	b
	1.76	8	multiplet	c
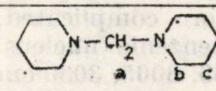	2.65	2	singlet	a
	2.31	8	multiplet	b
	1.40	12	multiplet	c
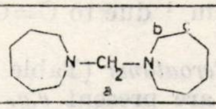	2.95	2	singlet	a
	2.56	8	multiplet	b
	1.56	16	singlet	c
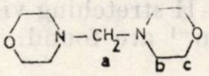	3.63	8	triplet	b
	2.86	2	singlet	a
	2.43	8	multiplet	c

^{1}H-NMR spectra of heterocyclic methylenebisamines with a single heteroatom correspond very well to the products obtained from the mechanism proposed by us. For example in ^{1}H-NMR spectrum of methylenebispyrrolidine registered in $CDCl_3$ all the three kinds of protons show three different signals (Table 4). A singlet at $\delta = 3.20$ ppm is due to CH_2 situated between nitrogen atoms (Table 4).

The deshielding effect is stronger than in the case of methylenebis (di-*n*-prophylamine), where propyl radicals have a stronger + I effect than the methylene groups in the pyrrolidine nucleus: one multiplet at $\delta = 2.55$ ppm due to protons from carbon near nitrogen atom and another multiplet at $\delta = 1.40$ ppm due to protons from other CH_2 groups in the nucleus.

In methylenebispiperidine (Table 2), protons from $N-CH_2-N$ are less deshielded than those in methylenebishexamethyleneimine (Table 4) and they in turn are less deshielded than in methylenebispyrrolidine.

The values in table 4 show that other signals are found in the same order.

The ^{1}H-NMR spectra of heterocyclicmethylenebisamines with two heteroatoms reflect the structure very well. For example in methylenebismorpholine (Table 4), the signal from protons of CH_2 between nitrogen atoms is at higher value than in methylenebispiperidine with a single heteroatom.

The neighbouring protons of oxygen are more deshielded than those of nitrogen.

EXPERIMENTAL

The secondary amines used as starting materials were pure commercial products, Fluka Merck, or Aldrich.

The bis(chloromethyl)ether was obtained through condensation of paraformaldehyde with hydrochloric acid in the presence of chlorosulphonic acid.[24]

Methylenebis(diethylamine) has been reported in a patent[10] and was synthesized from diethylamine and formaldehyde in 62% yield. Similary reports were found with 90% yield when water is azeotropically removed with benzene.[12]

Reaction of diethylamine with bis(chloromethyl)ether in petroleum ether proceeds with a slow rate as compared with that of di-*n*-buthyl amine.

Methylenebis(di-n-propylamine) has been reported in a paper which is concerned mainly cryoscopic studies.[15]

Methylenebis(di-iso-propylamine) was synthesized from di-*iso*-propylamine and formaldehyde (40%) in the molar ratio of 2 : 1.[13,14]

Condensation of di-*n*-propylamine with bis (chloromethyl)-ether was carried out in benzene.

Di-*iso*-propylamine reacts with bis(chloromethyl)ether more slowly than di-*n*-propylamine does.

Methylenebis(di-n-butylamine) has been reported in a German petent.[16] Reaction of di-*n*-butylamine with bis(chloromethyl)ether proceeds in very good yield.

Methylenebispyrrolidine has been synthesized from pyrrolidine and trioxymethylene.

By condensation of pyrrolidine with bis(chloromethyl)ether in hexane under reflux the hydrochloride of pyrrolidine results, as an oily mass which does not crystallize and is heavier than the solution of methylenebispyrrolidine in hexane.

Metylenebispiperidine is one of diamines synthesized much earlier by many authors. Putochin[10] suggested the intermediate piperidinomethanol which reacts with another molecule of piperidine conducting to the di-piperidinomethane.[7,11,17]

Reaction of piperidine with bis(chloromethyl)ether is very exothermic. Hydrochloride formation starts right at the begining of addition of the bis(chloromethyl)ether and its separation is very easy as well.

Of the *methylenebis(methylpiperidine)* only 4-methyl-piperidine is mentioned in the literature but it has not been characterized.[18]

Methylenebis(2,6-dimethylpiperidine) was not formed from piperidine and formaldehyde as mentioned in an article.[15]

In the new reaction described here we have synthesized it, the reaction is slower than at piperidine, due to steric hindrances. The yield is very small in this case.

Methylenebis(2-ethylpiperidine) was synthesized for the first time by the condensation of bis(chloromethyl)ether with 2-ethyl-piperidine in hexane under reflux. The reaction rate is slower than at 2-methylpiperidine and the yield is smaller.

Methylenebis(4-benzylpiperidine) is not mentioned in the literature. Reaction of 4-benzylpiperidine with bis(chloromethyl)-ether is very fast and a bulky precipitate is formed ; this requires the solvent to be in excess. The product as well as hydrochloride of 4-benzylpiperidine are solids and are separated by washing with water.

Methylenebismorpholine was synthesized previously from morpholine and formaldehyde in aqueous solution,[11] trioxymethylene or paraformaldehyde.[20,21]

Condensation of morpholine with bis(chloromethyl)ether was carried out in benzene under reflux. The reaction is slower than at piperidine but a good yield was obtained (Table 3).

Methylene-bis(N-methylpiperazine) was also synthesized for the first time by the condensation reaction of N-methyl-piperazine with bis(chloromethyl)ether, under the same conditions as described with piperidine and substituted piperidine.

Methylene-bis(N-phenylpiperazine) has not been reported. It results from the condensation reaction with bis-(chloromethyl)ether with N-phenylpiperazine in hexane under reflux. Soon after the addition of bis(chloromethyl)ether the precipitate is formed. The product and hydrochloride of *N*-phenylpiperazine (both solids) are separated by washing with water.

Methylenebis(N-benzylpiperazine) is known in the literature as resulting from the reaction of N-benzylpiperazine with formaldehyde in the molar ratio of 2 : 1.

Condensation of piperidine with bis(chloromethyl)ether in a molecular ratio of 6 : 1. In a three-necked flask provided with a reflux refrigerator, a stirrer, and funnel (which could be changed with a thermometer) 17.03 g piperidine (1/5 mol) and 50 ml petroleum ether were introduced. 3.83 g Bis(chloromethyl)-ether (1/30 mol) in 25 ml petroleum ether were gradually added under cooling and stirring. A white precipitate immediately appeared. The stirring was continued two hours at room temperature. After filtration, the filtrate was evaporated to remove the solvent. The remained liquid was distilled at 24—25 mm Hg and the fraction with b.p. 112—115° was isolated. The yield in methylenebispiperidine was 76%.

The precipitate was washed with petroleum ether and dried in vacuum. 7.6 g piperidine hydrochloride resulted. Yield 94%.

The other methylenebisamines were synthesized under similar conditions.

The UV spectra were recorded with a Specord-UV-Vis Carl Zeiss-Jena in methanol solution.

The IR spectra were obtained with the Specord IR-75 Carl Zeiss Jena in CS_2 CCl_4 and $CHCl_3$ solution or in KBr pellet.

The ^{1}H-NMR spectra were recorded with a Varian EM-360 spectrometer in $CHCl_3$. Proton absorption was measured in parts per million from TMS.

REFERENCES

[1] M. Iovu and G. Cîmpeanu, *Rev. Roumaine Chim.*, **19**, 881 (1974).

[2] M. Iovu and G. Cîmpeanu, *Rev. Chim. (Bucureşti)*, **27**, 373 (1976).

[3] M. Iovu, G. Cîmpeanu and N. Miclovici, *Rev. Roumaine Chim.* **18** 883 (1973).

[4] M. Iovu and G. Cîmpeanu, *Rev. Chim. (Bucureşti)*, **27**, 195 (1976).

[5] M. Iovu, G. Cîmpeanu and F. Avramescu, *Rev. Chim. (Bucureşti)*, **28**, 723 (1977).

[6] M. Kerfanto and D. Jegon, *Compt. rend.*, **261**, 2232 (1965).

[7] E. Knoevenagel, *Ber. dtsch. chem. Ges.*, **31**, 2586 (1899).

[8] A. Binz, and H. L. Pence, *J. Amer. Chem. Soc.*, **61**, 3134 (1939).

[9] A. P. Trentiev and E. G. Rukhadze, *Probl. org. sintezî Akad. Nauk S.S.S.R.*, **1965** 120 ; *Chem. Abstr.*, **64**, 8018 (1966).

[10] N. J. Putochin, *Ber. dtsch. Chem. Ges.*, **55**, 2749 (1922).

[11] R. D. Herlacke, R. D. Herloeker, M. P. Kleinhohoz, and F. M. Watkins, Pat. Amer., 2388058, (1965) *Chem. Abstr.* **40**, 1029 ^{6} (1946).

[12] Schmidt and Kohler, *Arch. Pharm.*, **240**, 232 (1902).

[13] G. Zinner, W. Kliegel and W. Ritter, *Ber. dtsch. Chem. Ges.*, **99**, 1678 (1967).

[14] J. F. Fernandez, and M. Jeane, *J. Chem. and Eng. Data*, **10**, 402 (1965) ; *Chem. Abstr.* **64**, 662b (1966).

[15] J. F. Fernandez, and R. Suter *J. Org. Chem.*, **32**, 447 (1967).

[16] H. Distler, R. Wader and H. Hagen, Pat. Germ. 2229644 ; *Chem. Abstr.*, **80**, 109578 (1974).

[17] D. Rehn and R. Kowatsch, *Zbl. Bact. Hyg. I Abt. Orig. A.*, **238**, 402 (1977).

[18] H. Bohme and E. Kulov, *Chem.-Ztg.*, **64**, 102 (1978).

[19] J. D. Rose and B.C.L. Weedon, *J. Chem. Soc.*, **1949**, 780.

[20] J. Burkus, *J. Org. Chem.*, **26**, 779 (1961) ; *Chem. Abstr.*, **55**, 23302 (1961).

[21] C. J. Thivlle and I. J. Tkatcentko, *J. Chem. Soc.*, **1879**, 377.

[22] R. D. Hill and G. Meakins, *J. Chem. Soc.*, **1958**, 760.

[23] M. Avram and G. D. Mateescu, "Infrared Spectroscopy" Wiley-Interscience, New-York, 1972.

[24] Organic Synthesis, vol. IV, Wiley, New York, 1966, p. 101.

Revue Roumaine de Chimie, 29, 4, 345–351 (1984)

SYNTHESIS OF 2-CYANO-2-ARYLAZO-METHYL-3,1-BENZOXAZIN-4(*H*)-ONES AND STUDIES OF THEIR SPECTRAL BEHAVIOUR

H.A. DESSOKI and A. ESSAWY *

Chemistry Department, Faculty of Science, Zagazig University, Benha, A. R. Egypt
* Faculty of Science, Zagazig University, Zagazig, A.R. Egypt

Received July 14, 1981

The UV-VIS spectral behaviour of some new azobenzoxazone derivatives is studied in solvents of different polarities. The different polarities of the solvents and the nature of the substituents in benzoxazone moiety give red or blue shifts according to the electron donor or acceptor ability of the substituted groups. The IR spectra are also recorded and discussed.

INTRODUCTION

From the literature dealing with the preparation and spectral studies of azo-compounds, [1–5] it seems that no work has been carried out on azo-compounds containing the benzoxazone moiety. Such compounds are prepared by the method described below. It seems of interest to investigate the absorption spectra of the prepared azobenzoxazone derivatives. The present paper is aimed to throw some light on the effect of the substituents attached to phenylazo moiety and of the polarities of the organic solvents used on the spectral behaviour of these compounds. It was also attempted to determine spectrophotometrically the azo compounds under investigation.

EXPERIMENTAL

The compounds used are derivatives of the 2 (α-cyano-α-phenylazo)methyl-3,1-benzoxazine-4(H)-one (Y) in which $X = H$ (I), *o*-Cl (II), *m*-NO_2 (III), *p*-CH_3 (IV) and *p*-OCH_3 (V).

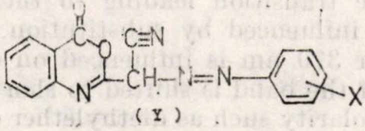

(Y)

These compounds were prepared by the action of aryldiazonium chlorides of 2-cyanomethyl-3,1-benzoxazine-4(H)-one.

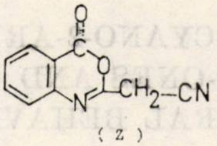

(Z)

Reaction of aryldiazonium chlorides with (Z) leads to the formation of the coupling products (I—V). Aryldiazonium chlorides were prepared by the addition of sodium nitrite solution (0.5 mole) to aromatic amine (0.5 mole) dissolved in conc. hydrochloric acid (20 ml) and water at 5°C.

The diazonium salt was then added to a solution of (Z) (0.5 mole) in 10% NaOH solution while cooling. The coloured solids obtained were filtered and recrystallized.

The solvents used for the spectral measurements were purified according to recommended procedures.[6] 10^{-3}M stock solutions were prepared by dissolving the accurately weighed amount of the material in the appropriate volume of the required solvent. Solutions of lower concentrations used for spectral measurements were obtained by accurate dilution. The spectra were recorded within the wavelength range 200—600 nm on a recording Beckman, Model 25 Spectrophotometer using 1 cm matched silica cells. The IR spectra were obtained on a Unicam Sp 1200 Spectrophotometer.

RESULTS AND DISCUSSION

The absorption spectra of benzoxazone can be considered as comprising five bands. The bands below 212 nm were assigned to the $\pi - \pi^*$ transition within the benzenoid system whereas those at 230, 250 and 305 nm are due to $\pi - \pi^*$transitions in the benzoxazone moiety.[7] The longest wavelength band within the 350—370 nm range is assigned to the $\pi - \pi^*$ transition within the azo group influenced by an intramolecular charge transfer.[8] Such an intramolecular CT would originate from the benzoxazone moiety and the substituted phenyl groups to the N = N linkage

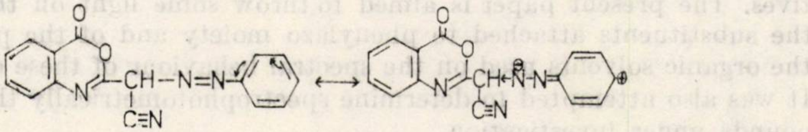

Though most of the absorption bands are influenced by changing the solvent and substituent, yet the most interesting effects are observed with CT bands.

The bands assigned to the $\pi - \pi^*$ transitions of the benzenoid system and the benzoxazone nucleus are shifted to red on increasing the polarity of the medium. This behaviour is in agreement with the $\pi - \pi^*$ nature of the electronic transition leading to these absorption bands. The bands are slightly influenced by substitution.

The CT band near 370 nm is influenced on changing the solvent polarity. The position of the band is shifted to shorter wavelength in the case of solvents of low polarity such as diethylether or cyclohexane rather than in ethanol which increases the polar structure of the compounds and facilitates the intramolecular charge transfer producing thus a red shift of the CT band. To verify whether the red shift is due to pure dielectric effects or to change in the strength of the hydrogen bond, the relation given by Gati and Szolay [9] is applied. This relation can be given as follows :

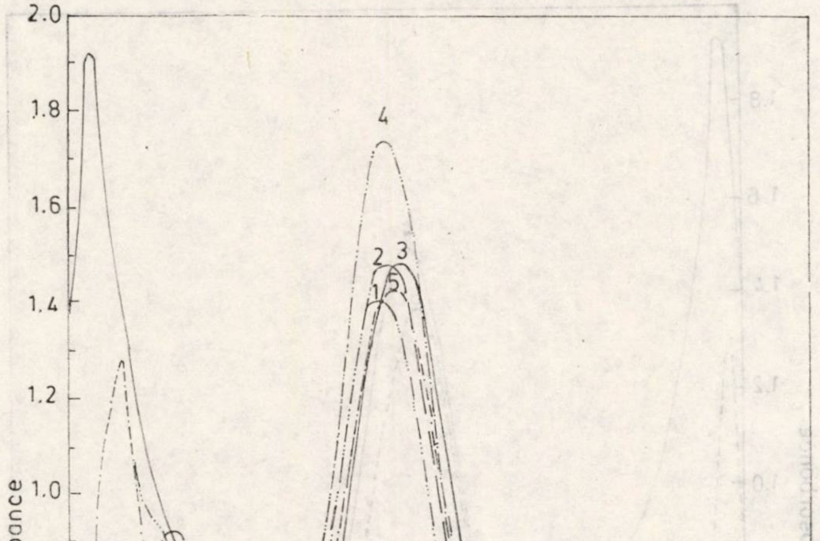

Fig. 1. — The absorption spectra of 5 × 10^{-5}M of azobenzoxazone derivatives in ethanol : 1. Compound I ; 2. Compound II ; 3. Compound III ; 4. Compound IV ; 5. Compound V.

$$\Delta\nu = (a - b)\left(\frac{n^2 - 1}{2n^2 - 1}\right) + b\left(\frac{D - 1}{D + 1}\right)$$

in which n and D are the refractive index and dielectric constant of the medium, a and b are constants.

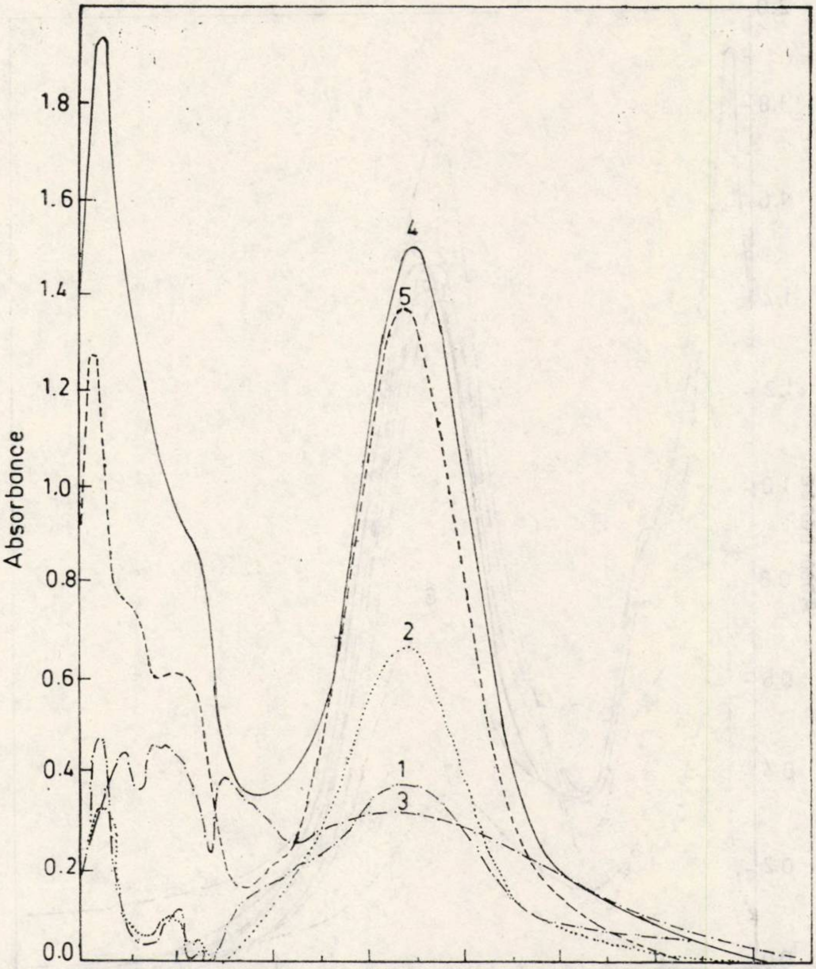

Fig. 2. — The absorption spectra of 2-Cyano-2-(p-anisylazo)methyl-3,1 (4H) Benzoxazone (5×10^{-5}M) in different solvents : 1. Ether ; 2. Carbon tetrachloride ; 3. Ethanol ; 4. Dioxane ; 5. Ethyleneglycol ; 6. Chloroform ; 7. Cyclohexane.

The plot of $\Delta\nu$ *vs* $\left(\dfrac{D-1}{D+1}\right)$ is not a strict linear relation indicating that the observed shifts are not only due to change in dielectric constant. Thus the changes in the solvation energies of the ground and excited states would play an important role in solvent shift. Similar results were obtained on using the dielectric functions given by Suppan.[10]

The position and extinction of the CT band are also influenced by the nature and position of the substituents on the benzenoid nucleus. The band is shifted towards red as the donor character of this substituent increases, so the compounds *e.g.* II, V show a band shifted towards the blue region in comparison to I due to the electron accepter character of the substituent which lowers the energy of the ground state of the molecule and hence increases the energy gap between the ground and excited states. On the contrary, a red shift of this band is observed for the compound possessing an electron donating group (*e.g.* CH_3).

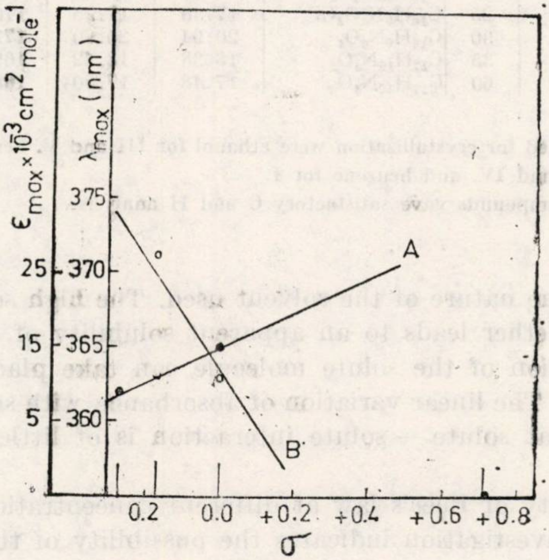

Fig. 3. — Compound V : A. Variation of λ_{max} with σ; B. Variation of ε_{max} with σ.

From Fig. 3, λ_{max} of the bands is shifted to longer wavelength as the Hammett constant σ of the substituent increases. This behaviour can be ascribed to a changed degree of overlap of molecular orbitals of the Φx and $-N=N-$ systems as the electronic nature of the substituent is changed. The linear variation of λ_{max} with σ of the substituent indicates the strong conjugation between x and $-N=N-$ *i.e.* the more or less planar configuration of the molecular part, involving these groups. A similar behaviour is observed with ε_{max} which decreases with the σ-constant.

The spectra of the compounds under investigation (Tables 1 and 2) indicate that both λ_{max} and ε_{max} of the absorption bands are readily influenced by the nature of the solvent used. The high solvation energy in ethanol and ether leads to an apparent solubility of the compounds and no association of the solute molecule can take place especially in dilute solutions. The linear variation of absorbance with solute concentration denotes that solute — solute interaction is of little importance in such solvents.

Table 1

Physical data of coupling products (I—V)

Compound*	m.p.°C	yield (%)	Mol. Formula	N (%)**		IR absorption KBr, cm^{-1}		
				Found	Calc.	$>C=O$	$>C=N$	$>C=N$
I	115	25	$C_{16}H_{10}N_4O_2$	19.40	19.31	1700	1635	2230
II	125	25	$C_{16}H_9N_4O_2Cl$	17.30	17.25	1705	1638	2230
III	115	30	$C_{16}H_9N_6O_4$	20.94	20.90	1710	1640	2230
IV	85	35	$C_{17}H_{12}N_4O_2$	18.38	18.42	1695	1630	2230
V	140	60	$C_{17}H_{12}N_4O_3$	17.48	17.50	1690	1630	2230

* Solvents used for crystallization were ethanol for III and V. benzene — light petrol (40 ~ 60°C) for II and IV, and benzene for I.

** All the compounds gave satisfactory C and H analysis.

The validity of Beer's law at different concentrations of the compounds under investigation indicates the possibility of their microdetermination. The spectrophotometric method can be used for the determination of small quantities (0.0059—0.032 mgm/ml) of the azo compounds under investigation.

The effect of substituents on the UV and visible spectral behaviour of such compounds is also supported by investigating their IR-spectra. The bands obtained are assigned using methods which are similar to those described by Looker [11] and considering the bands due to the aromatic and heterocyclic skeleton. [12] The positions of the bands for the C = N and C = O groups are observed at 1635, 1700 cm^{-1} for I, 1638, 1705 cm^{-1} for II, 1640, 1710 cm^{-1} for III, 1630, 1695 cm^{-1} for IV and 1630, 1690 cm^{-1} for V. These values indicate that the position of both bands shifts to lower wavenumbers with increased donor character of the substituents, and thus is in accord with common observations.

Table 2

λ_{max} and ε_{max} for azo benzoxazone derivatives (I–V)

Solvent	$\pi-\pi^*$		$\pi-\pi^*$		$\pi-\pi^*$		$\pi-\pi^*$		CT	
	λ_{max}	$\varepsilon \times 10^{-3}$	λ_{max}	$\varepsilon \times 10^{-3}$	λ_{max}	$\varepsilon \times 10^{-3}$	λ_{max}	$\varepsilon \times 10^{-3}$	λ_{max}	$\varepsilon \times 10^{-3}$
I. X = H										
EtOH	210	9.2	280	2.4	—	—	245	—	370	2.4
Ether	—	—	—	—	—	—	240	17.4	365	10.6
II. X = o-Cl										
EtOH	212	6.8	—	—	—	—	240	1.6	370	13.2
Ether	214	5.2	280	4.4	—	—	250	4.0	360	11.2
III. X = m-NO_2										
EtOH	—	—	—	—	—	—	246	9.0	367	11.4
Ether	—	—	—	—	—	—	242	18.2	350	11.2
IV. X = p-CH_3										
EtOH	212	38.4	305	7.8	261	17.6	230	26.0	373	29.9
Ether	—	—	295	11.2	250	18.8	—	—	363	28.2
CCl_4	—	—	—	—	—	—	—	—	365	29.7
$CHCl_3$	—	—	—	—	—	—	—	—	370	15.0
Dioxane	—	—	—	—	—	—	—	—	362	34.8
Cyclohexane	—	—	—	—	255	6.0	230	10.8	360	7.4
Ethyleneglycol	—	—	—	—	255	18.6	227	25.8	372	28.6
V. X = p-OCH_3										
EtOH	208	25.4	305		250	12.2	230	14.8	368	7.5
Ether	—	—	300	4.0	240	—	—	—	362	20.6
CCl_4	—	—	—	—	—	—	—	—	365	19.2
$CHCl_3$	—	—	—	—	—	—	—	—	368	21.0
Acetone	—	—	—	—	—	—	—	—	364	21.0
Cyclohexane	—	—	—	—	255	6.0	—	—	355	7.4
Ethyleneglycol	—	—	—	—	—	—	—	—	370	23.4

REFERENCES

[1] S. Nagakura and H. Baba, *Rept. Radiation Chem. Tokyo Univ.*, **5**, 19 (1950).
[2] G. Costa, *Gazz. chim. Ital.*, **85**, 548 (1956).
[3] H. Jaffe., S. Yeh and R. W. Gorder, *J. Mol. Spectroscopy*, **2**, 120 (1958).
[4] O. Neunhoffer and H. Paul, *J. prakt. Chem.*, **5**, 212 (1958).
[5] J. Kroner and H. Hock, *Chem. Ber.*, **101**, 1922 (1958).
[6] A. I. Vogel, "Practical Organic Chemistry", Longmans, London, 1964, p. 163, 166, 176.
[7] M. Mahmoud and M. A. El-Hashash, *Rev. Roumaine Chim.*, **24**, 1499 (1979).
[8] R. M. Issa *et al.*, *Z. phys. Chem. (Leipzig)*, **253**, **289** (1973); **256**, **257** (1957); **257**, **259** (1976); *Egypt. J. Chem.*, **18**, 63 (1975); **19**, 379 (1976).
[9] L. Gati and L. Szolay, *Acta. Phys. Chem.*, **5**, 87 (1959).
[10] P. Suppan, *J. Chem. Soc. (A)*, **1968**, 3125.
[11] H. H. Looker and W. W. Heennemann, *J. Org. Chem.*, **27**, 381 (1962).
[12] A. R. Katritzky, *J. Chem. Soc.*, **1957**, 2051, 2058; **1959**, 2670, 3674.

Revue Roumaine de Chimie, **29**, *4*, 353—365 (1984)

ÉTARD REACTION. XII *

OXIDATION OF DIBENZO[*b*, *f*]BICYCLO[3.2.1]OCTA-2,6-DIENE AND OF DIBENZO[*b*, *e*]BICYCLO[2.2.2]OCTA-2,5-DIENE WITH CHROMYL CHLORIDE

I. I. SCHIKETANZ, F. BADEA, ANA HANEŞ[a] and ILEANA NECŞOIU
Laboratory of Organic Chemistry, The Polytechnic Institute Bucharest, Romania

Received May 28, 1983

The Étard reaction of dibenzo[*b*, *f*]bicyclo[3.2.1]octa-2,6-diene (7) yields a complex which on hydrolysis with ice water led to a mixture of products containing as major product dibenzo[*b*, *f*]bicyclo[3.2.1]octa-2,6-dien-4-one (5). The filtrate remained after the removing of the Étard complex contains 7-chlorodibenzo[*b*, *e*]bicyclo[2.2.2]octa-2,5-diene (17) and dibenzo[*b*, *e*]bicyclo[2.2.2]octa-2,5-diene (8). Hydrocarbon 8 is about 10^4-10^5 less reactive than 7 and yields a mixture of about 28 products from which dibenzo[*b*, *e*]bicyclo-[2.2.2]octa-2,5-dien-7-one (6) and significant amounts of ketone 5 and anthraquinone were identified. The results are interpreted as proving the occurrence of a return from the initially formed ion pair.

INTRODUCTION

In the preceding paper of this series [1] we have shown that dibenzo [*c*, *g*]-bicyclo[4, 2, 0]octa-3,7-diene (**1**) treated with chromyl chloride yields a complex which decomposed with water produces as main reaction products (72.5%) compounds **2** — **5**, derived from dibenzo[*b*, *f*]bicyclo [3. 2.1] octa-2,5-diene (**7**), and small amounts of dibenzo[*b*, *e*]bicyclo [2.2.2] octa-2,5-dien-7-one (**6**), derived from the isomeric hydrocarbon, dibenzo [*b*, *e*] bicyclo [2.2.2] octa-2,5-diene (**8**) :

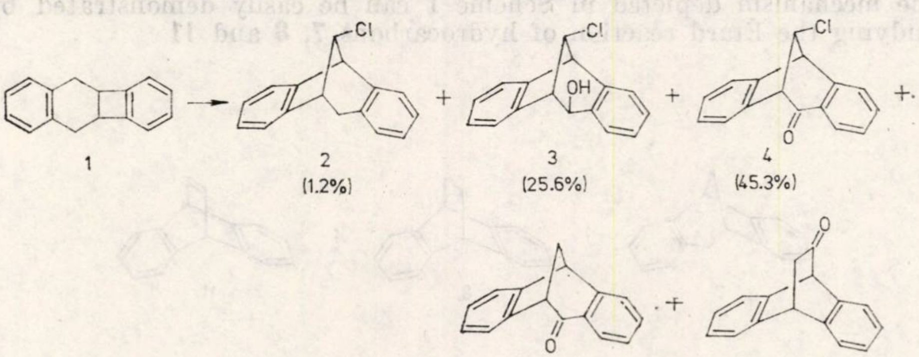

---

*) Part XI is reference [1]

[a] Deceased June 1982

The filtrate of the Étard complex contains only chloride **2**.

We considered that the major products of the Étard reaction **2, 3** and **4** can reasonably be explained through the following mechanism:

Scheme 1

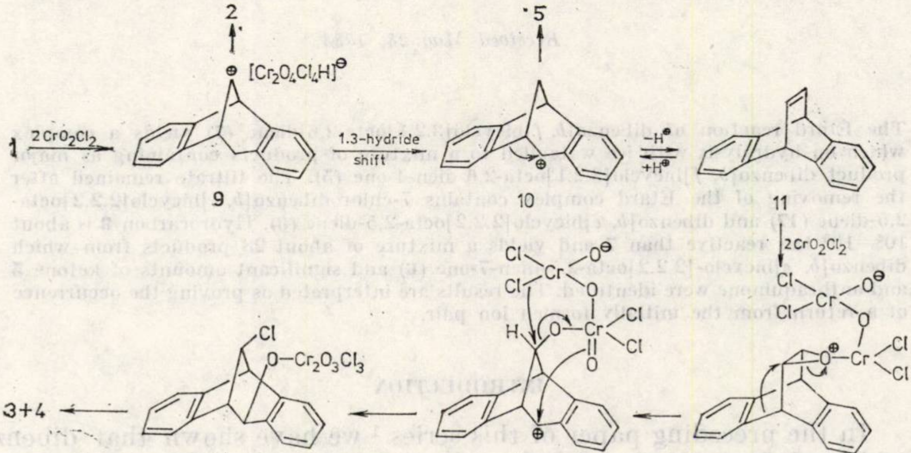
2
5
1
2CrO2Cl2
[Cr2O4Cl4H]⊖
1.3-hydride shift
−H⊕
+H⊕
9
10
11
2CrO2Cl2
12
13
14
3+4

The mechanism depicted in Scheme 1 can be easily demonstrated by studying the Étard reaction of hydrocarbons **7, 8** and **11**

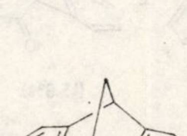
7 ;

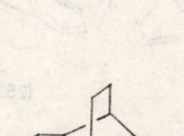
8 ;

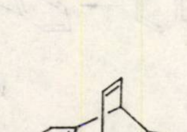
11

The results reported herein have ruled out the above mechanism. However the present data afforded a more complete picture of the initial steps of the Étard reaction.

RESULTS

Hydrocarbons **7**, **8** and **11** were prepared by the methods [2-4] described in Scheme 2, starting from anthracene:

Scheme 2

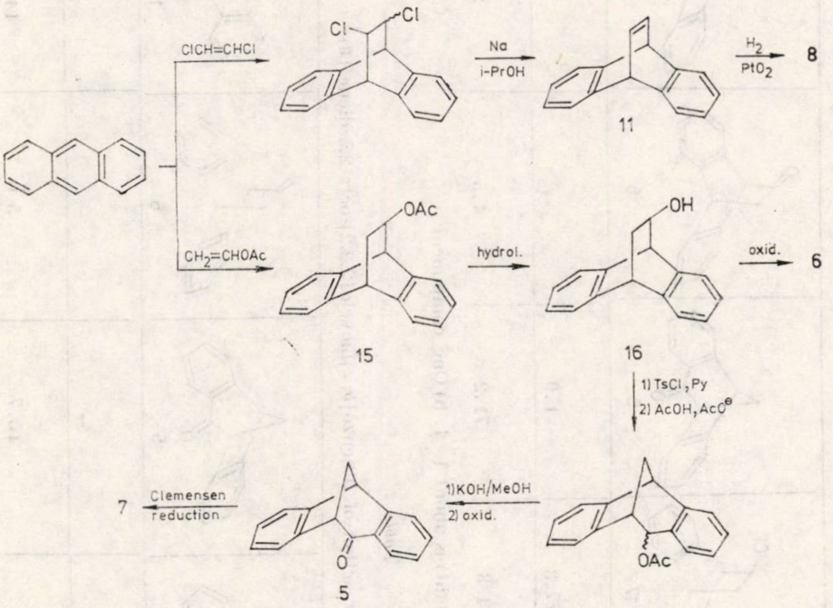
ClCH=CHCl
Cl
Cl
Na
i-PrOH
11
H_2
PtO_2
8
CH_2=CHOAc
OAc
15
hydrol.
OH
16
oxid.
6
1) TsCl, Py
2) AcOH, AcO⊖
OAc
1)KOH/MeOH
2) oxid.
O
5
Clemensen
reduction
7

The reaction of chromyl chloride with dibenzo [*b*, *f*]bicyclo[3.2.1]octa-2,6-diene (**7**) (in the ratio 2 : 1) is very fast. After adding the freshly prepared reagent at 0–5°, chromyl chloride was completely consumed in 2 hours. The reaction of the isomeric hydrocarbon **8** is sluggish and needs 100 hrs at room temperature or 8 hrs at 60°. By applying Eyring equation

$$k = \frac{k \cdot T}{h} e^{-\frac{\Delta G^{\neq}}{RT}} \tag{1}$$

and the data of Table 1 and Table 2 for the conversion of the two hydrocarbons, an approximate value of 10^4–10^5 for the rate ratio : rate **7** : rate **8** can be computed.

Both filtrate and the mixture of products obtained from the decomposition of the complex were gas-chromatographically analysed. The results of these analyses are given in Table 1 and Table 2.

In the Étard reaction of dibenzo[*b*, *e*]bicyclo[2.2.2]octa-2,5,7-triene, (**11**), the products were similar with those obtained from **7**. No chloroalcohol **3** or chloroketone **4** was identified.

Table 1

The products of the Étard reaction of dibenzo[*b*, *f*] bicyclo-[3.2.1]octa-2,6-diene (**7**)

Products	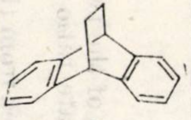 8	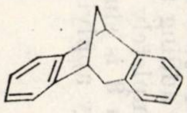 7	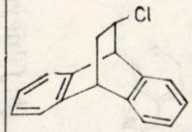 17	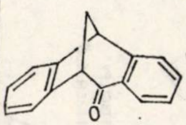 5	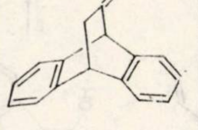 6	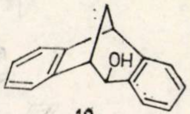 18	Un-identified
from a) filtrate	10.6	1.9	77.3	1.9	—	—	7.3 b)
from a) complex	0.3	0.7	14.8	71.2	4.5	8,1	—

Observations : a) The ratio filtrate : complex (weight : weight) is about 1 : 1. b) One component.

Table 2

The products of the Étard reaction of dibenzo[*b*, *e*]bicyclo[2.2.2]-octa-2,5-diene (**8**)

Products	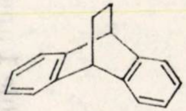 8	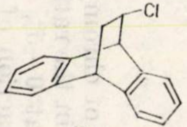 17	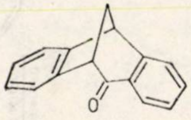 5	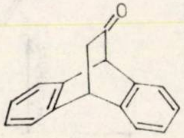 6	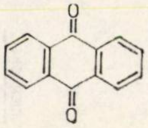 19	Unidentified
from a) filtrate	98.2	—	—	—	—	1.8 c)
from b) complex	20.4	7.6	15.7	5.0	14.8	36.5 d)

Observations : a) The recovered hydrocarbon **8** represents about 75%. b) The ratio filtrate : complex (weight : weight) is about 2 : 1. c) Two components. d) 22 components.

DISCUSSION

1. Alkenes as intermediates in Étard reaction

Previous works of our laboratory [5-10] as well as the results reported by others [11-15] have shown that alkenes and epoxides are intermediates in chromyl chloride oxidation of alkanes. Thus, our supposition that dibenzo [*b*, *e*]-bicyclo[2.2.2]octa-2, 5, 7-triene (**11**) is an intermediate in the oxidation of the polycyclic hydrocarbon **1** was plausible. The results reported in this paper clearly rule out the involvement of the hydrocarbon **11** in the formation of the main oxidation products observed in Étard reaction of **1**. However, if we can eliminate the polycyclic hydrocarbon **11** from the mechanism leading to the chloro derivatives **3** and **4**, we cannot completely rule out its involvement in the process of oxidation of the dibenzo[*c*, *g*]bicyclo[4.2.0]octa[3, 7]-diene (**1**). Indeed, a more thoroughly examination of the products formed either from the hydrocarbon [5,8,9] or the alkene or the epoxide [5,8] show that even if both alkenes and epoxides lead to the same products as the corresponding saturated hydrocarbon, alkenes and epoxides cannot be alone responsible for producing the main oxidation products. Let us consider, for example the oxidation of methylcyclopentane. [9]

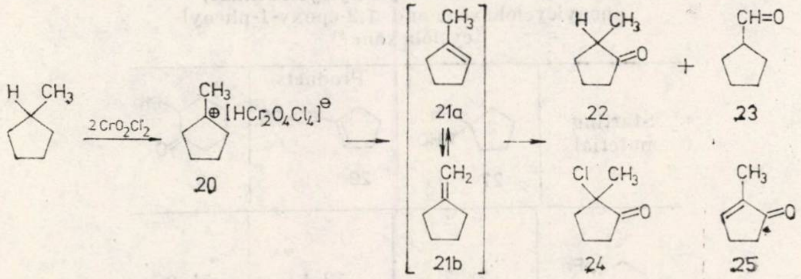

The reaction products where explained as resulting from complex **26a** or **26b**, formed from either **21a** or **21b**

Scheme 3

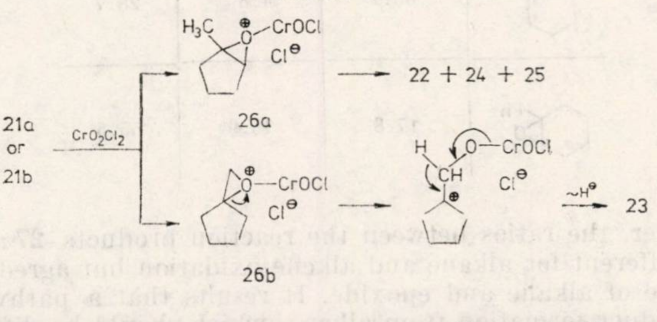

This interpretation was based on : a) Alkenes **21a** and **21b** oxidized with the same reagent give rise to the same products ; b) formylcyclopentane **23** is the main product (72%) formed in the oxidation of methylene cyclopentane; c) in the oxidation of alkenes, Freeman, Arledge and Yamachika[16–18] determined that the rate of oxidation is first order both in alkene and chromyl chloride, in agreement with the formation of a complex of type **12** or **26**. The comparison of the relative reactivities of complex formation with the relative rates of bromine and chlorine addition or expoxidation of alkenes[12] sustain the involvement of a three-membered ring intermediate, such as **26**.

Despite these facts, it has been shown[9] that in the oxidation of methylcyclopentane, 2-methyl-2-chlorocyclopentanone (**24**) is a main reaction product (31.2%) whereas in the oxidation of alkenes **21** it is a minor product (about 4.5%). Clearly, it seems that at least another route exists which leads to the chloroderivative **24** and *this route is specific for the saturated hydrocarbon and is unsignificant for the alkene.*

Later we compared the oxidation of phenylcyclohexane[8] and that of the corresponding alkene and epoxide. Again, the products of the Étard reaction are the same, as shown in Table 3:

Table 3

Étard reaction of 1-phenylcyclohexane, phenylcyclohexene and 1,2-epoxy-1-phenylcyclohexane[8)]

Starting material	Products		
	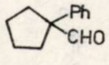 **27**	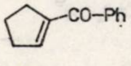 **28**	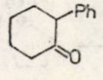 **29**
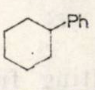	23.7	12.1	55.0
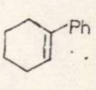	60.7	4.8	28.7
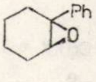	17.8	16.9	55.5

However, the ratios between the reaction products **27** : **28** : **29** are strikingly different for alkane and alkene oxidation but agree satisfactorily for those of alkane and epoxide. It results that a pathway should exist for product formation from alkene, which should be different from that of alkane, but will agree with the interpretation of the reaction products accepted so far.[11,12,19]

The pathway for product formation from alkane should resemble the pathway for product formation from epoxides. A plausible interpretation for the Étard reaction of phenylcyclohexane and 1,2-epoxy-1-phenylcyclohexane is given in scheme 4.

Scheme 4

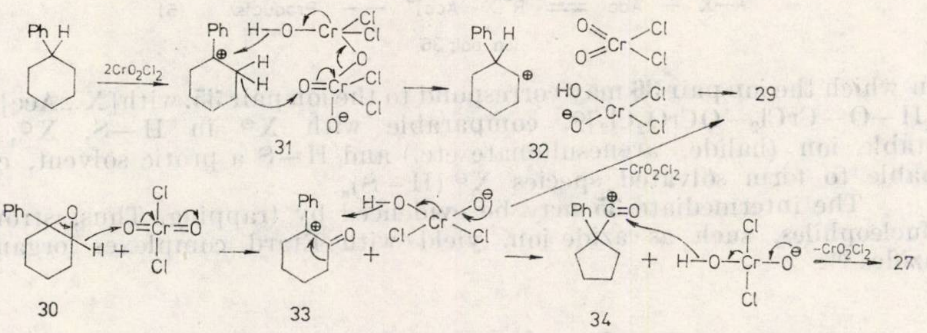

The counter ion of the initially formed Étard complex **30** is at the same time a hydride ion acceptor and a hydride ion donor. Thus, it can catalyse the otherwise unfavoured process (2)

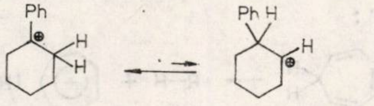
(2)

The transformation of the epoxide in ketone **29** is a Lewis acid catalysed reaction, which has been demonstrated independently.[8] The equilibrium (3) explains satisfactorily the difference between the catalytic effect of a typical Lewis acid catalyst and the action of chromyl chloride. Equilibrium (3):

$$\mathrm{Cr(VI)} + 2e \rightleftarrows \mathrm{Cr(IV)} \qquad (3)$$

is responsible for the cationic rearrangement (2) and also for the transformation of the epoxide **30** into the ketone **29**, and there from the similarity between the alkane and epoxide oxidation.

The reactions of Scheme 4 admit that the counter ion formed in the first step of Étard reaction may be a reducing agent for the carbocations involved in the oxidation process. The results of the present paper are a convincing proof for this interpretation.

2. The reversibility of the Étard reaction

The known data of the Étard reaction [11,12] agree that the first step in alkane oxidation is a hydride ion shift (4) resulting in the formation of an ion pair **35**:

$$\mathrm{R{-}H} + \mathrm{CrO_2Cl_2} \longrightarrow \underset{\text{ion pair 35}}{\mathrm{R^{\oplus}[HCr_2O_4Cl_4]^{\ominus}}} \qquad (4)$$

This process may be compared with an SN-1 ionization step such as (5):

$$R{-}X + \mathrm{Acc} \rightleftharpoons \underset{\text{ion pair } 36}{R^{\oplus}[X\cdots\mathrm{Acc}]^{\ominus}} \longrightarrow \text{Products} \qquad (5)$$

in which the ion pair **36** may correspond to the ion pair **35**, with $[X...Acc] = [H-O-CrCl_2-OCrO_2Cl_2]^{\ominus}$, comparable with $X^{\ominus}$ in $H-S$, $X^{\ominus}$, a stable ion (halide, arenesulfonate etc.) and $H-S$ a protic solvent, capable to form solvated species $X^{\ominus}(H-S)_n$.

The intermediate **35** may be evidenced by trapping. Thus, strong nucleophiles, such as azide ion, yield with Étard complexes organic azides [20]:

$$\mathbf{35} + N_3^{\ominus} \longrightarrow R{-}N_3 + Cr^{\mathrm{IV}} + Cr^{\mathrm{VI}} \qquad \mathbf{(6)}$$

Powerful hydride ion donors, such as eters [21,22] or cycloheptatriene [22] reform the initial hydrocarbon and generate a new complex, derived from the hydride donor:

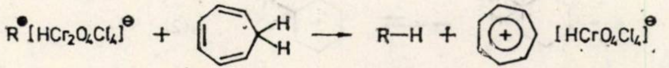

(7)

In the filtrate isolated after the removing of the Étard complex, organic chlorides are identified, occasionally accompanied by carbonyl compounds. [1,11,12,23] It is believed that the carbonyl compounds are formed during the working up of the complex, considering that moisture cannot be completely avoided. The chlorides, however, must result through ion pair collapse of the initially formed ion pair **35**:

$$\underset{\mathbf{35}}{R^{\oplus}[HCr_2O_4Cl_4]^{\ominus}} \longrightarrow R{-}Cl + HCl + CrO_2Cl_2 + CrO_2 \qquad (8)$$

Reaction (8) does not need the involvement of a polar or a protic solvent, Thus chloride R-Cl is found in the filtrate obtained before decomposing the complex with ice-water (or other decomposing agents [11,12]). The known data allow us to compare Étard reaction with an SN-1 solvolysis, in which the acceptor (or solvating agent) of the leaving group is chromyl chloride. However, in contrast with an SN-1 solvolysis, no internal return from ion pair **35** has been so far evidenced.

We believe that collapse to the chloride must be also accompanied by the re-formation of the hydrocarbon (internal return):

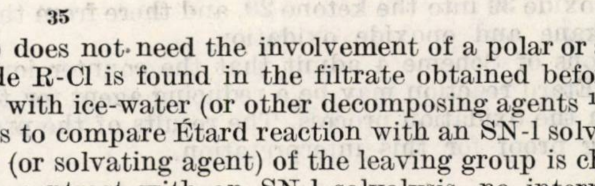

(9)

(10)

No electron transfer is needed in colapse (9). Formation of hydrocarbon R-H from the ion pair **35** in (10) involves a hydride ion shift from the counter ion $[HCr_2O_4Cl_4]^{\ominus}$ to the carbenium ion $R^{\oplus}$, and thus depends on the redox potential of Cr (IV). Reaction (10), as most of the internal returns from ion pairs are, [24–26] *is an invisible reaction*. In order to become visible it is necessary that the carbenium ion **35** would suffer a rearrangement before colapse:

Scheme 5

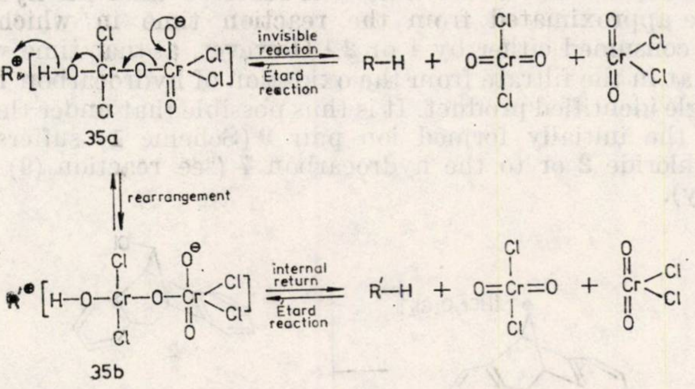

The rearrangement is a necessary but not sufficient condition for the identification of the internal return from ion pair **35**. Another condition is that the rearranged hydrocarbon R′-H should be less reactive toward chromyl chloride than the initial hydrocarbon R-H.

This is the case of the hydrocarbons **7** and **8**, the latter, as our results reported therein show, being 10^4-10^5 less reactive than **7**.

Indeed, in the oxidation of dibenzo[*b*, *f*]bicyclo[3.2.1]octa-2,6-diene (**7**) significant amounts of the isomeric hydrocarbon **8** are found in the filtrate. We believe that this reaction product is a typical return product from an ion pair **35**, as presented in Scheme 5. Another interpretation of its formation is an intermolecular hybride ion shift (Scheme 6):

Scheme 6

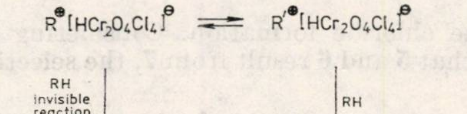

A first argument for the internal return interpretation of the results (Scheme 5) is based on the fact that both hydrocarbon **8** and chloride **17** are the main products found in the filtrate and that both are only minor components in the reaction mixture isolated after decomposing the Étard complex of hydrocarbon **7**. Thus, both **8** and **17** must be collapse products of the initially formed complex **35**. Other arguments are found by comparing the results of this work with those reported previously. The results reported herein thus demonstrate the similarity between chromyl chloride and aluminium chloride interaction with saturated hydrocarbons. In both processes the isomerisation of the initial hydrocarbon is observed. The two processes differ only in the side reactions of the intermediate carbocations.

3. Formation of halohydrine 3 and chloroketone 4

The formation of **3** and **4** from chloride **2** was considered as impossible because **2** is about 2–10 times less reactive than the hydrocarbon, as could be approximated from the reaction time in which chromyl chloride is consumed either by **1** or **2**.[1] However, at that time we did not consider that in the filtrate from the oxidation of hydrocarbon **1**, chloride **2** is the single identified product. It is thus possible that under the reaction conditions the initially formed ion pair **9** (Scheme 1) suffers collapse either to chloride **2** or to the hydrocarbon **7** (see reaction (9) and (10), respectively).

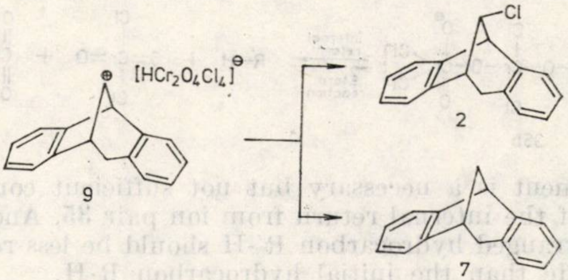

Hydrocarbon **7**, as our present results have indicated, is as reactive as hydrocarbon **1**, whereas **2** is less reactive. Thus, **2** is found in the filtrate whereas **7** is further transformed. If we take into account the data of table 1, it should be observed that the selectivity ratio S of the collapse:

$$S^{*} = \frac{/\text{Products of anion collapse of the ion pair}/}{/\text{Products of internal return}/} = \frac{\mathbf{5}+\mathbf{6}+\mathbf{17}+\mathbf{18}}{\mathbf{8}} = 17.2$$

is favourable to the chloride formation. Considering that **3** and **4** are formed from **2** and that **5** and **6** result from **7**, the selectivity factor S is:

$$S^{*} = \frac{\mathbf{2}+\mathbf{3}+\mathbf{4}}{\mathbf{5}+\mathbf{6}} = 16.76$$

which is similar to the selectivity factor determined for **7** in this work.

The similarity between the two values of the selectivity factor S determined independently in the chromyl chloride oxidation of hydro-

---

* Both filtrate and complex products are considered in the calculation

carbon 1[1] and hydrocarbon 7 (this work) is a clear indication that the internal return from the ion pair 35 is a general phenomenon occurring in Étard reactions.

4. Formation of anthraquinone 19

The formation of anthraquinone must involve the electrophilic attack of chromyl chloride at the bridgehead carbon-hydrogen bonds.

The most stable product which can be formed in this process is anthraquinone, also observed by Cristol [27] in the oxidation of hydrocarbon 37.

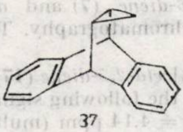

37

EXPERIMENTAL

Analytical gas-chromatographies were carried out on a Carlo Erba apparatus, type D, with FID, using a column ($L = 2$ m ; $Ø_i = 2$ mm) of 3 % NPGS chromosorb W silanized 60–80 mesh, $t = 190°$.

Preparative gas-chromatographies were carried out with a Carlo Erba apparatus type GV, HWD, using a column ($L = 3$ m ; $Ø_i = 6$ mm) of 10 % silicon OV17 anaprep. 30–50 mesh, $t = 205°$.

Starting materials

Dibenzo[b, f]bicyclo[3.2.1]*octa-2,6-diene* (**7**) was prepared [2b,c, 3] by the sequence of reactions presented in Scheme 2, starting from anthracene aduct with vinyl acetate. [4] Purified by sublimation (**7**) melts at 36–37°. Purity 99,5 % (gas-chromatography).

Dibenzo[b, e]bicyclo[2.2.2]*-octa-2,5-diene* (8) was obtained[2a] by elimination of chlorine from the anthracene aduct with 1,2-dichloroethene followed by catalytic hydrogenation of unsaturated hydrocarbon **11**. Recrystallized from ethanol, hydrocarbon **8** melts at 142 – 3°.

Chromyl chloride was prepared according to Sisler [28] and used immediately after distillation.

The Étard complex of dibenzo[b, f]bicyclo[3.2.1]-octa-2,6-diene (7)

In a 250 ml three-necked round-bottomed flask provided with a dropping funnel, a reflux condenser (with $CaCl_2$ tube), a thermometer and inert gas (nitrogen) inlet tube, placed in an ice-water bath, a solution of 3.0 g (14.5 mmols) hydrocarbon **7** in 30 ml dry CCl_4 was introduced.

To this solution, stirted with a magnetic stirrer, a solution of 4.5 g (29 mmols) chromyl chloride in 45 ml dry CCl_4 was added dropwise in the course of 2 hrs, in an inert gas atmosphere (nitrogen) at 0–5°C.

The reaction mixture was stirred at room temperature for 4 hrs, so that the chromyl chloride was completely consumed.

The complex was then filtered off under inert gas and thoroughly washed with dry CCl_4.

The complex was thus obtained as a brown, insoluble, hygroscopic powder. The complex was decomposed in ice-water in the presence of CH_2Cl_2. The organic layer was separated and the aqueous layer was extracted four times with 50 ml portions of CH_2Cl_2.

The filtrate of the Étard complex was washed with water, then with 5 % aq. $NaHCO_3$, dried over $MgSO_4$, yielding 1,5 g product after removal of solvent. The results of the gas-chromatography analysis are given in Table 1.

The Étard complex of dibenzo[b,e,]bicyclo[2.2.2]-octa-2,5-diene (8)

The complex was prepared from 3.10 g (15 mmols) hydrocarbon **8** in 40 ml dry CCl and 4.65 g (30 mmols) chromyl chloride in 50 ml dry CCl_4. The reaction time was 100 hrs at room temperature or 8 hrs at 60°. The chromyl chloride was not completely consumed. The complex was filtered off and worked-up as mentioned above. 0.8 g residue were obtained and identified by gas-chromatography (Table 2).

The red-coloured filtrate was washed with water, then with 5 % aq. $NaHCO_3$, dried over anhydrous $MgSO_4$ yielding 1.6 g residue after removal of solvent. The residue melted at 142° and it was identified as **8** (see Table 2).

Identification of the reaction products was done either by isolation of the individual products or by gas-chromatography (see below).

Dibenzo[b, f]bicyclo[3.2.1]*octa-2,6-diene* (**7**) and *dibenzo[b, e]bicyclo*[2.2.2]*-octa-2,5-diene* (**8**) were isolated by preparative gas-chromatography. Their ^{1}H-NMR spectra were identical to those of authentic samples. [29,30]

7-Chlorodibenzo[b, e]bicyclo[2.2.2]*octa-2,5-diene* (**17**) was isolated by gas-chromatography.

The ^{1}H-NMR spectrum displays the following signals : $\delta = 1.77$ ppm (multiplet H_8 cis) ; $\delta = 2.42$ ppm (multiplet H_8 trans) ; $\delta = 4.14$ ppm (multiplet H_4 and H_7) ; $\delta = 4.35$ (doublet H_1) ; $\delta = 7.15$ (multiplet, aromatic protons).
Elemental analysis : Found C, 79, 70 ; H, 5.68 ; Cl, 15.10.
Calculated for $C_{16}H_{13}Cl$; C, 79, 85 ; H, 5.44 ; Cl, 14.73 ;

Dibenzo[b, f]bicyclo[3.2.1]*cota-2,6-dien-4-one* (**5**) was isolated by gas-chromatography. The IR spectrum is characterized by $\nu = 1700$ cm^{-1} carbonyl band the ^{1}H-NMR spectrum is identical to that reported in literature. [28]

Dibenzo[b, e]bicyclo[2.2.2]*octa-2,5-dien-7-one* (**6**) and exo-*4-hydroxydibenzo[b,f]bicyclo* [3.2.1]*octa-2,6-diene* (**18**) : Gas chromatography retention times identical to those of authentic samples.

The IR spectrum of alcohol **18** is identical with the known spectrum of the compound. [3]

Anthraquinone (**19**) : Gas-chromatography retention time and IR spectrum identical to those of authentic samples.

REFERENCES

[1] I. I. Schiketanz, A. Hanes and I. Necsoiu, *Rev. Roumaine Chim* **22**, 1097 (1977).

[2] a. S. J. Cristol and N. Hause, *J. Amer. Chem. Soc.*, **74**, 2193 (1952).
b. S. J. Cristol, F. P. Parungo and D. E. Plorde, *J. Amer. Chem. Soc.*, **87**, 2870 (1965).
c. S. J. Cristol, J. R. Mihrig and G. Tiedeman, *J. Org. Chem.*, **37**, 3239 (1972).

[3] E. Cioranescu, A. Mihai, G. Mihai, M. Elian and C. D. Nenitzescu, *Studii Cercetări Chim. Acad. R.S.R.*, **14**, 161 (1965).

[4] S. Wawzonek and J. V. Hallum, *J. Org. Chem.*, **18**, 288 (1953).

[5] C. N. Rentzea, I. Necsoiu, M. Rentzea, A. Ghenciulescu and C. D. Nenitzescu, *Tetrahedron*, **22**, 3501 (1966).

[6] C. N. Rentzea, M. Rentzea, I. Necsoiu and C. D. Nenitzescu, *Rev. Roumaine Chim.*, **12**, 1495 (1967).

[7] C. N. Rentzea, M. Rentzea, I. Necsoiu and C. D. Nenitzescu, *Tetrahedron*, **24**, 4667 (1968).

[8] I. I. Schiketanz, I. Necsoiu, M. Rentzea and C. D. Nenitzescu, *Rev. Roumaine Chim.*, **13**, 1385 (1968).

[9] V. Przemetchi, I. Necsoiu, M. Rentzea and C. D. Nenitzescu, *Rev. Roumaine Chim.*, **14**, 1567 (1969).

[10] A. Ghenciulescu, I. Necsoiu, M. Rentzea and C. D. Nenitzescu, *Rev. Roumaine Chim.*, **14**, 1543 (1969).

[11] C. D. Nenitzescu, *Bull. Soc. chim. France*, **1968**, 1349.

[12] F. Freeman, in "Reviews on Reactive Species in Chemical Reactions", Freund Publ. House Ltd, Tel Aviv, p. 37.

[13] J. Rocek and J. C. Dorzs, *J. Amer. Chem. Soc.*, **92**, 6668 (1970).

[14] P. S. Kalsi, K. S. Kumar and M. S. Wadia, *Chem. and Ind.*, **1971**, 71.

[15] F. W. Bachelov and U. O. Cheriyan, *Canad. J. Chem.*, **54**, 3383 (1973).

[16] F. Freeman and N. J. Yamachika, *Tetrahedron Letters*, **1969**, 3615.

[17] F. Freeman, P. D. Mc Cart and M. J. Yamachika, *J. Amer. Chem. Soc.*, **92**, 6621 (1970).

[18] F. Freeman and K. W. Arledge, *J. Org. Chem.*, **37**, 2656 (1972).

[19] The interpretations based on radical or radical ions intermediates are not included in the discussion.

[20] I. Necsoiu and C. D. Nenitzescu, *Chem. and Ind.*, **1960**, 377.

[21] L. V. Sulima and I. P. Gragerov, *Zhur. obshchei Khim.*, **29**, 3825 (1959).

[22] I. Necsoiu, V. Przemetchi, A. Ghenciulescu, C. N. Rentzea and C. D. Nenitzescu, *Tetrahedron*, **22**, 3037 (1966).

[23] I. Necsoiu, A. Ghenciulescu, M. Rentzea, C. N. Rentzea and C. D. Nenitzescu, *Rev. Roumaine Chim.*, **12**, 1503 (1967).

[24] S. Winstein, E. Clippinger, A. H. Fainberg, R. Heck and G. C. Robinson, *J. Amer. Chem. Soc.*, **78**, 328 (1956); J. P. Hardy, A. Ceccon, A. F. Diaz and S. Winstein, *ibid.*, **94**, 1353, 2363 (1972).

[25] S. Winstein and A. H. Fainberg, *J. Amer. Chem. Soc.*, **86**, 459 (1958).

[26] S. Winstein and D. Trifan, *J. Amer. Chem. Soc.*, **74**, 1147, 1154 (1952).

[27] S. J. Cristol, A. A. Roberts and T. E. Mc Entee, *J. Org. Chem.*, **39**, 829 (1974).

[28] H. H. Sisler, "Inorganic Synthesis" vol. II, Mc Graw-Hill, New York, 1946, p. 205.

[29] S. J. Cristol, J. R. Mohrig and D. E. Plorde, *J. Org. Chem.*, **30**, 1956 (1965).

[30] S. J. Cristol, T. W. Russell, J. R. Mohrig and D. E. Plorde, *J. Org. Chem.*, **31**, 581 (1966).

Revue Roumaine de Chimie, 29, 4, 367–374 (1984)

DETERMINACIÓN DE Fe(III) POR POTENCIOMETRÍA COMPLEXOMÉTRICA. DETERMINACIÓN DE MEZCLAS BINARIAS DE Ca(II)–Pb(II), Ca(II)–Fe(III) Y Pb (II)–Fe(III).

DOLORES VAZQUEZ BARBADO
Departamento de Química analítica, Facultad de Ciencias, Universidad de Valladolid,
España

Recibido el 12 de Junio de 1981

Como continuación del trabajo anterior, se realiza un estudio sistemático de la determinación de Fe(III) por potenciometría complexométrica con ADTP y ANT, utilizando electrodo de Pt como indicador. Se determinan tambien mezclas de Ca(II), Pb(II) y Fe(III), proponiendo en cada caso el medio idóneo de valoración, así como los electrodos más adecuados para seguir la potenciometría. Se indica tambien la complexona más recomendable para cada mezcla.

As continuation of a previous paper, we have carried out a systematic study on the determination of Fe(III) by complexometric potentiometry with DTPA and NTA, using a Pt electrode as indicator. Also, the binary mixtures of Ca(II), Pb(II) and Fe(III) have been studied. The accurate media, the adequate electrodes for the potentiometry and the most accurate complexones were suggested in each case.

INTRODUCCIÓN

La titulación del Fe (III) con complexonas es conocida desde hace tiempo, Schwarzenbach la ha descrito realizándola a pHs 2 y 3 con tirón como indicador. [1]

No faltan referencias en cuanto a su determinación directa con AEDT [2] o con AEDT y ANT, [3] con otras complexonas como el ADCT [4-6] ó AEGT, [7] todas ellas con indicadores coloreados para la detección del punto final. No obstante se encuentran descritos métodos instrumentales para la localización del punto final de la determinación, [8,9] recomendando siempre la utilización de un electrodo de Pt como indicador en los métodos eléctricos.

Como continuación del trabajo anterior, se pretendió en un principio la utilización del electrodo de oro amalgamado para la potenciometria complexométrica del Fe (III). Ante la imposibilidad de obtener resultados satisfactorios, no quedó más remedio que utilizar uno de Pt como indicador frente a un calomelanos saturado como referencia. Las complexonas útiles para esta determinación fueron únicamente el ADTP y el ANT.

El electrodo de Pt, es uno de los llamados inertes, lo suficientemente conocido para que no sea necesario entrar en amplia discusión sobre su funcionamiento. Este electrodo cuando está sumergido en una disolución que contiene los estados oxidado y reducido de un sistema redox reversible, debe reflejar la proporción de los dos estados de oxidación. Por tanto su papel consiste únicamente en aceptar a proveer electrones.

El platino sumergido en una disolución que contiene iones Fe^{+3} y Fe^{+2}

$$Fe^{+3} + e^{-} \rightleftarrows Fe^{+2}$$

que de acuerdo con la ecuación de Nernst tendrá un potencial :

$$E = E^{0} + 0{,}0591 \log \frac{[Fe^{+3}]}{[Fe^{+2}]} \qquad (1)$$

Cuando se va añadiendo la complexona transcurre la siguiente reacción :

$$Y^{-4} + Fe^{+3} \rightleftarrows YFe^{-}$$

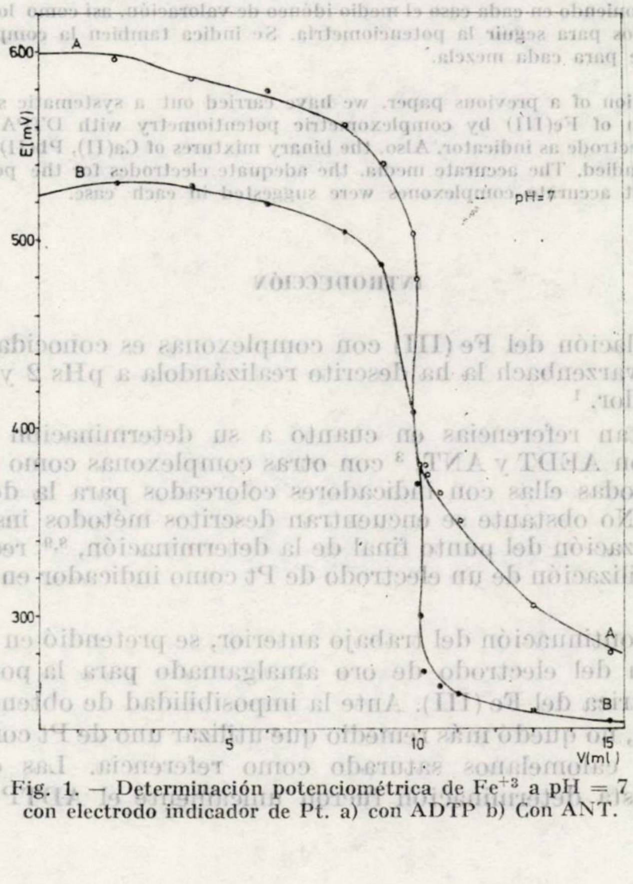

Fig. 1. — Determinación potenciométrica de Fe^{+3} a pH = 7 con electrodo indicador de Pt. a) con ADTP b) Con ANT.

cuya constante será :

$$K = \frac{[YFe^{-}]}{[Y^{-4}]\,[Fe^{+3}]} \qquad (2)$$

Combinando las ecuaciones (1) y (2) se obtiene que :

$$E = E^{0} = 0{,}0591 \log \frac{[YFe^{-}]}{K\,[Y^{-4}]\,[Fe^{+2}]}$$

englobando en K′ todo lo que permanece constante, la ecuación anterior se transforma en :

$$E = K' + 0{,}0591 \log \frac{[YFe^{-}]}{[Y^{-4}]}$$

El potencial varia con la concentración del complejo de Fe^{+3} y al de la complexona libre.

PARTE EXPERIMENTAL

Preparación de los electrodos

El de Pt se prepara soldando un hilo de Pt de 0,5 cm de longitud y 1 mm de diámetro a un tubo de vidrio. Se hace la conexión al pH-metro mediante un hilo de Cu unido al platino por estaño fundido.

El resto de los electrodos son los citados en el trabajo anterior.

Determinación de Fe^{+3}

El método de trabajo seguido es idéntico al expuesto para el Ca^{+2} y Pb^{+2}, tratando de conocer la influencia del pH del medio, así como la naturaleza de la solución reguladora empleada para conseguir ese pH.

Se trabaja añadiendo 2 ml de reguladora por cada 10 ml de solucion a calorar. En cada caso se representa graficamente E = f (ml) de YH_2^{-2}, obteniéndose con ello la curva potenciométrica correspondiente y el punto final de la determinación.

RESULTADOS Y DISCUSIÓN

Se comprueba que el Fe^{+3} es valorable directamente en medio ácido sin tamponar (PH = 2), aunque tambien es valorable a pH = = 6 y 7 de solución reguladora de trietanol amina y su sal nítrica. En la figura 1 se muestran los resultados de la determinación de Fe^{+3} con ADTP (A) y ANT (B) cuando el medio es de pH = 7., a pH = 6 y con el medio sin regular se obtienen resultados similares. Para el resto de los valores del pH no se obtuvieron valores reproducibles para el potencial, por lo que no resultaron útiles para la valoración.

Si se mantiene constante el volumen de disolución de Fe^{+3} a valorar, se observa que al modificar la concentración del catión, éste resulta valorable con ADTP hasta concentraciones de $5 \cdot 10^{-4}$M y con ANT hasta

10^{-3}M, tanto cuando el medio es ácido como a pH = 6 y 7. Los resultados se muestran en la tabla 1.

Los electrodos de PbO_2 y de oro amalgamado son inútiles para esta forma de determinar el Fe^{+3}.

Determinación conjunta de mezclas binarias de Ca(II), Pb(II), y Fe(III)

Modo de operar

Ca^{+2} y Fe^{+3}

Dado que el ADTP ha sido la complexona que ha permitido valorar a cada uno do estos dos cationes individualmente, se la pretende utilizar para su titulación conjunta, pers como cada uno de ellos requiere un electrodo indicador diferente, fué necesario preparar do, muestras idénticas A y B. En la muestra A se valoró el Fe^{+3} en presencia del Ca^{+2} a pH = 7- se observa entonces que se cometen grandes errores por exceso, por lo que el método fué dester rado.

Tabla 1

Valoración de Fe^{+3} con las diferentes complexonas y a distintas concentraciones

Molaridad	$5 \cdot 10^{-2}$	10^{-2}	10^{-3}	$5 \cdot 10^{-4}$
mg. Fe^{+3} puestos	28,03	5,60	0,56	0,28
mg. hallados con ADTP :				
pH = 2	28,06	5,62	0,57	0,27
pH = 6	28,06	5,61	0,55	0,28
pH = 7	27,78	5,61	0,57	0,28
%Error para el ADTP :				
pH = 2	+0,10	+0,35	+1,78	−3,51
pH = 6	+0,10	−0,17	−1,78	0,00
pH = 7	−0,89	−0,17	+1,78	0,00
mg. hallados con ANT :				
pH = 2	27,92	5,59	0,56	—
pH = 6	28,06	5,60	0,56	—
pH = 7	27,92	5,61	0,57	—
%Error para el ANT :				
pH = 2	−0,30	−0,17	0,00	—
pH = 6	+0,10	0,00	0,00	—
pH = 7	−0,30	+0,17	+1,78	—

El método definitivo es el siguiente : se preparan dos muestras idénticas A y B, en la A se valora el Ca^{+2} con ADTP a pH = 10 ($NO_3NH_4-NH_4OH$), añadiendo exceso de esta solución reguladora a fin de que precipite el hierro presente en forma de hidróxido, el electrodo indicador es uno de oro amalgamado y se requiere la presencia de una gota del complejo ADTP—Hg. No es necesario filtrar el precipitado para llevar a cabo la valoración. En la muestra B se valora el Fe^{+3} con ANT a pH = 7 de solución reguladora de trietanolamina y su sal nítrica. El electrodo indicador es uno de Pt.

Fe^{+3} y Pb^{+2}

Se preparan dos muestras idénticas A y B. En la A se determina el Fe^{+3} a pH = 2 sin regular el mismo, con ANT y electrodo de Pt como indicador. En la B, se valora el Pb^{+2}

a pH = 10 de $NO_3NH_4-NH_4OH$, en presencia de ácido tartárico, con ADCT y electrodo oro amalgamado como indicador. Se requiere la presencia de una gota de complejo de ADCT-Hg^{-2}

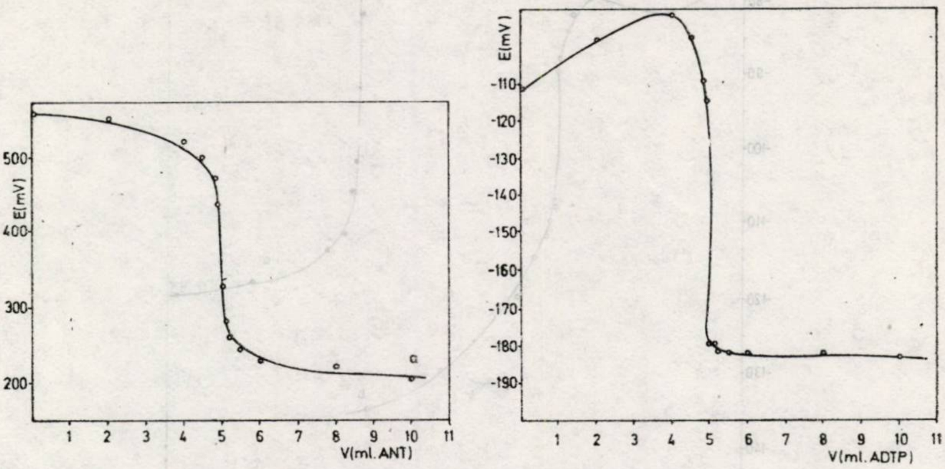

Fig. 2. — Determinación conjunta de Ca^{+2} y Fe^{+3} en la proporción 1 : 1 ; a) Ca^{+2} b) Fe^{+3}.

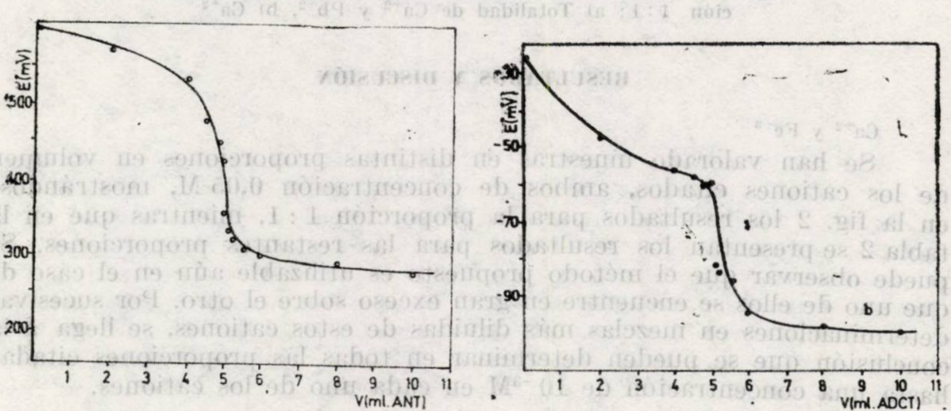

Fig. 3. — Determinación conjunta de Fe^{+3} y Pb^{+2} en proporción 1 : 1 ; a) Fe^{+3} b) Pb^{+2}.

Pb^{+2} y Ca^{+2}

Aquí se requiere únicamente el empleo de una complexona, el ADCT y un electrodo indicador único para los dos cationes : el de oro amalgamado, sin embargo es preciso preparar las dos muestras de siempre A y B idénticas.

En la muestra A se valora la totalidad de Ca(II) y Pb(II) a pH = 10 de $NO_3NH_4-NH_4OH$, en presencia de ácido tartárico y con una gota del complejo ADCT-Hg^{-2}. En la B se precipita el plomo como cromato de plomo en medio acético, añadiendo exceso de cromato potásico a la muestra. En la solución y sin necesidad de filtrar, se valora el Ca^{+2} como de costumbre a pH = 10 y electrodo de oro amalgamado como indicador.

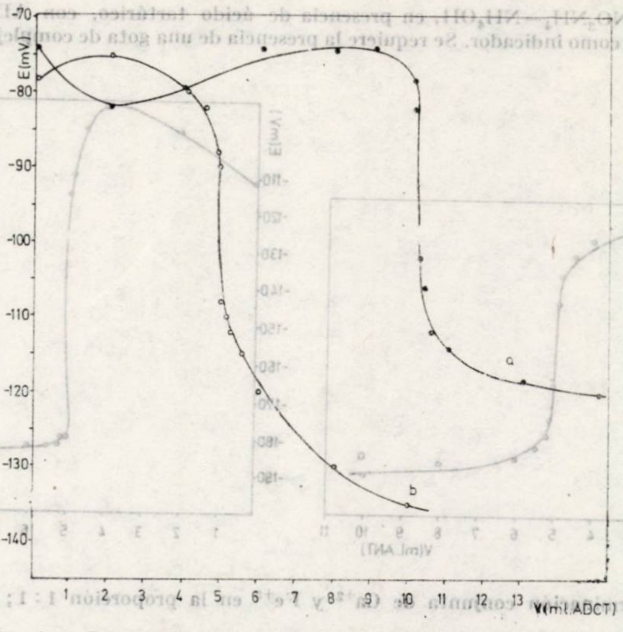

Fig. 4. — Determinación conjunta de Ca^{+2} y Pb^{+2} en proporción 1 : 1 ; a) Totalidad de Ca^{+2} y Pb^{+2}, b) Ca^{+2}

RESULTADOS Y DISCUSIÓN

Ca^{+2} y Fe^{+3}

Se han valorado muestras en distintas proporciones en volumen de los cationes citados, ambos de concentración 0,05 M, mostrándose en la fig. 2 los resultados para la proporción 1 : 1, mientras que en la tabla 2 se presentan los resultados para las restantes proporciones. Se puede observar que el método propuesto es utilizable aún en el caso de que uno de ellos se encuentre en gran exceso sobre el otro. Por sucesivas determinaciones en mezclas más diluidas de estos cationes, se llega a la conclusión que se pueden determinar en todas las proporciones citadas hasta una concentración de 10^{-3}M en cada uno de los cationes.

Fe^{+3} y Pb^{+2}

Como en el caso anterior se han titulado mezclas de ambos cationes, cada uno de ellos 0,05 M, y en distintas proporciones en volumen. En la fig. 3 se muestran los resultados para la proporción 1 : 1, y en la tabla 3 el resto de la proporciones estudiadas. Es posible valorar estas mezclas hasta una concentración $2 \cdot 10^{-3}$M en cada catión.

Pb^{+2} y Ca^{+2}

Es posible la valoración de mezcla de los cationes de concentración 0,05 M en cada uno de ellos, en distintas proporciones en volumen. En la fig. 4 están los resultados de la proporción 1 : 1 y en la tabla 4 las restantes proporciones. Estas mezclas se pueden valorar hasta una concentración $2 \cdot 10^{-3}$M en cada catión y en todas las proporciones.

Tabla 2

Determinación de mezclas binarias de Fe^{+3} y Ca^{+2} en distintas proporciones en volumen para una concentración de 0,05 en ambos

Muestras		mg. Fe^{+3} puestos	mg. Ca^{+2} puestos	mg. Fe^{+3} hallados	mg. Ca^{+2} hallados	Error	% Err.
1 : 1	A	14,03	—	14,03	—	0,00	0,00
	B	—	9,99	—	10,05	0,06	0,60
1 : 2	A	14,03	—	13,90	—	−0,13	0,92
	B	—	19,99	—	20,00	0,01	0,05
1 : 3	A	14,03	—	13,90	—	−0,13	0,92
	B	—	29,99	—	30,20	0,21	0,70
1 : 4	A	14,03	—	13,90	—	−0,13	0,92
	B	—	39,99	—	40,30	0,31	0,77
2 : 1	A	28,03	—	27,94	—	−0,09	0,32
	B	—	9,99	—	9,99	0,00	0,00
3 : 1	A	42,05	—	42,12	—	0,07	0,16
	B	—	9,99	—	10,05	0,06	0,60
4 : 1	A	56,07	—	56,07	—	0,00	0,00
	B	—	9,99	—	10,00	0,01	0,10

Tabla 3

Determinación de mezclas binarias de Fe^{+3} y Pb^{+2} en distintas proporciones en volumen para una concentración de 0,05 M en ambos

Muestras		mg. Fe^{+3} puestos	mg. Pb^{+2} puestos	mg. Fe^{+3} hallados	mg. Pb^{+2} hallados	Error	% error
1 : 1	A	14,03	—	14,03	—	0,00	0,00
	B	—	52,99	—	52,62	−0,37	0,69
1 : 2	A	14,03	—	13,97	—	−0,06	0,42
	B	—	105,99	—	105,76	−0,23	0,21
1 : 3	A	14,03	—	13,97	—	−0,06	0,42
	B	—	158,99	—	158,89	−0,10	0,06
1 : 4	A	14,03	—	13,97	—	−0,06	0,42
	B	—	211,99	—	211,52	−0,47	0,22
2 : 1	A	28,03	—	28,20	—	0,17	0,60
	B	—	52,99	—	53,13	0,14	0,30
3 : 1	A	42,05	—	42,29	—	0,24	0,49
	B	—	52,99	—	53,13	0,14	0,30
4 : 1	A	56,07	—	55,40	—	0,33	0,58
	B	—	52,99	—	52,62	−0,37	0,69

Tabla 4

Determinación de mezclas binarias de Pb^{+2} y Ca^{+2} en distintas proporciones en volumen para una concentración de 0,05 M en ambos

Muestras		mg. Pb^{+2} puestos	mg. Ca^{+2} hallados	mg. Pb^{+2} puestos	mg. Ca^{+2} hallados	Error	% error
1 : 1	A	52,99	—	53,13	—	0,14	0,26
	B	—	9,99	—	9,96	−0,03	0,30
1 : 2	A	52,99	—	52,62	—	−0,37	0,69
	B	—	19,99	—	20,11	0,12	0,60
1 : 3	A	52,99	—	52,62	—	−0,37	0,69
	B	—	29,99	—	30,17	0,18	0,60
1 : 4	A	52,99	—	53,13	—	0,14	0,26
	B	—	39,99	—	40,23	0,24	0,60
2 : 1	A	105,99	—	105,25	—	−0,74	0,70
	B	—	9,99	—	10,07	0,08	0,80
3 : 1	A	158,99	—	158,47	—	−0,52	0,32
	B	—	9,99	—	10,07	0,08	0,80
4 : 1	A	211,99	—	211,99	—	0,00	0,00
	B	—	9,99	—	9,96	−0,03	0,30

BIBLIOGRAFIA

[1] G. Schwarzenbach, "Komplexon-Methoden", Siegfried and Co., Zofingen, 1948.

[2] R. Přibil, Z. Kcudela y B. Matyska, *Chem. Listy*, **44,** 222 (1959).

[3] P. Wehber, *Z. analyt Chem.*, **158,** 321 (1959).

[4] F. Bermajo y M. Rey, *Anales real Soc. españ. Fís. Quím.*, **50 B,** 305 (1959).

[5] F. Bermejo y M. Rey, *Química e Industria*, **6,** 3 (1959).

[6] Z. Sir y R. Přibil, *Chem. listy*, **49,** 679 (1955).

[7] F. Bermejo y M. Paz, *Inform. Quím. Analítica*, **12,** 157 (1958).

[8] R. Přibil y B. Matyska, *Coll. Czech. Chem. Comm.*, **16,** 139 (1951).

[9] R. Patzak y G. Doopler, *Z. analyt. Chem.*, **156**, 248 (1957).

Revue Roumaine de Chimie, 29, 4, 375–382 (1984)

APLICACIONES DEL ELECTRODO DE ORO AMALGAMADO A LA DETERMINACIÓN COMPLEXOMÉTRICA DE Ca(II) Y Pb(II)

DOLORES VAZQUEZ BARBADO
Departamento de Química Analítica, Facultad de Ciencias, Universidad de Valladolid, España

Recibido el 12 de Junio de 1981

Se ha realizado un estudio metódico y sistemático de la determinación de Ca(II) y Pb (II) por potenciometria complexométrica con electrodo de oro amalgamado como indicator. Los agentes complejantes utilizados son del tipo del EDTA, tales como EGTA, DCTA, NTA y DTPA, proponiendo en cada caso el más idóneo, así como el medio de pH más apropiado para realizar la titulación.

A systematic study is reported on the determination of Ca(II) and Pb(II) by complexometric potentiometry with an amalgamated gold indicator electrode. EDTA type complex agents, as EGTA, DCTA, NTA and DTPA have been used. In each case, the more suitable, agent complex, together with the accurate pH are proposed in order to carry out the titration.

INTRODUCCION

La mayoría de los trabajos que se han realizado en complexometría se han llevado a cabo utilizando el EDTA como agente complejante, y diferentes sistemas indicadores para la detección del punto final.[1]

Así mismo en la literatura no faltan referencias a titulaciones potenciométricas con diferentes electrodos indicadores,[2-4] aunque el de mayor utilización ha sido el electrodo de gota de Hg para las potenciometrías complexométricas. A causa de las desventajas que presenta este electrodo líquido y el éxito con que ha sido utilizado para el mismo fin el de oro amalgamado[5] para Ca(II), Mg(II), Ba(II) y Sr(II) con EDTA, nos hemos propuesto su utilización para el presente trabajo.

Se pretende la determinación de Ca^{+2} y Pb^{+2} con complexonas del tipo del EDTA, tales como el EGTA, DCTA y DTPA.

El electrodo de gota de Hg en contacto con una disolución que contiene iones metálicos y una pequeña cantidad de complejo de Hg, posee un potencial que corresponde a la siguiente semipila :

$$Hg/\,HgY^{-4}//\,MY^{-}/\,M^{+2}$$

El potencial de este electrodo se puede obtener combinando la ecuación de Nernst para un electrodo de Hg con las ecuasiones que dan las constantes de estabilidad del complejo de Hg y la del complejo del catión que se está valorando, de donde se obtiene la siguiente expresión :

$$E = E^{0}_{HG} + 0{,}0296 \log \frac{(M^{+2})\ (Hgy^{-2})K_{MY}}{(MY^{=})K_{HgY}}$$

En esta ecuación se puede ver como el potencial del electrodo guarda una relación lineal con log (M^{+2}) y por tanto este electrodo sirve de indicador del pM en presencia de una cantidad fija de YHg^{-2}, con lo que la ecuación anterior se puede expresar como :

$$E = K + 0{,}0296 \log \frac{[M^{+2}]}{[MY^{-2}]}$$

En el caso en que el electrodo sea uno de oro amalgamado, todo transcurre de la misma forma, la diferencia es que habrá que sustituir el valor E^{0}_{Hg} por el de E^{0}_{Au-Hg} en las correspondientes expresiones del potencial de electrodo. Este electrodo tiene las ventajas de ser sólido y presentar interferencias mínimas frente a los halogenuros. Además de resultar útil como indicador en las potenciometrías complexométricas sino tambien para la determinación de una manera sencilla de las propiedades de los complejos bajo ciertas condiciones, como el cálculo de la cte. de estabilidad del catión que se está valorando.

Los valores del potencial del electrodo de oro amalgamado vendrá dado por las siguientes expresiones :

a) Para una solución ácida que no contiene más que el complejante y Hg^{+2} será :

$$E = E^{0}_{Au-Hg} + 0{,}0296 \log \frac{[HgY^{-2}]\O}{Y_{t} \cdot K_{HgY}}$$

donde Ø es una función de la concentración de H^{+} y de las ctes. de disociación de la complexona considerada como ácido.

b) Para la zona básica, manteniendo el resto de las condiciones experimentales idénticas, los potenciales de electrodo vienen limitados por la formación de HgO y la ecuación que da el valor del potencial es :

$$E = E^{0}_{Au-Hg} + 0{,}0296 \log \frac{K_{HgO}}{[OH^{-}]^{2}}$$

En la práctica, a pesar de todo, no se obtienen los valores que dan las expresiones matemáticas, debido al efecto salino de los distintos iones presentes en la disolución.

A medida que aumenta el pH de la disolución los potenciales se desplazan a la zona negativa, disminuyendo con ello el valor del salto del potencial en le punto final, por ello es indispensable realizar cada titulación a un pH óptimo, teniendo en cuenta la formación cuantitativa del complejo y la forma de la correspondiente curva potenciométrica.

En las titulaciones por potenciometria complexométrica con electrodo de oro amalgamado como indicador, es conveniente añadir unas gotas de ión Hg^{+2}, que añadiremos bajo la forma de HgY^{-2} en evitación de errores ; la única misión de este catión va a ser la de estabilizar el valor del potencial de electrodo, a la vez que va a seguir la actividad de los iones de la disolución.

Si se tienen en cuenta las ctes de estabilidad de los complejos de

Hg^{+2} y M^{+2}:

$$Hg^{+2} + Y^{-4} \rightleftharpoons HgY^{=} \qquad K = \frac{[HgY^{-2}]}{[Hg^{+2}]\,[Y^{-4}]}$$

$$M^{+2} + Y^{-4} \rightleftharpoons MY^{=} \qquad K' = \frac{[YM^{-2}]}{[M^{+2}]\,[Y^{-4}]}$$

y si además KK' (como en el caso de M^{+2} = Ca, Mg, Ba, Sr, Pb,. . .) se impide la reacción de desplazamiento total de M^{+2} sobre la pequeña cantidad de $HgY^{=}$, que permanece cte durante toda la valoración, con lo que la expresión del potencial del electrodo se puede escribir :

$$E = \text{cte.} - 0{,}0296 \log \, [Y^{-4}]$$

Esto implica que en el transcurso de la valoración, el potencial de electrodo está intimamente ligado a la concentración del agente complejamente libre, el cual se mantiene practicamente ctes durante la primera parte de la valoración, por formación del complejo MY^{-2}, pero en las proximidades del punto final la concentración de Y^{-4} aumenta bruscamente, y el potencial del electrodo disminuye, indicando de esta forma la situación del punto final.

PARTE EXPERIMENTAL

Preparación de los electrodos

El electrodo de oro amalgamado se ha preparado por un método que ha sido descrito por Verdejo[6] y se ha determinado su potencial normal del mismo modo que se propone enese trabajo.

Los electrodos de PbO_2 y MnO_2 se han preparado por deposición anódica sobre un electrodo de Pt de 2 × 0,75 cm² y 0,3 mm de espesor, unido a un tubo de vidrio por un hilo del mismo metal, y utilizando las mismas conexiones que para el de oro amalgamado. Las condiciones experimentales de deposición así como el cálculo del valor de sus potenciales normales son los descritos por Hulanicki.[7]

Determinación de Ca^{+2} y Pb^{+2}

Los cationes alcalinotérreos en condiciones normales no son electroactivos, pero pueden intervenir en procesos electroquímicos si se pone en juego un ión antagonista, representado aquí por el agente complejante ; Si hay presente en la disolución un catión electractivo, que dependiendo de la naturaleza de este último y del pH de la disolución formará un quelato más o menos estable que los que forman los cationes citados inicialmente, este ión que se ha introducido se comporta como un indicador electroquímico de la reacción de quelación, permitiendo detectar el punto final. Como ya se ha indicado aquí el ión que se introduce es el Hg^{+2} bajo la forma de HgY$^{=}$ para evitar errores, este ión junto al electrodo de oro amalgamado forma el sistema redox Hg^{+2}/Hg.

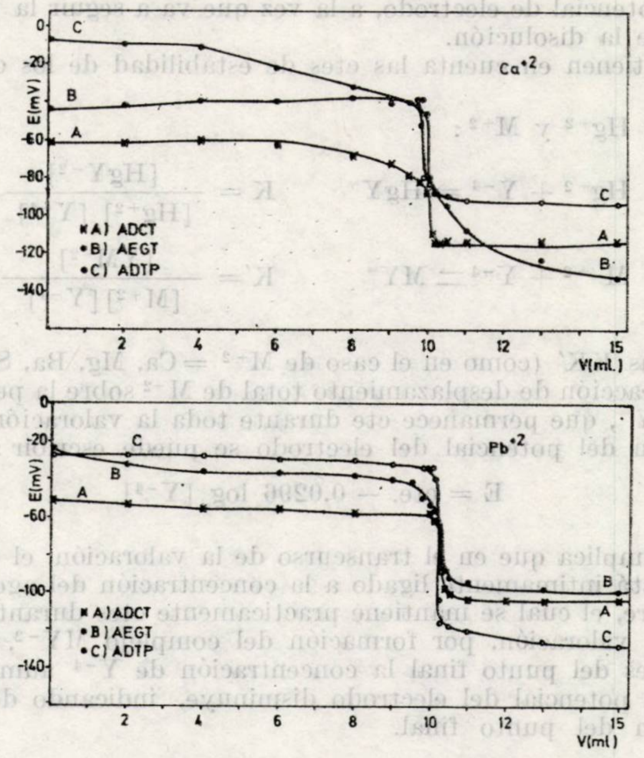

Fig. 1: — Determinación de Ca^{+2} (a) y Pb^{+2} (b) con electrodo indicator de oro amalgamado, a pH = 10 y con diferentes complexonas.

Como la estabilidad de los complejos de los cationes disminuye al hacerlo el pH, habrá que conocer cual es el medio óptimo de titulación, para ello se lleva a cabo una serie de valoraciones de volumenes iguales de disolución de cada uno de los cationes con todas y cada una de las complexonas, manteniendo el resto de las condiciones experimentales idénticas. Tambien se ha visto la posible influencia que para un determinado valor del pH puede tener la naturaleza de la solución reguladora empleada, resultando ser útiles solamente las mezclas de NO_3NH_4—NH_4OH de pH = 10. En la práctica se añaden 3 ml de sol. reguladora por cada 10 ml. de solución a valorar y una gota del complejo YHg^{-2}. Se representa E = f [ml. YH$_2^-$.] y se obtiene la correspondiente curva de titulación, obteniendo el valor del punto final a través de ella. Cuando se valora Pb^{+2}, además de realizar una serie de valoraciones en las condiciones indicadas, se efectua una segunda serie en la misma forma, pero añadiendo aprox. 1 gr. de ac. tartárico por cada 10 ml. de sol. de Pb^{+2} a valorar.

Se han preparado soluciones reguladoras del pH con NO_3NH_4—NH_4OH, para pH = =10, 9, 8'5 y 8; con trietanol amina y su sal nítrica para pH = 8'5, 8, 7 y 6; de pH = 5 de acetato etc.

Como muchos de los componentes de las soluciones reguladoras forman complejos con el Hg^{+2} o con el catión a valorar, se determinará cual debe ser la cantidad óptima que de ella es necesario añadir a 10 ml, de solución a valorar en cada caso, manteniendo el resto de las condiciones experimentales invariables.

RESULTADOS Y DISCUSION

Se observa que el comportamiento del electrodo de oro amalgamado es distinto segun la concentración de Hg del mismo, y en este tipo de potenciometria sólo resulta útil el que posee un contenido en Hg entre el 20 y 25% en peso, no apreciándose diferencias notables en ese intervalo de concentración en Hg, por lo se usarán indistintamente.

En la figura 1 se puede apreciar en las curvas A, B y C la determinación del Ca^{+2} con DCTA, EGTA y DTPA respectivamente, y en la misma figura las A′, B′ y C′ respectivamente para el Pb^{+2} en presencia de ac : tartárico. Apenas existen diferencias en las titulaciones de un determinado catión con cada una de las complexonas. El NTA no sirve para la determinación de estos cationes por potenciometría.

Es importante saber el límite mínimo de concentración al que es aplicable este método, para ello se realizan valoraciones de 10 ml. de solución de cada uno de los cationes con cada una de las complexomas a diferentes concentraciones, manteniendo el resto de las condiciones idénticas. En la tabla 1 se muestran los resultados obtenidos. Apenas existen diferencias, pero estas se deben a los diferentes valores del pK de los complejos que forman los cationes con las distintas complexonas.

Si se disminuye el valor del pH en cualquiera de las titulaciones que nos ocupan, el valor del salto del potencial en el punto final disminuye dificultando la valoración, pues el complejo se formará más lentamente

Tabla 1

Determinación da Ca^{+2}, con distintas complexonas para determinar la concentración mínima valorable

Molaridad	$5 \cdot 10^{-2}$	10^{-2}	10^{-3}	10^{-4}
mg. Ca^{+2} puestos	19,99	3,99	0,39	0,03
mg. hallados con ADCT	19,92	4,02	0,40	—
%Error con ADCT	−0,35	+0,75	+2,25	—
mg. hallados con AEGT	20,04	4,02	0,38	—
%Error con AEGT	+0,25	+0,75	−2,25	—
mg. hallados con ADTP	19,80	4,01	0,39	0,04
%Error con ADTP	−0,95	+0,50	0,00	+3,33

Idem. para Pb^{+2}

Molaridad	$5 \cdot 10^{-2}$	10^{-2}	10^{-3}	$5 \cdot 10^{-4}$
mg. Pb^{+2} puestos	105,99	21,19	2,11	1,05
mg. hallados con ADCT	106,30	21,26	2,13	—
%Error con ADCT	+0,29	+0,33	+0,95	—
mg. hallados con AEGT	105,87	21,17	2,10	—
%Error con AEGT	−0,11	−0,09	−0,47	—
mg. hallados con ADTP	105,67	21,29	2,10	1,06
%Error con ADTP	−0,30	+0,47	−0,47	0,95

y con mayor dificultad pues los protones compiten con el catión :

$$M^{+2} + YH_2^{-2} \rightleftharpoons MY^{-2} + 2H^+$$

Se realizan por tanto titulaciones de ambos cationes con cada una de las complexonas a diferentes valores del pH, obteniéndose para el calcio resultados totalmente semejantes para todas las complexonas; otro tanto ocurre para el caso del plomo. Los resultados que se obtienen son los siguientes : tanto para el Ca^{+2} como para el Pb^{+2} los únicos valores del pH a los que es posible la titulación para las complexonas estudiadas son 9 y 10, obtenidos con soluciones reguladoras de $NO_3NH_4—NH_4OH$.

Por otra parte, el aumento de la cantidad de solución reguladora de pH = 10 presente, conlleva una disminución del valor del salto del potencial en las proximidades del punto final, al mismo tiempo que se produce un desplazamiento de los valores hacia la región de los negativos; esto se puede explicar por la tendencia del ión Hg^{+2} a formar complejos con el NH_3.

$$Hg^{+2} + 2NH_3 \rightleftharpoons Hg(NH_3)_2^{+2}$$

cuya cte. K será :

$$K = \frac{[Hg(NH_3)_2^{+2}]}{[Hg^{+2}]\,[NH_3]^2}$$

Pero existe tambien la posibilidad de la reacción :

$$NH_3 + HgY^{-2} \rightleftharpoons NH_3HgY^{-2}$$

cuya cte. K′ será :

$$K' = \frac{[NH_3HgY^{-2}]}{[NH_3][HgY^{-2}]}$$

cuando tales complejos se forman, la variación del potencial debido exclusivamente a la solución reguladora viene dada por :

$$E = Cte + 0{,}0296 \log \frac{[NH_3HgY^{-2}]\,\varnothing\left(1 + \frac{H^+}{K_a}\right)}{[NH_3][Y^{-4}]K'_{NH_3HgY}{}^{-2}K_{HgY}{}^{-2}}$$

Además, se puede observar que la curva potenciométrica se desplaza hacia potenciales más altos al principio de la valoración, para volver hacia valores menores en cuanto se añaden los primeros ml. de complexona, por lo todo parece indicar que la complexona fuerza la disociación de complejo $Hg(NH_3)_2^{+2}$.

Si se valora por este método el Ca^{+2} en presencia de halogenuros, la posición del punto final se podría ver afectada por la formación de X_2Hg_2 sobre la superficie del electrodo, sin embargo, y tal como se aprecia en la figura 2 (Sólo se representan los resultados habidos para una complexona, pues para las demás es similar), la presencia de Cl^- y Br^- no afecta para nada la situación del punto final, pero hay una ligera modificación en el valor de los potenciales, todo ello para una concentración en X^- 20 veces superior a la de Ca^{+2}; sin embargo la presencia de I^- en este tipo de titulaciones, desvirtua por completo la forma de las curvas de titulación, tanto más cuanto mayor es la cantidad de I^- presente. Debido a esto no es posible determinar el punto final en presencia de yoduros (I^-), ya que el mercurio forma con este anión compuestos más estables que con los otros halogenuros.

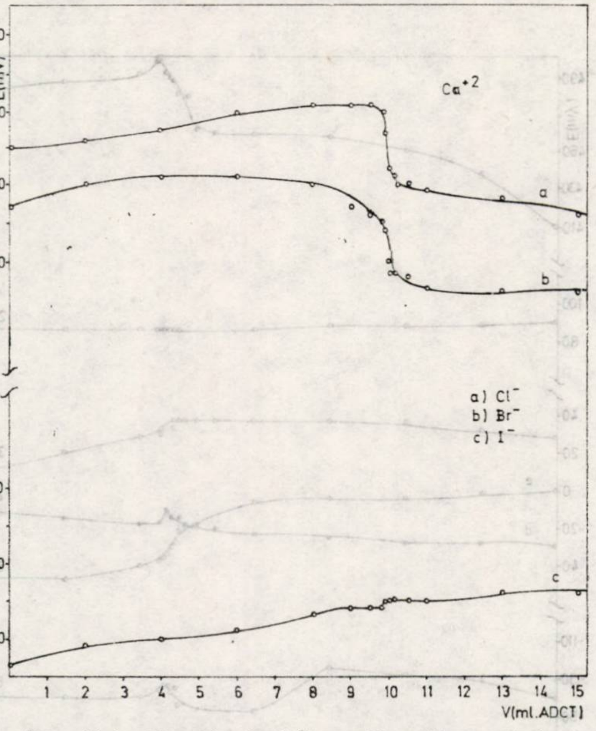

Fig. 2: — Determinación de Ca^{2+} a pH = 10, con electrodo de oro amalgamado y en presencia de a) Cl^-, b) Br^- y c) I^-.

Dado que varios autores [8-12] recomiendan la utilización de electrodos de PbO_2 y MnO_2 como indicadores en la potenciometria complexométrica de cationes, nos hemos propuesto aplicarlos tambien a nuestro trabajo, pero de entrada y por razones de índole práctico hubimos de renunciar al de MnO_2. Al trabajar con el de PbO_2, en las condiciones óptimas fijadas para cada catión y con cada una de las complexonas, no se obtuvieron resultados satisfactorios en ningún momento, según puede apreciarse en la figura 3, donde sólo se representan resultados para el DCTA pues para el resto de las complexonas es totalmente semejante.

Asimismo, como todos los electrodos llevan un soporte de Pt, se probó la posible influencia de este elemento en las determinaciones potenciométricas, sin obtener resultados favorables en los cationes y complexonas que nos ocupan (fig. 3). Teniendo en cuenta que Khalifa[13] afirma que es posible sustituir un electrodo de platino por uno de oro en una potenciometría sin que los resultados se alteren, se intentó tambien la utilización de un electrodo de oro sin ningún resultado práctico.[14] (Fig. 3)

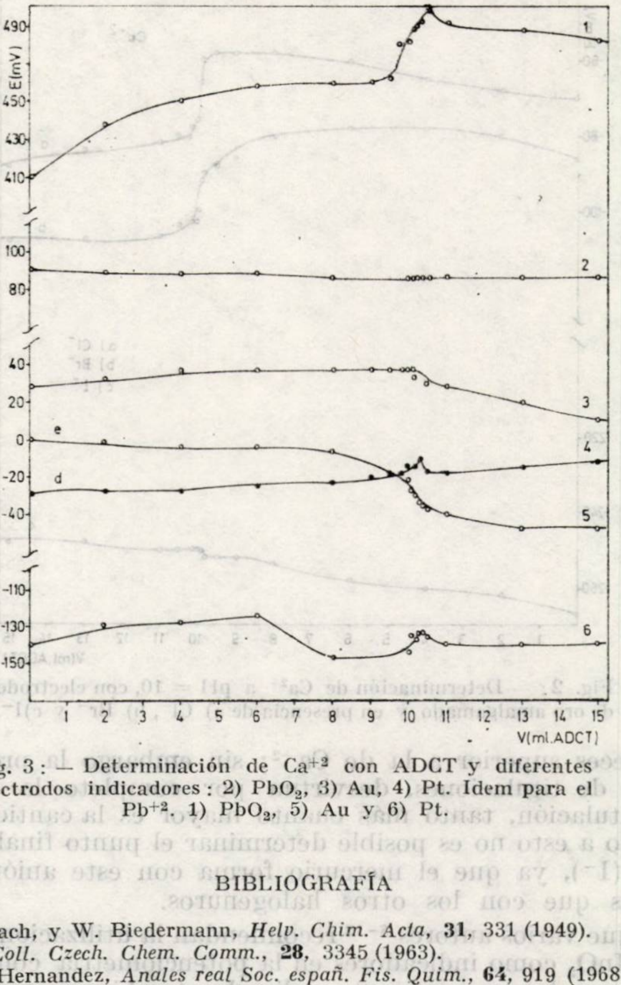

Fig. 3 : — Determinación de Ca^{+2} con ADCT y diferentes electrodos indicadores : 2) PbO_2, 3) Au, 4) Pt. Idem para el Pb^{+2}. 1) PbO_2, 5) Au y 6) Pt.

BIBLIOGRAFÍA

[1] G. Schwarzenbach, y W. Biedermann, *Helv. Chim. Acta*, **31**, 331 (1949).
[2] F. Strafelda, *Coll. Czech. Chem. Comm.*, **28**, 3345 (1963).
[3] F. Sierra y J. Hernandez, *Anales real Soc. españ. Fis. Quim.*, **64**, 919 (1968).
[4] P. Papastathopoulos, *Talanta*, **17**, 339 (1970).
[5] C. N. Reilley y R. W. Schmid, *Analyt. Chem.*, **30**, 947 (1948).
[6] C. Verdejo, Tesis Doctoral, Dpto. Quim. Anal., Univ. Valladolid (1975).
[7] A. Hulanicki y M. Trojanowicz, *Talanta*, **17**, 225 (1969).
[8] A. Hulanicki y M. Trojanowicz, *Talanta*, **23**, 503 (1976).
[9] T. Nomura y G. Nakagawa, *Japan Analyst*, **16**, 1314 (1967).
[10] C. Vandael, *Ind. Chim. belge*, **8**, 932 (1962).
[11] C. O. Huber y A. Dahnkek, *Analyt. Chem.*, **43**, 152 (1971).
[2] G. Kraft, *Z. analyt. Chem.*, **186**, 187 (1962).
[13] H. Khalifa y A. M. Daess, *Z. analyt. Chem.*, **169**, 272 (1958).
[14] Mª D. Vázquez, Tesis Doctoral, Dpto. Quim. Anal. Univ. Valladolid (1978).

Revue Roumaine de Chimie, **29**, *4*, 383–388 (1984)

SENSITISED COLOUR REACTION FOR SPECTROPHOTOMETRIC DETERMINATION OF URANIUM

SANJAY KUMAR, RAVI KANT and OM PRAKASH*
Department of Chemistry, University of Allahabad, Allahabad, India

Received July 14, 1981

Formation of a green ternary complex having λ_{max} at 620 nm has been reported between UO_2^{++}, CAS (chrome azurol S), and cetyltrimethylammnoium bromide (CTAB) over the pH range 3.7 to 5.7. The composition, $UO_2^{++}(CAS)_2(CTA)_4$, of the ternary complex has been established by Job's method of continuous variation and mole ratio method under certain essential experimental conditions. The ternary system obeys Beer's law between 0.15 and 3.8 ppm of uranium. A high molar absorptivity (81000 mol^{-1} cm^{-1}) and Sandell's sensitivity (0.003 γ/cm^2) have been obtained. A spectrophotometric method for the determination of uranium based on the formation of this ternary complex has been proposed. The method has been tested in the presence of several cations and anions. The mode of formation and structure of ternary complex have been discussed. The proposed method is sensitive, selective, precise and only few cations and anions interfere in the determination.

Chrome azurol S(tri sodium salt of 3''-sulpho-2'', 6''-dichloro-3,3'-dimethyl-4-hydroxy fuchsone-5,5'-dicarboxylic acid) has been employed as chromogenic reagent and as a metallochromic indicator for micro determination of several cations in solution.[1-5] Tremendous potentialities of cationic surfactants *viz.* cetyltrimethylammonium bromide and cetylpyridinium bromide for increasing sensitivity and selectivity of metal-dye colour reactions have now been well recognised.[6-14] It has been observed that strict control of experimental conditions is essential for establishing composition and for evaluation of the analytical parameters in order to use such ternary complex forming colour reactions for spectrophotometric determinations. The present paper outlines the essential conditions and applications of a new highly sensitive and selective colour reaction between chrome azurol S and uranium (VI) in the presence of cetyltrimethylammonium bromide. The proposed ternary complex forming reaction is highly sensitive and subject to less interference of foreign ions. The molar absorptivity value is also exceptionally high. The composition of ternary complex investigated has been established and analytical data for spectrophotometric determination of uranium (VI) have been evaluated under strict control of experimental conditions. An attempt has also been made for suggesting tentative structure and mode of formation of the ternary complex investigated.

---

* For correspondence.

EXPERIMENTAL

Reagents — A stock solution of uranyl nitrate was prepared by dissolving calculated amount in redistilled water. This solution was standardised gravimetrically by oxine as precipitating reagent. Working solutions were prepared by diluting this solution with redistilled water. A stock solution (2×10^{-4} M) of Chrome azurol S (CAS) was prepared by dissolving weighed amount in redistilled water. Working solutions were prepared by appropriate dilution of this solution. Freshly prepared solutions were always used. Cetyltrimethyl ammonium Bromide (CTAB) solution (10^{-3} M) was prepared by dissolving calculated amount in hot redistilled water. This solution was standardised by argentometric titration method. Acetate buffer solution was prepared from 0.2 M solutions of sodium acetate and acetic acid.

Apparatus — Absorbance measurements were made with Beckman (DU). Spectrophotometer against redistilled water blank. For pH measurements a. Leeds and Northrup direct reading pH meter with glass calomel electrode assembly was employed.

RESULTS AND DISCUSSION

Absorption Curves — In the pH range 4—6, maintained by acetate buffer, a pink-violet coloured binary chelate having λ_{max} at 585 nm is formed when uranyl nitrate and CAS solutions are mixed (Fig. 1, curve B). Curves A and C (Fig. 1) represent absorption spectra of CAS solution and a solution containing CAS and five fold excess of CTAB. When UO_2^{++}, CAS, and CTAB solutions were mixed in this pH range a green coloured ternary complex was formed immediately exhibiting λ_{max} at 620 nm (Fig. 1, curve D). The effect of pH on absorption characteristics of the ternary complex is shown in Fig. 2a by absorption spectra A, B, C, D and E at different pH's.

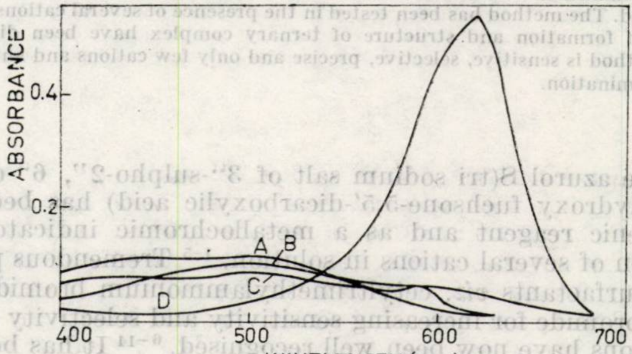

Fig. 1. — Change in absorption characteristics of CAS and binary complex of CAS with uranyl ion in the presence of CTAB. Final concentration of reactants : CAS, 1.33×10^{-5}M ; UO_2^{2+}, 0.66×10^{-5}M ; CTAB, 6.6×10^{-5}M ; and pH 4.5. A, CAS ; B, CAS + UO_2^{2+} ; C, CAS + CTAB and D. CAS + UO_2^{2+} + CTAB.

pH Stability Range — A number of solutions containing UO_2^{++}, CAS and CTAB in the ratio 1 : 2 : 10 were prepared at different pH's. Absorbance of these mixtures at 620 nm and λ_{max} are plotted againts pH in Fig. 2b and 2c respectively. The λ_{max} of ternary complex was constant between pH 2.8 and 7.8 but absorbance remained constant only over pH range 3.7–5.7. It has been observed that addition of 3 ml acetate buffer (0.2 M) had no appreciable effect on the colour and absorbance of the ternary complex solutions.

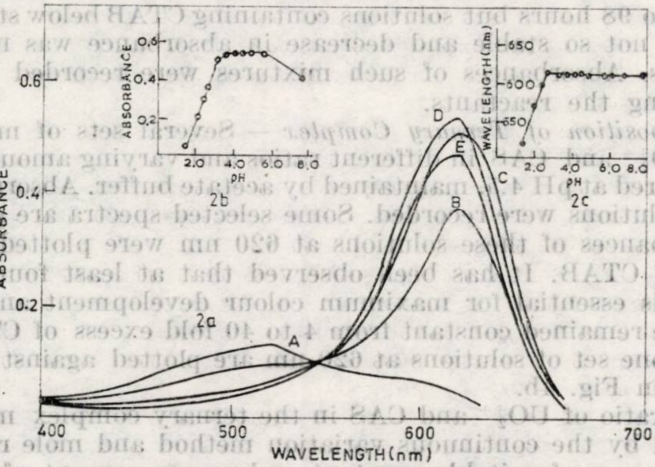

Fig. 2. — Effect of pH on absorption characteristics of ternary complex. Final concentration of reactants : CAS, 1.33 × 10^{-5}M ; UO_2^{2+}, 0.66 × 10^{-5}M ; and CTAB, 6.6 × 10^{-5}M. pH : A, 1.4 ; B, 2.8 ; C, 3.4 ; D, 4.2 ; E, 6.7.

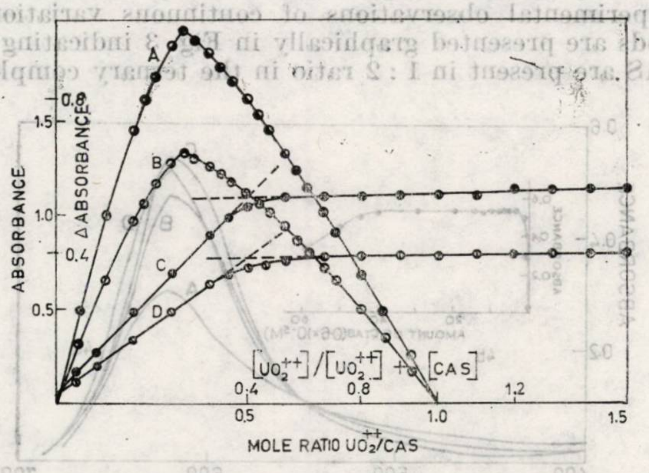

Fig. 3. — Job's plots (A and B). Original concentration of CAS and UO_2^{2+} and final concentration of CTAB : A, CAS (6.6 × 10^{-5}M), UO_2^{2+} (6.6 × 10^{-5}M), CTAB (8.0 × 10^{-5}M) and B, CAS (5.0 × 10^{-5}M), UO_2^{2+} (5.0 × 10^{-5}M), CTAB (6.0 × 10^{-5}M) ; pH 4.5, at 620 nm. Mole ratio plots. Final concentration of reactants : C, CAS (2.6 × 10^{-5}M), CTAB (1.56 × 10^{-4}M) ; and D, CAS (2.0 × 10^{-5}M), CTAB (1.20 × × 10^{-4}M) ; pH 4.5, at 620 nm.

The Effect of Time — The formation of green coloured ternary complex was instantaneous and ternary complex solution attains maximum absorbance within less than five minutes. The stability of ternary complex is greatly affected by the amount of CTAB. Ternary complex solutions containing CTAB in the stoichiometric ratio and above this ratio were stable up to 98 hours but solutions containing CTAB below stoichiometric ratio were not so stable and decrease in absorbance was noticed after 20 minutes. Absorbances of such mixtures were recorded immediately after mixing the reactants.

Composition of Ternary Complex — Several sets of mixtures containing UO_2^{++} and CAS in different ratios and varying amounts of CTAB were prepared at pH 4.5, maintained by acetate buffer. Absorption spectra of these solutions were recorded. Some selected spectra are given in Fig. 4a. Absorbances of these solutions at 620 nm were plotted against the amount of CTAB. It has been observed that at least four fold excess of CTAB is essential for maximum colour development and maximum absorbance remained constant from 4 to 40 fold excess of CTAB. Absorbances of one set of solutions at 620 nm are plotted against the amount of CTAB in Fig. 4b.

The ratio of UO_2^{++} and CAS in the ternary complex molecule was established by the continuous variation method and mole ratio method in the presence of suitable constant and excess amount of CTAB. The constant amount of CTAB was adjusted in such a manner that in each solution it was within 4 to 40 fold excess and absorbance of solutions was not a function of CTAB concentration. It was essential to observe this condition strictly for obtaining correct metal-dye ratio and reproducible results. Experimental observations of continuous variation and mole iatio methods are presented graphically in Fig. 3 indicating that uranyl ron and CAS are present in 1 : 2 ratio in the ternary complex molecule.

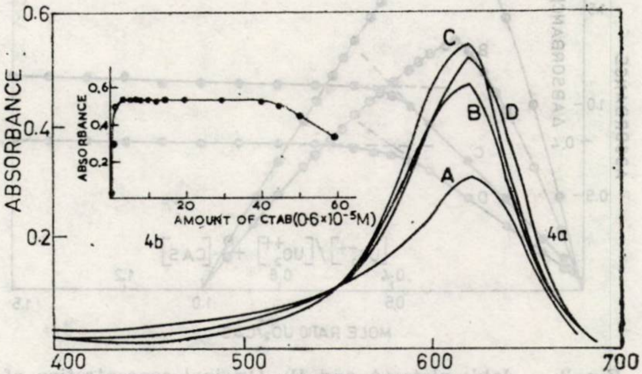

Fig. 4.(a) Final concentration of reactants : CAS, 1.33 × × 10^{-5}M ; UO_2^{2+}, 0.66 × 10^{-5}M ; CTAB : A, 0.30 × 10^{-5}M ; B, 0.60 × 10^{-5}M ; C, 1.80 × 10^{-5}M ; and D, 6.60 × 10^{-5}M. (b) Graph of absorbance versus amount of CTAB. Final concentration of reactants : CAS, 1.33 × 10^{-5}M ; UO_2^{2+}, 0.66 × 10^{-5}M ; pH 4.5, at 620 nm.

From Fig. 4b it can be concluded that four CTAB molecules are involved in the formation of one ternary complex molecule. Thus this ternary complex has been formulated as UO_2^{++} $(CAS)_2$ $(CTA)_4$.

Mode of Formation and Tentative Structures— Uranyl ion usually has a coordination number four which appears to be saturated by donors of two CAS molecules. Uranyl ion is initially bonded to the chromophore of CAS molecules through the phenolic oxygen and carboxylic oxygen and the ion-associating species are the CTAB cations. The CTAB cation forms its ion — association with the binary UO_2^{++} $(CAS)_2$ chelate primarily via the sulphonic acid group. Electrophilic reaction at this centre promotes electron withdrawal from the remaining carboxylic groups in the red-violet UO_2^{++} $(CAS)_2$ binary chelate along the conjugated bond system thus allowing ionisation of the remaining protons to produce an absorbing species similar to that of the blue green fully ionised CAS molecule. The resulting ternary complex may further associate with other two CTAB cations to produce final 1 : 2 : 4 ternary species as shown below.

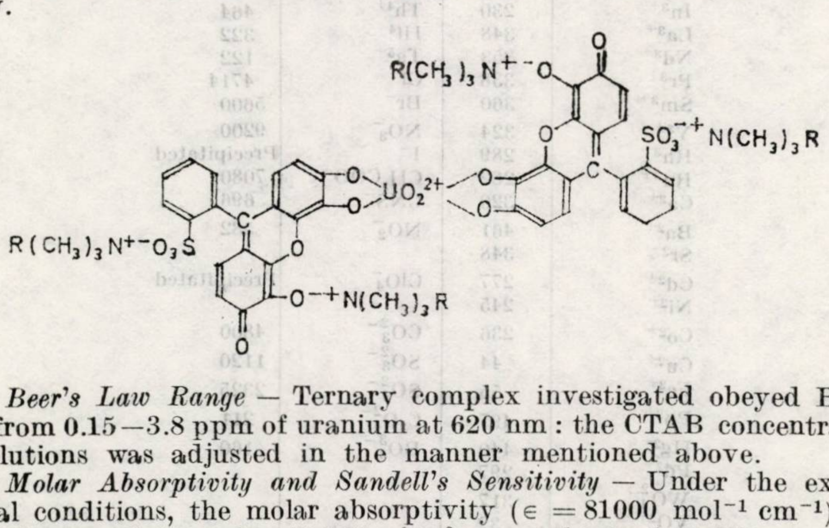

Beer's Law Range — Ternary complex investigated obeyed Beer's Law from 0.15—3.8 ppm of uranium at 620 nm : the CTAB concentration in solutions was adjusted in the manner mentioned above.

Molar Absorptivity and Sandell's Sensitivity — Under the experimental conditions, the molar absorptivity ($\in$ = 81000 mol^{-1} cm^{-1}) and Sandell's sensitivity value (0.003 γ/cm^2) were obtained at 620 nm.

Photometric Determination of Uranium (VI) — For spectrophotometric determination of uranium (VI), calibration curves were prepared by the following procedure. To solutions containing CAS and varying amounts of UO_2^{++}, was added suitable constant and excess amount of CTAB. pH of the solutions was maintained 4.5 by adding suitable amount of acetate buffer keeping total volume at 25 ml. Absorbance of each solution was recorded at 620 nm after 10 minutes and plotted against the amount of uranium. A suitable volume of sample solution containing uranium in the range (0.15 to 3.8 ppm) was treated with the same amounts of CAS and CTAB as used in the known solutions for preparing calibration curves. pH of the solution was adjusted 4.5 with acetate buffer keeping total volume at 25 ml. Absorbance was recorded at 620 nm. Knowing absorbance of the sample solution, its uranium concentration was determined directly from the calibration curves. The sample solution must be free from the following ions: Al^{3+}, Cu^{++}, Ga^{3+}, Fe^{++}, VO^{++}, ClO_4^-, Pt^{4+}. These ions can be removed from the sample solution by conventional methods.

Effect of Foreign Ions — The proposed method was tested in the presence of several cations and anions. Tolerance limit for different ions corresponding 2% change in absorbance is given in the following table:

Table 1

Effect of cations and anions on uranium determination
UO_2^{++} (6.6×10^{-6} M); CAS (1.3×10^{-5} M); CTAB (6.6×10^{-5} M); pH 4.5; Temp. 25°C

Foreign ion	Tolerance limit (ppm)	Foreign ion	Tolerance limit (ppm)
Al^{3+}	98	MoO_4^{2-}	371
Sb^{3+}	347	Pt^{4+}	Precipitated
Ga^{3+}	77	Zr^{4+}	195
In^{3+}	230	Th^{4+}	464
La^{3+}	348	Hf^{4+}	322
Nd^{3+}	353	Ta^{5+}	122
Pr^{3+}	338	Cl^-	4714
Sm^{3+}	360	Br^-	5600
Y^{3+}	324	NO_3^-	9200
Rh^{3+}	289	I^-	Precipitated
Ru^{3+}	282	CH_3COO^-	7080
Ca^{2+}	320	CNS^-	696
Ba^{2+}	461	NO_2^-	582
Sr^{2+}	348		
Cd^{2+}	277	ClO_4^-	Precipitated
Ni^{2+}	245		
Co^{2+}	236	CO_3^{2-}	4800
Cu^{2+}	44	SO_3^{2-}	1120
Fe^{2+}	55	SO_4^{2-}	2325
Pb^{2+}	497	$C_2O_4^{2-}$	211
Hg^{2+}	440	BO_3^{3-}	160
Pd^{2+}	297		
WO_4^{2-}	317		
VO^{2+}	32		
Zn^{2+}	209		

REFERENCES

[1] A. P. Martinov, V. P. Novak and B. E. Reznik. *Zhur. analit. Khim*, **33**, 51 (1978).
[2] R. K. Chernova, K. I. Gurev and E. G. Bolshakova, *Zhur. analit. Khim.*, **31**, 688 (1976).
[3] Nishida Hiroshi, *Bunseki Kagaku*, **24**, 261 (1975).
[4] Nishida Hiroshi, *Bunseki Kagaku*, **19**, 972 (1970).
[5] S. P. Mushran, Om Prakash and P. Sanyal, *J. prakt. Chem.*, **38**, 125 (1968).
[6] Y. H. Kulkarni and L. M. Good, *Analyt. Chem.*, **50**, 973 (1978).
[7] C. L. Lenog, *Analyst*, **102**, 293 (1977).
[8] H. Duchková, M. Malát and L. Čermáková, *Analyt. Lett.*, **9**, 487 (1976).
[9] N. S. Polvektov, R. S. Laver, L. A. Ovchar and S. F. Potapova, *Zhur. analit. Khim.*, **30**, 1106 (1975).
[10] Om Prakash, M. Malát and L. Čermáková, *Coll. Czech. Chem. Comm.*, **43**, 2536 (1978).
[11] Om Prakash, R. C. Gupta and S. P. Mushran, *Indian J. Chem.*, **18**, 535 (1979).
[12] R. Kant, O. Prakash and S. P. Mushran, *Analysis*, **8**, 56 (1979).
[13] O. Prakash, S. Kumar and S. P. Mushran, *Talanta*, **26**, 1167 (1979).
[14] S. Kumar, Om Prakash and S. P. Mushran, *Analyst*, **105**, 474 (1980).

Revue Roumaine de Chimie, **29**, *4*, 389–391 (1984)

COMPTES RENDUS

PER-OLOV LÖWDIN and B. PULLMAN (Eds), "New Horizons of Quantum Chemistry"; Proceedings of the Fourth International Congress of Quantum Chemistry, D. Reidel Publishing Company, London, 1983, 457 p.

The Fourth International Congress of Quantum Chemistry under the auspices of the International Academy of Quantum Molecular Science in Menton (France) was arranged at Uppsala University (Sweden) during the period June 14–19, 1982 , in close collaboration with the University of Florida. The Congress consisted of six symposia in various areas of quantum chemistry : quantum mechanical methods, time independent phenomena, time dependent phenomena, computational quantum chemistry, surfaces and catalysis, theory of large molecules and solids, quantum biology and quantum pharmacology.

These proceedings contain the text of the plenary lectures as well as the chairmen's introductions.

The range of problems within reach of today's quantum chemist is staggering, and the technical virtuosity shown in their solution is impressive. The full range and depth of the field is explored in clear expositions of the methodology employed, and the application of mathematical methods to a variety of complex chemical problems, including : energy transfer along alpha-helical proteins, hypervalency in XLi_n molecules ; nonadiabatic effects in slow atomic collisions ; low energy electron-molecule scattering ; the interpretation of molecular spectra from accurate *ab initio* calculations ; heterogeneous catalysis ; surface phenomena and surface crystallography ; treatment of large molecules and solid-state theory ; membrane proteins, molecular evolution, and the most complicated molecule found in quantum chemistry today, transfer RNA.

The book will be of interest to physical chemists, quantum chemists, organic chemists, molecular biologists, molecular pharmacologists and spectroscopists.

D. I. Marchidan

J. MORT and G. PFISTER (Eds), "Electronic Properties of Polymers", Wiley-Interscience Publication, New York, N. Y., 1982, 336 p.

The book "Electronic Properties of Polymers" comprises an up-to-date, cross-disciplinary review of the latest research into the properties and applications of polymers as electronic materials. The editors have invited research workers and experts in the various areas of research into polymers as electronic materials to review the current understanding and their actual or potential technologic application in hope that it will further highlight this rapidly developing and important field and stimulate current and new researches and ideas in the field.

The book is ordered around the electronic phenomenon nature and it deals with the following topics :

— Insulating polymers with photoelectric and triboelectric properties ;
— Pyroelectric and piezoelectric polymers as polyvinylidene fluoride ;
— Conjugated chain polymers (mainly polyacetylene) which can exhibit metallic-like conductivity.

The book is divided into seven chapters.

Chapter 1 — "Introduction" by J. Mort and G. Pfister (12 p).

Chapter 2— "Electronic states and triboelectricity" by J. J. Ritsko (45 p) discusses the progress made recently in the electronic spectroscopy of polymers and its interpretation in terms of the molecular structure of the polymers. Such information, particulary that involving molecular ion states, is used for quantitative understanding of triboelectricity.

Chapter 3 — "Charge storage" by E. M. Sessler (49 p) describes the charging and measuring techniques of polymer electrets, experimental results of real charge storage and dipole polarization and some of the more important applications of the polymer electrets. Piezoelectricity and pyroelectricity of polymers, especially polyvinylidene fluoride, is discussed by Y. Wada in chapter 4 ("Piezoelectricity and pyroelectricity", 52 p). Chapter 5 — "Energy transfer"

(53 p) by W. Klopffer discusses the energy transfer processes in polymer systems. Chapter 6 — "Photoelectronic properties of photoconducting polymers" by J. Mort and G. Pfister (51 p) deals with recent progress in understanding the photoelectronic properties, charge generation and charge transport in disordered organic solids. In the final chapter — "Conducting polymers : Polyacetylene" by D. Baeriswyl, G. Harbeke, H. Kiess and W. Meyer (60 p) recent work on conjugated organic polymers (notably polyacetylene) is presented. The most commonly proposed theoretical models and an account of the essential experimental results of conductivity, magnetic susceptibility and optical measurements are given. References are provided at the end of each chapter and allow the reader to pursue the subject more deeply. A subject index (10 p) ends this very interesting and highly useful book which will surely be favourably received by researchers who are working in the field of polymers as electronic materials.

Mircea Grigoraş

'A THERMODYNAMIC BYPASS GOTO LOG K", Monograph for Teachers No. 35, by P.A.H. Wyatt, The Royal Society of Chemistry, London, 1982, 70 p.

This volume is the 35th publication in the series of Monographs for Teachers which was launched in 1959 by the Royal Institute of Chemistry (UK) with the aim to present concise and authoritative accounts of selected well-defined topics in chemistry for those who teach the subject at GCE Advanced level and above.

Professor Wyatt's book follows the Guggenheim earlier monograph in the series (E. A. Guggenheim, Elements of Chemical Thermodynamics, 2nd edn RIC Monograph for Teachers, No 12, 1970), bearing a certain resemblance to it but having an important difference by inserting $\log_{10}$ K values in the tables, which reflects the attitude of the book and permits a good deal of chemistry to be discussed in quantitative terms before anything which passes for "thermodynamics" is tackled. Thus the end table can be treated in the same way as a table of logarithms before the pocket calculator revolution.

The first chapter entitled "Equilibrium Constants" gives a summary account of the calculational procedures involved in determining the K values. A classical reaction (in testing for carbon dioxide, after the initial precipitation of calcium carbonate from lime water further passage of the gas leads to disappearance of the precipitate due to the formation of soluble bicarbonate) is discussed. Concise information about activity scales and standard states is given.

The second chapter "Fixing Variables in Solving Equilibrium Constants" discusses the phase rule and some strange equilibrium such as $CaSiO_3$ (s) = CaO(s) + SiO_2 (s) or H_2O (s) = = H^2O (1).

The third chapter deals with the additivity of log K and the relationship to formation from the elements. Correlation with heat of reaction is pointed out.

Some worked examples have undeniable didactic advantages illustrating the way in which very simple calculations can amplify descriptive information in standard chemistry courses. At several points it is emphasized that the establishment of a tendency to change gives no information at all as to how fast a chemical reaction will occur : many substances can remain together indefinitely a long way removed from chemical equilibrium.

The fifth chapter "Energy and Entropy" is a condensed and very careful review of two important extensive properties : (thermodynamic) energy (U) and entropy (S). It is assumed that the reader has a working knowledge of the meanings of "heat", "work" and "absolute temperature", at least in terms of the gas scale.

The sixth chapter "The Gibbs Function" surveys the dependence of G for a gas upon its pressure, partial pressures and chemical potentials, chemical potentials in solutions and absolute activities.

Using the first example of the book the seventh chapter "Chemical Potentials and Activities in Chemical Equilibria" covers the dependence of K upon temperature, the route to the accurate calculation of equilibrium constants from thermal measurements only, and equilibrium constants in terms of absolute activities.

The end chapter of the book is an agreeable and original text on trends and perspectives in thermodynamics with an interesting final paragraph :

> "After all, we do not know how many more millions of years humanity will survive on this planet and, if some resources are limited, it cannot make much difference on that time-scale if they are exhausted within 100 years rather than extended for 200

years with careful husbandry, though obviously the short-term problems must be tackled sensibly. In either case there will be a stimulus to finding a longer term solution and, when eventually a continuous energy supply is tapped and a steady-state energy economy can be arrived at, it will not matter if the energy is not used with the highest efficiency, just as it is not really possible to waste water in the Highlands of Scotland : a new delivery soon arrives".

One more favourable word on Appendix containing log K, ΔH_f^θ, and S^0 values for a large number of elements and compounds in a table which can be used in much the same way as a table of logarithms.

This Monograph is intended primarily for teachers of chemistry at A-level or above, but it will undoubtedly be of value to a wider readership, including students themselves. The book is essential reading for anyone involved in teaching thermodynamics.

R. Bacaloglu
L. Cotarcă

NOTE POUR LES AUTEURS

La Revue Roumanie de Chimie publie des articles en anglais, français, russe, allemand ou espagnol. Les auteurs sont priés d'envoyer des articles et des comptes rendus inédits.

Les manuscrits seront dactylographiés à deux intervalles. La bibliographie, les tableaux et la légende des figures seront placés après le texte.

Si l'article fait partie d'une série numérotée, la partie précédente sera donnée comme première référence.

Chaque article sera précédé d'un résumé comprenant quinze lignes au maximum.

Les références bibliographiques dans le texte seront faites par des exposants sans parenthèses et paraîtront à la fin de l'ouvrage.

Les publications périodiques mentionnées dans la bibliographie seront présentés suivant les prescriptions internationales : le nom de l'auteur précédé de l'initiale de prénom, le titre du périodique abrégé conformément à « Chemical Abstracts » et souligné par une ligne, le numéro du tome indiqué par des chiffres arabes et souligné par deux lignes, suivi de la première page de l'article : à la fin, l'année de la parution sera placée entre parenthèses. Le numéro de la revue ne sera pas indiqué si les pages du volume sont numérotées consécutivement.

Les textes des livres ou traités inclueront : les nom des auteurs, l'initiale du prénom, le titre du livre entre guillemets et sans être souligné, le numéro du tome précédé par l'abréviation « vol. » (ou « Bd. »), le numéro de l'édition, les éditions (the publisher), la localité de la parution du livre, l'année de la parution et la page de la référence précédée(s) par l'abréviation « p » (ou « S »).

Les brevets seront indiqués comme suit : l'auteur ou la firme, le pays et le numéro du brevet, la date et la revue *(Chem. Abstr.)*. Par ex. : M. Jones (to Union Carbide Co.), Brit. Pat. 601 238, 2 Sept. 1959, cf. *Chem. Abstr.*, 54, 12808 (1960).

Les diagrammes seront tracés à l'encre de Chine sur papier calque. Les tableaux et les figures (en nombre strictement nécessaire), ainsi que les courbes dans les figures seront numérotés par des chiffres arabes. Leur explication sera donnée dans la légende des figures. Prière de ne pas inscrire les mêmes données dans les tableaux et les figures. Chaque tableau aura un titre. On indiquera dans le texte la place approximative des tableaux et des figures. Les formules chimiques seront incluses dans le texte : en outre, elles seront transcrites sur papier calque, à l'encre de Chine.

Les auteurs sont priés d'indiquer les caractères italiques (en soulignant les lettres au crayon), ainsi que tout autre caractère spécial : les préfixes *ortho*, *meta*, *para*, *cis*, *trans*, etc. seront soulignés pour indiquer leurs caractères italiques, et ne seront jamais écrits avec des majuscules.

Aucune correction à la main ne sera admise sur le manuscrit. Les corrections seront frappées à la machine. Les lettres grecques ou autres symboles spéciaux seront insérés à la main à l'encre clairement.

Le manuscrit sera signé par l'auteur.

Le titre-courant aura 50 lettres au maximum.

L'entière responsabilité du contenu des articles appartient aux auteurs.

Sur demande on peut obtenir une note plus complète.

PRINTED IN ROMANIA

ORSZÁGOS MŰSZAKI INFORMÁCIÓS KÖZPONT ÉS KÖNYVTÁR
1883

TRAVAUX PARUS AUX ÉDITIONS DE L'ACADÉMIE DE LA RÉPUBLIQUE SOCIALISTE DE ROUMANIE

ELENA CEAUŞESCU, **Cercetări in chimia şi tehnologia polimerilor**, 1983, 519 p.
N. ASANDEI, A. GRIGORIU, **Chimia şi structura fibrelor**, 1983, 395 p.
N. IONESCU, M. CĂLDĂRARU, **Oxidarea catalitică a olefinelor inferioare**, 1983.
C. CAŞCAVAL, **Studiul polimerilor prin piroliză şi cromatografie de gaze**, 1983, 220 p.
C. I. SIMIONESCU, F. DANEŞ, **Originea vieţii**, 1983, 110 p.
C. BODEA (sub redacţia), **Tratat de biochimie vegetală**, partea II, volumul IV, 1982, 408 p.
I. G. MURGULESCU, RODICA VÎLCU, **Introducere in chimia fizică**. Vol. III. Termodinamica Chimică, 1982, 624 p.
I. G. MURGULESCU, J. PĂUN, **Introducere in chimia fizică. Vol. I.3. Nucleul atomic, reacţii nucleare, particule elementare**, 1982, 606 p.
ELENA CEAUŞESCU, **Noi cercetări in domeniul compuşilor macromoleculari**, 1981, 536 p.
I. G. MURGULESCU, TATIANA ONCESCU, E. SEGAL, **Introducere in chimia fizică. Vol. II. 2. Cinematică chimică şi cataliză**, 1981, 1024 p.
V. DRĂGUŢAN, A. T. BALABAN, M. DIMONIE, **Metateza olefinelor şi polimerizarea prin deschidere de inel a cicloolefinelor**, 1981, 254 p.
LYDIA-MARIA VAICUM, **Epurarea apelor uzate cu nămol activ. Bazele biochimice**, 1981, 218 p.
I. GĂLĂŢEANU, **Procese şi metode radiochimice in energetica nucleară**, 1981, 234 p.
O. IORDACHE, **Procese polistocastice aplicate la fenomenele de transfer**, 1981, 186 p.
CR. SIMIONESCU, VALERIA GORDUZA, **Polimeri biocompatibili şi biologic activi**, 1980, 479 p.
ELENA CEAUŞESCU, **Polimerizarea stereospecifică a izoprenului**, 1979, 307 p.
CONST. GH. MACAROVICI, **Analiza chimică cantitativă anorganică**, 1979, 457 p.
M. FLORESCU, **Metode ştiinţifice in dezvoltarea industriei chimice moderne**, 1979, 256 p.
A. T. BALABAN, I. GĂLĂŢEANU, G. GEORGESCU, LIGIA SIMIONESCU, **Compuşi marcaţi şi radiofarmaceutici cu aplicaţii in medicina nucleară**, 1979, 495 p.
I. G. MURGULESCU, E. SEGAL, **Introducere in chimia fizică. Vol. II. 1. Teoria molecular cinetică a materiei**, 1979, 1036 p.
S. STERNBERG, FL. DANEŞ, **Termodinamica chimică aplicată**, 1978, 400 p.
I. G. MURGULESCU, V. EM. SAHINI, **Introducere in chimia fizică. Vol. I.2. Structura şi proprietăţile moleculare**, 1978, 604, p.
I. ZUGRĂVESCU, MAGDA PETROVANU, **N-ylid chemistry**, coédition avec McGraw-Hill International Book Company, U.S.A., 1977, 396 p.
I. G. MURGULESCU, **Introducere in chimia fizică. Vol. I.1. Atomi, molecule, legătură chimică**, 1976, 560 p.
ELENA CEAUŞESCU, **Research work on synthesis and characterization of macromolecular compounds. Contributions**, 1974, 251 p.
CR. SIMIONESCU, VIORICA RUSAN, V. POPA, **Chimia algelor marine**, 1974, 212 p., 1 pl.

1984 SEP 6

ISSN 0035-4090

I.P. INFORMATIA, cd. 2073

43 426

Lei 40
$ 75 (pour un abonnement annuel)

F1103 04
REFERALVA
R
66

ACADÉMIE DE LA RÉPUBLIQUE SOCIALISTE DE ROUMANIE

REVUE ROUMAINE DE CHIMIE

TOME 29
Nº 5
Mai 1984

EDITURA ACADEMIEI REPUBLICII SOCIALISTE ROMÂNIA

Rev. Roumaine Chim.

RRCHAX, 29, 5, p. 393–466 (1984), Bucarest

ACADÉMIE DE LA RÉPUBLIQUE SOCIALISTE DE ROUMANIE

COMITÉ DE RÉDACTION

Rédacteur en chef:

I. G. MURGULESCU, membre de l'Académie de la République Socialiste de Roumanie

Rédacteurs en chef adjoints:

A. T. BALABAN et V. EM. SAHINI, membres correspondants de l'Académie de la République Socialiste de Roumanie

Collège de rédaction:

EM. BRATU, ELENA CEAUŞESCU, ECATERINA CIORĂNESCU-NENITZESCU, CR. SIMIONESCU, membres de l'Académie de la République Socialiste de Roumanie: P. SPACU, membre correspondant de l'Académie de la République Socialiste de Roumanie: M. BANCIU, I. HAIDUC, M. GHEORGHIU. D. I. MARCHIDAN, I. MOLDOVAN, G. NIAC et D. SĂNDULESCU

La Revue Roumaine de Chimie paraît 10 fois par an. Toute commande de l'étranger pour les travaux parus aux Editions de l'Académie de la République Socialiste de Roumanie sera adressée à ILEXIM — Departamentul Export-Import Carte (Livres)/Departamentul Export-Import Presă (Revues), P.O.B. 136—137, télex 11226, 3, str. 13 Decembrie, 79517 Bucarest, Roumanie

Les manuscrits, les livres et les revues proposés en échange, ainsi que toute correspondance seront envoyés à la rédaction:

REVUE ROUMAINE DE CHIMIE

125, Calea Victoriei, 79717 Bucarest, Roumanie, téléphone 50 76 80

EDITURA ACADEMIEI REPUBLICII SOCIALISTE ROMÂNIA
125, Calea Victoriei, 79717 Bucarest, Roumanie, téléphone 50 76 80

ORSZÁGOS MŰSZAKI INFORMÁCIÓS KÖZPONT ÉS KÖNYVTÁR 1883

REVUE ROUMAINE DE CHIMIE

Tome 29, N° 5 Mai 1984

D. GEANĂ, A min-max formulation of the problem of phase equilibrium in chemical reacting systems . . . . 395–405 R

N. PETRESCU, LUCIA GANOVICI and MIRELA BRIȚCHI, Electrolytic copper refining from cuprous sulphate solutions containing organic nitriles . . . . 407–414 BC

MONIMUL HUQUE and D. SĂNDULESCU, Studies on aqueous electrolytes and nonelectrolytes. II. Effects of electrolytes on ultrasonic velocity, adiabatic compressibility and structure of aqueous solutions of polyvinyl alcohol (PVA) 415–421

ALEXANDRA GOCAN, ANA AURELIA BOTAR, A. BARABÁS, I. OPREAN, N. ȘERBAN and F. HODOȘAN, Exo- and endohormones. VIII. Methoxyallene in pheromone synthesis 423–428

M. RĂILEANU, S. FLOREA and MARINA SAHINI, Solvent effects. I. Solvent influence on the absorption spectra of some nitrophenothiazine-5-oxides and nitrophenothiazine-5,5-dioxides 429–435

VASILE LÖCSEI, Selective ester hydrolysis. Determination of ester groups in polyurethane elastomers . . . . 437–439 R

A. ALBEROLA, A. M. GONZALEZ and F. J. PULIDO, The reaction of *p*-quinones with triphenylstibine 441–446

SVETLANA DUMITRESCU, M. GRIGORAȘ and G. SURPĂȚEANU, On the polymerization of acetylenic derivatives. XXXV. Experimental and theoretical study on the radical polymerization of 9-ethynylanthracene 447–456

MIHAELA SPIRATOS, A. AIRINEI, G. I. RUSU and AGLAIA CIOBANU, Coordination polymers. VI. Preparation and characterization of some azomethine chelate polymers 457–460

M. VLASSA and MARIA KEZDI, Applications of phase transfer catalysis in the acridine series. II. Synthesis of some acridine ethers 461–463

COMPTE RENDU 465–466

Rev. Roumaine Chim. **29**, *5*, 393–466 (1984), Bucarest

Revue Roumaine de Chimie, **29**, *5*, 395–405(1984)

A MIN-MAX FORMULATION OF THE PROBLEM OF PHASE EQUILIBRIUM IN CHEMICAL REACTING SYSTEMS

D. GEANĂ
Dept. of Physical Chemistry, Polytechnic Institute,
Spl. Independenţei 313, Bucharest, Romania

Received March 30, 1983

An analysis of the problem of chemical and phase equilibrium formulated as a nonlinear geometric program is presented. One gives a rigorous statement of the geometric program, advanced previously (D. Geană, 1981) as a min-max problem. Some new aspects which arise are discussed in relation to some applications. The theory has a series of advantages, e.g. the uniqueness problem is formally solved and the phase-splitting enters the program in a natural way.

1. INTRODUCTION

In a previous work [1] we have presented a transformation of the problem of chemical and phase equilibrium (PCPE) in thermochemical systems, based on the duality theorem of geometric programming. Thus, a geometric primal program with a special form was obtained, which is named "*Y* formulation" of PCPE. Some simple applications of this program were presented in other papers. [2,3] The analysis of "Y formulation" of PCPE was directed, in the cited works, toward a reduction of the problem to a nonlinear equation system by using the method of Kuhn-Tucker multipliers.

The aim of this paper is to present an analysis of "*Y* formulation" of PCPE as a nonlinear (geometric) program. On purpose, we give a rigorous statement of the geometric program (eq. (31) in paper [1]) as a min-max problem and we will discuss new aspects which arise in relation to some applications. It must be mentioned that PCPE has recently been discussed by Gautam and Seider. [4] They used for solving PCPE a phase-splitting algorithm coupled to a Rand method. Some recent reviews on the theory and applications of chemical and phase equilibrium are also available. [5-8] The treatment given in the work [4] is based on the formulation (a) in our paper [1] (see eq. (8–10) therein). We believe that the "*Y*" program has a series of advantages, e.g. the uniqueness problems [9] are formally solved and the phase-splitting enters PCPE in a natural way.

2. THE MIN-MAX FORMULATION OF PCPE

We consider the thermodynamic statement (named (b) in the paper [1]) of PCPE for a system with N chemical species, F phases and $\mathcal{R}$ reactions:

$$\min_{n_i^{\Phi},\xi_k} G(n_i^{\Phi}) = \sum_{i,\Phi} n_i^{\Phi} \mu_i^{\Phi} \tag{1}$$

with restrictions

$$\sum_{\Phi} n_i^{\Phi} - \sum_{k} \nu_{ik}\xi_k = n_i^0, \ (i = 1,2..N) \qquad (k = 1,2..\mathcal{R}) \tag{2}$$

$$n_i^{\Phi} \geqslant 0 \qquad (\Phi = 1,2..F) \tag{3}$$

$$n_i^0 + \sum_{k} \nu_{ik}\xi_k \geqslant 0 \tag{4}$$

The notations are: n_i^{Φ} — mole number of species i in phase Φ, n_i^0 — initial mole number of species i in the system, ξ_k — extent of reaction k (De Donder variable of reaction k), ν_{ik} — stoichiometric coefficient of species i in reaction k.

The conditions for the existence of a solution of PCPE (1—4) are given by Duhem's theorem: [10] The equilibrium state of a closed system, for which the initial mole numbers (or mases) $n_1^0, n_2^0 \ldots n_N^0$ are known, is completely determined giving two independent variables, for any number of phase, components (= chemical species) and chemical reactions in the system. In general, the independent variables are T and P, but in practical cases one encounters other situations as for example adiabatic or isentropic conditions. For such cases the PCPE is solved with appropriate restrictions by using the same variables, T and P. [8]

Lately a research effort has been made whose aim is to construct a general thermodynamic theory of bodies obeying general thermokinetic processes. [11–14] Truesdell [11] suggested for this theory the name "rational thermodynamic". Bowen's work [12] and specially Müller's theory [13,14] arise at conditions of equilibrium which give a general background for the classical PCPE in systems as those of interest in this papers.

The thermodynamic formulation of PCPE (1—4) can be rewritten by introducing the set of indices: [1].

$$I_{NF} = \left\{ \begin{array}{ll} i = 1,2 \ .\ .\ N_1, & \Phi = 1, \ i \in I_1 \\ i = N_1 + 1, \ldots, N_2, & \Phi = 2, i \in I_2 \\ \cdot \quad \cdot \quad \cdot \quad \cdot \quad \cdot & \cdot \quad \cdot \\ i = N_{F-1} + 1, \ldots N_F, & \Phi = F, i \in I_F \end{array} \right\} \tag{5}$$

where $N_F = N \times F$. One obtains thus a geometric dual program: [1]

$$\min_{\xi_k} - \max_{n_i} v(n_i) \tag{6}$$

with restrictions:

$$\sum_{i=0}^{N_F} a_{ji}\, n_i = 0 \quad (j = 0,1, \dots N) \tag{7}$$

$$n_0 = 1\,;\; n_i \geqslant 0 \tag{8}$$

$$a_{00} = 1,\; a_{j0} = -n_j^0 - \sum_k \nu_{jk} \xi_k \leqslant 0 \;\; (k = 1,2, \dots \mathscr{R}) \tag{9}$$

where $a_{ji} (i = 1,2, \dots N_F,\; j = 1,2, \dots N)$ is a bloc formed of F unity matrix (each of dimension N).

The dual function $v(n_i)$ is defined:

$$v(n_i) \equiv \exp(-g) \equiv \exp(-G/RT) \tag{10}$$

and takes the form:

$$v(n_i) = \prod_{i=0}^{N_F} \left(\frac{c_i}{n_i} \right)^{n_i} \prod_{\Phi=1}^{F} (n_\Phi)^{n_\Phi} \tag{11}$$

A general model (or a constitutive equation in the language of rational thermodynamics[11]) for the chemical potential is:

$$\mu_i = \mu_i^0(T) + RT \,\ln\, C_i + RT \,\ln(n_i/n_\Phi) \tag{12}$$

$$c_i = \exp(-g_i^0)$$

$$g_i = \frac{\mu_i^0(T)}{RT} + \ln\, C_i \tag{13}$$

where C_i is a function dependent on T, P and n_i^Φ (composition of phase Φ) in the most general case. It is a function characteristic for the phase type (vapour, liquid, etc.) and will be determined by the ideal or real model considered (see for example[1-3]).

Based on the duality theorem of geometric programming[15,16] it is possible to associate with the dual problem (6−9) a corresponding primal program:

$$\min_{z_j} - \max_{\xi_k} \; p_0(z_j,\; \xi_k) = \prod_{j=1}^{N} z_j^{a_{j0}} \tag{14}$$

with restrictions

$$p_\Phi(z_j) = \sum_{i \in I_\Phi} c_i z_1^{a_{i1}} z_2^{a_{i2}} \dots z_N^{a_{iN}} \leqslant 1 \tag{15}$$

$$z_j > 0 \;\; (j = 1,2 \dots N) \tag{16}$$

$$a_{j0} \leqslant 0 \;\; (\Phi = 1,2 \dots F) \tag{17}$$

$$(k = 1,2 \dots \mathscr{R})$$

where p_0, p_Φ are called posinomials, and z_j are the primal variables.

Considering the special form of the matrix a_{ji}, the program (14—17) becomes:

$$\min_{z_j} - \max_{\xi_k} \; Y \equiv \ln \, p_0 = \sum_{j=1}^{N} -\left(n_i^0 + \sum_k \nu_{jk}\xi_k \right) \ln \, z_j \tag{18}$$

with restrictions

$$p_1(z_j) = c_1 z_1 + c_2 z_2 \ldots + c_{N_1} z_N \leqslant 1$$

$$p_2(z_j) = c_{N_1+1} z_1 + \ldots + c_{N_2} z_N \leqslant 1 \tag{19}$$

$$p_F(z_j) = c_{N_{F-1}+1} z_1 + \ldots + c_{N_F} z_N \leqslant 1$$

$$z_j > 0 \;\; (j = 1,2 \ldots N) \tag{20}$$

$$n_i^0 + \sum_k \nu_{jk}\xi_k \geqslant 0 \;\; (k = 1,2 \ldots \mathscr{R}) \tag{21}$$

The formulation (18—21) of PCPE was named in the paper [1], "Y formulation", and it represents rigorously a min-max program. In the previous paper [1] we used a formulation which referred only to the primal variables, z_j. Surely, it does not affect the stationarity conditions, for which the treatment given in the other papers [1-3] rests complete. It is better to writte eq. (19) in the form:

$$p_\Phi(z_j) = \sum_j c_{\Phi j} z_j \leqslant 1 \quad (\Phi = 1,2 \ldots F) \tag{19'}$$

$$(j = 1,2 \ldots N)$$

by introducing the matrix

$$c_{\Phi j} \equiv \exp(-\, g_{\Phi j}^0) \tag{12'}$$

where

$$g_{\Phi j}^0 = \frac{\mu_j^0(T)}{RT} + \ln \, C_{\Phi j} \tag{13'}$$

The physical meaning of the primal variables, z_j, results in the framework of duality theorem by relations between primal and dual variables. Thus, it can be shown that: [1]

$$X_{\Phi j} = c_{\Phi j} z_j \tag{22}$$

where $X_{\Phi j}$ are mole fractions (of species j in phase Φ). The eq. (19′) represents, in consequence, the well-known conditions:

$$\sum_j X_{\Phi j} \leqslant 1 \tag{23}$$

Moreover, eq. (19′) gives natural conditions for "phase splitting", thus:

(a) for the phases that coexist in the fixed conditions (T, P, n_i^0), eq. (19′) are satisfied by "$=$" sign

(b) for the phases that can not coexist in the fixed conditions (T, P, n_i^0), eq. (19′) are satisfied by "$<$" sign.

We stated that "Y formulation" solves also the uniqueness problem.[9] It can be observed that the "Y" function has not local stationarity points, the optimum being determined by restrictions (19′). In other words, the optimum solution (at equilibrium) is found on the frontier of the domain of variables and it is unique. Some examples which follow will clarify this point.

It must be mentioned that some general algorithms for solving the optimum problems with restrictions (as those given by eq. (19′)), as, for example the projected gradient method of Rosen,[17] use the Kuhn-Tucker stationarity conditions. In this case, the Kuhn-Tucker multipliers corresponding to eq. (19′) give directly the quantities of phases which coexist at equilibrium.[1]

3. EXAMPLES

We consider firstly the application of "Y formulation" to a phase equilibrium without chemical reactions. In this case $\xi_k = 0$, and eq. (11) becomes:[2]

$$\min_{z_j} \quad Y \equiv \ln \quad p_0(z_j) = \sum_{j=1}^{N} - n_i^0 \ln z_j \tag{11'}$$

Surely the restrictions (21) take the trivial form $n_i^0 > 0$.

For liquid-vapour equilibria, one uses the term "flash equilibrium" in the case when giving T, P an n_i^0, it is required to compute the composition of coexistent phases and their quantities.[18] As far as we know, this problem was raised by us in the literature in the form of a geometric program.[2] We called the problem (11′) with restrictions (19′, 20) a "phase equilibrium primal program". This formulation is more general, but it seems that there is no relation between this one and the formulations used in the literature on flash equilibrium (see [18] for example). In appendix we will present a demonstration of equivalence, the usual expressions from the literature[18] being in fact different possibilities of transformation of the problem (11′, 19′, 20). In this way, eq. (11′) which was obtained from (11) is a natural consequence of the Gibbs criterion of equilibrium.

Another simplification of the problem in the case of phase equilibria[2] is that coefficients $c_{\Phi j}$ in eq. (19′) do not contain further the standard chemical potentials ($\mu_j^0(T)$) which have the same values for all phases in the model adopted herein in eq. (12).

Example 1

Let us consider a liquid (L)-vapour (V) equilibrium with $N = 2$, analysed on the basis of classical thermodynamics using the concept of the "surface of dissipated Gibbs free energy" by Heidemann.[9] At

$P=1$ atm and given T, the vapor pressure of the chemical species is $P_1^s=2.8$ atm and $P_2^s=0.4$ atm. For the liquid phase (1) and the vapor (2) eq. (11′, 19′, 20) become:

$$\min_{z_1,\, z_2} Y = -n_1^0 \ln z_1 - n_2^0 \ln z_2$$

$$c_{11}z_1 + c_{12}z_2 \leqslant 1$$

$$c_{21}z_1 + c_{22}z_2 \leqslant 1$$

$$z_1 > 0, \; z_2 > 0$$

Assuming an ideal behaviour from eq. (13) it results:

$$c_{11} = 1/P_1^s; \quad c_{12} = 1/P_2^s; \quad c_{21} = P^{-1}; \quad c_{22} = P^{-1}$$

The problem was solved by using Rosen's method of projected gradient [16,17] for two situations: (a) $n_1^0 = n_2^0 = 0.5$ mole and (b) $n_1^0 = 0.8$, $n_2^0 = 0.2$ mole. Figures 1 and 2 present the solutions in the conditions given above in the plane $z_1 - z_2$. The results are given in Table 1. In the case

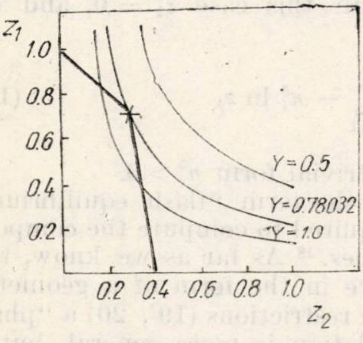

Fig. 1. Surface Y = constant for Example 1 with $n_1^0=n_2^0=0.5$ mole. Equilibrium with two phases.

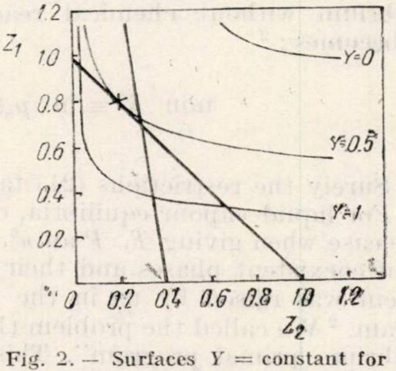

Fig. 2. — Surfaces Y = constant for Example 1 with $n_1^0 = 0.8$ and $n_2^0 = 0.2$ mole. Equilibrium with one phase.

Table 1

L — V equilibrium, $N = 2$, $P = 1$ atm, $P_1^s = 2.8$ atm, $P_2^s = 0.4$ atm

Problem	Initial approximation z_i	Optimum solution z_i^*	Phase amount λ_Φ	Mole fraction		Y^*
				liquid	vapour	
a	0.1	0.7	0.445	0.25	0.7	0.78032
	0.1	0.3	0.555	0.75	0.3	
b	0.1	0.8	0	—	0.8	0.5
	0.2	0.2	1	—	0.2	

presented in Fig. 1 (i.e. of equilibrium with two phases) the optimum is found at the intersection point of the restrictions. Function Y has the gradient in the cone generated by the gradients of restrictions.[16] In Fig. 2 the optimum solution corresponding to one phase equilibrium (vapor) is found in the tangent point of the second restriction to the curve $Y =$ constant. As can be observed there exists no problem related to uniqueness.

We have made similar calculations for other combinations n_1^0 and n_2^0 on condition $n_1^0 + n_2^0 = 1$ mole. The results are summarized in Fig. 3, which presents the dependence of the amount of liquid phase (λ_1) on n_1^0. One can remark that for $n_1^0 = 0.7$ the system reaches the dew-point, and at $n_1^0 = 0.25$ mole, the bubble point. For such simple cases we have obtained also the corresponding analytical conditions.[2]

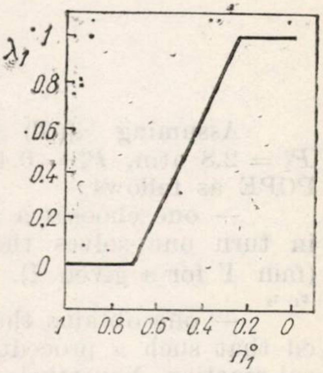

Fig. 3. — The dependence of the amount of liquid phase (λ_1) on n_1^0 for Example 1. The values λ_1 are calculated by Rosen's projected gradient method at equilibrium point.

Example 2

We consider the system with $N = 3$ given by benzene (1) — toluene (2) — o-xylene (3) at $P = 1$ atm and $T = 373$ K. The vapor pressures are: 1.78, 0.731 and 0.262 atm. respectively. The results obtained using the method of projected gradient are presented in Table 2.

Table 2

L — Vequilibrium. System benzene (1) — toluene (2) — o-xylene (3). $P = 1$ atm, $T = 373$ K

Component	Initial amount n_i^0	Optimum solution z_i^*	Mole fraction X_i	
			liquid	vapor
(1)	0.6	0.6545	0.3677	0.6545
(2)	0.3	0.2804	0.3836	0.2804
(3)	0.1	0.0651	0.2486	0.0651

Phase amount : $\lambda_L = 0.19$, $\lambda_V = 0.81$

Example 3

One considers the system from example 1 ($N = 2$, $F = 2$) with a chemical reaction $A \rightleftharpoons B$, where A is species 1 and B is species 2, analysed in other papers [3,9] too. The following program results :

$$\min_{z_1, z_2} - \max_{\xi} \; Y = -(n_1^0 - \xi)\ln z_1 - (n_2^0 + \xi)\ln z_2$$

with restrictions:

$$c_{11}z_1 + c_{12}z_2 \leqslant 1$$

$$c_{21}z_1 + c_{22}z_2 \leqslant 1$$

$$z_1 > 0,\ z_2 > 0$$

$$n_1^0 - \xi \geqslant 0\ ;\ n_2^0 + \xi \geqslant 0$$

Assuming $\mu_1^0(T) = \mu_2^0(T) = 0$ (therefore $\Delta^r G_T^0 = 0$), $P = 1$ atm $P_1^s = 2.8$ atm, $P_2^s = 0.4$ atm, $n_1^0 = 1$ mole, $n_2^0 = 0$ we have solved the PCPE as follows:

— one chooses a series of values for $\xi \in [0.1]$ and for each case in turn one solves the problem of phase equilibrium which results ($\min\limits_{z_1, z_2} Y$ for a given ξ).

— one obtains the value $\xi_{\max}$ by interpolation. It must be mentioned that such a procedure is applicable to systems with but one chemical reaction. Nevertheless, the above procedure offers a basis for an algorithm of solving the problem in systems with several reactions.

Figure 4 shows the results of calculations by means of function $Y(\xi)$. The optimum lies at $\xi = 0.875$, corresponding to an equilibrium in the liquid phase for which $z_1 = z_2 = 0.35$ and $X_1^L = 0.125$, $X_2^L = 0.875$. On the curve in Fig. 4 it was marked also the dew-point at $\xi = 0.3$ and the bubble point at $\xi = 0.75$ respectively. By comparing our Fig. 4 with Fig. 3 in Heidemann's work [9] one observes a perfect agreement, the values of functions differing by sign. This is a consequence of the primal-dual relation. For $\Delta^r G_T^0/RT = 0.8475$ and 1.5 respectively, the results are also identical to those of Heidemann [9] (see also our paper [3]).

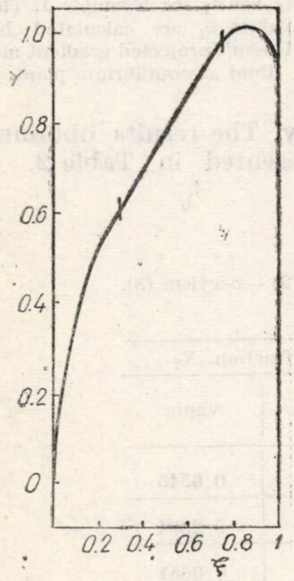

Fig. 4. — The dependence Y — ξ for Example 3. L — V equilibrium with reaction $A \rightleftarrows B$.

Example 4

This example is a ternary liquid-liquid equilibrium with chemical reaction and it was also analysed by Heidemann [9]. The species A_1, A_2 and A_3 react as follows:

$$A_1 + A_3 \rightleftarrows 2A_2$$

The PCPE becomes:

$$\min_{z_1, z_2, z_3,} - \max_{\xi} Y = -(n_1^0 - \xi)\ln z_1 - (n_2^0 + 2\xi)\ln z_2 - (n_3^0 - \xi)\ln z_3$$

$$\sum_{j=1}^{3} c_{\Phi j} z_j \geqslant 1 \quad (\Phi = 1,2) \qquad z_j > 0$$

$$n_1^0 - \xi \geqslant 0\ ;\ n_2^0 + 2\xi \geqslant 0\ ;\ n_2^0 - \xi \geqslant 0$$

At constants T and P and for $\mu_1^0 = \mu_2^0 = \mu_3^0$ (i.e. $\Delta^r G_T^0 = 0$) matrix $c_{\Phi j}$ takes the form:

$$c_{\Phi j} = 1/\gamma_{\Phi j}$$

being determined by the real model of the liquid phases. We adopted after Heidemann[9] a regular solution model:

$$\ln \gamma_{\Phi 1} = (\alpha/RT)\ X_{\Phi 2}(1 - X_{\Phi 1})$$

$$\ln \gamma_{\Phi 2} = (\alpha/RT)\ X_{\Phi 1}(1 - X_{\Phi 2})$$

$$\ln \gamma_{\Phi 3} = -(\alpha/RT)\ X_{\Phi 1}X_{\Phi 2}$$

considering as ideal the pairs $A_1 - A_3$ and $A_2 - A_3$. Phase separation appears for $\alpha/RT > 2$. It was taken $\alpha/RT = 4$. The procedure was similar to that used in Example 3. For $n_1^0 = n_3^0 = 0.5$ mole and $n_2^0 = 0$ the equilibrium is in the liquid phase 1, at $\xi = 0.05$, $z_1 = 0.5607$, $z_2 = 0.5054$ $z_3 = 0.3758$ and $X_1 = X_3 = 0.45$, $X_2 = 0.1$. The optimum value $Y_{\text{optim}} = 0.76892$. The results are in agreement with those of Heidemann[9]. It must observe that in our procedure no local minima appears, the solution being unique.

The method of projected gradient was in this case used iteratively for given ξ conforming to the algorithm:

(a) – with appropiate aproximations for $X_{\Phi j}$ one calculates $\gamma_{\Phi j}$ and the matrix $c_{\Phi j}$

(b) – the program min Y is solved for z_j

(c) – the new values of $X_{\Phi j}$ are computed

(d) – the convergence is tested: if $|X_{\Phi j}(\text{new}) - X_{\Phi i}(\text{old})| \leqslant \varepsilon$ the procedure ends, if not one goes to (a)

The computations obtained with different initial approximations for $X_{\Phi j}$ showed a good convergence. For $\Delta^r G_T^0/RT = -1$ and -2 respectively, we obtained the same results as Heidemann.[9]

In conclusion, the "Y formulation" of PCPE is suitable for different applications. The simple examples presented above show the agreement with previous results obtained on the basis of the thermodynamic formulation of PCPE. Some advantages of the new program have been pointed out. Work is in progress for applications to more complex systems.

APPENDIX

Let us consider a system of N chemical species and F phases. The program (11′, 19′, 20) can be solved by the method of Kuhn-Tucker multipliers.[15,16] One obtains the program:

$$Y_{KT} = \sum_{i=1}^{N} - n_i^0 \ln z_i + \sum_{\Phi=1}^{F} \lambda_\Phi \left(\sum_{i=1}^{N} c_{\Phi i} z_i - 1 \right) \qquad (A_1)$$

$$z_i > 0;\ \lambda_\Phi \geqslant 0$$

The stationarity conditions are :

$$\partial Y_{KT}/\partial z_i = 0 \quad (i = 1,\ N) \tag{A_2}$$

$$\partial Y_{KT}/\partial \lambda_\Phi = 0 \quad (\Phi = 1, \ldots F)$$

It results :

$$-(n_i^0/z_i) + \sum_{\Phi=1}^{F} \lambda_\Phi c_{\Phi i} = 0 \tag{A_3}$$

$$\sum_{i=1}^{N} c_{\Phi i} z_i - 1 = 0 \tag{A_4}$$

From (A_3) and (A_4) one obtains :

$$\sum_{\Phi=1}^{F} \lambda_\Phi = \sum_{i=1}^{N} n_i^0 = n^\circ \tag{A_5}$$

From (A_3) for z_i it becomes :

$$z_i = n_i^0 \Big/ \sum_{\Phi=1}^{F} \lambda_\Phi c_{\Phi i} \tag{A_6}$$

Now, by combining (A_4) and (A_6) it results :

$$\sum_i \frac{c_{\Phi i} n_i^0}{\sum_\Phi \lambda_\Phi c_{\Phi i}} - 1 = 0 \tag{A_7}$$

which represents a system of F equations in the unknowns λ_Φ. The Kuhn-Tucker multipliers give the amounts of phases at equilibrium. For 2 phases (e.g. liquid-vapour) eq. (A_7) and (A_5) become :

$$f_1(\lambda_1) = \sum_{i=1}^{N} \frac{c_{1i} n_i^0}{c_{2i} n^\circ + \lambda_1 (c_{1i} - c_{2i})} - 1 = 0 \tag{A_8}$$

$$f_2(\lambda_1) = \sum_{i=1}^{N} \frac{c_{1i} n_i^0}{c_{2i} n^\circ + \lambda_1 (c_{1i} - c_{2i})} - 1 = 0 \tag{A_9}$$

From (A_8, A_9) reults the well-known expression for flash-equilibrium [18] :

$$f(\alpha) = \sum_{i=1}^{N} \frac{w_i (1 - k_i)}{1 + \alpha (k_i - 1)} \tag{A_{10}}$$

with the notations :

$$w_i = n_i^0 / n^\circ$$

$$\alpha = \lambda_1 / n^\circ \tag{A_{11}}$$

$$k_i = c_{1i} / c_{2i}$$

REFERENCES

[1] D. Geană, *Rev. Roumaine Chim.*, **26**, 363 (1981).
[2] D. Geană, *Rev. Chim. (Bucureşti)*, **31**, 491 (1980).
[3] D. Geană, *Rev. Chim. (Bucureşti)*, **32**, 293 (1981).
[4] R. Gautam and W. D. Seider, *AIChE Journal*, **25**, 991 (1979).
[5] W. R. Smith, "Computational Aspects of Chemical Equilibrium in Complex Systems", in "Theoretical Chemistry: Advances and Perspectives", vol. 5, Academic Press, New York, 1980, p. 185.
[6] G. Eriksson, *Chem. Scr.*, *8*, 100 (1975); *Analyt. Chim. Acta*, **112**, 375 (1979).
[7] A. A. Bugaevsky, *Fizika molekul.*, **10**, 97 (1981).
[8] W. D. Seider, R. Gautam and C. W. White III, "ACS Symposium Series, No. 124", ed. by R. G. Squires and G. V. Reklaitis, 1980, p. 115.
[9] R. A. Heidemann, *Chem. Engng. Sci.*, **33**, 1517 (1978).
[10] I. Prigogine and R. Defay, "Chemische Thermodynamik", VEB Deutscher Verlag, Leipzig, 1962, p. 212.
[11] C. Truesdell, "Rational Thermodynamics", McGraw-Hill, New York, 1969.
[12] R. M. Bowen, *Arch. Rat. Mech. Anal.*, **24**, 370 (1967).
[13] I. Müller, *Z. Naturforsch.*, **28a**, 1801 (1973); *Journal de Mécanique*, **14**, 267 (1975).
[14] I. Müller, "Thermodynamics and Statistical Mechanics of Fluids and Mixtures of Fluids", Course given at the Scuola Estiva della Fisica Matematica, September 6–24, 1976, Universita di Bari.
[15] R. J. Duffin, E. L. Peterson and C. Zener "Geometric Programming-Theory and Applications", Wiley, New York, 1967.
[16] I. Marusciac, "Programare geometrică şi aplicaţii", Ed. Dacia, Cluj-Napoca, 1978.
[17] V. Dumitru, "Programare neliniară", Ed. Academiei, Bucureşti, 1975.
[18] E. J. Henley and E. M. Rosen, "Material and Energy Balance Computations", Wiley, New York, 1969.

Revue Roumaine de Chimie, 29, 5, 407–414 (1984)

ELECTROLYTIC COPPER REFINING FROM CUPROUS SULPHATE SOLUTIONS CONTAINING ORGANIC NITRILES

N. PETRESCU*, LUCIA GANOVICI** and MIRELA BRIȚCHI**

* Department of Metallurgy, Polytechnic Institute of Bucharest, Spl. Independenței 313, Romania

** Centre of Physical Chemistry, Spl. Independenței 202, Bucharest, Romania

Received June 24, 1983

Electrolytic copper refining from sulphuric solutions of cuprous sulphate was studied. The conditions of preparation of stable solutions of cuprous sulphate by adding organic nitriles and ammonia were established and the time dependence of their chemical composition was determined. It turns out that the concentration of cuprous ions had to be maintained above a certain level (20 g/l). In order to maintain a $[Cu^+]/[Cu^{2+}]$ ratio favourable to electrolysis, the procedures of transforming cupric ions into cuprous ones were studied. Our studies also extended over the influence of cuprous ion concentration, cathode current density, additives and temperature upon electrolysis.

Researches carried out during the past decade have demonstrated the organic solvents' property of solvating metallic ions and have thus opened up new horizons for the study of hydrometallurgic processes.[1–4] Such an example is the solvation of Ag^+ ions by organic nitriles which allows the electrolytic refining of silver in an aqueous Ag_2SO_4/H_2SO_4 solution containing nitriles.[2]

Cuprous ions are even more strongly solvated by nitriles in aqueous acidic solutions.

Due to the strong disproportionation tendency of cuprous ions:

$$2\,Cu^+ = Cu + Cu^{2+} \tag{1}$$

(equilibrium constant of the reaction, $K = 10^6 M^{-1}$), only extremely dilute aqueous cuprous sulphate solutions are obtainable. Muir et al.[4] have shown that by addition of 2–4 moles of organic nitriles per mole of cuprous ions in aqueous solutions of Cu_2SO_4 containing up to 180 g/l cuprous ions and 100 g/l H_2SO_4, the solutions become stable against disproportionation of Cu^+ ions ($K = 10^{-9} - 10^{-10}\,M^{-1}$, depending on concentration of nitriles).

The electrolytic refining of copper from cuprous electrolytes ensures some advantages which come directly from Faraday law: thus, for a given current the amount of copper deposited per unit time is twice that yielded by the conventional process.

Another advantage stems from the fact that cuprous sulphate is about twice more soluble in nitrile — water mixture than cupric sulphate in aqueous solutions.

The practical utilization of the electrolytic refining with cuprous ion-containing electrolytes has so far been restricted to current densities lower than those employed in the classic procedure. It was found that the operation voltage across cell terminals is higher, at the same current density, when cuprous sulphate electrolyte is employed.

One should also mention some of the drawbacks of electrolytic refining from cuprous electrolytes with organic nitriles : the tendency of cuprous sulphate acidic solutions that contain organic nitriles to oxidize slowly in the atmosphere to cupric sulphate, to hydrolyse slowly to ammonium acetate and to lose the volatile nitriles which are toxic and inflammable. One can overcome these drawbacks by conducting the process below 55° and by covering the electrolyte with a layer of kerosene.

EXPERIMENTAL

Electrolytic refining was conducted in small glass cells. The cathodes were made up of 35 × 20 mm electrolytic copper plate while the anodes, of thermally refined copper whose composition is listed in Table 1.

Table 1

Chemical composition of anodes (%)

Element	Cu	As	Sb	Pb	Zn	Ni	Sn	Fe	Al	S	Au	Ag
Content	99.465	0.078	0.170	0.040	0.005	0.006	—	0.038	0.002	0.056	0.0034	0.1015

The cell was equipped with one anode and one cathode 2.5 cm apart in the electrolyte, connected to a constant current power supply.

The composition of the electrolyte was as follows : 20—30 g/l Cu^+ as Cu_2SO_4, 150—200 g/l H_2SO_4, 240 g/l nitriles, about 18 g/l NH_3 and variable amounts of additives.

The organic nitriles that may be employed are : acetonitrile and acrylonitrile which are volatile (boiling points 81° and 78° respectively) and hydracrylonitrile which is much less volatile (boiling point 230°) and whose handling is less dangerous. Acetonitrile and hydracrylonitrile are relatively stable and cheap so that they are convenient for preparation of stable solutions of cuprous sulphate. In our experimental works we employed acetonitrile and covered the solutions with kerosene to avoid evaporation of this solvent.

The concentration of cuprous ions was determined by titration with 0.1 N $KMnO_4$ solution which oxidizes cuprous ions to cupric ions according to the reaction :

$$5\,Cu_2SO_4 + 2\,KMnO_4 + 8\,H_2SO_4 = 10\,CuSO_4 + K_2SO_4 + 2\,MnSO_4 + 8\,H_2O \qquad (2)$$

Titration was considered completed when the green solution turned dark beige.

The concentration of cupric solution was determined by titration with 0.1 N sodium thiosulphate solution in presence of starch and potassium iodide, according to the reaction :

$$2\,CuSO_4 + 4\,KI = 2\,CuI + 2\,K_2SO_4 + I_2 \qquad (3)$$

$$2\,Na_2S_2O_3 + I_2 = Na_2S_4O_6 + 2\,NaI \qquad (4)$$

Titration ended when the solution turned colourless.

The concentration of sulphuric acid was evaluated by titration with 0.1 N NaOH solution in presence of methyl-orange.

RESULTS AND DISCUSSION

A) Preparation of the electrolyte solutions and the evolution of their chemical composition

The electrolyte solution must contain 200 g/l H_2SO_4, 30 g/l cuprous ions, 240 g/l acetonitrile and about 18 g/l NH_3; monovalent copper ions are present in solution as $[CuAn_2]_2SO_4$ complexes where An stands for a nitrile or ammonia molecule.

The electrolyte solutions were prepared from cuprous oxide dissolved in sulphuric acid in presence of nitriles according to the reaction:

$$Cu_2O + 4\ An + H_2SO_4 = [CuAn_2]_2SO_4 + H_2O \qquad (5)$$

Five electrolyte solutions were prepared whose composition is given in Table 2. All solutions contained 240 g/l acetonitrile and about 18 g/l ammonia except for solution III prepared without ammonia.

The data in Table 2 show that shortly after preparation the concentration of Cu^+ ions is below 30 g/l (between 13 and 20 g/l), which proves that part of the copper originating in cuprous oxide was oxidised to Cu^{2+}. The overall concentration of Cu^+ and Cu^{2+} is on average 28.8 g/l (solutions III—V), the difference until 30 g/l being due to small amounts of cuprous oxide, left undissolved during solubilization.

The concentration of cuprous ions is higher in solutions with ammonia than in those without ammonia (solution III), which shows that ammonia contributes to stabilization of the cuprous complex and to fixation of a larger number of Cu^+ ions in complex ions.

Examination of the changes in the chemical composition of the solution during electrolysis has shown in all runs a marked increase of cuprous ion concentration within the first 24 hours of electrolysis, accompanied by a decrease of the concentration of cupric ions and sulphuric acid. The former effect is due to dissolution of copper at the anode and its fixation as cuprous complexes, while the decrease of sulphuric acid concentration is accounted for by depletion of a certain amount of acid at dissolution of copper. It was also found that the concentration of cuprous ions decreases and that of cupric ions increases in all solutions subjected to electrolysis for more than 24 hours which may be assigned to the instability of complex ions exposed to atmospheric oxygen. Although the electrolyte solution was covered with a kerosene layer, the oxidation process could not be completely stopped probably because of electrolyte agitation during the runs. When the concentration of cupric ions becomes higher than the concentration of cuprous ions, cupric sulphate is deposited on the anode and the current flow ceases. In order to avoid this effect several procedures were tested to decrease the concentration of cupric ions and to rise the concentration of cuprous ions.

a) *Addition of copper powder to the solution* rises the concentration of Cu^+ ions according to the reaction:

$$Cu + Cu^{2+} \rightleftharpoons 2\ Cu^+ \qquad (6)$$

The procedure was tested in solution I and brought about an increase of Cu^+ ions concentration from 22.7 to 26.8 g/l.

Table 2

Experimental data

Electrolyte solution	The electrolysis number	Experimental conditions*									Current efficiency (%)
		Current density (mA/cm^2)	Electrolyte agitation	Additives (p.p.m.)			Electrolysis duration (h)	Electrolyte correction	Change of Cu$^+$ concentr.		
				NaCl	Thiourea	Gelatin			Time after the analysis was effected (h)	Cu$^+$ (g/l)	
Solution I CH$_3$CN= 240 g/l NH$_3$= 18 g/l	1	10	still solution	0	0	0	21		0 21	17.7 30.6	99.1
	2	10	"	"	"	"	24		45	30.1	97.2
	3	10	"	"	"	"	24		69	28.4	93.5
	4	10	"	"	"	"	46		115	22.7	89.7
								Copper powder was added		26.8	
	5	10	"	"	"	"	24		139	22.4	88.2
	6	10	"	"	"	"	22		161	19.6	87.7
	7	10	"	"	"	"	27		188	14.6	88.3
	8	10	"	"	"	"	18		206	11.7	76.3
Solution II CH$_3$CN= 240 g/l	I	4	still solution	30	20	20	50		0 50	18.9 32.8	98.6
NH$_3$=18g/l	II	10	"	30	20	20	24		74	30.9	—
	III	10	magnetic stirring	30	20	20	51		125	22.1	99.5
	IV	15	"	30	20	20	24		148	12.0	82.2
	V	20	"	30	20	20	23		172	9.8	77.4

* Working temperature 27°

Table 2 (continued)

Electrolyte solution	The electrolysis number	Experimental conditions**											Current efficiency (%)
		Current density $\left(\frac{mA}{cm^2}\right)$	Electrolyte agitation	Additives (p.p.m.)			Electrolysis duration (h)	Electrolyte correction	Change of Cu^+, Cu^{2+}, H_2SO_4 concentr.				
				NaCl	Thiourea	Gelatin			Time after the analysis was effected (h)	Cu^+ (g/l)	Cu^{2+} (g/l)	H_2SO_4 (g/l)	
Solution III CH_3CN= 240 g/l NN_3 = 0	VI	10	recirculated	30	5	4	24		0 24	13.3 23.8	14.6 10.9	220.2 198.8	92.8
	VII	15	″	30	50	100	23		47	19.1	15.9	188.8	—
	VIII	10	″	30	50	100	24		71	16.2	25.1	183.8	92.7
	IX	20	″	30	50	100	24		95	13.0	31.6	183.1	—
								Bubbling with SO_2		25.4	16.2	196.0	
Solution IV CH_3CN= 240 g/l NH_3= 19 g/l	X	20	magnetic stirring	30	50	100	19		114	12.7	29.9	178.1	79.8
	XI	10	″	30	5	10	44		0 4	19.4 31.1	9.2 8.2	220.9 199.5	98.1
								H_2SO_4 added		30.5	9.2	219.4	
	XII	15	″	30	20	40	22		66	29.5	13.9	211.0	98.5
	XIII	20	″	30	20	40	24		90	26.4	18.6	207.4	95.4
	XIV	10	″	30	20	40	21	Bubbling with SO_2	111	27.9	9.5	223.0	98.5
								Bubbling with SO_2		36.5	11.3	230.0	
Solution V CH_3CN= 240 g/l NH_3= 19g/l	XV	10	″	30	20	40	22		133	10.8	40.6	213.7	82.3
	XVII	20	″	30	20	40	20		0 20	20.6 33.7	9.2 4.6	203.1 178.1	93.5
	XVIII	20	″	30	20	40	21	H_2SO_4 added	41	34.5	9.8	228.6	94.2
	XX	25	″	30	20	40	22		63	28.3	13.7	219.8	91.6
	XXI	15	″	30	20	40	46	H_2SO_4 added	109	27.9	22.6	240.7	96.0
	XXII	10	″	30	20	40	25		134	9.8	32.7	229.0	91.1

** All the electrolyses were effected at 27° except electrolysis XIV (37°) and electrolysis XV (47°).

Further electrolysis caused the concentration of Cu^+ to fall gradually although copper powder was still present in the electrolysis vessel. At Cu^+ ion concentrations below 11.7 g/l electrolysis ceased due to anodic polarization.

b) *Bubbling of SO_2 in the electrolyte* triggers the reduction reaction :

$$2\,CuSO_4 + SO_2 + 2\,H_2O \rightleftharpoons Cu_2SO_4 + 2\,H_2SO_4 \tag{7}$$

Applied to solutions III–V, SO_2 bubbling ensured an increase of cuprous ions concentration simultaneously with the decrease of the concentration of cupric ions.

c) *Correction of sulphuric acid concentration in the electrolyte* influences favourably the maintenance of cuprous ions concentration (solutions IV, V).

B) Electrolytic refining in cuprous sulphate electrolyte

In our experiments on electrolytic refining of copper the influence of the following parameters was studied : the concentration of cuprous ions, the current density, the stirring of the electrolyte, the additives and the electrolyte temperature.

The influence of cuprous ions concentration was studied in runs 1–8 with solution I at the same current density and temperature, without stirring and aditives. The results are listed in Table 2. One can notice that for Cu^+ ion concentrations higher than 30 g/l the current efficiency is 99% and remains above 90% even at lower Cu^+ ion concentrations.

Although an excess of copper powder was ensured in the electrolyte to reduce Cu^{2+} to Cu^+, the concentration of Cu^+ continued to decrease slowly during electrolyses 5–8 which resulted in a decreased current efficiency. A marked decrease in Cu^+ ion concentration triggers the anodic polarization and the current ceases to flow.

Figure 1 shows the dependence of the current efficiency on the concentration of cuprous ions.

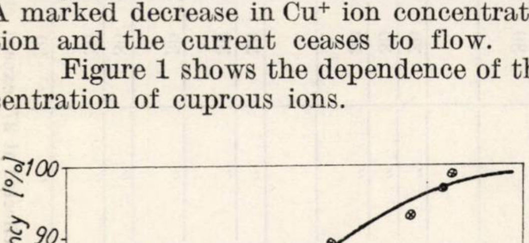

Fig. 1. — Current efficiency *vs* concentration of cuprous ions.

Our data show that in order to obtain high current efficiency electrolytes with Cu^+ ion concentrations higher than 20 g/l must be employed. The decrease of Cu^+ ion concentration requires the correction of the electrolyte compositions in order to transform cupric into cuprous ions.

The effect of agitation was studied in electrolyses I—X with solution II making use of a magnetic stirrer and a peristaltic pump. The electrolyte recirculation rate was 0.8 ml/minute. The electrolyses were conducted at the same temperature and current density, with natrium chloride, thiourea and gelatin as additives. The experiments showed that a relatively strong magnetic stirring yields uniform and compact deposits; in absence of stirring or with slowly recirculated electrolytes, the cathodic deposit was uneven, getting thicker at the bottom and sides where dendrite growth was manifest. All subsequent investigations were conducted under magnetic stirring.

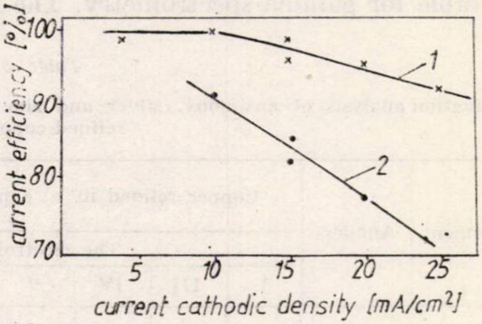

Fig. 2. — Current efficiency *vs* cathodic current density: 1. $[Cu^+] > 20$ g/l; 2. $[Cu^+] < 20$ g/l.

The influence of additives was studied in electrolyses III, VI, VIII and IX, conducted at a current density of 10 mA/cm², under stirring. The overall effect of additives employed (NaCl, thiourea and gelatin in variable amounts), was the improvement of the granulation and uniformity of the copper deposit whose aspect was vermicular. No significant difference could be noted in the aspect of the deposits obtained in the range of additives concentration employed in our experiments (Table 2).

The influence of current density. The current density in our investigations ranged from 4 to 25 mA/cm². The cuprous ion content of electrolytes covered two ranges of values, namely 20—33 g/l and 10—20 g/l. The results are listed in Table 2, which shows that the current efficiency decreases with the increase of current density; the decrease was stronger in electrolytes whose concentration of cuprous ions was below 20 g/l (Figure 2).

At low current densities the deposits are dense, uniform and of vermicular aspect. At current densities above 20 mA/cm² the vermicular elements are larger while at 25 mA/cm² dendrites grow at the ends of the cathode. Copper deposits of adequate quality were obtained at current densities of 15—20 mA/cm². At these values of the current densities, Brown et al. [5] reported a lower total capital cost for an acetonitrile-based process relative to the conventional electrorefining process, and an energy saving of 30—40%.

The influence of temperature. Electrolyses were conducted at a current density of 10 mA/cm² and temperatures between 27° and 47° (electrolyses III, IV, XV). At 37° the deposit was more uniform and its granulation finer than at lower temperatures, the other conditions being identical. At 47° the deposit was initially uniform, with fine grains, then its adherence became weaker and it was easily detached.

The optimum working temperature ranges from 27° to 37° provided that the electrolyte surface is covered with a kerosene layer.

The purity of cathodic copper was determined by neutron activation followed by gamma-spectrometry. Eight copper samples obtained in various conditions were analysed to determine the content of antimony, silver and zinc. The elements to be determined form radionuclides that are suitable for gamma-spectrometry. The results are given in Table 3.

Table 3

Activation analysis of antimony, silver and zinc content in anodes and in electrolytically refined copper (p.p.m.)

Element	Anodes	Copper refined in a cuprous sulphate electrolyte								Copper refined in a cupric sulphate electrolyte
		The electrolysis number								
		1	III	IV	V	VI	XII	XIII	XIV	
Sb	1700	1.5	2.6	3.0	2.3	1.4	0.9	2.4	1.1	1–6
Ag	1015	2.7	13.2	19.8	10.2	3.8	5.0	20.8	5.7	3–20
Zn	50	2.0	1.5	1.7	2.2	2.4	1.9	1.5	1.9	1–6

Examination of data in Table 3 shows that the impurities concentration in the refined copper obtained in our experiments is comparable to that in the copper refined with cupric electrolytes.

REFERENCES

[1] A. J. Parker, *Search*, **4**, 426 (1973).
[2] J. W. Diggle, A. J. Parker and J. Arevaamides, *Austral. J. Chem.*, **27**, 721 (1974).
[3] F. F. Farha and R. I. Iwamoto, *J. Electroanalyt. Chem.*, **8**, 55 (1964).
[4] D. M. Muir, A. J. Parker, J. A. Sharp and W. E. Waghorne, *Hydrometallurgy*, **1**, 61 (1975).
[5] A. P. Brown, R. O. Loutfy, G. M. Cook and N. P. Yao, *J. Metals*, **1981**, 49.

Revue Roumaine de Chimie, **29**, *5*, 415–421 (1984)

STUDIES ON AQUEOUS ELECTROLYTES AND NONELECTROLYTES. II[1]

EFFECTS OF ELECTROLYTES ON ULTRASONIC VELOCITY, ADIABATIC COMPRESSIBILITY AND STRUCTURE OF AQUEOUS SOLUTIONS OF POLYVINYL ALCOHOL (PVA)

MONIMUL HUQUE* and D. SĂNDULESCU**
Department of Engineering, Dakka, University, Dakka, Bangladesh
Department of Chemistry, Institute of Petroleum and Gas,
Blvd. București, No. 39, 2000 — Ploiești, Romania

Received December 6, 1982

In our previous work [1], data presented referred to the study of viscosity of aqueous solutions of PVA and electrolytes verifying the Jones-Dole equation and interpreting the values of coefficient '*B*'. In the present study the results obtained on the study of Ultrasonic velocity and its corresponding properties at different temperature, concentration of PVA and electrolytes have been presented. The results were interpreted through the effect on forming structure of solution.

In the last few years solutions of nonelectrolytes were studied with different views through different methods : heat capacity,[2–6] partial molar volume, [7,8] ultrasonic velocity, [9–11] coefficient of adiabatic compressibility[12,13] and temperature corresponding to the maximum velocity of sound .[15] These results show the theoretical importance of the obtained results to interprete the properties and structure of solutions.

In other works, the thermodynamic properties of the solution of electrolytes were studied by a good number of scientists keeping the views to the classification of nature and intensity of interactions in aqueous and nonaqueous solutions. [15,16]

In general, besides the usual methods of research in electrochemistry, these studies were limited to the density of aqueous solutions and the methods based on ultrasonic velocity, which permits the calculation of adiabatic compressibility, were not used. With the exception of a few limited research on the electrolyte-water solution, in general data referred to the effect of nonelectrolytes are not known. [17]

In this study experimental data with reference to ultrasonic velocity of aqueous solutions of NaCl and KCl in the presence of PVA have been presented. This study is a continuation of the study of these types of solutions by the viscometric method, [1,18,19] which permits to obtain, within certain limits, informations on interactions of different ions, Na^+ and K^+, in an aqueous solution of PVA.

EXPERIMENTAL SECTIONS

The solutions under study were made with redistilled water. The solutions were prepared at the required concentrations by the method followed in our previous study.[1,19] The density and the content of polymer (PVA) in solution were determined by the methods discussed in our earlier work.[19] Ultrasonic velocity in pure solvent and in solutions was determined by using a VI—31 type interferometer, made by the Polish Scientific Academy, the details of which were dicussed in our previous study.[19] The temperature of the solution was maintained constant by using an ultrathermostat with a digital thermometer.

RESULTS

The experimentally determined values of ultrasonic velocity through aqueous solutions of PVA in the presence of electrolytes (NaCl and KCl) at different concentrations of PVA and electrolytes are presented in Fig. 1. An examination of the data presented in figure 1 indicates that the velocity of propagation of the sound wave for a solution with NaCl is higher than that for a solution with KCl. The velocity of propagation increases with the increase of the concentration of electrolytes as well as with the rise of temperature (20°—40°C). It is observed that the addition of PVA into the solution modifies and complicates the change of propagation velocity as a function of electrolytes concentration. In addition to the usual tendency of increasing the velocity of propagation with the concentration of electrolytes even in the presence of PVA, the velocity of propagation of sound for a solution of 0—0.5 % PVA is smaller than that for an aqueous solution of electrolytes, but for a solution of higher concentration of PVA (1% PVA) the velocity of propagation of sound exceeds the value for the solution of electrolytes in pure water. These results are due to at least two simultaneous effects which appear in the presence of PVA as discussed below.

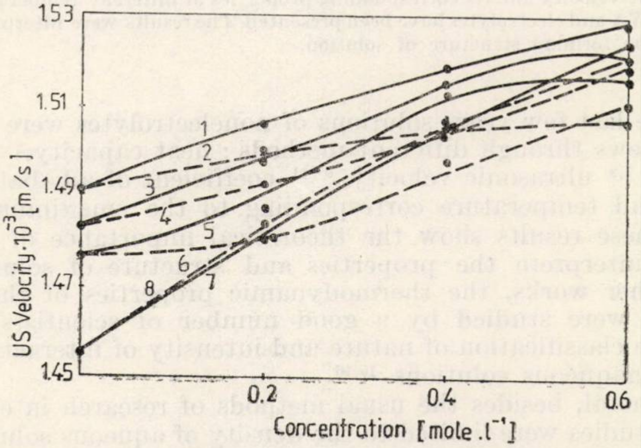

Fig. 1. — Variation of ultrasonic velocity with concentration of electrolytes at different concentrations of electrolytes, at different concentrations of PVA and at 20°C : 1, 3, 5, 7 for NaCl; 2, 4, 6, 8, for KCl; 1, 2 for 1.014% PVA; 3, 4 for 0.507% PVA; 5, 6 for 0.25% PVA; 7, 8 for 0% PVA.

Diagram u vs M_η (sound velocity vs molecular weight of PVA) at different temperatures leads us to a conclusion that at 20°C the effect of polymer molecular weight is relatively significant. The velocity of propagation decreases with the increase of PVA molecular weight. At a higher temperature (30°C), the effect of molecular weight has little importance and at 40°C the velocity of propagation is practically independent of the molecular weight. The velocity of propagation increases with the concentration of PVA for the solutions of both electrolytes (NaCl and KCl), keeping the order of increasing from KCl to NaCl. In general it is observed that in the case of PVA solution at higher concentration the effect of KCl on increasing the velocity of propagation becomes more important in comparison to that of NaCl.

DISCUSSION

According to the Newton — Laplace theory, the sound wave propagation is related to the density and adiabatic compressibility of the liquid, which can be represented mathematically by

$$K_s = -\left(\frac{\partial \ln V}{\partial \rho}\right)_s = \frac{1}{u^2 \rho}$$

where u is the velocity, v is the molar volume, ρ the density and s the entropy. The calculated values of K_s from the experimentally determined values of u and ρ, at different concentrations of PVA and electrolytes, are presented in Fig. 2. It is observed from the figure that the values of K_s decrease with the increase of concentration of electrolytes and temperature. This result is analogous with the result obtained by F. Gucker, D. Stubley, and D. Hill.[17] It is also observed that the change of K_s is almost similar for both electrolytes, but the value of K_s for a solution with KCl is always higher than that for a solution with NaCl, which can be explained by the formation of an intensive structure by Na^+. Sodium ion has the possibility to participate in the formation of H_2O—PVA linkages unlike KCl, i.e. K^+, chloride ion being the common ion for both the electrolytes.

A careful examination of the data presented in Fig. 2 shows that the addition of PVA in water has an effect of decreasing adiabatic compressibility. This effect is amplified by the addition of KCl and more by the addition of NaCl.

Increasing temperature has the effect of decreasing adiabatic compressibility, i.e. $\frac{\partial K_s}{\partial T}$ is negative. At the same time it annihilates the relative effects of electrolytes and of polymer (PVA).[19] The effect of decreasing K_s with temperature is maximum (absolute value) for pure water. This effect decreases with the decrease of the molecular weight of polymer (PVA). It is also observed that the effect of increasing K_s with the increase of the molecular weight of the polymer under study is significant at 20°C. At 30°C the effect of PVA molecular weight is relatively small and at 40°C the coefficient of adiabatic compressibility (K_s) is practically independent of the PVA molecular weight.

The interpretation of these results is not possible even qualitatively only by the formation or by the destruction of structure, appearing simultaneously by the modification of water structure, respectively the position of water molecules around the ions and also around the polymer chains. This part of conclusions can also be found in the work of other author.[20]

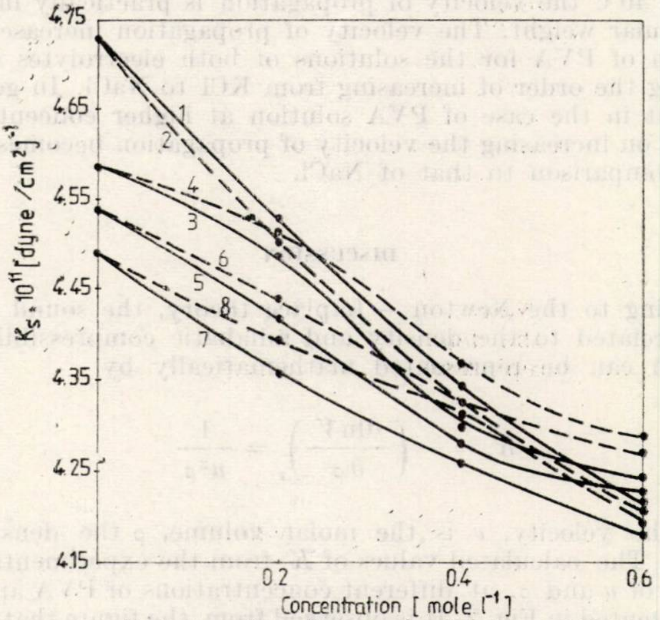

Fig. 2. — Variation of coefficient of adiabatic compressibility (K_s) with the concentration of electrolytes at different concentrations of PVA and at 20°C : 1, 3, 5, 7 for NACl; 2, 4, 6, 8 for KCl; 1, 2 for 0% PVA; 3, 4 for 0.25% PVA; 5, 6 for 0.507% PVA; 7, 8 for 1.0142% PVA.

It is well known that the velocity of propagation of sound wave depends upon the density and adiabatic compressibility of the medium. The interpretation of the experimentally determined values of velocity of sound wave propagation and respectively the K_s values of solutions under study can be evidently made by a known theory of Eyring.[21] According to the Eyring theory, in liquid medium sound wave propagates with an infinite velocity in molecules and with a velocity of kinetic theory of gases in intermolecular spaces, which leads to a conclusion indicating that the more compact structure has the effect of increasing velocity of propagation. Similarly it is understood that within certain limits, the increase of temperature leads to the breaking of hydrogen bonds, consequently decreases the intermolecular distances, and enhances the velocity of sound wave propagation. Beyond that limit of temperature the effect seems to increase the intermolecular distances and respectively, decreases the velocity of propagation. On the other hand, it can be said that the maximum density does not correspond to the maximum velocity of propagation because both properties represent a complicated function of temperature which is not completely known in case of water.

It is understood that the velocity of propagation increases with the increase of the concentration of electrolytes (NaCl and KCl), the increasing effect being higher in the case of NaCl. The velocity of propagation of sound wave also increases with the concentration of polymer (PVA). In this small range of molecular weight of the polymer under study the effect of molecular weight on the velocity of propagation of sound wave is relatively small. Similarly the variation of K_s is higher in the case of KCl and the values of K_s decrease with the increase of concentration and molecular weight of polymer (PVA).

Information on the electrolytes-water-polymer interactions have been obtained through the calculation of coefficients of partial molar adiabatic compressibility for electrolytes by using the equation

$$K_{s\varphi} = \frac{K_s - K_{s,0}}{C} + K_{s,0}\varphi$$

in which K_s, $K_{s,0}$ are the coefficients of adiabatic compressibility of water or aqueous solution of PVA with electrolytes and without electrolytes, respectively, φ is the partial molar volume of electrolytes in solution and C is the concentration of electrolytes.

Coefficients of apparent specific compressibility for polymer were calculated by using the equation

$$K_{s\varphi} = \frac{K_s - K_{s,0}}{W_2 \rho} + K_{s,0}\varphi$$

where K_s and $K_{s,0}$ are the coefficients of water compressibility or of an aqueous solution of electrolytes with PVA and without PVA respectively, W_2 is the weight fraction of the polymer in solution, ρ is the density and φ the partial specific volume of polymer in solution.

The values of $K_{s\varphi}$ for electrolytes are found to be negative. The smaller value for NaCl is analogous with the results obtained in a study on the solutions of electrolytes in pure water. [17] The value of $K_{s\varphi}$ for electrolytes decreases with the increase of polymer concentration and temperature but the effects of polymer become gradually smaller as shown in figure 3. The variation of the molecular weight of the polymer under study does not produce any significant effect on $K_{s\varphi}$ for electrolytes.

The coefficient of apparent specific adiabatic compressibility for polymer increases from a negative value to a positive one with the rise of temperature, the effect of which being greater in the case of KCl (Fig. 4). The increasing effect with the increasing concentration of electrolytes is decreased with the rise of temperature, which is in agreement with the the results observed in a previous work. [22] No significant difference is observed with the change of molecular weight of the polymer under study.

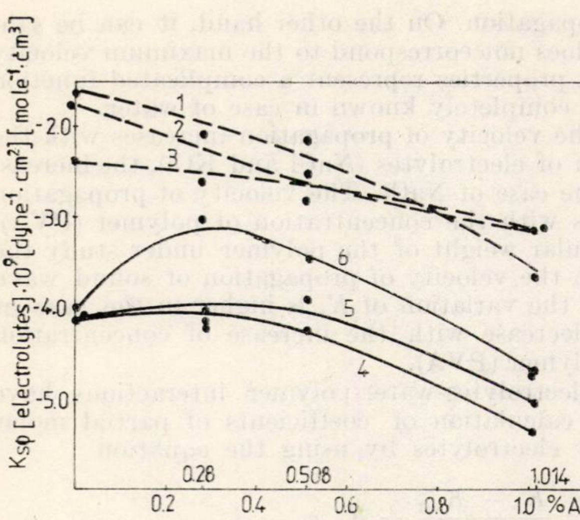

Fig. 3. — Variation of $K_{s\varphi}$ for electrolytes with a concentration of PVA at different concentrations of electrolytes and at 20°C : 1, 2, 3 for KCl ; 4, 5, 6 for NaCl ; 1, 4 for 0.2 mol. l^{-1} ; 2, 5 for 0.4 mole. l^{-1} ; 3, 6 for 0.6 mol. l^{-1}.

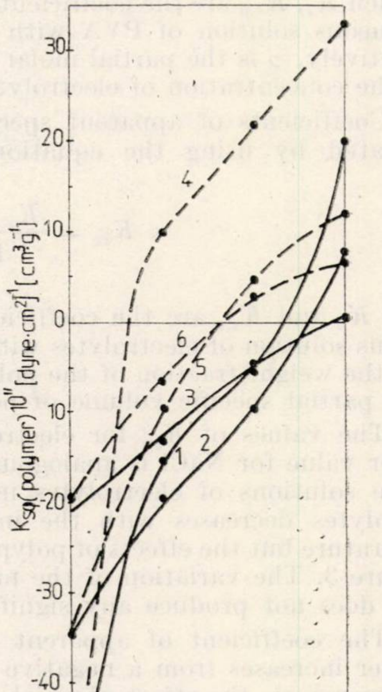

Fig. 4. Variation of $K_{s\varphi}$ for polymer with concentration of electrolytes at different concentrations of PVA and at 20°C : 1, 2, 3 for NaCl ; 4, 5, 6 for KCl ; 1, 4 for 0.25% PVA ; 2,5 for 0.507% PVA ; 3, 6 for 1.0142% PVA.

CONCLUSION

The study of sound wave propagation velocity in aqueous solutions of NaCl, KCl and polyvinyl alcohol has shown that the velocity increases with the increase of concentration of electrolytes and temperature. The effect of polymer on the propagation velocity of sound wave is complicated. It is found that the value for a solution having a concentration up to 1 % PVA is smaller than that for a solution of electrolytes in pure water. Solutions having concentrations of 1 % PVA or more have higher values than solutions of electrolytes in water.

The coefficient of adiabatic compressibility decreases with the rise of temperature and also with the increase of electrolytes concentration. The values are higher in the case of KCl. The coefficients of partial molar adiabatic compressibilities for electrolytes are found negative. The coefficient value of apparent specific adiabatic compressibility for polymer increases from a negative to a positive value with the increase of temperature. The increase of temperature annihilates the relative effect of polymer and electrolytes and also the effect of polymer molecular weight.

Data were interpreted with the help of the Eyring theory. Compact structure leads to an increase of sound wave propagation velocity.

REFERENCES

[1] Part. I. Monimul Huque and D. Săndulescu, *Rev. Roumaine Chim.* **29**, 1(1984).
[2] L. Stavely, K. Hart and W. Tupman, *Discuss. Faraday Soc.*, **15**, 130 (1953).
[3] A. Arnand, L. Avalikian and J. Morel, *J. Chem. Phys.*, **69**, 45 (1972).
[4] M. Murthy and S. Subrahmanyam, *Indian J. Pure Appl. Phys.*, **15**, 485 (1977).
[5] E. Arnett, W. Kover and J. Carter, *J. Amer. Chem. Soc.*, **91**, 4028 (1969).
[6] M. Murthy and S. Subrahmanyam, *Indian J. Chem.*, **A**, **16**, 558 (1978).
[7] V. Griffiths, *J. Chem. Soc.*, **1952**, 860.
[8] G. Malcom and J. Robinson, *Trans. Faraday Soc.*, **53**, 921 (1957).
[9] E. Baumgrtner and G. Artkinson, *J. Phys. Chem.*, **75**, 2337 (1971).
[10] H. Endo and O. Nomoto, *Bull. Chem. Soc. Japan.*, **46**, 3004 (1973).
[11] M. Blandamer, D. Carke, N. Hidden and N. Symons, *Chem. Com.*, 342 (1968).
[12] M. Murthy and S. Subrahmanyam, *J. Sol. Chem.*, **4**, 347 (1975).
[13] M. Murthy and S. Subrahmanyam, *Canad. J. Chem.*, **56**, 2412 (1978).
[14] M. Murthy and S. Subrahmanyam, *J. Acoust. Soc. Indian*, **5**, 88 (1977).
[15] R. Harney, "Water and Aqueous Solutions", Wiley, New York, 1972.
[16] F. Franks, "Water, A Comprehensive Treatise", Plenum Press, New York, 1973.
[17] F. Gucker, D. Stubley, and D. Hill, *J. Chem. Thermodynamics*, 7, 865 (1975).
[18] C. Holszky, C. Suciu and D. Săndulescu, *Rev. Roumaine Chim.*, **19**, 5 (1975).
[19] Monimul Huque, Ph. D. Thesis, Institutul de petrol și gaze, Ploiești, 1982.
[20] B. Jacobson, *Arkiv. Kemi.*, **2**, 177 (1950).
[21] H. Eyring and J. Kincoid, *J. Chem. Phys.*, **5**, 587 (1927); **6**, 626 (1938).
[22] J. Mathieson and B. Conway, *J. Soln. Chem.*, **3**, 455 (1974).

Revue Roumaine de Chimie, **29**, 5, 423—428 (1984)

EXO- AND ENDOHORMONES. VIII[1]

METHOXYALLENE IN PHEROMONE SYNTHESIS

ALEXANDRA GOCAN, ANA AURELIA BOTAR, A. BARABÂS, I. OPREAN,
N. ŞERBAN and F. HODOŞAN

Institute of Chemistry, 3400 Cluj-Napoca, Str. Fîntînele 30

Received January 27, 1983

A new approach to butterfly sex pheromone synthesis involving methoxyallene was developed and its preparative value investigated. As application examples 8-nonyn-1-ol ethers (V) were prepared and converted into the pheromone blend components *Z*—IXA, *E*—IXA and *Z*—IXB, respectively.

INTRODUCTION

The preparation of butterfly sex attractants *via* the coupling reactions with Grignard reagents represents a very suitable synthetic technique. It has the advantage that one can start with synthons already possessing the double bonds of desired configuration [2] or/and other pre-existing structural details. Recent improvements — *e.g.* utilization of Li_2CuCl_4 as cross-coupling catalyst [3] as well as that of tosyloxy derivatives [4] or allylic acetates [3] as coupling partners — stimulated the interest of pheromone chemists in this principle of synthesis. As examples we wish to mention two preparations starting with the same readily available protected bromo-alcohol $Br(CH_2)_6OR$ which by coupling *via* the corresponding Grignard compound, with *E*-2,*E*-4-hexadien-1-ol acetate or *E*-3-hexen-1-ol tosylate afforded the sex pheromones of the lepidopterous pests *Laspeyresia* [5-7] *pomonella* and *Rhyacionia buoliana* [8], respectively.

It is obvious that the scope of this synthetic method can be widened by employing new readily accessible and reactive synthons. Methoxyallene (I) fulfils these requirements owing, on the one hand to the easiness with which it can be prepared from methyl propargyl ether (II) [9] and, on the other hand, to its ability to react with Grignard reagents in the presence of copper(I) halides to give 1-alkynes in good yields. [10]

$$\underset{\text{II}}{HC\equiv C-CH_2OCH_3} \rightarrow \underset{\text{I}}{H_2C=C=CHOCH_3} \xrightarrow[\text{Cu(Cl, Br, I)}]{\text{RMgX}} R-CH_2-C\equiv CH$$

This chemical behaviour of methoxyallene (I) prompted us to develop a new approach to butterfly sex pheromone synthesis[11] which can be outlined as follows:

$$\underset{\mathrm{III}}{R^1O-(CH_2)_n-Hal} \xrightarrow{Mg} \underset{\mathrm{IV}}{R^1O-(CH_2)_n-MgHal} \xrightarrow{+H_2C=C=CHOCH_3\ (I)}$$

$$\underset{\mathrm{V}}{R^1O-(CH_2)_{n+1}-C\equiv CH} \rightarrow \underset{\mathrm{VI}}{R^1O-(CH_2)_{n+1}-C\equiv CM} \xrightarrow[-MY]{+YR^2}$$

$$\underset{\mathrm{VII}}{R^1O-(CH_2)_{n+1}-C\equiv C-R^2} \rightarrow \underset{\mathrm{VIII}}{AcO-(CH_2)_{n+1}-C\equiv C-R^2} \xrightarrow{+H_2}$$

$$\underset{\mathrm{IX}}{AcO-(CH_2)_{n+1}-CH=CH-R^2}$$

In order to demonstrate the preparative value of this route attempts were made to synthetize some 8-nonyn-1-ol ethers (V, $n=6$) and to convert them into three pheromones of the general formula IX ($n=6$). The other structural characteristics of these compounds, as well as those of their precursors, were the following:

a. $R^1 = Si(CH_3)_3$ A. $R^2 = C_3H_7$

b. $R^1 = C(CH_3)_3$ B. $R^2 = C_5H_{11}$

c. $R^1 = H$

The results of these investigations are reported in this paper.

RESULTS AND DISCUSSION

We started with $Br(CH_2)_6OH$ (IIIc) which was easily prepared from hexane-1,6-diol by continuous extraction method with HBr and petroleum ether.[12] The hydroxyl group protection to give IIIa or IIIb was carried out employing as reagents trimethylchlorosilane and iso-butylene, respectively. The corresponding Grignard compounds IVa and IVb (Hal = Br) reacted readily with methoxyallene (I), under the conditions reported by Meijer and Vermeer,[10] affording the terminal alkynes Va and Vb, respectively, in moderate yields of 50–60%.

The alkynol ethers Va and Vb could be alkylated following one of the known methods, *e.g.* metallation with lithium in liquid ammonia to give VI (M = Li) and subsequent treatment with an appropriate alkyl bromide (Y = Br) in the same reaction medium.[13]

Little attention has been paid so far to an alternative alkylation procedure, namely the action of alkyl tosylates on alkynyl Grignard compounds such as VI (M = MgBr).[14] We were tempted to explore also this route. Thus, employing *n*-propyl tosylate and starting with Va we obtained the disubstituted acetylenic compound VIIaA. In order to remove the excess reagent a saponification of the crude reaction product was carried out. During the work-up cleavage of the trimethylsilyl group occurred leading to a mixture of 8-dodecyn-1-ol (VIIcA) and 8-nonyn-l-ol (Vc) in a ratio of about 3 :2, the latter resulting from the unreacted Va. Removal of Vc by distillation afforded a sufficiently pure sample of VIIcA in a rather poor yield of about 30% (from Va). Acetylation of VIIcA with acetic anhydride in pyridine gave the acetate VIIIA.

When started with the *t*-butyl ether Vb, the saponification of the crude reaction product left the protecting group unaltered yielding a mixture of VIIbA and unreacted Vb in a similar ratio as in the previous case of about 3 :2. In contrast to the already mentioned hydroxy compounds (VIIcA and Vc) these ethers cannot be separated by distillation. Hence conversion of this mixture into that of the parent alcohols VIIcA and Vc, followed by separation as mentioned above, was necessary. We report here a roundabout way, *via* the direct acetylation and subsequent saponification of the resulted acetates.* A better result could be obtained by re-alkylation of the crude reaction product (VIIbA + Vb). This treatment augmented the ratio of the desired end poroduct up to 9 :1. After removal of the excess *n*-propyl tosylate by saponification and subsequent acetylation 8-dodecyn-l-ol acetate (VIIIA) could be readily isolated by vacuum distillation. This rather tedious way gave a satisfactory yield of about 70% from Vb.

When the alkylation reaction was carried out using *n*-pentyl tosylate a re-alkylation was superfluous due to the relatively high percentage of the resulted compound VIIbB in the crude reaction product. After removal of the excess alkylating reagent and subsequent acetylation the pure acetate VIIIb could be isolated by vacuum distillation. Unfortunately this purification was accompanied by an important loss of material thus sensibly lowering the overall yield (about 30% from Vb).

The hydrogenation of VIIIA and VIIIB to the geometrically pure *Z*-8-dodecen-l-ol acetate (*Z*-IXA) and *Z*-8-tetradecen-l-ol acetate (Z-IXB), respectively, was carried out employing Ni P-2 catalyst poisoned with ethylenediamine. The advantages of this highly stereoselective method, permitting conversions in yields of at least 90%, were already emphasized.[15]

In contrast to our previous observation[15] $LiAlH_4$ in diglyme[16] was found to be a suitable reagent to convert VIIcA into *E*-IXA (yield 75%).

The compounds *Z*-IXA, *Z*-IXB and *E*-IXA are components of pheromone blends released by females of some lepidopterous pests such as *Grapholitha funebrana* (*Z*-IXA + *E*-IXA)[17], *Grapholitha molesta* (*Z*-IXA + *E*-IXA)[18], *Pamene* spp. (*Z*-IXA)[19], *Spilonota ocellana* (*Z*-IXB)[20]. These compounds were found to be highly active in field experiments whose results will be published elsewhere.

---

* Conversion of t-butyl ethers directly into the corresponding alcohols is also feasible under certain conditions.

EXPERIMENTAL PART

Mass spectra were recorded on a Varian MAT SN-1 spectrometer at 70 eV and a source temperature of 210°, coupled to a Perkin-Elmer 990 gas-chromatograph. NMR-spectra were recorded on a Bruker WP-60 FT-NMR instrument equipped with a 14.1 kG electromagnet (60 MHz for ^{1}H, 15.086 MHz for ^{13}C); samples were dissolved in $CDCl_3$ and chemical shifts are related to internal TMS. Glc-analyses were performed on a Perkin-Elmer F 11 instrument.

6-Bromo-hexan-1-ol trimethylsilyl ether (IIIa): Trough a chilled solution of 6-bromo-hexan-1-ol (36.2 g, 200 mmoles) and 32.1 g (300 mmoles) of trimethylchlorosilane in 175 ml of dry benzene a stream of dry ammonia was passed for 2 hours at a rate of 100 ml/minute. The end of the reaction was checked by tlc on silica gel G. The resulted ammonium chloride was filtered and washed with three portions of 60 ml of benzene. From the combined filtrates the solvent was removed *in vacuo* at 15 mm and 40° (bath temperature) and the resulted crude trimethylsilyl ether IIIa distilled. The fraction boiling at 67—69° 2—3 mm or 92—95°/5 mm consisted of pure end product (purity 92—95%). Yield: 80—83%. $n^{18} = 1.4500$; IR (CCl_4): 760, 870, 895, 1120, 1270 cm^{-1} ($C-O-Si(CH_3)_3$).

6-Bromo-hexan-1-ol t-butyl ether (IIIb): It was prepared according to the general procedure reported previously.[15] Bp. 60—64°/1 mm or 78—80°/3—4 mm; $n^{19} = 1.4540$; ^{1}H-NMR (δ ppm); 1.16 (s, 9H, $-O-C(CH_3)_3$), 3.36 (t, 2H, J = 6 Hz, $-CH_2-O-$), 3.43 (t, 2H J = 6.6 Hz, $-CH_2-Br$); ^{13}C-NMR (carbon no. δ ppm): 1′/72.5, 2′/27.9, 1/61.5, 2/30.9, 3/28.4 4/33.3, 5/25.8, 6/34.1; ms (m/e): 223/221 $(M-CH_3)^+$, 165/163 $(Br-(CH_2)_6)^+$, 123/121 $(Br-(CH_2)_3^+$, 57 $(C(CH_3)_3)^+$.

8-Nonyn-1-ol trimethylsilyl ether (Va): A solution of Grignard compound in 370 ml of dry ethyl ether was prepared in the usual manner from 103 g (407 mmoles) of IIIa and 10 g (411 mmoles) of magnesium. The solution was cooled to the room temperature and 4 g (40 mmoles) of Cu_2Cl_2 were added. Thereafter a solution of 26 g (371 mmoles) of methoxyallene (I)[9] in 370 ml of dry ethyl ether was added dropwise under external ice cooling within 20—30 minutes. The reaction was brought to completion by stirring for 30 min. at room temperature. A solution of 74 g of ammonium chloride in 740 ml of water was then added dropwise under good external ice cooling. All operations were performed in an inert gas atmosphere and under vigorous stirring. The organic layer was separated and the aqueous one extracted with three portions of 100 ml ether. The combined ethereal solutions were washed with water and dried over $MgSO_4$. After removal of the solvent the residue was distilled at 2—3 mm using a short Vigreux column. The fraction collected at 70—71° contained the end product Va of 90—92% purity (glc). Yield: 43.5 g (50% from IIIa). $n^{20} = 1.4340$; IR (film): 3300 ($\equiv C-H$), 2160 ($C\equiv C$), 760, 870, 895, 1120, 1270 cm^{-1} ($C-O-Si-(CH_3)_3$); ^{1}H-NMR (δ ppm): 0.11 (s, 9H, $-Si(CH_3)_3$), 1.40 (s, 12H, $-(CH_2)_6-$), 1.92 (t, 1H, J = 2 Hz, $HC\equiv C-CH_2-$), 3.63 (t, 2H, J = 6 Hz, $-O-CH_2-$); ms (m/e): 197 $(M-CH_3)^+$, 103 $(CH_2=O-Si(CH_3)_3)^+$, 89 $(O-Si(CH_3)_3)^+$, 75 $(HO=Si(CH_3)_2)^+$, 73 $(Si(CH_3)_3)^+$.

8-Nonyn-1-ol t-butyl ether (Vb): The preparation was performed under the conditions used for Va. The Grignard compound solution in 500 ml of dry ethyl ether was prepared from 130.5 g (550 mmoles) of IIIb, 13.2 g (550 mmoles) of magnesium, 4.95 g (50 mmoles) of Cu_2Cl_2 and coupled with 35 g (500 mmoles) of methoxyallene (I). The pure end product Vb (95%) was obtained in a yield of 60 g (60% from IIIb). The purification was carried out by distillation at 75—80°/2 mm. $n^{17} = 1.4386$; IR (film): 3300 ($\equiv C-H$), 2160 ($C\equiv C$), 895, 1110, 1220 ($C-O-C(CH_3)_3$), ^{13}C-NMR (carbon no. δ ppm): 1′/72.5, 2′/27.6, 1/61.6, 2/30.6, 3/28.5, 4/26.2, 5/29.1, 6/28,8, 7/18.4, 8/84.0, 9/68.3; ms (m/e): 181 $(M-CH_3)^+$, 140 $(M-CH_2=C(CH_3)_2)^+$, 123 $(M-CO(CH_3)_3)^+$, 57 $(C(CH_3)_3)^+$.

8-Dodecyn-1-ol (VIIcA): 1) From Va: A solution of ethylmagnesium bromide in 150 ml of dry ethyl ether was prepared in the usual manner from 35 g (350 mmoles) of ethyl bromide and 8.5 (350 mmoles) of magnesium. A solution of 57 g (268 mmoles) of Va was then added. After the ethane evolution had subsided the boiling was continued for 2 hours. A solution of 150 g (701 mmoles) of *n*-propyl tosylate in 250 ml of dry ether was dropwise added within 2 hours, and refluxing continued for 8 hours. All operations were carried out in an inert gas atmosphere and under vigorous stirring. After cooling the resulted magnesium tosylate was removed by filtration. The solvent was removed by distillation and the residue refluxed for 4 hours under stirring with 500 ml of methanol containing 6% KOH. After cooling the resulted potassium tosylate was removed by filtration, the filtrate concentrated *in vacuo*, and the residue diluted with ether. The ethereal solution was washed successively with a saturated NaCl solution, dil. HCl, water, and finally dried over $MgSO_4$. The solvent was removed and the residue distilled at 2—3 mm using a short Vigreux column and rising the temperature gradually until the temperature at the column head attained 120° and the $\equiv C-H$ streching vibration band (3300 cm^{-1}) disappeared from the IR spectrum of the residue. In this way a complete removal of the more volatile Vc (resulted from the unreacted Va) could be performed. In the distillation flask remained the fairly pure compound VIIcA (purity 90—92 %). Yield : 14.7 g (30 %).

2) From Vb : The alkylation was performed as described above, using 280 mmoles of ethylmagnesium bromide (from 30.8 g of ethyl bromide and 6.8 g of magnesium) in 150 ml of dry ethyl ether, 55 g (280 mmoles) of Vb in 150 ml of dry ether, and 127 g (600 mmoles) of *n*-propyl tosylate in 300 ml of dry ether. The resulted mixture (VIIbA and unreacted Vb) was refluxed for 5 hours with 100 ml of acetic anhydride containing 1 ml of conc. sulfuric acid. After cooling the solution was poured onto ice and extracted with four portions of 100 ml of ether. The combined extracts were washed successively with aqueous Na_2CO_3, sat. NaCl solution, and dried over $MgSO_4$. The solvent was removed and the residue refluxed for 4 hours with 100 ml methanol containing 5% KOH. The solution was poured into a sat. NaCl solution, extracted with four portions of 75 ml of ether, the combined extracts washed with sat. NaCl solution and dried over $MgSO_4$. The solvent was removed and the resulted residue (mixture of VIIcA and Vc) purified as described above. The end product VIIcA of satisfactory purity (90—95 %) was thus obtained in a yield of 15 g (30 %), IR (CCl_4) : 3620 (OH) (no$\equiv$C—H stretching band was observable) ; ms (m/e) : 135 $(M - H_2O - C_2H_5)^+$.

8-Dodecyn-1-ol acetate (*VIIIA*) : 1) From Vb : The mixture of VIIbA and unreacted Vb, resulted from 105 g (536 mmoles) of Vb under the conditions described for the preparation of VIIcA, was re-alkylated. In the first alkylation reaction 53 ml (700 mmoles) of ethyl bromide, 17 g (700 mmoles) of magnesium and 300 g (1.4 moles) of *n*-propyl tosylate were used. Half of these amounts was used in the second alkylation. The crude reaction product (120 g) contained 70—75% VIIbA and less than 5% Vb. After acetylation by refluxing for $4\frac{1}{2}$ hours with 75 ml acetic anhydride and 1 ml conc. sulfuric acid and processing in the usual manner the crude reaction product was distilled *in vacuo* and the fraction passing at 118—120°/4—5 mm collected. The end product VIIIA (purity 89—91 %) was thus obtained in a yield of 88 g (73 %). n^{20}= 1.4493 ; IR (CCl_4) : 1060, 1250, 1740 cm^{-1} (C—O—$COCH_3$) (no$\equiv$C—H stretching band was observable) ; ^{1}H—NMR (δ ppm) ; 1.00 (t, 3H, J = 7 Hz, CH_3—CH_2—), 2.08 (s, 3H, —OCO—CH_3), 4.13 (t, 2H, J = 6.3 Hz, —O—CH_2—) ; ^{13}C—NMR (carbon no. δ/ppm) : 1'/171.3, 2'/21.0, 1/64.2, 2/29.0, 3/26.2, 4/29,0, 5/29.2, 6/29.5, 7/18.9, 8,9/79.8, 10/21.0, 11/22.9, 12/13.6 ; ms (m/e) ; 164 $(M - CH_3COOH)^+$, 61 $(CH_3COOH_2)^+$.

2) From the hydroxy compound VIIcA by acetylation with acetic anhydride in pyridine in the usual manner. The resulted end product exhibited the same analytical values as that obtained following the procedure described above.

8-Tetradecyn-1-ol acetate (*VIIIB*) : The procedure was similar to that used in the preparation of VIIcA. A re-alkylation as described for the preparation of VIIIA was unnecessary. Starting with 16.75 g (125 mmoles) of ethylmagnesium bromide, 19.6 g (100 mmoles) of Vb and 60.5 g (250 mmoles) of *n*-pentyl tosylate, the crude 8-tetradecyn-1-ol t-butyl ether (VIIbB) was obtained in a yield of 17.6 g (purity 75 %) ; ms(m/e) : 251 $(M-CH_3)^+$, 210 $(M - CH_2 = C(CH_3)_2)^+$, 57 $(C(CH_3)_3)^+$. Subsequent acetylation of this product by refluxing for 3 hours with 25 ml of acetic anhydride and 0.5 ml of conc. H_2SO_4 and processing as usual afforded 17 g of crude VIIIB (purity 77 %). A satisfactory purity could be achieved by vacuum distillation collecting the fraction boiling at 128—130°/2—4 mm ; yield 7.3 g (30 % from Vb) ; IR (film) : 1250, 1738 cm^{-1} ($OCOCH_3$) ; mm (m/e) : 252 $(M)^+$, 192 $(M-CH_3COOH)^+$, 61 $(CH_3COOH_2)^+$.

Z-8-Dodecen-1-ol acetate (*Z—IXA*) : The Ni P-2 catalyst was prepared according to the standard procedure [21] starting with 1.25 g (5 mmoles) of nickel acetate in 50 ml of ethanol and 0.189 g (5 mmoles) of sodium hydridoborate in 5 ml of ethanol. Ethylenediamine (1 ml ; 15 mmoles) and 11.2 g (5 mmoles) of 8-dodecyn-1-ol acetate (VIIIA) were added. The air was removed from the catalytic reduction apparatus by a rapid stream of hydrogen and the mixture shaken with hydrogen until 5 mmoles were absorbed. The catalyst was removed by filtration, the filtrate concentrated by vacuum distillation (15—20 mm) and the residue dissolved in 75 ml ether. The solution was washed with six portions of 15 ml dil. HCl and finally with water. After drying over $MgSO_4$ and removal of the solvent by distillation the end product *Z*-IXA was obtained in a yield of 10.5 g (93 %) ; isomer purity higher than 99 % ; n^{25} = 1.4436 ; IR (film) 1250, 1740 ($OCOCH_3$) ; H—NMR(δ ppm) : 0.90 (t, 3H, J = 7 Hz, CH_3—CH_2—), 2.02 (s, 3H, —$OCOCH_3$), 4.05 (t, 2H, J = 7 Hz, —OCH_2—), 5.35 (m, 2HC*H*=C*H*—) ; ^{13}C—NMR (carbon no./δ ppm) : 1'/171.0, 2'/21.0, 1/64.8, 2/28.8, 3/26.0, 4/29.8, 5/29.4, 6/29.4, 7/27.3, 8/129.6, 9/129.8, 10/29.3, 11/23.0, 12/13.8 ; ms (m/e) ; 166 $(M-CH_3COOH)^+$, 61 $(CH_3COOH_2)^+$.

***Z**-8-Tetradecen-1-ol acetate* (*Z—IXB*) : The procedure was identical with that used in the preparation of *Z*—IXA. Starting with 7.3 g of VIIIB the end product *Z*—IXB was obtained in a yield of 6.6 g (90 %); isomer purity higher than 99 %; $n^{25} = 1.4443$; ms (m/e): 194 $(M-CH_3COOH)^+$, 61$(CH_3COOH_2)^+$.

E-Dodecen-1-ol acetate (E-IXA): Into a mixture of 10 ml of dry THF and 80 ml of diglyme, 5 g (131 mmoles) of $LiAlH_4$ were introduced. The solvent was partially removed (about 7 ml) until the internal temperature reached 140°. The mixture was then colled to 0° and a solution of 7 g (38 mmoles) of VIIcA in 10 ml of diglyme was added in portions maintaining the temperature below 10°. The mixture was subsequently heated at 140–150° for 15 hours. The reaction was discontinued by dropwise addition of dil. H_2SO_4 under ice cooling. All manipulations were performed in an inert gas atmosphere and under vigorous stirring. The mixture was extracted with hexane and washed with sat. NaCl solution. After drying over $MgSO_4$ the solvent was removed by distillation. The residue (7.7 g) consisting of crude *E*-dodecen-1-ol was acetylated with acetic anhydride in pyridine under standard conditions and the reaction mixture processed as usual. From the crude *E*-IXA the volatile impurities were removed by heating *in vacuo* at 70–80°/2–3 mm. The resulted end product (6.7 g; 78 % from VIIcA) had a purity of 93–94 %; $n^{25} = 1.4408$; IR (film): 1250, 1740 cm^{-1} $(OCOCH_3)$, 980 cm^{-1} (trans $=C-H$); ^1H-NMR (δ ppm): 0.88 (t, 3H, J = 7.5 Hz, CH_3-CH_2-), 1.95 (s, 3H, $OCOCH_3$), 3.96 (t, 2H, J = 6.5 Hz, $-OCH_2-$), 5.30 (m, $-CH=CH-$); ^{13}C-NMR (carbon no./δ ppm): 1'/171.0, 2'/21.1, 1/64.8, 2/28.8, 3/26.1, 4/29.7, 5/29.3, 6/29.2, 7/32.8, 8/130.6, 9/130.8. 10/35.0, 11/22.9, 12/13.7; ms (m/e) 166 $(M - CH_3COOH)^+$, 61 $(CH_3COOH_2)^+$.

REFERENCES

[1] Part VII: N. Popovici, A. Barabás and F. Hodoşan, *Rev. Roumaine Chim.*, **28**, 995 (1983)

[2] H. J. Bestmann and O. Vostrowsky, "Chemistry of Insect Pheromones", in "Chemie der Pflanzenschutz- und Schädlingsbekämpfungsmittel", Bd. 6, Springer-Verlag, Berlin, 1980, p. 30.

[3] M. Tamura and J. Kochi, *Synthesis*, 303 (1971).

[4] G. Fouquet and M. Schlosser, *Angew. Chem.*, **86**, 50 (1974).

[5] H. J. Bestmann, J. Süss and O. Vostrowsky, *Tetrahedron Lett.*, 3329 (1978).

[6] D. Samains and C. Descoins, *Synthesis*, 388 (1978).

[7] E. P. Hodoşan, N. A. I. Popovici, M. Iacob and I. Ghizdavu, *Rom. Pat.* no. **76824**, 17.03. 1981 (appl. 19.01.1978).

[8] N. Popovici, A. A. Botar, A. Barabás, I. Oprean and F. Hodoşan, *J. prakt. Chem.*, **325**, 17 (1983); N. A. I. Popovici, F. P. Hodoşan, I. Ceianu and E. Maloş, *Rom. Pat.* no. **64552**, 19.04.1977 (appl. 8.02.1977).

[9] S. Hoff, L. Brandsma and J. F. Arens, *Rec. Trav. chim.*, **87**, 916 (1968).

[10] J. Meijer and P. Vermeer, *Rec. Trav. chim.*, **93**, 183 (1974).

[11] A. V. M. Gocan, A. A. Botar, M. Iacob, I. Ghizdavu and F. Hodoşan, *Rom. Pat.* no. **71284**, 12.05.1979 (appl. 4.06.1977).

[12] E. F. Degering and L. Boatright, *J. Amer. Chem. Soc.*, **72**, 5137 (1950).

[13] L. Brandsma, "Preparative Acetylenic Chemistry", Elsevier Publishing, Amsterdam, 1971, p. 29.

[14] "Methoden der organischen Chemie (Houben-Weyl)", Bd. V/2a, G. Thieme Verlag, Stuttgart, 1977, p. 447.

[15] A. A. Botar, A. Barabás, I. Oprean, J. Csonka-Horvai and F. Hodoşan, *Rev. Roumaine Chim.*, **28**, 741 (1983)

[16] R. Rossi and A. Carpita, *Synthesis*, 561 (1977).

[17] J. Granges and M. Baggiolini, *Rev. Suisse Vitic. Arboric.*, **3**, 93 (1971).

[18] W. L. Roelofs, A. Comeau and R. Selle, *Nature*, **224**, 723 (1969).

[19] H. P. Chambon and J. d'Anguillar, *Ann. Zool.–Ecol. Animal.*, **6**, 423 (1974).

[20] H. Arn, *Experientia*, **30**, 1142 (1974).

[21] H. C. Brown and C. A. Brown, *J. Amer. Chem. Soc.*, **85**, 1005 (1963).

Revue Roumaine de Chimie, **29**, *5*, 429–435 (1984)

SOLVENT EFFECTS. I. SOLVENT INFLUENCE ON THE ABSORPTION SPECTRA OF SOME NITROPHENOTHIAZINE-5-OXIDES AND NITROPHENOTHIAZINE-5,5-DIOXIDES

M. RĂILEANU*, S. FLOREA* and MARINA SAHINI**

* Craiova University, Chemistry Department, Str. A.I. Cuza, 13, Craiova, Romania
** Center of Physical Chemistry, Splaiul Independenţei, 202, Bucharest, Romania

Received September 16, 1981

Electronic absorption spectra were recorded in the 300–800 nm region for 3-nitro-, 3,7-dinitro-, 1,3,7,-trinitro- and 1,3,7,9-tetranitrophenothiazine-5-oxide and also for 3,7-dinitro-, 1,3,7-trinitro- and 1,3,7,9-tetranitrophenothiazine-5,5-dioxide. Having in view the solvatochromic and solvation type and using the solvent polarity scale of Dimroth and Reichardt, the nature of the absorption bands was established. With the help of IR spectra it was shown that the NH-group from 10 position forms intramolecular hydrogen bonds with the nitro groups from 1 and 9 positions. It was established that in some solvents the nitrophenothiazine-5-oxidic and nitrophenothiazine-5,5-dioxidic compounds exist in the form of three different species in equilibrium.

1. INTRODUCTION

The solvent nature influences the chemical reactivity through solvation, complexation or ionization of the substances and these processes manifest themselves in electronic spectra. [1]

In this paper we performed an absorption spectra study of some nitroderivatives of the phenothiazine (I) in solvents with different polarity and basicity. To study the behaviour of the nitrophenothiazinic compounds in solution, IR and electronic spectra were recorded.

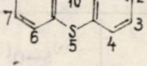

I

In this paper the solvent polarity was expressed by E_T polarity parameter of Dimroth and Reichardt.[2,3] The solvent polarity increases with their E_T value and the utilization of this scale allows the easy recognition of the absorption band nature of the substance in solution.

The names of the nitrophenothiazinic compounds studied were abbreviated as follows:

MNPS – 3-Nitrophenothiazine-5-oxide
DNPS – 3,7-Dinitrophenothiazine-5-oxide

DNPD — 3,7-Dinitrophenothiazine-5,5-dioxide
tNPS — 1,3,7,-Trinitrophenothiazine-5-oxide
tNPD — 1,3,7,-Trinitrophenothiazine-5,5-dioxide
TNPS — 1,3,7,9,-Tetranitrophenothiazine-5-oxide
TNPD — 1,3,7,9-Tetranitrophenothiazine-5,5-dioxide

2. SPECTRAL DATA INTERPRETATION

2.1. IR Spectra

5-Oxidic and 5,5-dioxidic nitrophenothiazinic compounds contain in their molecules $\rangle N{-}H$, $-NO_2$, $\rangle S \rightarrow O$, $\rangle SO_2$ groups. The structures of these compounds suggest that in solid state intermolecular hydrogen bonds ($\rangle S \rightarrow O \ldots H{-}N\langle$, $O \leftarrow \overset{|}{N} = O \ldots H{-}N\langle$)or intramolecular ones ($O \rightarrow \underset{|}{N} = O \ldots H{-}N\langle$) can appear.

Indeed, by studying the IR spectra of some benzo- and dibenzophenothiazines and their sulphoxides, Kudryavtseva *et al.* [4] found for N—H group from sulphoxides frequencies less than 3350 cm^{-1}, value recorded for the phenothiazine. [5] These frequency shifts toward lower values are explained by the existence of intermolecular hydrogen bonds $\rangle S \rightarrow O \ldots H{-}N\langle$.

To pursue the transformations of nitrophenothiazinic compounds in different solvents, it is important to know firstly the association type of these molecules in solid state. For this purpose IR spectra of MNPS, DNPS, tNPS and TNPS were recorded in solid state and the frequencies presenting an importance in this study are to be found in Table 1

Table 1

The IR absorption data of some nitrophenothiazine-5-oxides in solid state (cm^{-1})

Substance	Frequency values of some groups		
MNPS	$\nu_{N-H}(1) = 3270$ $\nu_{N-H}(2) = 3230$	$\nu_{S \rightarrow O}(1) = 1075$ $\nu_{S \rightarrow O}(2) = 1060$	$\nu_{NO_2}(1) = 1325$ $\nu_{NO_2}(2) = 1270$
DNPS	$\nu_{N-H}(1) = 3280$ $\nu_{N-H}(2) = 3235$	$\nu_{S \rightarrow O}(1) = 1080$ $\nu_{S \rightarrow O}(2) = 1030$	$\nu_{NO_2}(1) = 1330$ $\nu_{NO_2}(2) = 1285$
tNPS	$\nu_{N-H}(1) = 3330$ $\nu_{N-H}(2) = 3315$	$\nu_{S \rightarrow O}(1) = 1095$ $\nu_{S \rightarrow O}(2) = 1040$	$\nu_{NO_2}(1) = 1340$ $\nu_{NO_2}(2) = 1325$
TNPS	$\nu_{N-H} = 3220$	$\nu_{S \rightarrow O} = 1095$	$\nu_{NO_2}(1) = 1345$ $\nu_{NO_2}(2) = 1325$

In Table 1 one can observe that the absorptions of $N-H$, $S \rightarrow O$ and $O \leftarrow N=O$ groups in MNPS, DNPS and tNPS apperas doublets $\nu(1)$ and $\nu(2)$. In the case of $S \rightarrow O$ and $0 \leftarrow N=0$ vibrations the $\nu(1)$ values, which are higher, correspond to nitro and sulphoxidic groups without hydrogen bonds; the lower $\nu(2)$ values correspond to the same groups involved in hydrogen bonds.

TNPS presents only a single absorption for $N-H$ and $S \rightarrow 0$ groups and two values for the nitro group frequencies. The $\nu_{NO_2}(1) = 1345$ cm^{-1} value corresponds to the free nitro group whereas the lower value, $\nu_{NO_2}(2) = 1325$ cm^{-1}, shows the presence of associated nitro groups. Be cause in TNPS there is only a single $\nu_{S \rightarrow O}$ frequency with a high value (1095 cm^{-1}) comparatively to other corresponding values from the table, it results particularly convincing that in this substance the intermolecular hydrogen bonds with sulphoxidic group are absent (because the $N-H$ group is completely engaged in the formation of the intramolecular hydrogen bonds with nitro groups from the neighbouring 1 and 9 positions (chelate structure), as the formula II shows).

In tNPS one can observe two ν_{N-H} frequencies which are much higher in comparison with other corresponding frequencies from table 1. The $\nu_{N-H}(1) = 3330$ cm^{-1} value corresponds to $>S \rightarrow O \ldots H-N<$ intermolecular hydrogen bonds whereas the lower value, $\nu\ (2) = 3315$ cm^{22}, shows the existence of intermolecular hydrogen bonds between $N-H$ group and the nitro group from 1 position.

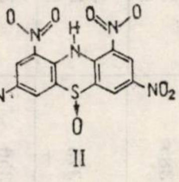

II

2.2. Electronic absorption spectra

In Table 2 the protic and aprotic solvents utilized in the electronic spectra recording are listed. These solvents are presented in increasing order of their polarity on Dimroth and Reichardt's scale; in the same table the substances studied in 300—800 nm region and the corresponding absorption maxima λ_{max} are presented.

The marked absorption from table 2 correspond to the nitrophenothiazinic anions resulted by the elimination of a proton from 10 position of the phenothiazinic nucleus. The other absorptions correspond to the unionized nitrophenothiazinic compounds which are unspecifically (dipole-dipole mechanism) or solvated by hydrogen bonds. One can observe that DNPD, tNPD and TNPD behave spectrally similarly to the series DNPS, tNPS and TNPS, as it was expected.

Table 2

The absorption maxima (λ_{max} in nm) for some nitrophenothiazinic compounds in different solvents

Solvent Substance	C_6H_6 $E_T = 34\cdot5$	$CH_3COOC_2H_5$ $E_T = 38\cdot1$	$CH_3COCH_2CH_3$ $E_T = 41\cdot3$	$HCON(CH_3)_2$ $E_T = 43\cdot8$	CH_3SOCH_3 $E_T = 45$	CH_3CH_2OH $E_T = 51\cdot9$	NaOH 0·25 *n* $H_2O/CH_3CH_2OH = 9/1$
MNPS	— 372 —	335–346 372 —	336–348 375 —	340–350 385 535*	340–350 395 535*	372 — 480*	— — 495*
DNPS	— 372 —	— 378 —	— 385 —	362 397 533*	358–365 399 535*	380 — 485*	— — 500*
DNPD	— 368 —	— 372 —	— 375 —	360 391 527*	358–365 593 532*	375 — 480*	— — 492*
tNPS	354 385–400 —	355 375–385 —	356 375–390 500*	358 385 500*	358–370 385 500*	358 375–390 480*	— — 480*
tNPD	352 385–400 —	353 375–385 —	356 375–390 500*	357 385 505*	358–365 385 505*	358 375–390 480*	— — 482*
TNPS	330 — 378 —	320–330 — 370 480*	320–330 — 370 480*	— 354 360–375 480*	— 358 365–380 480*	320–390 — 370 480*	— — — 480*
TNPD	330 — 378 —	320–330 — 370 —	320–330 — 370 480*	— 356 360–375 480*	— 356 370–385 480*	320–390 — 370 480*	— — — 480*

* The marked values are absorptions of the corresponding anions

In Table 3 the spectral data of Table 2 are explained.

Generally one can observe that the transition from the solvation by the dipole-dipole mechanism of the nitrophenothiazinic compounds to the solvation by the hydrogen bonds (>N−H... solvent) is determined by the increasing of the aprotic solvent basicity. The breaking of the chelatic structures in tNPS, tNPD, TNPS and TNPD molecules is also achieved by the basicity increase of the aprotic solvents. Indeed, the breaking of the chelated cycles by DMSO, which is more basic than MEC, is easily seen comparing the tNPS spectra in these two solvents, (Fig. 1).

Table 3

The solvation type, the absorption shift and the electronic transition nature

Substance	Absorption shift region (nm)	Absorption shift type	Electronic transition nature	Solvation type	Substance form
MNPS	335−46→372	Bathochromic	$\pi\to\pi^*$	By hydrogen bonds	Unionized
	372→395	Bathochromic	$\pi\to\pi^*$	Dipole — dipole	Unionized
	535→480	Hypsochromic	$n\to\pi^*$	By hydrogen bonds	Anion
DNPS	362→380	Bathochromic	$\pi\to\pi^*$	By hydrogen bonds	Unionized
	372→399	Bathochromic	$\pi\to\pi^*$	Dipole — dipole	Unionized
	533→485	Hypsochromic	$n\to\pi^*$	By hydrogen bonds	Anion
tNPS	354→358	Bathochromic	$\pi\to\pi^*$	Dipole — dipole	Chelate
	385−400→385	—	—	By hydrogen bonds	Unionized
	500→480	Hypsochromic	$n\to\pi^*$	By hydrogen bonds	Anion
TNPS	330→320−30	—	—	Charge transfer complex	Unionized
	354→358	Bathochocromic	$\pi\to\pi^*$	By hydrogen bonds	Unionized
	378→370	—	—	Dipole — dipole	Chelate
	480→480	—	—	By hydrogen bonds	Anion

In Figure 1 it can be observed how the 356 nm band in MEC, which corresponds to chelated tNPS molecules, becomes a shoulder in DMSO and the 385 nm band in DMSO, which corresponds to molecules solvated by hydrogen bonds with the solvent, becomes a shoulder in MEC.

In Table 3 bathochromic shifts are observed at MNPS, DNPS, tNPS and TNPS; these bathochromic shifts correspond to some $\pi\to\pi^*$ transitions. The anionic absorptions in aprotic solvents are hypsochromically shifted in protic solvents and correspond to some $n\to\pi^*$ electronic transitions. [2] Exceptions are TNPS and TNPD anions which constantly absorb at 480 nm in protic as well as in aprotic solvents; it results that the polarity of these anions is practically the same in fundamental or electronic excited state.

The compounds TNPS and TNPD are strong acceptors and form with benzene charge transfer complexes which absorb at 330 nm.

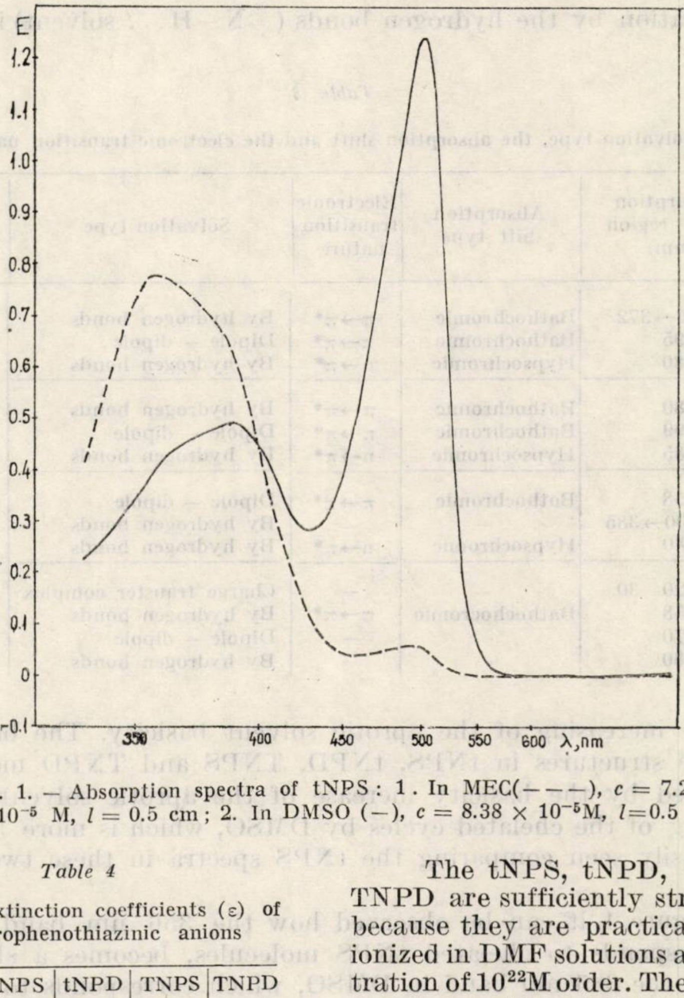

Fig. 1. – Absorption spectra of tNPS : 1 . In MEC(– – –), $c = 7.26 \times 10^{-5}$ M, $l = 0.5$ cm ; 2. In DMSO (–), $c = 8.38 \times 10^{-5}$M, l=0.5 cm.

The tNPS, tNPD, TNPS and TNPD are sufficiently strong acids, because they are practically totally ionized in DMF solutions at a concentration of 10^{22}M order. The molar extinction coefficients (ε) for the resulted anions are listed in Table 4.

Table 4

The molar extinction coefficients (ε) of some nitrophenothiazinic anions

Anion	tNPS	tNPD	TNPS	TNPD
ε	53488	53658	55263	55147

EXPERIMENTAL

The electronic absorption spectra were recorded with a Specord UV-VIS spectrophotometer at room temperature.

The IR spectra were recorded with a Carl Zeiss Jena UR-10 spectrophotometer as KBr pellets.

The nitrophenothiazinic compounds were prepared according to the methods described in references. [7,8]

The solution concentrations during the spectral recordings varied in $8.5 \times 10^{-5} - 10^{-5}$ M range.

REFERENCES

[1] M. Răileanu "Influenţa mediului asupra reactivităţii chimice", Ed. Scrisul Românesc, Craiova, 1981, p. 104–189.

[2] C. Reichardt, *Angew. Chem.*, **77**, 30(1965); *Angesw. Chem. Internat.* Ed. Engl., **4** 29(1965); C. Reichardt, and K. Dimroth, *Fortschr. chem. Forsch.*, **11**, 1 (1968).

[3] K. Dimroth, C. Reichardt, T. Siepmann and F. Bohlmann, *Liebigs Ann. Chem.*, 661, 1 (1963); K. Dimroth and C. Reichardt, *Z. analyt. Chem.*, **215**, 344 (1966).

[4] N. A. Kudryavtsova, Z. V. Pushkareva and V. F. Gryazev, *Khim. Geterosikl. Soedin. Akad. Nauk Latv. SSSR*, **1965**, 523; *Chem. Abstr.*, **64**, 2867a(1966).

[5] A. Turcu and M. Răileanu, *Rev. Roumaine Chim.*, **14**, 1579 (1969).

[6] D. P. Stevenson, C. M. Coppinger and J. W. Forbes, *J. Amer. Chem. Soc.*, **83**, 4350 (1961); G. H. Bresley and M. Kasha, *J. Amer. Chem. Soc.*, **77**, 4462 (1955).

[7] M. Răileanu, *Rev. Chim.* (Bucureşti), **33**, 1102 (1982)

[8] C. Bodea and M. Răileanu, *Studii şi Cercetări Chim. Fil. Cluj*, **1957**, 303.

Revue Roumaine de Chimie, 29, 5, 437–439 (1984)

SELECTIVE ESTER HYDROLYSIS. DETERMINATION OF ESTER GROUPS IN POLYURETHANE ELASTOMERS

VASILE LÖCSEI
ICECHIM, C.C.M.P., The "Solventul" Research Laboratory Str. Gării No. 25, R–1900,
Timişoara, Romania

Received September 7, 1982

The conditions for selective ester hydrolysis in urethanes were investigated in 83.5% aqueous DMSO. A fast, quantitative method for determination of esters in polyurethane elastomers is given. The method may have also some synthetic applications.

Elastomeric polyurethane /PU/ block copolymers consist of alternating blocks of flexible chains (polyesters or polyethers) often called "soft blocks or segments" and highly polar, relatively rigid blocks, "hard blocks or segments" containing urethane linkage.[1]

Our interest in determination of the hard segment size distribution (by HPLC) in these polymers,[2] prompted us to investigate the conditions for hydrolysis of ester groups without the interference of the urethane groups.

We chose DMSO as a hydrolysis medium for the following reasons. Efficient hydrolysis can be made only in homogeneous medium and DMSO is known to be one of the few solvents of PU. Generally, urethanes are hydrolysed at much slower rates than esters, but this is true only for low temperatures.[3] It is known that fast, low temperature hydrolysis of esters may be obtained in DMSO medium.[4]

No data concerning the hydrolysis of urethanes in this solvent are available.

EXPERIMENTAL

Biscarbamates of 4,4′-methylenedi(phenyl isocyanate), /MDI/

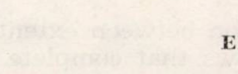

	R
I	$HO-(CH_2)_4-$
II	$CH_3-(CH_2)_6-COO-(CH_2)_4-$

as well as PU elastomers on the basis of poly(butylene adipate) diol M = 2000/PAB/, 1,4-butanediol /BD/ and MDI, with various PAB/BD/MDI molar ratios, namely; PU_1 1/2.4/3.4, PU_2 1/2/3, PU_3 1/0.6/1.6, were synthetized as described previously.[2] All other chemicals were of analytical reagent grade.

Generally, the *procedure used* in this work follows the back-titration method of Vinson and coworkers.[4] The recommended procedure for the PU analysis is given below.

Weigh accurately a PU sample cantaining approximately 1 milliequivalent ester and dissolve it in 40 ml of DMSO. Add exactly 8 ml of 0.5 M KOH (aqueous solution) and stir the reaction mixture magnetically at room temperature for 15 min. Dilute with 50 ml water, add Cresol Red indicator and titrate with standard 0.1 M HCl. A blank sample was similarly determined.

It must be noted than on working under these conditions, the heat of mixing DMSO—H_2O rises the temperature with 10—12°C.

Reaction time — extent of hydrolysis. In this investigation the moment when half of the base was added was considered as zero time and that of the dilution as final time. The samples were immediately titrated. Runs at 60°C were taken in a thermostat.

Extent of hydrolysis — excess of base. In all determinations the reaction time was 15 min. The concentration of the DMSO was 83.5% and the product [ester] [base] $= 1.7 \times 10^{-3}$ meq^2 ml^{-2} was the same at the beginning of every run. The extent of hydrolysis is defined as the ratio between the determined and the true saponification value.

RESULTS AND DISCUSSION

Table 1 shows the results for the saponification of urethane samples under the conditions of the recommended procedure. The relative standard deviation calculated for all the compounds used was 0.64%.

Table 1

Saponification of urethane samples

Compound	meq ester / g		Recovery %
	calculated	found	
II	2.93	2.92 ± 0.02^b	99.7
PU_1	6.26^a	6.30 ± 0.04	100.7
PU_2	6.55	6.49 ± 0.04	99.1
PU_3	7.82	7.74 ± 0.05	99.0

a Calculated on the basis of saponification value of parent polyester: 9.59 meq/g

b Errors are standard deviations for four determinations.

From the investigation of the correlation between extent of hydrolysis and reaction time, (see Fig. 1) it follows that complete hydrolysis occurs in ten minutes at room temperature.

Separate runs with addition of (I) to blank, at the same concentration as that resulted from hydrolysis of (II), together with no drift above 100% in runs with PU_2, proves that no interference from urethane occurs even after 30 min.

However, runs at 60°C give "conversions" higher than 100% already after 10 min, showing a competitive urethane hydrolysis.

Investigation of the influence of base excess on the extent of hydrolysis showed that in 15 min a complete saponification may be obtained already with 100% excess of base.

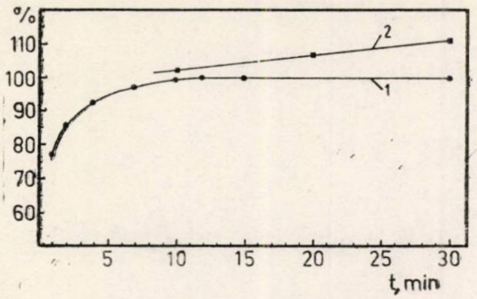

ig. 1. — Extent of hydrolysis *vs.* reaction time; at room temperature 1, at 60°C 2.

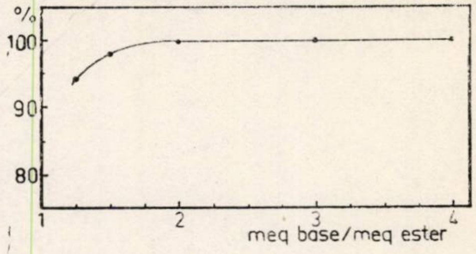

Fig. 2. — Extent of hydrolysis *vs.* excess of base.

Apart from its analytical interest, this method may have some synthetic applications in the preparation of hydroxyalkyl biscarbamates, as it was used by us for the synthesis of (I) from (II). [2]

REFERENCES

[1] A. Noshay and J. E. McGrath, "Block Copolymers. Overview and Critical Survey", Academic Press, New York, 1977, p. 365.
[2] V. Löcsei, O. Facsko and R. F. Pape, *Polym. Bull.*, **9**, 81 (1983).
[3] E. Schröder, J. Franz and E. Hagen, "Ausgewählte Methoden zur Plastanalytik", Akademie Verlag, Berlin, 1976, p. 586.
[4] J. A. Vinson, J. S. Fritz and C. A. Kingsbury, *Talanta*, **13**, 1973 (1966).

Revue Roumaine de Chimie, 29, 5, 441–446 (1984)

THE REACTION OF *p*-QUINONES WITH TRIPHENYLSTIBINE

A. ALBEROLA, A.M. GONZALEZ and F.J. PULIDO
Departamento de Química Orgânica de la Universidad de Valladolid y
de Investigaciones Químicas del C.S.I.C. Valladolid (Spain)

Received July 14, 1981

The reaction between a number of *p*-quinones and triphenylstibine afforded the corresponding diphenols and their 2-phenylderivatives in addition to pentavalent organoantimony compounds. From some of these reactions biphenyl and dimeric compounds have also been isolated. The reactions are temperature and solvent dependent. General reaction mechanisms via free radicals are proposed.

INTRODUCTION

The behavior of *p*-quinones when subjected to organometallic compounds, as organolithium [1,2] organomagnesium, [3,4] organoboron, [5,6] and organoaluminium,[7–13] was previously studied. Particularly, the reaction of the above mentioned quinones with triphenylaluminium produces a great variety of compounds, whose formation can be interpreted through homolytic reaction pathways.[11–13].

Apart from the reaction of *p*-quinones upon organophosphorus compounds,[14,15] no detailed study concerning the behavior of the above mentioned substances when treated with organometallic compounds which do not behave as Lewis acids, has been done. The behavior of 1,4-benzoquinone (Ia), toluquinone (Ib), 2,5-diphenyl-1,4-benzoquinone (Ic), 2,5-ditertbutyl-1,4-benzoquinone (Id) and 1,4-naphthoquinone (II) toward triphenylstibine (TPS) has been studied in order to determine whether the organoantimony compounds are capable of being used in substitution processes in the quinonoid nucleus and whether its smaller reactivity permits selective reactions of synthetic interest.

RESULTS

1,4-Benzoquinone (Ia) reacts with TPS in boiling ether producing an almost theoretical yield of hydroquinone (IIIa) and triphenylstibine dichloride (this being formed in the acid hydrolyis). Only a small portion of 2-phenylhydroquinone (IIIb)—8%—is isolated. 1,4-Naphthoquinone (II), under identical conditions, produces, 1,4-dihydroxy-2-phenylnapthalene and 1,4-dihydroxynaphthalene, readily oxidable to 2-phenyl-1,4-naphthoquinone (V) and 1,4-naphthoquinone (II) respectively. Triphenylstibine oxide and diphenylstibinic acid were also obtained.

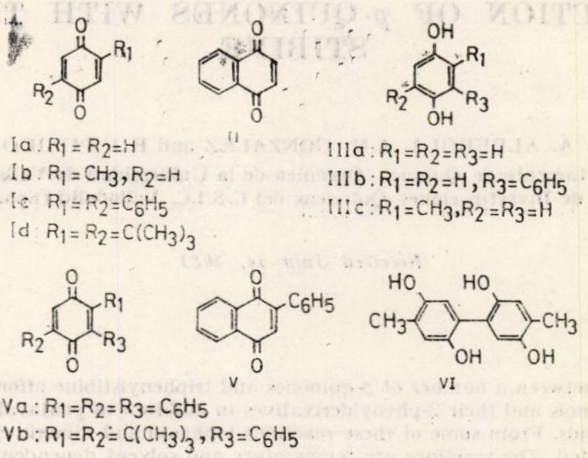

Fig. 1

When the reactions between *p*-quinones and TPS are carried out in refluxing benzene, the 1,4-benzoquinone comports itself differently and provides IIIb—82%—along with IIIa and triphenylstibine dichloride as minor products. Under these conditions, 1,4-naphthoquinone produced results similar to those obtained in ethereal solution. 2,5-Diphenyl-1,4-benzoquinone (Ic), in refluxing benzene, provides only 6% of triphenyl-1,4-benzoquinone (IVa), recovering the greater part of the initial quinone. The 2,5-ditertbutyl-1,4-benzoquinone (Id), which proves itself inactive in benzene, produces 2,5-ditertbutyl-3-phenyl-1,4-benzoquinone (IVb) — 23%—when the reaction is carried out in the presence of catalytic quantities of benzoyl peroxide. The behavior of toluquinone (Ib) is perceptively different and, in benzene solution, originates 2, 2′, 5, 5′-tetrahydroxy-4,4′-dimethylbiphenyl (VI) in addition to toluhydroquinone (IIIc) and diphenylstibinic acid. The reactivity of 2,5-diphenyl-1,4-benzoquinone increases if the reaction takes place in xylene yielding 60% of IVa ; under these conditions, one can also observe the formation of biphenyl resulting in the decomposition of triphenylstibine. The 2,5-ditertbutyl-1,4-benzoquinone shows itself totally inert when treated with TPS in refluxing xylene.

DISCUSSION

The UV spectrum of the mixture Ia-TPS (λmax$=430$ nm, log$\varepsilon = 1.30$), which is identical to that of 1,4-benzoquinone, suggests that an initial coordination of the organometallic compound to quinone forming a σ-complex does not take place in these reactions. The formation of no-arylated hydroquinones along with triphenylstibine halides, triphenylstibine oxides and phenylstibinic acid occurs as a consequence of the redox reaction which takes place in the hydrolysis (eq. 1).

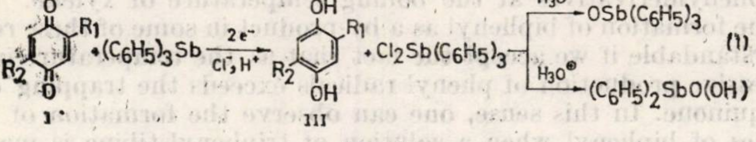

R1
R2
$+(C_6H_5)_3Sb$
2e⁻
Cl⁻, H⁺
OH
OH
$+Cl_2Sb(C_6H_5)_3$
$H_3O^{\oplus}$
$OSb(C_6H_5)_3$
$(C_6H_5)_2SbO(OH)$
(1)
I
III

Fig. 2

The formation of arylated hydroquinones (or arylated quinones resulting from the oxidation of the former) can be explained if we assume that the reaction is a 1,4 radical addition where the organoantimony acts as a potential source of phenyl radicals which are trapped by the *p*-quinone by virtue of its oxidation potential. The homolytic fission of the $Sb-C_6H_5$ bonds of TPS requires a temperature not lower than that of the refluxing benzene or the presence of an initiator as benzoyl peroxide (eq. 2).

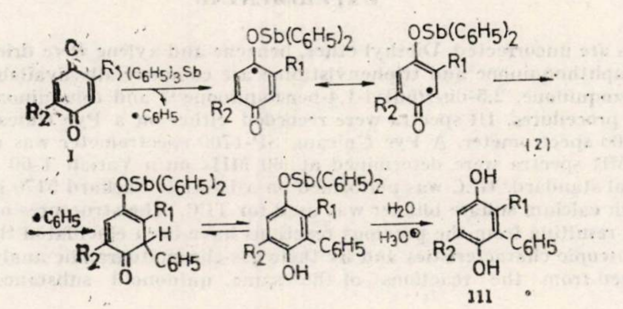

$(C_6H_5)_3Sb$
$\bullet C_6H_5$
$OSb(C_6H_5)_2$
R1
R2
I
(2)
H_2O
$H_3O^{\oplus}$
C_6H_5
OH
III

Fig. 3

The production of dimeric compounds must also be contemplated from the same point of view. The delocalization of the unpaired electron throughout the initial quinonoid nucleus – intermediate VII – permits to interpret the formation of 2, 2′, 5, 5′-tetrahydroxy-4,4′-dimethylbiphenyl upon its coupling of the two initial radicals (eq. 3).

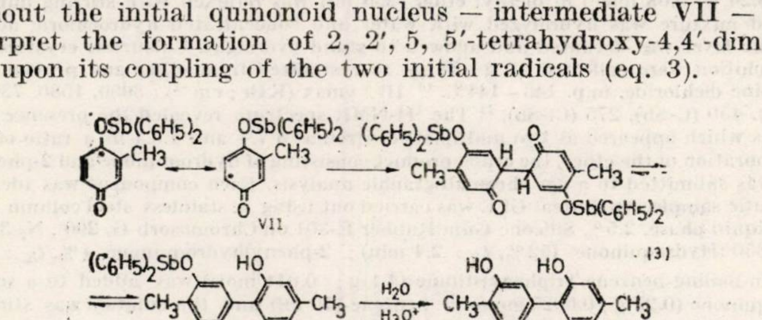

$OSb(C_6H_5)_2$
CH_3
VII
$(C_6H_5)_2SbO$
(3)
H_2O
H_3O^+
HO
OH
VI

Fig. 4

The final output of arylated hydroquinones (or arylated quinones) and consequently the trapping capacity of the quinone upon the phenyl

radicals depends on the oxidation potential of the used quinone. Thus, the 1,4-benzoquinone ($E_0 = 0.711$) leads to 82% of IIIb, in benzene solution while the 2,5-diterbutyl-1,4-benzoquinone ($E_0 = 0.554$) does not originate phenylderivatives at the boiling temperature of xylene.

The formation of biphenyl as a by-product in some of these reactions, is understandable if we accept the fact that as the temperature increases, the excessive production of phenyl radicals exceeds the trapping capacity of the quinone. In this sense, one can observe the formation of variable quantities of biphenyl when a solution of triphenylstibine is maintained in refluxing xylene for several hours.

We can finally conclude that TPS is a very slow generator of phenyl radicals when reacting with *p*-quinones and that consequently, the small concentration of the above mentioned radicals in solution yield very selective processes in which mono-arylated products, some of which have very acceptable outputs, are fundamentally produced.

EXPERIMENTAL

All m.ps are uncorrected. Diethyl ether, benzene and xylene were dried (Na). 1,4-Benzoquinone, 1,4-naphthoquinone and triphenylstibine are commercially available (Merck). 2,5-Diphenyl-1,4-benzoquinone, 2,5-di*tert*butyl-1,4-benzoquinone [16] and toluquinone [17] were prepared by established procedures. IR spectra were recorded either on a Pye Unicam SP-1000 or Pye Unicam SP-1100 spectrometer. A Pye Unicam SP-1700 spectrometer was used to obtain UV spectra. ^{1}H-NMR spectra were determined at 60 MHz on a Varian T-60 spectrometer using TMS as internal standard. GLC was performed on a Hewlett Packard 5170 gas chromatograph. Silicagel G with calcium sulfate blinder was used for TLC. The structures of the quinones and hydroquinones resulting from the previous reactions have been elucidated through their physical and spectroscopic characteristics and by their gas-chromatographic analysis using reference samples obtained from the reactions of the same quinonoid substances with triphenylaluminium. [12]

Reaction of triphenylstibine with 1,4-benzoquinone

a) In boiling ether. A mixture of 1,4-benzoquinone (2.16 g; 0.02 mole) and triphenylstibine (28.24 g; 0.08 mole) in diethyl ether (250 ml) was refluxed with stirring during 8 hrs. The cooled mixture was hydrolyzed with water and concentrated hydrochloric acid (1 : 1). The organic layer was decanted and allowed to stand overnight. Colourless crystals from the ethereal solution were collected (8 g; 94%), recrystallized from ether and proven to be triphenylstibine dichloride, m.p. 143–144°C. [18] IR : νmax (KBr; cm^{-1}) : 3050, 1580, 730 and 680 (aromatic), 450 (C-Sb), 275 (Cl-Sb). [19] The ^{1}H-NMR spectrum revealed the presence of aromatic protons which appeared as two multiplets centred at δ 7.4 and δ 8.1 in a ratio of 3H : 2H. After evaporation of the ether, the crude product consisting of hydroquinone and 2-phenylhydroquinone was submitted to a gas chromatographic analysis. Each component was identified by the authentic sample. Analytical GLC was carried out using a stainless steel column (3 mm × × 4 m); liquid phase, 2.5% Silicone Gum Rubber E-301 on Chromosorb G, 200°, N_2 35 ml/min, injection 350°. Hydroquinone (92%, t_R : 2.4 min); 2-phenylhydroquinone. (%, t_R : 19.2 min).

b) In boiling benzene. Triphenylstibine (4.1 g; 0.011 mole) was added to a solution of 1,4-benzoquinone (0.27 g; 0.0025 mole) in benzene (70 ml) and the solution was stirred at the reflux temperature of benzene during 16 hrs. The mixture was descomposed with water and concentrated hydrochloric acid (1 : 1) and the benzene phase was allowed to stand overnight. The colourless crystals that precipitated from the benzene solution were filltered off and recrystallized from ethanol to give 2-phenylhydroquinone (0.21 g; 45%), m.p. 96–98°. [20] IR : ν_{max} (nujol; cm^{-1}) : 3300, 1600, 1510, 1210, 740, 690. ^{1}H-NMR : δ (CD_3COCD_3) : 7.7 (8H, m, aromatic), 7.9 (1H, s, OH), 8.1 (1H, s, OH). The benzene fraction was removed by evaporation and the resulting oily solid was extracted with hot petroleum ether (40–60°). The insoluble residual oil (triphenylstibine-free) quickly solidified and was dried *in vacuo* to leave a brown solid

(0.22 g). The GLC of this solid indicated 22 % of hydroquinone and 78 % of 2-phenylhydroquinone. GLC analysis was conducted in the same manner as described in the case of boiling ether. Triphenylstibine dichloride could be detected from the original solution by means of TLC : (chloroform), $R_f = 0.45$.

Reaction of triphenylstibine with 1,4-naphthoquinone

a) In boiling ether. 1,4-Naphothquinone (0.4 g ; 0.0025 mole) dissolved in ether (80 ml) was treated with triphenylstibine (4.1 g ; 0.01 mole) and the reaction mixture was refluxed during 24 hrs, then cooled. The solution was hydrolyzed with a mixture of water and concentrated hydrochloric acid (1 : 1) .After filtration (filtrate"A"), the insoluble material (0.45 g) was extracted twice with 2 ml of dimethyl sulfoxide. The dimethyl sulfoxide-insoluble residue was filtered off (filtrate "B"), washed with water, dried and boiled with ethanol. The white powder (0.26 g), so obtained, was proven to be triphenylstibine oxide, m.p. 282—285°.[21] IR : νmax (CsI ; cm^{-1}) : 3050, 1580, 730, 680 (aromatic), 456 (C-Sb), 740, 660 (Sb-O-Sb).[21] The solubility of triphenylstibine oxide was such low that a saturated chloroform solution did not give ^{1}H-NMR spectrum (which could have aided in characterizing the product.) After careful evaporation of the filtrate "B", the residue was collected and washed with water, then it was boiled with ethanol to give diphenylstibine acid, m.p. 250—255°.[22] IR : νmax (CsI ; cm^{-1}) : 3200 (O-H), 1480, 1440, 730, 690 (aromatic), 440 (C-Sb), 745, 680 (Sb-O-Sb). ^{1}H-NMR : δ (CD_3SOCD_3) : 7.25 (4H, m, aromatic), 7.5 (5H, m, aromatic), 8.1 (1H, m, aromatic). The aqueous layer (filtrate "A") was separated and repeatedly extracted with ether. The solvent was removed from the combined ethereal solution. GLC of the residual material gave the following composition : 1,4-naphthoquinone 89 % ; 2-phenylnaphthoquinone 11 %. Analysis was carried out with the aid of a Hewlett Packard 5710A gas chromatograph which was equipped with 3 % OV-17 on Chromosorb Q, columns (3 mm + 4 mm), 250°, N_2 35 ml/min, injection 300°. 1,4-Naphthoquinone $t_R = 3.2$ min., 2-phenyl-1,4-naphthoquinone $t_R = 23.6$ min.

b) In boiling benzene. A benzene solution of triphenylstibine (4.1 g ; 0.012 mole) was added to a stirred solution of 1,4-naphthoquinone (0.5 g ; 0.003 mole) and the mixture was refluxed for 40 hrs. Upon working up as described in the case of boiling ether, the following products were identified (GLC) : 1,4-naphthoquinone, 87 % ; 2-phenyl-1,4-naphthoquinone, 13 %.

Reaction of triphenylstibine with 2,5-diphenyl-1,4-benzoquinone

a) In boiling benzene. The reaction of 2,5-diphenyl-1,4-benzoquinone (2.8 g ; 0.01 mole) with triphenylstibine (14.1 g ; 0.04 mole) was attempted in refluxing benzene solution (200 ml). After 48 hrs at the reflux temperature the usual hydrolytic work-up and GLC analysis yielded 94 % of 2,5-diphenyl-1,4-benzoquinone and 6 % of 2,3,5-triphenyl-1,4-bezoquinone. The identification and quantitative estimations of these compounds were achieved on a Hewlett Packard 5710A equipped with 3% OV—17 on Chromosorb Q, columns (3 mm × 4 m), 300° N_2 35ml/min, injection 350°. 2,5—diphenyl—1,4—benzoquinone t_R=8.0 mi ; 2,3,5—triphenyl—1,4—benzoquinone t_R=24.6 mi.

b) In boiling xylene. Triphenylstibine (5.6 g ; 0.016 mole) was added to a solution of 2,5-diphenyl-1,4-benzoquinone (1 g ; 0.04 mole) in xylene (100 ml) and the mixture was heated at the reflux temperature of xylene during 48 hrs. Working-up in the same manner as described in the case of boiling benzene the following products were identified (GLC) : 2,5-diphenyl-1,4-benzoquinone, 40 % ; 2,3,5-triphenyl-1,4-benzoquinone, 60 % and biphenyl (13 % from initial triphenylstibine). As usual, the compounds were analyzed by comparison of their t_R with that of authentic specimens.

Reaction of triphenylstibine with 2,5-ditertbutyl-1,4-benzoquinone

2,5-Di*tert*butyl-1,4-benzoquinone did not react with triphenylstibine when the reaction was carried out in refluxing benzene. Attempts to undergo the reaction at the reflux temperature of xylene failed. The reaction of 2,5- di*tert*butyl-1,4-benzoquinone (2.5 g ; 0.01 mole) with triphenylstibine (17 g ; 0.045 mole) was re-examined in the presence of catalytic amounts of benzoyl peroxide (0.011 g) and its was seen that 2,5-di*tert*butyl-3-phenyl-1,4-benzoquinone could be obtained in 23 % yield (GLC) when the reaction was carried out in refluxing benzene (100 ml) during 24 hrs. GLC analyses were performed using 3 % OV-17 on Chromosorb Q, columns (3 mm × 4 m), 250°, N_2 35 ml/mi, injection 350° ; 2,5-di*tert*butyl-1,4-benzoquinone $t_R = 2.4$ min ; 2,5-di*tert*butyl-3-phenyl-1,4-benzoquinone $t_R = 9.2$ min.

Reaction of triphenylstibine with toluquinone

A mixture of toluquinone (1 g ; 0.008 mole) and triphenylstibine (11.3 g ; 0.032 mole) in benzene (125 ml) was refluxed during 60 hrs. The hydrolysis (H_2O, HCl 1 : 1) of the mixture leaves a white powder (0.069 g), m.p. 250—255°. Its IR spectrum was superimposable on that of the diphenylstibinic acid obtained from the analogous reaction with 1,4-naphthoquinone. The organic layer was separated and washed with sat. $NaHCO_3$. After drying ($MgSO_4$) and evaporation, the crude reaction mixture was chromatographed on Silica Gel with a chloroform developer and yielded : 33.5 % of toluhydroquinone and 66.5 % of 2,2' 5,5'-tetrahydroxy-4,4'-dimethylbiphenyl. The identification of these compounds was achieved in the following way : toluhydroquinone, m.p. 126—128° [23] (benzene). IR : νmax (nujol ; cm^{-1}) : 3300, 1610, 1200, 875, 820. ^{1}H-NMR : δ (Cl_3CD) : 2.1 (3H, s, CH_3), 4.2 (1H, s, OH), 6.5 (3H, n, aromatic) ; 2,2' 5,5'-tetrahydroxy-4,4'-dimethylbiphenyl, m.p. 170—172° (ethanol). IR : νmax (nujol ; cm^{-1}) : 3150, 1605, 1200, 810. ^{1}H-NMR ; δ(Cl_3CD) : 2.1 (6H, s, CH_3), 4.5 (4H, s, OH), 6.5 (2H, s, 3 and 3' aromatic protons), 6.9 (2H, s, 6 and 6' aromatic protons). Oxidation of VI produces the corresponding quinone, m.p. 176—178° . [24]

REFERENCES

[1] H. M. Crawford, M. Lumpkin, and M. MacDonald, *J. Amer. Chem. Soc.*, **74**, 4087 (1952).

[2] H. M. Crawford, *J. Org. Chem.*, **36**, 3533 (1971).

[3] H. M. Crawford, *J. Amer. Chem. Soc.*, **70**, 1081 (1948).

[4] D. Cohen, L. Hewitt and T. Millar, *J. Chem. Soc.*, *(C)*, **1969**, 2266.

[5] G. W. Kabalka, *J. Organometal. Chem.*, **33**, C25 (1971).

[6] H. C. Brown, D. B. Bigley, S. K. Arora and N. M. Yoon, *J. Amer. Chem. Soc.*, **92**, 7161 (1970).

[7] A. Alberola, A. M. Gonzalez and J. A. Martinez de Ilarduya, *An. Quim.*, **73**, 1227 (1977)

[8] A. Alberola, A. M. Gonzalez and J. A. Martinez de Ilarduya, *An. Quim.*, **76**, 118 (1980).

[9] A. Arberola, A. M. Gonzalez and J. A. Martinez de Ilarduya, *An. Quim.*, **76**, 123 (1980).

[10] A. Alberola, A. M. Gonzalez, J. A. Martinez de Ilarduya and F. J. Pulido, *An. Quim.*, in press.

[11] A. Alberola, A. M. Gonzalez and F.J. Pulido, *An. Quim.*, **74**, 1147 (1978).

[12] A. Alberola, A. M. Gonzalez and F. J. Pulido, *An. Quim.*, **76C**, 199 (1980).

[13] A. Alberola, A. M. Gonzales, J. A. Martinez de Ilarduya and F. J. Pulido, *An. Quim.*, in press.

[14] M. M. Sidky, M. R. Mahran and Y. O. El-Khoshnieh, *Tetrahedron*, **30**, 47 (1974).

[15] E. A. C. Lucken, F. Ramirez, V. P. Catto, D. Rhum and S. Dershowitz, *Tetrahedron*, **22**, 637 (1966).

[16] K. Gurewitsch, *Chem. Ber.*, **32**, 2427 (1899).

[17] R. Schniter, *Chem. Ber.*, **20** 2283 (1887).

[18] J. F. Carson and F. F. Wong, *J. Org. Chem.*, **26**, 1467 (1961).

[19] G. Goel and E. Maslowsky, *Inorg. Chem.*, **10**, 2572 (1971).

[20] W. Borsche, *Liebigs Ann. Chem.*, **312**, 221 (1900).

[21] D. L. Venezky and C. W. Sink, *J. Organometal. Chem.*, **35**, 131 (1972).

[22] A. Michaelis and R. Reese, *Liebigs Ann. Chem.*, **233**, 59.

[23] R. Bamberger, *Liebigs Ann. Chem.*, **390**, 175 (1912).

[24] A. Fchiter and R. Ris, *Helv. Chim. Acta*, **7**, 808 (1924).

Revue Roumaine de Chimie, 29, 5, 447–456 (1984)

ON THE POLYMERIZATION OF ACETYLENIC DERIVATIVES. XXXV.[1]

EXPERIMENTAL AND THEORETICAL STUDY ON THE RADICAL POLYMERIZATION OF 9-ETHYNYLANTHRACENE

SVETLANA DUMITRESCU, M. GRIGORAŞ and G. SURPĂŢEANU
Polytechnic Institute of Iassy, Department of Organic and Macromolecular Chemistry, Iassy, 6600, Romania

Received November 3, 1982

A theoretical study using the MO (molecular orbital) calculations, EH (extended Huckel) noniterative procedure method was applied to the radical polymerization of 9-ethynylanthracene (9–EA). By theoretical results the radical polymerization mechanism proposed in scheme 2 with the formation of the dihydroanthracene units is energetically favorized. Experimentally, a mixture of polymers containing dihydroanthracene and polyene units was found. The steric and experimental factors could change the composition of the obtained polymers by a radical mechanism. The structures of all compounds using the UV and IR spectra were established.

INTRODUCTION

In some previous papers we showed that the polymerization of 9-ethynylanthracene (9–EA) by a ionic-coordinative mechanismus (Ziegler – Natta or phosphinic, arsinic and stibinic complexes of the transitional metals as catalyzers) leads to polymers with double-conjugated bonds in the main chain and anthryl group as adjacent substituent.[1–3]

The radical or ionic polymerization of 9–EA leads to complex structure polymers. [1].

In this paper we proposed to study the radical polymerization of 9–EA.

EXPERIMENTAL

The synthesis and purification of the 9-EA was made as described in paper. [2] The radical and thermal polymerization was carried out in joint-cap bottles under inert atmosphere (argon) in the absence of light, in the solution or in bulk. The polymerization using UV radiation was performed in a glass Pyrex ampoule by irradiation with a UV-500 W lamp ($\lambda > 350$ nm) of a solution of 9-EA in chloroform (10%). The conversion is of 25%. The polymers were precipitated with methanol, filtered and dried. The spectral measurements were performed as in the previous note. [2]

RESULTS AND DISCUSSIONS

The "spontaneous" polymerization of 9–EA

The pure monomer cannot be kept for a long time. Even in the absence of initiators it spontaneously polymerizes. Therefore, it was kept for a long time as anthryl-silver acetylide. The monomer was obtained just before utilization by the treatment of anthryl-silver acetylide with acid and then it was chromatographically purified. It was observed that the spontaneous polymerization of 9 – EA is slower in solution and inert medium than in the solid state and in air. The quantitative analysis of

Table 1

Elemental analysis of the product obtained by spontaneous polymerization of 9 – EA

Calc. for $(C_{16}H_{10})_n$	:	C,95.05%; H,4.95%
Found	:	C,91.12%; H.4.61%

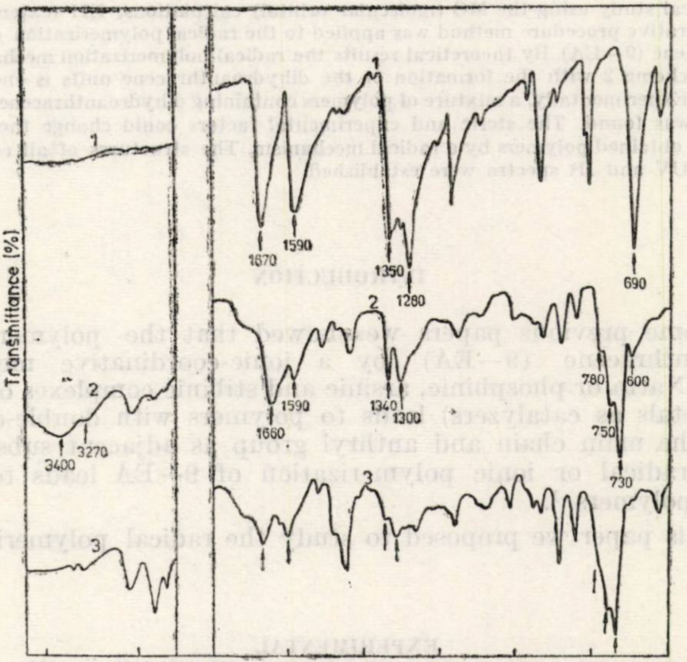

Fig. 1. – IR spectra (KBr pellet) : of 1) anthraquinone, 2) the product obtained by spontaneous polymerization of 9 – EA and 3) the product obtained by UV irradiation of 9 – EA.

the product obtained by spontaneous polymerization of 9 — EA shows a smaller percent content in carbon and hydrogen than their calculated values (Table 1). It follows that in this compound oxygen is bonded as oxidation micromolecular complexes or in polymers.

Figure 1 presents the IR spectra of the obtained product and of the anthraquinone. The appearance of the intensive bands at 1280, 1350 ($\nu C{=}O$), 1590 ($\nu C = C$) and 1670 cm ($\nu C = O$), in the polymer shows the anthraquinone presence in polymer. The UV irradiation of an undesired monomer solution leads to a compound with an IR spectrum similar to that of the spontaneously obtained compound (Fig. 1).

We shall present a simplified scheme which explains the polymerization of 9 — EA based on :

a) the presence in the polymers of monomer oxidation compounds ;

b) the slowness of the spontaneous polymerization of 9 — EA in the absence of the air and light, and

c) the available literature data on the photo-oxidation and photodimerization of anthracene.

Anthracene and its derivatives strongly absorb the UV radiations passing into singlet excited states (S*).[4]

In 9 — EA the conjugation between ethynyl group and anthracene ring has both bathochromic and hypsochromic effects, in respect to anthracene (Table 2).

Table 2

The UV molar extinction coefficients of 9 — EA and anthracene (solvent $-CHCl_3$)

9 — EA	255(166 000),263(240 000),313(1100),330(2240)
λ_{max} (ε_{max})	348(4470),364(8710),382(12100),403(11 000)
anthracene	253(170 000),313(1220),327(2650),342(5050),
λ_{max} (ε_{max})	359(7050),379(6650)

The probability of light absorption and formation of the states S* in this case are greater than for anthracene. This process may occur also in the presence of the light with $\lambda \geqslant 400$ nm. The disappearance of this excited state may occur by the interaction with the monomer ground state (A) or with oxygen (B) (dimerization of the anthracene and its derivatives is well known).

This occurs by the interaction between an excited and ground state molecule.[5-7]. Thermally and in the radiation absence the reaction is reversible. A more efficient way of disappearance of the excited state when the reaction occurs in air is by oxygen (B) contribution,[8-9] with the formation of singlet oxygen.[10]

Recently, Carlson et *al.*[10,11] have proposed a mechanism for the photo-oxidative destruction explanation of the polyolephins by the participation of anthracene and its derivatives absorbed from atmosphere. These compounds, under radiation influence, give the singlet oxygen which initiates the photo-oxidative destruction of the polymers.

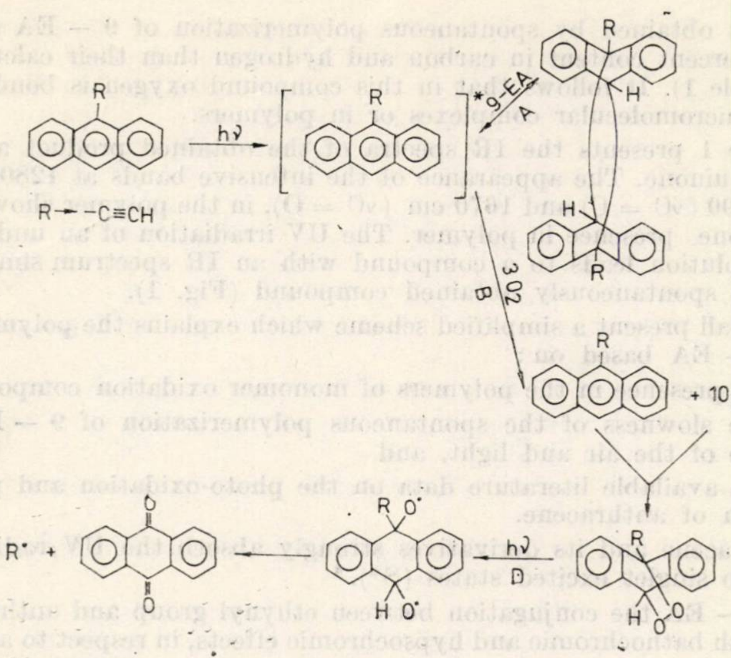

In our case the singlet oxygen interacts with a ground state monomer molecule giving an endoperoxide.[4,12,13] This is unstable and decomposes thermally or under radiation influence to anthraquinone and radicals able to initiate the spontaneous polymerization of 9 — EA.

Sugiyama *et al.* have demonstrated that the anthracene irradiation in CS_2 leads to bianthrone (29%) and anthraquinone (21%). As intermediate compounds, anthracene endoperoxide[14] appears.

Finally, the action of simultaneous light and oxygen on the 9 — EA causes its oxidation to anthraquinone and radical polymerization. The polymerization study should be performed in the absence of air and light.

Thermal and radical polymerization of 9—EA

The thermal and radical polymerization of 9 — EA in respect to other arylacetylenes at low temperatures occurs with good yield (Table 3).

Table 3

The radical polymerization of 9 — EA

Initiator	Conc. in mol %	Temp. °C	Time hrs	Solvent	Atmosphere	Yield %	Molecular weight
AIBN	2	90	0.5	bulk	argon	85.0	1120
BP	2	90	3.5	toluene	air	42.2	980
—	—	90	0.5	bulk	air	74.2	1000
—	—	90	0.5	bulk	argon	30.5	1420

The polymers obtained by a radical mechanism contain also dihydroanthracene units in the main chain. This was evidenced by IR spectroscopy.[1] The existence of the anthryl substituent as dihydroanthracene unit in the radical polymer obtained (PEA — R) is also demonstrated by comparison of its UV absorption spectra with those of an obtained polymer using Ziegler — Natta catalyzers (PEA — Z). In the last polymer the anthryl group is bound as adjacent substituent.[1] In figure 2 a clear difference between the absorption intensities of PEA — Z and PEA — R is observed.

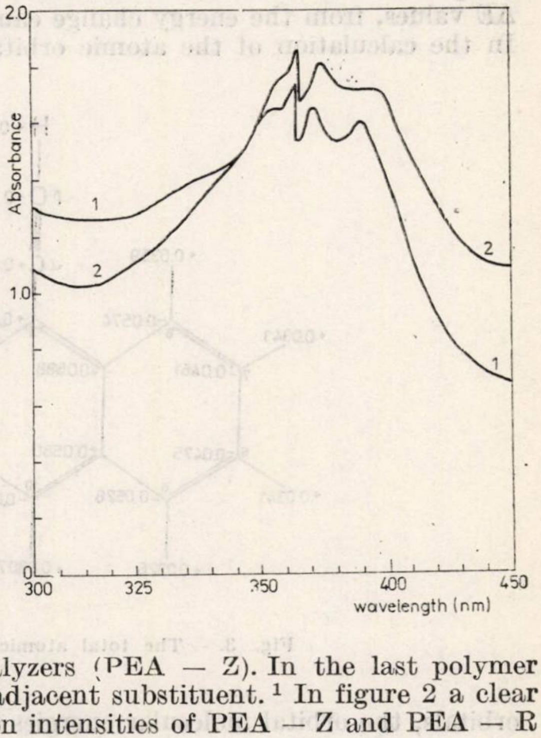

Fig. 2. — UV spectra ($CHCl_3$) of : 1) poly-9-EA obtained by radical mechanism (0.267 mmol/l) and 2) poly-9-EA obtained by Ziegler — Natta mechanism (0.207 mmol/l).

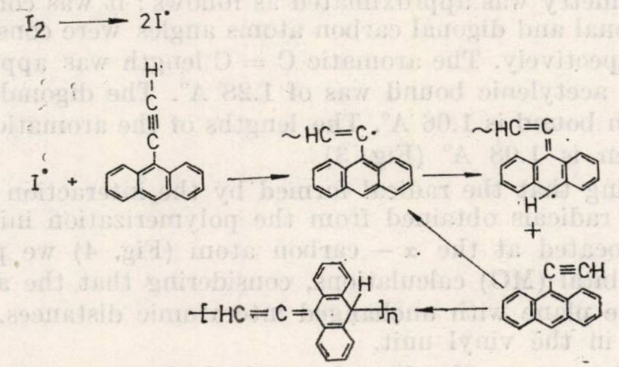

At a concentration of 0.267 mmol/l PEA — R shows a smaller absorption than PEA — Z at a concentration of 0.207 mmol/l at larger wavelengths. At smaller wavelengths an inversion of the absorption intensities takes place owing to the dihydroanthracene structure contribution. The dihydroanthracene structures do not absorb at wavelengths greater than 300 nm [15,16] due to interruption of the conjugation in the central anthracene ring.

In order to establish the polymerization mechanisms of 9 — EA in the presence of some radical initiators, we proposed to calculate the total ΔE values, from the energy change caused by the orbital interaction. [17,18] In the calculation of the atomic orbital coefficients from the molecular orbitals, the orbital molecular energies and total atomic charges, the EH (extended Hückel) noniterative procedure method was used. [19] The 9 — EA molecule geometry was approximated as follows : it was considered plane and the trigonal and digonal carbon atoms angles were considered of 120° and 180°, respectively. The aromatic C = C length was approximately of 1.39 A°. The acetylenic bound was of 1.28 A°. The digonal carbon atom and hydrogen bound is 1.06 A°. The lengths of the aromatic carbon atom and hydrogen is 1.08 A° (Fig. 3).

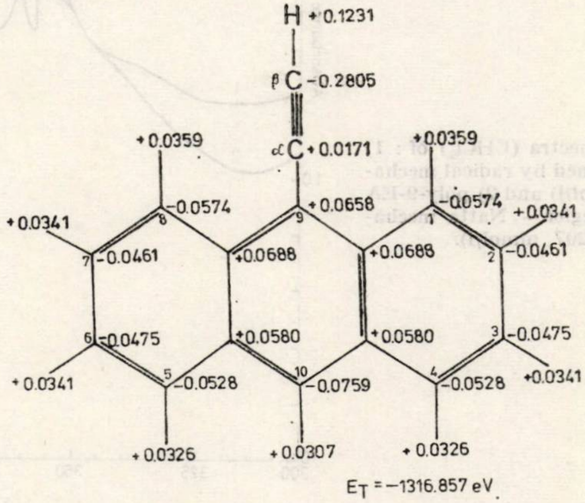

Fig. 3. — The total atomic charges in 9 — EA

Accepting that the radical formed by the interaction between 9 — EA and the radicals obtained from the polymerization initiator decomposition is located at the α — carbon atom (Fig. 4) we performed the molecular orbital (MO) calculations, considering that the aromatic rings remain in the plane with unchanged interatomic distances. The changes appear only in the vinyl unit.

Cα carbon atom, the formal unpaired electron carrier, is trigonal. The unpaired electron is placed in a p_z atomic orbital. The length between the radical carbon atom and the cycle is of 1.39 A°. The exocyclic double bound is of 1.34 A°. The bond lengths between trigonal carbon atom and exocyclic hydrogen are of 1.94 A° (Fig. 4). Taking into account that the carbon atom from the 10-position is formal unpaired electron carrier, we performed the MO calculation on the radicals presented in figure 5.

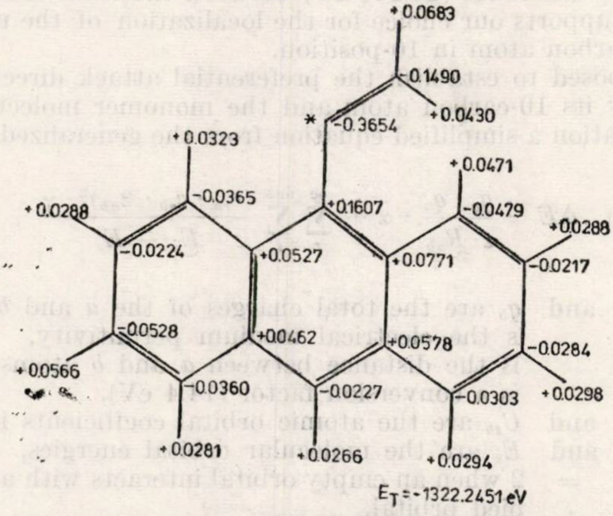
+0.0683
-0.1490
*
+0.0430
-0.3654
+0.0323
+0.0471
-0.0365
+0.1607
-0.0479
+0.0288
+0.0288
-0.0224
+0.0527
+0.0771
-0.0217
-0.0528
+0.0462
+0.0578
-0.0284
+0.0566
-0.0360
-0.0227
-0.0303
+0.0298
+0.0281
+0.0266
+0.0294
E_T = -1322.2451 eV

Fig. 4. — The total atomic charges in 9 — EA radical with unpaired electron at Cα carbon atom.

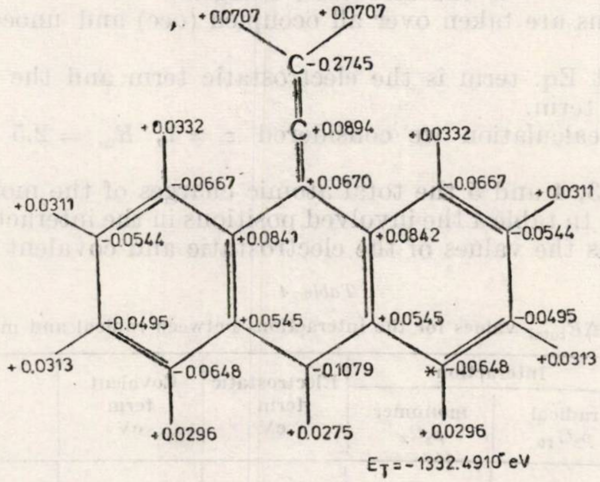
+0.0707
+0.0707
C -0.2745
+0.0332
C +0.0894
+0.0332
-0.0667
+0.0670
-0.0667
+0.0311
+0.0311
-0.0544
+0.0841
+0.0842
-0.0544
-0.0495
+0.0545
+0.0545
-0.0495
+0.0313
-0.0648
-0.1079
*
-0.0648
+0.0313
+0.0296
+0.0275
+0.0296
E_T = -1332.4910 eV

Fig. 5. — The total atomic charges in 9 — EA radical with unpaired electron at C_{10} carbon atom.

The aromatic cycles have been considered plane and all bond lengths remained unchanged. The only changes appear at the allenic system level bonded to the 9-position of the anthracene ring. The central carbon atom in the allenic system is digonal and the distance between this atom and the carbon atom in the 9-position is of 1.31 A°. The other double allenic bond was approximated at 1.34 A°. As we represented the radical geometries (Figs 4 and 5) we accepted that the interaction between the radical and the monomer molecule occurs at p_z orbital levels.

The large difference (10.246 eV) between the total energies given in Figs 4 and 5 supports our choice for the localization of the unpaired electron on the carbon atom in 10-position.

We proposed to establish the preferential attack direction between the radical by its 10-carbon atom and the monomer molecule. We used for ΔE calculation a simplified equation from the generalized perturbation theory.[20,21]

$$\Delta E = \frac{q_a \cdot q_b}{\varepsilon \cdot R_{ab}} \cdot \alpha + \sum_{r}^{\text{oc}} \sum_{s}^{\text{unoc}} \frac{(c_{ra} \cdot c_{sb} \cdot \beta_{ab})^2 \cdot \gamma}{E_r - E_s}$$

where :

q_a and q_b are the total charges of the a and b atoms,
ε is the electrical medium permitivity,
R_{ab} is the distance between a and b atoms,
α is a conversion factor (14.4 eV),
C_{ra} and C_{sb} are the atomic orbital coefficients in MO,
E_r and E_s are the molecular orbital energies,
γ = 2 when an empty orbital interacts with a double occupied orbital,
γ = 1 when a unielectron orbital interacts with an empty orbital or a double occupied orbital,
β_{ab} is the resonance integral.

The sums are taken over all occupied (occ) and unoccupied (unocc) orbitals.

The first Eq. term is the electrostatic term and the second one is the covalent term.

In our calculation we considered $\varepsilon = 1$, $R_{cc} = 2.5$ A° and $\beta_{cc} = 2.63$ eV. [22]

In Figs 3, 4 and 5 the total atomic charges of the molecular species are presented. In table 4 the involved positions in the interaction are specified, as well as the values of the electrostatic and covalent terms.

Table 4

The ΔE_{total} values for the interactions between radical and monomer

No.	Interaction		Electrostatic term eV	Covalent term eV	ΔE_{total} eV	
	radical p_zC_{10}	monomer p_zC_x				
1	C_{10}	C	−0.17424	−0.90190	−1.07614	I
2	C_{10}	C_{10}	+0.04708	−0.98386	−0.93678	II
3	C_{10}	C_4	+0.03283	−0.93146	−0.89863	III
4	C_{10}	C_1	+0.03571	−0.93037	−0.89466	IV
5	C_{10}	C_2	+0.02865	−0.89949	−0.87084	V
6	C_{10}	C_3	+0.02952	−0.89657	−0.86705	VI
7	C_{10}	C_α	+0.01051	−0.80511	−0.79460	VII

Depending on the sign of the electrostatic term, the only favorized interaction could be the $C_{10}-C_{\beta}$ interaction. The same interaction is favorized by the value of the total energy change. The sterical factors can stop this interaction. The interactions between radical by its carbon atom 10 and the molecule by its carbon atom 10 follow. This theoretical results suggest the polymerization mechanism presented in scheme 2. The initiator radical attacks the β position carbon atom in monomer and the new obtained radical by its C_{10} carbon atom attacks the β position monomer. The new radical could continue the polymerization. Because the radical initiators were the benzoyl peroxide and azobisis obutyronitrile it is possible that the energy differences between the radicals given in Figs 4 and 5 be more diminished. Therefore, the proposed mechanism does not exclude the possibility of polymerization at the triple bond level.

The studied radicals were prepared by formal addition of a hydrogen-atom to C_{β} carbon atom in 9—EA.

Experimentally it is observed that the polymer obtained by a radical mechanism contains dihydroanthracene and polyene units. The polyenic structures are obtained by the radicalic attack by its $C\alpha$ atom on the $C\beta$ carbon atom in monomer. The ratio of the band at 730 cm assigned to the polyenic structure and 750 cm absorbancies (assigned to the dihydroanthracene structure)[2] shows a larger polyenic content (scheme 3).

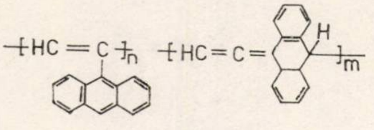

$n > m$

The used experimental conditions (solvent, temperature, initiator, etc.) could change the nature of the reaction products.

REFERENCES

[1] Part XXXIV, Sv. Dumitrescu, M. Grigoraş and C. I. Simionescu, *European Polymer J.*, in press.

[2] C. I. Simionescu, Sv. Dumitrescu, M. Grigoraş and I. Negulescu, *J. Macromol. Sci.—Chem.*, **A13**, 203 (1979).

[3] C. I. Simionescu, Sv. Dumitrescu, I. Negulescu, V. Percec, M. Grigoraş, I. Diaconu, M. Leancă and L. Goraş, *Vysokomol. Soedineniya*, **A16**, 790 (1974).

[4] N. P. Buu Hoi, P. Daudel, R. Daudel, P. Jacquignon, G. Morin, R. Muxart and C. Sandorfy, *Bull. Soc. chim. France*, **1951**, 132C.

[5] R. Calas and R. Lalande, *Bull. Soc. chim. France*, **1959**, 763.

[6] J. K. S. Wan, R. N. McCormick, E. J. Baum and J. N. Pitts jr., *J. Amer. Chem. Soc.*, **87**, 4409 (1965).

[7] A. Castellan, R. Lapouyade and H. Bouas-Laurent, *Bull. Soc. chim. France*, **1976**, 201, 210.

[8] O. L. Gijzeman, F. L Kaufman and G. Porter, *J. Chem. Soc. Faraday Trans.*, **69**, 708 (1973).

[9] E. Wasserman, V. J. Kuck, W. M. Delvan and W. A. Yager, *J. Amer. Chem. Soc.*, **91**, 104 (1969).

[10] J. Aspler, D. J. Carlson and D. M. Wiles, *Macromolecules*, **9**, 691 (1976).

[11] D. J. Carlson, A. Garton and D. M. Wiles, *Macromolecules*, **9**, 695 (1976).

[12] G. Meyer, *Ref. Gen. Cout. Plast.*, **49**, 443 (1972) ; G. Meyer, *Bull. Soc. chim. France*, **1970**, 702.

[13] B. Stevens, S. A. Perez and J. A. Ors, *J. Amer. Chem. Soc.*, **96**, 6846 (1974).

[14] N. Sugyiama, M. Iwata, M. Yoshioka, K. Yamada and H. Aoyama, *Bull. Chem. Soc. Japan*, **42**, 1377, 1379 (1969).

[15] E. L. May and E. Mosetting, *J. Amer. Chem. Soc.*, **73**, 130 (1951).

[16] D. D. Phillips and J. Cason, *J. Amer. Chem. Soc.*, **74**, 2934 (1952).

[17] G. Klopman, *J. Amer. Chem. Soc.*, **90**, 223 (1968).

[18] L. Salem, *J. Amer. Chem. Soc.*, **90**, 543 (1968).

[19] R. Hoffmann, *J. Chem. Phys.*, **39**, 1397 (1963), **40**, 2474, 2480 2745 (1964).

[20] G. Klopmann, "Chemical Reactivity and Reaction Paths", Wiley, New York, 1974, p. 55.

[21] K. Fukui, C. Nagata, T. Yonezawa, H. Kato and M. Morakuma, *J. Chem. Pys.*, **31**, 287 (1959).

[22] K. N. Houk, J. Sims, E. R. Duke, R. W. Strozier and Y. K. George, *J. Amer. Chem. Soc.*, **95**, 7287 (1973).

Revue Roumaine de Chimie 29, 5, 457–460 (1984)

COORDINATION POLYMERS. VI[1]

PREPARATION AND CHARACTERIZATION OF SOME AZOMETHINE CHELATE POLYMERS

MIHAELA SPIRATOS, A. AIRINEI, G.I. RUSU and AGLAIA CIOBANU
"P. Poni" Institute of Macromolecular Chemistry, R-6600 Iaşi, Romania

Received December 15, 1982
Completed September 28, 1983

Chelate polymers of azomethine complexes have been synthesized by interfacial polycondensation with organic diacid chlorides. Elemental analysis, magnetic, spectral and thermal properties as well as electrical conductivities of the polychelates are presented.

Synthesis and characterization of some polymers containing metal in the main chain have become of great importance in the last years because of the growing interest regarding their properties.

Our investigations concerning synthesis of chelate polymers from bisphenol complexes and aromatic acid chlorides are also situated on this line.[1–5]

The present communication describes the synthesis and properties of some chelate polymers derived from bis(2,4-dihydroxybenzaldehyde) ethylenediimine M^{2+} with aromatic diacid chlorides (terephthaloyl and isophthaloyl chlorides). The chelate polyesters correspond to the following general formula :

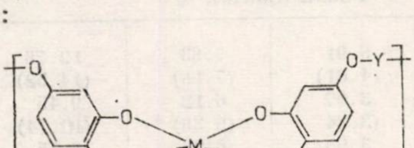

where : $M = Fe^{2+}$(I) ; Co^{2+}(II) ; Cu^{2+}(III) ; Z^{2+}(IV) for the chelates and : I_a, II_a, III_a, IV_a ; $Y = p-COC_6H_4CO-$
I_b, II_b, III_b, IV_b ; $Y = m-COC_6H_4CO-$
for the polymers.

EXPERIMENTAL

Bis(2,4-dihydroxybenzaldehyde) ethylenediimine Fe^{2+} (I) and bis(2,4-dihydroxybenzaldehyde)ethylenediimine Co^{2+}(II) were prepared by the reaction between 2 moles of resorcylic aldehyde in ethanol and 1 mole of iron or cobalt acetate respectively in water, added to the hot solution of 80 % ethylenediimine.

Bis(2,4-dihydroxybenzaldehyde)ethylenediimine Cu^{2+} (III) was synthesized as described elsewhere.[6] Bis(2,4-dihydroxybenzaldehyde)-ethylenediimine Zn^{2+} (IV) was obtained by heating an ethanolic solution of bis(2,4-dihydroxybenzaldehyde)ethylenediimine and zinc acetate in water for two hours on a water bath.

The chelate polyesters were synthesized from the chelates (I—IV) and the diacid chlorides by interfacial polycondensation.[7,8] In this method, 8.33×10^{-3} moles of complex salt in aqueous alkali (1.67×10^{-2} moles in 100 ml of water) reacted with 8.33×10^{-3} moles diacid chloride (terephthaloyl and isophthaloyl chlorides) in dichloromethane, in the presence of sodium lauryl sulfate, as dispersion agent. The mixture was vigorously stirred for 5—8 min and the polymers were isolated by precipitation in acetone. They were purified by repeated extractions with methanol and ethanol.

All the polymers are powdery in appearance, insoluble in water and in common organic solvents. Owing to their insolubility, molecular weight determinations are not possible by usual methods.

The water content of polychelates was estimated from the corresponding thermograms. The infrared and electronic absorption spectra, magnetic susceptibilities, thermogravimetrical and electrical conductivity measurements were carried out according to a previous work.[1]

RESULTS AND DISCUSSIONS

The analytical data (Table 1) show that the reaction between chelate monomer and aromatic acid chloride takes place at a molar ratio of 1 : 1.

The magnetic measurements established that all chelates and polychelates of Fe^{2+}, Co^{2+} and Cu^{2+} were paramagnetic. The paramagnetism of Fe^2 polymers is the result of an octahedral configuration achieved by the metal atom by coordination of two water molecules. The presence of water molecules is supported by the TG data and elemental analysis (Table 1).

Table 1

Elemental analysis, magnetic and thermal properties of chelate polyesters

Compound	C	H	N	M	μ_{eff} (MB)	T_d^* (°C)
	Found (Calcd.), %					
I	48.76 (49.25)	3.91 (4.61)	7.83 (7.18)	12.76 (14.32)		
I_a	54.95 (55.40)	3.97 (3.84	6.12 (5.38)	9.45 (10.74)	3.87	220
I_b	55.01 (55.40)	3.95 (3.84)	6.23 (5.38)	9.55 (10.74)		
II	44.15 (44.76)	5.35 (5.12	6.14 (6.52)	12.23 (13.73)		
II_a	51.26 (51.52)	5.06 (4.29)	5.76 (5.00)	9.27 (10.54)	1.88	155
II_b	50.67 (51.52)	4.33 (4.29)	5.67 (5.00)	9.46 (10.54)		
IV	47.63 (48.07)	3.94 (4.50)	6.76 (7.01)	15.85 (16.36)		
IV_a	54.78 (54.40)	3.56 (3.77)	5.45 (5.28)	11.76 (12.64)	diamagnetic	230
IV_b	53.85 (54.40)	3.56 (3.77)	5.79 (5.28)	11.53 (12.64)		

* Decomposition temperature taken as point of deviation from the base line of the TG curve.

The presence of nonequivalent ligands causes a strong distortion from the octahedral symmetry, proved by the absorption band at 450 nm and the smaller values of magnetic moment.[9]

The electronic reflexion spectra show the presence of absorption bands at 450–750 nm for the polymers II_a, II_b and the magnetic moment is specific to an octahedral configuration with low spin for the cobalt atom.[10–12]

The Cu^{2+} polymers show the magnetic moment of 1.34 MB and a strongly distorted octahedral configuration. The magnetic moment is much smaller as a result of the strong interaction between copper ion and the organic part of the polymer, leading to the decrease of the charge density on the copper atom.[13–14]

The Zn^{2+} polychelates were diamagnetic and show an absorption band at 375 nm specific to water adducts.[15,16]

IR absorption spectra of the polychelates exhibit a strong absorption band at about 1720 cm^{-1} assigned to C=O stretching frequency due to polyester formation and an absorption band at approximately 1615 cm^{-1} assigned to stretching frequency of C=N group. The last absorption band shifts towards lower frequency in polychelates (relating to ligand) due to involvement of nitrogen in coordination. A weak broad absorption band at about 3400 cm^{-1} confirms the presence of water molecules.

From thermograms, the weight loss, due to water molecules in polychelates, approaches the theoretical amounts for dihydrates (7–8%).

The decomposition temperature (Table 1) calculated from TG curves indicate the following thermal stability order :

$$Ni^{2+} > Zn^{2+} > Cu^{2+} > Fe^{2+} > Co^{2+}$$

The rapid change in weight on further heating after the water los hows the decomposition temperature of the ligand, the final decomposition product being the respective metal oxide in most cases.

Table 2

Electrical properties of polychelates

Sample	ΔT (°C)	ΔE (eV)	σ_{298K} ($\Omega^{-1}\cdot cm^{-1}$)	σ_0 ($\Omega^{-1}\cdot cm^{-1}$)
I_a	300–450	1.55	$6.12.10^{-8}$	$3.60.10^2$
I_b	300–450	1.50	$6.53.10^{-8}$	$5.66.10^2$
II_a	300–480	1.50	$7.33.10^{-8}$	$2.08.10^2$
II_b	300–480	1.50	$7.89.10^{-8}$	$3.50.10^2$
III_a	300–465	1.20	$1.17.10^{-8}$	$4.76.10^{-1}$
III_b	300–465	1.35	$2.20.10^{-8}$	$7.12.10^{-1}$
IV_a	300–475	1.75	$1.50.10^{-9}$	$1.61.10^2$
IV_b	300–465	1.80	$5.11.10^{-9}$	$4.50.10^2$
PBS	300–480	1.70	$8.06.10^{-9}$	$4.50.10^2$

The electrical resistivity of the coordination polymers was determined over a broad range of temperatures (Table 2).

Plots of $\ln \sigma$ (electrical conductivity) versus reciprocal temperature are linear and they satisfy the relation :

$$\sigma = \sigma_0 \cdot \exp(-\Delta E/2kT)$$

where σ_0 is the electrical conductivity at infinite temperature and ΔE is the activation energy. Values of σ_0, which provides a measure of carrier mobility and of activation energy of electrical conduction, ΔE, are given in Table 2.

The conductivities of polychelates, despite their metal content are rather low. Within the whole temperature range, the conductivity varied between $10^{-7}-10^{-10}\Omega^{-1} \cdot cm^{-1}$.

The values of activation energy increase in the following order: $Cu^{2+} < Co^{2+} < Fe^{2+} < Ni^{2+} < Zn^{2+}$.

The low conductivity of poly (Schiff bases) (PSB) can be attributed to the low molecular weight and the low extent of conjugation.

The sign of Seebeck coefficient is positive, indicating the predominance of holes as majority charge carriers and suggesting that the poly chelates are p-type semiconductors.

All the polychelates can be decomposed with dilute acids ; the original Schiff base (PSB) and appropriate metal salt are easily obtained

The geometry of the ligand, composition, high insolubility of the polychelates and their thermal stability indicate the polymeric nature of the compounds.

REFERENCES

[1] M. Spiratos, A. Airinei, G. I. Rusu and A. Ciobanu, *Polym. Bull.*, **6**, 243 (1982).

[2] M. Spiratos, A. Airinei and M. Bostan, *Mater. Plast.*, **16**, 137 (1979).

[3] M. Spiratos, A. Airinei and A. Ciobanu, *Rev. Roumaine Chim.*, **25** 1083 (1980).

[4] G. Singurel, A. Airinei, M. Spiratos and G. I. Rusu, *An. Stiinţ. Univ. "A.I. Cuza" Iaşi, Sect. 1b*, **26**, 103 (1980).

[5] M. Spiratos, G. I. Rusu, A. Airinei and A. Ciobanu, *Angew. Makromol. Chem.*, **107**, 33 (1982).

[6] P. Pfeiffer, E. Breith, E. Lübbe and T. Tsumaki, *Liebigs Ann. Chem.*, **503**, 84 (1933).

[7] W. M. Eareckson, *J. Polym. Sci.*, **40**, 399 (1959).

[8] L. V. Interrante and J. C. Bailar, jr., *Inorg. Chem.*, **3**, 1339 (1964).

[9] J. L. K. F. De Vries, J. M. Trooster and E. D. Boer, *J. Chem. Soc., Dalton Trans.*, **1974**, 1771.

[10] C. Busetto, F. Cariati, A. Fusi, M. Gulotti, F. Marazzoni, A. Pasini, R. Ugo and V. Valenti, *J. Chem. Soc., Dalton Trans.*, **1973**, 754.

[11] M. Calligaris, G. Nardin and L. Randaccio, *J. Chem. Soc., Dalton Trans.*, **1973**, 419.

[12] E. I. Ochiai, *J. Inorg. Nuclear Chem.*, **25**, 1727 (1973).

[13] V. V. Rode, L. I. Nekrasov, A. P. Terenteev and E. G. Rukhadze, *Vysokomol. Soedineniya*, **4**, 13 (1962).

[14] R. K. Kohli and P. K. Bhattacharya, *Bull. Chem. Soc. Japan*, **49**, 2872 (1976).

[15] G. E. Batley and D. P. Gaddon, *Austral. J. Chem.*, **20**, 887 (1967).

[16] A. Furuhashi and H. Yokota, *Bull. Chem. Soc. Japan*, **52**, 3753 (1979).

Revue Roumaine de Chimie, 29, 5, 461–463 (1984)

APPLICATIONS OF PHASE TRANSFER CATALYSIS IN THE ACRIDINE SERIES. II[1]

SYNTHESIS OF SOME ACRIDINE ETHERS

M. VLASSA and MARIA KEZDI
Institute of Chemistry Cluj-Napoca, str. Fîntînele 30, Romania

Received December 8, 1982

Aromatic acridine ethers were obtained by phase transfer catalytic reaction between 9-chloroacridine and substituted phenols $X-C_6H_4-OH$(where X=H, $m-CH_3$, $p-CH_3$, p-NH_2 and p-Cl), tetrabutylammonium bromide being used as the phase transfer catalyst.

Phase transfer catalysis showed itself excellently suited for C-alkylation of phenols with various reactants such as alkylhalides [2] dihalides, [3] epychlorohydrine, [4] alkyl sulphates [5] and more recently chloropyrydine and chloroquinolines. [6]

Continuing our studies[1,7] on phase transfer reactions in the acridine series we prepared ethers by the general reaction shown below : [8]

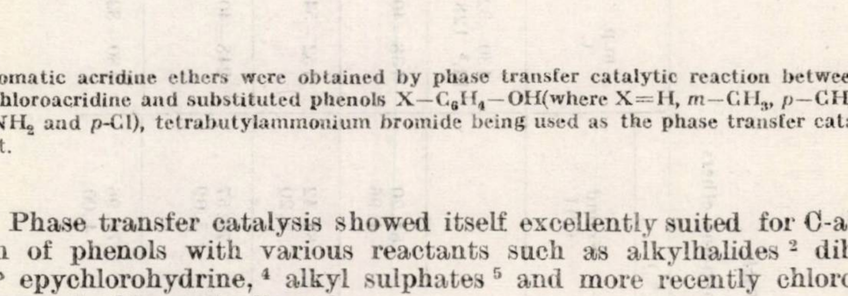

The results are shown in the Table.

EXPERIMENTAL

All m.p.'s were determined with a Boetius apparatus and are uncorrected. Infrared spectra were recorded in KBr pellets with a Unicam SP 200 G spectrophotometer.

General synthetic procedure : 6 ml of 50% aqueous sodium hydroxide solution, 2.3 mmoles of the appropriate phenol, 6 ml of toluene, 2.3 mmoles of 9-chloroacridine and 0.3 mmoles of tetrabutylammonium bromide were placed in a stoppered 100 ml flask and magnetically stirred for 4.5 hours at 85°C. The reaction mixture was then poured in 50 ml water and extracted with 3 × 25 ml of toluene. The organic layer was concentrated *in vacuo*, the residue taken up with 2N aqueous NaOH, filtered off, washed with water and dried.

To obtain analytically pure compounds, these crude products were recrystallized from ethanol-water.

Table

Aromatic acridine ethers

Starting phenol	Yield %	Analysis (%)		m.p. °C	IR absorption bands cm^{-1}
		Calcd. C/H	Found C/H		
Phenol	94			130–32 lit.[8] 128	3050,1620,1595,1560,1520,1442,1420, 1362,1230,1096,882,780
m-Cresol	61	84.21 5.25	84.20 4.96	138–40	3040,1615,1605,1556,1515,1440,1410, 1359,1250,1080,1020,940,782,772
p-Cresol	100		84.42 5.20	152–54	3050,1615,1600,1562,1518,1442,1420, 1369,1222,1096,1020,879,835,782,760
p-Aminophenol	44	79.72 4.90	79.57 5.09	248–40	3425,3300,3200,1630,1600,1560,1515, 1440,1420,1365,1218,1098,1020,890, 840,778
p-Chlorophenol	46	74.75 3.93	74.96 4.00	180–82	3030,1620,1582,1555,1518,1440,1418, 1360,1229,1080,1018,880,850,822,778

REFERENCES

[1] M. Vlassa, M. Kezdi and I. Goia, *Synthesis*, **1980**, 851.

[2] A. Mc Killop, Y.-C. Viout and R. P. Hug, *Tetrahedron*, **30**, 1379 (1974).

[3] E. d'Incan and P. Viout, *Tetrahedron*, **31**, 159 (1975).

[4] D. J. Nelson and E. A. Uschak, *J. Org. Chem.*, **42**, 3308 (1977).

[5] A. P. Bashall and J. F. Collins, *Tetrahedron Letters*, **1975**, 3489.

[6] H. Alsaidi, R. Gall and J. Metzger, *Synthesis*, **1980**, 921.

[7] M. Vlassa, I. Goia and M. Kezdi, Roum. Pat., 67031

[8] A. Albert "The Acridines" second edition, Edward Arnold Ltd., London, 1966, p. 282.

Revue Roumaine de Chimie, 29, 5, 465 (1984)

COMPTE RENDU

A. T. BALABAN, M. BANCIU, I. POGANY: *"Application of Physical Methods in Organic Chemistry"*, Ed. Ştiinţifică şi Enciclopedică, Bucharest, 1983, 287 p. (in Romanian)

The interaction between radiation and matter has become a useful and profitable analytical and research method currently used by practising chemists. This book is different from everything we have been offered so far. Beginning with the basic principles of spectroscopy, the book proceeds step by step to expose the five main spectroscopic methods (see below) and in this way it may be read without any spectroscopic knowledge. Although it contain principles and basic relations of spectroscopy and can be used independently, the authors intended it to be an application to another book (I. Pogany and M. Banciu, *"Physical Methods in Organic Chemistry"*, 1973) edited by the same publisher, also in Romanian.

There is a great task to cumulate in a short book both the principles and up-to-date information about spectroscopy, but the authors' experience in teaching, vehiculating and using spectroscopic data overcame the difficulties. The aim of the book is to show and to teach how one can correlate spectroscopic methods to elucidate the structure of organic (synthetic or natural) compounds and this is the content of the first chapter (10 pp). The book may be divided then into two parts. The first one refers to the general principles of common spectroscopic methods and their correlation, and the second covers several problems as models illustrating how they can be used. Therefore the next four chapters of the first part contain the essential of spectroscopy including many tables about IR (27 p.) UV-VIS (21 p.) ^{1}H-NMR-,^{13}C-NMR (40 p.) and mass spectrometry (30 p.). A special chapter (the 6th) is devoted to the integrated spectrometric methods and it is completed with tables compiling characteristic properties of each spectroscopic method. The same chapter includes a very interesting and useful synoptical table containing different spectroscopic properties of the main classes of organic compounds.

In the second part of the book (chapters 7 and 8, 140 p). sixty examples of organic structures are proposed to illustrate how one can use in practice the knowledge about different spectra to elucidate organic structures. Examples are selected very carefully either from the literature sources or (most of them) from the authors' long period of own research. The illustrating examples include the most important typs of organic compounds which the reader can meet in laboratory or industrial practice. The first fifteen models, each illustrated by UV-VIS, IR, ^{1}H-NMR, ^{33}C-NMR and mass spectra are discussed in detail by the authors, using sometimes also graph theoretical methods, in order to indicate the possibilities and the limits of each kind of spectra. The final 45 examples are offered to the reader to solve the problems helping him/her by gradual answers, to be found at the end of the book.

Each chapter is provided with a selected and representative bibliography, in several cases also with the latest monographs which provide the reader with supplementary reading. A special mention must be made about the graphical quality of tables, figures, formulas and spectra recorded under usual routine conditions which is very commendable and makes the reading attractive and easy.

Authors' thorough insight into the spectroscopy field and their long experience in research and teaching at the university level are reflected in the accuracy of the work and in the special attention given to definition terminology, chemical nomenclature and particularly to the educational side. Old subjects as for example UV-VIS spectroscopy are completed with modern aspects regarding the polarity of organic solvents or the incremental calculation of absorption maxima for conjugated multiple bonds. Many similar examples may be given. The whole book is permeated by the organic chemical philosophy, specially useful for students, proving that our knowledge about chemical bonds, intermediate reactive species (radicals, ions etc.), configuration and conformation of organic compounds, has a sound base which allows to understand and to predict the behaviour of unknown cases. Owing to these features the volume may be used as an excellent textbook for students of chemical faculties. The book will surely be of great use not only to chemistry students and teaching staff but also to anyone interested in the subject, be he a beginner or an old hand. In conclusion this is a very useful textbook for freshman wishing to obtain an accurate modern picture of the possibilities and limits in the combined use of spectroscopic methods to elucidate the structure of organic compounds.

An evidence of the interest aroused by this volume is the fact that it was out of print shortly after its publication so that many of those interested have failed to procure it. For this reason a second edition would be welcome.

Flavian Cuiban

ORSZÁGOS MŰSZAKI INFORMÁCIÓS KÖZPONT ÉS KÖNYVTÁR
1883

NOTE POUR LES AUTEURS

La Revue Roumaine de Chimie publie des articles en anglais, français, russe, allemand ou espagnol. Les auteurs sont priés d'envoyer des articles et des comptes rendus inédits.

Les manuscrits seront dactylographiés à double interligne. La bibliographie, les tableaux et la légende des figures seront placés après le texte.

Si l'article fait partie d'une série numérotée, la partie précédente sera donnée comme première référence.

Chaque article sera précédé d'un résumé comprenant quinze lignes au maximum.

Les références bibliographiques dans le texte seront faites par des exposants sans parenthèses et paraîtront à la fin de l'ouvrage.

Les publications périodiques mentionnées dans la bibliographie seront présentées suivant les prescriptions internationales : le nom de l'auteur précédé de l'initiale du prénom, le titre du périodique abrégé conformément à « Chemical Abstracts » et souligné par une ligne, le numéro du tome indiqué par des chiffres arabes et souligné par deux lignes, suivi de la première page de l'article ; à la fin, l'année de la parution sera placée entre parenthèses. Le numéro de la revue ne sera pas indiqué si les pages du volume sont numérotées consécutivement.

Les textes des livres ou traités incluront : le nom des auteurs, l'initiale du prénom, le titre du livre entre guillemets et sans être souligné, le numéro du tome précédé par l'abréviation « vol. » (ou « Bd. »), le numéro de l'édition, les éditions (the publisher), la localité de la parution du livre, l'année de la parution et la page de la référence précédée(s) par l'abréviation « p » (ou « S »).

Les brevets seront indiqués comme suit : l'auteur ou la firme, le pays et le numéro du brevet, la date et la revue (*Chem. Abstr.*). Par ex. : M. Jones (to Union Carbide Co.), Brit. Pat. 601 238, 2 Sept. 1959 ; cf. *Chem. Abstr.*, **54**, 12808 (1960).

Si la référence n'a pas été lue en original, on indiquera aussi la revue de référence consultée.

Les diagrammes seront tracés à l'encre de Chine sur papier calque. Les tableaux et les figures (en nombre strictement nécessaire) ainsi que les courbes dans les figures seront numérotés par des chiffres arabes. Leur explication sera donnée dans la légende des figures. Prière de ne pas inscrire les mêmes données dans les tableaux et les figures. Chaque tableau aura un titre. On indiquera dans le texte la place approximative des tableaux et des figures. Les formules chimiques seront incluses dans le texte ; en outre, elles seront transcrites sur papier calque, à l'encre de Chine.

Les auteurs sont priés d'indiquer les caractères italiques (en soulignant les lettres au crayon), ainsi que tout autre caractère spécial ; les préfixes *ortho, meta, para, cis, trans*, etc. seront soulignés pour indiquer leurs caractères italiques et ne seront jamais écrits avec des majuscules.

Aucune correction à la main ne sera admise sur le manuscrit. Les corrections seront tapées à la machine. Les lettres grecques ou d'autres symboles spéciaux seront insérés à la main à l'encre clairement.

Le manuscrit sera signé par l'auteur.

Le titre-courant aura 50 lettres au maximum.

L'entière responsabilité du contenu des articles appartient aux auteurs.

Sur demande on peut obtenir une note plus complète.

PRINTED IN ROMANIA

1984 SEP 6

TRAVAUX PARUS AUX ÉDITIONS DE L'ACADÉMIE DE LA RÉPUBLIQUE SOCIALISTE DE ROUMANIE

ELENA CEAUȘESCU, **Cercetări în chimia și tehnologia polimerilor** (Recherches de chimie et technologie des polymères), 1983, 519 p.

E. SEGAL, D. FĂTU, **Introducere în cinetica neizotermă** (Introduction à la cinétique non isotherme), 1983, 299 p.

N. IONESCU, M. CĂLDĂRARU, **Oxidarea catalitică a olefinelor inferioare** (L'oxydation catalytique des oléfines inférieures), 1983, 178 p.

C. CAȘCAVAL, **Studiul polimerilor prin piroliză și cromatografie de gaze** (L'étude des polymères par pyrolyse et chromatographie à gaz), 1983, 220 p.

C. I. SIMIONESCU, F. DENEȘ, **Originea vieții** (L'origine de la vie), 1983, 110 p.

C. BODEA (sous la direction de), **Tratat de biochimie vegetală** (Traité de biochimie végétale), IIe p., IV, 1982, 408 p.

I. G. MURGULESCU, RODICA VÎLCU, **Introducere în chimia fizică, Vol. III. Termodinamica chimică** (Introduction à la chimie physique, Vol. III, Thermodynamique chimique), 1982, 626 p.

I. G. MURGULESCU, J. PĂUN, **Introducere în chimia fizică, Vol. 1.3. Nucleul atomic, reacții nucleare, particule elementare** (Introduction à la chimie physique. Vol. 1.3. Noyau atomique, réactions nucléaires, particules élémentaires), 1982, 606 p.

ELENA JERCAN, **Analiza cromatografică** (Analyse chromatographique), 1982, 286 p.

ELENA CEAUȘESCU, **Noi cercetări în domeniul compușilor macromoleculari** (Nouvelles recherches dans le domaine des composés macromoléculaires), 1981, 536 p.

I. G. MURGULESCU, TATIANA ONCESCU, E. SEGAL, **Introducere în chimia fizică. Vol. II. 2 Cinetică chimică și cataliză** (Introduction à la chimie physique. Vol. II. 2. Cinétique chimique et catalyse), 1981, 1024 p.

V. DRĂGUȚAN, A. T. BALABAN, M. DIMONIE, **Metateza olefinelor și polimerizarea prin deschidere de inel a cicloolefinelor** (La métathèse des oléfines et la polymérisation par ouverture annulaire des cyclooléfines), 1981, 254 p.

LYDIA-MARIA VAICUM, **Epurarea apelor uzate cu nămol activ. Bazele biochimice** (L'épuration des eaux résiduelles à boue active. Les bases biochimiques). 1981, 218 p.

I. GĂLĂȚEANU, **Procese și metode radiochimice în energetica nucleară** (Processus et méthodes radiochimiques dans l'l'énergétique nucléaire), 1981, 234 p.

OCTAVIAN IORDACHE, **Procese polistocastice aplicate la fenomenele de transfer** (Processus polystochastiques appliqués aux phénomènes de transfert), 1981, 186 p.

CR. SIMIONESCU, VALERIA GORDUZA, **Polimeri biocompatibili și biologic activi** (Polymères biocompatibles et biologiquement actifs), 1980, 479 p.

ELENA CEAUȘESCU, **Polimerizarea stereospecifică a izoprenului** (La polymérisation stéréospécifique de l'isoprène), 1979, 307 p.

CONST. GH. MACAROVICI, **Analiza chimică cantitativă anorganică** (L'analyse chimique quantitative inorganique), 1979, 457 p.

M. FLORESCU, **Metode științifice în dezvoltarea industriei chimice moderne** (Méthodes scientifiques dans le développement de l'industrie chimique moderne), 1979, 256 p.

A. T. BALABAN, I. GĂLĂȚEANU, G. GEORGESCU, LIGIA SIMIONESCU, **Compuși marcați și radiofarmaceutici cu aplicații în medicina nucleară** (Composés marqués et radiopharmaceutiques à application en médecine nucléaire), 1979, 495 p.

I. G. MURGULESCU, E. SEGAL, **Introducere în chimia fizică, Vol. II. 1. Teoria molecular cinetică a materiei** (Introduction à la chimie physique. Vol. II. 1. La théorie moléculaire-cinétique de la matière), 1979, 1036 p.

S. STERNBERG, FL. DANEȘ, **Termodinamica chimică aplicată** (La thermodynamique chimique appliquée), 1978, 400 p.

I. G. MURGULESCU, V. EM. SAHINI, **Introducere în chimia fizică. Vol. I. 2. Structura și proprietățile moleculelor** (Introduction à la chimie physique. Vol. I.2. La structure et les propriétés des molécules), 1978, 604 p.

I. ZUGRĂVESCU, MAGDA PETROVANU, **N-ylid chemistry**, coédition avec McGraw-Hill International Book Company, U.S.A., 1977, 396 p.

I. G. MURGULESCU, **Introducere în chimia fizică. Vol. I. 1. Atomi, molecule, legătură chimică** (Introduction à la chimie physique. Vol. I.1. Atomes, molécules, liaison chimique), 1976, 560 p.

ELENA CEAUȘESCU, **Research work on synthesis and characterization of macromolecular compounds. Contributions**, 1974, 251 p.

CR. SIMIONESCU, VIORICA RUSAN, V. POPA, **Chimia algelor marine** (La chimie des algues marines), 1974, 212 p., 1 pl.

ISSN 0035–3930

I. P. „Informația" c. 2065

43 426

Lei 40

$ 75 (pour un abonnement annuel)

F1103
04
Vegyészet
REFERALVA

ACADÉMIE DE LA RÉPUBLIQUE SOCIALISTE DE ROUMANIE

REVUE ROUMAINE DE CHIMIE

TOME 29
N° 6
Juin 1984

EDITURA ACADEMIEI REPUBLICII SOCIALISTE ROMÂNIA
Rev. Roumaine Chim.
RRCHAX, 29, 6, p. 467 – 538 (1984), Bucarest

ACADÉMIE DE LA RÉPUBLIQUE SOCIALISTE DE ROUMANIE

COMITÉ DE RÉDACTION

Rédacteur en chef :

I. G. MURGULESCU, membre de l'Académie de la République Socialiste de Roumanie

Rédacteurs en chef adjoints :

A. T. BALABAN et V. EM. SAHINI, membres correspondants de l'Académie de la République Socialiste de Roumanie

Collège de rédaction :

EM. BRATU, ELENA CEAUȘESCU, ECATERINA CIORĂNESCU-NENITZESCU, CR. SIMIONESCU, membres de l'Académie de la République Socialiste de Roumanie ; P. SPACU, membre correspondant de l'Académie de la République Socialiste de Roumanie ; MARGARETA AVRAM, M. BANCIU, I. HAIDUC, D. I. MARCHIDAN, I. MOLDOVAN, G. NIAC et D. SĂNDULESCU

La Revue Roumaine de Chimie paraît 10 fois par an. Toute commande de l'étranger pour les travaux parus aux Editions de l'Académie de la République Socialiste de Roumanie sera adressée à ROMPRESFILATELIA—sectorul Export-Import Presă, P.O.Box, 12—201, télex 10376 prsfi r Bucarest, Calea Griviței nr. 64—66, Roumanie

Les manuscrits, les livres et les revues proposés en échange, ainsi que toute correspondance seront envoyés à la rédaction

REVUE ROUMAINE DE CHIMIE
125, Calea Victoriei, 79717 Bucarest, Roumanie, téléphone 50 76 80

EDITURA ACADEMIEI REPUBLICII SOCIALISTE ROMÂNIA
125, Calea Victoriei, 79717 Bucarest, Roumanie, téléphone 50 76 80

REVUE ROUMAINE DE CHIMIE

ORSZÁGOS MŰSZAKI INFORMÁCIÓS KÖZPONT ÉS KÖNYVTÁR
1983

Tome 29, N° 6 Juin, 1984

M. ANDRUH, C. I. LEPADATU and MARIA BREZEANU, Calculation of force constants for $[MCl_4]^{n-}$ complexes in the nuclear effective charge model 469–473
CONSTANȚA GHEORGHIU, CORNELIA GURAN, AURELIA MEGHEA and IOANA JITARU, Chromium (III) complex thiocyanates with biguanidine derivatives 475–482
DAN DONESCU, ION DEACONESCU and KRISTIANA GOȘA, Influence of coemulsifiers on the emulsion polymerization of vinyl acetate in the presence of hydroxyethylcellulose 483–488
MARIUS H. TERDIC, Disubstituted phenothiazones. II. New halogeno-3H-phenothiazin-3-ones 489–495
HOCINE KADI and D. P. LAZĂR, Identification of the aromatic hydrocarbons in some petroleum fractions. I. Experimental conditions in HPLC (in French) 497–505
LUMINIȚA VLĂDESCU and STELUȚA GHINEA, Separation and concentration of thiosulphate with ion-exchange resins . . . . 507–511 R
SVETLANA DUMITRESCU, M. GRIGORAȘ, G. SURPĂȚEANU and M. CONSTANTINESCU, On the polymerization of acetylenic derivatives. XXXVI. The cationic polymerization of 9-ethynylanthracene 513–520
GH. MANDRIC, GH. PETRACHE, ELENA PĂTRĂHĂU and TH. POPA, High-temperature polymers. V. Ordered benzothiazole-imide copolymers 521–530

IN MEMORIAM: MARGARETA AVRAM (1920–1983) 531–532

BOOK REVIEWS 533–537

Rev. Roumaine Chim. **29**, *6*, 467–538 (1984), Bucarest

Revue Roumaine de Chimie, **29**, *6*, 469–473 (1984)

CALCULATION OF FORCE CONSTANTS FOR $[MCl_4]^{n-}$ COMPLEXES IN THE NUCLEAR EFFECTIVE CHARGE MODEL

M. ANDRUH *, C. I. LEPADATU * and MARIA BREZEANU **
* Center of Physical Chemistry ICECHIM, Bucharest, Romania
** Polytechnical Institute, Splaiul Independenţei 202, Bucharest, Romania

Received March 24, 1983

The Mulliken population analysis is applied in calculating the force constants of $[MCl_4]^{n-}$ type ions. The calculus is made assuming that Ohwada's model is valid. The theoretical and experimental values are in good agreement.

1. INTRODUCTION

Theoretical prediction of force constants is a rather complex problem, which is one of the objects of vibrational analysis. In order to solve it, some models have been worked out, based on : i) perturbation approach ; ii) virial theorem ; iii) Hellmann-Feynman theorem.

The calculus is very tiresome, as it requires accurate knowledge concerning the wave functions and the orbital energies versusi nteratomic distances.[1]

A recent model suggested by Ohwada[2-6] involves a relatively simple method of calculating the force constants (bond stretching, angle deformation, bond-bond interaction, bond-angle interaction, angle-angle interaction) for different polyatomic molecules, as, e.g. XY_2, XY_3, XY_4, XY_5. The main input data for this model are the nuclear effective charges [7] of the atoms X and Y. In the case of homonuclear diatomic molecule, they are given by the relationship :

$$Z_i^* = Z_i e(1 - f_{ii})^{1/2} \tag{1}$$

where Z = the atomic number
e = the electronic charge
f_{ii} = the shielding factor [7]

According to Ohwada's model, the nuclear effective charge is determined by :

$$Z_i^* = \left(\frac{K_{ii} R_{ii}^3}{2} \right)^{1/2} \tag{2}$$

where K_{ii} is the force constant in the biatomic homonuclear molecule.

In order to calculate the force constants, the intramolecular potential function [1] is expanded to the second order in the displacements ΔR_{ij} and Δq_{jk}. The result is :

$$V = \frac{1}{2}\sum_{j(\neq i)} K_{ij}(\Delta R_{ij})^2 + \frac{1}{2}\sum_{j<k} H_{jk}(R_0\Delta\varphi_{jik})^2 + \sum_{j<k} k_{ij,\,ik}(\Delta R_{ij})(\Delta R_{ik}) + \tag{3}$$

$$+ \sum_{j\neq k} g_{ij,\,jik}(\Delta R_{ij})(R_0\Delta\varphi_{jik}) + \sum_{j\neq k\neq l} h_{jik,\,jil}(R_0\Delta\varphi_{jik})(R_0\Delta\varphi_{jil})$$

where : R_{ij}, q_{jk} = interatomic bonding and nonbonding distances, respectively

$\Delta\varphi_{jik}$ = variation in the angle between atoms j, i and k.
K = bond stretching force constant
H = angle deformation force constant
k = bond-bond interaction force constant
g = bond-angle interaction force constant
h = angle-angle interaction force constant

For XY_4 tetrahedral molecules, the force constants are computed according to Ohwada [4], using the following relationships :

$$K_{ij} = \frac{2Z_i^*Z_j^*}{R_0^3} + \sum_{j\neq k}\frac{Z_j^*Z_k^*}{q_0^3}(2s^2 - t^2) \tag{4}$$

$$H_{jik} = \frac{Z_j^*Z_k^*}{q_0^3}(2t^2 + s^2 + 1) \tag{5}$$

$$k_{ij,\,ik} = \frac{Z_j^*Z_k^*}{q_0^3}(2s^2 + t^2) \tag{6}$$

$$g_{ij,\,jik} = \frac{Z_j^*Z_k^*}{q_0^3}\,s\cdot t \tag{7}$$

$$h_{jik,\,jil} = \frac{2}{3}\,\frac{Z_j^*Z_k^*}{q_0^3} \tag{8}$$

$$\text{where } s = R_0(1 - \cos\varphi_{ijk})/q_0\ ;\ t = R_0\sin\varphi_{jik}/q_0 \tag{9}$$

R_0 = equilibrium bond length
q_0 = nonbonded distance

2. COMPUTATION OF FORCE CONSTANTS IN $(MCl_4)^{n-}$ COMPLEXES

When the relationships 4—8 are to be applied in the case of five-atoms tetrahedral molecules, they request, as input data, the knowledge of the nuclear effective charges, interatomic distances and of bond angles.

For simple CX_4 and SiX_4 type molecules (where X = H, F, Cl, Br, I), Z^* can be computed either on the basis of the vibration spectra of homonuclear diatomic molecules whose force constants are known (equation 2), or from those of heteronuclear diatomic molecules, when Z_i^* or Z_j^* are known :

$$K_{ij} = \frac{2Z_i^* Z_j^*}{R_{ij}^3} \qquad (4')$$

The work with such equations as (2) and (4′) when transition metal compounds are involved is difficult, because the vibration spectra of M_2 molecules are supposedly known, which is not always true.

Another side of the matter is that the nuclear effective charges used in the calculus are not the same, even for the same element, and are not constants, as they are supposed to be in Ohwada's works.

In the following, we shall assume that the nuclear charge of an atom is not constant. It varies versus the nature of the chemical bonds in the molecules under consideration.

Under these circumstances, it seems reasonable to use the "nuclear effective charge" of the metal ion determined by other methods : the differential ionization energy (which overevaluates the effective charge),[8,9] the nephelauxetic effect [9,10] and the Mulliken population analysis.[11]

For the chlorine atoms as a first approximation is used Ohwada's corrected nuclear effective charge, $Z_{Cl}^* = 1.759$

On the above stated basis, the force constants of the complex ions $[MCl_4]^{n-}$ (where M = Mn(II), Fe(III), Fe(II), Co(II), Ni(II)) can be computed. The values obtained by Mulliken's method [12] are used as the "nuclear effective charges" of the metallic ions. The results are listed in Table 1.

Table 1

The input data in Ohwada's model

—	R_0(Å)	Z_M^*
$MnCl_4^{2-}$	2.33	0.20
$FeCl_4^{2-}$	2.19	0.34
$FeCl_4^{2-}$	2.27	0.24
$CoCl_4^{2-}$	2.25	0.09
$NiCl_4^{2-}$	2.27	0.08

The results of the calculus, which used the relationships 4—8 are given in Table 2, where the force constants are expressed in mdyne/Å.

A check-up of those data has been accomplished by computing the four vibration frequencies (A_1, E, $2T_2$) by the GF method for each ion using the five constants K, H, k, g, h. These results have been compared with the experimental data wherever an assignment existed.

Table 2

The calculated force constants for $[MCl_4]^{n-}$ ions

	$MnCl_4^{2-}$	$FeCl_4^{-}$	$FeCl_4^{2-}$	$CoCl_4^{2-}$	$NiCl_4^{2-}$
K	0.517	0.731	0.587	0.581	0.476
H	0.303	0.364	0.327	0.336	0.327
k	0.217	0.260	0.234	0.240	0.234
g	0.061	0.074	0.066	0.068	0.066
h	0.086	0.104	0.093	0.096	0.093

The following matrix elements have been used in the calculus [13]:

$$F_{11} = K + 3k \qquad G_{11} = \mu_{Cl}$$

$$F_{22} = H - 2h \qquad G_{22} = 3\mu_{Cl}$$

$$F_{33} = K - 3k \qquad G_{33} = \mu_{Cl} + (4/3)\mu_M \tag{10}$$

$$F_{34} = \sqrt{2}g \qquad G_{34} = -(8/3)\mu_M$$

$$F_{44} = H \qquad G_{44} = 2\mu_{Cl} + (16/3)\mu_M$$

where μ_{Cl} and μ_M are the reciprocal masses of Cl and M, respectively.

The solutions of the secular equation [13]:

$$|GF - E\lambda| = 0 \tag{11}$$

$$E = \text{unit matrix}, \ \nu_i = \frac{\sqrt{\lambda_i}}{2\pi c}$$

are the frequencies of the normal vibration modes (Table 3)

Table 3

The calculated and experimental values for the four vibrations frequencies of $[MCl_4]^{n-}$ ions

	$\nu_1(cm^{-1})$		$\nu_2(cm^{-1})$		$\nu_3(cm^{-1})$		$\nu_4(cm^{-1})$	
	calc.	exp.	calc.	exp.	calc.	exp.	calc.	exp.
$MnCl_4^{2-}$	237	—	137	—	270	284	138	118
$FeCl_4^{-}$	270	330	150	106	295	378	180	133
$FeCl_4^{2-}$	249	—	143	—	279	286	151	119
$CoCl_4^{2-}$	250	—	144	—	280	297	145	130
$NiCl_4^{2-}$	238	—	143	—	276	289	114	112

The values in Table 3 show a good agreement of experimental [14]and calculated data. On the other hand, a perfect identity of experimental and calculated data cannot be expected, as in the used model neither any intermolecular interactions, in liquid or solid state, nor the influence of the cation on the vibration frequency are considered.

The use of the "nuclear effective charge" of the metallic ion computed according to Mulliken's method is more justifiable, as it varies with the metal-ligand bond type, stereochemistry of the metallic ion environment, and the amount of covalency of the metal-ligand bond.

REFERENCES

[1] C.J.H. Schute, *Structure and Bonding,* **9**, 213 (1971).
[2] K. Ohwada, *J. Chem. Phys.* **72**, 1 (1980).
[3] K. Ohwada, *J. Chem. Phys.*, **72**, 3663 (1980).
[4] K. Ohwada, *J. Chem. Phys.*, **73**, 5459(1981).
[5] K. Ohwada, *Spectrochim. Acta,* **37A**, 381 (1981).
[6] K. Ohwada, *Spectrochim. Acta,* **37A**, 873 (1981).
[7] N. J. Murrell, *J. Mol. Spectrosc.*, **4**, 446 (1960).
[8] C. K. Jørgensen, "Orbitals in Atoms and Molecules", Academic Press, London, 1962, p.85—92.
[9] C. K. Jørgensen, "Modern Aspects of Ligand Field Theory", North Holland Publ. Comp. Amsterdam, 1971, p. 131—139, 293—314.
[10] R. F. Fenske, K. C. Coulton, D. D. Radtke, C. C. Sweeney, *Inorg. Chem.*, **5**, 960 (1966).
[11] R. S. Mulliken, *J. Chem. Phys.*, **23**, 1841 (1955).
[12] R. F. Fenske, D. D. Radtke, *Inorg. Chem.*, **7**, 479 (1968).
[13] N. Nakamoto, "Infrared Spectra of Inorganic and Coordination Compounds", Wiley, New York, 1963, p. 45.
[14] D. W. James, M. J. Nolan, "Progress in Inorganic Chemistry", vol. 9, Interscience Publ., New York, 1968, p. 234.

Revue Roumaine de Chimie, **29**, *6*, 475–482 (1984)

CHROMIUM(III) COMPLEX THIOCYANATES WITH BIGUANIDINE DERIVATIVES

CONSTANȚA GHEORGHIU *, CORNELIA GURAN, AURELIA MEGHEA and IOANA JITARU
The Polytechnic Institute Bucharest, Department of Chemistry,
Laboratory of Inorganic Chemistry, 3–5 Polizu str., Bucharest, Romania

Received June 15, 1983

The present paper reports the results obtained in the synthesis and characterization of new chromium (III) complex thiocyanates having the general formula $[Cr(RBig)_2(NCS)_2]$ (NCS), where RBig were different biguanidine derivative ligands. The compounds were characterized by chemical and physico-chemical methods (electrical molar conductivity determinations, electronic spectra, vibrational spectra and electronic spin resonance spectra).

Chromium (III) complex thiocyanates have been intensely studied lately due to the many structural problems generated by these compounds and also to their large possible applicability in various fields.[1–12]

In a previous paper we presented thiocyanates with biguanidine derivatives $K[Cr(RBig)(NCS)_4]$ obtained by substitution of anionic ligands NCS^- from $K_3[Cr(NCS)_6]$ by RBig, under well stable working conditions.[13]

The study of the substituted reaction was continued and $[Cr(RBig)_2(NCS)_2](NCS)$ compounds were obtained, where RBig were the following biguanidine derivative ligands: N^1-chloropheny l-N^5-isopropylbiguanidine (paludrine), N^1-phenyl-, N^1-chlorophenyl- and N^1-tolybiguanidine (abridged in this paper: Pald, PhBig, ClPhBig and TBig). The compounds were characterized by chemical and physico-chemical methods (electrical molar conductivity determinations, electronic spectra, infrared vibration spectra and electronic spin resonance spectra).

RESULTS AND DISCUSSION

The reaction between $K_3[Cr(NCS)_6]$ and RBig derivatives develops by substitution of the NCS^- groups within the coordination sphere only under perfect anhydrization conditions both of the reagent and of the reaction medium. The substitution occurs owing to the higher basicity of the RBig derivatives than that of the NCS$^-$ anions.

---

* Deceased: March 28, 1983

Using anhydrous ethylic alcohol as solvent at 70—80°, under refluxion, at a molar ratio Cr : RBig 1 : 2, stable reddish-violet crystalline compounds $[Cr(RBig)_2(NCS)_2]$ (NCS) are obtained. The compounds are insoluble in water and soluble in solutions of ethylic alcohol, acetone, dimethylformamide.

When water is used as solvent, the$[Cr(NCS)_6]^{3-}$ anion is not destroyed, K^+ being substituted by protonated ligand molecules, $RBigH^+$.[14]

Elementary chemical analysis showed the atomic combining rations to be 1 Cr : 3 S : 13 N. The formulations also took into account the electrical molecular conductivity determinations which showed the new compounds to be electrolytes of type 1 : 1 (Table 1).

Table 1

Molar electric conductivity of the compounds: $[Cr(RBig)_2(NCS)_2](NCS)$

Compound	Conductivity $ohm^{-1}cm^2mol^{-1}$	Electrolyte type
$[Cr(Pald)_2(NCS)_2](NCS)$	79	1 : 1
$[Cr(PhBig)_2(NCS)_2](NCS)$	74.4	1 : 1
$[Cr(ClPhBig)_2(NCS)_2](NCS)$	75.3	1 : 1
$[Cr(TBig)_2(NCS)_2](NCS)$	81	1 : 1

For complete characterization the compounds were determined spectrophotometrically, assessing the distribution of their energy levels and stereochemistry.

The electronic reflection spectra of the compounds (Fig. 1, Table 2) showed four peaks at wavelengths of approximately 530, 410, 320 and 270 nm.

Table 2

Reflection spectra of the compounds: $[Cr(RBig)_2(NCS)_2](NCS)$

Compound	λ(nm) ${}^4A_{2g}\to{}^4T_{2g}(F)$	λ(nm) ${}^4A_{2g}\to{}^4T_{1g}(F)$	λ(nm) ${}^4A_{2g}\to{}^4T_{1g}(P)$	λ(nm) proprie to ligand
$[Cr(Pald)_2(NCS)_2](NCS)$	525	408	310	265
$[Cr(PhBig)_2(NCS)_2](NCS)$	535	410	320	270
$[Cr(ClPhBig)_2(NCS_2)]$ (NCS)	530	410	320	270
$[Cr(TBig)_2(NCS)_2]$ (NCS)	525	412	315	250
$K_3[(Cr(NCS)_6]$	550	410	310	—
$NH_4[Cr(NH_3)_2\ (NCS)_4]$	525	400	308	—

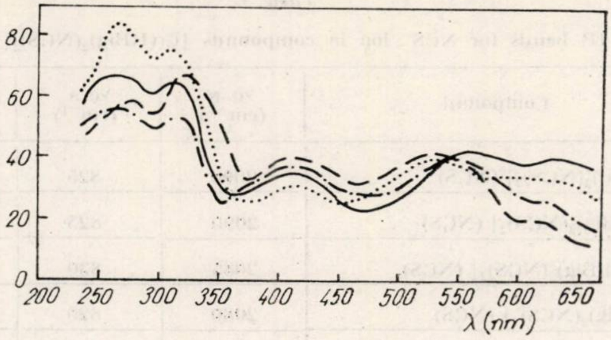

Fig. 1. — Reflection spectra of the compounds:

$[Cr(Pald)_2(NCS)_2](NCS)$ (. . . . .)
$[Cr(PhBig)_2(NCS)_2](NCS)$ (. . . . .)
$[Cr(ClPhBig)_2(NCS)_2](NCS)$ (— · — · — ·)
$[Cr(TBig)_2(NCS)_2](NCS)$ (————).

The first three peaks were assigned to spin transitions allowed for a d^3 ion in an octahedral field ($^4A_{2g} \rightarrow {}^4T_{2g}$, $^4A_{2g} \rightarrow {}^4T_{1g}$, $^4A_{2g} \rightarrow {}^4T_{1g}$).

The presence of the band at ~ 270 nm is due to the existence of the RBig ligands within the coordination sphere. These peaks are also to be found in the non-coordinated biguanidine derivatives at values very close to those found for the compounds discussed (Table 3). As a result of coordination the two peaks join and a single, large band appears.

Table 3

Ultraviolet bands of the ligands

RBig.HCl	λ max (nm)
Pald.HCl	230 258
PhBig.HCl	230 250.5
ClPhBig.HCl	232 258
TBig.HCl	241

A comparison of the data obtained by us with those of other compounds [9,15] (Table 2) shows that the geometry of the $[Cr(RBig)_2(NCS)_2](NCS)$ compounds is close to that of the $NH_4[Cr(NH_3)_2(NCS)_4]$ compound (octahedron with a slight tetragonal deformation).

The vibration and infrared spectra of the compounds studied were examined with a view to providing information on the mode of coordination of NCS^- ligands and on the presence of the organic RBig ligands (Table 4). This showed that the vibration bands specific to the RBig ligands can again be found at wavelengths displaced as a consequence of their coordination.

The stretching vibrations of bond ν_{C-S}, situated at 830–840 cm^{-1} do not establish precisely the nature of the bond between Cr^{3+} and the anionic NCS^- ligands. On the other hand, the broad band between 2080 and 2090 cm^{-1} specific to vibration ν_{C-N} confirms the existence of some Cr—NCS types of bonds. The frequency of the deformation vibration δ_{NCS}, was used, together with the ν_{C-S} and ν_{C-N} frequencies for determining the type of the bond. The presence of some bands at 480–490 cm^{-1} proves the existence of certain bonds mediated by nitrogen, the compounds being of isothiocyanate type.[16]

Table 4

IR bands for NCS⁻ ion in compounds $[Cr(RBig)_2(NCS)_2]$ (NCS)

Compound	ν_{C-N} (cm^{-1})	ν_{C-S} (cm^{-1})	δ_{NCS} (cm^{-1})
$[Cr(Pald)_2(NCS)_2]$ (NCS)	2090	825	490
$[Cr(PhBig)_2(NCS)_2]$ (NCS)	2090	825	480
$[Cr(ClPhBig)_2(NCS)_2]$ (NCS)	2085	830	480
$[Cr(TBig)_2(NCS)_2]$ (NCS)	2080	820	490
NCS^- (from KNCS)	2053	748	486

For identifying the NCS^- present outside the coordination sphere, the bands were compared with the modes of vibrations of ν_1, ν_2 and ν_3 in KNCS, present at 2035, 486 and 748 cm^{-1}.

The ν_{CN} band, specific to the non-coordinated ion, is covered by the ν_{CN} band due to vibration of the coordination ion. For the ν_2 frequencies, specific to the δ_{NCS} vibrations in the free and the coordinated ion, the differences are not too significant and no appreciation can be done in this connection. The ν_3 vibration frequency, specific to the C—S bond, appears within a range where bands of the RBig ligands are present (748 cm^{-1}). Therefore the only proof for the existence of the NCS^- ions non-coordinated in compounds $[Cr(RBig)_2(NCS)_2]$(NCS), is given by the data of molar electrical conductivity, as the compounds are electrolytes of type 1 : 1.

For characterizing the nature of the metal-ligand bond, in some of these complex thiocyanates their electronic spectra were analyzed according to the terms of the ligand field theory.

The absorption maxima, corresponding to the d—d transitions, were interpreted by using the approximations in the literature,[17] which for the d^3 ions in octahedral environment and spin-forbidden transitions

$$\begin{aligned}
\nu_1(^4A_{2g} \to {}^4T_{2g}) &= \Delta'_m + 2A(\beta_{35} - \beta_{55}) + 10\,B(\beta_{55} - \beta_{35}) = \Delta m \\
\nu_2(^4A_{2g} \to {}^4T_{1g}) &= \nu_1 + 12\,\beta_{35}B \qquad (1) \\
\nu_3(^4A_{2g} \to {}^2E_g) &= 9\,\beta_{55}B + 3\,\beta_{55}C = 21\,\beta_{55}B
\end{aligned}$$

where :

Δ'_m — the difference between the energy of the antibonding orbitals $E^*_g(\sigma)$ and $T^*_{2g}(\pi)$;

A, B, C — the Racah parameters for interelectronic repulsions ;

β — the nephelauxetic rations.

Ir $C \simeq 4B$, when $\beta_{33} = \beta_{55} = \beta_{35} = 1$ the formulas are reduced to the known ones.[18]

$$\nu_1 = \Delta'_m = \Delta_m$$

$$\nu_2 = \nu_1 + 12\,B$$

$$\nu_3 = 21\,B$$

On the basis of the first relation in formulas (2), considering that parameter Δ_m obeys the rule of medium environment,

$$\Delta_m = [MX_nY_{6-n}] \simeq \frac{n}{6}\Delta[MX_6] - \frac{6-n}{6}\Delta[\mathrm{MX}_6]$$

the splitting patameters Δ are obtained in purely octahedral complexes (Table 5).

The change of the Δ values from the compounds with PhBig to that with ClPhBig is probably due to the inductive effect of the chlorine group attached to the phenyl group. Owing to the free electrons of chlorine, an increase in the strength of the Cr(III)-N-bond is observed. As actually the nephelauxetic rations β_{35}, β_{33} and β_{55} are smaller than the unit and differ from one another, they were calculated on the basis of relation 2, taking $B = 0.920$ kK.[19]

Similarly, coefficients α_σ of the metal orbitals d for the E_g and T_{2g} states respectively were calculated on the basis of relations :

Table 5

Values of Δ parameter for the compounds $[Cr(RBig)_3]^{3+}$

Compound	Δ(kK)
$[Cr(PhBig)_3]^{3+}$	19.00
$[Cr(ClPhBig)_3]^{3+}$	19.51
$[Cr(TBig)_3]^{3+}$	19.00
$[Cr(Pald)_3]^{3+}$	19.00

$$\beta_{35} = \alpha_\sigma^2\alpha_\pi^2 Z^*/Z$$

$$\beta_{33} = \alpha_\sigma^4 \quad Z^*/Z$$

$$\beta_{55} = \alpha_\pi^4 \quad Z^*/Z$$

where Z^* and Z are the effective nuclear charge of the coordinated metal and of the free metallic ion respectively ; coefficient α_σ^2 was calculated considering $\alpha_\pi^2 = -1$ and $Z^*/Z = 0.89$.

Moreover, electronic density of the bond was calculated using relation $D = 3\,\alpha_\pi^2 + 4(1 - \alpha_\sigma^2) + 6(1 - \alpha_\pi^2)$ where 3, 4, 6 are the electrons in the molecular orbitals T_{2g}^* and E_g and T_{2g} respectively. The values of the β, α, D parameters, calculated for the complexes studied (Table 6) confirm that the Cr(III)-ligand bonds have a marked covalent character. This is in agreement with the value Δ in table 5 thus confirming the previous hypothesis in that the Cr—N bond is stronger due to the inducing effect of chlorine, in the case of the $[Cr(ClPhBig)_2(NCS)_2]$ (NCS) compound.

Table 6

Values of the β_{35}, β_{55}, α_σ^2 and D parameters

Compound	β_{35}	β_{55}	α_σ^2	D
$[Cr(PhBig)_2(NCS)_2]$ (NCS)	0.516	0.821	0.579	4.684
$[Cr(ClPhBig)_2(NCS)_2]$ (NCS)	0.500	0.820	0.561	4.756

Next to the electronic spectra, the electronic spin resonance spectra provide further information on the nature of the ligand in chromium (III) complex compounds.

Of the $[Cr(RBig)_2(NCS)_2]$ (NCS), compounds studied by the ESR method, the best solved spectrum was that obtained for the compound in which chlorophenylbiguanidine is the ligand (Fig. 2). For the $[Cr(Pald)_2(NCS)_2]$ (NCS) compound a relatively broad central line ($\sim$ 300 G) prevails in the spectrum, at $g \simeq 2$. In the ESR spectra of the $[Cr(PhBig)_2(NCS)_2]$ (NCS) and $[Cr(TBig)_2(NCS)_2]$ (NCS) compounds, an intense, broad line is predominant within the low field range ($g \simeq 4$), due to distorsion of the network (Fig. 3).

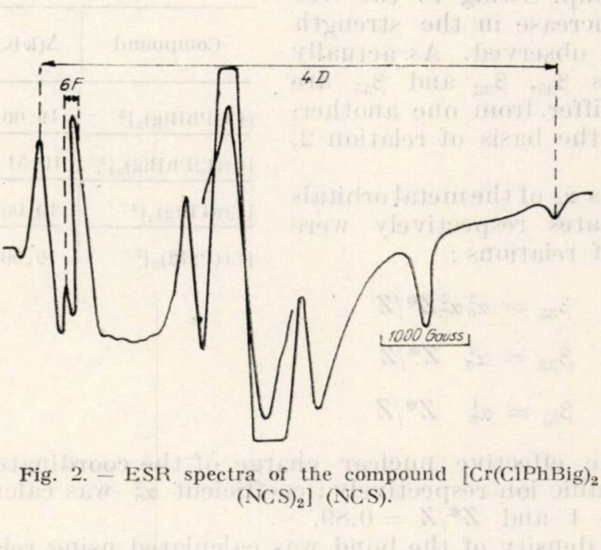

Fig. 2. — ESR spectra of the compound $[Cr(ClPhBig)_2(NCS)_2]$ (NCS).

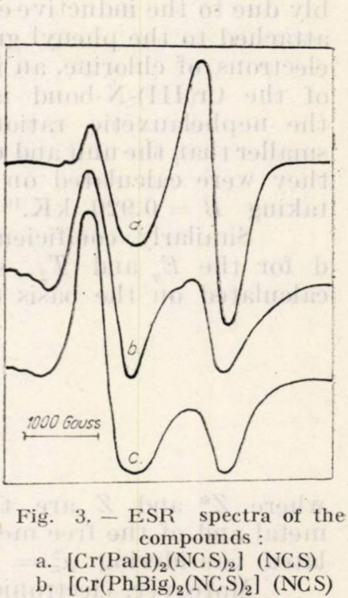

Fig. 3. — ESR spectra of the compounds :
a. $[Cr(Pald)_2(NCS)_2]$ (NCS)
b. $[Cr(PhBig)_2(NCS)_2]$ (NCS)
c. $[Cr(TBig)_2(NCS)_2]$(NCS).

The well solved spectrum of the $[Cr(ClPhBig)_2(NCS)_2]$ (NCS) compound permitted the calculation of the two anisotropic tensors of the spin Hamiltonian, D and E. A strong anisotropy is observed, determined by parameter D = 1168 G, and a very weak rhomboid anisotropy given by E = 20 G, attributed to the distortions of the crystalline network of this combination with the bulky ligands within the internal coordination sphere (Table 7).

The splitting parameter in zero-axial field, D, has close values for all the compounds $[Cr(RBig)_2(NCS_2)]$ (NCS) and of the same order of magnitude as an aminochlorocomplex.[20] Variation of this parameter is noted within the ligand series ClPhBig > PhBig > TBig > Pald.

The highest value, obtained for the combination with ClPhBig may be attributed to its more accentuated polarity and likewise to its more electronegative character introduced by the chlorine substituent. These brought about an advanced degree of crystallinity of the $[Cr(ClPhBig)_2(NCS)_2]$ (NCS) compound, a fact that permitted solving of the fine

Table 7

ESR spectral parameters for the compounds $[Cr(RBig)_2(NCS)_2]$ (NCS)

Compound	*g*		*D*(Gauss)	*E*(Gauss)
$[Cr(ClPhBig)_2(NCS)_2]$ (NCS)	1.989	4.588 6.479	1168	30
$[Cr(PhBig)_2(NCS)_2]$ (NCS)	1.997	4.473	918	—
$[Cr(TBig)_2(NCS)_2]$ (NCS)	2.031	4.415	862	
$[Cr(Pald)_2(NCS)_2]$ (NCS)	1.950	3.975	839	—
$[Cr(NH_3)_5\,Cl]Cl_2$ [20]	1.986		950	45

structure observed experimentally. In this case, evidence was found of a superfine structure by side satellites of the highly intense central line, attributed to the interaction with the magnetic nucleus of the $^{53}Cr(I = 3/2)$ in a natural proportion of 9.5%. The superfine splitting constant was $a_{hf} = 123$.

EXPERIMENTAL

I. Synthesis of the complex compounds $[Cr(RBig)_2(NCS)_2]$ (NCS)

Anhydrous $K_3[Cr(NCS)_6]$ and the biguanidine derivatives RBig are solved in anhydrous ethanol at pH = 7.5 and molar ratio 1 : 2. The mixture is refluxed for 2 hrs, then alcohol is removed by dry evaporation. Red-violet glues are obtained; this is water washed up to KNCS removal. The products are kept in vaccum desiccator until crystallization (2–3 days).

The compounds are soluble in ethanol, acetone, dimethylformamide and insoluble in water.

The chromium and sulphur were determined gravimetrically as Cr_2O_3 and $BaSO_4$ respectively, after having desintegrated the sample with oxygenated water in an ammoniacal medium. The nitrogen was determined by combustion using the micro-Dumas method.

Calcd. for : $[Cr(Pald)_2(NCS)_2]$ (NCS) ; $(C_{25}H_{32}N_{13}Cl_2S_3Cr)$:
Cr%, 6.75 ; S%, 12.62 ; N%, 24.30 ;
Found : 6.88 ; S% 12.69 24.06.

Calcd. for : $[Cr(PhBig)_2(NCS)_2]$ (NCS) ; $(C_{19}H_{22}N_{13}S_3Cr)$:
Cr%, 8.90 ; S%, 16.30 ; N%, 31.32 ;
Found : 8.96 ; 16.54 31.37 ;

Calcd. for : $[Cr(ClPhBig)_2(NCS)_2]$ (NCS) ; $(C_{19}H_{20}N_{13}Cl_2S_3Cr)$:
Cr%, 7.91 ; S%, 14.90 ; N%, 27.98 ;
Found : Cr%, 7.99 ; 14.74 ; 27.95 ;

Calcd.for : $[Cr(TBig)_2(NCS)_2]$ (NCS) ; $(C_{21}H_{26}N_{13}S_3Cr)$:
Cr%, 8.55 ; S%, 15.72 ; N%, 30.02,
Found : 8.55 ; 15.78 ; 29.92.

II. Electronic spectra

Reflection spectra have been recorded at room temperature using a spectrophotometer VSU 1, and as a referring material, magnesium oxide.

III. Vibrational spectra

IR Spectra have been obtained by means of a Zeiss UR 20 spectrophotometer using potassium bromide disk technique.

IV. ESR spectra

ESR spectra were registered in a solution of dimethylformamide, in the form of polycrystalline powders, by using a spectrophotometer of the type ART 5 – IFIN Bucharest in the 9060 MHz frequency ranges with a magnetic field modulation of 100 kHz.

V. Molar conductivity measurements

Measurements of molar electrical conductivity have been recorded with a Radelkis conductometer with a constant $K = 0.92$, in 10^{-3}M dimethylformamide solution at a temperature of 25°.

REFERENCES

[1] P. Spacu and A. Antonescu, *Studii și Cercetări Chim., Acad. RPR*, **8**, 73 (1960).
[2] I. Gănescu and G. Varhelyi, *Stud. Univ. Babeș Bolyai*, Chem, **2**, 89 (1969).
[3] I. Gănescu and Al. Popescu, *Rev. Roumaine Chim.*, **9**, 1343 (1970).
[4] R. Ripan, I. Gănescu and G. Varhelyi, *Rev. Roumaine Chim.*, **11**, 473 (1966).
[5] I. Gănescu, G. Varheley, and D. Oprescu, *Stud. Univ. Babeș Bolyai, Chem.*, **1**, 113 (1969).
[6] P. S. Glash, *J. Inorg. Nuclear Chem.*, **33**, 4199 (1971).
[7] I. Gănescu and G. Varhelyi, *Z. anorg. Chem.*, **439**, 282 (1978).
[8] C. L. Sharma, *J. Indian Chem. Soc.*, **58**, 119 (1981).
[9] F. Pruchnick and S. Wajda, *Roczniki Chem.*, **43**, 1379 (1969).
[10] I. Gănescu. M. Teodorescu and C. I. Lepădatu, *Z. phys. Chem (Frankfurt)* **74**, 11 (1971).
[11] G. C. Lalor, and H. Miller, *J. Inorg. Nuclear Chem.*, **40**, 305 (1978).
[12] M. Chsumano. *Inorg. Chem.*, **17**, 2222 (1978).
[13] C. Gheorghiu and C. Guran, *Analele Univ. Buc.*, **1**, 83 (1972).
[14] C. Guran and I. Jitaru, *Bul. Inst. Politeh. București*, in press.
[15] A.B.P. Lever, "Inorganic Electronic Spectroscopy", Ed. Elsevier, New York, 1968, p. 265.
[16] K. Nakamoto, "Infrared Spectra of Inorganic Coordination Compounds", Willey Interscience, 1970, p. 251.
[17] P. Spacu, and C. Lepădatu, *Z. phys. Chem (Frankfurt)*, **63**, 105 (1969).
[18] C. Griffits, "The Theory of Transition Metal Ions", Cambridge Univ. Press, Cambridge, 1960, p. 310.
[19] J. Csaszar and E. Horvath, *Acta Chem. Acad. Sci. Hung.*, **71**, 291 (1972).
[20] L. E. Mohrmann and B. B. Garrett, *Inorg. Chem.*, **13**, 357 (1974).

Revue Roumaine de Chimie, **29**, *6*, 483–488 (1984)

INFLUENCE OF COEMULSIFIERS ON THE EMULSION POLYMERIZATION OF VINYL ACETATE IN THE PRESENCE OF HYDROXYETHYLCELLULOSE

DAN DONESCU, ION DEACONESCU and KRISTIANA GOŞA
Center of Plastic Materials Research, Bucharest, Romania

Received December 8, 1982

The influence of coemulsifiers structure and concentration and of potassium persulphate (KPS) on maximum polymerization rate (R_{max}) was studied. As coemulsifiers nonyl phenols ethoxylated with 4, 8, 9, 12, 16 ethylene oxide mole were used (NFxEO). R_{max} presents a maximum when NF8EO was used. For all coemulsifiers, R_{max} decreases with its concentrations. This demonstrates the existence of a degradative chain transfer of coemulsifiers. Thus it was shown that $R_{max} \sim |NF8EO|_0\ .^{-6'0}$ and $R_{max} \sim |KPS_{0.8}$ The insoluble fractions concentrations of the final polymers decrease with the increase of coemulsifier concentration and with the increase of ethylene oxide concentration in NF × EO. This demonstrates that NF × EO act as chain transfer agents and that transfer reaction takes place on EO group.

INTRODUCTION

In previous papers [1,2] we have studied the kinetics of emulsion polymerization of vinyl acetate (VAc) with hydroxyethylcellulose (HEC) as protective colloid. The factors that influence the emulsion polymerization of VAc were established and the transfer of growing macroradicals with HEC macromolecules was evidenced. There are contributions[3–6] that reveal the possibility of utilizing the coemulsifiers in the emulsion polymerization of VAc in the presence of HEC.

This paper reports on a study of the effect of coemulsifiers on the evolution of polymerization of VAc.. Nonylphenolethoxylates (NFnEO) with various numbers of ethylene oxide were used as coemulsifiers.

EXPERIMENTAL

The experimental parameters were mentioned elsewhere [1,2] (temperature = 70°C, initiator-potassium persulphate (KPS)).

Coemulsifiers were commercial products utilized without any additional purification. The ethylene oxide content was determined by NMR.

---

* Paper presented at the 2nd National Congress of Chemistry, Bucharest, 1981

RESULTS AND DISCUSSION

Influence of coemulsifier composition and concentration on polymerization rate

To evidence the influence of coemulsifiers, a series of polymerizations were effected with constant concentration of VAc ($|VAc|_0 = 4.07$ mole/l), HEC ($|HEC|_0 = 4.37.10^{-2}$ mole us/l) and initiator ($|KPS|_0 = 2.3.10^{-3}$ mole/l). The results are shown in figure 1.

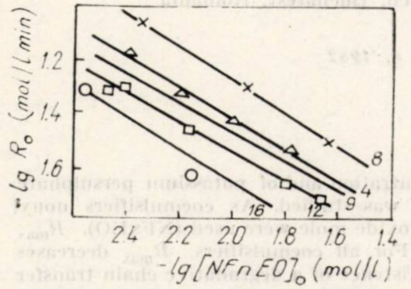

Fig. 1. — The polymerization rate versus the concentration of coemulsifiers (n = 8(×); 4(△); 9(▽); 12(□); 16(○)).

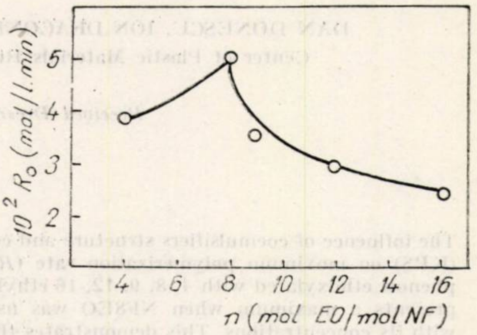

Fig. 2. — The variation of polymerization rate for coemulsifiers of different compositions $|NFnEO|_0 = 10^{-2}$ mol/l).

One can notice that utilization of coemulsifiers mentioned causes a decrease of polymerization rates with their concentration. This phenomenon was also evidenced in other systems of emulsion polymerization of VAc.[2,7-9] The decrease of polymerization rate is due to the degradative chain transfer which occurs with the emulsifier existing in the polymerization medium. The transfer yields radicals of lower activity. The slope of curve in figure 1 is about the same. The reaction order with respect to the coemulsifier is therefore -0.6 for NF8EO.

The way the polymerization rate is influenced by the degree of ethoxylation of coemuslifiers is shown in figures 1 and 2.

It is seen that the maximum of polymerization rate is reached at ethoxylation $n = 8$ of nonylphenols. Such curves with maximum of polymerization rate versus the increase of hydrophyilic part of the emulsifier were also found when ethylene oxide—propylene oxide block copolymers were used.[9] It is difficult to explain this phenomenon.[10] The modification of emulsifier structure changes the rate of splitting of the initiator and the interaction between monomer and emulsifier.

The concurrence of these phenomena gives the condition of maximum. The simple representation of an optimal balance of hydrophilic and hydrophobic (HLB) groups [3] dissimulates in fact all the complexity of the phenomena involved.

The maximum rate for a certain degree of ethoxylation of nonylphenoles employed as emulsifiers was obtained in the absence of HEC.[11]

Besides the polymerization rate, the degree of ethoxylation of coemulsifiers also affects the induction period (Fig. 3).

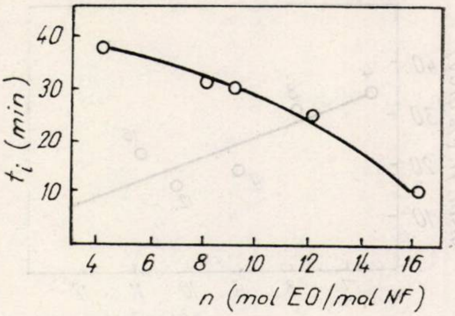

Fig. 3. — The variation of induction period versus coemulsifiers composition ($[NFnEO]_0 = 10^{-2}$ mol/l).

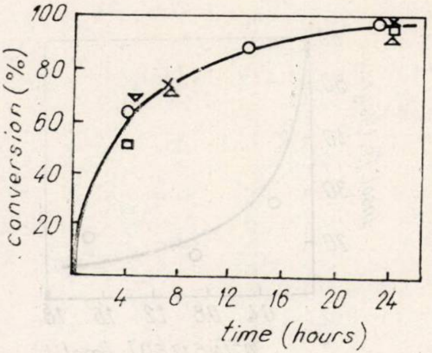

Fig. 4. — The evolution of conversion during polymerization of VAc in benzene in the absence (▽) and in the presence of coemulsifiers ($n = 16$ (⊙); (12(□); 8(⊗); 4(△)).

The induction period decreases with the increase of ethylene oxide content in the coemulsifier. The decrease of the interval after which the polymerization reaction starts with remarkable rate is due to modification of initiation rate either by modification of splitting rate of the initiator or by creating more favourable conditions of capturing the radicals initially formed.

In order to establish that the facts presented above stand only for emulsion polymerization, the influence of coemulsifiers in solution polymerization was studied. Polymerizations were conducted at 65°C in benzene. The concentration of VAc was 420 g/l, that of coemulsifiers 50 g/l and of initiator (AIBN) of 10 g/l (Fig. 4).

Unlike emulsion polymerization, the presence of coemulsifiers does not affect the evolution of solution polymerization. Even if the degradative chain transfer reaction occurs, the effect of low reactivity of newly formed radicals is not remarkable.

Effect of coemulsifier concentration and composition on the structure of obtained polymers

It was proved that in the presence of HEC the emulsion polymerization of VAc yields polymers that may separate into three fractions : soluble in water, soluble in benzene and insoluble.[2]

The first two fractions contain soluble grafted copolymers. Introduction of coemulsifiers into the polymerization system alters the ratio of these fractions due to the reaction of transfer. Thus the rising of coemulsifier concentration decreases the content of insoluble fraction (Fig. 5).

It turns out that these coemulsifiers play an additional role of transfer agents.

Examination of the structure of coemulsifiers and the value of chain transfer constant for various substances of similar structure [12,13] suggests that the transfer reaction occurs predominantly at ethylene oxide units. This is fully demonstrated if one analyzes the variation of insoluble polymer fraction formed in the presence of various coemulsifiers (Fig. 6) (Figures on curve correspond to the degree of ethoxylation of coemulsifiers).

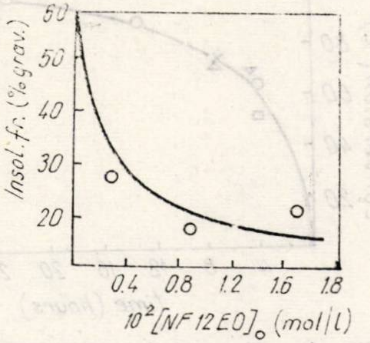

Fig. 5. — The dependence of insoluble polymer fraction on coemulsifiers (NF12EO) concentration (experimental condition in Fig. 1).

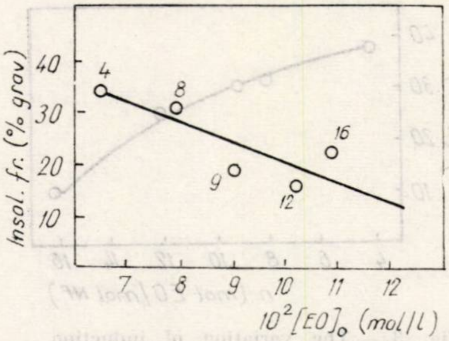

Fig. 6. — The influence of concentration of ethylene oxide units in polymerization medium on the insoluble polymer fraction ($[NFnEO]_0$ = 6.25 g/l) (the number — degree of ethoxylation).

It is noticeable that the increase of global ethylene oxide concentration in the polymerization medium causes the insoluble fraction to decrease. This phenomenon is similar to that observed when transfer agents are utilized in emulsion polymerization of VAc.[14]

Although in polymerization in solution the rate of monomer consumption is not affected by coemulgators, the structure of polymers changes (Fig. 7).

In conditions of solution polymerization adopted in this paper no insoluble polymer fractions were isolated. Due to the transfer to ethylene oxide protons, the concentration of soluble fraction in benzene rises with the degree of ethoxylation of nonylphenoles.

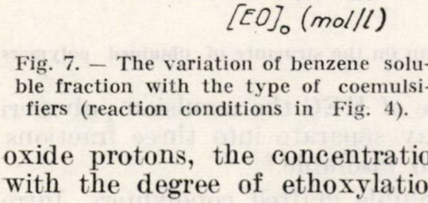

Fig. 7. — The variation of benzene soluble fraction with the type of coemulsifiers (reaction conditions in Fig. 4).

Influence of initiator concentration on polymerization rate

A study of kinetics of emulsion polymerization of VAc has revealed that the order of reaction with respect to the initiator depends on the conditions of polymerization: the nature of emulsifiers, of protective colloid [2,7,9,12] and that of electrolytes.[15] In the presence of HEC the order of reaction with KPS is 0.2. Introduction of NF8EO as coemulsifier yields an order of reaction of 0.8. (Fig. 8).

The value of the order of reaction deduced from figure 8 is identical with that for polymerization VAc in the presence of nonylphenol-ethoxylates as surfactants.[11] This coincidence suggests that the coemulsifiers alter the mechanism of initiation itself acting probably at the initial stage of formation and stabilization of macroradicals in aqueous phase.

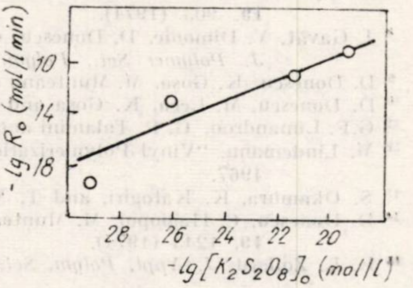

Fig. 8. — The reaction rate versus concentration of initiator $|NF8EO|_0 = = 1.12.10^2$ mol/l).

Influence of initiator concentration on the structure of the polymers

The increase of initiator concentration enlarges the number of radicals in the system and this increases the probability of chain transfer with HEC. The enhancement of this phenomenon alters the structure of polymer obtained in emulsion polymerization.

The analysis of the results in figure 9 reveals that the increase of initiator concentration rises the insoluble polymer fraction. This phenomenon is also observed when other protective colloids were used.[8]

It turns out that the presence of coemulsifiers studied does not preclude the chain transfer reactions of macroradicals with HEC.

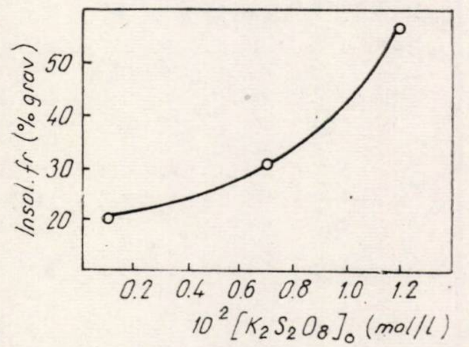

Fig. 9. — The correlation between the insoluble fraction and the concentration of initiator (reaction conditions in Fig. 8).

REFERENCES

[1] D. Donescu, K. Goşa, I. Deaconescu, M. Mazăre and N. Carp, Symposium on Emulsion Polymerization on Vinyl Acetate, Bethlehem, Pennsylvania, 1980.

[2] D. Donescu, I. Deaconescu, K. Goşa, M. Mazăre and I. Gavăţ, *Rev. Roumaine Chim.*, **25**, 975 (1980).

[3] G. G. Greth and J. E. Wilson, *J. Appl. Polym. Sci.*, **5**, 135 (1961).

[4] El. Elvine and Ph. C. Renther, Pat. Fr., 1 539 441 (1968); *Chem. Abstr.*, **71**, 12, 51318 (1969).

[5] Societa Edison, Pat. Brit. 1 044 915 (1966); *Chem. Abstr.*, **66**, 19240 (1967).

[6] Sicedison Societa par Azioni, Pat. Ital., 617 925 (1961); *Chem. Abstr.*, **58**, 13019 (1962).

[7] V. Dimonie, D. Donescu, M. Munteanu, C. Hagiopol and I. Gavăt, *Rev. Roumaine Chim.*, **19**, 903 (1974).

[8] I. Gavăt, V. Dimonie, D. Donescu, C. Hagiopol, M. Munteanu, K. Goşa and Th. Deleanu, *J. Polymer Sci., Polym. Symp.*, **64**, 125 (1978).

[9] D. Donescu, K. Goşa, M. Munteanu and I. Gavăt, *Rev. Roumaine Chim.*, **24**, 1399 (1979).

[10] D. Donescu, M. Leca, K. Goşa and M. Mazăre, *Mat. Plastice*, **3**, 146 (1980).

[11] G.F. Lunandron, G. P. Talamini and U. Grosso, *Europ. Polymer J.*, **11**, 437 (1975).

[12] M. Lindemann, "Vinyl Polymerization", vol. I, Ed. G. Ham, Marcel Dekker, New York, 1967.

[13] S. Okamura, K. Katogiri, and T. Motoyama, *J. Polymer Sci.*, **43**, 509 (1960).

[14] D. Donescu, C. Hagiopol, M. Munteanu, V. Dimonie and I. Gavăt, *Rev. Roumaine Chim.*, **19**, 1243 (1974).

[15] R. L. Zollard, *J. Appl. Polym. Sci.*, **24**, 1353 (1979).

Revue Roumaine de Chimie, **29**, *6*, 489–495 (1984)

DISUBSTITUTED PHENOTHIAZONES. II.

NEW HALOGENO-3H-PHENOTHIAZIN-3-ONES

MARIUS H. TERDIC
Institute of Chemistry, 3400–Cluj-Napoca,
Str. Fîntinele Nr. 30, Romania

Received February 15, 1983

Three general methods for the synthesis of some new halogenophenothiazones were extended. The methods involve : a) the thionation of halogeno-4′-hydroxy-diphenylamines follwed by oxidation with potassium dichromate (scheme 1 and table 1), b) condensation of zinc mercaptide of 2-aminothiophenols with halogeno-benzoquinones-(1,4) (scheme 2 and table 2) and c) the selective halogenation in position 4 of some monohalogenated phenothiazones (scheme 3 and table 3).

A new series of mono- and disubstituted 3H-phenothiazin-3-ones (phenothiazones) with bromine or chlorine atoms was prepared with the intention to perform a thorough physico-chemical study of these compounds. At the same time we expected to obtain more information about the possibilities and limits of the involved reactions for a better understanding of the reaction mechanisms. For this purpose we have extended three synthetic methods already described in our previous works. Among the compounds described in this paper, the monosubstituted phenothiazones in positions 6 and 9 have a peculiar importance. Firstly, these compounds have completed the series of the monobromo- and monochloro-isomers. Secondly, these substances may serve as starting materials for other reactions, such as selective halogenation in position 4 which is described in this work.

Method A (Thionation of halogeno-4′-hydroxy-diphenylamines followed by potassium dichromate oxidation)

By heating 4-methylaniline with hydroquinone in the presence of zinc chloride, Heller [2] has obtained 4-methyl-4′-hydroxy-diphenylamine. This reaction was later generalized by condensation of 2- and 3-methylaniline with hydroquinone and the obtained 2- and 3-methyl-4′-hydroxydiphenylamines were thionated and then oxidized yielding some monomethyl-phenothiyzones.[3]

Scheme 1

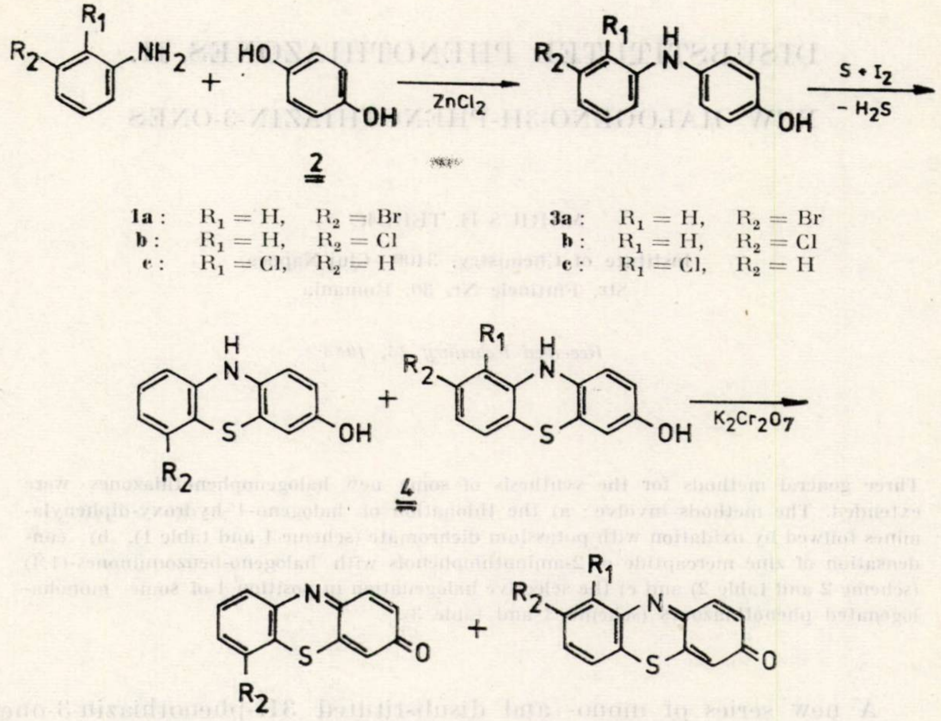

1a: $R_1 = H$, $R_2 = Br$
b: $R_1 = H$, $R_2 = Cl$
c: $R_1 = Cl$, $R_2 = H$

3a: $R_1 = H$, $R_2 = Br$
b: $R_1 = H$, $R_2 = Cl$
c: $R_1 = Cl$, $R_2 = H$

5a: $R_2 = Br$
b: $R_2 = Cl$

6a: $R_1 = H$, $R_2 = Br$
b: $R_1 = H$, $R_2 = Cl$
c: $R_1 = Cl$, $R_2 = H$

Similarly reacted 3-bromo- (**1a**), 3-chloro- (**1b**) and 2-chloroaniline (**1c**) with hydroquinone (**2**) in the presence of zinc chloride, but halogeno-4′-hydroxy-diphenylamines (**3a**−**c**) were obtained as brown oils. 2-Bromoaniline was completely charred in these conditions. By treating with sulphur in the presence of catalytic quantities of iodine in 1,2-dichlorobenzene at about 180°C, 3-bromo-(**3a**) and 3-chloro-4′-hydroxy-diphenylamine (**3b**) give a mixture of isomers, namely 6-bromo- and 8-bromo-, respectively 6-chloro- and 8-chloro-3-hydroxy-phenothiazine (**4**). These mixtures were not purified but they were oxidized with potassium dichromate in glacial acetic acid when 6-bromo- (**5a**) and 8-bromo-(**6a**), respectively 6-chloro- (**5b**) and 8-chloro-phenothiazone (**6b**) were obtained. The mixtures of monohalogenated phenothiazone isomers were separated by column chromatography on alumina using toluene as eluant. 2-Chloro-4′-hydroxy-diphenylamine (**3c**), having only one unoccupied *ortho*-position, gives on thionation followed by oxidation 9-chloro-phenothiazone (**6c**) as it is shown in scheme 1.

8-Bromo- (**6a**) and 8-chloro-phenothiazone (**6b**) are already known compounds, but they were obtained in a different way.[4] In table 1 the monohalogeno-phenothiazones obtained by this method are presented.

Table 1

Halogeno-phenothiazones obtained by method A

Compound		Yield %	m.p. °C	Halogen calcd.	Halogen found	IR[CO] cm^{-1}
6-Bromo-phenothiazone	**(5a)**	7.5	241–243	27.35	28.02	1628
8-Bromo-phenothiazone	**(6a)**	23.6	221–223	lit.[4]		1623
6-Chloro-phenothiazone	**(5b)**	4.2	236–239	14.33	15.27	1628
8-Chloro-phenothiazone	**(6b)**	16.8	215–216	lit.[4]		1630
9-Chloro-phenothiazone	**(6c)**	9.1	217–219	14.33	14.96	1629

Method B (Condensation of zinc mercaptide of 2-aminothiophenol with halogeno-*p*-benzo-quinones)

In previous works [1,3,4] we have presented this synthetic method of some phenothiazone derivatives and also some observations about the reaction mechanisms. The facility with which the zinc mercaptide of 2-aminothiophenol (ATPh) and its derivatives reacted with benzoquinones-(1,4) makes this method suitable for the synthesis of certain substituted phenothiazones with the substituent in well defined positions. However, the reaction proceeds generally with by-products and numerous impurities which decrease the yields. Moreover, the purification becomes more difficult so that only the chromatographic purification is efficient. The elucidation of the structure will be discussed in other work.

Scheme 2

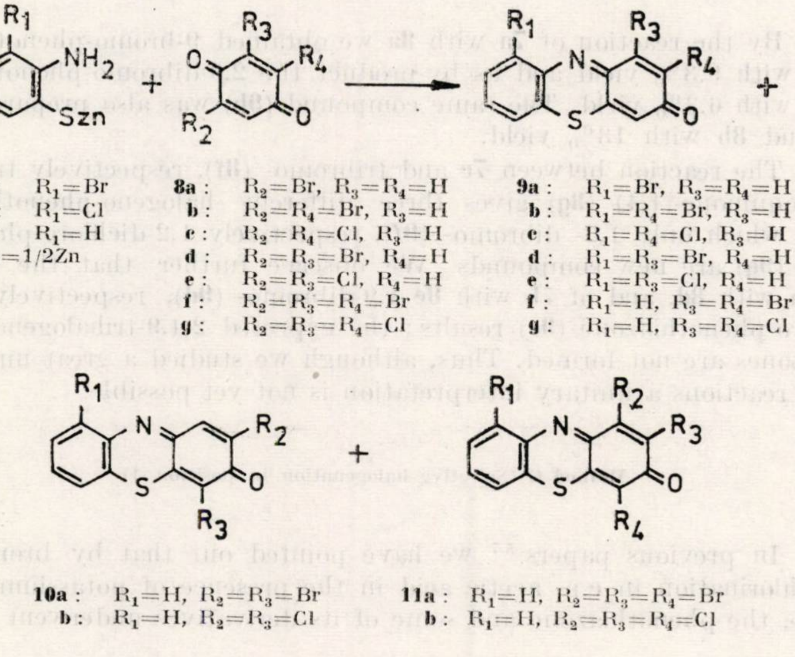

7a : R$_1$=Br
b : R$_1$=Cl
c : R$_1$=H
zn=1/2Zn

8a : R$_2$=Br, R$_3$=R$_4$=H
b : R$_2$=R$_4$=Br, R$_3$=H
c : R$_2$=R$_4$=Cl, R$_3$=H
d : R$_2$=R$_3$=Br, R$_4$=H
e : R$_2$=R$_3$=Cl, R$_4$=H
f : R$_2$=R$_3$=R$_4$=Br
g : R$_2$=R$_3$=R$_4$=Cl

9a : R$_1$=Br, R$_3$=R$_4$=H
b : R$_1$=R$_4$=Br, R$_3$=H
c : R$_1$=R$_4$=Cl, R$_3$=H
d : R$_1$=R$_3$=Br, R$_4$=H
e : R$_1$=R$_3$=Cl, R$_4$=H
f : R$_1$=H, R$_3$=R$_4$=Br
g : R$_1$=H, R$_3$=R$_4$=Cl

10a : R$_1$=H, R$_2$=R$_3$=Br
b : R$_1$=H, R$_2$=R$_3$=Cl

11a : R$_1$=H, R$_2$=R$_3$=R$_4$=Br
b : R$_1$=H, R$_2$=R$_3$=R$_4$=Cl

Condensing ATPh, Br- and Cl-ATPh (**7a**—**c**) with halogeno-benzoquinones-(1, 4) (**8a**—**g**) we obtained the halogeno-phenothiazones **9a**—**g**, **10a**—**b** and **11a**—**b**. Table 2 contains details upon a particular reaction performed by method B.

Table 2

Halogeno-phenothiazones obtained by method B

Starting compounds	Substituted-phenothiazone (substituent)	Yield %	m.p. °C	Halogene calcd.	Halogene found	IR[CO] cm^{-1}
7a+**8a**	9-Bromo- (**9a**)	9.3	216—217	27.35	26.89	1648
7a+**8b**	2,9-Dibromo- (**9b**)	6.3 (13)	234—236	43.07	42.93	1623
7b+**8c**	2,9-Dichloro- (**9c**)	13.6	243—245	25.13	24.73	1624
7a+**8d**	1,9-Dibromo- (**9d**)	28.6	214—218	43.07	43.53	1622
7b+**8e**	1,9-Dichloro- (**9e**)	7.3	206—208	25.13	26.00	1617
7c+**8f**	1,2-Dibromo- (**9f**)	2.2	215—218	43.07	43.38	1617
	2,4-Dibromo- (**10a**)	15.6	232	lit. [5]		1628
	1,2,4-Tribromo- (**11a**)	4.1	237—239	lit. [4]		1636
7c+**8g**	1,2-Dichloro- (**9g**)	5.0	225—227	25.13	25.13	1622
	2,4-Dichloro- (**10b**)	20.3	214—216	lit. [5]		1640
	1,2,4-Trichloro- (**11b**)	3.2	225—229	lit. [6]		1638

By the reaction of **7a** with **8a** we obtained 9-bromo-phenothiazone (**9a**) with 9.3% yield and as by-product the 2,9-dibromo-phenothiazone (**9b**) with 6.3% yield. The same compound (**9b**) was also prepared from **7a** and **8b** with 13% yield.

The reaction between **7c** and tribromo- (**8f**), respectively trichlorobenzoquinone-(1,4) (**8g**) gives three different halogeno-phenothiazones from which only 1,2- dibromo- (**9f**), respectively 1,2-dichloro-phenothiazone (**9g**) are new compounds. We observe further that the reaction of **7a** with **8d**, and of **7b** with **8e** 1,9-dibromo- (**9d**), respectively 1,9-dichloro-phenothiazone (**9e**) results ; the expected 2,4,9-trihalogeno-phenothiazones are not formed. Thus, although we studied a great number of such reactions a unitary interpretation is not yet possible.

Method C (Selective halogenation in position 4)

In previous papers [5,7] we have pointed out that by bromination or chlorination in c.p. acetic acid in the presence of potassium dichromate, the phenothiazone and some of its derivatives underwent an electrophilic halogenation in position 4. This halogenation method is now applied upon the monohalogeno-phenothiazones obtained by the methods A and B.

Scheme 3

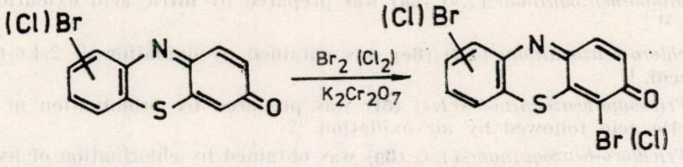

5a, **5b**, **9a**, **8a**

12a : 4,6-Dibromo-
b : 4,6-Dichloro-
c : 4,9-Dibromo-
d : 4,9-Dichloro-phenothiazone

The results of our experiments are shown in table 3.

Table 3

Halogeno-phenothiazones obtained by method C

Starting compound	Substituted-phenothiazone (substituent)		Yield %	m.p. °C	Halogen		IR[CO] cm^{-1}
					calcd.	found	
5a	4,6-Dibromo-	**(12a)**	55.5	238–239	43.07	42.51	1624
5b	4,6-Dichloro-	**(12b)**	30.8	238–241	25.13	24.90	1642
9a	4,9-Dibromo-	**(12c)**	23.6	235–236	43.07	43.05	1622
6c	4,9-Dichloro-	**(12d)**	45.5	246	25.13	*	1638

* This compound burns very difficultly

The reactions described in this paper by means of the methods A, B and C have not exhausted all the possibilities of synthesis. However, the new compounds have completed a number of series of simple substituted phenothiazones which will be used in other works.

EXPERIMENTAL

All melting points are corrected. The IR-spectra were recorded with a Carl Zeiss Jena UR-10 spectrophotometer ; the substances were prepared as KBr pellets.

Starting compounds

Zinc mercaptide of 2-amino-3-bromo-thiophenol (**7a**). The method of Dalgliesh and Mann [8] for the chloro-derivative was adapted with some modifications as follows : 2-Bromoaniline hydrochloride and sodium thiocyanate were boiled in chlorobenzene for 6 hours. The obtained (2-bromo-N-phenyl)-thiourea was cyclized with bromine in chloroform to give 2-amino-4-bromo-benzothiazole. This was heated in an autoclave with 20% aqueous hydroxide at 140–145°C and 3–3.5 bars (at higher temperature the product is decomposed) and the sodium 2-amino-3-bromo-thiophenolate was converted to the zinc salt with an aqueous solution of zinc chloride. The product is a yellowish powder.

Zinc mercaptide of 2-amino-3-chloro-thiophenol (**7b**) was obtained following the method of Dalgliesh and Mann [8] (see above). The last step, namely the alkaline splitting of 2-amino-4-chloro-benzothiazole was performed at 210–220°C (oil-bath temperature ; 160–170°C inside temperature and 9 bars pressure). **7b** was obtained as a white powder.

Zinc mercaptide of 2-amino-thiophenol (**7c**) was prepared from 2-mercapto-benzothiazole (Captax) by melting with potassium hydroxide. Yellowish powder .[9]

2-Bromo-benzoquinone-(1,4) (**8a**) was obtained by bromination of hydroquinone in chloroform-ethyl ether mixture followed by iron chloride oxidation.[10]

2,5-Dibromo-benzoquinone-(1,4) (**8b**) was prepared by bromination of hydroquinone in glacial acetic acid followed by iron chloride oxidation.[10]

2,5-Dichloro-benzoquinone-(1,4) (**8c**) was obtained by two successive additions of hydrochloric acid to benzoquinone-(1,4) and 2-chlorobenzoquinone-(1,4) and two oxidation reactions of 2-chloro- and 2,5-dichloro-hydroquinone with potassium dichromate and nitric acid. [11]

2,6-Dibromo-benzoquinone-(1,4) (**8d**) was prepared by nitric acid oxidation of 2,4,6-tribromophenol. [11]

2,6-Dichloro-benzoquinone-(1,4) (**8e**) was obtained by oxidation of 2,4,6-trichlorophenol with nitric acid. [12]

2,3,5-Tribromo-benzoquinone-(1,4) (**8f**) was prepared by bromination of hydroquinone in glacial acetic acid followed by air oxidation. [10]

2,3,5-Trichloro-benzoquinone-(1,4) (**8g**) was obtained by chlorination of hydroquinone in glacial acetic acid followed by iron chloride oxidation.[13]

Halogeno-phenothiazones

Method A

Halogeno-4′-hydroxy-diphenylamines (**3a** — **c**) 0.1 Moles of 3-bromo-, 3-chloro- or 2-chloroaniline (**1a** — **c**), 20 g hydroquinone and 2 g zinc chloride were heated at 180—190°C for 90 minutes. The reaction mixture was cooled, treated with 150 ml water and 20 ml concentrated hydrochloric acid and heated again on water-bath for 1 hour. On cooling the halogeno-4′-hydroxy-diphenylamine separated as brown oil which was pure enough for further reaction. Yield for **3a** 84 %, for **3b** 65 % and for **3c** 83 %.

Thionation of halogeno-4′-hydroxy-diphenylamines. 0.08 Moles of halogeno-4′-hydroxy-diphenylamines (**3a** — **c**), 4.86 g sulphur, 0.01 g iodine and 20 ml 1,2-dichlorobenzene were gently boiled for 1 hour. Hydrogen sulphide is evolved. The reaction mixture was cooled and then subjected to water distillation in order to remove all 1,2-dichlorobenzene. After cooling the supernatant layer was decanted and the dark coloured adhesive solid (or viscous oil) was weighed. The mixture of 6-bromo- and 8-bromo-3-hydroxy-phenothiazine is obtained with 89 % yield ; 6-chloro- and 8-chloro-3-hydroxyphenothiazine with 88 % and 9-chloro-3-hydroxy-phenothiazine with 75 % yield.

Oxidation of halogeno-3-hydroxy-phenothiazines. The mixture of halogeno-3-hydroxy-phenothiazine isomers (**3 g**) and potassium dichromate (**3 g**) were boiled in glacial acetic acid (100 ml) for 3 minutes. The red solution was cooled and precipitated with water, filtered off, dried and dissolved in 100—150 ml toluene. The dried solution was then purified by chromatography on 1 kg alumina (activity III) using toluene as eluant. (Dimensions of column : 50 × × 5.5 cm).

In the case of the mixtures of 6-bromo- (**5a**) and 8-bromo- (**6a**), respectively 6-chloro- (**5b**) and 8-chloro-phenothiazones (**6b**), from the chromatographic column the 6-halogeno-isomer was first eluted. The halogeno-phenothiazones obtained by this method are shown in table 1.

Method B

This method was described in detail in a previous paper.[4] The halogeno-phenothiazones obtained in this way are presented in table 2.

In the case of the mixtures of 1,2-, 2,4-dibromo- and 1,2,4-tribromo- (or chloro-) phenothiazones, from the chromatographic column the trisubstituted-phenothiazone **11a** (or **11b**) was first eluted, then 2,4-dibromo-(**10a**) or 2,4-dichloro- (**10b**) and at last the 1,2-dibromo-(or dichloro-)phenothiazone.

Method C

This method was also presented in detail in a previous work. [5] The dihalogeno-phenothiazones prepared by this method are shown in table 3.

ACKNOWLEDGEMENTS. For recording the IR-spectra the author is indebted to Miss Rodica Grecu and for the microanalytical analysis to Mrs. Maria Duma and Ileana Roșu.

REFERENCES

[1] Part I. M. H. Terdic and I. Valter, *Liebigs Ann. Chem.*, **1978**, 1285.
[2] G. Heller, *Liebigs Ann. Chem.*, **418**, 264 (1919).
[3] M. H. Terdic, *Liebigs Ann. Chem.*, **746**, 200 (1971).
[4] M. H. Terdic and C. Bodea, *Rev. Roumaine Chim.*, **13**, 833 (1968).
[5] M. H. Terdic and C. Bodea, *Rev. Roumaine Chim.*, **13**, 1241 (1968).
[6] Takao Mine, *Kogyo Kagaku Zasshi*, **67**, 149 (1964), *Chem. Abstr.*, **61**, 656 (1964).
[7] C. Bodea and M. H. Terdic, *Rev. Roumaine Chim.*, **13**, 1235 (1968).
[8] C. E. Dalgliesh and F.G. Mann, *J. Chem. Soc.*, **1945**, 893.
[9] A. W. Hofmann, *Ber. dtsch. chem. Ges.*, **13**, 20 (1880).
[10] E. Sarauw, *Liebigs Ann. Chem.*, **209**, 93 (1881).
[11] S. Levy and G. Schultz, *Liebigs Ann. Chem.*, **210**, 145 (1881).
[12] A. Faust, *Liebigs Ann. Chem.*, **149**, 153 (1869).
[13] H. Knapp and G. Schultz, *Liebigs Ann. Chem.* **210**, 174 (1881).

Revue Roumaine de Chimie, 29, 6, 497—505 (1984)

IDENTIFICATION D'HYDROCARBURES AROMATIQUES DE QUELQUES FRACTIONS PÉTROLIÈRES. I

CONDITIONS EXPÉRIMENTALES EN HPLC

HOCINE KADI et D. P. LAZĂR
Département de Génie chimique, Ecole Polytechnique, Université d'Alger, Algérie
Département de chimie physique, Faculté de technologie chimique, 71 Splai Bahlui, 6600 Jassy, Romania

Reçu le 11 mai 1983

The modern and powerful technique of high performance liquid chromatography (HPLC) has been used for the separation, identification and quantitative analysis of aromatic hydrocarbons from some fractions obtained after the primary distillation of the crude-oil of Hassi — Messaud (Algeria).

La technique moderne et efficace de la chromatographie HPLC[1] a été utilisée pour la séparation, l'identification et le dosage quantitatif d'hydrocarbures aromatiques de quelques fractions obtenues d'une première distillation du pétrole brut de Hassi—Messaoud (Algérie). La méthode chromatographique HPLC est suivie de la méthode de mesure de l'indice de réfraction, de la densité et du point d'aniline (méthode n.d. PA) de chaque fraction et de l'analyse spectroscopique IR des fractions étudiées.

1. OBJET DE LA RECHERCHE

La méthode principale de séparation et d'identification — méthode HPLC — comme les deux autres méthodes de contrôle, n.d.PA et IR, sont appliquées à une coupe pétrolière obtenue d'une première distillation à la raffinerie d'Alger. Cette coupe a une température initiale de distillation $t_i^\circ = 90°$ et une température finale $t_f^\circ = 209°$. La température initiale $t_i^\circ = 90°$ correspond au point d'ébullioscopie du 2-Méthyl hexane tandis que la température $t_f^\circ = 209°$ correspond au point d'ébullioscopie du 4-Méthyl indène.

Comme la coupe pétrolière 90°—209° comprend un nombre considérable de constituants individuels, nous avons procédé à son fractionnement par distillation VPE (vrai point d'ébullition)[2] pour obtenir 23 fractions séparées entre elles par une température d'ébullioscopie variant de 1,5° à 11,5° (voir Tableau 1).

Par la suite, chaque fraction est analysée par la méthode HPLC pour la séparation et l'identification des constituants individuels (cette méthode HPLC est suivie par des méthodes n.d.PA et IR).

2. CONDITIONS DE TRAVAIL EN HPLC

2.1. **Le chromatographe** utilisé est un HPLC WATERS Ass -440 comprenant deux pompes, un injecteur, deux systèmes de détection : UV (avec adsorption à 254 nm) et Refractive Index (RI).

2.2. Colonne

Après une série d'essais préliminaires, notre choix a porté sur une colonne μ BONDAPAK/C 18 (WATERS Ass) connue comme efficiente dans le cas de la séparation et de l'identification des hydrocarbures aromatiques .[3] Cette colonne est préremplie de microparticules solides ayant un diamètre de 10 nm. Les dimensions de la colonne sont : 30 cm de longueur, 0,4 cm de diamètre intérieur (catalogue WATERS 27324). La colonne μ BONDAPAK/C 18 est très efficace, elle produit des pics bien profilés et séparés de façon satisfaisante. Elle est garantie pour un nombre minimum de 9000 plateaux par mètre. Le garnissage de la colonne est apolaire. Elle doit donc être utilisée avec un éluent polaire en appliquant la chromatographie de partage en « phase inversée » .[4]

Les séparations chromatographiques sont faites à la température ambiante.

2.3. Sélection de la fraction utilisée pour l'optimisation et le test de la méthode HPLC

La fraction choisie doit répondre aux critères suivants :

1° être située à peu près au milieu de l'intervalle de température utilisé dans la méthode VPE, c'est-à-dire vers le milieu de l'intervalle 99° − 209°,

2° posséder une composition moyenne en pourcentage par rapport à la coupe pétrolière étudiée,

3° contenir des hydrocarbures aromatiques bien séparés par la chromatographie HPLC et faciles à identifier (c'est-à-dire que la fraction doit être facile à simuler à partir de constituants purs).

La fraction n° 7 a été sélectionnée sur la base de tous ces critères. Elle a $\mathring{t}_i = 137^\circ$ et $\mathring{t}_f = 145{,}5^\circ$ (voir Tableau 1) et contient trois hydrocarbures aromatiques identifiables.

2.4. Éluent

Nous utiliserons comme éluent un mélange binaire eau : acétonitrile[5] dans une gamme de débits 0,1 − 9,9 ml min^{-1}, sous une pression variable pouvant atteindre 290 atm. Il est indiqué d'éviter de travailler avec de grands débits. Ces derniers créent de très hautes pressions responsables de la diminution de l'efficacité de la colonne et même de la détérioration mécanique.[6]

Concentration de l'éluent. Nous avons testé un mélange binaire eau : acétonitrile à des rapports volumétriques différents (40 :60, 50 :50, 60 :40) avec des débits de 2, 3, 4, 5 et 6 ml min^{-1}. Les résultats de ces tests sont consignés dans les tableaux 2, 3 et 4, où R est un facteur de résolution particulier [7], défini par la relation :

$$R_C = \frac{\mathrm{OH} - \mathrm{O'H'}}{\mathrm{OA} - \mathrm{O'A'}} \qquad (1)$$

Tableau 1

Résultats de la redistillation VPE de la coupe primaire avec $t_i^\circ = 90°$ et $t_f^\circ = 209°$

Fraction N°	Temprature initiale t_i°	Température finale t_f°	$t_f^\circ - t_i^\circ$	Fraction N°	Temperature initiale t_i°	Température finale t_f°	$t_f^\circ - t_i^\circ$
1	90,0	99,0	9,0	13	172,0	175,0	3,0
2	99,0	103,5	4,5	14	175,0	178,0	3,0
3	103,5	115,0	11,5	15	178,0	182,0	4,0
4	115,0	123,5	8,5	16	182,0	184,5	2,5
5	123,5	131,0	7,5	17	184,5	188,0	3,5
6	131,0	137,0	6,0	18	188,0	191,0	3,0
7	137,0	145,5	8,5	19	191,0	197,5	6,5
8	145,5	151,0	5,5	20	197,5	200,5	3,0
9	151,0	157,5	6,5	21	200,5	202,0	1,5
10	157,5	164,5	7,0	22	202,0	205,0	3,0
11	164,5	169,0	4,5	23	205,0	209,0	4,0
12	169,0	172,0	3,0				

Tableau 2

Influence du débit et de la pression sur les valeurs t_R, R_C et R en utilisant l'éluent eau – acétonitrile = 60 : 40 (fraction n° 7)

Débit v (ml min^{-1})	Pression P (atm)	Temps de rétention t_R (s)	Facteur de rétention R_C	Résolution R
2	85,057	1. 1128 2. 1017 3. 696	0,85 1,00	1,14 4,46
3	136,092	1. 732 2. 657 3. 438	0,75 1,00	1,02 4,17
4	187,126	1. 552 2. 501 3. 336	0,72 1,00	* 3,44
5	238,160	1. 444 2. 399 3. 267	0,64 1,00	* 3,67
6	289,195	1. 336 2. 330 3. 222	0,65 1,00	* 3,60

* Difficile à déterminer

Tableau 3

Influence du débit et de la pression sur les valeurs t_R, R_C et R en utilisant l'éluent eau : acétonitrile = 50 : 50 (fraction n° 7)

Débit v (ml min^{-1})	Pression P (atm)	Temps de rétention t_R (s)	Facteur de rétention R_C	Résolution R
2	85,057	1. 585 2. 534 3. 399	0,82 1,00	1,21 3,10
3	136,092	1. 375 2. 348 3. 261	0,69 1,00	* 3,40
4	187,126	1. 279 2. 258 3. 195	0,69 1,00	— 2,80
5	238,160	1. 219 2. 204 3. 137	0,65 1,00	— 2,83
6	289,195	1. 177 2. 165 3. 126	0,60 1,00	— 2,60

* Difficile à déterminer

Tableau 4

Influence du débit et de la pression sur les valeurs t_R, R_C et R en utilisant l'éluent eau — acétonitrile = 40 : 60

Débit v (ml min^{-1})	Pression P (atm)	Temps de rétention t_R (s)	Facteur de rétention R_C	Résolution R
2	85,057	1. 294 2. 279 3. 231	0,49 1,00	— 1,68
3	136,092	1. 196 2. 186 3. 153	0,45 1,00	— 2,00
4	187,126	1. 147 2. 141 3. 117	0,36 1,00	— 2,29
5	238,160	1. 114 2. 108 3. 90	0,34 0,97	— 2,00
6	289,195	1. 96 2. 96 3. 75	0,00 0,00	0,00 0,00

avec $0 \leqslant R \leqslant 1$. La signification des grandeurs de la relation (1) est représentée par la fig. 1.

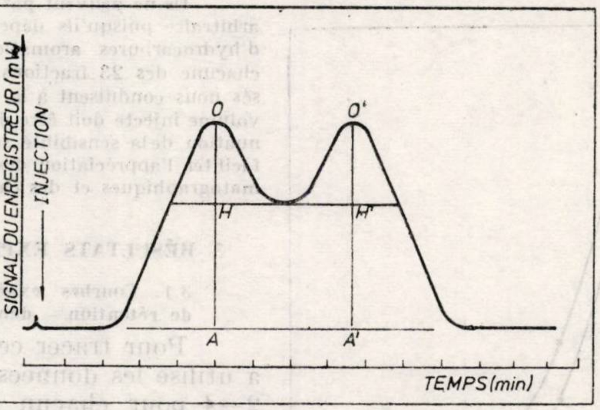
SIGNAL DU ENREGISTREUR (mV)
INJECTION
O
O'
H
H'
A
A'
TEMPS (min)

Fig. 1. — Définition du facteur de résolution R_C (cf. rel. (1)).

La grandeur $R = 2\left(\dfrac{t_{R_2} - t_{R_1}}{w_1 + w_2}\right)$ (2) représente la résolution[8] entre deux pics consécutifs, conformément à la fig. 2.

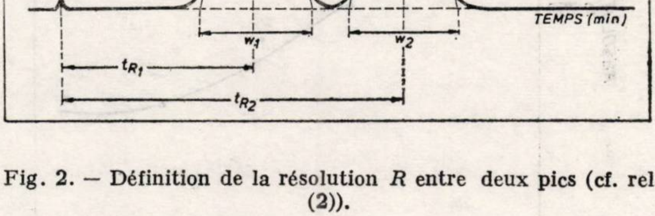
SIGNAL (mV)
INJECTION
$w_{h,1}$
$w_{h,2}$
w_1
w_2
t_{R_1}
t_{R_2}
TEMPS (min)

Fig. 2. — Définition de la résolution R entre deux pics (cf. rel. (2)).

D'après les résultats présentés par les tableaux 2—4, il résulte que l'éluent le plus indiqué est le mélange binaire eau — acétonitrile 60 :40, utilisé à un débit de 2 ml min^{-1}.

2.5. Volume de l'échantillon injecté et sensibilité des détecteurs

Ces deux paramètres sont interdépendants et exercent une grande influence sur la forme des pics et sur la résolution entre les pics.

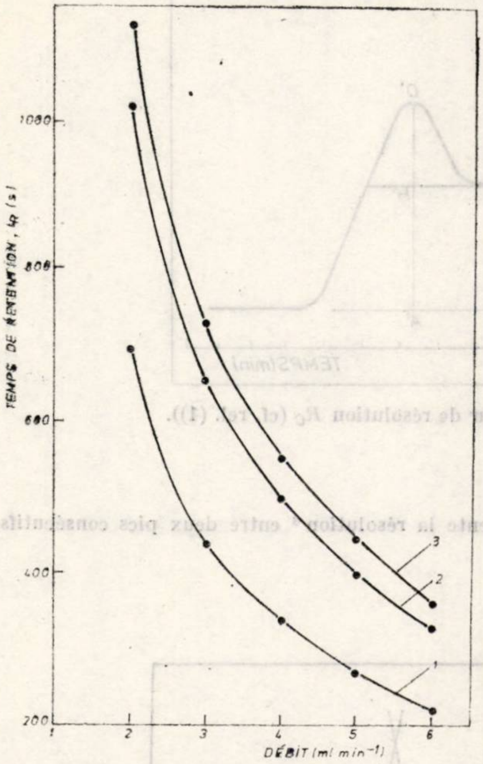

Fig. 3. — Courbes expérimentales « débit-temps de rétention »; éluent eau : acétonitrile = 60 :40, fraction n° 7;
1 — pic 1; 2 — pic 2; 3 — pic 3.

Ils ne peuvent pas être fixés de façon arbitraire puisqu'ils dépendent du nombre d'hydrocarbures aromatiques contenu par chacune des 23 fractions. Les tests réalisés nous conduisent à la conclusion que le volume injecté doit être de 5 μ 1, et l'atténuation de la sensibilité sera égale à 1, pour faciliter l'appréciation des séparations chromatographiques et des calculs.

3. RÉSULTATS EXPÉRIMENTAUX

3.1. Courbes expérimentales «temps de rétention — débit d'éluent»

Pour tracer ces courbes, on a utilisé les données des tableaux 2—4 pour chacun des trois rapports eau : acétonitrile. La figure 3 donne les courbes pour l'éluent sélectionné, eau : acétonitrile = 60 : 40.

3.2. Courbes expérimentales «résolution — débit»

Ces courbes sont tracées avec les données des tableaux 2 — 4. Dans la fig. 4 est représentée la courbe « résolution — débit » pour l'éluent eau : acétonitrile = 60 : 40.

Le facteur de résolution R (rel. 2) est donc une fonction décroissante du débit.[9] Pour obtenir une résolution satisfaisante entre les pics des hydrocarbures aroma-

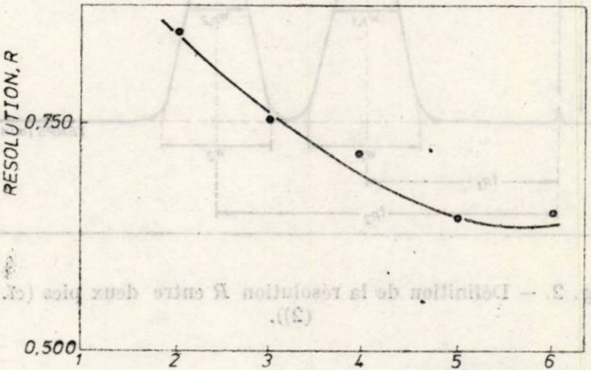

Fig. 4. — Courbes expérimentales « débit-résolution »; éluent eau-acétonitrile = 60 :40; fraction n° 7.

tiques appartenant à une même fraction, il faut que les séparations chromatographiques HPLC se fassent à de petits débits d'éluent.

3.3. Courbes expérimentales «pression — débit»

Dans la technique HPLC, la pression à laquelle l'éluent passe à travers la colonne est une fonction linéaire décroissante du débit de l'éluent.[10] Il est évident que des pressions très petites ou des pressions très grandes vont diminuer les performances de la colonne et les pressions élevées peuvent même causer la détérioration physique du garnissage de la colonne.

En conclusion, il est recommandé d'utiliser de petits débits (v. Fig. 5).

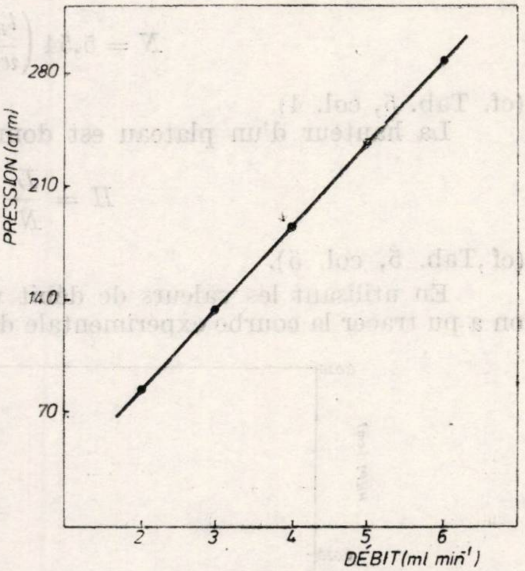

Fig. 5. — Courbe expérimentale « débit-pression ».

3.4. Efficacité de la colonne

Elle a été appréciée à l'aide des données chromatographiques obtenues à différents débits. Ces résultats se rapportent au constituant de la fraction nº 7, qui mannifeste le pic le plus haut.

Les résultats quantitatifs sont donnés par le tableau 5.

Tableau 5

Données quantitatives nécessaires pour le calcul du nombre de plateaux (N) et de la grandeur HEPT (H) pour $L = 30$ cm

Débit (cm min^{-1})	Temps de rétention t_R (cm)	Largeur du pic à la mi-hauteur w_h(cm)	Nombre de plateaux théoriques N	$H = \frac{L}{N}$ (cm)
2	18,8	0,95	2170	0,0138
3	12,2	0,70	1683	0,0178
4	9,2	0,60	1303	0,0230
5	7,4	0,50	1214	0,0247
6	6,1	0,40	1018	0,0295

où :

v = débit volumétrique de l'éluent, mesuré à la sortie de la colonne, en ml min^{-1},

$t_{R,i}$ = temps de rétention (non corrigé) du constituant « i » de l'échantillon analysé,

w_h = largeur du pic du constituant «i », mesurée à la mi-hauteur du pic en secondes,

N = nombre de plateaux théoriques,

L = longueur de la colonne, en cm.
H = hauteur d'un plateau théorique, en cm.

A l'aide des données du tableau 5, nous avons évalué l'efficacité de la colonne en calculant le nombre de plateaux théoriques de la colonne :

$$N = 5{,}54\left(\frac{t_{R_i}}{w_h}\right)^2 \tag{3}$$

(cf. Tab. 5, col. 4).

La hauteur d'un plateau est donnée par :

$$H = \frac{L}{N} \tag{4}$$

(cf ,Tab. 5, col. 5).

En utilisant les valeurs de débit v et de hauteur H du tableau 5, on a pu tracer la courbe expérimentale de van Deemter (Fig. 6), cette dernière nous a permis d'évaluer la valeur optimale du débit, v_{optim} ainsi que la hauteur minime d'un plateau théorique, $H_{\min}$ (sur le graphe le minimum en HETP ne figure pas),

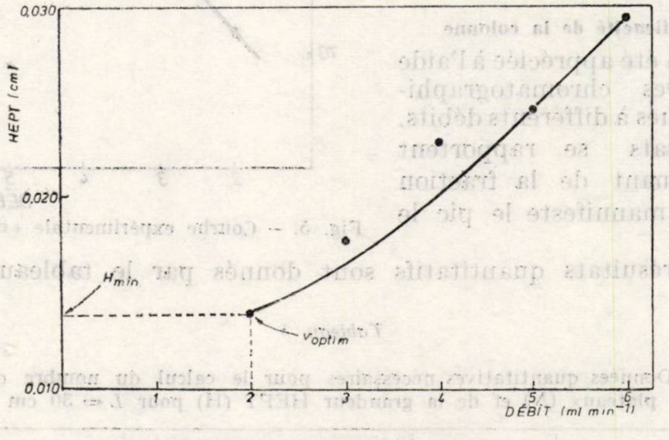

Fig. 6. — Courbe expérimentale van Deemter.

CONCLUSIONS

1°. L'obtention, par la méthode VPE, des 23 fractions rapportées par le tableau 1, a permis une analyse HPLC efficiente de la coupe pétrolière 99°—209°, qui constitue l'objet de cette recherche.

2°. Les conditions optimales d'utilisation de la technique HPLC sont :

a. dimension de colonne : 30 cm ; b. colonne : μ-BONDAPK/C 18 ; c. température de la colonne : ambiante ; d. éluent : eau : acétonitrile =

= 60 : 40 ; e. gradient : linéaire ; f. débit : 2 ml min $^{-1}$; g. détection : UV (254 nm) et Refractive Index (RI) ; h. échantillon : fraction n° 7 ; i. volume de l'échantillon : 5 μl.

BIBLIOGRAPHIE

[1] E. L. Johnston et R. Stevenson, "Basic Liquid Chromatography", VARIAN Associates, Inc., Palo Alto, California, 1978, p. 8–13.
[2] V. I. Robu, "Distilare – fracţionare", Editura Tehnică, Bucureşti, 1963, p. 170–175.
[3] E. L. Johnston et R. Stevenson, op. cit., p. 86–89, 92, 100, 110.
[4] E. L. Johnston et R. Stevenson, op. cit., p. 9–11, 96–97.
[5] E. L. Johnston et R. Stevenson, op, cit., p. 101.
[6] E. L. Johnston et R. Stevenson, op. cit., p. 44–64.
[7] S. E. Chitour, communication privée.
[8] E. L. Johnston et R. Stevenson, op. cit., p. 15–16.
[9] E. L. Johnston et R. Stevenson, op. cit., p. 18–19.
[10] E. L. Johnston et R. Stevenson, op. cit., p. 45.

Revue Roumanie de Chimie, **29**, *6*, 507–511 (1984)

SEPARATION AND CONCENTRATION OF THIOSULPHATE WITH ION-EXCHANGE RESINS

LUMINIŢA VLĂDESCU and STELUŢA GHINEA
National Institute of Chemistry, Laboratory of
Analytical Chemistry, Splaiul Independenţei 202, Bucharest, Romania

Received September 28, 1983

In this paper the ion exchange behaviour of $S_2O_3^{2-}$, SO_3^{2-} and SO_4^{2-} anions in the presence of strontium cations was studied. The working conditions for separation of the three anions were established on the basis of the results obtained using cation or anion exchange resins.

The analyst is often faced with the problem of quantitative determination of thiosulphate in the presence of SO_3^{2-} and SO_4^{2-} anions. Sulphate does not interfere in the methods for the determination of thiosulphate based on oxido-reduction reactions but the presence of sulphite gives positive errors.

The speciality literature indicates that the behaviour of thiosulphate differs from that of sulphate and sulphite anions in the presence of Sr^{2+} cations : in neutral solutions difficultly soluble strontium sulphate and sulphite precipitates form, whereas strontium thiosulphate is readily soluble in water.[1–4]

This property was used within an anionic exchange system for obtaining a solution that contains only sodium thiosulphate, starting from a sodium thiosulphate, sulphate and sulphite mixture.

The working conditions for separation of the three anions were established on the basis of the results obtained using cation or anion exchange resins.

EXPERIMENTAL

Chemicals and equipment

- Strongly acid cation exchange resin Vionit CS-3.
- Strongly basic anion exchange resin Vionit AT-1.
- Aqueous solutions of known titrum of $S_2O_3^{2-}$, SO_3^{2-}, SO_4^{2-}
- Aqueous solutions of 0.25, 0.50, 1.0 and 3.0 M $SrCl_2$ and 0.5 and 1.0 M $Sr(NO_3)_2$.
- Aqueous-ethanolic solution of 1 % α,α'-dipyridyl.
- Aqueous solution of 10^{-2}M $FeCl_3$ containing 1 M HCl.
- Aqueous solutions of 10^{-2}M Complexon III, 10^{-2} $Ba(NO_3)_2$.
- SPEKOL Carl Zeiss-Jena spectrophotometer.

The quantitative determination of the anions investigated was performed by spectrophotometry in the presence of $FeCl_3$ and α,α′-dipyridyl for sulphite and thiosulphate [5] and by indirect titration with Complexon III in the case of sulphate.[6]

The ion exchange took place in glass column, 15 cm long, 1 cm in diameter provided with stopcoks at bottom and funnel with ground joint at top. Known quantities of cation or anion exchanger were transferred into each column, purified, activated in H^+ or Cl^- ionic form, respectively, and washed with distilled water up to negative Cl^- test.

RESULTS AND DISCUSSION

With a view to establishing optimal working conditions, a study concerning the influence of the resin type, of strontium ion concentration and of the anion in the strontium salt, on the behaviour of thiosulphate, sulphite and sulphate in the course of ion exchange was carried out.

To this end, accurately measured volumes of the solution with known thiosulphate, sulphite and sodium sulphate titres were passed in turn through a strongly acid cation exchange resin, in ionic form Sr^{2+}. The quantity of anions that passed into effluent was measured after washing the column with distilled water.

Table 1

Influence of the type and form of the ion exchange resin, of the concentration and anion of the strontium salt and of the methanol content, on the ion exchange behaviour of $S_2O_3^{2-}$, SO_3^{2-} and SO_4^{2-} anions

Resin		Sr^{2+} solution			$S_2O_3^{2-}$		SO_3^{2-}		SO_4^{2-}	
Type	Ionic form	Salt	Conc M	MeOH 90 %	in sample mg	eluted mg	in resin mg	eluted mg	in resin mg	eluted mg
VIONIT CS-3	Sr^{2+}	—	—	—	1.12	1.14	0.80	—	0.96	—
			3	—	1.12	1.12	0.80	—	0.96	—
			1	—	1.12	1.10	0.80	—	0.96	—
	Cl^-	$SrCl_2$	0.5	—	1.12	1.14	—	—	—	—
VIONIT AT-1			0.25	—	1.12	1.10	—	—	—	—
			1	100 %	1.12	1.12	—	—	—	—
			1	—	1.12	1.11	0.80	—	0.96	—
		$Sr(NO_3)_2$	0.5	—	1.12	1.13	—	—	—	—

From table 1 it may be seen that sulphite and sulphate were retained in the resin under the form of strontium precipitate (also visible with the nacked eye) while thiosulphate was again found quantitatively in the effluent.

In the anion exchange experiments, known quantities of the studied anions were fixed in a strongly basic resin in the Cl^- form, by passing 100 ml strontium salt solutions in varied concentratios trough the resin, then measuring the quantity of anion not retained in the resin.

The results given in table 1 show that irrespective of the strontium salt used and the solution concentration, sulphate and sulphite remain in resin as strontium precipitates, whereas thiosulphate can be entirely found in the effluent. MeOH that diminished the solubility product of strontium sulphite and sulphate does not affect the behaviour of thiosulphate.

The elution curves in figure 1 show that thiosulphate is eluted from the anionite in an effluent volume which decreases with increase in the concentration of the strontium solution and that strontium nitrate proves to be a more efficient eluting agent than chloride.

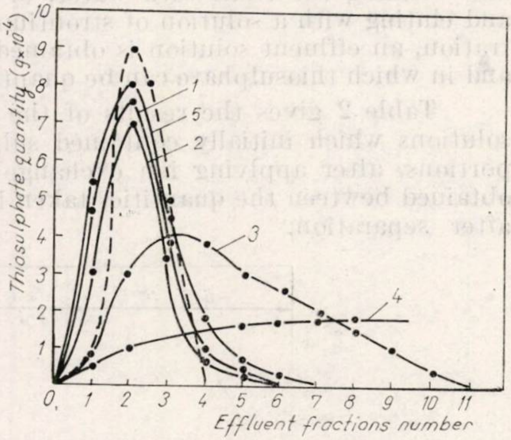

Fig. 1. — Elution curves of thiosulphate from an anion exchange resin in different experimental conditions. Eluent solutions : 1—3M $SrCl_2$; 2—1M $SrCl_2$; : 3—0.5M $SrCl_2$; 4—0.2M $SrCl_2$; 5—1M $Sr(NO_3)_2$.

The attempts to elute the sulphate and sulphite retained in resin led to the selection of the following elution systems.

In the case of sulphite it was found that after passing a solution of $FeCl_3$ 10^{-2}M containing 1M HCl and 1% α,α'-dipyridyl through an anion exchange resin, the effluent collected in graduated balloon may be used for indirect spectrophotometric determination of the sulphite retained in the resin.

Table 2

Results of $S_2O_3^{2-}$ content determination after ion exchange separation

$S_2O_3^{2-}$		Content in sample		Ion exchange procedure
In sample mg	Determined mg	SO_3^{2-} mg	SO_4^{2-} mg	
1.12	1.12	0.80	0.96	C
11.10	11.22	1.60	4.80	C
112.0	111.92	0.80	0.96	C
1.12	1.10	0.80	0.96	A
5.65	5.60	0.80	0.96	A

C = cation exchange method ; A = anion exchange method.

Sulphate can be eluted following solubilization of the precipitate, under the action of a HCl 4–6 M solution. At higher acid concentrations elution of the sulphate from the resin was more rapid.

Therefore, by passing the solution containing sulphate, sulphite and thiosulphate through a cation exchange resin in the Sr^{2+} ionic form and washing the resin with water, or through an anion exchange resin and eluting with a solution of strontium nitrate or chloride 0.5 M concentration, an effluent solution is obtained which contains only thiosulphate and in which thiosulphate can be quantitatively measured by any method.

Table 2 gives the results of the determinations of thiosulphate in solutions which initially contained sulphite and sulphate in varied proportions, after applying ion exchange methods. A good agreement was obtained bewteen the quantities taken in the sample and those determined after separation.

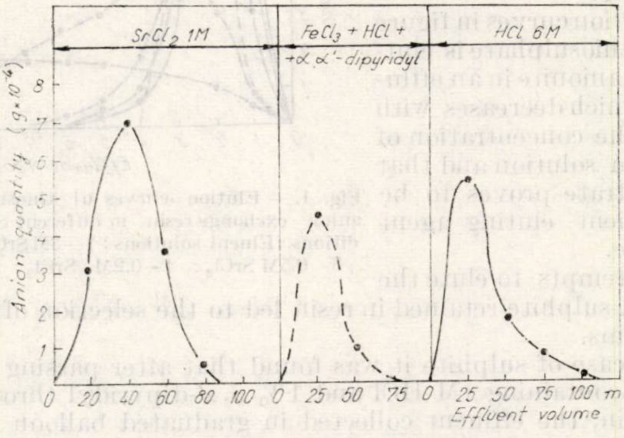

Fig. 2. Elution curves for anion exchange separation of $S_2O_3^{2-}-SO_3^{2-}-SO_4^{2-}$ anions mixture.

Figure 2 shows the elution curves obtained in the case of the anion-exchange method applied for separation of a synthetic mixture containing known quantities of sodium thiosulphate, sulphite and sulphate.

CONCLUSIONS

The experimental results show a different ion exchange behaviour of thiosulphate as compared with sulphate and sulphite in the presence of Sr^{2+} ions.

The working conditions for separation of the three anions were established on the basis of the results obtained using cation or anion exchange resins.

The procedure with anionite is recommended for solutions with low concentrations of thiosulphate permitting both its separation and concentration.

REFERENCES

[1] N. M. Selivanova and G. A Zubova, *Trudy Moskov. Khim. Tehn. Inst.*, **22**, 38 (1956).

[2] I. V. Kolosov, *Zhur. neorg. Khim.*, **10**, 2200 (1965).

[3] K. H. Lieser, *Z. anorg, Chem.*, **335**, 225 (1965).

[4] T. O. Denney and C. B. Monk, *Trans. Faraday Soc.*, **47**, 992 (1951).

[5] L. Vlădescu, *Bul. Inst. Politehn. București* (in press).

[6] C. Liteanu, "Chimia analitică cantitativă — Volumetria", Ed. Didactică și pedagogică, Bucharest, 1969.

Revue Roumaine de Chimie, **29**, *6*, 513–520 (1984)

ON THE POLYMERIZATION OF ACETYLENIC DERIVATIVES XXXVI[1]

THE CATIONIC POLYMERIZATION OF 9-ETHYNYLANTHRACENE

SVETLANA DUMITRESCU, M. GRIGORAŞ, G. SURPĂŢEANU
and M. CONSTANTINESCU

Polytechnic Institute of Jassy, Department of Organic and
Macromolecular Chemistry, Jassy-6600, Romania

Received November 3, 1982

A theoretical study using the MO calculations, EH (extended Huckel) noniterative procedure method was applied to the ionic polymerization of 9-ethynylanthracene. Theoretical results show that the ionic (cationic) polymerization follows the scheme 2,b — the dihydroanthracene units formation is energetically favoured. Experimentally, a mixture of polymers containing dihydroanthracene, 9,10-disubstituted anthracene and polyene units was founded. The sterical and experimental factors could change the composition of the obtained polymers by a cationic mechanism. The structure of polymers was established by using IR, UV and NMR spectra.

INTRODUCTION

In previous papers we studied the radical[1] and Ziegler-Natta[2] polymerization of 9-ethynylanthracene (9-EA). The polymerization of the same monomer using the phosphinic complexes of the transitional metals was presented in the paper[3].

The cationic polymerization of 9-vinylanthracene (9-VA) occurs with the isomerization and implication of the anthryl group in the main chain of the polymer as 9-methylene-9,10-dihydroanthracene units.[4]

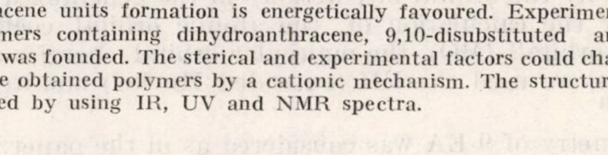

The poly-(9-vinylanthracene) is a copolymer which contains the above structural units.[4–6] The ratio of these units in the chain depends on the nature of the solvent, temperature, catalyst.[6]

In this paper we proposed to study the cationic polymerization of 9-EA.

EXPERIMENTAL

The 9-EA was synthesized as in paper [7] and 9-VA was synthesized by the Hawkins method.[8] As catalyst were used $TiCl_4$, $SnCl_4$ and BF_3 in toluene solutions. The polymerizations were performed in glass ampoules with inert medium, in the absence of light. The polymers were precipitated with methanol, filtrated and dried. In some cases the polymers were separated into two fractions : one insoluble in benzene (A) and another one soluble in benzene and insoluble in methanol (B). The 9-(α-chloro)vinylanthracene was obtained as intermediate product in the 9-EA synthesis. It was homopolycondensed in CH_2Cl_2 10% in the presence of $TiCl_4$ (molar ratio = 10/l), during 24 hrs. After precipitation with methanol a yellow product is separated. The conversion is of 47%.

The molecular weights of the polymer were measured in benzene solutions by the cryoscopy method. The spectral measurements were performed as in the previous paper.[3]

RESULTS AND DISCUSSION

In order to establish the polymerization mechanism of 9-EA in the presence of cationic catalysts we meant to calculate the ΔE_{total} (the energy change caused by the orbital interaction) in the generalized perturbation theory.[9,10] For the calculation of the atomic orbital coefficients from the molecular orbitals (MO), the molecular orbital energies and the total atomic charges, we used the EH (extended Huckel) non-iterative procedure method.[11]

The geometry of 9-EA was considered as in the paper.[1] The carbocation geometries with the positive charge localized on the C_α or C_{10} carbon atoms are identical to those of the respective radicals, as shown in previous paper.[1]

According to the type of representation of cation geometries and 9-EA molecule we acknowledged that the interactions could occur between the p_z orbitals belonging to the cation and the molecule of 9-EA. The larger difference (10.735 eV) between the total energies of both cations permit the localization of the positive charge on the 10-carbon atom (Fig. 1).

In order to elucidate the preferential attack between the cation by its 10-carbon atom and the monomer molecule we calculated the ΔE values using the following equation,[12] all the terms in this Eq. having the same signification as those presented in the paper.[1] The sums $\sum^{occ}$ and $\sum^{unocc}$ were performed for all double-occupied molecular orbitals in

$$\Delta E = \frac{q_a \cdot q_b}{\varepsilon \cdot R_{ab}} \cdot \alpha + \sum_r^{occ} \sum_s^{unocc} \frac{(C_{ra} \cdot C_{sb} \cdot \beta_{ab})^2 \cdot \gamma}{E_r - E_s}$$

9-EA and all empty molecular orbitals in the cation. This Eq. is applied with good results to the donor-acceptor interactions.[12]

In Figure 1 are presented the total atomic charges of all atoms belonging to the cation having the positive charge localized on the C_{10} carbon atom. In Table 1 are specified the interaction positions, the electrostatic and covalent term values and the energy ΔE_{total} values.

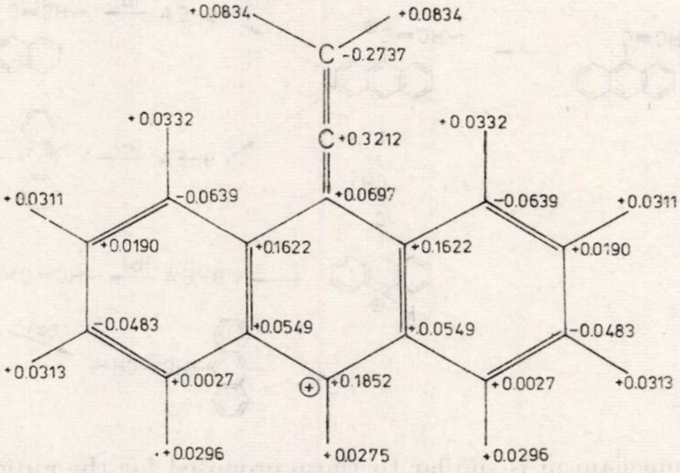
+0.0834
+0.0834
C -0.2737
C +0.3212
+0.0332
+0.0332
+0.0311
-0.0639
+0.0697
-0.0639
+0.0311
+0.0190
+0.1622
+0.1622
+0.0190
-0.0483
+0.0549
+0.0549
-0.0483
+0.0313
+0.0027
+0.1852
+0.0027
+0.0313
+0.0296
+0.0275
+0.0296

Fig. 1 — The atomic charges in 9-EA carbocation with the positive charge localized in the ring.

Table 1

The ΔE_{total} value for the interactions between cation and monomer, in eV, with $R_{ab} = 2.5$ A°, $\beta_{ab} = 2.63$ eV and $\varepsilon = 1$

Interaction		Electrostatic term eV	Covalent term eV	ΔE_{total} eV
Cation $p_zC^*_{10}$	Monomer p_zC_x			
C_{10}	C_{10}	−0.08095	−2.16860	−2.24955 I
C_{10}	C_β	−0.29921	−1.76373	−2.06294 II
C_{10}	C_4	−0.05631	−1.84152	−1.89783 III
C_{10}	C_1	−0.06122	−1.82490	−1.88612 IV
C_{10}	C_2	−0.04917	−1.69903	−1.74820 V
C_{10}	C_3	−0.05065	−1.68494	−1.73559 VI
C_{10}	C_α	+0.01823	−1.33973	−1.32150 VII

The interactions between the cation by its C_{10} carbon atom and the 9-EA molecule by its C_{10} carbon atom appear to be favoured; they are followed by the interaction between the C_{10} and C_β carbon atoms belonging to the same molecular species (Table 1). The other interactions are less probable.

The theoretical results suggest the following reaction mechanism (scheme 2).

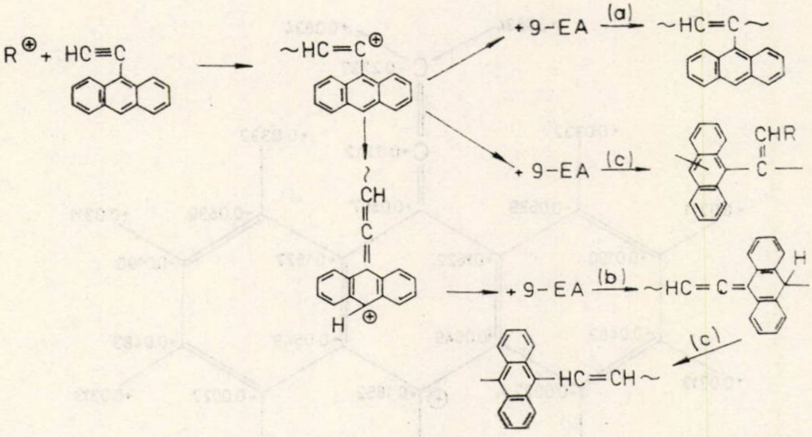

This mechanism is similar to those proposed for the radical polymerization of 9-EA. The dihydroanthracene and polyene units appear in this polymerization reaction.

The cationic polymerization was experimentally studied using some Lewis acids as catalysts. We analyzed the influence of concentration, the nature of catalyst and the polymerization temperature on the structure of the polymer obtained. The experimental conditions used in the polymerization reactions are presented in Table 2.

Table 2

The cationic polymerization of 9-ethynylanthracene

No.	Catalyst	Conc. cats. % mol	Time hr	Temp. °C	Conversion total	Conversion A	Conversion B	Molecular weight	A_{730}/A_{750} (A)	A_{730}/A_{750} (B)
1.	$TiCl_4$	5	3	20	77.8	64.8	13.0	—	3.56	2.56
2.	$TiCl_4$	5	3	0	59.2	39.2	20.0	—	3.02	2.21
3.	$TiCl_4$	5	3	−50	33.7	4.2	29.5	—	2.57	2.19
4.	$TiCl_4$	5	3	−80	81.8	—	21.8	1120	—	1.40
5.	$TiCl_4$	10	3	20	88.1	43.0	45.1	1200	2.42	2.36
6.	BF_3	a	3	20	49.3	3.3	46.0	1270	1.99	1.90
7.	$SnCl_4$	5	2	0	35.4	—	35.4	—	—	2.35
8.	$SnCl_4$	10	2	0	55.4	—	55.4	1320	—	2.58

Solvent = toluene ; gravimetric ratio solvent/monomer = 5/1 ; a) in the monomer solution some bubbles of BF_3 were added ; A = insoluble benzene fraction ; B = insoluble methanol fraction.

The cationic polymerization of all the studied arylacetylenes gives only soluble polymers with small weights. In the case of the 9-EA there were obtained insoluble fractions in organic solvents, when Ziegler-Natta,[1] phosphine complexes [3] and cationic catalyst were used. The insolubility of polyethynylanthracene (PEA) is explained by the greater rigidity of the polymer chain owing to the large volume of the anthryl adjacent substituents in polyenic structure. The content in the insoluble fraction of the cationic polymerization diminishes versus temperature of polymerization (the only soluble polymers were obtained only at −70°C) (Table 2).

The structure of PEA-C was determined according to its IR, NMR and UV spectra. In Figure 2 are presented the IR spectra of 9-VA (used as model for the polyenic structure), PEA-C, poly-9-vinylanthracene (PVA) obtained using a cationic catalyst and the poly (α-chloro) vinylanthracene formed by its homopolycondensation. In respect to 9-VA, in the spectra of PEA-C appear supplementary bands at 750 cm^{-1} ($\gamma C-H$ aromatic out of plane belonging to 9-allene, 9, 10-dihydroanthracene or 9,10-disubstituted anthracene) and at 1590 cm^{-1} ($\nu C=C$ belonging to 9-allene, 9,10-dihydroanthracene). The PVA contains the aromatic substituent as 9-methylen, 9,10-dihydroanthracene unit.[4]

The IR spectra similarity of PEA-C and PVA (Fig. 2) indicates the presence of 9-allene, 9,10-dihydroanthracene substituent in the acetylenic polymer. In respect to PVA, where $A_{730}/A_{750} > 1$, at PEA-C the same ratio is < 1. This fact indicates for PEA-C a similar structure with PVA, but with $m < n$.

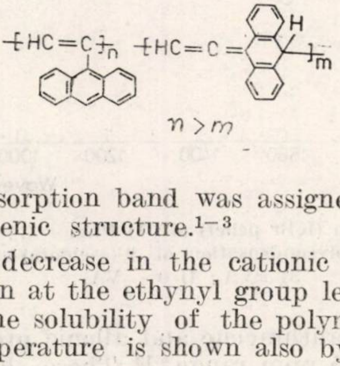

$n > m$

The 730 cm^{-1} absorption band was assigned to the 9-substituted anthryl group in polyenic structure.[1-3]

The temperature decrease in the cationic polymerization favours the 9-EA polymerization at the ethynyl group level and the central ring (Table 2). Therefore, the solubility of the polymer increases. A similar dependence versus temperature is shown also by the 9-VA in cationic polymerization.[6]

The theoretical results suggest that the cation formed by addition of the catalyst to the 9-EA in the β position, attacks the C_{10} carbon atom in 9-EA giving 9-allene, 9,10-dihydroanthracene units (Table 1). There follows the interaction between the C_{10} carbon atom in the cation and the C_β carbon atom in 9-EA. This interaction leads to polyenic units which were verified.

Probably, the experimental conditions could change the nature of the resulting polymers.

The NMR spectrum of PEA-C cannot provide supplementary data on the polymer structure. It has a wide signal placed within the 4−8.5

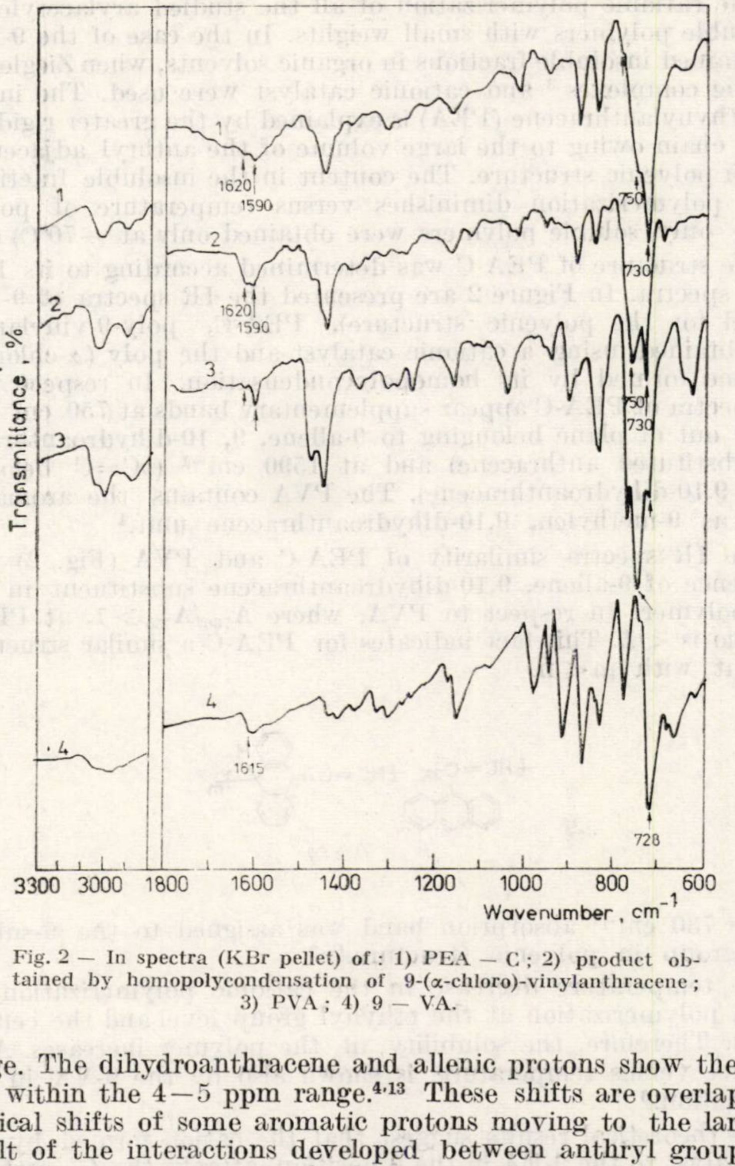

Fig. 2 — In spectra (KBr pellet) of: 1) PEA — C; 2) product obtained by homopolycondensation of 9-(α-chloro)-vinylanthracene; 3) PVA; 4) 9 — VA.

ppm range. The dihydroanthracene and allenic protons show the chemical shifts within the 4—5 ppm range.[4,13] These shifts are overlapped by the chemical shifts of some aromatic protons moving to the large field as a result of the interactions developed between anthryl groups as in the vinyl polymers containing the large aromatic substituents.[14,15]

In Figure 3 are presented the UV absorption spectra of PEA-C. In respect to PEA-Z,[2] the hypsochromic shift of the UV maximum at small wavelengths does not occur. This fact suggests the absence of the orderly structure in the polymer chain. Besides, at λ = 408 nm appears an absorption maximum assigned to the presence of the 9,10-disubstituted anthracenic ring. Unlike the anthracene and its 9-substituted derivatives the 9,10-disubstituted anthracene compounds absorb at wavelenghts larger than 400 nm.[16]

The 9,10-disubstituted units could appear in the polymers by: a) the aromatization of 9-ethynylidene-9,10-dihydroanthracene structures during the polymerization and the purification of the polymers;

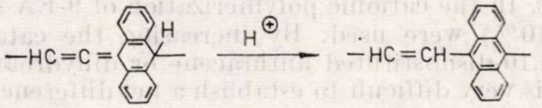

b) the polyalkylations of the anthracene rings by the Lewis acids action which have the properties of the Friedel-Crafts catalysts.

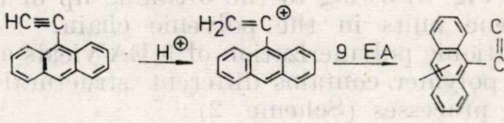

The IR (Fig. 2) and UV (Fig. 3) spectra of the polymer formed by polycondensation of 9-(α-chloro)vinylanthracene do not exclude the possibility of the polyalkylation reaction during the cationic polymerization of 9-EA.

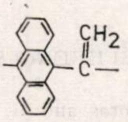

The introduction of an anthryl group in the polymers having as adjacent substituents the phenyl groups (polystyrene, poly-α-methylstyrene) has been performed by the alkylation of anthracene compounds

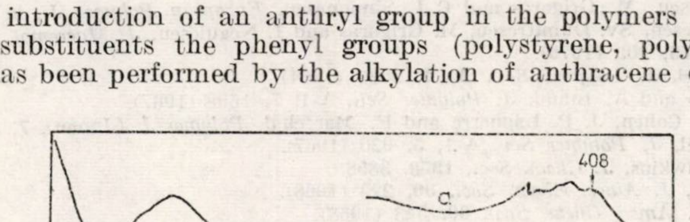

Fig. 3 — The electronic spectra ($CHCl_3$) of: a) the product obtained by homopolycondensation of 9-(α-chloro)-vinylanthracene (UV); b) PEA — C (UV) and c) PEA — C (visible range).

of the type A-CHX R (A=9-anthryl, X=OH, halogen, R=H, CH_3) with Friedel-Crafts catalysts.[17] In the interactions between the above anthracene compounds with the Friedel-Crafts catalysts carbocations of the $A-CH^{+}-R$ type appear. These cations are bounded by electrophile attack to the aromatic rings. The molar ratio anthracene/catalyst was equal to the unit. In the cationic polymerization of 9-EA small quantities of catalyst ($\leqslant 10\%$) were used. By increasing the catalyst quantities the content in 9,10-disubstituted anthracene or dihydroanthracene units increases too. It is very difficult to establish a net difference between these two structural units.

The 9-EA polymers obtained by ionic-coordinative polymerization show in the visible range an absorption maximum at 550 nm, assigned to a $\pi-\pi^*$ transition in the polyenic chain.[2,3] With respect to the polymers discussed above, PEA-C and PEA-R [1] show a decreasing absorption without maximum (Fig. 3) owing to the breaking up of the conjugation by dihydroanthracene units in the polyenic chain.

Finally, the cationic polymerization of 9 EA yields a complex polymer. The obtained polymer contains different structural units resulting from the following processes (Scheme 2):

a) the polymerization by ethynyl bond (the polyenic units)

b) the polymerization by ethynyl bond and central ring of the anthryl substituent (9-ethynylidene-9,10-dihydroanthracene units)

c) the aromatization of 9-ethynylidene 9,10-dihydroanthracene units and alkylation of anthracene groups.

REFERENCES

[1] Part XXXV-Sv. Dumitrescu, M. Grigoraş and G. Surpăţeanu, *Rev. Roumaine Chim.*, in press.

[2] Sv. Dumitrescu, M. Grigoraş and C. I. Simionescu, *European Polymer* J., in press.

[3] C. I. Simionescu, Sv. Dumitrescu, M. Grigoraş and I. Negulescu, *J. Macromol. Sci.-Chem*, **A13**, 203 (1979).

[4] R. H. Michel, *J. Polymer Sci.*, **A**, **4**, 2533 (1964).

[5] K. Morimoto and A. Inami, *J. Polymer Sci.*, A-1, **7**, 1699 (1967).

[6] C. Bunel, S. Cohen, J. P. Laguerre and E. Marechal, *Polymer J.* (Japan), **7**, 320 (1975).

[7] R. H. Michel, *J. Polymer Sci*, A-1, **5**, 920 (1967).

[8] E. G. E. Hawkins, *J. Chem. Soc.*, **1958**. 3858.

[9] G. Klopman, *J. Amer. Chem. Soc.*, **90**, 223 (1968).

[10] L. Salem, *J. Amer. Chem. Soc.*, **90**, 543 (1968).

[11] R. Hoffmann, *J. Chem. Phys.*, **39**, 1397 (1963), **40**, 2474, 2480, 2745 (1964).

[12] G. Klopman, "Chemical Reactivity and Reaction Paths", Wiley, New York, 1974, p. 55.

[13] P. J. Stang and R. J. Hargrove, *J. Org. Cehm.*, **40**, 657 (1975).

[14] D. J. Williams and W. W. Limburg, *Macromolecules*, **6**, 787 (1973).

[15] D. J. Williams, *Macromolecules*, **3**, 602 (1970).

[16] H. H. Jaffe and M. Orchin, "Theory and Applications of Ultraviolet Spectroscopy", Wiley, New Yrok, 1962, p. 316.

[17] M. G. Krakovyak, E. G. Anufrieva, T. D. Ananaeva, R. A. Gromova, V. B. Lusik and S. S. Skorokhodov, *Vysokomol. Soedineniya*, **A18**, 1494 (1976)

Revue Roumaine de Chimie, **29**, *6*, 521–530 (1984)

HIGH-TEMPERATURE POLYMERS. V[1]

ORDERED BENZOTHIAZOLE-IMIDE COPOLYMERS

GH. MANDRIC, GH. PETRACHE, ELENA PĂTRĂHĂU and TH. POPA
Institute of Macromolecular Chemistry "P. Poni",
Aleea Gr. Ghica Vodă 41-A, Jassy, Romania

Received January 27, 1983

A series of new polymers containing benzothiazole and imide rings with methylene and ether links between benzothiazole units was prepared. The synthesis was carried out by the two steps polycondensation reaction of benzothiazole rings containing diamines and aromatic dianhydrides. In the first step of reaction, polyamic acids were obtained ($\eta_{inh} = 0.4 - 1.64$ dl/g in N-methylpyrrolidone (NMP) at 20°C) that were then converted to polybenzothiazole-imides by thermal cyclodehydration. The prepolymers (polyamic acids) can be cast as films, which after cyclization exhibit high thermo-oxidative stability and good mechanical and electrical properties. The monomers, model compounds and polymers were characterized by infrared spectroscopy, viscosity, elemental and thermogravimetric analysis.

INTRODUCTION

Present demands of the industry have determined the necessity of obtaining heat-resisting polymers with a good retention of mechanical and electrical properties at high temperatures (200–300°C) for a long period of operation.

Among the organic polymers, those which contain aromatic and heterocyclic rings in the chain, [1–4] correspond the best to the conditions required for a thermostable polymer : high melting or softening point, resistance to pyrolysis, fireproofness and a good hydrolytic and thermo-oxidative stability.

The synthesis of ordered copolymers[5–8] represents a way of obtaining some polymers with various structures, so that no rearrangement of bonds occurs that permits a very great flexibility in yielding polymers.

By a judicious selection of the monomers containing aromatic and heterocyclic units, polymers with good thermal stability, crystallinity and high glass-transition temperature can be obtained.

Previously [1,8,9] we reported the synthesis of some ordered copolymers (polybenzimidazole-imides). This work is a continuation of our efforts in finding new ordered copolymers starting from diamines containing benzothiazole rings and aromatic dianhydrides.

DISCUSSION AND RESULTS

We have synthesized ordered copolymers with benzothiazole rings regularly alternating with imide rings or having aromatic units (*m*- or *p*-phenylene) between the benzothiazole and imide rings.

All these copolymers have atoms or groups of atoms, such as: –O– or –CH_2– between the benzothiazole rings which provide flexibility to the macromolecular backbone.

Unlike polybenzothiazoles, the polybenzothiazole-imides can be prepared by a two-step reaction, via a soluble and tractable precursor (polyamic acid) (I) that was converted to polybenzothiazole-imide (II) by a thermal cyclodehydration, in air, according to the following reactions:

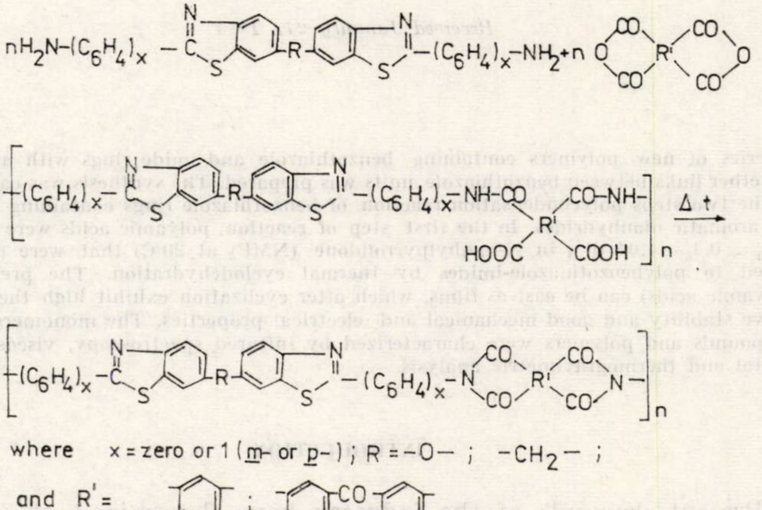

where x = zero or 1 (m- or p-); R = –O– ; –CH_2– ;

and R' =

Monomers and model compounds

As monomers there were used benzothiazole rings containing diamines and aromatic dianhydrides.

The diamines with the amine groups linked directly to the benzothiazole ring are intermediates in the obtention of the aromatic dimercapto-diamines and have the following structure:

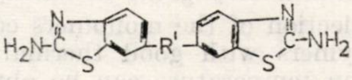

We have adapted a synthesis for simple (or *o*-amino substituted) benzothiazole using polyphosphoric acid (PPA) as a condensation agent and solvent, to yield diamino-benzothiazoles according to the reactions shown in the scheme:

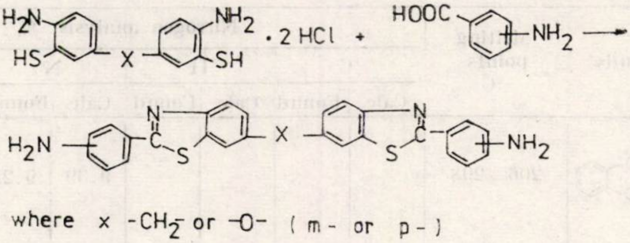

The diamines are easily soluble in a variety of solvents and are stable towards the effects of air-oxidation and solvolysis.

Some data on the melting points and elemental analysis of these diamines are found in table 1.

Table 1

Some characteristics of the monomers

Compound	Melting points °C	Elemental analysis, %				
			C	H	N	S
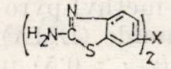 X = CH_2	258–264	Calc.	57.69	3.84	17.94	20.51
		Found	57.23	3.26	17.62	20.07
X = O	206–210	Calc.	53.50	3.18	17.83	20.38
		Found	52.64	3.41	17.24	19.06
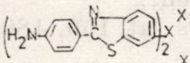 X = CH_2	274–279	Calc.	69.82	4.31	12.06	13.79
		Found	68.56	4.40	11.50	13.76
X = O	196–204	Calc.	66.95	3.86	12.01	13.73
		Found	66.24	3.48	11.84	13.28
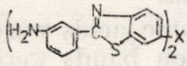 X = CH_2	236–242	Calc.	69.82	4.31	12.06	13.79
		Found	68.06	4.23	11.42	13.46
X = O	188–199	Calc.	66.95	3.86	12.01	13.73
		Found	66.05	3.33	11.68	13.46

The infrared spectra of heterocyclic diamines we prepared showed the absorption bands characteristic of amine groups at 3320 and 3450cm^{-1}.

Polyromellitic and benzophenonetetracarboxylic dianhydrides were used after recrystallization from acetic anhydride and pyromellitic dianhydride was sublimed before using.

In order to make possible the identification of the polymers and to investigate the imide formation from the polyamic acids, model compounds (amic acid and imide-benzothiazole) (M_1, M_2) were prepared (Table 2).

Table 2

Caracteristics of model compounds

Model compounds	Melting points °C	Nitrogen analysis, %							
		C		H		N		S	
		Calc.	Found	Calc.	Found	Calc.	Found	Calc.	Found
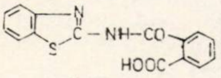 (M$_1$)	206–208	—	—	—	—	9.39	9.21	—	—
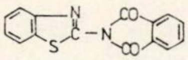 (M$_2$)	Sublimates	64.27	64.08	2.87	2.72	9.99	10.26	11.43	11.16

Polymers

The conditions of reaction, viscosity, thermal properties of polymers are summarized in table 3.

It was observed that the polymers in which the phenylene groups are inserted in the macromolecular chain have higher molecular weight ($\eta_{inh} = 0.39 - 1.64$) than the polymers without phenylene groups ($\eta_{inh} = 0.21 - 0.32$).

The results from elemental analysis are in agreement with the polymer structure assigned in table 4.

All the precursor polyamic acids (I) are soluble in N-methyl-pyrolidone (NMP), dimethylformamide (DMF) or dimethylacetamide (DMA). Some of them were cast from the clear viscous solutions ($\eta_{inh} > 0.5$) in NMP onto a glass plate, baked at 100°C for 20–25 min., and then removed from the glass plate while still plasticized with solvent.

The films were hung in an oven at 130°C for 4 hrs, at 150, 180, 210, 240 and 270°C for 30 min. and at 300°C for 1 hr.

The cured film was flexible, strong and of a light brown colour, insoluble in organic solvents but soluble in sulfuric acid.

Infrared spectra of the amic acid (M$_1$) and the polyamic acids were essentially the same, and the most characteristic absorption bands were found at 3300–3400 cm^{-1} (NH and OH stretching), 1700–1710 (CO stretching in carboxyl group) 1650 cm^{-1} (amide) I and 1550 cm^{-1} (amide II) (Figs. 1–3).

The conversion of the film from the amic acid — heterocycle copolymer to the imide-heterocycle copolymer and from the amic acid (M$_1$) to imide compound (M$_2$) was followed by infrared spectroscopy (Fig. 1–3).

Thus, the model compound (M$_1$) and the polyamic acids after thermal treatment showed the strong absorption bands at 1785 cm^{-1} due to symmetrical carbonyl stretching vibrations, at 1730 cm^{-1} due to asymmetrical carbonyl stretching vibrations and at 724 cm^{-1} possibly due to ring carbonyl deformations, and the absence of the amidic bands (at 1650 and 1550 cm^{-1}).

Table 3

Caracterization of polybenzothiazole-imides

No. Polymers *)	Aspect	Viscosity **) η inh dl/g	Films	TGA ***) Weight loss, %	
				400°	450°
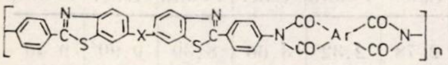					
I. X= -CH$_2$- ; Ar = 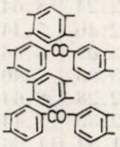	fibrous	1.64	flexible	0	3.2
II. X= -CH$_2$- ; Ar =	fibrous	0.77	flexible	0	2.8
III. X= -O- ; Ar =	fibrous	0.84	flexible	0	2.6
IV. X= -O- ; Ar =	fibrous	0.68	flexible	0	2.8
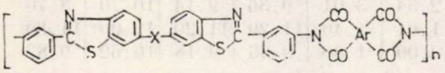					
V. X = -CH$_2$-; Ar = 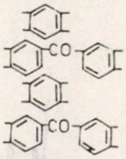	fibrous	0.53	flexible	0	3.8
VI. X = -CH$_2$-; Ar =	powder	0.39	brittle	0	2.9
VII. X = - O -; Ar =	fibrous	0.58	flexibile	0	2.4
VIII. X = - O -; Ar =	powder	0.46	brittle	0	2.5
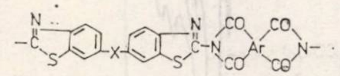					
IX. X =-CH$_2$- ; Ar = 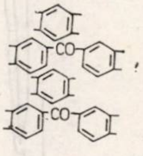	powder	0.21	brittle	0	4.3
X. X =-CH$_2$- ; Ar =	powder	0.32	brittle	0	3.8
XI. X =-O- ; Ar =	powder	0.29	brittle	0	3.9
XII. X =-O- ; Ar =	powder	0.31	brittle	0	3.8

*) The polymers were prepared in NMP, 16 hrs (3 hrs at 0° and 13 hrs at room temperature)

**) Inherent viscosity was measured at a concentration of 0.5 g/100 ml in N-methylpyrrolidone at 20°C.

***) Thermogravimetric analysis in air at a heating rate of 9°C/min. on "Derivatograph" Paulik-Paulik.

Thermogravimetric analysis of PBTh-I showed that in air the polymer decomposes above 400°C losing between 400–450°C, 2.4–4.3% of its weight (Table 3).

The temperatures of decomposition of the six copolymers obtained are given in table 5, in comparison with polybenzothiazole-imides and poly-benzothiazole-amide-imides described in the literature.[10] As can be seen from table 5, the copolymers containing phenylene rings in macro-

Table 4

Elemental analysis of benzothiazole-imide-copolymers

Polymers (Abbreviations)	Formula	Elemental analysis							
		C%		H%		N%		S%	
		Calc.	Found	Calc.	Found	Calc.	Found	Calc.	Found
I	$C_{37}H_{18}N_4O_4S_2$	68.73	68.24	2.78	2.32	8.66	8.39	9.90	9.40
II	$C_{44}H_{22}N_4O_5S_2$	70.40	72.26	2.93	3.33	7.46	7.08	8.53	8.26
III	$C_{36}H_{16}N_4I_5S_2$	66.66	64.88	2.46	2.24	8.64	8.20	9.87	9.26
IV	$C_{43}H_{20}N_4O_6S_2$	68.61	67.20	2.65	2.40	7.44	7.15	8.51	8.02
V	$C_3H_{18}N_4O_4S_2$	68.73	70.00	2.78	3.09	8.66	8.40	9.90	9.26
VI	$C_{44}H_{22}N_4O_5S_2$	70.40	70.46	2.93	3.65	7.46	7.08	8.53	7.99
VII	$C_{36}H_{16}N_4O_5S_2$	66.66	65.20	2.45	2.28	8.64	8.32	9.87	9.02
VIII	$C_{43}H_{20}N_4O_6S_2$	68.61	67.08	2.65	2.30	7.44	7.51	8.51	8.04
IX	$C_{25}H_{10}N_4O_4S_2$	60.72	59.06	2.02	1.84	11.33	11.18	12.95	11.60
X	$C_{32}H_{14}N_4O_5S_2$	64.21	63.26	2.34	3.01	9.36	9.14	10.70	8.70
XI	$C_{24}H_8N_4O_5S_2$	58.06	56.08	1.61	1.40	11.29	11.20	12.90	11.80
XII	$C_{31}H_{12}H_4O_6S_2$	62.00	61.20	2.00	1.80	9.33	9.18	10.62	9.82

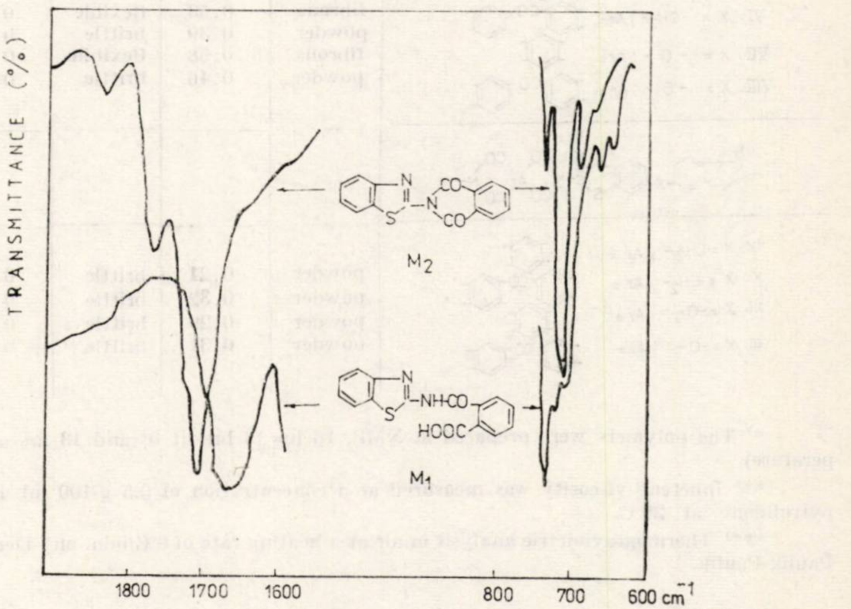

Fig. 1. — Infrared spectra of model compounds, M_1 and M_2 (KBr pellet).

molecular chain are more thermostable than those without phenylene rings and the copolymers with methylene or ether group in the chain are less thermostable than those without these groups.

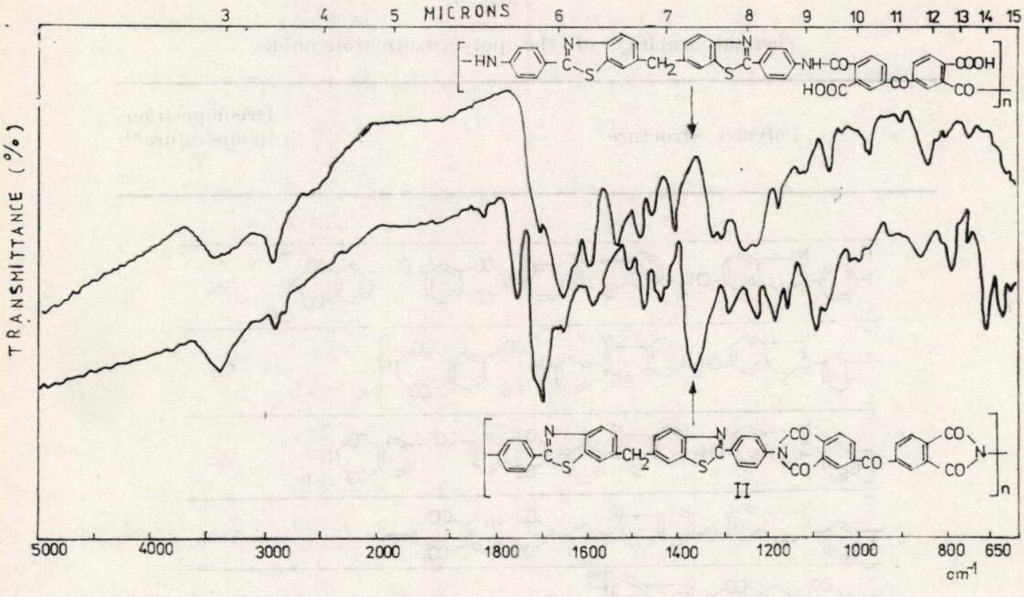

Fig. 12. — Infrared spectra of polyamic acid and polybenzothiazole-imide II (films).

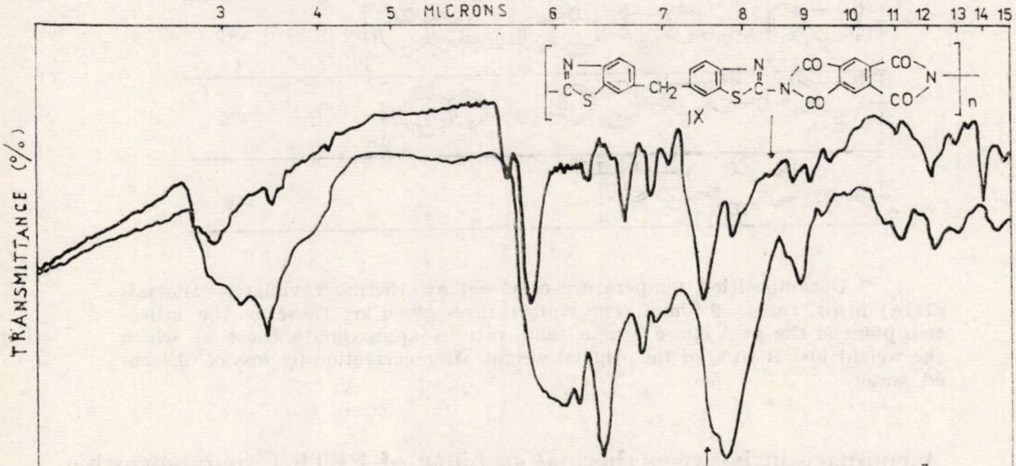

Fig. 3. — Infrared spectra of polyamic acid and polybenzothiazole-imide (IX) (films).

Table 5

Thermal stability of the polybenzothiazole-imides

Polymer structure	Decomposition temperature*) °C
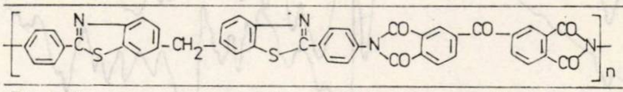	510
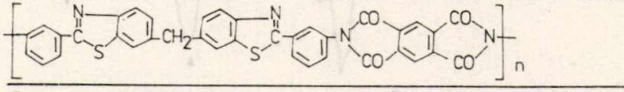	515
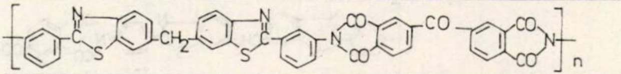	505
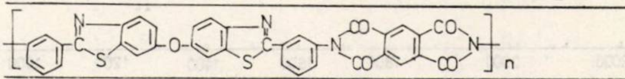	510
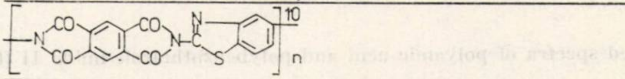	500
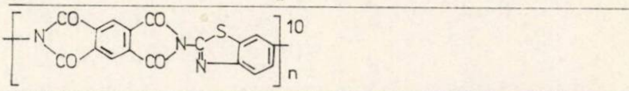	550
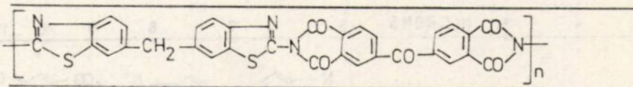	440
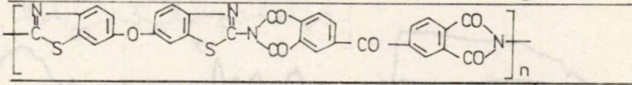	475
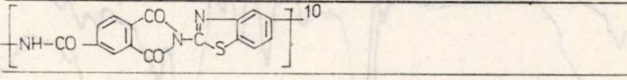	440

*) Decomposition temperature observed by thermogravimetric analysis (TGA) in air, rate $=9^\circ C/min$. The temperatures given are those at the inflection point in the TGA curve; these temperatures approximate those at which the weight loss is 10 % of the original weight after correction for loss of absorbed water.

A comparison between thermal stability of PBTh-I, polybenzothiazoles (PBTh) and polyimides (PI) showed that PBTh-I are more thermostable than PI and less thermostable than PBTh (Fig. 4).

Some electrical properties of the film PBTh-I are shown in table 6.

The fibers were readily spun from the solution of PBTh-I in N-methylpyrrolidone (conc. 15 %).

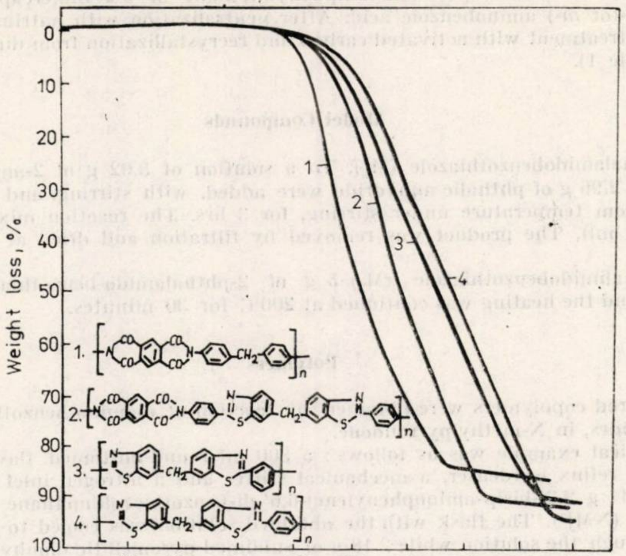

Fig. 4. — Thermal gravimetric analysis, curves for polyamide (1), polybenzothiazole-imide (2) and polybenzothiazoles (3,4)-(in air, at a heating rate of 9°C/min) (films).

Table 6

Electrical properties of the polybenzothiazole-imides

Polymer	Dielectric constant at 1 KHz	Dissipation factor, tg at 1 KHz	Volume resistivity ohm × cm	Dielectric strength kV/mm
PBTh–I(I)	2.4	0.68×10^{-3}	0.9×10^{15}	32
PBTh–I(II)	2.6	0.63×10^{-3}	0.4×10^{15}	35

EXPERIMENTAL

1. 4,4′-Diaminodiphenylmethane. This compound was obtained by condensation of aniline with formaldehyde in the presence of hydrochloric acid, separation by distillation and recrystallization from benzene, m.p. = 88–89°C.

2. 4,4′-Diaminodiphenylether.[11] It was prepared by reaction of natrium p-nitrophenolate with p-nitrochlorbenzene and the reduction of dinitric compound with iron and hydrochloric acid. The product obtained was purified by recrystallization from ethylic alcohol, m.p. 187–189°C.

3. *o-o′*-Dimercaptodiaminodiphenylmethane and *o,o′*-dimercaptodiaminodiphenylether. These were prepared by reaction of aromatic diamines with ammonium sulphocyanate bromine in acetic acid.

4. 2,2′-bis-(Aminobenzothiazolyl)methane and 2,2′-bis-(aminobenzothiazolyl)ether. These were obtained as intermediates at the synthesis of aromatic dimercaptodiamine.

5. 2,2′-bis-(*p*-(and *m*-)-aminophenylen)-6,6′-dibenzothiazolilmethane and 2,2′-bis(*p*-(and *m*-) aminophenylen)-6,6′-dibenzothiazolylether. These were obtained by condensation in poly

phosphoric acid of *o,o'*-dimercaptodiaminodiphenylmethane or *o-o'*-dimercaptodiaminodyphenylether with *p*-(or *m*-) aminobenzoic acid. After neutralization with natrium bicarbonate it was purified by treatment with activated carbon and recrystallization from dimethylformamide and water (Table 1).

Model Compounds

6. 2-Phthalamidobenzothiazole (M_1). To a solution of 3.02 g of 2-aminobenzothiazole in NMP (50 g) 2.96 g of phthalic anhydride were added, with stirring, and the reaction was continued at room temperature under stirring, for 3 hrs. The reaction mixture was poured into water (200 ml). The product was removed by filtration and dried at 40°C, for 48 hrs in vacuum.

7. 2-Phthalimidobenzothiazole (M_2) ·5 g of 2-phthalamido-benzothiazole were heated up to 200°C and the heating was continued at 200°C for 30 minutes.

Polymers

The ordered copolymers were obtained by reaction of diamino-benzothiazoles and aromatic dianhydrides, in N-methylpyrrolidone.

8. A typical example was as follows : a 300 ml round-bottomed flask, fitted with a thermometer, a reflux condenser, a mechanical stirrer and a nitrogen inlet tube was charged with 4.64 g 2,2'-bis(*p*-aminophenylene)-6,6'-di-benzothiazolilmethane in 50 ml N-methylpyrrolidone (NMP). The flask with the obtained solution was cooled to 0°C and nitrogen was passed through the solution while 2.18 g of sublimed pyromellitic dianhydride and 11.3 ml NMP, were added under stirring.

The flask content was kept below 0°C for 3 hrs and stirred for 13 hrs more at room temperature. The inherent viscosity of the solution of polyamic acid in NMP (conc. 0.5 % at 20°C) was 1.64 dl/g. Films were cast from the clear solutions onto a glass plate and then baked at 100°C for 30 min. and imidized by thermal treatment ; another part of the polymer was isolated by precipitating in methanol and water, and then dried at 40°C, under vacuum. Some of properties of PBTh-I copolymers are shown in table 3.

REFERENCES

[1] V. V. Korshak, A. I. Pavlov, Gh. Mandric and I. Zugrăvescu, *Rev. Roumaine Chim*, **22**, 1521, (1977).

[2] Gh. Mandric, M. Brumă and L. Stoicescu-Crivetz, *Materiale plastice*, **14**, 5 (1955).

[3] J. Preston and W..B Black, *J. Polymer Sci.*, *A-1*, **5**, 2429 (1967).

[4] J. Preston and W. B. Black, *J. Polymer Sci.*, *B*, **3**, 845 (1965).

[5] J. Preston and F. Dobinson, *J. Polymer Sci.*, *B*, **2**, 1171 (1964).

[6] J. Preston, *J. Polymer Sci.*, **A-1**, **4**, 529 (1966).

[7] J. Preston, W. F. DeWinter and W. B. Black, *J. Polymer Sci.*, **A-1**, **7**, 283 (1969).

[8] Gh. Mandric, A. I. Pavlov, V. V. Korshak and I. Zugrăvescu, *Rev. Roumaine Chim.*, **19**, 1783 (1974).

[9] C. Adam. Gh. Mandric, E. Pătrăhău and Th. Popa, Brevet R.S.R 63916. 16, 11, 1976.

[10] Yoshio Imai and Hiroshi Uchiyama, *Chem. High. Polymer*, **1970**, 305, 664.

[11] G. Caraculacu, M. Brumă and E. Caraculacu, Brevet R.S.R., 55089, 2.III.1972.

Revue Roumaine de Chimie, **29**, *6*, 531–532 (1984)

IN MEMORIAM

MARGARETA AVRAM

(1920 – 1983)

The death of Professor Margareta Avram on October 28, 1983 brought to an early end a career of outstanding achievements well known in Romania and internationally. Although ill for a long time, she continued to work prodigiously in the laboratory and to finish both scientific publications and a book on organic chemistry. Our chemical community loses by her disappearance a scientist with a high ethical and professional standard, who devoted her whole life with generosity to science and teaching. As a student of Costin D. Nenitzescu, she became, owing to her brightness, talent and hard work, one of his closest coworkers.

Born in Bistritza, Bistritza-Nasaud county, on January 2 1920, she spent her formative years at the Polytechnic from Bucharest, Department of Industrial Chemistry, graduating in 1942 as chemical engineer. In 1947 she acquired the Ph. D. degree under the guidance of Professor C. D. Nenitzescu, and in 1960 she was awarded for outstanding results in chemical research the title of D.Sc., equivalent to Dr. Habil.

Since 1945 when she was appointed to the chair of Organic Chemistry from the Polytehnic Institute, Bucharest, she climbed all didactical steps and was promoted in 1968 as full professor. Her teaching activity spanning over 35 years was devoted to transmitting the enthusiasm for organic chemistry (enthusiasm that she herself possessed to a great extent) ; her individual style and clarity of presentation provided a fascinating and always educative experience for her audience. She also pioneered in the Organic Chemistry Department of the Bucharest Polytechnic lectures regarding Natural Products (1956) and Pesticides (1960), and provided two basic books in the field of Pesticides (1974) and Infrared Spectroscopy (Romanian version, 1966 ; French translation, 1971 ; English translation, 1972). Until the last week of her life she worked assiduously on the Organic Chemistry textbook, a valuable reference book for all chemistry students.

Her research activity was profoundly marked by Professor C.D. Nenitzescu since her graduate days. Their cooperation was long and fruitful because Margareta Avram had an infatigable creative participation and a profound attachment for his research school.

After Prof. C. D. Nenitzescu's death, in 1970, together with Prof. Ecaterina Ciorănescu-Nenitzescu, she continued to lead activity and research in the chair of Organic Chemistry from the Polytechnic, Bucharest, and the Institute of Organic Chemistry, Bucharest, making important contributions for the development of basic and applied research. She supervised more than twenty Ph. D. theses and published more than 140 papers in chemistry journals both in Romania and abroad.

Professor Margareta Avram had a special interest in the chemistry of small rings, among which the cyclobutadiene problem was a favorite. Likewise she widened her contributions to chemistry by including research in various fields : Lewis acid-catalyzed isomerization of aliphatic hydrocarbons, organometallic complexes, reaction mechanisms, rearrangements of polycyclic compounds, synthesis and chemistry of Nenitzescu's hydrocarbon and benzoderivatives thereof.

Her wise counsel, encouragement and inspiration – dear to those who had the privilege to work directly with her – will be missed by many chemists.

Revue Roumaine de Chimie, **29**, *6*, 533–537 (1984)

COMPTES RENDUS

J. W. ROOT and K. A. KROHN (editors), "Short-lived Radionuclides in Chemistry and Biology", Advances in Chemistry Series No. 197, American Chemical Society, Washington, D. C. 1981 : 547 pp, cloth-bound, 73 $ for USA and 88 $ for export.

The 28 lectures presented at the symposium (Sept. 10–13, 1979) sponsored by the Division of Nuclear Chemistry and Technology, the Division of Physical Chemistry, and the Division of Biological Chemistry at the 178th Meeting of the American Chemical Society have been gathered in book-form. The lectures are grouped into five sections :

(i) Chemical Reaction Mechanisms, including P. P. Gaspar's "Recoil Chemistry and Mechanistic Studies with Polyvalent Atoms", F. Cacace's "Chemical Mechanistic Studies based on the Radioactive Decay of Multitritiated Molecules", Y. N. Tang's "Unusual Compounds Synthesized via Nuclear Recoil Methods" and C. A. Jones and W. S. Koski's "Charge Distribution in ^{13}N Ions Produced by the $^{12}C(d, n)^{13}N$ Reaction". The first communication emphasizes the fact that polyvalent atoms react forming reactive intermediates unlike univalent atoms. Product studies can afford information on the nature of these intermediates ; most of the recoil chemistry examined in this chapter involves ^{31}Si atoms, but some of the data also deal with ^{11}C atoms. The second chapter is an excellent and authoritative account of the unique method of generating $CT_3^{\oplus}$ cations by decay of CT_4 in gaseous or liquid systems (without any solvation shell because of the method by which they are produced) ; similarly, from p-$C_6H_4T_2$ one obtains a tritiated phenyl cation which undergoes automerization in gas phase (but not in liquid phase) ; other interesting reactions involve addition of $CT_3^{\oplus}$ to CO followed by various acetylations : of alcohols or of activated arenes (but not of benzene). The third lecture overlaps partly with the first two, but stresses the unusual intermediates (atoms, methyne, carbene, silylene, radicals) or compounds obtained by nuclear recoil methods, such as the new 1,2,3-pentatriene from 1,3-butadiene and recoil ^{11}C atoms formed *via* the $^{12}C(n,2n)^{11}C$ nuclear reaction. The fourth lecture reports the finding that ^{13}N ions are produced with high energies and with an electric charge of $+3$ or $+4$ but they do not react chemically till they have been slowed down by collisions and have remained with a charge of 0 or $+1$.

(ii) Kinetics and Chemical Reactions. From the six lectures in this section, the communication of J. W. Root and R. G. Manning, "Chemical Reactions of Nuclear Recoil ^{18}F Atoms with Gas-Phase Halocarbons" is a review of their ten years' investigations on the labelled products formed from these reactions ; this chapter is richly illustrated with tables and graphs. L. D. Spicer's lecture "Recoil Generated Radiotracers in Studies of Molecular Dynamics" stresses that the best theoretical rationalization of the results is based on the Rice-Ramsperger-Kassel-Marcus method for describing statistical energy redistribution and for calculating decomposition rate constants. E. R. Grant and J. Santamaria's paper "Dynamical Effects of High Rotational Excitation in Unimolecular Decomposition Activated by Hot Atom Substitution" and a paper by J. W. Root *et al.* "Limitations of the Moderated Nuclear Recoil Technique for investigating Thermal Hydrogen Abstraction Reactions by Atomic Fluorine" are of interest for hot atom chemists. A highly interesting paper by G. H. Kwei "Crossed Beam Studies of Chemical Kinetics Using Radiotracer Techniques" and another paper by C. A. Mathis and J. W. Root, "Radiotracer Studies of Unimolecular Energy Transfer" do not deal with short-lived radionuclides but with ^{14}C- and ^{3}H-labelled compounds ; these papers were included in order to provide a balanced technical overview and to suggest directions for future research.

(iii) ^{13}N Radiobiochemistry. This section includes ten papers, all of them dealing with ^{13}N, and some including also ^{11}C, ^{15}O and ^{18}F. The topics which are presented comprise "The Use of Isotopic Nitrogen as a Biochemical Tracer" by K. A. Krohn and C. A. Mathis (including a comprehensive historical account), a review on "The Chemical Form of ^{13}N Produced in Various Nuclear Reactions and Chemical Environments" by R. S. Tilbury, "Radiotracer Studies of Nitrogen Metabolism in Cynobacteria" by J. C. Meeks, "Use of ^{13}N in Studies of Denitrification" by J. M. Tiedje, R. B. Firestone, M. K. Firestone, M. R. Betlach, H. F. Kaspar and J. Sörensen (yielding results which are complementary to those obtained with ^{15}N), "The Feasibility of Producing ^{11}C, ^{13}N, ^{15}O and ^{18}F with Heavy-Ion Beams" by R. B. Firestone, M. K. Firestone, M. R. Betlach, and J. M. Tiedje, "^{13}N-Labeling of a Substituted Nitrosourea, Its Carbamate, and Nitrosocarbaryl : *In Vivo* and *In Vitro* Studies" by G. A.

Digenis et al., "Nitrogen and Carbon Assimilation in N_2-Fixing Plants : Short-Term Studies Using ^{13}N and ^{11}C" by K. R. Schubert and G. T. Coker III (both labeled N_2 and $NH_4^{\oplus}$ were tested with leguminous and actinorhizal plants, using HPLC for rapid measurement of amino acids after derivatization with *o*-phthaldialdehyde), "^{13}N as a Tracer for Studying Ammonia Uptake and Metabolism in the Brain" by A. J. L. Cooper, T. E. Duffy, J. M. McDonald and A. S. Gelbard (evidence was provided that free ammonia rather than $NH_4^{\oplus}$ enters the brain crossing the blood-brain barrier and that after 1—3 seconds most ammonia is incorporated into glutamine) and "^{13}N-Labelled L-Amino Acids : Enzymatic Syntheses and Metabolic Studies" by A. S. Gelbard, B. R. Freed, R. E. Reiman and A. J. L. Cooper (after reviewing the use of ^{18}F, ^{11}C, and ^{13}N-labeled amino acids for imaging tumors or organs, three methods for enzymatic syntheses of ^{13}N-labeled L-amino acids are described).

(iv) ^{11}C and ^{18}F Radiobiochemistry. This section starts with radiopharmaceuticals labeled with ^{11}C and ^{18}F. "Considerations Related to the Preparation of ^{11}C-Palmitate" by M. J. Welch, S. L. Wittmer, C. S. Dence and T. J. Tewson (a general introduction to the use of ^{11}C-labeled compounds is followed by details on the preparation of the title product for clinical and animal studies). M. E. Raichle's review, "Positron Emission Tomography Tracer Techniques", is a comprehensive review of the use of ^{15}O, ^{13}N, ^{11}C and ^{18}F *via* PET for human organ and tissue imaging ; color PET images of local cerebral blood flow are appended. G. D. Robinson Jr. describes in his paper "In Vivo Tracers for Studies of Myocardial Metabolism" labeled glucose analogs (^{18}F-DFG), $^{13}NH_3$, ^{11}C-fatty acids and amino acids, and discusses strategies for resolving current limitations due to the multiple biochemical pathways available to the label ; one of these is the use of ^{18}F-labeled fatty-acids having the fluorine attached to an odd-numbered carbon (no toxicity is then detected which would otherwise appear on conversion to fluorocitrate). "Tracer Studies with $^{13}NH_4^{\oplus}$, $^{42}K^{\oplus}$, and $^{28}Mg^{2\oplus}$: A Bug's Eye View of the Periodic Table" is the paper by S. Silver and R. D. Perry which concludes the section, but it does not actually pertain to this section (iv) ; it describes transport studies of cations through membranes.

(v) Microbiological and Environmental Applications. This section contains four papers in which mostly long-lived radionuclides are discussed and employed : "Radiometric Microbiologic Assays for the Measurement of Vitamin B_{12}, Folate and Niacin in Human Blood and Food" by M. F. Chen and P. A. McIntyre (a high sensitivity method using ^{14}C-labeled substrate and measuring $^{14}CO_2$ released by *Lactobacillus* proportionally to the amount of vitamins), "Environmental and Geochemical Applications of Mössbauer Spectroscopy" by T. Tominaga, "Ion Beam Analysis of Environmental Samples" by T. A. Cahill (the use of particle-induced X-ray emission and charged particle activation analysis allows environmental analyses and radioisotope dating), and "The Use of Stable Activable Tracers in Environmental Science" by W. D. Loveland.

The volume has a well-produced subject index. By providing a variety of communications involving short-lived radionuclides, the book succeeds in presenting an up-to-date account and bibliography for a very dynamic research front. Especially the medical applications of ^{11}C, ^{13}N, ^{15}O and ^{18}F, in connection with medical cyclotrons and positron-emission tomography introduce at present a new dimension into the study of physiological processes and diagnostic techniques, at low radiation doses for the living tissue and the patients, respectively. The volume is well-produced and highly recommended.

A. T. Balaban

G. S. EZRA, "Symmetry Properties of Molecules" (Lecture Notes in Chemistry, vol. 28), Springer-Verlag, Berlin—Heidelberg—New York, 1982, 202 pages, DM 39, 80 (soft-cover).

The aim of the present book is to give a critical exposition of the theory of the properties of rigid and nonrigid molecules. Several accounts of the subject, both technical and didactic, are now available, and an extensive discussion of nonrigid molecule symmetry has been going on since the classic papers of Hougen and Longuet-Higgins. There remains, however a need for a unifying survey of the problem. Previous treatments have tended to emphasize a particular viewpoint at the expense of a broader view.

Chapter 1 is devoted to a description of the derivation of the usual Wilson-Howard-Watson form of the molecular Hamiltonian, together with its generalization to nonrigid molecules. Particular attention is given to the introduction of molecular models. Some approaches to nonrigid molecule dynamics are also examined.

After a brief review of the fundamental symmetries of the complete molecular Hamiltonian, Chapter 2 gives a treatment of the symmetry properties of rigid molecules based upon the static molecular model. The formal theory is illustrated by application to the symmetry classification of states of diatomic molecules.

Chapter 3 then develops a unified approach to the symmetry properties of nonrigid molecules. The formalism is based on the properties of the semi-rigid molecular model, and is a straightforward generalization of the theory given in the preceding chapter. It is shown that previous approaches can by thereby encompassed within a unified scheme.

Chapter 4 applies the theory to derive character tables for various nonrigid molecular point groups. Recognition of semi-direct product structure allows a straightforward correlation which can be made between the irreducible representations of rigid and nonrigid molecular symmetry groups. Such correlations can be exploited in the general theory of vibrations in nonrigid molecules, but the details of this application have yet to be worked out.

The appendices develop in detail several important topics touched upon in the text. A glossary of mathematical symbols and abbreviations is included for the convenience of the reader.

The author presents in a systematic manner and at a high mathematical level the newest developments in the field of group theory. This book can be used with success by graduate students as well as by theoreticians to get quickly information in this area of theoretical chemistry.

Ursula Bologa

H. F. FRANZEN, "Second-Order Phase Transitions and the Irreducible Representation of Space Groups" (Lecture Notes in Chemistry, vol. 32), Springer-Verlag, Berlin—Heidelberg — New York, 1982, 98 pages (soft-cover).

Some properties of crystalline solids are directly related to the underlying of three-dimensional periodicities that characterize many crystalline materials. Such properties are: the directions and symmetry of diffraction (X-ray, neutron, electron), the transport phenomena, the anisotropy of thermal expansion and interaction of crystals with optical radiation. It is therefore important to understand such periodicities in order to explain the phenomenology of the interactions of crystalline solids.

The aim of the first four chapters (48 pages) is to discuss the three-dimensional periodicities in terms of space lattices, developed on the theory of symmetry in crystalline solids (the theory of space groups and their representations). The author presents in a suggestive and simple manner how to obtain all the 14 Bravais lattices. With the knowledge of the plane lattice types and their proper rotational symmetries the possible space lattices can be obtained by considering stacking of the plane lattices with various choices of stacking vector, so as to preserve axial symmetry.

The remaining half of the book is concerned with the thermodynamic and group theoretical techniques useful in the consideration of phase transitions which occur without the coexistence of two phases, i.e. without the nucleation and growth of a new phase. The transition under consideration occurs with a change of symmetry at a certain thermodynamic state during a continuous structure change through that state. Such structure changes may be of three types: order-disorder, displacive and a combination of order-disorder and displacive. It has been shown that in the latter case the ordering is incommensurate with the translation periodicity of the lattice. Landau's theory of the thermodynamics of second-order phase transitions is considered without symmetry and with consideration of symmetry applied to the NiAs-type to MnP-type phase transition.

The subject matter of the Lecture Notes presented in this volume has been incorporated in part in the lectures or courses in Solid State Chemistry taught several times in USA and in Western Germany during the last years. The first part of the book is a source of basic information in the field of Group Theory applied to Solid State Chemistry, useful for undergraduate students.

Ursula Bologa

P. BECKER, "Phosphates and Phosphoric Acid : Raw Materials, Technology, and Economics of the Wet Process" (Fertilizer Science and Technology Series, Volume 3), Marcel Dekker, Inc., New York, 1983, 608 pages, S. Fr. 253 (hard-cover).

Sixteen years have passed since 1968 when Marcel Dekker Inc. published A. V. Slack's book "Phosphoric Acid". During these years phosphoric acid technology advanced considerably, since production is growing at a rapid rate. World phosphoric rock consumption increased from 74 million metric tons in 1969 to 130 million metric tons in 1979, and it is estimated that about two thirds of this amount are now converted into wet process phosphoric acid. On the other hand, energy and raw material prices have increased, ore quality has changed. New construction materials and equipment and better knowledge of technology resulted in improved and larger-size production units. Environmental problems such as calcium sulfate disposal and fluorine emission became of primary importance in industrialized countries, often influencing the decision whether to implement a new project. There have been many improvements and developments in the use of lower-grade rocks, the control of pollution, and uranium recovery.

Many papers have been published on these subjects, and time has come to sum all this information in one book. The author had several primary goals : (i) To give an updated picture of phosphoric acid technology in today's economic situation ; (ii) To suggest methods for solving engineering and production problems which occur regularly in phosphoric acid production and to illustrate them with many examples ; (iii) To provide engineering and plant experience. (iv) To show how the various kinds of commercial phosphate concentrates apply to present technology, by presenting detailed tables of phosphoric rock analysis including specific industrial characteristics such as grinding capability, specific sulfuric acid consumption figures, filtration capacities, sludge formation from the concentrated acid, chemical and physical properties of produced acid. (v) To maintain a link between technology and economics.

From the foregoing it is obvious that the science of phosphates and the technology of phosphoric acid is somewhat esoteric. Words such as "technology" or "calculation", in this case, have to be employed very carefully. Sometimes traditional calculation methods can be used and sometimes one has to rely on experience and accept a simple estimation based on similar cases. The phosphate rock user lives in a permanent state of doubt and suspicion about phosphate rock composition and analysis. "Like human beings, phosphates are fascinating : they never behave consistently. They like to be treated differently every time." Whatever will happen in a plant or with the quality of commercial product the user's first reaction is : "Hasn't the rock changed?" In fact, the rock is sometimes a welcome scapegoat without a defender. From his own experience (thirty years spent in the dust and effluent gases of phosphoric plants, watching filter cakes and plugging pipes !), the author felt that there was a lack of practical information required to run a plant such as detailed material and heat balances, operating parameters and procedures, selection and sizing equipment. Answers to these problems were not available in the literature up to now.

The economics of manufacture is not forgotten : it is the object of two chapters. An appendix contains valuable information on the characteristics of approximately forty commercial phosphate rocks.

This book is written in a highly readable, attractive, colloquial manner, yet it provides excellent technical, scientific, economic, and managerial information. It will be a useful manual for any worker in the field : engineer technician, economist, and executive. Project engineers should find this volume to be a main source of helpful information.

Ursula Bologa

R. D. HARCOURT, "Qualitative Valence-Bond Descriptions of Electron-Rich Molecules : Pauling '3-Electron Bonds' and 'Increased-Valence' Theory" (Lecture Notes in Chemistry, vol. 30), Springer-Verlag, Berlin—Heidelberg—New York, 1982, 260 pages (soft cover).

It is well known that the electronic structure of a molecule can be represented by either the molecular orbital theory (MO) or the valence-bond theory (VB). Both theories are generally in agreement with experimental results with respect to bond properties : bond lengths, bond angles, dissociation energies, spin density distributions and bond orders. For a large class of molecules, the so-called "electron-rich" molecules, with more electrons than half the number of bonding orbitals, neither MO nor VB representations can account for some of the properties mentioned above.

The author of the book tries to demonstrate that for a more realistic qualitative electronic description of the ground-state of these molecules other representations have to be considered together with classical structures ("Lewis structures"). At the beginning of the book the author shows the usefulness of using the concepts of "Pauling 3-electron bond" and of Lewis "long-bond". It is argued that irrespective whether weights of the "long-bond" structures are larger or smaller, a more suitable description of the molecular systems must always be obtained when these structures are included rather than excluded.

Considering all these structures ("Lewis structures", Lewis "long-bond" structures, and structures with "Pauling 3-electron bond") to be in resonance, "increased-valence" structures are obtained. This term was introduced by the author in 1964. Such formulas contain the maximum number of bonding electrons and have the lowest energy.

Many examples are given of inorganic and organic molecules whose bond properties are explained. Some chapters are concerned with chemical bonding in transition metal complexes, free radicals and spin-paired bonding diradical reactions, intermolecular donor-acceptor complexes. For a clearer representation of electron distribution, the Green and Linnett formulas are used (with one bonding and two non-bonding electrons).

The author has the merit to bring up to date literature data till 1982 in the field of electronic structures by means of valence-bond theory. New arguments are presented for the existence of the "3-electron bond". The topic is organized in such a manner that every chapter anticipates what will be presented in the further chapters. Conclusions are drawn permanently and essential aspects are stressed. The formulas are written clearly. Sophisticated aspects of chemical bonding and molecular structure are presented systematically without elaborated mathematical treatment. The author has a remarkable pedagogical talent, therefore the reader has finally the satisfaction of understanding easily relatively complicated aspects of theoretical chemistry.

Ursula Bologa

ORSZÁGOS MŰSZAKI INFORMÁCIÓS KÖZPONT ÉS KÖNYVTÁR 1883

NOTE POUR LES AUTEURS

La Revue Roumaine de Chimie publie des articles en anglais, français, russe, allemand ou espagnol. Les auteurs sont priés d'envoyer des articles et des comptes rendus inédits.

Les manuscrits seront dactylographiés à double interligne. La bibliographie, les tableaux et la légende des figures seront placés après le texte.

Si l'article fait partie d'une série numérotée, la partie précédente sera donnée comme première référence.

Chaque article sera précédé d'un résumé comprenant quinze lignes au maximum.

Les références bibliographiques dans le texte seront faites par des exposants sans parenthèses et paraîtront à la fin de l'ouvrage.

Les publications périodiques mentionées dans la bibliographie seront présentées suivant les prescriptions internationales : le nom de l'auteur précédé de l'initiale du prénom, le titre du périodique abrégé conformément à « Chemical Abstracts » et souligné par une ligne, le numéro du tome indiqué par des chiffres arabes et souligné par deux lignes, suivi de la première page de l'article : à la fin, l'année de la parution sera placée entre parenthèses. Le numéro de la revue ne sera pas indiqué si les pages du volume sont numérotées consécutivement.

Les textes des livres ou traités inclueront : le nom des auteurs, précédés de l'initiale du prénom, le titre du livre entre guillemets et sans être souligné, le numéro du tome précédé par l'abréviation « vol. » (ou « Bd. »), le numéro de l'édition, les éditions (the publisher), la localité de la parution du livre, l'année de la parution et la page de référence précédée(s) par l'abréviation « p » (ou « S »).

Les brevets seront indiqués comme suit : l'auteur ou la firme, le pays et le numéro du brevet, la date de la revue *(Chem. Abstr.)*. Par ex. : M. Jones (to Union Carbide Co.). Brit. Pat. 610 238, 2 Sept. 1959 : cf. *Chem. Abstr.*, 54, 12808 (1960).

Si la référence n'a pas été lue en original, on indiquera aussi la revue de références consultée.

Les diagrammes seront tracés à l'encre de Chine sur papier calque. Les tableaux et les figures (en nombre strictement nécessaire), ainsi que les courbes dans les figures seront numérotés par des chiffres arabes. Leur explication sera donnée dans la légende des figures. Prière de ne pas inscrire les mêmes données dans les tableaux et les figures. Chaque tableau aura un titre. On indiquera dans le texte la place approximative des tableaux et des figures. Les formules chimiques seront incluses dans le texte ; en outre, elles seront transcrites sur papier calque à l'encre de Chine.

Les auteurs sont priés d'indiquer les caractères italiques (en soulignant les lettres au crayon), ainsi que tout autre caractère spécial : les préfixes *ortho*, *meta*, *para*, *cis*, *trans*, etc. seront soulignès pour indiquer leurs caractères italiques, et ne seront jamais écrits avec des majuscules.

Aucune correction à la main ne sera admise sur le manuscrit. Les corrections seront frappées à la machine. Les lettres grecques ou autres symboles spéciaux seront insérés à la main à l'encre clairement.

Le manuscrit sera signé par l'auteur.

Le titre courant aura 50 lettres au maximum.

L'entière responsabilité du contenu des articles appartient aux auteurs.

Sur demande on peut obtenir une note plus complète.

PRINTED IN ROMANIA

TRAVAUX PARUS AUX ÉDITIONS DE L'ACADÉMIE DE LA RÉPUBLIQUE SOCIALISTE DE ROUMANIE

ELENA CEAUȘESCU, **Cercetări în chimia și tehnologia polimerilor**, 1983, 519 p.
N. ASANDEI, A. GRIGORIU, **Chimia și structura fibrelor**, 1983, 395 p.
N. IONESCU, M. CALDARARU, **Oxidarea catalitică a olefinelor inferioare**, 1983, 178 p
C. CAȘCAVAL, **Studiul polimerilor prin piroliză și cromatograafie de gaze**, 1983, 220 p.
C. I. SIMIONESCU, F. DENES, **Originea vieții**, 1983, 110 p.
C. BODEA (editeur), **Tratat de biochimie vegetală**, II, Tome IV, 1982, 408 p.
I. G. MURGULESCU, RODICA VILCU, **Introducere în chimia fizică. Vol. III. Termodinamica chimică**, 1982, 624 p.
ELENA JERCAN, **Analiza cromatografică**, 1982, 286 p.
I. G. MURGULESCU, J. PĂUN, **Introducere în chimia fizică. Vol. I. 3. Nucleul atomic, reacții nucleare, particule elementare**, 1982, 606 p.
ELENA CEAUȘESCU, **Noi cercetări în domeniul compușilor macromoleculari**, 1981, 536 p.
I. G. MURGULESCU, TATIANA ONCESCU, E. SEGAL, **Introducere în chimia fizică. Vol. II. 2. Cinetică chimică și cataliză**, 1981, 1024 p.
V. DRĂGUȚAN, A. T. BALABAN, M. DIMONIE, **Metateza olefinelor și polimerizarea prin deschidere de inel a cicloolefinelor**, 1981, 254 p.
LYDIA-MARIA VAICUM, **Epurarea apelor uzate cu nămol activ. Bazele biochimice**, 1981, 218 p.
I. GĂLĂȚEANU, **Procese și metode radiochimice în energetica nucleară**, 1981, 234 p.
O. IORDACHE, **Procese polistocastice aplicate la fenomenele de transfer**, 1981, 186 p.
CR. SIMIONESCU, VALERIA GORDUZA, **Polimeri biocompatibili și biologic activi**, 1980, 479 p.
ELENA CEAUȘESCU, **Polimerizarea stereospecifică a izoprenului**, 1979, 307 p.
CONST. GH. MACAROVICI, **Analiza chimică cantitativă anorganică**, 1979, 457 p.
M. FLORESCU, **Metode științifice în dezvoltarea industriei chimice moderne**, 1979, 256 p.
A. T. BALABAN, I. GĂLĂȚEANU, G. GEORGESCU, LIGIA SIMIONESCU, **Compuși marcați și radiofarmaceutici cu aplicații în medicina nucleară**, 1979, 495 p.
I. G. MURGULESCU, E. SEGAL, **Introducere în chimia fizică, Vol. II. 1. Teoria molecular cinetică a materiei**, 1979, 1036 p.
S. STERNBERG, FL. DANEȘ, **Termodinamica chimică aplicată**, 1978, 400 p.
I. G. MURGULESCU, V. EM. SAHINI, **Introducere în chimia fizică. Vol. I. 2. Structura și proprietățile moleculelor**, 1978, 604 p.
I. ZUGRĂVESCU, MAGDA PETROVANU, **N-ylid chemistry**, coédition avec McGraw Hill International Book Company, U.S.A., 1977, 396 p.
I. G. MURGULESCU, **Introducere în chimia fizică. Vol. I. 1. Atomi, molecule, legătură chimică**, 1976, 560 p.
ELENA CEAUȘESCU, **Research work on synthesis and characterization of macromolecular compounds. Contributions**, 1974, 251 p.
CR. SIMIONESCU, VIORICA RUSAN, V. POPA, **Chimia algelor marine**, 1974, 212 p.,1 pl.

ISSN 0035–4090

I.P. INFORMAȚIA, cd. 2140

43 426

Lei 40.
$ 75 (pour un abonnement annuel)

F 1103

Veggészet

ACADÉMIE DE LA RÉPUBLIQUE SOCIALISTE DE ROUMANIE

REFERALVA

REVUE
ROUMAINE
DE
CHIMIE

TOME 29

N° 7

Juillet 1984

Rev. Roumaine Chim.

RRCHX. 29, 7, p. 539–622 (1984), Bucarest

EDITURA ACADEMIEI REPUBLICII SOCIALISTE ROMÂNIA

ACADÉMIE DE LA RÉPUBLIQUE SOCIALISTE DE ROUMANIE

COMITÉ DE RÉDACTION

Rédacteur en chef :

I. G. MURGULESCU, membre de l'Académie de la République Socialiste de Roumanie

Rédacteurs en chef adjoints ;

A. T. BALABAN et V. EM. SAHINI, membres correspondants de l'Académie de la République Socialiste de Roumanie

Collège de rédaction :

EM. BRATU, ELENA CEAUȘESCU, ECATERINA CIORĂNESCU-NENITZESCU, CR. SIMIONESCU, membres de l'Académie de la République Socialiste de Roumanie; P. SPACU, membre correspondant de l'Académie de la République Socialiste de Roumanie : M. BANCIU, MIRCEA GHEORGHIU, I. HAIDUC, D. I. MARCHIDAN, I. MOLDOVAN, G. NIAC et D. SĂNDULESCU

La Revue Roumaine de Chimie paraît 10 fois par an. Toute commande de l'étranger pour les travaux parus aux Editions de l'Académie de la République Socialiste de Roumanie sera adressée à ROMPRESFILATELIA — sectorul export — import presă P.O. Box 12—201, télex 10376 prsfi r București, Calea Griviței nr. 64—66

Les manuscrits, les livres et les revues proposés en échange, ainsi que toute correspondance seront envoyés à la rédaction.

REVUE ROUMAINE DE CHIMIE

125, Calea Victoriei, 79717 Bucarest, Roumanie, téléphone 50 76 80

EDITURA ACADEMIEI REPUBLICII SOCIALISTE ROMÂNIA
125, Calea Victoriei, 79717 Bucarest, Roumanie, téléphone 50 76 80

F 1103

ORSZÁGOS MŰSZAKI INFORMÁCIÓS KÖZPONT ÉS KÖNYVTÁR

REVUE ROUMAINE DE CHIMIE

Tome 29, N° 7 Juillet 1984

N. PETRESCU, MIRELA BRIŢCHI and LUCIA GANOVICI, Removal of antimony and arsenic from electrolytes by means of β-stannic acid . . . 541—547 R

P. FILIP, NICOLETA ŞTEFAN, F. CHIRALEU, I. G. DINULESCU and MARGARET AVRAM, Investigation in the cyclobutane series. LVI. Dimers of 1-alkyl-benzocyclobutadienes . . . . 549—555

P. FILIP, NICOLETA ŞTEFAN, F. CHIRALEU, I. G. DINULESCU, and MARGARETA AVRAM, Investigations in the cyclobutane series. LVII. On the behaviour of 1-alkyl-benzocyclobutadiene dimers toward the system t—BuOK—DMSO and air . . . . 557—560

MINODORA LECA and AURELIU LECA, Drag reduction of some ultra-high molecular weight polyacrylamides . . . . 561—566

CRISTOFOR I. SIMIONESCU and SILVIA BRĂNIŞTEANU, Ion exchange membranes based on grafted cellulose esters. I. Activation by peroxidation in view of grafting the cellulose esters . . . . 567—574 R

M. A. EL-KASABY and M. A. I. SALEM, Michael reaction of β (2-fluorenyl)-acrylic acid and its amides . . . . 575—582

ABDEL GHANI ALI EL-AGAMEY and LEVAN PETROVITSH ASATIANI, Synthesis of mono- and diacetylenic derivatives of silylferrocene . . . 583—588

A. CĂLUŞARU, Hydrogen isotope effects in the reaction of polarographic oxygen reduction . . . . 589—592

E. SEGAL, M. VLAD and V. POPA, Structural characteristics of the stoichiometric matrix . . . . 593—596

M. VLAD, V. POPA and E. SEGAL, On the kinetic model of the rate-determining step. II. Single-route systems with an arbitrary number of active intermediates . . . . 597—604

U. D. N. BAJPAI and ANIŢA AHI, Polymerization of acrylamide initiated by Fe^{2+}/bromate redox couple . . . . 605—612

BOUBEKEUR MAOUCHE, JOSÉ GAYOSO and OURIDA OUAMERALI, Diamagnetic susceptibility exaltations and aromaticities of unsaturated boron-nitrogen heterocycles . . . . 613—620

Comptes rendus . . . . 621—622

Rev. Roumaine Chim. 29, 7, 539—622 (1984), Bucarest

Revue Roumaine de Chimie, **29**, 7, 541–547(1984)

REMOVAL OF ANTIMONY AND ARSENIC FROM ELECTROLYTES BY MEANS OF β-STANNIC ACID

N. PETRESCU*, MIRELA BRIȚCHI** and LUCIA GANOVICI**

* Department of Metallurgy, The Polytechnic Institute of Bucharest, Spl. Independenței 313, Romania

** Centre of Physical Chemistry, Spl. Independenței 202, Bucharest, Romania

Received May 28, 1983

Experiments have been carried out for separating antimony and arsenic from hydrochloric and sulphuric solutions, by passing them through columns filled with pellets of β — stannic acid. The sulphuric solutions had compositions close to the composition of the electrolytes used for electrolytic refining of copper. The experiments have shown that the β — stannic acid is able to retain from solution the threevalent arsenic and antimony, according to a selective reaction. The maximum retaining capacity derived from the experimental data is 10.4 g Sb per 1 kg β — stannic acid and 5.3 g As per 1 kg β — stannic acid when each element is present separately in solution. When both arsenic and antimony are present in solution, the retaining capacity of 1 kg β — stanic acid changes to 5.16 g Sb and 6.4 g As. It was established that the reaction with β-stannic acid can be completely reverted for Sb in the presence of strong HCl solution and partially reverted for As.

The purity of copper obtained by electrolytic refining depends on the purity of the electrolytic solutions. [1] An important contribution to the impurifying of cathodic deposit is made by the floating slime, which is a very finely dispersed precipitate formed in the electrolytic solution. This consists of a mixture of antimony, arsenic and bismuth oxides and compounds in a ratio correlated to their relative content in the electrolyte. [1–3] For copper electrorefining impure anodes are used. During the dissolution of the anode its impurities pass into the solution together with copper. Some impurities such as lead and tin, form precipitates which settle down, forming the anodic slime; other impurities such as antimony, bismuth and arsenic form the floating slime. The formation of the floating slime depends on the concentration of these elements in the electrolyte solution and their valence state. The main role in the formation of the floating slime is played by pentavalent antimony when it exceeds 0.05 g/l. [3]

It is known that antimony, bismuth and arsenic pass from the anode into the solution in the form of threevalent ions. During the electrolysis of copper, the threevalent ions of antimony and arsenic are oxidized to pentavalent state by the atmospheric oxygen dissolved in the electrolyte. The threevalent bismuth is not oxidized by the oxygen from the electrolyte. To avoid the formation of the floating slime, conditions for the precipitation of these elements in form of crystalline antimony arsenate and bismuth arsenate must be ensured. In form of arsenates, antimony and bismuth are threevalent and arsenic is pentavalent. Consequently, the floating slime begins to form when the concentration of pentavalent antimony exceeds a certain value found to be 0.05 g/l. Below this concentration crystalline precipitates of antimony arsenate and bismuth arsenate are formed and these precipitates settle down.

A mean to maintain a low concentration of pentavalent antimony ions is to maintain a total concentration (threevalent and pentavalent ions) of antimony under the limit of 0.2 g/l. [3] In some works this limit concentration is established at a level of 0.5 g/l. [1] This can be achieved by the purification of the electrolyte using certain substances such as manganese oxide hydrate and stannic acid ($SnO_2 \cdot nH_2O$), which retain antimony, bismuth and arsenic.

Another mean to maintain a low concentration of pentavalent ions of antimony is to increase the amount of arsenic threevalent ions. This is because the oxidation rate of arsenic by the oxygen from the electrolyte is greater than the oxidation of antimony; this way conditions are ensured for the formation of arsenates. Experimentally it has been established that the formation of the floating slime during the electrorefining of copper can be avoided if the total concentration of arsenic in the electrolyte is maintained over 3 g/l. [3]

In the present work we have studied the first method of purification of the electrolytes, namely the removal of antimony and arsenic by β-stannic acid.

EXPERIMENTAL

Metastannic or β-stannic acid has the property to retain threevalent ions of antimony, bismuth and arsenic.

β-stannic acid has been prepared in our laboratory by direct action of HNO_3 33% on metallic tin, according to the reaction:

$$Sn + 4HNO_3 = H_2SnO_3 + 4NO_2 + H_2O$$

Pellets of β-stannic acid of 6–8 mm diameter and 2–4 mm height have been used. The pellets were obtained by pressing the powder in steel moulds under a pressure of 2050–3000 daN/cm^2 in a hydraulic press. The pellets must be very dense otherwise they break into pieces even in water.

The capacity of β-stannic acid to retain antimony and arsenic is strongly influenced by the physical state of absorbant. [4]

The electrolytic solutions containing either arsenic or antimony ions (or both) were passed through a glass column (11 mm diameter and 370 mm height) filled with 16 g pellets of β-stannic acid. The solutions were passed through the column by means of a peristaltic pump which kept a constant flow rate during the run. The output solutions from the column were analysed periodically and the antimony and arsenic concentrations determined.

In order to determine the antimony and arsenic in the electrolytic solutions which contain either antimony or arsenic ions, one used the analytical method of titration with $KBrO_3$ 0.01M and 0.01N in the presence of methyl-orange and starch. [2]

The amount of the antimony and arsenic is calculated by means of the following expressions :

$$g\ Sb/l = \frac{n T\, 60.875}{27.835}\ \frac{1000}{q}$$

$$g\ As/l = \frac{n T\, 37.461}{27.835}\ \frac{1000}{q}$$

where n = millilitres of $KBrO_3$ solution 0.01M or 0.01N used, T = grammes of $KBrO_3$ corresponding to 1 ml of solution, q = the volume of the analysed solution, generally 10 ml of solution.

The following experiments have been carried out :

1. Experiments to retain the antimony from the hydrochloric aqueous solutions having a content of 1.56 g/l — 1.60 g/l antimony. A series of experiments have been performed using the same column in order to verify the reversibility of the process and the possibility to reuse the β-stannic acid.

2. Experiments to retain the antimony from sulphuric solution of copper sulphate having the composition : 1.70 g/l (Sb^{3+}), about 150 g/l (H_2SO_4), Cu^{2+} = 40 g/l

3. Experiments to retain arsenic from hydrochloric aqueos solution having an arsenic content of 1.05 gAs/l.

4. Experiments to retain the arsenic from sulphuric solution of copper sulphate having the composition : 2.11 gAs/l, 40 gCu/l and about 150 gH_2SO_4/l.

5. Experiments to retain concomitantly the antimony and the arsenic from sulphuric solution of copper sulphate having the composition : 1.75 gSb/l, 2.57 gAs/l, 150 gH_2SO_4/l, 40 gCu/l.

RESULTS AND DISCUSSIONS

1. The retaining of the antimony from the electrolytic solutions by the β-stannic acid

In order to characterize the β-stannic acid from the point of view of its retaining capacity for the antimony threevalent ions, solutions containing only threevalent antimony ions were prepared and the solutions were passed over the β-stannic acid pellets at a constant flow rate.

The solutions which come out of the column were periodically analysed using the analytical method of titration with $KBrO_3$. The composition and the experimental results are shown in table 1.

In the runs la, 16 g of fresh β-stannic acid were used. The same β-stannic acid was reused in runs 1b, 1c and 2 after its regeneration with HCl 1 : 1. In all runs the solutions were passed through the column at a flow rate of 1.65 ml/min, the effective contact times ranging from 260 to 275 minutes. With the obtained experimental data the curves for the variation of the antimony amount in the solutions passed through the column vs. time were built up. The maximum quantity of antimony retained by 1 kg of β-stannic acid was calculated from the extended experimental curves. For the sake of illustration, figure 1 represents the curve for the variation of the antimony amount in the solutions passed through the column vs. time built up with the data from the run 1a.

The shaded area represents the maximum quantity of antimony which was retained by 16 g of β-stannic acid. For runs la, 1b and 1c (Table 1), an anverage value of 10.4 g Sb has been derived as the maximum retaining capacity for antimony in hydrochloric solutions, of 1 kg of β-stannic acid. The extraction of antimony from the β-stannic acid was

Table 1

The experimental results

Run	1a	1b	1c	2
The composition and the concentration of the sol. (g/l)	$Sb^{3+} = 1.60$	$Sb^{3+} = 1.58$	$Sb^{3+} = 1.56$	$Sb^{3+} = 1.70$ g/l $Cu^{2+} = 40$g/l $H_2SO_4 \cong 150$ g/l
The amount of Sb retained by the β-stannic acid during the effective time of the circ. of the sol. through the column (mg)	131	132	107	96
The amount of Sb obtained by reextraction with HCl 1 :1 (mg)	116	123	120	102
The maximum amount of Sb which can be retained by 1 kg of β-stannic acid (value obtained from the extended graph) (g)	11.31	9.5	10.43	7.8

effected with HCl 1 : 1. By comparing the experimental results in table 1 with the calculated values, one concludes that actually the whole retained quantity of antimony extracts with hydrochloric acid in the regeneration stage ; so the original amount of β-stannic acid can be reused several times without being poisoned. In the experimental run 2 (Table 1), the maximum capacity of the β-stannic acid to retain antimony, in a solution of different composition was studied. For that purpose we have used sulphuric solution of copper sulphate, having a concentration in Cu, H_2SO_4 and Sb, analogous to the electrolytic solutions used in industry, namely : 40 gCu/l, 150 gH_2SO_4/l and 1.70 gSb/l. The shape of curve for the varia-

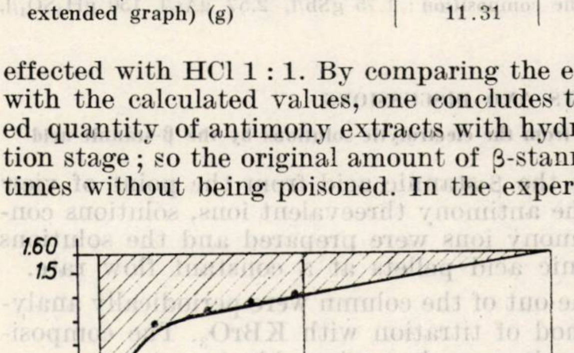

Fig. 1. — Variation of the antimony concentration in the solution passed over β-stannic acid pellets vs. time initial antimony concentration : 1.60 g/l ; the effective time of the circulation of the solution through the column : 270 minutes (experimental run 1a).

tion of the antimony amount in the solution which comes out of the column vs. time is similar to the curve represented in figure 1. For the maximum capacity to retain antimony in 1 kg of β-stannic acid a value of 7.8 g was obtained. This value is a little less than the values obtained in our previous experiments, where hydrochloric solutions were used, and only threevalent antimony was present. The retained antimony was extracted from the β-stannic acid with HCl 1 : 1. The quantity of extracted antimony from 16 g of β-stannic acid was 102 mg which is a little more than the amount of 96 mg derived from the plot (Table 1). The same issue results from the run 1c. The surplus of antimony can be ascribed to the amount of antimony retained in the previous experiments and which was not completely reextracted. From the analysis of the experimental data, one can conclude that the β-stannic acid has a good capacity to retain antimony both from hydrochloric solutions and from sulphuric solutions. The same quantity of β-stannic acid in the column can be reused several times ; the regeneration can be performed with acid solution of normality higher than the initial solutions.

2. The retaining of the arsenic from the electrolytic solutions by β-stannic acid

In order to characterize the β-stannic acid from the point of view of its capacity to retain arsenic threevalent ions experiments have been carried out with both hydrochloric solutions and sulphuric solutions. The composition of the solutions and the experimental results are shown in table 2.

Table 2

The experimental results

Run	3	4
The composition and the concentration of the sol. (g/l)	$As^{3+} = 1.05$	$As^{3+} = 2.11$ $Cu^{2+} = 40$ $H_2SO_4 \cong 150$
The amount of As retained by the β-stannic acid during the effective time of circ. of the sol. through the column (mg)	62	84
The amount of As obtained by reextraction with HCl 1 :1 (mg)	10	23
The maximum amount of As which can be retained by 1 kg of β-stannic acid (value obtained from the extended graph) (g)	5.3	7.3

In the experimental runs a quantity of 16 g of β-stannic acid was used, and then reused after the regeneration with HCl 1 : 1. In both experiments the solutions were circulated at the flow rate of 1.65 ml/min ; the effective times of the passing of the solutions were 250 and 245 minutes respectively. The exit electrolytic solutions were analysed and the obtained data have been used for plotting the curves for the variation of the arsenic concentration vs. time. In figure 2 such a curve was built up with the data obtained in the run 3.

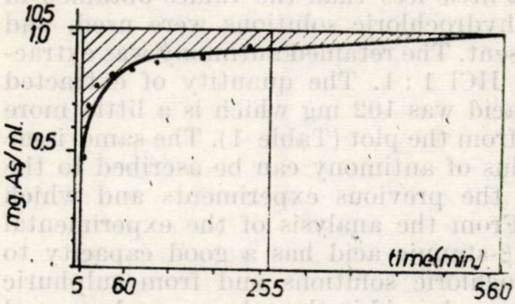

Fig. 2. — Variation of the arsenic concentration in the solution passed over β-stannic acid pellets vs. time. initial arsenic concentration : 1.05 g/l ; the effective time of the circulation of the solution through the column : 250 minutes (experimental run 3).

The maximum retaining capacity for the arsenic of 1 kg of β-stannic acid, from a hydrochloric solution is 5.3 g while from a sulphuric solution with copper sulphate is 7.3 g. To notice that the arsenic concentration in the sulphuric solution was double, 2.11 g/l.

The extraction of the arsenic from the pellets of β-stannic acid was performed with a hydrochloric acid 1 : 1. The results in the regeneration stage showed that the quantity of arsenic obtained was less than the amount of the retained arsenic (Table 2). In order to elucidate the problem of the arsenic reextraction, additional investigations are needed.

3. The concomitant retaining of antimony and arsenic with β-stannic acid

In order to characterize the retaining capacity of β-stannic acid for arsenic and antimony, when both elements are present, an experiment was made using a sulphuric solution of copper sulphate having the following composition : $Sb^{3+} = 1.75$g/l, $As^{3+} = 2.57$ g/l, $Cu^{2+} = 40$ g/l and $H_2SO_4 \cong 150$ g/l. A higher quantity of β-stannic acid namely 47.7 g was used. The solution was circulated over the fresh pellets with a flow rate of 1.60 ml/min. at an effective contact time of 285 minutes. The solution passed over the β-stannic acid pellets was analysed for the antimony and arsenic content separating these elements by the method of reduction of the arsenic with sodium hypophosphite. From the obtained data the curves for the variation of the antimony/arsenic concentration vs. time were plotted (Fig. 3). The values for the maximum capacity to retain the antimony and arsenic in 1 kg of β-stannic acid have been derived from the plots namely 5.16 g for antimony and 6.4 g for arsenic.

Experiments are in progress in our laboratory concerning the kinetics of the process and the determination of the partition of arsenic and antimony between solution and β-stannic acid in equilibrum conditions.

CONCLUSION

The experiments have shown that the β-stannic acid is able to retain the threevalent arsenic and antimony from solution, according to a selective reaction. The maximum retaining capacity derived from the experimental data, passing the solutions over β-stannic acid pellets (diameter 6–8 mm), is 10.4 gSb/kg β-stannic acid and 5.3 gAs/kg β-stannic, acid, when each element is present separately in solution. When both arsenic and antimony are present in solution, the retaining capacity of 1 kg β-stannic acid changes to 5.16 g Sb and 6.4 g As.

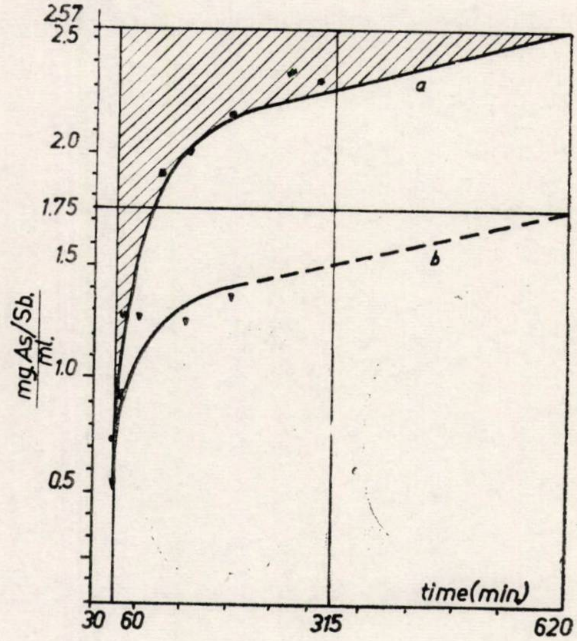

Fig. 3. — Variation of the arsenic/antimony concentration in the solution passed over β-stannic acid pellets vs. time. initial arsenic concentration : 2.57 g/l ; initial antimony concentration : 1.75 g/l ; the effective time of the circulation of the solution through the column : 285 minutes ; a) variation of the arsenic concentration ; b) variation of the antimony concentration

The reaction of β-stannic acid with antimony is reversible so that the antimony retained by the β-stannic acid can be put in solution using concentrated hydrochloric solutions. This way the same quantity of β-stannic acid can be used repeteadly for retaining new amounts of antimony.

The arsenic retained by the β-stannic acid has been recovered only partially by means of concentrated hydrochloric acid solution.

REFERENCES

[1] A. K. Biswas and U. G. Davenport, "Extractive Metallurgy of Copper", Pergamon, London, 1976, p. 511–523.

[2] C. W. Eichrodt, and J. H. Schleon, "Electrolytic Copper Refining" in "Copper, the Science and Technology of Metal its Alloys and Compounds", Hafner Pub. Comp., London, 1970, p. 171–173.

[3] N. F. R., Lindstrom, U.S.A. Patent, 3 753 877, 21 Aug. 1973 ;

[4] E. Petkova, D. Petrov, Kh. Vasilev, A. Tsanev, L. Tolinov, *Metallurgiya* (*Sofia*), **36**, 12 (1981).

[5] C. Liteanu and E. Hopîrtean, "Chimie analitică cantitativă—Volumetria", Ed. didactică și pedagogică, Bucharest, 1972, p. 370.

Revue Roumaine de Chimie, 29, 7, 549–555 (1984)

INVESTIGATION IN THE CYCLOBUTANE SERIES. LVI[1]

DIMERS OF 1-ALKYL-BENZOCYCLOBUTADIENES

P. FILIP [a], NICOLETA ȘTEFAN [a], F. CHIRALEU [a], I. G. DINULESCU [a]
and MARGARET AVRAM [b,*]

[a] Center of Organic Chemistry, Spl. Independenței 202 B, 76300 Bucharest 15, Romania
[b] Laboratory of Organic Chemistry, Polytechnic Institute-TCH, Spl. Independenței 313,
72206 Bucharest 16, Romania

Received July 21, 1983

A practical method for the synthesis of 1-alkyl-benzocyclobutadienes and their angular dimers starting with benzyne and trichloroethylene is presented.

The study of 1-alkyl-benzocyclobutadienes was limited to the 1-*t*-butyl-derivative, easy available by dehydrohalogenation of 1-bromo-1-*t*-butyl-benzocyclobutene.[2] Our interest in the synthesis of a range of 1-substituted benzocyclobutadienes and their dimers prompted us to investigate an accessible general route for the preparation of such compounds.

In this paper we present the synthesis of 1-methyl- and 1-isopropyl-benzocyclobutadiene (**1** and **2**, respectively), of their dimers (**4** and **5**, respectively) and the formation of the dibenzocyclooctatetraene derivative **7** in the course of attempts to obtain 1-phenyl-benzocyclobutadiene (**3**), respectively its dimer **6**.

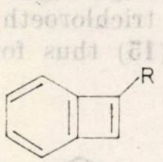

1, R = CH_3
2, R = $CH(CH_3)_2$
3, R = C_6H_5

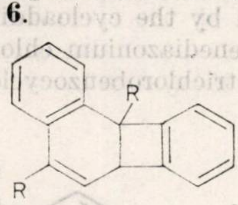

4, R = CH_3
5, R = $CH(CH_3)_2$
6, R = C_6H_5

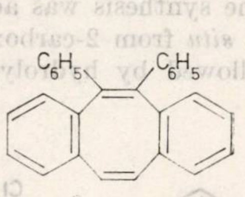

7

The earlier described method [2] for the generation of 1-*t*-butyl-benzocyclobutadiene by dehydrohalogenation with bases of 1-bromo-1-*t*-butyl-benzocyclobutene failed in the case of other alkyl derivatives (**8**) due to the tendency of the system to exocyclic elimination, [3] leading instead of 1-alkyl-benzocyclobutadienes to the corresponding alkylidene derivatives (**9**).

---

* Deceased in 1983

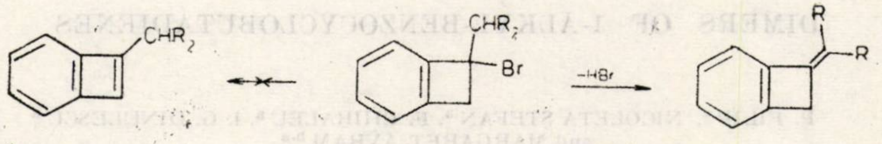

1, R = H
2, R = CH$_3$
8
9

The classical method of dehalogenation with lithium amalgam [4] of the corresponding dihalogenoderivatives **10** and **11** respectively needed the synthesis of a suitable precursor as the halogeno-benzocyclobutenones **12** or **13**.

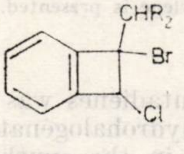

10, R = H
11, R = CH$_3$

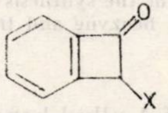

12, X = Br
13, X = Cl
14, X = H

While the obtention of **12** by bromination of **14** with NBS [5] gave mixtures of mono- and dihalogeno compounds, difficult to separate, a new route for the synthesis of the chloro ketone **13** was taken into account. The synthesis was achieved by the cycloaddition of benzyne (generated *in situ* from 2-carboxybenzenediazonium chloride [6]) to trichloroethylene, followed by hydrolysis of trichlorobenzocyclobutene (**15**) thus formed.

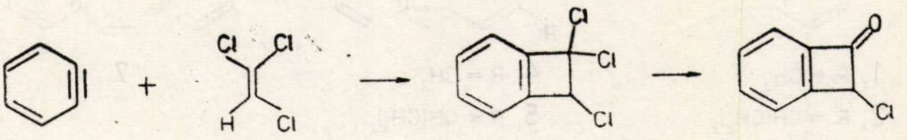

15
13

By treatment of the chloroketone **13** with excess of the corresponding Grignard reagents, in mild reaction conditions in order to prevent

secondary reactions, the 2-chloro-1-hydroxy-1-substituted benzocyclobutenes 16 (R = CH_3), 17 (R=$CH(CH_3)_2$) or 18 (R=C_6H_5) were obtained.

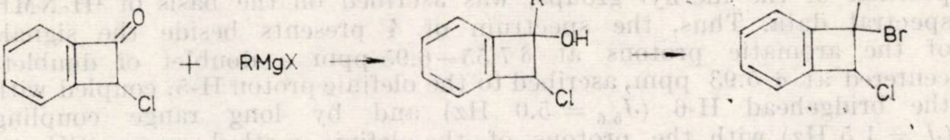

13

16, R = CH_3 10, R = CH_3

17, R = $CH(CH_3)_2$ 11, R = $CH(CH_3)_2$

18, R = C_6H_5 19, R = C_6H_5

Subsequent treatment of 16 and 17 with phosphorous tribromide gave the corresponding dihalogeno derivatives 10 and 11, respectively. In the case of isopropyl derivative 17, beside the expected bromoderivative 11, the 1-isopropylidene-2-chlorobenzocyclobutene (20) was formed in variable but apreciable amounts. Treatment of the latter (or of the crude reaction mixture) with anhydrous hydrobromic acid gave 11 in high yield.

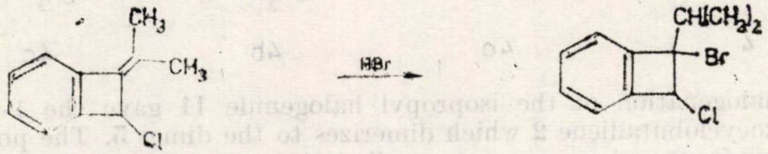

20

11

The structures of compounds 10, 11, 16—19 were ascribed on the basis of analytical and spectral data.

Some characteristic features of the hydroxy derivatives spectra merit to be underlined. Thus in the IR spectrum of the compounds 16, 17 and 18, the hydroxyl group absorption at 3575 cm^{-1}, invariable by dilution, indicates intramolecular association with chlorine atom. This fact evidences that the attack of the Grignard reagent to the carbonyl group occurs stereospecifically.

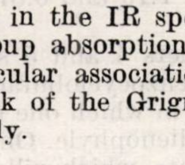

16 R = CH_3

17 R = $CH(CH_3)_2$

18 R = C_6H_5

By generation of 1-methyl-benzocyclobutadiene (**1**) from dihalogeno derivative **10** and lithium amalgam, in etehreal solution, the dimer **4** (white crystals, m.p. 98–100°) was obtained. The structure, namely the position of the methyl groups, was ascribed on the basis of ^{1}H-NMR spectral data. Thus, the spectrum of **4** presents beside the signals of the aromatic protons at δ 7.55–6.95 ppm a doublet of doublets centered at δ 5.93 ppm, ascribed to the olefinic proton H-5, coupled with the bridgehead H-6 ($J_{5,6} = 5.0$ Hz) and by long range coupling ($J = 1.5$ Hz) with the protons of the olefinic methyl group (CH_3-4). Another doublet of doublets centered at δ 3.75 ppm was attributed to the bridgehead proton H-6; this benzylic and allylic proton is coupled with H-5 ($J_{5,6} = 5.0$ Hz) and by long range coupling with the protons of CH_3-4 ($J = 1.5$ Hz). The signals of CH_3-4 appear as a triplet at δ 2.0 ppm, due to the long range couplings with H-5 and H-6 ($J = 1.5$ Hz); the bridgehead bonded CH_3-1 gave a singlet at δ 1.78 ppm. This spectral data excluded the isomeric structures **4a**–**4c**.

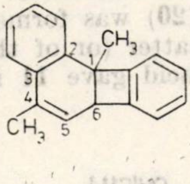

4

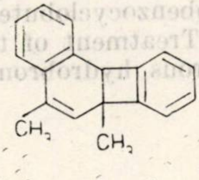

4a

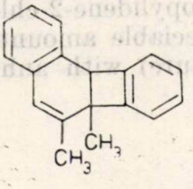

4b

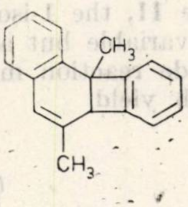

4c

Dehalogenation of the isopropyl halogenide **11** gave the 1-isopropyl-benzocyclobutadiene **2** which dimerizes to the dimer **5**. The positions of the two isopropyl groups were attributed on the basis of the following ^{1}H-NMR spectral data. The olefinic proton H-5 (δ 5.98 ppm) gave a doublet by coupling with the cyclobutene ring proton H-6 (δ 3.38 ppm; $J_{5,6} = 6.5$ Hz). The tertiary protons of the two isopropyl groups give rise to two multiplets centered at δ 2.93 and 2.52 ppm; the methyls appear as doublets ($J = 7.0$ Hz) at δ 1.16 and 0.87 ppm, by coupling with the tertiary protons.

The structure of the dimers **4** and **5** shows that the dimerisation of 1-methyl- and 1-isopropyl-benzocyclobutadiene (**1** and **2**, respectively) occurs by Diels-Alder reaction, in which one molecule takes part as diene partner and the other one as dienophyle. On structural grounds based on the stability of the transition state, which will be published, [7] the approach leading to the dimers with the alkyl groups in positions **1** and **4** is favoured.

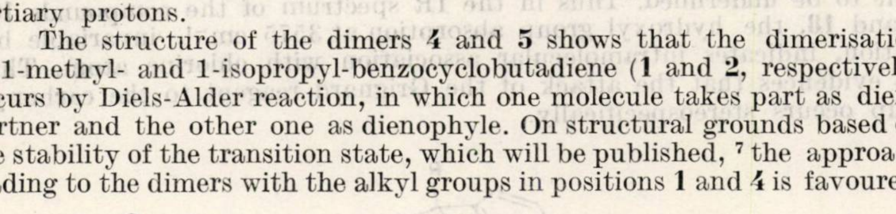

Attempts to obtain 1-phenyl-benzocyclobutadiene (**3**) using the above described route were unsuccessful. Treatment of **19** with lithium amalgam gave, instead of the expected phenyl-benzocyclobutadiene dimer **6** with dibenzobicyclo[4.2.0] octatriene skeleton, a white crystaline compound (m.p. 195°, ^{1}H-NMR signals δ 7.0–7.3 ppm), identified as diphenyl-dibenzocyclooctatetraene (**7**), earlier described in the literature as the reaction product of benzyne and phenylacetylene.[8]

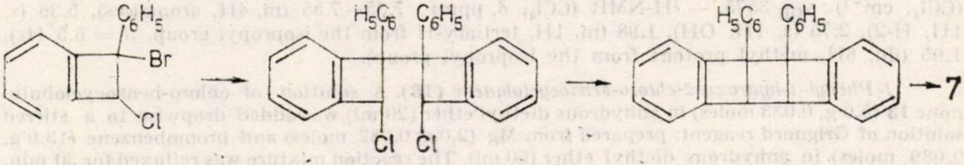

19 **21** **22**

The different course of this dehalogenation indicates that no phenyl-benzocyclobutadiene was formed as intermediate. The formation of **7** is explainable by a sequence of Wurtz reactions due to the greater reactivity of the bromine in **10**, involving the intermediates **21** and **22**.

Similar behaviour was observed also on dehalogenation of 1,2-dibromo-1-phenyl-2-methyl-benzocyclobutadiene[9] and seems to be characteristic for the phenyl derivatives. The isomerisation of dibenzotricyclooctatriene **22** to the dibenzocyclooctatetraene **7** is in agreement with the well-known properties of this system.[10]

EXPERIMENTAL

IR Spectra were recorded with a double beam Jena UR-20 spectrophotometer. ^{1}H-NMR spectra were performed with a Varian A 60-A spectrometer.

1,1,2-Trichlorobenzocyclobutene (**15**). To a stirred slurry of 2-carboxybenzenediazonium chloride (140 g, 0.88 moles) in trichloroethylene (1500 ml), propylene oxide (70 ml) was added and the mixture was maintained at 50° until gas evolution ceased (aprox. 8 hrs). The reaction mixture was worked-up by distillation, recovering the unreacted trichloroethylene at normal pressure and isolating under vacuum 40 g (25.5%), **15**, b.p. 89–93°/2 mm. Further purification of the trichlorobenzocyclobutene was done by distillation on a teflon spinning band column. ^{1}H-NMR (CCl$_4$, δ, ppm): 7.40 (m, 4H, aromatics), 5.73 (s, H-2).

2-Chloro-benzocyclobutenone (**13**). A mixture of trichlorobenzocyclobutene (**15**) (30.0 g, 0.14 moles), dimethylformamide (180 ml) and water (120 ml) was refluxed for 24 hours, poured into water (500 ml) and then extracted twice with methylene chloride. The organic layer was washed with water and after drying and solvent removal a brown oily residue was obtained. By vacuum distillation, 14.0g (63.5%) **13**, b.p. 101.5–103.5°/1mm, were obtained as colorless crystals with m.p. 59–60° (isopropanol). – C_8H_8ClO (152.5) Calcd.: C, 62.97; H, 3.30; Cl, 23.23. Found: C, 63.01; H, 3.51; Cl, 23.13. – IR (CCl$_4$, cm^{-1}): ν_{CO}1775, 1810.– ^{1}H-NMR (CCl$_4$, δ, ppm): 7.70–7.40 (m, 4H, aromatics), 5.73 (s, H-2).

1-Methyl-1-hydroxy-2-chloro-benzocyclobutene (**16**). A solution of chloro-benzocyclobutenone **13** (5.0 g, 0.033 moles) in diethyl ether (30 ml) was added dropwise to a stirred solution of Grignard reagent, prepared from Mg (1.46 g, 0.06 moles) and methyl iodide (8.6 g, 0.06 moles) in diethyl ether (40 ml). After one hour of stirring at room temperature, the reaction mixture was treated with 10 ml water and then with 30 ml saturated ammonium chloride solution. The product was extracted twice with diethyl ether and the organic layer after washing with water, drying and evaporation of the solvent, yielded 4.9 g (88.7%) **16**, colorless crystals, m.p. 42–43°. – C_9H_9ClO (168.6) Calcd.: C, 64.10; H, 5.38; Cl, 21.03. Found: C, 64.25; H, 5.59; Cl, 21.34. – IR (CCl$_4$, cm^{-1}): ν_{OH}3575. – ^{1}H-NMR (CCl$_4$, δ, ppm): 7.26 (m, 4H, aromatics), 5,26 (s, 1H, H-2), 2.81 (s, 1H, OH), 1.65 (s, 3H, CH$_3$).

1-Isopropyl-1-hydroxy-2-chloro-benzocyclobutene **(17)**. A solution of chloro-benzocyclobutenone **13** (5.0 g, 0.033 moles) in diethyl ether (30 ml) was added dropwise to a stirred solution of Grignard reagent, prepared from Mg (2.05 g, 0.082 moles) and isopropyl bromide (11.7 g, 0.095 moles) in anhydrous diethyl ether (50 ml). After addition of the ketone, the mixture was refluxed 30 min. and after cooling was treated with 20 ml water and 50 ml saturated ammonium chloride solution. The organic layer was washed with water and dried. Evaporation of the solvent yielded 5.4 g (83.8 %) crude **17** as yellow oil. The product was purified by column chromatography on silicagel with petroleum ether : diethyl ether 10 : 1 . — IR (CCl_4, cm^{-1}) : ν_{OH} 3575. — ^{1}H-NMR (CCl_4, δ, ppm) : 7.35—7.55 (m, 4H, aromatics), 5.36 (s, 1H, H-2), 2.75 (s, 1H, OH), 1.98 (m, 1H, tertiary-H from the isopropyl group, $J = 6.5$ Hz), 1.05 (dd, 6H, methyl protons from the isopropyl group).

1-Phenyl-1-hydroxy-2-chloro-benzocyclobutene **(18)**. A solution of chloro-benzocyclobutenone **13** (5.0 g, 0.033 moles) in anhydrous diethyl ether (20 ml) was added dropwise to a stirred solution of Grignard reagent, prepared from Mg (2.0 g, 0.082 moles) and bromobenzene (13.0 g, 0.089 moles) in anhydrous diethyl ether (50 ml). The reaction mixture was refluxed for 30 min. and after cooling was treated with 20 ml water and 50 ml saturated ammonium chloride solution. The organic layer was washed with water, dried and after the solvent removal, 9.4 g oily product were obtained. This crude product was chromatographied on alumina column separating two fractions. The first, eluated with petroleum ether, yielded, after solvent removal, 3.5 g diphenyl ; the second, eluated with petroleum ether : diethyl ether 10 : 1 afforded 3.3 g (43.0 %) **18**, colorless crystals, m.p. 68—69°. — IR (CCl_4, cm^{-1}) : ν_{OH}3565. — ^{1}H-NMR CCl_4, δ, ppm) : 7.2 (bs, 9H, aromatics), 5.31 (s, 1H, H-2), 3.41 (bs, 1H, OH).

1-Methyl-1-bromo-2-chloro-benzocyclobutene **(10)**. A solution of phosphorous tribromide (12.2 g, 0.045 moles) in anhydrous methylene chloride was added dropwise into a solution of alcohol **16** (4.9 g, 0.029 moles) in methylene chloride (50 ml). The reaction mixture was left for 24 hrs at room temperature and then refluxed for one hour. After cooling, the mixture was poured into ice-water. The product was extracted with methylene chloride and the organic layer was washed once with water then with 5 % sodium hydrogen carbonate and again with water. After drying and solvent removal, 5.6 g (83.2 %) **10**, dark yellow oil, were obtained. — ^{1}H-NMR (CCl_4, δ, ppm) : 7.15 — 7.50 (m, 4H, aromatics), 5.75 (s, 1H, H-2), 2.11 (s, 3H, from the methyl group).

1-Isopropyl-1-bromo-2-chloro-benzocyclobutene **(11)**. A solution of phosphorous tribromide (8.55 g, 0.031 moles) in anhydrous methylene chloride (50 ml) was added to a solution of alcohol **17** (2.85 g, 0.014 moles) in methylene chloride (50 ml). The mixture was worked up after 24 hrs by pouring into ice-water and extraction with methylene chloride. The organic layer was washed with water, 5 % sodium hydrogen carbonate solution and again with water. After drying and solvent removal, 2.55 g crude product containing bromochloro derivative **11** and alkene **20** were obtained. The crude product was treated with gaseous hydrobromic acid in 10 ml of methylene chloride and left for 24 hrs at room temperature. After adding 50 ml of methylene chloride the mixture was washed with water, 5 % sodium hydrogen carbonate solution. After drying and solvent removal, 2.75g (73.1 %) **11**, dark yellow oil, were obtained. — ^{1}H-NMR (CCl_4, δ, ppm) : 7.70 — 7.30 (m, 4H, aromatics), 5.76 (s, 1H, H-2), 2.17 (m, 1H, tertiary-H from the isopropyl group), 1.27 (d, 6H, CH_3 protons from the isopropyl group).

1-Phenyl-1-bromo-2-chloro-benzocyclobutene **(19)**. A solution of phosphorous tribromide (8.55 g, 0.031 moles) in methylene chloride (30 ml) was added to a solution of alcohol **18** (3.3 g, 0.014 moles) in 30 ml methylene chloride. After 24 hours the mixture was worked up in the same way as for the methyl derivative, obtaining 3.45 g (81.8 %) **19**, dark yellow oil. — ^{1}H-NMR (CCl_4, δ, ppm) : 7.20—7.60 (m, 9H, aromatics), 5.9 (s, 1H, H-2).

1,4-Dimethyl-dibenzo[b, g]bicyclo[4.2.0]octa-2,4,7-triene **(4)**. A mixture of bromochloroderivative **10** (3.5 g, 0.015 moles), 100 ml anhydrous diethyl ether and 66.0 g 0.5 % lithium amalgam was vigorously stirred for 24 hrs. The product was filtered and the organic layer was washed with water, dried and after solvent removal, 1.9 g crude product were obtained. The crude product was purified by column chromatography on alumina with petroleum ether, yielding 1.4 g (80.1 %), colorless crystals, m.p. 98—100°. — $C_{18}H_{16}$ (232.3) Calcd. : C, 92.06 ; H, 6.94. Found : C, 93.32 ; H, 7.21. — ^{1}H-NMR ($CHCl_3$, δ, ppm) : 6.95 — 7.55 (m, 8H aromatics), 5.93 (dd, 1H, H-5, $J_{5.6} = 5.0$ Hz, $J_{5.CH_3-4} = 1.5$ Hz), 2.00 (t, 3H, CH_3-4), 1.78 (s, 3H, CH_3-1).

1,4-Diisopropyl-dibenzo[b, g]bicyclo[4.2.0]octa-2,4,7-triene **(5)**. A solution of bromochloroderivative **11** (4 g, 0.019 moles) in 200 ml anhydrous dimethyl ether was stirred with 70 g 0.5% lithium amalgam for 24 hrs. After working up in the same way as for the methyl derivative, the reaction mixture was chromatographied with petroleum ether on a silicagel column yielding 1.8 g (80.0%) **5**, white crystals, m.p. 85–86°. – ^{1}H-NMR (CCl_4, δ, ppm) : 6.90–7.60 (m, 8H, aromatics), 5.98 (d, 1H, H-5, $J_{5,6} = 6.5$ Hz), 3.38 (d, 1H, H-6), 2.93 (m, 1H, tertiary-H from isopropyl group-4, $J = 7.0$ Hz), 2.52 (m, 1H, tertiary-H from isopropyl group-1, $J = 7.0$ Hz), 1.16 (d, 6H, CH_3 from isopropyl group-4), 0.87 (d, 6H, CH_3 protons from isopropyl group-1).

1,2-Diphenyl-dibenzo[e,g]cycloocta-1,3,5,7-tetraene **(7)**. A solution of phenyl derivative **19** (3.45 g, 0.012 moles) in 100 anhydrous diethyl ether was treated with 40 g 0.5% lithium amalgam and shaked for 24 hrs. By working up as above, 0.85 g (39.7%) **7**, white crystals, m.p. 194–195° (literature [8] 195°), were obtained.– ^{1}H-NMR ($CDCl_3$, δ, ppm) : 7.00–7.30 (m).

REFERENCES

[1] Part LV : A. Ghenciulescu, M. D. Gheorghiu, L. Enescu, I. G. Dinulescu and M. Avram, *Rev. Roumaine Chim.*, **29**, 49 (1984).

[2] a M. Avram, D. Constantinescu, I. G. Dinulescu and C. D. Nenitzescu, *Tetrahedron Letters*, **1969**, 5215 ; b. E. Mueller, H. Fetter and M. Sauerbier, *Synthesis*, **1970**, 82 ; c. M. Avram, D. Constantinescu, I. G. Dinulescu, O. Constantinescu-Simon, G. D. Mateescu and C. D. Nenitzescu, *Rev. Roumaine Chim.*, **15**, 1097 (1970) ; d. O. Constantinescu-Simon, I. G. Dinulescu, D. Constantinescu, P. Filip, F. Chiraleu and M. Avram, *Chem. Ber.*, **109**, 1287 (1976) ; e. O. Constantinescu-Simon, I. G. Dinulescu, F. Chiraleu, D. Constantinescu and M. Avram, *Chem. Ber.*, **109**, 1294 (1976) ; f. O. Constantinescu-Simon, I. G. Dinulescu, F. Chiraleu and M. Avram, *Chem. Ber.*, **109**, 1301 (1976) ; g. O. Constantinescu-Simon, F. Chiraleu and M. Avram, *Chem. Ber.*, **110**, 1335 (1977) ; h.O. Constantinescu-Simon, I. G. Dinulescu, F. Chiraleu and M. Avram, *Chem. Ber.*, **113**, 623 (1980).

[3] G. P. Newsoroff and S. Sternhall, *Australian J. Chem.*, **25**, 1669 (1972).

[4] C. D. Nenitzescu, M. Avram and D. Dinu, *Chem. Ber.*, **90**, 2541 (1957).

[5] M. P. Cava, D. Mangold and K. Muth, *J. Org. Chem.*, **29**, 2947 (1964).

[6] H. Wasserman and J. Solodar, *J. Amer. Chem. Soc.*, **87**, 4002 (1965) ; R. Osiewicz, Ph. D. Thesis, Case Western Reserve University, 1972.

[7] P. Filip to be published.

[8] M. Stiles, U. Burchardt and A. Haag, *J. Org. Chem.*, **17**, 4715 (1962).

[9] A. T. Blomquist and C. G. Bottomley, *Trans. N. Y. Acad. Sci.*, **24**, 823 (1962), cf. C A. **56**, 9981i (1962) ; A. T. Blomquist and C. G. Bottomley, *J. Amer. Chem. Soc.*, **87**, 86 (1965).

[10] M. Avram, D. Dinu and C. D. Nenitzescu, *Chem. and Ind.*, **1959**, 257 ; M. Avram, I. G. Dinulescu, D. Dinu, G. D. Mateescu and C. D. Nenitzescu, *Tetrahedron*, **19**, 309 (1963).

Revue Roumaine de Chimie, **29**, 7, 557–560 (1984)

INVESTIGATION IN THE CYCLOBUTANE SERIES. LVII[1]

ON THE BEHAVIOUR OF 1-ALKYL-BENZOCYCLOBUTADIENE DIMERS TOWARD THE SYSTEM t–BuOK–DMSO AND AIR

P. FILIP [a], NICOLETA ŞTEFAN [a], F. CHIRALEU [a], I. G. DINULESCU [a]
and MARGARET AVRAM [b,*]

[a] Center of Organic Chemistry, Spl. Independenţei 202B, 76300 Bucharest 15, Romania
[b] Laboratory of Organic Chemistry, Polytechnic Institute-TCH, Spl. Independenţei 313, 72206 Bucharest 16, Romania

Received July, 1983

The 1-alkyl-benzocyclobutadiene dimers in the presence of the system t-BuOK–DMSO and air afforded 6-hydroxy-derivatives and/or ketones with rearranged skeleton and/or oxidative degradation products. The course of the reactions is correlated with the size of the alkyl groups. Mechanistic aspects are discussed.

It was shown in a previous paper [2] that the dimer of t-butyl-benzocyclobutadiene (**1**) with dibenzobicyclo [4.2.0] octadiene skeleton, in the presence of the system potassium t-butoxide–dimethyl sulfoxide and air, undergoes oxidation accompanied by an anionic rearrangment leading to the ketone **2** with dibenzobicyclo [3.3.0] octadiene skeleton.

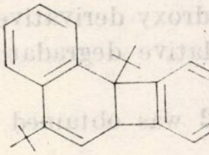

1

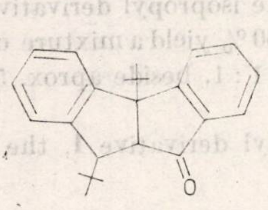

2

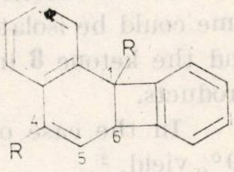

3, R = H
4, R = CH_3
5, R = $CH(CH_3)_2$

In order to have informations about the generality of this oxidative rearrangement and on the role of the alkyl group bonded at C-1, the behaviour of the unsubstituted benzocyclobutadiene dimer **3** as well as of the dimers of 1-methyl- and 1-isopropyl-benzocyclobutadiene (**4** and **5**, respectively) was investigated.

---

* Deceased in 1983

The reactions were carried out as earlier described [2] by stirring at room temperature the mixture of the hydrocarbon with t-BuOK and DMSO in the presence of air. The general results were listed in table 1

Table 1

Products distribution in the reaction of dimers 3, 4, 5 and 1[2] with system t-BuOK–DMSO–air

Dimer	Reaction time hrs	Unrearranged alcohol %	Rearranged ketone %	Oxidative degradation products %
3, R= H	0.5	—	—	100
4, R= CH_3	5	**6** 100	—	—
5, R= $CH(CH_3)_2$	2	**7** 25	**8** 25	50
1, R= $C(CH_3)_3$	12	—	**2** 60	40

The benzocyclobutadiene dimer 3, by treatment with t-BuOK–DMSO, after stirring for 0.5 hrs, gave a complex mixture of degradation products in quantitative yield.

In the reaction of methyl derivative 4, after 5 hars of reaction time, the hydroxy derivative 6 was obtained in almost quantitative yield.

In the reaction of the isopropyl derivative 5, after 2 hrs of reaction time could be isolated in 50% yield a mixture of the hydroxy derivative 7 and the ketone 8 in ratio 1 : 1, beside aprox. 50% oxidative degradation products.

In the case of t-butyl derivative 1, the ketone 2 was obtained in 60% yield. [2]

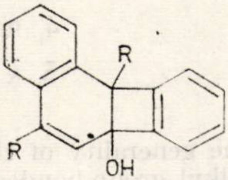

6, R = CH_3

7, R = $CH(CH_3)_2$

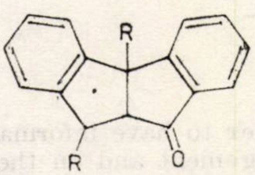

8, R = $CH(CH_3)_2$

2, R = $C(CH_3)_3$

For the anionic oxidative rearrangement of dibenzobicyclo [4.2.0]-octadiene system into dibenzobicyclo [3.3.0] octadiene system, the key intermediates **9**, **10** and **11** are postulated.

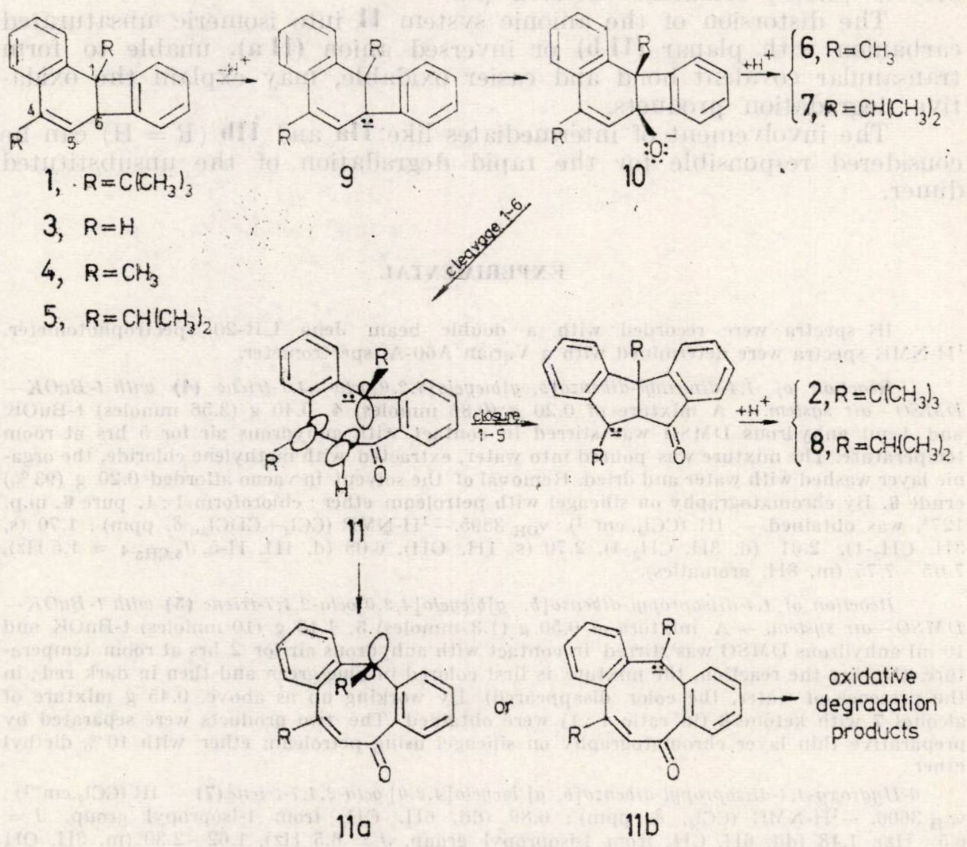
R
1
4
5
6
R
1, R=C(CH$_3$)$_3$
3, R=H
4, R=CH$_3$
5, R=CH(CH$_3$)$_2$
-H$^+$
R
R
9
R
:O:
R
10
+H$^+$
6, R=CH$_3$
7, R=CH(CH$_3$)$_2$
cleavage 1–6
R
O
H
R
11
closure 1–5
R
R
O
+H$^+$
2, R=C(CH$_3$)$_3$
8, R=CH(CH$_3$)$_2$
R
R
O
11a
or
R
R
O
11b
oxidative degradation products

The dimsyl base formed from t-BuOK and DMSO abstracts the allylic-benzylic proton (H-6) from the dimer molecule leading to the anionic intermediate **9**. The reaction of the later with oxygen leading the alkoxide anion **10** occurs rapidly. In the intermediate **10** the oxygen atom and the alkyl group are eclipsed.

When R is a bulky group such as t-butyl, the sterical repulsion favorizes the cleavage of 1–6 bond of the cyclobutene ring, leading to the intermediate anion with eight-membered ring **11**, which initially conserves the geometry of **10**. A small distorsion due to the formation of the carbonyl group creates a favorable geometry for the formation of 1–5 bond, yielding the rearranged ketone **2**.

When R is a less bulky group, as methyl for instance, the dibenzobicyclo [4.2.0] octadiene system is conserved and by protonation of **10** the hydroxy derivative **6** results.

The anion **10** bearing the middle sized isopropyl group can react according to the both above described possibilities. Thus, by protonation, the hydroxy derivative **7** is formed ; the cleavage of 1—6 bond can occur also leading to **11** ($R = CH(CH_3)_2$) which like the intermediate with t-butyl group, forms the 1—5 bond affording the ketone with dibenzobicyclo [3.3.0] octadiene skeleton **(8)**.

The distorsion of the anionic system **11** into isomeric unsaturated carbanion with planar **(11 b)** or inversed anion **(11 a)**, unable to form transanular covalent bond and easier oxidable, may explain the oxidative degradation products.

The involvement of intermediates like **11a** and **11b** ($R = H$) can be considered responsible for the rapid degradation of the unsubstituted dimer.

EXPERIMENTAL

IR spectra were recorded with a double beam Jena UR-20 spectrophotometer. ^{1}H-NMR spectra were determined with a Varian A60-A spectrometer.

Reaction of 1,4-dimethyl-dibenzo[b, g]bicyclo[4.2.0]octa-2,4,7-triene **(4)** *with t-BuOK—DMSO—air system.* — A mixture of 0.20 g (0.86 mmoles) **4**, 0.40 g (3.56 mmoles) t-BuOK and 4 ml anhydrous DMSO was stirred in contact with anhydrous air for 5 hrs at room temperature. The mixture was poured into water, extracted with methylene chloride, the organic layer washed with water and dried. Removal of the solvent in vacuo afforded 0.20 g (93 %) crude **6**. By chromatography on silicagel with petroleum ether : chloroform 1 : 1, pure **6**, m.p. 127°, was obtained. — IR (CCl_4, cm^{-1}) : ν_{OH} 3595. —^{1}H-NMR (CCl_4+CDCl_3, δ, ppm) : 1.70 (s, 3H, CH_3-1), 2.01 (d, 3H, CH_3-4), 2.70 (s, 1H, OH), 6.05 (d, 1H, H-5, $J_{5.CH_3\text{-}4} = 1.5$ Hz), 7.05—7.75 (m, 8H, aromatics).

Reaction of 1,4-diisopropyl-dibenzo[b, g]bicyclo[4.2.0]octa-2,4,7-triene **(5)** *with t-BuOK—DMSO—air system.* — A mixture of 0.50 g (1.3 mmoles) **5**, 1.10 g (10 mmoles) t-BuOK and 10 ml anhydrous DMSO was stirred in contact with anhydrous air for 2 hrs at room temperature. (During the reaction, the mixture is first colored in blue-green and then in dark red ; in the presence of water, the color disappeared). By working up as above, 0.45 g mixture of alcohol **7** with ketone **8** (in ratio 1 : 1) were obtained. The two products were separated by preparative thin layer chromatography on silicagel using petroleum ether with 10% diethyl ether.

6-Hydroxy-1,4-diisopropyl-dibenzo[b, g] bicyclo[4.2.0] octa-2,4,7-triene **(7)** — IR (CCl_4,cm^{-1}) ; ν_{OH} 3600. —^{1}H-NMR (CCl_4, δ, ppm) : 0.89 (dd, 6H, CH_3 from 1-isopropyl group, $J =$ 6.5 Hz), 1.18 (dd, 6H, CH_3 from 4-isopropyl group, $J = 6.5$ Hz), 1.62—2.30 (m, 3H, OH and two α tertiary protons from isopropyl groups), 6.00 (s, 1H, H-5), 7.16—7.70 (m, 8H, aromatics).

1,4-Diisopropyl-dibenzo[b,g]bicyclo[3.3.0]octadien-6-one **(8)**. — IR (CCl_4, cm^{-1}) : ν_{CO}1715— ^{1}H-NMR (CCl_4, δ, ppm ; $J_{4.5}$ and $J_{4.\alpha}$ were determined from spectra recorded in the presence of $Eu(DPM)_3$) : 0.60—1.40 (4d, CH_3 protons from isopropyl groups, $J = 7.0$ Hz), 2.00—3.00 (m, 2H, two α tertiary protons from isopropyl groups), 3.10 (m, 2H, H-4 and H-5, $J_{4.5} = 6.0$ Hz, $J_{4.\alpha} = 5.0$ Hz), 7.20—7.80 (m, 8H, aromatics).

REFERENCES

[1] Part LVI : P. Filip, N. Stefan, F. Chiraleu, I. G. Dinulescu and M. Avram, *Rev. Roumaine Chim.*, **29**, 549 (1984).

[2] O. Constantinescu-Simon, I. G. Dinulescu, D. Constantinescu, P. Filip, F. Chiraleu and M. Avram, *Chem. Ber.*, **109**, 1287 (1976).

Revue Roumaine de Chimie, **29**, 7, 561–566 (1984)

DRAG REDUCTION OF SOME ULTRA-HIGH MOLECULAR WEIGHT POLYACRYLAMIDES

MINODORA LECA and AURELIU LECA

Polytechnic Institute of Bucharest, Chemistry Department, Power Engineering Department, Splaiul Independenței No. 313, Romania

Received September 2, 1983

The drag reducing efficiency of some high and ultra-high molecular weight polyacrylamides has been determined. It has been found that these polyacrylamides verify the Virk's relation, but the reciprocal of the intrinsic concentration is not a linear function of intrinsic viscosity for the intrinsic viscosity range 8.4 to 33.8 dl/g.

The phenomenon of frictional drag reduction of liquids under turbulent flow conditions by dissolving trace amounts of high molecular weight polymers – Toms phenomenon – as well as its practical application has been extensively studied.[1–3] To be able to select the most efficient polymers, much effort has been made to develop a correlation between the polymer molecular structure and their drag reducing ability. It is now known that the most efficient are soluble, linear high molecular weight polymers.

The most important molecular parameter being the molecular weight, much work along this line has been performed.[4–6]

For dilute solutions in capillary tubes, Virk[7] found that the concentration dependence of drag reduction obeyed an equation which, in the modified form suggested by Little,[4] can be written:

$$\frac{DR}{DR_m} = \frac{c}{[c] + c} \tag{1}$$

where c is concentration, in wppm (weight parts per million), DR—per cent drag reduction, DR_m — the maximum drag reduction as $c \to \infty$ (a theoretical upper limit that can be obtained with a given sample at high concentrations) and $[c]$ – the Virk's intrinsic concentration. The validity of this equation has been tested for many drag reducing polymers both in capillaries and in laboratory-size pipes. $DR_m/[c]$ is a measure of polymer efficiency since it corresponds to the drag reduction per unit concentration at infinite dilution.[8] For polyethyleneoxide[4] and unhydrolysed polyacrylamide[9] $1/[c]$ is a linear function of polymer average molecular weight $\bar{M}$:

$$[c](\bar{M} - M_0) = A \tag{2}$$

suggesting a cutoff point in molecular weight M_0 below which no drag reduction takes place for the given flow conditions. More accessible is the correlation between $[c]$ and intrinsic viscosity $[\eta]$[10]:

$$[c]([\eta]-[\eta']) = D \tag{3}$$

where $[\eta']$ is the minimum intrinsic viscosity necessary to observe drag reduction in a given polymer series and flow conditions.

The purpose of this paper is to determine the drag reducing efficiency of some ultra-high molecular weight unhydrolysed polyacrylamides, to check the Virk's equation for them and to verify if relation (3) holds for a very large range of intrinsic viscosities (8.4 to 33.8 dl/g).

EXPERIMENTAL

Polyacrylamides (PAA) obtained by four different polymerization methods were tested : polymerization of a 10% aycrlamide solution with persulphate-bisulphite redox initiation system (sample 1), inverse suspension polymerization using the same initiation system (samples 2 and 3), photochemical polymerization of a 50% acrylamide solution with hydrogen peroxide as photosensitizer (samples 4, 5, 6 and 7) and radiochemical polymerization of a 50% acrylamide solution with γ ^{60}Co rays (samples 8 and 9).

Intrinsic viscosity was determined graphically in an aqueous 1N natrium nitrate solution at 30°C using a Ubbelohde viscometer ($k = 0.00488$). The viscosity average molecular weights $\overline{M}_v$ were calculated by means of the relation[11]:

$$[\eta] = 1.34 \times 10^{-3} \times \overline{M}_w^{0.57} \tag{4}$$

holding for $7 \times 10^5 < \overline{M}_w < 1.2 \times 10^7$, where $\overline{M}_w$ is the weight average molecular weight.

The characteristics of the nine samples are listed in table 1. $\overline{M}_v$ has not been computed for the samples 4 to 9, relation (4) being not valid for such high intrinsic viscosities.

Table 1

The characteristics of the polyacrylamide samples

Sample	$[\eta]$,dl/g	$\overline{M}_v \times 10^{-6}$	TR_m	$[c]$	$1/[c]$
1	8.4	4.589	28.0	8.63	0.116
2	8.8	4.979	31.5	7.65	0.131
3	9.6	5.800	35.5	6.15	0.162
4	17.0	—	40.6	1.74	0.575
5	20.4	—	39.1	0.91	1.098
6	20.4	—	37.6	0.43	2.295
7	20.4	—	37.5	0.93	1.073
8	20.5	—	—	—	—
9	33.8	—	—	—	—

The drag reduction properties of the polyacrylamide solutions were obtained in a simple laboratory vertical device composed of an 8 l cylindrical metallic tank having an overflow to measure the liquid level and a discharge connection to which a 0.65 cm diameter and 1.87 m long plastic pipe has been fixed. For one experiment a volume of 6.5 l of liquid was necessary. Gravity flow gave a Reynolds number of 12400. All the results were obtained for one pass through the pipe.

RESULTS AND DISCUSSION

The measurements made using the above installation do not allow to determine the drag reduction. As a measure of the efficiency the ratio of the flowing time t for a volume V of solution to the flowing time t_0 for the same water volume has been taken. The per cent reduction of the flowing time TR, which means the per cent increasing of the flow rate, has been also computed.

The dependence of TR on polymer concentration for the first seven samples is given in figure 1. As can be seen, as intrinsic viscosity — and hence molecular weight — increases TR becomes higher. The samples 5, 6 and 7, which have the same $[\eta]$, have the same efficiency in the limit of the experimental errors. This means that they also have almost the same molecular weight distributions. For very high intrinsic viscosities (samples 4—7) TR aquires maximum values for very small concentrations (6 to 10 wppm) compared to polyacrylamides 1—3 usually used as water drag reducers (40 to 50 wppm). The samples 8 and 9 were in such a small quantity so that TR at a concentration of 1 wppm were only determined. These values were 23.8 for sample 8, comparable to those of the samples 5—7 having the same $[\eta]$, and 26.9 for sample 9 which has a much higher $[\eta]$ (see Table 1).

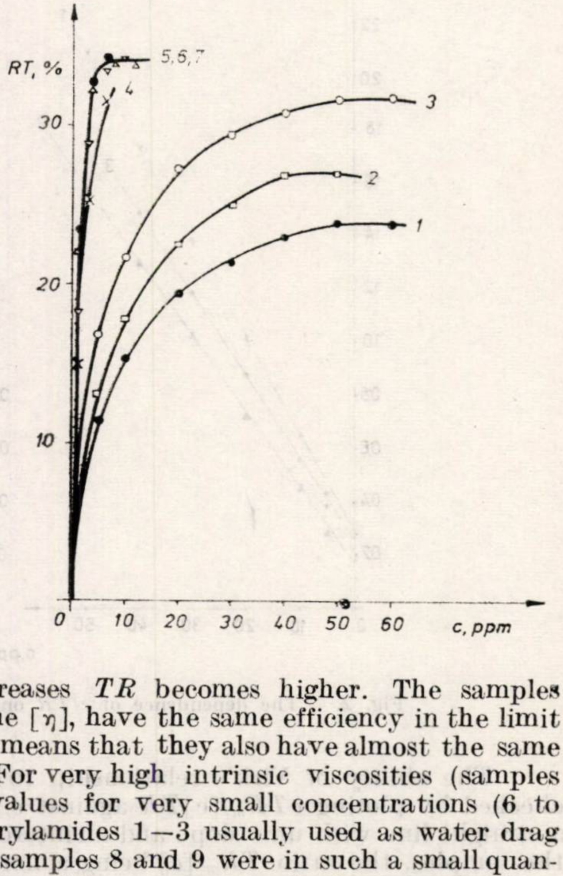

Fig. 1. — The dependence of TR on polymer concentration.

The Virk's equation (1) is verified both by the common high molecular weight PAA and by the ultra-high molecular weight ones (Fig. 2). The equation of the straight lines was calculated by the linear regression method. The correlation coefficients for the samples 1—3, for which we have 5 or 6 data points, have values ranging between 0.99936 and 0.99993. From the slopes and intercepts the corresponding TR_m and $[c]$ were computed (Table 1, columns 4 and 5). As figure 2 shows, the samples 5, 6 and 7 give the same straight line which has a correlation coefficient of 0.99847. From that we obtained $TR_m = 37.5$ and $[c] = 0.81$, very close to that obtained from the individual lines.

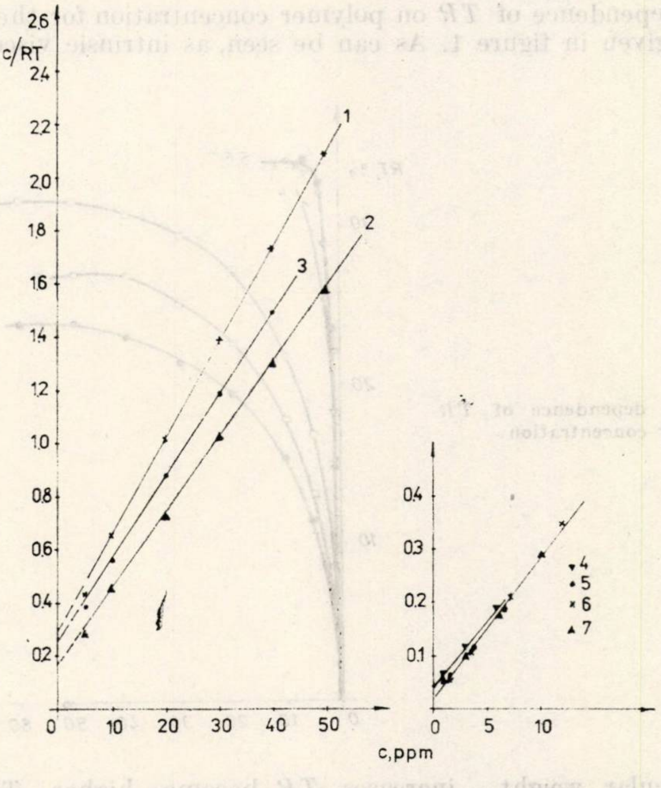

Fig. 2. — The dependence of c/TR on polymer concentration.

The ability of Virk's relationship to describe the data can also be checked by ploting $cTR_m/[c]TR$ against $c/[c]$, since equation (1) predicts a straight line with unit slope and an intercept of 1 in such a graph for all the samples, the ratio $TR_m/[c]$ being a normalization factor. As shown in figure 3, the data points fall very close to the predicted straight line.

Linear relations between $1/[c]$ and $\bar{M}_v$ and $1/[c]$ and $[\eta]$ have been found for PAA 1–3 in an earlier paper,[9] giving a cutoff molecular weight of 2.445×10^6 and 2.768×10^6 respectively. The difference has been explained by the fact that the highest molecular weights macromolecules in a sample play an even more important role in determining drag reducing ability than they do in determining intrinsic viscosity.[12] Introducing the ultra-high molecular weight PAA in the graph $1/[c] = f([\eta])$, figure 4, linear relation is not preserved. This may have two explanations : either the ultra-high molecular weight PAA have different molecular weight distributions having a high concentration of molecules with the lighest molecular weights,[12] or the coil density is smaller for very high molecular weights, hence the exponent *a* in the Mark-Houwink equation is bigger.

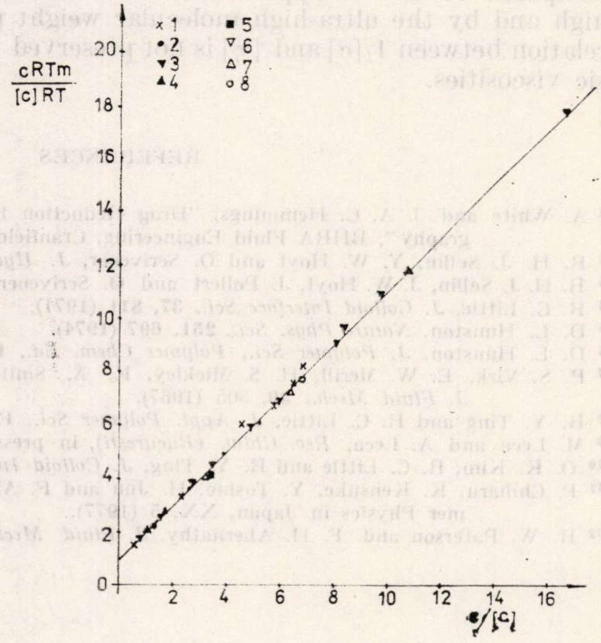

Fig. 3. — Data for the studied polyacrylamides compared to the prediction of Virk's equation.

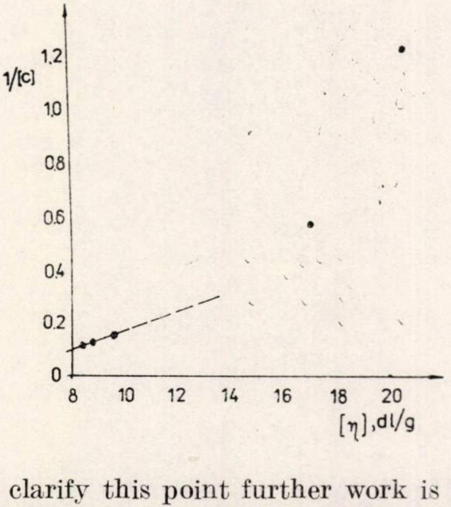

Fig. 4. — The dependence of $1/[c]$ on $[\eta]$ for the studied polyacrylamides.

To clarify this point further work is needed to correlate molecular weight distributions to drag reducing efficiency. Also, the drag reducing efficiency must be correlated with $[\eta]$ in water, not in aqueous 1 N natrium nitrate solution.

CONCLUSIONS

The ultra-high molecular weight polyacrylamides have a higher drag reducing efficiency than the high molecular weight ones and their maximum drag reduction is obtained at a much smaller concentration : 6 to 10 wppm compared to 40—50 wppm. The Virk's relation is verified both by the high and by the ultra-high molecular weight polyacrylamides. The linear relation between $1/[c]$ and $[\eta]$ is not preserved for the entire range of intrinsic viscosities.

REFERENCES

[1] A. White and J. A. C. Hemmings, "Drag Reduction by Additives. Review and Bibliography", BHRA Fluid Engineering, Cranfield, Bedford, England, 1976.

[2] R. H. J. Sellin, Y. W. Hoyt and O. Scrivener, *J. Hydraulic Res.*, **20**, 29 (1982).

[3] R. H. J. Sellin, J. W. Hoyt, J. Pollert and O. Scrivener, *J. Hydraulic Res.*, **20**, 235 (1982).

[4] R. C. Little, *J. Colloid Interface Sci.*, **37**, 811 (1971).

[5] D. L. Hunston, *Nature Phys. Sci.*, **251**, 697 (1974).

[6] D. L. Hunston, *J. Polymer Sci., Polymer Chem. Ed.*, **14**, 713 (1976).

[7] P. S. Virk, E. W. Merill, H. S. Mickley, K. A. Smith and E. L. Mollo-Christensen, *J. Fluid Mech.*, **30**, 305 (1967).

[8] R. Y. Ting and R. C. Little, *J. Appl. Polymer Sci.*, **17**, 3345 (1973).

[9] M. Leca and A. Leca, *Rev. Chim. (București)*, in press.

[10] O. K. Kim, R. C. Little and R. Y. Ting, *J. Colloid Interface Sci.*, **47**, 530 (1974).

[11] P. Chiharu, K. Kensuke, Y. Toshio, H. Jun and F. Akihisa, Reports on Progress in Polymer Physics in Japan, XX, 5 (1977).

[12] R. W. Paterson and F. H. Abernathy, *J. Fluid Mech.*, **43**, 689 (1970).

Revue Roumaine de Chimie, 29, 7, 567–574 (1984)

ION EXCHANGE MEMBRANES BASED ON GRAFTED CELLULOSE ESTERS. I

ACTIVATION BY PEROXIDATION IN VIEW OF GRAFTING THE CELLULOSE ESTERS

CRISTOFOR I. SIMIONESCU and SILVIA BRĂNIȘTEANU
Department of Polymer Chemistry, Polytechnical Institute of Jassy, 23 August 11, Romania

Received November 10, 1983

To obtain ion exchange membranes based on cellulose derivatives, the ionogen monomer was grafted on the support previously activated by hydroperoxidation. The thermal decomposition of hydroperoxide groups generated macroradicals able to initiate grafting. The hydroperoxidation reaction was studied by following the influence of ozonization duration, ozone concentration and nature of solvent used as medium for reaction development. The rate of thermal decomposition of hydroperoxide groups was found to depend on the duration of thermal treatment, temperature and catalytic action of ferrous ion. The obtained results allowed the choice of optimal ozonizing and grafting conditions for the synthesis of ion exchange membranes with avoidance of destruction of cellulose support to preserve the mechanical resistance of membranes.

INTRODUCTION

The obtainment of cellulose ion exchange membranes is conditioned by the possibilities of modifying the cellulose and cellulose derivatives as well as by their availability. Data reported in literature recommend cellulose grafting with ionogen monomers as one of the expecting methods for obtaining cellulose ion exchange membranes.[1-3]

The creation of active radical centers along the macromolecular chain can be accomplished by various chemical methods. Among these methods the introduction by oxidation with ozone of hydroperoxide groups allowing subsequently the grafting of monomer molecules deserves mention.[4-11]

The thermal decomposition of hydroperoxide groups in the presence of monomers to be grafted on cellulose chain favours the homopolymerization reaction, which results in additional difficulties connected with homopolymer removal.

The thermal decomposition of hydroperoxide group in the presence of monomers to be grafted on cellulose chain favours the homopolymerization reaction, which results in additional difficulties connected with homopolymer removal.

The addition of ferrous ion in the reaction medium catalyses the decomposition of hydroperoxide groups and eliminates the homopolymerization reaction.[12,13] The hydroperoxidation with ozone followed by thermal and catalytic decomposition of hydroperoxide groups takes place according to the following mechanism :

a) Hydroperoxidation :

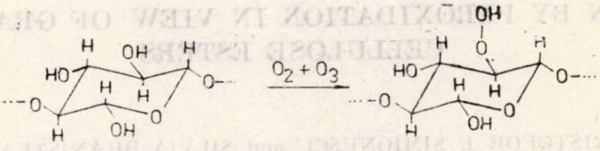

b) Thermal decomposition of hydroperoxide :

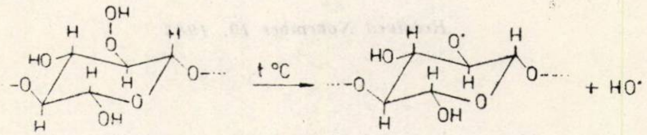

Homopolymerization :

$$HO^{\bullet} + nM \rightarrow HO-(M)_{n-1}-M^{\bullet}$$

c) Catalytic decomposition of hydroperoxide :

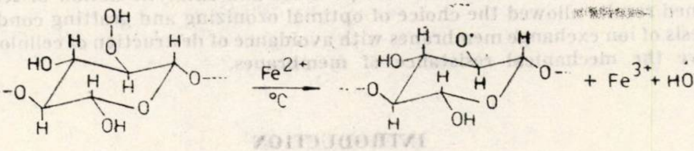

EXPERIMENTAL

The physico-chemical, mechanical and economical criteria for characterizing the ion-exchange membranes are numerous. Among these criteria the elasticity and permeability towards either ions or molecules of determined volume are extremely interesting.

To obtain such characteristics a series of cellulose esters have been synthesized. The acyl group, an aliphatic substituent has a plastifying effect which emphasizes with increasing volume of substituent. The membrane becomes more supple, elastic and permeable.[14] As cellulose esters we have used the commercial product Cellite 900 (Bayer), a secondary cellulose acetate and three esters synthesized by us : cellulose caprylate, laurate and palmitate, the acyl substituent containing 2, 8, 12 and 16 carbon atoms, respectively, in the aliphatic structure. In table 1 the composition of esters is given, the acyl radical to cellulose ratio having a significant influence on the hydroperoxidation degree.

The introduction of hydroperoxide groups into the cellulose support was accomplished by ozonization. In this view the samples were introduced in a glass cell in which an oxygen stream, containing ozone generated by a laboratory ozonizer, was introduced. The ozone occurs as a result of electrical discharges between two electrodes connected to an electric source of alternative current (tension 10.000 v), where the oxygen flows. The ozone concentration depends on the oxygen flow-rate and is determined iodometrically.

For the ion exchange membranes to possess low electrical resistance the ionogen group should be distributed uniformly over the membrane cross section and surface. For this reason the ozonization was carried out in homogeneous phase, by bubbling the ozonized oxygen stream through a 5% solution of cellulose ester in a volatile solvent. Thus, the cellulose chains are equally exposed to hydroperoxidation. The subsequent conversion of solution into a film of determined thickness and grafting with ionogen monomer in aqueous solution, uniformly over the film section will result in films with a good electrical conductivity.

Table 1

Composition of cellulose esters

Cellulose ester	Substitution degree, γ	Cellulose content, %	Acyl radical content, %	Acyl radical to cellulose ratio
Acetate (C_2)	2.20	49.0	51.0	1.04/1
Caprylate (C_8)	1.77	34.3	65.7	1.91/1
Laurate (C_{12})	1.44	31.6	68.4	2.16/1
Palmitate (C_{16})	0.80	42.0	58.0	1.38/1

The influence of solvent nature on the hydroperoxidation process as well as on the polymer destruction, the secondary reaction accompanying the peroxidation, was also investigated.

In the first part of the present paper the kinetics of ozonization of cellulose esters as a function of duration, ozone content of oxygen stream and solvent nature is reported.

The ozonization was carried out at the ambient temperature. The hydroperoxidation degree of samples was determined iodometrically.

In the second part of the paper the kinetics of thermal decomposition of hydroperoxide groups, in aqueous medium, in the absence and in the presence of Fe^{2+} catalyst, respectively, is investigated.

The obtained results allowed the settlement of optimal ozonizing and grafting conditions for cellulose esters with the purpose of obtaining ion exchange membranes with convenient properties.

RESULTS AND DISCUSSION

A. Study on ozonization kinetics

A.1. Influence of ozonization duration, ozone concentration in oxygen, substitution degree of cellulose esters and of the solvent nature on the ozonization degree of cellulose esters.

The peroxidation degree was followed during a time interval of 15–90 min, at ozone concentration in the oxygen stream of 2% (v/v) for 5 l/h flow rate and 1.2% (for 10 l/h). In figures 1 and 2 the variation of hydroperoxidation degree is depicted. As can be seen it is favourably influenced by higher values of the above mentioned parameters.

The cellulose content of esters largely determines the oxidation degree. The cellulose acetate and palmitate (curves 1 and 2) clearly distinguish from caprylate and laurate esters with a lower cellulose content. This fact confirms the resistance of parafinic residues towards the attack of oxygen and ozone. The caprylic and lauric esters having prevalently in composition aliphatic acyl residues will have less hydroperoxide groups. The cellulose laurate (31% cellulose) for instance, contains 44% peroxide groups, compared to cellulose acetate (49% cellulose), hydroperoxidated under the same conditions (the ozonizing duration 30 min, for a flow rate of 5 l O_2/h) (see Fig. 1).

The hydroperoxidation process is also influenced by the nature of solvent the cellulose is dissolved in. The study carried out on cellulose acetate, using acetone as solvent and the mixture methylene chloride-methanol (8: 2) led to the results depicted in Fig. 3.

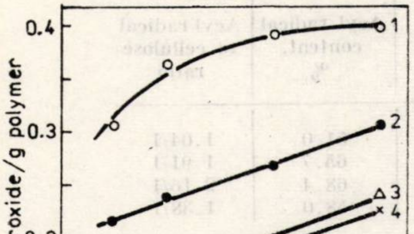

Fig. 1

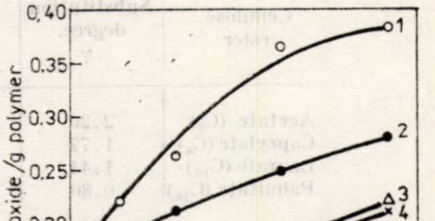

Fig. 2

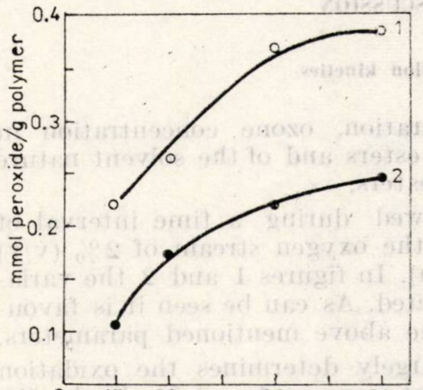

Fig. 1. — Influence of ozonizing duration on the hydroperoxidation degree, for 2 % ozone concentration (O_2 flow rate 5 l/h). 1. cellulose acetate (49 % cellulose) ; 2. cellulose palmitate (42 %, cellulose) ; 3. cellulose caprylate (34.3 % cellulose) ; 4. cellulose laurate (31.6 % cellulose).

Fig. 2. — Influence of ozonization duration on the hydroperoxidation degree for ozone concentration of 1.2 % (O_2 flow rate 10 l/h). 1 — cellulose acetate ; 2 — cellulose palmitate ; 3 — cellulose caprylate ; 4 — cellulose laurate.

Fig. 3. — Influence of solvent nature on the hydroperoxidation degree of cellulose acetate. Curve 1 — Acetone ; Curve ⟵ 2 — $CH_2Cl_2 - CH_3OH$ mixture (8 :2)

Since the acetone is an appropiate solvent for cellulose acetate, for the same concentration a more complete dissolution is attained and, consequently, the polymer is more exposed to the ozone attack.

A.2. Influence of ozonization on polymer destruction

The ion exchange ability of ion exchange membranes depends on the amount of ionogen polymer grafted on cellulose support, the grafting degree being determined, among other factors, by the concentration of hydroperoxidic groups introduced by ozonizing.

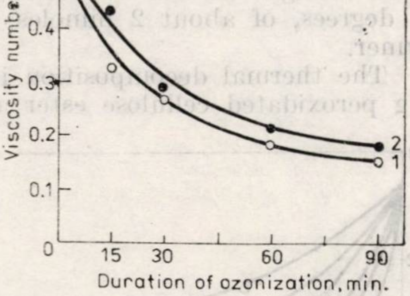

Fig. 4. — Influence of ozone concentration and of ozonizing duration on the destruction depth of cellulose acetate. Curve 1 — 2 % ozone ; Curve 2 — 1.2 % ozone.

The ozonization is an oxidation process of hydroxyl group accompanied by secondary reactions such as destruction and cross linking, which may sensibly affect the indices of mechanical resistance. The solvent nature influences the rate of the three reactions above mentioned.[15]

In the case of cellulose acetate the destruction degree was followed viscosimetrically, for a 5% solution in acetone. The obtained results given in Table 2 and Fig. 4, illustrate the destruction depth with prolonged ozonization duration and increased ozone concentration.

Table 2

Influence of ozonizing conditions on the depth of cellulose ester destruction

Flow rate $O_2 + O_3$, l/h	Ozonization duration, min	Reduced viscosity	Destruction depth, %	Obs.
—	—	0.548	—	Standard sample
5	15	0.325	37	
5	30	0.270	50	
5	60	0.182	67	
5	90	0.154	72	
10	15	0.438	14	
10	30	0.281	48	
10	60	0.217	61	
10	90	0.188	66	

The ozonization of the same product in solution of 8 : 2 methylene chloride-methanol mixture led to advanced cross-linking after 30 min treatment.

B. Kinetics of thermal decomposition of hydroperoxide groups

The rate of thermal decomposition of obtained hydroperoxides was investigated, since it influences the initiation rate of grafted copolymerization. The grafting of films of hydroperoxidated cellulose derivatives with ionogen monomers is to be performed in aqueous phase. For this reason, the thermal decomposition rate of hydroperoxide groups was studied in the presence of water, the influence of temperature, thermal treatment duration, absence or presence of catalyst (Fe^{2+} ion) on the process being followed. The cellulose esters have close hydroperoxidation degrees, of about 2 mmoles of hydroperoxide group per gram of polymer.

The thermal decomposition is carried out in a system containing **0.3** g peroxidated cellulose ester and 50 ml water or aqueous solution of ferrous sulphate of 0.2% concentration, by refluxing, under nitrogen stream. The results obtained are given in Figs 5—8.

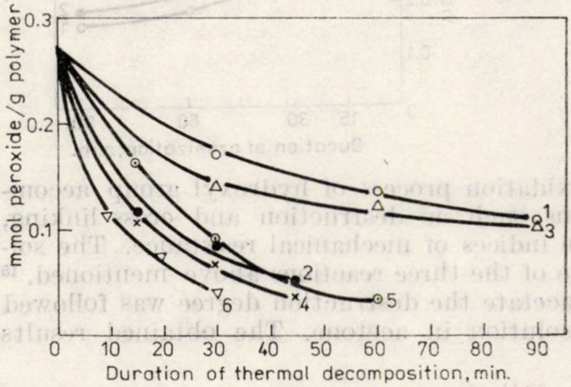

Fig. 5. — Decomposition rate of hydroperoxide groups for cellulose acetate. Curves 1,3,5 — heating in water at 70, 80 and 90°C. Curves 2,4,6 — heating in water in the presence of Fe^{2+} ion at 70, 80 and 90°C, respectively.

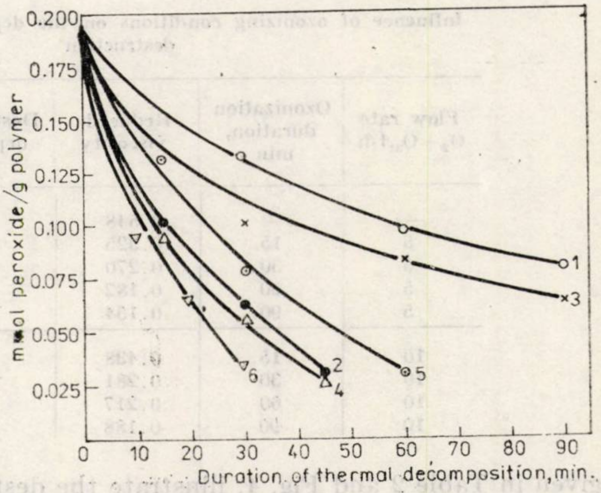

Fig. 6. — Decomposition rate of hydroperoxide groups for cellulose caprylate. Curves 1, 3, 5—heating in water at 70, 80 and 90°C. Curves 2,4, 6—heating in water and Fe^{2+} ion at 70, 80 and 90°C respectively.

The rate of thermal decomposition of hydroperoxides was studied at temperatures of 70, 80 and 90°C, respectively, the residual hydroperoxide groups being dosed iodometrically. The curves 1, 3, 5 represent the thermal decomposition rates of hydroperoxides in the presence of water at 70, 80 and 90°, respectively, while the curves 2, 4, 6 depict the decomposition rates in 0.2% aqueous solutions of ferrous sulphate at the same temperatures.

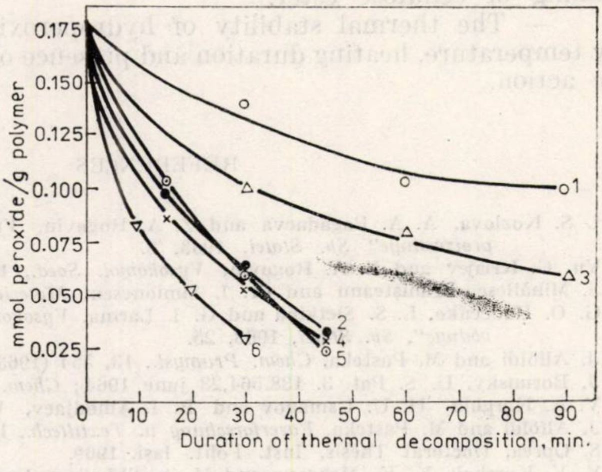

Fig. 7. — Decomposition rate of hydroperoxide groups for cellulose laurate. Curves 1, 3, 5— heating in water at 70, 80 and 90°C. Curves 2, 4, 6—heating in water and Fe^{2+} ion at 70, 80 and 90°C, respectively.

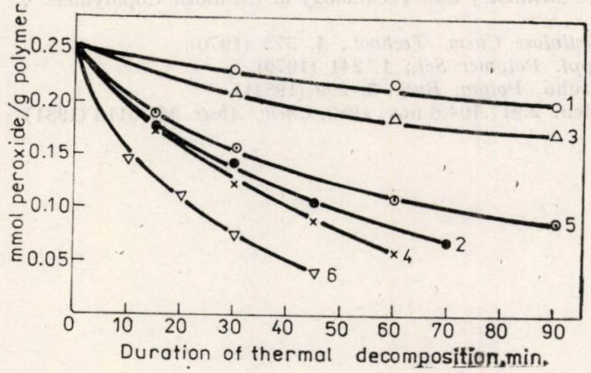

Fig. 8. — Decomposition rate of hydroperoxide groups for cellulose palmitate. Curves 1, 3, 5 — heating in water at 70, 80 and 90°C. Curves 2, 4, 6 — heating in water and Fe^{2+} ion at 70, 80 and 90°C, respectively.

The catalytic action of Fe^{2+} ion on the hydroperoxide decomposition is very clear; at the same temperature in the presence of Fe^{2+} ion the decomposition rate doubles. Consequently, the catalyst addition in the monomer solution when grafting the hydroperoxidated cellulose esters assures increased rates of grafting reaction at lower temperatures, or for shorter duration, and hinders the homopolymer formation.

CONCLUSIONS

— The activation of cellulose esters in view of grafting by introducing the reactive hydroperoxide groups was investigated.

— The hydroperoxidation degree was found to increase with prolonging ozonization duration, increasing ozone concentration and higher cellulose content of cellulose esters.

— The hydroperoxidation was carried out by bubbling the oxygen stream containing ozone into the polymer solution. The solvent nature was found to influence the peroxidation rate, destruction depth and crosslinking of cellulose ester.

— The thermal stability of hydroperoxide groups is conditioned by temperature, heating duration and presence of ferrous ion with catalytic action.

REFERENCES

[1] I. S. Kozlova, A. A. Pogadaeva and Z. A. Rogovin, *Vysokomol. Soed. "Tselluloza i ce proizvodnye" Sb. Statei*, 1963, 3.

[2] Yu. G. Kriajev and Z. A. Rogovin, *Vysokomol. Soed.*, **12**, 1847 (1961).

[3] S. Mihăilescu-Brănişteanu and Cr. I. Simionescu, *Materiale Plastice*, **10**, 295 (1973).

[4] G. O. Radcenko, L. S. Sletkina and G. I. Larina, *Vysokomol. Soed. "Tselluloza i ce proizvodnye", Sb. Statei*, 1963, 25.

[5] J. Alföldi and M. Pasteka, *Chem. Prumysl.*, **13**, 554 (1963).

[6] J. Borunsky, U. S. Pat. 3. 138.564,23 june 1964; *Chem. Abstr.*, **61**, 8478 (1964).

[7] V. A. Karghin, H. U. Usmanov and B. I. Aihodjaev, *Vysokomol. Soed.*, **1**, 149 (1959).

[8] J. Alföldi and M. Pasteka, *Faserforschung u. Textiltech.*, **14**, 389 (1963).

[9] S. Oprea, Doctorat Thesis, Inst. Polit. Iaşi, 1969.

[10] V. V. Korshak, K. K. Mozgova and M. A. Shkolina, *Vysokomol. Soed.*, **1**, 1573 (1959).

[11] A. Hebeish and J. T. Guthrie, "The Chemistry and Technology of Cellulosic Copolymers", New York, 1981, 146.

[12] P. Cremonesi and L. D'Angiuro, *Cellulose Chem. Technol.*, **4**, 373 (1970).

[13] H. Kubota and Y. Ogiwara, *J. Appl. Polymer Sci.*, **1**, 241 (1979).

[14] U. Tadashi, S. Yasuhiro and S. Mizuho, *Polym. Bull.*, **5**, 299 (1981).

[15] H. Arno and P. Eberhard, Ger. Offen. 2.917.104,6 nov. 1980, *Chem. Abstr.* **94**, 5113 (1981).

Revue Roumaine de Chimie, **29**, 7, 575–582 (1984)

MICHAEL REACTION OF β(2-FLUORENYL)-ACRYLIC ACID AND ITS AMIDES

M.A. El-KASABY and M.A.I. SALEM
Ain Shams University, Faculty of Science, Chem. Department, Cairo, A.R. Egypt

Received July 22, 1980
Revised June 30, 1983

β-(2-Fluorenyl)-acrylic acid and its amides react under Michael conditions with diethylmalonate, diethylsuccinate, ethyl phenylacetate, ethyl-acetoacetate, benzylmethyl ketone, acetylacetone, ethyl cyanoacetate and malonitrile to give cyclic or normal Michael adducts depending on the nature of the active methylene compound.

The only reported example dealing with the Michael reaction of methyl β-benzoylacrylate is its reaction with nitromethane[1]

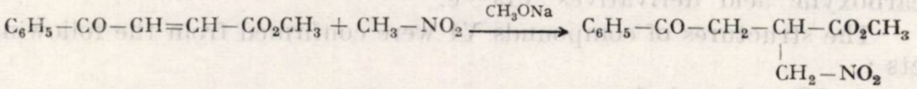

$$C_6H_5-CO-CH=CH-CO_2CH_3 + CH_3-NO_2 \xrightarrow{CH_3ONa} C_6H_5-CO-CH_2-\underset{\displaystyle CH_2-NO_2}{\underset{|}{CH}}-CO_2CH_3$$

This prompted us to extend the Michael addition of other active methylene compounds to β-aroylacrylic acids. It is found that in these acids the polarization of the olefinic double bond by ketone group outweights that caused by the carboxyl group; the keto group giving a more stable carbonium ion than the carboxyl group i.e. the α-carbon atom accepts the nucleophiles (donor in Michael condensation) more readily than the β-carbon atom.

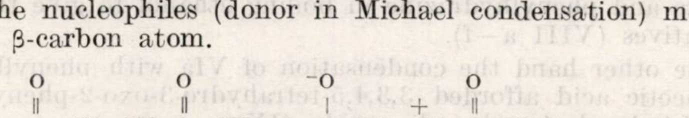

$$-\overset{O}{\overset{\|}{C}}-CH=CH-\overset{O}{\overset{\|}{C}}-OH \longrightarrow -\overset{^-O}{\overset{|}{C}}=CH-\overset{+}{C}H-\overset{O}{\overset{\|}{C}}-OH \text{ (more stable)}$$

$$-\overset{O}{\overset{\|}{C}}-CH=CH-\overset{O}{\overset{\|}{C}}-OH \longrightarrow -\overset{O}{\overset{\|}{C}}-\overset{+}{C}H-CH=\overset{^-O}{\overset{|}{C}}-OH \text{ (less stable)}$$

In continuation to our recent studies,[2,3] this work investigates the Michael reactions of β-(2-fluorenoyl)-acrylic acid (I). They have been studied in order to ascertain the mode of addition of activated methylene, since (I) could behave as an α, β-unsaturated acid or as an α, β-unsaturated ketone. The results presented in this communication concerning the addition of diethylmalonate,[4] diethylsuccinate[5] and ethyl phenylacetate to β-(2-fluorenoyl)acrylic acid (I) showed that in sodium methoxide solution the normal Michael adducts (II) were formed.

The structure II has been established from the following assignments :

(i) IR and ^{1}H-NMR spectra.[6,8]

The ^{1}H-NMR spectra of IIb show bands at values δ 4.50 (*2H* of $CH-COOH$ and $-CH-COOCH_3$); 3.55 (*9H* of three CH_3 groups) and 3.35 (*6H*) (*4H* of $CH-CH_2-CO-$ and $-CH-CH_2-COOCH_3$ and *2H* of $=C-CH_2-C=$)

(ii) Correct analytical data

(iii) *Chemically:*

a) — Alkaline hydrolysis of III a—c in boiling 5% alcoholic potassium hydroxide led to the dibasic acids (IIIa—c).

b) — Cyclization of IIa on boiling with acetic anhydride gives the dihydro-α-pyrone derivative (IV).

c) — Claisen condensation of IIa with aromatic aldehydes, namely benzaldehyde, anisaldehyde or *p*-chlorobenzaldehyde gave tricarboxylate derivatives (V a—c) respectively.

The ^{1}H—NMR spectrum of Va showed bands at δ values 7.45, 7.35 (*5H* of C_6H_5 group), 4.05—3.81 (*4H* of-$COO-CH_2-$group), 3.70 (*6H* of two CH_3 of ethyl ester), 3.55 (*1H* of $-CO-CH-CO-$), 3.40 (*1H* of $-CH-COOH$ and 6.85 (*1H* of $-CH-C_6H_5$).

On the other hand the addition of ethyl acetoacetate, benzyl methyl ketone, ethyl methyl ketone, acetylacetone and ethyl cyanoacetate to I, under the same conditions led to the formation of the 3-cyclohexen-1-carboxylic acid derivatives VIa—e.

The structures of compounds VI were confirmed from the following facts :

(i) IR spectral data

(ii) Chemically.

a) — Decarboxylation of VIa with alcoholic potassium hydroxide yields the 3-cyclohexen-1-carboxylic acid derivative (VII).

b) — The cyclohexene derivatives VI were condensed with hydrazine hydrate and phenylhydrazine in boiling ethanol to give the hydrazone derivatives (VIII a—f).

On the other hand the condensation of VIa with phenylhydrazine in glacial acetic acid afforded 3,3,4,5-tetrahydro-3-oxo-2-phenyl-6-(fluoren-2-yl)-2H-indazole-4-carboxylic acids (IX).

c) — The reaction of VIa with hydroxylamine hydrochloride yields the oxime derivatives (X) with elimination of the carbethoxy group.

Further, we investigated the reaction of β-(fluoren-2-yl)-N-arylacrylamides (XIa-c) with diethylmalonate under the same Michael conditions as above giving ethyl-3,4-dihydro-6-(fluoren-2-yl)-2-(arylcarbamoyl)2*H*-pyran-3-carboxylate derivatives (XIIa—c).

Hydrolysis of XIIa with a mixture of boiling hydrochloric acid and acetic acid yields a product identified to be IV by m.p. and mixed m.p. determination and by comparison of their IR spectra. Alkaline hydrolysis of XIIa using 5% alcoholic potassium hydroxide yields 3,4-dihydro-6-(fluoren-2-yl)-3-(N-phenyl carbamoyl)-2*H*-pyran-3-carboxylic acid (XIII).

By analogy with the recently reported reaction of chalcone,[7] acid I was condensed with malononitrile in the presence of ammonium acetate to give two products: the yellow 2-amino-3-cyano-4-carboxy-6 (fluoren-2′-yl)-hexahydropyridine (XV). The reactants underwent Michael addition then cyclization; moreover the reaction is accompanied by dehydrogenation.

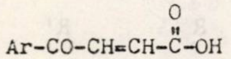

$$Ar-CO-CH=CH-\overset{O}{\overset{\|}{C}}-OH$$

(I)

Ar= $C_{13}H_9$-2

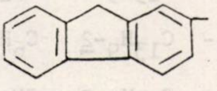

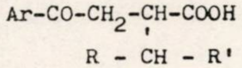

$$\begin{array}{l} Ar-CO-CH_2-\underset{|}{CH}-COOH \\ \qquad\quad R-CH-R' \end{array}$$

(II)

a)- Ar=$C_{13}H_9$-2 ;R=$CO_2C_2H_5$;R'=$CO_2C_2H_5$

b)- Ar=$C_{13}H_9$-2 ;R=CO_2CH_3;R'=$CH_2CO_2CH_3$

c)- Ar=$C_{13}H_9$-2 ;R=C_6H_5;R'=$CO_2C_2H_5$

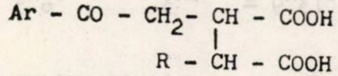

$$\begin{array}{l} Ar-CO-CH_2-\underset{|}{CH}-COOH \\ \qquad\qquad\quad R-CH-COOH \end{array}$$

(III)

a)- Ar= $C_{13}H_9$-2 ; R = H .

b)- Ar= $C_{13}H_9$-2 ; R = CH_3.

c)- Ar= $C_{13}H_9$-2 ; R = C_6H_5

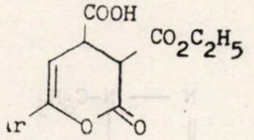

(IV)

Ar=$C_{13}H_9$-2

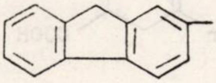

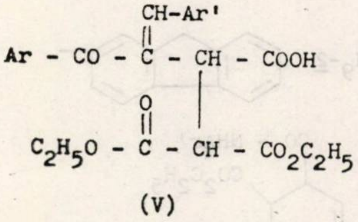

$$\begin{array}{l} \qquad\quad CH-Ar' \\ \qquad\quad \| \\ Ar-CO-C-CH-COOH \\ \qquad\qquad O \quad | \\ \qquad\qquad \| \quad | \\ C_2H_5O-C-CH-CO_2C_2H_5 \end{array}$$

(V)

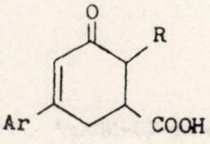

(VI)

a)- Ar = $C_{13}H_9$-2 ; Ar'= C_6H_5 .

b)- Ar = $C_{13}H_9$-2 ; Ar'=C_6H_4-CH_3-p

c)- Ar = $C_{13}H_9$-2;Ar'=C_6H_4-OCH_3-p

a)- Ar=$C_{13}H_9$-2 ; R=$CO_2C_2H_5$

b)- Ar=$C_{13}H_9$-2 ; R=C_6H_5

c)- Ar=$C_{13}H_9$-2 ; R= CH_3

d)- Ar=$C_{13}H_9$-2 ; R=CH_2-CO-CH_3

e)- Ar=$C_{13}H_9$-2 ; R= -C ≡ N

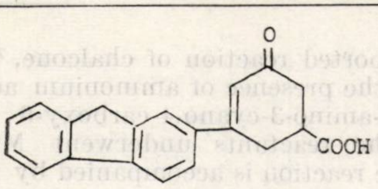
(VII)

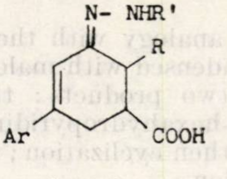
(VIII)

	Ar	R	R'
a)-	$C_{13}H_9$-$\underline{2}$	$CO_2C_2H_5$	H
b)-	$C_{13}H_9$-$\underline{2}$	C_6H_5	H
c)-	$C_{13}H_9$-$\underline{2}$	CH_3	H
d)-	$C_{13}H_9$-$\underline{2}$	$CO_2C_2H_5$	C_6H_5
e)-	$C_{13}H_9$-$\underline{2}$	C_6H_5	C_6H_5
f)-	$C_{13}H_9$-$\underline{2}$	CH_3	C_6H_5

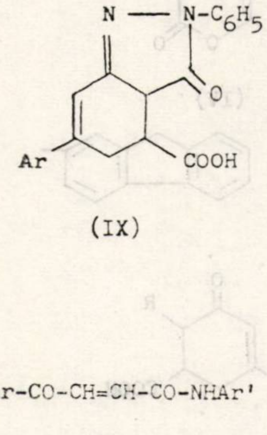
(IX)

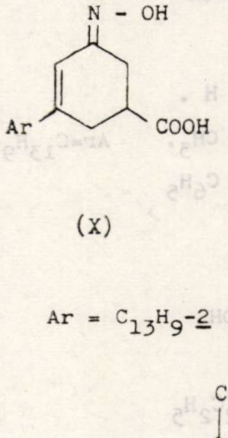
(X)

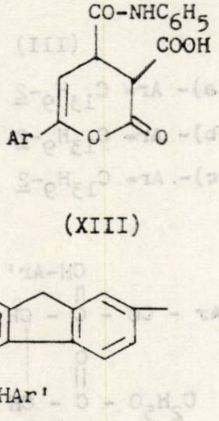
(XIII)

Ar = $C_{13}H_9$-$\underline{2}$ 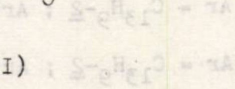

Ar-CO-CH=CH-CO-NHAr'

(XI)

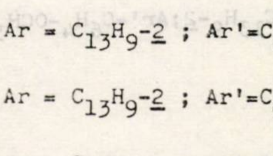
(XII)

a)- Ar = $C_{13}H_9$-$\underline{2}$; Ar'=C_6H_5

b)- Ar = $C_{13}H_9$-$\underline{2}$; Ar'=C_6H_4-CH_3-$\underline{p}$

c) Ar = $C_{13}H_9$-$\underline{2}$; Ar'=C_6H_4-OCH_3-$\underline{P}$

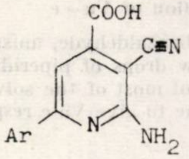

(XIV)

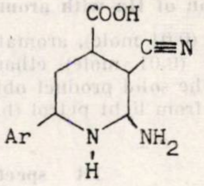

(XV)

Ar = $C_{13}H_9$-2

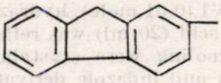

EXPERIMENTAL PROCEDURE

All m.p.'s are uncorrected. The IR spectra were obtained with a Perkin Elmer Infracord Model 577 using KBr pellet technique. The ^{1}H-NMR spectra were recorded with a Varian A60 spectrophotometer.

Base-catalyzed addition of active methylene compounds to β-(fluoren-2-yl) acrylic acids and their amides XIa–c. Formation of IIa–e; VIa-c and XIIa–c

A mixture of β-(fluoren-2-yl) acrylic acid (I) or its amides (XIa–c) (0.01 mole), the active methylene compound (0.01 mole), and sodium methoxide solution (0.015 mole) was heated at 180° for ten hours. The reaction mixture was poured into water then extracted with teher. The aqueous layer was acidified with ice-cold dilute hydrochloric acid. The oil which separated was triturated with light petrol (b.p. 80–100°). The solid obtained was crystallized from a suitable solvent to give the colourless Michael adducts IIa–e ; VIa–c and XIIa–c respectively.

IR Spectral data (cm^{-1})

Compound II : 3440 (OH of acid), 1720 (CO of acid), 1690–1680 (CO aroyl) and 1760–1750 (CO of ester).

Compound VI : 3480–3330 (OH of acid), 1730–1720 (CO of acid), 1680–1660 (CO, cyclohexene), 1610–1600 (C=C), 1690 (CO of acetyl) and 2225 (C=N) (for VIe only)

Compound XII : 3520 (NH of amide), 1640 (CO of amide), 1740 (CO of ester), 1710 (CO of pyrone) and 1610 (C=C).

Alkaline hydrolysis of IIa–c, VIa and XIIa. Formation of IIIa–c, VII and XIII

An alcoholic solution of IIa–c, VIa or XIIa (0.01 mole) was treated with aqueous potassium hydroxide solution (5%, 10 ml) and the reaction mixture was refluxed for ten hours. The cold mixture was acidified with dilute HCl. The solid obtained was crystallized from a suitable solvent to give IIIa–c, VII and XIII.

IR spectral data (cm^{-1})

Compound III : 3480–3460 (OH of acid), 1730–1720 (CO, acid), 1690–1680 (CO, aroyl).

Compound VII : 3450 (OH, acid) ; 1720 (CO, acid), 1670 (CO, cyclohexene) and 1600 (C=C).

Compound XIII : 5440 (OH or NH), 1660 (CO, amide), 1720 (CO, acid), 1700 (CO, pyrone) and 1600 (C=C).

Ring closure of IIa. Formation of IV

A solution of IIa (0.01 mole) in acetic anhydride (20 ml) was refluxed for eight hours. The solid obtained after concentration and crystallization from benzene gives IV as pale yellow crystals (yield 60%) m.p. 178°C. (Found C, 70.17 ; H, 4.70%. $C_{22}H_{18}O_{3}$ required : C, 69.84 ; H, 4.76%).

Condensation of IIa with aromatic aldehydes. Formation of Va—c

A mixture of IIa (0.01 mole), aromatic aldehydes, namely benzaldehyde, anisaldehyde or *p*-chlorobenzaldehyde (0.01 mole), ethanol (120 ml) and a few drops of piperidine were refluxed for six hours. The solid product obtained on evaporation of most of the solvent and cooling was crystallized from light petrol (b.p. 80—100°) or benzene to give Va-c respectively as colourless crystals.

IR spectra of V (cm^{-1})

3420—3380 (OH, acid), 1730—1720 (CO, acid), 1750—1740 (CO, ester), 1690—1680 (CO, aroyl) and 1610—1600 (C=C).

Condensation of VI with hydrazine hydrate and phenylhydrazine. Formation of VIIIa—h and IX

A mixture of VI (0.01 mole), hydrazine hydrate or phenylhydrazine (0.01 mole) and ethanol or glacial acetic acid (20 ml) was refluxed for six hours. The solid products formed after concentration and cooling were crystallized from a proper solventto give the hydrazone derivatives VIIIa—h and indazole derivative IX respectively as yellow crystals.

IR spectral data (cm^{-1})

Compound VIIIa—c : 3430—3390 (OH or NH), 1730—1724 (CO, acid), 1750—1735 (CO, ester), 1630—1618 (C=N) and 1610—1590 (C=C).

Compound VIIId—f :3480—3380 (OH, acid), 1730—1718 (CO, acid), 1750—1740 (CO, ester), 1630—1614 (C=N) and 1600—1590 (C=C).

Compound IX : 3450 (OH, acid), 1725 (CO, of acid), 1635 (C=N of indazole) and absence of NH.

Condensation of VI with hydroxylamine hydrochloride. Formation of X

A mixture of VIa (0.01 mole), hydroxylamine hydrochloride (0.01 mole) sodium acetate (2 g), ethanol (20 ml) and a few drops of water was refluxed for ten hours. The solid product formed after concentration and cooling was crystallized from toluene to give X as yellow rystals (yield 50%) m.p. 242°C.
(Found : C, 75.54 ; H, 5.30 ; N, 4.40. $C_{20}H_{17}NO_3$ required : C, 75.23 ; H, 5.33 ; N, 4.39%).

Acid hydrolysis of XII. Formation of IV

A solution of XIIa (0.01 mole) in a mixture of glacial acetic acid (15 ml) and conc. hydrochloric acid (15 ml) was refluxed for six hours. The reaction mixture was poured into ice. The solid which separated was filtered off and crystallized from benzene to give a product identified to be IV, m.p. 178°.

Reaction of malononitrile with I

A mixture of malononitrile (0.02 mole), β-(2-fluorenyl) acrylic acid (0.01 mole) and ammonium acetate (0.03 mole) was heated at 160—170°C for ten hours, then allowed to cool. The yellow oil obtained was washed with water, dried and then treated with ethanol. It was divided into two parts : *an ethanol soluble part* (*A*) and *an ethanol insoluble part* (*B*). The ethanol solution was concentrated. After standing overnight at room temperature, colourless crystals separated which, after crystallization from ethanol gave XV, m.p. 230° (yield 42%).
(Found : C, 72.28 ; H, 5.68 ; N, 12.55, $C_{20}H_{19}N_3O_2$ required : C, 72.07 ; H,5.70 ; N, 12.61%).
The ethanol insoluble part (B) was crystallized from xylene to give XIV as yellow crystals 250° (30%).
(Found : C, 73.59 ; H, 3.96 ; N, 12.80, $C_{20}H_{13}N_3O_2$ required : C, 73.39 ; H, 3.98 ; N, 12.84%).

IR spectrum of XIV (cm^{-1})

3470—3360 (NH or OH), 1730 (CO, acid 2228 (C≡N) and 1618 (C=N).

IR spectrum for XV (cm^{-1})

3450—3330 (NH or OH), 1730 (CO of acid, C≡N (2240) and 1610 (C=N).

Table 1

Physical Data of Compounds

Comp-ound.	M. Formula	m.p.°C	Solvent; Yield %	Analysis %		
				Found		Calcd.
IIa	$C_{24}H_{24}O_7$	188	E	C	68.12	67.92
			80	H	5.67	5.66
IIb	$C_{23}H_{22}O_7$	85	P	C	67.50	67.31
			86	H	5.35	5.36
IIc	$C_{27}H_{24}O_5$	234	T	C	75.93	75.70
			90	H	5.62	5.60
IIIa	$C_{19}H_{16}O_5$	210	T	C	70.19	70.37
			66	H	4.95	4.94
IIIb	$C_{20}H_{18}O_5$	133	B	C	71.20	71.00
			70	H	5.31	5.32
IIIc	$C_{25}H_{20}O_5$	182	B	C	75.18	75.00
			58	H	5.02	5.00
Va	$C_{31}H_{28}O_7$	156	P	C	72.50	72.65
			80	H	5.00	5.47
Vb	$C_{32}H_{30}O_8$	204	B	C	70.69	70.85
			70	H	5.55	5.54
Vc	$C_{31}H_{27}ClO_7$	241	B	C	88.28	88.07
			70	H	4.95	4.94
VIa	$C_{23}H_{20}O_5$	129	B	C	74.00	73.42
			80	H	5.33	5.32
VIb	$C_{26}H_{20}O_3$	182	B/E	C	82.40	82.10
			80	H	5.30	5.26
VIc	$C_{21}H_{18}O_3$	212	B/E	C	79.40	79.24
			84	H	5.67	5.66
VId	$C_{23}H_{20}O_4$	250	Bu	C	76.81	76.66
			82	H	5.53	5.55
VIe	$C_{21}H_{15}NO_3$	171	E	C	76.40	76.59
				H	4.56	4.55
			75	N	4.26	4.25
VII	$C_{20}H_{16}O_3$	250	T	C	80.17	78.95
			60	H	5.28	5.26
VIIIa	$C_{23}H_{22}H_2O_4$	149	T	C	70.92	70.77
				H	5.64	5.64
			75	N	7.20	7.10
VIIIb	$C_{26}H_{22}N_2O_2$	220	E	C	79.34	79.19
				H	5.56	5.58
				N	7.13	7.11

Table 1 (continued)

Compound	M. Formula	m.p.°C	Solvent; Yield %	Analysis %		
				Found		Calcd.
VIIIc	$C_{21}H_{20}N_2O_2$	250	AC	C	75.60	75.90
				H	6.00	6.03
			60	N	8.46	8.43
VIIId	$C_{26}H_{18}N_2O_2$	182	B	C	80.28	80.00
				H	4.65	4.62
			68	N	7.19	7.18
VIIIe	$C_{32}H_{26}N_2O_2$	250	B/E	C	81.88	81.70
				H	5.52	5.53
			66	N	5.98	5.95
VIIIf	$C_{27}H_{24}N_2O_2$	250	T	C	79.63	79.41
				H	5.89	5.88
			70	N	6.88	6.86
IX	$C_{27}H_{20}N_2O_3$	250	AC	C	77.70	77.14
				H	4.78	4.76
			75	N	6.63	6.66
XIIa	$C_{28}H_{23}NO_5$	193	E	C	74.32	74.17
				H	5.09	5.07
			80	N	3.11	3.09
XIIb	$C_{29}H_{25}NO_5$	149	B	C	74.70	74.52
				H	5.37	5.35
				N	2.97	2.09
XIIc	$C_{29}H_{25}NO_6$	132	E	C	72.26	72.05
				H	5.18	5.17
				N	2.88	2.89
XIII	$C_{26}H_{19}NO_5$	214	E	C	73.63	73.41
				H	4.45	H 4.47
				N	3.28	N 3.28

**E = Ethanol ; P = Light petrol (b.p 80—100) ; T = Toluene ; B = Benzene ; Bu = *n*-Butanol ; Ac = Acetic acid.

REFERENCES

[1] E. P. Kohler and H. J. Engelbrecht ; *J. Amer. Chem. Soc.*, **41**, 764 (1919).

[2] A. A. Sammour, M. I. B. Selim, E. A. Soliman, *U.A.R. J. Chem.*, **16**, 312 (1972).

[3] A. A. Sammour M.A.El Hashash, *J. prakt. Chem.*, **314**, 906 (1972).

[4] M. Harnik, *Israel. J. Chem.*, **3**, 1 (1965) ; *Chem. Abstr.*, **63**, 1748 (1965).

[5] A. A. Sammour, A. Rauf, M. El Kasaby and M. A. Salem, *Acta. Chim. Acad.*, **78**, 399 (**1973**).

[6] J. C. P. A. Schwarz, "Physical Methods in Organic Chemistry", Oliver and Boyd, Edinburgh, 1964.

[7] A. A. Sammour, Y. Akhnoukh and H. Jahine, *U.A.R.J. Chem.*, **13**, 421 (1970).

[8] L. J. Bellamy "The Infrared Spectra of Complex Molecules", Methuen, London, 1968.

Revue Roumaine de Chimie, 29, 7, 583–588 (1984)

SYNTHESIS OF MONO- AND DIACETYLENIC DERIVATIVES OF SILYLFERROCENE

ABDEL GHANI ALI EL-AGAMEY[a] and LEVAN PETROVITSH ASATIANI[b]
[a] Faculty of Education, Damiatta, Mansoura University, A.R. Egypt
[b] Faculty of Chemistry, Tbilissi University, Tbilissi, GSSR, USSR

Received July 20, 1983

Hydrosilation of ferrocene was carried out. Mono- and diacetylenic compounds of silylferrocene were prepared by the interaction of ferrocenylchlorosilane with mono- and dilithium acetylenic derivatives, respectively. Catalytic hydrogenation of the prepared compounds was studied. The constitution of products was investigated by means of IR and NMR spectroscopy.

Diverse utilities have been reported for ferrocene and ferrocene derivatives.[1,2] Ferrocenyl silane derivatives have recently become of increasing importance owing to their higher antiknock properties.[3] Keludza[4] reported that methylphenylferrocenylhydrosilane (I) increases the octane number. As a part of our program[5-7] directed for synthesis of ferrocene derivatives, we report here some chemical reactions of I. Compound I was prepared in a modified method, as a sole product, without the production of 1,1′-ferrocenedihydrosilane,[4] by using ferrocene and butyllithium in molar ratio (1 : 1) at room temperature, in dry hexane, and the chlorosilane was added to the reaction mixture at −40 to −45°C (Chart 1).

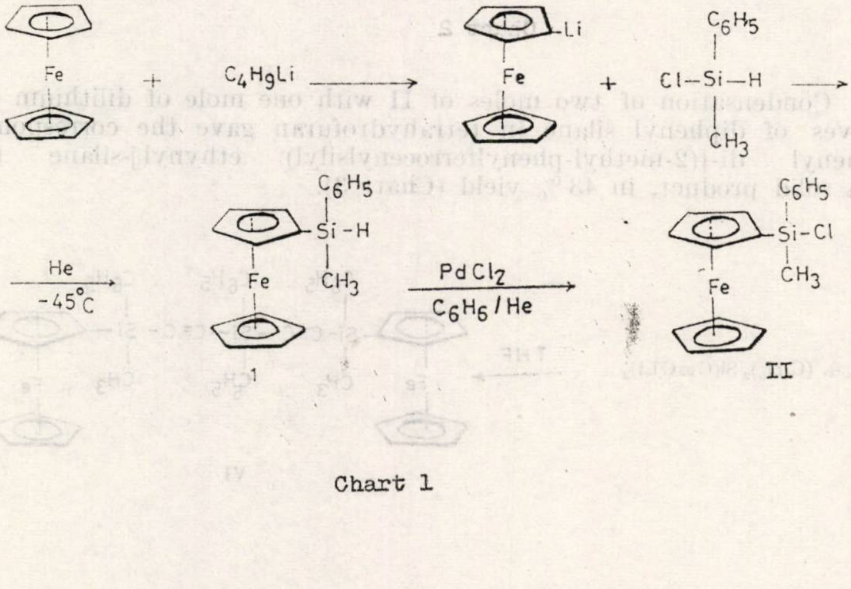

Chart 1

The IR spectrum[8-10] of I shows bands at 2140 cm^{-1} (Si—H); 3110 cm^{-1} (C—H ferrocene); 1430, 1260 and 740 cm (Si—AlK/Ar).

Methylphenylferrocenylchlorosilane (II) was prepared by the action of $PdCl_2$ on I according to Corriu [11] method. Chlorosilane II is sensitive to air oxidation, and then II purified by column chromatography under helium using benzene as an eluant (Chart 1).

Compound II reacted smoothly with lithium derivatives of phenyl-, triethylsilyl- and triphenylsilylacetylenes in dry tetrahydrofaran to give the corresponding disubstituted acetylenes III, IV and V respectively (Chart 2). These compounds could be obtained in pure form by TLC using pentane, pet. ether (40—60°C) and pet. ether (40—60°C) : benzene (3 : 1) as eluants for III, IV and V, respectively.

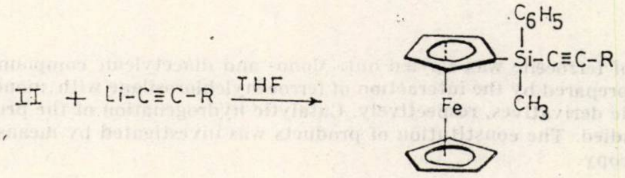

	R
III	C_6H_5-
IV	$(C_2H_5)_3Si-$
V	$(C_6H_5)_3Si-$

Chart 2

Condensation of two moles of II with one mole of dilithium derivatives of diphenyl silane in tetrahydrofuran gave the corresponding diphenyl di-[(2-methyl-phenylferrocenylsilyl) ethynyl]-silane (VI), as a solid product, in 43% yield (Chart 3).

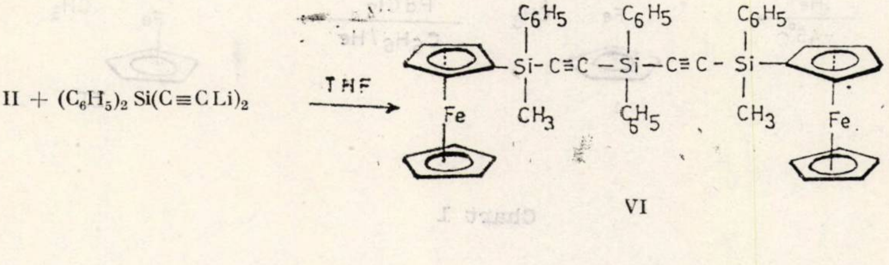

VI

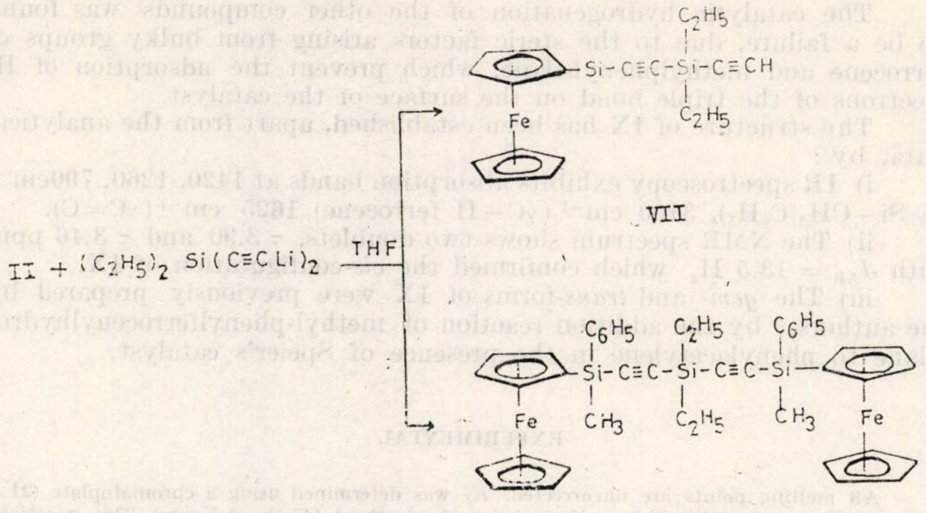
II + $(C_2H_5)_2$ Si(C≡CLi)$_2$
THF
C_2H_5
Si-C≡C-Si-C≡CH
Fe
C_2H_5
VII
C_6H_5
C_2H_5
C_6H_5
Si-C≡C-Si-C≡C-Si
CH_3
C_2H_5
CH_3
Fe
Fe
VIII

The infrared spectra of III–VI show absorption peaks at 1430, 1250, 740 cm^{-1} (Si–AlK/Ar) ; 2030–2060 cm^{-1} (C≡C) and 3100 cm^{-1} (C–H ferrocene).

Condensation of II with dilithium diacetylenic derivative of diethylsilane gives a mixture of the two dark red derivatives VII and VIII. Compound VIII could be received in pure form by fractional crystallization, whilst VII remains always contaminated with some VIII. The two products successfully isolated by TLC using octane (Chart 3).

The IR[8-10] of compound VIII showed absorption bands at 1445, 1260, 740 cm^{-1} (Si–alk/Ar) ; 2030–2060 cm^{-1} (C≡C) and 3100 cm^{-1} (C–H) ferrocene). In addition to the bonds mentioned above, compound VII has also bands 2040 and 3290 cm^{-1} corresponding to (–C≡C–) and (C–H), which suggests that the terminal group is C≡C–H and VII is a condensation product of one acetylonic group only.

In the present work we have examined the reactivity of the triple bonds of the prepared compounds ; partially catalytic hydrogenation of the triple bond to the corresponding olefinic derivatives using Lindlar catalyst (Pd–$CaCO_3$) was carried out.

The catalytic hydrogenation of compound III in the presence of (Pd–$CaCO_3$) successfully underwent the corresponding olefinic derivative with *cis*-configuration IX.

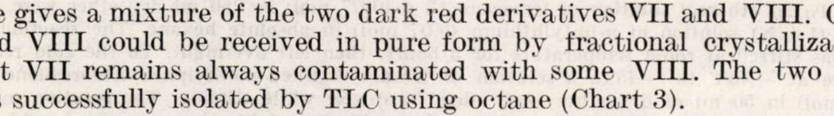
C_6H_5
Si-C≡C-C_6H_5
Fe
CH_3
+ H_2
Pd-$CaCO_3$
C_6H_5
Si-C=C-C_6H_5
H H
CH_3
Fe

IX

The catalytic hydrogenation of the other compounds was found to be a failure, due to the steric factors arising from bulky groups of ferrocene and methylphenylsilane, which prevent the adsorption of Π-electrons of the triple bond on the surface of the catalyst.

The structure of IX has been established, apart from the analytical data, by :

i) IR spectroscopy exhibits absorption bands at 1420, 1260, 790cm^{-1} (ν Si$-$CH$_3$/C$_6$H$_5$), 3100 cm^{-1} (νC$-$H ferrocene) 1625 cm^{-1} (νC$=$C).

ii) The NMR spectrum shows two doublets, τ 3.90 and τ 3.46 ppm with $J_{AB} = 13.5$ H$_z$ which confirmed the *cis*-configuration of IX.

iii) The *gem*- and *trans*-forms of IX were previously prepared by the authors,[5] by the addition reaction of methyl-phenylferrocenylhydrosilane to phenylacetylene in the presence of Speier's catalyst.

EXPERIMENTAL

All melting points are uncorrected. R_f was determined using a chromatoplate (21 × × 31 × 0.2) coated with a thin uniform layer of adsorbent (Al_2O_3 — 1.5 mm). The reactions were carried out under helium in dry THF. Purificaton and separation of the obtained products was done by TLC using Al_2O_3 of 1.2 mm thickness. Recorded yields correspond to the pure products. IR and NMR were measured on UR-20 and Perk-Elmer R-12, respectively. The acetylenes used were prepared according to known procedures[12-14].

Methylphenylferrocenylsilane (I) :

To an ethereal solution of ferrocene 13 g (0.07 mol) in 250 ml dry ether were added 50 ml (1.4 N) solution of n-butyllithium (0.07 mol) in absolute hexane. The reaction mixture was stirred at room temperature for 3 hours, then left overnight. To the cold reaction mixture at −40°C to −45°C, a solution of freshly distilled methylphenylchlorosilane 30 g (0.19 mol) in 50 ml of dry ether were added dropwise while stirring. The reaction mixture was stirred for another one hour at −45°C and set aside overnight, then poured on cold water and separated with ether, dried over anhydrous sodium sulphate. The ether was evaporated and the obtained residue was distilled as a sticky dark red oil with b.p. 177—178°C (1 mm Hg), yield 12.45 g (59%), $\eta_D^{20} = 1.6215$

$C_{17}H_{18}FeSi$ (306.3) Calcd. C 66.67 H 5.92 (Si—H) 0.34
Found C 66.63 H 5.67 (Si—H) 0.35

1-Phenyl-2-methylphenylferrocenylsilylethyne (III) :

To a solution of 1.5 g (0.014 mol) of phenyl lithium acetylide (prepared from 1.5 g (0.014 mol) of phenylacetylene and 0.11 g (0.016 mol) of lithium metal in 50 ml of tetrahydrofuran a solution of 4.8 g (0.014 mol) of II (prepared from 4.2 g (0.014 mol) of I and 3 g (0.017 mol) of $PdCl_2$ in 100 ml of dry benzene) was added with stirring. The reaction mixture was heated at 45—60°C for 3 hours, poured on cold water, extracted with ether and then dried over anhydrous sodium sulphate, then evaporated. The obtained residue was purified by thin layer chromatography using pentane as an eluant to give III as brownish oil with $R_f = 0.58$ (pentane), yield 4 g (74%).

$C_{25}H_{22}FeSi$ (406.4) Calcd. C 73.89 H 5.46
Found C 73.95 H 5.43

1-Triethylsilyl-2-methylphenylferrocenylsilylethyne (IV) :

To a solution of n-butyllithium (0.015 mol) (prepared from 0.2 g (0.03 mol) of lithium and 1.4 g (0.015 mol) of butylchloride) in 30 ml of absolute hexane, a solution of 2.1 g (0.015 mol) of triethylethynylsilane in 40 ml of absolute tetrahydrofuran was added. The reaction mixture was stirred, at room temperature for two hours and then a solution of 5.1 g (0.015 mol) of freshly prepared II in 100 ml of dry benzene, was added portionwise during a period of 30 min. The reaction mixture was stirred into ice-cold water, extracted with ether, dried using

Na_2SO_4 anhydrous. The oily product obtained after distilling off the ether was purified using thin layer chromatography (eluant pet. ether "40—60" to give yellowish brown oil of IV with $R_f = 0.48$ (pet. ether : benzene, 5 : 1), yield 4.46 g (77 %).

$C_{25}H_{32}FeSi_2$ (444.5) Calcd. C 67.55 H 7.26
Found C 68.11 H 7.49

Under similar experimental conditions, compound V was obtained.

1-Triphenylsilyl-2-methylphenylferrocenylsilylethyne (V) :

It was obtained as dark red oil after purification chromatographically using pet. ether : benzene, 3 : 1, $R_f = 0.36$ (pet. ether : benzene, 5 : 1) yield 78 %.

$C_{37}H_{32}FeSi_2$ (588.7) Calcd. C 75.49 H 5.48
Found C 75.44 H 5.76

Diphenyldi(2-methylphenylferrocenylsilylethynyl)silane (VI) :

To a solution of n-butyllithium (0.02 mol) (prepared from 0.31 g (0.04 mol) of lithium and 1.9 g (0.02 mol) of butylchloride) in 30 ml of absolute hexane, a solution of 2.3 g (0.01mol) of diphenyldiacetylsilane in 50 ml of dry tetrahydrofuran was added. The reaction mixture was stirred at room temperature for another 1 hour, and then a solution of 6.8 g (0.02 mol) freshly prepared II in 100 ml of absolute benzene was added portionwise during a period of 30 min. The reaction mixture was heated for two hours at 50—60°C, and then cooled, stirred into ice-cold water, extracted with ether, dried over anhydrous sodium sulphate. The oily product obtained after distilling off the ether was crystallized from pentane to give yellowish brown crystals with m.p. 208—209°C, yield 3.9 g (43 %).

$C_{50}H_{44}Fe_2Si_3$ (840.9) Calcd. C 71.42 H 5.27
Found C 71.35 H 5.53

Reaction of methylphenylferrocenylchlorosilane (II) with dilithium derivative of diethyldiacetylenylsilane :

To a solution of n-butyllithium (0.014 mol) (prepared from 0.2 g (0.028 mol) of lithium and 1.3 g (0.014 mol) of n-butylchloride in 30 ml of absolute hexane, a solution of 1 gm (0.007 mol) diethyldiacetylenylsilane in 50 ml of absolute THF was added. The reaction mixture was stirred at room temperature for another 20 min., and then of 4.8 g (0.014 mol) of freshly prepared (II) in 100 ml of absolute benzene were added portionwise during a period of 20 min. The reaction mixture was heated for 2 hours at 50—60°C, stirred into ice-cold water, extracted with ether, dried over anhydrous sodium sulphate. The oily product obtained after distilling off the ether was purified and then separated using the method of thin layer chromatography (eluant octane) into the two following products VII and VIII.

Diethylacetylenyl(2-methylphenylferrocenylsilylethynyl)-silane (VII) :

It was obtained as a sticky yellowish-brown oil, with $R_f = 0.57$ (octane), yield 3.1 g (50 %).

$C_{25}H_{28}FeSi_2$ (440.5) Cald. C 68.16 H 6.41
Found C 68.51 H 6.55

Diethyl-di(2-methylphenylferrocenylsilylethynyl)silane (VIII) :

It was obtained as yellowish crystals from octane with m.p. 213—215°C, yield 2.48 (40 %).

$C_{42}H_{44}Fe_2Si_3$(744.8) Calcd. C 67.73 H 5.95
Found C 67.55 H 5.76

Catalytic hydrogenation of 1-phenyl-2-methylphenylferrocenylsilylethyne (III). 1-Phenyl-2-methylphenylferrocenyl-silylethene (IX) :

A mixture of III (2.4 g) (0.006 mol) in absolute alcohol (50 ml) and 0.2 g Pd-$CaCO_3$ was shaken with hydrogen at room temperature and pressure (hydrogen absorbed 200 ml). The solution was filtered. The oily product obtained after evaporating the alcohol, was distilled to give 2.3 g (96 %) of 1-phenyl-2-methylphenylferrocenylsilylethene 9, b.p. 246—248°C (2 mm Hg).

$C_{25}H_{24}FeSi$ (408.4) Calcd. C 73.52 H 5.92
Found C 73.79 H. 5.90

REFERENCES

[1] A. N. Nesmeyanov, E. G. Perevalova and P. B. Galofna, *Izf. Akad. Hauk SSSR,* 740 (1956).

[2] A. N. Nesmeyanov, "Chemistry of Ferrocene", Hauk, Moscow (1969).

[3] C. Kh. Keludza, Ph. D. Thesis, Tbilisi University (1978).

[4] I. M. Gverdtsiteli, L. P. Asationi and C. Kh. Keludza, *Zh. Obshch. Khim.*, **46**, 861 (1976).

[5] L. P. Asationi, A. A. El-Agamey, and I. M. Gverdtsitili, *Bull. Akad. Nauk GSSR,* **90**, *1*, 172 (1978).

[6] *Ibid,* **90**, *3*, 589 (1978).

[7] L. P. Asationi, A. A. El-Agamey and M. A. Diab, *J. Polym. Sci.*, Under publication (1983).

[8] L. G. Bellamy, "The Infrared Spectra of Complex Molecules", Wiley, N.Y. (1970).

[9] Wilkinson, P. L. Pauson and F. A. Cotton, *J. Am. Chem. Soc.*, **74**, 6146 (1952).

[10] G. Wilkinson, *J. Am. Chem. Soc.*, **74**, 6146 (1952).

[11] R. Corriu, F. Larcher, G. Royo, *J. Organometal. Chem.*, **16**, 11 (1976).

[12] K. Schlögl, W. Strewrer, *Monatsch. Chem.*, **96**, 1520 (1965).

[13] M. Rosenblum, N. Braun, J. Papenmeier, *J. Organometal. Chem.*, **6**, 173 (1966).

[14] O. A. Nofikova, F. P. Koznetsofa and K. A. Korneva, *Zh. Obshch. Khim.*, **38**, 178 (1968).

Revue Roumaine de Chimie, **29**, 7, 589–592 (1984)

HYDROGEN ISOTOPE EFFECTS IN THE REACTION OF POLAROGRAPHIC OXYGEN REDUCTION

A. CĂLUŞARU

Institute of Chemical Research, Spl. Independenţei, No 202, 77208 Bucharest, Romania

Received December 7, 1983

The isotope effect of the half-wave potentials of the polarographic oxygen reduction was studied. It has been found that the isotope effect of the half-wave potential of the first reduction step increases from zero at pH(D) > 10 to 23 mV at pH(D) = 7.2, since the anion absorption becomes an important process at lower pH(D) values. The isotope effect of the second reduction step is 54 mV at all pH(D) values, owing to the high irreversibility of the second polarographic oxygen wave.

Although the isotopes are at the present time widely used in the study of polarographic processes, [1] since the works by Novak[2] and Heyrovsky,[3] concerning the reduction of O_2 and X_2O_2 ($X = H$ or D) in both H_2O and D_2O at $pX > 10$, no other work was devoted to this problem. However the kinetics of the two step oxygen reduction in normal water was thoroughly studied by several authors.[4–7] The general conclusion of these studies was that the second wave is always strongly irreversible, while the nature of the first wave depends on pH : for $pH > 10$ the wave is quasi-reversible and at lower pH values ($pH = 7$) the reduction is hindered by the process of anion adsorption.

Since, at $pX > 10$ the wave is quasi-reversible, it is possible to explain the coincidence of the half-wave potentials in the systems O_2/H_2O_2 and O_2/D_2O_2[2] :

$$ {}_0E_{1/2,O_2H_2O_2} - {}_0E_{1/2,O_2/D_2O_2} \simeq 0 \tag{1}$$

Therefore this diffusion-controlled wave is not accompained by a detectable isotope effect.

The second oxygen wave, corresponding to the systems H_2O_2/H_2O and D_2O_2/D_2O is irreversible ; this is why there is an isotope effect. For this case Novak found for the difference of the half-wave potentials :

$$E_{1/2,H_2O_2/H_2O} - E_{1/2,D_2O_2/D_2O} = 84 \text{ mV} \tag{2}$$

In the present work we studied the oxygen reduction at $pX = 7.2$ where both waves are accompained by isotope effects.

EXPERIMENTAL

The buffered Sörensen solution of phosphates in heavy water was prepared using D_3PO_4 and NaOD. The acid D_3PO_4 is obtained from P_2O_5 and D_2O and NaOD from metallic sodium and D_2O.

Since the interface of the reference electrode corresponds to two different solvents, H_2O and D_2O respectively, the problem is to know the potential difference due to solvent nature only at the anode. In order to determine this value we used Ti(IV) in normal and deuterated oxalic acids, where the reduction occurs quasireversibly, and therefore without detectable isotope effect in polarographic conditions.[8] As it is shown in Fig. 1, we found the value of 6 mV, which lies near the error limit of the polarographic method. However it agrees with the result obtained by Druker[9] according to whom the potential difference between calomel electrodes in H_2O and D_2O is 3.5 mV.

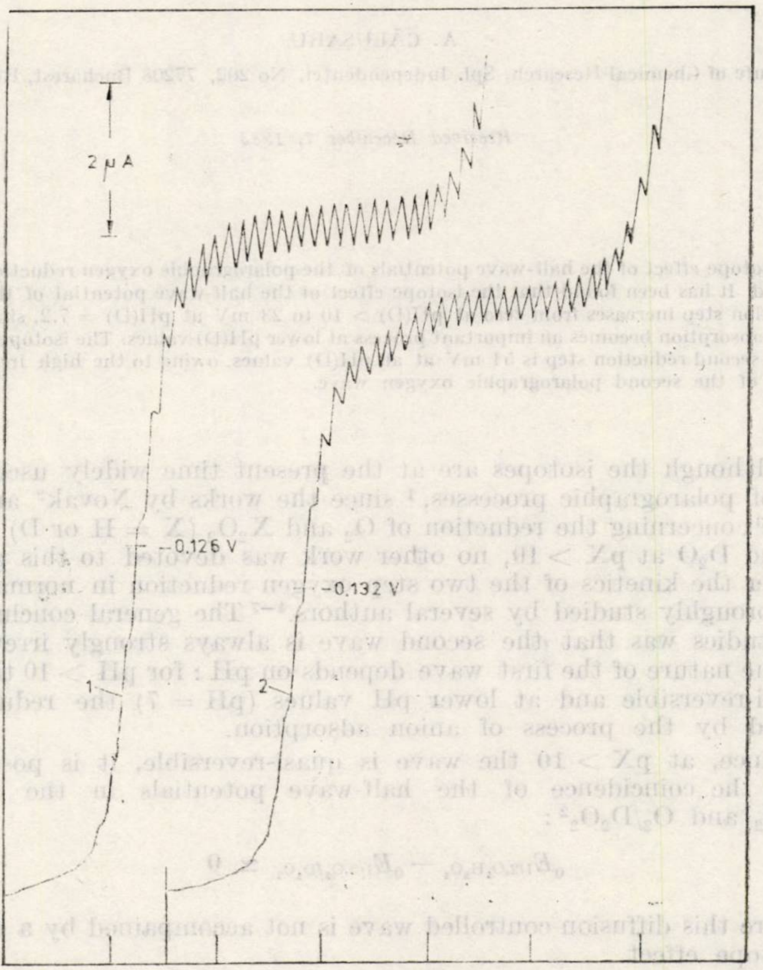

Fig. 1. – Polarograms corresponding to Ti(IV) 10^{-3}M reduction in oxalic acid, 2×10 M^{-1} : 1 – normal water solution and SCE in H_2O ; 2 – heavy water solution and SCE in D_2O. Start potential, 0 V; 100 mV/absc; temperature 24.5°C.

RESULTS AND DISCUSSION

In samples of normal and deuterated solutions buffered at $pX = 7.2$ (Fig. 2) it is a visible difference between the value of the half wave potentials corresponding to the first oxygen wave :

$$E_{1/2,O_2/H_2O_2} - E_{1/2,O_2/D_2O_2} = 23\ \text{mV} \tag{3}$$

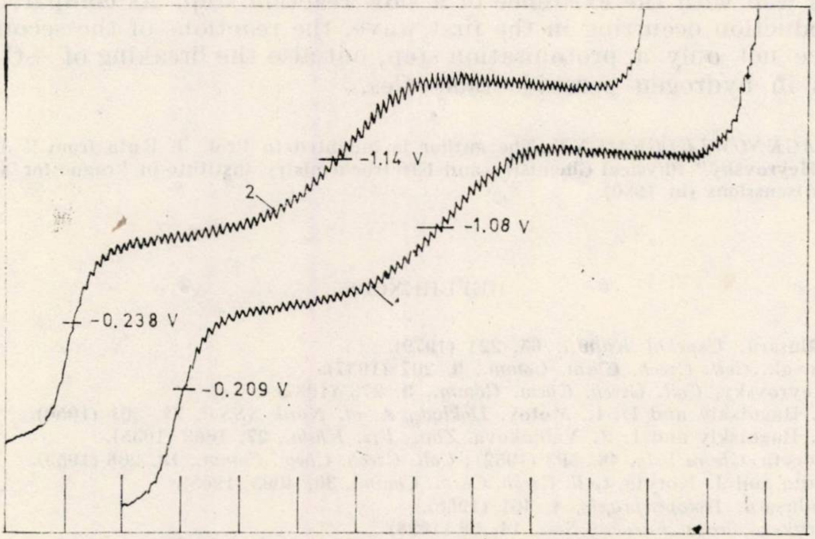

Fig. 2. — Polarograms corresponding to reduction of O_2 in Sörensen phosphate buffer of $pH = pD = 7.2$: 1 — normal water system ; 2 — heavy water system. Start potential, 0 V ; 200 mV/absc ; temperature, 23°C.

The same difference for the reaction process corresponding to the second wave is :

$$E_{1/2,H_2O_2/H_2O_2} - E_{1/2,D_2O_2/D_2O_2} = 54\ \text{mV} \tag{4}$$

If we carry out the recalculation of this value from the results by Novak, [2] using the mercury as reference electrode and the correction of 6 mV, we obtain the value 55 mV, in good agreement with the value given by (4).

These experimental values show that in conditions of the irreversibility corresponding to the both steps of oxygen reduction, isotope effects were found, which are different in magnitude.

For the first reduction step of oxygen the quasi-reversibility of the polarographic wave for $pX > 10$ indicates that no kinetic step can be found by the polarography. The absence of the influence of kinetics is also ascertained by the lack of isotope effect at $pX > 10$. At lower pX values the anion adsorption becomes stronger modifying the shape of the wave.[4-7] It is well known that on mercury electrode the simple anion adsorption-desorption kinetics in general is a very fast process and cannot be rate determining. However the field of the adsorbed anions influences the transfer process by lowering the rate of electrode reaction. This is why at $pX < 7$ the reaction mechanism changes and the isotope effect in the half-wave potentials increases from zero for $pX > 10$, to 23 mV at $pX = 7.2$.

The second oxygen reduction step corresponds to the reduction of water peroxides, which is irreversible at all pX values. This bahaviour agrees well with the existence of a slow reaction step. As compared with the reduction occurring in the first wave, the reactions of the second one involve not only a protonisation step, but also the breaking of $-O-O-$ bonds in hydrogen peroxide molecules.

ACKNOWLEDGEMENT. The author is indebted to Prof. J. Kuta from " J. Heyrovský" Physical Chemistry and Electrochemistry Institute in Prague for valuable discussions (in 1980).

REFERENCES

[1] A. Căluşaru, *Uspekhi Khimii*, **65**, 221 (1979).
[2] J. Novak, *Coll. Czech. Chem. Comm.*, **9**, 207 (1937).
[3] J. Heyrovsky, *Coll. Czech. Chem. Comm.*, **9**, 273 (1937).
[4] V. S. Bagotskiy and D. L. Motov, *Doklady Akad. Nauk SSSR*, **71**, 501 (1950).
[5] V. S. Bagotskiy and I. J. Yablokova, *Zhur. Fiz. Khim.*, **27**, 1663 (1935).
[6] J. Koryta, *Chem. listy*, **46**, 593 (1952); *Coll. Czech. Chem. Comm.*, **18**, 206 (1953).
[7] J. Kuta and J. Koryta, *Coll. Czech. Chem. Comm.*, **30**, 4095 (1965).
[8] A. Căluşaru, *Isotopenpraxis*, **4**, 401 (1968).
[9] C. Druker, *Trans. Faraday Soc.*, **14**, 59 (1928).

Revue Roumaine de Chimie, **29**, 7, 593–596 (1984)

STRUCTURAL CHARACTERISTICS OF THE STOICHIOMETRIC MATRIX

E. SEGAL*, M. VLAD[x] and V. POPA**

* Polytechnical Institute of Bucharest, Department of Physical Chemistry and Electrochemical Technology, Bd. Republicii 13, 70346, Romania

[x] Industrial Central for Medicinal Drugs, Cosmetics, Dyestuffs and Laquers, Bucharest, Bd. Ion Şulea 246, 78014, Romania

** Center of Physical Chemistry, ICECHIM – Bucharest, Splaiul Independenţei 202, 79611, Romania

Received July 21, 1983

In this paper some general relationships between the elements of a matrix $\mathbf{M}_{AB}$, with $C = \operatorname{rank} \mathbf{M}_{AB} < \min(A, B)$ are derived. The aquired equations are applied to complex chemical systems with linear dependent reactions.

Let

$$\mathbf{M}_{AB} = \| m_{ij} \|_{\substack{i=1,\ldots,A \\ j=1,\ldots,B}} \tag{1}$$

with

$$C = \operatorname{rank} \mathbf{M}_{AB} < \min(A,\ B) \tag{2}$$

This means that the vectors

$$\mathbf{m}_A^{(j)} = \begin{pmatrix} m_{1j} \\ \vdots \\ m_{Aj} \end{pmatrix},\ j = 1, \ldots, B \tag{3}$$

are linear dependent, that is

$$\sum_{j=1}^{B} \varepsilon_j \mathbf{m}_A^{(j)} = 0, \tag{4}$$

with at least one of the $\varepsilon_j \neq 0$.

Writing Eq. (4) in the matrix form

$$\mathbf{M}_{AB} \boldsymbol{\varepsilon}_B = \mathbf{0}_A \tag{5}$$

and making use of a convenient labelling of the matrix elements so that

$$\mathbf{M}_{AB} = \left\| \begin{array}{c:c} \mathbf{M}_{CC} & \mathbf{M}_{Cv} \\ \hdashline \mathbf{M}_{uC} & \mathbf{M}_{uv} \end{array} \right\|,\ u = A - C;\ v = B - C, \tag{6}$$

with

$$\operatorname{rank} \mathbf{M}_{CC} = C, \tag{7}$$

Eq. (5) yields

$$\left\| \begin{array}{c:c} \mathbf{M}_{CC} & \mathbf{M}_{Cv} \\ \hdashline \mathbf{M}_{uC} & \mathbf{M}_{uv} \end{array} \right\| \begin{pmatrix} \boldsymbol{\varepsilon}_C \\ \hdashline \boldsymbol{\varepsilon}_v \end{pmatrix} = \begin{pmatrix} \mathbf{O}_C \\ \hdashline \mathbf{O}_u \end{pmatrix}, \tag{8}$$

whence

$$\mathbf{M}_{CC}\, \boldsymbol{\varepsilon}_C + \mathbf{M}_{Cv}\, \boldsymbol{\varepsilon}_v = \mathbf{O}_C, \tag{9}$$

$$\mathbf{M}_{uC}\, \boldsymbol{\varepsilon}_C + \mathbf{M}_{uv}^{\varepsilon_v} = \mathbf{O}_u. \tag{10}$$

On the other side, (4) is a linear homogeneous system of A equations with B unknowns, ε_j, $j = 1,\ldots,B$[1]. As rank $\mathbf{M}_{AB} = \mathbf{C}$ from the general theory of such systems it follows that $v = B - C$ unknowns are arbitrary and the other C unknowns are linear combinations of the former.

Thus, we can take

$$\boldsymbol{\varepsilon}_v = \text{arbitrary}. \tag{11}$$

As $\mathbf{M}_{CC}$ is nonsingular, from (9) and (10) we get:

$$\boldsymbol{\varepsilon}_C = -\mathbf{M}_{CC}^{-1}\, \mathbf{M}_{Cv}\, \boldsymbol{\varepsilon}_v \tag{12}$$

and

$$(\mathbf{M}_{uv} - \mathbf{M}_{uC}\, \mathbf{M}_{CC}^{-1}\, \mathbf{M}_{Cv})\boldsymbol{\varepsilon}_v = \mathbf{O}_u. \tag{13}$$

By introducing the notation

$$\Xi_{uv} = \| \zeta_{ij} \|_{j = 1, \ldots, v}^{i = 1, \ldots, u} = \mathbf{M}_{uv} - \mathbf{M}_{uc}\, \mathbf{M}_{CC}^{-1}\, \mathbf{M}_{Cv}, \tag{14}$$

(13) becomes

$$\Xi_{uv}\, \boldsymbol{\varepsilon}_v = \mathbf{O}_u, \tag{15}$$

or, in scalar form

$$\sum_{j=1}^{v} \zeta_{ij}\, \varepsilon_{C+j} = 0, \quad i = 1, \ldots, u, \tag{16}$$

In (16) we may consider ζ_{ij} as unknowns, because ε_{c+j} are arbitrary; giving them convenient different values, ε_{c+j}^{k}, $\alpha = 1,2,\ldots$, we can construct a supradetermined system of $u\alpha > uv$ independent equations, the single solution of which is, naturally, the trivial one[1]

$$\zeta_{ij} = 0, \quad i = 1, \ldots, u; \quad j = 1, \ldots, v. \tag{17}$$

From (14) and (17) we get

$$\mathbf{M}_{uv} = \mathbf{M}_{uC}\, \mathbf{M}_{CC}^{-1} \mathbf{M}_{Cv}, \tag{18}$$

which is a general equation for matrices of the type considered above.

We consider now a complex chemical process, described by the mechanistic scheme

$$\sum_{i=1}^{S} \nu_{ij} A_i \rightleftarrows \sum_{i=1}^{S} \nu'_{ij} A_i, \;\; j = 1, \ldots, R, \tag{19}$$

$$\sum_{i=1}^{n} f_{ij} A_i = 0 \,; \;\; f_{ij} = \nu'_{ij} - \nu_{ij}, \tag{19'}$$

$$1 \leqslant \sum \nu_{ij}, \;\sum \nu'_{ij} \leqslant 3 \,; \;\; \nu_{ij}, \;\; \nu'_{ij} \geqslant 0 \;\; \forall i, j \tag{19''}$$

The elementary reactions (19) need not be linearly (algebrically) independent, but only ***physically independent***. That means that the stoichiometric vectors corresponding to these reactions

$$\mathbf{f}_S^{(j)} = \begin{pmatrix} f_{1j} \\ \vdots \\ f_{sj} \end{pmatrix}, \tag{20}$$

are not necessarily linearly independent.

If only K stoichiometric vectors are linearly independent, then the rank of the stoichiometric matrix[2-4]

$$\mathbf{F}_{SR} = \| \mathbf{f}_S^{(1)} \ldots \mathbf{f}_S^{(R)} \| = \| f_{ij} \|_{\substack{i = 1, \ldots, S \\ j = 1, \ldots, R}} \tag{21}$$

is K:

$$\text{rank } \mathbf{F}_{SR} = K \leqslant \min \;(R, S). \tag{22}$$

In this case the above considerations are valid, and we can write

$$\mathbf{F}_{SR} = \left\| \begin{array}{c:c} \mathbf{G}_{KK} & \mathbf{G}_{uK} \\ \hdashline \mathbf{G}_{Kv} & \mathbf{G}_{uv} \end{array} \right\|, \tag{23}$$

$$\text{rank } \mathbf{G}_{KK} = K \tag{24}$$

where from, by using (18)

$$\mathbf{G}_{uv} = \mathbf{G}_{uK}\, \mathbf{G}_{KK}^{-1}\, \mathbf{G}_{Kv} \tag{25}$$

We define now the partitions (submatrices)

$$\mathbf{\Phi}_{SK} = \left\|\begin{array}{c}\mathbf{G}_{KK}\\ \hline \mathbf{G}_{uK}\end{array}\right\| = \|\,\mathbf{f}_S^{(1)} \ldots \mathbf{f}_S^{(K)}\,\|, \tag{26}$$

$$\mathbf{\Phi}_{Sv} = \left\|\begin{array}{c}\mathbf{G}_{Kv}\\ \hline \mathbf{G}_{uK}\end{array}\right\| = \|\,\mathbf{f}_S^{(K+1)} \ldots \mathbf{f}_S^{(R)}\,\|. \tag{27}$$

From (27) and (25) we get

$$\mathbf{\Phi}_{Sv} = \left\|\begin{array}{c}\mathbf{G}_{Kv}\\ \hline \mathbf{G}_{uK}\mathbf{G}_{kk}^{-1}\mathbf{G}_{Kv}\end{array}\right\| = \left\|\begin{array}{c}\mathbf{G}_{KK}\mathbf{G}_{KK}^{-1}\mathbf{G}_{Kv}\\ \hline \mathbf{G}_{uK}\mathbf{G}_{KK}^{-1}\mathbf{G}_{Kv}\end{array}\right\| = \left\|\begin{array}{c}\mathbf{G}_{KK}\\ \hline \mathbf{G}_{uK}\end{array}\right\|\mathbf{G}_{KK}^{-1}\mathbf{G}_{Kv},$$

and taking into account (26):

$$\mathbf{\Phi}_{Sv} = \mathbf{\Phi}_{SK}\,\mathbf{G}_{KK}^{-1}\,\mathbf{G}_{Kv} = \mathbf{\Phi}_{SK}\,\mathbf{\Gamma}_{Kv}, \tag{28}$$

with

$$\mathbf{\Gamma}_{Kv} = \mathbf{G}_{KK}^{-1}\mathbf{G}_{Kv} = \|\,\gamma_{ij}\,\|\begin{array}{l} i=1,\ldots,K\\ j=1,\ldots,v\end{array} \tag{29}$$

Inserting Eqs. (26–27) into Eq. (28) we get

$$\|\,\mathbf{f}_S^{(K+1)} \ldots \mathbf{f}_S^{(R)}\,\| = \|\,\mathbf{f}_S^{(1)} \ldots \mathbf{f}_S^{(K)}\,\|\mathbf{\Gamma}_{Kv} \tag{30}$$

or

$$\mathbf{f}_S^{(K+\alpha)} = \sum_{\beta=1}^{K} \mathbf{f}_S^{(\beta)}\gamma_{\beta\alpha}, \quad \alpha = 1, \ldots, v = R - K. \tag{31}$$

Eqs. (30–31) give the expression of the linear dependent stoichiometric vectors in terms of the independent ones.

Eqs. (25), (28) and (30–31) are very important for the kinetic analysis of reaction networks[5,6].

REFERENCES

[1] G. Kurosh, "Higher Algebra", Mir Publishers, Moscow, 1972, p. 82–86.

[2] E. Jouguet, *J. Ecole Polytechnique II*, **21**, 61, 81 (1921).

[3] R. Aris, *Arch. Rational Mech. Anal.*, **19**, 81 (1965); **27**, 356 (1968).

[4] N. F. Stepanov, M. E. Erlykina and G. G. Filippov, "Metodele algebrei liniare in chimia fizică", Ed. Ştiinţifică şi Enciclopedică, Bucharest, 1980, p. 181–187.

[5] V. Popa, E. Segal and M. Vlad, *Rev. Roumaine Chim.*, in press.

[6] V. Vlad, V. Popa and E. Segal, *Rev. Roumaine Chim.*, in press.

Revue Roumaine de Chimie, **29**, 7, 597–604 (1984)

ON THE KINETIC MODEL OF THE RATE-DETERMINING STEP. II[1]

SINGLE-ROUTE SYSTEMS WITH AN ARBITRARY NUMBER OF ACTIVE INTERMEDIATES

M. VLAD*, V. POPA[x] and E. SEGAL**

* Industrial Central for Medicinal Drugs, Cosmetics, Dyestuffs and Laquers, Bucharest, Bd. Ion Şulea 246, 78014, Romania

[x] Center of Physical Chemistry, ICECHIM Bucharest, Splaiul Independenţei 202, 79611, Romania

** Polytechnical Institute of Bucharest, Department of Physical Chemistry and Electrochemical Technology, Bd. Republicii 13, 70346, Romania

Received July 21, 1983

In this note, the conditions within which the overall reaction rate of single-route systems with a rate-determining step may be expressed in the mass-action law form, are established. The treatment is free of restrictions concerning the number of active intermediates.

I. INTRODUCTION

In a previous paper [1] we presented a new derivation of the "step steady state" (Horiuti-Temkin) [2–10] conditions, for mono-route complex reactions, by means of a matricial formalism.

Thus, if the complex reaction in question is represented by the mechanistic scheme

$$\sum_{i=1}^{S_1} \alpha_{ij} A_i + \sum_{i=1}^{S_2} \beta_{ij} X_i \underset{k'_j}{\overset{k_j}{\rightleftarrows}} \sum_{i=1}^{S_1} \alpha'_{ij} A_i + \sum_{i=1}^{S_2} \beta'_{ij} X_i,$$

$$3 \geqslant \sum_{i=1}^{S_1} \alpha_{ij} + \sum_{i=1}^{S_2} \beta_{ij}, \ \sum_{i=1}^{S_1} \alpha'_{ij} + \sum_{i=1}^{S_2} \beta'_{ij} \geqslant 1 \, ; \ j = 1, \ldots, R-1 \, ; \tag{1}$$

$$\sum_{i=1}^{S_1} \alpha_{ic} A_i + \sum_{i=1}^{S_2} \beta_{ic} X_i \underset{k'_c}{\overset{k_c}{\rightleftarrows}} \sum_{i=1}^{S_1} \alpha'_{ic} A_i + \sum_{i=1}^{S_2} \beta'_{ic} X_i,$$

$$3 \geqslant \sum_{i=1}^{S_1} \alpha_{ic} + \sum_{i=1}^{S_2} \beta_{ic}, \ \sum_{i=1}^{S_1} \alpha'_{ic} + \sum_{i=1}^{S_2} \beta_{ic} \geqslant 1, \tag{2}$$

where A_i, $i = 1,\ldots,S_1$ are stable substances and X_i, $i = 1,\ldots,S_2$ are active intermediates, subscript c denoting the rate-determining step, we proved that the stoichiometric coefficients of the overall reaction,

$$\sum_{i=1}^{S_1} f_i A_i = 0, \tag{3}$$

are given by

$$\mathbf{f}_{S_1} = (\mathbf{a}^c_{S_1} - \mathbf{a}_{S_1R-1}\mathbf{b}^{-1}_{R-1R-1}\mathbf{b}^c_{R-1})\,\sigma_c. \tag{4}$$

Here, the following matrix notations have been used[1]

$$\mathbf{f}_{S_1} = \|f_i\|_{i=1,\ldots,S_1};\ \mathbf{a}^c_{S_1} = \|a_{ic}\|_{i=1,\ldots,S_1},\ \ a_{ic} = \alpha'_{ic} - \alpha_{ic}; \tag{5}$$

$$\mathbf{a}_{S_1R-1} = \|a_{ij}\|^{i=1,\ldots,S_1}_{i=1,\ldots,R-1},\ a_{ij} = \alpha'_{ij} - \alpha_{ij}; \tag{6}$$

$$\begin{aligned}\mathbf{b}_{S_2R} &= \|b_{ij}\|^{i=1,\ldots,S_2}_{j=1,\ldots,R} = \|\,\mathbf{b}^{(1)}_{S_2} \,\vdots\, \mathbf{b}^{(2)}_{S_2} \,\vdots\, \ldots \,\vdots\, \mathbf{b}^{(R-1)}_{S_2} \,\vdots\, \mathbf{b}^{(c)}_{S_2}\,\| = \\ &= \|\mathbf{b}_{S_2R-1} \,\vdots\, \mathbf{b}^{(c)}_{S_2}\| = \left\|\begin{array}{c|c} \mathbf{b}_{R-1R-1} & \\ \hline \mathbf{b}_{S_2-R+1R-1} & \mathbf{b}^{(c)}_{S_2}\end{array}\right\|,\ \ b_{ij} = \beta'_{ij} - \beta_{ij};\end{aligned} \tag{7}$$

$$\mathbf{b}^{(c)}_{R-1} = \|b_{ic}\|_{i=1,\ldots,R-1};\ \ b_{ic} = \beta'_{ic} - \beta_{ic}; \tag{8}$$

σ_c is the stoichiometric number of the rate-determining step.[2-4]

The above relationships are consequences of the single-route condition:

$$\text{rank}\ \mathbf{b}_{S_2R-1} = \text{rank}\ \mathbf{b}_{S_2R} = R - 1, \tag{9}$$

which, through a convenient labeling of the matrix elements b_{ij}, leads to

$$\text{rank}\ \mathbf{b}_{R-1R-1} = R - 1. \tag{10}$$

Within this framework, from the "intermediate" (Bodenstein)[4] steady-state conditions,

$$\frac{1}{\Omega}\frac{\mathrm{d}}{\mathrm{d}t}(X_i\Omega) = 0,\ \ i = 1,\ \ldots,\ S_2, \tag{11}$$

(Ω being the system extension), we got

$$r = r_c/\sigma_c, \tag{12}$$

$$r = r_i/\sigma_i,\ i = 1,\ldots R-1 \tag{12'}$$

(where σ_i is the stoichiometric number of the step i), i.e. the Horiuti Temkin[4,9] steady-state conditions.

Other analog derivations presented in literature[2–4,9,10] made use, more or less explicitly, of the restriction

$$S_2 = R-1,$$

whereas our derivation is free of this constraint.

Moreover, if. Eq. (13) and the quasi-equilibrium conditions

$$r_j = r_j^+ - r_j^- \cong 0, \;\; j = 1,\ldots,R-1 = S_2 \tag{14}$$

with

$$r_j^+ = k_j \prod_{i=1}^{S_1} A_i^{\alpha_{ij}} \prod_{i=1}^{S_2} X_i^{\beta_{ij}}; \;\; r_j^- = k_j' \prod_{i=1}^{S_1} A_i^{\alpha_{ij}'} \prod_{i=1}^{S_2} X_i^{\beta_{ij}'}, \tag{15}$$

hold, we could *prove* the validity of the mass-action law for the overall reaction

$$r = k \prod_{i=1}^{S_1} A_i^{n_i} - k' \prod_{i=1}^{S_1} A_i^{n_i'}. \tag{16}$$

We also got the expression for the overall kinetic parameters k, k', n_i, n_i' etc. in mechanistical therms.[1]

The famous Horiuti-Temkin relationships [2–4,9,10]

$$k/k' = K^{1/\sigma_c} \tag{17}$$

or

$$E - E' = \Delta H/\sigma_c \tag{17''}$$

are a simple corollary of the above treatment.

In this paper we are looking for the conditions within which our derivation of Eq. (16) may be extended to the general case

$$S_2 \geqslant R-1 \tag{18}$$

II. CONSISTENCY CONDITIONS

The problem reduces to the elimination of the unknown concentrations, X_i, $i = 1,\ldots,S_2$ from the R equations (12) and (14). To do this we shall write these in the form

$$r = r^+ - r^- = \frac{1}{\sigma_c}\left(k_c \prod_{i=1}^{S_1} A_i^{\alpha_{ic}} \prod_{i=1}^{S_2} X_i^{\beta_{ic}} - k_c' \prod_{i=1}^{S_1} A_i^{\alpha_{ic}'} \prod_{i=1}^{S_2} X_i^{\beta_{ic}'} \right); \tag{19}$$

$$\frac{k_j}{k_j'} = \prod_{i=1}^{S_1} A_i^{a_{ij}} \prod_{i=1}^{S_2} X_i^{b_{ij}}, \;\; j = 1,\ldots,R-1. \tag{20}$$

In the previous paper[1] we showed that in the case $S_2 = R-1$ the system (20) could be solved for X_i. If $S_2 > R-1$ this is no longer possible, the system being undetermined. In this case, from (20) one can find at most $R-1$ independent "complexions",[11] Γ_j,

$$\Gamma_j \overset{\Delta}{=} \prod_{i=1}^{S_2} X_i^{b_{ij}} = \frac{k_j}{k'_i} \prod_{i=1}^{S_1} A_i^{-a_{ij}}, \; j = 1, \ldots, R-1. \tag{21}$$

These complexions are independent in the sense that

$$1 \neq \prod_{j=1}^{R-1} \Gamma_j^{\varkappa_j}, \; \sum_j \varkappa_j^2 \neq 0, \tag{22}$$

or, through logarithmation

$$0 \neq \sum_{j=1}^{R-1} \varkappa_j \ln \Gamma_j, \; \sum_j \varkappa_j^2 \neq 0. \tag{23}$$

This is a natural consequence of the single-route condition (9). Indeed, through logarithmation of Eq. (21), we get

$$\ln \Gamma_j = \| \ln X_i \|_{S_2}^{+} \mathbf{b}_{S_2}^{(j)}, \; j = 1, \ldots, R-1 \tag{24}$$

The single-route condition (9) ensures the linear independence of the column vectors

$$\mathbf{b}_{S_2}^{(j)} = \| b \|_{i=1,\ldots,S_2} \tag{25}$$

and also the linear independence of the $\ln \Gamma_j$.

In order to put the reaction rate in an explicit form, in Eq. (19), it is necessary that the products $\prod_{i=1}^{S_2} X_i^{\beta_{ic}}$ and $\prod_{i=1}^{S_2} X_i^{\beta'_{ic}}$ may be expressed in the form

$$\prod_{i=1}^{S_2} X_i^{\beta_{ic}} = \prod_{j=1}^{R-1} \Gamma_j^{\eta_j}, \tag{26}$$

$$\prod_{i=1}^{S_2} X_i^{\beta'_{ic}} = \prod_{j=1}^{R-1} \Gamma_j^{\eta'_j}. \tag{26'}$$

or, taking into account Eq. (24)

$$\beta_{ic} \ln X_i = \sum_{j=1}^{R-1} \eta_j \ln \Gamma_j = \sum_{i=1}^{R-1} \sum_{i=1}^{S_2} \eta_j b_{ij} \ln X_i, \tag{27}$$

$$\beta'_{ic} \ln X_i = \sum_{j=1}^{R-1} \eta'_j \ln \Gamma_j = \sum_{j=1}^{R-1} \sum_{i=1}^{S_2} \eta'_j b_{ij} \ln X_i, \tag{27'}$$

whence

$$\sum_{i=1}^{S_2} (\ln X_i)\left(\beta_{ic} - \sum_{j=1}^{R-1} \eta_j b_{ij} \right) \equiv 0, \tag{28}$$

$$\sum_{i=1}^{S_2} (\ln X_i)\left(\beta'_{ic} - \sum_{j=1}^{R-1} \eta'_j b_{ij} \right) \equiv 0. \tag{28'}$$

Eqs. (28) and (28′) involve that

$$\beta_{ic} = \sum_{j=1}^{R-1} \eta_j b_{ij},\ i = 1, \ldots, S_2, \text{ or } \boldsymbol{\beta}_{S_2}^{(c)} = \sum_{j=1}^{R-1} \eta_j \mathbf{b}_{S_2}^{(j)}, \tag{29}$$

$$\beta'_{ic} = \sum_{j=1}^{R-1} \eta'_j b_{ij},\ i = 1, \ldots, S_2, \text{ or } \boldsymbol{\beta}_{S_2}^{\prime(c)} = \sum_{j=1}^{R-1} \eta'_j \mathbf{b}_{S_2}^{(j)}, \tag{29'}$$

with

$$\boldsymbol{\beta}_{S_2}^{(c)} = \begin{pmatrix} \beta_{1c} \\ \vdots \\ \beta_{S_2c} \end{pmatrix},\ \boldsymbol{\beta}_{S_2}^{\prime(c)} = \begin{pmatrix} \beta'_{1c} \\ \vdots \\ \beta'_{S_2c} \end{pmatrix}. \tag{30}$$

Eqs. (29) and (29′) represent the conditions within which the elimination of the unknown concentrations, X_i, of the active intermediates from the expression of the overall reaction rate, is possible. They express the fact that the vectors $\boldsymbol{\beta}_{S_2}^{(c)}$ and $\boldsymbol{\beta}_{S_2}^{\prime(c)}$ are linear combinations of the independent (base) vectors $\mathbf{b}_{S_2}^{(j)}, j = 1, \ldots, R-1$.

Thus, Eqs. (29) and (29′) may be expressed as follows

$$\text{rank } \|\mathbf{b}_{S_2}^{(1)} \vdots \ldots \vdots \mathbf{b}_{S_2}^{(R-1)} \vdots \boldsymbol{\beta}_{S_2}^{(c)} \| \equiv \text{rank } \| \mathbf{b}_{S_2R-1} \vdots \beta_{S_2}^{(c)} \| = R - 1, \tag{31}$$

$$\text{rank } \|\mathbf{b}_{S_2}^{(1)} \vdots \ldots \vdots \mathbf{b}_{S_2}^{(R-1)} \vdots \boldsymbol{\beta}_{S_2}^{\prime(c)} \| \equiv \text{rank } \| \mathbf{b}_{S_2R-1} \vdots \boldsymbol{\beta}_{S_2}^{\prime(2)} \| = R - 1. \tag{31'}$$

In fact, the conditions (29) and (29′) are not independent : the validity of one of them ensures automatically the validity of the other. This is a consequence of the single-route condition, (9).

Indeed, Eq. (9) involves

$$\mathbf{b}_{S_2}^{(c)} = \sum_{j=1}^{R-1} \varepsilon_j \mathbf{b}_{S_2}^{(j)}, \tag{32}$$

and, considering e.g. Eq. (29) valid, and taking into account that

$$\mathbf{b}_{S_2}^{(c)} = \boldsymbol{\beta}_{S_2}^{\prime(c)} - \boldsymbol{\beta}_{S_2}^{(c)}, \tag{33}$$

(which follows from (7)), we get :

$$\beta_{S_2}^{\prime(c)} = \mathbf{b}_{S_2}^{(c)} + \beta_{S_2}^{(c)} = \sum_{j=1}^{R-1} \eta'_j \mathbf{b}_{S_2}^{(j)}, \tag{29'}$$

with

$$\eta'_j = \varepsilon_j + \eta_j. \tag{34}$$

Similarly, assuming (29′) valid we get

$$\boldsymbol{\beta}^{(c)}_{S_2} = - \mathbf{b}^{(c)}_{S_2} + \boldsymbol{\beta}'^{(c)}_{S_2} = \sum_{j-1}^{R-1} \eta_j \mathbf{b}^{(j)}_{S_2}, \tag{29}$$

with

$$\eta_j = - \varepsilon_j + \eta'_j .$$

Obviously, in the case $S_2 = R-1$, the conditions (29), (29′) are automatically fulfilled as can be seem from their matrix transcriptions (31), (31′).

III. THE OVERALL RATE EQUATION

If and only if one of the conditions (29) or (29′) are fulfilled, the problem reduces to the elimination of the expressions $\prod_{i=1}^{S_2} X_i^{\beta_{ic}}$, $\prod_{i=1}^{S_2} X_i^{\beta'_{ic}}$ and Γ_j, $j = 1, \ldots, R-1$ from Eqs. (19), (21), (26) and (26′) which involve the determination of the numbers η_j, η'_j, $j = 1, \ldots, R-1$.

To do this, we write Eqs. (29) and (29′) in the form

$$\boldsymbol{\beta}^{(c)}_{S_2} = \mathbf{b}_{S_2 R-1} \boldsymbol{\eta}_{R-1} \tag{35}$$

$$\boldsymbol{\beta}'^{(c)}_{S_2} = \mathbf{b}_{S_2 R-1} \boldsymbol{\eta}'_{R-1} \tag{36}$$

where

$$\boldsymbol{\eta}_{R-1} = \begin{pmatrix} \eta_1 \\ \vdots \\ \eta_{R-1} \end{pmatrix}; \ \boldsymbol{\eta}'_{R-1} = \begin{pmatrix} \eta'_1 \\ \vdots \\ \eta'_{R-1} \end{pmatrix} \tag{37}$$

Partitioning in Eq. (35), we get

$$\left\| \begin{array}{c} \boldsymbol{\beta}^{(c)}_{R-1} \\ \hdashline \boldsymbol{\beta}^{(c)}_{S_2-R+1} \end{array} \right\| = \left\| \begin{array}{c} \mathbf{b}_{R-1\,R-1} \\ \hline \mathbf{b}_{S_2-R+1\,R-1} \end{array} \right\| \boldsymbol{\eta}_{R-1}, \tag{38}$$

where from

$$\boldsymbol{\beta}^{(c)}_{R-1} = \mathbf{b}_{R-1\,R-1} \boldsymbol{\eta}_{R-1}, \tag{39}$$

$$\boldsymbol{\beta}^{(c)}_{S_2-R+1} = \mathbf{b}_{S_2-R+1} \boldsymbol{\eta}_{R-1} \tag{40}$$

and, as rank $\mathbf{b}_{R-1\,R-1} = R - 1$ we get

$$\boldsymbol{\eta}_{R-1} = \mathbf{b}_{R-1\,R-1}^{-1}\boldsymbol{\beta}_{R-1}^{(c)}, \tag{41}$$

$$\boldsymbol{\beta}_{S_2-R+1} = \mathbf{b}_{S_2-R+1\,R-1}\mathbf{b}_{R-1\,R-1}^{-1}\boldsymbol{\beta}_{R-1}^{(c)}. \tag{42}$$

The identity (42) is a direct consequence of the resolvability conditions (29).[12]

Similarly, for η_j' we get

$$\boldsymbol{\eta}'_{R-1} = \mathbf{b}_{R-1\,R-1}^{-1}\boldsymbol{\beta}_{R-1}^{\prime(c)}. \tag{41'}$$

$$\boldsymbol{\beta}'_{S_2-R+1} = \mathbf{b}_{S_2-R+1\,R-1}\mathbf{b}_{R-1\,R-1}^{-1}\boldsymbol{\beta}_{R-1}^{\prime(c)}. \tag{42'}$$

Combining Eqs. (19), (21), (26) we have

$$r^+ = \frac{k_c}{\sigma_c}\prod_{i=1}^{S_1} A_i^{\alpha_{ic}} \prod_{j=1}^{R-1} \Gamma_j^{\eta_j} = \frac{k_c}{\sigma_c}\prod_{j=1}^{R-1}\left(\frac{k_j}{k_j'}\right)^{\eta_j}\prod_{i=1}^{S_1} A_i^{\alpha_{ic}-\sum\limits_{j=1}^{R-1} a_{ij}\eta_j} \tag{43}$$

where from, taking into account (41)

$$r^+ = \frac{k_i}{\sigma_c}\prod_{j=1}^{R-1}\left(\frac{k_j}{k_j'}\right)^{\sum\limits_{m=1}^{R-1}(\mathbf{b}_{R-1\,R-1}^{-1})_{jm}\,\beta_{mc}}\prod_{i=1}^{S_1} A_i^{\alpha_{ic}-\sum\limits_{j=1}^{R-1}\sum\limits_{m=1}^{R-1} a_{ij}(\mathbf{b}_{R-1\,R-1}^{-1})_{jm}\beta_{mc}}. \tag{44}$$

The expression of r^- results in an analogous way

$$r^- = \frac{k_c'}{\sigma_c}\prod_{j=1}^{R-1}\left(\frac{k_j}{k_j'}\right)^{\sum\limits_{m=1}^{R-1}(\mathbf{b}_{R-1\,R-1}^{-1})_{jm}\,\beta'_{mc}}\prod_{i=1}^{S_1} A_i^{\alpha'_{ic}-\sum\limits_{j=1}^{R-1}\sum\limits_{m-1}^{R-1} a_{ij}(\mathbf{b}_{R-1\,R-1}^{-1})_{jm}\beta'_{mc}}. \tag{44'}$$

From Eqs. (44) and (44′) the sought expression of the reaction rate results

$$r = k\prod_{i=1}^{S_1} A_i^{n_i} - k'\prod_{i-1}^{S_1} A_i^{n_i'}, \tag{45}$$

where

$$k = \frac{k_c}{\sigma_c} \prod_{j=1}^{R-1} \left(\frac{k_j}{k'_j} \right)^{\sum\limits_{j=1}^{R-1} (\mathbf{b}_{R-1\,R-1}^{-1})_{jm}\, \beta_{mc}} ; \tag{46}$$

$$k' = \frac{k'_c}{\sigma_c} \prod_{j=1}^{R-1} \left(\frac{k_j}{k'_j} \right)^{\sum\limits_{m=1}^{R-1} (\mathbf{b}_{R-1\,R-1}^{-1})_{jm}\, \beta'_{mc}} ; \tag{46'}$$

$$\mathbf{n}_{S_1} = \begin{Vmatrix} n_1 \\ \vdots \\ n_{S_1} \end{Vmatrix} = \boldsymbol{\alpha}_{S_1}^{(c)} - \mathbf{a}_{S_1 R-1} \mathbf{b}_{R-1\,R-1}^{-1} \boldsymbol{\beta}_{R-1}^{(c)},\ \boldsymbol{\alpha}_{S_1}^{(c)} = \begin{Vmatrix} \alpha_{1c} \\ \vdots \\ \alpha_{S_1 c} \end{Vmatrix}; \tag{47}$$

$$\mathbf{n}'_{S_1} = \begin{Vmatrix} n'_1 \\ \vdots \\ n'_{S_1} \end{Vmatrix} = \boldsymbol{\alpha}'^{(c)}_{S_1} - \mathbf{a}_{S_1\,R-1} \mathbf{b}_{R-1\,R-1}^{-1} \boldsymbol{\beta}_{R-1}^{(c)},\ \boldsymbol{\alpha}'^{(c)}_{S_1} = \begin{Vmatrix} \alpha'_{1c} \\ \vdots \\ \alpha'_{S_1 c} \end{Vmatrix} \tag{47'}$$

Eqs. (44—47) and (44′—47′) are formally identical with those obtained in the preceding paper.[1] Thus, the derivations of the Horiuti-Temkin relationships (17—17′) and the expressions in mechanistical terms of the activation energies and preexponential factors performed in the preceding paper are also valid for the case $S_2 > R-1$.

REFERENCES

[1] M. Vlad and E. Segal, *Rev. Roumaine Chim.*, **24**, 799 (1979).

[2] J. Horiuti, *Adv. Catalysis*, **9**, 339 (1957); *J. Catalysis*, **1**, 199 (1962); *Ann. N.Y. Acad. Sci.*, **213**, 5 (1973).

[3] J. Horiuti and T. Nakamura, *Z. phys. Chem. (Frankfurt)*, **11**, 358 (1957); *Adv. Catalysis*, **17**, 2 (1967).

[4] M. I. Temkin, *Doklady. Acad. Nauk. S,S,S,R.*, **152**, 156, (1963); **165**, 615 (1965); *Int. Chem. Eng.*, **11**, 709 (1971); *Ann. N.Y. Acad. Sci.*, **213**, 79 (1973); *Adv. Catalysis*, 28, 173, (1979).

[5] J. Happel, *Catal. Rev.*, **6**, 221 (1972).

[6] J. Happel and M. A. Hnatow, *Ann. N.Y. Acad. Sci.*, **213**, 206 (1973).

[7] J. Happel and R. S. Csuha, *J. Catalysis*, **20**, 132 (1971).

[8] J. Happel and R. S. Atkins, *Int. Eng. Chem. Fund.*, **9**, 11 (1970).

[9] M. Boudart, "Kinetics of Chemical Processes", Prentice Hall, Englewood Cliffs, New Jersey, 1968, Chapter 4, p. 81; in "Physical Chemistry : An Advanced Treatise", vol. 7, H. Eyring, W. Jost, and D. Henderson, Eds. Academic Press, New York, 1975, Chapter 7, p. 351; *J. Phys. Chem.*, **80**, 2869 (1976).

[10] K. Tamaru, "Dynamic Heterogeneous Catalysis", Academic Press, London, 1978, Chapter 1.

[11] F. Horn, *Proc. Roy. Soc. London A*, **334**, 299; 313; 331 (1973).

[12] E. Segal, M. Vlad and V. Popa, *Rev. Roumanie Chim.*, in press.

Revue Roumaine de Chimie, **29**, 7, 605–612 (1984)

POLYMERIZATION OF ACRYLAMIDE INITIATED BY Fe^{2+}/BROMATE REDOX COUPLE

U.D.N. BAJPAI and ANITA AHI

Department of Post-Graduate Studies & Research in Chemistry, Rani Durgawati University, Jabalpur, 482 001, M.P., India

Received October 10, 1983

The polymerization of acrylamide initiated by Fe^{2+}/bromate redox couple has been studied at 35 ± 0.2°C in nitrogen atmosphere. The effect of activator, catalyst, monomer, temperature, sulphuric acid concentration, organic solvents and various salts and surfactants has been studied. The rate may be expressed by the following equation $R_{p\alpha}$ [Bromate]$^{1/2}$[Monomer]$^{1/3}$. The overall energy of activation is 11.54 kcal/deg in the investigated range of temperature 30°–45°C.

I. INTRODUCTION

Redox initiated polymerization of vinyl monomers has been studied by several workers and an intensive review on the subject has recently been written by Misra and Bajpai.[1] The use of metal ions especially Fe^{2+}/Fe^{3+} as one of the redox components is very limited. Ferrous ions in conjunction with several oxidants have been found to form efficient redox systems for the polymerization of vinyl monomers in aqueous media. Pramanick et al.[2] employed this pair for the polymerization of methyl methacrylate in aqueous medium and showed that the efficiency of this system is very high with almost undetectable induction period. Initiation does take place at very low temperatures and a variety of vinyl monomers could be polymerized except acrylic acid, methacrylic acid and vinyl acetate. With this view and the developing applicability of polyacrylamide, in the present communication the polymerization of acrylamide using this redox pair has been investigated in aqueous medium at room temperature. This study also gives a change to compare the kinetic path of this polymerization process with similar systems.

RESULTS AND DISCUSSION

Palit et al.[4] demonstrated that the poly-methy lmethacrylate obtained by this redox system was incorporated with hydroxyl and bromine free radicals in the system. Thomas et al.[5] also suggested the reduction of BrO_3^- to Br^- by Fe^{2+}. Considering these points the following plausible mechanism may be given for the present study.

$$Fe^{2+} + BrO_3^- + H_2O \xrightarrow{k_d} Fe^{3+} + BrO_2^- + OH^{\bullet} + OH^- \qquad (a)$$

$$Fe^{2+} + BrO_2^- + H_2O \xrightarrow{k_d} Fe^{3+} + BrO^- + OH^{\bullet} + OH^- \qquad (b)$$

$$Fe^{2+} + BrO^- + H_2O \xrightarrow{k_d} Fe^{3+} + Br^- + OH^{\bullet} + OH^- \qquad (c)$$

$$\text{or} \longrightarrow Fe^{3+} + Br^{\bullet} + 2OH^- \qquad (d)$$

The $Br^{\bullet}$ and OH (say $R^{\bullet}$) may be responsible for the polymerization of acrylamide.

$$R^{\bullet} + M \longrightarrow R{-}M^{\bullet} \qquad (2)$$

$$R - M^{\bullet} + M \xrightarrow{k_p} R - M - M^{\bullet} \qquad (3)$$

$$R - M^{\bullet}_{n-1} + M \xrightarrow{k_p} R - M_n^{\bullet}$$

$$R - M_n^{\bullet} + R - M_n^{\bullet} \xrightarrow{k_t} \text{Polymer} \qquad (4)$$

Applying the steady state principle to the primary radical $R^{\bullet}$ as well as to the growing polymer radical $R{-}M_n^{\bullet}$ and taking radical reactivity as independent of radical size, we obtain,

$$-\frac{d[M]}{dt} = R_p = k_p[R - M_n^{\bullet}][M] \qquad (5)$$

$$\text{or } R_p = \left(\frac{k_d}{k_t}\right)1/2\ k_p[1]1/2[M] \qquad (6)$$

From equation (6) it is observed that R_p is directly proportional to [Bromate]$^{1}/_{2}$ [Acrylamide]. The order with respect to bromate has been found half (Fig. 2) but a little deviation has been seen in the case of the monomer.

Dependence of rate on bromate concentration

The initial rate of polymerization as well as the limiting conversion increase with the increase in concentration of the catalyst in the range $(2.4-8.7) \times 10^{-4}$ mol/l at fixed concentrations of acrylamide and ferrous amm. sulphate (Fig. 1). Increase in the amount of bromate brings about an increase in the numbers of free radicals thereby increasing both the rate and the total conversion. The order with respect to bromate was determined from the slope of the double logarithmic plot between initial rate and [Bromate] (Fig. 2) and was found to be 0.54.

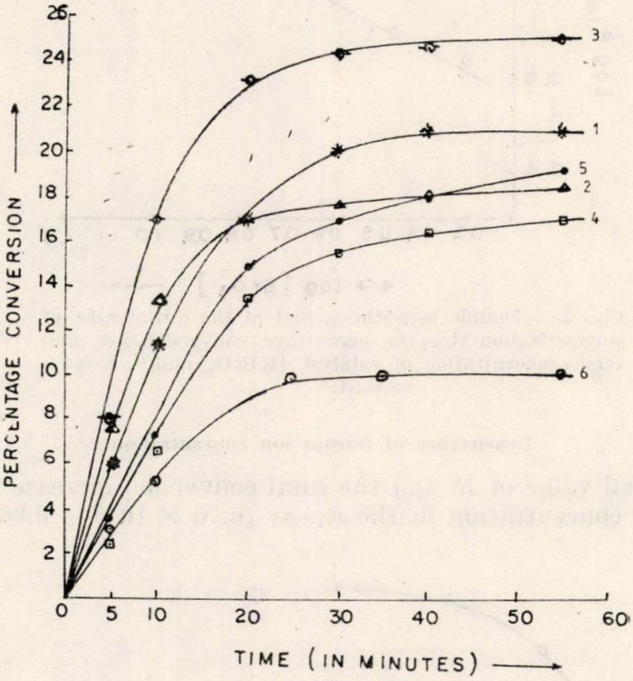

Fig. 1. — Time versus conversion curves for the polymerization of acrylamide at varying concentrations of catalyst. [Acrylamide] $= 10 \times 10^{-2}$ mol/l. ; [Ferrous Amm. Sulphate] $= 1.35 \times 10^{-3}$ mol/l

[$KBrO_3$] $= 7.4 \times 10^{-4}$ mol/l Temp. 35 ± 0.2°C

Control 1 – [$KBrO_3$] $= 7.4 \times 10^{-4}$ mol/l

2 – [$KBrO_3$] $= 10.95 \times 10^{-4}$ mol/l

3 – [$KBrO_3$] $= 8.76 \times 10^{-4}$ mol/l

4 – [$KBrO_3$] $= 4.138 \times 10^{-4}$ mol/l

5 – [$KBrO_3$] $= 5.84 \times 10^{-4}$ mol/l

6 – [$KBrO_3$] $= 2.92 \times 10^{-4}$ mol/l

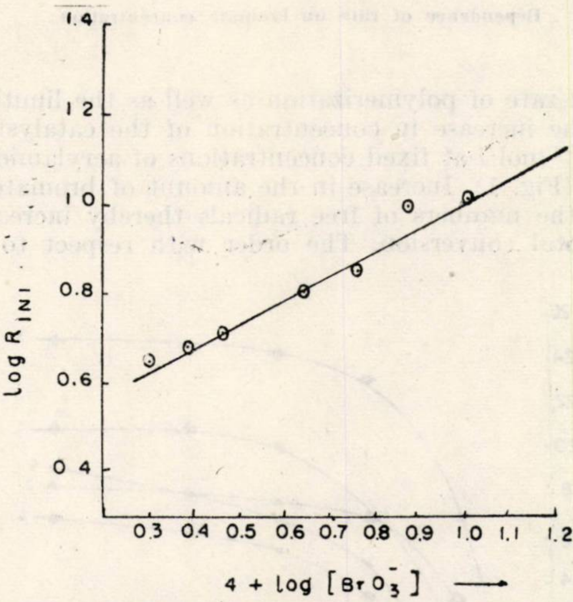

Fig. 2. — Double logarithmic plot of the initial rate of polymerization R_{INI} (in percentage conversion per min) versus concentration of catalyst. [$KBrO_3$] mol/l Slope= = 0.54.

Dependence of ferrous ion concentration

The initial value of R and the total conversion increase with increasing Fe^{2+} ion concentration in the range $(0.76 \times 10^{-3} - 0.96 \times 10^{-3})$ as

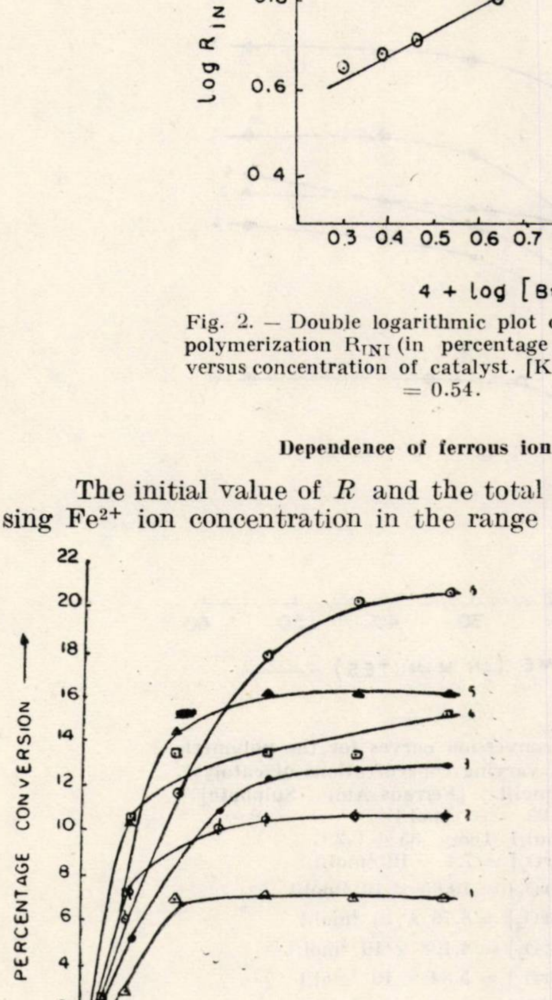

Fig. 3. — Plot of initial course of polymerization for various initial course of ferrous amm. sulphate. [Fe. Amm. Sulphate] =
= 7.68×10^{-4} mol/l — 1
= 2.4×10^{-3} mol/l — 2
= 2.0×10^{-3} mol/l — 3
= 1.92×10^{-3} mol/l — 4
= 0.96×10^{-3} mol/l — 5
= 1.35×10^{-3} mol/l — 6

is generally expected in redox polymerization, and is due to increase in the rate of generation of primary free radicals. But above this concentration of Fe^{2+}, the R_p was found to decrease (Fig. 3) which may be due to :

(a) chain termination by Fe^{3+} ions thus formed in the system;
(b) increase in the ionic strength of the medium which interferes in the normal polymerization process.
(c) the excess ferrous ions get involved in the oxidation of primary free radicals.

$$Fe^{2+} + (OH^{\bullet} \text{ or } Br^{\bullet}) \rightarrow Fe^{3+} + OH^{-} \text{ or } Br^{-}$$

Whatsoever the precise reason may be, the R_p has been found to decrease with increasing Fe^{2+} ion concentration.

Monomer dependence

The dependence of the rate of polymerization on monomer concentration was studied over the range (7.5×10^{-2} mol/l to 25.0×10^{-2} mol/l) and has been shown in Fig. 4). The rate of polymerization increases

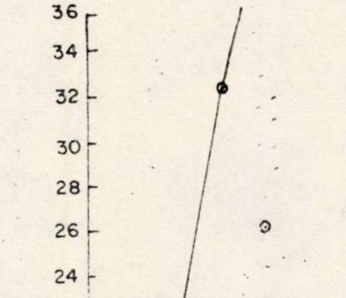

Fig. 4 — Plot of R_{INI} vs. [Monomer] in mol./l.

Fig. 5. — Double logarithmic plot of the initial rate of polymerization R_{INI} (mol./l/min) vs [Monomer], mol/l.
$[KBrO_3] = 7.4 \times 10^{-4}$ mol/l [Fe. Amm. Sulphate] = $= 1.35 \times 10^{-3}$ mol/l Slope = 1.33.

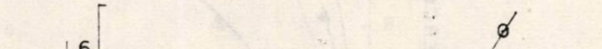

with increasing monomer concentration because of the increased availability of monomer molecules in the propagating step, resulting in an increase in the rate of polymerization. The monomer exponent as calculated from the log-log plot is 1.33 (Fig. 5).

The deviation from linearity as seen in Fig. 4 at higher concentration of monomer may be because of increased viscosity of the medium due to dissolved polymer. Misra et al. have observed similar behaviour.[6]

Temperature dependence

When the temperature of the medium was raised above 35°C, it was seen that the initial rate of polymerization increases and the maximum conversion falls (Fig. 6). At higher temperatures side reactions may set in thereby increasing the possibility of the primary radicals undergoing a change at a faster rate.

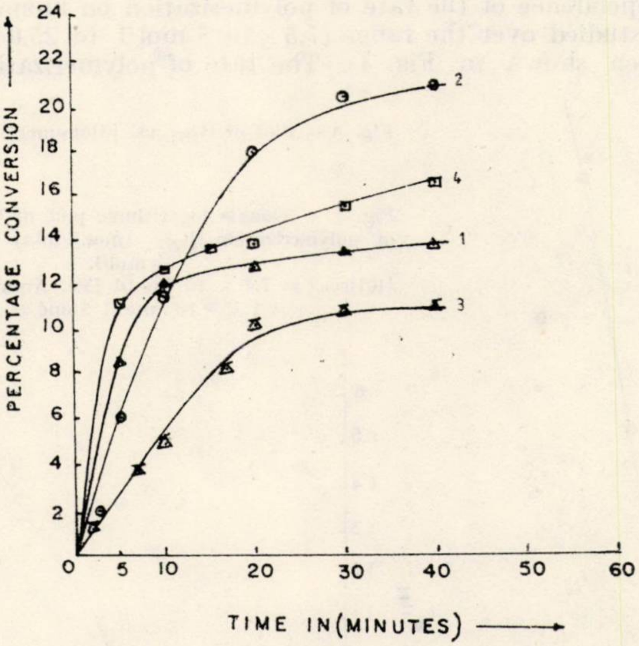

Fig. 6. — Time vs. concentration curves for the polymerization of acrylamide at varying temperatures.
[Monomer] = 10×10^{-2}mol/l
[KBrO$_3$] = 7.4×10^{-4}mol/l
[Fe.Amm.Sulphate] = 1.35×10^{-3} mol/l
30°C – 1 ; 35°C – 2 ; 40°C – 3 ; 45°C – 4

The overall energy of activation as calculated from the Arrhenius' plot (Fig. 7) is found to be 11.54 kcals/deg. mol. within the temperature range 30–45°C. This is in the same line as found in other redox systems.[7,8]

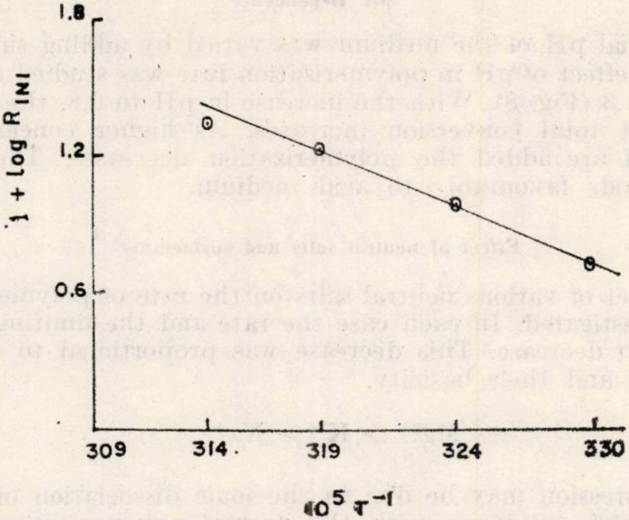

Fig. 7. — Arrhenius' plot [Monomer] = 10×10^{-2} mol/l [KBrO$_3$] = 7.4×10^{-4}mol/l; [Fe. Amm. Sulphate] = $1.35 \times \times 10^{-3}$mol/l Slope = 2.4×10^3

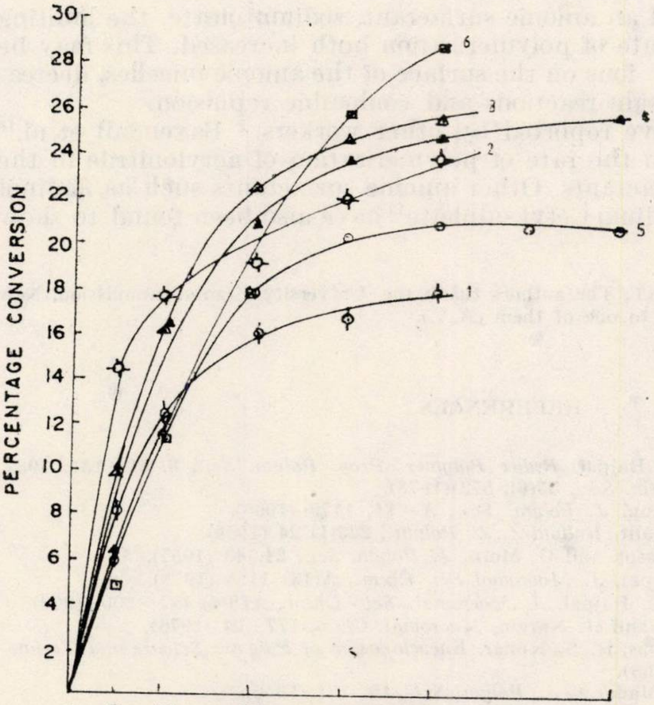

Fig. 8. Time vs conversion curves for the polymerization of acrylamide at varying pH.
[Monomer] = 10×10^{-2} mol/l; [KBrO$_3$] = 2.4×10^{-4} mol/l
[Fe. Amm. Sulphate] = $- 1.35 \times 10^{-3}$mol/l
pH =0.7 —1
=0.8 —2
=1.0 —3
=1.1 —4
=1.13 —5 control
=1.3 —6

pH Dependence

The initial pH of the medium was varied by adding sulphuric acid solution. The effect of pH in polymerization rate was studied over the pH range 0.7 to 1.3 (Fig. 8). With the increase in pH to 0.8, the polymerization rate and total conversion increases. As higher concentrations of sulphuric acid are added the polymerization decreases. The system in general responds favourably to acid medium.

Effect of neutral salts and surfactants

The effect of various neutral salts on the rate of polymerization has also been investigated. In each case the rate and the limiting conversion weré found to decrease. This decrease was proportional to the amount of salt added and their basicity.

$$Mg^{2+} > K^{+} > Na^{+}$$

The depression may be due to the ionic dissociation of the added electrolyte which interferes with the normal polymerization leading to premature termination of the growing polymer chain.

A cationic surfactant, CTAB, retards the rate of polymerization as well as the total conversion, below its CMC value. Polymerization was completely stopped at the CMC value.

In the presence of an anionic surfactant, sodium oleate, the limiting conversion and initial rate of polymerization both increased. This may be due to adsorption of H^{+} ions on the surface of the anionic micelles, decreasing the possibility of side reactions and coulombic repulsion.

Similar results have reported by other workers. [9] Baxendall et al.[10] also reported the rise in the rate of polymerization of acrylonitrile in the presence of anionic surfactants. Other anionic surfactants such as Jadinol PU[11], Cetevlon[12] and Sodium Cetyl sulphate[13] have also been found to show similar results.

ACKNOWLEDGEMENT. The authors thank the University Grants Commission, New Delhi for financial assistance to one of them (A.A.).

REFERENCES

[1] G. S. Misra and U. D. N. Bajpai, *Redox Polymer. Prog. Polym. Sci.*, **8**. 61−131, 1982.

[2] D. Pramanick; *J. Ind. Chem. Soc.*, **55(6)**, 572 (1978).

[3] R. A. Wallace, D. G. Young, *J. Polym. Sci.*, **A−14**, 1179 (1966).

[4] D. Pramanick and S. R. Palit, *Kolloid Z. Z. Polym.*, **229(1)** 24 (1969).

[5] W. M. Thomas, E. H. Gleason and G. Moro, *J. Polym. Sci.*, **24**, 43 (1957).

[6] G. S. Misra, U. D. N. Bajpai, *J. Macromol Sci. Chem.*, **A(13)** 1135 (1979).

[7] U. D. N. Bajpai and A. K. Bajpai, *J. Macromol. Sci−Chem.*, **A19(4)** 487−500 (1983).

[8] G. S. Miscra, J. S. Shzkla and H. Narain, *Macromol. Chem.* **177**., 21 (1976).

[9] S. R. Palit, T. Guha, R. Das, R. S. Konar, *Encyclopaedia of Polymer Science and Technology*, **2**, 229 (1965).

[10] J. H. Baxendale and W. Madaras, *J. Polym. Sci.*, **19**, 171 (1966).

[11] J. S. Shukla, D. C. Misra, *J. Polym. Sci.*, **11**, 751 (1973).

[12] S. R. Palit and R. S. Konar, *J. Polym. Sci.*, **58**, 85 (1962).

[13] S. R. Palit and R. S. Konar, *J. Polym. Sci.*, **Pt A−2**, 173 (1964).

Revue Roumaine de Chimie, **29**, 7, 613–620 (1984)

DIAMAGNETIC SUSCEPTIBILITY EXALTATION AND AROMATICITIES OF UNSATURATED BORON-NITROGEN HETEROCYCLES

BOUBEKEUR MAOUCHE, JOSÉ GAYOSO and OURIDA OUAMERALI

Université des Sciences et de la Technologie Houari Boumediene (U.S.T.H.B.) Institut de Chimie, Laboratoire de Chimie Quantique et Théorique B.P. n°9, Dar El Beida, Alger, Algérie

Received September 16, 1983

We have performed, in the Π-SCF framework, from zero field SCF eigen values and eigenvectors, using coupled Hartree-Fock perturbation technique, calculations of ring current contributions to diamagnetic susceptibilities of a series of eleven Boron-nitrogen unsaturated heterocycles and those of their homologous conjugated hydrocarbons. Our calculations have been at first carried out using the Π-SCF semiempirical Pople's method, with an original parametrization, well adapted to BN heterocyclic compounds, then with a modified version of this method which includes explicitly the σ polarization. The computed magnetic exaltation of borazine agrees quite well with the "experimental" value ($\Lambda\exp = -7.5\ 10^{-6}$emu). Our calculations show that the inclusion of σ polarization enhances the strength of ring currents, and consequently, increases appreciably the values of magnetic exaltations of NB molecules. It appears also that the replacement of a C-C bond by a BN bond in a polyacene molecule reduces strongly the magnetic exaltation and then the aromatic character of the heterocycle.

1 INTRODUCTION

Diamagnetism has recently evoked increasing interest in structural chemistry This can be attributed particularly to improvements in the accuracy of susceptibility measurements and to importance of this concept in the discussion of chemical bonding and aromaticity. Unfortunately, experimental or theoretical diamagnetic data for heterocyclic molecules containing boron and nitrogen atoms are very poor. Up to now, only borazine and some of its derivatives have received some attention. For these molecules, diamagnetic anisotropies have been determined[1–5] and SCF MO calculation on diamagnetic susceptibility has been published.[6] In this paper, we present a comparative study of the diamagnetic susceptibility exaltations and aromaticities of a series of 11 boron-nitrogen unsaturated heterocycles (Fig. 1) and of homologous conjugated hydrocarbons. The close resemblance observed for a number of physical properties of borazine and benzene and, as shown elsewhere,[7] the paralleled properties of the ground state and, to some extent, the lower excited state, of a series of a great number of boron-nitrogen unsaturated compounds and that of the homologous series of conjugated hydrocarbons, prompted us to examine the diamagnetic behavior of these two series of molecules.

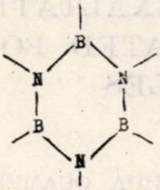

1-Borazine

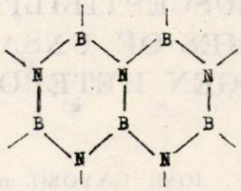

2-BN Naphthalene

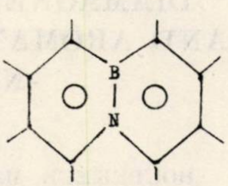

3-9,10 Borazaronaphthalene

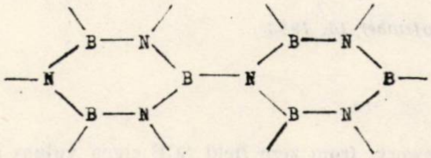

5 - BN Biphenyl

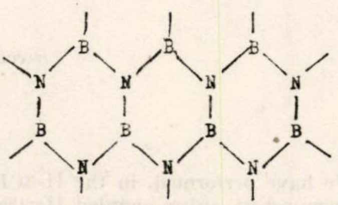

4 - BN Anthracene

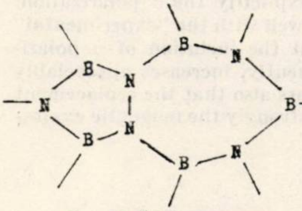

6 - BN (NN) Azulene

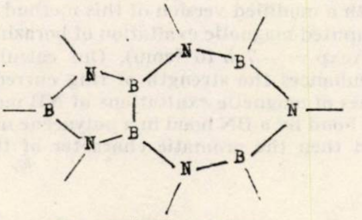

7 - BN (BB) Azulene

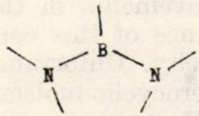

9 - BN (BB) Cyclopentadiene

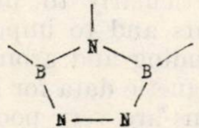

8 - BN (NN) Cyclopentadiene

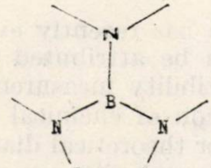

11 - BN(BB) - Fulvene

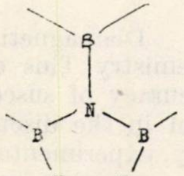

10 - BN (NN)- Fulvene

Fig. 1. — Molecular graphs and nomenclature of the BN unsaturated compounds considered in this work.

The diamagnetism of aromatic compounds is characteristic and can be explained in terms of the electronic structure associated with aromaticity. It is well known that aromatic compounds exhibit strong magnetic anisotropy ; the susceptibility measured normal to the plane is several times greater than that measured parallel to the plane of the ring. Moreover, the mean susceptibility is higher than the value expected on the basis of the incremental system derived theoretically or empirically. According to Pauling [8] and London, [9] only the susceptibility normal to the plane of the ring contributes to the high value of the mean diamagnetism, so, this term involves the diamagnetic effect of the delocalized π electrons that give rise to a molecular ring current in the aromatic system. This London susceptibility is closely related to the diamagnetic susceptibility exaltation introduced in magneto chemistry by Pacault [10] and which is generally considered as magnetic analog of the resonance energy. This susceptibility exaltation (Λ) may be defined as the difference between the molar susceptibility (χ_M) measured for a compound and that estimated (χ'_M), for a cyclopolyene of the same structure, using a Pascal like increment system

$$\Lambda = \chi_M - \chi_M' \tag{1}$$

Dauben et al. [11] have shown that the magnetic exaltation may be considered as a good *qualitative* aromaticity criterion. Furthermore, it has been shown, recently,[12] in our Laboratory, that the magnetic exaltation, Λ, may be transformed in a good *quantitative* aromaticity index, defined by the formula

$$\rho = K \frac{n\Lambda}{S^2} \tag{2}$$

where n is the number of π electrons S the total surface area of the cycles of the molecule under consideration and K a scaling constant which can be determined by reference to benzene ($\rho = 1$ for this compound).

Theoretically the susceptibility exaltations of cyclic conjugated compounds may be evaluated with the help of the Pauling-London "ring current" model. The "ring current" susceptibilities, χ_π^c, are simply related to the magnetic exaltations:

$$\Lambda = \frac{\chi_\pi^c}{3} \tag{3}$$

In this work, we have determined the magnetic exaltations of borazine, BN-analogs of naphtalene, anthracene, biphenyl, cyclopentadienyl anion and cation, fulvene, azulene and that of the homologous conjugated hydrocarbons. We have also considered the Dewar's borazaro Naphtalene which is an intermediate molecule between these two series (Fig. 1).

2 METHODS OF CALCULATION

Our calculations have been firstly carried out using the π-SCF semi-empirical method. [13] Secondly, we have used a method where the polarisation of the σ system is introduced in a simple and "natural" way by reducing the CNDO/2 method to the π system only. [14] It is well known that in BN-unsaturated compounds to a π charge transfer from the nitrogen lone pair to the empty boron p-orbital, there is, superimposed a strong electron withdrawing through the σ framework in opposite direction which leads, in most cases, to positive net charges on boron atoms and negative ones on nitrogen atoms. So, interaction between these two systems is too important to neglect the effect of the σ-polarisation on π structure in such molecules. This semiempirical procedure which has been worked out in our laboratory, has been termed $\pi(\sigma)$-SCF. In both cases the magnetic exaltations have been calculated, from zero field SCF eigenvalues and eigenvectors, using the so-called *coupled Hartree-Fock perturbation technique*. We recall below briefly the principle of this last method and this technique.

a) — $\pi(\sigma)$-SCF method — In planar conjugated molecules, the Roothaan hamiltonian matrix, F, can be separated into two sub-matrices : F_π and F_σ corresponding to the π and σ systems. The secular equation is then split up into a system of two interdependant equations which, in CNDO/2 approximations and for σ or π system, assume the form :

$$F_{rr} = -\chi_{rr} - \left(C_R + \frac{1}{2}(q_r - 1) \right) \gamma_{RR} - \sum_{S \neq R} C_S \gamma_{RS} \tag{4a}$$

$$F_{rs} = \beta^c_{rs} - \frac{1}{2} P_{rs} \gamma_{RS} \,;\; \chi_r = \frac{1}{2}(I_r + A_r) \tag{4b}$$

where C_R is the electronic charge on the atom R, q_r and χ_r the electronic density and electronegativity of the rth AO, and P_{rs} an element of the bond order matrix. When we reduce CNDO/2 method to π system only, the matrix elements F_{rr} and F_{rs} become :

$$F_{rr} = \bar{I}_r + \frac{1}{2} q_r \gamma_{rr} + \sum_{s \neq r} (q_s - \bar{n}_s) \gamma_{rs} \,;\; \bar{n}_s = C_{s\sigma} + n_s \tag{5a}$$

$$F_{rs} = \beta^c_{rs} - \frac{1}{2} P_{rs} \gamma_{rs} \,;\; \bar{I}_r = U_r - C_{r\sigma} \gamma_{rr} \,;\; U_r = -I_r - (n_r - 1) \gamma_{rr} \tag{5b}$$

These matrix elements have then the same form as in π-SCF Pople's method, provided that we neglect resonance integrals β^c_{rs}, corresponding to non bonded atoms. In equation (5), n_r is the number of electrons contributed to the π system by the A.O. r centered on the nucleus of atom R. The quantity U_r defined in (5b) may be considered as an ionization potential which corresponds to the neutral atom R in its Valence state for $n_r = 1$, to the cation of R for $n_r = 2$ and to the anion of this atom for $n_r = 0$. The one-centre Coulomb integral is calculated using the empirical Pariser[15] formula :

$$\gamma_{rr} = I^\delta_r - A^\delta_r \,;\quad \delta = 0, -1, +1 \leftrightarrow n_r = 0,1,2 \tag{6}$$

The two-centre electron repulsion integrals are evaluated using the Mataga-Nishimoto[16] relationship:

$$\gamma_{rs} = \frac{e^2}{\Gamma_{rs} + td_{rs}} \; ; \quad \Gamma_{rs} = \frac{2e^2}{\gamma_{rr} + \gamma_{ss}} \tag{7}$$

The σ charges are determined with the aid of the following simple empirical formula; (see ref.[17]).

$$C_{r\sigma} = k_\lambda \frac{\chi_s - \chi_r}{\chi_s + \chi_r} \tag{8}$$

where χ_r and χ_s are the Pauling electronegativities of the atoms R and S to which belongs, respectively, the A.O. r and s. The quantities t and k_σ appearing in Eqs. (7) and (8) are purely empirical parameters which have to be determined by fitting theoretical results to experimental ones.

b) — Coupled Hartree-Fock Perturbation Technique. — The technique used here is that developed by Stevens, Pitzer and Lipscomb.[18] In the framework of this technique, the core hamiltonian h, which is a function of the magnetic field H, may be expanded in the form of a Power series as

$$h = h^0 + Hh^1 + H^2h^2 + \dots \tag{9}$$

where h^0, h^1, h^2 are independent of H. The total magnetic susceptibility of the molecule is given by

$$\chi = -4 \sum_{i=1}^{m} \left(h^2_{ii} + \sum_{j=m+1}^{n} C^1_{ij} h^1_{ji} \right) \tag{10}$$

where the terms h^1_{ii} and h^2_{ii} are defined as follows:

$$h^2_{ii} = \langle \Psi^0_i | h^2 | \Psi^0_i \rangle \; ; \quad h^1_{ji} = \langle \Psi^0_j | h^1 | \Psi^0_i \rangle \tag{11}$$

In these expressions Ψ^0_i is the space part-of the ith spinorbital Φ^0_i of the nonperturbad system, m is the number of doubly occupied MO and n the total number of MO. The coefficients C^1_{ij} are independant of H; they determine the first order corrections Ψ^1_i of the non-perturbated MO Ψ^0_i. These coefficients are solutions of the following system of $m(n-m)$ linear inhomogeneous equations:

$$\sum_{k=1}^{m} \sum_{e=m+1}^{n} \left((\langle li | jk \rangle - \langle ki | jl \rangle) + (e^0_j - e^0_i) \delta_{jl} \delta_{ik} \right) C^1_{lk} = - h^1_{ji} \tag{12a}$$

$$i \in (1, m), \; J \in (m+1, n) \tag{12b}$$

$$\langle ij | kl \rangle = \iint \Psi^0_i(1) \Psi^0_j(1) \frac{e^2}{r_{12}} \Psi^0_k(2) \Psi^0_l(2) \, d\tau, \; d\tau_2 \tag{12c}$$

we can see, from $_0$equation (10) that the total susceptibility is the sum of two contributions, χ^d and χ^p, which have been called, respectively, diamagnetic and paramagnetic parts of the diamagnetic molecular susceptibility. From equation (10), χ^d and χ^p obviously defined as follows:

$$\chi = \chi^d + \chi^p \tag{13a}$$

$$\chi^p = -4 \sum_{i=1}^{m} \sum_{j=m+1}^{n} C^1_{ij} h^1_{ji} \quad \chi^d = -4 \sum_{i=1}^{m} h^2_{ii} \tag{13b}$$

3 RESULTS AND DISCUSSION

The B-N heterocycles considered in this work are portrayed in Fig. 1. Unfortunately, there are no generally accepted rules for naming inorganic ring systems. Therefore *we have used a simple nomenclature which consists in naming a Boron-Nitrogen unsaturated heterocycle by adding the "prefix" BN to the name of the isoelectronic conjugated hydrocarbon having the same molecular graph.* For example, following our nomenclature, Borazine would be termed BN-Benzene. The structural formulae of non alternant BN compounds, contains a homonuclear N-N or B-B bond. To avoid ambiguity, this homonuclear bond has been indicated after the "prefix" BN, in the name attributed to each non alternant heterocycle (see Fig. 1).

Table 1

Magnetic exaltations (Λ in −10 emu) in BN-insaturated heterocycles and in isoelectronic conjugated hydrocarbons

Molecule	Π-SCF	Π(σ)-SCF	Molecule	Π-SCF	Π(σ)-SCF
1 – Borazine	5.31	8.95	Benzene	10.22	10.69
2 – BN Biphenyl	10.75	18.44	Biphenyl	19.62	20.51
3 – BN Naphthalene	10.29	20.30	Naphthalene	22.07	23.10
4 – 9, 10 Borazaro-Naphthalene	19.37	21.45			
5 – BN Anthracene	15.08	32.57	Anthracene	34.68	27.43
6 – BN(NN)Azulene	1.99	6.24	Azulene	23.43	22.49
7 – BN(BB)Azulene	6.56	20.18			
8 – BN(NN)Cyclopentadiene	3.32	4.74	Cyclopenta-dienyl Anion	5.22	5.46
9 – BN(BB)Cyclopentadiene	−5.43	−15.97			
10 – BN(NN)Fulvene	2.47	2.74	Fulvene	−1.75	−1.77
11 – BN(BB)Fulvene	−3.39	−16.10			

COMMENTS: Π-SCF: Semiempirical Pople's method with a parameterization adapted to the treatment of unsturated boron-nitrogen compounds (see ref. 7). Π(σ)-SCF: Semiempirical Pople's method in which the valence ionisation potential I_B and I_N have been replaced by empirical parameters (I_B and I_N) which include σ polarization (see ref. 14 and this text). All the calculations have been carried out using the coupled Hartree-Fock perturbation technique proposed by Lipscomb et al. (see ref. 18).

The computed magnetic exaltations (Λ) of BN heterocycles are shown in Table 1. For comparative purposes, we have also reported in this table, the computed exaltations of the isoelectronic conjugated hydrocarbons. The magnetic aromaticity indexes (see Eq. 2) obtained using the theoretical exaltation values are given in table 2. The results listed in these two tables suggest the following remarks.

— According to the two methods, the magnetic exaltations of the BN unsaturated heterocycles are much smaller than the ones obtained for the isoelectronic conjugated hydrocarbons. The SCF Π methods, which take the effect of the σ polarization into account or which ignore it are then qualitatively consistent with the results given by the Hückel-London Theory[19]. The magnetic exaltation obtained for naphtalene is greater than the one obtained for 9,10-borazaronaphtalene. This indicates clearly that the replacement of a cc bond by a BN bond, reduces considerably the magnetic exaltation and the aromatic character of a polyacene.

— Classification in orders of magnitude of Λ given by the two methods is exactly the same for the hydrocarbons but is appreciably different for the BN unsaturated homologous heterocycles. The $\Pi(\sigma)$-SCF method only gives for the two series of molecules an analogous classification for the isotopological compounds.

The magnetic exaltations computed using the $\Pi(\sigma)$-SCF method appear to be greater in magnitude than the ones obtained with the help of the Π-SCF procedure. According to these results, it seems that the inclusion of σ polarization in the Π-SCF Pople's framework enhances the "strength of ring currents" and, consequently, increases the values of magnetic exaltations.

— On the basis of the results listed in table 2, it can be seen that, despite some numerical disagreement existing between the Π-SCF aro-

Table 2

Magnetic aromaticity indexes p (number without unit) in unsaturated heterocycles and of isoelectronic conjugated hydrocarbons

Molecule	Π-SCF	$\Pi(\sigma)$SCF	Molecule	Π-SCF	$\Pi(\sigma)$SCF
1 – Borazine	0.464	0.748	Benzene	1.000	1.000
2 – BN Biphenyl	0.470	0.771	Biphenyl	0.960	0.960
3 – BN Naphthalene	0.374	0.707	Naphthalene	0.900	0.901
4 – 9, 10 Borazaro-Naphthalene	0.790	0.836			
5 – BN Anthracene	0.342	0.706	Anthracene	0.880	0.665
6 – BN(NN)Azulene	0.068	0.205	Azulene	0.900	0.899
7 – BN(BB)Azulene	0.225	0.662			
8 – BN(NN)cyclopentadiene	0.662	0.904	Cyclopentadienyl anion	1.165	1.165
9 – BN(BB)cyclopentadiene	−0.722	−2.030			
10 – BN(NN)Fulvene	0.493	0.522	Fulvene	−0.391	−0.378
11 – BN(BB)Fulvene	−0.676	−3.070			

COMMENTS The surface arreas (*S*) appearing in Eq 2 have been calculated using idealized geometrics. All the cycles have been considered to be regular with numerical standard values for lengths of C–C (1.40Å) and B–N (1.44Å) bonds.

maticity indexes and the ones obtained using the $\Pi(\sigma)$-SCF method it seems necessary to attribute appreciable aromatic character to BN-polyacene and to BN-biphenyl. As for the two five membered heterocycles, our calculations show that the BN-(NN) – cyclopentadiene has an aromaticity index comparable to that of cyclopentadienyl anion, while the heterocycle with three boron atoms appears as antiaromatic. The two BN-fulvenes also can be distinguished clearly by their aromaticity index. It seems that the BN-(BB)-fulvene owing to its antiaromatic character, will be the real analog of the fulvene molecule. This result is in a good accord with that obtained through the MNDO study of the structural propreties of these molecules.[20] Turning now to the two BN-azulenes isomeres, it appears that these molecules are, at most, slightly aromatic (or pseudoaromatic).

— Lastly, it is noteworthy that the magnetic exaltation of borazine given by the SCF-Π and SCF-$\Pi(\sigma)$ methods are in very good agreement with that obtained experimentally ($\Lambda = -7.5$ 10 emu) by Dauben et al.[11]

REFERENCES

[1] M. Kubo, H. Watanabe and K. Ito, *J. Am. Chem. Soc.*, **86**, 1251 (1964).
[2] K. Lonsdale, *Nature*, **184**, 1060 (1959).
[3] K. Lonsdale and E. W. Toor, *Acta cryst.*, **12**, 1048 (1959).
[4] K. Muszkat, A. and B. Kirson, *Bull. Res. Council Israel* **Sect. A.**, **11**, 219 (1962).
[5] H. Watanabe, K. Ito and M. Kubo, *J. Am. Chem. Soc.*, **82**, 3294 (1960).
[6] D. W. Davies, *Trans. Farad. Soc.*, **57**, 2081 (1961).
[7] B. Maouche, these de 3e cycle, Alger, 1976.
[8] L. Pauling, *J. Chem. Phys.*, **4**, 2375 (1936).
[9] F. London, *J. Phys. Radium.*, **8**, 397 (1937).
[10] A. Pacault, *Ann. Chim.* (Paris), ser. XIII, 1946, 527; *Rev. Sci.*, 1948, 86, 38; *Bull. Soc. Chim. Fr.*, 1949, 16, 40 and 371.
[11] H. J. Dauben Jr., J. D. Wilson and J. L. Laity, *Org. Chem.*, **16**, 167 (1971).
[12] J. Gayoso and O. Ouamerali, *Rev. Roum. Chim.*, **26**, 7 (1981).
[13] J. A. Pople, *Trans. Farad. Soc.*, **49**, 1375 (1953).
[14] J. Gayoso, B. Maouche and A. Boucekkine, *C. R. Acad. Sci.*, Série C, **276**, 257 (1973).
[15] R. Pariser, *J. Chem. Phys.*, **21**, 568 (1953).
[16] N. Tyutyulkov, A. Gochev and F. Fratev, *Chem. Phys. Lett.*, **4**, 9 (1969).
[17] H. A. Hammond, *Theoret. Chim. Acta* (Berlin), **18**, 239 (1970).
[18] B. M. Stevens, P. M. Pitzer and W. N. Lipscomb, *J. Chem. Phys.*, **38**, 550 (1963).
[19] B. Maouche, Thèse d'Etat, Alger 1983.
[20] B. Maouche and J. Gayoso; *C.R. Acad. Sci.*, Paris 293, 141 (1981).

Revue Roumaine de Chimie, **29**, 7, 621–622 (1984)

COMPTES RENDUS

"Topics in Inorganic and Physical Chemistry" (Structure and Bonding, vol. 50), Springer–Verlag, Berlin–Heidelberg–New York, 1982, 178 pages, 98 DM (hard-cover).

Volume 50 in the Springer Series "Structure and Bonding" contains four contributions concerned with the chemistry of metal complexes, their structures, properties and applications, especially in biological systems.

J. A. Ibers, L. J. Pace, J. Martinsen and B. M. Hoffman are the authors of the first article entitled "Stacked Metal Complexes : Structures and Properties". This review discusses crystals that contain molecular stacks and are made of two components, at least one of which is a planar transition-metal chelate complex. One of the components may be considered as an electron donor, D, or its cation, D^{+P} ; the other an acceptor, A, or its anion, A^{-P}. Some of these compounds are primarily of structural interest, while others have unusual magnetic and electric properties.

"The Chemistry of Technetium : Toward Improved Diagnostic Agents" is written by M. J. Clarke, and P. H. Fackler.^{99m}Tc is now the preferred isotope for many diagnostic studies involving the imaging of internal organs by radioscintigraphic techniques because this element is continuously produced in some abundence during the operation of fission nuclear reactors, and because its chemistry is rich, even when limited to aqueous solutions. Recent synthetic methods are now available for preparing coordination complexes involving Tc(III), Tc(IV), and Tc(V).

An examination of the structure of lanthanide (III) ion complexes using nuclear magnetic resonance is made by R. J. P. Williams in his paper "The Chemistry of Lanthanide Ions in Solution and in Biological Systems". The importance of hydratation in both the inner and outher spheres is stressed. The structural data are used in an attempt to understand the stability constants and the rate of exchange of bound ligands.

The last survey, "Uranyl Photophysics" written by C. K. Jorgensen and R. Reisfeld deals with the extremely stable triatomic uranyl ion OUO^{+2}. The electron transfer bands of the uranyl group are due to the complicated manifold of excited levels by relativistic effects in linear symmetry. The lowest of these levels can live for longer than 1 millisescond (in the absence of adjacent hydrogen atoms) and has its own chemistry, reacting with many anions, univalent silver and thallium, in a way entirely different from the ground state. The spectroscopic and luminescent properties are compared with the hexafluorides and the dioxo complexes of quinquevalent and sixvalent uranium, neptunium, and americium with roughly octahedral species, and tungstates.

The present volume, like all the others in this series, is a very useful source of up-to-date information in coordination chemistry. By classifying and reviewing the structural data, the authors provide a firm basis for improving the understanding of the relation between physical properties and the structural features of these compounds. Consequently large applications in medicine and biology are possible, as it was shown above.

Ursula Bologa

"Structures Versus Special Properties" (Structure and Bonding, vol. 52), Springer–Verlag, Berlin–Heidelberg–New York, 1982, 202 pages, 108 DM (hard-cover).

The first paper, "Natural Optical Activity and the Molecular Hypothesis", is written by R. G. Woolley. The approach used in this article is well known in theoretical physics, but is novel as far as chemistry is concerned. It is based on the view that macroscopic matter is described by a suitable generalized formulation of quantum mechanics, namely Quantum Field Theory. Atoms and molecules are characterized as composite elementary excitations (or quasi-particles) of the macroscopic quantum-mechanical system which we call matter, and the spontaneously broken space inversion symmetry revealed by the existence of optical-isomerism is studied in this context.

L. Banci, A. Benici, C. Benelli, D. Gatteschi, and C. Zanchini are the authors of the next article entitled "Spectral-Structural Correlations in High-Spin Cobalt (II) Complexes". The spectral and magnetic properties of simple high-spin cobalt (II) complexes are reviewed with the aim of showing how to relate the experimental data to the electronic structure and the coordination geometry of the complexes. It is hoped that this may be of help to all research workers who need to characterize cobalt (II) complexes as a spectroscopic probe.

The third article, "Relationships Between Structure and Low-Dimensional Magnetism in Fluorides", written by A. Tressaud and J. M. Dance emphasizes the relationships between crystallographic features and dimensionality of the magnetic interaction in fluorides. The compounds involved are characterized by rings, chains, layers and three-dimensional arrangements of fluorinated MF_6 octahedra.

The last review, "Structure and Bonding in Organic Derivatives of Antimony (V", written by V. K. Jain, R. Bohra, and R. C. Mehrotra is concerned with structural chemistry of antimony (V) during the last decade (the last book on this subject appeared in 1970). It is shown that compounds of the type $SbL_nX_{5-n}(n = 1-5, X=\text{halogen}, L=\text{ligand})$, $RSbL_nX_{5-n}$ and $R_2SbL_nX_{2-n}$ have hexacoordinated environments around antimony which can be acquired either by chelation of the ligand or by molecular association.

Volume 52 in the Springer series "Structure and Bonding" is concerned with interesting aspects related to experimental and theoretical chemistry. All the articles are valuable sources of up-to-date information and key to the voluminous primary literature.

Ursula Bologa

"Light Scattering from Polymers", Advances in Polymer Science, vol. 48, Springer—Verlag, Berlin, Heidelberg, New York, 1983.

The present volume contains two papers, namely "Static and Dynamic Light Scattering from Branched Polymers and Biopolymers" and "Photon Correlation Spectroscopy of Bulk Polymers".

As it is known, the most probable conformation of a macromolecular chain is represented by a random coil. The usual method for determining the shape of macromolecules is static light scattering. The medium size of a macromolecular coil can be obtained by representing the experimental data in the well known. Zimm plot. Dynamic light scattering is a more recent technique, allowing access to information such as internal mobility or the translational motion of the mass centre. Needless to say that all measurements are performed using dilute polymer solutions.

The first article presents the mathematical models (the Flory-Stockmayer theory and the further developed cascade branching theory), describing randomly branched polymers. Using 242 references, most of them recent ones, various applications (polycondensation processes, substitution effects, vulcanization of chains) are reviewed.The experimental results were found in good agreement with the behaviour predicted by the cascade theory.

The second article deals with the development of the field of photon correlation spectroscopy from bulk polymers. The great majority of papers reviewed describe tests performed near the glass transition in polymers. It is important to notice that light scattering from bulk polymers is a very weak effect. Acccordingly, a strong laser is required to carry out measurements and special precautions have to be taken in sample preparation. These facts explain that the references quoted cover contributions made, in general, later than 1975.

Both papers present a high interest to all of those engaged in research activities in the field of physical chemistry of polymers.

Dan Sorin Vasilescu

ORSZÁGOS MŰSZAKI INFORMÁCIÓS KÖZPONT ÉS KÖNYVTÁR 1984

NOTE POUR LES AUTEURS

La Revue Roumaine de Chimie publie des articles en anglais, français, russe, allemand ou espagnol. Les auteurs sont priés d'envoyer des articles et des comptes rendus inédits.

Les manuscrits seront dactylographiés à double interligne. La bibliographie, les tableaux et la légende des figures seront placés après le texte.

Si l'article fait partie d'une série numérotée, la partie précédente sera donnée comme premiére référence.

Chaque article sera précédé d'un résumé comprenant quinze lignes au maximum.

Les références bibliographiques dans le texte seront faites par des exposants sans parenthèses et paraîtront à la fin de l'ouvrage.

Les publications périodiques mentionnées dans la bibliographie seront présentées suivant les prescriptions internationales : le nom de l'auteur précédé de l'initiale du prénom, le titre du périodique abrégé conformément à « Chemical Abstracts » et souligné par une ligne, le numéro du tome indiqué par des chiffres arabes et souligné par deux lignes, suivi de la première page de l'article ; à la fin, l'année de la parution sera placée entre parenthèses. La numéro de la revue ne sera pas indiqué si les pages du volume sont numérotées consécutivement.

Les textes des livres ou traités inclueront : le nom des auteurs, l'initiale du prénom, le titre du livre entre guillemets et sans être souligné, le numéro du tome précédé par l'abréviation « vol. » (ou « Bd. »), le numéro de l'édition, les éditions (the publisher), la localité de la parution du livre, l'année de la parution et la page de la référence précédée(s) par l'abréviation « p » (ou « S »).

Les brevets seront indiqués comme suit : l'auteur ou la firme, le pays et le numéro du brevet, la date et la revue (*Chem. Abstr.*). Par ex. : M. Jones (to Union Carbide Co)., Brit. Pat. 601 238, 2 Sept. 1959 ; cf. *Chem. Abstr.*, **54**, 12808 (1960).

Si la référence n'a pas été lue en original, on indiquera aussi la revue de références consultée.

Les diagrammes seront tracés à l'encre de Chine sur papier calque. Les tableaux et les figures (en nombre strictement nécessaire), ainsi que les courbes dans les figures seront numérotés par des chiffres arabes. Leur explication sera donnée dans la légende des figures. Prière de ne pas inscrire les mêmes données dans les tableaux et les figures. Chaque tableau aura un titre. On indiquera dans le texte la place approximative des tableaux et des figures. Les formules chimiques seront incluses dans le texte ; en outre, elles seront transcrites sur papier calque, à l'encre de Chine.

Les auteurs sont priés d'indiquer les caractères italiques (en soulignant les lettres au crayon), ainsi que tout autre caractère spécial : les préfixes *ortho, meta, para, cis, trans,* etc. seront soulignés pour indiquer leurs caractères italiques et ne seront jamais écrits avec des majuscules.

Aucune correction à la main ne sera admise sur le manuscrit. Les corrections seront tapées à la machine. Les lettres grecques on d'autres symboles spéciaux seront insérés à la main à l'encre clairement.

Le manuscrit sera signé par l'auteur.

Le titre-courant aura 50 lettres au maximum.

L'entière responsabilité du contenu des articles appartient aux auteurs.

Sur demande on peut obtenir une note plus complète.

PRINTED IN ROMANIA

1984 AUG 1 2

TRAVAUX PARUS AUX ÉDITIONS DE L'ACADÉMIE DE LA RÉPUBLIQUE SOCIALISTE DE ROUMANIE

ELENA CEAUŞESCU, **Cercetări în chimia şi tehnologia polimerilor**, 1983, 519 p.

N. ASANDEI, A. GRIGORIU, **Chimia şi structura fibrelor**, 1983, 395 p.

N. IONESCU, M. CĂLDĂRARU, **Oxidarea catalitică a olefinelor inferioare**, 1983.

C. CAŞCAVAL, **Studiul polimerilor prin piroliză şi cromatografie de gaze**, 1983, 220 p.

C. I. SIMIONESCU, F. DANES, **Originea vieţii**, 1983, 110 p.

C. BODEA (sub redacţia), **Tratat de biochimie vegetală**, partea II, volumul IV, 1982, 408 p.

I. G. MURGULESCU, RODICA VÎLCU, **Introducere în chimia fizică. Vol. III.** Termodinamica chimică, 1982, 624 p.

I. G. MURGULESCU, J. PĂUN. **Introducere în chimia fizică. Vol. I. 3. Nucleul atomic, reacţii nucleare, particule elementare**, 1982, 606 p.

ELENA CEAUŞESCU, **Noi cercetări în domeniul compuşilor macromoleculari**, 1981, 536 p.

I. G. MURGULESCU, TATIANA ONCESCU, E. SEGAL, **Introducere în chimia fizică vol. II. 2. Cinematică chimică şi cataliză**, 1981, 1024 p.

V. DRĂGUŢAN, A. T. BALABAN, M. DIMONIE, **Metateza olefinelor şi polimerizarea prin deschidere de inel a cicloolefinelor**, 1981, 254 p.

LYDIA-MARIA VAICUM, **Epurarea apelor uzate cu nămol activ. Bazele biochimice**, 1981, 218 p.

I. GALATEANU, **Procese şi metode radiochimice în energetica nucleară**, 1981, 234 p.

O. IORDACHE, **Procese polistocastice aplicate în fenomenele de transfer**, 1981, 187 p.

GR. SIMIONESCU, VALERIA GORDUZA, **Polimeri biocompatibili şi biologic activi**, 1980, 479 p.

ELENA CEAUŞESCU, **Polimerizarea stereospecifică a izoprenului**, 1979, 307 p.

CONST. GH. MACAROVICI, **Analiza chimică cantitativă anorganică**, 1979, 457 p.

M. FLORESCU, **Metode ştiinţifice în dezvoltarea industriei chimice moderne**, 1979, 256 p.

A. T. BALABAN, I. GĂLĂŢEANU, G. GEORGESCU, LIGIA SIMIONESCU, **Compuşi marcaţi şi radiofarmaceutici cu aplicaţii în medicina nucleară**, 1979, 495 p.

I. G. MURGULESCU, E. SEGAL, **Introducere în chimia fizică. Vol. II.1.Teoria molecular cinetică a materiei**, 1979, 1036 p.

S. STERNBERG, FL. DANEŞ. **Termodinamica chimică aplicată**, 1978, 400 p.

I. G. MURGULESCU, V. EM. SAHINI, **Introducere în chimia fizică. Vol. I.2. Structura şi proprietăţile moleculelor**, 1978, 604 p.

I. ZUGRĂVESCU, MAGDA PETROVANU, **N-ylid chemistry**, coédition avec McGraw Hill International Book Company, U.S.A., 1977, 396 p.

I, G. MURGULESCU, **Introducere în chimia fizică, Vol. I, 1. Atomi, moleculă, legătură chimică**, 1976, 560 p.

ELENA CEAUŞESCU, **Research work on synthesis and characterization of macromolecular compounds. Contributions**, 1974, 251 p.

CR. SIMIONESCU, VIORICA RUSAN, V. POPA, **Chimia algelor marine**, 1974, 212 p., 1 pl.

1984 AUG 3 1

ISSN 0035–4090

I.P. INFORMAŢIA cd. 2219

43 426

Lei 40

$ 75 (pour un abonnement annuel)

1103

Vegyészet
REFERALVA

ACADÉMIE DE LA RÉPUBLIQUE SOCIALISTE DE ROUMANIE

REVUE ROUMAINE DE CHIMIE

TOME 29
N° 8
Août 1984

Rev. Roumaine Chim.

RRCHAX, 29, 8, p. 623 – 716 (1984), Bucarest

EDITURA ACADEMIEI REPUBLICII SOCIALISTE ROMÂNIA

ACADÉMIE DE LA RÉPUBLIQUE SOCIALISTE DE ROUMANIE

COMITÉ DE RÉDACTION

Rédacteur en chef:

I. G. MURGULESCU, membre de l'Académie de la République Socialiste de Roumanie

Rédacteurs en chef adjoints :

A. T. BALABAN et V. EM. SAHINI, membres correspondants de l'Académie de la République Socialiste de Roumanie

Collège de rédaction :

EM. BRATU, ELENA CEAUŞESCU, ECATERINA CIORĂNESCU-NENITZESCU, CR. SIMIONESCU, membres de l'Académie de la République Socialiste de Roumanie : P. SPACU, membre correspondant de l'Académie de la République Socialiste de Roumanie : M. BANCIU, M. GHEORGHIU, I. HAIDUC, D. I. MARCHIDAN, I. MOLDOVAN, G. NIAC et D. SĂNDULESCU

La Revue Roumaine de Chimie paraît 10 fois par an. Toute commande de l'étranger pour les travaux parus aux Editions de l'Académie de la République Socialiste de Roumanie sera adressée à ROMPRESFILATELIA — sectorul export-import presă, P.O.Box 12—201, telex 10376 prsfi r, Calea Griviţei nr. 64—66, Bucarest, Roumanie

Les manuscrits, les livres et les revues proposés en échange, ainsi que toute correspondance seront envoyés à la rédaction :

REVUE ROUMAINE DE CHIMIE

125, Calea Victoriei, 79717 Bucarest, Roumanie, téléphone 50 76 80

EDITURA ACADEMIEI REPUBLICII SOCIALISTE ROMÂNIA
125, Calea Victoriei, 79717 Bucarest, Roumanie, téléphone 50 76 80

REVUE ROUMAINE
DE
CHIMIE

ORSZÁGOS MŰSZAKI INFORMÁCIÓS KÖZPONT ÉS KÖNYVTÁR 1883

Tome 29, N° 8 **Août, 1984**

V. POPA, E. SEGAL and M. VLAD, A new general form of Wegsheider's cyclicity conditions 625–629

NICOLETA ȘTEFAN, PETRU FILIP, ILIE G. DINULESCU, FILIP CHIRALEU and MARGARET AVRAM, Investigations in the cyclobutane series. LVIII. Stereoisomeric epoxides of the angular dimer of benzocyclobutadiene 631–638

G. IVAN and MARIA GIURGINCA, Influence of carbon black – antidegradant interaction on the behaviour of rubber compounds in thermo-oxidative degradation. . . . . 639–646 R

I. V. NICOLESCU, J. V. RAJAOFANOVA, LIGIA FRUNZĂ, FLORENTINA AVRAMESCU, RODICA MĂNĂILĂ, OLGA ȘERBAN, G. NEDELCU and V. BIDIAN, Activation of the natural zeolite clinoptilolite, structural properties and catalytic activity . . . . 647–654 R

ELENA CONSTANTINESCU and HILDEGARD DENGEL, Thermogalvanic cell with acqueous cesium chloride solutions (in German) 655–661

C. DODET, F. NOVILLE, M. CRINE and JEAN-PAUL PIRARD, A study of the texture of seabed nodules for potential use as catalysts (in French) . . 663–670

DUMITRU MĂNOIU, MARIA MĂNOIU, ILIE G. DINULESCU and MARGARET AVRAM, Friedel-Crafts acylation of alkynes. III. Reaction of 1-alkynes with acetyl chloride in the presence of silver perchlorate 671–676

C. ONISCU, AL. CECAL and E. HOROBA, Kinetic studies for the formation of a sulfamethine silver salt using radioisotopes (in German) 677–681

CLEOPATRA VASILIU OPREA, CLAUDIA NEGULIANU and FELICIA WEINER, Mechano-chemical modification of physical and chemical characteristics of poly(vinylchloride) suspension 683–692

E. BARRADO and R. PARDO, Use of an aged nitrate-selective electrode as halide-sensor in potentiometric titrations 693–698

S. STERNBERG, T. VIȘAN and ADINA COTÂRȚĂ, Electrochemical reactions of cupric and cupreous ions in lithium chloride – potassium chloride eutectic. II. Steady-state potentiostatic studies 699–706

METODIU RĂILEANU, Solvent effects. III. Solvent influence on the reaction of the phenothiazine with nitrous acid 707–713

BOOK REVIEWS 715–716

| Rev. Roumaine Chim. | **29**, *8*, 623–716 (1984), Bucarest

Revue Roumaine de Chimie, **29**, *8*, 625–629 (1984)

A NEW GENERAL FORM OF WEGSHEIDER'S CYCLICITY CONDITIONS

V. POPA*, E. SEGAL* and M. VLAD**

* Center of Physical Chemistry, ICECHIM — Bucharest, Splaiul Independentei 202, 79611, Romania

* Polytechnical Institute of Bucharest, Department of Physical Chemistry and Electrochemical Technology, Bd. Republicii 13, 70346, Romania

** Industrial Central for Medicinal Drugs, Cosmetics, Dyestuffs and Lacquers, Bucharest, Bd. Ion Şulea 246, 78014 Romania

Received July 21, 1983

On the basis of the previously derived properties [1] of the stoichiometric matrix a new form of the cyclicity conditions is found. The equivalence of this new form with the already established one [2] is proved.

The detailed balance principle [3] leads, under certain circumstances, to additional relationships between the rate constants, i.e. the well-known Wegsheider's cyclicity conditions. [2–6] In a previous paper, [2] a general form of these was derived for the reaction network

$$\sum_{i=1}^{S} \nu_{ij} A_i \underset{k'_j}{\overset{k_j}{\rightleftarrows}} \sum_{i=1}^{S} \nu'_{ij} A_i, \ j = 1, \ldots, R \tag{1}$$

$$1 \leqslant \Sigma\, \nu_{ij}, \Sigma\, \nu'_{ij} \leqslant 3 ; \ \nu_{ij}, \nu'_{ij} \geqslant 0 \ \ \forall_{i,j} \tag{1'}$$

The acquired relationships are

$$\frac{k_{K+\alpha}}{k_{K+\alpha}} = \prod_{j=1}^{K} \left(\frac{k_j}{k'_j} \right)^{[\mathbf{\Phi}^{+}_{VS} \mathbf{\Phi}_{SK} (\mathbf{\Phi}^{+}_{KS}\, \mathbf{\Phi}_{SK})^{-1}]_{\alpha j}} ; \quad \alpha = 1, \ldots, V = R - K \tag{2}$$

where

$$f_{ij} = \nu'_{ij} - \nu_{ij} ; \ i = 1, \ldots, S ; \ j = 1, \ldots, R$$

$$\mathbf{f}_S^{(j)} = \begin{pmatrix} f_{1j} \\ \vdots \\ f_{Sj} \end{pmatrix} ; \ j = 1, \ldots, R \tag{3}$$

are the stoichiometric vectors corresponding to the reactions (1),

$$\mathbf{F}_{SR} = \| \mathbf{f}_S^{(1)} \ldots \mathbf{f}_S^{(R)} \| = \| f_{ij} \|_{j=1,\ldots,R}^{i=1,\ldots,S} \tag{4}$$

is the stoichiometric matrix whose rank is K, and $\mathbf{\Phi}_{SK}$ and $\mathbf{\Phi}_{SV}$ are partitions of the $\mathbf{F}_{SR}$:

$$\mathbf{F}_{SR} = \| \mathbf{\Phi}_{SK} \,\vdots\, \mathbf{\Phi}_{SV} \| = \left\| \begin{array}{c|c} \mathbf{G}_{KK} & \mathbf{G}_{KV} \\ \hline \mathbf{G}_{uK} & \mathbf{G}_{uV} \end{array} \right\|, \; u = S - K, V = R - K, \tag{5}$$

with

$$\operatorname{rank} \mathbf{\Phi}_{SK} = \operatorname{rank} \mathbf{F}_{SR} = \operatorname{rank} \mathbf{G}_{KK} = K \tag{6}$$

Using some general properties of the stoichiometric matrix recently found, [1] we can derive a new form of these cyclicity conditions. In order to do this, we shall write the detailed balance conditions

$$k_j \prod_{i=1}^{S} \bar{A}_i^{\nu_{ij}} = k'_j \prod_{i=1}^{S} \bar{A}_i^{\nu'_{ij}}, \; j = 1, \ldots, R, \tag{7}$$

(for ideal systems which obey the mass-action law, with $\bar{A}_i$ denoting equilibrium concentrations), in a logarithmic form

$$\ln(k_j/k'_j) = \sum_{j=1}^{S} f_{ij} \ln \bar{A}_i = \| \ln \bar{A}_i \|_S^+ \, \mathbf{f}_S^{(j)}, \, j = 1, \ldots, K, \tag{7'}$$

$$\ln(k_{K+\alpha}/k'_{K+\alpha}) = \sum_{i=1}^{S} f_{i\,K+\alpha} \ln \bar{A}_i = \| \ln \bar{A}_i \|_S^+ \, \mathbf{f}_S^{(K+\alpha)}, \; \alpha = 1, \ldots, V. \tag{7''}$$

But we showed that [1]

$$\mathbf{f}_S^{(K+\alpha)} = \sum_{j=1}^{K} \mathbf{f}_S^{(j)} \gamma_{j\alpha}, \; \alpha = 1, \ldots, V, \tag{8}$$

where

$$\mathbf{\Gamma}_{KV} = \| \gamma_{ij} \| = \mathbf{G}_{KK}^{-1} \, \mathbf{G}_{KV} \tag{9}$$

Expressing in Eq. (7″) the linear dependent stoichiometric vectors by means of Eq. (8), we get

$$\ln(k_{K+\alpha}/k'_{K+\alpha}) = \sum_{j=1}^{K} \gamma_{j\alpha} \| \ln \bar{A}_i \|_S^+ \, \mathbf{f}_S^{(j)}, \tag{10}$$

and taking into account Eq. (7′)

$$\ln\left(k_{K+\alpha}/k'_{K+\alpha}\right) = \sum_{j=1}^{K} \gamma_{j\alpha} \ln(k_j/k'_j), \tag{11}$$

wherefrom, by means of Eq. (9) we get the sought for equations

$$\frac{k_{K+\alpha}}{k'_{K+\alpha}} = \prod_{j=1}^{K} \left(\frac{k_j}{k'_j}\right)^{(\mathbf{G}_{KK}^{-1}\,\mathbf{G}_{KV})_{j\alpha}} \tag{12}$$

Eqs. (12) has a much simpler form than these previously derived, (2). The equivalence between the two forms is easy to prove, as follows:

Using the identity [1]

$$\boldsymbol{\Phi}_{SV} = \boldsymbol{\Phi}_{SK}\,\mathbf{G}_{KK}^{-1}\,\mathbf{G}_{KV} = \boldsymbol{\Phi}_{SK}\,\boldsymbol{\Gamma}_{KV} \tag{13}$$

the exponents of Eqs. (2) become

$$[\boldsymbol{\Phi}^{+}_{VS}\,\boldsymbol{\Phi}_{SK}(\boldsymbol{\Phi}^{+}_{KS}\,\boldsymbol{\Phi}_{SK})^{-1}]_{\alpha j} = [\boldsymbol{\Gamma}_{VK}\,(\boldsymbol{\Phi}^{+}_{KS}\,\boldsymbol{\Phi}_{SK})\,(\boldsymbol{\Phi}^{+}_{KS}\,\boldsymbol{\Phi}_{SK})^{-1}]_{\alpha j} =$$

$$= [\boldsymbol{\Gamma}^{+}_{VK}]_{\alpha j} = [\boldsymbol{\Gamma}_{KV}]_{j\alpha} = [\mathbf{G}_{KK}^{-1}\,\mathbf{G}_{KV}]_{j\alpha},$$

q.e.d.

We can get a deeper insight into the mathematical aspects of the problem by means of an alternate derivation, using a sort of "axis transform". In order to do this we transcribe Eqs. (7) and (7′) in a matricial form

$$\mathbf{H}^{+}_{R} = \mathbf{P}^{+}_{S}\,\mathbf{F}_{SR}, \tag{14}$$

or, partitioning

$$\|\mathbf{H}^{+}_{K} \mid \mathbf{H}^{+}_{V}\| = \|\mathbf{P}^{+}_{K} \mid \mathbf{P}^{+}_{u}\|\,\mathbf{F}_{SR} \tag{14'}$$

where

$$\mathbf{H}^{+}_{K} = \|\ln(k_1/k'_1) \ldots \ln(k_K/k'_K)\|;\quad \mathbf{H}^{+}_{V} = \|\ln(k_{K+1}/k'_{K+1}) \ldots \ln(k_R/k'_R)\|;$$
$$\mathbf{P}^{+}_{K} = \|\ln \bar{A}_1 \ldots \ln \bar{A}_K\|;\quad \mathbf{P}^{+}_{u} = \|\ln \bar{A}_{K+1} \ldots \ln \bar{A}_S\|. \tag{15}$$

The multiplication of Eq. (14′) with a *square nonsingular* matrix, $\mathbf{N}_{RR}$, leads to an equivalent form

$$\|\mathbf{H}^{+}_{K} \mid \mathbf{H}^{+}_{V}\|\,\mathbf{N}_{RR} = \|\mathbf{P}^{+}_{K} \mid \mathbf{P}^{+}_{u}\|\,\mathbf{F}_{SR}\,\mathbf{N}_{RR}, \tag{16}$$

with

$$\text{rank } \mathbf{N}_{RR} = \mathrm{R}. \tag{16'}$$

We are looking for a particular form of the matrix $\mathbf{N}_{RR}$ which fulfills both (16′) and

$$\mathbf{F}_{SR}\,\mathbf{N}_{RR} = \left\| \begin{array}{c:c} \mathbf{G}_{KK} & \mathbf{O}_{KV} \\ \mathbf{G}_{uK} & \mathbf{O}_{uV} \end{array} \right\|. \tag{17}$$

Taking into account the partition (5), Eq. (17) may be written in the following form

$$\left\| \begin{array}{c:c} \mathbf{G}_{KK} & \mathbf{G}_{KV} \\ \hdashline \mathbf{G}_{uK} & \mathbf{G}_{uV} \end{array} \right\| \left\| \begin{array}{c:c} \mathbf{N}_{KK} & \mathbf{N}_{KV} \\ \hdashline \mathbf{N}_{VK} & \mathbf{N}_{VV} \end{array} \right\| = \left\| \begin{array}{c:c} \mathbf{G}_{KK} & \mathbf{O}_{KV} \\ \hdashline \mathbf{G}_{uK} & \mathbf{O}_{uV} \end{array} \right\|, \tag{17′}$$

which leads to

$$\mathbf{G}_{KK}\,\mathbf{N}_{KK} + \mathbf{G}_{KV}\,\mathbf{N}_{VK} = \mathbf{G}_{KK}, \tag{18}$$

$$\mathbf{G}_{uK}\,\mathbf{N}_{KK} + \mathbf{G}_{uV}\,\mathbf{N}_{VK} = \mathbf{G}_{uK}, \tag{19}$$

$$\mathbf{G}_{KK}\,\mathbf{N}_{KV} + \mathbf{G}_{KV}\,\mathbf{N}_{VV} = \mathbf{O}_{KV}, \tag{20}$$

$$\mathbf{G}_{uK}\,\mathbf{N}_{KV} + \mathbf{G}_{uV}\,\mathbf{N}_{VV} = \mathbf{O}_{uV}. \tag{21}$$

Multiplying Eqs. (18) and (20) with $\mathbf{G}_{KK}^{-1}$ and introducing the acquired expressions of $\mathbf{N}_{KK}$ and $\mathbf{N}_{KV}$ in Eqs. (19) and (20), respectively, we get the following equivalent system

$$\mathbf{N}_{KK} = \mathbf{I}_{KK} - \mathbf{G}_{KK}^{-1}\mathbf{G}_{KV}\,\mathbf{N}_{VK}, \tag{22}$$

$$(\mathbf{G}_{uV} - \mathbf{G}_{uK}\,\mathbf{G}_{KK}^{-1}\,\mathbf{G}_{KV})\,\mathbf{N}_{VK} = \mathbf{O}_{uK}, \tag{23}$$

$$\mathbf{N}_{KV} = -\,\mathbf{G}_{KK}^{-1}\,\mathbf{G}_{KV}\,\mathbf{N}_{VV}, \tag{24}$$

$$(\mathbf{G}_{uV} - \mathbf{G}_{uK}\,\mathbf{G}_{KK}^{-1}\,\mathbf{G}_{KV})\,\mathbf{N}_{VV} = \mathbf{O}_{uV}. \tag{25}$$

But we showed that [1]

$$\mathbf{G}_{uV} = \mathbf{G}_{uK}\,\mathbf{G}_{KK}^{-1}\,\mathbf{G}_{KV} \tag{26}$$

and from Eqs (23) and (25) it turns out that $\mathbf{N}_{VK}$ and $\mathbf{N}_{VV}$ are arbitrary and so there are $(VK + V^2)$ infinities of matrices, $\mathbf{N}_{RR}$, satisfying Eq. (17′):

$$\mathbf{N}_{RR} = \left\| \begin{array}{c:c} \mathbf{I}_{KK} - \mathbf{G}_{KK}^{-1}\,\mathbf{G}_{KV}\,\mathbf{N}_{VK} & -\,\mathbf{G}_{KK}^{-1}\,\mathbf{G}_{KV}\,\mathbf{N}_{VV} \\ \hdashline \mathbf{N}_{VK} & \mathbf{N}_{VV} \end{array} \right\|. \tag{27}$$

As we are looking for a nonsingular matrix of the form (27), the most convenient choice of the arbitrary matrices is

$$\mathbf{N}_{VK} = \mathbf{O}_{VK}, \tag{28}$$

$$\mathbf{N}_{VV} = \mathbf{I}_{VV}. \tag{29}$$

This results in the following expression of $\mathbf{N}_{RR}$:

$$\mathbf{N}_{RR} = \left\| \begin{array}{c|c} \mathbf{I}_{KK} & -\mathbf{G}_{KK}^{-1}\,\mathbf{G}_{KV} \\ \hline \mathbf{O}_{VK} & \mathbf{I}_{VV} \end{array} \right\|, \tag{30}$$

which, obviously, fulfills the condition

$$\det \mathbf{N}_{RR} = \begin{vmatrix} 1 & . & . & . & . & . & . & . \\ 0 & 1 & . & . & . & . & . & . \\ \vdots & 0 & . & . & . & . & . & . \\ \vdots & \vdots & & & & & & \vdots \\ \vdots & \vdots & & & & & & \vdots \\ 0 & 0 & . & . & . & . & . & 1 \end{vmatrix} = 1 \neq 0. \tag{31}$$

Combining Eqs. (14′), (17′) and (30), we get

$$\| \mathbf{H}_K^+ \,\vdots\, \mathbf{H}_V^+ \| \left\| \begin{array}{c|c} \mathbf{I}_{KK} & -\mathbf{G}_{KK}^{-1}\,\mathbf{G}_{KV} \\ \hline \mathbf{O}_{VK} & \mathbf{I}_{VV} \end{array} \right\| = \| \mathbf{P}_K^+ \,\vdots\, \mathbf{P}_u^+ \| \left\| \begin{array}{c|c} \mathbf{G}_{KK} & \mathbf{O}_{KV} \\ \hline \mathbf{G}_{uK} & \mathbf{O}_{uV} \end{array} \right\|, \tag{32}$$

wherefrom:

$$\mathbf{H}_K^+ = \mathbf{P}_K^+\,\mathbf{G}_{KK} + \mathbf{P}_u^+\,\mathbf{G}_{uK} \equiv \mathbf{P}_S^+\,\mathbf{\Phi}_{SK} \tag{33}$$

and

$$-\,\mathbf{H}_K^+\,\mathbf{G}_{KK}^{-1}\,\mathbf{G}_{KV} + \mathbf{H}_V^+ = \mathbf{O}_V. \tag{34}$$

The scalar transcription of Eqs. (33) leads to Eq. (7′). Taking into account Eq. (9), the scalar form of Eq. (34) leads to the cyclicity conditions (11) and (12).

Considering other possible forms of the matrix $\mathbf{N}_{RR}$ obeying Eq. (16), i.e., using other matrices $\mathbf{N}_{VK}$ and $\mathbf{N}_{VV}$, we can find sets of cyclicity conditions different from (11) and (12), but equivalent with these.

REFERENCES

[1] E. Segal, M. Vlad, V. Popa, *Rev. Roumaine Chim.*, **29**, 7 (1984).

[2] M. Vlad, E. Segal, *Rev. Roumaine Chim.*, **24**, 807 (1979).

[3] R. C. Tolman, *Phys. Rev.*, **23**, 699 (1924); *Proc. Nat. Acad. Sci. U.S.A.*, **11**, 436 (1925); "The Principles of Statistical Mechanics", Clarendon Press, Oxford, 1938, p. 163.

[4] R. Wegsheider, *Z. phys. Chem.*, **39**, 257 (1902).

[5] G. N. Lewis, *Proc. Nat. Acad. Sci. U.S.A.*, **11**, 179 (1925).

[6] J. Z. Hearon, *Bull. Math. Biophys.*, **15**, 121 (1953).

Revue Roumaine de Chimie, **29**, *8*, 631–638 (1984)

INVESTIGATIONS IN THE CYCLOBUTANE SERIES. LVIII[1]

STEREOISOMERIC EPOXIDES OF THE ANGULAR DIMER OF BENZOCYCLOBUTADIENE

NICOLETA ŞTEFAN,[a] PETRU FILIP,[a] ILIE G. DINULESCU,[a] FILIP CHIRALEU,[a] and MARGARET AVRAM[b,*]

[a] Center of Organic Chemistry, Spl. Independenţei 202B, 78100 Bucharest 12, Romania
[b] Laboratory of Organic Chemistry, Polytechnic Institute — TCH, Spl. Independenţei 313, 72206 Bucharest 16, Romania

Received September 28, 1983

The synthesis of *exo*-**2** and *endo*-**3** epoxides of the angular dimer of benzocyclobutadiene (**1**) are presented. The structure and stereochemistry of hydroxy and dihydroxyderivatives formed from **2** and **3** by the oxirane ring opening are discussed.

As part of our studies concerning the chemistry of benzocyclobutadiene dimers [2–6] with dibenzo [b.g] bicyclo[4.2.0]octa-2,4,7-triene skeleton (**1**), the synthesis of the epoxides with *exo* (**2**) and *endo* (**3**) oriented oxiranic ring as well as their behaviour in the oxirane ring opening reactions were investigated.

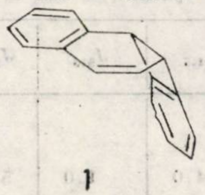
1

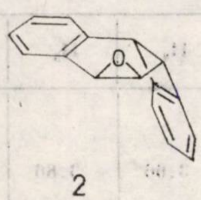

2

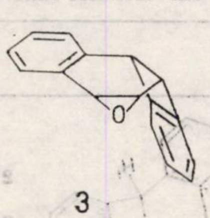

3

In a previous work [2] we proved that the electrophilic attack to the double bond of the dimer **1** occurs from the *exo* side of the molecule. Since the formation of the epoxidic ring takes place through the electrophilic attack of the peracid [7] we expected to obtain the *exo*-epoxide **2** on treatment of the dimer **1** with perbenzoic acid.

Indeed we obtain the *exo* epoxide **2** mixed with variable amounts of dihydroxyderivative **4**, the acid catalysed oxirane ring opening product of **2**.

---

[*] Deceased in 1983.

The dihydroxyderivative **4** is the sole reaction product when treating **1** with hydrogen peroxide in formic acid.

The *endo*-epoxide **3** was obtained from the earlier described bromohydroxyderivative **5** by treatment with natrium hydroxide in dimethylformamide solution.

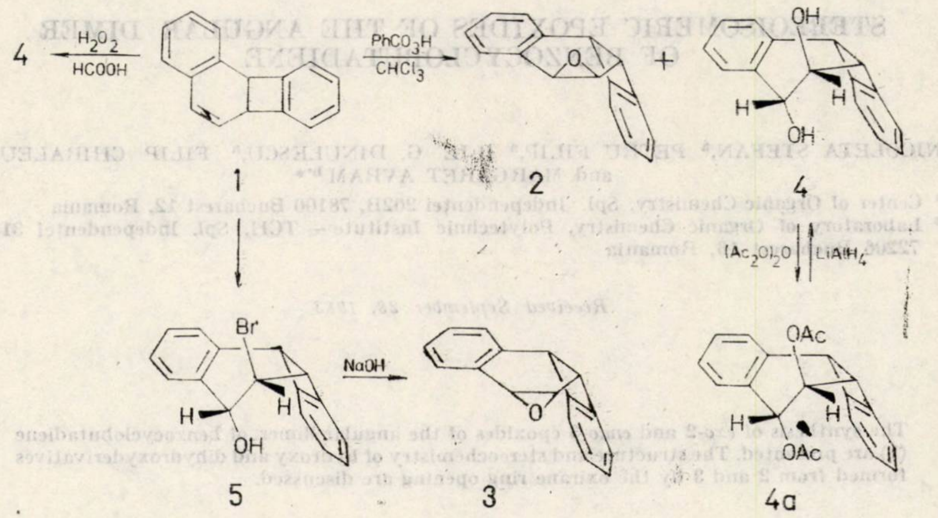

The structure and stereochemistry of the epoxides **2** and **3** were ascribed on the basis of the ^{1}H-NMR spectral data presented in table 1 and elemental analysis.

Table 1

The chemical shifts (δ, ppm) and coupling constants (Hz) of the epoxides **2** and **3**

		H_1	H_4	H_5	H_6	$J_{4.5}$	$J_{5.6}$	$J_{1.6}$
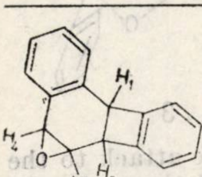	**2**	4.55	3.66	3.86	4.40	4.0	1.0	5.2
	3	4.58	3.63 —	3.90	4.06	4.0	4.0	5.5

* The coupling constants of **3** were obtained from the spectrum recorded in the presence of Eu(DPM)$_3$.

The values of the coupling constants between H-5 and H-6 protons gave informations about the orientation of the oxiranic ring in **2** and **3**.

For the *exo* orientation of the epoxidic ring, the expected dihedral angle between H-5 and H-6 protons evaluated from Dreiding models is about 70° which involves a low value for $J_{5,6}$. The experimental value for $J_{5,6}$ being 1.0 Hz the *exo* orientation of the oxiranic ring was attributed to **2**.

For the *endo* epoxide **3**, the molecular model shows a dihedral angle near 20°, corresponding to the observed value of 4.0 Hz for $J_{5,6}$. The same coupling constant was measured for the eclipsed epoxidic protons H-4 and H-5.

The formation of the *endo* epoxide **3** from **5** is a normal SNi substitution due to the favourable diaxial orientation of the hydroxy and bromine groups in **5**.

The tendency of **5** to intramolecular substitution was also observed during the reduction with lithium-aluminium hydride.

Thus aiming to obtain the benzylic alcohol **6** by reduction of bromine from **5** with lithium-aluminium hybride we obtained two positional isomeric hydroxyderivatives. They were separated by thin layer chromatography and identified as being the 4-hydroxyderivative **7** (m.p. 160°) and the 5-hydroxyderivative **6** (m.p. 138°).

The position of the hydroxy groups in **6** and **7** was established on the basis of the spectral data of their oxidation products, the ketones **8** and **9** respectively.

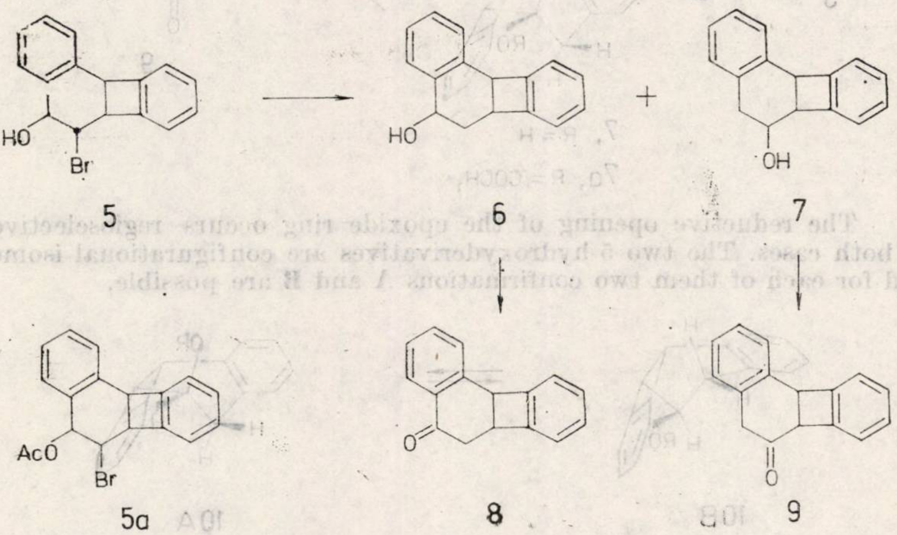

Thus, the carbonyl group frequency in **8** appears at 1700 cm^{-1} in accordance with the expected value for a benzylic ketone; in the IR spectrum of **9** the $\nu_{C=O}$ absorption at 1720 cm^{-1} indicates a saturated six membered ring ketone.

In the ^{1}H-NMR spectrum of **9** the geminal H-4 benzylic protons displayed an AB system (J_{AB} 17.0 Hz) while in the spectrum of **8** the geminal H-5 protons were observed as a complex ABX system formed by coupling with H-6.

The formation of the alcohol **7** in this reaction could be explained by the formation as an intermediate of the *endo*-epoxide **3**. This reaction is probably due to the basicity of lithium-aluminium hydride. This mechanism is supported also by the ring opening of *endo*-epoxide **3** with lithium-aluminium hydride.

The reduction of the *exo*-epoxide **2** and of the *endo*-epoxide **3** with lithium-aluminium hydride gave the 5-hydroxyderivatives **10** and respectively **7**, both characterized as acetoxyderivatives (**10a**, **7a**).

The oxidation of 5-hydroxyderivatives **10** and **7** afforded the same ketone **9**.

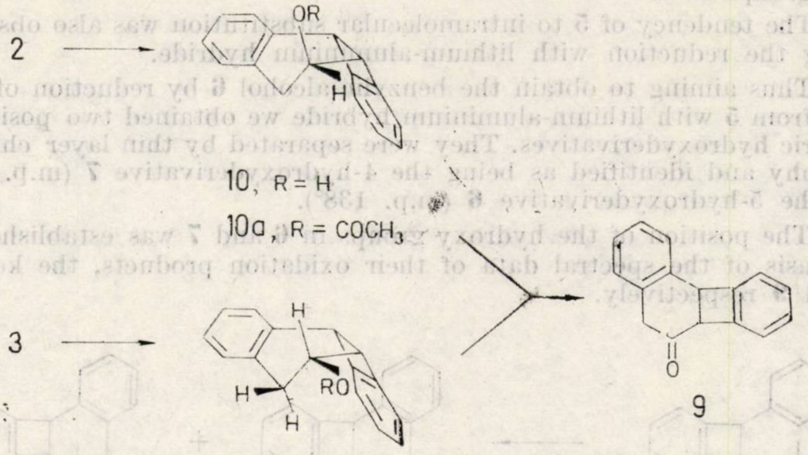

10, R = H

10a, R = COCH$_3$

7, R = H

7a, R = COCH$_3$

9

The reductive opening of the epoxide ring occurs regioselectively in both cases. The two 5-hydroxyderivatives are configurational isomers and for each of them two confirmations **A** and **B** are possible.

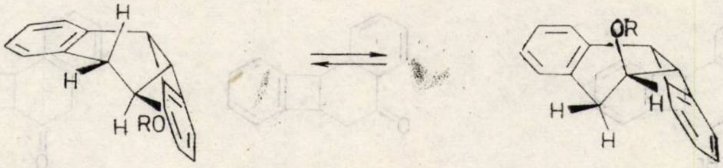

10B

10A

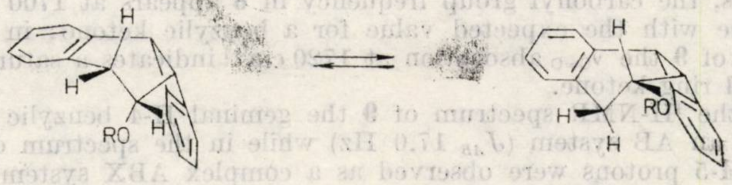

7B

7A

The analysis of ^{1}H-NMR spectra of the acetoxyderivatives **10a** and **7a** offers arguments concerning the conformations of these compounds. Thus the ^{1}H-NMR spectrum of the **5**-*exo*-acetoxyderivative **10a** shows for the H-5 proton ($\delta = 5.55$ ppm) a quartet with two different coupling constants of 3.0 and 4.0 Hz.

The examination of the Dreiding molecular models of **10A** and **10B** shows that in the conformer **10A** the *endo*-equatorial orientation of the H-5 proton is in agreement with the displayed spectrum; consequently the 5-acetoxy group in **10a** and 5-hydroxy group in **10** respectively has the *exo*-axial orientation as in **10A** conformer.

In the ^{1}H-NMR spectrum of the 5-*endo*-acetoxyderivative **7a** for H-5 proton, two different coupling constants are visible having values of 5.15 and 11.5 Hz. These values are in agreement with the dihedral angles for the **7A** conformer in which the protons at C-4 and C-5 are axial.

The acid catalysed oxiranic ring opening of the *exo*- and *endo*- epoxides **2** and **3** in the presence of the formic acid was investigated.

In both cases unisolable formylderivatives are formed which after hydrolysis gave the corresponding dihydroxyderivatives. From the *exo*-epoxide **2** the dihydroxyderivative **4** (m.p. 230–232°) was formed. The *endo*-epoxide **3** gave a mixture of two dihydroxyderivatives **11** and **12**.

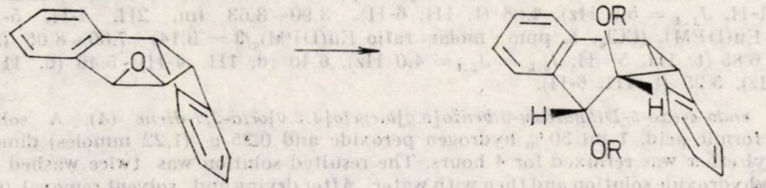

2

4, R = H

4a, R = COCH$_3$

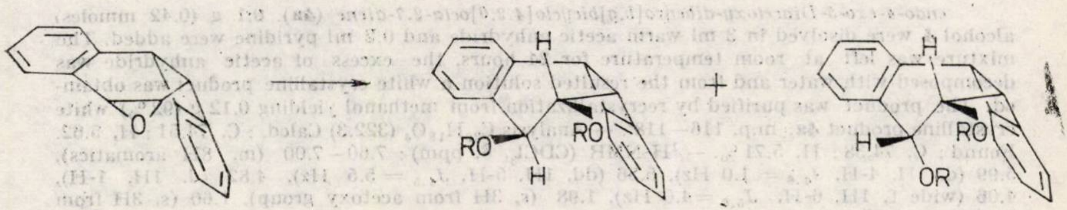

3

11, R = H

11a, R = COCH$_3$

12, R = H

12a, R = COCH$_3$

All the dihydroxyderivatives were treated with acetic anhydride to give the diacetates which were analyzed by spectroscopic methods. The diacetoxyderivative **11a** results also by the acetolysis of the bromoacetoxyderivative **5a**[3,8] in the presence of potassium acetate.

All these diacetoxyderivatives have an **A** type conformation. The arguments for the conformation of the skeleton and for the orientation of the acetoxy group in **4a**, **11a** and **12a** are presented in the following paper. [8]

EXPERIMENTAL

IR spectra were recorded with a double beam Jena UR-20 spectrophotometer. ^{1}H-NMR spectra were determined with a Varian A60-A spectrometer.

exo-4,5-Epoxy-dibenzo[b,g]bicyclo[4.2.0]octa-2,7-diene (**2**). 1.0 g (4.89 mmoles) benzocyclobutadiene dimer **1** was dissolved in 20 ml trichloromethane and a chloroformic solution containing 1.38 g (10 mmoles) perbenzoic acid was added. The mixture was left at room temperature for 24 hours. Water was added and the organic layer was quickly washed with 2 % natrium hydroxide solution. After washing with water, drying and solvent removal, the crude product was recrystallized from pethroleum ether/diethyl ether, yielding 0.3 g (28 %) epoxide **2**, m.p. 102°. — Analysis : $C_{16}H_{12}O$ (220.2) Calcd. : C, 87.24 ; H, 5.49. Found : C, 86.99 ; H, 5.78 %. — ^{1}H-NMR (CCl_4, δ, ppm) : 7.00—7.50 (m, 8H aromatics), 4.55 (d, 1H, 1-H, $J_{1.6} = 5.2$ Hz), 4.40 (d, 1H, 6-H), 3.86 (dd, 1H, 5-H, $J_{4.5} = 4.0$ Hz, $J_{5.6} = 1.0$ Hz), 3.66 (d, 1H, 4-H).

endo-4,5-Epoxy-dibenzo[b.g]bicyclo[4.2.0.]octa-2,7-diene (**3**). A solution of 8.3 ml 0.1 N natrium hydroxide (containing 0.83 mmoles natrium hydroxide) was gradually added to a stirred solution of 0.25 g (0.83 mmoles) bromohydrine **5** in 15 ml dimethylformamide. After 2 hours at room temperature from the resulted solution 0.15 g (83 %) **3** as a white product, m.p. 109° was crystallized. — Analysis $C_{16}H_{12}O$ (220.2) Calcd. : C, 87.24 ; H, 5.49. Found : C, 87.05 ; H, 5.71 %. — ^{1}H-NMR (CCl_4, δ, ppm) : 7.00—7.50 (m, 8H aromatics), 4.58 (d, 1H, 1-H, $J_{1.6} = 5.5$ Hz), 4.06 (t, 1H, 6-H), 3.90—3.63 (m, 2H, 4-H, 5-H). ^{1}H-NMR with $Eu(DPM)_3$ (CCl_4, δ, ppm ; molar ratio $Eu(DPM)_3$/**3** = 0.14) : 7.00—8.05 (m, 8H aromatics), 6.85 (t, 1H, 5—H, $J_{4.5} = J_{5.6} = 4.0$ Hz), 6.40 (d, 1H, 4-H), 5.46 (d, 1H, 1-H, $J_{1.6} = 5.5$ Hz), 5.25 (t, 1H, 6-H).

endo-4-exo-5-Dihydroxy-dibenzo[b.g]bicyclo[4.2.0]octa-2,7-diene (**4**). A solution of 3 ml 98 % formic acid, 1 ml 30 % hydrogen peroxide and 0.25 g (1.22 mmoles) dimer **1** in 35 ml diethyl ether was refluxed for 4 hours. The resulted solution was twice washed with 50 % natrium hydroxide solution and then with water. After drying and solvent removal 0.25 g (86.2 %) white crystalline product **4** m.p. 230—232° (decn.) were obtained. — Analysis $C_{16}H_{14}O_2$ (238.2) Calcd. : C, 80.65 ; H, 5.90. Found : C, 80.38 ; H, 6.23 %. — ^{1}H-NMR ($CDCl_3$ + DMSO -d_6, δ, ppm) ; 7.65—7.10 (m, 8H aromatics), 4.83 (d, 1H, 1-H, $J_{1.6} = 5.5$ Hz), 4.56 (d, 1H, 4-H, $J_{4.5} = 8.5$ Hz), 3.81 (dd, 1H, 6-H, $J_{5.6} = 8.5$ Hz), 3.53 (dd, 1H, 5-H).

endo-4-exo-5-Diacetoxy-dibenzo[b.g]bicyclo[4.2.0]octa-2,7-diene (**4a**). 0.1 g (0.42 mmoles) alcohol **4** were disolved in 3 ml warm acetic anhydride and 0.2 ml pyridine were added. The mixture was left at room temperature for 24 hours, the excess of acetic anhydride was decomposed with water and from the resulted solution a white crystalline product was obtained. The product was purified by recrystallization from methanol yielding 0.12 g (92 %) white crystalline product **4a**, m.p. 116—118°. — Analysis $C_{20}H_{18}O_4$ (322.3) Calcd. : C, 74.51 ; H, 5.62. Found : C, 74,38 ; H, 5.71 %. — ^{1}H-NMR ($CDCl_3$, δ, ppm) : 7.60—7.00 (m, 8H aromatics), 5.99 (d, 1H, 4-H, $J_{4.6} = 1.0$ Hz), 5.56 (dd, 1H, 5-H, $J_{4.5} = 5.5$ Hz), 4.82 (d, 1H, 1-H), 4.06 (wide t, 1H, 6-H, $J_{5.6} = 4.0$ Hz), 1.98 (s, 3H from acetoxy group), 1.60 (s, 3H from acetoxy group).

Reduction of bromohydrine **5** *with lithium-aluminium hydride*. A solution of 2.0 g (6.68 mmoles) bromohydrine **5** in 150 ml tetrahydrofurane was refluxed with 2.0 g (52.69 mmoles) lithium-aluminium hydride. The excess of lithium-aluminium hydride was decomposed, the precipitate was filtered off and after the solvent removal a mixture (1.35 g, 92 %) of two alcohols **6** and **7** yielded. The pure alcohols were obtained by thin layer chromatography (Silicagel G, after Stahl, eluent dichloromethane with 45 % vol. acetone).

endo-4-Hydroxy-dibenzo[b.g]bicyclo[4.2.0]octa-2,7-diene (**6**), m.p. 160°.—Analysis $C_{16}H_{14}O$ (222.2), Calcd. : C, 86.65 ; H, 6.34. Found : C, 86.71 ; H, 6.54 %.— IR (CS_2, cm^{-1}) : ν_{OH}3585.— ^{1}H-NMR ($CDCl_3$, δ, ppm) : 7.00—7.50 (m, 8H aromatics), 4.81 (*t*, 1H, 4-H, $J_{4.5} = 4.5$ Hz), 4.69 (d, 1H, 1-H, $J_{1.6} = 5.2$ Hz), 4.09 (q, 1H, 6-H), 2.30 (*t*, 2H, 5-H, $J_{5.6} = 5.2$ Hz) 1.30 (wide s, 1H from hydroxyl group).

endo-5-Hydroxy-dibenzo[b.g]bicyclo[4.2.0]octa-2,7-diene (**7**), m.p. 138°.— Analysis $C_{16}H_{14}O$ (222.2) Calcd. : C, 86.65 ; H, 6.34. Found : C, 86.45 ; H, 6.42 %. — IR (CS_2, cm^{-1}) : ν_{OH} 3620.— ^{1}H-NMR ($CDCl_3$, δ, ppm) : 7.50—6.85 (m, 8H aromatics), 4.66 (d, 1H, 1-H, $J_{1.6} = 4.5$ Hz), 4.45—4.00 (m, 2H, 5-H, 6-H), 2.69 (dq, 1H, 4-$H_{(e)}$, $J_{4(a).4(e)} = 14$ Hz, $J_{4(e).5} =$ 4 Hz, $J_{4(e).6} = 2$ Hz), 2.50 (dd, 1H, 4-$H_{(a)}$, $J_{4(a).5} = 11$ Hz), 1.91 (s, 1H from hydroxyl group).

Dibenzo[b.g]bicyclo[4.2.0] octa-2,7-dien-5-one (**9**). A solution of 1.0 g (4.50 mmoles) **7** or **10** in 20 ml pyridine was treated with the complex formed from 1.0 g chromic anhydride and 10 ml pyridine, and the mixture was left at room temperature for 24 hours with occasional stirring. The mixture was diluted with water, extracted with diethyl ether and the ethereal solutions were washed with 2 % hydrochloric acid solution and then with water. After drying and solvent removal 0.66 g (65 %) **9**, white crystalline product with m.p. 141° (from methanol) were obtained. — Analysis $C_{16}H_{12}O$ (220.2) Calcd. : C, 87.24 ; H, 5.49. Found : C, 87.38 ; H, 5.60 %.— IR (CCl_4, cm^{-1}) : $\nu_{C=O}$ 1700.—^{1}H-NMR ($CDCl_3$, δ, ppm) : 7.50—6.90 (m, 8H aromatics), 4.97 and 4.37 (AB system, 2H, 1-H, 6-H, $J_{1.6} = 4.5$ Hz), 3.56 and 3.41 (AB system, 2H, 4-H, $J_{gem.} = 17.0$ Hz).

Dibenzo[b.g]bicyclo[4.2.0]octa-2,7-dien-4-one (**8**). A solution of 0.4 g (1.80 mmoles) alcohol **6** in 10 ml pyridine was oxidized with the complex formed from 1 g chromic anhydride and 10 ml pyridine in the same way as for the ketone **9**, yielding 0.25 g (70 %) **8**, m.p. 128° (from methanol). — Analysis $C_{16}H_{12}O$ (220.2) Calcd. : C, 87.24 ; H, 5.49. Found : C, 87.40 ; H, 5.28 %. — IR (CCl_4, cm^{-1}) : $\nu_{C=O}$1720. — ^{1}H-NMR ($CDCl_3$, δ, ppm) : 7.80 (d, 1H aromatic, $J = 7.0$ Hz), 7.60—6.90 (m, 7H aromatics). 4.76 (d, 1H, 1-H, $J_{1.6} = 5.0$ Hz), 4.31 (m, 1H, 6-H), 3.08 and 2.88 (AB part of an ABX system, 2H, 5-H, $J_{gem.} = 16.0$ Hz, $J_{5.6} = 4.0$ Hz).

exo-5-Acetoxy-dibenzo[b.g]bicyclo[4.2.0]octa-2,7-diene (**10a**). A solution of 1.8 g (8.17 mmoles) *exo* epoxide **2** and 50 ml anhydrous diethyl ether was refluxed with 0.5 g (13.17 mmoles) lithium-aluminium hydride for 8 hours. The excess of lithium-aluminium hydride was decomposed, the precipitate was filtered off and after the solvent removal the crude alcohol **10** was acetylated as below yielding 1.6 g (74.8 %) crude acetoxyderivative from which by column chromatography on neutral alumina with diethyl ether pure **10a** was isolated ; m.p. 141°. — Analysis $C_{18}H_{16}O_2$ (264.3) Calcd. : C, 81.79 ; H, 6.10 ; Found : C, 81.8 ; H, 5.63 %. — ^{1}H-NMR ($CDCl_3$, δ, ppm) : 7.85—7.45 (m, 8H aromatics), 5.55 (q, 1H, 5-H), 4.68 (d, 1H, 1-H, $J_{1.6} = 5.0$ Hz), 4.01 (m, 1H, 6-H), 2.85 (m, 1H, 4-$H_{(e)}$, $J_{4(e).4(a)} = 16.0$ Hz, $J_{4(e).5(e)} = 4.0$ Hz, $J_{4(e).6} = 1.5$ Hz), 2.55 (dd, 1H. 4-$H_{(a)}$, $J_{4(a).5} = 3.0$ Hz), 1.91 (s, 3H from acetoxy group).

endo-5-Acetoxy-dibenzo[b.g]bicyclo[4.2.0]octa-2,7-diene (**7a**). A solution of 0.2 g (0.90 mmoles) alcohol **7** in 4 ml acetic anhydride and 0.2 ml pyridine was left at room temperature for 24 hours. The excess of acetic anhydride was decomposed with water and the organic compound was extracted with dichloromethane. The organic layer was washed with water until neutral. Drying and solvent removal yielded 0.2 g (84 %) **7a**, m.p. 87° (methanol). — Analysis $C_{18}H_{16}O_2$ (264.3) Calcd. : C, 81.79 ; H, 6.10. Found : C, 81.83, H, 6.22 %. — ^{1}H-NMR (CCl_4, δ, ppm) : 7.60—7.00 (m, 8H aromatics), 5.25 (m, 1H, 5-H, $J_{5.6} = 6.15$ Hz, $J_{4(e).5} = 5.15$ Hz, $J_{(4a).5} = 11.5$ Hz), 4.75 (d, 1H, 1-H), 4.32 (wide t, 1H, 6-H), 2.80 (m, 1H, 4-H), 2.13 (s, 3H from acetoxy group).

endo-4-endo-5-Diacetoxy-dibenzo[b.g]bicyclo[4.2.0]octa-2,7-diene (**12a**). An ethereal solution of 0.55 g (2.49 mmoles) *endo* epoxide **3** and 20 ml 98 % formic acid was refluxed for 8 hours. The diethyl ether and the formic acid were removed and the residue was reduced with lithium-aluminium hydride yielding 0.4 g (67 %) colourless oil. This crude product was acetylated by treatment with acetic anhydride and small amounts of pyridine yielding 0.4 g (74 %), a mixture of two diacetoxyderivatives **11a** and **12a** in 1 : 1 molar ratio, colourless oil. One of these has the same ^{1}H-NMR spectrum with the diacetoxyderivative obtained by acetolysis of the bromoacetoxyderivative **5a**[3]. The structure of this compound is discussed in the next paper.[8] The ^{1}H-NMR data ($CDCl_3$, δ, ppm) for the second diacetoxyderivate **12a** are : 7.55—7.10 (m, 8H aromatics), 6.23 (dd, 1H, 4-H, $J_{4.5} = 3.0$ Hz, $J_{4.6} = 1.0$ Hz), 5.54 (dd, 1H, 5-H, $J_{5.6} = 6.5$ Hz), 4.76 (d, 1H, 1-H, $J_{1.6} = 6.0$ Hz), 4.25 (t, 1H, 6-H), 2.05 (s, 3H from acetoxy group at C_5), 1.55 (s, 3H from acetoxy group at C_4).

REFERENCES

[1] Part LVII : P. Filip, N. Stefan, F. Chiraleu, I. G. Dinulescu and M. Avram, *Rev. Roumaine Chim.*, **29**. 557 (1984).

[2] N. Stefan, I. G. Dinulescu, F. Chiraleu and M. Avram, *Rev. Roumaine Chim.*, **20**, 1473 (1975).

[3] N. Stefan, I. G. Dinulescu and M. Avram, *Rev. Roumaine Chim.*, **21**, 107 (1976).

[4] O. Constantinescu-Simon, I. G. Dinulescu, D. Constantinescu, P. Filip, F. Chiraleu and M. Avram, *Chem. Ber.*, **109**, 1287 (1976).

[5] O. Constantinescu-Simon, I. G. Dinulescu, F. Chiraleu, D. Constantinescu and M. Avram, *Chem. Ber.*, **109**, 1294 (1976).

[6] O. Constantinescu-Simon, I. G. Dinulescu, F. Chiraleu and M. Avram, *Chem. Ber.*, **109**, 1301 (1976).

[7] P. D. Bartlett, *Rec. Chem. Progr.*, **18**, 111 (1957).

[8] N. Stefan, P. Filip, F. Chiraleu and M. Elian, *Rev. Roumaine Chim.*, in press.

Revue Roumaine de Chimie, **29**, 8, 639–646 (1984)

INFLUENCE OF CARBON BLACK—ANTIDEGRADANT INTERACTION ON THE BEHAVIOUR OF RUBBER COMPOUNDS IN THERMO-OXIDATIVE DEGRADATION

G. IVAN and MARIA GIURGINCA
Research Institute for Rubber and Plastics Processing, R–79628 Bucharest, Romania

Received September 25, 1983

In the present work, the interaction of antidegradants with carbon black was investigated using spectroscopic methods in conjunction with accelerated ageing tests of binary systems as well as of rubber base compounds. For this purpose, in experimental program N,N′-disubstituted-p-phenylenediamines (with alkyl, aryl and alkyl + aryl substituents) were included as antidegradants and representative products for channal, furnace and thermal types of carbon black were selected as fillers.
On the basis of the experimental results, some correlations were emphasized between the characteristics of carbon black (specific surface area, oxygen content, pH), the formation of oxidation products of diamines and the amount of adsorbed diamine.

The action of various atmospheric factors and, at the same time, the interaction of the antidegradants with other ingredients of the compound leads to the reduction of their active concentration. In fact, protecting action is realized not by the amount of the antidegradant introduced in mix but by the quantity effectively acting at one time. Because the carbon black is used in an important amount and its large surface area is able to adsorb significant quantities of protecting agent, several authors payed attention to the possibility of interference of carbon black in antidegradant system but, till now, a consensus does not exist and some authors consider it has a stabilizing effect while the other enhance its pro-oxidant capability.[1–4] That controversy is generated, in part at least, by the complex structure and topochemistry of the carbon black itself : beside its large surface area which is able to adsorb physically important quantities of low molecular substances, chemical functions (phenol, quinone, carboxyl, free radical species) present on the surface could participate in various reactions including redox reactions, or as catalytic agent.

The present work was conducted in an attempt to contribute to a better understanding of the influence of the interaction carbon black — antidegradant, in the presence or in the absence of an elastomer, using various types of carbon black and different N,N′-disubstituted p-phenylenediamines as antidegradants.

EXPERIMENTAL

In experiments described in the present work, the following materials were used :

— natural and synthetic polyisoprenes, and styrene-butadiene rubber, all of commercial grade ; for the experiments in solution and for mixes rubber — carbon black in oxygen absorption testing, the raw rubbers were previously purified by successive extractions ;

— various types of carbon black (as presented in Table 1) were used in an amount of 30—40 phr ;

— the antidegradants (presented in Table 2) were introduced always in a proportion of 2 phr.

Table 1

The carbon blacks used in investigation of their influence on degradation

Type of carbon black	Content, %		Average diameter[1] Å	Average surface area[2] $m^2.g^{-1}$	pH
	H	O			
HAF Rebonex H Romanian product	.29	.62	310	82	8.1
ISAF Rebonex I Romanian product	.27	.88	265	108	8.3
FEF Carbodis 50 Romanian product	.32	.42	495	45	8.0
SRF R300 Romanian product	.32	.38	736	33	8.8
MPC Carbomet Romanian product	.58	3.10	295	122	3.7
MT Thermax Vanderbilt USA	.31	.05	4210	7.9	9.6

[1] Electron microscopy ; [2] BET

Table 2

Antidegradant types

Symbol	Chemical name	Commercial name Supplier
77PD	N,N′-di-(1,4-dimethylpentyl)-p-phenylenediamine	Santoflex 77 Monsanto Co., USA
IPPD	N-isopropyl, N′-phenyl-p-phenylenediamine	Santoflex IP Monsanto Co., USA
DMBPPD	N-(1,3-dimethylbutyl)-N′-phenyl-p-phenylenediamine	Santoflex 13 Monsanto Co., USA
DPPD	N,N′-diphenyl-p-phenylenediamine	Permanax DPPD Vulnax, France

For the evaluation of the oxygen absorption a Warburg apparatus (VEB Ilmenau, German DR) was used; electronic spectra were recorded on a Specord UV—VIS spectrophotometer (Carl Zeiss, Jena, German DR); e.s.r. spectra were obtained using an ART—6 apparatus (IFIN, Bucharest, Romania).

For tests on vulcanizates, simplified recipes were adopted, based on general purpose rubbers. The vulcanized samples were aged (Geer oven) for 3 days at 90°C, in ozone chamber (MAST Ozone Cabinet; 50°C, 50 pphm, 20 % elongation), or fatigued by repeated flexing (DeMattia flex tester; crack appearance method).

RESULTS AND DISCUSSIONS

Carrying on the experiments, three aspects were followed: the influence of the carbon black alone on elastomer degradation, the interaction of carbon black itself with substituted p-phenylenediamines, and the influence of carbon black upon vulcanizate degradation.

1. *The influence of the carbon black alone* was checked in natural rubber (NR) compounds containing 30 phr of various types of carbon black. The kinetic curves recorded in oxygen absorption test (Warburg technique) at 100—150°C reveal (Figure 1) that the MPC reduces the induction period of thermo-oxidative process while the other carbon blacks increase it, and the increasing effect (i.e. protecting effect) is more enhanced for FEF, SRF and MT blacks.

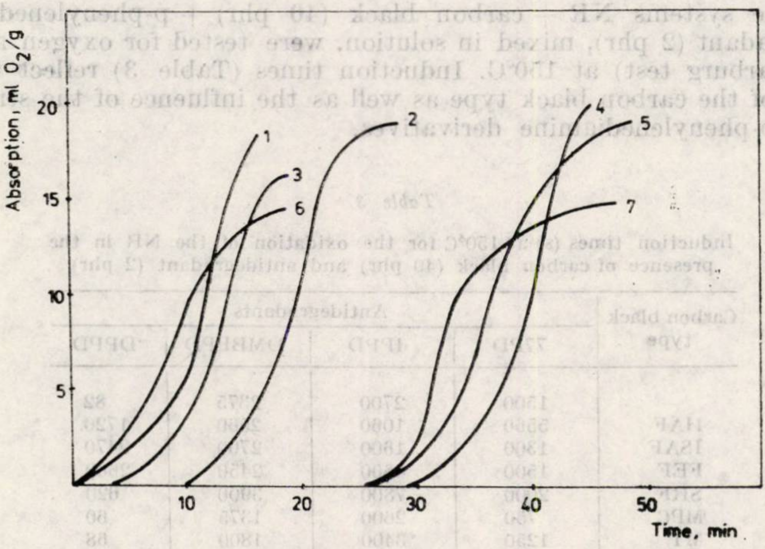

Fig. 1. — Oxygen absorption at 150°C by NR (1), NR+HAF (2), NR+ISAF (3), NR+FEF (4), NR+SRF (5), NR+MPC (6), and NR+MT (7).

2. *Interaction of carbon black with disubstituted p-phenylenediamines* was studied in squalene or in natural rubber (solution in carbon tetrachloride). The antidegradant was introduced in an amount of 2 phr and then mixed with 40 phr of carbon black for 16 hours. After separation of the carbon black, the content of the free antidegradant was determined

spectroscopically observing that the rest is of 15 to 45% of the initial amine content. The most important quantity was adsorbed by MPC because of its large surface area in conjunction with acid character of the surface. MT carbon black adsorbs the smallest quantities and for this carbon black was observed that the increase of the aromaticity of the antidegradant leads to an increase of the adsorbed amount, in agreement with literature data.[5]

Spectroscopical investigation of the extracted antidegradant revealed that it is partly transformed in oxidation products with semiquinone or quinonediimine structure.[6] Responsible for this oxidation could be oxygen bearing groups and the extractible substances (heavy aromatics) adsorbed on carbon black surface. In order to have a more accurate information, these tests were repeated using carbon black previously extracted with acetone for 24 hours; spectroscopical investigation of the diamines separated after contact with carbon black showed that the antidegradants preserve their initial structure and no oxidation was observed. Based on these results it is justified to afford to the influence of the heavy aromatics adsorbed on carbon black surface, the main responsibility for oxidative transformation of an amount of the protecting agent introduced in mix.

The systems NR + carbon black (40 phr) + p-phenylenediamine antidegradant (2 phr), mixed in solution, were tested for oxygen absorption (Warburg test) at 150°C. Induction times (Table 3) reflect the influence of the carbon black type as well as the influence of the structure of the p-phenylenediamine derivatives.

Table 3

Induction times (s) at 150°C for the oxidation of the NR in the presence of carbon black (40 phr) and antidegradant (2 phr)

Carbon black type	Antidegradants			
	77PD	IPPD	DMBPPD	DPPD
—	1500	2700	2375	82
HAF	5560	1060	2560	1720
ISAF	1300	1600	2700	2470
FEF	1500	4600	2450	2660
SRF	2000	7800	3900	620
MPC	750	2600	1375	60
MT	1250	3400	1800	68

The same ternary systems rubber + carbon black + antidegradant were tested in dry form. The stock was realized in a Brabender Plastograph P13S (Brabender OHG, FR Germany),mixing with 60 rpm, at 100°C for 10 minutes followed by a 24 hours rest. In Soxhlet extraction acetone is able to remove a quantity of antidegradant superior to the amount observed by solution mixing. That fact may indicate that in dry mixing, a part of the carbon black surface (or of active sites of this surface) is blocked by polymer chains, i.e. in dry mixing a lower quantity of antidegradant may be consumed by interaction with filler.

Electronic spectra of the acetone extracts obtained from the compounds realized by dry mixing reveal the presence of the derivatives resulting by oxidation of diamines as shown in Table 4.

Table 4

Absorption bands in electronic spectra of acetone extracts

Diamines	Absorption bands, nm			
Carbon blacks	77PD	IPPD	DMBPPD	DPPD
HAF	345 476	417 455	417 588	435
ISAF	385 417 500	417	425	455
FEF	385 417 500	385 408 588	435	455 625
SRF	377 408 476	408 571	455	455
MT	408 500	385 408 555	408 435 714	408 435 625
Reference	408 476	420 560 720	435	455 625

The e.s.r. spectra of the same extracts present an intensification of the signal for the case of IPPD, DMBPPD and DPPD, and a major distortion of the signal for the 77PD (Fig. 2). These alterations of the e.s.r. spectra may be attributed to the formation of quinonediimines from the diamines offering capabilities for an extended conjugation (particularly this is the case for DPPD). For the case 77PD, the modification of the spectrum and the significant increase of the band width support the hypothesis that in this case results a mixture of oxidation products: a semiquinone plus a quinonediimine.

3. *The influence of the carbon black upon vulcanizate degradation* was investigated in simplified recipes based on NR and SBR (Table 5). The carbon black type influences the vulcanization in known manner (optimal vulcanization time increases in order furnace black < channel black < thermal black) while, at usual low dosage (2 phr) the nature of the diamine protecting agent seems to exhibit a certain influence on the rheometric curves.

Typical ageing (thermo-oxidation for 72 hours at 90°C; ozone chamber test) and fatigue (DeMattia flexing) tests were carried out: for a first series of experiments, for the same antidegradant, various carbon blacks were tested, and in a second series of experiments the filler was constant and the protecting agent was variable.

For the same carbon black the decrease of performances in thermo-oxidative ageing is lower when protection is ensured by IPPD. DeMattia test indicated that in circumstances of flexing fatigue, the best results are obtained using DMBPPD. The antiozonant protection is better ensured by IPPD and DMBPPD and this capability is more enhanced in dynamic tests in ozone cabinet. These results indicate that for all rubbers and

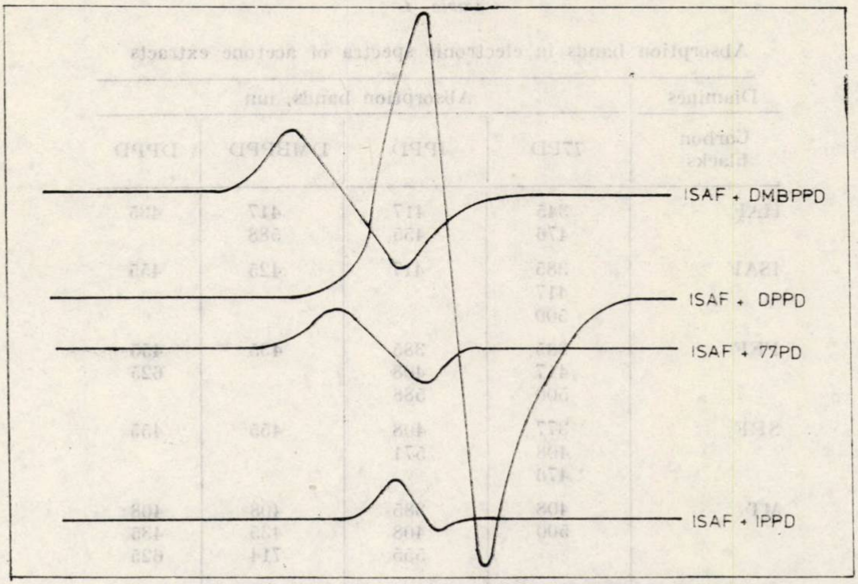

Fig. 2. — The e.s.r. spectra of acetone extracts from NR+ISAF+diamine compounds.

Table 5

Experimental recipes

Components	Recipes 1	2	3	4
Natural rubber RSS 3	100	—	—	50
Synthetic polyisoprene Carom 2230, Romanian product		100	—	—
Styrene-butadiene rubber Carom 1500, Romanian product	—	—	100	50
Carbon black (various types)	40	40	40	40
Protecting agent (various types)	2	2	2	2
Aromatic processing oil	4	4	4	4
Zinc oxide	5	5	5	5
Stearic acid	2	2	2	2
Benzothizyl-2-cyclohexyl sulphenamide	1	1	—	.5
Benzothiazyl disulfide	—	—	3	1.5
Sulfur	3	3	2	2.5

carbon black types, the unsymmetrically substituted p-phenylenediamines (N-alkyl, N′-aryl) ensure the highest protection effect (an example for NR compounds filled with HAF is illustrated in Figure 3).

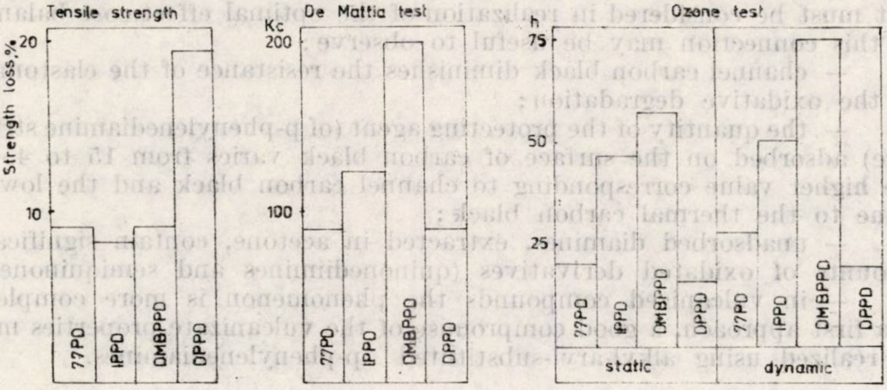

Fig. 3. — Ageing and flexing test results for NR+HAF+diamine compounds.

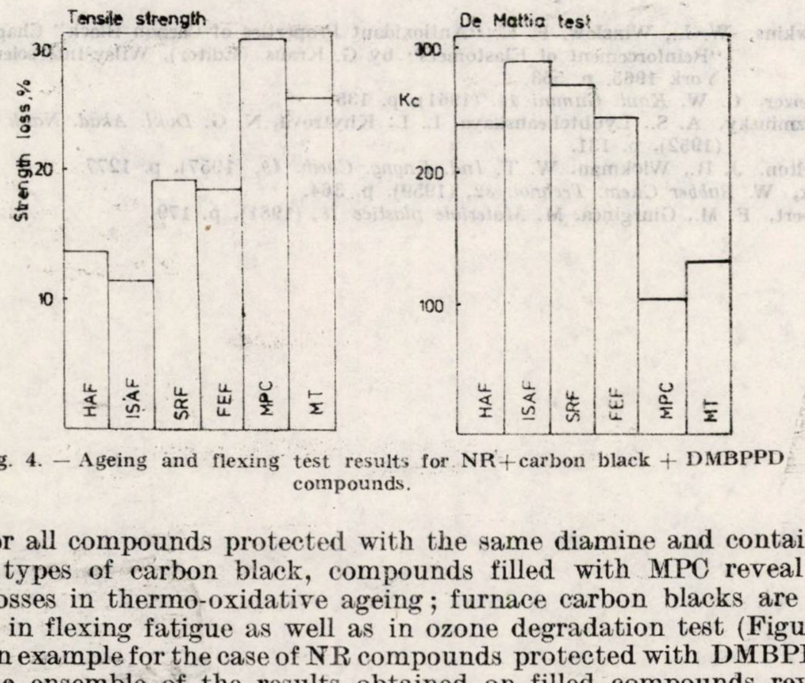

Fig. 4. — Ageing and flexing test results for NR+carbon black + DMBPPD compounds.

For all compounds protected with the same diamine and containing various types of carbon black, compounds filled with MPC reveal the higher losses in thermo-oxidative ageing; furnace carbon blacks are also superior in flexing fatigue as well as in ozone degradation test (Figure 4 shows an example for the case of NR compounds protected with DMBPPD).

The ensemble of the results obtained on filled compounds reveals a more complicated behaviour of the vulcanizates due to the interference of the carbon black (mainly depending of its type) with the antidegradant (for which the most important is the nature of the substituents at aminic nitrogen).

CONCLUSIONS

In use of rubber products a complex of factors could influence the durability of the vulcanizates. The data presented enhance the interference of carbon black with protection system of the compound and this fact must be considered in realization of the optimal effect-cost balance. In this connection may be useful to observe :

— channel carbon black diminishes the resistance of the elastomers to the oxidative degradation ;

— the quantity of the protecting agent (of p-phenylenediamine structure) adsorbed on the surface of carbon black varies from 15 to 45%, the higher value corresponding to channel carbon black and the lowest value to the thermal carbon black ;

— unadsorbed diamines, extracted in acetone, contain significant amounts of oxidated derivatives (quinonediimines and semiquinones) ;

— in vulcanized compounds the phenomenon is more complex ; in a first approach, a good compromise of the vulcanizate properties may be realized, using alkyl-aryl-substituted p-phenylenediamines.

REFERENCES

[1] Hawkins, W. L., Winslow, F. H. "Antioxidant Properties of Carbon Black" Chapter 17 in "Reinforcement of Elastomers" by G. Kraus (Editor), Wiley-Interscience, New York 1965. p. 563.

[2] Sweizer, C. W. *Kaut. Gummi 14.* (1961), p. 135.

[3] Kuzminsky, A. S., Lyubtcheanskaya, L. I., Khytrova, N. G. *Dokl. Akad. Nauk SSSR 82*, (1952), p. 131.

[4] Shelton. J. R., Wickman. W. T. *Ind. Engng. Chem. 49*, (1957), p. 1277.

[5] Cox, W. *Rubber Chem. Technol. 32*, (1959), p. 364.

[6] Albert, F. M., Giurginca, M. *Materiale plastice 18*, (1981), p. 179.

Revue Roumaine de Chimie, **29**, *8*, 647–654 (1984)

ACTIVATION OF THE NATURAL ZEOLITE CLINOPTILOLITE, STRUCTURAL PROPERTIES AND CATALYTIC ACTIVITY

I. V. NICOLESCU*, J. V. RAJAOFANOVA**, LIGIA FRUNZĂ***, FLORENTINA AVRAMESCU*, RODICA MĂNĂILĂ***, OLGA ŞERBAN*, G. NEDELCU* and V. BIDIAN****

* Polytechnical Institute, Faculty of Chemical Technology, Bucharest, Romania
** Polytechnical Institute, Madagascar
*** Institute of Physics and Technology of Materials, Bucharest — Măgurele, Romania
**** Research Institute of Nonmetallic Materials, Cluj-Napoca, Romania

Received September 23, 1983

The work reports on the dependence between the structural properties and the catalytic activity of the natural zeolite clinoptilolite, in its initial form or activated either by decationization, ammoniation-deammoniation or by direct or indirect dealumination. A relation is found between the lattice modification by decationization and dealumination and the catalytic activity in the test reaction of *iso*-propylbenzene dealkylation.

1. INTRODUCTION

Since the crystalline synthetic zeolites are more and more used as catalysts or as supports for catalysts in different processes of hydrocarbon transformation, the investigations developed concerning the utilization to the same purpose of activated natural zeolites and zeolitic volcanic tuffs, particularly of those with clinoptilolite (CP) or mordenite structure.[1–5]

It was shown that H-CP has a high catalytic activity in the reactions of olefine isomerization[6] and of alcohol dehydratation.[7]

The catalytic activity of natural zeolites depends essentially on the chemical composition, the form and the dimensions of the channels, on the degree of crystallinity and on the method and conditions of activation. The activation of the natural zeolite is aimed at : a) the rise of the total acidity by decationization (substitution of Na^+, K^+, Ca^{2+} ions with H^+); b) the modification of the SiO_2/Al_2O_3 ratio by dealumination of the natural or decationized product.

This work presents some experimental results concerning the activation of the natural zeolite from Mîrşid, considering the physico-structural properties as well as the catalytic activity.

2. EXPERIMENTAL RESULTS AND DISCUSSION

The chemical composition of the natural parent zeolite (ZN_0) is given in Table 1. The SiO_2/Al_2O_3 molar ratio has the value 9.3.

The surface area of the zeolite calcined at 460–500°C is 27 m^2/g. TG and TDA data evidence three endothermic peaks (Fig. 1) : the main one, at 117°C, is due to dehydration and dehydroxylation, while the other smaller ones, at 680 and 860°C, are probably due to the decomposition of some carbonates or inclusion materials. The weight losses are 12.7 %. The (Si, Al)O framework of the parent zeolite was found to be thermally stable up to 700°C.

Table 1

Chemical composition of the natural zeolite clinoptilolite ZN_0

SiO_2 %	Al_2O_3 %	Fe_2O_3 %	CaO %	MgO %	K_2O %	Na_2O %	Losses at 110°C, %g
69.50	12.50	0.75	2.95	1.05	2.90	0.80	9.45

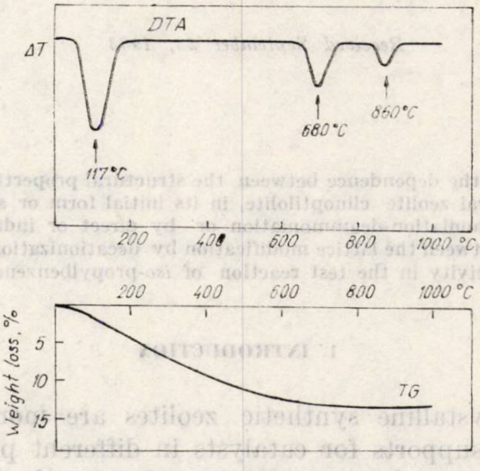

Fig. 1. — DTA and TG plots for natural zeolite ZN_0.

The samples were characterized by XRD and IR spectroscopy.

ZN_0 has a high crystallinity degree. The relative intensities (I_{rel}) and interplanar distances d(Å) of the main diffraction lines are coincident, within 0.6–1 %, with those of the natural zeolite clinoptilolite from ASTM cards 24–319, 21–131 and from Amirov's data [8] (Fig. 2).

IR spectra were obtained in the range 400–1800 cm^{-1} of the lattice fundamental vibration modes. The absorption maxima are given in Table 2. There are four main maxima assigned to the bending of the internal (Si, Al)O_4 tetrahedra at 420–500 cm^{-1}, to the asymmetric stretching of the same tetrahedra at 950–1250 cm^{-1} and to external linkages modes at 500 – 650 cm^{-1} (double ring) and at 750 – 820 cm^{-1} (symmetric stretching).[6] The peak at 1640 cm^{-1} is due to a harmonic of Si-O stretching and to the physisorbed water deformation mode (curve 1, Fig. 3).

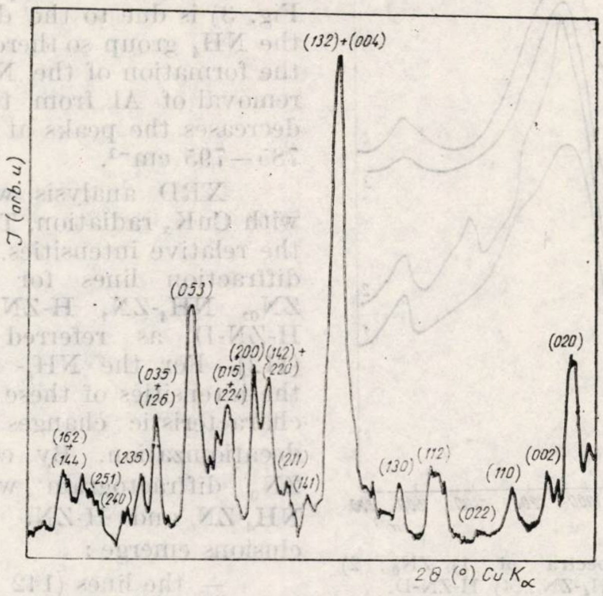

Fig. 2. – XRD plot for natural zeolite ZN_0.

Table 2

The position of IR absorption maxima

Sample	Position, cm^{-1}						
ZN_0	460	520	605	790	1050b	1200sh	1640

b – broad, sh – shoulder.

2.1. CLINOPTILOLITE ACTIVATION AND CHARACTERIZATION OF THE RESULTING PRODUCTS

In order to obtain a higher activity and different types of zeolites, we used several activation techniques : decationization, deammoniation and dealumination of the natural, clinoptilolite-type zeolite.

The decationization to the NH_4-ZN form was performed by ionic exchange with a 2n NH_4Cl solution for 2 – 6 h, at 90°C. H-ZN was obtained by calcinating the NH_4-form at 450 – 500°C.

Both H-ZN and ZN_0 were dealuminated with HCl solution 80 – 90°C, for 6 h to the H-ZN-D and ZN-D forms respectively.

The IR spectra of these samples are similar to that of the natural zeolite, having the four main maxima at 450 – 470, 585 – 605, 785 – 795, and 1050–1070 cm^{-1} (Fig. 3). Nevertheless they differ by the relative intensities, as referred to the 1050–1070 cm^{-1} maximum (Table 3). These maxima were attributed following Flanigen et al.,[6] as already discussed. The peak at 1410 cm^{-1} in the spectrum of NH_4-ZN (curve 2, Fig. 3) is due to the deformation of the NH_4 group so thereby confirming the formation of the NH_4-form. The removal of Al from the framework decreases the peaks at 585–605 and 785–795 cm^{-1}.

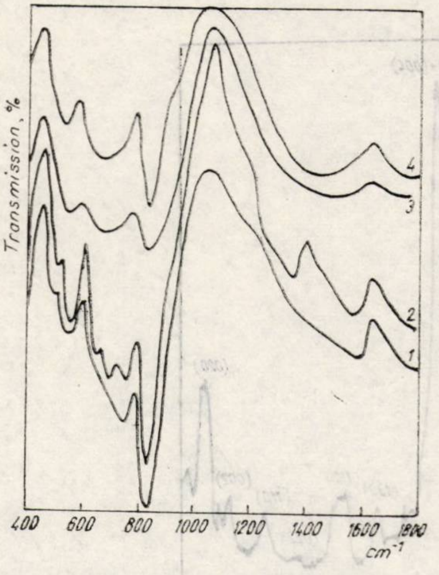

Fig. 3. — IR spectra of 1) ZN_0; 2) H-ZN; 3) NH_4-ZN; 4) H-ZN-D.

XRD analysis was performed with CuK_α radiation. Table 4 collects the relative intensities of the main diffraction lines for the samples ZN_0, NH_4-ZN, H-ZN, ZN-D and H-ZN-D, as referred to the line (112). For the NH_4- and H-forms, the intensities of these lines undergo characteristic changes due to the decationization. By comparing the ZN_0 diffractogram with those of NH_4-ZN and H-ZN, several conclusions emerge:

— the lines (142 + 220), (020), (110), (002) and (132+004) increase noticeably by exchanging Na^+, K^+, Ca^{2+} with H^+ and NH_4^+.

— the lines (200), (053) and (224) show a decreasing tendency, particularly in the H-form. The details of intensity variation suggest that the substitution with H^+ and NH_4^+ may take place in cationic sites having different symmetry. The reference line (112) is insensitive to decationization and dealumination processes. The intensity variations due to decationization have been explained by the analysis of the structure factors for the corresponding reflexes.

Table 3

The intensities of IR maxima referred to the 1050–1070 cm^{-1} peak

Sample	450–470	585–605	785–795
ZN_0	0.72	0.40	0.20
NH_4-ZN	0.79	0.40	0.21
H-ZN	0.67	0.32	0.28
H-ZN-D	0.73	0.28	0.23

Weak additional lines appear when the alkaline cations are exchanged with H^+, which could not be indexed on the basis of the clinoptilolite elementary cell. They might be attributed to the ordering of the present cations on the cationic sublattice.

Dealumination of H-ZN brings about an intensity decrease of the diffraction lines (Table 4) suggesting a slight disorder of the (Si, Al)O framework in decationized and dealuminated zeolites. This effect is much weaker with ZN-D sample.

Table 4

The intensities of XRD lines referred to the $(11\bar{2})$ line

Sample	002	110	142+220	020	132+ 004	053	224	035+ 126	200
ZN_0	0.81	0.83	2.10	2.53	8.95	3.58	1.84	1.37	1.56
NH_4-ZN	1.21	1.27	4.45	4.37	10.94	4.02	2.07	1.37	0.87
H-ZN	1.28	1.45	2.60	4.18	10.59	2.97	1.33	1.07	0.72
ZN-D	1.04	1.57	1.74	4.39	10.89	2.56	1.15	0.80	1.09
H-ZN-D	0.89	1.41	2.00	3.69	9.90	2.28	0.80	0.78	0.95

The intensity variation of the diffraction lines at dealumination suggests a preferential distribution of Al on certain sites of the (Si, Al) sublattice.

2.2. CATALYTIC ACTIVITY OF THE ACTIVATED ZEOLITES

The catalytic activity of the zeolites prepared by different activation techniques from the natural clinoptilolite was appreciated by the reaction of *iso*-propylbenzene (IPB) dealkylation with the formation of benzene and propene, a characteristic test for hydrocarbon cracking. The reaction takes place with the participation of protonic acidic sites as well as of Lewis acidic ones :

a) $C_6H_5\text{-}C_3H_7 + H^+(SK) \dashrightarrow (C_3H_7)^+ + C_6H_6 + SK^{(-)}$

b) $(C_3H_7)^+ + SK^{(-)} \dashrightarrow C_3H_6 + H^+(SK)$

c) $C_6H_5\text{-}C_3H_7 + SK \dashrightarrow C_3H_6 + (C_6H_5)^+ + SK; H$

d) $(C_6H_5)^+ + SK; H \dashrightarrow C_6H_6 + SK$

where H^+ is a protonic site and SK, the catalyst surface.

This test was carried out in dynamic regime, between 340 and 500°C, at a space velocity of $1-3\ h^{-1}$, for a reaction time of 15—60 min. A certain grannulation (1.6—2.6 mm) and volume of the catalyst bed ($10\ cm^3$) were chosen to eliminate the influence of internal and external diffusion. The liquid products were chromatographically analysed using a 4 m column (3 mm diameter), and bentone+di-iso dodecylphtalate/chromosorb 60/80 W as stationary phase.

The catalysts were selected after their total activity as referred to the reaction time (15, 30, 45, 60 min) at constant temperature (460°C) and space velocity ($1\ h^{-1}$). It was evaluated from the concentration of benzene (the main reaction product) and of the untransformed IPB and represented in Fig. 4. As secondary products, there were identified : toluene, ethylbenzene, xylenes and di-*iso*-propylbenzenes.

Several facts are emerging from the data in figure 4 :

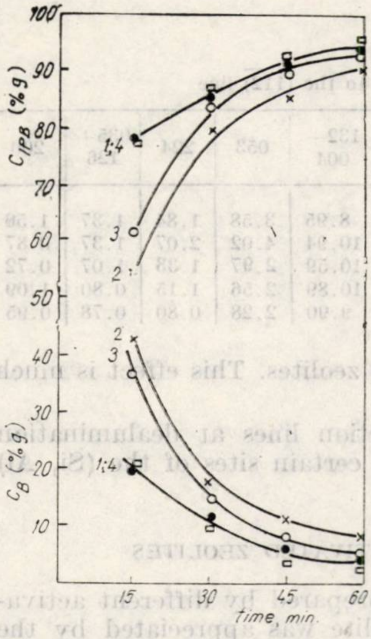

Fig. 4. — Total activity of modified zeolites vs. reaction time : 1) ZN_0 ; 2) H-ZN ; 3) H-ZN-D ; 4) ZN-D.

— the reaction intensity falls after 15 min ; after 45 min, the benzene concentration remains constant due to the convering of the catalyst surface by coke and tar.

— the parent zeolite (calcined at 500°C) shows a minimum of activity ($C_B = 20.5\%$) while H-ZN has a maximal one ($C_B = 43.5\%$).

— the dealumination of ZN_0 or H-ZN yields catalysts with a low activity.

Thus, the catalysts with a high activity in the reaction are obtained not by dealumination but by decationization of the natural zeolite.

As it was shown above, the relative intensity of certain diffraction lines can be considered as a sensitive indicator of the cationic exchange extent. Table 5 presents the activity increase by decationization in parallel with the relative intensity diminution of the (200) line, due to the cation removal. This parallelism extends to the dealuminated samples too, although the intensity variation in this case cannot be explained in a straightforward manner.

The catalyst H-ZN was selected for the study of the yield, conversion and selectivity versus the variation of operational parameters; the temperature range was 340—500°C, the reaction time 20 min and the space velocity 1—3 h^{-1}. The contact time τ_c was calculated on the basis of the above data.

Table 5

Catalytic activity and relative intensities of the (200) line

Catalyst	Treatment	I_{rel} of (200) line	Activity C_B, %g
H-ZN	decationized	0.72	43.5
H-ZN-D	decationized, dealuminated	0.95	37.0
ZN-D	dealuminated	1.09	1.2
ZN_0	(calcined at 500°)	1.16	20.5

The variation of the conversion (X_A, %mole) and of the benzene yield (R_B, %mole) as functions of the contact time and reaction temperature are given in figure 5 and 6 respectively: the best results are obtained for a temperature of 460—500°C and a medium contact time.

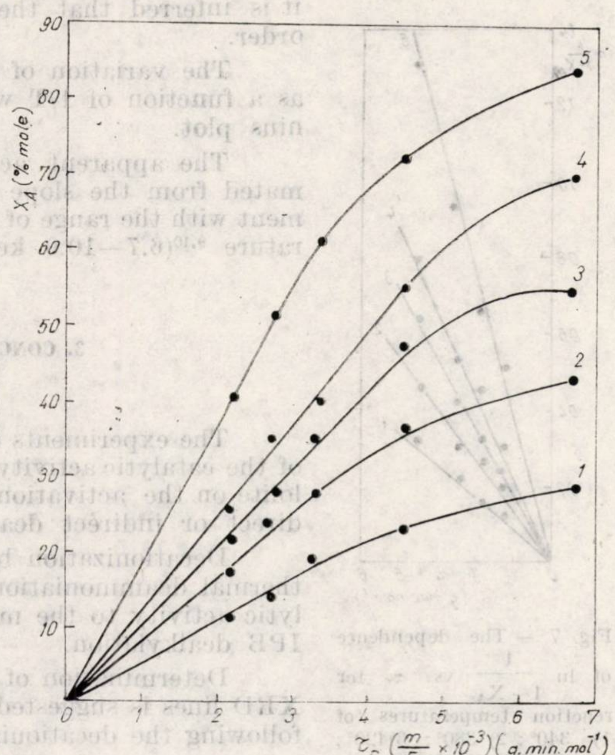

Fig. 5. — Conversion X_A vs. contact time τ_c for different reaction temperatures: 1) 340°; 2) 380°; 3) 420°; 4) 460°; 5) 500°C.

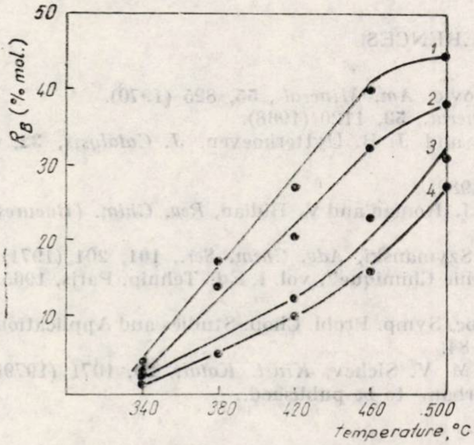

Fig. 6. — Variation of the yield R_B as a function of reaction temperature for $\tau_c = (6.71 - 2.24) \times 10^{-3}$ g.min. mole^{-1}

From the experimental data, the apparent rate constant and activation energy were calculated under the assumption that the slow step of the process is the transformation of adsorbed IPB. The $\ln \frac{1}{1 - X_A}$ vs.

τ_c dependence is shown in figure 7 for temperatures of 340 – 500°C and $\tau_c < 4.5 \times 10^{-3}$ g.min.mole^{-1}. From the linearity of the dependence it is inferred that the reaction is of the first order.

The variation of the apparent rate constant as a function of 1/T which shows a linear Arrhenius plot.

The apparent activation energy was estimated from the slope as 8.5 kcal/mole, in agreement with the range of values reported in the literature [9,10](6.7 – 10.0 kcal/mole).

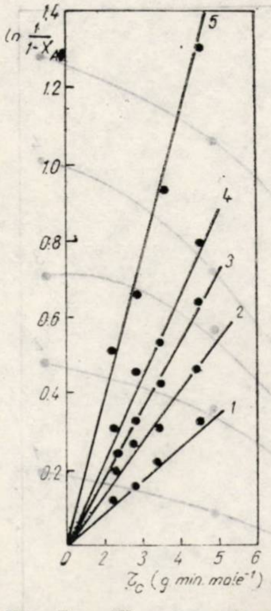

Fig. 7. – The dependence of $\ln \frac{1}{1 - X_A}$ vs. τ_c for reaction temperatures of 1) 340°; 2) 380°; 3) 420°; 4) 460°; 5) 500°C.

3. CONCLUSIONS

The experiments evidenced the dependence of the catalytic activity of natural zeolite clinoptilolite on the activation method (decationization, direct or indirect dealumination).

Decationization by ammoniation followed by thermal deammoniation confers an optimal catalytic activity to the modified zeolite in the test IPB dealkylation.

Determination of the relative intensities of XRD lines is suggested as a sensitive method for following the decationization process.

REFERENCES

[1] J. A. Berger, J. C. Chandler and P. Zubovic, *Am. Mineral.*, **55**, 825 (1970).

[2] A. B. Merkle and M. Slaughter, *Am. Mineral.*, **53**, 1120 (1968).

[3] E. J. Detrekoy, P. A. Jacobs, D. Kallo and J. B. Uytterhoeven, *J. Catalysis*, **32**, 442 (1974).

[4] J. V. Rajaofanova : Thesis, Bucharest (1982).

[5] A. Damian, A. Bâldea, A. Abrudeanu, J. J. Roman and V. Bidian, *Rev. Chim. (București)*, **31**, 656 (1980).

[6] E. M. Flanigen, H. Khatami and H. A. Szymanski, *Adv. Chem. Ser.*, **101**, 201 (1971).

[7] P. Wurthier : "Le Petrole, Rafinage et Genie Chimique", vol. I, Ed. Tehnip, Paris, 1965, p. 15.

[8] S. T. Amirov et al., in : "Clinoptilolite. Proc. Symp. Probl. Cliop. Studies and Applications", Metsniereva, Tbilisi, 1974, p. 84.

[9] V. V. Goncharuk, N. E. Scheratnik and M. V. Sichev, *Kinet. Katal.*, **20**, 1071 (1979).

[10] I. V. Nicolescu, Hoa Huu Thu and O. Serban, to be published.

Revue Roumaine de Chimie **29**, *8*, 655–661 (1984)

THERMOKETTEN MIT WÄSSRIGEN CESIUMCHLORID LÖSUNGEN

ELENA CONSTANTINESCU und HILDEGARD DENGEL*
Polytechnisches Institut Bukarest, Institut für Chemie, Splaiul Independenţei 313 Cod 77206, Rumänien
* Universität Galatz, Bdul. Republicii 47, Rumänien

Eingegangen 23. November, 1983

Anhand der potentiometrischen Methode wurden Soret-Koeffizienten und molare Überführungswärmen von wässrigen Cesiumchloridlösungen für sechs Konzentrationen bestimmt. Es wurde die Konzentrationsabhängigkeit der Soret-Koeffizienten und der molaren Überführungswärmen wiedergegeben. Für die Konzentration 0,001 Mol.kg^{-1} wurde die ionische Überführungsentropie des Iones Cs$^+$ errechnet.

By using potentiometric measurements to double thermogalvanic cells, the Soret coefficients and transfer molar heats to aqueous cesium chloride solutions were determined. The dependence of Soret coefficients and transfer molar heats on concentrations were presented. For the concentration 0.001 mol.kg^{-1} the transfer ionic heat and the transfer ionic entropy for the Cs$^+$ ion were obtained.

In der gegenwärtigen Arbeit werden die Ergebnisse von potentiometrischen Messungen an thermogalvanischen Doppelzellen mit wässrigen Cesiumchloridlösungen wiedergegeben. Als Bezugslösung mit bekanntem Soret-Koeffizienten wurde eine wässrige Kaliumchloridlösung gewählt. Die der Forschung unterworfene thermogalvanische Doppelzelle war der Form :

$$\underset{(T_1)}{Hg/Hg_2Cl_2,}\ KCl(m),\ \underset{(T_2)}{Hg_2Cl_2/Hg/Hg_2Cl_2,}\ CsCl(m),\ \underset{(T_1)}{Hg_2Cl_2/Hg} \qquad (1)$$

$$\text{wo}: T_1 < T_2$$

Die Temperaturen T_1 und T_2 wurden so gewählt, dass die mittlere Temperatur stets 25,00 °C beträgt :

$$\frac{T_1 + T_2}{2} = 25{,}00°C$$

Die Molalitäten der beiden Elektrolytlösungen haben den gleichen Wert.

In einer früherem Arbeit wurden die Gleichungen für die Errechnung des Soret-Koeffizienten (σ^{MCl}) und der molaren Überführungswärme (Q^{*MCl})

der wässrigen Alkalimetalchloridlösungen ausgehend von dem Anfangswert der thermoelektrischen Kraft (ε_0) abgeleitet.

Für die wässrigen Cesiumchloridlösungen erhält man folgende Gleichungen:

$$\sigma^{\mathrm{CsCl}} = \frac{2RT\ t_{\mathrm{K+}}^{\mathrm{KCl}} \cdot \sigma^{\mathrm{KCl}} \cdot B^{\mathrm{KCl}} \cdot F\varepsilon_0}{2RT \cdot t_{\mathrm{Cs+}}^{\mathrm{CsCl}} \cdot B^{\mathrm{CsCl}}} \tag{2}$$

$$-Q^{*\mathrm{CsCl}} = \nu RT^2 \cdot B^{\mathrm{CsCl}} \cdot \sigma^{\mathrm{CsCl}} \tag{3}$$

wo:

$$B^{\mathrm{KCl}} = 1 + \left(\frac{\mathrm{d} \ln \gamma_{\pm}^{\mathrm{KCl}}}{\mathrm{d} \ln m}\right) P, T \tag{4}$$

$$B^{\mathrm{CsCl}} = 1 + \left(\frac{\mathrm{d} \ln \gamma_{\pm}^{\mathrm{CsC}}}{\mathrm{d} \ln m}\right) P, T \tag{5}$$

Hierin bedeutet: $R =$ die universelle Gaskonstante, F die Faradaysche Konstante, $t_{\mathrm{K+}}^{\mathrm{KCl}}$ die Ionenüberführungszahl des Iones K^+ in der KCl Lösung, $t_{\mathrm{Cs+}}^{\mathrm{CsCl}}$ die Ionenüberführungszahl des Iones Cs^+ in der CsCl Lösung, T die mittlere Temperatur (298,15 K), σ^{KCl} — der Soret-Koeffizient der KCl Lösung, σ^{CsCl} — der Soret-Koeffizient der CsCl Lösung, ν die Ionenzahl in welche ein Molekül CsCl dissoziert.

DER EXPERIMENTELLE TEIL

Die Arbeitszelle wurde in einer früheren Arbeit beschrieben[2,3]. Die Substanzen aus welchen die Elektroden und die Lösungen dargestellt wurden stammen direkt aus dem Handel, wobei der höchstmögliche Reinheitsgrad gewählt wurde: (KCl—U.C. Belgien, $\mathrm{Hg_2Cl_2}$—Merck, CsCl—Carlo-Erba), das Quecksilber wurde im Vakum distilliert. Die Lösungen wurden aus dreifach distilliertem Wasser hergestellt.

Für die Bestimmung der Anfangswerte der E.M.K. wurde eine Feussnerpotentiometer welche eine Messgenauigkeit von 1.10^{-6} V gewährleistet, in Gebrauch genommen. Als Nullinstrument wurde ein Lichtgalvanometer von der Sensibilität 4.10^{-9} A/mm verwendet. Die Temperaturen wurden mit Termometern mit Zentelgraden gemessen. Die Temperierung wurde mit drei Ultrathermostaten nach Höppler unternommen.

ERGEBNISSE UND DISSKUSIONEN

Es wurden doppelte Thermoketten mit wässrigen CsCl — Lösungen im Konzentrationsbereich $5.10^{-1} \div 1.10^{-3}$ $\mathrm{Mol.kg^{-1}}$ für sieben Werte des Temperaturgradientes studiert.

In Tabelle 1 sind die mit dem Asymetriepotential korrigierten Anfangswerte der E.M.K., für drei experimentelle unabhängige Versuche, wiedergegeben.

Die Daten aus Tabelle 1 zeigen eine gute Übereinstimmung für die in wässrigen CsCl—Lösungen gegebener Konzentration und demselben Temperaturgradient, individuellen Zahlenwerte der Anfangswerte der

Tabelle 1

Experimentelle Werte für die CsCl — Lösungen $E_0 . 10^3$ (Volt)

ΔT°C	Konzentration Mol.kg^{-1}								
		0,500			0,100			0,050	
1	0,033	0,034	0,032	0,038	0,037	0,037	0,039	0,040	0,040
2	0,067	0,062	0,067	0,077	0,079	0,077	0,090	0,091	0,087
3	0,102	0,107	0,100	0,117	0,121	0,123	0,127	0,130	0,129
5	0,160	0,167	0,169	0,194	0,198	0,199	0,209	0,215	0,216
7	0,236	0,235	0,233	0,267	0,269	0,270	0,293	0,297	0,295
9	0,287	0,285	0,284	0,321	0,325	0,327	0,367	0,360	0,362
12	0,428	0,429	0,432	0,469	0,468	0,470	0,489	0,487	0,490
		0,010			0,005			0,001	
1	0,041	0,042	0,042	0,044	0,046	0,047	0,050	0,048	0,049
2	0,103	0,105	0,102	0,117	0,116	0,119	0,133	0,137	0,138
3	0,150	0,157	0,159	0,172	0,176	0,173	0,193	0,197	0,192
5	0,237	0,233	0,239	0,259	0,260	0,262	0,289	0,285	0,288
7	0,317	0,320	0,319	0,350	0,349	0,351	0,376	0,375	0,379
9	0,395	0,397	0,399	0,422	0,420	0,418	0,503	0,506	0,509
12	0,515	0,512	0,511	0,572	0,577	0,579	0,664	0,660	0,662

E.M.K., was für ein gutes Entdecken des Anfangsstadium der doppelten Thermokette spricht und zugleich eine zufriendenstellende Konsistenz prüfung unabhängiger Messungen darbietet.

In Konformität mit der Vorzeichenvereinbarung, welche der E.M.K. ein positives Vorzeichen zuschreibt, wenn der Elektrod in der kühleren Seite der CsCl Lösung positiver ist, als der in der kühleren Seite der KCl-Lösung, wurden für alle Anfangswerte der E.M.K. der studierten Doppelketten, positive Werte gefunden. Die erhaltenen positiven Werte ordnen sich in das allgemeine Verhalten der wässrigen Alkali- und Erdalkalichloridlösungen ein. [1-7]

Die graphische Darstellung der Funktion $E_0 = f(\Delta T)$ führt zu Graden positiver Steilheit, was für einen linearen Anstieg der Anfangswerte der E.M.K. (E_0) mit dem Zunehmen der Temperaturdifferenz, für alle der Forschung unterworfenen wässrigen CsCl-Lösungen gegebener Konzentration, spricht.

In Abbildung 1 ist die Kurvenschar, für verschiedene Molalitäten der CsCl — Lösungen wiedergegeben, welche eine lineare Abhängigkeit des Anfangswertes der E.M.K. (E_0) von der Temperaturdifferenz (ΔT) zeigt, und das charakteristische Gesetz für das Anfangsstadium der Thermoketten bestätigt. [8,9]

Die Thermokraft ε_0 wurde ausgehend von dem arithmetischen Mittetlwert, als auch dem anhand der Gradegleichung linearisierten Wert errechnet.

Der Soret-Koeffizient σ^{CsCl} und die molare Überführungswärme Q^{*CsCl} der wässrigen CsCl-Lösungen wurden mit den Zahlenwerten von ε_0 bestimmt. Die Werte der Grossen ε_0, σ^{CsCl} und Q^{*CsCl} für verschiedene Werte der Molalität des Elektrolyten sind in Tabelle 2 und 3 zusammengestellt.

Die zur Bestimmung des Soret-Koeffizienten und der Überführungswärme notwendigen Hilfsgrössen als auch die entsprechenden Werte für das Bezugsalz, stammen aus der Literatur. [6,10,11]

Die Zahlenwerte aus Tabelle 2 und 3 zeigen eine gute Übereinstimmung zwischen den Werten der Soret-Koeffizienten und der molaren Überführungswärmen die ausgehend von dem arithmetischen Mittel der Anfangsthermokraft ($\varepsilon_{0\,\mathrm{med}}$) und diejenigen, welche mit dem anhand der Gradegleichung linearisierten Werte, ($\varepsilon_{0\,\mathrm{Ec.\,dr}}$) errechnet wurden.

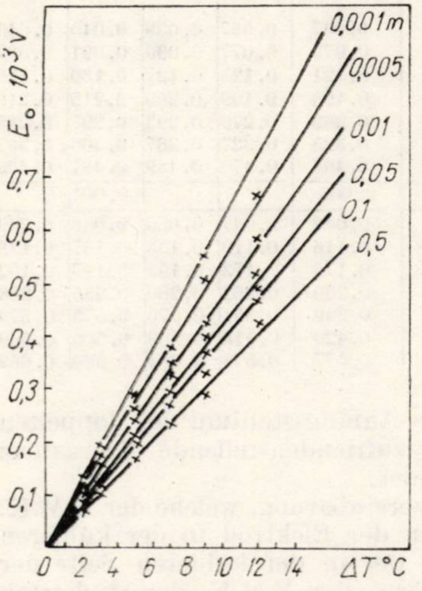

Abb. 1. — Die Veränderung des Anfangswertes der E.M.K. in Abhängigkeit vom Temperaturgradienten für verschiedene Konzentrationen der wässrigen CsCl-Lösungen.

Die für die Soret-Koeffizienten und molaren Überführungswärmen der wässrigen CsCl-Lösungen erhaltenen Zahlenwerte gliedern sich in den Bereich für die entsprechenden Werte der wässrigen Elektrolytlösungen ein [12] Gleichfalls bemerkt man, dass die Zahlenwerte der Soret-Koeffizienten als auch der molaren Überführungswärmen mit dem Anwachsen der Konzentration der CsCl-Lösung abnehmen. Änliche Abhänigkeiten wurden auch von anderen Forschern beobachtet[13] und zwar für eineinwertige Elektrolyten als auch bei mehrwärtigen Elektrolyten bei kleinen Konzentrationen.

Wenn man die Soret-Koeffizienten und die molaren Überführunswärmen in Abhänigkeit von der Quadratwurzel der Molalität aufzeichnet, erhält man Kurven die in Abbildung 2 und 3 wiedergegeben sind.

Bei kleinen Konzentrationswerten wird eine lineare Abhänigkeit der Soret-Koefizienten als auch der molaren Überführungswärmen von der Quadratwurzel der Molalität bemerkt, was für die CsCl — Lösungen eine analoge Gesetzmässigkeit mit den von Agar [14] als auch Helfand und Kirkwood [15] demonstrierten Formeln bestätigt.

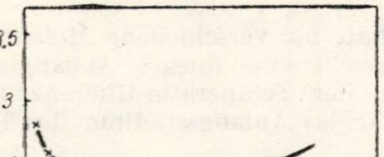

Abb. 2. — Die Abhängigkeit des Soret-Koeffizienten der CsCl-Lösungen von der Quadratwurzel der Molalität.

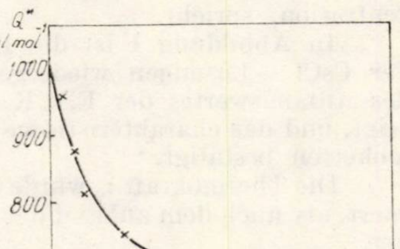

Abb. 3. — Die Abhängigkeit der molaren Überführungswärmen des CsCl von der Quadratwurzel der Molalität des Lösungen.

Tabelle 2

Soret Koeffizienten der wässrigen CsCl-Lösungen

Nr. crt.	m Mol. kg^{-1}	$-\sigma^{CsCl}\ 10^3 grd^{-1}$				
		1	2	3	med.	Ec.dr.
1	0,001	2,80	2,82	2,81	2,81	2,46
2	0,005	2,59	2,61	2,63	2,61	2,68
3	0,010	2,42	2,45	2,45	2,44	2,51
4	0,050	2,32	2,34	2,33	2,33	2,36
5	0,100	2,36	2,37	2,8	2,37	2,37
6	0,500	2,43	2,45	2,44	2,43	2,40

Tabelle 3

Molaren Überführungswärmen der wässrigen CsCl-Lösungen

Nr. crt.	m Mol.kg^{-1}	Q_1^*	Q_2^*	Q_3^*	$Q_{med.}^*$	$Q_{Ed.dr.}^*$
		cal.Mol.$^{-1}$				
1	0,001	958,5	963,3	958,8	960,2	241,6
2	0,005	872,0	879,5	884,6	878,7	903,8
3	0,010	804,5	814,3	815,4	811,4	835,2
4	0,050	748,6	757,1	752,2	752,6	761,4
5	0,100	708,7	713,9	714,5	712,4	713,8
6	0,500	706,1	709,9	705,3	717,1	968,0

Bei grösseren Konzentrationen der CsCl-Lösungen werden Abweichungen von der Linearität beobachtet. Dergleiche Abweichungen wurden im allgemeinen bei Alkali —und Erdalkalihalogenieden für Konzentrationen die grösser als 0,5 m sind beobacht,[16] bei $CdCl_2$-Lösungen [17] und bei einigen Polyelektrolytlösungen [18] erscheinen solche Abweichungen von der Linearität auch bei kleineren Konzentrationen. Diese Abweichungen der molaren Überführungswärme von der Linearität können den Veränderungen in der sekundären Hydratierungssphäre der Ionen die mit dem Ansteigen der Konzentration stattfinden, zugeschrieben werden. Diese Veränderungen in der sekundären Hydratierungssphäre sind um so bregreifbarer je weniger das Ion primär hydratiert ist und je stärker es die Wasserstruktur auf grössere Strecken zerstört, was der Fall des Iones Cs^+ ist.

Mit Hilfe des Wertes der molaren Überführungswärme Q^{*CsCl} für die Konzentration 0,001 m, welcher als entsprechender Wert für die unendliche Verdünnung angenommen wurden

$$Q^{*CsCl} \approx {}^*Q^{0CsCl}$$

hat man die konventionelle ionische Überführungswärme und die konventionelle ionische Überführungsentropie des Iones Cs^+ bestimmt.

Als Bezugsgrösse wurde die ionische Überführungswärme für Cl^- nach Haase und Mitarbeiter

$$^*Q^0_{Cl^-} = 1700 \text{ cal.Mol}^{-1} \text{ genommen.}$$

Die ionische Überführungswärme des Iones Cs^+ wurde mit folgender Formel bestimmt:

$$*Q^0_{Cs^+} = *Q^{0CsCl} - *Q^0_{Cl^-}$$

Mit dem Zahlenwert der ionischen Überführungswärme wurde die ionische Überführungsentropie für unendliche Verdünnung mit dem Ausdruck

$$*S^0_{Cs^+} = \frac{*Q^0_{Cs^+}}{T} + S^{\emptyset}_{Cs^+}$$

errechnet, wo $S^{\emptyset}$ die ionische Überführungstandardentropie darstellt.

Man bemerket eine gute Übereinstimmung zwischen unseren Rezultaten und Literaturwerten, welche von Messungen mit einfachen Thermoketten mit Ag/AgCl, Cl^- Elektroden stammen.[4]

Tabelle 4

Konventionelle ionische Überführungswärmen und Überführungsentropien bei 25°C

m Mol.kg^{-1}	$*Q^0_{Cs^+}$ · cal.Mol^{-1}				$*S^0_{Cs^+}$ cal.grd^{-1} Mol^{-1}		
	Eigene Daten		Literaturdaten[4]		Eigene Daten		Literaturdaten[4]
	a	b	c	d	e	f	g
0,001	−739	−859	−884	−780	29,32	28,92	29,20

a und e — wurden mit den arithmetischen experimentellen Mittelwerten erhalten
b und f — wurden ausgehend von den anhand der Gradegleichung linearisierten Werten experimenteller Wert
c — experimenteller Wert
d — wurde mit den Werten der konventionellen ionischen und Standardentropien erhalten.

SCHLUSSFOLGERUNGEN

Die unternommenen E.M.K. Messungen an doppelten Thermoketten mit wässrigen CsCl-Lösungen bei einer mittlerem Temperatur von 25,00°C, haben uns Daten zur Berechnung von Soret-Koeffizienten, molare Überführungswärmen dieser Lösungen, als auch für die Erhaltung der ionischen, konventionellen Überführungswärme und ionischen konventionellen Überführungsentropie des Iones, Cs^+, geliefert.

LITERATURHINWEISE

[1] E. Constantinescu und H. Dengel, *Rev. Roumaine Chim.*, **27**, 47 (1982).
[2] Fl. Bărbulescu, E. Constantinescu und H. Dengel, *Buletinul I.P.B.* Seria Chimie-Metalurgie, XLI, 19 (1979).
[3] Fl. Bărbulescu, E. Constantinescu und H. Dengel, *Rev. Chim.* (Bucureşti) **31**, 258 (1980).

[4] R. Haase und K. Hoch, Z. phys. Chem (Frankfurt), **46**, 63 (1965).

[5] I. G. Murgulescu, Fl. Bărbulescu und E. Constantinescu, *Rev. Roumaine Chim.*, **13**, 841 (1968).

[6] T. Ideka, *Bull. Chem. Soc. Japan*, **38**, 407 (1965).

[7] T. Ideka, H. Ohe und S. Kawamura, *Bull. Chem. Soc. Japan*, **41**, 2858 (1968).

[8] Ch. Moreau und G. Lepoutre, *J. Chem. Phys.*, **52**, 498 (1955).

[9] R. C. Srivastava, *J. Indian Chem. Soc.*, **40**, 585 (1963).

[10] T. Ideka „Some Aspects of Electrochemistry in Non-isothermal Systems", Kaimeido Printing Co., Shizouka, 1961.

[11] H. S. Harned und B. B. Owen „The Physical Chemistry of Electrolytic Solution" Reinhold Publishing Corp., New York, 1958.

[12] B. D. Butler und J. C. R. Turner, *J. Phys. Chem.* **69**, 3598 (1965).

[13] P. N. Snowdon und J. C. R. Turner, *Trans. Faraday Soc.*, **56**, 456 (1960).

[14] L. G. Longsworth und J. N. Agar, „The Structure of Electrolytic Solutions", Ed. Hamer Wiley, New York, 1959, p. 213.

[15] E. Helfand und J. G. Kirkwood, *J. Chem. Phys.*, **32**, 857 (1960).

[16] J. Chanu und L. Mousselin, *Electrochim. Acta.*, **14**, 207 (1969).

[17] J. Demichowicz-Piogoniowa, *Bull. Acad. Polon. Sci., Ser. Sci. Chim.*, **13**, 1 (1965).

[18] J. N. Agar und V. M. M. Lobo, *Electrochim. Acta*, **20**, 319 (1975).

[illegible] Jones [illegible] Phys. [illegible] 46, 85 (1934).

[illegible] Margenau [illegible] 18, 851 [illegible]

[illegible] (1950).

[illegible] 57 (1950).

[illegible] (1963).

[illegible] (1962).

[illegible] 49 (1949).

[illegible]

[illegible] (1961).

[illegible] Pergamon Press, New York [illegible]

[illegible] 69, [illegible] (1965).

[illegible] 56, 456 (1960).

[illegible]

[illegible] New York [illegible]

[illegible] (1962).

[illegible] (1962).

[illegible] 13 [illegible] (1963).

[illegible] 78, [illegible] (1957).

Revue Roumaine de Chimie, **29**, *8*, 663—670 (1984)

ÉTUDE DE LA TEXTURE DES NODULES OCÉANIQUES EN VUE DE LEUR UTILISATION COMME CATALYSEURS

CLAUDE DODET, FRANCIS NOVILLE, MICHEL CRINE et JEAN-PAUL PIRARD
Université de Liège, Unité Applications du Centre de Recherches sur la Catalyse
Institut de Chimie Industrielle Rue A. Stévart, 2-B-4000, Liège, Belgique

Reçu : 23 février 1983
Révisé : 7 décembre 1983

Les nodules océaniques possèdent une **texture poreuse remarquable** qui permet d'envisager leur utilisation comme catalyseurs ou adsorbants.
En vue de confirmer les résultats obtenus par l'analyse des isothermes d'adsorption-désorption d'azote, des échantillons de nodules calcinés entre 25 et 725° C sous courant d'azote, d'hydrogène et d'oxygène on été examinés par diffractométrie des rayons X.

INTRODUCTION

La découverte récente et la récupération des nodules océaniques procurent un matériau de faible coût, intéressant pour beaucoup d'industries. En effet, de par leur composition riche en éléments métalliques tels que le manganèse, le fer et surtout le nickel, le cuivre et le cobalt, les nodules sont d'un très grand intérêt pour la métallurgie. [1,2]

En chimie également, ce matériau peut trouver des applications intéressantes en catalyse et en adsorption, car il possède des propriétés texturales assez remarquables et une réactivité non négligeable. Une des applications catalytiques envisagées est l'hydrotraitement à température et pression élevées des coupes pétrolières lourdes, domaine où ils peuvent entrer en compétition avec les catalyseurs classiques. [3,4] L'utilisation des nodules comme catalyseurs d'oxydation a également été envisagée. [5]

Dans une étude récente, [6] nous avons mis en évidence par l'analyse des isothermes d'adsorption-désorption d'azote, la texture poreuse remarquable des nodules océaniques extraits de l'Océan Pacifique au large des côtes de Californie par le Consortium Ocean Mining Associates.

Nous avons constaté que les nodules bruts possèdent une surface spécifique élevée (de l'ordre de 85 m^2/g). Calcinés sous hydrogène, sous azote ou sous oxygène, ils conservent leur porosité élevée jusqu'à des températures pouvant atteindre 500° C ce qui permet d'envisager leur utilisation comme catalyseur pour des réactions relativement sévères. Au-dessus de 500°C, la texture poreuse disparaît progressivement.

Bien que l'étude approfondie de la structure complexe des nodules océaniques bruts soit entreprise depuis de nombreuses années, il nous a paru intéressant, vu l'importance des applications envisagées dans le domaine de la catalyse, de confirmer les résultats de l'analyse des isothermes d'adsorption-désorption par une étude des mêmes échantillons par diffractométrie des rayons X. Nous voulons ainsi esquisser le comportement des nodules dans des milieux gazeux semblables à ceux régnant dans un réacteur catalytique.

EXPÉRIMENTATION

1. MÉTHODE

Nous avons utilisé, pour la détermination des spectres de diffraction des poudres, un diffractomètre Philips avec monochromateur et anticathode de cuivre.

2. PRÉPARATION DES ÉCHANTILLONS

Un lot représentatif de nodules a été broyé, puis tamisé, les grains dépassant 250 µm étant renvoyés au broyage. Les mesures furent effectuées sur la fraction de grains dont le diamètre était compris entre 170 et 250 µm.

Le traitement thermique sous courant gazeux de certains échantillons fut réalisé dans des fours à température contrôlée (±5 °C). Les échantillons traités sous courant d'hydrogène furent conservés sous atmosphère d'argon, tandis que ceux traités sous courant d'azote ou d'oxygène furent conservés à l'air.

3. RÉSULTATS

Nous avons déterminé les spectres de diffraction d'un échantillon de nodule brut, d'une série d'échantillons calcinés sous courant d'azote pendant 24 heures aux températures de 135, 215, 335, 525 et 725 °C, d'une série d'échantillons calcinés sous courant d'hydrogène pendant 24 heures aux températures de 130, 215, 335 et 520 °C, d'un échantillon calciné sous courant d'oxygène pendant 24 heures à la température de 420 °C.

DISCUSSION

1. L'étude approfondie de la structure complexe des nodules océaniques bruts est entreprise depuis de très nombreuses années. D'après les travaux les plus récents, parmi la vingtaine de minéraux d'oxyde de magnésium (IV) connus, il n'y a que trois qui existent en quantité appréciable dans les nodules de manganèse. Ce sont la todorokite, la birnessite et le δ-MnO_2.

Ces composés étant relativement mal définis, les données spectrales publiées dans la littérature peuvent être légèrement différentes selon les auteurs. Au tableau 1, nous avons reportés les spectres de diffraction des principaux minéraux rencontrés dans les nodules. [9,10]

L'examen du spectre de diffraction que nous avons obtenu sur les nodules bruts montre une structure mal cristallisée — raies larges et de faible intensité. Les solides amorphes ou mal cristallisés possèdent une texture poreuse plus importante en raison des défauts d'empilage.

Tableau 1

Spectres de diffraction des principaux minéraux présents dans les nodules polymétalliques

Todorokite MnO_2		Birnessite MnO_2		Delta-MnO_2 MnO_2	Hausmannite Mn_3O_4		Magnétite Fe_3O_4		Braunite Mn_2O_3		Hématite Fe_2O_3		Manganosite MnO		Quartz α SiO_2	
d(pm)	I/I_1	d(pm)	I/I_1	d(pm) I/I_1	d(pm)	I/I_1	d(pm)	I/I_1	d(pm)	I/I_1	d(pm)	I/I_1	d(pm)	I/I_1	d(pm)	I/I_1
956	10	727	10													
					486	5			492	7						
480	8															
															426	3
		360	4		336				336	3					334	10
319	4															
311	5								308	9						
					298		297	3								
									276	9	270	10				
					254	10	253	10	249	10	252	7	257	6		
246	2	244	7	244											246	
240	4															
234	3														228	
223	3												222	10		
					210		210								213	
									204	6						
198	3															
193	2															
178	1								179	3	170	4			182	2
174	1				172		172									
					162		162									
									154	8			157	6	154	
					149	6	149	4								
142	3	142	7	142												
139	2												134		138	

Les raies les plus intenses peuvent être attribuées à la todorokite et au quartz α, tandis que quelques raies de très faible intensité peuvent être attribuées à la birnessite et au δ-MnO_2 (tableau 2).

La birnessite posséderait une structure lamellaire formée successivement de couches d'octaèdres d'oxyde de manganèse — distantes d'environ 0,72 nm — et de couches d'eau entre lesquelles sont intercalés des ions métalliques bivalents tandis que la todorokite posséderait une structure formée de tunnels de diamètre de l'ordre de 0,6 nm à 0,7 nm compris entre des doubles chaînes d'octaèdres d'oxyde de manganèse. Ces tunnels seraient remplis d'ions métalliques et de molécules d'eau.

Ce résultat est en bon accord avec l'étude de la texture poreuse par les isothermes d'adsorption-désorption d'azote (tableau 3).
Celle-ci a permis de montrer que les nodules bruts possèdent une surface spécifique élevée (85 m^2/g) et des pores de rayon de 0,7 nm et 1,7 nm environ, dits « en fente », c'est-à-dire constitués par la superposition de plaquettes cristallines parallèles entre elles mais séparées par de très petites particules ou par des défauts d'empilement.

2. Les traitements thermiques altèrent considérablement les spectres de diffraction. Pour les échantillons calcinés sous azote à 135° C, 215° C

Tableau 2

Principales propriétés texturales des nodules calcinés sous courant gazeux

Brut d(pm)	Cal. 525°C d(pm)	Cal. 725°C d(pm)	Hydr. 335°C d(pm)	Hydr. 520°C d(pm)
980 Todorokite		980		*980*
		930		**921**
730 Birnessite				
		708		*708*
	490 Mn_3O_4	**487** Mn_3O_4		
482 Todorokite				
448				
420 Quartz α	420 Quartz α		420 Quartz α	*426* Quartz α
337 Quartz α	330 Quartz α		330 Quartz α	333 Quartz α
320 Todorokite	320	319	320	
		306 Mn_2O_3		
	298 Mn_3O_4	**298** Mn_3O_4,Fe_3O_4		
		287		
		273 Mn_2O_3,Fe_2O_3		
	253 Mn_3O_4	**255** Mn_3O_4,Fe_3O_4 Fe_2O_3	**254** MnO	**254** MnO
	246 Mn_3O_4(?)	248 Mn_2O_3		
246 Todorokite				
244 δ-MnO_2 Birnessite	*240*	234		
222 Todorokite			222 MnO	219 MnO
		212 Mn_2O_4		
		209 Mn_3O_4		
		203 Mn_2O_3		203
198 Todorokite				
		162 Mn_3O_4		
			156 MnO	**156** MnO
		154 Mn_2O_3		
		149 M_3O_4,Fe_3O_4		

Les valeurs **en caractères gras** représentent les raies les plus intenses.
Les valeurs en italique représentent des raies très faibles.

et 335° C, et sous oxygène à 420° C, toutes les raies disparaissent, à l'exception de celles attribuées au quartz.

La structure des nodules est ainsi complètement disloquée par le départ des groupements hydroxydes et de l'eau d'hydratation sous l'action de l'élévation de température (fig. 1).

On observe en parallèle une augmentation de la surface spécifique mais la texture de pores « en fente » se maintient en partie lors des traitements thermiques, car même pour les nodules calcinés à température élevée, on retrouve une certaine fraction de pores de 0,7 nm et 1,7 nm de rayon (fig. 2).

Pour les échantillons chauffés à 525 °C et 725 °C, l'on constate une recristallisation progressive des nodules allant de pair avec une rapide diminution de la surface spécifique (tableau 3). Les raies les plus intenses peuvent être attribuées au Mn_3O_4, au Mn_2O_3, au Fe_3O_4 et au Fe_2O_3 ou à des cristaux mixtes isomorphes Fe_2O_3 — Mn_2O_3. L'étude du système Fe_2O_3 — Mn_2O_3 montre l'existence d'une série de cristaux mixtes isomorphes du sesquioxyde de manganèse pour les concentrations moléculaires allant de 0 à 1 mole de Fe_2O_3 par mole de Mn_2O_3. La substitution

Tableau 3

Spectres de diffraction des nodules bruts, des nodules calcinés sous azote à 525°C et 725°C et sous hydrogène à 335°C et 520°C

Echantillon	S_{BET}(m²/g)	V_P(cm³/g)	r_{max}(nm)
Brut	85	0,177	0,8—1,7
Cal. 135°C	117	0,227	0,8—1,7
Cal. 215°C	102	0,361	1,7
Cal. 335°C	111	0,304	1,7
Cal. 525°C	73	0,395	1,7—4,0
Cal. 725°C	18	0,265	1,7—20,0
Brut	85	0,177	0,8—1,7
Hydr. 130°C	114	0,328	1,7
Hydr. 215°C	109	0,475	1,7—3,5
Hydr. 335°C	73	0,741	3,5—7,0
Hydr. 520°C	39	0,444	3,5—10,0
Oxyd. 420°C	102	0,329	1,7

Cal. = échantillon calciné sous courant d'azote.
Hydr. = échantillon calciné sous courant d'hydrogène.
Oxyd. = échantillon calciné sous courant d'oxygène.
S_{BET} = surface spécifique BET.
V_P = volume poreux.
r_P = rayons des pores (valeur des maxima de la courbe de distribution).

des atomes de manganèse par des atomes de fer dans le réseau se produit sans variation visible des dimensions réticulaires. [10]

L'oxyde de manganèse IV (MnO_2) perd progressivement de l'oxygène lorsqu'il est chauffé au-delà de 200 °C. [10]

A 725 °C, les raies attribuées au quartz α ont disparu car le quartz α se transforme en quartz β à 573 °C. [10]

3. Lors des traitements thermiques des nodules sous courant d'hydrogène à 130 °C, la même évolution est observée, disparition des raies attribuées aux composés du manganèse, maintien des raies attribuées au quartz α. A 335 °C et 520 °C, l'on constate également une recristallisation progressive des nodules allant de pair avec une diminution de la surface spécifique (tableau 3). Dans ce cas, les raies les plus intenses peuvent être attribuées au MnO, ce qui correspond à un degré d'oxydation plus petit du manganèse en présence d'hydrogène.

Signalons que les raies qui n'ont pas été attribuées proviennent probablement de composés alumino-silicates. Le nombre de composés de ce type rencontrés dans les nodules de différentes origines est tellement important qu'il ne nous était pas possible de nous avancer plus en avant.

Notons également que les échantillons chauffés à 725 °C et 520 °C sous azote et à 525 °C sous hydrogène s'orientent lorsqu'ils sont soumis au champ magnétique d'un aimant. On peut attribuer cette propriété à la présence de Mn_2O_3, Mn_3O_4, Fe_3O_4 et MnO qui ont une susceptibilité magnétique plus élevée que le MnO.

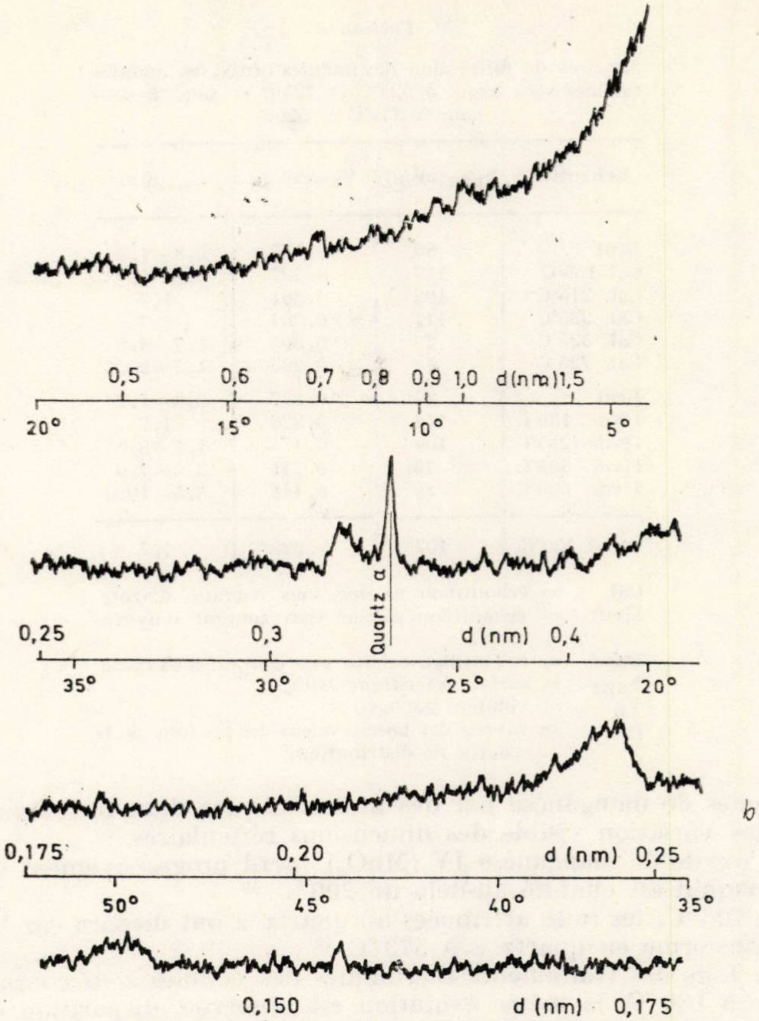

Fig. 1. — Spectre de diffraction d'un échantillon calciné à 335°C sous courant d'azote.

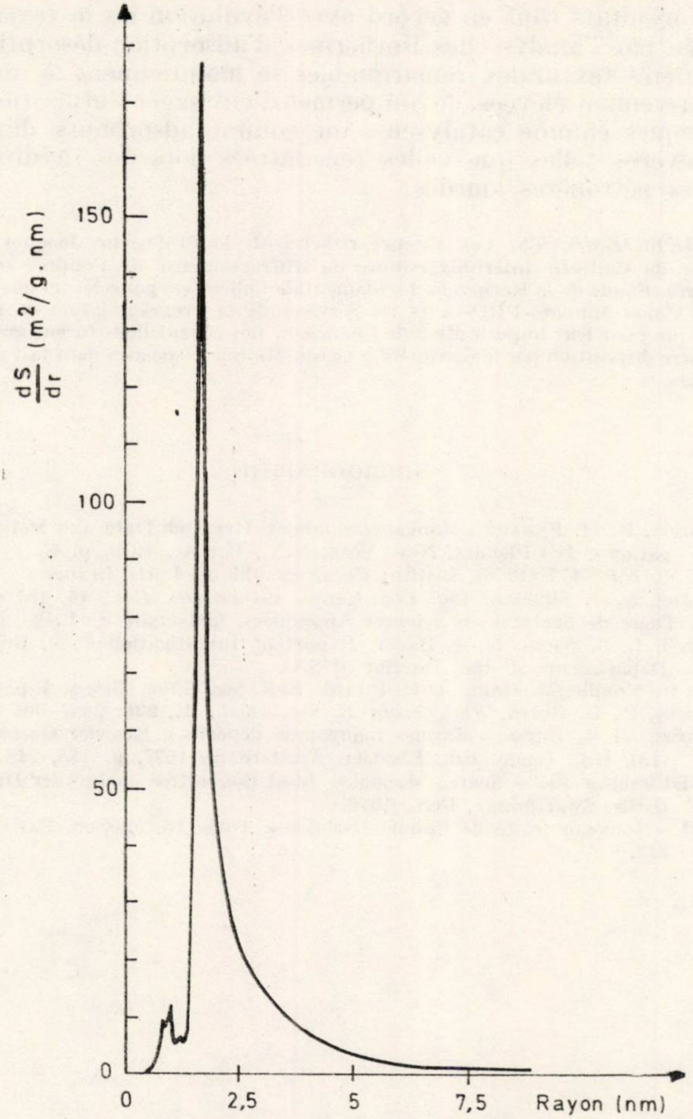

Fig. 2. — Courbe de distribution de la surface spécifique en fonction du rayon de pore pour un échantillon calciné à 335°C sous courant d'azote.

CONCLUSIONS

Cette étude montre par des mesures de diffractométrie des rayons X que la structure des nodules océaniques bruts est peu cristalline et que cette structure se disloque complètement lorsque les nodules sont traités thermiquement sous azote, sous hydrogène ou sous oxygène à des températures inférieures à 300—400 °C. A température plus élevée, une structure cristalline différente se reforme progressivement.

Ces résultats sont en accord avec l'évolution de la texture poreuse déterminée par l'analyse des isothermes d'adsorption-désorption d'azote. Ces propriétés texturales remarquables se maintiennent à des températures relativement élevées, ce qui permet d'envisager l'utilisation des nodules océaniques comme catalyseurs ou comme adsorbants dans des conditions sévères telles que celles rencontrées lors des hydrotraitements des coupes pétrolières lourdes.

REMERCIEMENTS. Les auteurs remercient le Professeur Jacques THOREZ, Directeur du Collectif Interuniversitaire de Diffractométrie de Poudres aux Sciences de la Terre (Fonds de la Recherche Fondamentale Collective) pour les mesures des spectres et l'Union Minière, l'IRSIA et les Services de la Programmation de la Politique Scientifique pour leur importante aide financière. Les échantillons furent gracieusement mis à notre disposition par le Consortium Ocean Mining Associates dont fait partie l'Union Minière.

BIBLIOGRAPHIE

[1] R. K. Sorem, R. H. Fewkes, « Manganese nodules, Research Data and Methods of Investigation », IFI/Plenum, New York, N.Y., U.S.A., 1979, p. 65.
[2] *Oceanis* **3** (8), 356–477 (1976), Institut Océanographique, Paris, France.
[3] C. D. Chang, A. J. Silvestri, *Ind. Eng. Chem., Process Des. Dev.*, **15**, 161 (1976).
[4] C. Dodet, Thèse de doctorat en Sciences Appliquées, Université de Liège, Belgique, 1983.
[5] E. F. Ferell, L. J. Nicks, D. J. Bauer, Report of Investigation 8330, Bureau of Mines, Department of the Interior (USA).
[6] C. Dodet, F. Noville, M. Crine, J. P. Pirard, *Bull. Soc. Chim. Belges*, à paraître en 1983.
[7] V. M. Burns, R. G. Burns, *Phil. Trans R. Soc. Lond., A.*, **286**, 283–301 (1977).
[8] R. G. Burns, V. M. Burns, « Marines manganese deposits », Elsevier Oceanography series (15), G.P. Gasby Ed., Elsevier, Amsterdam, 1977, p. 185, 248.
[9] « Powder Diffraction file — Search Manual ». Joint Committee on Powder Diffraction Standards, Swarthmore, Pen., 1976.
[10] P. Pascal, « Nouveau traité de Chimie Minérale ». Tome 16, Masson, Paris, 1960, p. 747, 813.

Revue Roumaine de Chimie, **29**, *8*, 671–676 (1984)

FRIEDEL-CRAFTS ACYLATION OF ALKYNES. III[1]

REACTION OF 1-ALKYNES WITH ACETYL CHLORIDE IN THE PRESENCE OF SILVER PERCHLORATE

DUMITRU MĂNOIU,[a] MARIA MĂNOIU,[a] ILIE G. DINULESCU[b] and MARGARET AVRAM[b, *]

[a] Institute of Research Technological Engineering and Design for Rafineries, Ploiești, Romania
[b] Laboratory of Organic Chemistry, Polytechnic Institute—TCH, Spl. Independenței 313, 72206 Bucharest 16, Romania

Received July 21, 1983

The behaviour of acylvinyl cations, generated from alkynes, acetyl chloride and $AgClO_4$, was investigated. In methylene chloride chloro-dienic ketones, β-chloro-α, β-unsaturated ketones and allenic ketones are formed. In the presence of benzene β-phenylated α, β-unsaturated ketones are formed in high yield. In cyclohexane α, β-unsaturated ketones are formed by hydride abstraction ; the reaction was acompanied in this case by isomerisation at equilibrium of the solvent.

INTRODUCTION

As part of our research concerning the chemistry of acylvinyl cations generated from acetylenes and acetyl chlorides, in the previous papers we reported on their behaviour in the $AlCl_3$ catalysed reaction in homogenous solution of non nucleophilic halogenated solvents,[2] saturated hydrocarbons or nucleophilic aromatic solvents.[1] It was shown [1,2] that the vinyl cations, generated in the course of these reactions, react with the present nucleophilic species ($AlCl_4^-$, benzene, acetylene) according to their nucleophilicity. Using benzene as nucleophilic solvent, coupled acylation with phenylation occurs, but the amount of phenylated unsaturated ketones is diminished, due to the competition between benzene and $AlCl_4^-$ in capturing the intermediate vinyl cation.

As a sequel to our studies, it was considered of interest to investigate the behaviour of the acetylvinyl cations, generated from acetylene and acetyl chloride in the absence of an efficient nucleophile as $AlCl_4^-$. Being known the low nucleophilicity of perchlorate ion, ClO_4^-, toward organic cations and the fact that ClO_4^- does not form covalent bonds with carbon atoms, the use of $AgClO_4$ for the generation of the acylating reagent was considered the most appropriate.

---

[*] Deceased in 1983

In this paper we present the results obtained in the reaction of acetyl chloride and 1-alkynes in the presence of $AgClO_4$. In order to compare the results with those obtained in the $AlCl_3$ catalysed reactions, the experiments were performed in non nucleophilic halogenated solvents or/and benzene and also in saturated hydrocarbons such as cyclohexane. The following 1-alkynes were used : propyne, 1-butyne and 1-hexyne.

REACTION OF 1-ALKYNES WITH ACETYL CHLORIDE AND $AgClO_4$ IN THE PRESENCE OF HALOGENATED SOLVENTS

The reaction of propyne and 1-hexyne with acetyl chloride in non nucleophilic halogenated solvents was performed in dichloromethane and dichloroethane at −50°.

In the reaction of propyne a crude reaction product was obtained, for which, by glc analysis, the presence of two major components in a ratio 1 : 8 was evidenced. They were isolated by preparative gas chromatography and identified as being the *E*-β-chloro-α, β-unsaturated ketone **2** and the dienic chloroketone **3**. Higher condensation products (aprox. 5%) were not identified.

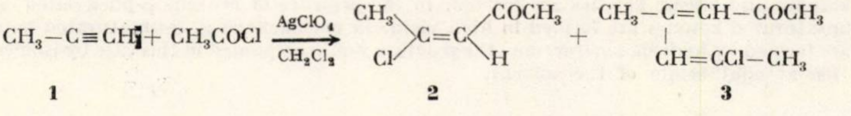

$$CH_3-C\equiv CH + CH_3COCl \xrightarrow[CH_2Cl_2]{AgClO_4} (CH_3)(Cl)C=C(COCH_3)(H) + CH_3-C(=CH-COCH_3)-CH=CCl-CH_3$$

1 **2** **3**

The reaction of 1-hexyne (**4**), in the same conditions, gave a more complex reaction mixture, in which not all the components could be identified. Three major components (totalising 60%), present in ratio 1 : 2 : 1 according to the gas chromatographic analysis, were isolated and identified as the *E*-β-chloro-α, β-unsaturated ketone **5**, the dienic chloroketone **6** and the allenic ketone **7**.

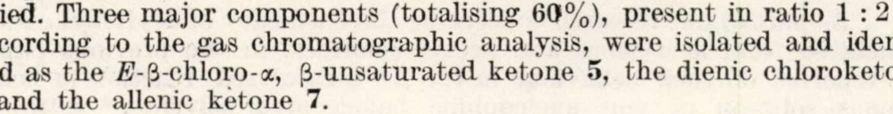

$$C_4H_9-C\equiv CH + CH_3COCl \xrightarrow[CH_2Cl_2]{AgClO_4} (C_4H_9)(Cl)C=C(COCH_3)(H) + C_4H_9-C(=CH-COCH_3)-CH=CCl-C_4H_9 +$$

4 **5** **6**

$$C_3H_7-CH=C=CH-COCH_3$$

7

The formation of β-chloro-α, β-unsaturated ketones (**2**, **5**) as well as chloro-dienic ketones (**3**, **6**), identical with those obtained in the previously described $AlCl_3$ catalysed reaction, needs comments. Unlike the $AlCl_3$ catalysed reaction, in which $AlCl_4^-$ furnishes the chloride ion, in the reaction occurring in the presence of $AgClO_4$, the issue of the halogenated compounds is explainable only by halogen ion abstraction from the halogenated solvent. [3] It is to notice that when CCl_4 is used, no chloride abstraction was observed. The general course of the reaction can be described as presented in scheme 1 for 1-hexyne.

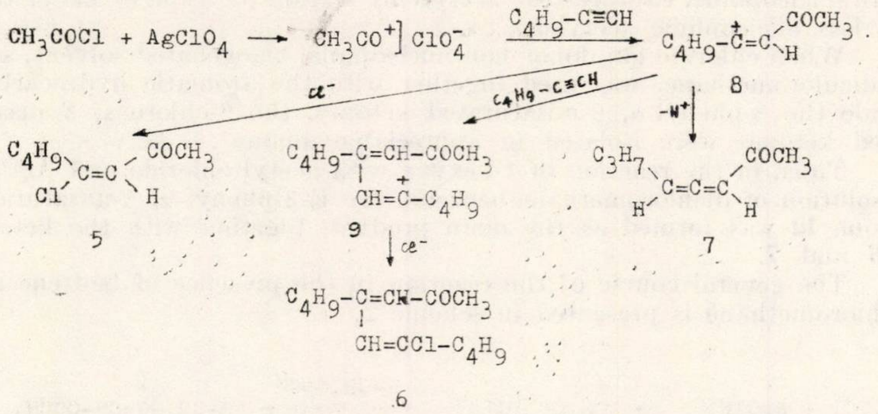
CH3COCl + AgClO4 → CH3CO+] ClO4−
C4H9−C≡CH
C4H9−C+=C(COCH3)H
8
−H+
Cl−
C4H9−C≡CH
C4H9(Cl)C=C(COCH3)H
5
C4H9−C=CH−COCH3 / CH=C+−C4H9
9
Cl−
C3H7(H)C=C=C(COCH3)H
7
C4H9−C=CH−COCH3 / CH=CCl−C4H9
6

Scheme 1.—Reaction of 1-hexyne with acetyl chloride and $AgClO_4$ in halogenated solvents.

As shown in scheme 1, the acylation of the alkyne occurs regioselectively leading to the acylvinyl cation **8**. The reaction of **8** with the nucleophilic acetylene gives rise to a new vinyl cation **9**. The intermediate **8**, as the dienic intermediate **9**, abstracts chloride ion from the solvent, leading to the stable halogenated final reaction products **5** and **6** respectively. The acylvinyl cation resulted from higher alkylacetylenes, except propyne, gives acylallenic compounds like **7** by loss of a proton. The isolation of acylallenes in this reaction supports the previous assumption that the intermediate formation of acylallenes explains the issus of isomeric β-chloro-β, γ-unsaturated ketones formed in the $AlCl_3$ catalysed acylation of higher 1-alkynes.[1,2]

REACTION OF 1-ALKYNES WITH ACETYL CHLORIDE AND $AgClO_4$ IN THE PRESENCE OF AROMATIC HYDROCARBONS

The reactions of the alkynes with acetyl chloride and $AgClO_4$ in the presence of aromatic hydrocarbons were performed using benzene-CCl_4 mixture and the same experimental conditions as those used in the above described experiments.

In the reaction of propyne and 1-butyne in benzene-CCl_4 mixture at −60°, the previously described [1] β-phenyl-α,β-unsaturated ketones **10** (97.0 % *E* and 3.0 % *Z* isomer) and **11** (83.0 % *E* and 4.7 % *Z* isomer) were obtained.

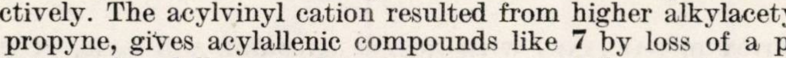

$$R-C\equiv CH + CH_3COCl \xrightarrow[C_6H_6]{AgClO_4} \begin{matrix} R \\ C_6H_5 \end{matrix}\!\!>C=C<\!\!\begin{matrix} COCH_3 \\ H \end{matrix} + \begin{matrix} R \\ C_6H_5 \end{matrix}\!\!>C=C<\!\!\begin{matrix} H \\ COCH_3 \end{matrix}$$

$R=CH_3$	**10** *E* (97.0 %)	**10** *Z* (3.0 %)
$R=C_2H_5$	**11** *E* (83.0 %)	**11** *Z* (4.7 %)
$R=C_4H_9$	**12** *E* (70.0 %)	

It is to notice that neither dienic nor isomeric β-phenyl-β, γ-unsaturated ketones were identified in these conditions. The benzene molecule, more nucleophilic, captures the acetylvinyl cation (of type **8**) faster than the less nucleophilic acetylene.

When chloride ion donor non nucleophilic halogenated solvent, such as dichloromethane, was used together with the aromatic hydrocarbon, beside the β-phenyl-α, β-unsaturated ketones, the β-chloro-α, β-unsaturated ketones were isolated in appreciable amount.

Thus, in the reaction of 1-hexyne with acetyl chloride and $AgClO_4$, in solution of dichloromethane-benzene, the E-β-phenyl-α, β-unsaturated ketone **12** was formed as the main product, together with the ketones **5**, **6** and **7**.

The general course of the reaction in the presence of benzene and dichloromethane is presented in scheme 2.

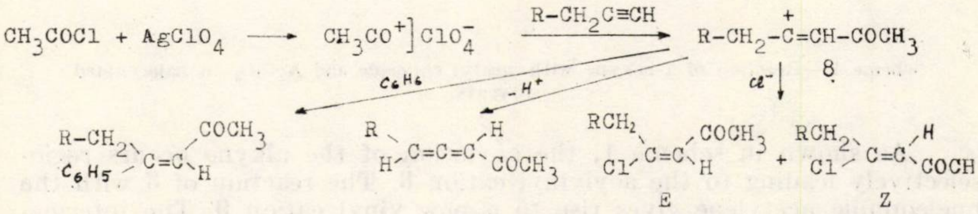

Scheme 2. — Reaction of 1-alkynes with acetyl chloride and $AgAlO_4$ in benzene-methylene chloride solution.

REACTION OF 1-ALKYNES WITH ACETYL CHLORIDE AND $AgClO_4$ IN THE PRESENCE OF SATURATED HYDROCARBONS

Attempts to evidence intermolecular hydride ion transfer from saturated hydrocarbons to the acylvinyl cations generated in the reaction of 1-alkynes and acetyl chloride in the presence of $AlCl_3$ were unsuccessful,[1] due to the presence of the chloride ion donor $AlCl_4^-$. Consequently, in order to have informations about the ability of the acetylvinyl cations to abstract hydride ions from saturated hydrocarbons, their generation in the absence of any nucleophile seemed appropriate.

For this purpose, a mixture of phenylacetylene, cyclohexane and $AgClO_4$ was reacted with acetyl chloride at room temperature. The glc analysis of the solvent shows that isomerisation of cyclohexane in methylcyclopentane occurred in the ratio corresponding almost to the equilibrium mixture.[4]

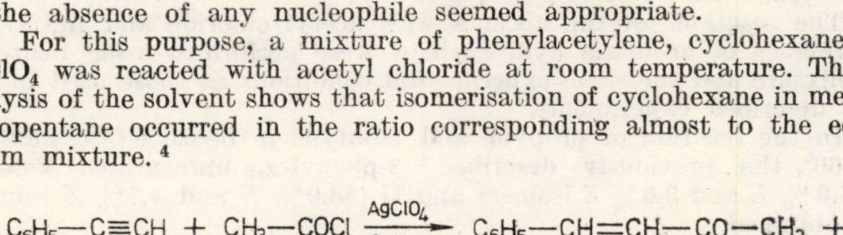

$$C_6H_5-C\equiv CH + CH_3-COCl \xrightarrow[C_6H_{12}]{AgClO_4} C_6H_5-CH=CH-CO-CH_3 +$$

13

In the heavy reaction products it was isolated benzylidene acetone **(13)** together with a mixture of isomers with formula $C_{12}H_{22}$ (three isomers not separated), formed from cyclohexane by hydride ion abstraction.[4]

EXPERIMENTAL

IR Spectra were recorded with a C. Zeiss double beam UR-20 spectrophotometer. ^{1}H-NMR spectra were determined with Tesla-60 and Varian A-60A spectrometers. Glc analysis and glc preparative separations were carried out as earlier described.[1,2]

Standard procedure. A suspension of 2.27 g (11.0 mmoles) $AgClO_4$ in 15 ml halogenated solvent (or a solution of 2.27 g (11.0 mmoles) $AgClO_4$ in 15 ml halogenated solvent and 15 ml aromatic hydrocarbon), well stirred and cooled, was treated with 0.78 g (10.0 mmoles) acetyl chloride and, after 10 min. with 0.40 g (10.0 mmoles) propyne ; the mixture was stirred for 30 min. The separated AgCl was filtered, the filtrate washed with water, dried and the solvent removed in vacuo. The crude reaction product was analysed gas chromatographically.

Reaction of propyne with acetyl chloride and $AgClO_4$ in dichloromethane. Working as above, at −15°, two compounds in ratio 1 : 8 were formed : *E*-4-chloro-pent-5-en-2-one (**2**), identical with the previously described product,[2] and the new ketone **3**.

2-Chloro-1,4-dimethyl-hepta-2,4-dien-6-one (**3**). IR (CCl_4, cm^{-1}) : $\nu_{C=C}$ 1628, ν_{CO} 1700 ; ^{1}H—NMR (CCl_4, δ, ppm) : 2.31 (CH_3CO), 6.08 (=CH—CO), 6.37 (H—C=CCl).

Reaction of 1-hexyne with acetyl chloride and $AgClO_4$ in dichloromethane. The reaction was carried out according to the standard proecedure, at −50°. After working up, the major components (totalising 60 % from the crude reaction product), present in ratio 1 : 2 : 1, were isolated and found as being the previously described[2] chloroketones **5** and **6** together with the new ketone **7**.

Octa-3,4-dien-2-one (**7**). IR (CCl_4, cm^{-1}) : ν_{CO} 1685, $\nu_{C=C=C}$ 1950 ; ^{1}H-NMR (CCl_4, δ, ppm) : 0.94 (CH_3), 1.2—2.5 (CH_2), 6.5 (CH=C=CH).

Reaction of propyne with acetyl chloride and $AgClO_4$ in benzene. Working as above, in the crude reaction product the previously described[1] phenylated ketones **10** *E* (97.0 %) and **10** *Z* (3.0 %) were evidenced by glc.

Reaction of 1-butyne with acetyl chloride and $AgClO_4$ in benzene. Working as above, in the crude reaction product, isolated in 67 % yield, the earlier described[1] phenylated ketones **11** *E* (83.0 %) and **11** *Z* (4.7 %), together with 12.3 % polymeric compounds, were evidenced by glc.

Reaction of 1-hexyne with acetyl chloride and $AgClO_4$ in dichloromethane-benzene solution. In the crude reaction product, the previously described[1,2] chloroketones **5**, mixture of 18 % isomer *E* and 3 % isomer *Z*, together with allene **7** (8 %) and phenylated ketone **12** (70 %) were identified.

Reaction of phenylacetylene with acetyl chloride in cyclohexane. Into a suspension of 8.0 g (38.7 mmoles) $AgClO_4$ in 4.0 g (38.7 mmoles) phenylacetylene and 25 ml cyclohexane, 3.0 g (38.6 mmoles) acetyl chloride were dropped in 15 min. under vigorous stirring, at 25°. The mixture was stirred for 30 min. The AgCl was filtered and the solvent was removed on water bath. Analysis of the distilled fraction shows a content of 24.7 % methylcyclopentane together with 75.3% cyclohexane. From the residue, two components were separated by preparative glc.

Benzalacetone (**13**), b.p. 125°/6 mm. IR (CCl_4, cm^{-1}) : ν_{CO} 1673, 1697, $\nu_{C=C}$ 1612, 1627 ; ^{1}H-NMR (CCl_4, δ, ppm) : 5.0—5.9 (=C—H, J = 10.4 Hz).

Hydrocarbon $C_{12}H_{22}$ (mixture of isomers). Analysis : $C_{12}H_{22}$ Calcd : C, 86.74 ; H, 13.25. Found : C, 87.12 ; H, 14.87 %.

REFERENCES

[1] Part II: D. Mănoiu, M. Mănoiu, I. G. Dinulescu and M. Avram, *Rev. Roumaine Chim.*, **29**, 201 (1984).

[2] D. Mănoiu, M. Mănoiu, I. G. Dinulescu and M. Avram, *Rev. Roumaine Chim.*, **29**, 193 (1984).

[3] E. H. White, H. P. Tiwari and M. J. Todd, *J. Amer. Chem. Soc.*, **90**, 4734 (1968); W.S. Johnson, M. B. Gravestock, R. J. Pany and D. A. O'Koril, *J. Amer. Chem. Soc.*, **94**, 8604 (1972).

[4] C. D. Nenitzescu and I. P. Cantuniari, *Ber. dtsch. Chem. Ges.*, **66**, 1907 (1933).

Revue Roumaine de Chimie, **29**, *8*, 677–681 (1984)

KINETISCHE UNTERSUCHUNG DES HERSTELLUNGSPROZESSES EINES SULFAMETHIN-SILBERSALZES UNTER VERWENDUNG VON RADIOISOTOPEN

C. ONISCU, AL. CECAL und E. HOROBA

Fakultät für chemische Technologie des Polytechnischen Instituts, Splaiul Bahlui-71, 6600 – Iaşi, Rumänien

Eingegangen am 26. November 1983

Die Arbeit stellt ein kinetisches Studium der Synthesereaktion von Sulfamethin-Natriumsalz mit Silbernitrat vor, durch die man Sulfamethin-Silbersalz erhält. Im Hinblick auf die Verfolgung des zeitlichen Ablaufs dieser Reaktion wurde eine Silbernitratlösung mit ^{110}Ag verwendet. Es wurden die Geschwindigkeitskonstanten und die Aktivierungsenergie für die entsprechenden Reaktionen zweiter Ordnung bestimmt.

A kinetical study on the synthesis of the sulfamethine silver salt from the corresponding sodium salt and silver nitrate is reported. The reaction development in time was followed by means of a silver nitrate solution with ^{110}Ag, as tracer. For the second order reactions the rate constants and the activation energy were established.

EINFÜHRUNG

Die antiseptischen Eigenschaften der Silbersalze sind seit längerem bekannt, wobei man bei der Anwendung des Nitrats dieses Metalls positive Ergebnisse erzielte bei der Behandlung von schweren Verbrennungen, u.a durch die heilenden, antiinfektiösen Eigenschaften des Silbers. Nach Entdeckung der Sulfamide und im speziellen der Sulfadiazine wurde begonnen, diese auf breiter Basis für die Behandlung schwerer Verbrennungen zu nutzen[1–5].

In dieser Arbeit wird vorgeschlagen, das Sulfamethin-Silbersalz, eines der aktivsten Sulfonamide, charakterisiert durch ein breites antibakterielles Spektrum und schnelle Absorption, durch Synthese zu erhalten. Die Kinetik dieser Reaktion unter verschiedenen Versuchsbedingungen wurde durch eine Methode verfolgt, die auf der Verwendung von Radioisotopen beruht.[6–12]

EXPERIMENTELLER TEIL

Das Natriumsalz von Sulfamethin wurde erhalten durch Auflösung des Sulfamethins in einer Lösung von Natriumhydroxid. Die beiden Substanzen befanden sich in einem striktäquimolaren Verhältnis und der pH-Wert des Reaktionsgemisches (in 3-fach destiliertem Wasser, ohne Chlor) wurde auf 7—7,2 gehalten. Die Endkonzentration der Lösung des Natriumsalzes von Sulfamethin war 1.10^{-3}M. Das markierte Silbernitrat $^{110}AgNO_3$ in fester Form mit einer spezifischen Aktivität von $1,5.10^7$ Bq/g, wurde von IFIN Bukarest geliefert. Aus diesem Salz wurde eine Lösung von 1.10^{-3} M hergestellt, die in den nachfolgenden Experimenten benutzt wurde.

Aus der Reaktion des Natriumsalzes von Sulfamethin mit dem Silbernitrat ging das Silbersalz von Sulfamethin hervor, im Niderschlag von weisser Farbe. Längere Zeit bei Tageslicht gelassen, nimmt dieser einen hellbraunen Farbton an, wahrscheinlich, durch den teilweisen Zerfall dieser chemischen Verbindung.

Die Experimente wurden in konischen Zentrifugenreagenzglässern durchgeführt; jede Serie bestand aus 6—8 solcher Reagenzglässer. Das totale Volumen betrug jedesmal 10 mal, wobei die Konzentration der an der Reaktion beteiligten Substanzen variierte.

Die kinetischen Untersuchungen wurden mit mehreren molaren Verhältnissen durchgeführt (Silbernitrat-Natriumsalz von Sulfamethin), 2 : 1, 1 : 1, 1 : 2 und 1 : 5 bei 294,2 K. Für das Verhältnis 1 : 5 die Experimente bei Temperaturen von 301,7; 305,6 und 313,4 K ausgeführt und man hat die Reaktion bei zwei verschiedenen pH-Werten (4,4 und 7,0) untersucht bei einer Temperatur von 294,2 K. Ebenfalls wurde diese Reaktion im statischen Zustand und durch Schütteln in einer Zeitspanne von 2 Stunden im dynamischen Zustand (pH = 7,0) verfolgt.

Im Rahmen einer Versuchsserie wurde je ein Reagenzglass genommen und der Inhalt in einem Zeitintervall von 15 min zentrifugiert (1500 U/min) um den Niederschlag, Sulfamethin-Silbersalz (mit ^{110}Ag) von der Lösung zu trennen. Aus dieser Lösung wurden 0,5 ml entnommen und in einen Porzellantiegel gefüllt. Nach Verflüchtigung der Lösung mit Hilfe einer infrarotlampe wurde die Aktivität des verbliebenen Rückstandes gemessen wobei eine Szintilla-Ionssonde NaI(T1) angeschlossenen an einen VA—M—14 Vakutronik Zähler, verwendet wurde.

ERGEBNISSE UND DISKUSSION

Im ersten Teil, wurde die Reaktionsordnung bestimmt, die das Reaktionssystem Sulfamethinol-Natriumsalz und mit ^{110}Ag markiertes Silbernitrat, charakterisiert. Die Ausgangskonzentration der Lösung betrug 1.10^{-3} M und die Arbeitstemperatur 294,2 K.

In diesem Sinne wurden Reaktionsgemische mit verschiedenen molaren Verhältnissen zwischen den Reaktanten hergestellt.

In allen Fällen lief die Reaktion nach einer Kinetik zweiter Ordnung ab, die durch die Gleichung:

$$1/R = 1/R_0 + kt, \tag{1}$$

beschrieben werden kann, wobei R_0 die Ausgangsaktivität und R diejenige zu einem gegebenen Zeitpunkt, entsprechend der entnommenen Proben aus dem Reaktionssystem. k ist die Geschwindigkeitskonstante und t bezieht sich auf die Reaktionszeit. Für die verschiedenen reaktanten Systeme betrug die notwendige Zeit zum Erreichen des Reaktionsgleichgewichts 2—3 Stunden. Aus der graphischen Darstellung von: $1/R = f(t)$, entsprechend der Gleichung (1) ergeben sich Geraden, aus deren Steigungen die Geschwindigkeitskonstanten errechnet wurden. Die entsrprechenden Werte sind in Tabelle 1 wiedergegeben.

Man stellt fest, dass die Reaktionsgeschwindigkeit relativ klein ist.

Im weitern wurde der Einfluss der Temperatur auf die Reaktionsgeschwindigkeit verfolgt. In diesem Sinne wurden aus den Ausgangslösungen mehrere Gemische hergestellt, bei denen das molare Verhältnis zwischen Silbernitrat (mit ^{110}Ag) und dem Natriumsalz von Sulfamethin 1 : 5 betrug. Es wurde bei Temperaturen von 294,2 ; 301,7 ; 305,6 und 313,4 K

Tebelle 1

Die Geschwindigkeitskonstanten für die Reaktion der Bildung von Sulfamethin-Silbersalz, bei 294,2 K

Molaren Verhältnissen : Silbernitrat-Natriumsalz von Sulfamethin	k (l.mol^{-1}.h^{-1})
2 : 1	$2,86 \cdot 10^{-7}$
1 : 1	$3,25 \cdot 10^{-7}$
1 : 2	$2,93 \cdot 10^{-7}$
1 : 5	$3,20 \cdot 10^{-7}$

gearbeitet. Für jede Arbeitstemperatur wurde die Geschwindigkeitskonstante der jeweiligen Reaktion bestimmt. Die gefundene Werte sind in Tabelle 2 gezeigt.

Durch die graphische Darstellung von $\ln k = f(1/T)$ erhielt man eine Arrhenius Gerade, aus deren Steigung die Aktivierungsenergie für den gegebenen Prozess errechnet wurde (Abb. 1).

Tabelle 2

Die Geschwindigkeitskonstanten in Abhängigkeit von der Temperatur des Reaktionssystems Silbernitrat-Natriumsalz von Sulfamethin in Verhältnis 1 : 5

Temperatur (K)	k(l.mol^{-1}.h^{-1})
294, 2	$3,20 \cdot 10^{-7}$
301, 7	$3,45 \cdot 10^{-7}$
305, 6	$4,47 \cdot 10^{-7}$
313, 4	$6,50 \cdot 10^{-7}$

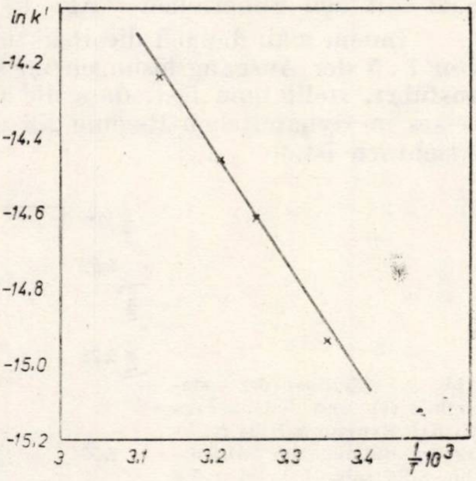

Abb. 1. — Wechselbeziehung zwischen dem Logarithmus der Geschwindigkeitskonstanten und der Temperatur bei der Reaktion von Silbernitrat mit Natriumsalz von Sulfamethin (1 : 5). →

Aus dieser Darstellung wurde ein Wert von 28,8 KJ/Mol für die Aktivierungsenergie gefunden.

Danach wurde auch der Einfluss anderer Parameter auf die Kinetik des Bildungsprozesses von Sulfamethin-Silbersalz verfolgt. Die Untersuchungen wurden mit den Ausgangslösungen (1.10^{-3} M) durchgeführt, aus denen Gemische von Silbernitrat (mit ^{110}Ag) und Sulfamethin-Natriumsalz in Verhältnis 1 : 5 hergestellt wurden.

Was den Einfluss des pH-Wertes auf die Reaktionsgeschwindigkeit anbetrifft (Abb. 2) stellt man fest, dass für den sauren pH-Wert von 4,4 im Puffer Essigsäure-Natriumazetat, die Reaktionsgeschwindigkeit wiedergegeben durch die Geschwindigkeitskonstante) 3,5 mal kleiner ist als bei dem neutralen pH-Wert von 7,0. In Anwesenheit des Puffergemisches

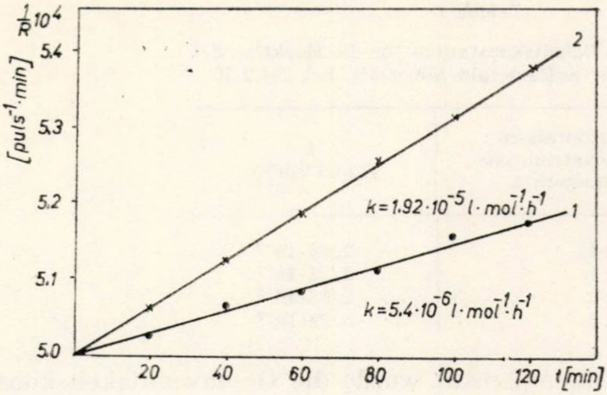

Abb. 2. — Kinetische Darstellung des Bildungsprozesses von Sulfamethin-Silbersalz in Abhängigkeit von pH-Wert (1) pH=4,4 und (2) pH=7,0.

ist eine schwache Dissoziation der Essigsäure und eine alkoholische Hydrolyse des Natriumazetats möglich, während die resultierenden Natriumkationen Inhibitoren für den gegebenen Prozess darstellen, d.h., für den gegenseitigen Austausch der Natriumionen aus dem Sulfamethin-Salz mit den Silberionen ^{110}Ag.

Indem man danach die Reaktion bei demselben molaren Verhältnis von 1 : 5 der Ausgangslösungen im statischen und dynamischen Regime ausführt, stellt man fest, dass die Geschwindigkeit des gegebenen Prozesses im dynamischen Regime 2,6 mal grosser ist, was aus dem Abb. 3 ersichtlich ist.

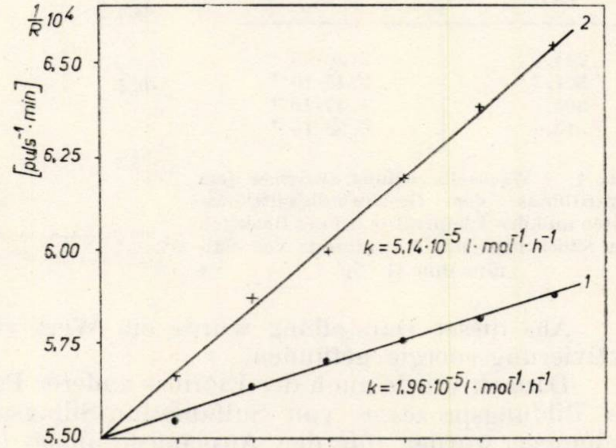

Abb. 3. — Einfluss der statischen (1) und dynamischen (2) Arbeitsweise auf die Kinetik der Bildung von Sulfamethin-Silbersalz, bei pH = 7,0

Diese Tatsache wird dadurch erklärt, dass beim Schütteln sich die Geschwindigkeit der Zusammenstösse zwischen den reaktanten Molekülen vergrössert, was eine Vergrösserung der Reaktionsgeschwindigkeit zur Folge hat.

Schlussfolgerung kann man auf Grund der aussgeführten kinetischen Untersuchung als Parameter des chemischen Prozesses zur Bildung von Sulfamethin-Silbersalz festhalten : optimale Temperatur rund 310 K; pH = 7,0 ; Dauer = 2 Stunden und dynamische Arbeitsweise.

LITERATUR

[1] B. J. Sandmen, *J. Pharm. Sci.*, **63**, 948 (1974).

[2] J. E. Coward und H. S. Rosenkranz, *Chemother. (Basel)*, **21**, 231 (1975).

[3] H. S. Rosenkranz und J. E. Coward, *Antimicrob. Agents Chemother.*, **5**, 119 (1974).

[4] C. L. Fox und S. M. Modak, *Antimicrob. Agents Chemother.*, **5**, 582 (1974).

[5] V. S. Fedorova und E. A. Levina, *Zhur. khim. Farm.*, **90**, 150 (1976).

[6] C. J. Collins, *Adv. Phys. Org. Chem.*, **2**, 3 (1963).

[7] A. N. Nesmeianov, R. K. Freifilina und L. I. Zakharkin, *Doklady Akad. Nauk S.S.S.R.*, **88**, 199 (1951).

[8] B. N. Neiman und G. I. Feklisov, *Doklady Akad. Nauk S.S.S.R*, **90**, 583 (1953).

[9] M. B. Neiman, *Zhur. fiz. Khim.*, **28**, 1235 (1954).

[10] M. B. Neiman und D. Gál, "The Kinetic Isotope Methods and its Application", Akadémiai Kiádo, Budapest, 1971, p. 37.

[11] L. Melander, "Isotope Effects on Reaction Rates", Roland Press, New York, 1960, p. 54.

[12] Al. Cecal, V. Sunel und L. Ghimiciu, *J. Radional. Chem.*, **78**, 247 (1983).

Revue Roumaine de Chimie, **29**, *8*, 683–692 (1984)

MECHANO-CHEMICAL MODIFICATION OF PHYSICAL AND CHEMICAL CHARACTERISTICS OF POLY(VINYL CHLORIDE) SUSPENSION

CLEOPATRA VASILIU OPREA, CLAUDIA NEGULIANU and
FELICIA WEINER

Polytechnic Institute of Iassy, Department of Organic and Macromolecular Chemistry, Iassy, Calea 23 August No. 11A, Romania

Received April 27, 1983

The paper deals with the modification of some physical and chemical characteristics of poly(vinyl chloride)-suspension subjected to mechanical action by vibratory milling and cryolysis in the presence of aromatic diamines of the *p*-phenylenediamine and benzidine types. Under these conditions the reaction is noticed between the polymer destruction fragments and diamines. The final products thus obtained show some new properties compared to the support polymer. Thus, they can be coloured by diazotizing and coupling reactions and their stability to the action of some physical and chemical agents is improved.

INTRODUCTION

The chemical reactions carried out in the presence of solid substances proceed especially at their surface; hence their nature is decisive for the participation at different chemical reactions. The mechanical work of the micro- and macromolecular solid substances was demonstrated to result in the internal energy increase of the system and, consequently, occurrence of the excited states which cause profound modifications in the structural edifice. At the same time heat evolvements, electrizations, electronical mechano-emissions, triboluminescence, etc. are produced.

Based on the fact that the mechano-chemical degradation of poly(vinyl chloride) takes place by homolytic splitting of C—C bond and occurrence of free radicals and that the amines introduced during working may act as radicalic acceptors, in the present paper the change in the structure and properties of this polymer by cryolysis and vibratory milling in the presence of *p*-phenylendiamine and benzidine was studied.

By mechano-chemical reaction between the destruction fragments and the above mentioned derivatives the poly(vinyl chloride) was coloured in a large colour scale by diazotizing and coupling with suitable components.

EXPERIMENTAL

1.1. RESEARCH TECHNIQUES

The mechano-activation by vibratory milling was achieved in a laboratory mill, model LS—60, supplied by VEB—Kefama Katzute Thuringem RDG equipped with steel vessels and milling parts, valves for gas admission and evacuation, thermostating jacket.The reaction mixture consisting of PVC—S and diamines was introduced together with the balls into the milling vessels which were then sealed. The air was removed by means of a vacuum pump and by passing an inert gas (nitrogen) previously purified and dried. The milling was performed under nitrogen atmosphere.

The reaction temperature was kept constant, $18 \pm 2°C$, by thermostating with water in the reaction vessel jacket.

The filling ratio ($\eta = \frac{a}{b} \times 100$) was 0.4 %, with a — as monomer or polymer quantity and b — as balls quantity.

The reaction products were taken out quantitatively from the milling vessels by methanol removal. The obtained suspension was filtered, the products extracted with methanol in a Soxhlet apparatus for separating the unreacted diamine and dried to a constant weight. The samples were purified by solving in cyclohexanone since a touch of metal from the equipment walls appears in the reaction mixture. The insoluble portion was removed by filtration; the filtrate was precipitated in methanol, washed for removing the cyclohexanone remainders, dried to constant weight and analysed.

The cryolysis was carried out with a polymer solution in cyclohexanone and diamine. The reactions were carried out in the presence of air, in V_2A ampoules ($Ø = 40$ mm, length $= 200$ mm) with threaded cap.

The freezing temperature was $-196°C$, the thawing temperature 80°C, a cycle needs 15 minutes (10 minutes for thawing and 5 minutes for freezing). When the reaction was finished, the polymer was precipitated with methanol, filtered, extracted in methanol in a Soxhlet apparatus and dried till constant weight.

1.2. INFLUENCE OF CERTAIN FACTORS ON THE REACTION BETWEEN PVC—S AND AROMATIC DIAMINES

1.2.1. Mechanical treatments

The effects of the mechanical treatments within different periods of time were characterized by observing the following properties: the molecular weight, the amount of chemically bound diamine, the degree of degradation, the amount of chlorine. For this purpose, a series of syntheses have been carried out covering a wide range of treating times, namely: 1—96 hours for milling, 10—60 cycles for cryolysis. The amount of chemically bound diamine in the samples obtained by synthesis, the fraction soluble in cyclohexanone, was calculated from the nitrogen content determined by the Kjeldahl method. The molecular weight was obtained by viscosimetry, [1] and the chlorine percentage according to Schöniger's method. [2]

The degree of degradation was expressed in terms of the relation: M_∞ / M_τ, where M_∞ denotes the limiting molecular weight and M_τ the actual average molecular weight. The data are illustrated in Fig. 1

The period of time of milling is noticed to play a decisive role on the reaction efficiency. Thus, for both vibratory milling and cryolysis the molecular weight decreases gradually with increasing milling times. One evidences the fact that the vibratory milling is more efficient than is the cryolysis, for a molecular weight $\overline{M} = 32.000$ is obtained after 6 hours milling, while for the same period of time of the cryolysis (60 cycles) a value of $\overline{M} = 50.000$ is obtained. For longer times of milling (24—96 hours) the concentration of chlorine in the sample, the fraction soluble in cyclohexanone was found to decrease from 55.07% to 39.83% while the amount of the chemically bound diamine increases (0−5.46%) (Table 1). By prolonging the milling time up to the limit : $M_\infty = 18{,}600$, the degree of degradation is noticed to increase continuously, in accordance with the variation of the contents of chlorine and chemically bound diamine, arriving at the limiting value $\varphi = 1$ at 96 hours (Fig. 1). The data characterizing the effects of the mechanical treatments covering different periods of time were also confirmed spectrophotometrically. Thus, the occurrence of new bands (1490−1600 cm^{-1}) within the recorded IR spectra is noticed, which may be attributed to the C≡N bond.

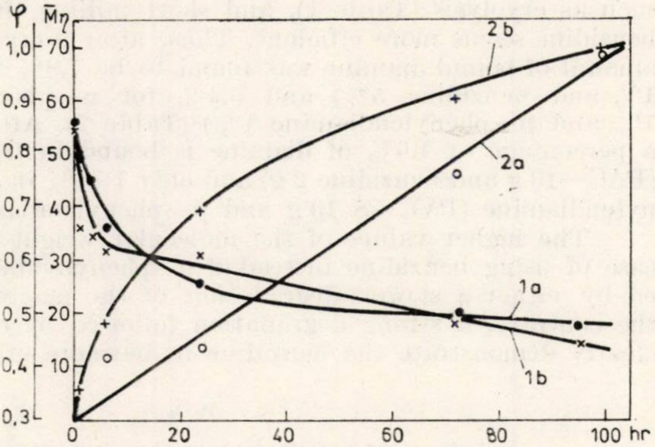

Fig. 1. — Influence of the mechanical work duration on the reaction efficiency for the system PVC−S (10 g)+ benzidine (a. 1 g and b. 2 g) activated by vibratory milling : 1a, 1b, $-M_n$; 2a, 2b−φ.

Table 1

Influence of the mechanical work duration on the reaction effectiveness for the system PVC −S + diamine

Sample	Duration and type of the mechanical work	M.10^{-3}	Amount of	
			chemically bound diamine %	chlorine %
PVC− S + benzidine	vibratory milling hours			
(10g) (2g)	0	54.97	0	55.07
(soluble fraction)	24	26.00	4.6	—
	72	20.00	4.8	43.46
	96	18.00	5.46	39.83
PVC− + *p*-phenylen−	0	54.97	0	55.07
diamine	24	9.00	1.78	42.35
	72	8.25	5.39	46.35
(10g) (1g)	96	6.35	5.40	29.20
(soluble fraction)				
PVC− S + benzidine (1%) (1g)	cryolysis, number of cycles			
	0	54.97	0	—
	20	51.80	4.33	
	60	50.24	6.30	

1.2.2. Diamine Nature

The results indicate the efficiency of the reaction between PVC—S and the special aromatic diamines, *p*—phenylendiamine and benzidine, to be also dependent on the diamine nature. Thus, under milder conditions such as cryolysis (Table 1), and short milling times (till 24 hours), the benzidine seems more efficient. Thus, after a cryolysis of 60 cycles, the amount of bound diamine was found to be 7.8% for benzidine (PVC—S 1% and benzidine 5%) and 5.4% for p—phenylendiamine (PVC—S 1% and *p*—phenylendiamine 1%) (Table 2). After 24 hours of milling a percentage of 4.6% of diamine is bound in the presence of benzidine (PAC—10 g and benzidine 2 g) and only 1.78% in the presence of *p*—phenylendiamine (PVC—S 10 g and *p*—phenylendiamine 1g).

The higher values of the molecular weight and chlorine content in case of using benzidine instead of *p*—phenylendiamine might be explained by either a slower degradation of the macromolecular chain or, on the contrary, a strong degradation followed by crosslinking. These data clearly demonstrate the benzidine to be more efficient.

Table 2

Influence of the diamine nature on the effectiveness of the reaction activated by cryolysis in the system PVC—S and diamine

Sample	Number of cycles	$M.10^{-3}$	Amount of chemically bound diamine %
PVC—S + benzidine (1%) (5%)	0	54.97	0
	40	49.85	6.05
	60	57.39	7.80
PVC—S+*p*-phenylen- (1%) diamine (1%)	0	54.97	0
	30	—	3.48
	40	49.47	5.40
PVC—S+benzidine (1%) (1%)	0	54.97	0
	20	51.80	4.33
	60	50.24	6.3

1.2.3. Diamine Amount

In order to observe the influence of the amount of diamine added to the reaction medium, the syntheses were carried out by both cryolysis and vibratory milling with variable amounts of diamine. The cryolysis was carried out with solutions of polyvinylchloride suspension in cylohexanone 1% in which benzidine in variable amounts (1—5 g), and in the case of vibratory milling the amounts of benzidine were (1—3 g). After 60 cryolysis cycles from the diamine amount introduced (5 g and 1 g respectively), 7.8% and 6.3% repectively were chemically bound. The data are shown in Figs. 2, 3 and Table 2. The molecular weights obtained by cryolysis (Table 2) also evidence the favourable effect of having a maximum amount of diamine.

Fig. 2. — Influence of the *p*-phenylendiamine amount on the molecular weight variation for the sample synthesized by vibratory milling in the system : PVC—S (10g) + diamine (1. —1 g ; 2. —3 g) at variable work duration (1—96) hours.

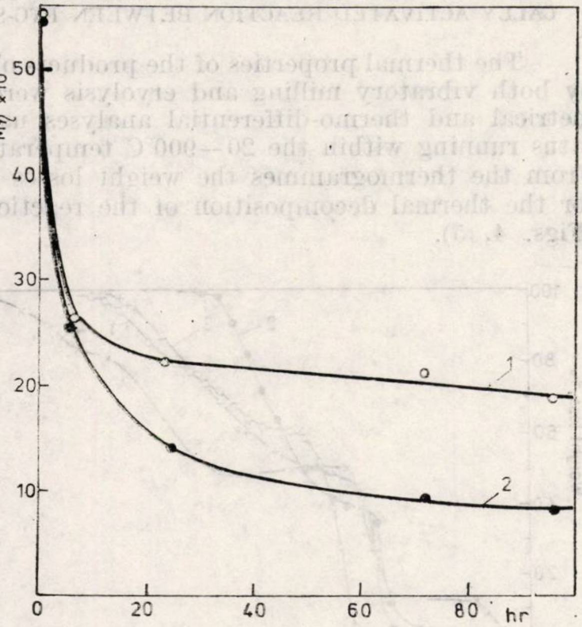

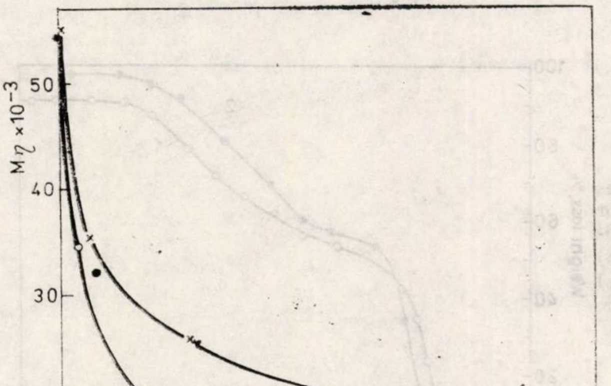

Fig. 3. — Influence of the benzidine amount on the molecular weight variation for the samples synthesized by vibratory milling at different work durations : 1. PVC—S (10 g) + (1 or 2 g) diamine 2. PVC—S (10 g) + 3 g diamine.

On the contrary, with vibratory milling covering long periods of time (24—96 hours), the data indicate increasing of degradation degrees with increased amounts of diamine. Under these conditions the activation of diamine might be supposed to play a decisive role, hence determining the direction of the process, by its concentration.

1.3. THERMAL CHARACTEZATION OF THE PRODUCTS OF THE MECHANO-CHEMICALLY ACTIVATED REACTION BETWEEN PVC-S AND AROMATIC DIAMINES

The thermal properties of the products obtained mechano-chemically by both vibratory milling and cryolysis were followed by thermo-gravimetrical and thermo-differential analyses using an Erdeli-Paulik apparatus running within the 20—900°C temperature range in inert medium. From the thermogrammes the weight losses and the activation energies for the thermal decomposition of the reaction products were calculated (Figs. 4, 5).

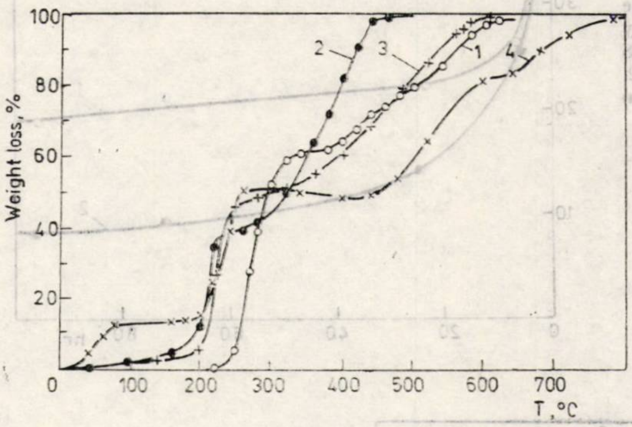

Fig. 4. — Variation of weight losses with decomposing temperature: 1. PVC—S; 2 PVC—S + 2 g benzidine milled for 24 hours; 3. PVC—S + 2 g benzidine milled for 72 hours; 4. PVC—S + 2g benzidine milled for 96 hours.

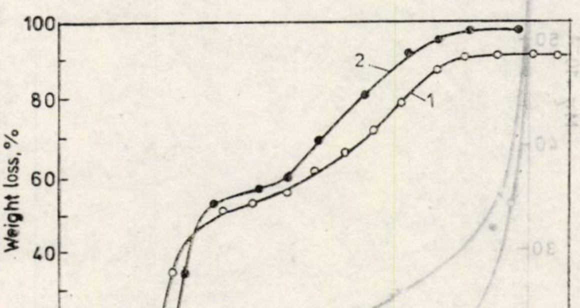

Fig. 5. — Variation of weight losses with decomposing temperature for the samples submitted to mechanical activation by cryolysis (60 cycles) in the system: 1. PVC—S(1%) + benzidine (5%); 2. PVC—S (1%) + *p*-phenylendiamine (1%).

In the case of reaction activated by vibratory milling the exprimental data indicate the sample synthesized in the presence of benzidine, at a 96 hours duration, to be the most stable system (Fig. 4, curve 4). Till 450°C this polymer loses only 50% of its weight while the poly (vinyl-chloride) taken as reference standard attains the same value at a temperature of 300°C.

In continuing the analysis with products synthesized by cryolysis two samples have been selected, one of them obtained in the presence of *p*-phenylendiamine, the other in the presence of benzidine (Fig. 5). Once again it is observed that introduction into the macromolecular chains aromatic diamines units improves the thermal stability of the original polymer (Table 3).

Table 3

Activation energy values the thermal decomposition of the products of the reaction between PVC−S and aromatic diamines activated mechano-chemically by vibratory milling and cryolysis

Sample	Amount of the diamine	Type of the mechanical work	Duration of the mechanical work	Activation energy(kcal/mol)
PVC−S	—	—	0	32.4
PVC−S+ pFDA	2 g	vibratory	24 hrs	34.78
PVC−S+ Benz.	2 g	milling	3 hrs	38.44
PVC−S+ Benz.	2 g	milling	24 hrs	45.76
			number of cycles	
PVC−S+ pFDA	1 %	cryolysis	60	33.8
PVC−S+ Benz.	5%	cryolysis	60	38.1

It is known that on milling of polymers in metallic environments, small amounts of iron in an activated state pass into the system.[3,4] Its ability to react with degradation fragments of polymers has been checked by means of Mössbauer spectroscopy. A spectrum has been recorded on an ELRON type Mössbauer spectrophotometer of a polymer synthesized by milling for 96 hours in the presence of benzidine (Fig. 6). The data obtained were then processed on an IBM 3703/1 computer.

The Mössbauer spectrum shows four sub-networks, two of them showing magnetic order. The Mössbauer parameters (Table 4) indicate the presence of α-Fe in both of the magnetic networks : 32% α-Fe almost pure in the first network 39% less pure in the latter. The other two networks (non-magnetic) may be attributed to the Fe^{3+} ions in a network different from the cubic one. Two unequivalent positions of Fe^{3+} ions, hence two possibilities of bonding in the system thus appear. The Mössbauer spectrum of the same sample, which was not purified by dissolution and precipitation, is similar to the previous one. An increase in the α-Fe content of a higher purity (54%) and a decrease in the second α-Fe component (29%) is noticed. Furthermore, the second phase of α-Fe shows a magnetic hyperfine field of only 316 KOE (compared to 333 KOE) (Table 4) which represents an increase of inhomogeneity in the α-Fe network.

Table 4

Mössbauer parameters characterizing the PVC—S samples worked mechanically by vibratory milling

Sample	Under-networks	δ(mm/s)	ΔE_Q(mm/s)	H(KOe)	Surface %	Obs.
PVC(10g) + Benz. (2g)	1.	-0.233 ± 0.016	0.042 ± 0.022	336 ± 0.2	32	α—Fe
worked by vibratory	2.	-0.163 ± 0.014	0.032 ± 0.018	325 ± 0.2	39	α—Fe
milling 96 hours	3.	0.133 ± 0.011	0.805 ± 0.013	—	25	
(portion soluble in cyclohexanone)	4.	-0.281 ± 0.013	0.753 ± 0.014	—	4	
ibidem, crude product	1.	-0.213 ± 0.002	0.042 ± 0.002	338 ± 0.3	54	α—Fe
	2.	-0.189 ± 0.006	0.026 ± 0.005	316 ± 0.7	29	α—Fe
	3.	0.158 ± 0.001	0.829 ± 0.002	—	14	
	4.	-0.223 ± 0.002	0.796 ± 0.004	—	3	

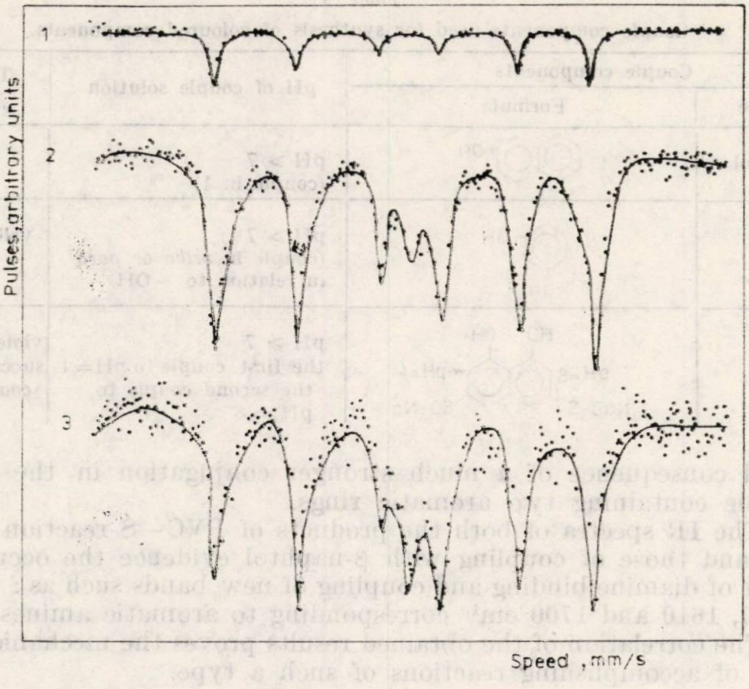

Fig. 6. — Mössbauer spectrum for:
1. blank sample (Fe_2O_3); 2. the soluble fraction of the product synthesized by vibratory milling in the system PVC—S +2 g benzidine, 96 hours; 3. the unfractioned polymer synthesized by vibratory milling in the system PVC—S+2 g benzidine, 96 hours.

1.4. DIAZOTIZING AND COUPLING WITH DYES

The data obtained evidence the fact that by mechano-chemical synthesis carried out in the presence of aromatic diamines, a thermal stabilization of the original polymer becomes possible also improving its abilities of colouring. For investigating these properties the final products have been coloured by diazotizing and coupling with different components thus producing a series of coloured polymers.

The coupling components used are listed in Table 5. Because of containing aromatic amine residues, these may be successively diazotized which yields increasing degrees of colouring.

The fastening of the aromatic amine residues to the PVC—S degradation fragments by mechano-chemically activated reactions discussed in the paper, was evidenced by using chemical and spectrophotometrical methods. Of the selected diamines the benzidine proved to be the most reactive compound which can be acccounted for by the labilization of the aminic hydrogens hence by their higher withdrawal capacity in the presence of certain radicalic particles or activated chlorine atoms capable of giving condensation reactions. The labilization of hydrogens is the

Table 5

Couple components used for synthesis of coloured components.

Couple components		pH of couple solution	The colour realized
Name	Formula		
β-Naphtol	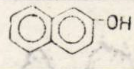	pH > 7 (couple in 1)	red
Resorcin	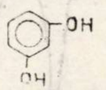	pH > 7 (couple in *ortho* or *para* in relation to —OH)	yellow
Acid H	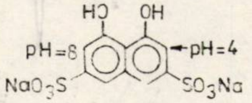	pH ⩾ 7 the first couple to pH=4 the second couple to pH = 8	violet (after two successive couples)

natural consequence of a much stronger conjugation in the benzidine molecule containing two aromatic rings.

The IR spectra of both the products of PVC—S reaction with diamines and those of coupling with β-naphtol evidence the occurrence as a result of diamine binding and coupling of new bands such as : the bands at 3400, 1610 and 1700 cm^1 corresponding to aromatic amines. [5]

The correlation of the obtained results proves the mechanical energy ability of accomplishing reactions of such a type.

CONCLUSIONS

1. The activation by vibratory milling and cryolysis of the reaction between PVC—S destruction fragments and aromatic diamines was proved.

2. The factors influencing the efficiency of the reaction between PVC—S and aromatic diamines are the type of mechanical activation, the period of stressing, nature and amount of diamines.

3. The reaction products have been characterized chemically, spectrophotometrically and by thermo-gravimetric and thermo-differential analyses.

4. By diazotizing the synthesized products and coupling with different components their colouring in a large tone scale becomes possible.

REFERENCES

[1] Cl. Vasiliu Oprea, Cl. Negulianu, M. Popa and Cr. Simionescu, *Plaste und Kautschuk*, **9**, 604, (1977).

[2] W. Schöniger, *Mikrochim. Acta.*, **3**, 449, (1961).

[3] Cr. Simionescu, Cl. Vasiliu Oprea, "Mecanochimia compuşilor meacromoleculari", Ed. Acad,. Bucharest, 1967, p. 55.

[4] N. K. Baramboim, "Mechanochimia vysocomolecularnyi soedinenii", Ed. Himia, Moskva, 1971, p. 70.

[5] M. Avram and Gh. D. Mateescu, "Spectroscopia în IR—aplicaţii în chimia organică", Ed. Tehnică, Bucharest, 1966.

Revue Roumaine de Chimie, **29**, *8*, 693–698 (1984)

USE OF AN AGED NITRATE-SELECTIVE ELECTRODE AS HALIDE-SENSOR IN POTENTIOMETRIC TITRATIONS

E. BARRADO and R. PARDO
Departamento de Química Analítica, Facultad de Ciencias Valladolid, Spain

Received October 10, 1983

The observed response of halides on the Philips-IS-561-Nitrate-Selective Electrode remains constant even if its membrane is aged and cannot be used to determine the nitrate ion. This effect permits its use in potentiometric titrations of halides with silver(I) sulfate solution. The end point is located by the second derivative procedure and the titration is suitable for iodide, bromide and chloride concentrations over 0.004, 0.007 and 0.04 mM respectively.

INTRODUCTION

In a previous paper, [1] a study of behaviour and interferences of the liquid membrane Nitrate-Selective electrode IS-561-Philips was carried out. Theoretically, greater interferences will be expected from those anions with similar properties to nitrate ion. This prevision was experimentally proved for the oxoanions, which were the chemical species with higher selectivity coefficients and due to membrane mechanism.

In the halide case, their interfering action increases with the ionic radius, because the nitrate ion is very voluminous.

Although their selectivity coefficients vary considerabily with the activities of interfering and primary ions in the solutions, the obtained values found by the mixed solutions method, [2] when the halides were in solution in concentration next to 10^{-2} M are 8.10^{-4} of fluoride, 4.10^{-3} of chloride, 5.10^{-2} of bromide and 1.0 of iodide ion.

The interferent action of these elements (with the exception of fluoride, which on the other hand does not interfere seriously) may be removed, by treatment with silver ions, adding silver sulfate solution.

In this paper a study of the possibility of using the Nitrate-Selective Electrode as electrochemical sensor of halides, in the same way as Motonaka et al.[3] have applied an Iodide-Selective Electrode, is reported.

EXPERIMENTAL

APPARATUS

A digital ion-activity meter (Philips PW–9414) was used with a Philips IS–561–NO_3^- selective electrode and a Philips R44/2–SD/1 double junction saturated calomel reference elec trode, with its outer chamber filled with saturated KCl solution. The pH was measured with a Radiometer 29-pH-meter and a Radiometer GK 2401 C glass electrode.

REAGENTS

All chemicals used were of analytical-reagent grade. Distilled, deionized water used throughout.

For the stock iodide solution 0.2500 g potassium iodide was dissolved in 100 mL water. Stock bromide and chloride solutions were prepared by dissolving 0.5550 and 0.9312 g of their respective potassium salt, in 100 mL water. For the silver (I) solution, 3.5 g silver (I) sulfate were dissolved in 1 liter water. This solution was stored in the dark and must be previously standardized versus iodide or bromide standard solutions.

PRELIMINARY CONSIDERATIONS

The determination of halides (especially iodide) with accuracy and precission, cannot be carried out by using a direct measurement with nitrate-selective electrode after multipoint calibration (4) because of two reasons :

a) First, the measured potentials of the iodide solutions are not reproducible, since the membrane is getting active to this anion and great potentials shifts are produced. Therefore, it is very difficult to obtain a calibration line. These potentials shifts can be visualized by comparing two titrations of similar samples carried out with two different nitrate membranes, a new one (Figure 1, solid line) and the other one "aged" by its use as nitrate-selective (Figure 1, dashed line).

b) Lastly, although the "memory effect" for the primary ion is nearly null,[5] when the membrane is used to measure halide ions, the "memory effect" increases with the selectivity coefficient.

According to this, the direct potentiometry cannot be used and all measurements were performed by using a potentiometric titration with silver (I) ion.

Therefore, in this paper a nitrate-selective electrode whose membrane is aged and cannot be used to determine the nitrate ion because its slope is decreased and its detection limit becomes very great, is employed as halide-selective electrode in potentiometric titrations since its response to halides follows the considerations above indicated.

Notwithstanding, silver (I) nitrate is not suitable as titrating reagent because the presence of nitrate ions in the halide solutions causes a decrease of the emf jumps obtained in the titration.

The proposed method is very recommendable when the sample to titrate contains interfering species of halide-selective electrodes, which does not interfere to nitrate-selective electrode.

RECOMMENDED PROCEDURE

Add 100 mL halide solution into a 250—mL beaker. Place the reference and selective. electrodes into it and titrate with 0.02—0.04 M silver (I) sulfate solution. The selective electrode senses the decrease of the halide concentration according to the reaction :

$$X^- + Ag^+ = AgX \downarrow$$

Continuous stirring is required, and near the end-point the titratant must be added in 0.20 mL increments each 30—60 seconds.

The end-point is located from the second derivative of the titration curve, as shown in Fig. 1.

RESULTS AND DISCUSSIONS

POTENTIOMETRIC TITRATIONS OF PURE HALIDE SOLUTIONS

The results observed in a set of titrations of pure halide solutions, are shown in Table 1. According to the selectivity coefficients found for the nitrate electrode, the iodide ion can be titrated in a concentration range comprised between 0.004 – 0.6 mM with a mean recovery of 98.28% and a standard deviation of 2.95%; the bromide ion between 0.007 – 0.4 mM with a mean recovery of 98.71% and a standard deviation of 3.62%, and the chloride ion between 0.04 – 0.2 mM with a mean recovery of 99.56% and a standard deviation of 0.37%.

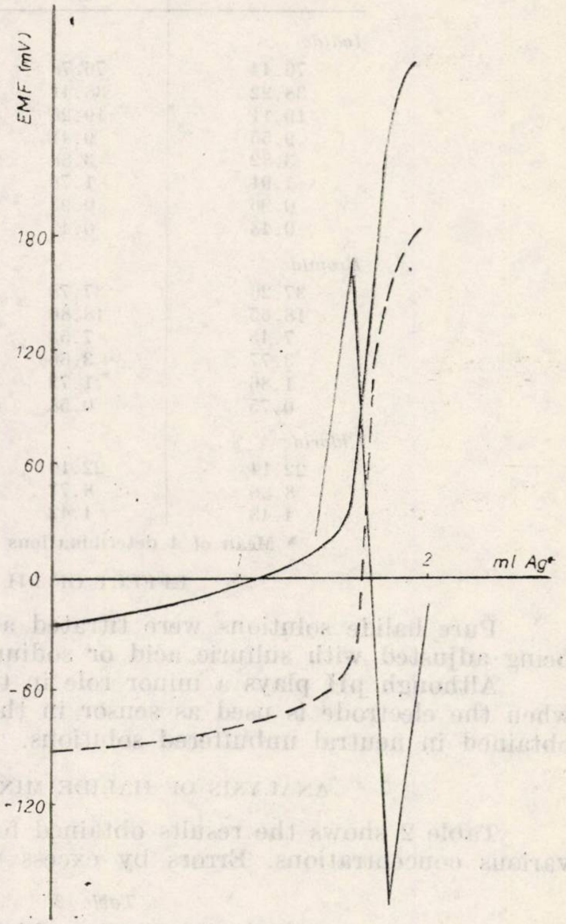

Fig. 1. — Potentiometric titration of iodide with Ag_2SO_4 and a Nitrate-Selective Electrode as sensor. Solid line : new membrane, dashed line : aged membrane. The endpoint is detected by the second derivative procedure.

When the halide concentrations are smaller than the indicated ones, there are not appreciable emf jumps. When the concentrations are greater, the errors due to dilution increase, because silver (I) sulfate is a slightly soluble salt (a Ag_2SO_4 saturated solution has a concentration of $2 - 4 . 10^{-2}$ M), and therefore is necessary a considerable volume of titratant to reach the equivalence point.

Table 1

Potentiometric titrations of halides with silver (I) sulfate

Halide added (mg)	Halide recovered (mg)[a]	Error (%)
Iodide		
76.44	76.78	+0.44
38.22	38.41	+0.48
19.11	19.26	+0.49
9.55	9.41	−1.51
3.82	3.88	+1.39
1.91	1.78	−6.96
0.96	0.93	−2.72
0.48	0.45	−5.65
Bromide		
37.26	37.78	+1.40
18.65	18.86	+1.80
7.45	7.53	+1.06
3.77	3.66	−3.10
1.86	1.72	−7.62
0.75	0.58	−22.15
Chloride		
22.14	22.10	−0.15
8.86	8.77	−0.96
4.43	4.42	−0.20

[a] Mean of 4 determinations

EFFECT OF PH

Pure halide solutions were titrated at various pH values, the pH being adjusted with sulfuric acid or sodium hydroxide (Fig. 2).

Although pH plays a minor role in the determination of nitrate, [1] when the electrode is used as sensor in this titration, best results were obtained in neutral unbuffered solutions.

ANALYSIS OF HALIDE MIXTURES

Table 2 shows the results obtained for a set of halide mixtures at various concentrations. Errors by excess were observed for the halide

Table 2

Potentiometric titrations of halide mixtures

ADDED (mg)			RECOVERED (mg)[a]			ERROR (%)		
I^-	Br^-	Cl^-	I^-	Br^-	Cl^-	I^-	Br^-	Cl^-
10.94	25.08		11.47	24.97		+4.84	−0.44	
10.94	18.63		11.50	18.61		+5.12	−0.11	
10.94	5.02		11.51	5.00		+5.21	−0.41	
2.73	18.63		2.59	18.68		−5.13	+0.27	
2.73	2.54		2.96	2.43		+8.42	−4.33	
10.94		22.14	10.96		22.00	+0.18		−0.63
5.47		22.14	5.63		22.22	+3.68		+0.36
	5.02	8.86		5.22	8.47		+3.98	−4.34
10.94	5.02	8.86	11.53	5.00	7.67	+5.39	−0.40	−13.43
5.47	18.63	4.43	5.63	18.03	3.00	+2.93	−3.22	−32.28

[a] Mean of 2 results

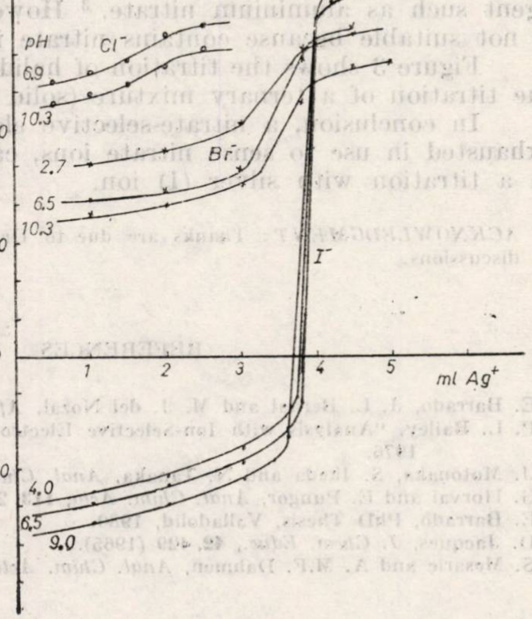

Fig. 2. — Effect of PH on the potentiometric titrations.

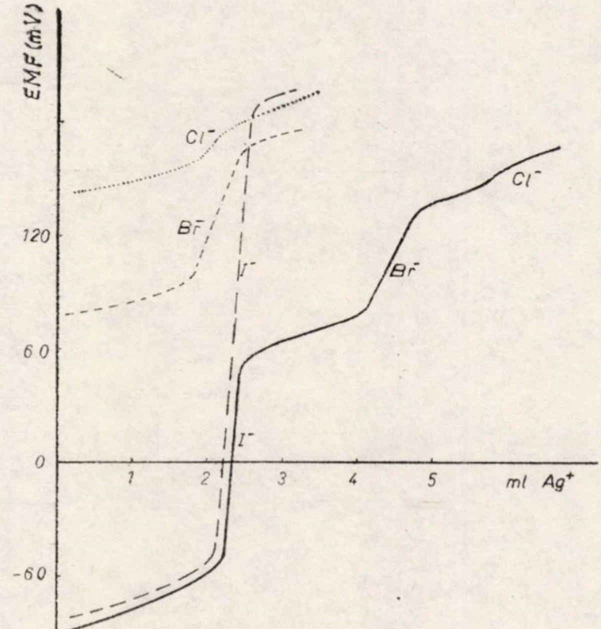

Fig. 3. — Potentiometric titrations of pure halide solutions (dashed lines) and a ternary mixture (solid line).

with smaller solubility product (iodide), while errors by deffect appeared for the other two halide ions (chloride and bromide). Those effects are due to co-precipitation[6,7] and can be eliminated by adding a coagulating agent such as aluminium nitrate. [3] However, in our case that reagent is not suitable because contains nitrate ions.

Figure 3 shows the titration of halide separately (dashed lines) and the titration of a ternary mixture (solid line).

In conclusion, a nitrate-selective electrode which slowly becomes exhausted in use to sense nitrate ions, can be utilized as halide sensor in a titration with silver (I) ion.

ACKNOWLEDGMENT: Thanks are due to Dr. P. Sánchez Batanero for fruitful discussions.

REFERENCES

[1] E. Barrado, J. L. Bernal and M. J. del Nozal, *Afinidad*, **38**, 96 (1981).

[2] P. L. Bailey, "Analysis with Ion-Selective Electrodes", Heyden and Son Ltd., London, 1976.

[3] J. Motonaka, S. Ikeda and N. Tanaka, *Anal. Chim. Acta*, **105**, 417 (1979).

[4] G. Horvai and E. Pungor, *Anal. Chim. Acta*, **113**, 287 (1980).

[5] E. Barrado, PhD Thesis, Valladolid, 1980.

[6] D. Jacques, *J. Chem. Educ.*, **42**, 429 (1965).

[7] S. Mesaric and A. M.F. Dahmen, *Anal. Chim. Acta*, **64**, 431 (1973).

Revue Roumaine de Chimie, **29**, *8*, 699–706 (1984)

ELECTROCHEMICAL REACTIONS OF CUPRIC AND CUPREOUS IONS IN LITHIUM CHLORIDE – POTASSIUM CHLORIDE EUTECTIC. II [1]

STEADY-STATE POTENTIOSTATIC STUDIES

S. STERNBERG, T. VIŞAN and ADINA COTÂRŢĂ*

Chair of Physical Chemistry and Electrochemical Technology, The Polytechnic, Bucharest, Romania

* Institute of Chemical and Biochemical Energetics, Bucharest, Romania

Received March 10, 1983

Steady-state potentiostatic measurements have been carried out in $LiCl-KCl-CuCl_2-CuCl$ melts on graphite electrodes at 500 °C. The obtained cathodic limiting current of Cu^{2+} reduction was found to be linearly proportional to cupric chloride concentration. At anodic polarization, current/potential curve exhibits the existence of two separated processes : Cu^+/Cu^{2+} oxidation and chlorine discharge. Symmetric shape of $i-E$ curves near the equilibrium potential is due to fast electrochemical reactions of redox couple Cu^{2+}/Cu^+. The orders of cathodic and anodic reaction of this couple were determined as well as kinetic parameters such as exchange current densities and standard rate constant.

INTRODUCTION

Molten systems containing mono- and divalent (Cu^{2+} and Cu^{2+}) copper ions dissolved in the $LiCl-KCl$ eutectic solvent are interesting for the possible implementation of high-capacity batteries.[2,3] Thus, the cells of the type $Li/CuCl_2$, $CuCl$, carbon ($t = 500°C$) work on the basis of the redox reaction

$$Cu^{2+} + e \rightleftharpoons Cu^+ \qquad (1)$$

In the previous paper [4] we showed that in dilute copper chloride solutions on metallic (platinum) electrodes the two cyclic voltammetry anodic peaks can be superposed, *i.e.* the following processes take place simultaneously :

$$Cu^+ - e \rightarrow Cu^{2+} \qquad (2)$$

$$Cl^- - e \rightarrow 1/2\ Cl_2 \qquad (3)$$

In the cathodic direction, apart from partial reduction

$$Cu^{2+} + e \rightarrow Cu^+ \qquad (4)$$

the deposition reaction of metallic copper can occur

$$Cu^{+} + e \rightarrow Cu \qquad (5)$$

These sequential electrochemical reactions have been also confirmed by galvanostatic investigations both on platinum and carbon electrodes. [1] The present paper reports on the results of the research by steady-state potentiostatic method, of electrode processes in $LiCl-KCl-CuCl_2-CuCl$ melts on spectral carbon (graphite).

EXPERIMENTAL

Table 1 shows the $LiCl-KCl-CuCl_2-CuCl$ systems studied. Cu^{2+} and Cu^{+} ions concentrations were calculated using a recent value of density of the solvent.[5] The working melts were prepared by dissolving the corresponding amounts of $CuCl_2$ and CuCl anhydrous salts in the purified and melted LiCl–KCl (1 : 1) eutectic. The actual concentrations are likewise influenced by the disproportionating reaction

Table 1

The composition of molten systems investigated by steady-state potentiostatic method ($t = 500°C$)

System	$c_{CuCl_2} \times 10^5$, mol/cm^3	$c_{CuCl} \times 10^5$, mol/cm^3
$LiCl-KCl-CuCl_2$	60.2	—
$LiCl-KCl-CuCl_2-CuCl$		
A	8.38	8.57
B	16.57	16.9
C	32.3	32.3
D	61.9	59.4
E	75.0	76.02
F	88.9	88.8
G	114.0	103.0
H	158.0	142.0
I	246.0	23.6
J	108.7	14.76

$$CuCl_2 \rightarrow CuCl + 1/2\,Cl_2 \qquad (6)$$

The same electrolysis cell previously described [1] was used for all systems. The working electrode was made of spectral graphite rod sealed in Pyrex glass on its cylindrical part; thus, a 0.25 cm^2 constant surface area was exposed in the melt. Before the experiments, the working surface was polished on emery paper, washed and dried. The counterelectrode was a carbon rod with a large surface area. The reference electrode consisted of an Ag wire immersed in a LiCl–KCl–AgCl 1 M melt, all introduced into a glass sheath.

In all determinations the temperature was kept constant at 500 ± 5 °C.

Steady-state measurements were made with a usual potentiostatic assembly. The P.A.R. potentiostat used, Model 173, was provided with a P.A.R. digital coulometer Model 179, with the posssibility of compensating the ohmic drop across the cell. The polarization curves were obtained by increasing the voltage at any potential and allowing the current to arrive at a constant value between readings. Usually, the current became stationary within 2–3 min.

RESULTS AND DISCUSSION

In Figures 1—2 are presented some potentiostatic i — E curves in LiCl—KCl—$CuCl_2$—CuCl systems. Steady-state measurements gave reproducible results for obtaining these complete polarization curves. Figure 1 also gives the polarization curve in solvent LiCl—KCl eutectic and in a melt where only $CuCl_2$ was added. In LiCl—KCl eutectic, within a very large potential range (about 2.5—2.8 V), no important current appears, this being indicative of the absence of any electrode process; the only reactions that appear are the discharge reactions of Li^+ or Cl^- ions at the ends of potential interval. The dissolution of cupric chloride in the melt leads to a significant change of i — E curve (see curve 2 in Fig. 1).

Starting with equilibrium potential in cathodic direction, the reduction process of Cu^{2+} ion, existing in great amount in this system, gives a relatively high diffusion limiting current. At more negative potentials a second polarization wave appears, which corresponds to the further reduction of Cu^+ ion.

At anodic polarization, a wave due to oxidation of the monovalent copper ion (resulting from the disproportionation reaction (6)) is noticed; the chlorine anodic discharge appears in this system, as well as in all LiCl—KCl—$CuCl_2$—CuCl solutions, starting only with the +1.5 V potentials.

The study goes on with the systems A up to H (see Table 1) in which Cu^{2+} and Cu^+ concentrations are practically equimolecular. We also studied two systems in which Cu^{2+} concentration exceeds seven or

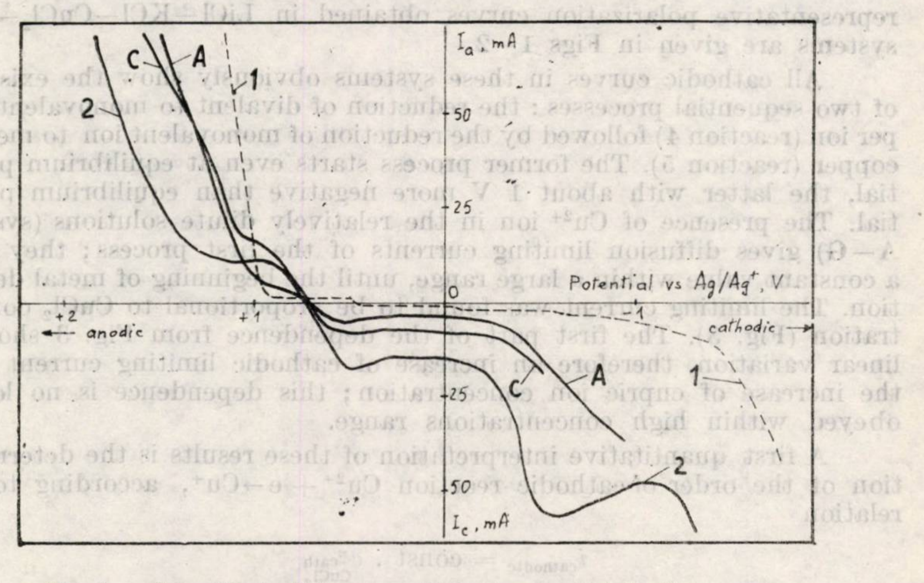

Fig. 1. — Current/potential curves obtained potentiostatically on graphite electrode at 500°C. 1—LiCl—KCl eutectic solvent; 2—LiCl—KCl—$CuCl_2$ with $c_{CuCl_2} = 60.2 \times 10^{-5}$ mol/cm^3. The letters denote the LiCl—KCl—$CuCl_2$—CuCl systems according to Table 1.

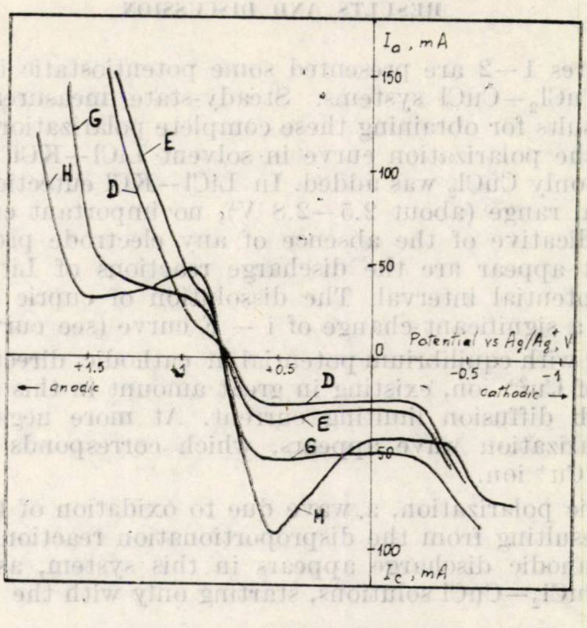

Fig. 2. — Curent/potential curves obtained potentiostatically on graphite electrode at 500°C. The implication of the letters is the same as that of Table 1.

ten times that of Cu^+ concentration (systems I and J in Table 1). Some representative polarization curves obtained in $LiCl-KCl-CuCl_2-CuCl$ systems are given in Figs 1—2.

All cathodic curves in these systems obviously show the existence of two sequential processes : the reduction of divalent to monovalent copper ion (reaction 4) followed by the reduction of monovalent ion to metallic copper (reaction 5). The former process starts even at equilibrium potential, the latter with about 1 V more negative than equilibrium potential. The presence of Cu^{2+} ion in the relatively dilute solutions (systems A—G) gives diffusion limiting currents of the first process ; they have a constant value within a large range, until the beginning of metal deposition. The limiting current was found to be proportional to $CuCl_2$ concentration (Fig. 3). The first part of the dependence from Fig. 3 shows a linear variation, therefore an increase of cathodic limiting current with the increase of cupric ion concentration ; this dependence is no longer obeyed within high concentrations range.

A first quantitative interpretation of these results is the determination of the order of cathodic reaction $Cu^{2+} + e \rightarrow Cu^+$, according to the relation

$$i_{\text{cathodic}} = \text{const} \; . \; c^{n_{\text{cath}}}_{\text{CuCl}_2} \qquad (7)$$

where n_{cath} is the order of electrochemical reaction. Figure 4 gives the cathodic current density at two different overpotentials as a function of diva

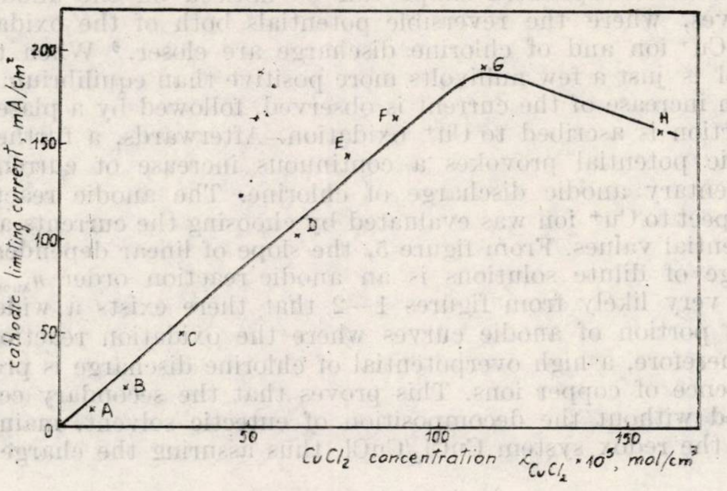

Fig. 3. — Plot of cathodic limiting current versus $CuCl_2$ concentration.

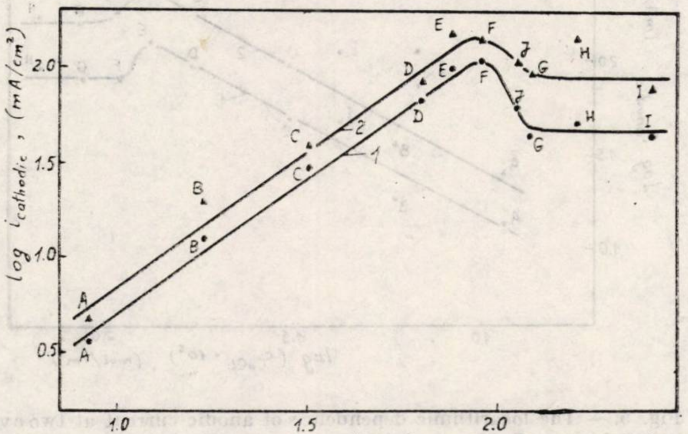

Fig. 4. — The logarithmic dependence of cathodic current at two overpotentials on $CuCl_2$ concentration. $1-\eta = 50$ mV ; $2-\eta = 75$ mV.

lent copper ion concentration in logarithmic coordinates. For small concentrations range a reaction order $n_{\text{cath}} = 1.2$ was found, whereas at higher concentrations n_{cath} had zero or negative reaction orders. The shape of the curves in figures 3—4 can be explained by the appearance of complex compounds within the range of high $CuCl_2$ concentrations, a phenomenon that provokes the decrease of effective concentration of copper ions taking part in the electrode process.

A more complicated shape can be noticed on the anodic part of i-E curves, where the reversible potentials both of the oxidation reaction of Cu^+ ion and of chlorine discharge are closer.[6] When the anodic potential is just a few millivolts more positive than equilibrium potential, a sudden increase of the current is observed, followed by a plateau region. This portion is ascribed to Cu^+ oxidation. Afterwards, a further increase of anodic potential provokes a continuous increase of current, due to supplementary anodic discharge of chlorine. The anodic reaction order with respect to Cu^+ ion was evaluated by choosing the currents at different overpotential values. From figure 5, the slope of linear dependence within the range of dilute solutions is an anodic reaction order $n_{\text{anodic}}=1.1$. It appears very likely from figures 1—2 that there exists a wide range of the first portion of anodic curves where the oxidation reaction (2) prevails. Therefore, a high overpotential of chlorine discharge is produced by the presence of copper ions. This proves that the secondary cells can be recharged without the decomposition of eutectic solvent, mainly on the basis of the redox system $CuCl_2/CuCl$, thus assuring the charge/discharge cycles.

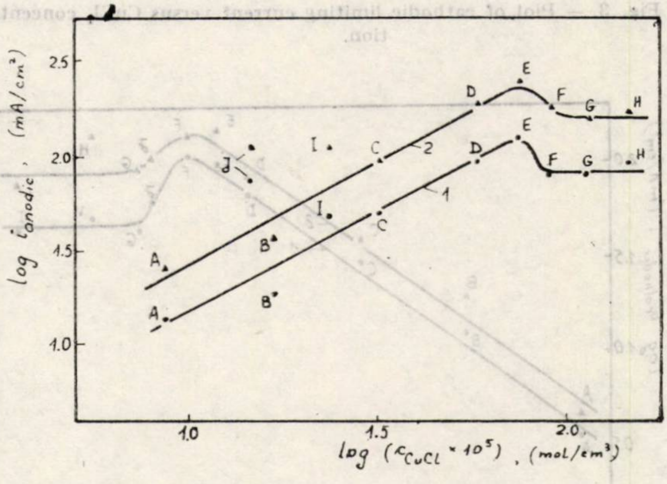

Fig. 5. — The logarithmic dependence of anodic current at two overpotentials on CuCl concentration 1. $\eta = 100$ mV; 2. $\eta = 200$mV.

An analysis of kinetic parameters was also tried. The values of the exchange current densities for Cu^{2+}/Cu^+ couple may be estimated according to the relationship

$$\eta = \frac{RT}{zF} \cdot \frac{i}{i_0} \tag{8}$$

where R, T, F have their usual meaning, z is the number of electrons which participate at the electrochemical process and i — the current at a given overpotential η. The relation holds true for low overpotentials, of the 10—20 mV order. From the slopes of i—E curves near equilibrium potential, the exchange current densities i_0 were calculated using relation (8). Generally, cathodic and anodic values of i_0 (calculated in this way) are equal. Figure 6 shows the dependence of cathodic exchange currents on copper ions concentration, choosing the transfer coefficient $\alpha = 1/2$. As can be seen from this figure the linear dependence $i_0 = f$ (conc.) is not respected for higher concentrations of copper ion. This behaviour supports very well the hypothesis of complex compounds formation in the melt.

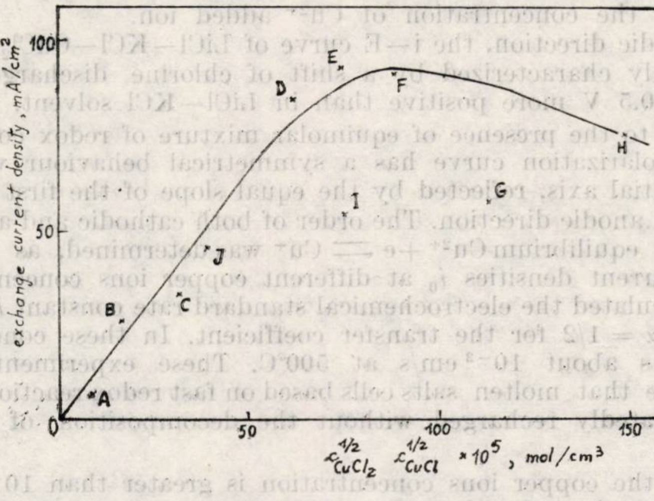

Fig. 6. — Plot of cathodic exchange current densities versus copper ions con centration.

Figure 6 allows one to determined also the electrochemical standard rate constant k_s^0, on the basis of the wellknown relation in electrochemical kinetics

$$i_0 = zFk_s^0 c^{\alpha}_{CuCl_2} \cdot c^{1-\alpha}_{CuCl} \tag{9}$$

The mean value of k_s^0 of about 10^{-3} cm/s resulted from the slope of linear portion of the dependence plotted in figure 6.

The value of α coefficient equal to 1/2 is justified by symmetrical shape of i—E curve corresponding to redox couple Cu^+/Cu^+ in all melts of Cu^{2+} and Cu^+ equimolecular composition and by the equal values of both cathodic and anodic exchange currents.

CONCLUSIONS

Polarization curves on spectral graphite electrodes have been obtained in $LiCl-KCl-CuCl_2-CuCl$ melts (equimolar Cu^{2+}/Cu^+ ratio) by steady-state potentiostatic method at 500°C. Two systems used as electrolytes for molten salts rechargeable batteries were also investigated by this technique.

At cathodic polarization, two well-separated waves are observed for the reduction of Cu^{2+} and subsequently of Cu^+ on graphite. The obtained cathodic limiting currents for the first wave are almost linearly proportional to the concentration of Cu^{2+} added ion.

In anodic direction, the i$-$E curve of $LiCl-KCl-CuCl_2-CuCl$ system is mainly characterized by a shift of chlorine discharge potential with about 0.5 V more positive than in $LiCl-KCl$ solvent.

Owing to the presence of equimolar mixture of redox couple $CuCl_2$/$CuCl$, the polarization curve has a symmetrical behaviour with regard to the potential axis, reflected by the equal slope of the first portions in cathodic and anodic direction. The order of both cathodic and anodic reaction for the equilibrium $Cu^{2+} + e \rightleftharpoons Cu^+$ was determined, as well as the exchange current densities i_0 at different copper ions concentrations. It was also calculated the electrochemical standard rate constant k_s^0 by using a value of $\alpha = 1/2$ for the transfer coefficient. In these conditions, the k_s^0 value was about 10^{-3} cm/s at 500°C. These experimental findings clearly prove that molten salts cells based on fast redox reaction Cu^{2+}/Cu^+ can be repeatedly recharged without the decomposition of $LiCl-KCl$ solvent.

When the copper ions concentration is greater than 10^{-3} mol/cm^3, the experimental results showed a value of zero or negative for electrochemical reaction order and lower exchange current densities. This remarkable behaviour may be ascribed to the formation of complex compounds with corresponding decrease of copper ions in the melts.

REFERENCES

[1] Part I, S. Sternberg, V. Petrescu, T. Vişan and A. Cotârţă, *Rev. Roumaine Chim.*, **28**, 565 (1983).

[2] S. Sternberg, S. Petrescu and V. Petrescu, Romanian Patent No. 68529 (1978).

[3] S. Sternberg, T. Vişan, V. Petrescu and S. Petrescu, Romanian Patent No. 68604 (1978).

[4] S. Sternberg and T. Vişan, "IIIrd Int. Conf. on Molten Salt Chem. — Proceedings" — Wrocław-Karpacz, Poland, 1979", p. 299.

[5] Nguyen Duc Hung, *Z. phys. Chem. (Leipzig)*, **262** 304 (1981).

[6] B. F. Markov, "Termodynamika rasplavlennikh solevikh smesey", Naukova Dumka, Kiev, 1974.

Revue Roumaine de Chimie, **29**, *8*, 707– 713 (1984)

SOLVENT EFFECTS. III[1]

SOLVENT INFLUENCE ON THE REACTION OF THE PHENOTHIAZINE WITH NITROUS ACID

METODIU RĂILEANU
Craiova University, Str. A.I. Cuza 13, Craiova, Romania

Received March 31, 1983

In different media nitrous acid transforms the phenothiazine into phenothiazine-5-oxide, 3-nitro- and 3,7-dinitrophenothiazine-5-oxide, 3,7-dinitrophenothiazine or into phenazathionium cation. This result is explained by the transformation of nitrous acid in different solvents into nitric acid, nitrogen dioxide or into nitrosonium cation. Some substitution and oxidation mechanisms of the phenothiazine in the presence of the mentioned reactant species were proposed.

1. INTRODUCTION

From the analysis of the synthetic methods of some phenothiazinic derivates it results that the phenothiazine reactions with nitrous acid are different according to the reaction medium. Indeed, by treating a suspension of the phenothiazine (I) in glacial acetic acid with sodium nitrite 3,7-dinitrophenothiazine (II)[2] results. The same substance is obtained also by addition of sodium nitrite and acetic acid to a solution of the phenothiazine in chloroform.[3] In dimethylformamide (DMF) – acetic acid mixture sodium nitrite transforms the phenothiazine(I) under more energetic conditions into 3,7-dinitro- and 1,3,7-trinitrophenothiazine mixture.[4] The addition of the phenothiazine(I) in a mixture of 50% sulphuric acid in glacial acetic acid and sodium nitrite determines the formation of the phenazathionium cation(III). [5]

In this work it was found that in some solvents the nitrous acid can also convert the phenothiazine(I) into phenothiazine-5-oxide(IV), 3-nitrophenothiazine-5-oxide(V) and into 3,7-dinitrophenothiazine-5-oxide(VI).

All these syntheses convincingly show that the mechanism of the reaction between phenothiazine(I) and nitrous acid depends on medium (solvent, acidity, reactant concentration, etc.).

2. RESULTS AND DISCUSSION

The different reactions between the phenothiazine (I) and nitrous acid can be understood and explained having in view the transformation possibilities of this acid in the corresponding reaction medium. Indeed, in various conditions the nitrous acid can generate the following reactant species[6]:

$$2HNO_2 \rightleftharpoons N_2O_3 + H_2O \tag{1}$$

$$N_2O_3 \rightleftharpoons NO + NO_2 \tag{2}$$

$$2NO_2 + H_2O \rightarrow HNO_3 + HNO_2 \tag{3}$$

The nitrogen oxide resulted in reaction (2) is easily oxidized by the atmospheric oxygen passing into nitrogen dioxide. The nitrogen trioxide forms in concentrated sulphuric acid the nitrosonium cation, NO^+:

$$N_2O_3 + 3H_2SO_4 \rightarrow 2NO^+HSO_4^- + H_3O^+HSO_4^- \tag{4}$$

The latter in aqueous medium is converted into nitrous acid:

$$NO^+ + 2H_2O \rightarrow HNO_2 + H_3O^+ \tag{5}$$

Phenothiazine (I) has a very mobile electronic system and that is why it can be converted into phenothiazinyl cation-radical (VII)[7,9], phenazathionium cation (III)[4,8–12] or into phenothiazine-5-oxide[5,13] according to the nature and strength of the oxidant.

Table 1

The products obtained from phenothiazine with nitrous acid in different solvents or in solvent mixtures

Reaction medium	Phenothiazine quantity (mmoles/l)	Nitrite concentr. (mmoles/l)	Product				
			II	III	IV	V	VI
CH_3Cl_3	—	—	+				
CH_3COOH	50.20	724.60	+				
CH_3COOH 10%	50.20	724.60	+				
CH_3COOH 20%	50.20	724.60	+		+*		
HCOOH 56%	55.78	322.00			+		
H_3PO_4 37%	62.75	724.60			+		
H_2SO_4 2%	50.20	579.70	+		+**		
H_2SO_4 14%	50.20	579.70			+		
H_2SO_4 50%	50.20	579.70				+	+
$HClO_4$ 37%	50.20	579.70				+	
H_2SO_4 50% in CH_3COOH	100.40	579.70		+			

* Substance traces; ** Little substance

In this paper a particular selectivity of the phenothiazine oxidation with nitrogen dioxide, nitric acid and nitrosonium cation was established.

In the substitution reactions of the phenothiazine(I), if the reactants exhibit also oxidative properties, the ring substitution is generally preceded by oxidation.

Table 1 presents the obtained products from the phenothiazine(I) and nitrous acid in different reaction media.

One can observe in this table that in chloroform, acetic acid and in 10% acetic acid the nitrous acid converts the phenothiazine(I) into 3,7-dinitrophenothiazine(II). It may be admitted that in these solvents the nitration agent is nitrogen dioxide, NO_2, which results from reactions (1) and (2) and the nitration can be explained by the reaction mechanism presented in scheme 1.

Scheme 1

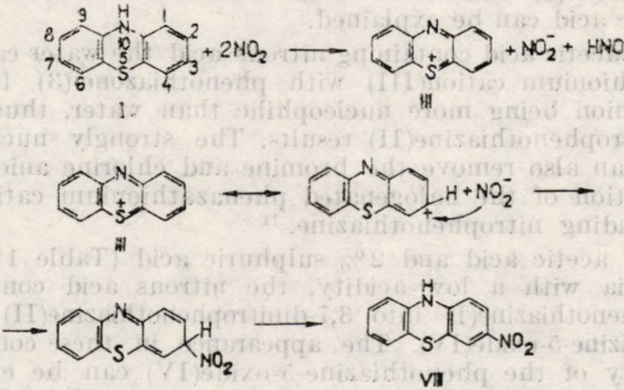

The 3-nitrophenothiazine(VIII) from scheme 1 is further converted by a similar mechanism into 3,7-dinitrophenothiazine(II).

This nitration mechanism which implies the formation of the phenazathionium cation(III) and its nucleophilic substitution with nitrite anions is also admitted by Silberg and Diudea, [4] but these authors do not specify that the authentic oxidant in the reaction is the nitrogen dioxide which is reduced by phenothiazine(I), turning into nitrite anion, NO_2^-, and nitrous acid (Scheme 1).

The appearance of the nitrite anion in solution by reducing the nitrogen dioxide with phenothiazine(I) can be deduced from the occurrence conditions of the 3,7-dinitrophenothiazine(II) in phenothiazine-chloroform-acetic acid-sodium nitrite system, [3] where acetic acid converts integrally during the reaction the sodium nitrite into nitrous acid. The sodium nitrite is insoluble in chloroform, but the nucleophilic nitration of the phenazathionium cation(III) takes place whitout stirring, because nitrite anions appear in the solution as a result of the reduction of nitrogen dioxide with phenothiazine(I) (Scheme 1).

Silberg and Diudea [4] obtained a 3,7-dinitro-(II) and 1,3,7-trinitrophenothiazine mixture in phenothiazine-dimethylformamide(DMF)-acetic acid—sodium nitrite system in which the ratio DMF/acetic acid =

4/1(V/V), using a great nitrite excess. Because the sodium nitrite is soluble in DMF, it may be concluded that in this system most of the nitrite anions preceed from the dissolved salt and only a smaller fraction from these results on reduction of the nitrogen dioxide with phenothiazine(I).

The nitrogen dioxide is a strong oxidant, because it can oxidize also 3,7-dinitrophenothiazine(II) by extracting two electrons and one proton forming the 3,7-dinitrophenazathionium cation, [4] which turns then into 1,3,7-trinitrophenothiazine. Indeed, the 3,7-dinitrophenothiazine is oxidized more heavily than the phenothiazine(I), because the two nitro groups determine a decrease of the electronic density of the ring.

The selectivity of nitrogen dioxide in the oxidation reactions of some phenothiazinic compounds exhibits by electron and proton capture from the ring and not by donation of the oxygen atoms. In this manner the absence of the phenothiazine-5-oxide(IV) in the reaction between the phenothiazine(I) and nitrous acid in chloroform, [3] in acetic acid and in 10 % acetic acid can be explained.

In 10 % acetic acid containing nitrous acid the water cannot attack the phenazathionium cation(III) with phenothiazone-(3) formation, [9,14] the nitrite anion being more nucleophilic than water, thus practically only 3,7-dinitrophenothiazine(II) results. The strongly nucleophilic nitrite anions can also remove the bromine and chlorine anions from the 3 and 7 position of the halogenated phenazathionium cations, forming the corresponding nitrophenothiazine. [11]

In 20 % acetic acid and 2 % sulphuric acid (Table 1), which are aqueous media with a low acidity, the nitrous acid converts prevalently the phenothiazine(I) into 3,7-dinitrophenothiazine(II) and partly into phenothiazine-5-oxide(IV). The appearance in these conditions of a small quantity of the phenothiazine-5-oxide(IV) can be explained by nitric acid formation from nitrogen dioxide and water according to reaction (3). Indeed, it was shown in a recent paper, [5] that the 0,5 % nitric acid in glacial acid rapidly oxidizes the phenothiazine (I), without nitration, forming phenothiazine-5-oxide(IV).

The nitric acid is also a selective oxidant with respect to the phenothiazinic ring and stronger than the nitrogen dioxide; it does not require hydrogen to turn into nitrous acid and can oxidize the phenothiazine by oxygen donation, forming phenothiazine-5-oxide(IV) (Scheme 2).

Scheme 2

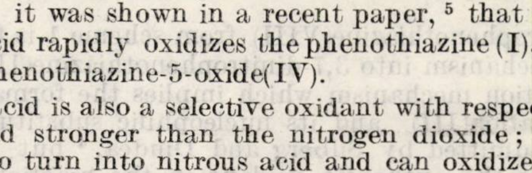

The phenothiazine-5-oxide(IV) can also be obtained by phenothiazine oxidation with hydrogen peroxide [13] in ethanol or by alkylhydroperoxides [15] in ether, but very diluted nitric acid oxidizes the phenothiazinic sulphur at room temperature even in 2—3 minutes. [5] The nitric acid easily converts also 3,7-dinitro-(II)[3] and 1,3,7,-trinitrophenothiazine [4] into corresponding 5-oxides.

In 56 % formic acid, 37 % phosphoric acid and 14 % sulphuric acid the phenothiazine(I) forms with nitrous acid only phenothiazine-5-oxide (IV) (Table 1). It may be admitted that in these media the concentration of the nitric acid is greater and the high oxidation rate to the sulphoxide does not permit the appearance of the 3,7-dinitrophenothiazine(II) according to the mechanism shown in scheme 1. One can thus conclude than an increase of the medium acidity determines an increase of the nitric acid concentration.

Because in these systems the phenothiazone-(3) does not appear, the sulphoxide oxygen a cannot proceed from the reaction with the phenazathionium cation(III), [9] but from the nitric acid which rapidly oxidizes the heterocyclic sulphur. Also in 10 % acetic acid, which is an aqueous medium, the phenothiazine(I) does not yield phenothiazine-5-oxide(IV) (Table 1), because in this medium with low acidity the nitrous acid cannot generate the nitric acid in necessary concentration for the direct oxidation of the phenothiazinic sulphur.

In more acidic media, as 37 % perchloric acid or 50 % sulphuric acid, the concentration of the nitric acid resulted according to the reaction (3) appreciably increases and determines an electrophilic nitration of the phenothiazine-5-oxide(IV), [16] resulting thus 3-nitro-(V) and 3,7-dinitrophenothiazine-5-oxide(VI).

The nitration of the phenothiazine-5-oxide(IV) with nitrous acid in 37 % percloric acid and in 50 % sulphuric acid shows that the appearance of the nitric acid in these strongly acidic media is undisputed. At the same time it was experimentally demonstrated that the phenothiazine-5-oxide(IV) cannot be nitrated by nitrous acid in aqueous acetic acid, because in this low acidity solution the formation of the nitric acid according to reaction (3) is probably very slow.

In 50 % sulphuric acid dissolved in glacial acetic acid the nitrous acid converts the phenothiazine(I) into phenazathionium cation(III) as it was demonstrated in a recent work. [5] In this anhydrous acidic mixture the nitrous acid generates the nitrosonium cation, NO^+, (according to reaction 4), which oxidizes the phenothiazine(I), forming probably the phenothiazinyl cation-radical(VII) ; the latter turns by disproportionation [12] into phenazathionium cation(III) (Scheme 3).

Scheme 3

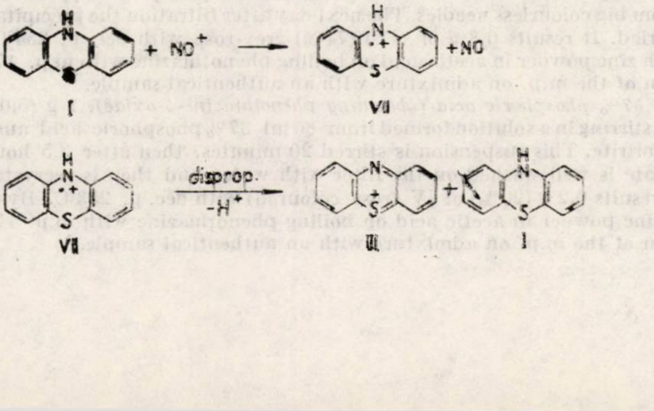

The monoelectronic oxidation of the phenothiazine(I) is easily to admit, because the reduction of the nitrosonium cation to the nitrogen oxide requires a single electron and the phenothiazinic oxidation potential is low (only 4.36 eV[17]).

In these conditions the phenothiazine nitrosation cannot be achieved, because the electrophilic nitrosonium cations do not attack the resulted phenazathionium cation(III).

During the performed experiments it was possible to find that in water-sulphuric acid—nitrous acid system for the same concentration of the nitrous acid the formation of the nitric acid according to reaction (3) is catalyzed by the increase of the sulphuric acid concentration.

Succintly it is possible to conclude that depending on the reaction medium the nitrous acid can be converted into nitrogen dioxide, nitric acid or into nitrosonium cation. These reactive species attack phenothiazine(I) through different oxidation and substitution mechanisms.

The reaction between phenothiazine(I) and nitrous acid points out convincingly that for some organic syntheses the reaction medium plays a determinant role.

3. EXPERIMENTAL

The reaction of phenothiazine(I) with nitrous acid:

a) *In glacial acetic acid (obtaining 3,7-dinitrophenothiazine).* This synthesis represents a modification of the method described by Kehrmann and Nossenko.[2] 1 g (5,2 mmoles) of I is solved in warm glacial acetic acid and the obtained solution is cooled up to room temperature 5 g (72.46 mmoles) of sodium nitrite were added in a minute under stirring. The solution is coloured in dark-red and after 5 minutes the separation of a precipitate begins (violaceus splendid needles). After 4 hours the suspension is filtered off and the precipitate is washed on the filter with 50% acetic acid. water and then dried. It results 0.7 (48%) of II (chocolate coloured) with m.p. 288—290°C (lit.[2] 275°C).

$C_{12}H_7O_4N_3S(289)$: *calcd.*: N 14.23; *found*: N 14.16%

b) *In 20% acetic acid (obtaining a mixture of 3,7-dinitrophenothiazine and phenothiazine-5-oxide).* In 100 ml of 20% acetic acid 5 g (72.46 mmoles) of sodium nitrite are introduced under stirring then 1 g (5.02 mmoles) of phenothiazine. The dark-red coloured suspension is stirred 20 minutes then is left over night. The next day lilac coloured acicular crystals of 3,7-dinitrophenothiazine were observed along with few white plate-shaped crystals of phenothiazine-5-oxide. The suspension is filtered off, the precipitate is washed with water, then three times with methanol which extracts easily the phenothiazine-5-oxide. The chocolate coloured precipitate left on the filter is dried. It results 0.4 g of II (28%) with m.p. 279—280°C. In alcoholic solution water is added and the obtained precipitate is filtered off and is recrystallyzed from 50% methanol. It results IV in small amount, very impure, with dec. p. 210°C (violent decomposition).

c) *In 56% formic acid (obtaining phenothiazine-5-oxide).* 1 g (5.02 mmoles) of I is introduced under stirrring in a solution formed from 90 ml 56% formic acid and 2 g (28.98 mmoles) sodium nitrite. After a few minutes of stirring the precipitate appears at the microscope-as formed from big colourless needles. The next day after filtration the precipitate is washed with water and dried. It results 0.8 g of (IV) (74%) grey-rose with dec. p. 254°C (lit.[2] 257°C). By reducing with zinc powder in acetic acid on boiling phenothiazine with m.p. 179—180°C results; no depression of the m.p. on admixture with an authentical sample.[5]

d) *In 37% phosphoric acid (obtaining phenothiazine-5-oxide).* 1 g (5.02 mmoles) of I is added under stirring in a solution formed from 80 ml 37% phosphoric acid and 4 g (57.97 mmoles) sodium nitrite. This suspension is stirred 20 minutes, then after 3.5 hours is filtered off; the precipitate is well washed on the filter with water and then is recrystallized from 66% ethanol. It results 0.2 g (20%) of IV (rose coloured) with dec. p, 253°C. By reducing the substance with zinc powder in acetic acid on boiling phenothiazine with m.p. 179—180°C results; no depression of the m.p. on admixture with an authentical sample.[5]

e) *In 2% sulphuric acid (obtaining a mixture of 3,7-dinitrophenothiazine and phenothiazine-5-oxide).* 1 g (5.02 mmoles) of I is added under stirring in a solution formed from 100 ml 2% sulphuric acid and 4 g (57.97 mmoles) sodium nitrite. After four hours the red coloured suspension is filtered, the precipitate is washed with water and crystallyzed from 30 ml, 66% ethanol. From the filtrate little precipitate deposits on cooling (having dec. p. 251°C) which is phenothiazine-5-oxide. [5] The precipitate left on the filter is washed three times with methanol and dried. It results 0.2 of II with m.p. 279—280°C (lit.[2] 276°C); no depression of the m.p. on admixture with an authentical sample. [2]

f) *In 14% sulphuric acid (obtaining phenothiazine-5-oxide),* 1 g (5.02 mmoles) of I is added under stirring in a mixture formed from 100 ml 14% sulphuric acid and 4 g (57.97 mmoles) sodium nitrite. A cream coloured suspension appeared at once in which colourless plate shaped crystals were observed at microscope. Twenty four hours later the suspension. is filtered off, the precipitate is washed with water and is recrystallized from 60% ethanol. It results 0.4 g (37%) of IV yellow-rose coloured and with dec. p. 252—255°C (lit.[5] 257°C). By boiling with zinc powder in acetic acid the substance is transformed into phenothiazine with m.p. 179—180°C; no depression of the m.p. on admixture with an authentical sample. [5]

g) *In 50% sulphuric acid (obtaining a mixture of 3-nitro- and 3,7-dinitrophenothiazine-5-oxide).* 1 g (5.02 mmoles) of I is introduced under stirring in a solution formed from 100 ml of 50% sulphuric acid and 4 g (57.97 mmoles) sodium nitrite. At the beginning the suspension is coloured in dark-red but a minute after a yellow colour appears gradually and a crystalline yellow precipitate deposits. The suspension is stirred 15 minutes and after 0.5 hours is filtered. The precipitate is washed on the filter with ethanol and is recrystallized from 100 ml glacial acetic acid. By filtration of the hot solution it remains on the filter 0.15 g (10%) of VI with dec. p. 307—308°C (lit.[3] 309°C) From the acetic solution 0.4 g (31%) of V (m.p. 288—289°C with slight decomposition). (lit.[18] 285°C) were obtained. The substances V and VI are spectrally and chromatographically identical with authentical samples. [18]

h) *In 37% perchloric acid (obtaining 3-nitrophenothiazine-5-oxide).* 1 g (5.02 mmoles) of I is introduced under stirring in a solution formed of 100 ml of 37% perchloric acid and 4 g (57.97 mmoles) sodium nitrite. At the beginning the solution is dark-red coloured, but a few minutes after yellow crystals deposit which at microscope appear as radial aggregate. The suspension is stirred for 10 minutes, and 40 minutes later is filtered off, the precipitate is washed with water and dried. It results 1.2 g (92%) of V (m.p. 286—287°C with decomposition) (lit.[18] 285°C); the substance V is spectrally and chromatographically identical with an authentical sample. [18]

i) In 10% acetic acid (obtaining 3,7-dinitrophenothiazine). The proceeding is the same as in b). It results 0.4 g (28%) of II with m.p. 286°C; no depression of the m.p. on admixture with an authentical sample. [3]

REFERENCES

[1] Part. II. M. Răileanu, S. Florea and N. Mureşan, *Rev. Roumaine Chim.*, **28**, 363 (1983).
[2] F. Kehrmann and O. Nossenko, *Ber. dtsch. chem. Ges.*, **46**, 2809 (1913).
[3] C. Bodea and M. Răileanu, *Studii şi Cercetări Chim. Acad. RPR. Fil. Cluj*, 1957, 303.
[4] I. A. Silberg and M. V. Diudea, *Rev. Roumaine Chim.*, **25**, 1329 (1980).
[5] M. Răileanu, *Rev. Chim. (Bucureşti)*, **34**, 113 (1983).
[6] C. D. Neniţescu, "Chimie generală", Ed. didactică şi pedagogică, Bucharest, 1972, p. 740—743.
[7] J. Craig, M. E. Tate, E. W. Denovan and W. P. Rogers, *J. Med. Pharm. Chem.*, **2**, 669 (1960).
[8] J. Billon, *Bull. Soc. Chim. France*, **1960**, 1784.
[9] J. H. Shine and E. E. Mach, *J. Org. Chem.*, **30**, 2130 (1965).
[10] J. Daneke and H. W. Wanzlich, *Liebigs Ann. Chem.*, **740**, 52 (1970).
[11] I. A. Silberg and M. V. Diudea, *Rev. Roumaine Chim.*, **25**, 1229 (1980).
[12] M. V. Diudea, *Rev. Roumaine Chim.*, **26**, 725 (1981).
[13] H. Gilman and R. D. Nelson, *J. Amer. Chem. Soc.*, **75**, 5482 (1953).
[14] C. Bodea and M. Răileanu, *Studii şi Cercetări Chim. Acad. RPR. Fil. Cluj, 1960*, 325.
[15] C. Bodea and I. Silberg, *Studii şi Cercetări Chim. Acad. RPR. Fil. Cluj, 1963*, 317.
[16] M. Răileanu and A. Turcu, *Rev. Roumaine Chim.*, **11**, 1423 (1966).
[17] D. A. Kearns and M. Calvin, *J. Chem. Phys.*, **34**, 2026 (1961).
[18] M. Răileanu, *Rev. Chim. (Bucureşti)*, **33**, 1102 (1982).

Revue Roumaine de Chimie, **29**, 8, 715—716 (1984)

COMPTES RENDUS

JAROSLAV SESTAK, "Thermophysical Properties of Solids", Academia, Prague, 1984, 440 p.

The book is dedicated to some modern aspects concerning the physical chemistry of the solid state whose applied variant is known as material science. The author, Dr. Jaroslav Sestak, principal scientific worker at the Institute of Physics in Prague, is a distinguished scientist with internationally recognized activity. He presents in an original manner, on the healthy background of heterogeneous kinetics and thermodynamics some problems neglected in the recent books in spite of their both theoretical and practical importance. Among them one has to notice : metastable and unstable states (mainly for glasses), rational thermodynamics including the heating rate and nonisothermal kinetics. The book written at a high theoretical level, fulfils at the same time the condition of accessibility. The problems concerning experimental tehniques are equally considered.

The book id based on a very rich and up to date literature, including references to the authors contributions. The scientific contribution of some Romanian group of research are equally mentioned. The author proposes the following contents :

Chapter 1. Introduction and preliminary remarks to individual chapters
Chapter 2. Characterization and preparation of solid samples
Chapter 3. The use of thermal analysis in the study of the behaviour of materials and substances
Chapter 4. Measurement, calibration and regulation of temperature
Chapter 5. Thermodynamic principles
Chapter 6. Thermodynamics of phase equilibria, phase diagrams
Chapter 7. The theory of phase transitions
Chapter 8. Mechanism and kinetics of heterogeneous non-catalyzed reactions
Chapter 9. Kinetics of processes under non isothermal conditions
Chapter 10. The kinetic theory of glass formation in quenched melts
Chapter 11. Calorimetry : the determination of changes in thermal properties
Chapter 12. The theory and practice of differential thermal analysis
Chapter 13. Measurements of non-thermal properties
Chapter 14. Mathematical analysis of curves and the use of computers
Chapter 15. APPENDIX

The book is meant to meet the requirements of the students and teaching people interested in solid-state physical chemistry, as well as to the research workers involved in the field, and should be found on their working desks. It is an open window to the modern aspects of heterogeneous kinetics and thermodynamics.

E. Segal

SÁNDOR FLISŽAR, "Charge Distributions and Chemical Effects. A New Approach to the Electronic Structure and Energy of Molecules", Springer-Verlag, Berlin, 1983, 205 pages, 115 DM (44. 7 US $), hard-cover.

The approach presented in this monograph goes back to the fundamentals in that it is exclusively based on interactions involving nuclear and electronic charges. The problem of calculating the energy of molecules is reduced to consider its electrostatic aspects. A description of the molecules is given in terms of charge distributions, and attention is focussed on the relationships between charge and the physical and chemical properties.

A convenient way of extracting atomic charges is offered by Mulliken's population analysis, which is rooted in the LCAO formalism. A superficial inspectation of charge results seems to be wrong, e.g. the electron population of -1.07 e on the methane carbon atom. Thus serious doubts appear on the ability of the Mulliken scheme to obtain meaningful charge distributions, suitable for the discussion of real physical problems.

The author of the book tries to solve these discrepancies by assuming that the assignment of the overlap population terms need not follow the original Mulliken half-and-half partitioning scheme in cases involving heteronuclear overlap partners. Another idea is that the changes in electron population occur "most reluctantly", thus keeping them as small as possible. One can obtain new sets of atomic chrges which are closely linked to, and easily deduced from the original Mulliken populations. When derived from different wave functions, modified atomic charges are obtained, related to their original Mulliken counterparts.

The relative ordering of the carbon charges deduced by this method for a number of compounds is the only one which corresponds to the ordering determined from comparison with experimental quantities, namely $^{13}C-NMR$ chemical shifts, energies of atomization, and ionization potentials of alkanes. Charge-related chemical effects are discussed in terms of net charges deduced from the "generalized Mulliken scheme" involving the modified partitioning of overlap populations.

An important aspect is that inductive effects of alkyl groups are explained quantitatively by means of electron distribution of alkanes. The interpretation of these effects is rooted in an important result, namely the C^+-H^--polarity in saturated hydrocarbon systems. It follows that the hydrogen atoms "retain" electrons in CH_x groups ($X = 0, 1, 2, 3$), being thus the "electron reservoirs" of the molecules. The electron retention in CH_x groups decreases in the order $CH_3 > CH_2 > CH > C$. Consequently, intramolecular charge transfers occur in the direction $CH_2 \rightarrow CH_3$ and $CH \rightarrow CH_2$. A quaternary carbon atom "loses" about three times, and a CH group about twice as much electronic charge to each adjacent CH_3 group as a CH_2 group. It is equivalent to say that the electron-releasing abilities of the alkyl groups decrease as follows : tert-butyl>iso-propyl>ethyl>methyl.

The aim of the book is to develop a useful approach based on accurate empirical correlations : charge distributions versus $^{13}C-NMR$ and $^{17}O-NMR$ shifts, although the significance or generality of such correlations is not known. The approach does not leave sources of errors because it does not postulate special effects. The agreement between theory and experiment is demonstrated for over 100 molecules. The results are encouraging for further investigations in other classes of molecules (e.g. those containing nitrogen atoms). The book is a beginning in this area of research. Organic and physical chemists should develop new aspects of charge-properties relationships.

The book is highly readable and clear. Its ten chapters are :

1. Electronic charge distributions
2. Charge analysis of simple alkanes
3. A modified population analysis
4. Charge analysis involving nuclear magnetic resonance shifts.
5. The molecular energy, a theory of electron density
6. Energy analysis of saturated hydrocarbons
7. On the role of vibrational energies
8. Unsaturated hydrocarbons
9. Energy analysis of oxygen-containing compounds
10. Conclusion and assessment

At the end of each chapter are given comprehensive bibliographies of articles and books and the subject. Author and subject indices are included. Diagrams and formulas are presented clearly. The printing is excellent.

Ursula Bologa

NOTE POUR LES AUTEURS

La Revue Roumaine de Chimie publie des articles en anglais, français, russe, allemand ou espagnol. Les auteurs sont priés d'envoyer des articles et des comptes rendus inédits.

Les manuscrits seront dactylographiés à deux intervalles. La bibliographie, les tableaux et la légende des figures seront placés après le texte.

Si l'article fait partie d'une série numérotée, la partie précédente sera donnée comme première référence.

Chaque article sera précédé d'un résumé comprenant quinze lignes au maximum.

Les références bibliographiques dans le texte seront faites par des exposants sans parenthèses et paraîtront à la fin de l'ouvrage.

Les publications périodiques mentionnées dans la bibliographie seront présentés suivant les prescriptions internationales : le nom de l'auteur précédé de l'initiale de prénom, le titre du périodique abrégé conformément à « Chemical Abstracts » et souligné par une ligne, le numéro du tome indiqué par des chiffres arabes et souligné par deux lignes, suivi de la première page de l'article : à la fin, l'année de la parution sera placée entre parenthèses. Le numéro de la revue ne sera pas indiqué si les pages du volume sont numérotées consécutivement.

Les textes des livres ou traités inclueront : les nom des auteurs, l'initiale du prénom, le titre du livre entre guillemets et sans être souligné, le numéro du tome précédé par l'abréviation « vol. » (ou « Bd. »), le numéro de l'édition, les éditions (the publisher), la localité de la parution du livre, l'année de la parution et la page de la référence précédée(s) par l'abréviation « p » (ou « S »).

Les brevets seront indiqués comme suit : l'auteur ou la firme, le pays et le numéro du brevet, la date et la revue (*Chem. Abstr.*) Par ex. : M. Jones (to Union Carbide Co.), Brit. Pat. 601 238, 2 Sept. 1959 ; cf. *Chem. Abstr.*, **54**, 12808 (1960).

Les diagrammes seront tracés à l'encre de Chine sur papier calque. Les tableaux et les figures (en nombre strictement nécessaire), ainsi que les courbes dans les figures seront numérotés par des chiffres arabes. Leur explication sera donnée dans la légende des figures. Prière de ne pas inscrire les mêmes données dans les tableaux et les figures. Chaque tableau aura un titre. On indiquera dans le texte la place approximative des tableaux et des figures. Les formules chimiques seront incluses dans le texte : en outre, elles seront transcrites sur papier calque, à l'encre de Chine.

Les auteurs sont priés d'indiquer les caractères italiques (en soulignant les lettres au crayon), ainsi que tout autre caractère spécial : les préfixes *ortho, meta, para, cis, trans,* etc. seront soulignés pour indiquer leurs caractères italiques et ne seront jamais écrits avec des majuscules.

Aucune correction à la main ne sera admise sur le manuscrit. Les corrections seront frappés à la machine. Les lettres grecques ou d'autres symboles spéciaux seront insérés à la main à l'encre clairement.

Le manuscrit sera signé par l'auteur.

Le titre-courant aura 50 lettres au maximum.

L'entière responsabilité du contenu des articles appartient aux auteurs.

Sur demande on peut obtenir une note plus complète.

PRINTED IN ROMANIA

ORSZÁGOS MŰSZAKI INFORMÁCIÓS KÖZPONT ÉS KÖNYVTÁR
1833

TRAVAUX PARUS AUX ÉDITIONS DE L'ACADÉMIE DE LA RÉPUBLIQUE SOCIALISTE DE ROUMANIE

1984 NOV 1

ELENA CEAUŞESCU, **Cercetări în chimia şi tehnologia polimerilor**, 1983, 519 p.
N. ASANDEI, A. GRIGORIU, **Chimia şi structura fibrelor**, 1983, 395 p.
N. IONESCU, M. CĂLDĂRARU, **Oxidarea catalitică a olefinelor inferioare**, 1983
C. CAŞCAVAL, **Studiul polimerilor prin piroliză şi cromatografie de gaze**, 1983, 220 p.
C. I. SIMIONESCU, F. DENEŞ, **Originea vieţii**, 1983, 110 p.
C. BODEA (sub redacţia), **Tratat de biochimie vegetală**, II, Vol. IV, 1982, 408 p.
I. G. MURGULESCU, RODICA VÎLCU, **Introducere în chimia fizică Vol. III. Termodinamica chimică**, 1982, 624 p.
I. G. MURGULESCU, J. PĂUN, **Introducere în chimia fizică. Vol. I.3. Nucleul atomic, reacţii nucleare, particule elementare**, 1982, 506 p.
ELENA CEAUŞESCU, **Noi cercetări în domeniul compuşilor macromoleculari**, 1981, 536 p.
I. G. MURGULESCU, TATIANA ONCESCU, E. SEGAL, **Introducere în chimia fizică Vol. II, 2. Cinetică chimică şi cataliză**, 1981, 1024 p.
V. DRĂGUTAN, A. T. BALABAN, M. DIMONIE, **Metateza olefinelor şi polimerizarea prin deschidere de inel a cicloolefinelor**, 1981, 254 p.
LYDIA-MARIA VAICUM, **Epurarea apelor uzate cu nămol activ. Bazele biochimice**, 1981, 218 p.
I. GĂLĂŢEANU, **Procese şi metode radiochimice în energetica nucleară**, 1981, 234 p.
O. IORDACHE, **Procese polistocastice aplicate la fenomenele de transfer**, 1981, 186 p.
CR. SIMIONESCU, VALERIA GORDUZA, **Polimeri biocompatibili şi biologic activi**, 1980, 479 p.
ELENA CEAUŞESCU, **Polimerizarea stereospecifică a izoprenului**, 1979, 307 p.
CONST. GH. MACAROVICI, **Analiza chimică cantitativă anorganică**, 1979, 457 p.
M. FLORESCU, **Metode ştiinţifice în dezvoltarea industriei chimice moderne**, 1979, 256 p.
A. T. BALABAN, I. GĂLĂŢEANU, G. GEORGESCU, LIGIA SIMIONESCU, **Compuşi marcaţi şi radiofarmaceutici cu aplicaţii în medicina nucleară**, 1979, 495 p.
I. G. MURGULESCU, E. SEGAL, **Introducere în chimia fizică. Vol. II. 1. Teoria molecular cinetică a materiei**, 1979, 1036 p.
S. STERNBERG, FL. DANEŞ, **Termodinamica chimică aplicată**, 1978, 400 p.
I. G. MURGULESCU, V. EM. SAHINI, **Introducere în chimia fizică, Vol. 1.2. Structura şi proprietăţile moleculelor**, 1978, 604 p.
I. ZUGRĂVESCU, MAGDA PETROVANU, **N-ylid chemistry**, coédition avec McGraw Hill, International Book Company, U.S.A., 1977, 396 p.
I. G. MURGULESCU, **Introducere în chimia fizică. Vol. I.1. Atomi, molecule, legătură chimică** 1976, 560 p.
ELENA CEAUŞESCU, **Research work on synthesis and characterization of macromolecular compounds. Contributions**, 1974, 251 p.
CR. SIMIONESCU, VIORICA RUSAN, V. POPA, **Chimia algelor marine**, 1974, 212 p., 1 pl.

ISSN 0035–4090

I. P. Informaţia c. 2284

43 426

Lei 40
$ 75 (pour un abonnement annuel)

F 1103 64 66 Vegyészet

ACADÉMIE DE LA RÉPUBLIQUE SOCIALISTE DE ROUMANIE

REVUE ROUMAINE DE CHIMIE

REFERÁLVA

TOME 29

Nos 9—10

Septembre — Octobre 1984

EDITURA ACADEMIEI REPUBLICII SOCIALISTE ROMÂNIA

Rev. Roumaine Chim. RRCHAX, **29**, *9—10*, p. 717—806 (1984), Bucarest

ACADÉMIE DE LA RÉPUBLIQUE SOCIALISTE DE ROUMANIE

COMITÉ DE RÉDACTION

Rédacteur en chef:

I. G. MURGULESCU, membre de l'Académie de la République Socialiste de Roumanie

Rédacteurs en chef adjoints:

A. T. BALABAN et V. EM. SAHINI, membres correspondants de l'Académie de la République Socialiste de Roumanie

Collège de rédaction:

EM. BRATU, ELENA CEAUŞESCU, ECATERINA CIORĂNESCU-NENITZESCU, CR. SIMIONESCU, membres de l'Académie de la République Socialiste de Roumanie; P. SPACU, membre correspondant de l'Académie de la République Socialiste de Roumanie; M. BANCIU, M. D. GHEORGHIU, I. HAIDUC, D. I. MARCHIDAN, I. MOLDOVAN, G. NIAC et D. SĂNDULESCU

La Revue Roumaine de Chimie paraît 10 fois par an. Toute commande de l'étranger pour les travaux parus aux Editions de l'Académie de la République Socialiste de Roumanie sera adressée à « ROMPRESFILATELIA » — sectorul Export-Import Presă, P.O. Box 12—201 télex 10376 București, Calea Griviței nr. 64—66, Roumanie

Les manuscrits, les livres et les revues proposés en échange, ainsi que toute correspondance seront envoyés à la rédaction:

REVUE ROUMAINE DE CHIMIE
125, Calea Victoriei, 79717 Bucarest, Roumanie, téléphone 50 76 80

EDITURA ACADEMIEI REPUBLICII SOCIALISTE ROMÂNIA
125, Calea Victoriei, 79717 Bucarest, Roumanie, téléphone 50 76 80

ORSZÁGOS MŰSZAKI INFORMÁCIÓS KÖZPONT ÉS KÖNYVTÁR 1883

REVUE ROUMAINE DE CHIMIE

Tome 29, N°s 9—10 Septembre—Octobre, 1984

ALEXANDRU C. RĂZUȘ, EMERIC BARTHA, ZSOLT ARVAY and ALICE-MARIE GLATZ, Synthesis of *para*-substituted benzylcyclopropyl ketones . . . 719

S. STERNBERG, A. MATEESCU, V. BRÂNZOI and L. APĂTEANU, Electrode processes in $PbSO_4/PbO_2$ system . . . . 727 R

A. VELENIK, T. ŽIVKOVIĆ and N. TRINAJSTIĆ, On bond orders and bond energies in conjugated systems 737

CONSTANȚA GHEORGHIU, CORNELIA GURAN and MARCELA MUNTEAN, Chromium hexammine complexes with biguanidine derivatives 741

CONSTANȚA GHEORGHIU, CORNELIA GURAN and AURELIA MEGHEA, Molybdenum(V) oxo-thiocyano compounds with biguanidine derivatives 747

ROBERT SCHWARTZ, ANIKÓ JUHÁSZ and PETRONELA COLȚEA, The synthesis of 3β-acetoxy-B-nor-androst-5-en-3β-ol-17-one and 3β-acetoxy-B-nor-pregn-5-en-3β-ol-20-one 755

I. FENEȘAN, V. MUREȘAN, A. BARABÁS and M. BOGDAN, 2-Arylsulphonylamido-2-thiono-5,5-dimethyl-1,3,2-dioxaphosphorinanes 761

M. A. HASSAN, M. EL-KADY, M. EL-BORAI and A. A. ZBD EL-MOATY, Base catalyzed additions of dehydroacetic acid and its 3-cinnamoyl derivatives 769

F. SĂNDESCU and CR.I. SIMIONESCU, New solvent systems for acrylic copolymers . . . . 773 R

M. M. HUSAIN, D. K. SINGH and O. P. MATHUR, A correlation of lattice energy and equilibrium interionic distance of alkali metal hydrides 789

IOAN SĂNDULESCU, VASILE PÂRVULESCU and SORIN STRAJA, An attempt of explaining hydrogenation/dehydrogenation of ethylbenzene-ethylcyclohexane on $Pd-Mn/\gamma Al_2O_3$ and $Mn/\gamma Al_2O_3$ catalysts 793

CANDIN LITEANU, GHEORGHE RĂDULESCU and MARIA MOISE, Study of the rectification properties of heterogeneous membranes. VIII('). Behaviour of the bipolar unitary membrane system ı cationite R—H and anionite R—OH 799

Rev. Roumaine Chim. **29**, *9—10*, 717—806 (1984), Bucarest

Revue Roumaine de Chimie, **29**, *9 – 10*, 719 – 725 (1984)

SYNTHESIS OF *para*-SUBSTITUTED BENZYLCYCLOPROPYL KETONES*

ALEXANDRU C. RĂZUS, EMERIC BARTHA, ZSOLT ARVAY
and ALICE-MARIE GLATZ

Centre of Organic Chemistry, Spl. Independenței 202 B, R – 78100, Bucharest, Romania

Received April 10, 1984

A new method for the synthesis of benzylcyclopropyl ketones is reported. Isopropyl magnesium bromide or chloride was used as transmetallation agent in the condensation of substituted sodium phenylacetates with ethyl cyclopropanecarboxylate. The synthesis offers the advantage of using readily available starting materials and gives satisfactory yields of ketones.

For studies of the solvolysis in cyclopropylcarbinylic systems, we required benzylcyclopropyl carbinols **2** whose forerunners are the respective benzylcyclopropyl ketones **1**.

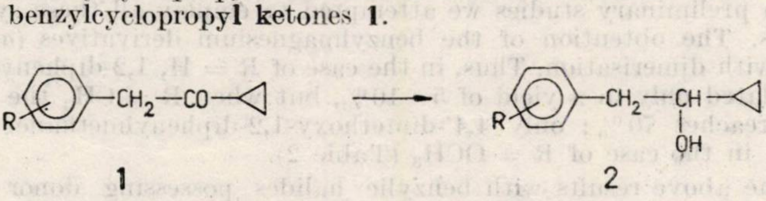

The synthesis of several such ketones is the subject of this paper. The ketones **1** have previously been prepared by the following three methods :[1,2]

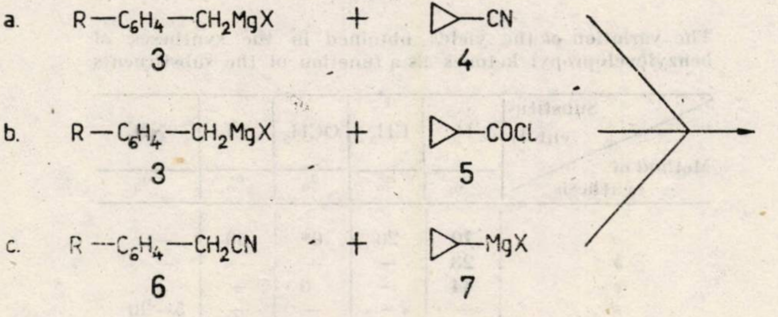

Scheme 1

---

* Partially reported at the Symposium of the Centenary of Polytechnical Institute, Bucharest, December 1981.

As shown in Table 1 the yields are heavily dependent on the method of synthesis and the substrate structure (nature of the *para*-substituent R).

Table 1

Syntheses of some benzylcyclopropyl ketones **2**

R	Method	Yields * %	Reference
H	*a*	70	1
H	*b*	23	1
H	*c*	44	1
$p-Cl$	*a*	65	2
$p-CH_3$	*a*	27	2

*In the case of method *a*, the reported yield includes the formation of the organomagnesium derivative.

The first two methods (*a* and *b*) are partially adequate for our purposes ; more or less advanced Wurtz dimerisation occurs in the synthesis of organomagnesium derivative **3** with significant loss in yields of the resulting ketones. The third method (c) is not more effective because of the difficulty in obtaining the starting material [3] (cyclopropylmagnesium bromide) and the poor yields in the condensation with the nitrile.

In preliminary studies we attempted to employ all these synthetic methods. The obtention of the benzylmagnesium derivatives (*a* and *b*) occurs with dimerisation. Thus, in the case of R = H, 1,2-diphenylethane was isolated only in a yield of 5–10%, but when $R = CH_3$ the dimerisation reaches 70% ; only 4,4′-dimethoxy-1,2-diphenylmethane is the product in the case of $R = OCH_3$ (Table 2).

The above results with benzylic halides possessing donor substituents suggested the use of benzylic halides containing acceptor substituents. However, the reaction of the latter halides is strongly affected by the small solubility of the halides and also by the secondary reactions.

Table 2

The variation of the yields obtained in the syntheses of benzylcyclopropyl ketones as a function of the substituents

Substituent R / Method of synthesis	H	CH_3	OCH_3	Cl	NO_2
	%	%	%	%	%
a	70	20	0*	60	—
b	23	—	—	—	—
c	44	—	0	—	0
d	—	—	—	—	5–20
e	—	—	0	—	0
f	83.5	80	75	70	0

* 0% represents the fact that the method does not give results.

The inactivity of starting materials and the modest yields obtained in the above synthetical routes suggested different syntheses of benzylcyclopropyl ketones.

The first is an adaptation of the general method for cyclopropyl ketone synthesis,[4] namely the condensation of the arylacetic acid halides with trimethylcyclopropylsilane (method *d*). The condensations of arylacetic acid derivatives (nitrile or alkali salts) with cyclopropylcarboxylic acid ester or halide (methods *e* and *f*) are alternative approaches to be used.

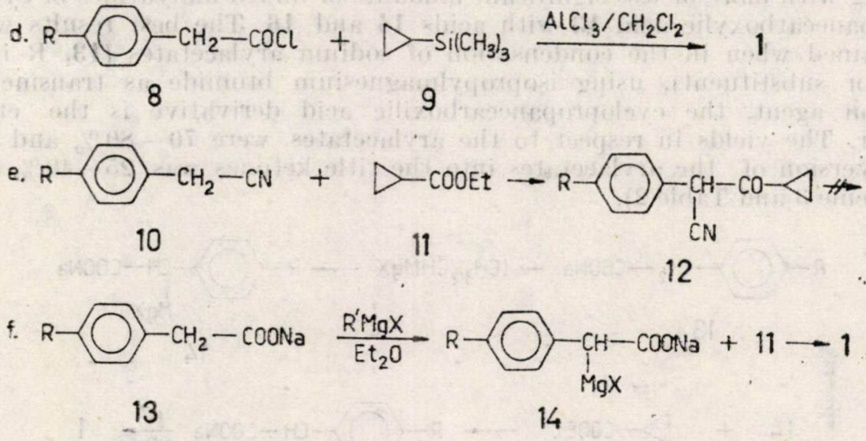
d. R–C6H4–CH2–COCl + ▷–Si(CH3)3 → 1
AlCl3/CH2Cl2
8
9
e. R–C6H4–CH2–CN + ▷–COOEt → R–C6H4–CH(CN)–CO–◁ ↛ 1
10
11
12
f. R–C6H4–CH2–COONa → R–C6H4–CH(MgX)–COONa + 11 → 1
R'MgX
Et2O
13
14

Scheme 2

The starting materials for the last three methods (*d*, *e* and *f*) are benzyl and cyclopropane derivatives.* The condensation of acid halide **8** with silane **9** (method *d*), in known conditions [4] gave a very complex mixture of products; nevertheless at lower temperature and at short reaction times we isolated about 20 % pure ketones after several column chromatographic separations. Only the *p*-nitrobenzylcyclopropyl ketone (**1**, $R = p - NO_2$) was prepared in this way, because this ketone is not available by any other methods. The condensation of benzyl cyanides **10** with ethyl cyclopropanecarboxylate [6] (method *e*) occurs in good yields (50 – 60 %). We obtained ketonitriles **12**, which have been separated, purified and described.

Unfortunately it was found impossible to promote further conversion of nitriles into carboxylic acids; the acid hydrolysis of the nitrile group was accompanied by ring opening and the alkaline saponification of the ketonitrile **12** gave scission leading to the formation of two acids (arylacetic and cyclopropanecarboxylic acids, respectively).

The method *f* consists in the condensation of ethyl cyclopropanecarboxylate with a metallic derivative of sodium arylacetate [5](**13**) obtained by transmetallation at the α-position.

---

* In the course of this work we tried several methods for the obtention of unsaturated ketones whose cyclopropanation would give ketones of type **1**. These experiments did not succeed.

The condensation of substituted sodium arylacetate (**13**, R = OCH_3) with ethyl cyclopropanecarboxylate was carried out in the presence of phenyllithium as transmetallation agent. The reaction occurs with the exclusive formation of the respective deoxybenzoin (see ^1H-NMR spectrum in the experimental part).

In an alternative synthesis isopropylmagnesium halides have been used as transmetallation agents in the condensation of cyclopropanecarboxylic acid halide with substituted sodium phenylacetate (**13**, R = H, CH_3O). The product of this reaction is *p*—R benzylcyclopropyl ketone along with more or less significant amounts of mixed anhydrides of cyclopropanecarboxylic acid **13** with acids **14** and **16**. The best results were obtained when in the condensation of sodium arylacetates (**13**, R is a donor substituent), using isopropylmagnesium bromide as transmetallation agent, the cyclopropanecarboxilic acid derivative is the ethyl ester. The yields in respect to the arylacetates were 70—80% and the conversion of the arylacetates into the title ketones was 25—40% (see Scheme 3 and Table 2).

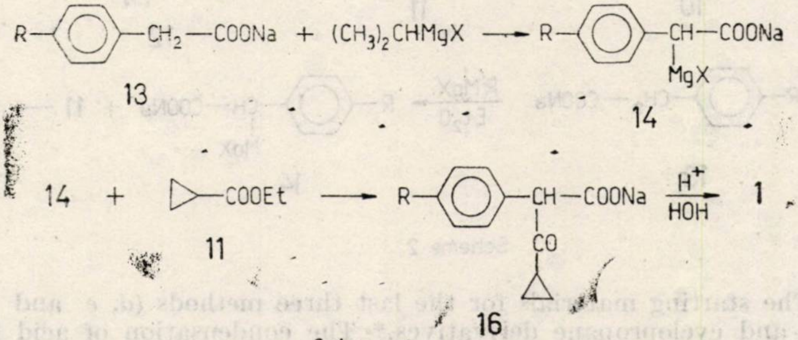

Scheme 3

It is notable that the use of arylacetates (**13**) with an acceptor substituent (NO_2, CN or COOH) in *para* position, as starting materials, leads to unexpected results. The substituents with an electron-withdrawing electronic effect would favour the proton elimination of the CH_2 group from the *para* position and thus would facilitate the transmetallation leading to better results than in the case of donor substituents. Surprisingly however, these compounds gave the condensation products of ethyl cyclopropanecarboxylate with the organomagnesium compounds (namely diisopropyl-cyclopropyl carbinol and isopropyl cyclopropyl ketone) instead of the transmetallation products (**14**), and the arylacetic salts were recovered unchanged. The explanation for the different behavior in this case seems to be complexation of the acceptor substituents with the organomagnesium derivatives.

EXPERIMENTAL

All melting points are uncorrected. ^1H-NMR spectra were recorded with a Varian A 60—A spectrometer, using TMS as internal standard. The v.p.c. analyses were carried out on a Willy Giede model 18—3 gas-chromatograph using a 1 m× 4 mm column packed with 7% Carbowax 20M and 13% ethyleneglycolsuccinate on Chromosorb W (60—80 mesh); the column temperature was 175°. IR spectra were recorded on a UR—20 Carl Zeiss Jena spectrophotometer.

A. *Syntheses of starting materials* were performed by standard methods. Detailed experimental procedures appear in the following. Sodium arylacetates (**13**) were obtained from the corresponding arylacetic acids by adding a NaOH solution into their aqueous suspension in the presence of phenolphthalein. The aqueous solutions were concentrated at normal pressure and then dried in vacuo or azeotropically with benzene. They were kept in a desiccator.

Arylacetic acids were prepared from the corresponding nitriles by alkaline or acidic hydrolysis. *Phenylacetic acid* had m.p. 75° (water; lit.[7] m.p. 77°); *p-Methylphenylacetic acid,* m.p. 92° (from water; lit.[9] m.p. 93°), was obtained by hydrolysis of nitrile **6** ($R = CH_3$). The nitrile (**6**) was obtained by photochemical bromination of *p*-xylene [2] and treatment of the resulted bromide with sodium cyanide in methanol/water; *p-chlorophenylacetic acid,* m.p. 106° (from water; lit.[10] m.p. 106°), was prepared by alkaline hydrolysis of the nitrile **6** ($R = Cl$); for the *synthesis of homoanisic acid* two different pathways were used: a) the reduction of *p*-anisaldehyde with natrium borohydride, substitution with bromine (PBr_3 in benzene [11]), treatment of the *p*-methoxybenzyl bromide with sodium cyanide, followed by alkaline saponification of the nitrile **6** ($R = OCH_3$); b) the chloromethylation of anisole,[12] treatment with sodium cyanide and saponification of the nitrile which gave the acid, m.p. 79—83°. The product is a mixture of two isomers (*ortho* 33% and *para* 67%, v.p.c. analysis). The homoanisic acid (*para*-isomer) was obtained by three successive recrystallizations from water (for the last recrystallization the solution was kept at 40°), yield 30—35%, m.p. 84—85° (lit. m.p. 86—87°); *p-nitrophenylacetic acid* was obtained by the nitration of benzylcyanide **6** ($R = H$), followed by acidic hydrolysis and water recrystallization, m.p. 151° (lit.[3] m.p. 151°). Its acid halide (**8**) was prepared in the usual manner, b.p. 45—47° (lit.[23] b.p. 46°); *p-aminophenylacetic acid.* The reduction of the *p*-nitrophenylacetic acid with hydrazine hydrate in the presence of Raney-nickhel in ethanol gave the desired product; m.p. 199—200° (lit.[24] m.p. 199—200°).

p-Cyanophenylacetic acid. The substitution of the amino group by cyano group was performed by means of Sandmeyer reaction [15] starting from the ethyl ester of *p*-aminophenylacetic acid. Water recrystallization gave a compound with m.p. 150° (lit. m.p. 152°); *homoterephthalic acid* was obtained from *p*-cyanophenylacetic acid by alkaline hydrolysis; water recrystallization gave a product with m.p. 237° (lit.[17]m.p. 236—237°).

Ethyl cyclopropanecarboxylate (**22**): γ-butyrolactone (1 mole), thionyl chloride (1.1 mole) and zinc chloride (1 g)[18] were stirred at 120—130° for 3—5 hours. The resulting mixture was worked up according to literature [19]. In this manner we obtained 60—65 g of ester; b.p. 135—140° (lit.[19] b.p. 136°); *Cyclopropanecarboxylic acid,* $b.p._{16}$ 90—91°, and its *acid chloride,* $b.p._{30-40}$ 40—45°, were obtained by literature methods,[21] *cyclopropylbromide,* b.p. 68—70° (lit. p.b. 69—71°), was prepared from cyclopropanecarboxylic acid as indicated[3], *cyanocyclopropane* (**4**), $b.p._{60}$101° (lit. b.p. 142—147°), was obtained starting from 1-bromo-3-chloropropane. Using trimethylvinylsilane [22] and methylene iodide we obtained *cyclopropyltrimethylsilane* (**9**), b.p. 98° (lit. 93°); yield 35—40%.

B. *Condensation of the acid chloride* **8** *with cyclopropyl-trimethylsilane* **9**. (*Method d*)

p-Nitrobenzylcyclopropyl ketone **1** ($R = NO_2$). In a solution of 5.85 g (0.05 moles) of cyclopropyltrimethylsilane and 10 g (0.05 moles) acid chloride **8** in 50 ml methylene chloride, 7.35 g (0.055 moles) anhydrous aluminium chloride were added in portions at $\leqslant 10°$ under stirring (approximately 30 min.). The mixture was stirred for 2 hours at 10—15° and then poured into a saturated solution of sodium chloride and ice. The organic layer was separated, the aqueous solution was extracted with methylene chloride and the organic solutions were washed with sodium hydrogen carbonate, dried over anhydrous magnesium sulfate and the solvent was removed in vacuo. The residual oil, 8 g, was purified via column chromatography (a 1.5 × 20 cm column, packed with neutral alumina, eluent ether) to give 2 g of product. The second purification on a column (1.4 × 40 cm column, packed with neutral alumina, eluent petroleum ether-ethylic ether 4 : 1) gave 0.5 g colorless crystals, m.p. 62°.

^1H—NMR *spectrum* ($CDCl_3$, δ ppm): 0.71—1.33 (m, 4H cyclopropyl); 2.03 (m, 1H cyclopropyl α—CO); 4.00 (s, 2H CH_2 α—CO); 7.40 and 8.20 (AA′BB′ system from the aromatic protons, $J_{AB} = 9.0$ Hz).

IR *spectrum* (CS_2, CCl_4, cm^{-1}): $\gamma_{CH\ aromatic}$ 855 (m); $\nu_{NO_2\ sym.}$ 1352 (vs); $\nu_{NO_2\ assym.}$ 1536 (m); $\nu_{C=O}$ 1711 (vs).

C. *Condensation of nitriles with ethyl cyclopropane carboxylate.* (*Method e*)

The synthesis of the ketonitrile **12** ($R = OCH_3$)[6] was performed in natrium ethoxide solution (50 ml dry ethanol and 0.1 atom-g sodium) by dropwise addition of a mixture of 15.9 g (0.1 mole) nitrile **6** ($R = OCH_3$) and 11.7 g (0.1 mole) of ethyl cyclopropanecarboxylate, then the mixture was heated at reflux for 5 hours under magnetical stirring. The reaction mixture was cooled at room temperature and poured into 250 ml of water. The aqueous phase was extracted twice with 100 ml ether and acidified with hydrochloric acid. The organic layer was washed with water and dried over anhydrous magnesium sulfate. The concentration in vacuo gave 11.5 g of ketonitrile **12**, m.p. 52°.

^1H-NMR *spectrum* ($CDCl_3$, δ ppm) : 0.68—1.28 (m, 4H cyclopropyl) ; 2.01 (m, 1H cyclopropyl α—CO) ; 3.75 (s, 3H OCH_3 group) ; 4.73 (s, 1H CH α in respect to CO and CN) ; 6.95 and 7.21 (AA′BB′ system from the aromatic nucleus, $J_{AB} = 8.5$ Hz).

IR *spectrum* (CS_2, CCl_4, cm^{-1}) : $\gamma_{C-H\ arom.}$ 705 (s) ; 742 (m) ; $\nu_{C=O}$ 1706 (vs).

D. *Condensation of organometallic sodium arylacetate derivatives* (**13**) *with ethyl cyclopropane carboxylate* **11** (*Method f*)

General procedures

The organomagnesium derivatives of sodium arylacetate (**14**) were prepared (in Ivanov's conditions **5**) in a round-bottomed three-necked flask fitted with mechanical stirrer, dropping funnel and reflux condenser (drying $CaCl_2$ tube).

Formation of ketones

1 Mole ester **11** dissolved in four times its volume of anhydrous ether was added dropwise to 1 mole of organomagnesium derivative under stirring, and then the mixture was heated at reflux for three hours. The reaction mixture was poured slowly in cold diluted hydrochloric acid. The ethereal layer was separated and the aqueous solution was extracted twice with ether. The combined ethereal solutions were dried over anhydrous magnesium sulfate and the ether was removed in vacuo. The residual oil was heated at 100° for 10—15 min (water bath), dissolved in ether, washed with a saturated sodium hydrogen carbonate solution and with water ; the ethereal solution was dried over anhydrous magnesium sulfate, concentrated and fractionated in vacuo. The first fraction contains unreacted ethyl cyclopropanecarboxylate, by a small amount of an intermediate fraction and, finally, the ketone fraction. The ketones were analysed by v.p.c., IR and ^1H-NMR spectra.

The resulted alkaline aqueous solution after ethereal extraction was acidified with diluted hydrochloric acid and the unreacted arylacetic acid was recovered pure enough (IR and ^1H-NMR spectra analyses) to be used in another experiment.

Benzylcyclopropyl ketone **1** ($R = H$). An ethereal solution of ethyl cyclopropanecarboxylate was added with stirring to an ethereal suspension of organomagnesium sodium phenylacetate, obtained from 39.5 g (0.25 moles) of **12**. The treatment of the reaction mixture in the usually manner gave 13.9 g ketone **1**, b.p. $_{30-35}$[3] 158—160° (98% purity, v.p.c. determined) ; yield 67% and a conversion of 40% in respect to sodium phenylacetate. ^1H-NMR *spectrum* (CCl_4, δ ppm) : 0.40—1.20 (m, 4H cyclopropyl) ; 1.80 (m, 1H cyclopropyl α—CO) ; 3.63 (s, 2H CH_2 group α CO) ; 7.1 (s, 5H aromatics). IR *spectrum* (CS_2, CCl_4, cm^{-1}) : $\gamma_{CH\ arom.}$ 705 (s) ; 742 (m) ; $\nu_{C=O}$ 1706 (vs). 13.5 g ethyl cyclopropanecarboxylate and 13.7 g phenylacetic acid were also recovered.

p-Methylbenzylcyclopropyl ketone **1** ($R = CH_3$). Starting from 38 g (0.21) moles) of sodium *p*-methylphenylacetate **13** ($R = CH_3$) and working in the above described conditions 16.5 g of ketone **1** ($R = CH_3$) were obtained ; b.p.$_5$ 110—120° ; yield 70.2% (49% conversion in respect to the sodium salt **13**). ^1H-NMR *spectrum* (CCl_4, δ ppm) : 0.47—1.10(m, 4H cyclopropyl) ; 1.83 (m, cyclopropyl α—CO) ; 2.30 (s, 3H *p*—CH_3) ; 3.60 (s, 2H CH_2 group CO) ; 7.03 (s, 4H aromatics). IR *spectrum* (CS_2, CCl_4, cm^{-1}) : $\gamma_{CH\ arom.}$ 815 (s) ; $\nu_{C=O}$ 1708 (vs). 11.5 g of ethyl cyclopropanecarboxylate, 1.7 g of an intermediate fraction and 11.7 g *p*-phenylmethylacetic acid were also obtained.

p-Chlorophenylcyclopropyl ketone **1** ($R = Cl$). Reaction of 60 g (0.3 moles) of sodium *p*-chlorophenylacetate **13** ($R = Cl$) working as in the usually manner results in 21.3 g of ketone **1** ($R = Cl$), b.p.$_{5-6}$ 130—136° ; m.p. 40—42° (v.p.c. purity 96%) was obtained ; yield 70% (conversion 37.6% in respect to *p*-chlorophenylacetic acid). ^1H-NMR *spectrum* (CCl_4, δ ppm) : 0.46—1.23 (m, 4H cyclopropyl) ; 1.83 (m, 1H cyclopropyl α—CO) ; 3.66 (s, 2H CH_2

group α CO); 7.10 (m, 4H aromatics). IR *spectrum* (CCl_4, CS_2 cm^{-1}) : $\gamma_{CH\ arom.}$ 804 (s); $\nu_{C=O}$ 1711 (vs); 15 g ethyl cyclopropanecarboxylate and 23 g *p*-chlorophenylacetic acid were also recovered.

p-Methoxybenzylcyclopropyl ketone **1** (R = OCH_3). From 29 g sodium salt **13** (R = OCH_3) working as above 11.9 g ketone **1** (R = OCH_3), b.p.$_1$ 121–125°, were obtained; yield 84.5% (conversion 41.3% in respect to **13**). ^{1}H–NMR *spectrum* (CCl_4, δ ppm) : 0.46–1.10 (m, 4H cyclopropyl); 1.85 (m, 1H cyclopropyl α–CO); 3.60 (s, 2H group CH_2 α–CO); 3.70 (s, 3H OCH_3 group); 6.71 and 7.02 (AA′BB′ aromatic system, $J_{AB} = 9.0$ Hz). IR *spectrum* (CS_2, CCl_4, cm^{-1}) : $\gamma_{CH\ arom.}$ 824 (s); $\nu_{C=O}$ 1704 (vs), 7.3 g ethyl cyclopropanecarboxylate and 13.4 g homoanisic acid were recovered.

REFERENCES

[1] H. Hanack and H. M. Ensslin, *Liebigs Ann. Chem.*, **697**, 100 (1966).
[2] M. Cussac, A. Boncherle and J. Hache, *Eur J. Med. Chem.—Chim. Ther.*, **10**, 112 (1975).
[3] J. S. Meeck and D. T. Osuga, *Org. Synth.*, **43**, 9 (1963).
[4] M. Grignon-Dubois, J. Dunognés and R. Calas, *Synthesis*, **1976**, 737.
[5] D. Ivanov, N. Marecoff and E. Zidaroff, *Rev. Chim. Acad. R.P.R.*, **7**, 985 (1962) and further references therein.
[6] P. B. Russel and G. H. Hitchings, *J. Amer Chem. Soc.*, **73**, 3763 (1951).
[7] R. Adams and A. F. Thal, Organic Syntheses coll. vol. 1, 436(1941).
[8] T. R. Lewis and S. Archer, *J. Amer. Chem. Soc.*, **73**, 211 (1951).
[9] D. Schoringin, *Ber. dtsch. chem. Ges.*, **43**, 1941 (1910).
[10] C. Viel, R. Dorne and P. Rumpf, *Bull. Soc. Chim. France*, **1966**, 1956.
[11] G. Wittig and H. Zimmermann, *Chem. Ber.*, **86**, 637 (1953).
[12] A. Müller, M. Mészáros, M. Zempert-Stréter and J. Száva, *J. Org. Chem.*, **16**, 1013 (1951).
[13] G. R. Robertson, Organic Syntheses coll. vol. 1, 406(1941).
[14] D. Balcon and A. Furst, *J. Amer. Chem. Soc.*, **75**, 4334 (1953).
[15] Y. Kominato, *Kumamoto Med. J.*, **6**, 139 (1954); *Chem. Abstr.*, **50**, 306 i (1956).
[16] G. Fileti and M. Basso, *Gazz. Chim. Ital.*, **21**, 61 (1958).
[17] H. Krieger, *Suomen Kem. B*, **31**, 161 (1958).
[18] W. Reppe, *Liebigs Ann. Chem.*, **596**, 1(1955).
[19] S. C. Bunce and R. A. Kent, *Organ. Prep. Proc. Internat.*, **6**, 193 (1974).
[20] M. J. Schlatter, *J. Amer. Chem. Soc.*, **63**, 1733 (1941).
[21] a) L. I. Smith and E. R. Rogier, *J. Amer. Chem. Soc.*, **73**, 4047 (1951).
b) L. I. Smith and S. McKenzie, jr., *J. Org. Chem.*, **15**, 74 (1950).
[22] Motonori Kanazashi, *Bull. Chem. Soc. Jpn.*, **26**, 493 (1953); *Chem. Abstr.*, **49**, 1158 c (1956).
[23] R. J. Rowson and J. T. Harrison, *J. Org. Chem.*, **35**, 2057 (1970).
[24] G. Ross Robertson, Organic Syntheses coll. vol. 1, 52 (1941).

Revue Roumaine de Chimie, **29**, *9 — 10*, 727—735 (1984)

ELECTRODE PROCESSES IN $PbSO_4/PbO_2$ SYSTEM

S. STERNBERG *, A. MATEESCU **, V. BRÂNZOI * and L. APĂTEANU ***

* Polytechnic Institute of Bucharest, Romania
** Acumulatorul Entreprise — Bucharest, Romania
*** Biochemical and Chemical Energetics Institute — Bucharest, Romania

Received January 21, 1984

In order to obtain information on the electrode processes in $PbSO_4/PbO_2$ system, in sulphuric acid solutions, a porous microelectrode was obtained by a few successive recyclings.

During formation, initially it is the rhombic form ($\alpha-PbO_2$) of the lead bioxide which deposits. Then, during the cycles, electrochemical recrystallization of PbO_2 occurs following the scheme :

$$\alpha-PbO_2 \rightleftarrows PbSO_4 \rightleftarrows \beta-PbO_2$$

The amount of $\alpha-PbO_2$ which exists on the electrode, at the *i* cycle was determined using the equation :

$$Q_{i\alpha} = Q_{(i-1)\alpha} - Q_{(i-1)\alpha} U_\alpha + Q_i - Q_{i-1}$$

The efficiency of $\alpha-PbO_2$ to $\beta-PbO_2$ transformation for the 10th cycle was :

$$\eta_{10\alpha} = \frac{Q_{10\alpha}}{Q_{10}} = 28.9\%$$

In order to reproduce in laboratory the electrode processes which occur in the lead-sulphuric acid battery, it is necessary to obtain a porous ,,microelectrode'' able to simulate the pasted electrodes from the batteries. For the negative $Pb/PbSO_4$ electrode, this microelectrode is described in other papers.[1-6]

The present paper reports on some results concerning the electrochemical behaviour of the positive $PbSO_4/PbO_2$ electrode, on a porous "microelectrode" obtained from pure lead by a few repeated cyclings.

EXPERIMENTAL PART

The experiments were carried out by means of linear voltammetry of low rate, using a 173-Model (Princeton Applied Research) potentiostat/galvanostat with a 179-Model Digital Coulometer. The potential — current curves were registered by means of an X—Y recorder.

As pulses generator, an Orion — EMG 1117/2 Low Frequency Generator was used. The electrochemical cell and the scheme of the electronic device were described in detail in the previous papers.[4,7]

The pure lead electrodes were of cylindrical form with a 1.5 mm diameter, the surface exposed to electrolyte being of about 50 mm². The polarization curves were registered in the (800 ÷ 1650) mV anodic potential range.

All potentials were measured versus the $Hg/Hg_2SO_4/H_2SO_4$ electrode. The potential scan rates were in the $(0.75 \div 7.5)$ mV/sec range, and the electrolytes were sulphuric acid solutions of different concentrations. For each cyclical voltammogram, the total anodic (Q_a) and cathodic (Q_c) amount of electricity was registered by means of the digital coulometer.

RESULTS AND DISCUSSIONS

Figure 1 shows the polarization curves obtained on the pure lead microelectrode in sulphuric acid solution of 1.245g/cm³ density, at a potential scan rate of 1.75 mV/sec.

The potential was scanned from + 800 mV to + 1650 mV and back to + 800 mV, this scanning resulting in successive cycles (on the figure was indicated the number of cycle and the total amounts of electricity Q_a and Q_c, respectively).

Figure 1 shows that, in order to obtain voltammograms with a reproducible shape a few recyclings are necessary. At the end of about 6—7 cycles, a characteristic shape of the polarization curves is obtained, with an anodic (A) peak corresponding to the reaction of PbO_2 formation from $PbSO_4$, and a cathodic (B) peak corresponding to the PbO_2 reduction to $PbSO_4$. As the recycling proceeds, the shape of voltammograms is maintained and there are only the Q_a and Q_c capacities which increase. Thus, it is obvious that information concerning the electrode processes cannot be obtained only from one or two cycles. It is necessary to obtain a porous "microelectrode" which forms by some recyclings and partially simulates the positive electrode from the acid battery, obtained by the electrodes formation from "paste". Using the electricity amount, Q_c, it is possible to calculate the thickness of the porous layer, for the 10th cycle, which is of about 3 μ. Our results, generally refer to the 10th cycle.

Table 1

The variation of the voltameograms parammnters obtained on pure lead, in 1.24 g/cm³ H_2SO_4 solution, as a function of the scan rate

Cycle duration (sec)	I_{p_A} (mA)	I_{p_B} (mA)	E_{p_A} (mV)	E_{pB} (mV)	$\frac{Q_a}{Q_c}$
60	8.8	13.2	1470	1040	5.72
120	6.6	15.1	1470	1050	7.98
155	5.9	15.4	1430	1050	8.83
195	3.7	15.7	1420	1060	10.11
246	3.5	15.9	1420	1080	10.23
333	3.4	16.1	1410	1080	17.89
495	3.2	16.9	1370	1080	20.87

Previous measurements have shown that 10 cycles are enough to obtain reproducible voltammograms. The anodic peak is followed by a great increase of current coresponding to the discharge of the gaseous oxygen. The anodic Q_a capacity is much higher than the cathodic one, $Q_a \gg Q_c$ (see Figure 3 and Table 1), owing to the discharge of the gaseous oxygen.

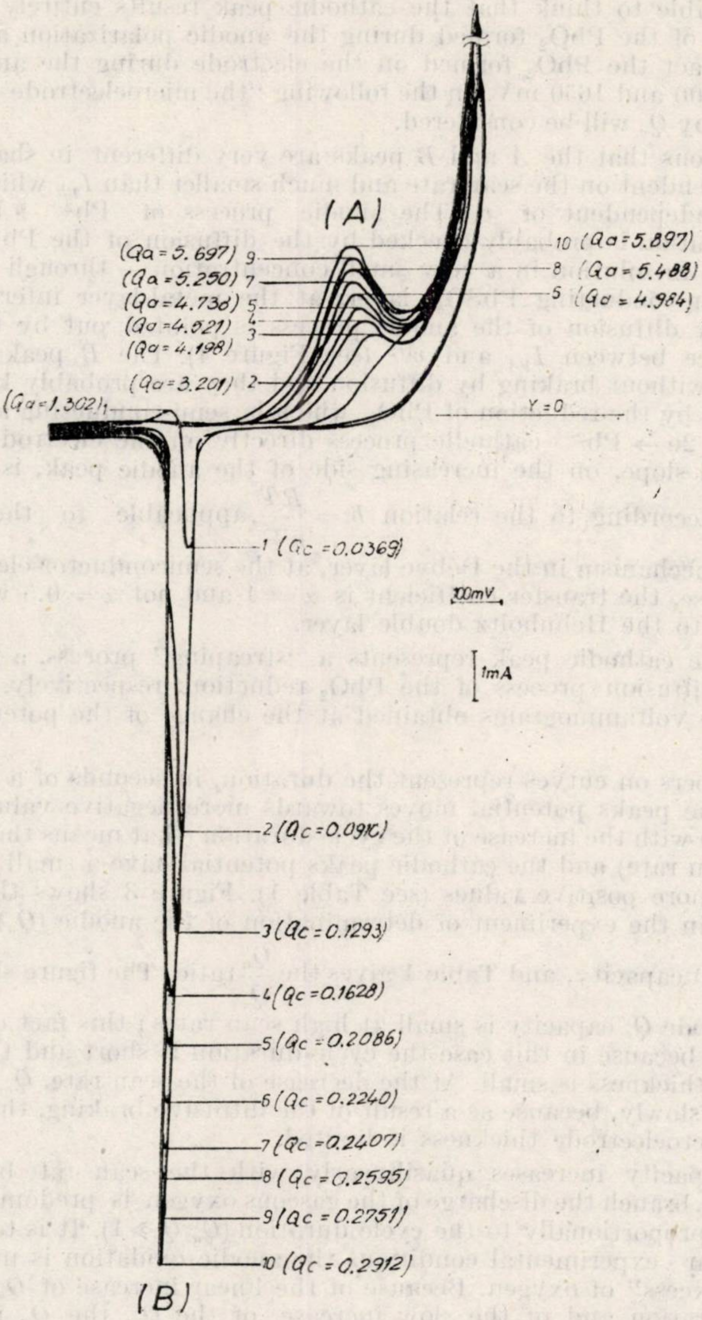

Fig.1. — Voltammograms obtained on pure lead, in 1.245 g/cm^3 H_2SO_4 solution, by a few (10) successive recyclings. On voltammograms are indicated the number of cycle and the Q_a and Q_c amounts of electricity in *C*, for each cycle. The scan rate = 1.75 mV/cm.

It is possible to think that the cathodic peak results entirely from the reduction of the PbO_2 formed during the anodic polarization and represents in fact the PbO_2 formed on the electrode during the anodic scan between 800 and 1650 mV. In the following "the microelectrode capacity" designed by Q_c will be considered.

It is obvious that the A and B peaks are very different in shape. Thus, I_{pA} is dependent on the scan rate and much smaller than I_{pB} which is practically independent of v. The anodic process of $Pb^{2+} \rightarrow Pb^{4+} + 2e$ transformation is probably checked by the diffusion of the Pb^{2+} ions — which are in solution in a very small concentration — through the pores of the non-conducting $PbSO_4$ layer, at the metal-layer interface. The control by diffusion of the anodic process is pointed out by the linear dependence between I_{pA} and $v^{1/2}$ (see Figure 4). The B peaks are very "sharp", without braking by diffusion and they are probably kinetically controlled by the reduction of PbO_2, which is semi-conducting and allows a $Pb^{4+} + 2e \rightarrow Pb^{2+}$ cathodic process directly on the electrode surface. The Tafel slope, on the increasing side of the anodic peak, is of about 30 mV, according to the relation $b = \frac{RT}{n\mp}$, applicable to the charge transfer mechanism in the Debye layer, at the semiconductor electrodes [9]; in this case, the transfer coefficient is $\alpha = 1$ and not $\alpha = 0.5$ which corresponds to the Helmholtz double layer.

Hence, the cathodic peak represents a "streaping" process, a non-braking by diffusion process of the PbO_2 reduction, respectively. Figure 2 shows the voltammograms obtained at the change of the potential scan rate.

The numbers on curves represent the duration, in seconds of a cycle.

The anodic peaks potential moves towards more negative values at the same time with the increase of the cycle duration (that means the decrease of the scan rate) and the cathodic peaks potential have a small deviation towards more positive values (see Table 1). Figure 3 shows the results obtained in the experiment of determination of the anodic (Q_a) and cathodic (Q_c) capacity, and Table 1 gives the $\frac{Q_a}{Q_c}$ ratio. The figure shows that the electrode Q_c capacity is small at high scan rates; this fact could be explained because in this case the cycle duration is short and the microelectrode thickness is small. At the decrease of the scan rate, Q_c increases relatively slowly, because as a result of the diffusive braking, the increase of the microelectrode thickness is limited.

The Q_a capacity increases quasilinearly with the scan rate because on the anodic branch the discharge of the gaseous oxygen is predominant and increases proportionally to the cycle duration ($Q_a/Q_c \gg 1$). It is to mention that in our experimental conditions the anodic oxidation is made with a high "excess" of oxygen. Because of the linear increase of Q_a with the cycles duration and of the slow increase of the Q_c, the Q_a ratio will increase with the decrease of the scan rate, as it is shown in Table 1.

The PbO_2 layer is more compact for the first cycles but with the cycles repeating it becomes more and more porous.[4]

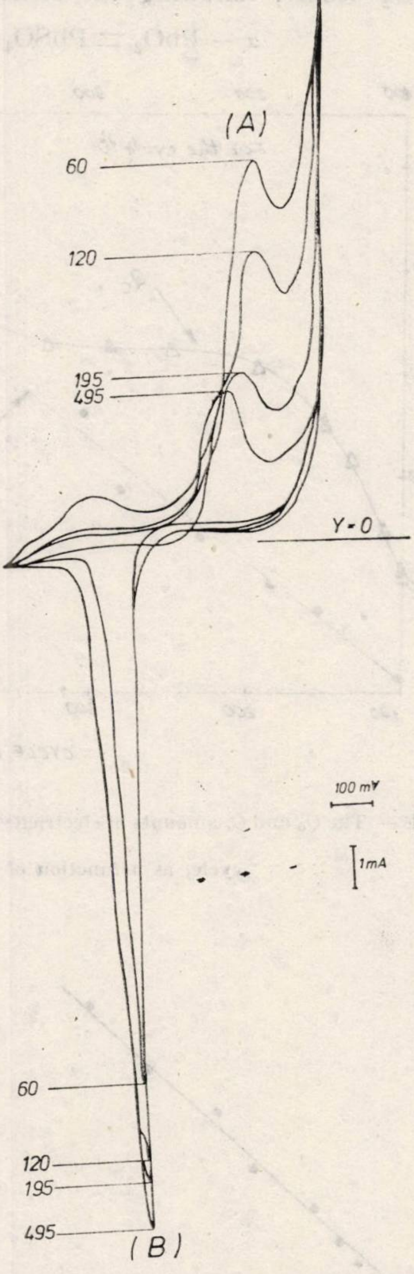

Fig. 2. — Characteristic voltammograms for the 10th cycle, obtained on pure lead, in 1 245 g/cm^3 H_2SO_4 solution, at the potential scan. The number on curves represents the duration of a cycle, in seconds.

We can suppose that, initially, it is the rhombic form of the lead bioxide, that means the $\alpha-PbO_2$, which deposits [8] on the microelectrode, during its formation.

During the charge-discharge cycles, an electrochemical recrystallization of $\alpha-PbO_2$ occurs, following the scheme:

$$\alpha - PbO_2 \rightleftarrows PbSO_4 \rightleftarrows \beta - PbO_2 \tag{1}$$

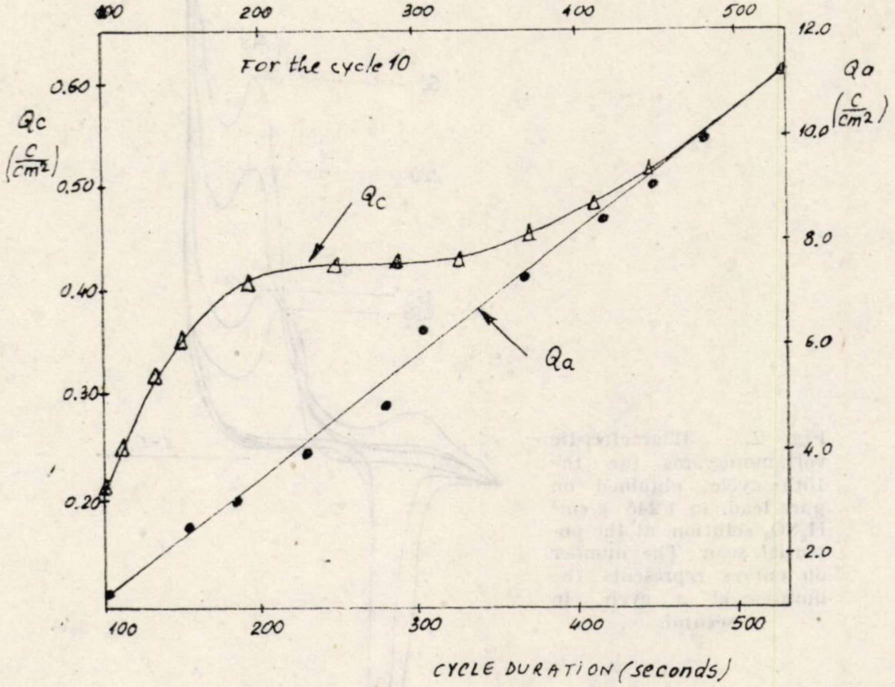

Fig. 3. — The Q_a and Q_c amounts of electricity $\left(\text{in } \frac{C}{cm^2}\right)$ determined for the 10th cycle, as a function of cycles duration.

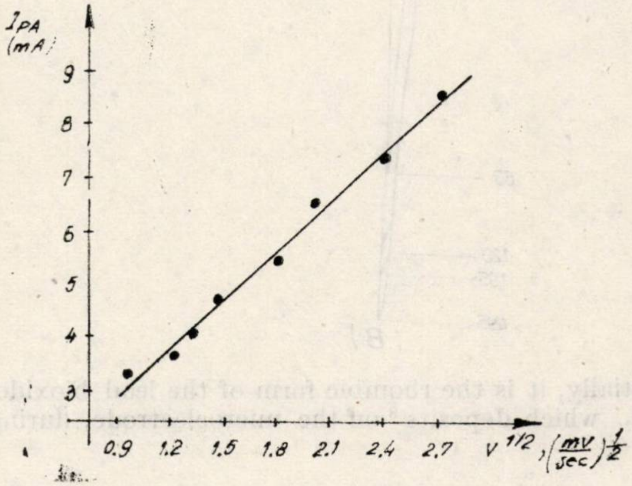

Fig. 4. — Anodic peak height dependence on the scan rate.

As a result of this transformation, according to the theory of Dasoian and Aguf,[8] at each recycling, a $U_\alpha \cong 0{,}3$ fraction of $\alpha-PbO_2$ turns into $\beta-PbO_2$. According to the phase composition determinations of the active mass formed on the positive electrodes [10] we propose for U_α the 0.2 value. Let us note by $Q_1, Q_2 \ldots Q_i$ the PbO_2 amounts formed at each cycle and by $Q_{1\alpha}, Q_{2\alpha}, \ldots, Q_{i\alpha}$, the $\alpha-PbO_2$ amounts remained at the end of each cycle. The $Q_{i\alpha}$ amount which forms on the microelectrode at the i cycle, is :

$$Q_{i\alpha} = Q_{(i-1)\alpha} - Q_{(i-1)\alpha} \cdot U_\alpha + Q_i - Q_{i-1} \tag{2}$$

Q_i and Q_{i-1} are $Q_{cathodic}$, for the i and $i-1$ cycle, which are directly determined from the experiment.
$(Q_i - Q_{i-1})$ is the "primary" $\alpha-PbO_2$ which appears at each cycling as long as $Q_{cathodic}$ did not reach a constant value. For the first ten cycles the following equations were obtained and can be used to calculate the percentage of $\alpha-PbO_2$, $\eta_\alpha = \dfrac{Q_{i\alpha}}{Q_i} \cdot 100$

$$Q_{1\alpha} = Q_1 ; \ \eta_\alpha = 100\% \tag{3}$$

$$Q_{2\alpha} = Q_1 - Q_1 U_\alpha + Q_2 = Q_2 - Q_1 U_\alpha ; \ \eta_{2\alpha} = 91{,}9\% \tag{4}$$

$$Q_{3\alpha} = Q_3 - (Q_1 + Q_2)\, U_\alpha + Q_1 U_\alpha^2 ; \ \eta_{3\alpha} = 81.3\% \tag{5}$$

$$Q_{4\alpha} = Q_4 - (Q_1 + Q_2 + Q_3)\, U_\alpha + (2Q_1 + Q_2)\, U_\alpha^2 - Q_1 U_\alpha^3 ;$$

$$\eta_{4\alpha} = \frac{Q_{4\alpha}}{Q_4} = 72.1\% \tag{6}$$

$$Q_{5\alpha} = Q_5 - (Q_1 + \ldots + Q_4)\, U_\alpha + (3Q_1 + 2Q_2 + Q_3) U_\alpha^2 -$$
$$-(3Q_1 + Q_2)\, U_\alpha^3 + Q_1 U_\alpha^4 ;$$

$$\eta_{5\alpha} = \frac{Q_{5\alpha}}{Q_5} = 60.00\% \tag{7}$$

Similarly, we obtained for $\eta_{i\alpha}$ the following values :

$$\eta_{6\alpha} = 56.8\% ; \ \eta_{7\alpha} = 45.8\% ; \ \eta_{8\alpha} = 44.4\% ; \ \eta_{9\alpha} = 39.4\% ;$$
$$\eta_{10\alpha} = 28.9\%$$

Figure 5 shows the voltammograms obtained for two extreme concentrations. The two voltammograms are represented at different scales, because at low concentrations the anodic and cathodic currents have high values. It is to point out, from table 2, that the anodic and cathodic peaks heights and the Q_a and Q_c amounts of electricity increase with the decrease of the concentrations (the increase of the pH). The explanation of this behaviour results from figure 5. At the increase of the pH the whole zone of lead oxidation moves towards more electronegative values.

This behaviour results from the movement of the oxygen discharge potential to more electronegative values, when the pH increases. Thus, the beginning (the shoulder) of the (*A*) peak moves with about 300 mV and the zone of the intense evolution of the gaseous oxygen, too. The scan

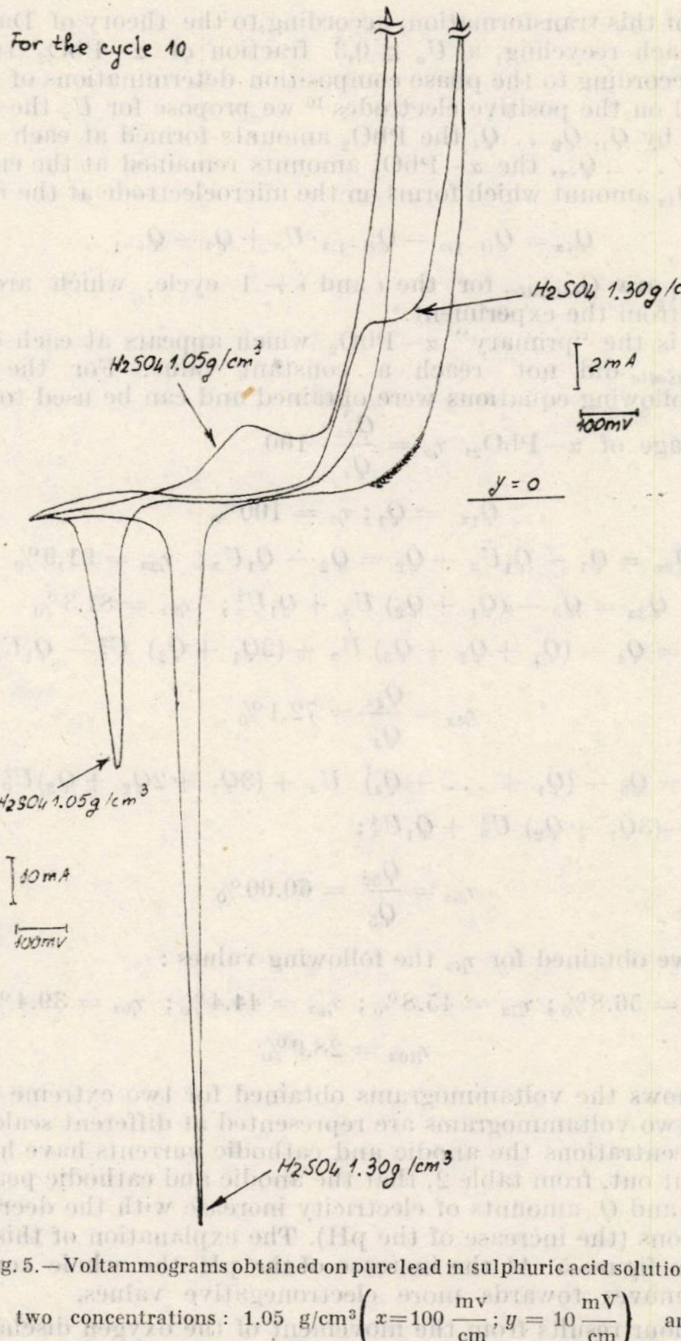

Fig. 5.—Voltammograms obtained on pure lead in sulphuric acid solutions of two concentrations: 1.05 g/cm³ $\left(x=100\ \frac{\text{mv}}{\text{cm}};\ y=10\ \frac{\text{mV}}{\text{cm}} \right)$ and 1.30 g/cm³ $\left(x=100\ \frac{\text{mV}}{\text{cm}};\ y=2\ \frac{\text{mV}}{\text{cm}} \right)$.

range remains contant, hence the oxidation zone is more extended when the solution pH increases. The ratio $Q_{c_{1\cdot05}}/Q_{c_{1\cdot30}}$, hence only a part of this oxygen is used to obtain PbO_2, and the rest evolves as gaseous oxygen.

Table 2

The variation of the voltammograms parameters obtained on pure lead in sulphuric acid solutions of different concentrations (the scan rate = 1.75 mV/sec)

Density of H_2SO_4 solution (g/cm^3)	I_{p_A} (mA)	I_{p_B} (mA)	E_{p_A} (mV)	E_{p_B} (mV)	$\frac{Q_a}{Q_c}$
1.05	14.2	49	1250	930	26.5
1.10	11.8	41	1320	980	24.3
1.15	10.6	36	1350	990	24.0
1.20	9.3	31.4	1370	1180	23.8
1.25	8.7	28.9	1380	1180	18.5
1.30	8.4	25.8	1470	1180	17.4

By this way it is possible to explain the increase of the ratio Q_a/Q_c with the decrease of the concentration, too.

CONCLUSIONS

In order to obtain conclusive information concerning the electrode processes in $PbSO_4/PbO_2$ system, in sulphuric acid solutions, it is necessary to obtain a microporous electrode, which could be obtained by a few successive recyclings.

The anodic branch of voltammograms is controlled by diffusion and the cathodic one is kinetically controlled.

At the decrease of H_2SO_4 concentration, the lead oxidation process moves towards more electronegative values.

REFERENCES

[1] F. F. Sharpe, *J. Electrochem. Soc.* **2** (1977).

[2] S. Sternberg, V. Brânzoi, L. Apăteanu, *Rev. Roumaine de Chim.*, (under press).

[3] A. A. Abdul Azim, K. M. El-Sobki, A. A. Khedr, *Corrosion Science*, **17**, 415 (1979).

[4] S. Sternberg, V. Brânzoi, L. Apăteanu, A. Mateescu, *Rev. Roumaine de Chim.* **6**, 583 (1983).

[5] B. K. Mahato, *J. Electrochem. Soc.*, **126**, 365 (1979).

[6] K. R. Bullock, and W. T. Tiedeman, *J. Electrochem Soc.* **10** (1980).

[7] A. Mateescu, L. Marinescu, *Rev. Chim.* **32**, 688 (1981).

[8] M. A. Dasoian, I. A. Aguf, "Sovremennaia teoria svintsovogo accumuliatora" Leningrad 1975, p. 128.

[9] V. A. Myamlin, Pleskov, "Electrochemistry of Semiconductors", Yu. V. Plenum Press, New York, 1967.

[10] S. Sternberg. A. G. Mateescu, *Rev. Chim.*, **33**, 243 (1982).

Revue Roumaine de Chimie, **29**, *9 – 10*, 737–740 (1984)

ON BOND ORDERS AND BOND ENERGIES IN CONJUGATED SYSTEMS[1]

V. VELENIK,[a] T. ŽIVKOVIĆ[b] and N. TRINAJSTIĆ[c]

[a] Faculty of Pharmacy and Biochemistry, The University of Zagreb, 41000 Zagreb, Croatia, Yugoslavia

[b] The Rugjer Bošković Institute, P.O.B. 1016, 41001 Zagreb, Croatia, Yugoslavia

[c] Department of Chemistry, University of South Carolina, Columbia, South Carolina 29208, U.S.A. ; permanent address : The Rugjer Bošković Institute, P.O.B. 1016, 41001 Zagreb, Croatia, Yugoslavia

Received February 10, 1984

The contribution of a particular molecular bond to the total π-electron energy is discussed.

In the Hückel theory the contribution of the bond orders to the total π-electron energy may be given as [2],

$$E_\pi = 2 \sum_{i<j} p_{ij}\, \beta_{ij} \tag{1}$$

where p_{ij} are π-bond orders, while β_{ij} are the resonance integrals between atoms i and j. In the simple Hückel model [3] $\beta_{ij} = \beta = \text{const.}$ for adjacent carbon atoms, and $\beta_{ij} = 0$ otherwise. The contribution of the bond (i, j) to the total π-electron energy (in β units) is therefore $2p_{ij}$. However, in this study we will show that the energy change ΔE_{ij} due to the removal of the bond (i, j) from the molecule is well approximated by the bond order p_{ij} alone and not $2p_{ij}$ as expected from (1). This problem was studied by several people [4–7] without a definitive answer.

A partial differentiation of E_π with respect to β_{ij} yields

$$\frac{\partial E_\pi}{\partial \beta_{ij}} = 2 \cdot p_{ij} \tag{2}$$

According to relation (1) the total π-electron energy E_π does not depend explicitly on the bond orders p_{ij} between atoms which are not connected to each other. On the other hand, the energy E_π is the absolute minimum with respect to the variation over all physicaly realizable bond orders p_{ij}. In order to minimize E_π, the bond orders p_{ij} between the adjacent carbon atoms should be as large as possible, since they explicitly enter relation(1). Different bond orders are not independent from each other, and hence as a result the bond orders between atoms which are not connected tend to be relatively small. In the simplest approximation we may put $p_{ij} \approx 0$ whenever atoms i and j are not connected to each other, i.e. whenever $\beta_{ij} = 0$. Consider now bond order p_{ij} as a function of the resonance integral β_{ij} for a particular bond (i, j). When atoms i and j are not connected to each other, then $\beta_{ij} = 0$ and as assumed above $p_{ij} = 0$. When atoms i and j are first neighbours, then $\beta_{ij} = \beta$, and $p_{ij} = p_{ij}(\beta)$ is the bond order of the bond (i, j). The simplest assumption for the intermediate case is obtained by the linear extrapolation.

$$p_{ij}(\beta_{ij}) = \frac{\beta_{ij}}{\beta} p_{ij}(\beta) \qquad (3)$$

From relations (2) and (3) follows,

$$\frac{E_\pi}{\partial \beta_{ij}} = \frac{2\beta_{ij}}{\beta} p_{ij}(\beta) \qquad (4)$$

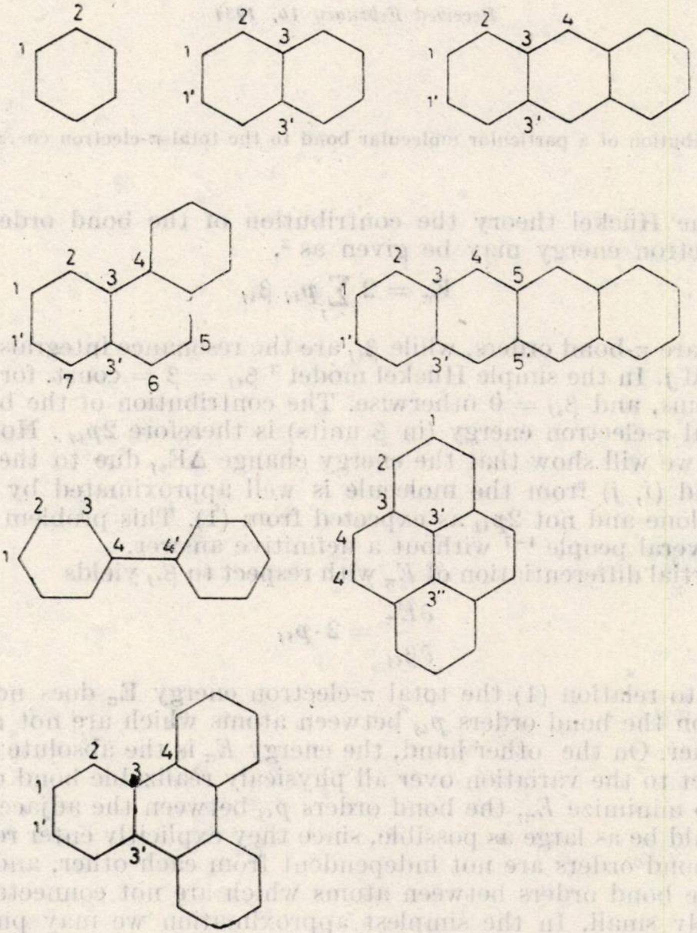

Fig. 1.— Graphs of molecules studied. Numbers denote those bonds for which the bond energies were computed using formula (5).

Let ΔE_{ij} be the difference in energy between the molecules with and without the (i, j) bond,

$$\Delta E_{ij} = E_\pi(\beta_{ij} = \beta) - E_\pi(\beta_{ij} = 0) \tag{5}$$

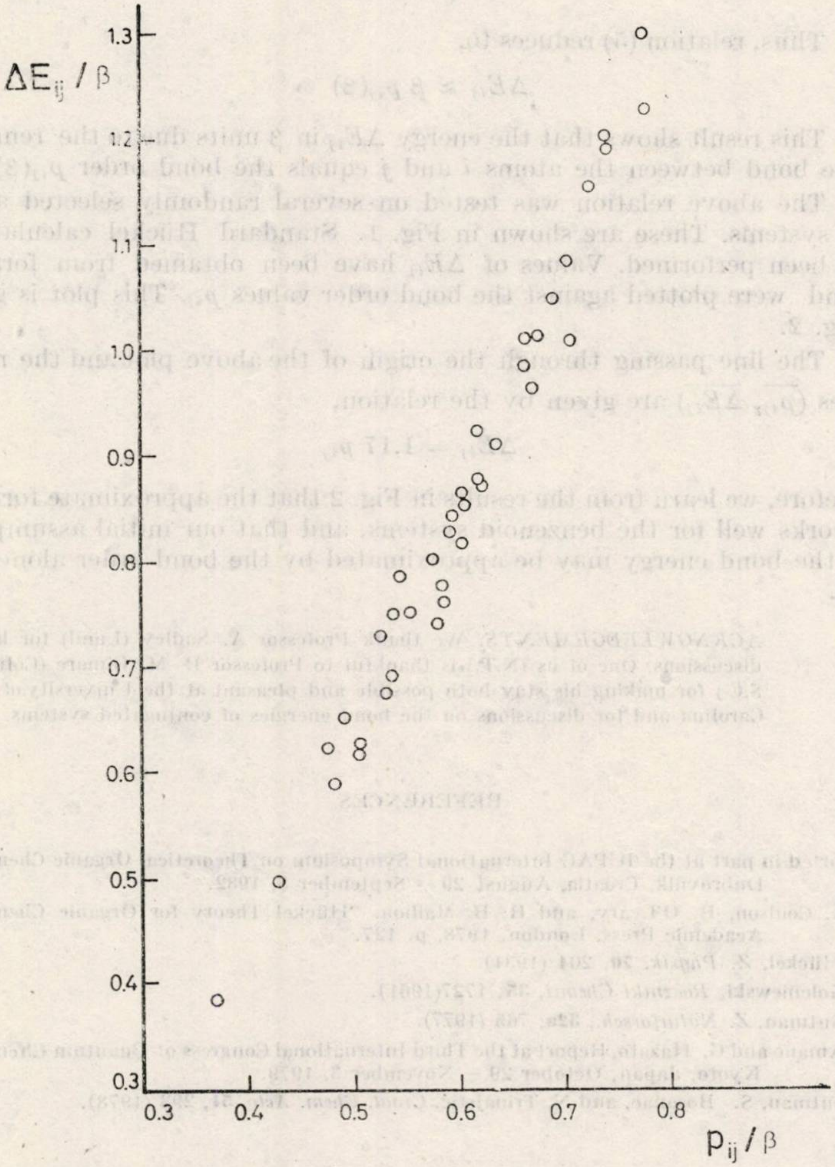

Fig. 2. — Bond energies (in β units) *vs.* bond orders of a randomly selected set of conjugated molecules whose graphs are given in Fig. 1.

The energy $E_\pi(\beta_{ij})$ may be considered as a function of the parameter $\beta_{ij'}$, and using (4) one obtains,

$$E_\pi(\beta_{ij}=\beta) \approx E_\pi(\beta_{ij}=0) + \int_0^\beta \frac{\partial E_\pi}{\partial \beta_{ij}} \mathrm{d}\beta_{ij} \approx E_\pi(\beta_{ij}=0) + \beta p_{ij}(\beta) \quad (6)$$

Thus, relation (5) reduces to,

$$\Delta E_{ij} \approx \beta\, p_{ij}(\beta) \quad (7)$$

This result shows that the energy ΔE_{ij} in β units due to the removal of the bond between the atoms i and j equals the bond order $p_{ij}(\beta)$.

The above relation was tested on several randomly selected alternant systems. These are shown in Fig. 1. Standard Hückel calculations have been performed. Values of ΔE_{ij} have been obtained from formula (5) and were plotted against the bond order values p_{ij}. This plot is given in Fig. 2.

The line passing through the origin of the above plot and the mean values $(\overline{p_{ij}}, \overline{\Delta E_{ij}})$ are given by the relation,

$$\Delta E_{ij} = 1.17\, p_{ij} \quad (8)$$

Therefore, we learn from the results in Fig. 2 that the approximate formula (7) works well for the benzenoid systems, and that our initial assumption that the bond energy may be approximated by the bond order alone was valid.

ACKNOWLEDGEMENTS. We thank Professor A. Sadley (Lund) for helpful discussions. One of us (N.T.) is thankful to Professor B. M. Gimarc (Columbia, S.C.) for making his stay both possible and pleasant at the University of South Carolina and for discussions on the bond energies of conjugated systems.

REFERENCES

[1] Reported in part at the IUPAC International Symposium on Theoretical Organic Chemistry, Dubrovnik, Croatia, August 29 – September 3, 1982.

[2] C. A. Coulson, B. O'Leary, and R. B. Mallion, "Hückel Theory for Organic Chemists," Academic Press, London, 1978, p. 127.

[3] E. Hückel, *Z. Physik*, **70**, 204 (1931).

[4] A. Golebiewski, *Roczniki Chemii*, **35**, 1727(1961).

[5] I. Gutman, *Z. Naturforsch.*, **32a**, 765 (1977).

[6] T. Amano and G. Hazato, Report at the Third International Congress of Quantum Chemistry, Kyoto, Japan, October 29 – November 3, 1979.

[7] I. Gutman, S. Bosanac, and N. Trinajstić, *Croat. Chem. Acta*, **51**, 293 (1978).

Revue Roumaine de Chimie, **29**, *9 — 10*, 741—746 (1984)

CHROMIUM HEXAMMINE COMPLEXES WITH BIGUANIDINE DERIVATIVES

CONSTANȚA GHEORGHIU*, CORNELIA GURAN and MARCELA MUNTEAN
Polytechnic Institute Laboratory of Inorganic Chemistry, Bucharest, Romania

Received June 15, 1983

The present paper reports the results obtained in the synthesis and characterization of new chromium (III) complex thiocyanates having the general formula $[Cr(RBig)_3](NCS)_3$, where RBig are the different biguanidine derivative ligands. The compounds were characterized by chemical and physico-chemical methods (electrical molar conductivity determinations, electronic and vibration al spectra and X-ray spectra).

One of the most characteristic features of chromium (III) chemistry is its great ability to form coordination compounds. Some of these compounds are applicable in various fields. The speciality literature has published numerous data on the complex thiocyanates of chromium (III), in view of the highly interesting theoretical and practical aspects of this group of compounds.[1-7] In order to obtain new chromium (III) complex thiocyanates, a study was carried out on the reaction between $K_3[Cr(NCS)_6]$ and various biguanidine derivative ligands (RBig), using water and ethanol as solvents. [8-10]

When water is used as solvent, biguanidine salts $(RBigH)_3$ $[Cr(NCS)_6]$ are obtained, irrespective of the molar ratios considered and the pH of the solution.

In anhydrous ethyl alcohol, pH 7—7.5, the substitution occurs within the coordination sphere, by 1, 2 or 3 molecules of biguanidine derivative ligand which, in this case, is a bidentate ligand.

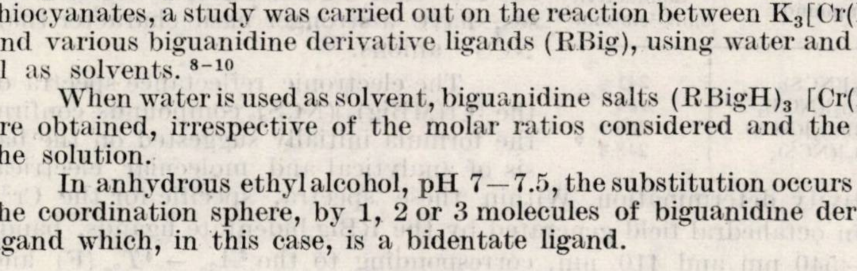
$(RBigH)_3[Cr(NCS)_6]$
t = 70°
pH = 5
water
molar ratio 1 : 1
t=70°
pH=7,5
anh ydrous ethanol
$K_3[Cr(NCS)_6]+RBig$
anhydrous ethano
molar ratio 1 : 3
t = 70°
pH = 7,5
molar ratio 1 : 2
t = 70°
pH = 7.5
anhydrous etha nol
$K[CrRBig(NCS)_4]$
+RBig
$[Cr(RBig)_2(NCS)_2](NCS)$
+RBig
$[Cr(RBig)_3](NCS)_3$

The present paper describes the isolation and characterization of some new compounds of general formula $[Cr(RBig)_3](NCS)_3$, where RBig are the following biguanidine derivatives : N′-chlorophenyl —, N^5-isopropyl-, N′-phenyl-, N′-chlorophenyl-, N′-tolylbiguanidine (abridged in the paper as Pald, PhBig, ClPhBig, TBig).

---

* Deceased March 28, 1983

RESULTS AND DISCUSSION

A new series of compounds of the $[Cr(RBig)_3](NCS)_3$ type was isolated as a result of the reaction between $K_3[Cr(NCS)_6]$ and biguanidine derivatives under the form of bases, in anhydrous ethylic alcohol, pH 7—7.15, for Cr :Big molar ratios of 1 : 3. These compounds are very stable and have a high solubility in ethylic alcohol, acetone and dimethylformamide.

The atomic combination ratios, 1Cr : 3S : 18N were determined by elementary chemical analysis.

Also taking into consideration the determination of the molar electric conductivity, which gives the electrolytic nature of these compounds (electrolytes of type 1 : 3), the following formula was suggested $[Cr(RBig)_3](NCS)_3$ (Table 1).

Table 1

Molecular electrical conductivity data of the obtained compounds in DMF solution, 10^{-3}M

Compound	Conductivity $ohm^{-1}cm^2mol^{-1}$
$[Cr(Pald)_3](NCS)_3$	241
$[Cr(PhBig)_3](NCS)_3$	184
$[Cr(ClPhBig)_3](NCS)_3$	205
$[Cr(TBig)_3](NCS)_3$	248.4

Under the perfect anhydrization conditions of the reaction medium, pH 7—7.5, the six NCS^- groups within the coordination sphere were substituted by three molecules of biguanidine derivative ligands.

The substitution was facilitated by the fact that biguanidines, N-organic bases, have a stronger basic character than NCS^- anions.

The electronic reflectance spectra of the $[Cr(MBig)_3](NCS)_3$ compounds confirm the formula initially suggested on the basis of analytical and molecular electrical conductivity determination. Within these spectra, specific for the Cr^{3+} ion in an octahedral field generated by the RBig bidentate ligands, bands at 530—540 nm and 410 nm, corresponding to the $^4A_{2g} \rightarrow {}^4T_{2g}$ (F) and $^4A_{2g} \rightarrow {}^4T_{1g}$ (F) transitions were evidenced (Table 2, Fig. 1.).

Table 2

Electronic spectra of the obtained compounds $[Cr(RBig)_3](NCS)_3$

Compound	λ(nm), ν(cm^{-1}) $^4A_{2g} \rightarrow {}^4T_{2g}$(F)	λ(nm), ν(cm^{-1}) $^4A_{2g} \rightarrow {}^4T_{1g}$(F)
$[Cr(Pald)_3](NCS)_3$	455(21970)	350(28570)
$[Cr(PhBig)_3](NCS)_3$	453(22070)	345(28980)
$[Cr(ClPhBig)_3](NCS)_3$	452(22120)	345(28980)
$[Cr(TBig)_3](NCS)_3$	452(22120)	350(28570)
$[Cr(NH_3)_6]^{3+}$	465(21500)	350(28570)
$[Cr\ en_3]^{3+}$	460(21740)	350(28570)

A comparison of the data obtained by us for the $[Cr(RBig)_3](NCS)_3$ compounds with the published data for other chromium (III) amine complexes $[Cr(NH_3)\ ]^{3+}$, $[Cr(en)_3]^{3+}$ [11,12] shows that the absorption bands shift towards shorter and shorter wavelengths decreasing with increase of the basicity of the ligand within the coordination sphere. This attests to the higher basicity of the RBig ligands and their listing in the spectrochemical series to the right of etylendiamine.

The vibration spectra in infrared light of the complex thiocyanates were examined with a view to obtaining a complete characterization. On the basis of IR spectra some conclusions can be drawn on the mode of coordination of the NCS^- ligands at the central metal ion (Cr^{+3}). On the other hand, the presence of organic ligands within or outside the coordination sphere can be evidenced. [13-15]

Fig. 1. — Electronic spectra of the compounds :
$[Cr(Pald)_3](NCS)_3$ ····
$[Cr(PhBig)_3](NCS)_3$ —·—·
$[Cr(ClPhBig)_3](NCS)_3$ — — —
$[Cr(TBig)_3](NCS)_3$ ———

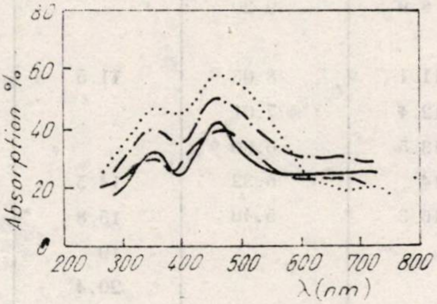

Analysis of the IR spectra of the $[Cr(RBig)_3](NCS)_3$ compounds shows that the bands specific for the ν_{CN}, δ_{NCS} and ν_{CS} modes of vibration are to be found at values characteristic of the presence of the ionic NCS^- groups (2050—2065)cm^{-1}, 470—485 cm^{-1} and 745—750 cm^{-1}) (Fig. 2).[13]

Shift of the specific vibration bands of the RBig ligands is observed following coordination effect, e.g. the vibration bands specific for the CN, NCN, NH_2 groups appear within the 1540 cm^{-1}, 1500 cm^{-1} and 1600, 1630 cm^{-1} respectively.

The X-ray diffraction spectra of some of the complex chromium (III) thiocyanates prepared by us were examined in order to obtain further data regarding their crystalline structure.

Table 3 presents the structural parameters determined experimentally : θ-diffraction angles and interplanar distances d(Å) for compounds $K_3[Cr(NCS)_6]$, $[Cr(TBig)_3](NCS)_3$ and $[Cr(TBig)_2(NCS)_2]$ (NCS). Compound $K_3[Cr(NCS)_6$ is characterized by an accentuated crystalline character, with thick lines within the 2.70 Å, 2.93 Å, 3.14 Å ranges, whereas the compound $[Cr(TBig)_3](NCS)_3$ is slightly crystallized as revealed by the diffractogram aspect with less marked characteristic 2.93 Å, 2.86 Å and 2.79 Å lines.

A comparison of the data obtained shows that the diffractogram of the $[Cr(TBig)_2(NCS)_2](NCS)$ compound, which includes the mixed TBig and NCS ligand contains lines belonging both to the $K_3[Cr(NCS)_6]$ and to the $[Cr(TBig)_3]\ (NCS)_3$ compounds.

Table 3

X-ray data of the compounds: $K_3[Cr(NCS)_6]$, $[Cr(TBig)_2(NCS)_2](NCS)$, $[Cr(TBig)_3](NCS)_3$

$K_3[Cr(NCS)_6]$		$[Cr(TBig)_2(NCS)_2](NCS)$		$[Cr(TBig)_3](NCS)_3$	
2θ°	d(Å)	2θ°	d(Å)	2θ°	d(Å)
6	14.24	6	15.76		
		6.5	14.24	7	13.38
		7.5	11.93		
8.9	9.20			9	9.40
				10.4	8.83
11.1	8.03	11.5	7.89	11	8.18
12.4	7.01			12.2	7.13
13.5	6.60				
14	6.32	14.5	6.14*		
16.3	5.40	15.8	5.74		
		19	4.81	19	4.76
		20.4	4.48***		
		21.2	4.18		
22.8	3.96	22.5	3.96		
24	3.76	24.3	3.70*		
25	3.55				
25.5	3.47	25.4	3.50*		
				26.5	3.37
27	3.29	27.5	3.25	27	3.29
29	3.14*				
29.2	3.05				
30.8	2.93**		2.91	30.5	2.93**
31.4	2.86	31		31.2	2.86*
32.5	2.70***	32.4	2.76	32.7	2.79*
		33.5	2.68		
		34.7	2.50		
36	2.49	36.3	2.48		
39	2.33				
41	2.22	41.2	2.18		
43	2.09			43.5	2.08
44.5	2.03				
47.5	1.90				
48.3	1.87				
49.6	1.85	49.5	1.85		
50.4	1.81				

* — weak band
** — strong band
*** — very strong band

Compound $[Cr(TBig)_2(NCS)_2](NCS)$ presents intermediary crystallization as compared to the other two compounds, evidenced by lines 2.91Å and 2.76 Å; in addition it is characterized by a crystalline structure of its own, presenting the characteristic 4.48 Å and 6.14 Å lines.

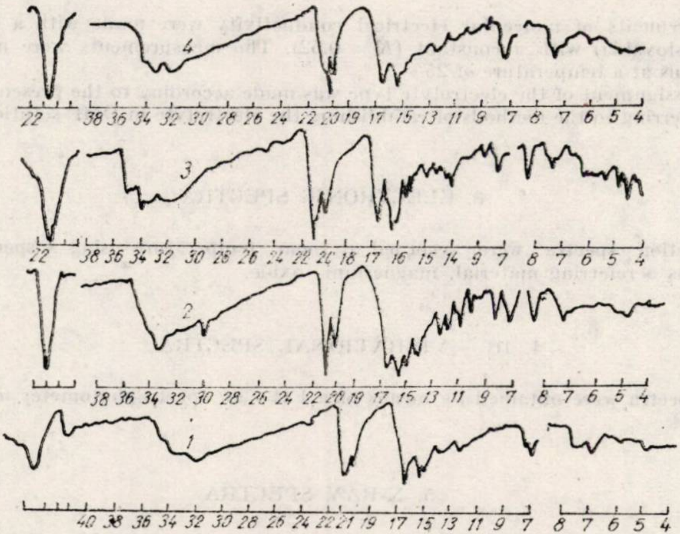

Fig. 2. — Infrared spectra of the compounds:
1. $[Cr(Pald)_3](NCS)_3$
2. $[Cr(PhBig)_3](NCS)_3$
3. $[Cr(ClPhBig)_3](NCS)_3$
4. $[Cr(TBig)_3](NCS)_3$

EXPERIMENTAL

1. SYNTHESIS OF THE COMPLEX COMPOUNDS $[Cr(RBig)_3](NCS)_3$

Anhydrous $K_3[Cr(NCS)_6]$ and the biguanidine derivatives RBig (molar ratio 1 : 3) are solved in anhydrous ethanol at pH = 7.5.

The mixture is refluxed for 2 hrs, then the alcohol is distilled. Red — violet glues are obtained, which are water washed up to KNCS removal. The products are kept in vacuum desiccator until crystallization (2—3 days).

The compounds are soluble in ethanol, acetone, dimenthyl-formamide and insoluble in water.

The chromium and sulphur were determined gravimetrically as Cr_2O_3 and $BaSO_4$ respectively, after having been disintegrated the samples with oxygenated water in an ammoniacal medium. The nitrogen was determined by combustion using the micro-Dumas method.

Calcd. for: $[Cr(Pald)_3](NCS)_3$; $C_{36}H_{48}N_{18}S_3Cl_3Cr$
Found: Cr %5.31; S% 9.38; N%25.74
Cr % 5.22; S% 9.50; N% 25.90

Calcd. for: $[Cr(PhBig)_3](NCS)_3$; $C_{27}H_{33}N_{18}S_3Cr$
Found: Cr % 6.86; S% 12.70; N% 33.29
Cr % 6.80; S% 12.81; N% 33.52.

Calcd. for: $[Cr(ClPhBig)_3(NCS)_3$; $C_{27}H_{30}N_{18}S_3Cl_3Cr$
Found: Cr % 6.03; S % 11.40; N% 29.23
Cr %6.20; S% 11.35; N% 29.38.

Calcd. for: $[Cr(TBig)_3]\ (NCS)_3$; $C_{39}H_{39}N_{18}S_3Cr$
Cr% 6.51 ; S% 12.03 ; N%31.55
Cr% 6.45 ; S %12.11 ; N% 31.60.

2. MOLECULAR CONDUCTIVITIES

Measurements of molecular electrical conductivity were made with a Conductometer (II) (Czechoslovakia) with a constant ($K = 0.52$). The measurements were made in 10^{-3}M DMF solutions at a temperature of 25°

The assignment of the electrolyte type was made according to the present indication in literature referring to the methods of establishing the electrolyte in DMF solutions.[16,17]

3. ELECTRONIC SPECTRA

Reflection spectra were recorded at room temperature using a spectrophotometer VSU_1, and as a referring material, magnesium oxide.

4. IR – VIBRATIONAL SPECTRA

IR spectra were obtained by means of a UR–20 spectrophotometer using potassium bromide disk.

5. X-RAY SPECTRA

X-ray spectra were determined on crystalline powder ⩽ 63 μm, using a TUR-M-62, 40 KV, 18 mA diffractometer, in Cu K-radiation.

REFERENCES

[1] P. Spacu and A. Antonescu, *Studii şi Cercetări Chim., Acad. R.S.R.*, **8**, 73 (1970).

[2] R. Ripan, I. Gănescu and Cs. Varhelyi, *Rev. Roumaine Chim.*, **11**, 473 (1966).

[3] I. Gănescu and Cs. Varhelyi, *Z. anorg. Chem.*, **439**, 282 (1978).

[4] P. S. Glash, J. *Inorg. Nuclear Chem.*, **33**, 4199 (1971).

[5] I. Gănescu, M. Teodorescu and C. Lepădatu, *Z. phys. Chem. (Frankfurt)*, **74**, 11 (1971).

[6] G. C. Lalor and H. Miller, *J. Inorg. Nuclear Chem.* **40**, 305 (1978).

[7] M. Cusumano, *Inorg. Chem.*, **17**, 2222(1978).

[8] C. Gheorghiu and C. Guran, *Analele Univ. Bucureşti*, **1**, 83 (1972).

[9] C. Gheorghiu, C. Guran, A. Meghea and I. Jitaru, *Rev. Roumaine de Chim.* 1984, in press.

[10] C. Guran and L. Băloiu, *Bul. I. P.B.*, 1984 in press.

[11] A.B.P. Lever, "Inorganic Electronic Spectroscopy", Interscience Publishers New York 1968, p. 265.

[12] B. N. Figgis, "Introdction to Ligand Fields", Interscience Publishers, New York 1967, p. 156.

[13] R. A. Bailey, S. L. Kozak and T. W. Michesen, *Coordin. Chem. Rev.*, **6**, 407 (1971).

[14] A. Sabatini and I. Bertini, *Inorg. Chem.* **4**, 959 (1965).

[15] A. H. Norbury and A.J.P. Sinha, *Inorg. Chem.* **6**, 339 (1967).

[16] D. J. Phillips and S. Y. Zyref, *J. Amer. Chem. Soc.* **83**, 1806 (1961).

[17] I. F. Jonug, R. D. Gillord and G. Wielkinson, *J. Chem. Soc. (A)*, **1964**, 2176.

Revue Roumaine de Chimie, 29, 9 – 10, 747–754 (1984)

MOLYBDENUM(V) OXO-THIOCYANO COMPOUNDS WITH BIGUANIDINE DERIVATIVES

CONSTANȚA GHEORGHIU*, CORNELIA GURAN and AURELIA MEGHEA
Polytechnic Institute, Laboratory of Inorganic Chemistry,
Splaiul Independenței 87, Bucharest, Romania

Received June 15, 1983

The present paper deals with a series of new Mo(V) coordination compounds of the form $RBigH_2[MoO(NCS)_5]$, where RBig stands for biguanidine derivatives. They were characterized by elementary chemical analysis, molecular electrical conductivity measurements, electronic and vibrational spectra. Using the ESR data from polycrystalline powders and DMF solutions, assumptions regarding the geometry of the compounds are made.

Molybdenum (V) coordination compounds with the NCS^- ion as a ligand have been studied to a great extent lately, due particularly to their possibilities of being applied to analytical purposes.

It has been experimentally found that in 1–9 M HCl or H_2SO_4 solutions molybdenum precipitates quantitatively in the form $[MoO(NCS)_5] \cdot 2BH$.[1,2]

In less acid solutions (under 1 N) molybdenum is also isolated quantitatively, but the precipitate analysis in this case shows that a mixture is separated to Mo(V) and Mo (VI).

Eremin and others [1-5] synthesized and characterized a series of oxothiocyanate species of Mo(V) and Mo(VI) with several amines : tetramethyl-, tetraethyl-, tetrabutylamine, ε-caprolactame, antipyrene pyridine, acridine, pyramidon, 2,2′-dipyridyl, o-phenanthroline. The isolated compounds retain 2, 3 or 4 base molecules, being of the types $MoO(NCS)_5 \cdot 2R_4N$; $MoO(NCS)_6 \cdot 3R_4N$; $MoO(NCS)_4 \cdot 2Dipy$; $MoO(NCS)_3 \cdot 4$ ε-caprolactame, or $MoO(NCS)_3 \cdot 4$ antipyrene in the case of dipyridyl, caprolactame and antipyrene.

For an optimum separation of Mo(V) coordination compounds in the form of oxospecies, the folowing conditions are necessary :

— the reaction medium should have a concentration of 1–9 N HCl or H_2SO_4;

— the concentration of SCN^- should be higher than, or equal to 1% ;

— the Mo : base ratio should be 1 : 3.

---

* Deceased March 28, 1983

Most of research papers, in the field of Mo oxothiociano complex species chemistry focus on the possibilities of dosing the material in the form of those compounds.[6–13]

This paper presents the results of our research concerning the synthesis and characterization of new Mo(V) compounds having a general formula of the form $RBigH_2[MoO(NCS)_5]$. The ligands that have been used, represented by "RBig", are the following biguanidine derivatives: N^1-chlorophenyl-N^5-isopropyl- N^1-phenyl-, N^1-chlorophenyl-, N^1- tolylbiguanidine, namely:

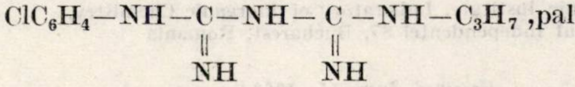

$ClC_6H_4-NH-\underset{\underset{NH}{\|}}{C}-NH-\underset{\underset{NH}{\|}}{C}-NH-C_3H_7$,paludrine, Pald

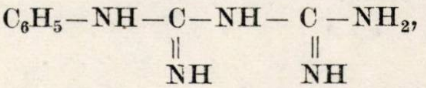

$C_6H_5-NH-\underset{\underset{NH}{\|}}{C}-NH-\underset{\underset{NH}{\|}}{C}-NH_2$, PhBig

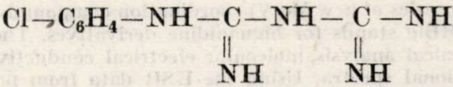

$Cl\to C_6H_4-NH-\underset{\underset{NH}{\|}}{C}-NH-\underset{\underset{NH}{\|}}{C}-NH_2$, ClPhBig

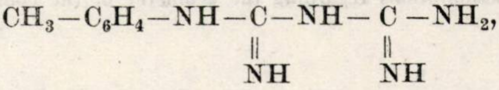

$CH_3-C_6H_4-NH-\underset{\underset{NH}{\|}}{C}-NH-\underset{\underset{NH}{\|}}{C}-NH_2$, TBig

RESULTS AND DISCUSSION

As will be shown in the experimental part, a series of dark red-violet compounds are separated by treating with biguanidine derivates a solution obtained through the action of KSCN on MoO_3 in an acid medium. The thiocyanic acid, obtained as a result of the reaction between KSCN and HCl, behaves as a reducer for the molybdenic acid.

On the basis of the elementary chemical analysis and determinations of the molar electric conductivity (Table 1) the combining atomic ratios have been established as 1Mo : 4.955 S : 10 N, as well as their electrolytic nature. Cerimetrical determinations have confirmed the +5 state of oxidation of molybdenum in those compounds. On the basis of this data we have suggested the formulation $RBigH_2[MoO(NCS)_5]$.

Table 1

Molar electrical conductivity of the compounds $RBigH_2[MoO(NCS)_5]$, in DMF solution, $10^{-3}M$

Compound	Molar conductivity $cm^2\Omega^{-1}\ mol^{-1}$, 25°C
$PaldH_2[MoO(NCS)_5]$	180
$PhBigH_2[MoO(NCS)_5]$	170
$ClPhBigH_2[MoO(NCS)_5]$	175
$TBigH_2[MoO(NCS)_5]$	181

We mention that the reaction efficiency is rather small, owing to the fact that the experiment was made with a ratio Mo : base lower than 2.5 — the optimum value for quantitative separation of Molybdenum.

The spectrophotometric measurements carried out on the dark red-violet powder samples confirm the formulation of these compounds as monomers, namely $\mathrm{RBigH_2[MoO(NCS)_5]}$. The first transition of crystalline field $2B_2 \rightarrow 2E(\mathrm{I})$ occurs with frequencies of about 14 000 cm^{-1}, the electron being promoted from the d_{xy} orbital to d_{xz} or d_{yz}; the second transition of spin permitted, $2B_2 \rightarrow 2B_1$, occurs with frequencies of about 20.000 cm^{-1} and is due to the jump made by the electron between orbitals d_{xy} and $d_{x^2-y^2}$ The third transition of crystalline field is covered, as a rule, by a transition with transfer of charge which is considerably more powerful, and occurs with frequencies of ~24 000 cm^{-1} (Table 2, Fig. 1).

Table 2

Electronic spectra of the compounds $\mathrm{RBigH_2[MoO(NCS)_5]}$

Compound	${}_2B_2 \rightarrow {}^2E(\mathrm{I})$ ν(cm^{1-})	${}^2B_2 \rightarrow {}^2B_1$ ν(cm^{-1})
$\mathrm{PaldH_2[MoO(NCS)_5]}$	13800	20000
$\mathrm{PhBigH_2[MoO(NCS)_5]}$	14200	20800
$\mathrm{ClPhBigH_2[MoO(NCS)_5]}$	14600	21100
$\mathrm{TBigH_2[MoO(NCS)_5]}$	13700	21200
$\mathrm{H_2[MoOBr_5]}$	14390	21320
$\mathrm{H_2[MoOCl_5]}$	15150	22600

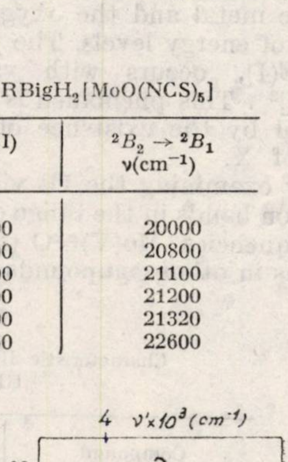

Fig. 1. — Electronic spectra of the compounds :
··· Pald $\mathrm{H_2}$ $\mathrm{[MoO(NCS)_5)}$
---- $\mathrm{PhBigH_2[MoO(NCS)_5]}$
—·—· $\mathrm{ClPhBigH_2[MoO(NCS)_5]}$
—$\mathrm{TBigH_2[MoO(NCS)_5]}$

For comparison, the table also presents the bands of the free acids $H_2[MoOCl_5]$ and $H_2[MoOBr_5]$.[14] It can be seen that by substituting NCS^- for the anionic ligands Br^- or Cl^- within the coordination sphere, the absorption bands shift towards lower and lower wave lengths. This fact is in accordance with the position of the NCS^- anionic ligand in the spectrochemical series ($Br^- < Cl^- < NCS^-$), in which NCS^- is situated to the right of anions Br^- and Cl^-.

In each of the cases under discussion, the spectrum is characteristic of the interaction of the ligand-fields within the orbitals of the central metallic ion.

The ion $[MoO(NCS)_5]^{2-}$ has the structure of an undeformed octahedron, due probably to the close positions occupied in the spectrochemical series by the donor atoms O and N.

According to the theory of Balhausen and Gray [14] the π-bond between the metal and the oxygen exerts a considerable influence on the position of energy levels. The position of the band due to the transition ${}^2B_2 \to {}^2E(\mathrm{I})$, occurs with values of $\sim$ 14 000 cm^{-1} for all the ions $[MoOX_5]^{2-}$. This phenomenon is to be expected, as the split of level ${}^2T_{2g}$ is generated by the existence of the π bond Mo—O, irrespective of the nature of X.

By examining the IR vibration spectra one notices the presence of absorption bands in the range of 950—980 cm^{-1} characteristic of the vibration frequencies Mo(V)=O (occurring in all the oxohalomolybdates (V) as well as in other compounds of Mo(V)) [15–17] (Table 3).

Table 3

Characteristic IR frequencies of the compounds $RBigH_2[MoO(NCS)_5]$

Compound	$\nu_{Mo(V)=O}$ (cm^{-1})	ν_{CN} (cm^{-1})	δ_{NCS} (cm^{-1})	ν_{CS} (cm^{-1})
$PaldH_2[MoO(NCS)_5]$	965	2060	485	825
$PhBigH_2[MoO(NCS)_5]$	970	2060	485	812
$ClPhBigH_2[MoO(NCS)_5]$	960	2060	475	820
$TBigH_2[MoO(NCS)_5]$	950	2065	490	820

Also, one notices the presence of vibrations characteristic of biguanidine, such as vibrations of groups CN, NCN and NH_2 respectively, in the ranges of 1540 cm^{-1}, 1500 cm^{-1} and 1100 cm^{-1}, 1830 cm^{-1} respectively.

The bands of 485 cm^{-1}, 800 — 835 cm^{-1}, 2100 — 2080 cm^{-1}, have been attributed to the deforming vibrations δ_{NCS} and the lengthening vibrations ν_{CS} and ν_{CN} according to.[18] The ν_{CN} band has a wide range and for all compounds it occurs with values around 2060 cm^{-1}.

Taking also into consideration the position of bands ν_{CN} and δ_{NCS}, we can say that between Mo(V) and NCS^- ligands, nitrogen links are established.

The monomer combinations of the type $RBigH_2[MoO(NCS)_5]$ are characterized by a particularly intense paramagnetism, evinced by the spectra of spin electronic resonance.[19]

The compounds $RBigH_2[MoO(NCS)_5]$ in polycrystalline powders manifest isotropic signals of singlet with a factor $g = 1.94$ characteristic of the coordination of Mo^{5+} with O—or N-donor ligands.
Since in the Mo(V) combinations in which sulphur is the donor atom, g is 1.97, it follows that in the case of our compounds NCS^- coordinates through nitrogen, as shown also in the analysis of IR vibration spectra (Table 4).

Table 4

ESR data of the compounds $RBigH_2[MoO(NCS)_5]$

Compound	Monomers-powders		Monomers in DMF	
	g	a_{iz} (Gauss)	g	a_h
$PaldH_2[MoO(NCS)_5]$	1.940	24.7	1.941	—
$PhBigH_2[MoO(NCS)_5]$	1.942	35.6	1.939	49.3
$ClPhBigH_2[MoO(NCS)_5]$	1.944	36.9	1.938	51.2
$TBigH_2[MoO(NCS)_5]$	1.944	48.2	1.936	49.1

The ESR parametres for oxothiocyanospecies do not evince the existence of a tetragonal distorsion as is the case of bromine oxospecies. This is probably due to the neighbouring positions of oxygen and nitrogen as donors in the spectrochemical series.

In the case of bromineoxospecies,[20] the biguanidonium ions do not exert a very strong influence on the ESR spectral parametres. On the other hand, for oxothiocyanospecies, while the g-factor has a very small variation (1.940 — 1.944) being characteristic of the internal coordination sphere, the breadth of the (a_{iz}) line is practically doubled.

Thus, the influence is made evident of the ligand in the external coordination sphere on the electronic density of the complex oxoanion $[MoO(NCS)_5]^{2-}$. It may be seen that, owing to a higher degree of symmetry of anion $[MoO(NCS)_5]^{2-}$ versus $[MoOBr_5]^{2-}$ (to which a tetrahedral structure has been assigned, with a tetragonal distortion), ligands $RBigH_2^{2+}$ exert a stronger influence on the distribution of electronic density in the complex oxoanion. As the coordination capacity of the organic ligand is strengthened in the series Pald $<$ PhBig $<$ ClPhBig $<$ TBig, by increasing its donor power, the interactions of the central ion in the internal coordination sphere are altered, the covalent nature of the metal-ligand bond decreases, which leads to widening the ESR line.

In a solution of dimethylformamide, intense isotropic signals can be obtained, in which the main line is accompanied by six components of hyperfine structure due to the interaction with the magnetic nuclei of isotopes ^{95}Mo and ^{97}Mo ($I = 5/2$). In this case, both the g-factors and the hyperfine splitting constants have close values, for the four combinations, $RBigH_2[MoO(NCS)_5]$, as, due to their electrolytic nature, the influence of the protonated ligand is considerably diminished.

By comparing the ESR parameters of these oxo-isothiocyanomolybdates with the ones of the corresponding oxo-bromine-molybdates previously described, as well as with other data in the literature (shown in Table 5), one notices a dependence similar to the ligand sequence in the spectrochemical series : F^-, NCS^-, Cl^-, Br^-, through an increase of the *g*-factor and a decrease of the hyperfine splitting constant.[21-22] The graphic representation of the two parametres dependence (Fig. 2) shows an increase in the covalence degree of the metal-ligand bond, from F^- towards Br^-, rendered by narrowing the hyperfine splitting.

Table 5

ESR data of $[MoOX_5]^{2-}$ species

Species	g	a_h (Gauss)	Literature
$[MoOF_5]^{2-}$	1.906	70	22
$[MoO(NCS)_5]^{2-}$	1.938	50	*
$[MoOCl_5]^{2-}$	1.948	47	22
$[MoOBr_5]^{2-}$	1.993	42	20

* This paper

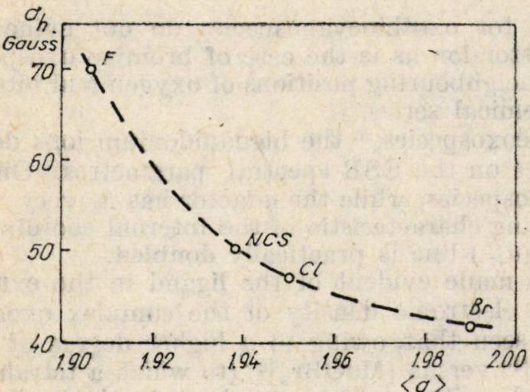

Fig. 2. — The dependence of parameters $a_h - g$.

In a future paper we shall present data concerning the tendency of polymerization of the Mo(V) oxospecies, under the influence of several solvents.

EXPERIMENTAL

I. SYNTHESIS OF THE COMPLEX COMPOUNDS $RBigH_2[MoO(NCS)_5]$

5 g MoO_3 are solved in a solution obtained by solving 4 g KOH in 10 ml water ; 25 ml concentrated HCl are added slowly. The final solution is heated over a hot water bath.

A concentrated solution of potassium thiocyanate is prepared by solving 15 g KSCN in 15 ml water which are added to the hot solution molybdenic acid.

The dark red solution is diluted with 30 ml water and is heated over a hot water bath for 2 hours, stirring continuously. The ligands are then added, in the form of chlorhydrates, solved in water, in a molar ratio Mo : RBig.HCl = 1 : 1.

The compounds are thus separated as dark red-violet glues which crystallize if kept on ice.

They are then water -washed, and dried up in desiccator over P_4O_{10}.

The compounds are soluble in ethanol, acetone, dimethylformamide and insoluble in water.

The molybdenum and sulphur were determined gravimetrically with 8-hydroxypuinoline and barium chloride respectively, after having disintegrated the samples with oxygenate water in an ammoniacal medium.

The (V) — state of oxidation of molybdenum was checked by cerimetrical titration. The nitrogen was determined by combustion, using the micro-Dumas method.

Pald $H_2[MoO(NCS)_5]$ calcd : Mo%,	13.61 ;	S%, 24.31 ;	N%, 21.29 ;
$(C_{11}N_5H_{18}Cl[MoO(NCS)_5])$found :	13.75 ;	24.15 ;	31.29 ;
PhBig$H_2[MoO(NCS)_5]$ calcd : Mo%,	15.40 ;	S%, 27.57 ;	N% 24.10 ;
$(C_8N_5H_{13}[MoO(NCS)_5])$ found :	15.45 ;	27.32 ;	24.14.
ClPhBig$H_2[MoO(NCS)_5$calcd : Mo%,	14.52 ;	S%, 25.99 ;	N%, 22.70
$(C_8N_5H_{12}Cl[MoO(NCS)_5]$ found :	14.58 ;	25.90 ;	22.78.
TBig$H_2[MoO(NCS)_5]$ calcd : Mo%,	15.02 ;	S%, 26.89 ;	N%, 23.49 ;
$(C_9N_5H_{15}[MoO(NCS)_5])$	15.10	26.85 ;	23.59

II. MOLECULAR CONDUCTIVITIES

Measurements of molecular conductivity were made with a conductometer (II) (Czechoslovakia) with a constant ($K = 0.52$). The measurements were made in 10^{-3}M dimetylformamide solutions at a temperature of 25°.

III. ELECTRONIC SPECTRA

Reflection spectra where recorded at room temperature with a VSU_2 spectrophotometer, in the 360—1000 nm range, in MgO pellets.

IV. VIBRATIONAL SPECTRA

IR spectra were registered with a UR 20 spectrophotometer, in the 400—4000 mm range, in potassium bromide pellets.

V. ESR SPECTRA

ESR spectra were registered in a solution of dimethylformamide, in the form of polycrystalline powders, by using a spectrophotometer of the type ART 5 — IFIN Bucharest, in the X (9060 MHZ) frequency range with a magnetic field modulation of 100 KHz.

REFERENCES

[1] Iu. G. Eremin and E. F. Kolokova, *Zhur. analit. Khim.*, **27**, 1293 (1972).
[2] Iu. G. Eremin and E. F. Kolikova, *Zhur. analit. Khim.*, **27**, 1297 (1972).
[3] Iu. G. Eremin and E. F. Kolikova, *Zhur. neorg. Khim.*, **20**, 1587 (1975).
[4] Iu. G. Eremin and E. F. Kolikova, *Zhur. neorg. Khim.*, **20**, 3287 (1975).

[5] Iu. G. Eremin and E. F. Kolikova, *Zhur. neorg. Khim.*, **16**, 2426 (1971).
[6] Pandu Ranga Rao, *Mikrokim Acta,* **1**,81 (1968).
[7] L. P. Greenland, *Analyt. Chim. Acta,* **69**, 335(1974).
[8] C. J. Horn and T. M. Brown, *Inorg. Chem.*, **11**, 1970 (1972).
[9] I. N. Marov, *Doklady Akad. Nauk. S.S.S.R.*, **181**, 111 (1968).
[10] Iu. G. Eremin, *Zhur. anal. Khim.*, **31**, 732 (1976).
[11] K. Nytko, *Mikrochem* J.,**25**, 548 (1980).
[12] N. Monidipa, *Talanta* **24**, 698 (1977).
[13] P. K. Agasyan and E. R. Nikolaeva, *Zhur. analit. Khim.*, **33**, 730 (1978).
[14] H. B. Gray and C. Hare, *Inorg. Chem.*, **1**, 363 (1962).
[15] M. C. Chakravarti, *J. Inorg. Nuclear Chem.*, **35**, 3644 (1973).
[16] M. C. Chakravarti, *Indian J. Chem.*, **11**, 601 (1973).
[17] H. K. Saha, *J. Indian Chem. Soc.*, **53**, 30 (1976).
[18] K. Nakamoto, "Infrared Spectra of Inorganic Coordination Compounds", Willey New-York, 1970, p. 187.
[19] C. Gheorghiu, A. Meghea and C. Guran, *Rev. Chim. (București)*, **33**, 743 (1982).
[20] D. I. Phillips and S. V. Tyrec, *J. Amer. Chem. Soc.*, **83**, 1806 (1961).
[21] C. Gheorghiu, C. Guran and A. Meghea, "The First National Congress of Chemistry Bucharest", 1981.
[22] B. A. Goodman and R. D. Johnston, *Adv. Inorg. Chem. Radio Chem.* **13**, 252 (1970).

Revue Roumaine de Chimie, **29**, *9 – 10*, 755–759 (1984)

THE SYNTHESIS OF 3β-ACETOXY-B-NOR-ANDROST-5-EN-3β-OL-17-ONE AND 3β-ACETOXY-B-NOR-PREGN-5-EN-3β-OL-20-ONE

ROBERT SCHWARTZ*, ANIKÓ JUHÁSZ and PETRONELA COLȚEA
Chemical and Pharmaceutical Research Institute, Str. Fabricii No.126,
3400 Cluj-Napoca, Romania

Received November 10, 1983

A new synthetic method emerging from diosgenin via B-nor-diosgenin was elaborated in order to obtain biologically active steroid hormones with a five-membered B ring.

In two previous papers[1,2] we reported the synthesis of 3β-acetoxy-B-nor-cholest-5-ene and of some of its derivatives. In order to extend the study of B-nor-steroids the synthesis of other non-cholesterol derivatives was necessary. For this purpose two methods are available:

1) Where the structure of the compounds permits, the degradation of the "normal" derivative was performed[3-6] (e.g. 3β-acetoxy-androst-5-en-3β-ol-17-one,[7-10] 3β-acetoxy-pregn-5-en-3β-ol-20-one,[7,11,12] cortisone[13,14] etc. to the corresponding B-nor-derivatives). B-nor-Pregnane derivatives were synthetized from 3β-acetoxy-B-nor-androst-5-en-3β-ol-17-one too,[11] building the 17β-side chain. The method gave poor yields.

2) The synthesis of a key intermediate from an easy available raw material thus obtaining the desired product. This posibility was not yet reported in the literature.

The most important starting material for the synthesis of the biologically active steroids belonging to the "normal" series is the diosgenin obtained from the plant Dioscorea. We chose this material for our purposes.

Starting from diosgenin **1**, contracting the B ring according to the known methods,[1,7,10] the B-nor-diosgenin **8** was obtained. The 3β-hydroxyl group of diosgenin was protected as acetate **2** and an epoxide was formed at the C_5-C_6 double bond **3**. The subsequent oxidation with chromium trioxide yielded the 5α-hydroxy-6-ketone **4**. The Baeyer-Villiger oxidation of the hydroxy-ketone with peracetic acid gave the keto-acid **5**. Treating **5** with benzoyl chloride in pyridine the 5,6-lactone **6** was obtained. The pyrolysis of **6** was performed at about 180°C yielding 3β-acetoxy-B-nor-diosgenin **7**. The decarboxylation was feasible also refluxing the lactone in a solvent with higher boiling point (e.g. toluene, xylene etc.). Acetate **7** was hydrolyzed in alkaline solution giving 3β-hydroxy-derivate **8**.

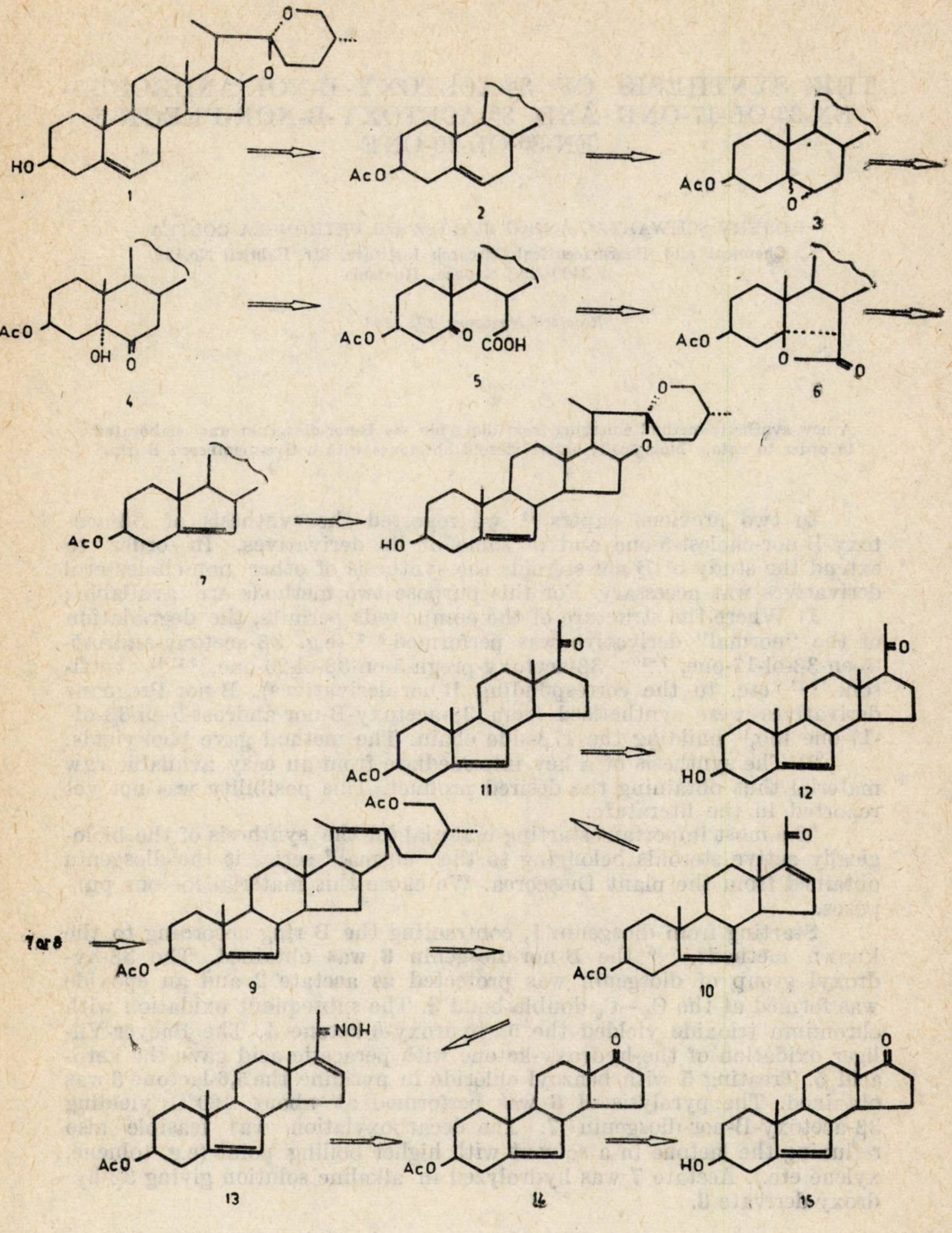
HO
1
AcO
2
AcO
O
3
AcO
OH
O
4
AcO
O
COOH
5
AcO
O
O
6
AcO
7
HO
O
O
8
AcO
O
11
HO
O
12
AcO
AcO
9
7 or 8
AcO
O
10
NOH
AcO
13
O
AcO
14
O
HO
15

3β-Acetoxy- **7** or 3β-hydroxy-B-nor-diosgenin **8** refluxed gently in acetic anhydride in the presence of pyridine and acetyl chloride (obtained from acetic anhydride and hydrogen chloride) was transformed in 3β-acetoxy-B-nor-pseudodiosgenin **9**. This was oxidized with chromium trioxide (without isolation of the product) and then hydrolyzed selectively to give 3β-acetoxy-B-nor-pregn-5,16-diene-3β-ol-20-one **10**, which proved to be an excellent key intermediate for our purposes. This intermediate permits :

— the production of B-nor-pregn-5-ene derivatives **11**, **12** after selective hydrogenation of $C_{16}-C_{17}$ double bond in the presence of Raney-Ni as catalyst;

— it is possible to obtain the B-nor-dehydroepiandrosterone acetate **14** through B-nor-pregnenolone acetate oxime **13** and its Beckmann rearrangement, the B-nor-dehydroepiandrosterone acetate being the most important starting material for androgens and some estrogens.

EXPERIMENTAL

Melting points are uncorected. The IR (KBr) spectra were recorded with a SPECORD 75 IR and the UV (methanol) spectra with a SPECORD UV VIS Carl Zeiss Jena spectrophotometer. The completion of the reactions and the purity of the prepared compounds were checked by TLC.

A) RING CONTRACTION

3β-Acetoxy-5,6-oxido-diosgenin **3**

To a suspension containing 100 g (0.219 mol) of diosgenin acetate, 24 g (0.292 mol) of sodium acetate and 600 ml of chloroform 375 ml of peracetic acid (14.5%) were added dropwise at −10 — −5°C. The mixture was stirred 90 min. at −10°C and worked-up, washed with sodium hydrogen carbonate solution then with water. The evaporation of the dried chloroformic solution gave the crude mixture of 5α, 6α — and 5β, 6β-oxides **3**.Recrystallization from methanol afforded 98.9 g of **3**, m.p. 231—232°C, $[\alpha]_{\Delta}^{20}: -121°$ ($CHCl_3$). yield 95%, ν_{max} 2950, 2925, 2862, 1712, 1437, 1362, 1237, 1092, 1062, 1025, 962 cm^{-1}.

3β, 5α-Dihydroxy-6-keto diosgenin-3β-acetate **4**

To a solution of 98.9 g (0.209 mol) of **3** in 760 ml of acetone 57 g (0.570 mol) of chromic anhydride dissolved in 76 ml of water were added in such a way that the mixture was maintained under a slow reflux. The reaction was completed in 30 min. The mixture was poured into 4.2 l of cold water. The solid product was filtered, washed with water and recrystallized from methanol to give 88.9 g (yield 87%) of **4**, m.p. 280—283°C, $[\alpha]_{\Delta}^{20}: -125°$ ($CHCl_3$), anal. calc. for $C_{29}H_{44}O_6$, C : 71.28%, H : 9.07%, found C : 71.46%, H : 9.25%, ν_{max} : 3492, 3485, 2937, 2925, 2862, 1725, 1700, 1437, 1362, 1350, 1262, 1225, 1150, 1135, 1050, 1025 cm^{-1}.

3β-Acetoxy-5-keto-5,6-seco-diosgenin-6-oic acid **5**

To a solution of 88.9 g (0.181 mol) of **4** in 177.4 ml of chloroform, 72.3 ml of peracetic acid (14.5%) were added under stirring and cooling in a water-bath. The mixture was left 48 hours at room temperature. After working-up (washing with water and evaporating the dried chloroformic solution) a colourless oil was obtained which crystallized from n-hexane afforded 74.8 g (81%) of **5**, m.p. 170—172°C, $[\alpha]_{\Delta}^{20}: -7.2°$ ($CHCl_3$), anal. calc. for $C_{29}H_{44}O_7$, C : 69.01%, H : 8.78%, found C : 69,16%, H : 9.04%, ν_{max} : 3325, 2941, 2930, 2890, 1737, 1700, 1450, 1425, 1392, 1175, 1137 cm^{-1}.

3β-Acetoxy-5α-hydroxy-B-nor-diosgenin-6β-carboxylic acid lactone **6**

74.8 g (0.148 mol) of acid **5** were dissolved in 281.5 ml of pyridine. To this solution 81.2ml (0.698 mol) of benzoyl chloride were added and the mixture was allowed to stand at room temperature for 20 hours. The mixture was poured into 4.5 l of water, and an oily substance separated, which crystallized in standing and was filtrated. The solid product was recrystallized from diethyl ether to give 46.8 g (yield 64%) of lactone **6**, m.p. 170–172°C, $[\alpha]_{\Delta}^{20}$: −20.1° ($CHCl_3$), anal. calc. for $C_{29}H_{42}O_6$, C : 71.57%, H : 8.70%, found C : 71.58%, H : 8.62%, ν_{max} : 2950, 2937, 2881, 1800, 1735, 1456, 1375, 1242, 1187, 1151, 986, 900 cm^{-1}.

3β-Acetoxy-B-nor-diosgenin **7**

Lactone **6** (46.8 g, 0.096 mol) was pyrolyzed at 180°C for 30 min. The crude product recrystallized from chloroform-methanol gave 32.6 g (yield 76%) of **7**, m.p. 180–181°C, $[\alpha]_{\Delta}^{20}$: −173° ($CHCl_3$), anal. calc. for $C_{28}H_{42}O_4$,C : 75.97%, H : 9.56%, found C : 75.75%, H : 9.82%, ν_{max} : 3050, 2956, 2910, 2875, 2858, 1731, 1643, 1452, 1440, 1390, 1362, 1350, 1250, 1090, 1068, 1036, 981, 900 cm^{-1}.

Acetate **7** was hydrolyzed in 5% methanolic potassium hydroxide solution affording 19.7 g (yield 67%) of **8**, m.p. 170–171°C, $[\alpha]_{\Delta}^{20}$: −187° ($CHCl_3$), anal. calc. for $C_{26}H_{40}O_3$,C : 77.95%, H : 10.06%, found C : 78.07%, H : 10.33%, ν_{max} : 3400, 3037, 2952, 2927, 2862, 1636, 1453, 1385, 1361, 1247, 1175, 1151, 1110, 1062, 987, 900 cm^{-1} :

B) *Degradation of 3β-acetoxy-B-nor-diosgenin* **7**

Pseudomerization

To a solution obtained from 32.6 g (0.073 mol) of **7** and 115.4 ml of acetic anhydride, 4.7 ml of pyridine and 7.5 ml of acetic anhydride containing 1.5 g of hydrogen chloride were added. The mixture was gently refluxed for 8–8.5 hours and oxidized without isolation of the 3β-acetoxy-B-nor-pseudodiosgenin **9**. Analytical data of **9**, which was isolated only for characterization, are m.p. 90–91°C, $[\alpha]_{\Delta}^{20}$: −80° ($CHCl_3$), anal. calc. for $C_{30}H_{44}O_5$, C :7.34%, H : 9.15%, found C :74.85%, H :9.68%, ν_{max} : 3036, 2950, 2937, 2900, 2850, 1731, 1681, 1437, 1362, 1236, 1041 cm^{-1}.

Oxidation

To the reaction mixture, 39.1 ml of water and 15.3 g (0.153 mol) of chromic anhydride dissolved in 20.2 ml of water were added under continuous stirring and cooling. The oxidation temperature was 30–32°C. The mixture was stirred one hour at this temperature. The excess of chromic anhydride was decomposed with 16.3 ml of methanol.

Hydrolysis

The above mixture was treated with 7.1 ml of water, 11.7 ml of acetic acid and 7.8 g of sodium hydroxide and refluxed for 2 hours. The crude product was precipitated with 978 ml of water, filtered, washed, dried and recrystallized from methanol to give 14.1 g (yield 55%) of **10**, m.p. 162.5–164°C, $[\alpha]_{\Delta}^{20}$: −61.6° ($CHCl_3$), λ_{max} : 208 (6883.4), 242 (7842.3), 322 (44.5) nm, anal. calc. for $C_{22}H_{30}O_3$, C : 77.15%, H : 8.83%- found C : 77.02%, H : 9.09%, ν_{max} : 3025, 2956, 2931, 2912, 2850, 2825, 1715, 1650, 1573, 1443, 1362, 1343, 1310, 1238, 1212, 1181, 1150, 1100, 1012 cm^{-1}.

20-Oximino-3β-acetoxy-16-dehydro-B-nor-pergnenolone **13**

14.1 g (0.041 mol) of **10** were suspended in 79 ml of anhydrous ethanol. To this suspension 16.3 ml (0.202 mol) of pyridine and 4.8 g (0.068 mol) of hydroxylamine hydrochloride were added. The mixture was refluxed for one hour and cooled afterwards in a refrigerating bath of salt and ice for 5—6 hours. The precipitate was filtered, washed with water and recrystallized from chloroform — methanol to give 12 g (yield 81%) of **13**, m.p. 202—205°C, $[\alpha]_{\Delta}^{20}$: —56.8° ($CHCl_3$), λ_{max} : 208 (9008.24), 238 (13798.34) nm, anal. calc. for $C_{22}H_{31}O_3N$, C : 73.91%, H : 8.74%, N : 3.91%, found C : 73.84%, H : 8.92%, N : 3.89%, ν_{max} : 3518, 3406, 3027, 2962, 2942, 2860, 1700, 1600, 1575, 1448, 1423, 1375, 1362, 1325, 1306, 1268, 1115, 1075, 1025, 990 cm^{-1}.

3β-Acetoxy-B-nor-androst-5-en-17-one **14**

12 g (0.033 mol) of **13** were dissolved in 76.8 ml anhydrous benzene. The solution was cooled at 0— +2°C and 4.5 ml (0.055 mol) anhydrous pyridine were added. To the reaction mixture 6 ml (0.065 mol) phosphorus oxychloride were added dropwise during 30—35 min. under stirring and at +2 — +5°C. The stirring was continued for other 3 hours. 48 ml of aqueous hydrochloric acid solution 1 :1 were dropped in under stirring and cooling. After stirring one hour the mixture was allowed to stand at room temperature in order to separate the two layers that were formed. The organic layer was separated, washed to neutrality with water, concentrated to a small volume and steam distillated to give the crude product. After recrystallization from acetone, 9.9 g (yield 94%) of **14** were obtained, m.p. 135—136°C, $[\alpha]_{\Delta}^{20}$: —51° ($CHCl_3$), anal. calc. for $C_{20}H_{28}O_3$, C : 75.91%, H : 8.91%, found C : 75.70%, H : 9.48%, ν_{max} : 3025, 2937, 2900, 2856, 2837, 1737, 1725, 1613, 1437, 1412, 1373, 1347, 1237, 1037 cm^{-1}.

Acetate **14** was hydrolyzed in a solution of 5% methanolic potassium hydroxide to give 3β-hydroxy derivative **15**, m.p. 142—145°C, $[\alpha]_{\Delta}^{20}$: —60.2° ($CHCl_3$), anal. calc. for $C_{18}H_{26}O_2$, C : 78.78%, H : 9.55%, found C : 79.11%, H : 9·81%, ν_{max} : 3437, 3027, 2962, 2926, 2851, 1727, 1687, 1628, 1450, 1435, 1361, 1352, 1238, 1081 cm^{-1}.

C) HYDROGENATION

3β-*Acetoxy-B-nor-pregnenolone* **11**

14 g (0.040 mol) of **10** were hydrogenated in 840 ml of methanol using 5.8 g of Raney-Ni as catalyst under stirring and at 45—50°C. The hydrogenolysis of the $C_{16}—C_{17}$ double bond was completed in one hour. After filtration of the catalyst the methanolic solution was concentrated under reduced pressure. The crude product was recrystallized from methanol to give 13.3 g (yield 95%) of **11**, m.p. 120—121°C, $[\alpha]_{\Delta}^{20}$: —22.2° ($CHCl_3$), anal. calc. for $C_{22}H_{32}O_3$, C : 76.70%, H : 9.36%, found C : 77.06%, H : 9.62%, ν_{max} : 3037, 2937, 2925, 2912, 2875, 2847, 1715, 1687, 1447, 1425, 1375, 1338, 1231, 1023 cm^{-1}.

Acetate **11** was hydrolyzed in alkaline solution giving 3β-hydroxy-derivative **12**[12].

REFERENCES

[1] R. Schwartz and A. Juhász, *Revista de Chimie* (Bucureşti), **32** (7), 685 (1981).

[2] R. Schwartz, A. Juhász, S. Selinger and L. Moraru, *Rev. Roumaine de Chim.*, **28**, 5, 499 (1983).

[3] W. G. Dauben and G. J. Fonken, *J. Amer. Chem. Soc.*, **78**, 4736 (1956).

[4] K. Tanabe and Y. Morisawa, *Chem. Pharm. Bull.*, **11**, 536 (1963).

[5] H. Lettre and A. John., *Ann. Chem.*, **608**, 43 (1957).

[6] L. Knof, *Ann. Chem.*, **657**, 171 (1962).

[7] J. F. Kerwin (to Smith Klein and French Laboratories) *U.S.Patent* 3.334.140 (august 2, 1967); cf. *Chem. Abstr.*, **67**, 100332 m (1967).

[8] F. Sorm, *Allgemeine und praktische Chemie*, **19**(9), 303 (1968).

[9] J. Joska and F. Sorm, *Coll. Czech. Chem. Comm.*, **23**, 1377 (1958).

[10] J. Fried and J. A. Edwards, "Organic Reactions in Steroid Chemistry", Vol 2, van Nostrand Reinhold Company, New-York, 1972, p. 429.

[11] J. Joska, A. A. Achrem, J. Fajkos and F. Sorm, *Coll. Czech. Chem. Comm.*, **26**, 2050 (1961).

[12] R. Schwartz and A. Juhász, *Revista de Chimie* (Bucureşti) 1983 under press.

[13] V. Sanda, J. Fajkos and F. Sorm, *Coll. Czech. Chem. Comm.*, **39**(5), 1377 (1874).

[14] V. Sanda, J. Fajkos, F. Sorm and A. Protiva, *Coll. Czech. Chem. Comm.*, **37** (8), 2807 (1972).

Revue Roumaine de Chimie, **29**, *9 — 10*, 761—768 (1984)

2-ARYLSULPHONYLAMIDO-2-THIONO-5,5-DIMETHYL-1,3,2-DIOXAPHOSPHORINANES

I. FENEȘAN,*[,a] V. MUREȘAN[a], A. BARABÁS[a] and M. BOGDAN[b]
[a] Institute of Chemistry, str. Fîntînele 30, 3400 Cluj-Napoca, Romania
[b] Institute of Isotopic and Molecular Technology, Cluj-Napoca, Romania

Received November 7, 1983

2-Arylsulphonylamido-2-thiono-5,5-dimethyl-1,3,2-dioxaphosphorinanes of structure **9** (Y = H ; X = H, CH_3, OCH_3, F, Cl, and Br) were synthesized and characterized. According to their IR, ^{1}H-, ^{13}C— and ^{31}P—NMR spectra all these compounds exist almost exclusively in the amido-thionic tautomeric form, **9**. Methylation of **9** (Y = H) under kinetic control (with CH_2N_2) afforded approx. equal amounts of the amido-thionic N-methyl (**9**, Y = Me) and the imido-thiolic S-methyl (**9**′, Y = Me) derivatives, whereas methylation under thermodynamic control (with Me_2SO_4) afforded mainly the N-methyl derivative **9**, Y = Me, with only small amounts of the S-methyl tautomer **9**′, Y = Me. Diastereotopic magnetic nonequivalence between axial and equatorial 5-methyl groups and methylenic protons (4.6) of the phosphorinane ring was observed and discussed in the context of literature data on related compounds.

INTRODUCTION

There is a marked interest in the recent chemical literature on the saturated phosphorus heterocycles with 5-membered[1-13] or 6-membered[14-20] rings. Prepared from phosphorus chlorides **1** (Z = 0, S, or lone electron pair) upon reaction with appropriated diols, thiols or amino-alcohols **2** (X = 0, S, or NH) to give the chloro-substituted heterocycles **3**, from which a large series of derivatives **4** can be prepared upon substitution of the chlorine atom by another groups, they have been known for some time.[21-23]

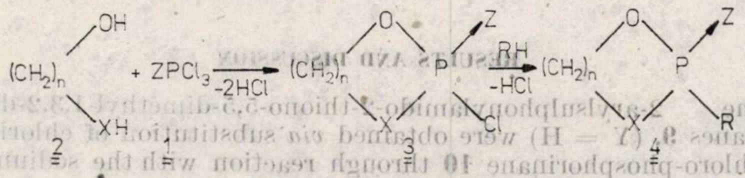

The newly aroused interest can be partly explained by the diastereomerism and diastereotopic magnetic nonequivalence phenomena observed on these compounds. Indeed, the chemically equivalent protons H_a and H_b in compounds like **5**[1,3] or **6**[15], or the chemically equivalent methyl groups Me_a and Me_b in **6**[18,19] or **7**[4] appear diastereotopically nonequivalent, affording different chemical shifts and different coupling constants to the phosphorus. The magnitudes of these parameters served as starting data for a series of interesting studies on the conformation of these heterocycles.[10-13,18,19] The introduction of an enantiotopic* carbon in the ring, as shown in compound **8**, results in the appearance of a second center of enantiotopy at the phosphorus and will thus lead to the appearance of diastereomers.[2,5-7] Similar diastereomerism was induced[20] in the dioxaphosphorinanes like **6**, by creating an asymmetric center at position 5 of the ring, by replacing one of the 5-methyl substituents through a chloromethyl group.

---

* to whom correspondence should be addressed

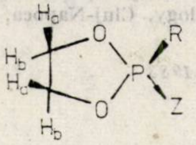
Ha
O
R
Hb
Ha
P
O
Z
Hb

5

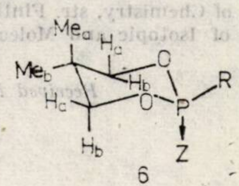
Mea
Ha
O
Meb
Hb
R
Hc
O
P
Hb
Z

6

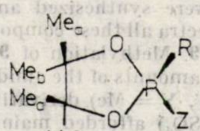
Mea
O
R
Meb
P
Mea
O
Z
Meb

7

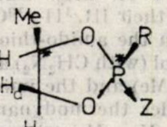
Me
O
R
H
P
Ha
O
Z
Hb

8

As a sequel to our previous work on phosphorylated sulphonylamides[24-33] we wish to report here on 2-arylsulphonylamido-2-thiono-5,5-dimethyl-1,3,2-dioxaphosphorinanes **9** (Y = H, CH_3; X = H, CH_3, OCH_3, F, Cl and Br).

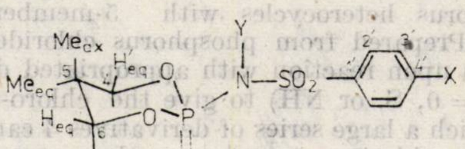
Y
Meax
H'eq
2'
3'
Meeq
5
4
O
N—SO2
X
Heq
6
O—P
Hax
S

9

RESULTS AND DISCUSSION

The 2-arylsulphonylamido-2-thiono-5,5-dimethyl-1,3,2-dioxaphosphorinanes **9**, (Y = H) were obtained *via* substitution of chlorine from the 2-chloro-phosphorinane **10** through reaction with the sodium salt of the appropriate sulphonylamide, **11** :

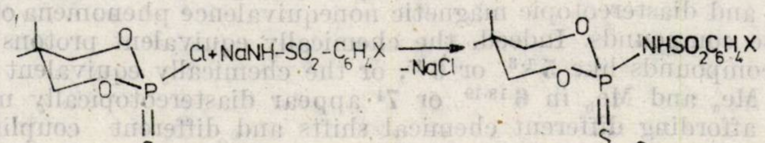
O
Cl+NaNH-SO2-C6H4X
O
NHSO2C6H4X
-NaCl
O
P
O
P
S
S

10 **11** **9**

Compound **10** was prepared from neopentyl glycol and thiophosphoryl chloride, as described in the literature.[15]

Compounds **9** were obtained with yields of 30—40%, when the reaction was carried out at room temperature in highly polar aprotic solvents (dimenthylformamide, acetonitrile). No reaction occurs in solvents of low polarity, whereas increased reaction temperature (100°) has led to decomposition marked by evolution of hydrogen sulphide.

Compounds **9**(Y = H) are white crystalline solids characterized by the data given in Table 1. Two tautomeric formulae **9** or **9′** could be taken into discussion for representing their molecular structure.

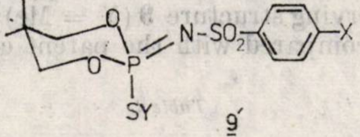

9′

Table 1

Physical constants and analytical data for the 2-arylsulphonyl amido-2-thiono-5,5-dimethyl-1,3,2-dioxaphosphorinanes

Formula			m.p. °C	Yield %	Analytical figures ; % found/(% calcd.)			
No.	Y.	X			C	H	P	S
9	H	H	152	32	41.29 (41.11)	4.95 (5.01)	9.70 (9.63)	19.76 (19.95)
9	H	CH_3	135.5	30	43.03 (42.97)	5.35 (5.40)	9.32 (9.23)	19.20 (19.12)
9	H	OCH_3	147	30	41.18 (41.02)	4.99 (5.16)	8.56 (8.81)	18.08 (18.25)
9	H	F	129.5	35	39.01 (38.93)	4.02 (4.45)	9.02 (9.12)	18.70 (18.89)
9	H	Cl	155	40	37.31 (37.13)	4.16 (4.24)	8.53 (8.70)	17.96 (18.02)
9	H	Br	181	40	33.06 (33.00)	3.70 (3.77)	7.05 (7.73)	16.08 (16.02)
9	CH_3	H	106	50	42.91 (42.97)	5.39 (5.41)	9.20 (9.23)	19.21 (19.12)
9	CH_3	Cl	98	85	38.76 (38.97)	4.85 4.91	8.23 (8.37)	—
9′	CH_3	H	108	50	42.87 (42.97)	5.43 (5.41)	9.18 (9.23)	19.10 (19.12)

All spectra recorded by us (IR, $^1H^-$, $^{31}P^-$ and ^{13}C—NMR) indicated that in moderately concentrated solutions these compounds appear almost exclusively as thiono-tautomers **9**. Thus, in the IR-spectra of compounds

9 characteristic absorption bands were observed for the following substructures : P = S (665 cm^{-1})[15] ; SO_2 sym. stretching (1175–1180) ; SO_2 asym. str. (1385–1390) ; associated NH str. (3100–3300) and free NH str. (3365–3380 cm^{-1}). No absorption was observed in the region (2200–2500 cm^{-1}) where S–H stretching vibrations usually appear. All compounds **9** (Y = H) afforded ^{31}P-chemical shifts (see Table 2) of about 52 ppm, characteristic for monothiono phosphorus compounds. Similar values (54–55 ppm) were measured [18,34] for a number of related 2-thiono-5,5-dimethyl-1,3,2-dioxaphosphorinanes. A methylation product of **9** (X, Y = H), which presumably has an imido-thiolic structure **9′** (X =H. Y = Me) afforded a ^{31}P-chemical shift at 28.5 ppm, whereas the N-methylated derivatives preserving structure **9** (Y = Me) have their phopshoru-slightly deshielded as compared with the parent compounds **9** (Y = H)s

Table 2

^{1}H- and ^{31}P–NMR Spectra of the 2-arylsulphonylamido-2-thiono-5,5-dimethyl-1,3,2-dioxaphosphorinanes in $CDCl_3$.

Formula			^{1}H-Chemical shifts (ppm)								^{31}P–Chem. shift (ppm)
No.	Y	X	5,5–$(CH_3)_2$		4,6–CH_2		Y	2′	3′	X	
			ax.	eq.	ax.	eq.					
9	H	H	1.22	1.09	4.20		[a]	[b]	[b]	[b]	52.39
9	H	CH_3	1.20	1.09	4.19		[a]	7.85	7.32	2.44	52.40
9	H	OCH_3	1.20	1.09	4.19		[a]	7.89	6.96	3.88	52.94
9	H	F	1.21	1.09	4.20		[a]	7.98[c]	7.20[d]	—	52.57
9	H	Cl	1.21	1.10	4.19		[a]	7.90	7.50	—	52.53
9	H	Br	1.21	1.10	4.20		[a]	7.80	7.70	—	[e]
9	CH_3	H	1.21	1.02	4.30[f]	4.06[g]	3.00[h]	[b]	[b]	[b]	58.60
9	CH_3	Cl	1.27	1.05	4.33[i]	4.10[j]	3.04[h]	7.92	7.54	—	57.89
9′	CH_3	H	1.19	1.01	4.15		2.37[k]	[b]	[b]	[b]	28.48

[a] signal not found ; [b] pattern not analysed ; [c] J_{HF} = 4.9 Hz ; [d] J_{HF} = 8.5 Hz ; [e] not recorded ; [f] J = 19.0 Hz ; [g] J_{PH} = 8.9 Hz ; J_{ax-eq} = 10.3 Hz ; [h] J_{PH} = 10.5 Hz ; [i] J_{PH} = 19.6 Hz ; [j] J_{PH} = 7.8 Hz ; J_{ax-eq} = 10.1 Hz ; [k] J_{PH} = 16.8 Hz.

These results clearly indicate that the amido thionic tautomers **9** (Y = H) are thermodynamically more stable than their imido-thiolic counterparts **9′** (Y = H). Derivatives of the less stable imido-thiolic tautomers could be however obtained in methylation experiments under kinetic control. Thus, methylation of **9** (X, Y = H) with diazomethane afforded a mixture of two products in approximately equal amounts, which could be separated chromatographically. One of them (m.p. 106°) afforded ^{31}P- and ^{1}H–NMR spectra consistent with formula **9**(X= H, Y = Me), whereas an imido-thiolic structure **9′** (X = H, Y = Me) could be assigned to another component (m.p. 108°). Analogously, methylation of **9** (X = Cl, Y = H) with diazomethane afforded two components with structures according to **9**(Y = Me, X = Cl) and **9′** (Y = Me, X=Cl) respectively, as shown by ^{1}H– and ^{13}C–NMR spectra. Methylation of **9** (X = Cl, Y = H) with dimethylsulphate (thermodynamic control) afforded a product consisting mostly of **9** (Y = Me, X = Cl) with only small amounts of **9′** (Y = Me, X = Cl) as shown by ^{13}C–NMR spectra.

Analogous methylation experiments on 2-arylsulphonylamido-2-thiono-1,3,2-dioxaphospholanes always afforded only one product with amido-thionic structure.[33]

The ^1H-NMR spectra of compounds **9** (see Table 2) are in good agreement with those of other similar dioxaphosphorinanes.[16,18,19,34] The diastereotopic magnetic nonequivalence of the methylenic protons in positions 4 and 6 is much less pronounced in compounds **9** ($Y = H$) than in other (e.g. 2-aryloxy-[34]) phosphorinanes; in compounds **9** ($Y=H$) these protons (expected to afford the AB part of an ABX spin system) yielded only deceptively simple patterns with only two strong lines of unequal height, along with some barely decelable ones. A comparison with computed ABX spectra [35] indicated a chemical shift difference $\delta_A - \delta_B$ of about 0.05 ppm. The frequency difference between the two strong lines (about 14 Hz) is most probably due to the P—H coupling, as an analogous separation was found between the lines of the proton-undecoupled ^{31}P-spectra. The diastereotopic nonequivalence of the methylene protons is slightly increased by S-methylation; in compound **9′** ($Y = Me$) the lower and broader of the two strong lines appears as a slightly resolved doublet, the separation of its lines from the another strong line being of 12 and 15 Hz respectively; these values were found in the proton-undecoupled ^{31}P-spectrum of **9′** ($Y = Me$) too. Finally, N-methylation produced a powerful diastereotopic nonequivalence of the methylenic protons, with all eight lines of the AB part of an ABX system appearing separately in the spectra of compounds **9**($Y=Me$; $X=H$, Cl). An important difference between the P—H coupling constants of the axial and equatorial protons also appears, paralelling the chemical shift difference due to magnetic nonequivalence (see also refs.[16,18,34])

A marked influence of solvent polarity on the chemical shifts of the dioxaphosphorinane ring substituents was observed; e.g. the signals of the equatorial and axial 5-Me substituents (separated in $CDCl_3$ by 0.1 ppm for **9** ($Y = H$) and by 0.2 ppm for **9** and **9′** ($Y = Me$)) appeared totally merged in DMSO-d_6. Such changes were associated [18] with conformational equilibra of the dioxaphosphorinane ring.

$^{13}C-NMR$—Data on compounds **9** and **9′** are summarized in Table 3. The chemical shifts of carbons of the dioxaphosphorinane ring are in good agreement with the data reported in the literature.[18] The magnetic nonequivalence between the axial and equatorial 5-methyl groups for compounds **9**($Y = H$) is at the limit of resolution in our experimental conditions; it is however sensibly increased both by N-methylation (**9** ($Y = Me$)) and S-methylation (**9′** ($Y = Me$)).

Compounds **9** ($Y = H$) are fairly strong monobasic acids due to proton Y; they dissolve readily in aqueous sodium bicarbonate under gas evolution, forming water-soluble sodium salts. Table 4 summarizes the pK values measured for their dissociation in aqueous ethanol. From these experimental data, pK-values for pure water and for ethanol-water mixtures of different concentrations can be computed according to a procedure given by Ismailov.[36,37] The following numerical expression of the Ismailov-Hammet equation for compounds **9**($Y = H$) was obtained after mathematical processing of the experimental pK-values according to refs.[36-38] :

$$pK_{(X)M} = 1.505 + \lg f^0_H + 0.329 \lg f^0_{el} - (1.086 + 1.555 \lg f^0_{el}) \cdot \tau \quad \text{(eq.1)}$$

Table 3

^{13}C—NMR Spectra of the 2-arylsulphonylamido-2-thiono-5,5-dimethyl-1,3,2-dioxaphosphorinanes in acetone-d_6

Formula			Chemical shifts of carbons (δ, ppm)									
No.	Y	X	5,5—$(CH_3)_2$ eq.	5,5—$(CH_3)_2$ ax.	5—C	4,6 — CH_2O	1′	2′	3′	4′	X	Y
9	H	H	21.7		33.0[a]	77.9[b]	142.3	129.7	128.1	134.2	—	—
9	H	CH_3[c]	21.6		33.0[a]	77.7[a]	139.4	130.1	128.0	144.8	21.6	—
9	H	OCH_3	21.6		33.0[a]	77.8[a]	133.8	130.3	114.8	164.1	56.1	—
9	H	F	21.6	21.7	33.0[d]	77.9[e]	138.4[f]	131.2[g]	116.7[h]	166.0[i]	—	—
9	H	Cl	21.4	21.6	32.9[a]	77.9[e]	140.7	129.8	129.8	139.6	—	—
9	H	Br	21.4	21.6	33.0[a]	77.9[a]	141.4	132.9	130.0	128.2	—	—
9	CH_3	Cl	21.25	22.18	32.3[d]	78.3[h]	140.4	129.9	129.2	135.5	—	34.9[j]
9′	CH_3	Cl	20.0	21.7	32.9[a]	78.5[a]	143.6	129.7	128.6	138.1	—	10.9[k]

[a] J_{PC} = 6.6 Hz; [b] J_{PC} = 9 Hz; [c] δ_X = 21.6 (see ref. 33) a practically identical spectrum was obtained in $CDCl_3$; [d] J_{PC} = 5.8 Hz; [e] J_{PC} = 7.5 Hz; [f] J_{CF} = 3.8 Hz; [g] J_{CF} = 10 Hz; [h] J_{CF} = 23.3 Hz; [i] J_{CF} = 252.4 Hz; [j] J_{CP} = 3.3.Hz; [k] J_{CP} = 4.2 Hz.

Table 4

Experimental and computed (in parentheses) pK-values for compounds 9 (Y=H)

Compound **9**, X =	Hammet σ- values for X	pK — Values in aqueous ethanol			
		0%	40%	60%	80%
OCH_3	−0.268	— (1.801	2.256 (2.214)	2.427 (2.488)	3.122 (3.107)
CH_3	−0.170	— (1.685)	2.175 (2.074)	2.333 (2.361)	2.898 (2.931)
H	0.000	— (1.503	2.037 (1.832)	2.147 (2.140)	2.663 (2.626)
F	0.062	— (1.436)	1.985 (1.743)	2.296 (2.059	2.378 (2.514)
Cl	0.226	— (1.261)	1.573 (1.509)	1.805 (1.846)	2.293 (2.219)
Br	0.232	(1.254)	1.448 (1.501)	1.723 (1.838)	2.253 (2.208)

where $pK_{(X)M}$ represents the pK of the given compound **9**(X) in the medium M, f^0_H and f^0_{ei} are activity coefficients [36,37] and σ the Hammet constant of the given X substituent. The measured pK values are in fair agreement with those calculated by eq. 1 (shown in Table 4 between parentheses).

The substituents X in position 4′ of the aromatic ring increase the acidity of compounds **9** (Y = H) at an extent directly proportional to their Hammet $\rho-\sigma$ constants, that is to their electron-attracting inductive effect. The pK$-\sigma$ plots drawn for all three concentrations (40, 60, 80%) from Table 4 showed a very high degree of linearity, with linear correlation coefficients very closely approaching unity. This type of dependence between the nature of the substituents X and the acidity of the compounds, invariably found for various classes of phosphorylated arylsulphonylamides,[24–30, 32, 38] is in accordance with theoretical predictions; electron-withdrawing substituents should stabilize the anion resulted from acidic dissociation of the sulphonylamides and thus promote dissociation.

The various substituents on the phosphorus also exert their specific influence on the acidity of the phosphorylated sulphonyl-amides.[32] Among the compounds of the general formula **12** investigated by us, the following series of increasing acidity could be established:

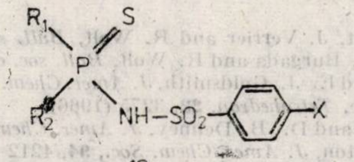

12

R_1:	C_2H_5	C_2H_5	C_6H_5	C_6H_5	C_2H_5O	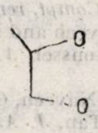	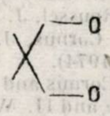	C_6H_5O.
R_2:	C_2H_5	C_2H_5O	C_2H_5O	C_6H_5	C_2H_5O			C_6H_5O;

(The comparison is subject of some approximation, as not all of the pK-values used were obtained in the same set of experimental conditions).

EXPERIMENTAL PART

Preparation of the 2-arylsulphonylamido-2-thiono-5,5-dimethyl-1,3,2-dioxaphosphorinanes 9 (Y = H); (*general method*): 50 mmoles of 2-chloro-2-thiono-5,5-dimethyl-1,3,2-dioxaphosphorinane[15], (**10**) and 50 mmoles of the sodium salt of the appropriated arylsulphonylamide **11** were placed in a reaction flask equipped with mechanical stirrer and protected from moisture by calcium chloride; 100 ml of dimethylformamide were added and the mixture stirred at room temperature for 2 hrs. The solvent was removed *in vacuo*. The residue consisted from product **9**, along with unreacted arylsulphonylamide **11**, which could be removed by several repetitions of the following operations: the residue was taken up in 100 ml of saturated aqueous $NaHCO_3$, the undissolved solid material filtered off, and the product **9** reprecipited by adding concentrated hydrochloric acid to the filtrate. Finally, recrystallization from hexane : n-propanol (3 : 1) afforded analytically pure samples of compounds **9** (Y = H), as characterized in Table 1.

Methylation of compounds **9** (*Y = H; X = H, Cl*) *by diazomethane*: 10 mmoles of **9**(Y = H) were dissolved in 20 ml of dry ethyl ether in a moisture-protected flask and 20 mmoles of diazomethane contained in 60 ml of dry ether were dropped into. After 24 hrs standing, the solvent was removed and the residue eluted through a silica gel column (50 × 3 cm) with dry benzene. The amido-thionic tautomer **9** (Y = Me) elutes first, followed by the imido-thiolic tautomer **9′** (Y = Me). After removing the solvent *in vacuo*, the analytically pure compounds were obtained by recrystallization from hexane – *n*-propanol as above.

Methylation of compound **9** *($Y = H$; $X = Cl$) by dimethylsulphate* : 2 g of compound **9** ($Y = H$; $X = Cl$) were dissolved in 20 ml of saturated $NaHCO_3$ solution and 5 g dimethylsulphate were dropped into at room temperature during 2 hrs. After 12 hrs standing, the reaction product was removed from the mixture by extraction with 25 ml benzene. The separated organic layer was dried over anhydrous magnesium sulphate and concentrated *in vacuo*. The crude white crystalline residue was analysed by $^{13}C-NMR$.

Analyses and spectra : Elementary analyses were effected by standard methods. IR-Spectra were recorded in CCl_4 solutions with an UR–10 Carl Zeiss Jena double beam spectrophotometer with salt optics in the region between 400–3600 cm^{-1}. NMR-Spectra were recorded on a Bruker WP–60 FT-NMR instrument at a field of 14 kG (60 MHz for ^1H, 24.28 MHz for ^{31}P and 15.086 MHz for ^{13}C). Chemical shifts are given downfields from internal TMS for ^1H and ^{13}C, respectively from external D_3PO_4 for ^{31}P.

Dissociation constants were determined potentiometrically, as described in ref. 38. The EMF-values of the following chains were measured at 25 ± 0.01 °C in a thermostat : Ag/AgCl (saturated), KCl (satd.) ; HCl 10^{-2}M/glass electrode Ag/AgCl (satd.) KCl (satd.) ; $HA(c_1)KA(c_2)$/glass electrode. HA = compounds **9** ($Y = H$), $c_1 = 10^{-2}M$, $c_2 = 0.5 \times 10^{-2}M$. The solvents used were ethanol in water at the concentrations of 40, 60 and 80% respectively.

REFERENCES

[1] D. Gagnaire, J. B. Robert, J. Verrier and R. Wolf, *Bull. soc. chim. France*, **1966**, 3719.

[2] H. Germa, M. Sanchez, R. Burgada and R. Wolf, *Bull. soc. chim. France*, **1970**, 612.

[3] P. Haake, J. P. McNeal and E. J. Goldsmith, *J. Amer. Chem. Soc.*, **90**, 715 (1968).

[4] B. Fontal and H. Goldwhite, *Tetrahedron*, **22**, 3275 (1966).

[5] D. Z. Denney, G. Y. Chen and D. B. Denney, *J. Amer. Chem. Soc.*, **91**, 6838 (1969).

[6] R. H. Cox and M. G. Newton, *J. Amer. Chem. Soc.*, **94**, 4212 (1972).

[7] R. H. Cox, B. S. Campbell and M. G. Newton, *J. Org. Chem.*, **37**, 1557 (1972).

[8] J. Devillers and J. Navech, *Bull. soc. chim. France*, **1970**, 4341.

[9] R. Burgada and C. Laurenço, *Compt. rend.*, **273C**, 1536 (1971).

[10] J. Devillers, J. Roussel, J. Navech and R. Burgada, *Org. Magn. Reson.*, **5**, 511 (1973).

[11] J. Devillers, M. Cornus, J. Roussel, J. Navech and R. Burgada, *Org. Magn. Reson.*, **6**, 205 (1974).

[12] J. Devillers, M. Cornus and J. Navech, *Org. Magn. Reson.*, **6**, 211 (1974).

[13] W. G. Bentrude and H. W. Tan, *J. Amer. Chem. Soc.*, **98**, 1850 (1976).

[14] R. S. Edmundson and J. O. L. Wrigley, *Tetrahedron.*, **20**, 2781 (1964).

[15] R. S. Edmundsnon, *Tetrahedron*, **21**, 2379 (1965).

[16] K. D. Bartle, R. S. Edmundson and D. W. Jones, *Tetrahedron*, **23**, 1701 (1967).

[17] D. Gagnaire and J. B. Robert, *Bull. soc. chim. France*, **1967**, 2240.

[18] J. P. Dutasta, A. Grand, J. B. Robert and M. Taieb, *Tetrahedron Letters*, **1974**, 1659.

[19] J. P. Majoral and J. Navech, *Bull. soc. chim. France*, **1971**, 95.

[20] W. S. Wadsworth jr. and Y. G. Tsay, *J. Org. Chem.*, **39**, 984 (1974).

[21] H. J. Lucas, F. W. Mitchell jr. and C. N. Scully, *J. Amer. Chem. Soc.*, **72**, 5491 (1950).

[22] R. L. McConnel and H. W. Coover, *J. Org. Chem.*, **24**, 630 (1959).

[23] A. E. Arbuzov and M. M. Azanovskaya, *Izvest. Akad. Nauk SSSR*, **1949**, 473 ; **1951**, 544.

[24] L. Almási, R. Popescu and L. Paskucz, *Rev. Roumaine Chim.*, **24**, 3, 741 (1979).

[25] L. Almási, N. Popovici and J. Zsakó, *Chem. Ber.*, **106**, 1384 (1973).

[26] L. Almási and R. Popescu, *Chem. Ber.*, **108**, 156 (1975).

[27] L. Almási and A. Hantz, *Chem. Ber.*, **96**, 3148 (1963).

[28] L. Almási and A. Hantz, *Rev. Roumaine Chim.*, **9**, 433 (1964).

[29] J. Zsakó, L. Almási, M. Giurgiu and A. Hantz, *Zhurn. Obhschei Khim.*, **35**, 1866 (1965).

[30] L. Almási, R. Popescu and R. Grecu, *Tetrahedron*, **33**, 1327 (1977).

[31] A. Barabás, R. Popescu, V. Mureşan and L. Almási, *Org. Magn. Reson.*, **10**, 35 (1977).

[32] L. Almási, V. Mureşan and A. Varabás, *Z. anorg. allg. Chem.*, **458**, 62 (1979).

[33] A. Barabás, V. Mureşan and L. Almási, *Org. Magn. Reson.*, **12**, 313 (1979).

[34] M. Vlassa and A. Barabás, *J. prakt. Chem.*, 1983 (in press).

[35] E. D. Becker, "High Resolution NMR. Theory and Chemical Applications", Acad. Press, New-York, 1969, p. 161.

[36] N. A. Ismailow, "Elektrohimia rastvorov", Izd. Kharkowsk. Univ., Kharkow, 1959, p. 795.

[37] W. W. Alexandrow and N. A. Ismailow, *Zhurn. Fiz. Khim.*, **32**, 404 (1958).

[38] J. Zsakó, M. Giurgiu, L. Almási and A. Hantz, *Rev. Roumaine Chim.*, **11**, 1019 (1966).

Revue Roumaine de Chimie, **29**, *9 – 10*, 769–772 (1984)

BASE CATALYZED ADDITIONS OF DEHYDROACETIC ACID AND ITS 3-CINNAMOYL DERIVATIVES

M. A. HASSAN, M. EL-KADY, M. EL-BORAI, and A. A. ZBD EL-MOATY

Chemistry Department, Faculty of Science, Ain Shams University,
Cairo, Egypt

Received October 10, 1983

Base catalyzed addition of dehydroacetic acid (**1**) to some chalcones was investigated. Condensations of 3-cinnamoyl-4-hydroxy-6-methyl-2-pyrone (**3**) with hydrazines, acetylacetone, diethyl malonate, etyhl acetoacetate and ethyl phenyl acetate were studied. The structures of the products were established by elemental analysis and spectroscopic evidences.

As an extension of our previous work [1-3] base catalyzed addition of dehydroacetic acid (**1**) to some chalcones gives the Michael adducts, namely 3,5-diarylpentan-1-(4′-hydroxy-6′-methyl-2′-oxopyran-3′-yl)-1,5-diones (**2a – d**). The IR spectra of compounds **2** showed bands at 1000, 1640, 1710, and 3220 cm^{-1} attributable to the stretching frequencies of C–O–C, (α-pyrones), C = 0 (1,5-diketones), and OH group respectively. The ^1H-NMR spectrum of **2b** in $CDCl_3$ showed signals at δ 1.73 (*m*, 1H, $Ar'-CH-$), 2.3 (*s*, 3H, C_6-CH_3), 3.6 (*d*, 4H, $COCH_2$), 4.12 (*s*, 3H, $Ar'-OCH_3$), 5.7 (*s*, 1H, C_5-H) and 6.8–7.6 ppm (*m*, 9H, $Ar-H$).

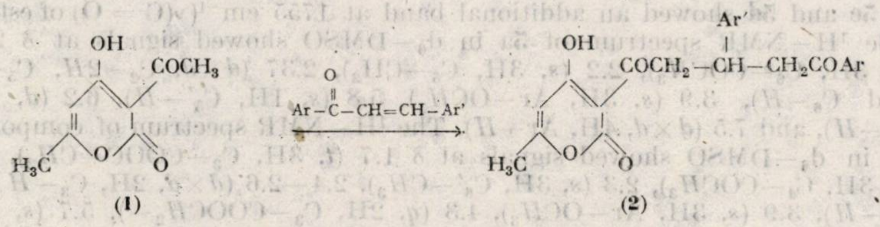

a) $Ar = Ar' = C_6H_5$
b) $Ar = C_6H_5$; $Ar' = C_6H_4-OCH_3-p$
c) $Ar = C_6H_4\text{-}OCH_3-p$; $Ar' = C_6H_5$
d) $Ar = Ar' = C_6H_4-OCH_3-p$

Claisen-Schmidt condensation [4] of dehydroacetic acid (**1**) with aromatic aldehydes in boiling chloroform in the presence of piperidine gives 3-cinnamoyl-4-hydroxy-6-methyl-2*H*-pyran-2-ones (**3**a–d), which con-dense with phenylhydrazine in boiling acetic acid to give 5-aryl-1-phenyl-3-(4′-hydroxy-6′-methyl-2′-oxopyran-5′-yl)-2-pyrazolines (**4a**—**d**). The IR spectra of compounds **3** showed bands at 1000, 1600, 1650, 1705, and 3230 cm^{-1} attributable to the stretching frequencies of C—O—C, C = C, C = O (α-pyrones), C = O (α, β-unsaturated ketones) and OH respectively, while the IR spectra of **4** showed the absence of ν(C =**O**) (of *α*, β-unsaturated ketones). The ^{1}H—NMR spectrum of **3b** in $CDCl_3$ showed signals at δ 2.24 (*s*, 3H, C_6—CH_3), 4.2 (*s*, 3H, Ar—OCH_3), 5.87 (*s*, 1H, C_5—*H*),7.3 (*d*×*d*, 4H, Ar—*H*), and 8.1 ppm (*d*×*d*, 2H, C*H*=C*H*), while the ^{1}H—NMR spectrum of **4**a in d_6—DMSO showed signals at δ2.18 (*s*, 3H, C_6—CH_3), 3.3—4.0 (*m*, 3H, C_4—H_2 and C_5—*H*), 6.1 (*s*, 1H, C_5—*H*), and 6.9—7.3 ppm (*m*, 10H, Ar,—*H*).

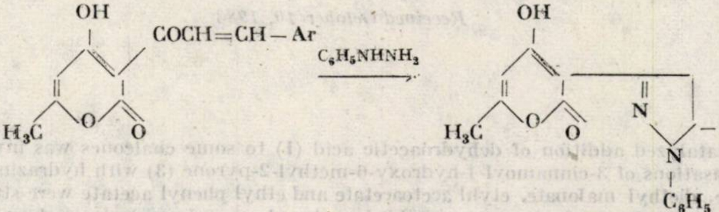

(3) **(4)**

a) Ar = C_6H_5 ; b) Ar = C_6H_4—OCH_3—*p*
c) Ar = C_6H_5—O_2CH_2—3,4— ; d) Ar = C_6H_4—NO_2—*p*

Base catalyzed cycloaddition of acetyl acetone on **3b** or **3c** in the presence of sodium methoxide at 170° gives 6-acetyl-5-aryl-3-(4′-hydroxy-6′-methyl-2′-oxopyran-3′-yl)-cyclohex-3-en-1-ones (**5a** and **5b**). Also base catalyzed cycloaddition of diethyl malonate, ethyl acetoacetate, and ethyl phenylacetate to **3** gives 4-aryl-5, 6-dihydro-6-(4′-hydroxy-6′-methyl-2′-oxopyran-3′-yl)-3-carbethoxy (or acetyl/or phenyl)-2*H*-pyran-2-ones (**5c**—**f**) respectively. The IR spectra of compounds **5a** and **5b** showed bands at 1000, 1650, 1685, 2260—2980, and 3220 cm^{-1} attributable to the stretching frequencies of C—O—C, C = O (α-pyrones), C =O (cyclohexanone), aliphatic CH, and CH respectively, while IR spectra of **5c** and **5d** showed an additional band at 1755 cm^{-1}(ν(C = **O**) of ester). The ^{1}H—NMR spectrum of **5**a in d_6—DMSO showed signals at δ 2.12 (*s*, 3H, C_6—COCH_3), 2.2 (*s*, 3H, C_6—CH_3), 2.37 (*d*×*d*, C_2—2*H*, C_5—*H* and C_6—*H*), 3.9 (*s*, 3H, Ar—OCH_3), 5.8 (*s*, 1H, C_5'—*H*), 6.2 (*d*, 1H, C_4—*H*), and 7.5 (*d*×*d*, 4H, Ar—*H*). The ^{1}H—NMR spectrum of compound **5c** in d_6—DMSO showed signals at δ 1.7 (*t*, 3H, C_3—COOC—CH_3), 2.2 (*s*, 3H, C_4—COCH_3), 2.3 (*s*, 3H, C_6'—CH_3), 2.4—2.6 (*d*×*d*, 2H, C_3—*H* and C_4—*H*), 3.9 (*s*, 3H, Ar—OCH_3), 4.3 (*q*, 2H, C_3—COOCH_2—), 5.7 (*s*, 1H, C_5'—*H*), 6.2 (*s*, 1H, C_5—*H*), and 7.5 (*d*×*d*, 4H, Ar—*H*).

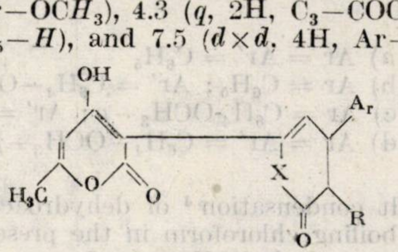

(5)

Table 1

Physical data of compounds **2–5**

Compound	M.p. °C	Mol. formula	Analysis % Calcd./Found		
			C	H	N
2a	95	$C_{23}H_{20}O_5$	73.40	5.32	—
			73.53	5.23	—
2b	91	$C_{24}H_{22}O_6$	70.94	5.42	—
			71.03	5.37	—
2c	100	$C_{24}H_{22}O_6$	70.94	5.42	—
			70.88	5.36	—
2d	88	$C_{25}H_{24}O_7$	68.81	5.50	—
			69.02	5.43	—
3a	128	$C_{15}H_{12}O_4$	70.31	4.67	—
			70.25	4.71	—
3b	203	$C_{16}H_{14}O_5$	67.13	4.89	—
			67.04	4.92	—
3c	185	$C_{18}H_{12}O_6$	63.79	4.32	—
			63.82	4.27	—
3d	243	$C_{15}H_{11}NO_6$	59.80	3.65	4.65
			59.94	3.58	4.72
4a	178	$C_{21}H_{18}N_2O_3$	76.36	5.45	7.76
			76.43	5.37	7.59
4b	148	$C_{22}H_{19}N_2O_4$	70.40	5.07	7.47
			70.52	5.13	7.31
4c	186	$C_{22}H_{18}N_2O_5$	67.69	4.62	7.18
			67.73	4.60	7.06
4d	208	$C_{21}H_{17}N_3O_5$	67.20	4.53	10.74
			67.34	4.58	10.67
5a	201	$C_{21}H_{20}O_6$	68.48	5.43	—
			68.32	5.51	—
5b	231	$C_{21}H_{18}O_7$	65.97	4.71	—
			66.11	4.68	—
5c	206	$C_{21}H_{20}O_8$	63.00	5.00	—
			63.12	4.78	—
5d	249	$C_{20}H_{17}NO_9$	57.83	4.10	3.37
			57.96	4.14	3.22
5e	236	$C_{20}H_{16}O_8$	62.50	4.17	—
			62.63	4.13	—
5f	208	$C_{24}H_{20}O_6$	71.29	4.95	—
			71.34	4.82	—

a) X	R	Ar
a) CH_2	$COCH_3$	$C_6H_4-OCH_3-p$
b) CH_2	$COCH_3$	$C_6H_3-O_2CH_2-3,4-$
c) O	$CO_2C_2H_5$	$C_6H_4-OCH_3-p$
d) O	$CO_2C_2H_5$	$C_6H_4-NO_2-p$
e) O	$COCH_3$	$C_6H_3-O_2CH_2-3,4-$
f) O	C_6H_5	$C_6H_4-OCH_3-p$

EXPERIMENTAL

All melting points are uncorrected. The IR spectra were determined on a Unicam SP 200 G spectrometer using KBr wafer technique and the ^1H-NMR spectra were recorded on a Bruker WP—80 Cw spectrophotometer.

3,5-Diaryl-pentan-1-(4'-hydroxy-6'-methyl-2'-oxopyran-3'-yl)-1,5-diones (**2a—d**)

To a solution of dehydroacetic acid (**1**) (0.012 mol) in alcoholic potassium hydroxide 2.0 g KOH (in 50 ml ethanol), chalcones (0.01 mol) in ethanol (20 ml) were added and then the reaction mixture was allowed to stand 7 days at room temperature. The reaction mixture was poured into dilute hydrochloric acid, and the solid product which separated was filtered and) crystallised from benzene-light petrol mixture to give **2a—d** as colourless crystals (yields 50—53% (cf. Table 1).

2-Cinnamoyl-4-hydroxy-6-methyl-2-pyrones (**3a—d**)

A solution of dehydroacetic acid (0.01 mol), aromatic aldehyde, namely benzaldehyde, anisaldehyde, piperonal, or *p*-nitrobenzaldehyde, piperidine (5 drops) in chloroform (30 ml) was refluxed for 4 hrs. The yellowish red product which separated after distillation the water-chloroform azeotrope was filtered off and recrystallized from benzene to give **3a—d** as yellow crystals respectively (yields 56—62%) (cf. Table 1).

5-Aryl-1-phenyl-3-(4'-hydroxy-6'-methyl-2'-oxopyran-3'-yl)-2-pyrazolines (**4**a—d)

A solution of **3** (0.01 mol) and phenylhydrazine in acetic acid (30 ml) was refluxed for 6 hrs. The product which separated after concentration and cooling was filtered off and crystallized from acetic acid-ethanol mixture to give **4a—d** as yellow to orange crystals (yields 42—56%) (cf. Table 1).

6-Acetyl-5-aryl-3(4'-hydroxy-6'-methyl-2'-oxopyran-3'-yl)-cyclohex-3-en-1-ones (**5**a *and* **5**b), *and 4-aryl,-5,6-dihydro-6-(4'-hydroxy-6'phenyl-2'-oxopyran-3'-yl)-3-carbethoxy (or acetyl/or phenyl)-2H-pyran-2-ones* (**5**c—f)

A mixture of **4** (0.01 mol), acetylacetone, diethyl malonate, ethyl acetoacetate,or ethyl phenyl acetate (0.012 mol), and sodium methoxide (0.022 mol) was heated in a sealed tube for 4 hrs at 170°. The mixture was poured into dilute hydrochloric acid. The solid products which separated were filtered and recrystallized from acetic acid-ethanol mixture to give **5a—f** as pale yellow crystals (yields 38—47%) (cf. Table 1).

REFERENCES

[1] M. A. Hassan, A. A. Afifi and S. H. Eltamany, *Pakistan J. Sci. Ind. Res.*, **20**, 79 (1977).

[2] A. Sammour, A. Raouf, M. Elkassaby, and M. A. Hassan, *J. Prakt. Chem.*, **315**, 1175 (1973).

[3] A. Sammour, A. Raouf, M. Elkassaby, and M. A. Hassan, *Acta Chim. Acad. Sci. Hung.*, **83**, 209 (1974).

[4] V. K. Mahesh, and R. S. Gupta, *Indian J. Chem.*, **12**, 956 (1974).

Revue Roumaine de Chimie, 29, 9 – 10, 773–788 (1984)

NEW SOLVENT SYSTEMS FOR ACRYLIC COPOLYMERS*

F. SĂNDESCU[a] and CR. I. SIMIONESCU[b]
[a]Industrial Central for Chemical Fibres and Yarns, Săvineşti, Romania
[b]Institute of Macromolecular Chemistry "P. Poni", Iaşi, Romania

Received October 11, 1983

The properties of $CP/CE/H_2O$ ternary systems have been studied, establishing their optimal compositions as solvents for acrylic copolymers.

The study of the rheological, optical and spinning properties of the polymer solutions prepared with these solvents evidences the fact that these solutions contain a higher amount of polymer at similar values of the absolute viscosity and may be processed at higher velocities and lower temperatures as compared to the solutions obtained on the basis of the reference solvent CE/H_2O.

INTRODUCTION

The aqueous solutions of ethyleneglycol carbonate (CE) with a concentration of 85–87% is the solvent used for producing certain types of acrylic fibres. It presents important industrial advantages such as a low cost price in comparison with other solvents, easy handling owing to its reduced toxicity, possibilities of recuperation of wet wastes, etc.[1]

On the other hand, the limited solving capacity of CE/H_2O with respect to acrylic copolymers requires some restrictions related to the selection of solving and spinning parameters.

This is the reason why the attention was focused on the study of new solvent systems with an increased capacity of solving acrylic copolymers and whose behaviour during spinning is closer to that of solutions of copolymers in DMF. Consideration has been given to the ternary solvent 1,2 propyleneglycol carbonate/ethyleneglycol carbonate/H_2O ($CP/CE/H_2O$).[7,8]

EXPERIMENTAL

First the binary solvent systems CP/H_2O and CP/CE were studied. The behaviour of the binary system CE/H_2O is known from literature [1–6,13,14]. The optimal miscibility limits were established for the binary systems studied and on this basis the ternary system $CP/CE/H_2O$ was investigated.

---

* Paper presented at the 29th Symposium of Macromolecules, IUPAC, Bucharest, September 5–9, 1983.

RESULTS AND DISCUSSIONS

THE BINARY SYSTEM CP/H_2O

The limited solubility in CP/H_2O can be accounted for in terms of the structural characteristics of its molecule. The volume of the CP molecule is larger than that of the CE molecule and this probably results in a more reduced stability of the CP hydrated complexes in comparison with those of CE. Several authors point out the relationship between the solvation effect and the mobility of ions. However, they are at the same time in favour of a careful interpretation of these results since besides solvent molecules in a first sphere, there are other molecules of a second or even of a more distant one.[11] On the other hand, the information concerning viscosity, density and refraction index enables a qualitative evaluation of the hydrogen linkage association between components.[11]

The data referring to the binary system CP/H_2O, from which one may infer that the optimal miscibility range corresponds in this case to the ratio (4 : 96), are presented in Fig. 1. The difference from the system CE/H_2O (where the optimal range corresponds to 87 : 13) is evident and can be explained in terms of the larger volume of the CP molecule, which results in a reduced stability of the CP hydrated complexes in comparison with those of CE.

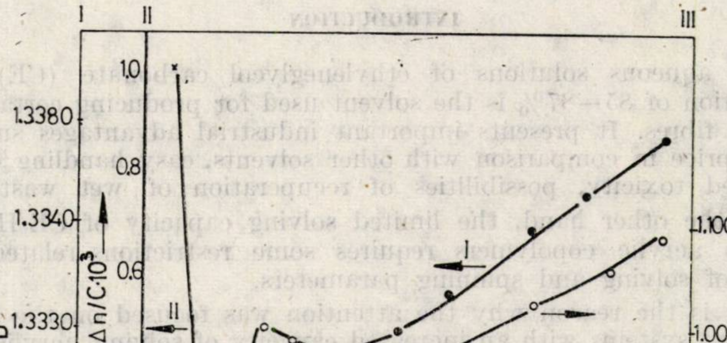

Fig. 1. — The variation of the refraction index and of density as a function of the concentration of the aqueous solutions of CP at 70°C.
(● — ●) — the integral curve for the refraction index ; (x — x) — the differential curve ; (○ — ○) — the curve of density variation.

THE BINARY SYSTEM CP/CE

The fact that the two components can be mixed on the whole range of concentrations may be explained in accordance with the mixotrope series : two solvents are the more miscible with each other, the more their chemical structures resemble.[11]

The phenomenon of mutual dissolution implies the appearance of certain attraction forces between the two types of molecules ; the component A may dissolve into B only if the attraction forces among the molecules of either A or B are smaller or equal to the forces of attraction between the molecules of A and B. Conversely, miscibility decreases considerably. These intermolecular forces, also known as van der Waals forces, are forces of orientation, induction and dispersion and increase with the dipole moment and molecule polarizability.[11]

$$F_0 = \frac{2\mu_1^2 \mu_2^2}{3K.Tr^6} \tag{1}$$

$$F_i = \frac{2\alpha \mu^2}{r^6} \tag{2}$$

$$F_d = \frac{3\alpha^2 I}{4 r^6} \tag{3}$$

where F_0, F_i, F_d are the forces of orientation, induction and dispersion, respectively, μ_1, μ_2 are the values of the electric dipole moments, α is the molecule polarizability, K is Boltzmann's constant, T is the absolute temperature, I is the ionization energy and r is the distance between the two electric charges in the molecule.

The molecular polarizability can be determined from the refractometric data on the basis of Lorenz-Lorenz law [11,12] :

$$R_m = \frac{n^2 - 1}{n^2 + 2} \cdot \frac{M}{d} = \frac{4}{3} \pi \alpha N \tag{4}$$

where R_m is the molecular refraction, n is the refraction index, M is the molecular mass, d is the density, N is Avogadro's number and α is the molecule polarizability.

By introducing $k = \frac{3}{4\pi N}$ (5) in relationship (4) follows :

$$\alpha = k \cdot R_m \tag{6}$$

The molecular polarizability increases in direct proportion with molecular refraction, which can be explained by the fact that the molecular refraction in visible spectrum characterizes electron movements in the molecule.[10-12]

The inductive effect of CH_3 in the CP molecule confers it a more accentuated polar character in comparison with the CE molecule :

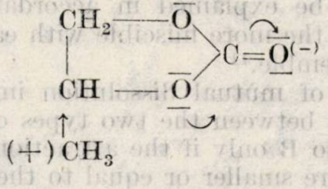

Experimental refractometric measurements confirm the higher values of the molecular refraction in the case of CP as compared with CE and, consequently, the more accentuated polarizability of the former. This is presented in Table 1.

Table 1

Molecular refraction for CP and CE, calculated from experimental data at 70°C

Solvent	CP	CE
R_m(70°C)	21.84	17.42

The behaviour of the binary system CP/CE also results from the data presented in Fig. 2 and Fig. 3. The inflexion points and the minima on the curves correspond to 10, 20, 40 and 60% CP in CE ; these concentrations may also be observed on the diagram illustrating the variation of the specific refraction with the composition of the mixture presented

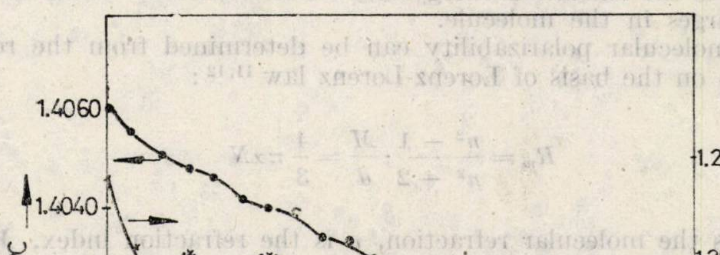

Fig. 2. — The variation of the refraction index and density for CP/CE binary systems at 70°C.

in Fig. 4. The specific refraction, r, was calculated from the experimental data, using the following formula:

$$r = \frac{n^2 - 1}{n^2 + 2} \cdot \frac{1}{d} \tag{7}$$

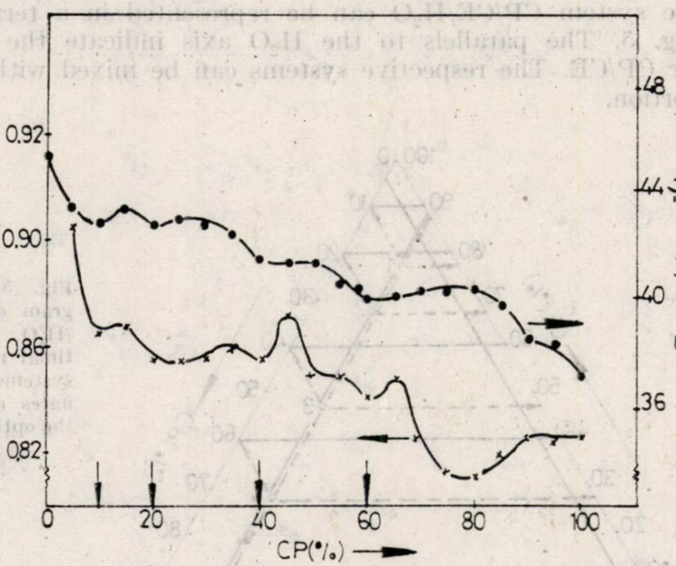

Fig. 3. — The variation of viscosity and surface tension for CP/CE binary systems at 70°C.

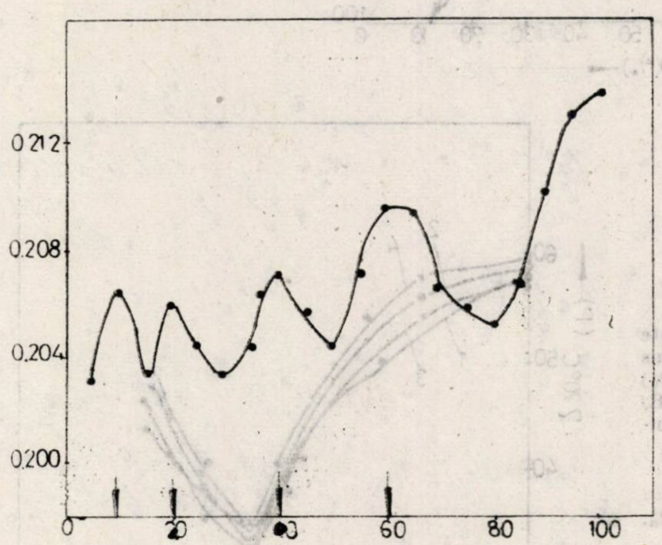

Fig. 4. — The variation of the specific refraction as a function of CP/CE mixture composition.

The maximal values of r, correlated with the values of α indicate the increase of intermolecular forces in the case of the respective compositions.

THE TERNARY SYSTEM CP/CE/H_2O

After having determined the optimal miscibility ranges of the binary systems and taking into account the information provided by references,[13-14] according to which in the case of CE/H_2O the optimal ratio is 87 : 13, the system CP/CE/H_2O can be represented in a ternary diagram as in Fig. 5. The parallels to the H_2O axis indicate the optimal miscibility for CP/CE. The respective systems can be mixed with water in any proportion.

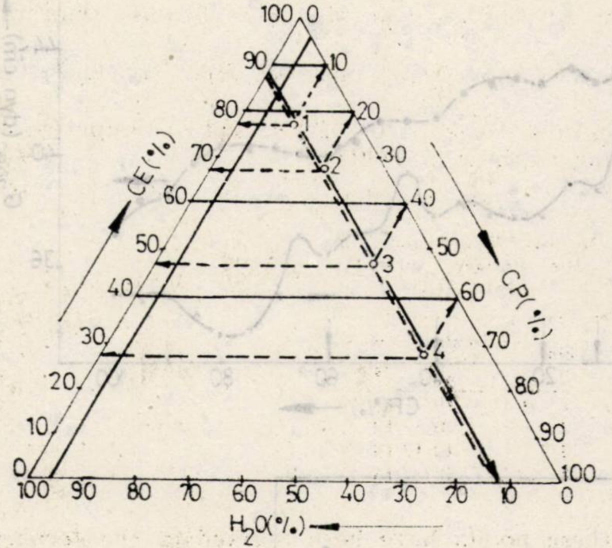

Fig. 5. — The ternary diagram of the system CP/CE//H_2O. —— the domains of optimal miscibility of the binary systems; — — — the coordinates of the points marking the optimal solvents for acrylic copolymers.

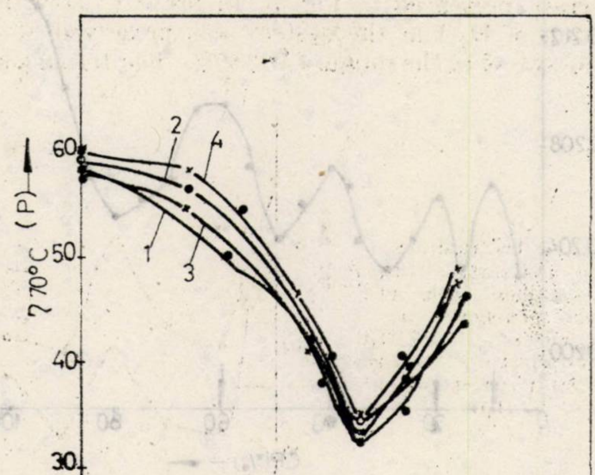

Fig. 6. — The absolute viscosity of some solutions of acrylic copolymer (14%) in ternary solvent CP/CE//H_2O with different compositions: 1 — CP = 10%; 2— CP = 20%; 3— ;CP = = 40%; 4 — CP = 60%.

In order to establish the proportions in which the ternary system CP/CE/H_2O is an adequate solvent for PAN and its copolymers, equiconcentrated solutions were prepared and their absolute viscosities were determined. The same content of CP in the system at the above-established concentrations was preserved, varying the amount of water and adding complementary amounts of CE.

The amount of water did not exceed 18% because above this concentration, no matter what the value of the CP/CE ratio is, polymer solvation becomes slow and the viscosities of the solutions are increasingly higher, as shown in Fig. 6. The data in Fig. 6 point out the following:

— the binary systems CP/CE are less adequate solvents than the ternary ones;

— for all the ternary systems, the optimal H_2O concentration is 13%.

Consequently, the optimal solvents for PAN and its copolymers have compositions according to those in Table 2.

Table 2

Optimal compositions for the ternary solvent CP/CE/H_2O.

No.	Composition of CP/CE/H_2O
1.	10/77/13
2.	20/67/13
3.	40/47/13
4.	60/27/13

The coordinates of these points have been marked in the ternary diagram presented in Fig. 5. In order to confirm these data, the concentration of H_2O in the system was preserved at 13%, whereas the CP/CE ratio varied in the range of 0—80%. The ternary systems thus obtained were

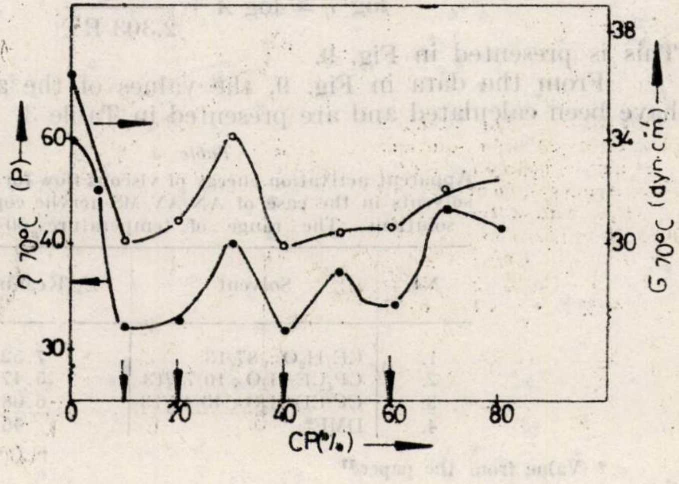

Fig. 7. — The absolute viscosity and surface tension of solutions with 14% acrylic copolymer as a function of CP/CE/H_2O ternary mixture composition for a content of 13% H_2O.

subsequently used for preparing several equiconcentrated polymer solutions whose absolute viscosities and surface tensions were determined and represented in Fig. 7.

From the data presented here, the following conclusions can be drawn :

— In the case of the binary solvent CE/H_2O (87 : 13), the polymer solutions present higher viscosity as compared with the equiconcentrated solutions in ternary solvent.

— By correlating the data concerning the surface tension of polymer solutions with spinnability, [9, 13, 15, 16] it is expected that the surface tension values observed in the case of polymer-ternary solvent solutions should result in a better spinnability in comparison with equivalent solutions of polymer in CE/H_2O.

THE STUDY OF THE $CP/CE/H_2O$ TERNARY SYSTEM PROPERTIES AT OPTIMAL COMPOSITION

RHEOLOGICAL PROPERTIES

The flow properties of the solutions constituted by acrylic copolymers and CE/H_2O were dealt with in a previous paper.[17] In the following section we propose to study the polymer/$CP/CE/H_2O$ systems, particularly two cases of mixture proportions : 10/77/13 and 40/47/13.

In this study a Rheotest RV viscometer was used. The analysed solutions were prepared by using a ternary copolymer of acrylonitrile — vinyl acetate — α—methyl styrene (AN/VA/MS).

The flow diagrams, in double logarithmic plot ($\log\eta/\log\dot{\gamma}$), for the two solvents mentioned above and compared with the reference solvent CE/H_2O ($T = 70°C$), are presented in Fig. 8. The flow curves of the three types of solution show that the viscosity of the solutions of polymer in CE/H_2O is higher than that of the solutions of polymer in $CP/CE/H_2O$ over the whole range of concentrations and shear rates investigated.

The quantitative evaluation of the three types of solutions was made in terms of the apparent activation energy of viscous flow, calculated as the slope of the straight line :

$$\log \eta = \log A + \frac{E_k}{2.303\ RT} \qquad (8)$$

This is presented in Fig. 9.

From the data in Fig. 9, the values of the activation energy, E_k, have been calculated and are presented in Table 3.

Table 3

Apparent activation energy of viscous flow for various solvents in the case of AN/AV/MS acrylic copolymer solutions. The range of temperature 50—80°C

No.	Solvent	E_k(Kcal.mol^{-1})
1.	CE/H_2O : 87/13	7.52
2.	$CP/CE/H_2O$: 10/77/13	5.47
3.	$CP/CE/H_2O$: 40/47/13	6.08
4.	DMF*	45

* Value from the paper [17]

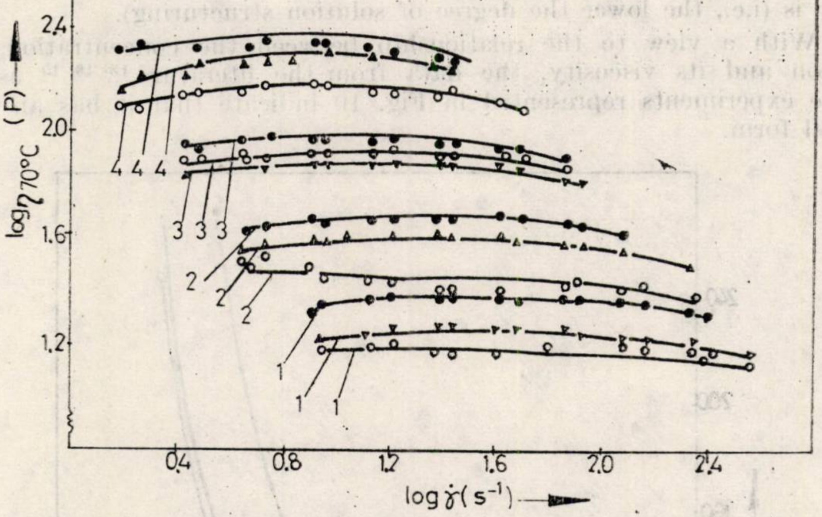

Fig. 8. — Flow curves for equiconcentrated solutions in the following solvents : (● — ●) — CE/H_2O : 87/13 ; (○ — ○) — $CP/CE/H_2O$: 10/77/13 ; (Δ — Δ) — $CP/CE/H_2O$: 40/47/13 and for the following polymer concentrations : 1 — 12 % ; 2 — 14 % ; 3 — 16 % ; 4 — 18 %.

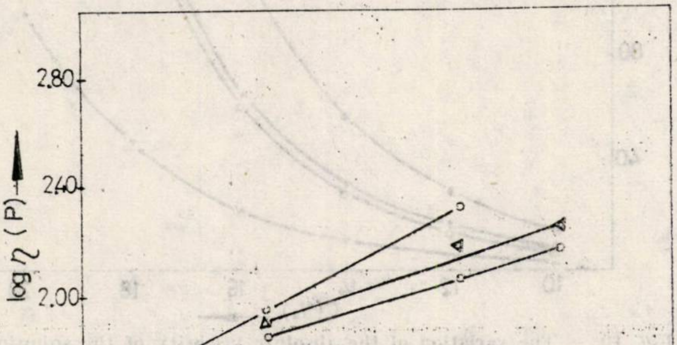

Fig. 9. — The determination of the apparent activation energy of viscous flow for solutions with 16 % AN/AV/MS ternary copolymer. (● — ●) — CE/H_2O : 87/13 ; (○ — ○) — $CP/CE/H_2O$: 10/77/13 ; Δ — Δ — $CP/CE/H_2O$: 40/47/10.

The different values of E_k in the four solvents are due to both the activation energy of each solvent and the different structures of the polymer solutions formed with the respective solvents. It is generally admitted that the activation energy, E_k, is the lower, the lower the solution viscosity is (i.e., the lower the degree of solution structuring).

With a view to the relationship between the concentration of a solution and its viscosity, the data from the literature,[13, 18, 19] as well as the experiments represented in Fig. 10 indicate that it has an exponential form.

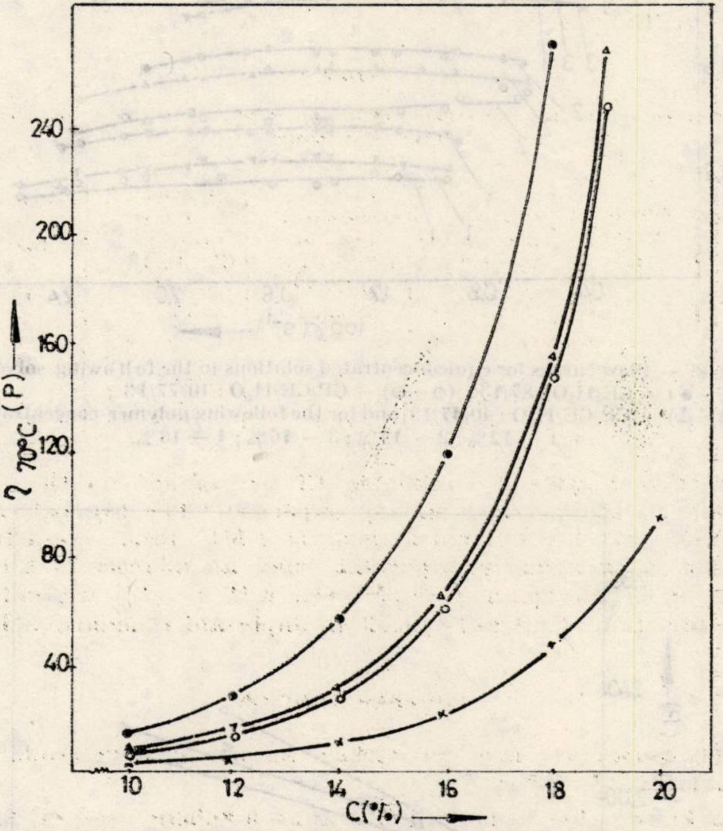

Fig. 10. — The variation of the absolute viscosity of the spinning solution as a function of concentration for :
(● — ●) — CE/H_2O : 87/13 ; (o—o) — $CP/CE/H_2O$: 10/77/13 ;
(△—△) — $CP/CE/H_2O$: 40/47/13 ; (x—x) — DMF.

There is a relationship between the increase of a solution viscosity and the change in the flow mechanism, which is determined by the increase of the number of links appearing among molecular aggregates. The literature mentions the formation of the fluctuating networks within concentrated solutions and whose movement is conditioned by energy barriers.[20] The amount of polymer chains becomes comparable with the amount of solvent molecules and there appears a competition between macromolecular chains concerning the interaction with the solvent molecules. This leads to the modification of the level of the energetic interactions existing among the molecules which were not solvated by the solvent. The establishment of a relationship between the viscosity of the polymer solution and its concentration presents interest from a practical point of view, as the increase of polymer concentration results in the decrease of the amount of solution, as well as the growth of unit productivity.

From the data in Fig. 10 one can determine the concentrations corresponding to every solvent for a certain level of absolute viscosity, as presented in Table 4.

Table 4

Polymer concentrations corresponding to the respective solvents for a certain level of viscosity

No.	Absolute viscosity (p)	Polymer concentration in CE/H_2O (%)	Polymer concentration in $CP/CE/H_2O$ 10/77/13 (%)	Polymer concentration in $CP/CE/H_2O$ 40/47/13 (%)	Polymer concentration in DMF (%)
1.	40	13	14.9	14.6	17.5
2.	60	14.1	16.0	15.5	18.6
3.	80	14.9	16.6	16.4	19.4

The solvent systems containing CP are almost on the same level with regard to the polymer solving capacity. They are better solvents than CE/H_2O (87 : 13), but not as good as DMF. From a practical point of view this is particularly important, since an increase of the polymer concentration in the spinning dope, even with 1–2%, without a subsequent modification of viscosity, leads to important economic achievments.

SURFACE TENSION

Some researchers consider surface tension as a determining factor for spinnability.[9, 15, 16, 23–28]

It is known that in normal conditions a spheric drop of fluid can be elongated within the limits of $\pi/2$ of its initial diameter. By continuing the elongation beyond the limit mentioned above, the fluid drop breaks into smaller drops that have a marked tendency to assume a spheric shape, since this geometric form is characterized by minimal surface tension.

If the kinetic energy of the fluid is sufficiently high, the drop tends to assume a cylindric, elongated form that is stable only in specific conditions. The value of the energy barrier, E, necessary for passing from the cylindric to the spheric form is given by the following formula :

$$E = 2\sigma \cdot \Pi \cdot r^2 \tag{9}$$

where σ is the surface tension of the polymer solution ($\text{dyn} \cdot \text{cm}^{-1}$) and r is the spinnerette channel radius (cm).

Other authors [13] consider spinnability as the capacity of axial deformation of a fluid without loss of compactness. The velocity of the deformation is equivalent to that of flow in determined conditions.

Consequently, after having exceeded the energy barrier necessary for passing from the cylindric to the spheric form, the life of the cylindric filament will be determined by the ratio between viscosity and surface tension, which is responsible for the thinning of the cylinder. The critical velocity of forming filaments of length l is given by the following formula :

$$V_{cr} = \frac{2\pi}{3\eta} \cdot \frac{l}{d_f} \tag{10}$$

where η is the viscosity of the polymer solution ($\text{g} \cdot \text{cm}^{-1} \cdot \text{s}^{-1}$) and d_f is the diameter of the filament (cm). Formula (10) can be used when calculating the minimal viscosity of polymer solutions such that they satisfy the condition of spinnability.

The study of the surface tension of polymer melts and solutions is a relatively new field that has developed only in recent years and is very important for the study of certain properties related to polymer processing. Polymers are characterized by lower values of the surface tension in comparison with micromolecular substances. These values decrease with the increase of the relative molecular mass.

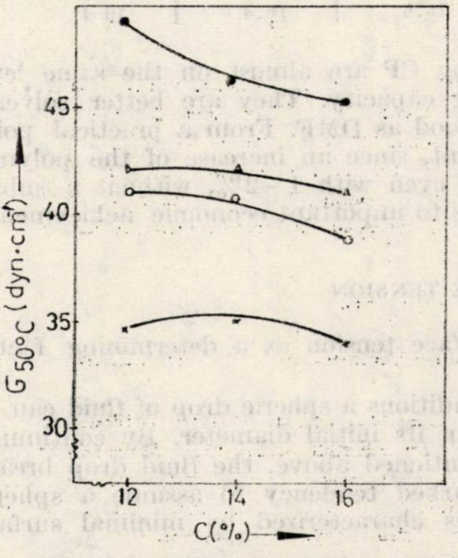

Fig. 11. — The surface tension of solutions of AN/AV/MS copolymers in various solvents and at various concentrations.
(● — ●) — CE/H_2O : 87/13 ; (o — o) — $CP/CE/H_2O$: 10/77/13 ; (△ — △) — $CP/CE/H_2O$: 40/47/13 ; (x — x) — DMF.

The decrease of the surface tension is due to the reduction of the surface enthropy, which, in its turn, is determined by the fact that the chain mobility is limited by conformation and configuration reasons.[21]

In the case of the solvents containing CP, the experimental measurements present values situated between CE/H_2O and DMF. This is represented in Fig. 11.

Based on the data presented in Fig. 10 and Fig. 11 and by means of formulae (9) and (10), the values of the energy barriers to be exceeded during spinning processes, as well as the critical velocities of producing filaments of length $l = 1$ m from polymer solutions (concentration 16%) have been calculated. These values refer to the extrusion through a spinnerette whose channel diameter is of 80 μ and the data thus obtained are presented in Table 5.

Table 5

The values of the energetic barrier, E, and of the critical velocity of formation of filaments in the spinning process ; $l = 1$ m ; $d_f = 80 \cdot 10^{-6}$m ; $C_{polymer} = 16\%$.

Solvent/ Parameter	CE/H_2O 87/13	$CP/CE/H_2O$ 40/47/13	$CP/CE/H_2O$ 10/77/13	DMF
E (erg.10^2)	4.52	4.12	3.90	3.42
V_{cr}(m/s)	30.43	53.6	56.2	135.7

It can be noted that the solvents containing CP have advantageous properties in comparison with CE/H_2O, with respect to both the energy barrier and the velocity of forming filaments, though they do not equal the performance of DMF.

GELATION TEMPERATURE

The physic and structural behaviour of polymer systems can be described in terms of thermodynamic laws. The change in the variation with temperature of certain mechanic, electric or optical properties indicates the change of the character of particles movements or the shift of a thermodynamic system from one state to another.[22]

In the present case, the variation of optical and flow properties are studied.

The curves indicating the variation of the refraction index of polymer solutions with temperature present several inflexion points and the curves associated with the variation of turbidity with the same parameter present maxima. The temperatures corresponding to modifications of optical properties may be interpreted as changes of the state of polymer solutions, not in the sense of phase transitions, but as structural transformations. The temperatures corresponding to the modification of the optical properties of polymer solutions are presented in Table 6.

The temperatures in Table 6 should be interpreted as boundary domains between two structural states of the polymer solutions. It can be observed that the domains move towards lower values with the increase of the amount of CP in the solvent.

With a view to the flow properties of the studied solutions, we found out the following (Fig. 12) :

— the solutions present an inferior temperature limit below which the flow does not occur any more, the solutions being gelated. These temperatures are marked by the dotted line in Fig. 12.

— the curves representing the variation of viscosity with temperature present inflexion points which can be interpreted as optimal temperatures for the processing of these solutions. The corresponding values are presented in Table 7. The increase of temperature above

Table 6

Temperatures at which the modifications of the optical properties of polymer solutions occur (°C)

Solvent Method of study	CE/H_2O 87/13	CP/CE/H_2O 10/77/13	CP/CE/H_2O 40/47/13
Variation of the refraction index with temperature	32	27.5	24
Variation of the turbidity with temperature	33	26	22.5

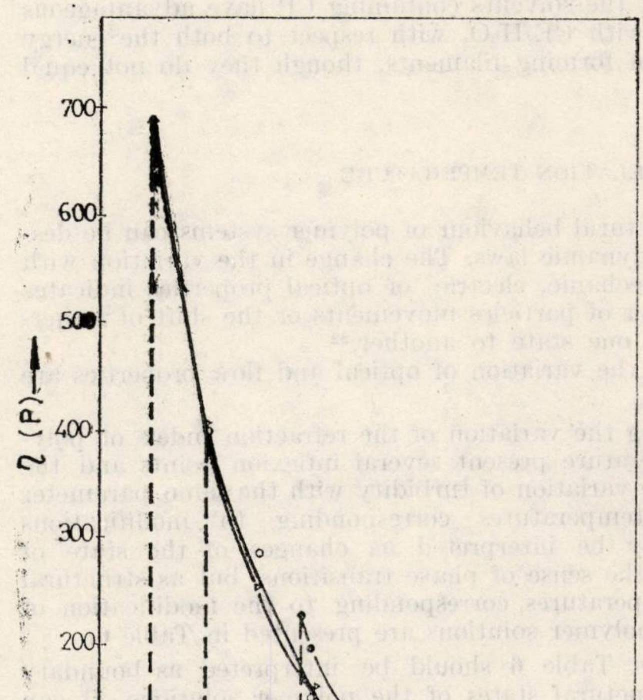

Fig. 12. — The variation of the absolute viscosity with temperature in the case of equiconcentrated polymer solutions. (● — ●) — CE/H_2O : 87/13; (○ — ○) — CP/CE/H_2O : 10/77/13; (△ — △) — CP/CE/H_2O : 40/47/10.

this limit has no sense for the processing of these solutions since flow properties change insignificantly. Lower temperatures are not indicated since minor temperature variations lead to major viscosity variations.

Table 7

Temperatures limiting the flow and optimal temperatures for spinning polymer solutions (°C)

Solvent / Method of study	CE/H_2O 87/13	$CP/CE/H_2O$ 10/77/13	$CP/CE/H_2O$ 40/47/13
Temperature limiting the flow	38	20	10
Optimal temperature for spinning	50	37	24

A certain discordance between the temperature limiting the flow of polymer solutions and those at which the sense of the variation of optical properties changes, can be observed. This difference is positive for CE/H_2O and negative for $CP/CE/H_2O$ and increases with the content of CP in the system. This may be explained by the difference in the elastic properties of polymer solutions : in the case of the systems CE/H_2O the flow stops before visible structural modifications occur, whereas in the systems $CP/CE/H_2O$ the elasticity reserves of the solutions allow the occurrence of flow even below the temperatures at which structural modifications of the system have been observed.

The temperatures given in Table 7 are particularly useful from the technological point of view and confirm the fact that the use of solvents containing CP is also advantageous with respect to energy, allowing spinning at temperatures lower than those used in the case of CE/H_2O solvents.

CONCLUSIONS

1. The properties of $CP/CE/H_2O$ ternary systems have been studied and their optimal compositions as solvents for PAN and its copolymers have been established.

2. At similar values of the absolute viscosity, the solutions of polymer in $CP/CE/H_2O$ solvents contain 10–15% more polymer comparatively with solutions based on CE/H_2O.

3. The spinnability of the solutions of polymer in $CP/CE/H_2O$ solvents is superior to that of equivalent solutions based on CE/H_2O, this resulting in the possibility of increase of spinning velocities.

4. The presence of CP in the $CP/CE/H_2O$ ternary solvent allows for the substantial lowering of the temperatures necessary for the processing of polymer solutions.

5. The advantages enumerated at points 2–4 have particularly positive consequences, not only economic, but also with respect to the quality of the resulted fibres.

REFERENCES

[1] M. Ionescu et al. (CFS Săvineşti), RDG Pat. no. 52814, December 20, 1966.

[2] M. Gilman and S. Hooper (Ind. Rayon Corp.), France Pat. no. 1 092 674, April 26, 1955.

[3] J. M. Terpay (Ind. Rayon Corp.), France Pat. no. 1 065 710, May 20, 1954.

[4] J. M. Terpay (Ind. Rayon Corp.), France Pat. no. 1 090 816, April 4, 1955.

[5] H. Bruson and G. S. Hooper (Ind. Rayon Corp.), France Pat. no. 1 038 663, September 30, 1953.

[6] G. A. McFarren (Ind. Rayon Corp.), France Pat. no. 1 043 100, November 5, 1953.

[7] F. Săndescu (CFS Săvineşti), Brevet RSR, no.79 698, May 25, 1982.

[8] F. Săndescu (CFS Săvineşti), Brevet RSR, no. 79 699, May 24, 1982.

[9] H. F. Mark, S. M. Atlas and E. Cernia, "Man-made fibres", vol. I, Interscience Publ., New York, 1967.

[10] C. D. Nenițescu, "Chimie organică", vol. I—II, Ed. Didactică şi Pedagogică, Bucharest, 1975.

[11] M. Răileanu, "Rolul solvenților în reacțiile compuşilor organici", Ed. Scrisul Românesc, Craiova, 1976.

[12] K. Ladislau, "Analiza fizico-chimică", Ed. Didactică şi Pedagogică, Bucharest, 1969.

[13] S. P. Papkov, "Fiziko-himiceskie osnovy iskustvennyh, i sinteticeskih volokon", Ed. Himia, Moskow, 1972.

[14] A. A. Tager, *Vysokomol. Soedineniya*, **13**, 2 (1971).

[15] A. Ziabicki, *Him. Volokna*, **2**, 8 (1964).

[16] A. Ziabicki, "Fundamentals of Fibre Formation", Interscience Publ., London, New York, 1976.

[17] F. Săndescu and D. Feldman, *Acta Polymerica* **30**, 166 (1979).

[18] K. E. Perepelkin, "Karbotsepnye sinteticeskie volokna", Ed. Himia, Moskow, 1973.

[19] F. N. Kelly and F. Bueche, *J. Pol. Sci.* **50**, 549 (1961).

[20] V. G. Aldoşin and S. I. Frenkel, *Vysokomol. Soedineniya*, **4**, 116 (1962).

[21] W. Berger, K. Olbricht and H. W. Kammer, *Faserforsch. u. Textiltechnik*, **27**, 9(1976).

[22] I. Petrea, "Termodinamica statistică a macromoleculelor", Ed. Didactică şi Pedagogică, Bucharest, 1968.

[23] E. M. Beplodrov and T. I. Sumakov, *Zavodskaia laboratoria*, **12**, 1483, (1971).

[24] H. W. Kammer, *Faserforsch. u. Textiltechnik*, **28**, 27 (1977).

[25] C. Michels, *Faserforsch. u. Textiltechnik*, **27**, 639 (1976).

[26] E. Helfand, *Macromolecules*, **9**, 307 (1976).

[27] T. Weber and E. Helfand, *Macromolecules*, **9**, 311 (1976).

[28] B. V. Ozerovski, I. V. Kalmykov, U. G. Gaturov and V. P. Rosheiupkin, *Vysokomol. Soedineniya* (**A 19**), 1437 (1977).

Revue Roumaine de Chimie, **29**, *9 – 10*, 789–792 (1984)

A CORRELATION OF LATTICE ENERGY AND EQUILIBRIUM INTERIONIC DISTANCE OF ALKALI METAL HYDRIDES

M. M. HUSAIN, D. K. SINGH and O. P. MATHUR
Chemistry Department, Lucknow University,
Lucknow — 226007, U.P., India

Received December 7, 1983

A general relation involving the lattice energy, U_0, and equilibrium interionic distance, r_0, has been proposed for alkali metal hydrides. The observed product, U_0r_0, is nearly constant with an average value of 482 kcal.mole^{-1}. Å. Likewise, the statistical analysis reveals a satisfactory linear relationship between U_0 and $1/r_0$ data. The lattice energy, U_0, of francium hydride, obtained from the two relations has been found to be 149 and 153 kcal.mole^{-1} respectively.

INTRODUCTION

The lattice energy, U_0, relations with various physico-chemical properties viz., absolute melting point [1,2](T_m), absolute boiling point [1](T_b), equilibrium interionic distance [3,4] (r_0), molar entropy[3,4] (S°) and coefficient of thermal expansion [5](α) in some well-defined groups of similar inorganic compounds have been reported earlier from this laboratory.

In view of a ready interaction of solid alkali metal hydrides with atmospheric moisture, the experimental studies on most of their physical properties appear to lack in literature. Probably, on account of this limitation, theoretical estimates of different useful data in the case of these compounds have been reported by various workers.[6-9] As such, it seems desirable to examine a general dependence of lattice energy, U_0, data on their appropriate lattice properties. A $U_0 - r_0$ relationship of this interest has, therefore, been investigated in the compact family of ionic compounds,[11] comprising hydrides of alkali metals.

RESULTS AND DISCUSSION

The fact that lattice energy, U_0, for different members of a family of similar ionic compounds is inversely proportional to the corresponding equilibrium distance of counter ions, r_0, tends to observe a fair constancy of the product, U_0r_0. The maintenance of such a trend viz.,

$$U_0r_0 \approx \text{constant} \tag{i}$$

has been reported for alkali metal halides,[3] alkali metal hydroxides[1] and alkaline earth halides.[4]

In order to examine the validity of eqn (i) in the family of alkali metal hydrides, the required data [10] on U_0 and r_0^* together with their corresponding products of U_0r_0 are summarized in Table 1.

One may further estimate the product, U_0r_0, from the existing data on Born exponents,[11] n, in the case of the concerned hydrides by the following equation :

$$U_0 = \frac{Ae^2N}{r_0}\left(1 - \frac{1}{n}\right) \tag{ii}$$

where different terms used have the usual meaning. The Madelung constant, A, of alkali hydride crystals is assumed to be the same as that of NaCl crystal, since all of them possess sodium chloride type lattices. Thus, the theoretically estimated products, U_0r_0, for concerned hydrides have been derived from eqn (ii) by using the following constants : $A = 1.748$; $n = 5.24$ (NaH), 5.85 (KH), 6.63 (RbH) and 6.97 (CsH). On the basis of this alternative treatment, the values of U_0r_0 of NaH to CsH in terms of kcal.mole^{-1}. Å are also shown in Table 1.

Table 1

Product of U_0 and r_0 of alkali metal hydrides

Alkali hydride *	U_0 (k cal.mole^{-1})	r_0 (Å)	U_0r_0** (kcal.mole^{-1}.Å)
NaH	193	2.44	471(468)
KH	165	2.85	470(479)
RbH	162	3.02	489(491)
CsH	156	3.19	498(495)
		Average	482(483)

* LiH is excluded in the present study, since Li$^+$ ion is wellknown to have characteristic differences from other alkali metal cations. This is also evident from its lower value of $U_0r_0 \approx 448$ kcal.mole^{-1}.Å and the vitiated behaviour of LiH in Fig. 1 as compared to the remaining alkali hydrides.

** The observed values U_0r_0 preceding parentheses are according to eqn (i) while those within parentheses refer to those obtained from eqn (ii) taking into account their Born exponents, n.

A comparative account of the products, U_0r_0, obtained from eqns (i) and (ii) for different alkali hydrides may be seen from Table 1. One may note a similar trend of the constancy of U_0r_0 in the two cases. The average values of U_0r_0 from the two different approaches aie found to be approximately 482 kcal.mole^{-1}, Å and 483 kcal.mole^{-1}.Å respectively. The corresponding U_0r_0 values observed from the two view points of each hydride appear to be in close agreement. The maximum and minimum deviations from the average $U_0r_0 \approx 482$ are about 2.5% and 3% respectively, whereas the respective departures from $U_0r_0 \approx 483$ are 3% and 2.5%. A general constancy of U_0r_0 in the hydrides of alkali metals thus appears to be convincingly established.

---

* The equilibrium interionic distances, r_0, are the experimentally observed values.

Moreover, it seems interesting now to compare the products, U_0r_0, for solid alkali metal halides,[3] hydroxides[1] and hydrides which are 520, 500 and 480 kcal.mole^{-1}. Å respectively. The three separate families of similar ionic compounds possessing the common alkali metal cations differ only in the anion moiety. It thus appears probable that the difference in U_0r_0 values in the case of the three groups of compounds is due to electronegativity difference of the anions concerned.

The linear relationship between the corresponding U_0 and $1r_0$ data (assuming U_0 and $\frac{1}{r_0}$ as dependent and independent variables respectively) has been worked out from the statistical approach, given by the following general form :

$$U_0 = a + b\,\frac{1}{r_0} \tag{iii}$$

in which a and b are the usual constants whose values have been obtained from the known data [10] of U_0 and r_0. Putting these values, the final form of eqn (iii) stands as under :

$$U_0 = 37.75 + 375\,\frac{1}{r_0} \tag{iv}$$

Eqn (iv) gives the values of regression coefficient (b) as 375. Further, the correlation coefficient (r) is 0.99 which shows a meaningful linear relationship between U_0 and $\frac{1}{r_0}$.

One may now demonstrate a potential utility of relations (i) and (iv) to estimate the unreported lattice energy, U_0, of FrH from the knowledge of its interionic distance, r_0. In order to compute r_0 of FrH, the logarithms of molecular weights, log M, have been plotted against the corresponding experimental r_0 values of LiH, NaH, KH, RbH and CsH. The points for different alkali metal hydrides appear to fall on a straight line, except for somewhat an anamolous behaviour in the case of LiH. This is shown in Fig. 1.

The log M of FrH =2.25 corresponds its r_0 value to be equal to 3.25 Å in Fig. 1. Assuming the validity of relation, $U_0r_0 \approx 482.5$ kcal··mole^{-1}. A (Table 1) and r_0 to be 3.25 Å gives the U_0 of FrH equal to 149 kcal.mole^{-1}. On the other hand, the statistically derived relation (iv) yields its U_0 value to be 153 kcal.mole^{-1}. Both of these estimated U_0 data are lower than U_0 of CsH (156 kcal.mole^{-1}), as one should expect from a general consideration of decreasing trend of U_0 with increasing r_0 values of alkali hydrides, down the group. Thus an inclusion of either one of the predicted U_0 values of FrH amongst the U_0 data of companion hydrides shows a normal trend. A deviation of about 3% in the U_0 values, obtained from the two proposed relations, appears to be encouraging, perhaps in lending a reasonable support to the estimated lattice energy, U_0, of francium hydride.

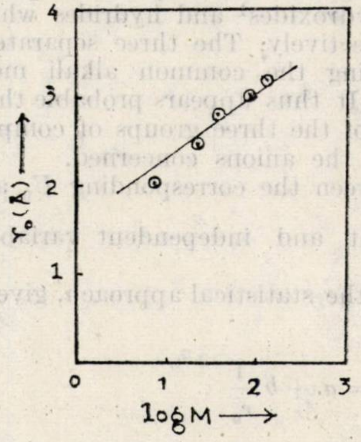

Fig. 1. — r_0 vs. log M plot of alkali metal hydrides.

ACKNOWLEDGEMENT. The authors are grateful to Prof. V. S. Misra, Head, Department of Chemistry, Lucknow University, for research facilities. (D.K.S.) is thankful to CST, U.P., Lucknow and (O.P.M.) feels obliged toUGC, New Delhi for financial support.

REFERENCES

[1] M. M. Husain, A. Gupta and D. K. Singh, *J. Indian Chem. Soc.*, **56**, 930 (1979).
[2] D. K. Singn, M. M. Husain and O. P. Mathur, *J. Indian Chem. Soc.*, **60**, 407 (1983).
[3] M. M. Husain, A. Gupta and S. N. Misra, *Z. phys. Chem.* (Frankfurt), **91**, 67 (1974).
[4] M. M. Husain, A. Gupta and S. N. Misra, *Rev. Roum. Chim.*, **24**, 809 (1979).
[5] D. K. Singh, M. M. Husain and O. P. Mathur, *J. Indian Chem. Soc.*, (In Press).
[6] L. Dass and S. C. Saxena, *Indian J. Pure appl., Phys.*, **3**, 494 (1966).
[7] C. M. Kachhava and S. C. Saxena, *Mol. Phys.*, **7**, 465 (1964).
[8] L. Dass and C. M. Kachhava, *Proc. Indian Natl. Sci. Akad.*, Part A, **43**, 110 (1977).
[9] V. Kumar and C. M. Kachhava, *Chem. Abstr.*, **74**, 46500 u (1971).
[10] Y. K. Syrkin and M. E. Dyatkina, "Structure of Molecules and the Chemical Bond", Dover Publications, Inc., New York, 1964, p. 329.
[11] J. Sherman, *Chem. Revs.*, **11**, 93 (1932).

Revue Roumaine de Chimie, **29**, *9 – 10*, 793–798 (1984)

AN ATTEMPT OF EXPLAINING HYDROGENATION/ DEHYDROGENATION OF ETHYLBENZENE-ETHYLCYCLOHEXANE ON Pd-Mn/γAl_2O_3 AND Mn/γAl_2O_3 CATALYSTS

IOAN SĂNDULESCU, VASILE PÂRVULESCU and SORIN STRAJA
Department of Chemical Technology and Catalysis, Polytechnic Institute,
Str. Polizu 1, Bucharest, Romania

Received October 10, 1983

The pulse chromatographic hydrogenation/dehydrogenation of ethylbenzene/ethylcyclohexane follows an equilibrium reaction. For the Pd–Mn/γAl_2O_3 and Mn/γAl_2O_3 catalysts both hydrogenation of ethylbenzene and dehydrogenation of ethylcyclohexane show an increasing conversion for decreasing contact times. An explanation of these unusual experimental results is attempted.

The conversion and the selectivity of the styrene hydrogenation on Pd–Mn/γAl_2O_3 catalysts, for a given Mn concentration (1.0% Mn), are functions of the interaction between the two other metals. The experimental results depending on the catalyst nature, and their selectivity and activity correlation with their structural properties have been already published.[1,2] The styrene hydrogenation presents, for the above catalysts, high conversion and selectivity to ethylbenzene, and as a by-product, ethylcyclohexane is formed in a small amount.

For these catalysts and Mn/γAl_2O_3 catalyst, the use of both ethylbenzene and ethylcyclohexane as reactant lead to an increase of the conversion for decreasing contact times. From the ethylbenzene hydrogenation over Pd–Mn/γAl_2O_3 and Mn/γAl_2O_3 catalysts under the operating conditions given in our presions paper [1] results only ethylcyclohexane. The process is reversible since from ethylcyclohexane we obtained ethylbenzene.

The aim of this paper is an attempt to explain the experimental results concerning the ethylbenzene/ethylcyclohexane hydrogenation/dehydrogenation process.

THE OPERATING CONDITIONS

We used a fixed bed, catalytic chromatographic microreactor, its length being 2.1 cm and cross sectional area 0.1 cm^2. The catalyst particle had an average diameter of 300 μm. The hydrogen was used as a carrier, and the reactant, ethylbenzene or ethylcyclohexane, was fed through single injection having an input signal with a triangular shape. We investigated the behaviour of the Pd(X%)–Mn(1.0%)/γAl_2O_3 and Mn(1.0%)/γAl_2O_3 catalysts, where X is 0.1, 0.3 and 0.5.

THE REACTOR MODEL

The mathematical model adopted [3] is that of the pseudohomogeneous dimensional isothermal reactor with axial dispersion. Because of the small radius of the catalyst particle, the effectiveness factor was assumed equal to unit. The material balance for each molecular species is :

$$\frac{\partial c_i}{\partial t} + u_z \frac{\partial c_i}{\partial z} = D_i \frac{\partial^2 c_i}{\partial z^2} + V_{Ri} \qquad (1)$$

where c_i is the concentration of the ith component, D_i and V_{Ri} are its axial dispersion coefficient and generation rate respectively, and u_z is the superficial gas velocity. The axial coordinate is denoted by z and the time by t , as usually.

The boundary conditions are :

$$c_{ie} = c_i - \frac{D_i \partial c_i}{u_z \partial z} \qquad \text{for } z = 0 \qquad (2)$$

$$D_i \frac{\partial c_i}{\partial z} = 0 \qquad \text{for } z = L \qquad (3)$$

where L is the reactor length and c_{ie} is the concentration of the ith species before entering the reactor. Equation (2) stands for the entrance condition and (3) for the exit one.

The initial conditions are :

$$c_i = c_{io} \qquad \text{for } t = 0 \qquad (4)$$

To solve the two point boundary value problem, we have discretized along the reactor axis through a five point collocation technique using orthogonal polynomials. The set of ordinary differential equations which resulted, because of its stiffness, was integrated with the Gear package. [5]

RESULTS AND DISCUSSIONS

The most surprising fact is the increase in conversion when the gas flow rate is increasing, no matter the feed of the catalytic reactor, ethylbenzene or ethylcyclohexane, as shown in Figs. 1—4.

The phenomenom observed by us is similar with that presented by Schweich and Villermaux,[6] and because every fixed bed reactor is more or less a chromatographic reactor, it aroses problems of the same nature. The variation of the axial dispersion, even between zero and infinite, cannot account for such results. From thermocouple measurements it may be asserted that temperature fluctuations can be neglected. Because of the small amount of the injected gas with respect to the hydrogen carrier, the volumetric flow rate may be taken as constant during an injection. The effect of the surface coverage, pointed out by Schweich and Villermaux,[6] has not been detected for this class of catalysts, to our knowledge.

The key to this problems seems to be the kinetic mechanism.

The stoechiometric equation is :

$$A \rightleftharpoons B + 3H_2$$

where A stands for ethylcyclohexane and B for ethylbenzene, and thus the generation rate of A is the same as for B but with the opposite sign.

We tested the usual models, their kinetic parameters being identified through a Marquardt search routine.[7] To illustrate them we have listed in Table 1 our results for Pd (0.1%)—Mn(1.0%)/γAl_2O_3 catalyst at 40°C and 62°C.

Table 1

The kinetic models analyzed for Pd(0.1%)—Mn(1.0%)/γAl_2O_3 catalyst

$$V_{RA} = 5.17\times 10^{-2}[B] - 6.23\times 10^{-3}[A] \qquad T = 40°C \qquad (5)$$

$$V_{RA} = 1.28\times 10^{-6}[B]\,[H_2) - 6.23\times 10^{-3}[A] \qquad T = 40°C \qquad (6)$$

$$V_{RA} = \frac{2.57\times 10^{-4}[B]\,[H_2] - 1.24[A]}{(1 + 10^{-2}[A] + 3.69\times 10^{-3}[B])^2} \qquad T = 40°C \qquad (7)$$

$$V_{RA} = \frac{1.61\times 10^{-3}[B]\,[H_2]}{1 + 10^{-2}B} - \frac{7.78[A]}{1 + 10^{-2}A} \qquad T = 40°C \qquad (8)$$

$$V_{RA} = \frac{1.61\times 10^{-3}[B]\,[H_2]}{1 + 1.37\times 10^{-3}[B] + 4.53\times 10^{-5}[B]^2} - \frac{7.79[A]}{1 + 1.34\times 10^{-3}[A] + 4.52\times 10^{-5}[A]^2} \quad T = 40°C \qquad (9)$$

$$V_{RA} = \frac{1.61\times 10^{-3}[B]\,[H_2]}{1 + 1.37\times 10^{-3}[B] + 1.22\times 10^{-4}[B]^2} - \frac{7.79[A]}{1 + 1.34\times 10^{-3}[A] + 1.22\times 10^{-4}[A]^2} \quad T = 62°C \qquad (10)$$

Note : V_{RA}, in mmol/m^3
Concentrations, in mmol/m^3

Table 2

The kinetic models analyzed for Mn (1.0%)/γAl_2O_3 catalyst

$$V_{RA} = \frac{1.61\times 10^{-3}[B]\,[H_2]}{1 + 1.58\times 10^{-3}[B] + 2.24\times 10^{-6}[B]^2} - \frac{7.79[A]}{1 + 1.58\times 10^{-3}[A] + 2.24\times 10^{-6}[A]^2} \qquad T = 52°C \qquad (11)$$

$$V_{RA} = \frac{1.61\times 10^{-3}[B]\,[H_2]}{1 + 1.58\times 10^{-3}[B] + 10^{-5}[B]^2} - \frac{7.79[A]}{1 + 1.58\times 10^{-3}[A] + 10^{-5}[A]^2} \qquad T = 62°C \qquad (12)$$

Note : V_{RA}, in mmol/m^3
Concentrations, in mmol/m^3

The simplest model, the reversible first order reaction, predicts a decreasing conversion when the gas flow rate increases, no matter the numerical values of the kinetic parameters. Taking the direct reaction of first order and the inverse one of second order (first order with respect to B and first order with respect to the hydrogen), we may get the desired shape of the curve relating conversion to the gas flow rate only when the reactants vary strongly. In our case the hydrogen decreases with less than 0.1%, thus the reverse reaction has a pseudo first order kinetics and there is no significant difference between the two cases presented above.

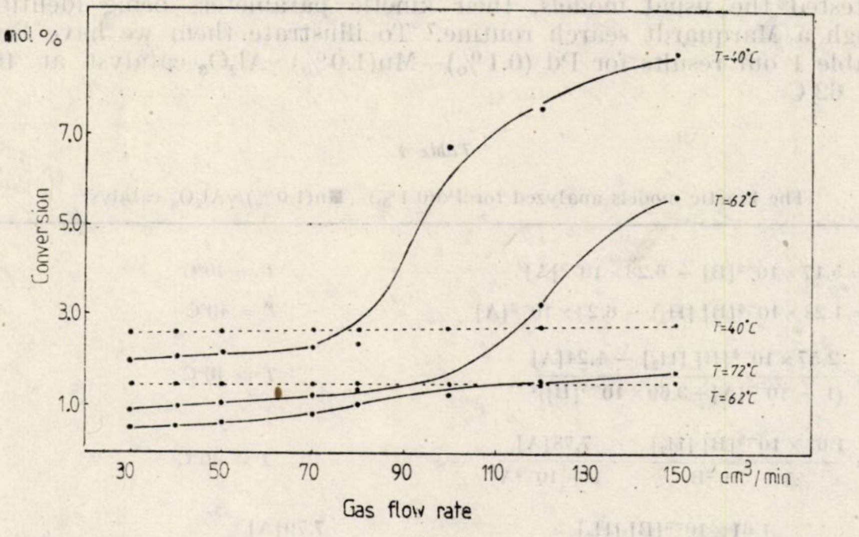

Fig. 1

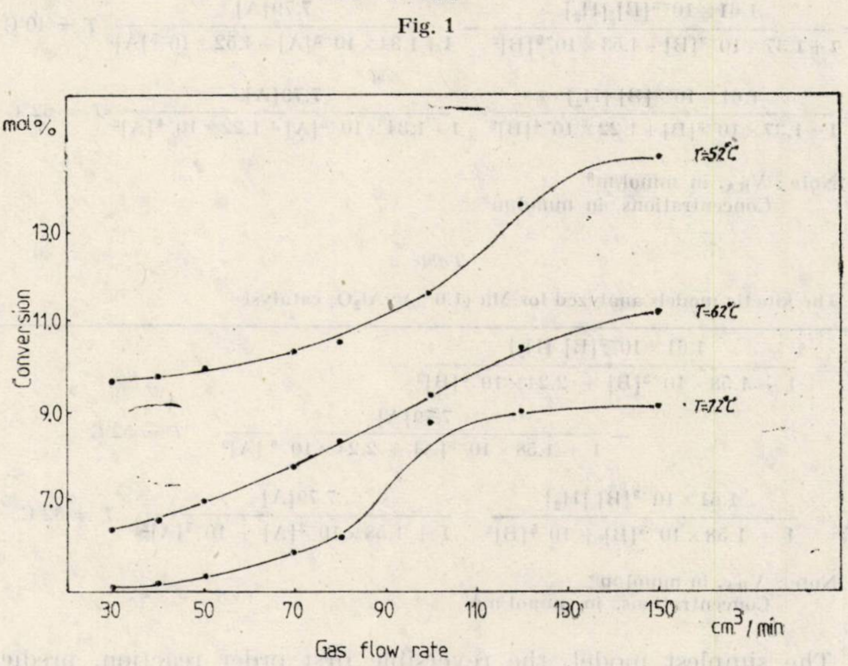

Fig. 2

Figures 1 — 4. Variation of ethylbenzene-ethylcyclohexane conversion depending on flow rate and temperature.

1. — catalyst Pd (0.1%)—Mn(1.0%)/γAl_2O_3
2. — catalyst Pd (0.3%)—Mn (1.0%)/γAl_2O_3
3. — catalyst Pd(0.5%)—Mn(1.0%)/γAl_2O_3
4. — catalyst Mn(1.0%)/γAl_2O_3

(——) experimental values ; (— —) predicted values.

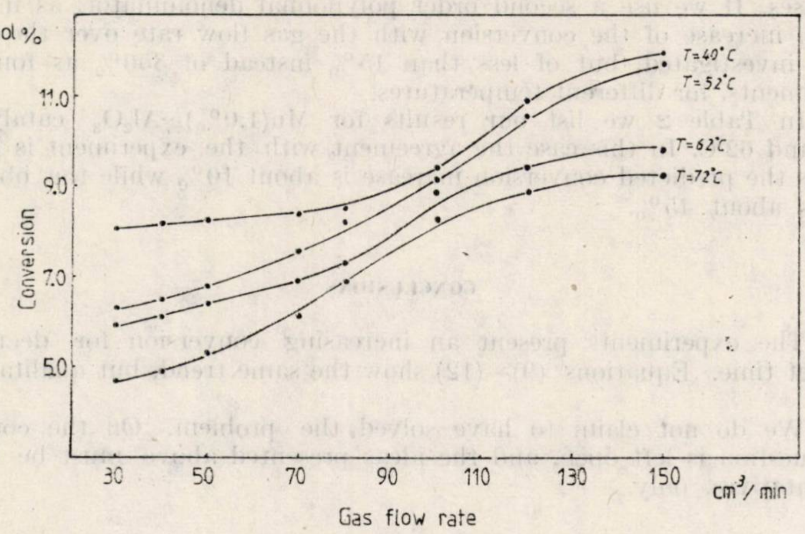

Fig. 3

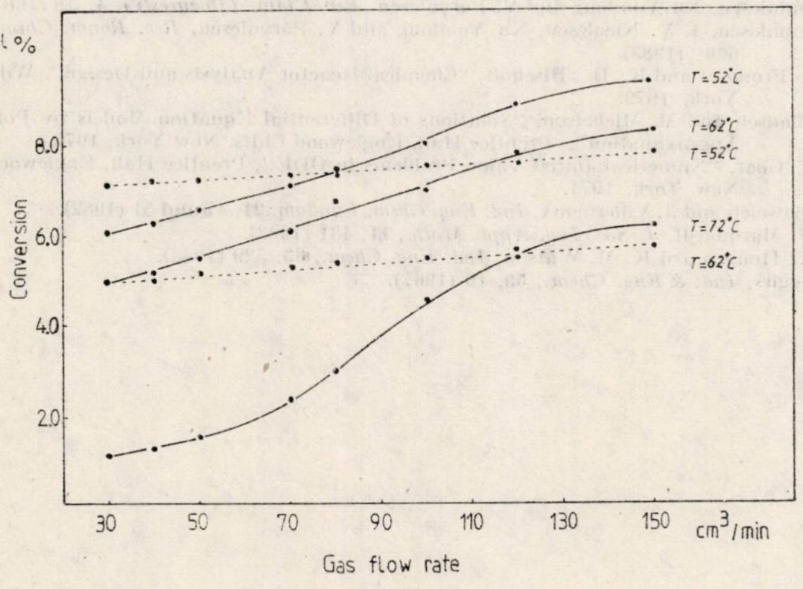

Fig. 4

Instead of the homogeneous models, introducing the kinetics of the heterogeneous catalysis,[8] the results are of the same type. Qualitatively, all of them predict an inverse dependence between the conversion and the gas flow rate than the experimental one, and must be rejected. If we adopt the Michaelis-Menten [9] kinetics for enzymatic reactions, the conversion decreases with the gas flow rate up to 70 cm^3/min, and thereafter increases. If we use a second order polynomial denominator, as in [9], we get an increase of the conversion with the gas flow rate over the whole range investigated, but of less than 15% instead of 350% as found in experiments, for different temperatures.

In Table 2 we list our results for Mn(1.0%)/γAl_2O_3 catalyst at 52°C and 62°C. In this case the agreement with the experiment is better, that is the predicted conversion increase is about 10% while the observed one is about 45%.

CONCLUSIONS

The experiments present an increasing conversion for decreasing contact time. Equations (9)—(12) show the same trend, but qualitatively, only.

We do not claim to have solved the problem. On the contrary the question is left open, and the ideas presented above must be taken, as tentatives, only.

REFERENCES

[1] I. Săndulescu, Xu Yondong and V. Pârvulescu, *Rev. Chim. (București)*, **4**, 31 (1983).

[2] I. Săndulescu, I. V. Nicolescu, Xu Yondong and V. Pârvulescu, *Rev. Roum. Chim.*, **28**, 7, 669 (1983).

[3] G. F. Fromont and K. B. Bischoff, "Chemical Reactor Analysis and Design", Wiley, New York, 1979.

[4] J. Villadsen and M. Michelson, "Solutions of Differential Equation Models by Polynomial Approximation", Prentice Hall, Englewood Cliffs, New York, 1978.

[5] C. W. Goar, "Numerical Initial Value Problems in ODE", Prentice Hall, Englewood Cliffs, New York, 1971.

[6] D. Schweich and J. Villermaux, *Ind. Eng. Chem. Fundam.* **21**, 47 and 51 (1982).

[7] D. W. Marquardt, *J. Soc. Ind. Appl. Math.*, **11**, 431 (1963).

[8] O. A. Hougen ard K. M. Watson, *Ind. Eng. Chem.*, **35**, 529 (1943).

[9] J. Higgirs, *Ind. & Eng. Chem.*, **59**, 19 (1967).

Revue Roumaine de Chimie, **29**, *9 — 10*, 799—806 (1984)

STUDY OF THE RECTIFICATION PROPERTIES OF HETEROGENEOUS MEMBRANES. VIII(′). BEHAVIOUR OF THE BIPOLAR UNITARY MEMBRANE SYSTEM: CATIONITE R—H AND ANIONITE R—OH

CANDIN LITEANU *, GHEORGHE RĂDULESCU ** and MARIA MOISE **
* Department of Chemical Technology, University of Cluj-Napoca, str. Arany Janos 11, Cluj-Napoca, Romania
** Superior Education Institute of Oradea, str. Armatei Roșii 5, Oradea, Romania

Received November 1, 1983

The paper elaborates the rectification properties of the bipolar unitary membrane system, apart from the ordinary bipolar membranes or the "sandwich" and "mosaic" types respectively. The bipolar unitary membrane system consists of a preliminary anionitic and cationitic resin blend mixture. For this type of membrane characteristic curve, the rectification output, the rectification coefficient and other parameters have been studied to characterize the rectification process in the above mentioned system.

I. INTRODUCTION

A series of both experimental and theoretical papers have been published on the current rectification phenomenon by means of the membranes.[1-24]

Using the analogy made by Reiss [1] and Fuller [2] between the electron excess and deficit in Si and Ge containing impurities which correspond to semiconductors of type n and p, on the one hand, and between the proton excess and deficit coressponding to acidic and basic solutions, on the other hand, Lovrecek, Despic and Bockris [3] have experimentally shown for the first time the possibility to rectify the alternating electric current by means of type p and n electrolyte junctions consisting of two membranes: cationite—H and anionite—OH.

The problem of the electric current rectification of bipolar double membranes, systems formed by joining an anionitic membrane with a cationitic one, is of interest due to the analogy between both artificial membranes and biological ones and to the complete analogy of the bipolar membranes with the semiconductor diode.[4]

As a rule, a p—n type electrolyte junction may be obtained in whatever system possessing a slightly mobile anion and a mobile cation, associated with an alternate phase possessing a slightly mobile cation and a mobile anion.

(′) Part VII: Gh. Rădulescu, C. Liteanu and M. Moise: Scientific papers. (A), Inst. Inv. Sup. Oradea, *1978*, 159 (Romania).

The rectification effects are better obtained when the difference between the ion mobilities is greater, being necessary that sparingly dissociable products be formed at the interface.[9]

It is known that the semiconductors case both for a direct region and for the inverse one is given by the following equation:

$$I=I_0\left[\exp\left(\frac{eV}{kT}\right)-1\right] \tag{1}$$

where I stands for the total junction current and I_0 representes the sum of the two field currents, k being Boltzman's constant ($k = 1.38\times10^{-23}$ Jgrd^{-1}) and e, the elementary charge ($e = 1.602\times10^{-19}$C).

For $V > \frac{kT}{e} \simeq 0.026$ (at room temperature), the parenthesized unit of equation (1) may be neglected, the equation becoming:

$$I = I_0 \exp\left(\frac{eV}{kT}\right) \tag{2}$$

Considering that equation (2) describes the theoretical characteristic under the above conditions and comparing it to the experimental characteristic which may be usually expressed in the form:

$$I=I_0 \exp\left(\frac{eV}{\eta kT}\right) \tag{3}$$

it is possible to estimate the deviation from the theoretical predictions because the deviation of the experimental characteristic coefficient η from the unity indicates the deviation of the experimental characteristic from the ideal reactification characteristic.

A plot of $\ln I = f(V)$, respectively,

$$\ln I = \ln I_0 + \frac{eV}{kT} \tag{4}$$

for the considered membrane system enables the determination of the value.

Similarly, by applying equation (5) to such a system with p–n ionic junction[10]:

$$\frac{I}{V} = Ae^{-Vq/kT} \tag{5}$$

and plotting $\log I/V = f(V)$, the relation describes with a good approximation the rectification phenomenon in the unitary membrane system, a fact which confirms the correctness of the assumption underlying the statistical theory regarding rectification system formed by two bipolar membranes.[10]

II. APPARATUS AND PROCEDURE

The membrane unitary system was prepared using Romanian exchange ions of the type "vionite". Both anionite and cationite used were turned into a granularity passing through a sieve of 60 μ. An anionite-cationite blend corresponding to the weight report ratio of 1 :1 was prepared.

The support was formed of modified cellulose acetate dissolved in acetone and formamide.[25]

The cellulose acetate is poured on a glass plate and then the mixture of the ionic champers is added and homogenized. After drying, the membrane is detached from the glass plate, then it is soaked in water and placed between two platinum electrodes with 1 cm^3 surface [16] The whole system is closed by paraffining in order to provide a constant humidity which is important for obtaining good rectification effects in the same way as in the other studies. [5–10, 15, 1] The membrane thickness was of 0.1 mm.

III. EXPERIMENTAL RESULTS

Figure 1 illustrates the membrane fixation scheme and figure 2 shows the curve of the continuons current tension — current.

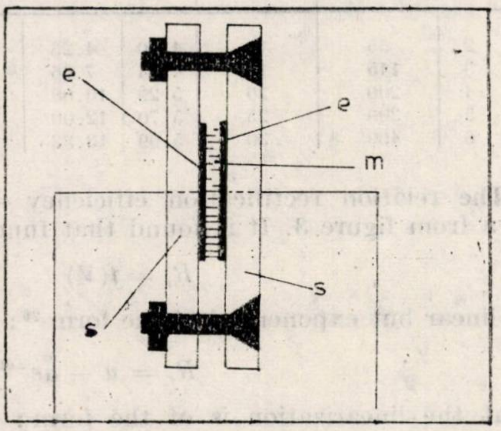

Fig. 1. — Scheme of membrane fixation : m — membrane ; e — platinum plates ; s — support of plastic material.

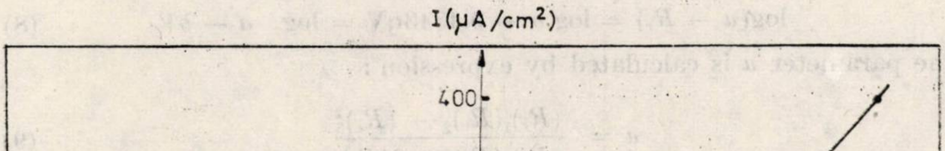

Fig. 2. I—V direct current characteristic curve.

From the values I_d (direct current) and I_i (invers current) the rectification output $\varphi = \frac{I_d}{I_i}$ is calculated and the redressing of the efficiency according to the relation[5]

$$R_r = 100 \cdot \frac{I_d - I_i}{I_d}$$

for different applied tensions. Table 1 shows I_d, I_i values as well as the other parameters characteristic of the rectification process.

Table 1

The values of some rectification process parameters

V	I_d (A/cm²)	I_i (A/cm²)	ln I_d	$\varphi = \frac{I_d}{I_i}$	R_r (%)	log (I_d/V)	log (I_i/V)
1	2	3	4	5	6	7	8
2	55	13	4.00	4.23	76.0	1.43	0.81
3	115	15	4.74	7.66	86.9	1.58	0.69
4	200	20	5.29	10.00	90.0	1.69	0.69
5	300	25	5.70	12.00	91.6	1.77	0.69
6	400	30	5.99	13.33	92.5	1.82	0.69

The relation rectification efficiency — tension, is represented by curve a from figure 3. It is found that function :

$$R_r = f(V) \tag{6}$$

is not linear but exponential of the form [26] :

$$R_r = u - ae^{-qV} \tag{7}$$

so that the linearization is of the form :

$$\log(u - R_r) = \log a - 0.4343\mathrm{qV} = \log \quad a - bV \tag{8}$$

The parameter u is calculated by expression :

$$u = \frac{(R_r)_1(R_r)_2 - (R_r)_3^2}{(R_r)_1(R_r)_2 - 2(R_r)_3} \tag{9}$$

where $(R_r)_1$ and $(R_r)_2$ correspond to two values V_1 and V_2 arbitrarily selected on curve $R_r = f(V)$, and $(R_r)_3$ is the value corresponding to $V_3 = (\mathrm{V}_1 + V_2)/2$. In expression (9), the values R_r, respectively V are chosen in such a way that $u > (R_r)_{\max}$

By the least square method on the basis of those six pairs of value V, log $(93 - R_r)$ (columns 1 and 3, table 2), are obtained : $\log a = 1.95$, and $b = -0.372$, so that equations (6) and (7) have the form (curve a, figure 3)

$$R_r = 93 - 89.2\mathrm{e}^{-0.856\mathrm{V}} \tag{10}$$

and (curve b, figure 3)

$$\log\ (93 - R_r) = 1.95 - 0.372\mathrm{V} \tag{11}$$

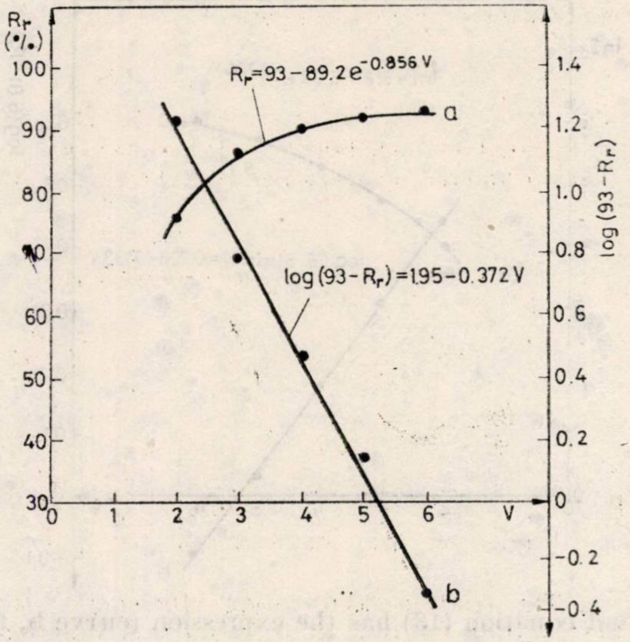

Fig. 3. a) $R_r = f(V)$ exponential curve : b) Linearization of $R_r = f(V)$ exponential curve.

Considering equation (4), the relation $\ln I = f(V)$ is represented by curve a in figure 4. It is found that this relation is not linear but exponential in its form :

$$\ln\ I = u - ae^{-qV} \tag{12}$$

so that the linearization is

$$\begin{aligned}\log\ (u - \ln I) &= \log\ a - 0.4343\mathrm{qV} = \\ &= \log a - \mathrm{bV}\end{aligned} \tag{13}$$

expression in which parameter u is calculated by expression (9).

Hence it results that the coefficient value η reflecting the deviation of the rectification parameters of the p—n ionic junction from those of the electric junction p—n semiconductors, is not constant. Therefore :

$$\eta = f(V) \tag{14}$$

To establish the structure of this function out of the equation derivative (12) and considering the function slope (4), it results :

$$\frac{\mathrm{d}\ln I}{\mathrm{d}V} = aqe^{-qV} = \frac{e}{\eta kT} = \frac{40}{\eta} \tag{15}$$

By the least square method on the basis of those five pairs of V values, log (6.81—ln I) (columns 1 and 5, table 2), are obtained : $\log a = 0.708$ and $b = -0.133$ so that equation (12) has the expression (curve a, figure 4) :

$$\ln\ I = 6.81 - 5.02\ e^{0.306V} \tag{16}$$

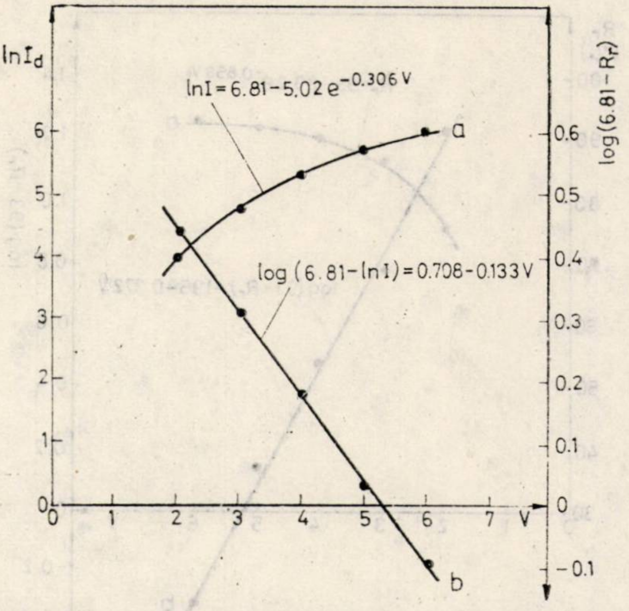

Fig. 4. a) $\ln I = f(V)$ exponential curve : b) Linearization of $\ln I = f(V)$ exponential curve.

and equation (13) has the expression (curve b, figure 4) :

$$\log\ (6.81 - \ln I) = 0.708 - 0.133\ V \tag{17}$$

Table 2

Linearization of exponential expressions

V	$(u - R_r)$ $(93 - R_r)$	$\log\ (93 - R_r)$	$(u - \ln I)$ $(6.81 - \ln I)$	$\log\ (6.81 - \ln I)$	$\dfrac{d\ln I}{dV}$	η
1	2	3	4	5	6	7
2	17.0	1.23	2.80	0.44	13.88	2.88
3	6.1	0.78	2.07	0.31	5.19	7.70
4	3.0	0.47	1.52	0.18	2.52	15.87
5	1.4	0.14	1.11	0.04	1.07	37.38
6	0.5	−0.30	0.82	−0.09	0.46	86.95

On the basis of η values (column 7, table 2) obtained from the five values $\dfrac{d\ln I}{dV}$ (column 6, table 2), calculated after (15), the exponential curve is obtained in figure 5.

By the least square method, expression :

$$\eta = \frac{40}{aq} e^{qV} = 0.55\ e^{0.368V} \tag{18}$$

is deduced for equation (15).

Consequently also function (14) has an exponential character, similar to the functions (7) and (12).

Taking into account expression (4) from relation (16) it results that for $V = 0$, $\ln I = 1.79 = \ln I_0$ and so, $I_0 = 5.8\ \mu\text{A/cm}^2$.

From expresion (18) it is found that for $V = 0$, $\eta = 0.55$.

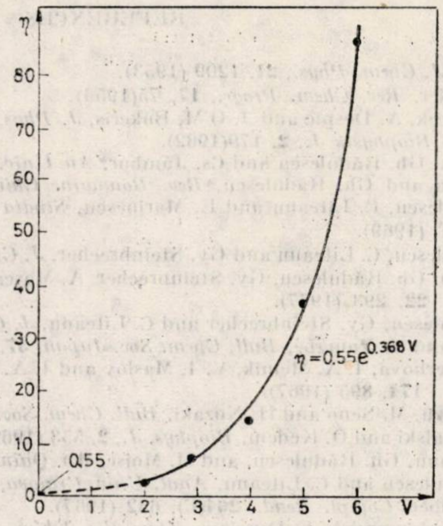

Fig. 5. $\eta = f(V)$ exponential curve.

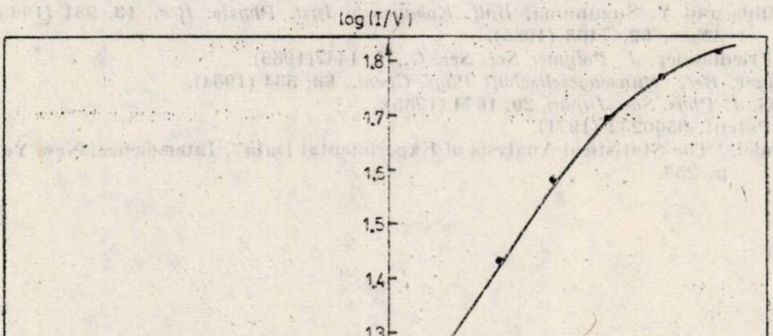

Fig. 6. log (I/V) = $f(V)$ curve.

By applying equation (5) in linearized form $\log (I/V) = \log A - bV$ on the basis of the data from table 1 (columns 7 and 8) as it was observed in figure 6, this relation describes the rectification phenomenon in this bipolar unitary membrane system, with a good aproximation.

REFERENCES

[1] H. Reiss, *J. Chem. Phys.*, **21**, 1209 (1953).

[2] C. S. Fuller, *Rec. Chem. Progr.*, **17**, 75(1956).

[3] B. Lovrecek, A. Despic and J. O'M, Bokcris, *J. Phys. Chem.*, **63**, 750 (1959).

[4] A. Mauro, *Biophysik J.*, **2**, 179(1962).

[5] C. Liteanu, Gh. Rădulescu and Cs. Jámbor, *An. Univ. Craiova*, **1**, 175(1969).

[6] C. Liteanu and Gh. Rădulescu, *Rev. Roumaine Chim.*, **14**, 1257 (1969).

[7] Gh. Rădulescu, C. Liteanu and E. Marinescu, *Studia Univ. Babeș-Bolyai, Chem.*, **14**, (2) 33 (1969).

[8] Gh. Rădulescu, C. Liteanu and Gy. Steinbrecher, *J. Chim. Phys.*, **68**, 1412 (1971).

[9] C. Liteanu, Gh. Rădulescu, Gy. Steinbrecher, A. Mascaş and M. Preda, *Rev. Roumaine Chim.*, **22**, 293 (1977).

[10] Gh. Rădulescu, Gy. Steinbrecher and C. Liteanu, *J. Chim. Phys.*, **68** 1403 (1971).

[11] M. Seno and T. Yamabe, *Bull. Chem. Soc. Japan*, **37**, 668 (1964).

[12] A. I. Tchernova, I. A. Melnik, V. I. Maslov and I. A. Zotov, *Doklady Akad. Nauk S.S.S.R.*, **174**, 895 (1967).

[13] K. Shimizu, M. Seno and H. Nozaki, *Bull. Chem. Soc. Japan*, **41**, 803 (1968).

[14] A. Katchalski and O. Kedem, *Biophys. J.*, **2**, 553 (1962).

[15] C. Liteanu, Gh. Rădulescu, and M. Moise, *An. Quim.*, **74**, 693 (1978).

[16] Gh. Rădulescu and C. Liteanu, *Anal. Univ. Craiova*, **1**, 181 (1970).

[17] S. Schreiber, *Compt. Rend.*, **264(C)**, 652 (1967).

[18] V. N. Maslov and A. V. Ovodova, *Zhur. Fiz. Khim.*, **34**, 413 (1960).

[19] B. Lovrecek and B. Kunst, *Nature*, **189**, 804 (1961).

[20] B. Lovrecek and B. Kunst, *Croat. Chem. Acta*, **34**, 137, 219 (1962; **35**, 7(1963).

[21] J. Oshida and Y. Sugunuma, *Bull. Kobayaschi Inst. Physic. Rev.*, **13**, 961 (1963); *Chem. Abstr.*, **62**, 7408 (1965).

[22] H. J. Friedlander, *J. Polymer Sci. Ser. C.*, **4**, 1447(1969).

[23] P. Läuger, *Ber. Bunsengesellschaft Phys. Chem.*, **68**, 534 (1964).

[24] S. Ohki, *J. Phys. Soc. Japan*, **20**, 1674 (1965).

[25] U. S. Patent, 3560232 (1971).

[26] J. Mandel, "The Statistical Analysis of Experimental Data", Interscience, New York, 1964, p. 253.

NOTE POUR LES AUTEURS

La Revue Roumaine de Chimie publie des articles en anglais, français, russe, allemand ou espagnol. Les auteurs sont priés d'envoyer des articles et des comptes rendus inédits.

Les manuscrits seront dactylographiés à double interligne. La bibliographie, les tableaux et la légende des figures seront placés après le texte.

Si l'article fait partie d'une série numérotée, la partie précédente sera donnée comme première référence.

Chaque article sera précédé d'un résumé comprenant quinze lignes au maximum.

Les références bibliographique dans le texte seront faites par des exposants sans parenthèses et paraîtront à la fin de l'ouvrage.

Les publications périodiques mentionnées dans la bibliographie seront présentées suivant les prescriptions internationales : le nom de l'auteur précédé de l'initiale du prénom, le titre du périodique abrégé conformément à « Chemical Abstracts » et souligné par un ligne, le numéro du tome indiqué par des chiffres arabes et souligné par deux lignes, suivi de la première page de l'article ; à la fin, l'année de la parution sera placé entre parenthèses. Le numéro de la revue ne sera pas indiqué si les pages du volume sont numérotées consécutivement.

Les textes des livres ou traités inclueront : le nom des auteurs, l'initiale du prénom, le titre du livre entre guillemets et sans être souligné, le numéro du tome précédé par l'abréviation « vol. » (ou « Bd »), le numéro de l'édition, les éditions (the publisher), la localité de la parution du livre, l'année de la parution et la page de la référence précédée(s) par l'abréviation « p » (ou « S »).

Les brevets seront indiqués comme suit : l'auteur ou la firme, le pays et le numéro du brevet , la date et la revue *(Chem. Abstr.)*. Par ex. : M. Jones (to Union Carbide Co), Brit. Pat. 601 238, 2 Sept. 1959 ; cf. *Chem. Abstr.*, **54**, 12808 (1960).

Si le référence n'a pas été lue en original, on indiquera aussi la revue de référence consultée.

Les diagrammes seront tracés à l'encre de Chine sur papier calque. Les tableaux et les figures (en nombre strictement nécessaire) ainsi que les courbes dans les figures seront numérotés par des chiffres arabes. Leur explication sera donnée dans la légende des figures. Prière de ne pas inscrire les mêmes données dans les tableaux et les figures. Chaque tableau aura un titre. On indiquera dans le texte la place approximative des tableaux et des figures. Les formules chimiques seront incluses dans le texte ; en outre, elle seront transcrites sur papier calque, à l'encre de Chine.

Les auteurs sont priés d'indiquer les caractères italiques (en soulignant les lettres au crayon), ainsi que tout autre caractère spécial ; les préfixes *ortho*, *meta*, *para*, *cis*, *trans*, etc. seront soulignés pour indiquer leurs caractères italiques et ne seront jamais écrits avec des majuscules.

Aucune correction à la main ne sera admise sur le manuscrit. Les corrections seront tapées à la machine. Les lettres grecques ou d'autres symboles spéciaux seront insérés à la main à l'encre clairement.

Le manuscrit sera signé par l'auteur.

Le titre-courant aura 50 lettres au maximum.

L'entière responsabilité du contenu des articles appartient aux auteurs.

Sur demande on peut obtenir une note plus complète.

PRINTED IN ROMANIA

TRAVAUX PARUS AUX ÉDITIONS DE L'ACADÉMIE DE LA RÉPUBLIQUE SOCIALISTE DE ROUMANIE

GH. MARCU, **Chimia compuşilor coordinativi**, 1984, 415 p.
E. CORDOŞ, C. MANOLIU, **Spectrometria de absorbţie şi fluorescenţă atomică**, 1984, 178 p.
C. BODEA, **Tratat de biochimie vegetală**, p. II, vol. 5, 1984, 438 p.
ELENA CEAUŞESCU, **Cercetări în chimia şi tehnologia polimerilor**, 1983, 519 p.
N. ASANDEI, A. GRIGORIU, **Chimia şi structura fibrelor**, 1983, 395 p.
N. IONESCU, M. CĂLDĂRARU, **Oxidarea catalitică a olefinelor inferioare**, 1983.
C. CAŞCAVAL, **Studiul polimerilor prin piroliză şi cromatografie de gaze**, 1983, 220 p.
C. I. SIMIONESCU, F. DANEŞ, **Originea vieţii**, 1983, 110 p.
C. BODEA (sub redacţia), **Tratat de biochimie vegetală**, partea II, volumul IV, 1982, 408 p.
I. G. MURGULESCU, RODICA VÎLCU, **Introducere în chimia fizică. Vol. III, Termodinamica chimică**, 1982, 624 p.
I. G. MURGULESCU, J. PĂUN, **Introducere în chimia fizică, Vol. I.3. Nucleul atomic, reacţii nucleare, particule elementare**, 1982 606 p.
ELENA JERCAN, **Analiza cromatografică**, 1982, 286 p.
ELENA CEAUŞESCU, **Noi cercetări în domeniul compuşilor macromoleculari**, 1981, 536 p.
I. G. MURGULESCU, TATIANA ONCESCU, E. SEGAL, **Introducere în chimia fizică. Vol. II. 2. Cinematică chimică şi cataliză**, 1981, 1024 p.
V. DRĂGUŢAN, A. T. BALABAN, M. DIMONIE, **Metateza olefinelor şi polimerizarea prin deschidere de inel a cicloolefinelor**, 1981, 254 p.
LYDIA-MARIA VAICUM, **Epurarea apelor uzate cu nămol activ. Bazele biochimice**, 1981, 218 p.
I. GĂLĂŢEANU, **Procese şi metode radiochimice în energetica nucleară**, 1981, 234 p.
O. IORDACHE, **Procese polistocastice aplicate la fenomenele de transfer**, 1981, 186 p.
CR. SIMIONESCU, VALERIA GORDUZA, **Polimeri biocompatibili şi biologic activi**, 1980, 479 p.
ELENA CEAUŞESCU, **Polimerizarea stereospecifică a izoprenului**, 1979, 307 p.
CONST. GH. MACAROVICI, **Analiza chimică cantitativă anorganică**, 1979, 457 p.
M. FLORESCU, **Metode ştiinţifice în dezvoltarea industriei chimice moderne**, 1979, 256 p.
A. T. BALABAN, I. GĂLĂŢEANU, G. GEORGESCU, LIGIA SIMIONESCU, **Compuşi marcaţi şi radiofarmaceutici cu aplicaţii în medicina nucleară**, 1979, 495 p.
I. G. MURGULESCU, E. SEGAL, **Introducere în chimia fizică . Vol. II. 1. Teoria molecular cinetică a materiei**, 1979, 1036 p.
S. STERNBERG, FL. DANEŞ, **Termodinamica chimică aplicată**, 1978, 400 p.
I. G. MURGULESCU, V. EM. SAHINI, **Introducere în chimia fizică. Vol. 1.2. Structura şi proprietăţile moleculare**, 1978, 604 p.
I. ZUGRĂVESCU, MAGDA PETROVANU, **N-ylid chemistry**, coédition avec McGraw-Hill International Book Company, U.S.A., 1977, 396 p.
I. G. MURGULESCU, **Introducere în chimia fizică. Vol, I.1. Atomi, molecule, legătură chimică**, 1976, 560 p.
ELENA CEAUŞESCU, **Research work on synthesis and characterization of macromolecular compounds. Contributions**, 1974, 251 p.
CR. SIMIONESCU, VIORICA RUSAN, V. POPA, **Chimia algelor marine**, 1974, 212 p., 1 pl.

ISSN 0035–4090

I. P. INFORMAŢIA, c. 2327

43 426

Lei 40
$ 75 (pour un abonnement annuel)

F1103

66 Vegyészet

04

ACADÉMIE DE LA RÉPUBLIQUE SOCIALISTE DE ROUMANIE

REFERÁLVA

REVUE ROUMAINE DE CHIMIE

TOME 29

N°s 11—12

Novembre — Décembre 1984

| Rev Roumaine Chim. | RRCHAX, **29**, *11–12*, p. 807 – 914 (1984), Bucarest

EDITURA ACADEMIEI REPUBLICII SOCIALISTE ROMÂNIA

ACADÉMIE DE LA RÉPUBLIQUE SOCIALISTE DE ROUMANIE

COMITÉ DE RÉDACTION

Rédacteur en chef :

I. G. MURGULESCU, membre de l'Académie de la République Socialiste de Roumanie

Rédacteurs en chef adjoints :

A. T. BALABAN et V. EM. SAHINI, membres correspondants de l'Académie de la République Socialiste de Roumanie

Collège de rédaction :

EM. BRATU, ELENA CEAUŞESCU, ECATERINA CIORĂNESCU-NENITZESCU, CR. SIMIONESCU, membres de l'Académie de la République Socialiste de Roumanie ; P. SPACU, membre correspondant de l'Académie de la République Socialiste de Roumanie ; M. BANCIU, M. GHEORGHIU, I. HAIDUC, D. I. MARCHIDAN, I. MOLDOVAN, G. NIAC et D. SĂNDULESCU.

La Revue Roumaine de Chimie paraît 10 fois par an. Toute commande de l'étranger pour les travaux parus aux Editions de l'Académie de la République Socialiste de Roumanie sera adressée à « ROMPRESFILATELIA » — sectorul export-import presă P.O. Box 12—201, telex 10376 prsfi r Bucureşti, calea Griviţei nr. 64—66.

Les manuscrits, les livres et les revues proposés en échange, ainsi que toute correspondance seront envoyés à la rédaction :

REVUE ROUMAINE DE CHIMIE

125, Calea Victoriei, 79717 Bucarest, Roumanie, téléphone 50 76 80

EDITURA ACADEMIEI REPUBLICII SOCIALISTE ROMÂNIA

125, Calea Victoriei, 79717 Bucarest, Roumanie, téléphone 50 76 80

REVUE ROUMAINE DE CHIMIE

ORSZÁGOS MŰSZAKI INFORMÁCIÓS KÖZPONT ÉS KÖNYVTÁR 1883

Tome 29, Nos 11–12 **Novembre-Décembre 1984**

I. G. MURGULESCU and EUGENIA SĂLĂGEAN, Estimation of thermodynamic properties of molten alkaline earth metal halides . . . . 809–815 R

VASILE T. CIORBA, SIMONA BĂDILESCU, AURELIA MEGHEA, IOSIF SCHIKETANZ and ALEXANDRU T. BALABAN. A new method for preparing polyphenylpyrylium salts with 7,7′, 8,8′-tetracyano-*para*-quinodimethane radical-anions 817–827

I. TEOREANU, H. BĂLĂȘOIU and MARCELA MUNTEAN, The influence of manganese oxides additives on the vitrification of clinker and Portland cement . . . . 829–832 R

S. STERNBERG, V. BRÂNZOI and LILIANA APĂTEANU, Polarization behaviour of the lead microelectrode in sulphuric acid solution . . . . 833–841 C

S. STERNBERG and D. GEANĂ, Calculation of phase diagrams of molten salt mixtures from electromotive force measurements 843–855

DUMITRU MĂNOIU, MARIA MĂNOIU, ILIE G. DINULESCU and MARGARET AVRAM, Friedel-Crafts acylation of acetylenes. IV. On the non selectivity of acylvinyl cations in aromatic substitution 857–860

NICOLETA ȘTEFAN, PETRU FILIP, FILIP CHIRALEU and MIHAI ELIAN, The stereochemistry of some dibenzo [*b*, *g*] bicyclo [4.2.0] octadiene derivatives 861–865

E. CORDOȘ and LIANA MUREȘAN, Analogic device for derivation of spectral curves in flame photometry 867–875

G. SURPĂȚEANU, Distribution of atomic charges in cycloimmonium ylides 877–882

R. S. SINDHU, and R. P. SINGH, Potentiometric studies on the complexes of Pr(III), Nd(III), Sm(III), Gd(III), Tb(III), Dy(III) and Ho(III) with 2'-hydroxychalcone 883–885

SPIRIDON OPREA, ABDELKRIM AZZOUZ, EMIL DUMITRIU and NICOLAE BÎLBĂ, Catalytic transformations of aromatic hydrocarbons. VI. Study of the activity of zeolites modified with polyvalent elements (in French) 887–893

BOOK REVIEWS. 895–896

AUTHOR INDEX. 897–907

SUBJECT INDEX 909–914

Rev. Roumaine Chim. **29**, *11–12*, 807–914 (1984). Bucarest

Revue Roumaine de Chimie, **29**, *11–12*, 809–815 (1984)

ESTIMATION OF THERMODYNAMIC PROPERTIES OF MOLTEN ALKALINE EARTH METAL HALIDES

I. G. MURGULESCU and EUGENIA SĂLĂGEAN

Received July 14, 1983

Thermodynamic properties — expansion and compressibility coefficients, entropies and heat capacities of ternary molten electrolytes (alkaline earth metal halides) have been estimated, in order to prove the suitability of Buehler-Hirschfelder-Curtiss' and Thiele's equations under Stilinger's assumptions to such liquids.

In a previous paper, [1] the adequacy of Buehler-Hirschfelder and Curtiss' equation of state, to thermodynamic properties prediction of molten binary ionic liquids, has been proved. Essentially, we followed Yosim's [2] way upon Thiele's equation of state, using like him, Stilinger's hypotheses to define the perfect hypothetical liquid with identical particles.

In this paper we follow the same way to the estimation of thermodynamic properties of molten alkaline earth metal halides. The hypothetical identical spheres fluid was made up through an arithmetical mean radius.

THE EQUATIONS OF STATE

For the sake of simplicity, we use B.H.C.'s and Thiele's equations of state, that proved to be good enough in the thermodynamic properties estimation of binary molten electrolytes. As B.H.C.'s equation contains a structure factor γ, we take it $2^{1/2}$, for reasons mentioned elsewhere, [1] so that the equation for a liquid with three ions may be written :

$$pV = 3RT\frac{1}{1-\dfrac{2^{5/6}3^{1/3}N^{1/3}\bar{r}}{V^{1/3}}} \tag{1}$$

The second equation of state considered here, namely Thiele's equation is :

$$pV = 3RT\frac{1+x+x^2}{(1-x)^3} \tag{2}$$

where

$$x = \frac{4\pi N\bar{r}^3}{V} \tag{3}$$

THE THERMAL EXPANSION COEFFICIENTS

The two equations mentioned above, give the following expressions for the thermal expansion coefficients:

$$\alpha_{BHC} = \frac{1}{T} \frac{1 - \dfrac{2^{5/6} 3^{1/3} N^{1/3} \bar{r}}{V^{1/3}}}{1 - \dfrac{2}{3} \dfrac{2^{5/6} 3^{1/3} N^{1/3} \bar{r}}{V^{1/3}}} \tag{4}$$

$$\alpha_T = \frac{1}{T} \frac{1 - x^3}{(1 + 2x)^2} \tag{5}$$

The experimental values of the expansion coefficients were obtained from Janz's [4] data on temperature dependence of liquid densities:

$$\rho = a - bT \tag{6}$$

$$\alpha = \frac{b}{\rho} \tag{7}$$

Table 1 shows the calculated and experimental values of the thermal expansion coefficients.

Table 1

The expansion coefficients of molten alkaline earth metal halides at their melting points

Salt	T_m, K	V cm^{3}mol^{-1}	$\bar{r}$, Å	$\alpha \cdot 10^4$, K^{-1}				
				exp	eq(4)	Δ%	eq(5)	Δ%
MgF_2	153	25.64	1.123	2.16	2.51	16.5	1.79	−17.1
$MgCl_2$	987	56.68	1.323	1.80	4.28		3.05	
$MgBr_2$	984	70.36	1.517	1.83	4.39		3.14	
MgI_2	923	91.45	1.657	2.04	4.67	128.9	3.34	63.6
CaF_2	1691	29.99	1.237	1.50	1.89	26.4	1.38	−8.1
$CaCl_2$	1046	53.21	1.536	2.07	2.66	28.4	2.00	−3.4
$CaBr_2$	1003	63.69	1.630	1.60	2.78	73.7	2.09	30.7
CaI_2	1057	85.46	1.770	2.18	2.89	32.6	2.12	−2.6
SrF_2	1673	35.61	1.283	2.13	2.11	−1.1	1.51	−29.1
$SrCl_2$	1146	58.22	1.583	2.12	2.41	13.8	1·82	−14.1
$SrBr_2$	916	66.72	1.677	2.01	2.78	38.7	2.16	7.3
SrI_2	788	84.91	1.817	2.16	3.25	50.3	2.51	16.2
BaF_2	1593	41.89	1.357	2.39	2.19	−8.1	1.57	−34.1
$BaCl_2$	1235	65.63	1.657	2.15	2.16	0.7	1.65	−23.3
$BaBr_2$	1150	74.82	1.750	2.33	2.15	−7.7	1.68	−27.8
BaI_2	1013	92.42	1.890	2.26	2.32	2.6	1.85	−18.1

Table 1 shows that:

— Both equations fail for Mg halides

— Equation (1) gives better values for Ba halides, while equation (2) is better for Ca and Sr halides.

— The results are inferior to those for alkaline halides, but have the correct order of magnitude.

THE ISOTHERMAL COMPRESSIBILITY COEFFICIENTS

The expressions of the isothermal compressibility coefficients derived from the two equations of state are:

$$\beta_T = \frac{V}{3RT} \frac{1 - \dfrac{2^{5/6}3^{1/3}N^{1/3}\bar{r}}{V^{1/3}}}{1 - \dfrac{2}{3}\dfrac{2^{5/6}3^{1/3}N^{1/3}\bar{r}}{V^{1/3}}} \tag{8}$$

or

$$\beta_T = \frac{V}{3R}\left(1 - \frac{2^{5/6}3^{1/3}N^{1/3}\bar{r}}{V^{1/3}}\right)\alpha_{\mathrm{BHC}} \tag{8'}$$

and

$$\beta_T = \frac{V}{3RT}\frac{(1-x)^4}{(1+2x)^2} \tag{9}$$

or

$$\beta_T = \frac{V}{3R}\frac{(1-x)^4}{1-x^3}\alpha_T \tag{9'}$$

The above mentioned equations must be thermodinamically equivalent two by two; but, taking into account Coulson's[5] recommendation to use smaller radius in compressibility calculations, the two equations for the compressibility coefficient, derived from the same equation of state would produce different results, according to the α value used. The explicit presence of α in the expression of the isothermal compressibility coefficient, suggests the lack of reliability of equations (8) and (9) (i.e. of recalculation of α with smaller radius).

So, although equations 8′ and 9′ with previously estimated α values, seems to be more trustful, we used equations (8) and (9) as well.

The compressibility radius has been assimilated to the arithmetical mean of polarisability radii of the three ions, which are very close to Coulson's compressibility radii, at least for the anions.

The experimental reference values for the isothermal compressibility coefficients were obtained by ultrasound speed measurements due to Bockris et al.[6]

The estimated and experimental results are tabulated in table 2.

Table 2

The isothermal compressibility of some molten alkaline earth metal halides, at their melting points

Salt	T_m K	V cm^{3}mol	$\bar{r}$ Å	$\beta_T \cdot 10^{11}$ cm^{2}dyne^{-1}								
				exp	eq 8	Δ%	eq 8′	Δ%	eq 9	Δ%	eq 9′	Δ%
$MgBr_2$	984	70.36	1.275	14.70	5.64	−61.6	4.08	−72.2	5.00	−65.9	3.26	−77.7
MgI_2	923	91.45	1.434	11.30	7.04	−37.7	5.29	−53.2	5.86	−48	4.06	−64.0
$CaCl_2$	1046	53.21	1.289	1.26	2.65	110.3	1.45	15.1	1.84	46	1.03	−18.6
$CaBr_2$	1003	63.69	1.384	1.61	3.14	94.8	1.76	9.2	2.11	30.9	1.21	−24.7
CaI_2	1057	85.46	1.544	2.75	3.76	36.9	2.37	−13.9	2.45	−10.9	1.55	−43.6
$SrCl_2$	1146	58.12	1.347	1.26	2.46	95.4	1.37	8.7	1.64	30.1	0.95	−24.9
$SrBr_2$	916	66.72	1.442	1.31	3.14	139.4	1.69	29.6	1.96	49.0	1.14	−13.0
SrI_2	788	84.91	1.602	1.79	3.99	122.9	2.31	29.0	2.32	29.4	1.45	−19.2
$BaCl_2$	1235	65.63	1.417	1.27	2.43	91.7	1.35	6.3	1.58	24.4	0.92	−27.8
$BaBr_2$	1150	74.82	1.512	1.58	2.65	68.0	1.43	−9.7	1.61	2.2	0.94	−40.4
BaI_2	1013	92.42	1.671	1.48	3.08	107.9	1.70	14.9	1.71	15.5	1.06	−28.6

Polarisability radii of ions : $r_{Mg^{2+}} = 0.448$ Å ; $r_{Ca^{2+}} = 0.777$ Å ;
$r_{Sr^{2+}} = 0.951$ Å ; $r_{Ba^{2+}} = 1.116$ Å ;
$r_{Cl^-} = 1.545$ Å ; $r_{Br^-} = 1.688$ Å ;
$r_{I^-} = 1.927$ Å

As expected, a very great discrepancy is to be noted between the experimental and the β values with equations (8) and (9). Using equations (8′) and (9′), the agreement is better but not altogether satisfactory.

THE ENTROPY

According to Yosim, the entropy for a rigid spheres fluid is :

$$S_l = S_g - \int_{V_l}^{V_g} \frac{P}{T}\,\mathrm{d}V \tag{10}$$

where :

S_g is the molar entropy of a rigid spheres gas
V_g is the molar volume of the gas, at the melting point and 1 atm.
V_l is the molar volume of the liquid at the melting point.

The two chosen equations of state produce the following expressions for the molar liquid entropies :

$$S_l = S_g - 9R \ln \left(\frac{V_g}{V}\right)^{1/3} \frac{1 - \dfrac{2^{5/6}3^{1/3}N^{1/3}\,\bar{r}}{V_g^{1/3}}}{1 - \dfrac{2^{5/6}3^{1/3}N^{1/3}\,\bar{r}}{V^{1/3}}} \tag{11}$$

$$S = S_g - 3R\left[\ln\frac{V_g}{V_l}\frac{1-x_g}{1-x} + \frac{3x}{1-x} + \frac{3x^2}{2(1-x)^2}\right] \tag{12}$$

In the above relationship, x_g stands for x calculated with the molar volume of the gas; in fact the term x_g may be neglected.

For the molar entopy of the gas, the entropy of a mixture of three perfect monoatomic gases, with the ionic weights was taken:

$$S_g = (2.5\,R\ln T + 1.5\,R\ln M_+ - 2.31) +$$

$$+ 2(2.5\,R\ln T + 1.5\,R\ln M_- - 2.31) + 2.81 \tag{13}$$

The experimental reference entropies were estimated from temperature dependence of solid heat capacity, where such data were available, [7] and molar entropies of fusion. [8] Concerning salts for which such data are lacking, the entropy of the solid at its melting point was calculated with the standard heat capacity.

The comparison between experimental and calculated values of entropies is presented in table 3.

Table 3

The molar entropies of molten alkaline earth metal halides at their melting points

Salt	T_m K	V cm³mol⁻¹	V cm³mol⁻¹	$\bar{r}$ Å	S, cal.mol⁻¹K⁻¹				
					exp	eq 11	Δ %	eq 12	Δ %
MgF_2	1536	25.64	126070	1.123	54.80	51.18	−6.6	60.92	11.2
$MgCl_2$	987	56.68	80934	1.423	56.40	59.24	3.1	69.47	21.2
MgBr	984	70.36	80688	1.517	57.41*	65.07		75.42	
MgI_2	923	91.45	75700	1.657	58.98*	68.93		79.08	
CaF_2	1691	29.99	132580	1.237	55.38	50.45	−8.9	57.46	3.7
$CaCl_2$	1046	53.21	90760	1.536	56.46	49.91	−11.6	53.84	−4.5
$CaBr_2$	1003	63.69	82300	1.630	61.18*	56.28		60.25	
CaI_2	1057	85.46	86730	1.770	68.24*	63.09		68.63	
SrF_2	1673	35.61	137300	1.283	52.38*	55.71		64.16	
$SrCl_2$	1146	58.12	93970	1.583	58.25	53.84	−7.5	57.76	−0.8
$SrBr_2$	916	66.72	75160	1.677	57.64*	55.98		58.10	
SrI_2	788	84.91	64830	1.817	61.81*	59.08		60.99	
BaF_2	1593	41.89	130730	1.357	62.23	57.41	−7.7	65.67	5.5
$BaCl_2$	1235	65.63	101360	1.657	59.94	55.86	−6.8	59.08	−1.4
$BaBr_2$	1150	74.82	94370	1.750	67.32*	59.28		60.76	
BaI_2	1013	92.42	83130	1.890	68.59*	61.26		61.43	

* Approximative experimental values.

Table 3 reveals a good fit between experimental and calculated entropies, for fluorides and chlorides; for bromides and iodides, the comparison is inconclusive, due to the lack of experimental information.

THE HEAT CAPACITY

The heat capacity results from the entropy, using the relationship :

$$Cp = T\left(\frac{\partial S}{\partial T}\right)_P = Cp_g - T\frac{\partial}{\partial T}\left(\int_{V_g}^{V_g}\frac{P}{T}\,\mathrm{d}V\right) \tag{14}$$

With the two equations of state, we get for the heat capacity :

$$Cp = 15 + 3RT\left[\frac{\alpha_l}{1-\dfrac{2^{5/6}3^{1/3}N^{1/3}\bar{r}}{V^{1/3}}} - \frac{1}{T\left(1-\dfrac{2^{5/6}3^{1/3}N^{1/3}\bar{r}}{V_g^{1/3}}\right)}\right] \tag{15}$$

and

$$Cp = 15 + 3RT\alpha_l\frac{1+x+x^2}{(1-x)^3} - 3R \tag{16}$$

In the derivation of the above formulae, we put T^{-1} for α_g and neglected terms in V_g^{-1}.

The calculated and Janz's experimental heat capacity values are given in table 4.

Table 4

The heat capacities of molten alkaline earth metal halides at their melting points

Salt	T_m K	V_l cm^{3}mol^{-1}	V_g cm^{3}mol^{-1}	$\bar{r}$ Å	Cp, cal · mol^{-1}K^{-1}				
					exp	eq. 15	Δ%	eq. 16	Δ%
MgF_2	1536	25.64	126070	1.123		22.01		22.289	
$MgCl_2$	987	56.68	80934	1.423	22	21.43	− 2.6	20.82	− 5.4
$MgBr_2$	984	70.36	80688	1.517	24	21.27	−11.3	20.47	−14.7
MgI_2	923	91.45	75700	1.657	24	21.23	−11.6	20.50	−14.6
CaF_2	1691	29.99	132580	1.237	—	22.77	—	25.63	
$CaCl_2$	1046	53.21	90760	1.536	23.6	23.13	− 2.0	28.53	+20.9
$CaBr_2$	1023	63.69	82300	1.630	27	23.07	−14.4	28.46	+ 5.4
CaI_2	1057	85.46	86730	1.770	24.7	22.71	− 8.0	26.58	+ 7.2
SrF_2	1679	35.61	137300	1.283	—	22.38	—	23.84	
$SrCl_2$	1146	58.12	93970	1.583	27.2	23.14	−15.0	28.63	+ 5.3
$SrBr_2$	916	66.72	75160	1.677	27.8	23.31	−16.0	30.34	+ 9.1
SrI_2	788	84.91	64830	1.817	26.3	23.22	−11.7	30.31	+15.2
BaF_2	1593	41.89	130730	1.357	—	22.38	—	23.99	
$BaCl_2$	1235	65.63	101360	1.657	26.3	23.24	−11.6	29.35	+11.6
$BaBr_2$	1150	74.82	94370	1.750	25.6	23.43	− 8.5	31.06	+21.3
BaI_2	1013	92.42	83130	1.890	27	23.50	−13.0	32.23	+19.4

The inspection of table 4, shows that equation 1 underestimates the heat capacity while equation (2) overestimates it, the former being slightly better.

CONCLUSIONS

The two equations of state tried in thermodynamic properties prediction of molten alkaline earth metal halides show no such performances as for alkaline halides; but in spite of the many simplifying assumptions made, the equations give the correct order of magnitude for all the properties estimated, being meanwhile two of the simplest known state equations for liquids.

REFERENCES

[1] I. G. Murgulescu and Eugenia Sălăgean, *Rev. Roum. Chimie*, **29**, 143 (1984).
[2] S. Y. Yosim and B. B. Owens, *J. Chem. Phys.*, **41**, 2032 (1964).
[3] F. H. Stilinger jr., *J. Chem. Phys.*, **35**, 1581 (1961).
[4] G. Janz "Molten Salts Handbook", Academic Press New York, 1967.
[5] C. A. Coulson, "Valence", Oxford University Press, Oxford 1959.
[6] J. O'M Bockris, A. Pilla and J. Barton, *Rev. Chim. Acad. RPR*, **7**, 59 (1962).
[7] M. Kh. Karapetyants, "Chemical Thermodynamics", Mir. Moscow, 1978.
[8] Termicheskie Constanti Veschestv, Vipusk IX AN. S.S.S.R. Moskwa, 1979.

Revue Roumaine de Chimie, **29**, *11–12*, 817–827 (1984)

A NEW METHOD FOR PREPARING POLYPHENYLPYRYLIUM SALTS WITH 7,7′, 8,8′-TETRACYANO-*para*-QUINODIMETHANE RADICAL-ANIONS

VASILE T. CIORBA, SIMONA BĂDILESCU, AURELIA MEGHEA,
IOSIF SCHIKETANZ and ALEXANDRU T. BALABAN*

Polytechnic Institute, Organic Chemistry Department, Splaiul Independenței 313,
76206 Bucharest, Romania

Received May 7, 1984

A new method is presented for obtaining polyphenylpyrylium salts with 7,7′, 8,8′-tetracyano-*para*-quinodimethane ($TCNQ^{\cdot -}$) radical-anions from TCNQ and pyrylium pseudobases (1,5-enediones) or their enol-ethers in acetonitrile. The anions may be either $TCNQ^{\cdot -}$ or $(TCNQ_2)^{\cdot -}$. These salts have been characterized by elemental analysis, IR, UV–VIS, and ESR spectra. Their electrical conductivity is low, and they have deep colours (blue, green, violet).

INTRODUCTION

Charge-transfer (CT) complexes involving quinones and related systems have long been known.[2] The existence of donor-acceptor (D–A) interactions is proved by characteristic electronic absorption bands (CT-bands). In general the donor D is a Lewis base possessing π- or n-electrons, while the acceptor A is a π- or a v-acid possessing a vacant orbital. Sometimes the CT complex may present ESR evidence for the D–A interaction.

More than twenty years ago, Acker and Hertler[3] prepared 7,7′,8,8′-tetracyano-*para*-quinodimethane (TCNQ, **1**). The $C(CN)_2$ groups have a high electronegativity and moreover, unlike quinonic oxygen atoms, are able to delocalize the negative charge of the anion-radical **2** of TCNQ. A highly interesting feature of CT complexes involving TCNQ is their high electrical conductivity (much higher than of both donor and acceptor); such highly conducting solids have been called "organic metals", or one-dimensional conductors[4] because their electrical conductivity in single crystal is very anisotropic. During the last years, symposia in this area were held,[5] and a new journal started to appear.[6]

---

* Correspondence author. The present paper is to be considered as Part V in the series: "Molecular Complexes with Aromatic Cations as Electron Acceptors". Part IV in this series is ref.[1].

Among CT complexes of TCNQ having as donors aromatic hydrocarbons, phenols, aromatic amines, compounds of nitrogen, phosphorus or arsenic, polymers etc., those which led to the most promising results are with sulphur or selenium derivatives :[7] tetrathiofulvalene (TTF) or its selenium-congener. The recent discovery of Bechgaard *et al.* concerning the possibility to stabilize supraconducting states of organic perchlorates gave further impetus to the active research on CT complexes involving such congeners.[8]

According to the electrical conductivity one may divide solids into several groups as indicated and exemplified in Table 1.

Table 1

Electrical conductivity of solids at room temperature

Material	Example	Conductivity ($ohm^{-1} \cdot cm^{-1}$)
Metal	Copper	6×10^5
1D-Conductor	$TTF^{\cdot +}$ $TCNQ^{\cdot -}$	10^3
Conductor	Graphite	7×10^2
Semiconductor	Germanium	$0{\cdot}5 - 40$
Insulator	Sulphur	10^{-22}

Depending on the nature of the donor and in the reaction conditions, there exist three types of CT complexes with TCNQ : (i) π-complexes obtained by mixing hot solutions of donor and acceptor in appropriate solvents (THF, $CHCl_3$, CH_2Cl_2, etc.) and cooling the mixture ; their electrical resistivity is high and they present weak ESR signals ; (ii) simple 1 : 1 complexes, usually obtained from metallic or organic iodides and $Li^+TCNQ^{\cdot -}$; though at room temperature the electrical conductivity and ESR absorption of such salts are low, these properties are enhanced by elevated temperature and pressure so that in some cases one can obtain semiconducting or 1D-conducting systems ; and (iii) complex salts $M^+(TCNQ_2)^{\cdot -}$ or less often $M^{2+}(TCNQ_3)^{2-}$; their electrical resistivity is low ($10^{-2} - 10^{-3}$ ohm ·cm) and significant ESR absorption is manifest ; both phenomena are anisotropic in single crystals.

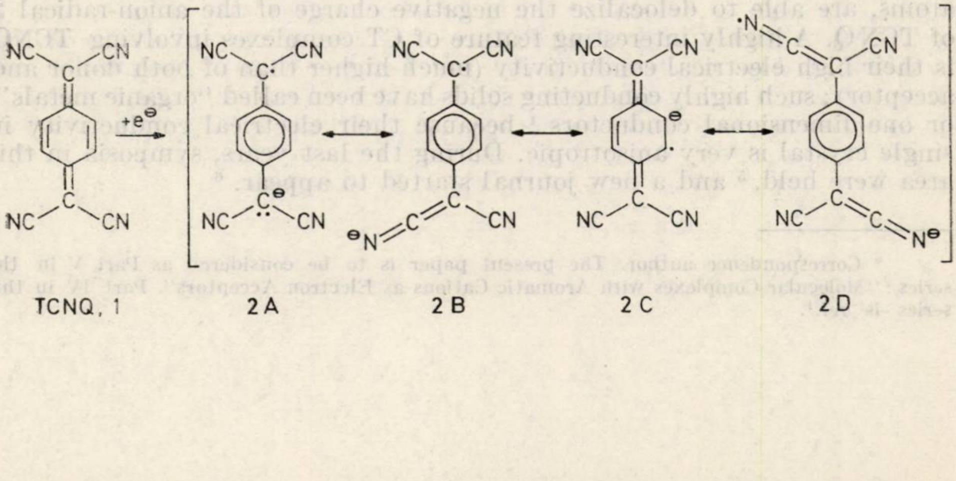

TCNQ, 1 2A 2B 2C 2D

An interesting feature of 1 : 1 CT complexes involving TCNQ is the disproportionation of $\mathrm{TCNQ}^{\cdot-}$ radical-anions leading to 1 : 2 (D—A) complexes **3** (sometimes even on recrystallization attempts from acetonitrile) :

$$2\,\mathrm{TCNQ}^{\cdot-} \rightleftarrows \mathrm{TCNQ}^{2-} + \mathrm{TCNQ}$$

$$\mathrm{D^{+}TCNQ^{\cdot-}} + \mathrm{TCNQ} \rightleftarrows \underset{\mathbf{3}}{\mathrm{D^{+}(TCNQ_2)^{\cdot-}}}$$

Though spectral data and conductivity measurements in solution indicate reversible dissociation, complete delocalization may occur in the solid in such 1 : 2 complexes **3** as suggested by formula $(\mathrm{TCNQ_2})^{\cdot-}$.

As an example of 1 : 2 complexes, $\mathrm{Et_3NH^{+}(TCNQ_2)^{\cdot-}}$(**4**) can be prepared by several methods, [8a,9] namely :

1) $\mathrm{Et_3NH^{+}Cl^{-}} + \mathrm{Li^{+}TCNQ^{\cdot-}} \longrightarrow \mathrm{Et_3{}^{+}NH\,TCNQ^{\cdot-}} \xrightarrow[50\%]{\mathrm{TCNQ}} \mathbf{4}$

2) $3\,\mathrm{Et_3NH^{+}I^{-}} + 2\,\mathrm{TCNQ} \longrightarrow \mathbf{4} + \mathrm{I_2}$

3) $\mathrm{Et_3N} + \mathrm{H^{+}TCNQ^{\cdot-}} \longrightarrow \mathbf{4}$

These methods can be applied to "onium" salts and to heterocycles.

CHARGE-TRANSFER COMPLEXES OF POLYPHENYLPRYLIUM WITH TCNQ

Only two types of CT complexes of TCNQ involving pyrylium cations have so far been described, namely **5**, [7a,10] starting from a pyrylium salt and lithium TCNQ in anhydrous acetonitrile under inert gas atmosphere, and **6** [11] from TCNQ and substituted 4,4′-bipyranylidenes.

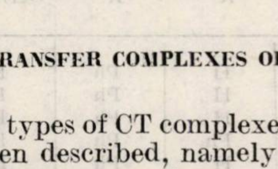

where R = Me or Ph
n = 1 or 2

5

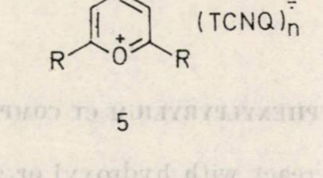

where R = H, Me, Ph or
2-thienyl

6

The present paper describes a larger variety of seven new CT complexes **7** between TCNQ and polyphenylpyrylium systems in both 1 : 1 and 2 : 1 molar ratios (di-, tri-, isomeric, tetra-, and pentaphenyl-substituted pyrylium cations) obtained *via* a new method, and attempts correlations between structure and properties.

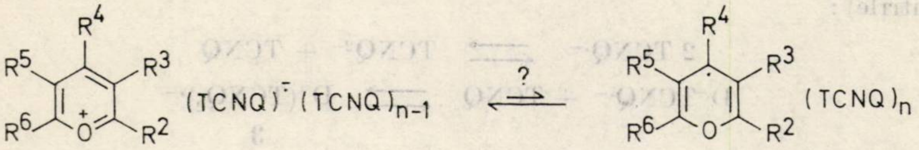

7 a-g •

7A a-g •

Table 2 presents the structures **7a–g*** of the new CT complexes which can be visualized as if a TCNQ molecule had abstracted an electron from a donor pyranyl free radical, as indicated by structure **7A**.

Table 2

Structures of pyrylium cations and derivatives thereof for obtaining salts **7**

No.	R^2	R^3	R^4	R^5	R^6	Derivatives[a]	n[b]
7a	Ph	H	H	H	Ph	P[c]	2
7b	Ph	H	Ph	H	Ph	P	2
7c	Ph	H	3-nitrophenyl	H	Ph	P	2
7d	Ph	Ph	H	Ph	Ph	E, P	2
7e	Ph	Ph	Ph	H	Ph	E, P	2
7f	Ph	Ph	Ph	Ph	Ph	E, M, P	2
7g	Ph	Ph	Ph	Ph	Ph	E, M, P	1

---

a — Abbreviations : P = pseudobase ; E = Ethoxy-enol-ether ;
M = Methoxy-enol-ether.

b — Number of TCNQ moles in **7**.

c — Not isolated.

A NEW SYNTHESIS OF TCNQ–POLYPHENYLPYRYLIUM CT COMPLEXES

Pyrylium salts **8** are known to react with hydroxyl or alkoxyl anions.[12–14] Scheme 1 presents a summary of the main reactions, assuming that nucleophilic attack occurs only at positions 2 and 6 in symmetrically aryl-substituted pyrylium salts.

When alkyl substituents are present in positions 2 and 6, the resulting keto-enolic pseudobase (or 1,5-enedione) usually undergoes further intra- (leading to phenols) or intermolecular condensations (leading to dimers or to undefined polymers). Therefore alkyl-substituted pseudobases

---

* Small letters **a-g** indicate different substituents according to Table 2 ; capital letters **A–E** indicate limiting resonance structures.

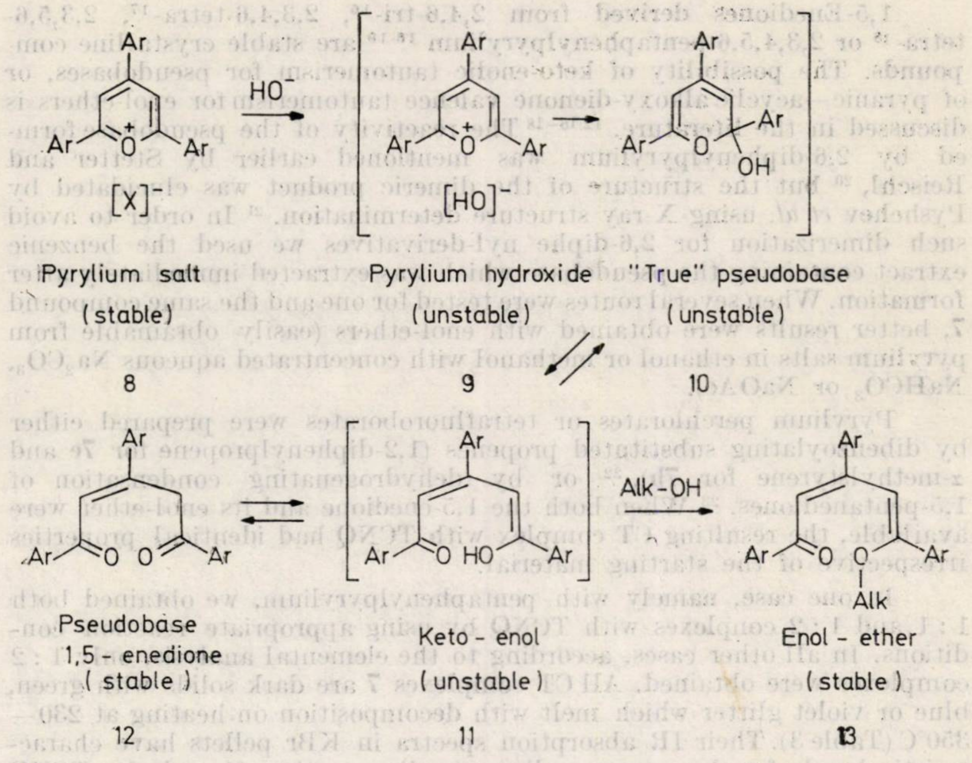
HO⁻
[X]⁻
[HO]⁻
Pyrylium salt
(stable)
8
Pyrylium hydroxide
(unstable)
9
"True" pseudobase
(unstable)
10
Alk-OH
Pseudobase
1,5-enedione
(stable)
12
Keto-enol
(unstable)
11
Enol-ether
(stable)
13

SCHEME 1

are unstable and we used only pyrylium salts where the 2 and 6 substituents are aryl groups.

The basic idea of the new synthesis is the following: since TCNQ is a Lewis acid and since 1,5-enediones **12** or their enol-ethers **13**[15] are pseudobase derivatives, one can imagine a reaction of these two reagents leading to CT complexes **7**.

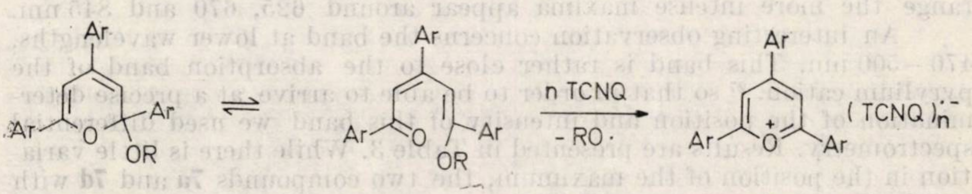
n TCNQ
- RO·
(TCNQ)$_n^{\cdot -}$
7

Unlike the synthesis of **5** which required preformation of the lithium salt of TCNQ under carefully controlled oxygen-free conditions, the new synthesis can be carried out in the presence of air, and starts from stable, conservable 1,5-enediones or enol-ethers as indicated in Table 2.

1,5-Enediones derived from 2,4,6-tri-[16], 2,3,4,6-tetra-[17], 2,3,5,6-tetra-[18] or 2,3,4,5,6-pentaphenylpyrylium [16,19] are stable crystalline compounds. The possibility of keto-enolic tautomerism for pseudobases, or of pyranic—acyclic alkoxy-dienone valence tautomerism for enol-ethers is discussed in the literature. [12,15–18] The reactivity of the pseudobase formed by 2,6-diphenylpyrylium was mentioned earlier by Stetter and Reischl, [20] but the structure of the dimeric product was elucidated by Pyshchev *et al.* using X-ray structure determination. [21] In order to avoid such dimerization for 2,6-diphe nyl-derivatives we used the benzenic extract containing the pseudobase which was extracted immediately after formation. When several routes were tested for one and the same compound **7**, better results were obtained with enol-ethers (easily obtainable from pyrylium salts in ethanol or methanol with concentrated aqueous Na_2CO_3, $NaHCO_3$ or NaOAc).

Pyrylium perchlorates or tetrafluoroborates were prepared either by dibenzoylating substituted propenes (1,2-diphenylpropene for **7e** and α-methylstyrene for **7b**), [22] or by dehydrogenating condensation of 1,5-pentanediones. [23] When both the 1,5-enedione and its enol-ether were available, the resulting CT complex with TCNQ had identical properties irrespective of the starting material.

In one case, namely with pentaphenylpyrylium, we obtained both 1 : 1 and 1 : 2 conplexes with TCNQ by using appropriate reaction conditions. In all other cases, according to the elemental analysis, only 1 : 2 complexes were obtained. All CT complexes **7** are dark solids with green, blue or violet glitter which melt with decomposition on heating at 230—350°C (Table 3). Their IR absorption spectra in KBr pellets have characteristic bands for the corresponding pyrylium cation [24] and the TCNQ radical-anion. [25,26]

This new synthesis could be general, starting from TCNQ and pseudobases of heterocyclic compounds.

ELECTRONIC ABSORPTION SPECTRA

The electronic absoption spectra in dry acetonitrile present several ill-differentiated maxima in the visible region; in the long-wavelength range the more intense maxima appear around 625, 670 and 845 nm.

An interesting observation concerns the band at lower wavelengths, 470—500 nm. This band is rather close to the absorption band of the pyrylium cation, [27] so that in order to be able to arrive at a precise determination of the position and intensity of this band we used differential spectrometry. Results are presented in Table 3. While there is little variation in the position of the maximum, the two compounds **7a** and **7d** with unsubstituted 4 position (which are the most bathochromically shifted) reveal an extremely intense absorption; the molar extinction coefficient is higher by at least an order of magnitude than for the other CT complexes.

In agreement with literature data, [28] the electronic absorption spectra and the ESR spectra (see next Section) of TCNQ salts with organic cations indicate that salts with radical-anions may have a partial charge transfer, measured by the transfer ratio ρ : for a donor $D^{\cdot}$, when ρ is 1, one has the true salt $D^{\cdot +}(TCNQ_n)^{\cdot -}$, but with $\rho < 1$ one obtains charge-transfer complexes $D^{\rho\cdot +}(TCNQ_n)^{\rho\cdot -}$.

Table 3

Melting points and absorption characteristics for one of the visible absorption bands of **7**, and longest-wavelegth band of the corresponding perchlorates. [a]

Pyrylinm cation		CT complex **7**				Perchlorate
		m.p. (°C)	λ_{max} (nm)	ν_{max} (cm^{-1})	ε	λ_{max} (nm)
a	2,6-Diphenyl	250	478	20,900	1,130	415
b	2,4,6-Triphenyl	270	490	20,400	200	408
c	2,6-Diphenyl-4-(3-nitrophenyl)	275	492	20,300	300	—
d	2,3,5,6-Tetraphenyl	280	480	20,800	7,300	—
e	2,3,4,6-Tetraphenyl	235	492	20,300	84	412
f	2,3,4,5,6-Pentaphenyl	350	480	20,800	90	—
g	2,3,4,5,6-Pentaphenyl*	279	485	20,600	100	—

---

[a] For **7** in CH_3CN ; for perchlorates in CH_3COOH [27].
* 1 : 1 CT complex ; all other cases are 1 : 2 complexes.

ELECTRON SPIN RESONANCE (ESR) SPECTRA

No ESR data were reported for compounds **5**. We investigated ESR spectra of several solid salts **7** and determined their g-factor and the number of free spins by comparison with diphenylpicrylhydrazyl as standard. Results are presented in Table 4.

In comparing tri-, tetra-, and pentaphenyl-derivatives **7**, one can observe from Table 4 that the triphenyl-derivative **7b** has the highest spin concentration (17%), while with increasing number of phenyl groups the spin concentration decreases reaching 1.7% for the 1 :1 CT complex of pentaphenylpyrylium **7g**, and 1.5% for the 1 : 2 complex **7f**. This range of values agrees with literature data for other CT complexes of TCNQ.[26]

Table 4

ESR data of some salts **7**.

Compound	Mol. weight	Mol. spin number (× 10^{23})	g value	Calculated CT ratio (%)
DPPH	399	6.00	2.0037	100.0
7b $(TCNQ)_2$	725	1.02	2.0028	16.9
7d $(TCNQ)_2$	801	0.17	2.0026	2.8
7f $(TCNQ)_2$	877	0.09	2.0026	1.5
7g $(TCNQ)$	669	0.10	2.0026	1.7

The g-values indicate that the spin density is mainly associated with carbon atoms, as required by contribution from limiting structures **2A**–**2C** (with smaller contributions for **2D**) for the anion. The contribution of limiting structure **7A** for the complex is considered to be negligible in the ground state therefore $\rho \approx 1$ i.e. the structure is essentially salt-like, but it may be important in the electronically excited state responsible for the band around 480 nm.

ELECTRICAL CONDUCTIVITY

Electrical conductivity measurements were effected at room temp. with compressed powdered samples using the method of four points. Results, which are presented in Table 5, indicate that these compounds are intermediates between insulators and semiconductors.

Table 5

Conductivity data for some compounds **7**.

	CT Complex	Conductivity ($ohm^{-1} \cdot cm^{-1}$)
7d	2,3,5,6,-Tetraphenylpyrylium ($TCNQ_2$)	3.4×10^{-7}
7f	2,3,4,5,6-Pentaphenylpyrylium (TCNQ)	1.7×10^{-7}
7g	2,3,4,5,6-Pentaphenylpyrylium ($TCNQ_2$)	2.5×10^{-12}

CONCLUSIONS

A new synthesis for charge-transfer pyrylium salts having $TCNQ^{\cdot -}$ or $(TCNQ_2)^{\cdot -}$ radical-anions was described. It consists in treating the pyrylium pseudobase or its enol-ether with TCNQ in refluxing acetonitrile. The resulting compounds having 2–5 aryl groups were studied by UV-VIS, IR, ESR methods; they are poor electrical conductors.

EXPERIMENTAL SECTION

Infrared spectra were recorded with Jena UR–10 and SPECORD–71–IR instruments in KBr pellets. UV–VIS spectra were determined with a SPECORD UV–VIS Jena spectrophotometer. ^1H–NMR spectra were recorded at 60 MHz with Varian A–60 A and Varian EM–360–L instruments. Differential spectrophotometry was carried out with a Unicam SP–700 instrument which had in the solvent cell a solution (matched in concentration) of the respective pyrylium perchlorate in the same solvent (acetonitrile). ESR spectra were recorded with weighed amounts of solid samples using DPPH as standard for the number of spins.

Acetonitrile was specially purified by repeated distillations, drying over phosphorus pentoxide and calcium hydride. It was stored over molecular sieves.

Solid pseudobases (m.p.'s given) were obtained from 2,4,6-triphenylpyrylium fluoroborate (m.p. 119°), 2,3,5,6-tetraphenylpyrylium (m.p. 148°, dec.), and 2,3,4,5,6-pentaphenylpyrylium (m.p. 169°) according to literature data.[16–19]

5-Ethoxy-1,2,4,5-tetraphenyl-2,4-pentadien-1-one

A suspension of 1.8 g (4 mmol) of 2,3,5,6-tetraphenylpyrylium perchlorate in 35 ml refluxing ethanol was treated with a saturated solution of excess (5 g) sodium acetate hydrate in hot water. The resulting clear solution deposits on cooling the crystalline enol-ether, m.p. 158.5°. Anal. $C_{31}H_{26}O_2$ requires C, 86.48 ; H, 6.09. Found : C, 85.78 ; H, 6.67%.

UV (MeOH, nm, lg ε) : 353 (4.11) ; 233 (4.30) ; 204 (4.70).

IR (KBr, cm^{-1}) : 1240 ; 1670 ; 2980 ; 3040.

^1H-NMR ($CDCl_3$, δ, ppm) : 1.28 (t, 3H) ; 3.95 (q, 2H) ; 6.98 (s, 1H) ; 7.1 – 7.9 (m, 20 H).

5-Ethoxy-1,2,3,5-tetraphenyl-2,4-pentadien-1-one

A suspension of 2,3,4,6-tetraphenylpyrylium perchlorate (0.5 g) in 30 ml refluxing ethanol was treated with a saturated solution of 0.5 g Na_2CO_3 in 5 ml water. The resulting red solution deposits on cooling the yellow crystalline enol-ether, m.p. 69°.

IR (KBr, cm^{-1}) : 1360 ; 1670 ; 3050.

^1H-NMR ($CDCl_3$, δ ,ppm) : 1.28 (t, 3H) ; 3.95 (q, 2H) ; 6.30 (s, 1H) : 6.9 – 7.9 (m, 20 H)

5-Ethoxy-1,2,3,4,5-pentaphenyl-2,4-pentadiene-1-one

In a suspension of 2 g pentaphenylpyrylium bromide in refluxing ethanol (30 ml), a solution of 3 g sodium acetate in 5 ml water was added, and the refluxing was continued till a clear solution resulted. On gradual cooling pale yellow crystals (m.p. 147°) separated, which were filtered off and washed with water. Anal. $C_{37}H_{30}O_2$ requires : C, 87.71 ; H, 5.96. Found : C, 87.93 ; H, 6.14%.

IR (KBr, cm^{-1}) : 1250 ; 1670 ; 2980 ; 3050.

UV (MeOH, nm, lg ε) : 409 (4.19) ; 298 (4.32) ; 204 (4.79).

^1H-NMR ($CDCl_3$, δ, ppm) : 1.28 (t, 3H) ; 3.95 (q, 2H) ; 6.95 – 7.55 (m, 25 H).

The CT complex 2,6-diphenylpyrylium (TCNQ), 7a

A two-phase system (water — ethyl ether) was used in which 100 mg of 2,6-diphenylpyrylium perchlorate was stirred 20 min at 5°C with sodium hydrogen carbonate. The cold ethereal layer, having a blue fluorescence, was dried over magnesium sulphate and was treated with 90 mg TCNQ in acetonitrile at 40°C. The CT complex separated after concentration of the solution at reduced pressure as black crystals with reddish glitter, m.p. 250°, dec. Anal. $C_{41}H_{21}N_8O$ requires : C, 76.73 ; H, 3.30 ; N, 17.48. Found : C, 76.62 ; H, 3.22 ; N. 17.18%.

IR (KBr, cm^{-1}) : 1280 ; 1600 ; 2200 ; 3027.

The CT complex 2,4,6-triphenylpyrylium $(TCNQ)_2$, 7b

1,3,5-Triphenyl-1,5-pentendione (200 mg) dissolved in one ml warm acetonitrile was added to a clear refluxing saturated solution of TCNQ in 10 ml acetonitrile. The black crystalline product which separated was filtered off after cooling and washed with 15 ml acetonitrile. The m.p. 270° dec., agrees with literature data.[10]

A similar procedure was followed for obtaining the 2,6-diphenyl-4-(3-nitrophenyl)-pyrylium $(TCNQ)_2$ complex, **7c**, deep green, m.p. 275°, dec.

The CT complex 2,3,5,6-tetraphenylprylium $(TCNQ)_2$, 7d

To a solution of 200 mg TCNQ in 30 ml refluxing acetonitrile was added a solution of 400 mg enol-ether **13d** (Alk = Et) in 4 ml acetonitrile. After refluxing for 30 min. and similar work-up as above, the deep green salt **7d** was obtained, m.p. 280°, dec.

The CT complex 2,3,4,6-tetraphenylpyrylium $(TCNQ_2)$, 7e.

An analogous method was used for the dark green **7e**,m.p. 248°, dec. Anal. $C_{36}H_{28}N_8O$ requires : C, 80.19 ; H, 3.68 ; N, 14.13. Found : C, 79.89 ; H. 3.38 ; N, 15.34%.

IR (KBr, cm^{-1}) : 1250 ; 1600 ; 2150 ; 3027.

The CT complexes of 2,3,4,5,6-pentaphenylpyrylium with TCNQ (7f and 7g)

The two complexes were obtained from the pseudobase or from the methoxy or ethoxy enol-ethers of pentaphenylpyrylium. When using equimolar amounts of the methoxy-derivative [m.p. 181 ; Anal. $C_3 H_2 O_2$ requires : C, 87.77 ; H, 5.73. Found : C, 87.48 ; H. 5.71 %. ; H—NMR ($CDCl_3$, δ, ppm) : 3.58 (s, 3H, methoxy) ; 6.73—7.90 (m, 25 H, aromatic)] and TCNQ, the blue-violet 1 : 1 complex **7g** was obtained, m.p. 279°, dec. Anal. $C_{47}H_{29}N_4O$ requires : C, 84.28 ; H, 4.36 ; N, 8.36. Found : C, 84.51 ; H, 4.39 ; N, 7.97%.

In all other cases, when using an excess of TCNQ, the dark-violet 1 : 2 complex was isolated, m.p. 350°, dec.

Anal. $C_{59}H_{33}N_8O$ requires : C, 81.45 ; H, 3.82 ; N, 12.88. Found : C, 81.16 ; H, 3.98 ; N, 11.96%.

IR (KBr, cm^{-1}) : 1350 ; 1540 ; 3027.

Yields for products **7a**—**7g** were about 60—80%.

AKNOWLEDGEMENTS. Thanks are addressed to Prof. Dr. W. Ruppel and Dr. Geserich (Institut für angewandte Physik der Universität Karlsruhe) for conductivity measurements, to Prof. Dr. I. Pogany for optical spectra and to Drs. M. D. Gheorghiu and F. Chiraleu for ^1H—NMR spectra.

REFERENCES

Preceding part in the series, S. Bădilescu, L. Manu, and A. T. Balaban, *Rev. Roumaine Chim.* **24**, 947 (1979).

[1] G. Briegleb, "*Elektronen-Donator-Acceptor-Komplexe*", Springer Verlag, Berlin, 1961 ; E. M. Kosower, "An Introduction to Physical Organic Chemistry", Wiley, New York, 1969, p. 301 ; R. Foster, "Organic Charge-Transfer Complexes", Academic Press, London, 1969.

[3] D. S. Acker, R. W. Hertler, R. J. Harder, W. Mahler, L. R. Melby, R. E. Benson , and W. E. Machel, *J. Amer. Chem. Soc.*, **82**, 6408 (1960) ; D. S. Acker and W. R. Hertler, *J. Amer. Chem. Soc.*, **84**, 3370 (1962).

[4] F. H. Herbstein, "*Perspectives in Structural Chemistry*", Academic Press, New York, 1971, vol. IV, p. 166.

[5] "Organic Conductors and Semiconductors", Proc. Int. Conf. Siófok, Hungary, 1976, Akadémiai Kiadó, Budapest and Spinger Verlag, Berlin, 1977 ; *Chemica Scripta*, **17**, No. 1—5 (1981) : "The International Conference of Low Dimensional Synthetic Metals", Helsingör, Denmark, 1980.

[6] "Synthetic Metals", Elsevier-Sequoia, Lausanne, **1** (1979/1980).

[7a] Q. R. Melby, R. J. Harder, W. R. Hertler, W. Mahler, R. E. Benson, and W. E. Machel, *J. Amer. Chem. Soc.*, **84**, 3374 (1962) ; b. J. Ferraris, D. O. Cowan, V. Walatka, Jr., and J. H. Perlstein, *J. Amer. Chem. Soc.*, **95**, 948 (1973) ; c. R. C. Wheeland and J. L. Gillson, *ibid.* **98**, 3916 (1976) ; d. J.-M. Fabre, M. Vigroux, E. Torreilles, and L. Giral, *Tetrahedron Lett.*, **21**, 607 (1980).

[8] K. Bechgaard, K. Carneiro, F. B. Rasmussen, M. Olsen, G. Rindorf, C. S. Jacobsen, H. J. Pedersen, and J. C. Scott, *J. Amer. Chem. Soc.*, **103**, 2440 (1981).

[9] R. Buvet, P. Dupuis, J. Néel, and J. Périchon, *Bull. Soc. Chim. France*, **11**, 3991 (1969).

[10] M. Feldman and S. Winstein, *Tetrahedron Lett.*, **1962**, 853 ; W. J. Siemons, P. E. Bierstedt, and R. G. Kepler, *J. Chem. Phys.*, **39**, 3528 (1963) ; B. H. Klanderman and D. C. Hoesterey, *ibid.*, **51**, 377 (1969).

[11] H. Strzelecka, W. Schönfelder, and J. Rivory, *Mol. Cryst. Liq. Cryst.*, **52**, 611 (1979) ; J. Alizon, G. Berthet, J. P. Blanc, P. Durand, J. Gallice, and C. Thibaud, *Magn. Reson. Relat. Phenom.*, Proc. Congr. AMPERE **20**, 439 (1979).

[12] A. T. Balaban, A. Dinculescu, G. N. Dorofeenklo, G. W. Fischer, A. V. Koblik, V. V. Mezheritskii, and W. Schroth, "Pyrylium Salts. Syntheses, Reactions, and Physical Properties", Academic Press, New York, 1982, p. 68.

[13] J. W. Bunting, *Adv. Heterocyclic Chem.*, **25**, 1 (1979).

[14] J. M. Risley, R. L. van Etten, C. Uncutza, and A. T. Balaban, *J. Amer. Chem. Soc.*, (in press).

[15] G. Doddi, S. Fornarini, G. Illuminati, and F. Stegel, *J. Org. Chem.*, **44**, 4496 (1979).

[16] J. A. Berson, *J. Amer. Chem. Soc.*, **74**, 358 (1952).

[17] G. Rio and Y. Fellion, *Tetrahedron Lett.*, **1962**, 1213.

[18] J.-J. Basselier, *Ann. Chim. (Fr.)*, **6**, 1131 (1961).

[19] H. Pütter and W. Dilthey, *J. prakt. Chem.* (2) **107**, 149 (1929).

[20] H. Stetter and A. Reischl, *Chem. Ber.*, **99**, 1253 (1980).

[21] A. I. Pyshchev, N. G. Bokii, and Yu. T. Struchkov, *Tetrahedron*, **34**, 2131 (1978).

[22] A. T. Balaban and C. D. Nenitzescu, *Liebigs Ann. Chem.*, **625**, 74 (1959).

[23] Review : A. T. Balaban, W. Schroth, and G. Frischer, *Adv. Heterocyclic Chem.*, **10**, 241 (1969).

[24] A. T. Balaban. G. D. Mateescu, and M. Elian, *Tetrahedron*, **18**, 1083 (1962).

[25] A. D. Bandrauk, K. D. Truong, V.R. Salares, and J.H. Bernstein, *J. Raman Spectrosc.*, **8**, 5 (1979).

[26] V. Kampars, I. Gudele, and O. Neilands, *Teor. Eksp. Khim.*, **16**, 415 (1980); M. Tanaka, *Bull. Chem. Soc. Japan*, **51**, 1001 (1978).

[27] A. T. Balaban, V. E. Sahini, and E. Keplinger, *Tetrahedron*, **9**, 163 (1960).

[28] J. B. Torrance, *Acc. Chem. Res.*, **12**, 79 (1979).

Revue Roumaine de Chimie, 29, 11–12, 829–832 (1984)

THE INFLUENCE OF MANGANESE OXIDES ADDITIVES ON THE VITRIFICATION OF CLINKER AND PORTLAND CEMENT

I. TEOREANU*, H. BĂLĂȘOIU** and MARCELA MUNTEAN*
* Polytechnic Institute of Bucharest, Str. Polizu no. 1
** Center of Physical Chemistry, Spl. Independenței no. 202, Bucharest, Romania

Received January 13, 1984

The consequences of the presence of manganese ions on the formation of clinker have always been one of the main concerns of the Portland cement chemistry. [1–8] This paper is meant to bring new information on the modifications induced by adding manganese oxides (analyzed as manganese dioxide) on the vitrification degree of the Portland cement clinker, as correlated to the proportions used and to their distribution in the main clinker phases.

1. EXPERIMENTAL INVESTIGATION

In order to obtain this information, clinkers were prepared with a variable MnO_2 content (0 %, 0.5 %, 1 % and 3 %, in gravimetric percents against the crude mixture), using $CaCO_3$, SiO_2, Al_2O_3 and Fe_2O_3 of analytical purity as raw materials. The synthesized clinkers had the following modular parameters : $S_K = 0.96$; $M_{Si} = 2.2$ and $M_{Al} = 2.0$. The crude mixtures were isolated with analytical accurateness and were prepared and homogenized by a planetary mill; an important specific surface was thus obtained, the mixtures having $R_{0063} = 0\,\%$. The burnt samples were shaped by pressing at 10 MPa. As both the existing information and the preliminary trials show that half of the clinker synthesis having the given modular characteristics is already complete at 1350°, we burnt the clinkers using this temperature as the maximum synthesis temperature for 30 minutes.

Porosimetric analyses were made on the clinkers by means of an image analyser microscope. A × 100 magnification was used ; the possible errors produced by the selection of the investigated field were corrected by 8 determinations made at 3 levels for each sample.

In order to obtain information on the manganese distribution among clinker phase constituents, electronic microprobe was analysed.

Chemical analyses were also made for the silicate phases separated by selective chemical attack using a 5 % salicilic acid in methanol solution (which solves the calcium silicates). The data thus obtained confirmed, on the one hand the results of the electronic microprobe analysis and on the other evidenced the correlation between the MnO_2 addition proportion and the alite relative content in the silicate phases (against the MnO_2-free clinker). An interdependence was established between the share of mineralizing acid and the degree of vitrification of the clinker.

2. RESULTS AND THEIR INTERPRETATION

The results of the porosimetric analyses are shown in Table 1.

The study of the data in table 1 clearly shows that for increasing manganese dioxide shares, though the relative pore number increases their corresponding volume decreases, as a consequence of the porosity spectrum shifting towards small size pores. While the number of small pores increases that of the large pores decreases, owing both to the viscous-plastic particle displacement (i.e. their rearrangement into more compact positions, with the fragmentation of the initial, large pores, which become more thoroughly filled with the liquid phase) and to the solving-noncrystallization processes accompanied by solid-liquid interactions which take place in the vitrification system (implying also substance displacement). By processing the data in table 1 in terms of relative capacity of the synthesized clinkers (taken into consideration through the volumetric relative mass against the volumetric mass of the 3% MnO_2 clinker), the dependence of the vitrification degree of the manganese dioxide share added (Fig. 1) can be measured. A marked influence on the degree of vitrification can be noted even for small shares of manganese dioxide ; judging from

Table 1

Values of porosimetric analyses

Determined value	for clinkers containing :			
	0% MnO_2	0.5% MnO_2	1.0% MnO_2	3% MnO_2
The pore number/mm² and size : s [mm]²				
0–2 μm	126	147	480	545
2–4 μm	79	108	309	332
4–8 μm	44	45	103	122
8–16 μm	37	19	62	49
16–32 μm	23	8	32	31
32–64 μm	16	15	11	11
64–128 μm	17	17	10	10
> 128 μm	6	4	3	1
The total pore number/mm²	348	363	1010	1101
Average pore diameter [mm]	0.0318	0.0242	0.0167	0.0147

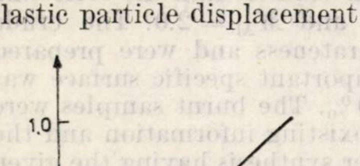

Fig. 1. — Relative volumetric mass (ρ_r) variation with the percentage of manganese dioxide.

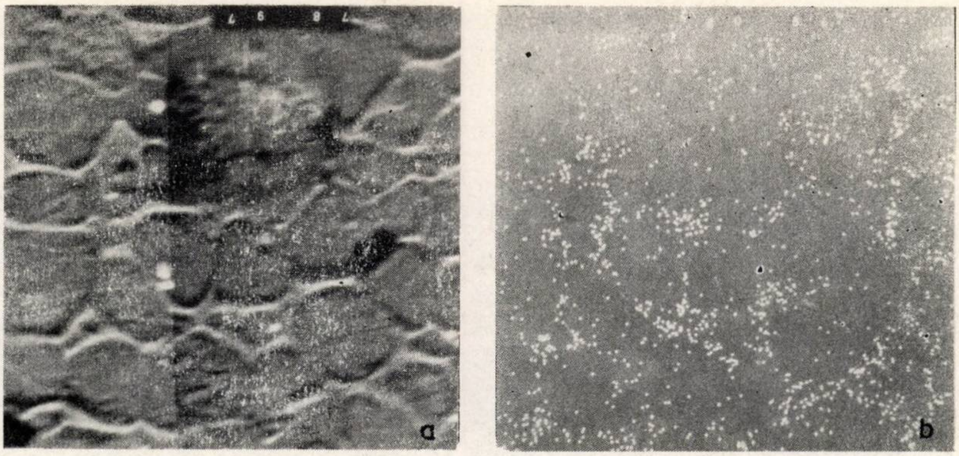

Fig. 2. — Electronomicroscopical images of the MnO_2 free samples : a. image of the mineral composition ; b. image of the iron distribution.

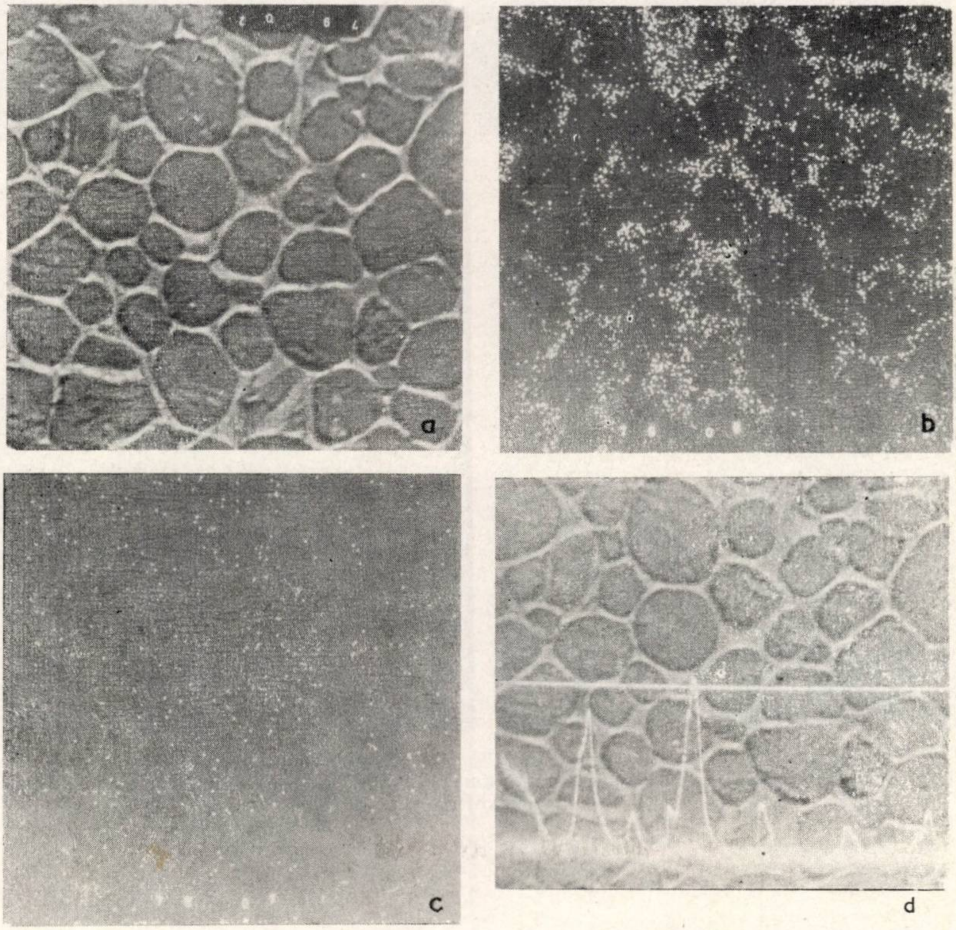

Fig. 3. — Electronomicroscopical images of the 0.5% MnO_2 samples : a. mineral composition image ; b. iron distribution image ; c. manganese composition image ; d. iron and manganese variation concentration.

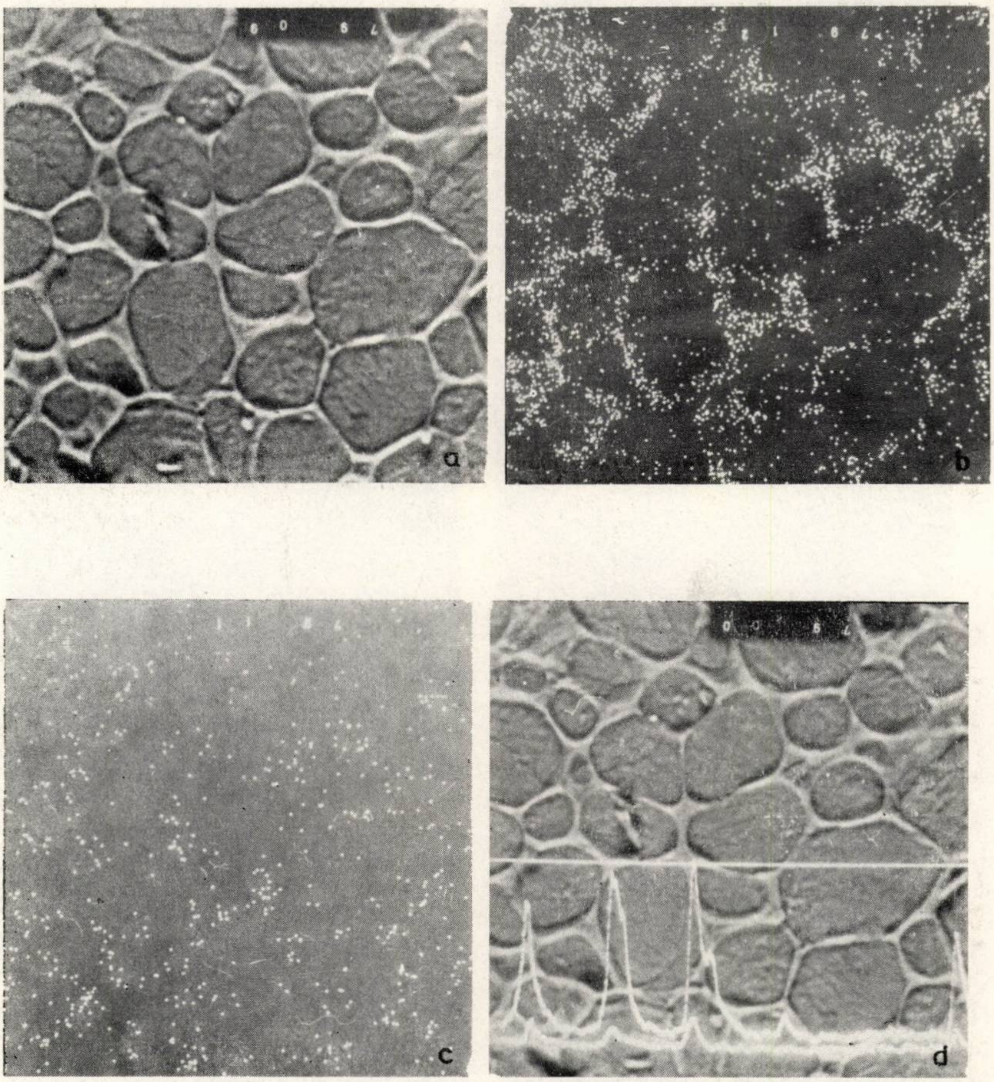

Fig. 4. — Electronomicroscopic images of the 1 % MnO_2 samples : a. mineral composition images ; b. iron distribution image ; c. manganese distribution image ; d. iron and manganese concentration variation.

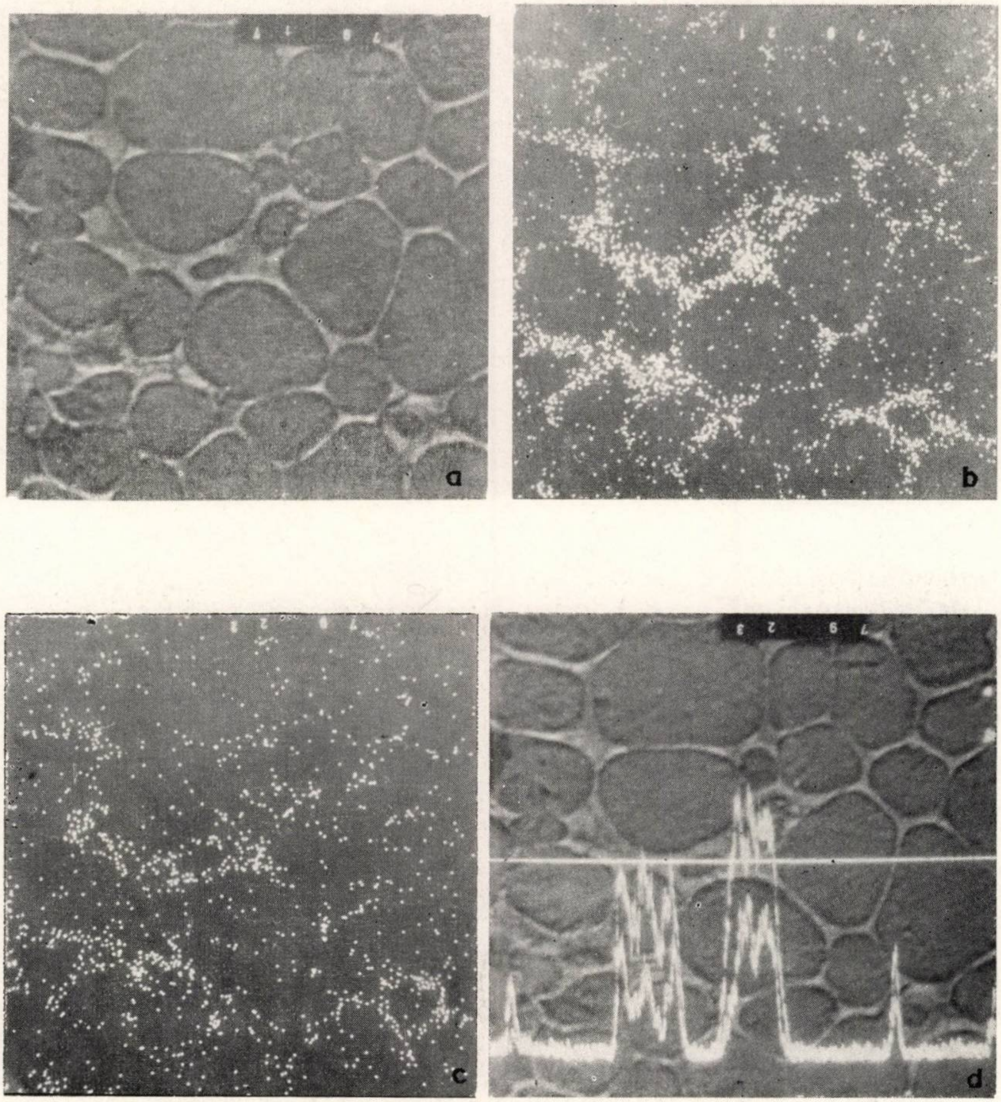

Fig. 5. — Electronomicroscopic images of 3% MnO_2 samples : a. mineral composition images ; b. iron distribution image ; c. manganese distribution image ; d. iron and manganese concentration variation.

the $\rho_r = f(\%MnO_2)$ curve slope this influence is somewhat attenuated for shares larger than 0.5–1 %MnO_2. This proves MnO_2 to be a strong fusing agent. This conclusion is confirmed by the preponderance of the manganese dioxide in the intermediary phaseas shown by the images taken with the electronic microprobe (congruent with the data drawn from the chemical analyses) (Figs. 2–5).

The increase of the vitrification degree with the manganese dioxide share used in the crude mixture does not imply the continuous modification of the mineral composition of the clinker. A rush occurrence of the liquid phase (melt) in the system favours alite formation. The presence of MnO_2 in the system also modifies the thermal equilibrium relationships, especially in high quantities. Its predilect distribution into the intermediary phase (in ferrite calcium aluminate [1,5]) may cause a behaviour of the synthesized clinker similar to ironportland clinkers, with a lower M_{Al}, which at quick cooling, is characterized by a lower alite content. Under these circumstances it is possible that the 3 % MnO_2 clinkers, which have the advantage of the presence of this oxide during the vitrification process, present disadvantages as concerning the alite content. The chemical analysis data obtained were processed in terms of alite relative content in the silicate phase (against, as already mentioned, the MnO_2 additive free clinker), figure 6 shows the image of the relative alite content variation against the degree of vitrification and the MnO_2 share in the clinker. It has been noted that in clinkers having a MnO_2 content up to 1 %, the relative alite content is maintained over that of the standard clinker — the maximum MnO_2 positive effect corresponds to a 0.5 % addition. It was also noted that this MnO_2 percentage has a very strong influence on the clinker vitrification process. Although the respective information is not available it is supposed that percentages higher than 1 % MnO_2 have a negative influence on their bonding characteristics. This conclusion agrees with the literature data regarding the hardening behaviour of certain cements mineralized with manganese oxides. [3]

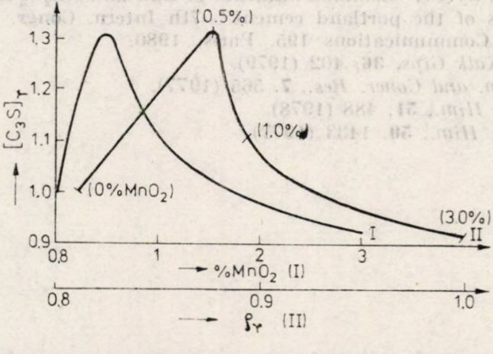

Fig. 6. — Alite relative content variation in the silicate phases of the clinckers as a function of the MnO_2 percentage and corresponding to their degree of vitrification.

3. CONCLUSIONS

a. The manganese oxides, mainly MnO_2, strongly influence the degree of vitrification of the clinker, even in relatively small percentages (0.5%), their fusing capacity being thus proved. The clinker capacity increases with the shifting of the porosity spectrum towards smaller size pores.

b. Manganese oxides are distributed in the intermediate phases, mainly in the ferrite aluminate one.

c. The manganese oxides, by facilitating the occurrence of the liquid phase (melt) in the Portland cement clinker systems, can favour the alite formation. But, they also simultaneously modify the phase thermal equilibrium relationships, thus resulting in mineral composition modifications and maintenance of the cooling thermal treatment system; for higher MnO_2 percentages, the clinkers can behave similarly to low M_{Al} clinkers. These clinkers especially when suddenly cooled, show a diminished alite content, for a quarternary basical composition ($CaO-Al_2O_3-Fe_2O_3-SiO_2$) identical to that of the standard cement. In such cases a great percentage of MnO_2 is added to the Fe_2O_3 when the interstitial phase is formed.

d. The most suitable manganese oxides share in the clinker, which favours the corresponding cement properties, must not be over 1%.

REFERENCES

[1] H. Hornain. *Rev. Mat. Constr.*, 671–672, 203–218 (1971).

[2] B. V. Voljenskii, "Mineralizatory v stroitelinyi promyshlenosti". Stroizd., Moskva, 1964,p. 48.

[3] M. Georgescu and. A. Puri, *Mat. Constr.*, **12**, 177 (1982).

[4] V. Volkov, and M. M. Sycev, "Common influence of BaO and Mn_2O_3 on the obtaining and the properties of the portland cement". 7th Intern. Congr. on the Chem. Cement. Vol. II. Communications 195. Paris, 1980.

[5] O. Knöfel, *Zement Kalk Gips*, **36**, 402 (1979).

[6] R. A. Kennerly, *Cem. and Concr. Res.*, **7**, 565 (1977).

[7] I. Malinin. *J. Prikl. Him.*, **51**, 488 (1978).

[8] V. Volkov, *J. Prikl. Him.*, **50**, 1433 (1977).

Revue Roumaine de Chimie, 29, *11–12*, 833–841 (1984)

POLARIZATION BEHAVIOUR OF THE LEAD MICRO-ELECTRODE IN SULPHURIC ACID SOLUTION

*S. STERNBERG, *V. BRÂNZOI and **LILIANA APĂTEANU

* Chair of Physical Chemistry, The Polytechnic Institute of Bucharest, str. Polizu no. 1

** Institute of Chemical and Biochemical Energetics, Bucharest, 77208, Splaiul Independenţei no. 206, Romania

Received April 27, 1983

The lead electrode (the negative plate) behaviour during the functioning cycles of the lead acid battery was studied by microelectrode technique. The lead microelectrode was cycled within the ($-860 \div -1170$ mV) potential range, using different potential scan rates. The microelectrode capacity (the cycle life index respectively) increases with the increasing number of cycles. A maximum value is obtained at the 150 cycle ; after that the capacity begins to decrease because the microelectrode is sulphated.
There is a similitude between the microelectrode behaviour during the cycling and that of the lead electrode during the battery functioning.

INTRODUCTION

The special importance of the lead acid batteries like power sources has determined the great development of the studies concerning the behaviour of the positive and negative plates during the functioning cycles of the battery. The most studies were made on the positive plate ; for this reason the literature is full of information on its behaviour during the lead acid battery charging or discharging.

Because of poor and incomplete data about the lead electrode behaviour, any study concerning the negative plate behaviour during the battery functioning completes and enriches this information.

The battery test was the only method to determine the discharging capacity of the lead active mass and to maintain the lead electrode capacity during the functioning cycles. Mahato [1,2] proposed for the first time, the microelectrode technique like a determination and test method of the lead electrode behaviour during the acid battery functioning. In the elaboration of this method one starts from the fact that during the potentiostatic cycling of the microelectrode, within the $-1170 \div -860$ mV range (*vs* the $Hg/Hg_2SO_4/H_2SO_4$ 1M electrode), a change of its capacity occurs.

The cycle life index (η), in order to characterize the lead electrode activity during the battery functioning, was introduced and defined as :

$$\eta = \frac{Qf - Qs}{Qo}$$

where *Qo* and *Qf* are the initial and final capacity of the electrode respectively.

In fact, the electrode cycle life index shows the discharging capacity of the lead active mass and the capacity maintenance during the functioning cycles.

The simple quick measurement, the elimination of the complex factors related to the battery test and the economy of materials, substances and time are the major advantages of this technique.

In his works, Mahato was interested only in the technical aspect of the microelectrode utilization in order to establish a similitude between the life time index of the lead microelectrode and the life time of the pasted electrodes from the acid batteries.

In the present work we have used the lead microelectrode technique in order to obtain fundamental informations concerning the mechanism of the $Pb \rightarrow Pb^{2+}$ redox process.

For this purpose, the shape of the anodic and cathodic polarization curves and the coulometrically determined evolution in time of the microelectrode capacity were studied.

EXPERIMENTAL

The microelectrode technique was used. For this purpose an ORION type low frequency generator coupled with a Princetown applied research model 179 potentiostat, a test cell with three electrodes and an X—Y recorder were used (see the schematical representation of the electronic device in Fig. 1).

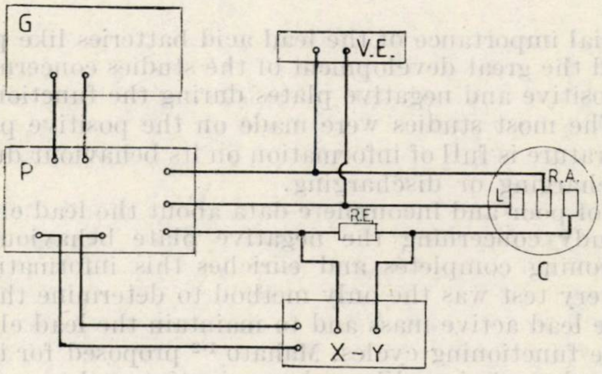

Fig. 1. — Scheme of the electronic device, used in the microelectrode technique.
G — pulse generator, *p* — potentiostat, *x*—*y* — register
c — working cell, *V*—*E* — electronic voltmeter, *R*—*E* standard — load.

By summation of the triangular pulses of the generator with the continuous and constant-pulse of the potentiostat, a potential scanning from —1170 mV to —860 mV and back to —1170 mV, of the lead microelectrode occurs (this is a cycle).

The potential scan rate could be changed as a function of the frequency of the generator pulse. Several potential scan rates were used and many determinations where carried out for each potential scan rate till reproducible results were obtained. The potentiograms were automatically registered by means of an x—y recorder, and the working electrode potential was measured by an electronic voltmeter, *vs.* an $Hg/Hg_2SO_4/H_2SO_4$ 1M referencee electrode. For electrochemical polarizations, a single compartment cell was used; the lead microelectrode of 2 mm diameter and 1.5 cm length in the middle of the cell, was surrounded by a platinum gauze as counterelectrode. This arrangement of the two electrodes creates, during the cycling a uniform, intense electric field.

A Haber-Luggin capillary was used to assure the binding between the cell compartment and the reference electrode. A sulphuric acid solution of 1.24 g/cm^3 density was used as basic electrolyte.

RESULTS AND DISCUSSIONS

Figure 2 shows the lead microelectrode potentiogram in sulphuric acid solution of 1.24 g/cm^3 density, at 150 mV/min potential scan rate.

Analysis of the curve shows that on the anodic increasing curve a (B) maximum of the oxidation current appears within the $-970 \div -860$ mV potential range. This maximum corresponds to the lead dissolution and to the formation of the passive lead sulphate layer. On the (AB) increasing side of the maximum, the active dissolution of lead occurs, resulting in the marked increase of the current density. The Pb^{2+} ions formation combined with the potential removal to more positive values leads to the nonconductor lead sulphate formation, which hinds the dissolution process.

The further potential removal to more electropositive values leads to the decrease of the free surface and of the current density. We are on the (BC) decreasing side of the current maximum, which represents in fact the active-passive transition zone. At the end of this zone the lead microelectrode surface is covered with a dense, compact layer of lead sulphate resulting in the electrode passivation — the current density decreases to a very small value which represents the passivation current. Within this range the electrode process is controlled by the diffusion through the semipermeable layer of lead sulphate. This potential scanning range, from —1170 mV to —860 mV, simulates the lead-acid battery discharge according to the overall equation:

$$Pb \rightarrow Pb^{2+} + 2e \xrightarrow{HSO_4^-} PbSO_4 + H^+ + 2e$$

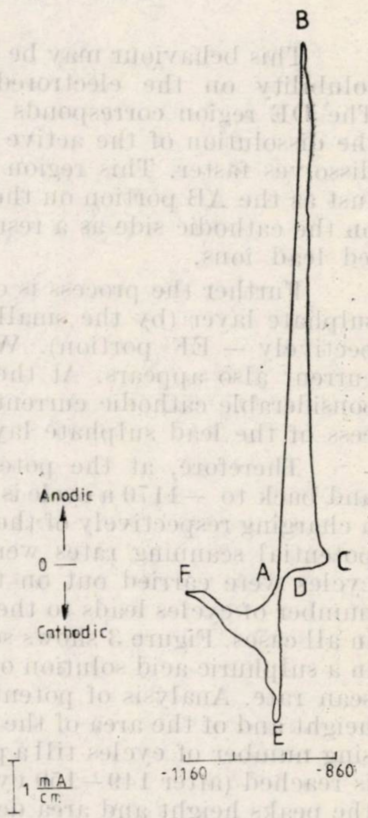

Fig. 2. — The lead microelectrode potentiogram in a sulphuric acid solution of 1.24 g/cm^3 density, registered after 150 cycles, at 150 mV/min potential scan rate.

This discharge process of the lead electrode in sulphuric acid is controlled by the formation of a passive lead sulphate layer on the electrode surface.[2–6]

The reverse potential scanning from −860 mV to −1170 mV leads to the appearance of an (E) reduction current maximum within the −940 mV ÷ −1020 mV potential range. This potential scanning from −860 mV to −1170 mV, simulates the negative electrode charging of the lead acid battery. So, the charging or the cathodic reduction of the lead microelectrode involves the electroreduction of the lead sulphate to metallic lead. The conventional reduction process occurs by a chemical dissolution of the lead sulphate to Pb^{2+} ions succeeded by the electroreduction of Pb^{2+} ions to metallic lead according to the following equations :

$$PbSO_4 + H^+ \rightarrow HSO_4^- + Pb^{2+} \text{ (chemical dissolution)} \quad (2)$$

$$Pb^{2+} + 2e \rightarrow Pb \text{ (electroreduction)} \quad (3)$$

This behaviour may be explained by the control of the lead sulphate solubility on the electroreduction process — reaction (3) respectively. The DE region corresponds to the reduction of Pb^{2+} ions resulted from the dissolution of the active portion of the lead sulphate layer ; this one dissolves faster. This region is predominantly controlled by activation just as the AB portion on the anodic side, but the peak current is smaller on the cathodic side as a result of the limited concentration of the dissolved lead ions.

Further the process is controlled by the slow dissolution of the lead sulphate layer (by the small concentration of the resulted lead ions respectively — EF portion). Within the (EF) range a diffusion limiting current also appears. At the reverse potential sweep it is found that a considerable cathodic current maintains, showing that the reduction process of the lead sulphate layer is not finished up.

Therefore, at the potential sweep from — 1170 mV to — 860 mV and back to —1170 a cycle is obtained equivalent to a discharging, and to a charging respectively of the lead electrode from the acid battery. Several potential scanning rates were used and for each rate a number of 150 cycles were carried out on the lead microelectrode. The increase of the number of cycles leads to the increase of the lead microelectrode capacity, in all cases. Figure 3 shows some potentiograms of the lead microelectrode in a sulphuric acid solution of 1.24 g/cm³ density, at 150 mV/min potential scan rate. Analysis of potentiogram in figure 3 shows the increase of the height and of the area of the anodic and cathodic maxima with the increasing number of cycles till a practically constant value of the peak height is reached (after 149—150 cycles, in our case). If the cycling is going on, the peaks height and area decrease (see Table 1). The existence of a maximum as a function of the number of cycles can be explained on the basis of the results reported by Popova and Kabanov.[7] They showed that the lead sulphate dissolution may occur with very high rates.

Because of this high electroreduction rate a considerable activation of the new-formed lead layers occurs, resulting in their interpenetration and in the formation of a deposit with a small efficient area which will

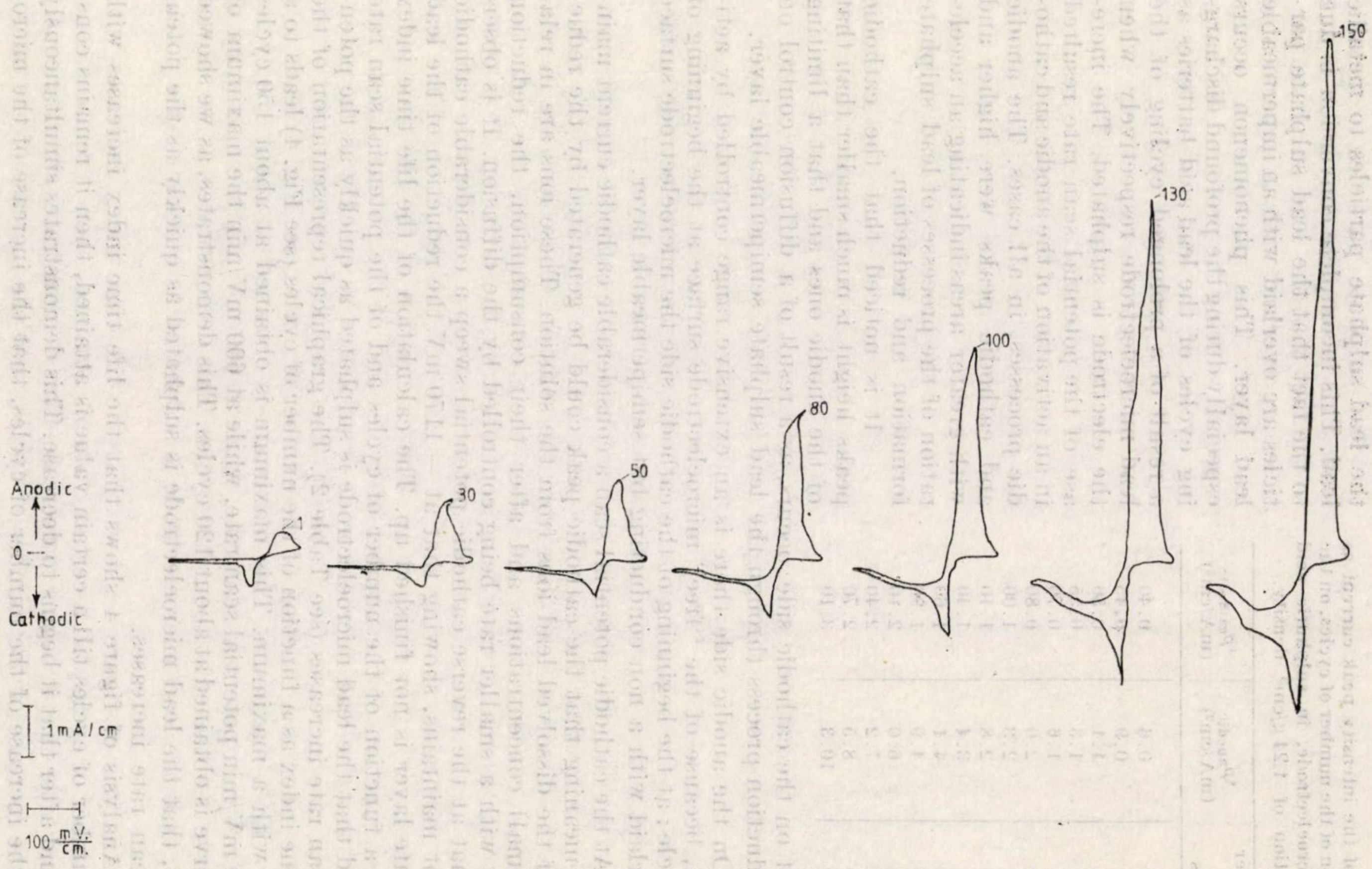

Fig. 3. — The lead microelectrode voltammograms as a function of the number of cycles, in a sulphuric acid solution of 1.24 g/cm density, at 150 mV/min potential scan rate.

Table 1

Values of the intensity peak current as a function of the number of cycles, on the lead microelectrode, in sulphuric acid solution of 1.24 g/cm^3 density.

Number of cycles	$i_{p_{\text{anodic}}}$ (mA/cm^2)	$i_{p_{\text{cathodic}}}$ (mA/cm^2)
10	0.6	0.40
20	0.9	0.45
30	1.1	0.50
40	1.3	0.55
50	1.6	0.70
60	2.0	0.80
70	2.3	1.00
80	2.8	1.10
90	3.4	1.40
100	4.1	1.60
110	4.9	1.90
120	6.0	2.10
130	7.2	2.40
140	8.5	2.70
150	10.3	3.10

generate an incomplete conversion of the lead sulphate particles to metallic lead. This incomplete conversion is due to the fact that the lead sulphate particles are overlaid with an impermeable lead layer. This phenomenon occurs especially during the profound discharging cycles of the lead acid batteries as a result of a prolonged cycling of the lead microelectrode respectively when the electrode is sulphated. The increase of the potential scan rate resulted in an activation of the anodic and cathodic processes, in all cases. The anodic and cathodic peaks were higher and with greater areas indicating an acceleration of the processes of lead sulphate formation and reduction.

It is noticed that the cathodic peaks height is much smaller than that of the anodic ones and that a limiting current on the cathodic side occurs, as a result of a diffusion control on the reduction process through the lead sulphate semipermeable layer.

On the anodic side there is an extensive range controlled by activation, because of the "free" microelectrode surface at the beginning of the cycle ; at the beginning of the cathodic side the microelectrode surface is overlaid with a non conducting but semipermeable layer.

At the cathodic potential scan a considerable cathodic current maintains, meaning that the cathodic peak could be generated by the reduction of the dissolved lead ions from the solution. These ions are in relative small concentrations and after their consumption, the reduction occurs with a smaller rate being controlled by the diffusion. It is observed that at the reverse cathodic potential sweep a considerable cathodic current maintains, showing that at $-$ 1170 mV the reduction of the lead sulphate layer is not finished up. The calculation of the life time index (η) as a function of the number of cycles and of the potential scan rate showed that the lead microelectrode is sulphated as quickly as the potential scan rate increases (see Table 2). The graphical representation of the life time index as a function of the number of cycles (see Fig. 4) leads to a curve with a maximum. This maximum is obtained at about 150 cycles at 150 mV/min potential scan rate, while at 600 mV/min the maximum of the curve is obtained at about 120 cycles. This demonstrates, as we showed before, that the lead microelectrode is sulphated as quickly as the potential scan rate increases.

Analysis of figure 4 shows that the life time index increases with the number of cycles till a certain value is attained, then it remains constant and after that it begins to decrease. This demonstrates simultaneously with the increase of the number of cycles, that the increase of the microelectrode capacity occurs.

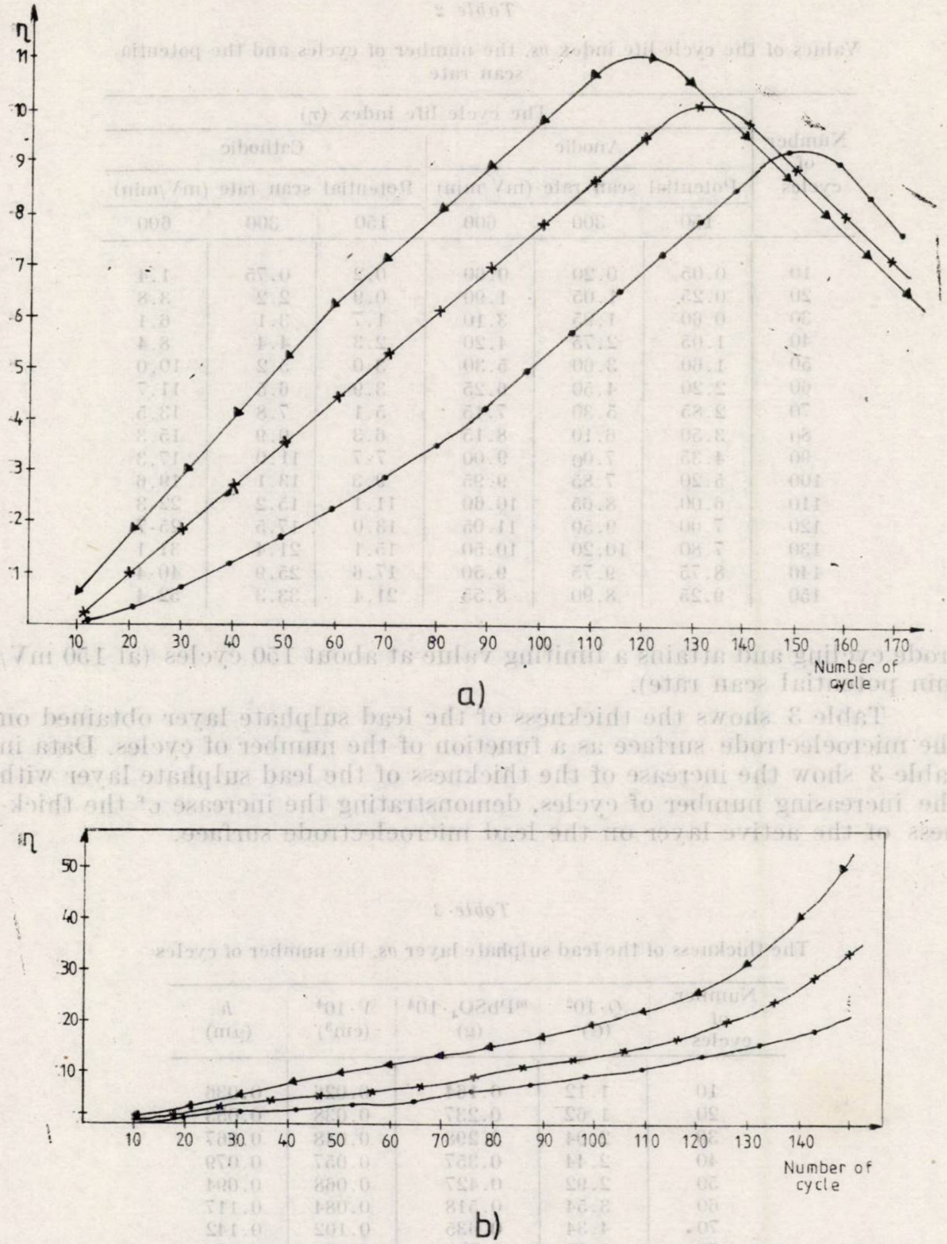

Fig. 4. The cycle life index vs. the number of cycles, at different potential scan rates, a) anodic ; b) cathodic (▲) 600 mV/min ; (x) 300 mV/min ; (.) 150 mV/min.

In fact there is an increase of the thickness of the active layer on the lead electrode surface, which participates in the charging and discharging reactions. This active layer thickness increases with the microelec-

Table 2

Values of the cycle life index *vs.* the number of cycles and the potentia. scan rate

Number of cycles	The cycle life index (η)					
	Anodic			Cathodic		
	Potential scan rate (mV/min)			Potential scan rate (mV/min)		
	150	300	600	150	300	600
10	0.05	0.20	0.60	0.2	0.75	1.4
20	0.25	1.05	1.90	0.9	2.2	3.8
30	0.60	1.95	3.10	1.7	3.1	6.1
40	1.05	2.75	4.20	2.3	4.4	8.4
50	1.60	3.60	5.30	3.0	5.2	10.0
60	2.20	4.50	6.25	3.9	6.5	11.7
70	2.85	5.30	7.15	5.1	7.8	13.5
80	3.50	6.10	8.15	6.3	9.9	15.3
90	4.35	7.00	9.00	7·7	11.0	17.3
100	5.20	7.85	9.95	9.3	13.1	19.6
110	6.00	8.65	10.60	11.1	15.2	22·3
120	7.00	9.50	11.05	13.0	17.5	25·7
130	7.80	10.20	10.50	15.1	21.4	31·1
140	8.75	9.75	9.50	17.6	25.9	40·4
150	9.25	8.90	8.55	21.4	33.3	52·4

trode cycling and attains a limiting value at about 150 cycles (at 150 mV/min potential scan rate).

Table 3 shows the thickness of the lead sulphate layer obtained on the microelectrode surface as a function of the number of cycles. Data in table 3 show the increase of the thickness of the lead sulphate layer with the increasing number of cycles, demonstrating the increase of the thickness of the active layer on the lead microelectrode surface.

Table 3

The thickness of the lead sulphate layer *vs.* the number of cycles

Number of cycles	$Q\cdot 10^2$ (C)	$^{m}\mathrm{PbSO}_4\cdot 10^4$ (g)	$V\cdot 10^4$ (cm^3)	h (μm)
10	1.12	0.164	0.026	0.036
20	1.62	0.237	0.038	0.053
30	2.04	0.298	0.048	0.067
40	2.44	0.357	0.057	0.079
50	2.92	0.427	0.068	0.094
60	3.54	0.518	0.084	0.117
70	4.34	0.635	0.102	0.142
80	5.23	0.765	0.123	0.170
90	6.20	0.907	0.146	0.202
100	7.35	1.075	0.173	0.240
110	8.58	1.255	0.202	0.280
120	9.93	1.453	0.234	0.325
130	11.45	1.675	0.270	0.375
140	13.17	1.927	0.311	0.432
150	15.05	2.202	0.355	0.493

It is to mention that, to determine the thickness of the lead sulphate layer, we used the coulometric part of the potentiostat ; this one automatically registers the quantity of electricity which passes through the cell.

Using Faraday's laws we calculated the mass of the deposited lead sulphate and then the layer thickness. We observed once more that the limiting value of the active layer thickness is obtained after a certain number of cycles, as a function of the potential scan rate (see Table 3). Finally, we conclude that :

— The increase of the number of cycles leads to the increase of the microelectrode capacity (in all cases). In fact, the height of the layer, on the microelectrode surface, increases with the number of cycles.

— At the potential scan from -1170 mV to -860 mV a maximum of current appears, corresponding to the lead dissolution and to the lead sulphate formation.

This potential scan very well simulates the discharging of the lead electrode from the lead acid battery.

— At the reverse potential sweep from -860 mV to -1170 mV, a maximum of cathodic current appears corresponding to the reduction of Pb^{2+} ions to metallic lead. This reverse potential sweep very well simulates the charging of the lead microelectrode from the lead acid battery.

— The increase of the potential scan rate leads to the anodic and cathodic activation (in all cases). The anodic and cathodic maxima of current are more pronounced.

— The life time index (η) increases with the increase of the number of cycles until a maximum value is attained ; then it begins to decrease. At higher potential scan rates, the maximum value of the life time index is attained after a smaller number of cycles indicating that the lead microelectrode is more rapidly sulphated and that the lost of the discharging and of the charging capacity of the lead microelectrode earlier occurs.

REFERENCES

[1] B. K. Mahato, *J. Electrochem. Soc.*, **11**, 124 (1977).

[2] B. K. Mahato, *J. Electrochem. Soc.*, **7**, 128 (1981).

[3] B. K. Mahato, *J. Electrochem. Soc.*, **127**, 8, (1980).

[4] J. Burbank, A. C. Simion, and E. Willihnganz in "Advances in Electrochemistry and Electrochemical Engineering", vol. 8, P. Delahay and C. W. Tobias, Editors, Wiley New York 1970.

[5] P. Ruetschi, *J. Electrochem. Soc.*, **120**, 331 (1973).

[6] A. Winsel, U. Hullmeine, and E. Voss, *J. Power Sources*, **2**, 369 (1977/78).

[7] T. J. Popova și B. N. Kabanov, *Zhur. Priklado Khim.*, **32**, 326 (1959).

Revue Roumaine de Chimie, **29**, *11–12*, 843–855 (1184)

CALCULATION OF PHASE DIAGRAMS OF MOLTEN SALT MIXTURES FROM ELECTROMOTIVE FORCE MEASUREMENTS

S. STERNBERG and D. GEANĂ
Chair of Physical Chemistry, Polytechnic Institute, Spl. Independenţei 313, Bucharest, Romania

Received May 23, 1983

One presents a method of calculation of phase diagrams in binary molten salt mixtures on the basis of electromotive force measurements in formation cells. The excess thermodynamic properties correlated by a Redlich-Kister equation were used for computing the solid-liquid phase diagrams of AgCl –KCl, AgCl –RbCl and AgCl –NaCl systems. A detailed analysis of the calculation is presented together with an algorithm. On this basis a computer program in FORTRAN was written.

INTRODUCTION

The recent progress in computer technology has created a major interest in the computation and correlation of the phase diagrams of binary and multicomponent systems. At present, an important amount of experimental data in relation to solid-liquid equilibrium is available. The computation of solid-liquid equilibria implies a series of aspects, but one can consider two great directions:

— the correlation of experimental data related to solid-liquid equilibria with the aid of a thermodynamic model

— the calculation of solid-liquid phase diagrame, eventually with implications of liquid-liquid and/or solid-solid equilibria.

Different variants of calculation, numerical (or graphic) methods and other details related to solid-liquid equilibria computations are presented and discussed in literature. [1–10] An important progress was possible by the development of computer programs for mathematical representation of thermodynamic properties of multicomponent phases and for the calculation of phase diagrams in binary and ternary systems.

In this paper we present a method of calculation of phase diagrams in binary molten salt mixtures on the basis of electromotive force measurements (emf) in formation cells. The method is similar to that used by Pelton and coworkers [8–10] in the calculation of phase diagrams from enthalpies of mixing.

In two preceding works [11,12] we have discussed the correlation of thermodynamic excess properties, obtained from emf measurements in formation cells, by using the Redlich-Kister and Wilson equations. The results of these correlations were used for computing the solid-liquid phase diagrams of AgCl—KCl, AgCl—RbCl and AgCl—NaCl systems. Some preliminary results were reported elsewhere.[13] A detailed analysis is presented in this paper together with an algorithm of calculation. Based on this algorithm a computer program in FORTRAN was written.

THERMODYNAMIC MODEL OF SOLID-LIQUID EQUILIBRIUM

For a theoretical treatment of solid-liquid equilibrium,[14] one applies usually the thermodynamic criterion based on the minimization of Gibbs free energy function (free enthalpy). Recently, the general application of this criterion to phase equilibria in chemical reacting systems was analysed.[15] A multicomponent system (c components) with two phases (S, L) may be described by the free enthalpy function :

$$G(T, P, n_i^S, n_i^L) = \sum_{i=1}^{c} n_i^S \mu_i^S + \sum_{i=1}^{c} n_i^L \mu_i^L \tag{1}$$

where μ_i are chemical potentials.

The mole numbers are obeyed to the restriction of closed system :

$$n_i^S + n_i^L = n_i^0 \quad (i = 1, 2, \ldots c) \tag{2}$$

and non-negativity

$$n_i^S \geqslant 0 \, ; \; n_i^L \geqslant 0 \tag{3}$$

where n_i^0 are the initial amounts of components.

At equilibrium the function G for constant T, P must reach the minimum [subject to restrictions (2)] :

$$\min G_{T,P}(n_i^S, n_i^L) \tag{4}$$

Taking into account the restrictions and by applying the conditions for a minimum :

$$\partial G / \partial n_i^L = 0 \quad (i = 1, 2, \ldots c) \tag{5}$$

one obtains a non-linear equations system

$$\mu_i^S = \mu_i^L \; (i = 1, 2, \ldots c) \tag{6}$$

The problem of solid-liquid equilibrium is, therefore, to determine the values n_i^S and n_i^L which minimize (1) for given T, P and n_i^0, with the constraints (2), (3). The problem is largely known in formulation (6). One can observe that this problem is a particular case of the general theory of phase equilibrium in chemical reaction systems.[15]

The results of such calculations can be finally expressed by the compositions of phases at equilibrium, for example by mole fractions in the liquid (X_i) and in the solid phase (Y_i).

Since the model of chemical potential of the components has a special form in chemical thermodynamics, another type of calculation of equilibrium is more known, that based on equations (6) without restrictions (2). The chemical potentials are expressed in all the cases (ideal and real) as functions of T, P and phase composition as it results :

$$\mu_i^S(T, P, Y_1, Y_2 \dots Y_{c-1}) = \mu_i^L(T, P, X_1, X_2, \dots X_{c-1})\ (i = 1, 2, \dots c) \quad (7)$$

respectively a non-linear system of c equations with $2c$ unknowns. Generally, one chooses T, P and a number of unknowns which make the system compatible (c equations in c unknowns). In the case of a binary system ($c = 2$), T and P are usually fixed, but X_1, Y_1, are calculated. For a ternary system, one chooses T, P and a mole fractions (for example Y_1), the other unknowns being calculated by solving (7). Surely in calculations the value for X_i, Y_i must be in the domain $[0, 1]$. Such calculations are usualy called phase diagrams calculations.

In the case of melting equilibria, equations (7) become by using the activity function, the Schröder-van Laar equations : [14]

$$\ln \frac{Y_i\gamma_i^S}{X_i\gamma_i^L} = f_i(T, T_i^0, \Delta^t H_i^0, \Delta^t C_{p,i}) \quad (8)$$

where γ_i are the activity coefficients, and the function f_i is dependent on T and the parameters T_i^0 (melting temperature), $\Delta^t H_i^0$ (melting enthalpy) and $\Delta^t C_{p,i}$ (change in molar heat capacity). For an expression of $\Delta^t C_{p,i}$ of the form

$$\Delta^t C_{p,i} = C_{p,i}^L - C_{p,i}^S = \Delta a_i + \Delta b_i T + \Delta c_i T^{-2} \quad (9)$$

the function f_i becomes

$$f_i = \frac{\Delta^t H_i^0}{R}\left(\frac{1}{T} - \frac{1}{T_i^0}\right) - \frac{\Delta a_i}{R}\left(\frac{T_i^0}{T} - 1 - \ln\frac{T_i^0}{T}\right)$$

$$-\frac{\Delta b_i}{2R}\left(\frac{T_i^{0\,2}}{T} - 2T_i^0 + T\right) - \frac{\Delta c_i}{2R}\left(\frac{1}{T} - \frac{1}{T_i^0}\right)^2 \quad (10)$$

The activity coefficients are functions related to the excess thermodynamic properties :

$$\gamma_i^L(T, P, X_1, X_2 \dots X_{c-1}) = \exp[\mu_{i,L}^E/RT] \quad (11)$$

$$\gamma_i^S(T, P, Y_1, Y_2, \dots Y_{c-1}) = \exp[\mu_{i,S}^E/RT]$$

In the calculation of phase equilibria we need expressions of the functions γ_i^L, and γ_i^S respectively. The expressions of these functions may be obtained on the basis of a solution model from statistical thermodynamics (the case of regular model of solution is largely used) or may be empirical. The problem of mathematical representation of thermodynamic excess properties was discussed in the literature. [4,6] We have suggested the equations Redlich-Kister and Wilson for molten salt mixtures. [11,12]

It must be remarked that the functions μ_i^E are generally obtained by the correlation of experimental data from binary systems. The data used in molten salt mixtures are enthalpies of mixing and emf of cells. Generally such data are available at constant temperature. In another work [11] we have suggested a procedure for obtaining the temperature functions $\mu_i^E(T, X_i)$ from emf measurements. Unfortunately emf data are rarely available in a temperature range, the work of Pelton and Flengas [16] being an exception. As an alternative one can use a simultaneous correlation of emf and heat of mixing data. [10,11] The problem is more complicated for ternary (or with $c > 3$) systems where the experimental data are scarce. In such systems one uses interpolation formulas, for example those suggested by Kohler [17] or Toop, [18] by which the calculation of properties in ternary systems is made from the corresponding binary data.

The calculations of solid-liquid phase diagrams based on equations $(7-10)$ can by classified in two classes:

a) Calculation of the composition of coexistent phases at equilibrium if the functions γ_i^S and γ_i^L for binary systems are available from other surfaces. [2]

b) Calculation of the phase equilibrium compositions and the parameters in γ_i^E functions if the excess functions (μ_i^E and eventually S_i^E) of the liquid and the phase diagram are available from other sources. [9,10] In some calculations the parameters of excess entropy function of the liquid are obtained too. The calculations in this class may be named correlations of solid-liquid phase diagrams.

The method presented in this work is from the second class. We remark that the binary systems with eutectic represent an important particular case for both the classes of calculation because $\gamma_i^S = 1$ $(i = 1, 2, \dots c)$. For such systems in the calculations of (b) type [10] one determines S^E (liquid).

CALCULATION OF PHASE DIAGRAMS IN MOLTEN SALT BINARY SYSTEMS

The experimental data used in calculation of phase diagrams of molten salt are the activities obtained by electrochemical methods (emf's), heats of mixing etc. The calculation procedure which will be presented, is based on both data types. For the excess enthalpy, the Redlich-Kister equation [19] was used:

$$G^E = X_1X_2[A + B(X_1 - X_2) + C(X_1 - X_2)^2 + \dots] \qquad (12)$$

where A, B, C are the parameters of the model.

If one assumes a linear dependence of temperature for the parameters [11], eq. (12) becomes:

$$G^E = X_1X_2[(A_0 + A_1T) + (B_0 + B_1T)(X_1 - X_2) + \\ + (C_0 + C_1T)(X_1 - X_2)^2 + \ldots] \quad (13)$$

The activity coefficients are given by

$$RT \ln \gamma_1 = X_2^2[A + B(3X_1 - X_2) + C(X_1 - X_2)(5X_1 - X_2) + \ldots] \quad (14)$$

$$RT \ln \gamma_2 = X_1^2[A + B(X_1 - 3X_2) + C(X_2 - X_1)(5X_2 - X_1) + \ldots] \quad (15)$$

and by similar equations for the model (13).

For the liquid phase we used a model (12) or (13) dictated by available experimental data. For the solid phase the used model is (12). One calculates the values A, B, C for the solid phase which minimize the objective function:

$$\min Q = \sum_k \left(1 - \frac{X_{1,k}(\text{calc})}{X_{1,k}(\text{exp})}\right)^2 + \sum_k \left(1 - \frac{Y_{1,k}(\text{calc})}{Y_{1,k}(\text{exp})}\right)^2 \quad (16)$$

$$(k = 1, 2, \ldots N)$$

The mole fractions are calculated by eqns. (8—11).

The minimization of Q (for the parameters A, B, C of the solid phase) represents a problem of parameters estimation. [20] There are algorithms for solving such problems which were discussed in literature. [20,21] We chose the Hooke-Jeeves algorithm, for its simplicity. [21]

The non-linear equation system (8) was solved by Marquardt's method [22] which is shortly reviewed in appendix. The calculation of phase diagram was made with the following algorithm:

(a) — Input of initial data: properties of pure components (T_i^0, $\Delta^t H_i^0, \Delta^t C_{p,i}$), Redlich-Kister parameters of liquid phase (A_0, A_1, B_0, B_1, C_0,C_1) experimental phase diagram ($T_k(\text{exp})$, $X_{1,k}(\text{exp})$, $Y_{1,k}(\text{exp})$).

(b) — Initial estimation of Redlich-Kister parameters of solid phase: A, B, C (eventually $A = B = C = 0$).

(b) — Initial estimation of Redlich-Kister parameters of solid phase: A, B, C (eventually $A = B = C = 0$).

(c) — Calculation by Marquardt's method [22] of the phase diagram at temperatures $T_k(\text{exp})$: $X_{1,k}(\text{calc})$, $Y_{1,k}(\text{calc})$.

(d) — Calculation of Q by eq. (16).

(e) — New estimations of A, B, C parameters of the solid phase by using Hooke-Jeeves method.

(f) — Convergence test: if ΔA, ΔB, $\Delta C \leqslant \varepsilon$ the procedure is ended (by going to (g)), if the convergence is not achieved the procedure is repeated from (c).

(g) — Output of results: A, B, C parameters for the solid phase, the value of Q function, the calculated compositions of the phases.

For systems with eutectic the calculation is much simplified.[3-10] For such systems we used a modification in the above algorithm by which one solves eqns (8–11) particularised for $Y_i = 1$, $\gamma_i^S = 1$. The solution of nonlinear equation for each component was obtained in this case by a "brute-force" method.[23]

Based on the above presented algorithm a FORTRAN program was written.

EXAMPLES

Emf measurements in formation cells with molten salts AgCl–KCl and AgCl–RbCl, at different temperatures,[16] have been correlated[11] for excess properties on the basis of Redlich-Kister equation (13). The calculated values of Redlich-Kister parameters from eq. (13) are taken from table 2 of our paper.[11] Based on these data, the eutectic diagram was calculated. The used thermochemical data are given in table 1. The phase diagrams for AgCl–KCl and AgCl–RbCl are presented in Figs. 1 and 2 respectively. The experimental curves are shown too.[24] As can be observed, the agreement between the calculated and experimental diagrams is good. The errors at the eutectic temperature are between 5–15° and those for eutectic composition are < 0.02. It can be noticed that differences of a few degrees in T_i^0 frequently encountered in literature have only a minor effect upon calculation. A similar effect is observed for a difference of ± 100 cal/mole in $\Delta^t H_i^0$.

Table 1

Thermochemical data[25, 26]

Salt	T°	ΔH°	C_P^S	C_P^L
	K	kcal/mole	cal/mole.K	
AgCl	724	3.08	$14.88 + 10^{-3}T - 2.7 \cdot 10^5 T^{-2}$	16
KCl	1037	6.35	$9.89 + 5.2\ 10^{-3}T + 0.77\ 10^5 T^{-2}$	17.49
RbCl	995	5.67	$11.5 - 2.49\ 10^{-3}T$	17.56
NaCl	1074	6.69	$8.88 - 5.69\ 10^{-3}T$	16.5

The above presented algorithm was used for calculating the phase diagrams of KCl–NaCl and AgCl–NaCl systems. The phase diagram of the first system was calculated by Lin and coworkers[9,10] based on the heat of mixing in liquid phase:

$$\Delta H_{am} \equiv H^E = X_1 X_2 (-0.4896 - 0.065\, X_2),\ \text{kcal/mol} \tag{17}$$

We have made a similar calculation for testing our program, using the thermochemical data from the above work (see table I, p. 28 in [9]). The agreement is very good, the excess free entalphy being:

$$G^E = Y_1 Y_2 (2.853 + 0.152\, Y_2 - 0.076\, Y_2^2),\ \text{kcal/mol} \tag{18}$$

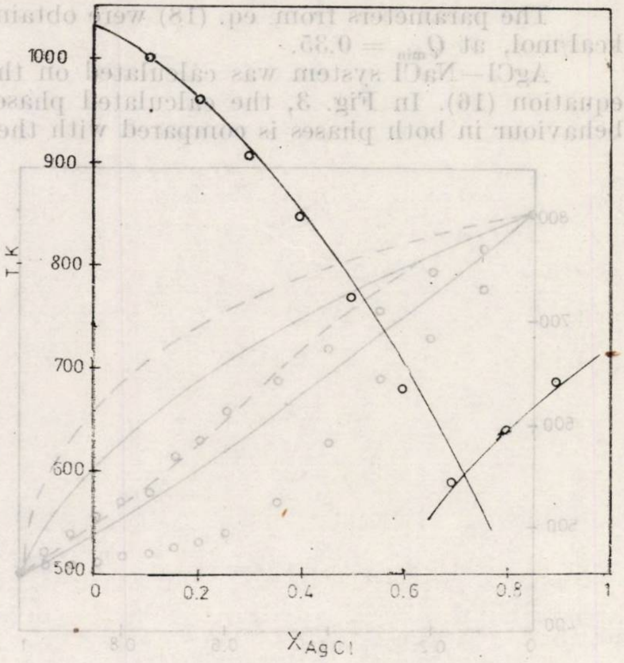

Fig. 1. —Solid-liquid phase diagram of KCl —AgCl system (—) calculated ; (0) experimental.

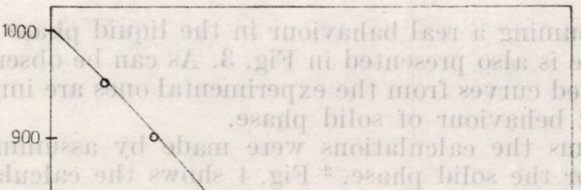

Fig. 2. — Solid-liquid phase diagram of RbCl —AgCl system (—) calculated ; (0) experimental.

The parameters from eq. (18) were obtained for ΔA, ΔB, $\Delta C \leqslant 0.01$ kcal/mol, at $Q_{\min} = 0.35$.

AgCl—NaCl system was calculated on the basis of Redlich-Kister equation (16). In Fig. 3, the calculated phase diagram assuming ideal behaviour in both phases is compared with the experimental diagram [24].

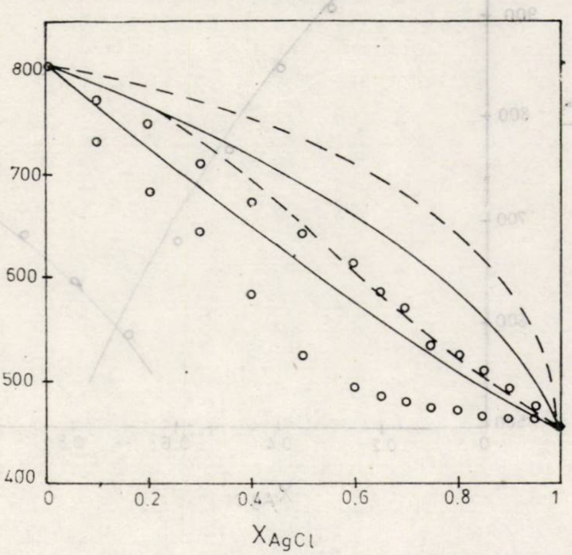

Fig. 3. — Solid-liquid phase diagram of NaCl-AgCl system.
(—) calculated assuming ideal behaviour in both phases; (— —) calculated assuming real liquid phase and ideal solid phase; (0) experimental.

A calculated diagram assuming a real bahaviour in the liquid phase and the ideality of solid phase is also presented in Fig. 3. As can be observed the deviations of calculated curves from the experimental ones are important, suggesting the real behaviour of solid phase.

For different systems the calculations were made by assuming a regular solution model for the solid phase. [2] Fig. 4 shows the calculated phase diagram with a Redlich-Kister model for the liquid phase (13) and assuming a regular solution model for the solid phase. Two situations are presented which differ by the parameter of the regular model, $A = 1000$ cal/mole and $A = 2000$ cal/mole respectively. It can observed that for $A = 2000$ cal/mole the calculated diagram is close to the experimental one, but the agreement is not satisfactory.

Therefore the phase diagram for AgCl—NaCl system was calculated with the above presented algorithm. In Fig. 5 one compares the calculated and experimental diagrams. For the solid phase we used a Redlich-Kister equation (12) assuming $S^E(\text{solid}) = 0$. For the excess free enthalpy the resulted equation is :

$$G^E(\text{solid}) = Y_1 Y_2 (1750 + 422(Y_1 - Y_2) + 1281(Y_1 - Y_2)^2), \text{ cal/mol} \quad (19)$$

It can be remarked that the solidus calculated curve is in very good agreement with the experimental one. The calculated liquidus curve shows deviations which at $T = 600$ K are $\simeq 0.1$ in mole fraction. The minimization criterion has the value $Q_{\min} = 0.57572$ by using 14 temperature values for calculation.

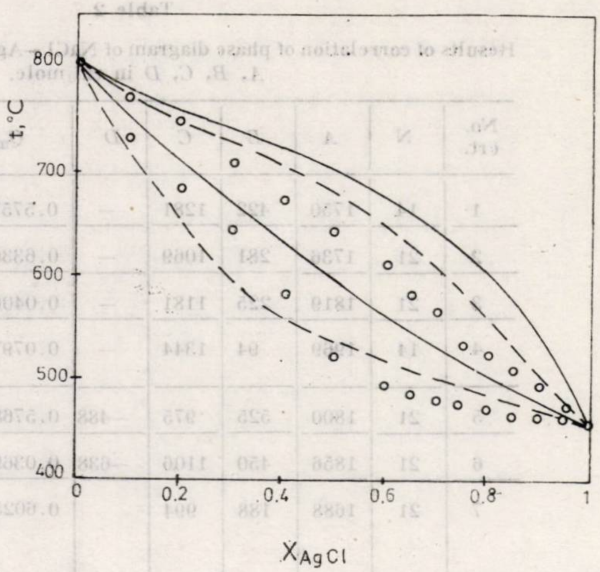

Fig. 4. — Solid-liquid phase diagram of NaCl—AgCl system.
(—) calculated for real liquid phase and regular solid solution (A = 1000 cal/mole);
(— —) calculated for real liquid phase and regular solid solution (A = 2000 cal/mole);
(0) experimental.

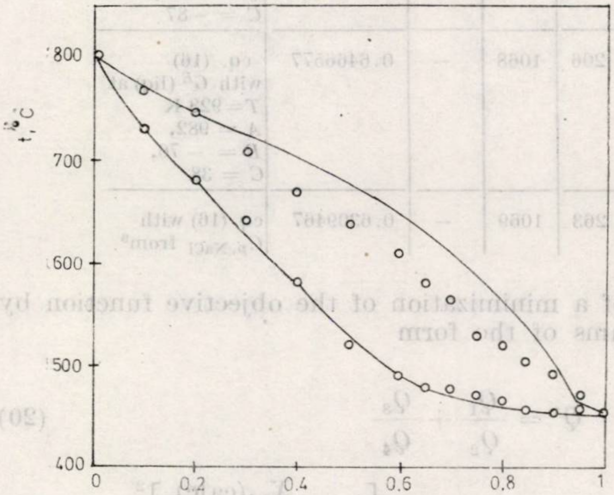

Fig. 5. — Solid-liquid phase diagram of NaCl—AgCl system.
(—) calculated by minimization of function Q with A, B, C parameters of solid phase from eq. (19); (0) experimental.

We have analysed the influence of the following factors on the accuracy of calculation:

a) the growth of the number of temperature values in the correlation. The necessary data were obtained by linear interpolation using the experimental measured values.[24] In table 2 the obtained results of correlation are presented (in the second row). We can remark some modifications by comparison with eq. (19) (see also the first row in table 2), but the value of $Q_{\min} = 0.6336$.

Table 2

Results of correlation of phase diagram of NaCl —AgCl system. Parameters A, B, C, D in cal/mole.

No. crt.	N	A	B	C	D	$Q_{\min}$	Observations
1	14	1750	422	1281	—	0.5757161	eq. (16)
2	21	1736	281	1069	—	0.6336258	eq. (16)
3	21	1819	225	1181	—	0.0406273	eq. (20 –24)
4	14	1969	94	1344	—	0.07974738	eq. (25) $\Delta A, \Delta B, \Delta C \leqslant 20$
5	21	1800	525	975	−488	0.5768161	eq. (16)
6	21	1856	450	1106	−638	0.03690481	eq. (20 –24)
7	21	1688	188	994		0.6025659	eq. (16) with G^E (liq) at $T=1073$ K $A=910$; $B=-107$, $C=-87$
8	21	1743	206	1068	—	0.6466577	eq. (16) with G^E (liq) at $T=923$ K $A=982$, $B=-76$, $C=38$
9	21	1763	263	1069	—	0.6309467	eq. (16) with $C_{p,\mathrm{NaCl}}$ from[9]

b) the application of a minimization of the objective function by weighing the terms in sums of the form

$$Q' = \frac{Q_1}{Q_2} + \frac{Q_3}{Q_4} \tag{20}$$

$$Q_1 = \sum_k X_{1,k}(\exp)[1 - X_{1,k}(\exp)]\left[1 - \frac{X_{1,k}(\mathrm{calc})}{X_{1,k}(\exp)}\right]^2 \tag{21}$$

$$Q_2 = \sum_k X_{1,k}(\exp)\ [1 - X_{1,k}(\exp)] \tag{22}$$

$$Q_3 = \sum_k Y_{1,k}(\exp)\ [1 - Y_{1,k}(\exp)]\left[1 - \frac{Y_{1,k}(\mathrm{calc})}{Y_{1,k}(\exp)}\right]^2 \tag{23}$$

$$Q_4 = \sum_k Y_{1,k}(\exp)\ [1 - Y_{1,k}(\exp)] \tag{24}$$

The results are presented in the third row of table 2 but the calculated phase diagram is not better.

Another correlation function was:

$$Q'' = \sum_k \left[X_{1,k} - X_{1,k}(\exp)\right]^2 + \sum_k \left[Y_{1,k} - Y_{1,k}(\exp)\right]^2 \qquad (25)$$

The results are given in table 2 (row 4). A little influence on the accuracy of calculation can be noticed.

c) the growth of the number of Redlich-Kister parameters in γ functions. We tried the calculations with 4 and 5 parameters for the solid phase (rows 5 and 6 in table 2). The effect on the accuracy of calculation is not important. The fifth parameter was null in the calculations. Probably the using of the orthogonal functions [4] may be more concludent.

d) the use for the liquid phase of an excess function G^E, independent of temperature (assuming S^E (liquid) $= 0$). The results in table 2 (rows 7, 8) obtained with $G^E(T = 1073\ \mathrm{K})$ and $G^E(T = 923\ \mathrm{K})$ respectively show a decrease in the accuracy of correlation. Therefore it is necessary to use the excess entropy of liquid phase in calculations if there is available.

e) the changes in the function $\Delta^t C_{p,\mathrm{NaCl}}$ influence slightly the accuracy of correlation as can be seen from table 2 (row 9). Deviations of ±100 cal/mole in the values of melting enthalpies of components show a little influence on the calculated phase diagram.

Certainly the problems which appear in the calculations of solid-liquid phase diagrams are numerous. Some aspects were discussed in this work, and the study of a great number of systems will lead to general conclusions. It must be remarked that the accuracy of correlations in binary systems is very important for the treatment of multicomponent systems.

APPENDIX

Marquardt's method [22] for solving a nonlinear equation system is a combination of two known procedures, Newton-Raphson method and the method of steepest descent.

Consider the system of nonlinear equations:

$$F(x) = 0 \qquad (A_1)$$

Expanding in a Taylor's series:

$$F^{k+1} = F^k + J_k \xi + \dots \qquad (A_2)$$

where J^k is the Jacobian at iteration k, and

$$\xi = x^{k+1} - x^k \qquad (A_3)$$

Neglecting the terms of higher order, for the solution $F^{k+1} = 0$, it results

$$J^k \xi = -F^k \qquad (A_4)$$

or

$$\xi = -(J^k)^{-1} F^k \qquad (A_5)$$

Taking f_i as elements of the vector $F(x)$ and

$$Q = \sum_i f_i^2 \tag{A_6}$$

there exists the relation

$$2J^T F = \nabla Q \tag{A_7}$$

where ∇Q is the gradient vector of the function Q, and the superscript T denotes transposition for a matrix.

Multiplying (A_4) by $2J^T$ one obtains:

$$2J^T J\, \xi = -2J^T F \tag{A_8}$$

dropping the iteration index.

Eq. (A_8) can be written

$$G\xi = -\nabla Q \tag{A_9}$$

where $G = 2J^T J$. If J is a singular matrix, G is also singular and eq. (A_9) can be modified to

$$(G + \lambda I)\xi = -\nabla Q \tag{A_{10}}$$

I is the unity matrix and λ is a nonnegative scalar.

Eq. (A_{10}) can be solved

$$\xi = -(G + \lambda I)^{-1}\nabla Q \tag{A_{11}}$$

For $\lambda = 0$ it results the Newton-Raphson method, but if λ is large, the diagonal terms in the matrix $(G + \lambda I)$ are dominant resulting the method of steepest descent.

REFERENCES

[1] R. Haase, and H. Schönert, "Solid-Liquid Equilibrium", Pergamon Press, Oxord, 1969.

[2] L. Kaufmann and H. Bernstein, "Computer Calculation of Phase Diagrams", Acad. Press, New York, 1970.

[3] L. Filipescu and E. Pincovschi, "Echilibrul solid-lichid", Ed. Tehnică, Bucharest, 1980.

[4] C. W. Bale and A. D. Pelton, *Metall. Trans.*, **5**, 2323 (1974).

[5] K. Nakanishi, *Ind. Eng. Chem. Fundam.*, **9**, 449 (1970).

[6] J. Marimi and K. Nakanishi, *Fluid Phase Equil.*, **1**, 153 (1977).

[7] M. Malinovsky, *Chem. Zvesti*, **25**, 92 (1971).

[8] A. D. Pelton and C. W. Bale, *CALPHAD*, **1**, 253 (1977).

[9] P. L. Lin, C. W. Bale and A. D. Pelton, in "Proc. of Symp. on Calculation of Phase Diagrams and Thermochemistry of Alloy Phases" ed. Y. A. Chang, J. F. Smith, held in Milwaukee, Wisconsin, Sept. 17–18, 1979, p. 26.

[10] P. L. Lin, A. D. Pelton and C. W. Bale, *J. Amer. Ceram. Soc.*, **62**, 414 (1979).

[11] S. Sternberg and D. Geană, *Rev. Roumaine Chim*, **24**, 279 (1979).

[12] S. Sternberg and D. Geană, *Rev. Roumaine Chim.* **24**, 1083 (1979),

[13] S. Sternberg and D. Geană, in "Proc. of 30th Meeting of International Society of Electrochemistry", Trondheim, Norway, August 26–31, 1979, p. 233

[14] I. Prigogine and R, Defay, "Chemische Thermodynamik", VEB Deutsche Verl. Leipzig, 1962.

[15] D. Geană, *Rev. Roumaine Chim.*, **26**, 363 (1981).

[16] A. D. Pelton and S. N. Flengas, *J. Electrochem. Soc.*, **117**, 1130 (1970).

[17] F. Kohler, *Mh. Chem.*, **91**, 738 (1960).

[18] G. W. Toop, *TMS-AIME*, **233**, 850 (1965).

[19] O. Redlich and A. T. Kister, *Ind. Eng. Chem.*, **40**, 345 (1945).

[20] J. H. Seinfeld and L. Lapidus, "Mathematical Methods in Chemical Engineering", vol. 3, Prentice Hall, New Jersey, 1974, p. 382.

[21] V. Dumitru, "Programare neliniară", Ed. Academiei, Bucharest, 1975.

[22] E. J. Henley and E. M. Rosen, "Mathematical and Energy Balance Computations", Wiley, New York, 1969, p. 202.

[23] H. Herman, Electrochemistry, in "Computer in Chemistry and Instrumentation", vol. 2, ed. J. S. Matsson, H. B. Mark jr., H. C. Mac Donald jr. M. Dekker Inc., New York, 1972.

[24] N. K. Voskresenskaya, "Spravochnik po plavosti sistem iz bezvodykh neorganicheskih solei", vol. 1, Izd. Akad. U.S.S.R., Moskow, 1961.

[25] M. Blander, "Molten Salt Chemistry", Interscience Publ., New York, 1964.

[26] I. G. Murgulescu and C. Telea, *Rev. Roumaine Chim.*, **22**, 683 (1977).

Revue Roumaine de Chimie, 29, 11–12, 857–860 (1984)

FRIEDEL-CRAFTS ACYLATION OF ACETYLENES. IV[a]

ON THE NON SELECTIVITY OF ACYLVINYL CATIONS IN AROMATIC SUBSTITUTION

DUMITRU MĂNOIU,[a] MARIA MĂNOIU,[a] ILIE G. DINULESCU[b]
and MARGARET AVRAM[b,*]

[a] Institute of Research Technological Engineering and Design for Refineries, Ploeşti, Romania
[b] Laboratory of Organic Chemistry, Polytechnic Institute —TCH, Spl. Indpendenţei 313, 72206 Bucharest 16, Romania

Received July 21, 1983

The reaction of propyne with propionyl chloride and $AgClO_4$ in aromatic hydrocarbons with different nucleophilicities or in mixture of such hydrocarbons evidences that the acylvinyl cation reacts statistically and unselectively with the aromatic partners.

Aiming to extend the area of knowledge concerning the reactivity of acylvinyl cations generated in the reaction of 1-alkynes with acyl chlorides in the presence of $AgClO_4$, [1] their behaviour toward aromatic partners with different nucleophilicities seemed of interest.

In this paper we present the results obtained in the coupled acylation-arylation reaction of propyne with propionyl chloride using as aromatic partners benzene, toluene, mesitylene and mixtures of these solvents.

The experiments were performed according to a standard procedure (see experimental part). The product distribution was established on the basis of glc analysis of the crude reaction mixture; the compounds were identified by comparison with authentical samples or isolated and the structure ascribed on the basis of analytical and spectral data.

The reaction of propyne with propionyl chloride and $AgClO_4$ carried out in benzene-CCl_4 mixture afforded a mixture of two isometric compounds. The major component (92%) was isolated and identified as *E*-5-phenyl-hex-4-en-3-one (**1**); for the minor component (6.8%) the structure of *Z* isomer **2** was ascribed.

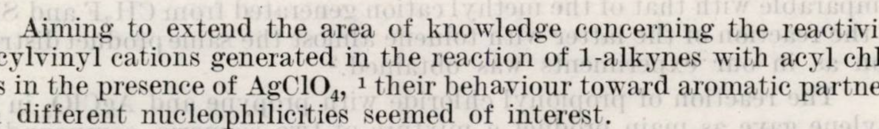

1 **2**

The reaction of propyne with propionyl chloride and $AgClO_4$ carried out in the same experimental conditions but using as solvent toluene-CCl_4 mixture gave a crude reaction product (52%) containing three major components (totalising 92%) beside two minor (8%) with greater retention times. The major components were isolated and identified as being *ortho*, *para* and *meta* isomers of 5-tolyl-hex-4-en-3-one (**3**), in ratio 3.2 : 1.7 : 1.0.

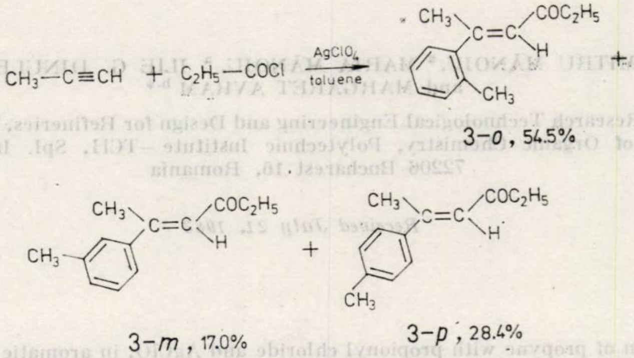
$CH_3-C\equiv CH + C_2H_5-COCl \xrightarrow[\text{toluene}]{AgClO_4}$
CH_3
COC_2H_5
$C=C$
H
+

3-*o*, 54.5%

3-*m*, 17.0%

3-*p*, 28.4%

This result evidences that the acylvinyl cation is an efficient electrophile in aromatic substitution with low positional selectivity. The orientation effect of the methyl group from the aromatic partner is inoperant due to the "hot" nature of the free acylvinyl cation. This behaviour is comparable with that of the methyl cation generated from CH_3F and SbF_5. In the reaction of the latter with toluene almost the same product distribution as in our experiments was obtained.[2]

The reaction of propionyl chloride with propyne and $AgClO_4$ in mesitylene gave as main product a mixture of two isomeric compounds in ratio 6.7 : 1.0. These compounds were isolated and identified as being *E*-5-mesityl-hex-4-en-3-one (**4**) and its *Z* isomer (**5**).

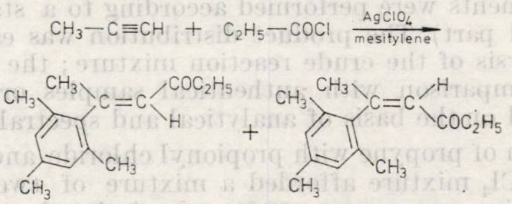
$CH_3-C\equiv CH + C_2H_5-COCl \xrightarrow[\text{mesitylene}]{AgClO_4}$
CH_3
COC_2H_5
$C=C$
H
+

4, 87.0%

5, 13.0%

The high reactivity of the acylvinyl cation in the electrophilic aromatic substitution, evidenced by the low positional selectivity when toluene is used as aromatic partner, prompted us to investigate the reaction of propyne with propionyl chloride and $AgClO_4$ in the presence of mixtures of aromatic hydrocarbons with different nucleophilicities in order to establish, if existent, the degree of selectivity toward the aromatic hydrocarbons.

Considering that the difference of basicity between benzene and toluene is of the order of 10^2 and between benzene and mesitylene is $2.8 \cdot 10^5$, it was assumed that if the acylvinyl cation presents selectivity, the reaction with more basic hydrocarbon will be preferred.

Using the standard procedure described in the experimental part, the reactions of propyne with propionyl chloride and $AgClO_4$ were performed in mixtures of benzene-toluene 1 : 1 and 1 : 14 and benzene-mesitylene 1 : 1 and 14 : 1. The reaction products were analysed by glc and identified by comparing with authentical samples obtained in the above described reactions.

Thus, the reaction performed in benzene-toluene 1 : 1 afforded 45.8 % phenylated ketones **1** and **2** together with 54.2 % tolylketones **3** (*ortho*, *para* and *meta* isomers in ratio 2.7 : 1.5 : 1.0). From these data the calculated value of the selectivity ratio S_T/S_B was found 1.47.

Using as aromatic partner a mixture of benzene-toluene 1 : 14, 9.6 % phenylketones (**1** and **2**) and 89.4 % **3** were obtained; the selectivity ratio S_T/S_B was found 1.34.

In the reactions performed in mixture of benzene and mesitylene (with greater difference of basicity) comparable results were obtained. Thus, using benzene-mesitylene in ratio 1 : 1 a mixture of 43.8 % phenylketones (**1** and **2**) and 56.2 % mesitylketones **4** and **5** were obtained. The selectivity ratio calculated from these data was 1.93. With a mixture of benzene-mesitylene 14 : 1, 83.0 % phenylketones (**1** and **2**) and 17.0 % mesitylketones **4** and **5** were obtained; the selectivity ratio is $S_M/S_B = 2.69$.

These data evidence also that the acylvinyl cation presents a low selectivity toward the aromatic partners. Such low selectivity was observed in few cases, for instance in the methylation of benzene in gaseous phase ($S_T/S_B = 1.8$). [2]

The results obtained in this study evidence that the "hot" acylvinyl cation reacts statistically and unselectively with the aromatic partners.

EXPERIMENTAL

IR spectra were recorded with a double beam C. Zeiss UR-20 spectrophotometer. ^{1}H-NMR were determined with Tesla-60 and Varian A60-A spectrometers. Glc analysis and glc preparative separations were carried out as earlier described. [3,4]

Standard procedure. The reactions were carried out using the previously described standard procedure.[1]

Reaction of propyne with propionyl chloride and $AgClO_4$ in benzene. Working according to the general procedure, a crude reaction product was obtained in 65 % yield. In this product, by means of glc the ketones **1** (92 %) and **2** (8 %) were evidenced. These new compounds were separated by preparative glc.

E-5-Phenyl-hex-4-en-3-one (**1**), b.p. 110°/5mm. IR (CCl_4, cm^{-1}) : ν_{CO} 1696, $\nu_{C=C}$ 1602; ^{1}H-NMR (CCl_4, δ, ppm) : 1.0 (CH_3), 2.40 (CH_2), 2.42 ($CH_3-C=$), 6.35 ($H-C=$), 7.28 $(C_6H)_5$; UV (EtOH; λ max nm, ε) : 210 (4900), 200 (6150), 280 (15700). Analysis : $C_{12}H_{14}O$ Calcd. : C, 82.75; H, 8.04. Found : C, 82.02; H, 8.70 %.

Z-5-Phenyl-hex-4-en-3-one (**2**), b.p. 130°/5 mm. ^{1}H-NMR (CCl_4, δ ppm) : 0.78 (CH_3), 1.96 (CH_2), 2.07 ($CH_3-C=$), 7.09 (C_6H_5).

Reaction of propyne with propionyl chloride and $AgClO_4$ in toluene. From the crude reaction products, isolated in 52 % yield, a fraction containing the three major components (totalising 92 %) was separated by glc and found to be a mixture of *ortho, meta* and *para*-isomers of 5-tolyl-hex-4-en-3-one (**3**), b.p. 110 –135°/5 mm.
Analysis : $C_{13}H_{16}O$ Calcd. : C, 82.97; H, 8.51. Found : C, 82.51; H, 8.17 %.

Further glc separation afforded the pure components.

3-*ortho*, 54.5 %, mixture of *Z* and *E* isomers (separated by thin layer chromatography). IR (CCl_4, cm^{-1}) : ν_{CO} 1695, $\nu_{C=C}$ 1620 ; UV (EtOH ; λ max nm, ε) : 215 (6700), 225 (6700), 286 (10700). — *E*-**3**-*o*, 47.9 %. ^1H-NMR (CCl_4, δ, ppm) : 1.10 (CH_3), 1.81 (CH_2), 2.17 ($Ar-CH_3$), 2.30 ($CH_3-C=$), 6.01 ($H-C=$), 7.03 (aromatic). — *Z*-**3**-*o*, 6.6 %. ^1H-NMR (CCl_4, δ, ppm) : 2.00 ($CH_3-C=$), 2.16 ($Ar-CH_3$), 6.09 ($H-C=$), 7.01 (aromatic).

3-*para*, 28.4 %. IR (CCl_4, cm^{-1}) : ν_{CO} 1690, $\nu_{C=C}$ 1605 ; ^1H-NMR (CCl_4, δ, ppm) : 0.99 (CH_3), 2.38 (CH_2), 2.41 ($CH_3-C=$), 6.30 ($H-C=$), 7.12 (aromatic) ; UV (EtOH ; λ max nm, ε) : 225 (2500).

3-*meta*, 17.0 %. IR (CCl_4, cm^{-1}) : ν_{CO} 1690, $\nu_{C=C}$ 1605 ; ^1H-NMR (CCl_4, δ, ppm) : 1.00 (CH_3), 2.27 ($Ar-CH_3$), 2.38 (CH_2), 2.41 ($CH_3-C=$), 6.30 ($H-C=$), 7.04 (aromatic).

Reaction of propyne with propionyl chloride and $AgClO_4$ in mesitylene. Working as above a mixture of **4** and **5** was separated by glc ; b.p. 125 –132°/5 mm. Analysis : $C_{15}H_{20}O$ Calcd : C, 82.17 ; H, 9.21. Found : C, 82, 33 ; H, 9.25 %. Further glc separation afforded the pure components.

E-5-Mesityl-hex-4-en-3-one (**4**), 87.0 %. IR (CCl_4, cm^{-1}) : ν_{CO} 1695, $\nu_{C=C}$ 1620 ; ^1H-NMR (CCl_4, δ, ppm) : 1.00 (CH_3), 2.07 (o-CH_3), 2.16 (p-CH_3), 2.21 ($CH_3-C=$), 5.90 ($H-C=$), 6.70 (aromatic) ; UV (EtOH ; λ max nm, ε) : 223 (24100), 273 (3260).

Z-5-Mesityl-hex-4-en-3-one (**5**), 13.0 %. IR (CCl_4, cm^{-1}) : ν_{CO} 1690, $\nu_{C=C}$ 1620 ; ^1H-NMR (CCl_4, δ, ppm) : 0.75 (CH_3), 1.83 (CH_2), 1.90 ($CH_3-C=$), 2.01 (o-CH_3), 2.15 (p-CH_3), 6.08 ($H-C=$), 6.65 (aromatic) ; UV (EtOH ; λ max nm, ε) : 222 (22704), 278 (1490).

Reaction of propyne with propionyl chloride and $AgClO_4$ in benzene-toluene. Working as above but using as aromatic hydrocarbons 15 mmoles benzene and 15 mmoles toluene, a mixture of 45.8 % phenylated ketones **1** and **2** with 54.2 % tolylketones **3** (*ortho*, *para* and *meta* isomers in ratio 2.7 : 1.5 : 1.0) was obtained. With 15 mmoles benzene and 210 mmoles toluene, 9.6 % phenylated ketones **1** and **2** and 89.4 % **3** (mixture of isomers) were obtained.

Reaction of propyne with propionyl chloride and $AgClO_4$ in benzene-mesitylene. Using 15 mmoles benzene and 15 mmoles mesitylene a mixture of 43.8 % phenylketones **1** and **2** and 56.2 % mesitylketones (**4** and **5**) were obtained. With 210 mmoles benzene and 15 mmoles mesitylene, 83.0 % phenylketones (**1** and **2**) and 17.0 % mesitylketones (**4** and **5**) were evidenced.

REFERENCES

[1] Part III : D. Mănoiu, M. Mănoiu, I. G. Dinulescu and M. Avram, *Rev. Roumaine Chim.*, **29**, 671(1984).

[2] R. C. Dunbar, J. Scen, E. Melby and G. A. Olah, *J. Amer. Chem. Soc.*, **95**, 7200 (1973).

[3] D. Mănoiu, M. Mănoiu, I. G. Dinulescu and M. Avram, *Rev. Roumaine Chim.*, **29**, 201 (1984).

[4] D. Mănoiu, M. Mănoiu, I. G. Dinulescu and M. Avram, *Rev. Roumaine Chim.*, **29**, 193 (1984).

Revue Roumaine de Chimie **29**, *11–12*, 861–865 (1984)

THE STEREOCHEMISTRY OF SOME DIBENZO[*b*, *g*] BICYCLO[4.2.0]OCTADIENE DERIVATIVES

NICOLETA ŞTEFAN*, PETRU FILIP, FILIP CHIRALEU and MIHAI ELIAN
*Center of Organic Chemistry, Spl. Independentei 202B, 78100 Bucharest 12, Romania

Received December 11, 1983

The stereochemistry of five mono- and diacetoxyderivatives with dibenzo[*b*, *g*]bicyclo[4.2.0]octadiene skeleton was studied by ^{1}H-NMR spectroscopy, revealing the preference of the system for one of the two possible conformations.

In the previous work,[1] concerning the reactivity of the angular dimer of benzocyclobutadiene **1**, we reported the synthesis of monoacetoxyderivatives **2** and **3** and diacetoxyderivatives **4**, **5** and **6**.

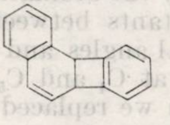
1

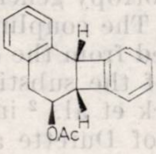

2

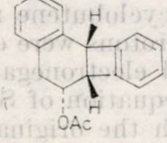

3

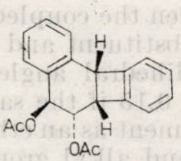

4

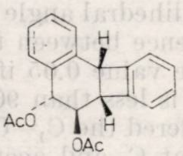

5

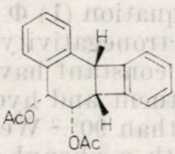

6

In the present paper we establish the stereochemistry of acetates **2**–**6** by ^{1}H-NMR – spectroscopy.

Two stereoisomeric 5-substituted derivatives and four 4,5-disubstituted derivatives are possible in this system. For the bicyclooctane skeleton in compounds **2**–**6** two different conformations **A** and **B** are possible.

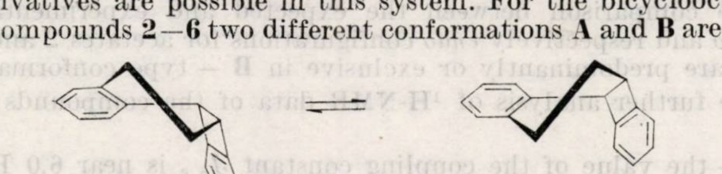
A B

First we analysed the ^{1}H-NMR spectral data of the monoacetoxyderivatives **2** and **3** for which the possible conformations are presented below.

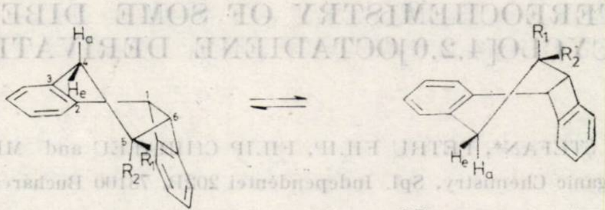

2A: R$_1$= OAc , R$_2$= H
3A: R$_1$= H , R$_2$= OAc

2B: R$_1$= OAc , R$_2$= H
3B: R$_1$= H , R$_2$= OAc

The criteria chosen to differentiate between these conformations were: the values of the coupling constants $J_{4,5\,cis}$ and $J_{4,5\,trans}$, the presence of a long-range coupling between H-6 and one of the H-4 protons and the presence on an acetoxy group at higher field due to the interaction with the aromatic ring of the benzocyclobutane moiety.

Examination of the Drieding molecular models shows that a long-range coupling could exist only for the conformation **B** in which H-6 and equatorial H-4 protons are favourably oriented. Only in **3A** the signal of the acetoxy group could appear at higher field in the ^{1}H-NMR spectrum due to the magnetic anisotropy generated by the aromatic ring from the benzocyclobutene moiety. The coupling constants between the H-4 and H-5 protons were evaluated from the dihedral angles and the orientation and electronegativity of the substituents at C_4 and C_5. We have used the equation of Streefkerk et al., [2] in which we replaced the coefficients with the original ones of Durette and Horton. [3]

$$J_{\mathrm{H,H}} = (7.8-1.0\cos\Phi + 5.6\cos 2\Phi)\ (1 - \Sigma f_i \cdot \Delta\chi_i) \qquad (1)$$

In equation (1) Φ is the dihedral angle between the coupled protons, $\Delta\chi_i$ is electronegativity difference between the substituent and hydrogen and f_i is a constant having the value 0.05 if the dihedral angle between the substituent and hydrogen is less than 90° and 0.15 if the same angle is greater than 90°.[2] We considered the C_4-C_5 fragment as an ethane substituted with a phenyl group at C_4 and acetoxy and alkyl groups at C_5.

The calculated values for the coupling constants $J_{4,5}$ as well as the above mentioned criteria regarding the long-range coupling and high field acetoxy group signal in every conformation and for a rapidly equilibrating mixture of equally populated conformers are presented in table 1.

The comparison between the expected and experimental values shows *exo* and respectively *endo* configurations for acetates **2** and **3**. Both acetates are predominantly or exclusive in **B** — type conformation.

The further analysis of ^{1}H-NMR data of the compounds **2** and **3** showed:

a — the value of the coupling constant $J_{5,6}$ is near 6.0 Hz for an *exo-axial* orientation of the H-5 proton and 3.0 Hz for an *endo-equatorial* orientation of the same proton, b — a dependence of the difference between the chemical shifts of H-5 and H-6 protons and the orientation of the acetoxy group at C_5 was observed. For an *endo* orientation of the acetoxy group the chemical shifts are 5.25 ppm for H-5 proton and 4.3 ppm for H-6 proton, the difference between them being $\Delta\delta = 1.0$ ppm, while for an *exo* orientation of the acetoxy group at C_5 the difference between the chemical shifts is $\Delta\delta = 1.5$ ppm ($\delta_{H-5} = 5.55$ ppm, $\delta_{H-6} = 4.0$ ppm).

These data were used as supplementary arguments for structure determination of the diacetates **4**, **5** and **6**. For the 4,5-diacetoxy-dibenzo[*b*, *g*]bicyclo[4.2.0]octadiene four different configurations are possible, each one having two conformations which could be at equilibrium (**IA**—**IVB**). The structures of the diacetates **4**—**6** were established from the ¹H-NMR experimental data in comparison with the data evaluated for the structures **IA**—**IVB**.

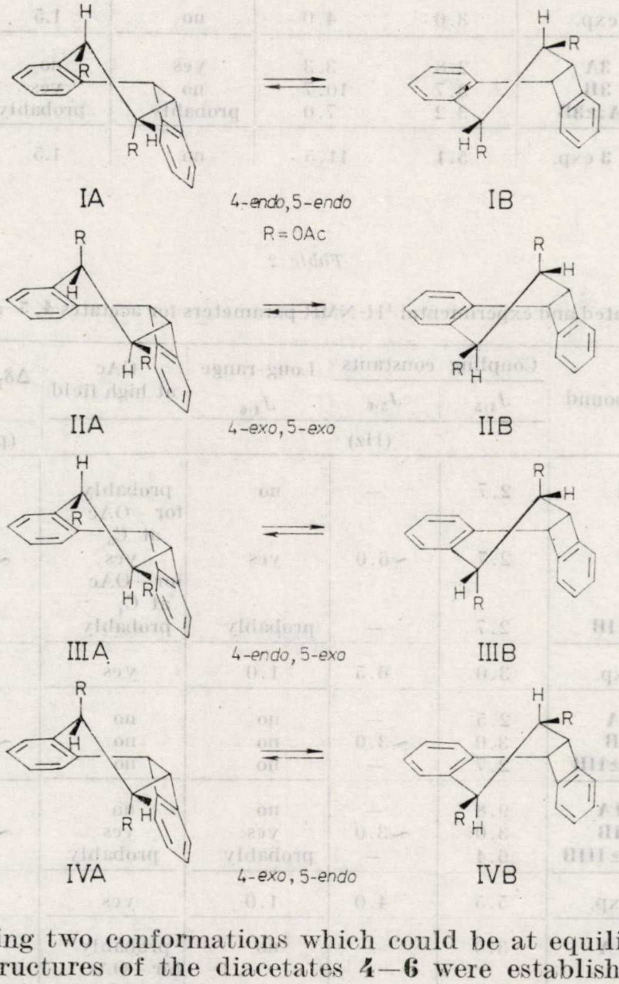

Table 2 presents the values of the ¹H-NMR parameters to differentiate between the possible structures of the diacetates **4**—**6**.

Table 1

Estimated and experimental ^{1}H-NMR parameters for acetates **2** and **3**

Compound	Coupling constants $J_{4,5}$		OAc at high field	$J_{4,6}$ long-range
	$J_{4,5\,cis}$	$J_{4,5\,trans}$		
	(Hz)			(Hz)
2A	3.7	10.7	no	no
2B	2.8	3.3	no	yes
2A$\rightleftarrows$**2B**	3.2	7.0	no	probably
2 exp.	3.0	4.0	no	1.5
3A	2.8	3.3	yes	no
3B	3.7	10.7	no	yes
3A$\rightleftarrows$**3B**	3.2	7.0	probably	probably
3 exp.	5.1	11.5	no	1.5

Table 2

Estimated and experimental ^{1}H-NMR parameters for acetates **4**, **5** and **6**

Compound	Coupling constants		Long-range	OAc at high field	$\Delta\delta_{H_5-H_6}$
	$J_{4,5}$	$J_{5,6}$	$J_{4,6}$		
	(Hz)				(ppm)
IA	2.7	—	no	probably for –OAc at C_5	—
IB	2.7	~6.0	yes	yes for –OAc at C_4	~1.0
IA$\rightleftarrows$**IB**	2.7	—	probably	probably	—
6 exp.	3.0	6.5	1.0	yes	1.3
IIA	2.5	—	no	no	—
IIB	3.0	~3.0	no	no	~1.5
IIA$\rightleftarrows$**IIB**	2.7	—	no	no	—
IIIA	9.8	—	no	no	—
IIIB	3.0	~3.0	yes	yes	~1.5
IIIA$\rightleftarrows$**IIIB**	6.4	—	probably	probably	—
5 exp.	5.5	4.0	1.0	yes	1.5
IVA	3.0	—	no	probably for –OAc at C_5	—
IVB	9.8	~6.0	no	no	~1.0
IVA$\rightleftarrows$**IVB**	6.4	—	no	no	—
4 exp.	9.0	6.0	no	no	1.0

The values of $J_{4,5}$ were calculated in the same way as for monoacetates **2** and **3** and the values of $J_{5,6}$ and $\Delta\delta_{5,6}$ were assumed, for the **B** — type conformation, to be the same as for the monoacetates.

Using these data, the following assignments were made: in the diacetate **6**, the acetoxy groups have a *cis-endo* configuration the skeleton having **B** conformation; the diacetate **5** is probably a mixture of the two conformers **IIIA** and **IIIB**, the acetoxy groups have a *trans*-4-*endo*-5-*exo* configuration, and in the diacetate **4** the skeleton has a **B** conformation and the acetoxy groups have a *trans*-4-*exo*-5-*endo* configuration.

The study of the stereochemistry of mono- and diacetates **2**—**6** with dibenzo[*b*, *g*]bicyclo[4.2.0]octadiene skeleton reveals the preference of the system for a **B** — type conformation, which is probably energetically favoured over an **A**—type conformation in which the molecule is more crowded. The difference in free energy, between conformers is about 0.5 kcal/mol (calculated from the experimental coupling constant $J_{4,5}$). For the others compounds discussed in this paper, this difference is probably higher than 1.5 kcal/mol, therefore the population of an **A**—type conformation is negligible.

EXPERIMENTAL

The ^{1}H-NMR spectra were recorded on a Varian A-60A spectrometer, using TMS as internal standard.

In the case of monoacetates **2** and **3**, in order to make correct signal assignments, the ^{1}H-NMR spectra of the five cycloaliphatic protons were simulated using a program written in BASIC, implemented on a Hewlett-Packard—9830A desk-top calculator.

exo-5-Acetoxy-dibenzo[b, g]bicyclo[4.2.0]octa-2,7-diene (**2**).
^{1}H-NMR ($CDCl_3$, δ, ppm) : 7.85 —7.45 (m, 8H aromatics), 5.55 (q, 1H, 5-H), 4.68 (d, 1H, 1-H, $J_{1,6} = 5.0$ Hz), 4.01 (m, 1H, 6-H), 2.85 (m, 1H, 4-$H_{(e)}$, $J_{4(e),4(a)} = 16.0$ Hz, $J_{4(e),5(e)} = {}$ $= 4.0$ Hz, $J_{4(e),6} = 1.5$ Hz), 2.55 (dd, 1H, 4-$H_{(a)}$, $J_{4(a),5} = 3.0$ Hz), 1.91 (s, 3H, acetoxy group).

endo-5-Acetoxy-dibenzo[b, g]bicyclo[4.2.0]octa-2,7-diene (**3**).
^{1}H-NMR (CCl_4, δ, ppm) : 7.60 —7.00 (m, 8H aromatics), 5.25 (m, 1H, 5-H, $J_{5,6} = 6.15$ Hz, $J_{4(e),5} = 5.15$ Hz, $J_{4(a),5} = 11.5$ Hz), 4.75 (d, 1H, 1-H), 4.32 (broad t, 1H, 6-H), 2.80 (m, 1H, 4-H), 2.13 (s, 3H, acetoxy group).

exo-4-endo-5-Diacetoxy-dibenzo[b, g]bicyclo[4.2.0]octa-2,7-diene (**4**).
^{1}H-NMR (CCl_4, δ, ppm) : 6.80 —7.50 (m, 8H aromatics), 5.62 (d, 1H, 4-H, $J_{4,5} = 9.0$ Hz), 4.69 (d, 1H, 1-H, $J_{1,6} = 5.0$ Hz), 4.27 (t, 1H, 6-H, $J_{1,6} = 5.0$ Hz), 2.06 and 2.09 (s, 6H, acetoxy groups).

endo-4-exo-5-Diacetoxy-dibenzo[b, g]bicyclo[4.2.0]octa-2,7-diene (**5**).
^{1}H-NMR ($CDCl_3$, δ, ppm) : 7.60 —7.00 (m, 8H aromatics), 5.99 (d, 1H, 4-H, $J_{4,6} = 1.0$ Hz), 5.56 (dd, 1H, 5-H, $J_{4,5} = 5.5$ Hz), 4.82 (d, 1H, 1-H), 4.06 (broad t, 1H, 6-H, $J_{1,6} = 4.0$ Hz) 1.98 (s, 3H, acetoxy group), 1.60 (s, 3H, acetoxy group).

endo-4-endo-5-Diacetoxy-dibenzo[b, g]bicyclo[4.2.0]octa-2,7-diene (**6**).
^{1}H-NMR ($CDCl_3$, δ, ppm) : 7.55 —7.10 (m, 8H aromatics), 6.23 (dd, 1H, 4-H, $J_{4,5} = 6.5$ Hz), 4.76 (d, 1H, 1-H, $J_{1,6} = 6.0$ Hz), 4.25 (t, 1H, 6-H), 2.05 (s, 3H, acetoxy group at C_5), 1.55 (s, 3H, acetoxy group at C_4).

REFERENCES

[1] N. Ştefan, P. Filip, I. G. Dinulescu, F. Chiraleu and M. Avram, *Rev. Roumaine Chim.*, **29**, 631(1984).
[2] D. G. Streefkerk, M.J.A. de Bie and J. F. G. Vliegenthart, *Tetrahedron*, **29**, 833 (1973).
[3] P. L. Durette and D. Horton, *Org. Magn. Resonance*, **3**, 417 (1971).

Revue Roumaine de Chimie, **29**, *11–12*, 867–875 (1984)

ANALOGIC DEVICE FOR DERIVATION OF SPECTRAL CURVES IN FLAME PHOTOMETRY

E. CORDOŞ and LIANA MUREŞAN

Department of Chemistry, "Babeş-Bolyai" University
Cluj-Napoca, Str. Arany Janos 11, Romania

Received Jannuary 21, 1984

The noise influence upon the derivative is reduced by the use of integrated value of the signal instead of its momentary value. The integrated signal at a given wavelength is subtracted from the integrated value at the next wavelength. The derivative results by plotting these differences as a function of wavelength. The derivation and plotting operation is automatically performed by an analogic device controlled by a logic circuit. The device has been tested with good results, both on synthetic curves and on emission spectral lines.

Derivative spectroscopy is a technique frequently mentioned in recent years. The derivatives of different orders of absorption or emission spectra are efficient means to emphasize the fine spectral structure, to resolve overlaped bands or to eliminate the effect of a relatively high background. [1,2] The derivation of spectral curves could be implemented electronically, analogically [3,4] or digitally [5,6] upon the photodetector signal, operation often coupled with wavelength modulation. [7,8] Emphasizing by derivation, the distinctive features of a spectrum are accomplished at the expense of worsening the signal to noise ratio, thus limiting the applicability of this technique. [9]

The decrease of signal to noise ratio is determined by the manner in which the derivation is implemented. As shown by one of the authors [10] the noise influence is considerable when the derivation is made continuously either analogically or digitally. In fact, by derivation the slope of the spectral curve is determined in a certain point of it, at a given moment. If, in the considered point, in the moment of derivation, the noise fluctuates rapidly, its slope could be very high and consequently its derivative. This way, noise contribution to the final value of the measurement becomes much higher than those of the signal. The things look like the noise fluctuations are more amplified in detriment of the signal and, respectively, signal to noise ratio. For this reason the derivation is considered useful only for curves having a high signal to noise ratio and a certain diminishing of this ratio does not affect the final results.

In the present paper a method of spectra derivation is presented in which the noise influence is much reduced by using the integrated value of the photodetector signal over a given time interval, instead that of a momentary value. The principle of the method is illustrated in figure 1.

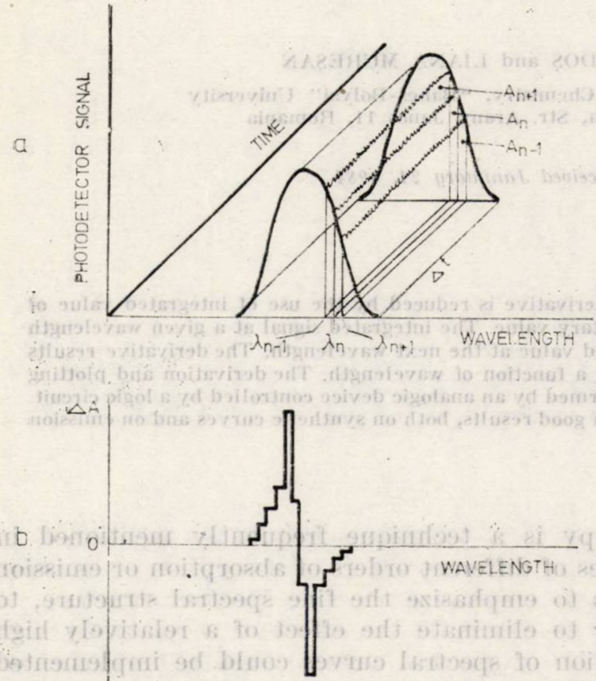

Fig. 1. — The principle of derivation of a spectral curve by previous time integration of photodetector signal.
a — A spectral curve and signal derivation in time.
b. — The first derivative of the curve from a.

The amplified and conditioned detector signal is integrated over a time interval Δt, at the wavelength λ_{n-1} (Fig. 1a). The result is the area A_{n-1}, materialized electronically by an integrated signal. The spectrophotometer is then moved at the wavelength λ_n and the integration is repeated. From the resulted area A_n, the area A_{n-1} is substracted. The difference $\Delta A_n = A_n - A_{n-1}$ is recorded and the wavelength changed at λ_{n+1} where the signal is integrated and the difference $\Delta A_{n+1} = A_{n+1} - A_n$ is obtained. The sequence of operations is then continued for the rest of spectrum.

The correlation of ΔA with the derivative of the spectral curve on the given interval could be made considering the output current of the measuring instrument as the sum of the effects produced by various sources. This output current comprises the useful signal and a background. Both the signal and the background have variations whose resultant is the noise. For a given wavelength λ_n:

$$I_n = f(S_n) + \Phi(N_n) + \theta(F_n) \qquad (1)$$

where I_n = photodetector signal
S_n = signal nonaltered by noise
F_n = continuous component of the background
N_n = the noise
f, Φ, θ = functions representing the time dependence of the variables above mentioned.

Integrating equation (1) in the $\Delta t = t_{n+1} - t_n$ time interval one obtains the area A_n:

$$A_n = \int_{t_n}^{t_{n+1}} I_n = \int_{t_n}^{t_{n+1}} f(S_n) + \int_{t_n}^{t_{n+1}} \Phi(N_n) + \int_{t_n}^{n+1} \theta(F_n) \tag{2}$$

Since the noise has a statistical nature the integer of function would be zero if Δt is much longer than noise period. On the other hand both signal and the continuous component of the background are constant at a given wavelength so that equation (2) becomes:

$$A_n = aS_n + bF_n \tag{3}$$

where a and b are constants.

The difference between two consecutive areas is:

$$\Delta A = A_{n+1} - A_n = aS_{n+1} - aS_n + bF_{n+1} - bF_n \tag{4}$$

Since the background does not change with the wavelength, $F_{n+1} = F_n$ and equation (4) is reduced at:

$$\Delta A = a(S_{n+1} - S_n) \tag{5}$$

The signal derivative for two consecutive wavelengths is:

$$\frac{\Delta S}{\Delta \lambda} = \frac{S_{n+1} - S_n}{\lambda_{n+1} - \lambda_n} \tag{6}$$

Substituting equation (5) into (6):

$$\frac{\Delta S}{\Delta \lambda} = \frac{\Delta A}{a(\lambda_{n+1} - \lambda_n)} \tag{7}$$

The denominator of the left fraction is a constant, $k = 1/a(\lambda_{n+1} - \lambda_n)$, therefore:

$$\frac{\Delta S}{\Delta \lambda} = k\Delta A \tag{8}$$

respectively the derivative of the signal in $\Delta\lambda$ wavelength interval is proportional to the difference between integrals of the photodetector signal at λ_n and λ_{n+1}.

The value of this derivative is not affected by noise or, at least, the noise influence could be reduced below a selected limit by using a proper Δt integration time.

Representing ΔA as a function of wavelength, the derivative curve from figure 1b is obtained. The step form is due to the monochromator advancing in $\Delta\lambda$ increments. Decreasing $\Delta\lambda$ respectively by integrating the spectra in more points the derivative curve approaches the ideal continuous derivative.

EXPERIMENTAL

The derivative is obtained by means of an analogic-digital circuit, with the block diagram given in figure 2.

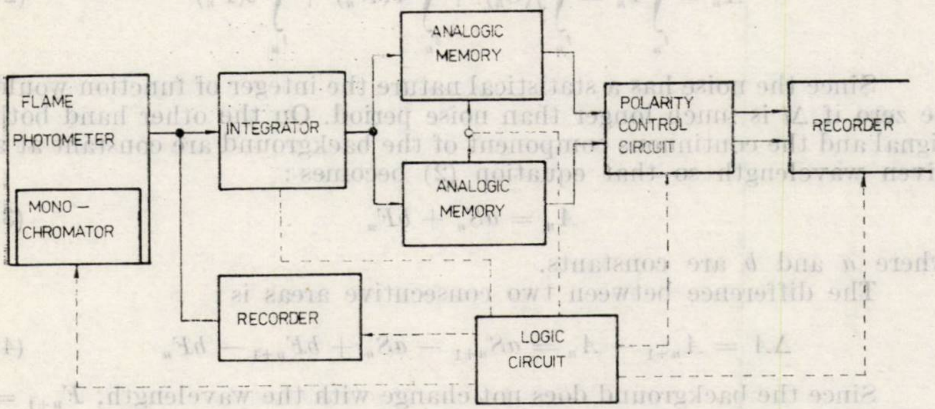
ANALOGIC MEMORY
FLAME PHOTOMETER
MONO-CHROMATOR
INTEGRATOR
POLARITY CONTROL CIRCUIT
RECORDER
ANALOGIC MEMORY
RECORDER
LOGIC CIRCUIT

Fig. 2. — The block diagram of the system for derivation by differentiating the integrated photodetector signal.

The analogic circuit controls the operations of the analogic part and that of the signal source. The signal generated by the photomultiplier is integrated and stored in a pair of analog memories. The memories output is connected to a polarity control circuit and further to a floating input recorder. A logic cricuit provides for the scan to the next wavelength of the spectrophotometer monochromator. At the same time the logic circuit provides for the integration time, stores alternatively the integrated signal in the memories and properly connects the recorder by means of the polarity control circuit. A second recorder monitors the output signal of the spectrophotometer.

The analogic circuit diagram is given in figure 3.

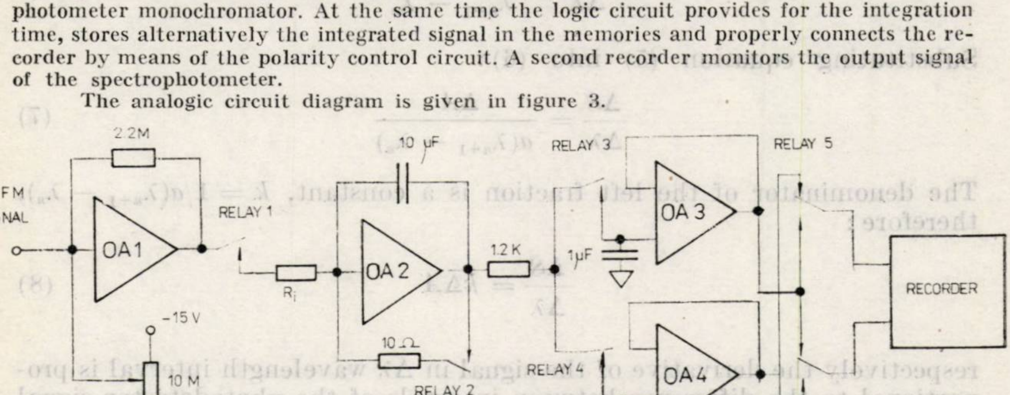
2.2M
FM SIGNAL
OA1
RELAY 1
10 µF
OA 2
R_i
1.2 K
10 Ω
RELAY 2
-15 V
10 M
+15 V
RELAY 3
OA 3
1µF
RELAY 5
RECORDER
RELAY 4
OA4
1µF
RELAY 6

Fig. 3. — The diagram of the analogic circuit. OA 1- OA 5, operational amplifiers Burr-Brown 1012.
Relays 1—6 Heath EU 800 JD.

The photomultiplier current is converted to voltage by OA 1 amplifier, with a sensitivity of $4.5 \cdot 10^{-7}$ A at 1 V output voltage, sufficient for measuring the photocurrents usually obtained in emission photometry. The resulted voltage is applied, through a relay, to the integrator built from the OA 2 amplifier, with a 10 μF capacitor in the feedback loop. The integrating time, respectively the time during which the signal is applied to the amplifier input is controlled through relay 1. The R_i resistor allows the adjustment of integrator sensitivity and the relay 2 shorts the integrating capacitor at the end of one period. The integrated signal is alternatively applied, through relays 4 and 5, to the sample and hold circuits, wired from OA 3 and OA 4 amplifiers, which stores the voltage in the 1 μF condensors connected at the noninverting inputs. The 1.2 kΩ resistor and the 1 μF capacitor gives a time constant much smaller than integrating time, so that the sampling and hold operation does not affect the signal value. The stored voltages are substracted one from another by using a floating input recorder. The relays 5 and 6 form a polarity control circuit, so that the difference between signals provided by OA 3 and OA 4 is always maintained at a positive sign.

The functioning of analogic circuit relays are controlled by the logic circuit from figure 4.

The mean part of this circuit is a timing circuit (TC) with the diagram given in reference 6. For the sake of simplification the main inputs and outputs of the circuit were identified by the same symbols as in the above mentioned reference. The timing circuit provides the time intervals and the basic sequence for relays operation. The TC circuit is activated through monostables M_1 and M_2 which form the start system of the circuit. The monostables provide a short delay in which different parts of the circuit and the relays are brought in the proper state. The start is given manually, through M_1. After the TC circuit is activated, the pulses applied at clock input are divided and modulated yielding the output waveforms shown in figure 5. The pulses provided by QFF 5 and the counter DCU 2 control the integration time. The DCU 2 gives also the pulses from monochromator scanning after each integration. The sampling time is provided by SD 3, being alternatively applied by the flip-flop FF 2 to the sample and hold circuits. The same flip-flop changes the polarity before each measurement. The SD 4 output, reversed by G 10 opens the relay 2, so that the capacitor could perform the integration, and closes it discharging the capacitor after each integration allowing for a new integration. After each integration the pulses from SD 4 reactivate, through M_2, the TC circuit input.

The logic circuit is such that performs a cycle of 10 pairs of integrations, sufficient for derivation of an atomic emission or absorption line. The number of integrations is decided by the counter DCU 1 and the flip-flop FF 1. The last one blocks, through gate G 3, the access of the signals at the TC start, after 20 integrations. If necessary the number of integration pairs could be increased by using additional decimal counters of flip-flops.

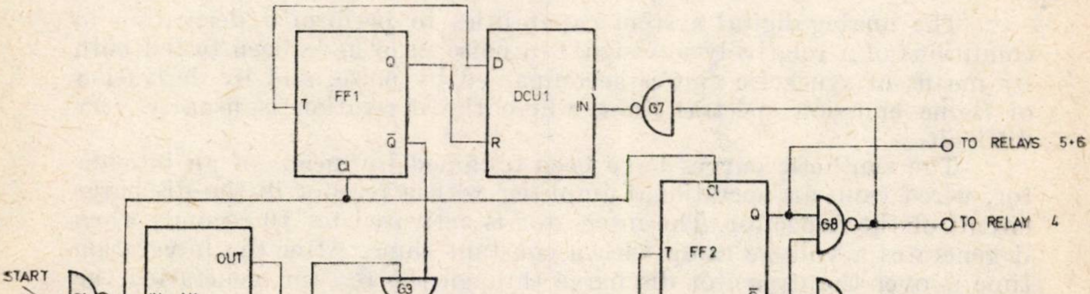

Fig. 4. — The diagram of the logic circuit.

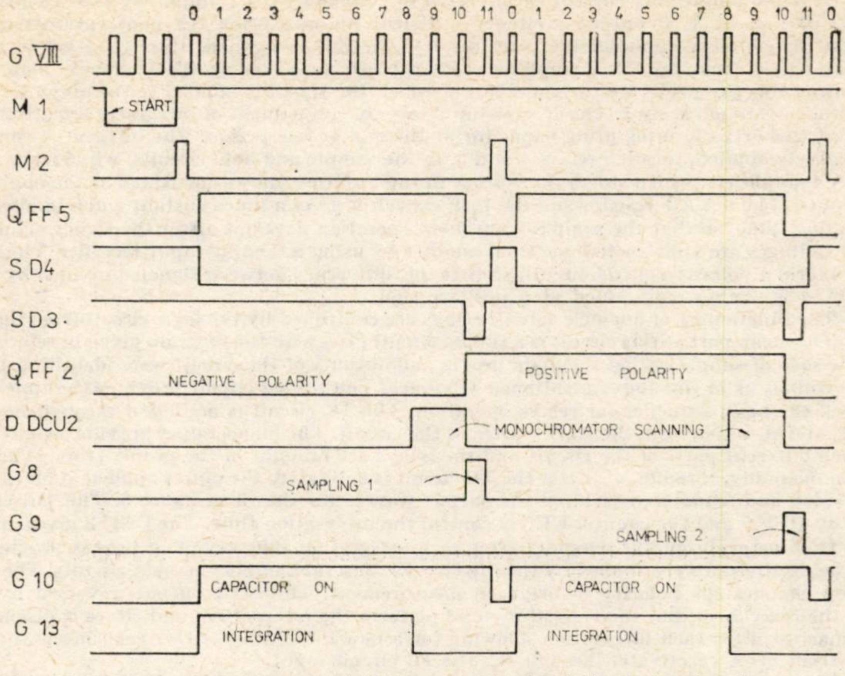
0 1 2 3 4 5 6 7 8 9 10 11 0 1 2 3 4 5 6 7 8 9 10 11 0
G VIII
M 1
START
M 2
Q FF 5
S D4
SD3
Q FF 2
NEGATIVE POLARITY
POSITIVE POLARITY
D DCU2
MONOCHROMATOR SCANNING
G 8
SAMPLING 1
G 9
SAMPLING 2
G 10
CAPACITOR ON
CAPACITOR ON
G 13
INTEGRATION
INTEGRATION

Fig. 5. — Waveforms at the mean outputs of the logic circuit.

RESULTS AND DISCUSSIONS

The analog-digital system capabilities to perform a derivation in conditions of a relatively low signal to noise ratio have been tested both by means of synthetic curves accompanied by noise, and by derivation of flame emission spectral lines, where the derivation is usually very difficult.

The synthetic curves have been obtained by means of an integrator, wired from an operational amplifier with a resistor in the discharge circuit of the capacitor. The integrator is activated for 10 seconds when it generates a voltage ramp with a constant slope. After the integration time is over the capacitor discharge through the resistor, generating the descending part of the curve with a variable slope (Fig. 6 a).

By connecting at the summing point of the OA1 amplifier (Fig. 3) both the synthetic curve generator and a sinewave generator a synthetic noisy curve is obtained (Fig. 6 b).

The derivative of noiseless curves shows the expected feature (Fig. 6c). To the linear rising portions of the curve corresponds the horizontal part of the derivative while to the falling portion corresponds the second part of the derivative, which tends to zero as the synthetic curves approach the horizontal.

The noise influence on the derivative is a function of its frequency and amplitude reported to the integration time and signal amplitude. As a measure of this influence could be considered the lower frequency limit at which the noise alters the derivative amplitude with a given value. In the present case a 10% change in derivative amplitude has been considered in determining the frequency limit. The results are given in figure 7

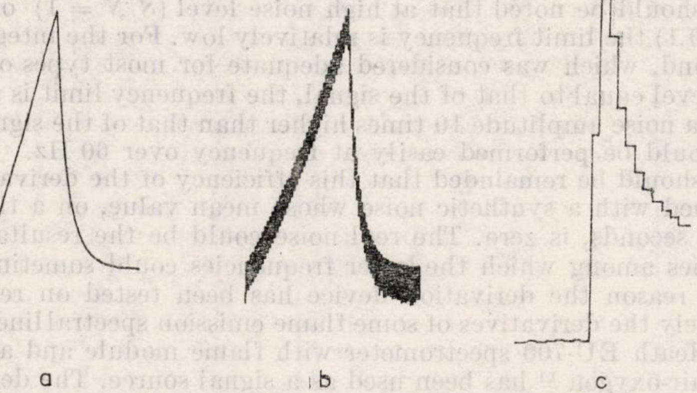

Fig. 6. — a — Synthetic curve; b — Synthetic curve with noise; c — Derivative.

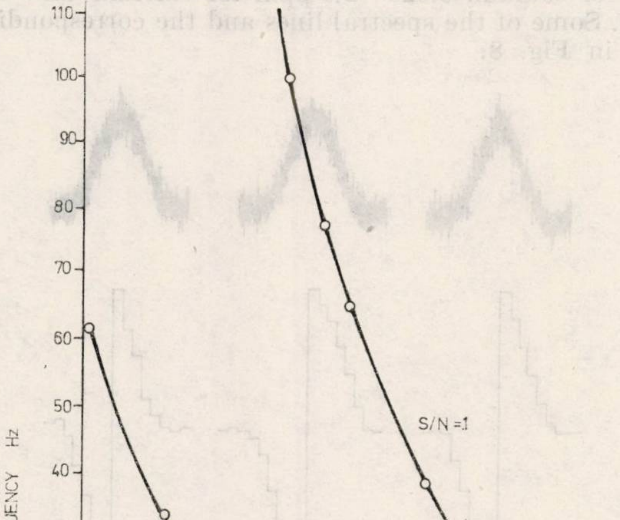

Fig. 7. — The low frequency limit of the derivation device at various signals to noise ratios.

where the working limits at low frequencies are plotted as a function of integration time, at three values of signal to noise ratio. Each point (Fig. 7) represents the mean of 30 determinations.

As expected, the frequency limit decreases with the increase of signal to noise ratio and of the integration time.

It should be noted that at high noise level ($S/N = 1$) or very high ($S/N = 0.1$) the limit frequency is relatively low. For the integration time of a second, which was considered adequate for most types of signals, at a noise level equal to that of the signal, the frequency limit is about 8 Hz. Even at a noise amplitude 10 times higher than that of the signal the derivation could be performed easily at frequency over 60 Hz.

It should be remainded that this efficiency of the derivative system is obtained with a synthetic noise whose mean value, on a time interval of a few seconds, is zero. The real noise could be the resultant of more frequencies among which the lower frequencies could sometimes prevail. For this reason the derivation device has been tested on real systems, respectively the derivatives of some flame emission spectralline were recorded. A Heath EU-700 spectrometer with flame module and a burner for methan-air-oxygen [11] has been used as a signal source. The derivative for sodium, calcium and manganese were recorded in the concentration ranges 0.005 – 1 ppm for sodium, 0.025 – 2.5 ppm for calcium and 0.1 – 10 ppm for manganese. Some of the spectral lines and the corresponding derivatives are given in Fig. 8.

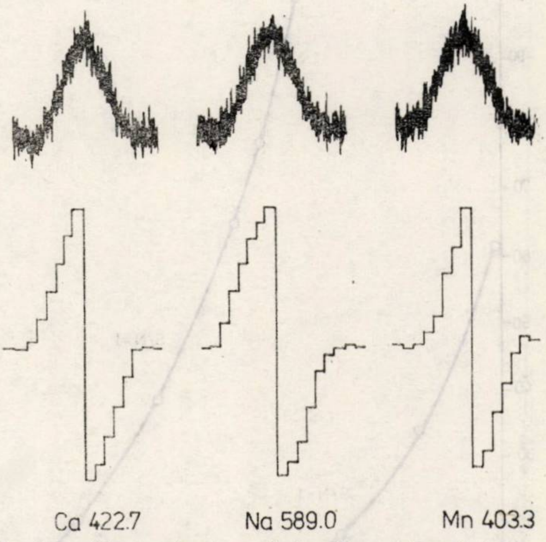

Fig. 8. – Flame atomic emission lines (above) and corresponding derivatives (below).

It could be concluded that the present system could perform the derivation in conditions which noise made it impossible by point by point techniques. The noise immunity makes the circuit very useful for weak signals, burried in a spectral noise much more intense, as it is the case in trace analysis by atomic emission or absorption in flame.

REFERENCES

[1] A. T. Giese and C. S. French, *Appl. Spectrosc.*, **9**, 78 (1955).
[2] R. N. Hager, *Analyt. Chem.*, **45**, 1131 A (1973).
[3] G. L. Collier and F. Singleton, *J. Appl. Chem.*, **6**, 495 (1956).
[4] E. C. Olson and C. D. Alway, *Analyt. Chem.*, **32**, 370 (1960).
[5] A. Savitzky and M. J. Golay, *Analyt. Chem.*, **36**, 1627 (1964).
[6] J. Steiner, Y. Termonia and J. Deltour, *Analyt. Chem.*, **46**, 1906 (1972).
[7] T. C. O'Haver, *Analyt. Chem.*, **51**, 91 A (1979).
[8] D. T. Williams and R. N. Hager, *Appl. Optics*, **9**, 1597 (1970).
[9] J. E. Cahill, *Intern. Lab.*, **10**(1) 64 (1980).
[10] E. Cordoș, S. R. Crouch and H. V. Malmstadt, *Analyt. Chem.*, **40**, 1812 (1968).
[11] E. Cordoș, L. N. Kékedy and R. Hui, Romanian Patent 67867, 30 Dec. 1977.

Revue Roumaine de Chimie, **29**, *11–12*, 877–882 (1984)

DISTRIBUTION OF ATOMIC CHARGES IN CYCLOIMMONIUM YLIDES

G. SURPĂŢEANU

Organic Chemistry Department, Polytechnic Institute Jassy, Splai Bahlui 71, Jassy 6600 Romania

Received July 25, 1983
Revised February 20, 1984

The binding energies of the nitrogen 1s electron have been measured for a series of azaaromatic heterocyclic methylides (cycloimmonium ylides). As azaheterocycle, pyridine isoquinoline, pyradazine, phthalazine and cinnoline are used. The ylide carbon substituents are cyano and carbomethoxy groups. A linear correlation between the binding energies measured by ESCA method and charges of nitrogen atoms by CNDO/2 procedure method has been established. A slope of $k = 18.4$ eV with a correlation coefficient $r^2 = 0.86$ has been found. In every case the calculated charge on the ylide carbon atom is smaller than the one of the heteroatom of substituent (nitrogen of nitril group or oxygen of the carbomethoxy one).

A previous ESCA study (electron spectroscopy for chemical analysis) on the distribution of the charges in a series of pyridinium methylides has been carried out.[1,2] The negative charge usually represented at ylide carbon atom is delocalized on the whole carbanion. The same delocalization is possible for the positive charge on the all azaaromatic heterocycle.[3–5]

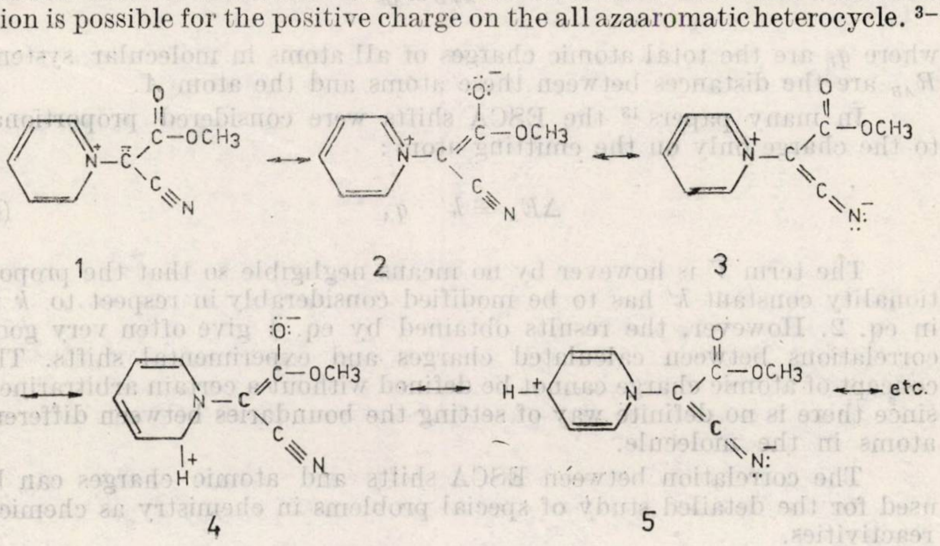

The purpose of these papers was to appreciate the total atomic charges on the nitrogen and carbon ylide atoms.

The correlation between electronic binding energies 1s and total atomic charges in organic compounds has been often announced.[6,8]

Briefly, in ESCA method, the electronic binding energies 1s ΔE_A, of the atom A in a molecular system, is calculated as:

$$\Delta E_A = E_{\mathrm{X\,ray}} - E_{\mathrm{kin}} \tag{1}$$

where $E_{\mathrm{X\,ray}}$ is the quantum energy of the characteristic X-rays used to eject the electrons and E_{kin} is the measured kinetic energy of the ejected electrons.[9]

This method may be applied to measure the kinetic energies of electrons in all elements except hydrogen.

There are in literature,[10–12] several examples of how ESCA spectra reflect the charge distribution in molecules and thus may become a new tool for the study of chemical bonding.

Siegbahn et al.[9] proposed equation 2 which correlates the electronic binding energy with the total atomic charges q_A and the molecular potential V, of an atom A in a molecular system:

$$\Delta E_A = k \cdot q_A + V + l \tag{2}$$

The constants k and l have been determined using experimental data. When the atomic charges are calculated by the CNDO/2 procedure method these constants have the following values: $k = 21.5$ eV and $1 = -1.7$ eV

$$V = \sum_{A \neq B} \frac{q_A}{R_{AB}} \tag{3}$$

where q_B are the total atomic charges of all atoms in molecular system, R_{AB} are the distances between these atoms and the atom A.

In many papers[13] the ESCA shifts were considered proportional to the charge only on the emitting atom:

$$\Delta E_A = k' \cdot q_A \tag{4}$$

The term V is however by no means negligible so that the proportionality constant k' has to be modified considerably in respect to k in in eq. 2. However, the results obtained by eq. 4 give often very good correlations between calculated charges and experimental shifts. The concept of atomic charge cannot be defined without a certain arbitrariness since there is no definite way of setting the boundaries between different atoms in the molecule.

The correlation between ESCA shifts and atomic charges can be used for the detailed study of special problems in chemistry as chemical reactivities.

RESULTS AND DISCUSSIONS

In the present paper, which describes a study of series of cycloimmonium ylides, the chemical shifts of the nitrogen 1s level, have been correlated with the charge on the nitrogen atom calculated by means of CNDO/2 procedure method.[14]

In order to obtain the functions of the type:

$$(\Delta E_A - V - 1) = f(q_A) \tag{5}$$

the total atomic charges of nitrogen atoms in the series of disubstituted carbanion cycloimmonium ylides presented in Table 1, have been calculated.

Table 1

Geometries of ylides

No.		Length	Å	Angle	0
1	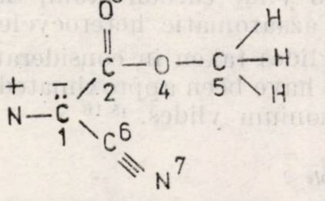 O 3 H C O C H + 2 4 5 H N C 1 C 6 N 7	$\overset{+}{N}-\overset{-}{C}_1$ C_1-C_2 C_2-O_4 C_2-O_4 O_4-C_5 C_5-H C_1-C_6 C_6-N_7	1.41 1.48 1.22 1.34 1.43 1.09 1.42 1.13	$C_2C_1C_6$ $O_3C_2O_4$ $C_2O_4C_5$ $C_1C_6N_7$ HC_5O_4	120 120 105 180 109.28
2	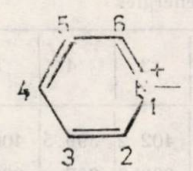	N_1-C_2 C_2-C_3 C_3-C_4 $C-H$	1.37 1.39 1.39 1.08	$C_5C_4C_3$ $C_4C_3C_2$ $C_2N_1C_6$	119 120.5 120
3	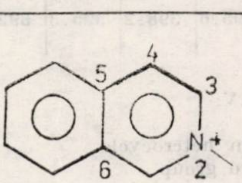	N_2-C_1 N_2-C_3 C_3-C_4 C_4-C_5 $C-H$	1.37 1.37 1.39 1.39 1.08	$C_1N_2C_3$ $N_2C_3C_4$	120 119.5
4	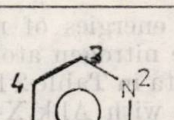	N_1-N_2 N_2-C_3 C_3-C_4	1.36 1.37 1.39	$C_3N_2N_1$ $N_2N_1C_6$ $N_2C_3C_4$	120 120 119.3

Table 1 (continued)

No.		Length	Å	Angle	0
5	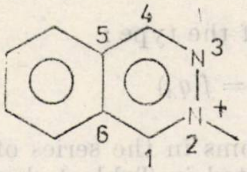	N_1-N_3 N_2-C_1 C_1-C_6 C_5-C_6 $C-H$	1.36 1.37 1.39 1.39 1.08	$C_1N_2N_3$ $N_2N_3C_4$ $C_4C_5C_6$	120 120 119.3
6	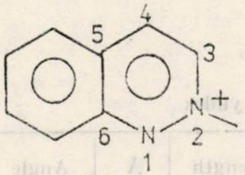	N_1-N_2 N_2-C_3 C_3-C_4 $C-H$	1.36 1.37 1.39	$N_1N_2C_3$ $N_2C_3C_4$ $C_3C_4C_5$	120 120 119.3

All studied cycloimmonium ylides have the same carbanion, cyano and carbomethoxy groups bonded to ylide carbon atom, the difference between them being the nature of azaaromatic heterocycle.

In Table 1 the geometries of ylides taken in considerations in calculations are given. These geometries have been approximated by analogy to other previous studied cycloimmonium ylides. [15,16]

Table 2

The electronic binding energies

Ylides		1	2	3	4	5
Electronic	N^+	400.2	399.3	402.2	399.5	400.8
binding	N^0	0	0	399.9	397.0	398.8
energies ΔE in (e.V.)	N^-	396.5	395.6	398.2	395.3	392.5

Reference : N in $NaNO_2$ 407.2 e.V.
N^+ : the positive nitrogen atom
N^0 : the second nitrogen atom in heterocycle
N^- : the nitrogen atom in cyano group

Table 2 gives the measured binding energies of nitrogen 1a electron in eV. As reference chemical shift, the nitrogen atom in $NaNO_2$ has been considered (407.2 eV). The numerical data in Table 2 have been obtained using a spectrometre AEI—ES—200 B with Al.k.X-ray. The cyclommonium ylides with sodium nitrate, simultaneously, were deposed on the sound at 120 K, to avoid the decomposition of the products in experimental conditions.

The experimental values of binding energies of nitrogen 1s electron in cyano groups in cycloimmonium ylides have always larger values than cyano groups in other organic compunds. [17] That means a large charge on the nitrogen atom in cyano group in cycloimmonium ylides.

The calculated total atomic charges, using CNDO/2 procedure method prove this point of view.

Table 3 gives the charges of nitrogen ylide carbon and oxygen atoms, together with potentials of nitrogen atoms in cycloimmonium ylides.

The charges of cyclic nitrogen ylide atoms have in all studied ylides positive subunitary values.

The charges of ylide carbon atoms have negative values in the range 0.1551 –0.2580. The most negative charged atoms are oxygen atoms in carbomenthoxy group. Similar nagtive values have the nitrogen atoms in cyano groups.

Table 3

Charges and potentials*

Ylides	N^+		N°		N^-		C^- charge	O(C=O) charge
	charge	potential	charge	potential	cahrge	potential		
1.	+0.1113	−1.0804	—	—	−0.1550	+0.4130	−0.2572	−0.4102
2.	+0.0980	−0.9901	—	—	−0.1494	+0.4908	−0.2580	−0.4135
3.	+0.1922	−1.8807	−0.0890	+1.9911	−0.1535	+0.8410	−0.2132	−0.3755
4.	+0.1862	−2.0833	−0.1114	+0.2179	−0.1660	+0.8488	−0.2253	−0.3950
5.	+0.2794	−2.3997	−0.1690	+3.3489	−0.2408	+1.7798	−0.1551	−0.4281

* for meaning of N^+, N°, N^- see footnote at Table 2
C^- : the ylide carbon atom

All these data prove the delocalisation of the positive and negative charges on the azaaromatic heterocycle and carbanion, respectively.

Next, in order to obtain a correlation as in equation 5 the quantities $(\Delta E_A - V - 1)$ have been calculated. The respective values for all types of nitrogen atoms in cycloimmonium ylides in table 4 are given.

By a graphic representation of $(\Delta E_A - V - 1)$ versus q_N a linear relationship has been obtained. Using the least square method that correlation may be given by the following equation :

$$(\Delta E_k - V - 1) = k \cdot q_N + C \quad (6)$$

where $k = 18.14$ eV, $C = 400.57$ eV and the correlation coefficient $r^2 = 0.86$.

All these data permit to appreciate that the positive and negative charges usually represented on the N—C bond are strongly delocalized on the azaheterocycle and carbanion respectively.

Table 4

Values of $(\Delta E_A - V - 1)$ eV*

Ylides / $(\Delta E_A - V - 1)$	N^+	N°	N^-
1.	402.9804	—	397.769
2.	401.9901	—	396.8092
3.	405.7807	399.6089	399.0590
4.	403.2833	398.4821	396.1512
5.	404.8997	396.6511	397.4202

---

* for meaning of N^+, N°, N^- see footnote at Tabele 2

The most negative charged are nitrogen and oxygen in substituents bonded to ylide carbon atoms. Thus, the ylide carbon atoms have negative subunitary values. The chemical behaviour of cycloimmonium ylides proves this point of view. There are in literature[3] many cases in which the disubstituted carbanion cycloimmonium ylides are nucleophilic reagents at the nitrogen or oxygen atoms belonging to the substituents bonded to ylide carbon atom. The ylides may react by their resonance structures 2 and 3 with different electrophiles.

REFERENCES

[1] J. P. Catteau, A. Lablache-Combier, J. Grimblot, M. Nastasi and J. Streith, *Tetrahedron*, **31**, 2909 (1975).

[2] J. P. Catteau, P. Karafiloglu, A. Lablache-Combier, N. Lethan and G. Surpățeanu, *Tetrahedron*, **32**, 461 (1976).

[3] G. Surpățeanu, J. P. Catteau, P. Karafiloglu and A. Lablache-Combier, *Tetrahedron*, **32**, 2647 (1976).

[4] A. W. Johnson, "Ylide Chemistry" Academic Press-New York, 1966.

[5] I. Zugrăvescu, M. Petrovanu, "N-ylide chemistry", McGraw-Hill, London, 1976.

[6] R. Nordberg, R. G. Albrindge, T. Bergmark, E. Ericson, J. Hedman, C. Nordling, K. Siegbahn and B. J. Lindberg, *Arkiv för kemi*, **28**, 19, 257 (1967).

[7] J. C. Carver, R. C. Gray, and D. M. Hercules, *J. Amer. Chem. Soc.*, **96**, 22, 6851 (1974).

[8] W. L. Jolly and W. B. Perry, *J. Am. Chem. Soc.*, **95**, 5442 (1973).

[9] K. Siegbahn, C. Nordling, G. Johansson, J. Hedman, P. F. Heden, K. Hamrin, U. Gelius, T. Bergmark, L. O. Werme, R. Manne and Y. Baer, "ESCA Applied to Free Molecules", North Holland, Amsterdam, 1971.

[0] M. E. Schwartz, J. D. Switalski and R. E. Stronski, "Electron Spectroscopy", North Holland, Amsterdam, 1972.

[11] J. M. Dereppe, R. Touillaux, A. Schanek and M. Van Meerssche, *Ind. Chim. Belg.*, **38**, 247 (1973).

[12] U. Gelius, *Physica Scripta*, **9**, 133 (1974).

[13] M. E. Schwartz, *Chem. Phys. Letts*, **5**, 50 (1970).

[14] J. A. Pople, D.L.Beveridge, "Approximate Molecular Orbital Theory", McGraw-Hill, London, 1970.

[15] G. Surpățeanu, M. Constantinescu, C. Luchian, M. Petrovanu, I. Zugrăvescu and A. Lablache-Combier, *Rev. Roum. Chim.*, **26**, 8, 1169 (1981).

[16] I. Zugrăvescu, M. Constantinescu, G. Surpățeanu, A. Lablache-Combier and L. Devos, *Rev. Roum. Chim.*, **24**, 7, 1089 (1979).

[17] J. M. Hollander, D. N. Hendrikson and W. L. Jolly, *J. Chem. Phys.*, **49**. 3315 (1968).

Revue Roumaine de Chimie, **29**, *11–12*, 883–885 (1984)

POTENTIOMETRIC STUDIES ON THE COMPLEXES OF Pr(III), Nd(III), Sm(III), Gd(III), Tb(III), Dy(III) AND Ho(III) WITH 2′-HYDROXYCHALCONE

R. S. SINDHU* and R. P. SINGH**

* Chemistry Department, M. S. College, Saharanpur, 247002, India
** Chemistry Department, Delhi University, Delhi, 110007, India

Received December 19, 1983

Potentiometric studies have been carried on out metal complexes of Pr(III), Nd(III), Sm(III), Gd(III), Tb(III), Dy(III) and Ho(III) with 2′-hydroxychalcone in 50% (*v*/*v*) dioxane-aqueous medium at 35 ± 0.1° and ionic strength $\mu = 0.1$ M ($NaClO_4$). The stability constant of the metal complexes has been determined by the method of Bjerrum and Calvim as modified by Irvin and Rossotti. The order of stability constant was found to be : Pr(III) < Nd(III) < Sm(III) > Gd(III) < Tb(III) < Dy(III) < Ho(III).

INTRODUCTION

The chalcones are highly biologically important compounds. The germicidal, bactericidal, fungicidal and carcinogenic action of chalcones and analogous compounds have been reported by various workers.[1–11] Welson and co-workers [12] observed that methoxy and hydroxy chalcones can check up the destruction of adrenaline. Besides their importance in biological fields, they have been used as analytical reagents for the spectrophotometric estimations of a number of metal ions [13,14] The sability constants of the complexes of some bivalent metal ions and trivalent metal ions with 2′-hydroxychalcone have been reported earlier.[15–17] But no work has been done on the complexes of title metal ions with 2′-hydroxychalkone. The present paper is aimed at determining the stability constant of this metal ion with 2′-hydroxychalcone.

EXPERIMENTAL

2′ – Hydroxychalone (I) was prepared by the method reported in literature[18] and was crystllized twice before use.

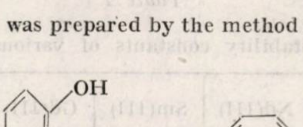

(I)

The solutions of the metal perchlorates were prepared using metal carbonates or oxides of A. R. grade. All these were titrated complexometrically by EDTA titrations.[19] All other chemicals used were reagents of either DDH or Ar or equivalent quality. A Backman pH meter model SS –2 with a glass electrode and a calomel electrode assembly was used for pH measurements. The pH meter readings in 50% dioxane-water medium were corrected using the method of Van Uitert and Hass. [20] A thermostat MLW (type NBE) GDR was used for constant temperature (35 ± 0.1°).

Tetramethyl ammonium hydroxide (TMAH) (E. Merck) was used as titrant. Its solution was standardized with potassium hydrogen phthalate.

The following solutions (total volume 20 ml) were titrated against TMAH $\left(\frac{N}{20}\right)$.

(i) 1.0 ml $HClO_4$ (0.01 M) + 1.0 ml $NaClO_4$(2.0 M) + 10 ml dioxane + 8 ml water.

(ii) 1.0 ml $HClO_4$ (0.01 M) + 1.0 ml $NaClO_4$ (2.0 M) + 10 ml 2'-hydroxychalkone (0.01 M) in dioxane + 8 ml water.

(iii) 1.0 ml $HClO_4$ (0.01 M) + 1.0 ml $NaClO_4$ (2.0 M) + 1 ml metal perchlorate (0.01 M) + 10 ml 2'-hydroxychalkone (0.01 M) + 7 ml water.

The experiments were performed in duplicate and results were found to be reproducible. The proton-ligand stability constant and the metal ligand stability constants (log K_1 and log K_2) were calculated by the Bjerrum Calvim method as modified by Irving-Rossotti. [21]

RESULTS AND DISCUSSIONS

From the titration curves of solutions (i) and (ii) $\bar{n}_A$ values at various 'B' values (pH-meter reading) were calculated and a curve between 'B' and the corresponding $\bar{n}_A$ values was plotted. The value of pK_1^H was evaluated by half integral method as well as from the plot of log $\left(\frac{\bar{n}_A}{1 - n_A}\right)$ vs. B. Both these values agree well. The value of proton-ligand stability constant is in agreement with that reported in the literature [15,16] (in slightly different conditions). From the titration curves of solutions (ii) and (iii), n and pL values were calculated. The n values were plotted against the corresponding pL values to get the formation curves of metal complexes – ion equilibria. From these curves, the values of stability constants could be directly read by half integral method. The pK_1^H of the ligand and the log K_1 and log K_2 of the complexes are given in Table 1. The second step stability constants for Pr(III), Nd(III) could not be evaluated because of precipitation of metal ions probably due to metal ion hydrolysis. The order of stability constant (log K_1) was found to be Pr(III) < Nd(III) < Sm(III) > Gd(III) < Tb(III) < Dy(III) < Ho(III). This order agrees well to that reported earlier. [22]

Table 1

Stepwise stability constants of various complexes

H^+	Pr(III)	Nd(III)	Sm(III)	Gd(III)	Td(III)	Dy(III)	Ho(III)
Log K_1 12.00	8.20	8.42	8.65	8.50	8.60	8.80	9.1
Log K_2 –	–	–	7.52	7.32	7.42	7.50	7.70

REFERENCES

[1] J. K. Fatan and R. G. Davies, *Ann. App.*, **37**, 473 (1950).

[2] S. S. Mishra, *Proc. Nat. Acad. Sci. (India)*, **40A**, 468, 1970.

[3] S. S. Mishra, *J. Indian Chem. Soc.*, **50**, 68, (1973).

[4] S. S. Mishra and Dinkar, *J. Indian Chem. Soc.*, **49**, 637 (1972).

[5] J. Russki and H. Clarke, *J. Amer Chem. Soc*, **61**, 2651 (1939).

[6] N. P. Buu — Hoi and N. D. Xuong, *J. Org. Chem.*, **23**, 39, (1958).

[7] S. C. Kushwaha, Diwakar and J.B. Lal, *Indian J. Chem.*, **5**, 82 (1967).

[8] W. B. Geiger and J. E. Conn., *J. Amer Chem. Soc.*, **67**, 112 (1945).

[9] E. Schraufstatter and S. Dentosoh, *Z. Naturforsch*, **4B**, 430 (1948).

[10] P. F. Devitt, A, Timoney and M. A. Vickars, *J. Org. Chem.*, **26**, 4941 (1961).

[11] S. V. Tsukerman, V. P. Izrikan and U. F. Lavrushin, *Akad. Nauk Latv.*, USSR 527 (1965), *Chem. Abs*, **64**, 676e (1966).

[12] C. W. Wilson and D. E. Flayd, *J. Pharmocol Exptl. Therap.*, **95**, 399 (1949).

[13] K. Shyamsuner, *Proc. Indian Acad Sci.*, **4**, 241 (1964).

[14] K. Shyamsunder, *Proc. Indian Acad. Sci.*, **2**, 90 (1968).

[15] P. V. Khadikar, S. N. Kakkar and D. D. Berge, *Indian J. Chem.*, **13**, 844 (1975).

[16] S. Jagannatha Swamy and P. Lingaih, *Indian J. Chem.*, **16** A, 723 (1978).

[17] R. S. Sindhu and R. P. Singh, *Talanta* (communicated).

[18] F. W. Feursteem and S. Van Kostunecki, *Ber. dt. Chem. Ges.*, **31**, 715 (1898).

[19] H. A. Flaschka, "EDTA Titations" Pergamon Press, New York p. 78.

[20] L. G. Van Uitart and C. G. Hass, *J. Amer Chem. Soc.*, **75**, 451 (1953).

[21] H. Irving and H. S. Rossotti, *J. Amer. Chem. Soc.*, **76**, 2910 (1954).

[22] S. N. Dubey and B. C. Bhuyan, *Indian J. Chem.*, **21A**, 442 (1982).

Revue Roumaine de Chimie, 29, *11—12*, 887—893 (1984)

TRANSFORMATIONS CATALYTIQUES D'HYDROCARBURES AROMATIQUES. VI

ÉTUDE DE L'ACTIVITÉ DE ZÉOLITES MODIFIÉES AVEC DES ÉLÉMENTS POLYVALENTS

SPIRIDON OPREA, ABDELKRIM AZZOUZ, EMIL DUMITRIU et NICOLAE BÎLBĂ
Section de Technologie chimique organique, Institut Polytechnique de Jassy, Bahlui Stînga 71, Jassy 6600, Roumanie

Reçu le 21 septembre 1983
Révisé le 7 mai 1984

Le processus de disproportionation du toluène a été réalisé sur des catalyseurs du type faujasitique modifiés avec des cations La^{3+} et Co^{2+}. L'étude a porté sur l'influence de l'échange cationique ainsi que sur celle de la nature du cation de compensation sur la structure cristalline. L'étude cinétique effectuée sur ces catalyseurs a permis de déterminer les constantes de vitesse et d'adsorption du toluène ainsi que les énergies d'activation et d'adsorption du toluène. Les résultats obtenus ont démontré que l'échange avec le cobalt est plus avantageux du point de vue de l'activité mais moins sélectif que l'échange avec le lanthane.

The disproportionation of toluene on faujasite type catalysts modified by ionic exchange with La^{3+} and Co^{2+} was carried out. The influence of the cation nature and degree of ionic exchange on the crystalline structure of catalyst was studied. The rate constants and toluene adsorption constant as well as the energy of activation were determined by kinetic studies. The experimental data have shown the catalyst exchanged with Co^{2+} to have a better activity but a poorer selectivity than the catalyst exchanged with La^{3+}.

INTRODUCTION

La réalisation pratique du processus de disproportionation du toluène en benzène et xylènes montre que le mélange de produits de réaction contient, en plus de ceux-ci, des composés comme les triméthylbenzènes, des produits de condensation et bien d'autres. L'analyse chromatographique des gaz évacués met en évidence la formation du méthane. D'autre part, il faut mentionner que la formation de coke accompagne inconditionnellement tous les processus ayant lieu sur des catalyseurs du type zéolitique. Cette grande distribution des produits de réaction démontre que le processus global comporte, en plus des réactions principales de disproportionation du toluène et d'isomérisation des xylènes, une série d'autres transformations comme la disproportionation des xylènes, la déméthylation des alkylbenzènes, le craquage et bien d'autres. [1]

La formation des triméthylbenzènes n'a lieu qu'à des conversions relativement élevées du toluène, ce qui signifie que dans des conditions modérées les réactions de disproportionation des xylènes se déroulent avec des constantes de vitesse suffisamment petites pour ne pas être observables. Les triméthylbenzènes deviennent décelables à des températures plus grandes que 350°C.

Le déroulement des réactions secondaires est étroitement lié à leur cinétique sur chaque catalyseur et particulièrement à l'activité de celui-ci. L'activité catalytique dans le processus de disproportionation du toluène est, à son tour, étroitement liée à l'acidité de la surface catalytique, tandis que la sélectivité par rapport au processus principal est proportionnelle au nombre de centre Brönsted de la surface du catalyseur respectif. Dans le meme ordre d'idées, la nature du cation de compensation ainsi que la cristallinité de la zéolite ont une influence remarquable sur l'activité catalytique, fait qui se reflète sur les performances technologiques.

Le but de ce présent article a été d'étudier la corrélation des propriétés physico-chimiques de certains catalyseurs avec leurs activités dans la disproportionation du toluène. Pour une meilleure interprétation de l'activité catalytique une série d'expériences cinétiques ont été effectuées. Ces expériences ont eu recours à des catalyseurs à base de faujasite du type Y échangé avec des cations La^{3+} ou Co^{2+} et les résultats obtenus ont permis de comparer les activités de ces catalyseurs.

PARTIE EXPÉRIMENTALE

Les catalyseurs ont été préparés à partir du faujasite NaY (LZ-Y52, fourni par la firme Ventron) ayant un rapport molaire SiO_2/Al_2O_3 de 4,74 mol/mol. Préalablement, la zéolite de départa été transformée en NH_4NaY avec un taux d'échange d'environ 59 %. L'échange cationique proprement dit a été effectué avec des solutions aqueuses 10 % de $La(NO_3)_3 \cdot 6H_2O$ ou $CoCl_2 \cdot 6H_2O$. Les taux d'échange finals ont été déterminés à l'aide d'un flammephotomètre du type AAS-1 (Carl-Zeiss Jena) et une valeur d'environ 72 % d'ions Na^+ substitués a été obtenue pour les deux catalyseurs.

Les échantillons contenant les produits de réaction ont été analysés par chromatographie en phase gazeuse à l'aide d'un appareil du type Chrom-4 doté d'un détecteur FID. La colonne chromatographique consistait en Chromosorb WAWS supportant du dinonylphtalate et de la bentone 34. La détection des traces de produits a été réalisée par la méthode de l'étalon interne au cyclohexane.

La structure cristalline de la zéolite initiale (LZ-Y52) ainsi que celle des échantillons échangés ont été examinées par la méthode de diffraction des rayons X. L'analyse a été effectuée utilisant la radiation filtrée K_α du cuivre. L'appareil utilisé est du type TUR M-62(RDA),

RÉSULTATS ET DISCUSSIONS

La zéolite de départ est du type NaY ayant comme formule générale :

$$Na^+_{56}(AlO_2^-)_{56} \cdot (SiO_2)_{136} \cdot 264\ H_2O \tag{1}$$

Il est admis que dans la structure tridimensionnelle de la zéolite Y, les cations Na^+ occupent seulement certaines positions (I, I', II, II' et III). [2] A la température ambiante, l'échange avec des cations bi et trivalents est partiel, le taux maximal étant de 70 %. Les isothermes d'échange cationique sont du type *d*. Ceci correspond, en principe, à la non-occupation des positions se trouvant dans les prismes hexagonaux et qui sont au nombre de 16. L'occupation des positions de la cellule sodalitique par des cations ayant une grande capacité d'hydratation est très probable. Les cations La^{3+} en sont un bon exemple.

Les cations Co^{2+} ($r = 7{,}8 \times 10^{-2}$ nm) et La^{3+}($r = 1{,}15 \times 10^{-1}$ nm) introduisent une modification dans le champ électrostatique du réseau cristallin,conséquence logique de la compensation partielle des charges.

L'analyse par diffraction des rayons X des échantillons testés a permis de mettre en relief certains aspects liés aux modifications produites lors de l'échange cationique. La figure 1 présente la variation de l'intensité relative des lignes de diffraction ($100\ I/I_0$, où I_0 représente la plus grande intensité) en fonction de l'angle de diffraction de Bragg (θ).

Il ressort clairement de cette figure que par rapport à la zéolite initiale, la zéolite ayant été échangée avec des cations La^{3+} présente un déplacement du plan [311] de $d = 7{,}46 \times 10^{-1}$ nm à $d = 7{,}20 \times 10^{-1}$ nm, accompagné d'une réduction de l'intensité limite de diffraction.

Les échantillons prétraités avec des cations NH$_4^+$ présentent une meilleure cristallinité que celle des échantillons échangés directement sous la forme La^{3+}. Il en résulte que l'échange intermédiaire avec NH$_4^+$ joue un rôle important dans la conservation de la cristallinité. De même, l'échantillon modifié avec Co^{2+} et ayant été prétraité avec du chlorure d'ammonium conserve sa cristallinité initiale. D'autre part, ce catalyseur ne présente aucune modification des plans de diffraction. Cette modification des plans de diffraction est liée à la nature du cation de compensation. Ce fait est dû à la dimension du rayon ionique ainsi qu'à la capacité d'hydratation de celui-ci.

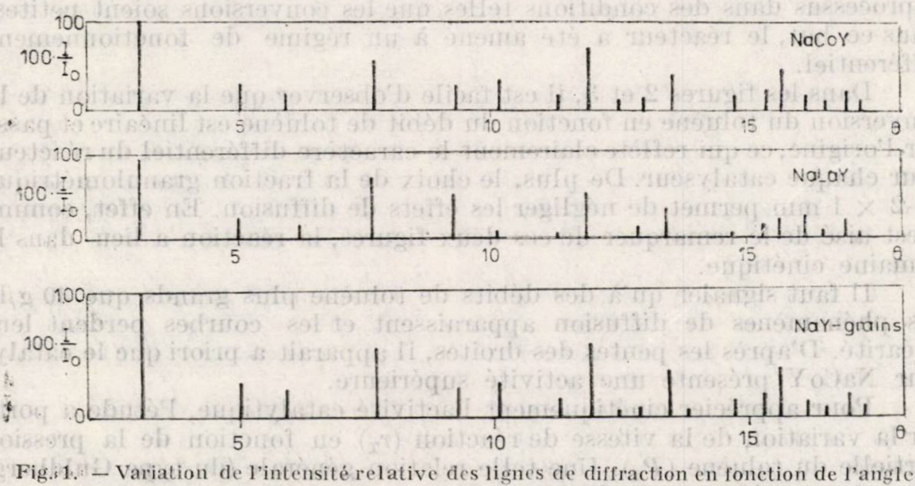

Fig. 1. — Variation de l'intensité relative des lignes de diffraction en fonction de l'angle de diffraction de Bragg, pour les deux catalyseurs et pour la zéolite de départ.

Il ressort de ces observations que même l'activité catalytique peut être influencée par la nature du cation introduit ainsi que par les modifications provoquées par celui-ci dans la structure de la zéolite. La substitution des cations monovalents (Na$^+$) par des cations bi et trivalents a pour effet une augmentation remarquable de l'activité catalytique. Ces cations ont une action favorisante des mécanismes ioniques, action due au champ électrostatique créé et à son effet polarisant des molécules adsorbées.

De même, il faut mentionner qu'une série de cations, comme c'est le cas du cation La^{3+}, présentent une grande capacité d'hydratation, ce qui aboutit, dans les conditions d'une activation thermique, à la création de groupements acides du type $-SiOH$ conformément aux réactions suivantes [3,4] :

$$Co^{2+}(OH_2) \overset{\Delta}{\rightleftarrows} [Co(OH)]^{+} + H^{+} \tag{2}$$

$$La^{3+}(OH_2)_2 \overset{\Delta}{\rightleftarrows} [La(OH)(OH_2)]^{2+} + H^{+} \tag{3}$$

$$La(OH)(OH_2)^{2+} \overset{\Delta}{\rightleftarrows} [La(OH)_2]^{+} + H^{+} \tag{4}$$

Le nombre de groupements hydroxyliques est plus grand dans le cas de l'échange cationique avec des éléments trivalents. Il en résulte que les zéolites échangées avec le lanthane devraient manifester une activité supérieure à celle des zéolites modifiées avec le cobalt.

D'habitude, la réaction de disproportionation du toluène est accompagnée d'une série de réactions secondaires qui impliquent des transformations ultérieures des produits principaux. Une des méthodes classiques de suivre l'activité d'un catalyseur par rapport à la réaction principale, quand celle-ci possède une vitesse suffisamment grande, consiste à réaliser le processus dans des conditions telles que les conversions soient petites. Dans ce but, le réacteur a été amené à un régime de fonctionnement différentiel.

Dans les figures 2 et 3, il est facile d'observer que la variation de la conversion du toluène en fonction du débit de toluène est linéaire et passe par l'origine, ce qui reflète clairement le caractère différentiel du réacteur pour chaque catalyseur. De plus, le choix de la fraction granulométrique $1-2 \times 1$ mm permet de négliger les effets de diffusion. En effet, comme il est aisé de le remarquer de ces deux figures, la réaction a lieu dans le domaine cinétique.

Il faut signaler qu'à des débits de toluène plus grands que 30 g/h, des phénomènes de diffusion apparaissent et les courbes perdent leur linéarité. D'après les pentes des droites, il apparaît a priori que le catalyseur NaCoY présente une activité supérieure.

Pour apprécier cinétiquement l'activité catalytique, l'étude a porté sur la variation de la vitesse de réaction (r_T) en fonction de la pression partielle du toluène (P_T). Une telle relation générale (du type Guldberg-Waage) se présente sous la forme :

$$r_T = k \cdot P_T^{\alpha} \tag{I}$$

et peut s'appliquer aux réactions contrôlées cinétiquement sans tenir compte du mécanisme intime du processus catalytique. Vu les étapes élémentaires du processus catalytique, même dans le cas où la réaction est l'étape déterminante, il faut prendre en considération le processus d'adsorption. Etant donné que l'étude a été réalisée à de petites conversions du toluène (sous 2 % mol.), il n'est pas nécessaire de prendre en considération l'adsorption compétitive entre le toluène et les xylènes ou le benzène.

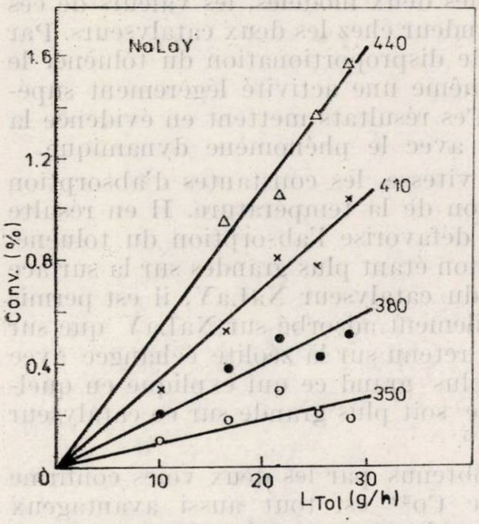

Fig. 2. — Influence de la variation du débit de toluène sur la conversion de celui-ci (WHSV = 5,72 h^{-1}) sur le catalyseur NaLaY.

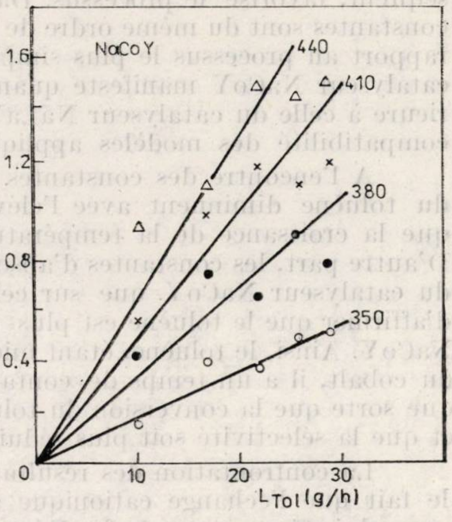

Fig. 3. — Influence de la variation du débit de toluène sur la conversion de celui-ci (WHSV = 5,72 h^{-1}) sur le catalyseur NaCoY.

Ces considérations permettent d'appliquer un modèle cinétique simplifié du type Langmuir-Hinshelwood ayant la forme :

$$r_T = \frac{k(K_T P_T)^2}{(1 + K_T P_T)^2} \tag{II}$$

La vitesse de réaction (r_T) a été mesurée pour chaque modèle en faisant varier la pression partielle du toluène. Les résultats obtenus ont permis de déterminer les constantes de vitesse de réaction (k) ainsi que celle d'adsorption du toluène (K_T) qui dont présentées dans le tableau 1.

Tableau 1

Valeurs des constantes de vitesse et d'adsorption du toluène pour les deux catalyseurs et pour les deux modèles

T(°C)	Constante de vitesse 10^{14} k(mol/g.h)				K_T (atm^{-1})	
	selon l'équation (I)		selon l'équation (II)			
	NaCoY	NaLaY	NaCoY	NaLaY	NaCoY	NaLaY
350	4,19	2,31	3,71	2,13	21,08	14,29
380	6,73	4,79	6,78	4,34	16,00	11,50
410	10,11	7,97	9,77	8,82	15,00	8,95
440	13,24	13,37	12,54	14,86	13,97	7,57

Il résulte de ce tableau que l'élévation de la température entraîne la croissance des valeurs des constantes de vitesse, ce qui se traduit par le fait que l'apport thermique augmente la vitesse de réaction et, par conséquent, favorise le processus. Dans les deux modèles, les valeurs de ces constantes sont du même ordre de grandeur chez les deux catalyseurs. Par rapport au processus le plus simple de disproportionation du toluène, le catalyseur NaCoY manifeste quand même une activité légèrement supérieure à celle du catalyseur NaLaY. Ces résultats mettent en évidence la compatibilité des modèles appliqués avec le phénomène dynamique.

A l'encontre des constantes de vitesse, les constantes d'absorption du toluène diminuent avec l'élévation de la température. Il en résulte que la croissance de la température défavorise l'absorption du toluène. D'autre part, les constantes d'absorption étant plus grandes sur la surface du catalyseur NaCoY que sur celle du catalyseur NaLaY, il est permis d'affirmer que le toluène est plus facilement adsorbé sur NaLaY que sur NaCoY. Ainsi, le toluène, étant mieux retenu sur la zéolite échangée avec du cobalt, il a un temps de contact plus grand ce qui explique en quelque sorte que la conversion du toluène soit plus grande sur ce catalyseur et que la sélectivité soit plus réduite [1,5].

La confrontation des résultats obtenus par les deux voies confirme le fait que l'échange cationique avec Co^{2+} est tout aussi avantageux que celui effectué avec La^{3+}. Néanmoins le processus nécessite une énergie d'activation plus petite sur NaCoY que sur NaLaY. Ceci démontre que NaCoY est en fait un catalyseur plus actif que NaLaY dans le processus de disproportionation du toluène (tableau 2).

Tableau 2

Valeurs des énergies d'activation (ΔE), des chaleurs d'absorption du toulène (Q) ainsi que celles de l'ordre de réaction (α)

Donnécs	NaCoY	NaLaY
Energie d'activation (kJ/mol)		
— selon l'équation (I)	44,85	71,04
— selon l'équation (II)	46,82	75,27
Chaleur d'adsorption (kJ/mol)	8,37	31,21
« Ordre de réaction »	0,39	0,51

En ce qui concerne les chaleurs d'absorption, la valeur obtenue sur le catalyseur à base de La^{3+} est plus grande (31,18 kJ/mol) que celle obtenue sur l'autre catalyseur, ce qui prouve encore une fois que le toluène est mieux adsorbé sur NaLaY que sur NaCoY.

Comme prévu, les valeurs des exposants de la pression partielle du toluène (exposants qui équivalent en fait à l'ordre de réaction en cinétique formelle) sont fractionnaires. Des valeurs présentées dans le tableau 2 (0,39 pour NaCoY et 0,51 pour NaLaY) il résulte que la dépendance entre la vitesse de réaction et la pression partielle du toluène est plus accentuée chez le faujasite échangé avec des cations La^{3+} que chez celui ayant été modifié par des ions Co^{2+}. Ceci compense en quelque sorte la différence existant entre les valeurs des énergies d'activation, ce qui fait que la vitesse de réaction soit approximativement la même sur les deux catalyseurs.

CONCLUSION

Cette étude a permis de constater que la cinétique du processus principal de disproportionation du toluène ainsi que celles des réactions secondaires dépendent énormément des particularités observées dans le comportement de chaque catalyseur, particularités dues en premier lieu à la nature du cation de compensation.

La détermination des constantes de vitesse et d'adsorption ainsi que celle des énergies d'activation et d'adsorption du toluène ont donné une image assez claire de l'activité des catalyseurs testés. Les résultats obtenus sont en bonne concordance avec ceux obtenus par d'autres auteurs pour des catalyseurs similaires.[6-10]

BIBLIOGRAPHIE

[1] S. Oprea, A. Azzouz, E. Dumitriu et M. Constantinescu, *Bull. Soc. chim. belges*, **92**, 289 (1983.
[2] Y. Y. Huang, J. E. Benson et M. Boudart, *Ind. Eng. Chem. Fundamentals*, **8**, 346 (1969).
[3] J. W. Ward, *J. Phys. Chem.*, **72**, 4211 (1968).
[4] D. W. Breck, « Zeolite Molecular Sieves », Wiley, New York, 1974, p. 460—480.
[5] S. Oprea. A. Azzouz, E. Dumitriu et V. Pescaru, « Lucrările celei de-a IX-a sesiuni de comunicări științifice a Centrului de cercetare Rm. Vîlcea, Voineasa, 2—4 iunie 1983 ».
[6] N. Goidea, D. Goidea et G. Șerban, *Rev. Chim. (București)*, **24**, 497 (1973).
[7] T. Iwamura, S. Otani et M. Sato, *Bull. Jap. Petr. Inst.*, **13**, 116 (1971).
[8] S. B. Shashidhar et R. P. Suresh, *Ind. Eng. Chem. Prod. Res. Dev.*, **20**, 106 (1981).
[9] L. E. Aneke, L. A. Gerritsen, J. Eilers et R. Trion, *J. Catalysis*, **59**, 37 (1979).
[10] Y. Izumi et T. Shiba, *Kogyo Kagaku Zasshi*, **66**, 1817 (1963).

Revue Roumaine de Chimie, 29, *11–12*, 895 (1984)

COMPTES RENDUS

W. KLÖPFFER, "Introduction to Polymer Spectroscopy", (Polymers. Properties and Applications, vol. 7), Springer-Verlag, Berlin, 1984, 184 pages, 98 DM (hard-cover).

In order to obtain complete information on polymers, chemists must combine polymer chemistry with spectroscopy. Because of the elevated molecular mass some physical properties of polymers are different from those of monomers and oligomers, so that not all methods available for the latter are applicable to the former. As a consequence of this distinction it becomes necessary to study polymers in a different way with spectroscopic methods.

The author defines polymer spectroscopy as "the science of quantum resonance interactions of electromagnetic radiations with polymers". The information obtained thereby is classified into :

i) experimental (structural and dynamic)
ii) theoretical.

The former one is the scope of the present book. The principal methods reviewed are :

i) electronic spectroscopy (electron spectroscopy for chemical analysis, i.e. ESCA, UV and IR absorption spectroscopy, fluorescence and phosphorescence).
ii) vibrational spectroscopy (Raman, IR and UV spectroscopy)
iii) spin-resonance spectroscopy (electron spin resonance, ^{1}H–NMR and ^{13}C–NMR).

The main purpose of the book is a didactic one, because it has taken shape from several series of lectures at the Ecole Polytechnique Federale (Lausanne) and at the University of Fribourg in Switzerland. In contrast to other books on this subject, equal weight is given to each technique. Much emphasis is given to understanding the basic processes and mechanisms involved in each method. Both similarities and differences between low and high molecular mass compounds with regard to their spectra have been elaborated. At the end of each chapter the strengths as well as the limitations of the methods are delineated.

The monograph is a useful survey to polymer researches not specialized in spectroscopy or even to specialists in one or the other spectroscopic techniques wishing to orient themselves outside their own field of research. The most important monographs on the subject are listed at the end of each chapter.

The review is highly readable and systematically presented in an elementary fashion ; attention is drawn on the understanding of the basic phenomena. Like all the other books in the series "Polymers. Properties and Applications" it is excellently printed. Formulas, diagrams and tables are drawn clearly. Together with the other volumes in this series it is a main source of fundamental knowledge in the field of polymer science.

Ursula Bologa

INDEX DES AUTEURS

A

ABDEL GHANI ALI EL-AGAMEY and LEVAN PETROVITSH ASATIANI, Synthesis of mono- and diacetylenic derivatives of silylferrocene . . . 583
AHI ANITA, voir BAJPAI U.D.N. . . . 605
AIRINEI A., voir SPIRATOS M. . . . 457
ALBEROLA A., and A. M. GONZALES, F. J. PULIDO, The reaction of *p*-quinones with triphenylstibine . . . 441
ALBU B., voir POPESCU D. . . . 253
ANDREI A., voir LUCA C. . . . 67
ANDREI C., and E. MOLDOVAN, G. ANDREI, G. NICOLESCU, V. DOBRESCU, Alternating copolymers of maleic anhydride with ethylene and vinyl acetate — ion exchangers . . . 13
ANDREI GEORGETA, voir ANDREI C. . . . 13
ANDRUH M. and C. I. LEPĂDATU, MARIA BREZEANU, Calculation of force constants for $[MCl_4]^{n-}$ complexes in the nuclear effective charge model . . . 469
ANGELESCU N., voir TEOREANU I. . . . 113
APĂTEANU L., voir STERNBERG S. . . . 727
— voir STERNBERG S. . . . 833
ARVAY ZSOLT, voir RĂZUȘ A. C. . . . 719
AVRAM MARGARET, voir GHENCIULESCU A. . . . 49
— voir MĂNOIU D. . . . 193
— , voir MĂNOIU D. . . . 201
— , voir ȘTEFAN N. . . . 631
— , voir MĂNOIU D. . . . 671
— , voir ȘTEFAN N. . . . 549
— , voir ȘTEFAN N. . . . 557
— , voir MĂNOIU D. . . . 857
AVRAMESCU F., voir NICOLESCU I. V. . . . 647
AZZOUZ ADELKRIM, voir OPREA S. . . . 887

B

BACALOGLU R. and I. HAVLIK, C. CSUNDERLIK, Synthesis and characterization of substituted 2-(aryl-azoarylamino)-4,6-dichlor- and 2-chlor-4,6-bis (arylazoarylamino)-1,3,5-triazines (in German) . . . 185
BADEA F., voir SCHIKETANZ I. I. . . . 353
BAHADUR P. and K. SINGH, A. GUPTA, Influence of added salt on the adsorption characteristics of alkaline earth metal soaps at benzene-water interface . . . 323
BALABAN A. T., voir UNCUȚA C. . . . 121

BĂLĂŞOIU M., voir ZAHARESCU M. 241

BÂLDEA A. and G. NIAC, Kinetics of lignite and lignite char gasification with carbon dioxide and steam 175

BALLY I., voir UNCUŢA C. 121

BALU I., voir ZUCA ŞTEFANIA 309

BARABÁS A., voir GOCAN A. 423

— , voir FENEŞAN I. 761

BARBADO D. VAZQUES, Determination of Fe(III) by complexometric potentiometry. Determination of the binary mixtures of Ca(II)—Pb(II), Ca(II)—Fe(III) and Pb(II)—Fe(III) (in Spain) 367

— , Applications of the amalgamated gold electrode to the complexometric determination of Ca(II) and Pb(II) 375

BARRADO E. and R. PARDO, Use of an aged nitrate-selective electrode as halide-sensor in potentiometric titrations 693

BARTHA E., voir RĂZUŞ A. C. 719

BAJPAI U. D. N. and ANITA AHI, Polymerization of acrylamide initiated by Fe^{2+}/ bromate redox couple 605

BEZDADEA M., voir SIMIONESCU CR. I. 77

BIDIAN V., voir NICOLESCU I. V. 647

BÎLBĂ N., voir MIHĂILĂ Gh. 261

— , voir OPREA S. 887

BOGDAN M., voir FENEŞAN I. 761

BORCAN R., voir ZUCA ŞTEFANIA 233

BORDEIANU R., voir CEAUŞESCU E. 3

BOTAR A. A., voir GOCAN A. 423

BRĂNIŞTEANU S., voir SIMIONESCU Cr. I. 567

BRÂNZOI V., voir STERNBERG S. 727

— , voir STERNBERG S. 833

BREZEANU MARIA, voir ANDRUH M. 469

BRIŢCHI M., voir PETRESCU N. 407

— , voir PETRESCU N. 541

BUTUFEI OLGA and I. GAVĂT, Polyaminochlorquinones. I. Polycondensation of chloranil with piperazine 19

BUZDUGAN E., voir CEAUŞESCU E. 3

C

CĂLUŞARU A., Hydrogen isotope effects in the reaction of polarographic oxygen reduction 589

CARP M., voir CIOCHINĂ A. 151

CASPI E., voir SIMON Z. 83

CEAUŞESCU ELENA, and R. BORDEIANU, P. GHIOCA, R. STANCU, I. CERCHEZ, E. BUZDUGAN, Dilute block copolymer systems. III. Hardness of oil-extended butadiene-styrene block copolymers 3

CECAL Al. and N. MIHAI, Radiochemical study on the corrosion kinetics of the carbon-steel OL-32 315

— , voir ONISCU C. 677

CERCASOV C. and F. CORNEA, M. CIUREANU, M. HILLEBRAND, V. Em. SAHINI, E. VOLANSCHI, ESR and ^{1}H-NMR spectra of some nitro-substituted thiobenzamides 25

CERCHEZ I., voir CEAUȘESCU E. 3
CHIFU E. and C. GHEORGHIU, I. STAN, Surface mobility of surfactant solutions. XI. Numerical analysis for the Marangoni and the gravity flow in a thin liquid layer of triangular section 31
CHIRALEU F., voir UNCUȚA C. 121
— , voir FILIP P. 549
— , voir FILIP P. 557
CHIRALEU F., voir ȘTEFAN N. 631
— , voir ȘTEFAN N. 861
CHIRIAC C. I., A new convenient method for the synthesis of aromatic hydrazides directly from acids using ethylene chlorophosphite as reagent 219
— , Synthesis of aromatic thioureas under mild conditions using a new condensation reaction 329
CIOBANU A., voir SPIRATOS M. 457
CIOCHINĂ A. and M. CARP, RODICA VÎLCU, Thermal conductivimeter for nonmetallic solids 151
CIUREANU M., voir CERCASOV C. 25
COLȚEA PETRONELA, voir SCHWARTZ R. 755
CONSTANTINESCU ELENA and HILDEGARD DENGEL, Thermogalvanic cell with aqueous cesion chloride solution (in German) 655
CONSTANTINESCU M., voir DUMITRESCU S. 513
CONȚESCU ADRIANA, voir SPACU P. 99
CONTINEANU IULIA, and D. I. MARCHIDAN, The enthalpies of combustion and formation and D-alanine, L-alanine, D,L-alanine and β-alanine 43
CORDOȘ E. and LIANA MUREȘAN, Analogic device for derivation of spectral curves in flame photometry 867
CORNEA FELICIA, voir CERCASOV C. 25
COTÂRȚĂ ADINA, voir STERNBERG S. 699
CRINE M., voir DODET C. 663
CRIȘAN D., voir ZAHARESCU MARIA 241
CRIȘAN MARIA, voir ZAHARESCU MARIA 241
CSUNDERLIK C., voir BACALOGLU R. 185

D

DEACONESCU I., voir DONESCU D. 483
DENGEL H., voir CONSTANTINESCU E. 655
DESSOKI H. A. and A. ESSAWY, Synthesis of 2-cyano-2-arylazo-methyl-3,1-benzoxazin-4(*H*)-ones and studies of their spectral behaviour 345
DIMITRIU E., voir VÎLCU RODICA 131
DINULESCU I. G., voir GHENCIULESCU A. 49
— , voir MĂNOIU D. 193
— , voir MĂNOIU D. 201
— , voir ȘTEFAN N. 631
— , voir MĂNOIU D. 671
— , voir FILIP P. 549
— , voir FILIP P. 557
— , voir MĂNOIU D. 857
DOBRESCU VIORICA, voir ANDREI C. 13

DODET C. and F. NOVILLE, M. CRINE, JEAN-PAUL PIRARD, A study of the texture of seabed nodules for potential use as catalysts (in French) 663

DONESCU D., and I. DEACONESCU, KRISTIANA GOȘA, Influence of coemulsifiers on the emulsion polymerization of vinyl acetate in the presence of hydroxyethylcellulose 483

DRĂGĂNOIU MIHAELA, voir STERNBERG S. 105

DRĂGHICI C., voir UNCUȚA C. 121

DRANGA D., voir MIHĂILĂ Gh. 261

DUMITRESCU SVETLANA and M. GRIGORAȘ, G. SURPĂȚEANU, On the polymerization of acetylenic derivatives XXXV. Experimental and theoretical study on the radical polymerization of 9-ethynylanthracene 447

— , On the polymerization of acetylenic derivatives XXXVI. The cationic polymerization of 9-ethynylanthracene 513

DUMITRIU E., voir OPREA S. 887

E

El-BORAI M., voir HASSAN M.A. 769

ELIAN M., voir ȘTEFAN N. 861

El-KADY M., voir HASSAN M. A. 769

El-KASABY M. A. and M. A. I. SALEM, Michael reaction of β(2-fluorenyl)-acrylic acid and its amides 575

ENESCU L., voir GHENCIULESCU A. 49

ESSAWY A., voir DESSOKI H. A. 345

F

FAZAKAS JÁNOS, Effect of atomisation temperature on the sensitivity of lead in atomic absorption spectrometry under electrothermal atomisation and tube wall or platform vaporization (in French) 207

FENEȘAN I. and V. MUREȘAN, A. BARABÁS, M. BOGDAN, 2-Arylsulphonylamido-2-thiono-5,5-dimethyl-1,3,2-dioxaphosphorinanes 761

FILIP P. and ȘTEFAN N., F. CHIRALEU, I. G. DINULESCU, M. AVRAM, Investigation in the cyclobutane series. LVI. Dimers of 1-alkylbenzocyclobutadienes 546

FILIP P. and N. ȘTEFAN, F. CHIRALEU, I. G. DINULESCU, M. AVRAM, Investigation in the cyclobutane series. LVII. On the behaviour of 1-alkyl-benzocyclobutadiene dimers toward the system t-BuOK-DMSO in air. . . . 557

— , voir ȘTEFAN NICOLETA 631

— , voir ȘTEFAN NICOLETA 861

FLOREA S., voir RĂILEANU M. 429

FRUNZĂ LIGIA voir NICOLESCU I. V. 647

G

GALAȘIU I., voir ZUCA ȘTEFANIA 309

GAOVNICI L., voir PETRESCU N. 407

— , voir PETRESCU N. 541

GHENCIULESCU AURELIA and M. D. GHEORGHIU, L. ENESCU, I. G. DINULESCU, MARGARET AVRAM, Regio- and stereoselective bromine addition to 2-chloro-*endo*-benzocyclobutenonorbornene 49

GHEORGHIU CĂLIN, voir CHIFU E. 31

GHEORGHIU CONSTANȚA and C. GURAN, A. MEGHEA, I. JITARU, Chromium (III) complex thiocyanates with biguanidine derivatives 475

— and C. GURAN, M. MUNTEANU, Chromium hexammine complexes with biguanidine derivatives 741

— , C. GURAN, A. MEGHEA, Molybdenum (V) oxo-thiocyano compounds with biguanidine derivatives 747

GHEORGHIU M. D., voir A. GHENCIULESCU 49

GHINEA STELUȚA, voir VLĂDESCU LUMINIȚA 507

GHIOCA P., voir CEAUȘESCU E. 3

GIURGINCA M., voir IVAN Gh.. 639

GLATZ ALICE MARIE, voir RĂZUȘ A. C. 719

GOCAN A. and A. BOTAR, A. BARABÁS, I. OPREAN, N. ȘERBAN, F. HODOȘAN, Exo- and endohormones VIII. Methoxyallene in pheromone synthesis. . 423

GONZALES A. M., voir ALBEROLA A. 441

GOȘA KRISTIANA, voir DONESCU D. 483

GOȘA V., voir POPESCU DOMNINA 253

GRIGORAȘ M., voir DUMITRESCU SVETLANA 447

— , voir DUMITRESCU SVETLANA 513

GUG VICTORIA, voir ROMAN L. 211

GUPTA A., voir BAHADUR P. 323

GURAN C., voir GHEORGHIU CONSTANȚA 475

— , voir GHEORGHIU CONSTANȚA 741

— , voir GHEORGHIU CONSTANȚA 747

H

HANEȘ A., voir SCHIKETANZ I. I. 353

HASSAN M. A. and M. El-KADY, M. El-BORAI, A. A. ZBD El-MOATY, Base catalyzed additions of dehydroacetic acid and its 3-cinnamoyl derivatives. 769

HAVLIK I., voir BACALOGLU R. 185

HILLEBRAND MIHAELA, voir CERCASOV C. 25

HODOȘAN F., voir GOCAN A. 423

HOROBA E., voir ONISCU C. 677

HUQUE MONIMUL and D. SĂNDULESCU, Studies on aqueous electrolytes and nonelectrolytes. I. Effects of electrolytes on viscosity and structure of aqueous solutions of polyvinyl alcohol 55

HUQUE MONIMUL and D. SĂNDULESCU, Studies on aqueous electrolytes and nonelectrolytes. II. Effects of electrolytes on ultrasonic velocity, adiabatic compressibility and structure of aqueous solutions of polyvinyl alcohol (PVA) 415

HUSAIN M. M. and D. K. SINGH, O. P. MATHUR, A correlation of lattice energy and equilibrium interionic distance of alkali metal hydrides. 789

I

IONESCU N., voir POPESCU D. 253

IONIȚĂ S., voir LANGFELD H. W. 295

IOVU M. and M. IQBAL, Condensation of bis(chloromethyl)ether with secondary amines. A new reaction 333

IQBAL M., voir IOVU M. 333

IVAN G. and M. GIURGINCA, Influence of carbon black—antidegradant interaction on the behaviour of rubber compounds in thermo-oxidative degradation. . 639

J

JITARU IOANA, voir GHEORGHIU CONSTANȚA 475

JUHÁSZ ANIKÓ, voir SCHWARTZ R. 755

K

HADI HOCINE and D. P. LAZĂR, Identification of the aromatic hydrocarbons in some petroleum fractions. I. Experimental conditions in HPLC (in French). . . 497

KANT RAVI, voir KUMAR SANJAY 383

KEZDI MARIA, voir VLASSA M. 461

KUMAR SANJAY amd RAVI KANT, OM PRAKASH, Sensitised colour reaction for spectrophotometric determination of uranium. 383

L

LANGFELD H. W. and S. IONIȚĂ, On the quaternization of p-amino-phenylazo-azols. I. Mechanism of 2-(4′-aminophenylazo)-azol alkylation (in German). . . 295

LAZĂR D. P., voir KADI HOCINE 497

LECA A., voir LECA M. 561

LECA MINODORA and A. LECA, Drag reduction of some ultra-high molecular weight polyacrylamides 561

LEPĂDATU C. I., voir ANDRUH M. 469

LITEANU C. and Gh. RĂDULESCU, MARIA MOISE, Study of the reactification properties of heterogeneous membranes. VIII. Behaviour of the bipolar unitary membrane system : cationite R—H anionite R—OH 799

LÖCSEI V., Selective ester hydrolysis. Determination of ester groups of polyurethane elastomers 437

LUCA C., and G. SEMENESCU, A. ANDREI, Consideration on the equilibrium state of metal/oxide electrolyte system 67

— , voir MIHĂILĂ Gh. 261

M

MĂNĂILĂ R., voir NICOLESCU I. V. 647

MANDRIC Gh. and Gh. PETRESCU, E. PĂTRĂHĂU, Th. POPA, High-temperature polymers V. Ordered benzothiazole-imide copolymers 521

MĂNOIU D. and MARIA MĂNOIU, I. G. DINULESCU, MARGARET AVRAM, Friedel-Crafts acylation of alkynes. I. The reaction of 1-alkynes with acetyl chloride. $AlCl_3$-complex in the presence of halogenated nonnucleophilic solvents. 193

— and MARIA MĂNOIU, I. G. DINULESCU, MARGARET AVRAM, Friedel-Crafts acylation of alkynes. II. The reaction of 1-alkynes with acetyl chloride. $AlCl_3$-complex in aromatic and saturated hydrocarbons as solvents 201
— and MARIA MĂNOIU, I. G. DINULESCU, MARGARET AVRAM, Friedel-Crafts acylation of alkynes. III. Reaction of 1-alkynes with acetyl chloride in the presence of silver perchlorate 671
— and MARIA MĂNOIU, I. G. DINULESCU, MARGARET AVRAM, Friedel-Crafts acylation of acetylenes. IV. On the non selectivity of acylvinyl cations in armonic substitution 857
MĂNOIU MARIA, voir MĂNOIU D. 193
— , voir MĂNOIU D. 201
— , voir MĂNOIU D. 671
— , voir MĂNOIU D. 857
MAOUCHE BOUBEKEUR and J. GAYOSO, O. OUAMERALI, Diamagnetic susceptibility exaltations and aromaticities of unsaturated boron-nitrogen heterocycles 613
MARCHIDAN D. I., voir CONTINEANU IULIA 43
MASCAȘ A. and S. STERNBERG, Thermal conductivity of $Co(NO_3)_2 \cdot 6H_2O - nH_2O$ system 165
MATEESCU A., voir STERNBERG S. 727
MATHUR O. P., voir M. M. HUSAIN 789
MEGHEA A., voir GHEORGHIU C. 475
— , voir GHEORGHIU C. 747
MIHAI N., voir CECAL Al. 315
MIHĂILĂ Gh. and N. BÎLBĂ, D. DRANGA, C. LUCA, Vapour-liquid equilibrium at atmospheric pressure of the toluene-acetic anhydride and acetic anhydride-*o*-xylene systems 261
MIHALAȘ G. I., voir SIMON Z. 53
MOISE MARIA, voir LITEANU C. 799
MOLDOVAN E., voir ANDREI C. 13
MOSER V., voir ZAHARESCU M. 247
MUNTEAN M., voir GHEORGHIU C. 741
MUREȘAN LILIANA, voir CORDOȘ E. 867
MUREȘAN V., voir FENEȘAN I. 761
MURGULESCU I. G. and EUGENIA SĂLĂGEAN, Equations of state for ionic liquids. 143
— and EUGENIA SĂLĂGEAN, Estimation of thermodynamic properties of molten alkaline earth metal halides 809

N

NEAGOE S., voir NEGOIU D. 267
— , voir NEGOIU D. 275
NECȘOIU ILEANA, voir ȘCHIKETANZ I. I. 353
NEDELCU G., voir NICOLESCU I. V. 647
NEGOIU D. and S. NEAGOE, MARIA NEGOIU, Contributions to the chemistry of thiocomplexes. I. Complex combinations of Pd(II) with 4-(arylsulfonyl)-thiobenzamides 267

NEGOIU D. and S. NEAGOE, I. ȘARAMET. Contributions to the chemistry of thiocomplexes II. Complex combinations of Pt(II), Cu(I), Au(III) and Hg(II) with 4-(arylsulfonyl)-thiobenzamides 275

NEGOIU MARIA, voir NEGOIU D. 267

NEGULIANU CLAUDIA, voir VASILIU OPREA Cl. 683

NIAC G., voir BÂLDEA A. 175

NICOLESCU GALINA, voir ANDREI C. 13

NICOLESCU I. V. and J. V. RAJAOFANOVA, L. FRUNZĂ, F. AVRAMESCU, R. MĂNĂILĂ, O. ȘERBAN, G. NEDELCU, V. BIDIAN, Activation of the natural zeolite clinoptilolite, structural properties and catalytic activity. 647

NOVILLE F., voir DODET C. 663

O

OANCEA D., voir POPESCU D. 253

OUAMERALI OURIDA voir MAOUCHE BOUBEKEUR 613

ONISCU C. and AL. CECAL, E. HOROBA, Kinetic studies for the formation of a sulfamethine silver salt using radioisotopes (in German) 677

OPREA S. and A. AZZOUZ, E. DUMITRIU, N. BÎLBĂ, Catalytic transformations of aromatic hydrocarbons. VI. Study of the activity of zeolites modified with polyvalent elements (in French) 887

OPREAN I., voir GOCAN A. 423

P

PARDO R., voir BARRADO E. 693

PÂRVULESCU V., voir SĂNDULESCU I. 793

PĂTRĂHĂU E., voir MANDRIC Gh. 521

PATRON LUMINIȚA, voir SPACU P. 99

PĂUNESCU N., A spectrophotometric study of uranyl complexes formed in the UO_2^{2+} — Cl^- —acetone system. 289

PETRACHE Gh., voir MANDRIC Gh. 521

PETRESCU N., and L. GANOVICI, M. BRIȚCHI, Electrolytic copper refining from cupreous sulphate solutions containing organic nitriles 407

PETRESCU N. and M. BRIȚCHI, L. GANOVICI, Removal of antimony and arsenic from electrolytes by means of β-stannic acid 541

PETROVITSH ASATIANI L., voir ABDEL GHANI ALI 583

PIRARD J. P., voir DODET C. 662

POPA TH., voir MANDRIC Gh. 521

POPA V., voir SEGAL E. 593

— , voir VLAD M. 593

POPA V. and E. SEGAL, M. VLAD, A new general form of Wegsheider's cyclicity conditions 625

POPESCU D. and D. OANCEA, V. GOȘA, N. I. IONESCU, B. ALBU, The explosive combustion of propylene. III. The explosive combustion of propylene in a constant volume bomb 253

PULIDO F. J., voir ALBEROLA A. 441

R

RĂDULESCU Gh., voir LITEANU C. 799
RĂILEANU M. and S. FLOREA, MARINA SAHINI, Solvent effects. I. Solvent influence on the absorption spectra of some nitrophenothiazine-5-oxides and nitrophenothiazine-5,5-dioxides 429
RĂILEANU M., Solvent effect III. Solvent influence on the reaction of the phenothiazine with nitrous acid 707
RAJAOFANOVA J. V., voir Nicolescu I. V. 647
RĂZUȘ C. A. and E. BARTHA, Z. ARVAY, A. M. GLATZ, Synthesis of *para*-substituted benzylcyclopropyl ketones. 719
ROMAN L. and M. ȘERBAN, V. GUG, Mercaptothiadiazole derivatives-sensitive reagents for the potentiometric determination of Hg (II) (in German). . . 211
RUSU G. I., voir SPIRATOS M. 457

S

SAHINI V. Em., voir CERCASOV C. 25
SAHINI MARINA, voir RĂILEANU M. 429
SĂLĂGEANU E., voir MURGULESCU I. V. 143
— , voir MURGULESCU I. V. 809
SALEM M. A. I., voir El-KASABY M. A. 575
SĂNDULESCU F. and Cr. I. SIMIONESCU, New solvent systems for acrylic copolymers 773
SĂNDULESCU D., voir HUQUE MONIMUL 55
— , voir HUQUE MONIMUL. 415
SĂNDULESCU I. and V. PĂRVULESCU, S. STRAJA, An attempt of explaining hydrogenation/dehydrogenation of ethylbenzene - ethylcyclohexane on Pd –Mn/γ Al_2O_3 and Mn/γ Al_2O_3 catalysts 793
ȘARAMET I., voir NEGOIU D. 275
SCHIKETANZ I. I. and F. BADEA, A. HANEȘ, I. NECȘOIU, Etard reaction XII. Oxidation of dibenzo [*b*, *f*] bicyclo[3,2,1]octa-2,6-diene and of dibenzo[*b*,*e*] bicyclo[2,2,2] octa-2,5-diene with chromyl chloride 353
SCHWARTZ R. and A. JUHÁSZ, P. COLȚEA, The synthesis of 3β-acetoxy-B-nor-androst-5-en-3β-ol-17-one and 3β-acetoxy-B-nor-pregn-5-en-3β-ol-20-one . 755
SEGAL E., and M. VLAD, V. POPA, Structural characteristics of the stoichiometric matrix 593
— , voir M. VLAD. 598
— , voir POPA V. 625
SEMENESCU G., voir LUCA C. 67
ȘERBAN M., voir ROMAN L. 211
ȘERBAN N., voir GOCAN A. 423
ȘERBAN OLGA, voir NICOLESCU I. V. 647
SHARMA B. K., voir SHARMA M. K. 223
SHARMA M. K. and B. K. SHARMA, On the aging of turpentine (montan wax) in water emulsions as functions of viscosity and particle size distribution. . . 223
SHOUKRY M. M., Potentiometric studies on transition metal chelates of aceto-acetanilide 283
SIMIONESCU Cr. I. and M. BEZDADEA, Matrix polymerization in the presence of urea 77

SIMIONESCU Cr. I. and S. BRĂNIŞTEANU, Ion exchange membranes based on grafted cellulose esters. I. Activation by peroxidation in view of grafting the cellulose esters 567
SIMIONESCU Cr. I., voir SĂNDESCU F. 773
SIMON Z. and G. I. MIHALAŞ, E. CASPI, Structure-binding affinity correlations for iodo- and selenoestrogen analogs and mapping of the estrogen receptor by the MTD-method 83
SINDHU R. S. and R. P. SINGH, Potentiometric studies on the complexes of Pr(III), Nd(III), Sm(III), Gd(III), Tb(III), Dy(III) and Ho(III) with 2'-hydroxychalcone 883
SINGH D. K., voir HUSAIN M. M. 789
SINGH K., voir BAHADUR P. 323
SINGH R. P., voir SINDHU R. S. 883
SPACU P. and L. PATRON, A. CONŢESCU, Coordination compounds of Co(II) (d^7) with tryptophan 99
SPIRATOS M. and A. AIRINEI, G. I. RUSU, A. CIOBANU, Coordination polymers VI. Preparation and characterization of some azomethine chelate polymers. 457
STAN I., voir CHIFU E. 31
STANCU R., voir CEAUŞESCU E. 3
STRAJA S., voir SĂNDULESCU I. 793
ŞTEFAN N., voir FILIP P. 549
— , voir FILIP P. 557
— , and P. FILIP, I. G. DINULESCU, F. CHIRALEU, M. AVRAM, Investigation in the cyclobutane series. LVIII. Stereoisomeric epoxides of the angular dimer of benzocyclobutadiene 631
— and P. FILIP, F. CHIRALEU, M. ELIAN, The stereochemistry of some dibenzo [*b, g*] bicyclo [4,2,0] octadiene derivatives 861
STERNBERG S. and M. DRĂGĂNOIU, Thermodynamic activity of $ZnSO_4$ in ternary systems. I. $ZnSO_4 + Me_2^ISO_4 + H_2O$ and $ZnSO_4 + Me^{II}SO_4 + H_2O$ systems 105
— , voir MASCAŞ A. 165
— and T. VIŞAN, A. COTÂRŢĂ, Electrochemical reactions of cupric and cupreous ions in lithium chloride — potassium chloride eutectic. II. Steady-state potentiostatic studies 699
— and A. MATEESCU, V. BRÂNZOI, L. APĂTEANU, Electrode processes in $PbSO_4/PbO_2$ system 727
— and V. BRÂNZOI, L. APĂTEANU, Polarization behaviour of the lead microelectrode in sulphuric acid solution 833
— and D. GEANĂ, Calculation of phase diagrams of molten salt mixtures from electromotive force measurements 843
SURPĂŢEANU G., voir DUMITRESCU SVETLANA 447
— , voir DUMITRESCU SVETLANA 513
— , Distribution of atomic charges in cycloimmonium ylides. 877

T

TĂVALĂ T., voir ZAHARESCU M. 247
TEOREANU I. and N. ANGELESCU, D. ŢUCLEA, $CA-CA_2$ Aluminous cement hydration kinetics and the nature of its hydration products (in French). 113
TERDIC H. M., Disubstiuted phenothiazones II. New halogeno-3H-phenothiazin-3-ones 489

TRINAJSTIĆ N., voir VELENIK A. 737
ŢUCLEA D., voir TEOREANU I. 113

U

UNCUŢA C. and I. BALLY, C. DRĂGHICI, F. CHIR ALEU, A. T. BALABAN, Heterocyclic organoboron compounds. XVII. Axial chirality of boron chelates evidenced by ^{1}H-NMR spectroscopy in the presence of chiral additives 121

V

VASILIU-OPREA Cl. and C. NEGULIANU, F. WEINER, Mechano-chemical modification of physical and chemical characteristics of poly-(vinylchloride) suspension 683
VELENIK A. and T. ŽIVKOVIĆ, N. TRIANJSTIĆ, On bond orders and bond energies in conjugated systems 737
VÎLCU R. and E. DIMITRIU, A correlation between surface tension and the adiabatic compressibility 131
— , voir CIOCHINĂ A. 151
VIŞAN T., voir STERNBERG S. 699
VLAD M., voir SEGAL E.. 593
— , voir POPA V.. 625
— and V. POPA, E. SEGAL, On the kinetic model of the rate-determining step. II. Single-route systems with an arbitrary number of active intermediates 597
VLĂDESCU L. and S. GHINEA, Separation and concentration of thiosulphate with ion-exchange resins 507
VLASSA M. and M. KEZDI, Application of phase transfer catalysis in the acridine series. II. Synthesis of some acridine ethers 461
VOLANSCHI E., voir CERCASOV C.. 25

W

WEINER F., voir VASILIU OPREA Cl. 683

Z

ZAHARESCU M. and M. BĂLĂŞOIU, M. CRIŞAN, D. CRIŞAN, T. TĂVALĂ, V. MOSER, The influence of the properties of ferric oxides on the formation of Mn—Zn ferrite 247
ZBD El-MOATY A. A., voir HASSAN M. A. 769
ŽIVKOVIĆ T., voir VELENIK A. 737
ZUCA ŞT. and R. BORCAN, Viscosity of certain charge-unsymmetrical molten chloride mixtures : $CaCl_2$-(Na, K, Rb, Cs)Cl 233
— and I. GALASIU, I. BĂLU, On anode effect in aluminium electrolysis. . 309

INDEX DES SUJETS

1984

-3β-Acetoxy-B-nor-androst-5-en-3β-ol-17-one and 3β-acetoxy-B-nor-pregn-5-en-3β-ol-20-one, The synthesis of —, R. SCHWARTZ, A. JUHÁSZ and P. COLȚEA . . 755

Acetylenes IV. On the non selectivity of acylvinyl cations in aromatic substitution, Friedel-Crafts acylation of —, D. MĂNOIU, M. MĂNOIU, I. G. DINULESCU and M. AVRAM 857

Acetylenic derivatives XXXV. Experimental and theoretical study on the radical polymerization of 9-ethynyl-anthracene, On the polymerization of —, S. DUMITRESCU, M. GRIGORAȘ and G. SURPĂȚEANU 447

Acetylenic derivatives XXXVI. The cationic polymerization of 9-ethynylanthracene, On the polymerization of —, S. DUMITRESCU, M. GRIGORAȘ, G. SURPĂȚEANU and M. CONSTANTINESCU 513

D-Alanine, L-alanine, DL-alanine and β-alanine, The enthalpies of combustion and formation of —, I. CONTINEANU and D. I. MARCHIDAN. 43

Alkaline earth metal soaps at benzene-water interface, Influence of added salt on the adsorption characteristics of —, P. BAHADUR, K. SINGH and A. GUPTA 323

Alkynes I. The reaction of 1-alkynes with acetyl chloride. $AlCl_3$-complex in the presence of halogenated nonnucleophilic solvents, Friedel-Crafts acylation of —, D. MĂNOIU, M. MĂNOIU, I. G. DINULESCU and M. AVRAM . . 193

Alkynes II. The reaction of 1-alkynes with acetyl chloride. $AlCl_3$-complex in aromatic and saturated hydrocarbons as solvent, Friedel-Crafts acylation of —, D. MĂNOIU, M. MĂNOIU, I. G. DINULESCU and M. AVRAM. . . . 201

Alkynes III. Reaction of 1-alkynes with acetyl chloride in the presence of silver perchlorate, Friedel-Crafts acylation of —, D. MĂNOIU, M. MĂNOIU, I. G. DINULESCU and M. AVRAM 671

Aluminium electrolysis, On anode effect in —, Ș. ZUCA, I. GALAȘIU and I. BĂLU. . . 309

Aluminous cement hydration kinetics and the nature of its hydration products (in French), I. TEOREANU, N. ANGELESCU and D. ȚUCLEA 113

Amalgamated gold electrode to complexometric determination of Ca(II) and Pb(II), Application of the — (in Spain), DOLORES VAZQUES BARBADO. . . 375

p-Aminophenylazo-azols I. Mechanism of 2-(4′-amino-phenylazo)-azol alkylation, On the quaternization of — (in German), H. W. LANGFELD and S. IONIȚĂ. 295

Analogic device for derivation of spectral curves in flame photromey, E. CORDOȘ and L. MUREȘAN 867

Antimony and arsenic from electrolytes by means of β-stannic acid, Removal of —, N. PETRESCU, M. BRIŢCHI and I. GANOVICI 541

Aqueous electrolytes and nonelectrolytes. I. Effects of electrolytes on viscosity and structure of aqueous solutions of polyvinyl alcohol, Studies on —, M. HUQUE and D. SĂNDULESCU 55

Aqueous electrolytes and nonelectrolytes. II. Effects of electrolytes on ultrasonic velocity, adiabatic compressibility and structure of aqueous solutions of polyvinyl alcohol (PVA), Studies on —, M. HUQUE and D. SĂNDULESCU. . 415

Aromatic hydrazides directly from acids using ethylene chlorophosphite as reagent, A new convenient method for the synthesis of —, C. I. CHIRIAC. . . . 219

Aromatic hydrocarbons VI. Study of activity of zeolites modified with polyvalent elements, Catalytic transformations of — (in French), S. OPREA, A. AZZOUZ, E. DUMITRIU and N. BÎLBA 887

Aromatic hydrocarbons in some petroleum fractions. I. Experimental conditions in HPLC, Identification of the — (in French), H. KADI and D. P. LAZĂR. . 497

2-(Aryl-azoarylamino)-4,6-dichlor- and 2-chlor-4,6-bis-(aryl-azoarylamino)-1,3,5-triazines, Synthesis and characterization of substituted — (in German), R. BACALOGLU, I.HAVLIK and C. CSUNDERLIK 185

2-Arylsulphonylamido-2-thiono-5,5-dimethyl-1,3,2-dioxaphosphorinanes, I. FENEŞAN, V. MUREŞAN, A. BARABÁS and M. BOGDAN 761

Azomethine chelate polymers, Coordination polymers VI. Preparation and characterization of some —, M. SPIRATOS, A. AIRINEI, G. I. RUSU and A.CIOBANU 457

Benzylcyclopropyl ketones, Synthesis of *para*-substituted —, A. C. RĂZUŞ, E. BARTHA, Z. ARVAY and A.-M. GLATZ 719

Binary mixtures of Ca(II)—Pb(II), Ca(II)—Fe(III) and Pb(II)—Fe(III). Determination of Fe(III) by complexometric potentiometry, Determination of — (in Spain), DOLORES VAZQUES BARBADO 367

Bromine addition to 2-chloro-*endo*-benzocyclobutenonorbornene, Regio- and stereoselective —, A. GHENCIULESCU, M. D. GHEORGHIU, L. ENESCU, I. G. DINULESCU and M. AVRAM 49

Book reviews 389, 390, 465, 533, 534, 535, 536, 536, 715, 895

Carbon black-antidegradant interaction on the behaviour of rubber compounds in thermo-oxidative degradation, Influence of —, G. IVAN and M. GIURGINCA 639

bis(Chloromethyl)ether with secondary amines. A new reaction, Condensation of —, M. IOVU and M. IQBAL 333

Chromium (III) complex thiocyanates with biguanidine derivatives, C. GHEORGHIU, C. GURAN, A. MEGHEA and I. JITARU 475

Chromium hexammine complexes with biguanidine derivatives, C. GHEORGHIU, C. GURAN and M. MUNTEAN 741

Complexes of Pr(III), Nd(III), Sm(III), Gd(III), Tb(III), Dy(III) and Ho(III) with 2-hydroxy chalcone, Potentiometric studies on the —, SINDHU R. S. and R. P. SINGH 883

Conjugated systems, On bond orders and bond energies in —, A. VELENIK, T. ŽIVKOVIĆ and N. TRINAJSTIĆ 737

Copper refining from cuprous sulphate solutions containing organic nitriles, Electrolytic —, N. PETRESCU, L. GANOVICI and M. BRIŢCHI. 407

Corrosion kinetics of the carbon-steel OL-32, A radiochemical study on the — (in French), Al. CECAL and N. MIHAI 315

Cupric and cupreous ions in lithium-chloride-potassium chloride eutectic II. Steady-state potentiostatic studies, Electrochemical reactions of —, S. STERNBERG, T. VIȘAN and A. COTÂRȚĂ 699

2-Cyano-2-arylazo-methyl-3,1-benzoxazin-4(*H*)-ones and studies of their spectral behaviour, Synthesis of —, H. A. DESSOKI and A. ESSAWY 345

Cyclobutane LVI. Dimers of 1-alkyl-benzocyclobutadiene, Investigation in the —, P. FILIP, N. ȘTEFAN, F. CHIRALEU, I. G. DINULESCU and M. AVRAM . 549

Cyclobutane. LVII. On the behaviour of 1-alkyl-benzocyclobutadiene dimers toward the system t-BuOK-DMSO and air, Investigations in the —, N. ȘTEFAN, P. FILIP, I. G. DINULESCU, F. CHIRALEU and M. AVRAM . . . 557

Cyclobutane LVIII. Stereoisomeric epoxides of the angular dimer of benzocyclobutadiene, Investigations in the —, N. ȘTEFAN, P. FILIP, I. G. DINULESCU, F. CHIRALEU and M. AVRAM 631

Cycloimmonium ylides, Distribution of atomic charges in —, G. SURPĂȚEANU . . . 877

Dehydroacetic acid and its 3-cinnamoyl derivatives, Base catalyzed additions of —, M. A. HASSAN, M. El-KADY, M. El-BORAI and A. A. ZBD El-MOATY 769

Diamagnetic susceptibility exaltations and aromaticities of unsaturated boron-nitrogen heterocycles, B. MAOUCHE, J. GAYOSO and O. OUAMERALI 613

Dibenzo (*b*, *g*) bicyclo(4.2.0) octadiene derivatives the stereochemistry of some —, N. ȘTEFAN, P. FILIP, F. CHIRALEU and M. ELIAN 861

Dilute block copolymer systems. III. Hardness of oil-extended butadiene-styrene block copolymers, ELENA CEAUȘESCU, R. BORDEIANU, P. GHIOCA, R. STANCU, I. CERCHEZ and E. BUZDUGAN 3

Disubstituted phenothiazones. II. New halogeno-3H-phenothiazin-3-ones, M. H. TERDIC 489

Electrode processes in $PbSO_4/PbO_2$ system, S. STERNBERG, A. MATEESCU, V. BRÂNZOI and L. APĂTEANU 727

Emulsion polymerization of vinyl acetate in the presence of hydroxyethylcellulose, Influence of coemulsifiers on the —, D. DINESCU, I. DEACONESCU and U. GOȘA 483

Equilibrium state of metal/oxide electrolyte system, Considerations on the —, C. LUCA, G. SEMENESCU and A. ANDREI 67

Étard reaction XII. Oxidation of dibenzo [*b*, *f*] bicyclo [3, 2, 1] octa-2,6-diene and of dibenzo [*b*, *e*] bicyclo [2.2.2] octa-2,5-diene with chromyl chloride, I. I. SCHIKETANZ, F. BADEA, A. HANEȘ and I. NECȘOIU 353

Exo- and endohormones VIII. Methoxyallene in pheromone synthesis, A. GOCAN, A. A. BOTAR, A. BARABÁS, I. OPREAN, N. ȘERBAN and F. HODOȘAN 769

Ferric oxides on barium hexaferrite formation, The influence of the properties of —, M. ZAHARESCU, M. BĂLĂȘOIU, M. CRIȘAN, D. CRIȘAN, T. TĂVALĂ and N. BRÎNZAN 241

Ferric oxides on the formation of Mn—Zn ferrite. The influence of the properties of—, M. ZAHARESCU, M. BĂLĂȘOIU, M. CRIȘAN, D. CRIȘAN, T. TĂVALĂ and V. MOSER 247

Force constants for $[MCl_4]^n$ — complexes in the nuclear effective charge model, Calculation of —, M. ANDRUH, C. I. LEPĂDATU and M. BREZEANU . . . 469

Halide-sensor in potentiometric titrations, Use of an aged nitrate-selective electrode as — , E. BARRADO and R. PARDO 693

Heterocyclic organoboron compounds XVII. Axial chirality of boron chelates evidenced by $^{1}H-NMR$ spectroscopy in the psesence of chiral additives, C. UNCUŢA, I. BALLY, C. DRĂGHICI, F. CHIRALEU and A. T. BALABAN 121

Heterogeneous membranes VIII. Behaviour of the bipolar unitary membrane system: cationite R—H and anionite R—OH, Study of the rectification properties of —, C. LITEANU, Gh. RĂDULESCU and M. MOISE 799

High-temperature polymers V. Ordered benzothiazole-imide copolymers, Gh. MANDRIC, Gh. PETRACHE, E. PĂTRĂHĂU and Th. POPA Hydrogenation/dehydrogenation of ethylbenzene-ethylcyclohexane on $Pd-Mn/\gamma Al_2O_3$ and $Mn/\gamma Al_2O_3$ catalysts, An attempt of explaining —, I. SĂNDULESCU, V. PÂRVULESCU and S. STRAJA 793

Hydrogen isotope effects in the reaction of polarographic oxygen reduction, A. CĂLUŞARU 589

Iodo- and selenoestrogen analogs and mapping of the estrogen receptor by the MTD-method, Structure-binding affinity correlations for—, Z. SIMION, G. I. MIHALAŞ and E. CASPI 83

Ion exchange membranes based on grafted cellulose esters I. Activation by peroxidation in view of grafting the cellulose esters, C. I. SIMIONESCU and S. BRĂNIŞTEANU 567

Ionic liquids, Equations of state for —, I. G. MURGULESCU and E. SĂLĂGEANU . . 143

Kinetics of lignite and lignite char gasification with carbon dioxide and steam, A. BĂLDEA and G. NIAC 175

Lattice energy and equilibrium interionic distance of alkali metal hydrides, A correlation of —, M. M. HUSAIN, D. K. SINGH and O. P. MATHUR . . . 789

Lead microelectrode in sulphuric acid solution, Polarization behaviour of the —, S. STERNBERG, V. BRÂNZOI and L. APĂTEANU 833

Maleic anhydride with ethylene and vinyl acetate — ion exchangers, Alternating copolymers of —, C. ANDREI, E. MOLDOVAN, G. ANDREI, G. NICOLESCU and V. DOBRESCU 13

Matrix polymerization in the presence of urea, Cr. I. SIMIONESCU, and M. BEZDADEA 77

Mercaptothiadiazole derivatives-sensitive reagents for the potentiometric determination of Hg(II) (in German), L. ROMAN, M. ŞERBAN and V. GUG 211

Metal chelates of acetoacetanilide, Potentiometric studies on transition — , MOHAMED M. SHOUKRY 283

Michael reaction of β(2-fluorenyl)-acrylic acid and its amides, M. A. El-KASABY and M. A. I. SALEM 575

Min-max formulation of the problem of phase equilibrium in chemical reacting systems, D. GEANĂ 395

Molybdenum(V) oxo-thiocyano compounds with biguanidine derivatives, C. GHEORGHIU, C. GURAN and A. MEGHEA. 747

Molten alkaline earth metal halides, Estimation of thermodynamic properties of —, I. G. MURGULESCU and E. SĂLĂGEAN 809

Molten chloride mixtures: $CaCl_2-(Na, K, Rb, Cs)Cl$, Viscosity of certain charge-unsymmetrical —, Ş. ZUCA and R. BORCAN 233

Molten salt mixtures from electromotive force measurements, Calculation of phase diagrams of —, S. STERNBERG and D. GEANĂ 843

Mono- and diacetylenic derivatives of silylferrocene, Synthesis, of —, ABDEL GHANI ALI El-AGAMEY and LEVAN PETROVITSH ASATIANI 583

Natural zeolite clinoptilolite, structural properties and catalytic activity, Activation of the—, I. V. NICOLESCU, J. V. RAJAOFANOVA, L. FRUNZĂ, F. AVRAMESCU, R. MĂNĂILĂ, O. ŞERBAN, G. NEDELCU and V. BIDIAN

Polyacrylamides, Drag reduction of some ultra-high molecular weight —, M. LECA and A. LECA 561

Polyaminochlorquinones. I, Polycondensation of chloranil with piperazine, O. BUTUFEI and I. GAVĂT 19

Polymerization of acrylamide initiated by Fe^{2+}/bromate redox couple, U.D.N. BAJPAI and ANITA AHI 605

Polyurethane elastomers, Selective ester hydrolysis, Determination of ester groups in —, V. LÖCSEI 437

Poly(vinylchloride)suspension, Mechano-chemical modification of physical and chemical characteristics of —, Cl. VASILIU-OPREA, C. NEGULIANU and F. WEINER 683

Propylene. III. The explosive combustion of propylene in a constant volume bomb. The explosive combustion, D. POPESCU, D. OANCEA, V. GOŞA, N. I. IONESCU and B. ALBU 253

p-Quinones with triphenylstibine, The reaction of—, A. ALBEROLA, A. M. GONZALES and F. J. PULIDO 441

Sensitivity of lead in atomic absorption spectrometry under electrothermal atomisation and tube wall or platform vaporization (in French) Effect of atomisation temperature on the —, J. FAZAKAS 207

Solvent effects I. Solvent influence on the absorption spectra of some nitrophenothiazine-5,-oxides and nitrophenothiazine-5,5-dioxides, M. RĂILEANU, S. FLOREA and M. SAHINI 429

Solvent effects. III. Solvent influence on the reaction of the phenothiazine with nitrous acid, M. RĂILEANU 707

Solvent systems for acrylic copolymers, New —, F. SĂNDESCU and Cr. I. SIMIONESCU 773

Stoichiometric matrix, Structural characteristics of the —, E. SEGAL, M. VLAD and V. POPA 593

Sulfamethine silver salt using radioisotopes, Kinetic studies for the formation of a —, C. ONISCU, Al. CECAL and E. HOROBA 677

Surface tension and the adiabatic compressibility, A correlation between —, R. VÎLCU and El. DIMITRIU 131

Surfactant solutions. XI. Numerical analysis for the Marangoni and the gravity flow in a thin liquid layer of triangular section. Surface mobility of —, E. CHIFU, C. GHEORGHIU and I. STAN 31

Texture of seabed nodules for potential use as catalysts, A study of the —, (in French) C. DODET, P. NOVILLE, M. CRINE and J. P. PIRARD 663

Thermal conductivimeter for nonmetallic solids, A. CIOCHINĂ, M. CARP and R. VÎLCU 151

Thermal conductivity of $Co(NO_3)_2 .6\ H_2O - nH_2O$ system, A. MASCAŞ and S. STERNBERG 165

Thermogalvanic cell with acqueous cesium chloride solutions (in German), E. CONSTANTINESCU and H. DENGEL 655

Thernary systems. I. $ZnSO_4 + Me^I_2SO_4 + H_2O$ and $ZnSO_4 + Me^{II}SO_4 + H_2O$ systems, Thermodynamic activity of $ZnSO_4$ in —, S. STERNBERG and M. DRĂGĂNOIU 105

Thiobenzamides nitrosubstituted, ESR and ^{1}H—NMR spectra of some —, C. CERCASOV, F. CORNEA, M. CIUREANU, M. HILLEBRAND, V. Em. SAHINI and E. VOLANSCHI 25

Thiocomplexes. I. Complex combinations of Pb(II) with 4-(arylsulfonyl)-thiobenzamides, Contributions to the chemistry of—, D. NEGOIU, S. NEAGOE and M. NEGOIU 267

Thiocomplexes II. Complex combinations of Pt(II), Cu(I), Au(III) and Hg(II) with 4-(arylsulfonyl)-thiobenzamides, Contributions to the chemistry of—, D. NEGOIU, S. NEAGOE and I. ŞARAMET 275

Thiosulphate with ion-exchange resins, Separation and concentration of — (in French), L. VLĂDESCU and S. GHINEA 507

Thioureas under mild conditions using a new condensation reaction, Synthesis of aromatic —, C. I. CHIRIAC. 329

Toluene-acetic anhydride and acetic anhydride — *o*-xylene systems, Vapour-liquid equilibrium at atmospheric pressure of the —, Gh. MIHĂILĂ, N. BÎLBĂ, D. DRANGA and C. LUCA 261

Tryptophan, Coordination compounds of Co(II) (d^7) with —, S. SPACU, L. PATRON and A. CONŢESCU — 99

Turpentine (montan wax) in water emulsions as functions of viscosity and particle size distribution, On the aging of —, M. K. SHARMA and B. K. SHARMA 223

Uranium. Sensitised colour reaction for spectrophotometric determination of —, S. KUMAR, R. KANT and OM PRAKASH 383

Uranyl complexes formed in the $UO_2^{2+} - Cl^- -$acetone system, A spectrophotometric study of —, N. PĂUNESCU 289

Wegscheider's cyclicity conditions, A new general form of —, V. POPA, E. SEGAL and M. VLAD. 625

ORSZÁGOS MŰSZAKI INFORMÁCIÓS KÖZPONT ÉS KÖNYVTÁR
1983

NOTE POUR LES AUTEURS

La Revue Roumaine de Chimie publie des articles en anglais, français, russe, allemand ou espagnol. Les auteurs sont priés d'envoyer des articles et des comptes rendus inédits.

Les manuscrits seront dactylographiés à double interligne. La bibliographie, les tableaux et la légende des figures seront placés après le texte.

Si l'article fait partie d'une série numérotée, la partie précédente sera donnée comme première référence.

Chaque article sera précédé d'un résumé comprenant quinze lignes au maximum.

Les références bibliographiques dans le texte seront faites par des exposants sans parenthèses et paraîtront à la fin de l'ouvrage.

Les publications périodiques mentionnées dans la bibliographie seront présentées suivant les prescriptions internationales : le nom de l'auteur précédé de l'initiale du prénom, le titre du périodiqué abrégé conformément à « Chemical Abstracts » et souligné par une ligne, le numéro du tome indiqué par des chiffres arabes et souligné par deux lignes, suivi de la première page de l'article ; à la fin, l'année de la parution sera placée entre parenthèses. Le numéro de la revue ne sera pas indiqué si les pages du volume sont numérotés consécutivement.

Les textes des livres ou traités inclueront : le nom des auteurs, l'initiale du prénom, le titre du livre entre guillemets et sans être souligné, le numéro du tome précédé par l'abréviation « vol. » (ou « Bd. »), le numéro de l'édition, les éditions (the publisher), la localité de la parution du livre, l'année de la parution et la page de la référence précédée(s) par l'abréviation « p » (ou « S »).

Les brevets seront indiqués comme suit : l'auteur ou la firme, le pays et le numéro du brevet, la date et la revue (*Chem. Abstr.*). Par ex. : M. Jones (to Union Carbide Co.), Brit. Pat. 601 238, 2 Sept. 1959 ; cf. *Chem. Abstr.*, **54**, 12808 (1960).

Si la référence n'a pas été lue en original, on indiquera aussi la revue de référence consultée.

Les diagrammes seront tracés à l'encre de Chine sur papier calque. Les tableaux et les figures (en nombre strictement nécessaire) ainsi que les courbes dans les figures seront numérotés par des chiffres arabes. Leur explication sera donnée dans la légende des figures. Prière de ne pas inscrire les mêmes données dans les tableaux et les figures. Chaque tableau aura un titre. On indiquera dans le texte la place approximative des tableaux et des figures. Les formules chimiques seront incluses dans le texte ; en outre, elles seront transcrites sur papier calque, à l'encre de Chine.

Les auteurs sont priés d'indiquer les caractères italiques (en soulignant les lettres au crayon), ainsi que tout autre caractère spécial ; les préfixes *ortho, meta, para, cis, trans*, etc. seront soulignés pour indiquer leurs caractères italiques et ne seront jamais écrits avec des majuscules.

Aucune correction à la main ne sera admise sur le manuscrit. Les corrections seront tapées à la machine. Les lettres grecques ou d'autres symboles spéciaux seront insérés à la main à l'encre clairement.

Le manuscrit sera signé par l'auteur.

Le titre-courant aura 50 lettres au maximum.

L'entière responsabilité du contenu des articles appartient aux auteurs.

Sur demande on peut obtenir une note plus complète.

PRINTED IN ROMANIA

1985 MAR 14

TRAVAUX PARUS AUX ÉDITIONS DE L'ACADÉMIE DE LA RÉPUBLIQUE SOCIALISTE DE ROUMANIE

ELENA CEAUȘESCU, **Cercetări în chimia și tehnologia polimerilor**, 1983, 519 p.

N. ASANDEI, A. GRIGORIU, **Chimia și structura fibrelor**, 1983, 395 p.

N. IONESCU, M. CĂLDĂRARU, **Oxidarea catalitică a olefinelor inferioare**, 1983, 178 p.

C. CAȘCAVAL, **Studiul polimerilor prin piroliză și cromatografie de gaze**, 1983, 220 p.

C. I. SIMIONESCU, F. DENEȘ, **Originea vieții**, 1983, 110 p.

C. BODEA (editeur), **Tratat de biochimie vegetală**, II, Tome IV, 1982, 408 p.

I. G. MURGULESCU, RODICA VÎLCU, **Introducere în chimia fizică**, **Vol. III. Termodinamica chimică**, 1982, 624 p.

ELENA JERCAN, **Analiza cromatografică**, 1982, 286 p.

I. G. MURGULESCU, J. PĂUN, **Introducere în chimia fizică. Vol. I. 3. Nucleul atomic, reacții nucleare, particule elementare**, 1982, 606 p.

ELENA CEAUȘESCU, **Noi cercetări în domeniul compușilor macromoleculari**, 1981, 536 p.

I. G. MURGULESCU, TATIANA ONCESCU, E. SEGAL, **Introducerea în chimia fizică. Vol. II. 2. Cinetică chimică și cataliză**, 1981, 1024 p.

V. DRĂGUȚAN, A. T. BALABAN, M. DIMONIE, **Metateza olefinelor și polimerizarea prin deschidere de inel a cicloolefinelor**, 1981, 254 p.

LYDIA-MARIA VAICUM, **Epurarea apelor uzate cu nămol activ. Bazele biochimice**, 1981, 218 p.

I. GĂLĂȚEANU, **Procese și metode radiochimice în energetica nucleară**, 1981, 234 p.

O. IORDACHE, **Procese polistocastice aplicate la fenomenele de transfer**, 1981, 186 p.

CR. SIMIONESCU, VALERIA GORDUZA, **Polimeri biocompatibili și biologic activi**, 1980, 497 p.

ELENA CEAUȘESCU, **Polimerizarea stereospecifică a izoprenului**, 1979, 307 p.

CONST. GH. MACAROVICI, **Analiza chimică cantitativă anorganică**, 1979, 457 p.

M. FLORESCU, **Metode științifice în dezvoltarea industriei chimice moderne**, 1979, 256 p.

A. T. BALABAN, I. GĂLĂȚEANU, G. GEORGESCU, LIGIA SIMIONESCU, **Compuși marcați și radiofarmaceutici cu aplicații în medicina nucleară**, 1979, 495 p.

I. G. MURGULESCU, E. SEGAL, **Introducere în chimia fizică, Vol. II. 1. Teoria molecular-cinetică a materiei**, 1979, 1036 p.

S. STERNBERG, FL. DANEȘ, **Termodinamica chimică aplicată**, 1978, 400 p.

I. G. MURGULESCU, V. EM. SAHINI, **Introducere în chimia fizică. Vol. I. 2. Structura și proprietățile moleculelor**, 1978, 604 p.

I. ZUGRĂVESCU, MAGDA PETROVANU, **N-ylid chemistry**, coédition avec McGraw-Hill International Book Company, U.S.A., 1977, 396 p.

I. G. MURGULESCU, **Introducere în chimia fizică. Vol. I. 1. Atomi, molecule, legătură chimică**, 1976, 560 p.

ELENA CEAUȘESCU, **Research work on synthesis and characterization of macromolecular compounds. Contributions**, 1974, 251 p.

CR. SIMIONESCU, VIORICA RUSAN, V. POPA, **Chimia algelor marine**, 1974, 212 p., 1 pl.

ISSN 0035—3930

I.P. INFORMAȚIA C. 2399

43 426

Lei 40

$ 75 (pour un abonnement annuel)